NATURE ENVIRONMENT & POLLUTION TECHNOLOGY

A Multidisciplinary, International Journal on Diverse Aspects of Environment

Technoscience Publications

website: www.neptjournal.com

INSTRUCTIONS TO AUTHORS

Scope of the Journal

The Journal publishes original research/review papers covering almost all aspects of environment like monitoring, control and management of air, water, soil and noise pollution; solid waste management; industrial hygiene and occupational health hazards; biomedical aspects of pollution; conservation and management of resources; environmental laws and legal aspects of pollution; toxicology; radiation and recycling, etc.

Format of Manuscript

- The manuscript (mss) should be typed in double space leaving wide margins on both the sides.
- First page of mss should contain only the title of the paper, name(s) of author(s) and name and address of Organization(s) where the work has been carried out along with the affiliation of the authors.

Nature Environment and Pollution Technology
Vol. 24, No. (1), March 2025

CONTENTS

The Journal is Currently **Abstracted and Indexed** in:

- CNKI Scholar (China National Knowledge Infrastructure)
- Scopus Cite Score (2023) 1.2
- Scopus®, SJR (2023) 0.204
- Index Copernicus (2022) = 132.21
- Indian Science Abstracts, New Delhi, India
- Chemical Abstracts, U.S.A.
- Pollution Abstracts, U.S.A.
- Elsevier Bibliographic Databases
- Paryavaran Abstract, New Delhi, India
- Zoological Records
- CAB Abstracts, U.K.
- Electronic Social and Science Citation Index (ESSCI)
- Indian Citation Index (ICI)
- CrossRef (DOI)
- EBSCO: Environment Index™
- ProQuest, U.K.
- Google Scholar
- DOAJ
- Zetoc
- J-Gate
- Environment Abstract, U.S.A.
- Centre for Research Libraries
- Elektronische Zeitschriftenbibliothek (EZB)
- CSA: Environmental Sciences and Pollution Management
- Access to Global Online Research in Agriculture (AGORA)
- Present in UGC-CARE List (Group II)

- WorldCat (OCLC)
- British Library
- Connect Journals (India)
- Indian Science
- JournalSeek
- Research Bible (Japan)
- SHERPA/RoMEO
- Directory of Science
- AGRIS (UN-FAO)
- Ulrich's (Refereed) database
- NAAS Rating 2024 = 5.33

- UDL-EDGE (Malaysia) Products like i-Journals, i-Focus and i-Future

www.neptjournal.com

Nature Environment and Pollution Technology

Green Marketing Practices and Sustainability Performance of Manufacturing Firms: Evidence from Emerging Markets

Derrick Nukunu Akude[1]†, John Kwame Akuma[2], Emmanuel Addai Kwaning[2] and Kojo Agyekum Asiama[3]

[1]Department of Marketing, Ghana Communication Technology University, PMB 100, Tesano, Accra, Ghana

[2]Department of Accounting and Finance, Ghana Communication Technology University, PMB 100, Tesano, Accra, Ghana

[3]Department of Accounting and Finance, Data Link Institute of Business and Technology, Tema, Ghana

†Corresponding author: Derrick Nukunu Akude; dakude@gctu.edu.gh

ABSTRACT

This study investigates the relationship between green marketing practices and the sustainability performance of manufacturing firms in emerging markets. A self-administered questionnaire was used to collect data from 270 respondents, and the analysis was conducted using Smart PLS-SEM (version 4). The results demonstrate a significant positive relationship between green internal marketing and the overall sustainability performance of the firms. Specifically, green marketing communication was found to positively influence both environmental and social performance, although it did not have a significant effect on financial performance. Likewise, the adoption of green products substantially improved environmental performance but did not significantly impact financial or social performance. Additionally, the study supports a positive association between green strategy implementation and sustainability performance. These findings underscore the critical role of integrating green marketing practices into sustainability initiatives. The research provides valuable insights for managers and policymakers, emphasizing the need for a holistic approach to green marketing to enhance environmental and social outcomes, even if financial benefits are not immediately apparent. This study contributes to the growing body of knowledge on sustainable business practices and offers practical implications for achieving long-term sustainability in manufacturing firms.

INTRODUCTION

According to Akuma et al. (2024), the implementation of relevant management practices helps to enhance the performance of manufacturing firms. Such practices include green marketing practices (GMP). The adoption of green marketing strategies has emerged as a significant global issue, compelling businesses, consumers, and governments to acknowledge the environmental impacts of their actions across various sectors (Gupta & Gupta 2020, Szabo & Webster 2021), including the manufacturing industry (Muisyo et al. 2022). The detrimental effects of overproduction, carbon emissions, and hazardous waste generated by organizations, particularly within the manufacturing sector, have led stakeholders to pressure companies into adopting, implementing, and monitoring environmentally sustainable practices (Baah et al. 2021, Dai et al. 2022). Consequently, industrial firms are required to adopt sustainable practices that balance environmental, financial, and social performance metrics (Shabbir & Wisdom 2020). Notably, green marketing practices (GMP) not only help protect the environment but also enhance company reputation (Bahta et al. 2021), attract environmentally conscious entrants (Umrani et al. 2022), foster customer loyalty (Justavino-Castillo et al. 2022), reduce costs, ultimately leading to increased profits and improved firm performance (Ren & Hussain 2022). Furthermore, green marketing practices are essential for companies aiming to achieve sustainable business operations (Szabo & Webster 2021).

The interrelationship between certain dimensions of GMP and sustainability performance (SsP) is accentuated in prose, where scholars indicated the vital role of GMP in achieving sustainability performance (Chung 2020, Mele et al. 2019, Shabbir & Wisdom 2020). This implies that GMP can drive operating efficacy as well as cost savings through resource optimization and waste decrease initiatives (Mishra et al. 2020). For instance, green products (Hossain & Khan 2018) and green marketing communication (Mahmoud et al. 2017) were established to have significant positive affiliations with economic performance. However, the consequence of green strategy (GS) as well as green internal marketing (GIM) practices on sustainability performance (SsP) has not been sighted in the literature. Meanwhile, Vilkaite-Vaitone et al. (2022) recommend that these aspects of green marketing practices should be considered by scholars. This is because while GS ensures that a firm regularly engages its stakeholders on appropriate green practices, GIM encourages firms to constantly explain their green practices in their annual reports as well as at workshops. These will, in turn, boost the sustainability performance of firms (Vilkaite-Vaitone et al. 2022)

It must be noted that since scholars have focused on limited areas of green marketing practices and sustainability performance, this has led to a limited understanding of the concepts (Ren & Hussain 2022). Consequently, Mehraj & Qureshi (2020) explained that the majority of the studies on GMP have mainly scrutinized the consequence of green marketing (GM) on green consumer behavior, green manufacturing initiatives, as well as organizational performance (Shabbir & Wisdom 2020).

Moreover, several sources have explored the consequence of aspects of green marketing practices such as product, price, and promotion as well as place on various aspects of sustainability performance, including environmental, economic, and social performance (Qalati et al. 2023). However, the influence of green strategy, green internal marketing, green product as well as green marketing communication from an integrated perspective on sustainability performance remains inconclusive. The influence of Green strategy and green internal marketing practices in particular, on sustainability performance has not been sighted in the literature. Meanwhile, Vilkaite-Vaitone et al. (2022) recommend that these aspects of green marketing practices should be considered at the strategic, tactical as well as operational levels of a firm.

Moreover, there is an international demand for research examining the impact of green marketing within the manufacturing sector, given its significant role in waste production, greenhouse gas emissions, and the enhancement of firms' overall sustainability performance (Baah et al. 2021).

Furthermore, the manufacturing industry is recognized as one of the most polluting sectors in both developed and developing nations (Javeed et al. 2020). Consequently, green marketing has garnered significant attention in developed countries (Papadas et al. 2019, Han et al. 2019, Mehraj & Qureshi 2020). However, only a small number of manufacturing firms in developing countries focus on green practices due to the limited presence of corporate green strategies (Hassan & Jaaron 2021). According to Javeed et al. (2020), there is an urgent need for manufacturing firms in developing countries to invest in adopting green policies and green marketing practices to reduce their environmental footprint and meet rising consumer expectations. It is clear that organizational strategies are ineffective without the involvement of employees, as they are essential to strategy implementation (Li et al. 2022, Mahmood et al. 2021, Ren & Hussain 2022).

While research has extensively explored the relationship between green marketing practices (GMP) as well as economic performance (Jones et al. 2021, Lee & Wang 2019), there is a noticeable gap concerning the association between GMP and financial performance. It's important to distinguish between economic performance, which focuses on how these practices contribute to improving GDP and the welfare of individuals, and financial performance, which assesses their impact on boosting the sales and profits of firms (Le et al. 2024). Understanding the financial implications of GMP is crucial for firms seeking to justify investments in sustainability initiatives and demonstrate their business value to stakeholders. By aligning green marketing efforts with financial objectives, firms can leverage sustainability as a driver of competitive advantage as well as profitability in the marketplace (Ofori 2021).

This investigation aims to address the aforementioned gaps by investigating the interplay among green marketing practices, as well as the sustainability performance of manufacturing firms within the setting of emerging nations. By scrutinizing how green marketing practices influence the overall sustainability performance among firms, this research seeks to provide insights into the underlying processes driving green marketing practices to achieve overall performance. Ultimately, the findings of this investigation have the potential to inform how green marketing practices enhance firm performance and contribute to the theoretical understanding of green marketing practices as well as sustainability performance. Explicitly, the objectives of this investigation are:

- To assess the relationship between green strategy and sustainability performance.
- To examine the association between green internal marketing and sustainability performance.
- To evaluate the link between green products and sustainability performance.
- To examine the affiliation among green marketing communication as well as sustainability performance.

Subsequent sections of the paper will include literature summaries on green marketing practices, as well as firm performance, followed by the presentation of the investigation's methodology. Analysis and results will be provided in subsequent sections, with the paper concluding by discussing the findings and their theoretical and practical implications.

LITERATURE REVIEW

Theoretical Foundation and Hypotheses

Green marketing practices and sustainability performance constitute a complex interplay within the domain of manufacturing industries. This literature review aims to synthesize existing theoretical frameworks and literature to elucidate the relationships between these constructs.

Stakeholder theory (ST): The Stakeholder Theory (ST) posits that firms are accountable to various stakeholders, including customers, employees, and communities, and must consider their interests in decision-making processes (Freeman 2010). From this perspective, adopting green marketing practices serves to meet the expectations of environmentally conscious stakeholders, thereby enhancing the firm reputation, legitimacy, and, ultimately, sustainability performance (Lee & Park 2019). Cogdill et al. (2017) have recently revised the theory, asserting that companies should not solely concentrate on enhancing their stock price without also taking into account the diverse groups and individuals impacted by the company's operations. These individuals might eventually become clients or might be willing to assume some of the organization's risks (Cogdill et al. 2017). Recent advancements in stakeholder theory underscore the dynamic and interconnected nature of stakeholder relationships, emphasizing the significance of dialogue, engagement, and collaboration between organizations as well as their stakeholders (Bansal & Roth 2020).

Stakeholder theory has diverse applications across various domains, including corporate governance, strategic management, and sustainability. Organizations that adopt a stakeholder-oriented approach tend to focus on enduring value creation, balancing the interests of multiple stakeholders to enhance organizational resilience and legitimacy (Fassin & Van Rossem 2022). Moreover, stakeholder theory provides a framework for addressing emerging challenges such as climate change, social inequality, and technological disruption, encouraging organizations to adopt proactive and inclusive strategies for sustainable development (Crane et al. 2023).

Resource-based view theory (RBV): The RBV proposes that sustainable competitive advantage can be derived from valuable, rare, as well as non-substitutable resources (Barney 1991). Green marketing capabilities, such as eco-design and green supply chain management, can be viewed as strategic resources that contribute to superior sustainability performance (Chen et al. 2023). Topical advancement within RBV highlights the importance of resource orchestration, path dependence, and the role of context in shaping resource-based strategies (Eisenhardt & Martin 2021).

RBV theory has significant implications for strategic management practices, informing decisions related to resource allocation, diversification, and innovation. Organizations that leverage their unique resources and capabilities can achieve superior performance and resilience in dynamic markets (Arend & Bromiley 2022)

Triple Bottom Line framework (TBL): The TBL framework emphasizes the interconnectedness of economic, social, as well as environmental outcomes (Elkington, 1997). Green marketing practices contribute to the environmental dimension of the Triple Bottom Line, which, in turn, can positively influence financial performance. Initially focused on expanding the scope of organizational performance measurement beyond financial metrics, TBL has evolved to encompass broader notions of sustainability, corporate citizenship, and stakeholder engagement (Bansal & DesJardine 2020). Recent progress within TBL indicates the importance of integrated reporting, materiality assessment, and the role of technology in advancing sustainability practices (Lozano et al. 2023).

However, debates persist regarding the trade-offs between economic growth and sustainability, as well as the challenges of measuring and valuing non-financial impacts (Savitz & Weber 2021). Scholars also discuss the role of governance structures, incentives, and accountability mechanisms in driving TBL implementation and effectiveness (Moneva et al. 2022). It is worthy of note that the TBL provides a roadmap for integrating sustainability into strategic decision-making processes, product development, and supply chain management, fostering resilience as well as innovation (Eccles & Serafeim 2024).

Green marketing practices are intricately linked within the context of sustainability performance. Theoretical

frameworks such as stakeholder theory, resource-based theory, as well as the triple bottom line framework, offer valuable insights into the underlying mechanisms driving green marketing practices to the sustainability performance of firms. By understanding these relationships, manufacturing firms can design and implement effective green marketing strategies to enhance sustainability performance outcomes.

Green Marketing Practices and Sustainability Performance

Empirical evidence indicates a complex relationship between green marketing practices and sustainability performance. Numerous studies have demonstrated the positive effects of green marketing initiatives on various sustainability performance dimensions, encompassing environmental, social, and economic aspects (Lai & Cheng 2020, Sarkar & Rajendran 2022). Nevertheless, there are limited studies that examine the relationship between green marketing initiatives and the broader dimensions of sustainability performance, including environmental, social, and financial aspects, from a comprehensive perspective.

Green marketing practices have been shown to positively impact the sustainability performance of manufacturing firms (Qalati et al. 2023, Braik et al. 2023). These practices, encompassing the use of eco-friendly materials, production methods, packaging, pricing, distribution channels, and promotion, can enhance a firm's brand image and fortify its market position (Hamali & Micael 2022).

Consequently, Qalati et al. (2023) determined that environmentally sustainable practices have a direct impact on green employee integration, environmental sustainability, and overall firm performance. In a similar vein, Demessie & Shukla (2023) found that a green marketing strategy enhances firm performance by providing a competitive advantage. Additionally, Braik et al. (2022) reported that the adoption of green marketing practices, such as green products and green placement, improves environmental performance, while green promotion boosts economic performance. Likewise, Li et al. (2020), in their study of Chinese manufacturing firms, noted that proactive green marketing initiatives were linked to better environmental management practices and enhanced overall sustainability performance.

Moreover, Wang et al. (2021) focused on the influence of green product design on the sustainability performance of the electronics industry. Their findings revealed that integrating environmental considerations into product design not only enhanced market competitiveness but also contributed to reduced environmental impacts throughout the product life cycle. This underscores the significance of proactive environmental stewardship in achieving sustainable manufacturing practices.

However, the effectiveness of green marketing practices in driving sustainability performance is contingent upon several factors, such as green strategy, green internal marketing, green product as well as green marketing communication (Vilkaite -Vaitone et al. 2022).

Green Strategy Implementation and Sustainability Performance

Recent studies have highlighted the optimistic relationship between green strategy implementation and sustainability performance across various industries and organizational contexts (Feng et al. 2023, Jabbour et al. 2021). Green strategies encompass a range of practices, including eco-friendly product design, resource efficiency measures, renewable energy adoption, and supply chain sustainability initiatives. Organizations that prioritize green strategies often experience reduced environmental footprint, enhanced brand reputation, and improved stakeholder relationships, ultimately contributing to long-term financial viability and resilience (Sarkis et al. 2022).

Enhanced resource efficiency, cost savings through waste reduction and energy conservation, regulatory compliance, access to green markets, and innovation-driven competitive advantage are the mechanisms that underpin the relationship between green strategy and sustainability performance (Bocken et al. 2020, Lai et al. 2024). Furthermore, organizational factors such as leadership commitment, employee engagement, organizational culture, and stakeholder pressure play vital roles in shaping the effectiveness of green strategy implementation as well as its impact on sustainability performance (Dangelico & Pujari 2023).

Despite the potential benefits, organizations encounter various challenges in implementing green strategies and translating them into tangible sustainability performance improvements. These challenges include high initial investment costs, lack of expertise and resources, resistance to change, complexity of supply chain management, and the trade-offs between environmental objectives and short-term financial goals (Lu et al. 2021, Zhu et al. 2024). Consequently, the following hypotheses have been proposed,

H$_1$: There is a statistically significant relationship between green strategy as well as sustainability performance.

H$_{1a}$: There is a statistically significant relationship between green strategy as well as financial performance.

H$_{1b}$: There is a statistically significant relationship between green strategy as well as environmental performance.

H₁c: There is a statistically significant relationship between green strategy as well as social performance.

Green Internal Marketing Practices and Sustainability Performance

Research has demonstrated the optimistic relationship between green internal marketing practices as well as various dimensions of sustainability performance (Huang et al. 2021, Xie et al. 2023). Green internal marketing encompasses activities such as employee training, communication of sustainability goals and values, recognition of eco-friendly behaviors, and participation in green teams or committees. Organizations that effectively implement green internal marketing strategies tend to experience improved employee engagement, morale, and commitment to sustainability objectives, leading to enhanced environmental performance, cost savings, and innovation (Chen et al. 2022, Liu et al. 2024).

Green internal marketing initiatives create a sense of organizational identity and shared purpose around sustainability goals, fostering a culture of environmental responsibility as well as innovation (Zhang et al. 2020). Moreover, by providing employees with the necessary knowledge, skills, and resources to adopt sustainable behaviors both at work and in their personal lives, green internal marketing contributes to the diffusion of pro-environmental attitudes and practices throughout the organization (Chen et al. 2021). Leadership support, employee involvement, communication effectiveness, and organizational climate for sustainability are critical drivers that influence the effectiveness of green internal marketing efforts and their impact on sustainability performance outcomes (Li et al. 2023).

Nonetheless, organizations encounter challenges in implementing effective green internal marketing strategies. These include resistance to change, lack of employee awareness or motivation, communication barriers, and the need for continuous reinforcement and evaluation of green initiatives (Chen & Huang 2022). Consequently, the following hypotheses have been proposed,

H₂: There is a statistically significant relationship between green internal marketing as well as sustainability performance.

H₂a: There is a statistically significant relationship between green internal marketing as well as financial performance.

H₂b: There is a statistically significant relationship between green internal marketing as well as environmental performance.

H₂c: There is a statistically significant relationship between green internal marketing as well as social performance.

Green Products and Sustainability Performance

There exists a positive relationship between the adoption of green products and various dimensions of sustainability performance (Chen et al. 2021, Hsu et al. 2023). Green products encompass a range of offerings, including eco-friendly goods, energy-efficient appliances, organic foods, and sustainable packaging materials. Organizations that invest in developing and marketing green products often experience enhanced brand reputation, customer loyalty, and market competitiveness, leading to improved environmental outcomes, resource efficiency, and financial performance (Wu et al. 2024).

Green products help mitigate environmental impacts by reducing resource consumption, minimizing pollution, and promoting circular economy principles (Zhang et al. 2021). Moreover, green products contribute to sustainable consumption patterns by raising consumer awareness, shifting preferences towards eco-friendly alternatives, and fostering pro-environmental behaviors (Chang et al. 2022). Organizational factors such as innovation capabilities, supply chain management practices, and stakeholder engagement also play crucial roles in driving the adoption and diffusion of green products and their impact on sustainability performance outcomes (Tong & Zhao 2020).

However, organizations face challenges in developing and marketing green products effectively. These challenges include high development costs, limited consumer demand or willingness to pay premium prices, regulatory uncertainties, and the need for supply chain transparency and certification (Lin et al. 2023). By addressing these challenges and leveraging opportunities for collaboration, innovation, and market differentiation, organizations can capitalize on the growing demand for sustainable products and drive positive environmental and social impacts (Huang et al. 2024). Consequently, the following hypotheses have been proposed,

H₃: There is a statistically significant relationship between green products and sustainability performance.

H₃a: There is a statistically significant relationship between green products as well as financial performance.

H₃b: There is a statistically significant relationship between green products as well as environmental performance.

H₃c: There is a statistically significant relationship between green products as well as social performance.

Green Marketing Communication and Sustainability Performance

The positive relationship between green marketing

communication strategies, as well as various dimensions of sustainability performance, is grounded in extant literature (Chen et al. 2021, Lai et al. 2023). Green marketing communication encompasses a range of activities, including advertising, public relations, social media engagement, and corporate sustainability reporting. Organizations that adopt transparent, authentic, and credible green marketing communication strategies often experience improved brand reputation, customer loyalty, and market share, leading to enhanced environmental performance, stakeholder trust, and financial resilience (Zhang et al. 2022, Wang et al. 2024).

Effective green marketing communication helps raise awareness about environmental issues, educate consumers about sustainable choices, and shape attitudes and behaviors toward more eco-friendly alternatives (Luo et al. 2020). Moreover, by providing transparent information about sustainability practices, certifications, and product attributes, green marketing communication enhances consumer trust, reduces perceived risk, and strengthens brand loyalty (Lin et al. 2021). Organizational factors such as leadership commitment, employee engagement, and stakeholder collaboration also play critical roles in driving the effectiveness of green marketing communication efforts and their impact on sustainability performance outcomes (Chang et al. 2023).

However, there is the challenge of greenwashing, where organizations exaggerate their environmental commitments, as well as consumer skepticism, information overload, and the need for consistent messaging across different channels

(Wang & Chen 2024). By addressing these challenges and leveraging opportunities for storytelling, co-creation, and digital engagement, organizations can build trust, credibility, and authenticity in their green marketing communication efforts, driving positive environmental and social impacts (Hsu et al. 2022). Consequently, the following hypotheses have been proposed.

H$_4$: There is a statistically significant relationship between green marketing communication as well as sustainability performance.

H$_{4a}$: There is a statistically significant relationship between green marketing communication as well as financial performance.

H$_{4b}$: There is a statistically significant relationship between green marketing communication as well as environmental performance.

H$_{4c}$: There is a statistically significant relationship between green marketing communication as well as social performance.

Fig. 1 shows the relationship of green marketing practices and sustainable performance through the proposed hypotheses.

MATERIALS AND METHODS

Survey Instrument

The survey instrument was created by selecting a questionnaire
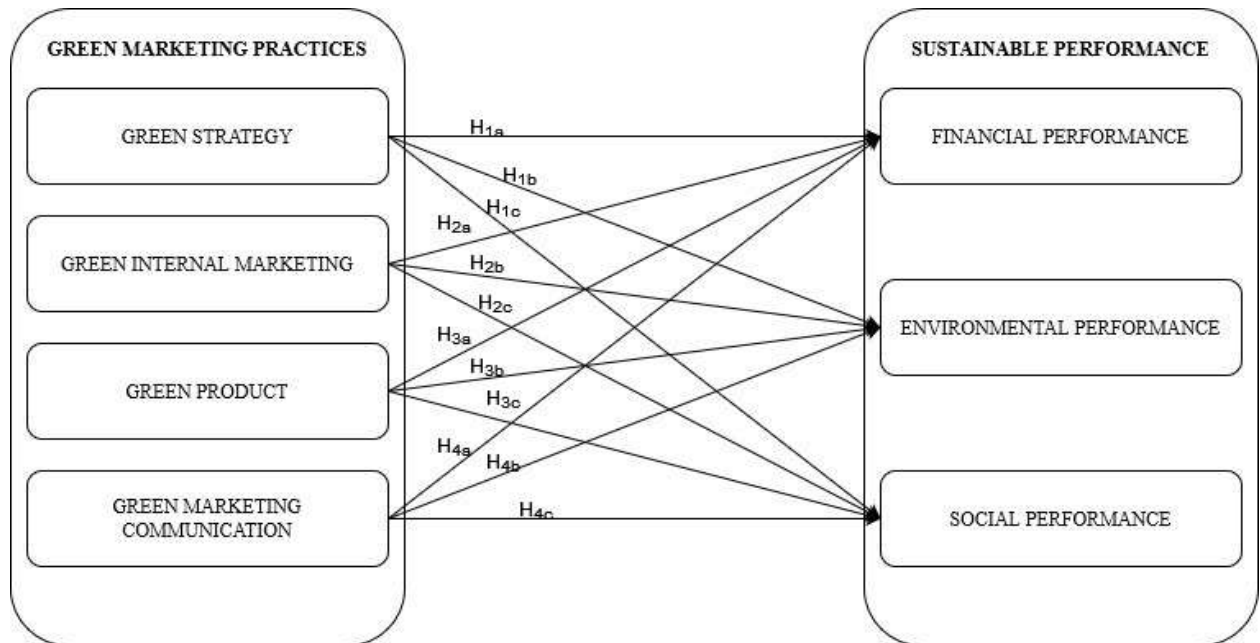
Fig. 1: Authors' own construct (2024).

from the literature to assess the research model's constituent parts. Using information from a survey sample, the study assessed the validity as well as reliability of the instrument and tested the proposed relations. The question types used to assess green marketing practices have been modified (Mahmoud et al. 2017, Hossain & Khan 2018, Vilkaite-Vaitone et al. 2022). Additionally, the questions used for sustainability performance were modified (Hasan & Ali 2017). For the investigation, a 5-point Likert scale was used. It is worthy of note, that two academic faculties (marketing and finance) assessed the content validity of the initial survey.

Sampling and Data Collection

This cross-sectional survey design targeted 634 manufacturing firms registered with the Association of Ghana Industries (AGI) as of 2024. These firms were categorized based on their respective products. The study relied on the Krejcie & Morgan (1970) formula below to determine the minimum sample size.

$$S = \frac{X^2 NP(1 - P)}{d^2(N - 1) + X^2 P(1 - P)}$$

Where:

S = the required sample size.

X^2 = the table value of chi-square for 1 degree of freedom at the desired confidence level (3.841)

N = the population size

P = the population proportion assumed to be 0.5 since this would provide a maximum sample size

d = the degree of accuracy expressed as a proportion (0.05)

According to the sample size determination formula by Krejcie & Morgan (1970), with a target population of 634 registered manufacturing firms, the minimum sample size required for this survey at a 95% confidence level and a 0.05 margin of error is 242. To achieve this target, 282 questionnaires were distributed via Google Forms, using stratified and simple random sampling techniques. A total of 270 questionnaires were retrieved, yielding a response rate of 95.7%. Each questionnaire was completed by a manager from the respective firms. The manufacturing firms in the study are well-known both domestically and abroad for their visibility and adoption of sustainable practices. Participants received a cover letter outlining the study's objectives and eligibility before the commencement of the survey. Participants were asked informally by researchers about whether they were interested in taking part in the study. After expressing interest, those who requested to fill out the questionnaire were asked to do so voluntarily.

Profile of Respondents

In total, 270 valid responses were collected and used for statistical analysis. Of these, 64.5% (n=174) were males, and 35.5% (n=96) were females, indicating a higher number of male respondents compared to females. The study employed the age classifications recommended by Yarlagadda et al. (2015), namely young adults (<31 years), middle-aged adults (31 to 50 years), and senior adults (>50 years) (Table 1).

The study reveals that 39% (n=104) of the respondents were young adults, 53% (n=142) were middle-aged adults, and 8% (n=24) were senior adults, indicating that middle-aged managers comprised the majority of respondents. This suggests that the respondents are mature and experienced, making them well-positioned to provide insights into the management accounting practices of manufacturing firms.

Regarding the positions held by the respondents, 16.7% (n=45) were Chief Executive Officers (CEOs) or General Managers, 58.7% (n=158) were senior managers, 12.5% (n=34) were board members, and 12.1% (n=33) were middle-level managers. This indicates that senior managers and CEOs together constituted 75.4% (n=203) of the respondents. These top-level employees, with their extensive experience, are thus capable of providing high-quality responses regarding their green marketing practices.

Data Analysis

The statistical analysis was carried out using Smart PLS (version 4.0) software in an attempt to compare the interrelationship between green marketing practices and sustainability performance outcomes (Ringle et al. 2022). PLS-SEM was used because it is more flexible in handling

Table 1: Profile of respondents.

Details	Classes	Frequency	Percentage
Gender	Male	174	64.5%
	Female	96	35.5%
Age	< 30 years	104	39%
	31 and 50 years	142	53%
	> 50 years	24	8%
Highest qualification	Degree	174	64.5%
	Masters	35	12.9%
	Pre-Secondary	23	8.7%
	Diploma	29	10.7%
	Secondary	9	3.2%
Position	Chief Executive Officer	45	16.7%
	Senior Manager	158	58.7%
	Board Member	34	12.5%
	Middle-level Manager	33	12.1%

Source: Field Survey (2024)

various modeling challenges than the difficult and strict assumptions relating to the use of multivariate statistics (Boonlertvanich 2019).

Hair et al. (2019) suggested that pointers assessing a concept in the structural model ought to be 0.70 for an investigation that utilizes validated concepts to guarantee the dependability of the research items. This is due to the indication explaining more than 50% of the variance of the indicator. Because this investigation utilized validated constructs from prior research, a reliability test was conducted utilizing the indicators, employing a minimal reliability criterion of 0.70.
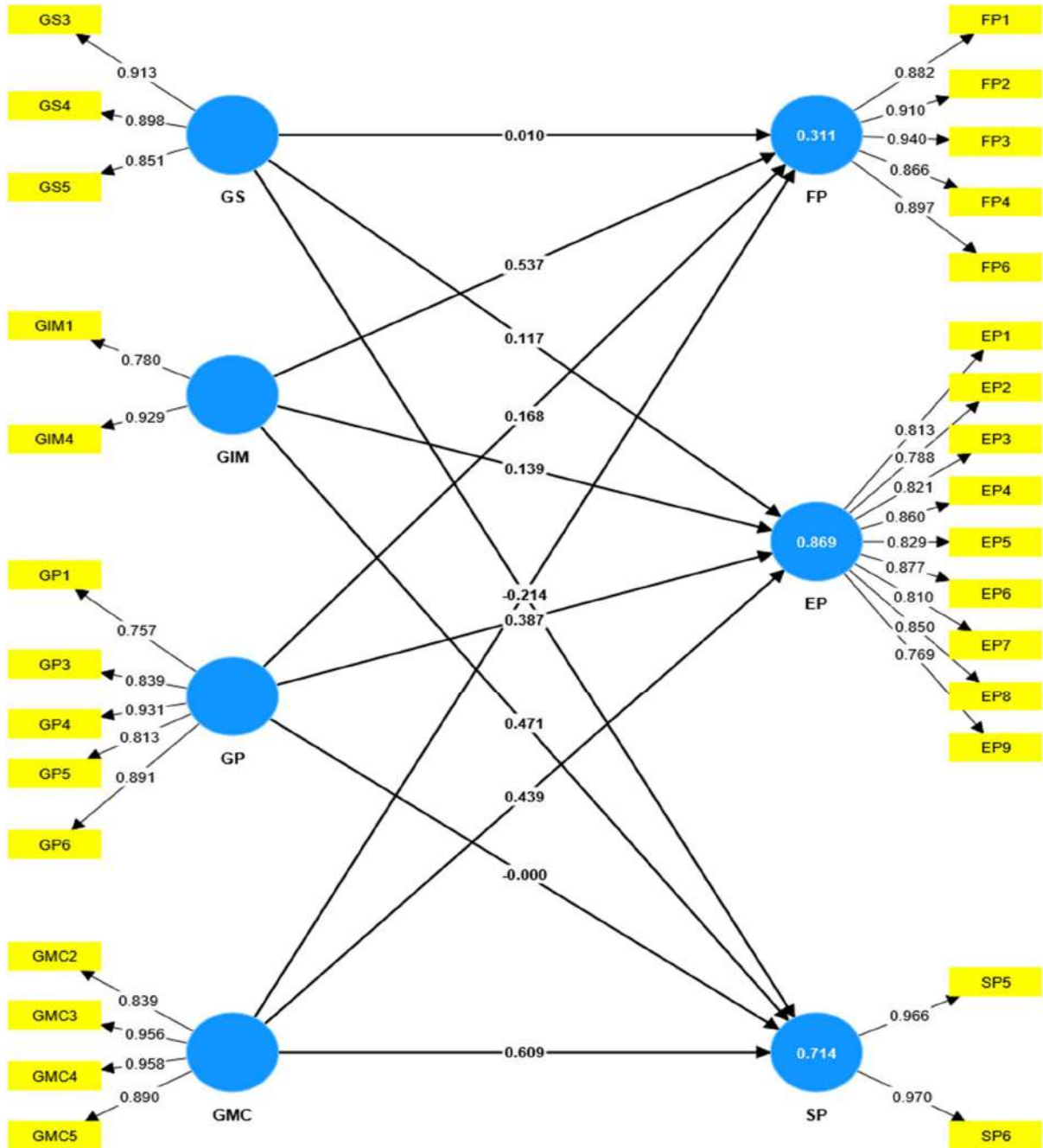
Fig. 2: Measurement model.

Evaluation of Measurement Model

We appraised the measurement model using PLS-SEM (version 4) (Fig. 2). Seven components made up the conceptual outline of this investigation, namely, environmental performance, financial performance, green internal marketing, green marketing communication, green product, green strategy, and social performance.

RESULTS

To assess the measurement model, the construct reliability, convergent validity, and discriminant validity of the seven constructs were evaluated (Hair et al. 2019, Hanafiah 2020). Reliability is established if Cronbach's alpha, composite reliability (rho_a), and composite reliability (rho_c) are all above 0.7 (Table 2). Additionally, to establish convergent validity, the average variance extracted (AVE) must exceed 0.5 (Ringle et al. 2022).

Table 2 demonstrates that items, as well as constructs in this investigation, had adequate degrees of convergent validity as well as reliability on each of the seven constructs used in this investigation. We used the most conservative method, the heterotrait-monotrait (HTMT) ratio, to evaluate the discriminant validity (Henseler et al. 2015). The HTMT ratio has also recently been proven to be a better evaluation standard in comparison to other conventional appraisal techniques (Henseler et al. 2015). To prove discriminant validity, each concept's HTMT ratio needs to be less than 0.9. (Ringle et al. 2022). The findings of HTMT are presented in Table 5, which reveals a satisfactory discriminant validity (Table 3).

Evaluation of the Structural Model

The structural model must be appraised to scrutinize the interrelationship between green marketing practices as well

Table 2: Cronbach alpha, Composite Reliability Rho_a, and Composite Reliability rho_c.

	Cronbach's alpha	Composite reliability (rho_a)	Composite reliability (rho_c)	Average variance extracted (AVE)
EP	0.914	0.914	0.933	0.700
FP	0.941	0.948	0.955	0.809
GIM	0.856	0.879	0.902	0.698
GMC	0.932	0.945	0.952	0.832
GP	0.905	0.922	0.933	0.778
GS	0.869	0.878	0.938	0.884
SP	0.933	0.936	0.968	0.937

Note: EP = Environmental performance, FP = Financial performance, GIM = Green internal marketing, GMC = Green marketing communication, GP = Green product, GS = Green strategy, SP = Social performance.

Table 3: Discriminant validity assessment (HTMT).

	EP	FP	GIM	GMC	GP	GS
FP	0.525					
GIM	0.866	0.591				
GMC	0.805	0.325	0.775			
GP	0.831	0.418	0.826	0.576		
GS	0.821	0.336	0.899	0.752	0.719	
SP	0.759	0.584	0.756	0.832	0.479	0.568

as sustainability performance. Consequently, the hypotheses of the investigation were tested.

Collinearity Assessment

Collinearity among latent variables is assessed through the Variance Inflated Factor (VIF) (Table 4). Implicatively, VIF ≥ 5 specifies a probable collinearity problem (Hair et al. 2011). The results presented in Table 6 revealed that all the values are below 5; therefore, the model does not have any potential collinearity problem. Consequently, the model is free of common method bias (Kock 2015).

The significance of the path coefficients should be evaluated, together with the R-square (R^2) and Stone-Geisser criterion (Q^2), for green marketing practices and sustainability performance to appraise the structural model (Hair et al. 2017). The R^2 values of 0.777 for environmental performance are regarded as excellent scores in the behavioral sciences (Rasoolimanesh et al. 2017). This indicates that 77.7% of the four predictors are explained by the variance in environmental performance. Moreover, The R^2 value of 0.330 for financial performance is regarded as a medium score (Rasoolimanesh et al. 2017). This indicates

Table 4: Inner VIF.

	VIF
GIM -> EP	3.919
GIM -> FP	3.919
GIM -> SP	3.919
GMC -> EP	2.307
GMC -> FP	2.307
GMC -> SP	2.307
GP -> EP	2.160
GP -> FP	2.160
GP -> SP	2.160
GS -> EP	2.806
GS -> FP	2.806
GS -> SP	2.806

that 33.0% of the four predictors are explained by the variance in financial performance. Furthermore, The R^2 value of 0.670 for social performance is regarded as an excellent score (Rasoolimanesh et al. 2017). This indicates that 67.0% of the four predictors are explained by the variance in social performance. The variances, as explained, were above the minimum threshold R^2 assessment of 25% (Hair et al. 2016).

According to Ali et al. (2018), the assessment of Q^2 ought to be greater than zero to show that a structural model is prognostic, in this situation, we observed a Q^2 assessment of 0.772 for environmental performance, 0.310 for financial performance, and 0.663 for social performance. These numbers demonstrate the model's good predictive capabilities.

Green internal marketing has a positive effect on environmental, financial, and social performance, respectively. Moreover, green marketing communication has a positive effect on environmental and social performance, respectively. However, green marketing communication has a negative effect on financial performance. Furthermore, the green product has a positive effect on environmental and financial performance respectively. However, the green product has a negative effect on social performance. Also, green strategy has a negative effect on financial and social performance, respectively. However, a green strategy has a positive effect on environmental performance. It is worthy of note that green internal marketing influenced financial performance the most. Green marketing communication also influenced social performance the most. In addition, green products influenced environmental performance the most.

Hypotheses Testing (Direct Effect)

As a conclusion of the direct effect, nine of the twelve hypotheses were supported: green internal marketing to environmental performance ($\beta = 0.143$, $p < 0.05$), green internal marketing to financial performance ($\beta = 0.769$, $p < 0.05$), green internal marketing to social performance ($\beta = 0.474$, $p < 0.05$), green marketing communication to environmental performance ($\beta = 0.343$, $p < 0.05$), green marketing communication to social performance ($\beta = 0.643$, $p < 0.05$). However, green marketing communication to financial performance is insignificant ($\beta = -0.140$, $p = 0.139$), and green product to environmental performance is significant ($\beta = 0.400$, $p < 0.05$). However, green product to financial performance is insignificant ($\beta = 0.082$, $p = 0.116$). Also, green product to social performance is insignificant ($\beta = -0.084$, $p = 0.060$), green strategy to environmental performance ($\beta = 0.133$, $p < 0.05$), green strategy to financial performance ($\beta = -0.242$, $p < 0.05$) and green strategy to social performance ($\beta = -0.240$, $p < 0.05$) were supported (Table 5).

The investigation also appraised the effect size (f2), which is a measure of whether a certain exogenous construct significantly affects an outcome variable. Subject to Cohen's (1988) suggestion, the result of the investigation revealed that green marketing communication has a large effect size on social performance. Moreover, the green product has a medium effect size on environmental performance. Nevertheless, green internal marketing and green marketing communication have a small effect size on financial performance and environmental performance, respectively.

Table 5: Hypotheses analysis.

	Original sample (O)	f-square	T statistics (|O/STDEV|)	P values	Decision
GIM -> EP	0.143	0.024	2.082	0.037	Significant
GIM -> FP	0.769	0.225	13.089	0.000	Significant
GIM -> SP	0.474	0.173	7.193	0.000	Significant
GMC -> EP	0.343	0.229	10.522	0.000	Significant
GMC -> FP	-0.140	0.013	1.481	0.139	Insignificant
GMC -> SP	0.643	0.543	13.904	0.000	Significant
GP -> EP	0.400	0.332	8.898	0.000	Significant
GP -> FP	0.082	0.005	1.571	0.116	Insignificant
GP -> SP	-0.084	0.010	1.884	0.060	Insignificant
GS -> EP	0.133	0.028	2.930	0.003	Significant
GS -> FP	-0.242	0.031	3.054	0.002	Significant
GS -> SP	-0.240	0.062	5.114	0.000	Significant

DISCUSSION

Grounded on the stakeholder theory, resource-based theory, as well as the triple bottom line framework, the investigation contrasts the relationships between green marketing practices and the sustainability performance of manufacturing firms. Our results provide actual evidence for the crucial part that green marketing practices play a critical role in channeling the sustainability performance of manufacturing firms.

Overall, nine of the twelve hypotheses were supported, the study noted the presence of a significant positive relationship between green internal marketing as well as environmental performance. Similarly, the relationship between green internal marketing as well as financial performance, and green internal marketing as well as social performance were also significant. In addition, there is a significant positive connection between green marketing communication and environmental performance, as well as green marketing communication and social performance. However, the relationship between green marketing communication and financial performance is insignificant. Moreover, the relationship between green products and environmental performance is positively significant. However, the relationship between green products as well as financial performance is insignificant.

Similarly, the relationship between green products as well as social performance is insignificant. The relationship between green strategy as well as environmental performance is positively significant, while the relationship between green strategy as well as financial performance as well as green strategy, and social performance was negatively significant (Table 5). The result of the investigation revealed that green marketing communication has a large effect size on social performance. Moreover, the green product has a medium effect size on environmental performance. Nevertheless, green internal marketing, as well as green marketing communication have a small effect size on financial performance and environmental performance, respectively.

Implicatively, manufacturing firms who engage in green internal marketing (like looking at environmental achievements of job seekers and contractors before engaging them as well as annual presentation of environmental reports) are more likely to enhance their environmental performance (EP), financial performance (FP) and social performances (SP). The improvements in EP include using machines that consume less energy, the routine use of recycled materials, winning more environmental awards, and fewer environmental complaints from the public. Improvement in FP includes higher sales, profits, cash flows, and market share, while that of SP includes more implementation of corporate social responsibilities as well as maintaining

cleaner environments for residents through regular clean-up exercises.

Consequently, incorporating green marketing communication (like using eco-friendly items that decay easily like paper in packaging products, putting eco-friendly information on websites, as well as engaging in green advertisements) leads to an enhancement in the EP and SP of manufacturing firms. The improvements in EP include using machines that consume less energy, the routine use of recycled materials, winning more environmental awards and fewer environmental complaints from the public, while that of SP includes more implementation of corporate social responsibilities as well as maintaining cleaner environments for residents through regular clean-up exercises. However, green marketing communication does not enhance the financial performance of manufacturing firms in developing countries.

Using green products (like the production and sale of green products, using raw materials that are safe for the environment and health of consumers to produce goods, producing energy-efficient goods that reduce environmental pollution, use of quality energy efficient appliances as well as production of toxic-free products) contribute to the EP of manufacturing firms. The enhancements in EP include using machines that consume less energy, the routine use of recycled materials, winning more environmental awards and fewer environmental complaints from the public. However, green products do not contribute to both the financial and social performance of manufacturing firms.

Moreover, the practice of green strategy (like incorporating green marketing as a culture as well as promotion of environmental preservation) has a positive significant influence on EP. This means as firms practice green strategy (GS), their EP improves. This EP includes more use of machines that consume less energy, the routine use of recycled materials, winning more environmental awards, and fewer environmental complaints from the public. The study, however, found a negative but significant impact of GS on both financial performance (FP) and social performance (SP). Thus, the more manufacturing firms practice GS, the worse their FP and SP will be, and vice versa. These firms should, therefore, integrate their green strategies with costing since it has the likelihood of lowering the FP and SP.

Green marketing practices play a pivotal role in shaping the sustainability performance of manufacturing firms, offering opportunities to reduce environmental impacts, enhance stakeholder relationships, and drive competitive advantage. By embracing sustainability as a core business imperative and integrating green principles into their

marketing strategies, manufacturing firms can contribute to a more environmentally responsible and socially conscious marketplace while securing long-term profitability, agility, and resilience in an increasingly sustainability-focused world. Overall, the findings suggest that manufacturing firms can effectively leverage green marketing practices to enhance their sustainability performance to meet growing consumer demand for sustainable products, comply with regulatory requirements, and enhance corporate reputation.

CONCLUSIONS

The empirical findings of this study underscore the pivotal role of green marketing practices in enhancing the sustainability performance of manufacturing firms. Green internal marketing and green strategy exhibit significant positive relationships with sustainability performance, indicating that internal efforts to align organizational practices with environmental objectives and strategic orientations toward sustainability yield substantial benefits. The significant positive effects of green marketing communication on both environmental and social performance further illustrate the critical role of effective communication in fostering a corporate culture attuned to sustainability goals and enhancing external stakeholder engagement.

Contrarily, the findings reveal that the relationship between green marketing communication and financial performance, as well as the relationship between green products and both financial and social performance, is not significant. These results suggest that while green marketing initiatives contribute positively to environmental and social dimensions of sustainability, their direct impact on financial outcomes remains limited. This highlights a potential area for further investigation and strategic refinement, as firms might need to explore more integrative approaches that concurrently address financial performance while pursuing sustainability goals.

Overall, the study emphasizes the importance of adopting comprehensive green marketing strategies that not only focus on environmental and social dimensions but also strive to align these efforts with financial performance metrics. Manufacturing firms aiming to achieve sustainable growth must, therefore, consider a balanced approach, integrating green marketing practices across all facets of their operations to foster long-term sustainability and competitive advantage.

Theoretical Implications

Our study establishes a critical linkage between green marketing practices as well as the sustainability performance of manufacturing firms. Consequently, this study adds to the investigation of green marketing practices as well as sustainability performance. This investigation enhances the pertinent inquiry by focusing on the aforementioned constructs.

Furthermore, the conceptualization of the link between green marketing practices as well as the sustainability performance of manufacturing firms offers a new direction for inquiry to increase knowledge of sustainability performance while also empowering manufacturing firms to adopt green marketing initiatives in an attempt to be competitive.

By analyzing the connection between green marketing practices as well as the sustainability performance of manufacturing firms, this research significantly adds to the body of literature. To make sure that the inquiry is pertinent and legitimate in the particular context of interest, the modified measurement of latent constructs in the study is essential. This can result in a more precise and detailed understanding of the connections between the different constructs and offer insightful information.

Manufacturing firms that effectively integrate sustainability into their marketing strategies can develop unique capabilities, such as eco-design, green branding, and environmental certifications, which enhance their sustainability performance. By aligning marketing strategies with sustainability goals, manufacturing firms can build trust and legitimacy with stakeholders, leading to enhanced reputation and long-term relationships.

The adoption of green marketing practices by manufacturing firms can be influenced by institutional pressures from regulatory agencies, industry associations, and societal norms. As green marketing practices become more widespread, they contribute to the mainstreaming of sustainability within the manufacturing sector, driving broader societal change.

Managerial Implications

The findings of this analysis have a lot of implications for the ability of manufacturing firms and businesses to make critical green marketing practices and sustainability performance decisions.

Firstly, it facilitates the reduction of environmental footprints throughout the product lifecycle, from raw material extraction to end-of-life disposal. By incorporating sustainability criteria into product design, production processes, and supply chain management, firms can minimize resource consumption, pollution, and waste generation, thereby mitigating environmental risks and improving ecological efficiency.

Furthermore, green marketing practices contribute to stakeholder engagement and relationship building. By

transparently communicating their sustainability initiatives and achievements, manufacturing firms can foster trust and loyalty among environmentally conscious consumers, investors, and communities. This not only enhances brand equity but also strengthens social license to operate and reduces reputational risks associated with environmental controversies.

One of the key managerial implications of green marketing practices is the need for strategic alignment between sustainability objectives and overall business goals. Manufacturing firms must integrate environmental considerations into their strategic planning processes, ensuring that sustainability initiatives are aligned with core competencies, market positioning, and long-term growth objectives. This requires proactive engagement from top management, clear articulation of sustainability priorities, and allocation of resources to support green initiatives across the organization.

Green marketing practices offer manufacturing firms opportunities for innovation and differentiation in increasingly competitive markets. By investing in eco-design, sustainable sourcing, and green technologies, firms can develop innovative products and processes that reduce environmental impacts while meeting customer needs and preferences. This not only enhances market competitiveness but also strengthens brand identity and fosters customer loyalty, driving long-term profitability and market share growth.

Effective green marketing practices can also serve as a strategic tool for risk management, helping manufacturing firms mitigate environmental risks and regulatory compliance challenges. By proactively addressing environmental issues through transparent communication, stakeholder engagement, and responsible product stewardship, firms can reduce the likelihood of environmental liabilities, reputational damage, and regulatory sanctions. This requires proactive monitoring of environmental trends, adoption of best practices, and integration of sustainability into risk assessment and management processes.

Transparency and accountability are essential principles underpinning effective green marketing practices. Manufacturing firms must communicate transparently with stakeholders about their sustainability initiatives, performance, and progress towards environmental goals. This requires robust reporting mechanisms, adherence to sustainability standards and certifications, and engagement with external stakeholders, including investors, customers, NGOs, and regulatory bodies. By demonstrating accountability for their environmental impacts and commitments, firms can build trust, credibility, and long-

term relationships with stakeholders, enhancing brand reputation and market legitimacy.

LIMITATIONS AND RECOMMENDATIONS FOR FUTURE RESEARCH

First, only manufacturing firms in Ghana were included in our research sample. The universality of the findings should be confirmed in follow-up investigations using diverse samples. To provide a more thorough explanation of this link, future research could expand on additional potential components like organizational culture, IT integration, regulatory environment, consumer awareness, and education.

Longitudinal studies from other cultures and nations at various stages of development may be included in future studies. Such multi-country analysis allows researchers to compare mean responses and the strength of correlations, which contributes to a more comprehensive knowledge of green marketing practices and their effects on the sustainability performance of manufacturing firms.

Delving into consumer perceptions, attitudes, and behaviors towards green marketing messages and sustainable products can enhance understanding of drivers and barriers to adoption, informing more targeted marketing strategies.

Examining the dynamics of multi-stakeholder collaborations and partnerships aimed at advancing sustainability goals within manufacturing ecosystems can shed light on effective strategies for collective action and impact.

Also, future studies may consider exploring the application of circular economy principles, such as product lifecycle extension, remanufacturing, and closed-loop systems, in driving sustainability performance and creating shared value for manufacturing firms and their stakeholders.

REFERENCES

Akuma, J.K., Tackie, G., Idun, A.A.A. and Kwaning, E.A., 2024. Management accounting practices and sustainability performance of manufacturing firms in Ghana. *American Journal of Industrial and Business Management*, 14(2), pp.214-241.

Ali, F., Rasoolimanesh, S.M., Sarstedt, M., Ringle, C.M. and Ryu, K., 2018. An assessment of the use of partial least squares structural equation modeling (PLS-SEM) in hospitality research. *International Journal of Contemporary Hospitality Management*, 30(1), pp.514–538. https://doi.org/10.1108/IJCHM-10-2016-0568

Arend, R.J. and Bromiley, P., 2022. Dynamic capabilities and competitive advantage: A review and research agenda. *Journal of Management*, 48(1), pp.81-109.

Baah, C., Opoku-Agyeman, D., Acquah, I.S.K., Agyabeng-Mensah, Y., Afum, E., Faibil, D. and Abdoulaye, F.A.M., 2021. Examining the correlations between stakeholder pressures, green production practices, firm reputation, environmental and financial performance: Evidence from manufacturing SMEs. *Sustainable Production and Consumption*, 27, pp.100-114.

Bahta, D., Yun, J., Islam, M.R. and Bikanyi, K.J., 2021. How does CSR enhance the financial performance of SMEs? The mediating role of firm reputation. *Economic Research-Ekonomska Istraživanja*, 34(1), pp.1428-1451.

Bansal, P. and DesJardine, M.R., 2020. Triple bottom line: A review of the literature and analysis of trends. *Business Ethics Quarterly*, 30(2), pp.211-237.

Bansal, P. and Roth, K., 2020. Beyond stakeholders: Toward a pluralistic view of corporate sustainability. *Journal of Business Ethics*, 167(3), pp.393-406.

Barney, J., 1991. Firm resources and sustained competitive advantage. *Journal of Management*, 17(1), pp.99–120.

Bocken, N.M., Short, S.W., Rana, P. and Evans, S., 2020. A literature and practice review to develop sustainable business model archetypes. *Journal of Cleaner Production*, 65, pp.42-56.

Boonlertvanich, K., 2019. Service quality, satisfaction, trust, and loyalty: The moderating role of main-bank and wealth status. *International Journal of Bank Marketing*, 37(1), pp.278–302. https://doi.org/10.1108/ijbm-02-2018-0021

Chang, H.L., Lin, Y.F. and Chou, C.C., 2023. The effects of green product innovation on green brand equity: The mediating role of green brand image. *Journal of Cleaner Production*, 331, pp.129908.

Chen, X., Geng, Y., Zhao, R. and Sarkis, J., 2023. Aligning circular economy practices and sustainable development: A bibliometric and content analysis. *Journal of Cleaner Production*, 344, pp.130228.

Chen, Y. and Huang, J., 2022. Green internal marketing and green innovation performance: The mediating role of green psychological capital and the moderating role of green dynamic capabilities. *Journal of Business Research*, 145, pp.616-627.

Chen, Y., Chang, C. and Huang, Y., 2023. Green marketing strategy, green innovation, and corporate sustainable performance: Evidence from Taiwanese manufacturing firms. *Journal of Business Ethics*, 172(3), pp.525–543.

Chen, Y., Huang, J. and Han, Y., 2021. The impact of green internal marketing on employees' pro-environmental behavior: The moderating roles of green organizational identity and green organizational climate. *Journal of Business Ethics*, 176(2), pp.429-447.

Chen, Y., Xie, Y. and Cui, Y., 2021. Green product design and innovation: The role of eco-innovation capability and green strategy. *Journal of Business Research*, 134, pp.685-693.

Chung, K.C., 2020. Green marketing orientation: Achieving sustainable development in green hotel management. *Journal of Hospitality Marketing & Management*, 29(6), pp.722–738. https://doi.org/10.1080/19368623.2020.1693471

Cogdill, R.P., Knight, T.P. anderson, C.A. and Drennen III, J.K., 2017. The financial returns on investments in process analytical technology and lean practices: Benchmarks and case study. *Journal of Pharmaceutical Innovation*, 2(1-2), pp.38-50.

Crane, A., Palazzo, G. and Spence, L.J. (Eds.), 2023. *The Oxford Handbook of Corporate Social Responsibility: Psychological and Organizational Perspectives*. Oxford University Press.

Dai, Z., Zhu, H. and Zhang, X., 2022. Dynamic spillover effects and portfolio strategies between crude oil, gold, and Chinese stock markets related to new energy vehicles. *Energy Economics*, 109, pp.105959.

Dangelico, R.M. and Pujari, D., 2023. Stakeholder engagement and sustainability performance: The mediating role of organizational culture. *Business Strategy and the Environment*, 32(1), pp.263-276.

Eccles, R.G. and Serafeim, G., 2024. The future of corporate reporting: Integrated, interactive, and intelligent. *Harvard Business Review*, 102(3), pp.76-85.

Eisenhardt, K.M. and Martin, J.A., 2021. Dynamic capabilities: Current debates and future directions. *Academy of Management Perspectives*, 35(1), pp.89-106.

Elkington, J., 1997. *Cannibals with Forks: The Triple Bottom Line of 21st Century Business*. New Society Publishers.

Fassin, Y. and Van Rossem, A., 2022. Stakeholder management and corporate performance: A meta-analysis. *Journal of Business Ethics*, 175(1), pp.1-23.

Faul, F., Erdfelder, E., Buchner, A. and Lang, A.-G., 2009. Statistical power analyses using G*Power 3.1: Tests for correlation and regression analyses. *Behavior Research Methods*, 41, pp.1149-1160. Download PDF.

Feng, Y., Liu, H., Dai, Z. and Li, Y., 2023. Green practices and environmental performance: The roles of green innovation and green capability. *Journal of Cleaner Production*, 341, pp.130779.

Freeman, R.E., 2010. *Strategic Management: A Stakeholder Approach*. Cambridge University Press.

Gupta, S. and Malik, A., 2019. Green marketing: Boon or bane. *International Journal of Management, Technology, and Social Sciences (IJMTS)*, 4(2), pp.1-10.

Hair, J.F., Sarstedt, M., Ringle, C.M. and Gudergan, S., 2017. Advanced issues in partial least squares structural equation modeling. https://nls.ldls.org.uk/welcome.html?ark:/81055/vdc100044101027.0(000001).

Hair, J., Risher, J., Sarstedt, M. and Ringle, C., 2019. When to use and how to report the results of PLS-SEM. *European Business Review*, 31(1), pp.2-24. https://doi.org/10.1108/EBR-11-2018-0203.

Hair, J.F., Jr, Hult, G.T.M., Ringle, C. and Sarstedt, M., 2016. *A Primer on Partial Least Squares Structural Equation Modeling (PLS-SEM)*. Sage publications.

Han, M., Lin, H., Wang, J., Wang, Y. and Jiang, W., 2019. Turning corporate environmental ethics into firm performance: The role of green marketing programs. *Business Strategy and the Environment*, 28(6), pp.929–938. https://doi.org/10.1002/bse.2290.

Haque, A. and Bhuiyan, N., 2021. The role of green marketing in achieving sustainable supply chain management: A conceptual framework. *International Journal of Engineering Business Management*, 13, pp.1-13.

Hart, S.L., 1995. A natural-resource-based view of the firm. *Academy of Management Review*, 20(4), pp.986–1014.

Hassan, A. and Jaaron, A., 2021. Total quality management for enhancing organizational performance: The mediating role of green manufacturing practices. *Journal of Cleaner Production*, 308, pp.127366. 25 July 2021. https://doi.org/10.1016/j.jclepro.2021.127366.

Henseler, J., Ringle, C.M. and Sarstedt, M., 2015. A new criterion for assessing discriminant validity in variance-based structural equation modeling. *Journal of the Academy of Marketing Science*, 43(1), pp.115–135. https://doi.org/10.1007/s11747-014-0403-8.

Hossain, A. and Khan, M.Y.H., 2018. Green marketing mix effect on consumers buying decisions in Bangladesh. *Marketing and Management of Innovations*, 4(December 2018), pp.298-306. https://doi.org/10.21272/mmi.2018.4-25.

Hsu, C.W., Chang, H.L. and Lai, K.H., 2022. Green marketing communication, environmental knowledge, and green purchase intention: The moderating role of green brand equity. *Journal of Business Research*, 134, pp.685–693.

Hsu, C.W., Chang, H.L. and Lai, K.H., 2023. Green product innovation and firm performance: The roles of green dynamic capabilities and green regulatory pressure. *Journal of Business Research*, 174, pp.116–128.

Huang, Y., Guo, H. and Huo, B., 2024. The effects of green product development on the environmental and economic performance of firms. *Journal of Cleaner Production*, 388, pp.127818.

Huang, Y., Li, Y. and Huo, B., 2021. The influence of green internal marketing on employees' green behavior and organizational performance. *Business Strategy and the Environment*, 30(4), pp.2419–2432.

Huang, Y., Li, Y. and Huo, B., 2023. The influence of green internal marketing on employees' green behavior and organizational

performance. *Business Strategy and the Environment*, 30(4), pp.2419–2432.

Jabbour, C.J., Lopes de Sousa Jabbour, A.B., Kannan, D., Singh, S.K. and Gunasekaran, A., 2021. Green supply chain management, green technology innovation, and environmental performance: The moderating roles of green corporate strategy and environmental collaboration. *Transportation Research Part E: Logistics and Transportation Review*, 150, pp.102184.

Javeed, S.A., Latief, R. and Lefen, L., 2020. An analysis of relationship between environmental regulations and firm performance with moderating effects of product market competition: Empirical evidence from Pakistan. *Journal of Cleaner Production*, 254, pp.120197. https://doi.org/10.1016/j.jclepro.2020.120197.

Justavino-Castillo, M.E., Gil-Saura, I., Fuentes-Blasco, M. and Moliner-Velazquez, B., 2022. How to increase company loyalty: Using relational variables and sustainable practices to segment the maritime transport sector. *Economic Research-Ekonomska Istrazivanja*, pp.1–24. https://doi.org/10.1080/1331677X.2022.2142830.

Krejcie, R.V. and Morgan, D.W., 1970. Determining sample size for research activities. *Educational and Psychological Measurement*, 30(3), pp.607-610.

Lai, K.H., Wong, C.W., Cheng, T.C. and Lun, V.Y., 2024. Green operations practices and environmental performance: The moderating roles of green innovation and green process management. *Journal of Cleaner Production*, 365, pp.130796.

Le, T.T., Le, M.H., Nguyen Thi Tuong, V., Nguyen Thien, P.V., Tran Dac Bao, T., Nguyen Le Phuong, V. and Mavuri, S., 2024. Prestige over profit, corporate social responsibility boosts corporate sustainable performance: Mediation roles of brand image and brand loyalty. *Journal of Global Responsibility*, 15(2), pp.215-244.

Lee, M. and Park, S., 2019. The effect of green marketing strategy on corporate sustainability performance: The mediation role of stakeholder collaboration. *Sustainability*, 11(3), pp.592.

Li, S., Jiang, X. and An, M., 2020. Green marketing strategy, environmental management practices, and corporate sustainability: Empirical evidence from Chinese manufacturing firms. *Sustainability*, 12(8), pp.3411.

Li, Y., Wu, H., Huo, B. and Huang, Y., 2022. Empowering employees to support corporate sustainability: The roles of green internal marketing and green organizational identification. *Business Strategy and the Environment*, 32(1), pp.234–246.

Li, Y., Wu, H., Huo, B. and Huang, Y., 2023. Empowering employees to support corporate sustainability: The roles of green internal marketing and green organizational identification. *Business Strategy and the Environment*, 32(1), pp.234–246.

Lin, Y.F., Chang, H.L. and Lai, K.H., 2021. The effects of green marketing communication on brand equity and purchase intention: The mediating roles of green brand attitude and green brand credibility. *Journal of Business Ethics*, 172(2), pp.339–353.

Lin, Y.F., Chang, H.L. and Lai, K.H., 2023. Effects of green supply chain management and green product development on firm performance: The moderating role of external support. *Journal of Cleaner Production*, 333, pp.130280.

Liu, Z., Zhou, J. and Huang, Y., 2024. The impact of green internal marketing on employees' green innovation behavior: The roles of green job satisfaction and green psychological empowerment. *Journal of Cleaner Production*, 335, pp.130566.

Lozano, R., Huisingh, D., Ceulemans, K. and Lozano, F.J., 2023. The development of sustainability reporting: A historical overview. *Journal of Cleaner Production*, 302, pp.127082.

Lu, Y., Shan, M. and Zhang, X., 2021. Economic effects of corporate environmental responsibility: A literature review and research agenda. *Business Strategy and the Environment*, 30(3), pp.1629–1648.

Luo, X., Chen, C.C. and Xu, S., 2020. Green marketing, greenwash and the

impact on environmental behavior intention. *Management Decision*, 58(1), pp.129–147.

Mahmoud, T.O., 2017. Impact of green marketing mix on purchase intention. *International Journal of Advanced and Applied Sciences*, 5(2), pp.127–135. https://doi.org/10.21833/ijaas.2018.02.020.

Mehraj, D. and Qureshi, I.H., 2020. Determinants of green marketing mix in developing economies: Conceptualization and scale validation approach. *Business Strategy & Development*, 3(4), pp.522–530. https://doi.org/10.1002/bsd2.114.

Mele, P., Gomez, J. and Garay, L., 2019. To green or not to green: The influence of green marketing on consumer behaviour in the hotel industry. *Sustainability*, 11(17), pp.4623. https://doi.org/10.3390/su11174623.

Mishra, P. and Sharma, P., 2014. Green marketing: Challenges and opportunities for business. *BVIMR Management Edge*, 7(1), pp.35–41. http://ijiet.com/wp-content/uploads/2013/07/71.pdf.

Mishra, P., Sharma, P. and Kumar, A., 2020. Green marketing and sustainable development: A review. *Global Business Review*, 21(2), pp.450–468.

Moneva, J.M., Ortas, E. and Gallego-Álvarez, I., 2022. Corporate governance and sustainability: A systematic review and research agenda. *Business Strategy and the Environment*, 31(1), pp.584–600.

Muisyo, P.K., Su, Q., Hashmi, H.B.A., Ho, T.H. and Julius, M.M., 2022. The role of green HRM in driving hotels' green creativity. *International Journal of Contemporary Hospitality Management*, 34(4), pp.1331–1352.

Ofori, D., 2021. Opportunities and challenges of green marketing. In: *Green Marketing in Emerging Markets: Strategic and Operational Perspectives*, pp.251–276.

Ottman, J., 2017. *The New Rules of Green Marketing: Strategies, Tools, and Inspiration for Sustainable Branding*. Routledge.

Papadas, K.-K., Avlonitis, G.J., Carrigan, M. and Piha, L., 2019. The interplay of strategic and internal green marketing orientation on competitive advantage. *Journal of Business Research*, 104, pp.632–643. https://doi.org/10.1016/j.jbusres.2018.07.009.

Porter, M.E. and Kramer, M.R., 2011. Creating shared value. *Harvard Business Review*, 89(1/2), pp.62–77.

Ren, Z. and Hussain, R.Y., 2022. A mediated–moderated model for green human resource management: An employee perspective. *Frontiers in Environmental Science*, 10, pp.973692.

Ringle, C.M., Wende, S. and Becker, J.-M., 2022. SmartPLS 4. Oststeinbek: SmartPLS GmbH. http://www.smartpls.com.

Sarkar, S. and Rajendran, C., 2022. Green marketing orientation, sustainability, and competitive advantage in the context of Indian manufacturing firms. *Management Decision*, 60(2), pp.276–298.

Sarkis, J., Cohen, M.J., Dewick, P. and Schröder, P., 2022. Circular economy: A research agenda for supply chain sustainability. *Annals of Operations Research*, pp.1–22.

Savitz, A.W. and Weber, K., 2021. *The triple bottom line: How today's best-run companies are achieving economic, social, and environmental success—And how you can too*. John Wiley & Sons.

Schiederig, T., Tietze, F. and Herstatt, C., 2012. Green innovation in technology and innovation management – An exploratory literature review. *R&D Management*, 42(2), pp.180–192.

Shabbir, M.S. and Wisdom, O., 2020. The relationship between corporate social responsibility, environmental investments and financial performance: Evidence from manufacturing companies. *Environmental Science and Pollution Research*, 27(32), pp.39946–39957. https://doi.org/10.1007/s11356-020-10217-0.

Sikandar Ali Qalati, B., Barbosa, B. and Iqbal, S., 2023. The effect of firms' environmentally sustainable practices on economic performance. *Economic Research-Ekonomska Istraživanja*, 36(3), pp.2199822. DOI: 10.1080/1331677X.2023.2199822.

Szabo, S. and Webster, J., 2021. Perceived greenwashing: The effects of

green marketing on environmental and product perceptions. *Journal of Business Ethics*, 171, pp.719–739.

Tong, X. and Zhao, Q., 2020. Green product innovation strategy and corporate environmental performance: The mediation effect of green supply chain collaboration. *Journal of Cleaner Production*, 267, pp.121844.

Vilkaite-Vaitone, N., Skackauskiene, I. and Díaz-Meneses, G., 2022. Measuring green marketing: Scale development and validation. *Energies MDPI*, 15, pp.718. https://doi.org/10.3390/en15030718.

Wang, H., Li, Y., Wang, Y. and Huang, Y., 2024. The impact of green marketing communication on environmental and economic performance: The moderating role of environmental management capabilities. *Journal of Business Research*, 188, pp.720–730.

Wang, Y., Wang, L. and He, H., 2021. The impact of green product design on sustainable performance: Evidence from Chinese manufacturing firms in the electronics industry. *Sustainability*, 13(15), pp.8500.

Wu, H., Zhu, Y. and Huo, B., 2024. The effect of green product development on firm performance: A dynamic capability view. *Journal of Business Research*, 188, pp.720–730.

Xie, Y., Guo, H. and Zhang, Y., 2023. How does green internal marketing improve firms' environmental performance? A resource orchestration perspective. *Journal of Cleaner Production*, 327, pp.129431.

Zhang, Y., Li, Y. and Huo, B., 2022. Green product design and development: A bibliometric analysis and research agenda. *Journal of Cleaner Production*, 328, pp.129706.

Zhang, Y., Zhang, L., Wang, H. and Li, X., 2020. Green internal marketing, green organizational identity, and green service behavior. *Journal of Business Ethics*, 163(4), pp.677–691.

Zhang, Y., Zhang, L., Wang, H. and Li, X., 2021. Effects of green product design on firm environmental and economic performance: The mediating role of green supply chain management. *Journal of Cleaner Production*, 292, pp.125962.

Zhang, Y., Zhang, L., Wang, H. and Li, X., 2022. Green internal marketing, green organizational identity, and green service behavior. *Journal of Business Ethics*, 171, pp.719–739.

Zhu, Q., Lai, K.H. and Wong, C.W., 2024. Green supply chain management and firm performance: The moderating roles of green information sharing and environmental uncertainty. *Journal of Business Research*, 146, pp.503–515.

Study of Biological Treatment of Rice Mill Wastewater Using Anaerobic Semicontinuous Reactors (ASCR)

R. K. Singh†[iD] and S. Bajpai

Department of Civil Engineering, National Institute of Technology, Raipur, Chhattisgarh, India
†Corresponding author: Raj Kishore Singh; rksingh.phd2019.ce@nitrr.ac.in

ABSTRACT

Anaerobic digestion (AD) of industrial wastewater has drawn researchers' attention due to biofuel's recovery in the form of biomethane. This study introduced two anaerobic semi-continuous reactors (ASCR)- R1 and R2 for bioremediation of the rice mill wastewater (RMWW). The alkali treatment of the substrate in reactors R1 and R2 was done by dry NaOH and $Ca(OH)_2$, respectively. Both reactors were loaded with 80% of the RMWW and 20% of the cow-dung-fed biogas plant sludge (BGPS) for 16 days of stabilization at mesophilic temperatures (18℃ to 42℃). A small amount of jaggery and white rot fungi (*Phanerochaete chrysosporium*) were also added into both reactors for the bacterial growth and removal of the biorefractory organics (lignin and phenol) present in RMWW, respectively. The impact of variations in the hydraulic retention time (HRT) and organic loading rate (OLR) upon the anaerobic biodegradation of RMWW was studied in three operating phases (OP) I, II, and III. The highest BOD, COD, lignin, and phenol removal achieved in reactors R1 and R2 were 94%, 92%, 84%, and 82%, as well as 93%, 91%, 82%, and 80%, respectively, in OP I. The highest biomethane yield in both reactors was 0.005 L.g^{-1} COD in OP II. The results of the three operating phases reveal that a high HRT and low OLR give the maximum pollutant removal efficiency and the highest biomethane yield. The novelty of this research paper is the significant removal of the biorefractory organics lignin and phenol from the RMWW with the help of white rot fungi and specific bacterial strains *Bacillus* sp., *Pseudomonas* sp., *Enterobacter* sp., *Actinomycetes* sp. and *Streptomycetes* sp. present in the inoculum. The digestates from reactors were rich in macro and micronutrients viz., N, P, K, Cu, Zn, Fe, etc., essential for plant growth.

INTRODUCTION

The rapid growth of the population, accompanied by economic progress through industrialization and urbanization, has resulted in sustainability challenges and climate change. The accelerating consumption of resources has resulted in the total waste generation of approximately 12×10^3 million tons (MT) due to anthropogenic activities in the year 2020, which is anticipated to be enhanced to 19×10^3 million tons per year (MT.yr^{-1}.) by 2025 (Duan et al. 2021). As per the Central Pollution Control Board (CPCB) report, nearly 72,368 million liters per day (MLD) of wastewater was produced by Class 1 cities and Class 2 towns in India in 2022. This wastewater consists of municipal and industrial wastewater, of which only 28% is remediated, and there is a broad gap of 72% of the untreated wastewater (Bassi et al. 2022). The huge amount of waste generated by various industries has led to an undeniable confrontation between industrial development and ecological sustainability. Industrial effluents have harmful effects on biodiversity because of their ambulant character. They are generally discharged into surface water bodies without appropriate treatment, creating consequential adverse damage (Alderson et al. 2015). Environmental sanitation is essential for the sound health of the citizens of a nation.
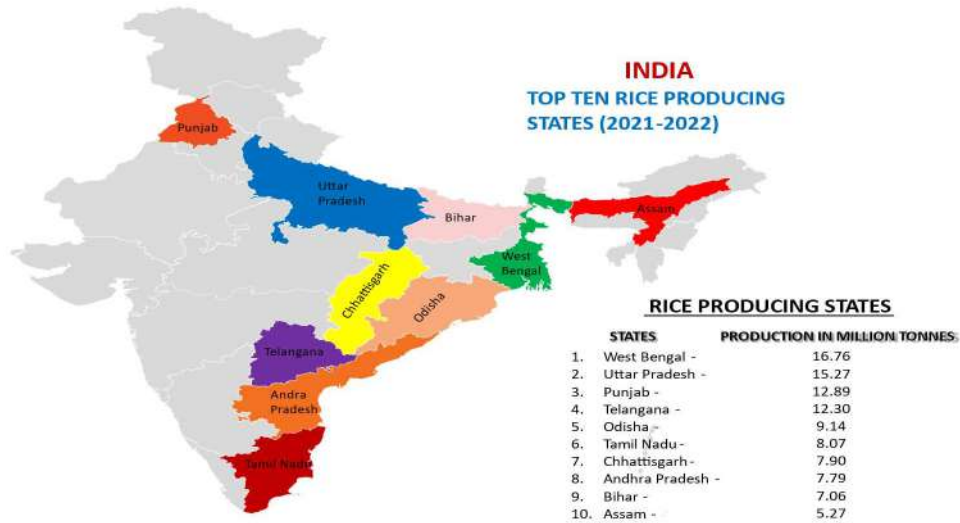
Fig. 1: Map of India showing the top ten rice-producing states in the financial year 2021-2022.

In the current era, agro-industries have gained momentum in size to fulfill people's food demands with a quickly growing population. Rice production from paddy milling is a progressively rising agro-industry and plays a pivotal role in the global circular economy. Rice is a staple food for a larger global population (Veluchamy & Kalamdhad 2017). The global rice production in the financial year (FY) 2021-22 was 513.06 MT. India produced 130.29 MT of rice in FY 2021-22, after China, which produced 148.99 MT in FY 2021-22. India's contribution to global rice production was 25.39%, whereas China's was 29.04% in FY 2021-22. Thus, India and China collectively contributed to more than half (54.43%) of the world's total rice production in FY 2021-22 (Paddy Outlook- March 2023). Asian countries contribute more than 90% of global rice production (Yusrin et al. 2024). India is the world's second-largest producer of rice and the largest consumer and exporter of rice. It stands first in the world regarding total acreage under rice cultivation. Besides fulfilling the domestic rice needs, India exports rice (basmati and non-basmati) to 150 countries worldwide (Annamalai & Johnson 2023). Fig. 1 shows a map of India showing the top ten rice-producing states in the financial year 2021-2022.

There are approximately 1,30,000 rice mills in India including Chhattisgarh, to date. The rice mills operating in India generally have two types- raw/white rice mills and parboiled rice mills, producing raw/white and parboiled rice, respectively (Singh & Bajpai 2023). The rice mills, producing parboiled rice discharge an enormous amount of wastewater in paddy soaking during the paddy parboiling process. Varshney (2012) investigated that one parboiled rice mill discharges 20×10^6 liters of wastewater per year in India. Thus, 57850 rice mills producing parboiled rice

(COINDS 2008) release approximately 11.57×10^9 L.yr^{-1}. of wastewater in India.

There are two methods for rice mill wastewater (RMWW) treatment- physicochemical and biological. The physicochemical methods are cost-intensive and produce huge quantities of sludge, whose safe disposal becomes a big problem. On the contrary, the biological methods generate less sludge and are cost-effective (Singh & Bajpai 2023). Biological methods are capable of recovering green energy in the form of biomethane, biohydrogen, and bioelectricity with the help of anaerobic digestion (AD), dark fermentation (DF), and microbial fuel cells (MFCs) techniques, respectively, apart from pollutant removal from the wastewater (Kumar & Deswal 2021). In this study, biological treatment of rice mill wastewater has been performed using two anaerobic semi-continuous reactors (ASCR). The AD process involves microbes (obligate and facultative anaerobes) that grow in the absence of molecular oxygen and use organic substrates as food resources. The microbes metamorphose the organic substrate into oxidized matter (digestate), new bacterial cells, energy for their life cycles, and biogas comprising mainly biomethane (CH_4) and carbon dioxide (CO_2) gases.

Various research works have been performed on the RMWW treatment (Xin et al. 2018). The treated wastewater discharged from the various industrial wastewater treatment plants (IWWTP), still comprises some deleterious toxins and becomes harmful to various ecosystems. (Dhanasekar & Sasivarman 2016, Nain et al. 2015). Hence, an imperative need is to evolve a novel, high-performance, and cost-effective technique that can dexterously remediate industrial wastewater, including RMWW (Hu et al. 2018, Yuan et al. 2012). Anaerobic digestion (AD) is a rational, practicable,

and cost-effective technique for remediating RMWW. Liu et al. (2018) recommended the AD process as an eco-friendly biological treatment process. The AD process has many merits over physicochemical treatment processes (Mao et al. 2015). The AD process curtails the use of the comprehensive land area, does not give rise to an obnoxious smell, and diminishes organic load and pathogenic microbes while generating biomethane and digestate to be used as organic fertilizers as the end products of microbial metabolism (Weng et al. 2014). AD process is cost-effective compared to other treatment technologies adopted for remediating RMWW because it yields biomethane and digestate as organic manure at the end of the biochemical reactions. In the AD system, biomethane gas can be generated from various agricultural and organic

Table 1: Recent research papers (2015-2023) on anaerobic digestion of rice mill wastewater (RMWW) and similar effluents.

S. No.	Title of papers	Conclusions	Reference
1.	Treatment of parboiled rice manufacturing wastewater using anaerobic fixed-film bed reactor packed with special media.	The study examined the anaerobic digestion of RMWW using an ASFBR at varied OLRs. Biopac media yielded BOD/COD removal (83.0%-92.7%)/ (80.2%-89.0%), surpassing fugino spiral media (79.4%-90.6%)/(76.7%-86.1%). Biopac-packed reactors showed superior pollutant removal efficiency across all OLRs.	Giri & Satyanarayan (2015)
2.	Rice mill wastewater treatment by up-flow anaerobic sludge blanket reactor.	The examination utilized a UASB digester to treat RMWW across three phases at hydraulic retention times (HRTs) of 20 h, 14 h, and 10 h. COD removal efficiencies of 97%, 89%, and 86% were achieved in phases I, II, and III, respectively. Despite a lower HRT and higher OLR, the best operating condition achieved an 86% COD reduction, indicating OLR's influence on removal efficiency.	Saini et al. (2016)
3.	Robust performance of a novel anaerobic biofilm membrane bioreactor with mesh filter and carbon fiber (ABMBR) for low to high-strength wastewater treatment	The anaerobic biofilm membrane reactor (ABMR) with mesh filter and carbon fiber effectively remediated low to high-strength wastewater. It maintained a stable COD reduction efficiency of 95% and produced biomethane at 290 mL/g COD. The reactor showed resilience to organic load changes, with minimal membrane fouling and dominance of aceticlastic methanogens like Methanosaeta in the biofilm.	Li et al. (2017)
4.	Digestive performance of sludge with different crop straws in mesophilic anaerobic digestion.	The study investigated the anaerobic digestion of various crop straws with sludge under mesophilic conditions, focusing on hydrolytic behavior and methane production. Wheat straw exhibited the highest biomethane potential (BMP) at $0.462 \, L.g^{-1}$ VS, while corn cob had the lowest at $0.368 \, L.g^{-1}$ VS due to its hemicellulosic content. Corn cob digestion resulted in the highest volatile solids (VS) removal at 68.8%, surpassing corn, wheat, and rice straw-loaded digesters.	Chen et al. (2019)
5.	Comparative evaluation of methanogenesis suppression methods in microbial fuel cell during rice mill wastewater treatment.	The study explored RMWW treatment using microbial fuel cells (MFCs) and assessed methanogenesis suppression's impact on COD removal and bioelectricity. Air exposure led to the highest power density (656.10 mW/m³), followed by ultrasonication ($525.62 \, mW.m^{-3}$), while heat treatment resulted in the lowest ($312.43 \, mWm^{-3}$). However, heat treatment exhibited the highest COD removal efficiency (85.22%).	Raychaudhuri & Behera (2020)
6.	Methane production test of the anaerobic sludge from rice parboiling industries with biodiesel glycerol from rice bran oil in Brazil.	The research explored glycerol's impact on biomethane generation from the anaerobic digestion of RMWW. Using four digesters with varying glycerol proportions, a 1% addition resulted in the highest biomethane production (945.23 mL) and COD removal (77%), which is attributed to the methanogenic bacteria's prolonged stationary phase.	Lourenco et al. (2021)
7.	Effect of rice winery wastewater as a co-substrate to enhance anaerobic digestion of molasses for methane production.	In this investigation, rice winery wastewater (RWWW) and molasses were anaerobically co-digested with various concentrations and increased OLR (1.875 to 13 g COD/L). The highest COD removal rate, 90.20 ± 0.44 to $92.65 \pm 0.38\%$, and maximum methane contents of $69.14 \pm 1.4\%$ were observed at feeding OLR of 7 to 13 g $COD.L^{-1}$ and at 3.75 g $COD.L^{-1}$, respectively. However, only molasses at OLR 18.5 g $COD.L^{-1}d^{-1}$ negatively affected anaerobic digestion.	Khan et al. (2022)
8.	Sequential anaerobic-aerobic treatment of rice mill wastewater and simultaneous power generation in a microbial fuel cell.	In this research, the performance of two microbial fuel cells- one with a biological cathode (MFC_B) and the other with an abiotic cathode (MFC_A) treating RMWW anaerobically was compared. MFC_B exhibited lower power density ($379.53 \, mW.m^{-3}$ vs. MFC_A's $791.72 \, mW.m^{-1}$). However, MFC_B demonstrated higher COD removal efficiency (96.8% vs. MFC_A's 88.4%), highlighting its potential for efficiency.	Raychaudhuri & Behera (2023)

wastes viz. rice straw, fruits and vegetable wastes, food wastes, dairy farm effluents, slaughterhouse wastes, and high and medium-strength industrial wastewaters, etc. (Naik et al. 2022, Agrawal et al. 2023, Kesharwani & Bajpai 2020, Tsegaye et al. 2022, Kalantzis et al. 2023). Biomethane gas is a sustainable, renewable, and eco-friendly energy source having zero carbon footprint and contributing significantly to the circular economy. The research findings (conclusions) of the anaerobic digestion of rice mill wastewater and similar effluents recently carried out by various researchers during 2015-2023 are given in Table 1.

The RMWW comprises an immense amount of inorganic and organic pollutants. It comprises high chemical oxygen demand (COD), biochemical oxygen demand (BOD), total solids (TS), total organic solids (TOS), total dissolved solids (TDS), total suspended solids (TSS), total alkalinity (TA), total hardness (TH), and moderate volatile fatty acids (VFA), sodium (Na), potassium (K), lignin and phenol, etc. However, the concentration of pollutants in RMWW depends on the varieties of paddy soaked, the extent of parboiling, and additives used to improve the marketability of the produced rice. The rice millers usually add urea (NH_2CONH_2) and common salt (NaCl) in the soaking tank at the time of parboiling as additives to impart the glazing to rice and inhibit the boiling point of soaking water respectively, which aggravates the pollutant concentration of the RMWW (Pradhan & Sahu 2004). Transferring this wastewater without proper treatment into surface water bodies can harm freshwater and seawater ecosystems as well as onto land surfaces, deteriorate the terrestrial ecosystem, and eventually pollute the groundwater by contaminant transport. Hence, developing novel, affordable, efficient, environment-friendly, and sustainable techniques for remediating agro-industrial wastewater, including RMWW, is a prerequisite to achieving a sanitary environment.

The aim of this research is focused on the AD of RMWW in an anaerobic semi-continuous reactor (ASCR) with different OLR and HRT conditions by splitting the entire study into three operating phases, namely operating phase I (OP I): varying the HRT and keeping the OLR constant, operating phase II (OP II): varying both the OLR and HRT, and operating phase III (OP III): varying the OLR and keeping HRT constant, aimed at determining the most optimal conditions for biogas and biomethane generation as well as a substantial removal of the pollutants viz., BOD, COD, TS, TDS, TSS, TOS, lignin, and phenol, etc. from the RMWW. The novelty of this research paper is the substantial removal of the two potent biorefractory organics- lignin and phenol from the RMWW by White rot fungi (*Phanerochaete chrysosporium*), as well as lignin and phenol removing microbial species viz., *Bacillus* sp., *Pseudomonas* sp.,

Enterobacter sp., *Actinomycetes* sp., *Streptomycetes* sp. and *Aspergillus* sp. present in the cow-dung fed biogas plant sludge (BGPS), used as inoculum.

MATERIALS AND METHODS

Chemicals and Instruments Used

All chemicals and reagents of analytical grade (97 to 99% purity) were used for the experimental works. The glassware used was manufactured from borosilicate glass. The weight measurements during the conduction of experiments were done using the analytical balance present in the lab. The deionized water was used for analyses. The segregation and quantification of the constituents of the biogas (viz., CH_4 and CO_2) generated from bioreactors were performed with the aid of the Gas Chromatography (GC) Apparatus.

Additives Used

White rot fungi (*Phanerochaete chrysosporium*) and jaggery (*Saccharum officinarum*) were used as additives to the substrate (RMWW) of the lab-scale bioreactors. *Phanerochaete chrysosporium* was used to degrade the biorefractory organics lignin and phenol, and it was collected from the Biotechnology Department, Pandit Ravishankar Shukla University, Raipur, Chhattisgarh, India. Jaggery was used to enhance the metabolism of the microorganisms present in the BGPS. It was purchased from the local market of Raipur.

Properties of Jaggery

Jaggery is rich in carbon and energy. It stimulates the metabolic activity of the bacteria and boosts the reproduction of new bacterial cells by cell division, thereby enhancing the bacterial growth rate in the anaerobic reactors. It balances the dehydrogenase activity, especially in case of temperature drop in the winter season, and facilitates the smooth functioning of the bioreactor (Aralkar et al. 2023). The dehydrogenase activity is associated with the anaerobic biodegradability of organic compounds by microbial activity. It can be a good indication of the microorganism activity (Hongwei et al. 2002). In the lab-scale anaerobic digester, the biogas production was increased by 36.8% when cattle dung (3.00 kg) was supplemented by 30 g of jaggery @10 g jaggery/kg of cow dung (Masih et al. 2019). The physicochemical properties and nutritional content of jaggery are shown in Table 2.

Collection of RMWW Sample and its Characterization

The RMWW samples were collected from a nearby rice mill for feeding in reactors and their physicochemical analyses.

Table 2: Physicochemical characteristics and nutritional content of Jaggery.

S. No.	Parameters	Unit	Range of Values
1.	pH	-	5.8-6.4
2.	Density	g.cm^{-3}	1.5
3.	Viscosity	Centipoise[cP]	807
4.	Melting point	K	460
5.	Molecular mass	g.mol^{-1}	342
6.	Carbohydrate	%	83.90-97.20
7.	Reducing sugar	%	10.50
8.	Total sugar	%	87.50-95.40
9.	Sucrose	%	76.55-89.48
10.	Iron [Fe]	µg.mL^{-1}	1.60-2.50
11.	Copper [Cu]	µg.mL^{-1}	0.17-8.50
12.	Zinc (Zn)	µg.mL^{-1}	0.10-1.76
13.	Cobalt [Co]	µg.mL^{-1}	9.90
14.	Manganese [Mn]	µg.mL^{-1}	0.35-1.66
15.	Iodine [I]	µg.mL^{-1}	0.01

(Aralkar et al. 2023, Sharifi-Rad et al. 2023)

Their physicochemical characteristics were determined in the Environmental Engineering Lab, NIT Raipur, as per the standard methods by APHA, AWWA, and WWF (2017) 23rd Edition, except for the CHNSO analysis (C/N ratio of dry RMWW) performed at Pt. Ravi Shankar Shukla University, Raipur. Fifteen RMWW samples were collected on different days and seasons- monsoon, pre-monsoon, post-monsoon, summer, and winter from January 2022 to March 2023. The samples were taken in low-density polyethylene (LDPE) bottles of 1.0-liter (L) capacity each. Three LDPE bottles of 1.0 L capacity were used for each sampling. The first bottle was filled with absolute RMWW for determining pH, EC, turbidity, sulfate, chloride, lignin, BOD, TS, TOS, TIS, TDS, TSS, DO, TA, TH, Ca-hardness, Mg-hardness, and VFA. The second bottle was filled with RMWW acidified with Conc. H_2SO_4 for determining COD, total Kjeldahl nitrogen (TKN), nitrate (NO_3), phosphate (PO_4), oil and grease, phenol (C_6H_5OH), etc. The third bottle was filled

Table 3: Physicochemical characteristics of RMWW.

S. No.	Parameters	Unit	Range of Values	Mean value
1.	pH	-	5.28 - 6.08	5.64
2.	Color	-	Faint brown to Faint yellow	-
3.	Electrical Conductivity [EC]	µS.cm^{-1}	5.65 - 7.50	6.84
4.	Turbidity	NTU	39.4 - 43.8	40.5
5.	Total Alkalinity [TA]	mg.L^{-1} as CaCO$_3$	2,251 - 2,467	2,356
6.	Total Hardness [TH]	Mg.L^{-1} as CaCO$_3$	2,320 - 2,537	2,440
7.	Calcium Hardness [Ca- H]	mg.L^{-1} as CaCO$_3$	1,833 - 1,964	1,906
8.	Mg- Hardness (Mg-H)	mg.L^{-1} as CaCO$_3$	487 – 573	534
9.	Chemical Oxygen Demand [COD]	mg.L^{-1}	5,145 - 5,427	5,274
10.	Biochemical Oxygen Demand [BOD]	mg.L^{-1}	3,410 - 3,785	3,612
11.	Total Kjeldahl Nitrogen [TKN]	mg.L^{-1}	45 – 65	54
12.	Total Solids (TS)	mg.L^{-1}	3,837 - 4,200	4,078
13.	Total Organic Solids [TOS]	mg.L^{-1}	2,847 - 3,180	3,068
14.	Total Inorganic Solids [TIS]	mg.L^{-1}	990 - 1,020	1,010
15.	Total Dissolved Solids [TDS]	mg.L^{-1}	2,733 - 3,060	2,958
16.	Total Suspended Solids [TSS]	mg.L^{-1}	1104 - 1,140	1120
17.	Dissolved Oxygen [DO]	mg.L^{-1}	0.9 - 2.0	1.5
18.	Chloride [Cl]	mg.L^{-1}	673 – 850	746
19.	Sulfate [SO$_4$$^{3-}$]	mg.L^{-1}	61 – 78	71
20.	Oil & Grease	mg.L^{-1}	14 – 24	18
21.	Nitrate [NO$_3$$^{-}$]	mg.L^{-1}	19 -29	23
22.	Orthophosphate [PO$_4$$^{3-}$]	mg.L^{-1}	82 – 94	87
23.	Lignin	mg.L^{-1}	122 - 141	138
24.	Phenol [C$_6$H$_5$O]	mg.L^{-1}	12 -20	16
25.	Sodium [Na]	mg.L^{-1}	70 – 82	79
26.	Potassium [K]	mg.L^{-1}	450 – 550	496
27.	Volatile Fatty Acids [VFA]	mg.L^{-1}	290 – 350	318
28.	VFA/Alkalinity ratio	-		0.13
29.	Carbon	%		22.449
30.	Nitrogen	%		1.821
31.	Carbon/Nitrogen [C/N] ratio	-		12.3

Table 4: Physicochemical characteristics of BGPS.

S. No.	Parameters	Unit	Mean value
1.	pH	-	7.5
2.	Color	-	Black
3.	Carbon	%	32.904
4.	Nitrogen	%	2.297
5.	C/N ratio	-	14.3
6.	VFA	$mg.L^{-1}$	115
7.	Alkalinity	$mg.L^{-1}$ as $CaCO_3$	2675
8.	VFA/Alkalinity ratio	-	0.04
9.	COD	$mg.L^{-1}$	21,695

with RMWW acidified with Conc. HNO_3 for determining sodium (Na) and potassium (K). All bottles filled with wastewater samples were preserved in the Lab refrigerator at 4°C temperatures to maintain the sample's integrity. The wastewater for feeding in anaerobic reactors was also collected from the same rice mill in three plastic cans of 10 L capacity each. The physicochemical parameters of each sample were analyzed in triplicate and their mean value was taken. The range of values and the mean value of each parameter are shown in Table 3.

Inoculum Used for Reactors

Biogas plant sludge (BGPS) was used as inoculum for the reactors. It was taken from the biogas plant operated by Sarda Dairy (Vachan Milk) Limited, Kharora, Chhattisgarh, India. It is a cow dung-fed biogas plant of a 2000 m³ capacity with two anaerobic digesters- each producing 1000 m³ of biogas

daily. The physicochemical examination of BGPS was done as per the standard methods by APHA in the Lab, except for the CHNSO analysis (C/N ratio of BGPS) that was done at IIT Bombay. The physicochemical characteristics of BGPS are shown in Table 4.

Experimental Set-up for Anaerobic Digestion of RMWW

Two anaerobic semi-continuous reactors (ASCR)- R1 and R2 of 35 L capacity each and made of high-density polyethylene (HDPE) provided with feed inlets on their top for feeding the substrate (RMWW) and inoculum (BGPS), were taken for AD of the wastewater. In both reactors, 24 L of RMWW (80%) and 6 L of BGPS (20%), i.e., 30 L of the mix along with 24 g jaggery @ 1 g jaggery/L and 24 g white-rot fungi (*Phanerochaete chrysosporium*) @ 1 g fungi/L were fed from their feed inlets. The substrate pH of reactors R1 and R2 were adjusted to 7.0 by adding 24 g NaOH@ 1 g $NaOH.L^{-1}$ and 12 g $Ca(OH)_2$@ 1 g $Ca(OH)_2.L^{-1}$, respectively. The clearance volume left in both reactors above the substrate and inoculum mix was 35 L-30 L= 5 L, which was left for the biogas released in the process of AD. The biogas produced in both reactors was volumetrically measured by the water displacement techniques in the inverted measuring cylinders of 1 L capacity each. In both reactors, manual feeding was accomplished in semi-continuous mode through their feed inlets. The effluent samples for analyses were collected from taps provided in both reactors- R1 and R2. The blending of substrate, co-substrate, and inoculum was performed manually before feeding the reactors. The anaerobic reactors- R1 and R2 were kept in the ambient atmosphere at mesophilic
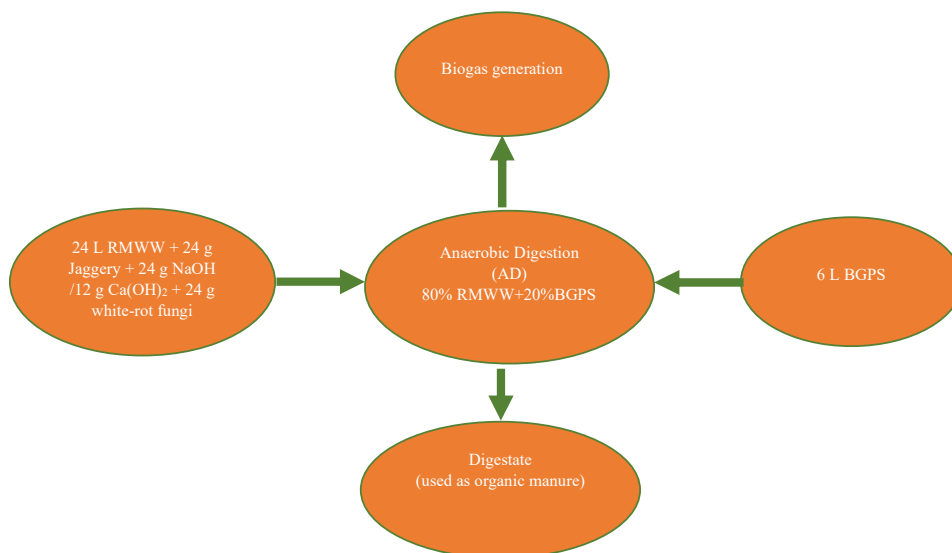
Fig. 2: Schematic diagram of biogas generation from AD of RMWW.

temperatures (18°C to 42°C). The biogas generation began 16 days after the date of feeding the reactors. After attaining constant and steady biogas generation for consecutive 4 days, the organic loading was started, and the biogas generation was recorded daily. Fig. 2 depicts a schematic diagram of biogas generation from anaerobic digestion of rice mill wastewater. The cumulative sum of daily biogas generation from both reactors was found every 10 days after the end of each HRT. Furthermore, BOD, COD, TS, TOS, TDS, TSS, lignin, and phenol contents of the reactors' substrate (RMWW) were determined, which were 3725, 5425, 4194, 3177,3059,1135, 135, and 19 mg.L^{-1} respectively at the time of loading the reactors- R1 and R2. The organic loading capacity of both reactors was 7.50 kg COD.m^{-3}·d^{-1} each.

The stationary condition of the bioreactors- R1 and R2 was maintained for the subsequent 16 days for stabilization of the substrate. Fig. 3a and 3b exhibit the bioreactors- R1 and R2 used for the experimental analyses delineating the feed inlets for loading substrate into the reactors as well as gas pipes, gas valves, and effluent collection taps for collecting biogas and reactor effluent. The biogas generated from the reactors R1 and R2 were conveyed through the gas pipes and collected in the inverted measuring cylinders. Fig. 4 shows additives used in anaerobic reactors- R1 and R2.

Operating Phases of Anaerobic Reactors- R1 and R2

After 16 days of stabilization of the anaerobic bioreactors- R1 and R2, the biogas generation commenced. After confirming the stabilization, the OLR was initiated after 4 d of the arrival of steady biogas production, and every OLR was capered to the upcoming loading after safeguarding 9 d of consistent biogas generation. The research was split into three operating phases, namely operating phase I (impact of changing HRT and keeping OLR constant), operating phase II (impact
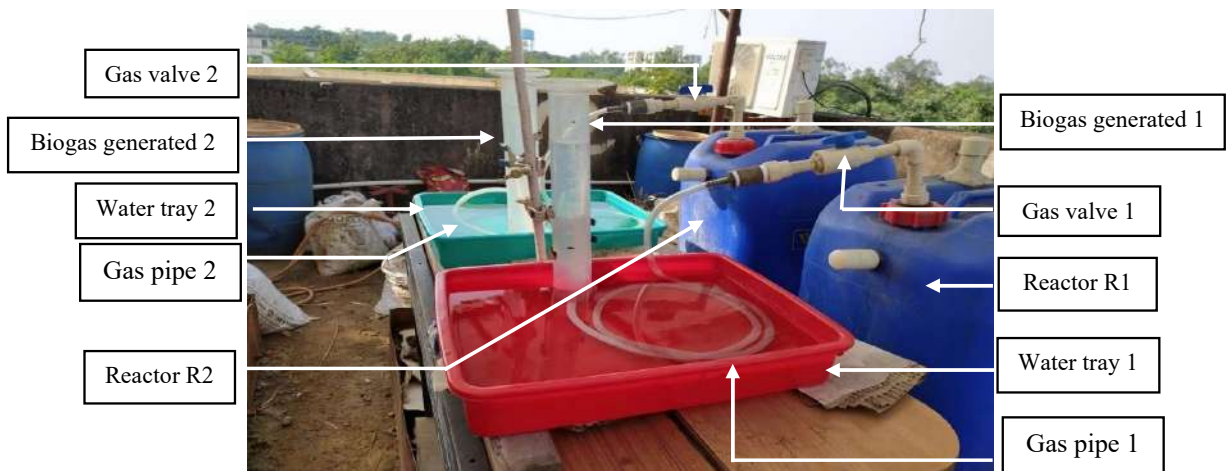
Fig. 3a: Lab-scale anaerobic reactors R1 and R2 showing biogas.

Fig. 3b: Lab-scale anaerobic reactors R1 and R2 showing feed inlets and effluent collection taps.

Jaggery   Calcium hydroxide   Sodium hydroxide   White-rot fungi
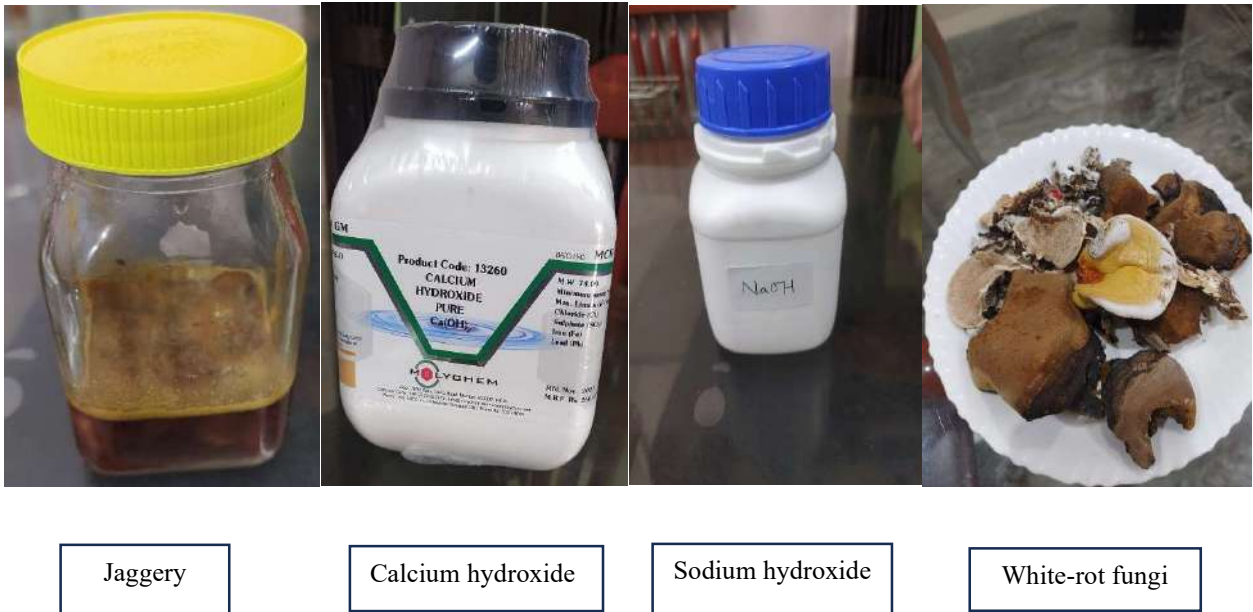
Fig. 4: Ca(OH)$_2$, NaOH, Jaggery, and White-rot fungi used as additives in reactors- R1 and R2.

of changing both OLR and HRT), and operating phase III (impact of changing OLR and keeping HRT constant) based on enhancing and diminishing the influent organic load (Veluchamy & Kalamdhad 2017). The biogas generation was monitored daily based on the HRT and OLR conditions, and the pollutants (BOD, COD, lignin, phenol, TS, TSS, TOS, and TDS) removal efficiencies of both reactors were found. The bioreactors- R1 and R2 were run for a total duration of 370 d in three operating phases, as mentioned below:

Operating Phase I (OP I): In this phase, OLR remained constant at 3.25 kg COD.m^{-3}.d^{-1}, and HRT was varied from 10 d to 110 d. The bioreactors' start-up time was 16 d from the date of feeding, and their smooth functioning, along with the invariable biogas production, commenced 4 d after the start-up time. As a result, the OLR was started after 20 d (16 d+4 d), i.e., after the constant and steady biogas generation. Thus, the total days of bioreactors' run in OP I = 110 + 20 = 130 d.

Operating Phase II (OP II): In OP II, OLR was varied from 1.50 to 7.32 kg COD.m^{-3}.d^{-1}, and HRT was varied from 10 d to 150 d. Thus, the total days of the bioreactors' run in this phase, including the commencement of the smooth functioning of the bioreactors and constant and steady biogas generation = 150 d + 20 d = 170 d.

Operating Phase III (OP III): In OP III, OLR was varied from 1.55 to 7.25 kg COD.m^{-3}.d^{-1} in 10 segments, and HRT was kept constant for each OLR at 5 d. Thus, the total days of the bioreactors' run in this phase, including the commencement of the smooth functioning of the bioreactors

and constant and steady biogas generation = 50 d + 20 d = 70 d.

Hence, the total duration of the bioreactors' run in all three phases = 130 d +170 d + 70 d = 370 d.

Effluent Analyses and Biogas Measurement

In OP I, the effluents were collected from reactors R1 and R2 after an HRT of 10 d, 20 d, 30 d, 40 d, 50 d, 60 d, 70 d, 80 d, 90 d, 100 d, and 110 d for the physicochemical analyses with the help of the effluent collection taps provided in them as shown in Fig. 3b, when OLR was kept constant at 3.25 kg COD.m^{-3}.d^{-1}. In OP II, the effluents were collected from the reactors after an HRT of 10 d, 20 d, 30 d, 40 d, 50 d, 60 d, 70 d, 80 d, 90 d, 100 d, 110 d, 120 d, 130 d, 140 d, and 150 d for analyses, when OLR was varied from 1.50 to 7.32 kg COD.m^{-3}.d^{-1}. Eventually, in OP III, effluents were collected from the reactors after a constant HRT of 5 d each time, when OLR was varied from 1.55 to 7.25 kg COD.m^{-3}.d^{-1}. The pH, VFA, Alkalinity, BOD, COD, lignin, phenol, TS, TSS, TOS, and TDS of the effluents collected in each operating phase after each HRT from reactors R1 and R2 were determined in the Lab as per the standard methods by APHA, AWWA, and WWF (2017) 23rd Edition. The VFA/Alkalinity ratio and pH of the reactors' substrate were regularly monitored after each HRT in all three phases. The values were found within permissible limits each time, which reflects that both reactors were operating satisfactorily in all three phases. Pollutants (BOD, COD, TS, TSS, TOS, TDS, lignin, and phenol) removal percentages of the effluents

were determined after each HRT to know the comparative performances of both reactors. The volumes of biogas generated from both reactors- R1 and R2 were separately measured by the inverted measuring cylinders by the water displacement techniques, as shown in Fig. 3a. The biogas generated from both reactors mainly comprised CH_4 and CO_2, which were 51% and 49% respectively as analyzed by Gas Chromatography (GC).

RESULTS AND DISCUSSION

Impact of OLR and HRT Variations

Organic Loading Rate (OLR): It expresses the amount of suspended and dissolved organic materials fed into the reactor per cubic meter of its volume per day. It is expressed in kg $COD.m^{-3}.d^{-1}$ or g $COD.L^{-1}.d^{-1}$. The organic loading is done in a semi-continuous mode in this study. When OLR is increased, the volume of the biogas production is increased to an appreciable extent. However, the reactor's performance and equilibrium of the biochemical process are degraded.

Hydraulic Retention Time (HRT): The average retention time for which wastewater is retained in the bioreactor is referred to as HRT. It is expressed in day (d). The HRT depends upon OLR, process temperature, substrate characteristics, and microbial growth rate.

In this investigation, the mesophilic anaerobic degradation of RMWW was carried out in the ambient atmospheric conditions of NIT Raipur in changing OLR and HRT conditions. The pH, VFA, alkalinity, and VFA/Alkalinity ratio, as well as BOD, COD, lignin, phenol, TS, TSS, TOS, and TDS removal of the effluents from both reactors, were examined by the optimization of OLR and HRT conditions.

Experimental Outcomes

Tables 5a, 5b, 5c, and 6a, 6b, 6c illustrate the experimental findings of RMWW treatment in three operating phases using two anaerobic semi-continuous reactors (ASCR)- R1 and R2, respectively, in which the pH adjustment of the substrate to 7.0 is done by blending NaOH and $Ca(OH)_2$ respectively with the substrate. In Operating Phase I, the OLR was kept constant in both reactors R1 and R2 at 3.25 kg $COD.m^{-3}.d^{-1}$ for the entire HRT (10 d to 110 d), and pollutant removal, as well as biogas generation, was inspected under varying HRT conditions. In Operating Phase II, the HRT was changed from 10 d to 150 d, and the OLR was changed from 1.50 to 7.32 kg $COD.m^{-3}.d^{-1}$. In Operating Phase III, the HRT was kept constant at 5 d, and the OLR was changed from 1.55 to 7.25 kg $COD.m^{-3}.d^{-1}$. The pollutant (BOD, COD, lignin, phenol, TS, TSS, TOS, and TDS) removal and biogas generation from both reactors were examined in all three operating phases. The highest BOD removal percentages achieved in reactors R1 and R2 were 94% and 93% respectively, in Operating Phase I of both reactors, shown in Tables 5a and 6a, respectively.

Behavior of pH, VFA, and Alkalinity in Different Operating Phases

Fig. 5 illustrates the pH variation in the biological treatment

Table 5a: Operating Phase I: Varying HRT from 10 d to 110 d and keeping OLR constant at 3.25 kg $COD.m^{-3}.d^{-1}$ (R1).

HRT [d]	10	20	30	40	50	60	70	80	90	100	110
OLR [g $COD.m^{-3}.d^{-1}$]						3.25					
BOD removal [%]	65	76	85	94	93	94	94	93	93	94	94
COD removal [%)]	62	74	82	92	91	92	92	91	91	92	92
Lignin removal [%]	39	51	68	84	83	84	84	83	83	84	84
Phenol removal [%]	36	49	65	82	81	82	82	81	81	82	82
TSS removal [%]	56	65	75	88	87	88	88	87	87	88	88
TOS removal [%]	58	69	79	92	91	92	92	91	91	92	92
TDS removal [%]	58	71	81	92	91	92	92	91	91	92	92
Biogas generation [$L.d^{-1}$]	07.51	07.81	08.32	08.52	08.51	08.50	08.51	08.51	08.49	08.49	08.50
Biogas yield [$L.g^{-1}$ COD]	0.007	0.007	0.008	0.008	0.008	0.008	0.008	0.008	0.008	0.008	0.008
Biomethane generation ($L.d^{-1}$)	03.81	03.92	04.21	04.32	04.32	04.31	04.32	04.32	04.31	04.31	04.31
Biomethane yield ($L.g^{-1}$ COD)	0.003	0.003	0.004	0.004	0.004	0.004	0.004	0.004	0.004	0.004	0.004
pH	7.6	7.7	7.6	7.5	7.4	7.3	7.2	7.1	7.1	7.0	6.9
VFA [$mg.L^{-1}$ as CH_3COOH]	85	82	78	73	72	65	59	54	47	44	40
Alkalinity [$mg.L^{-1}$ as CaCO]	894	882	877	861	852	830	795	786	760	750	734
VFA/Alkalinity ratio	0.09	0.09	0.09	0.08	0.08	0.08	0.07	0.07	0.06	0.06	0.05

Table 5b: Operating Phase II: Varying OLR from 1.50 to 7.32 kg COD.m^{-3}.d^{-1} and HRT from 10 d to 150 d (R1).

HRT [d]	10	20	30	40	50	60	70	80	90	100	110	120	130	140	150
OLR [g COD.m^{-3}·d^{-1}]	1.50	2.50	3.25	3.75	4.25	4.75	5.25	5.50	5.75	6.00	6.25	6.50	6.75	7.00	7.32
BOD removal [%]	92	91	90	89	87	85	83	82	81	80	78	76	74	73	71
COD removal [%)]	90	89	88	87	86	84	82	81	80	78	77	75	73	72	70
Lignin removal [%]	82	80	78	76	74	73	71	69	68	66	64	61	59	57	54
Phenol removal [%]	80	77	76	74	73	71	69	66	65	64	62	59	56	55	52
TSS removal [%]	89	88	87	86	85	84	82	81	80	79	77	75	73	71	70
TOS removal [%]	86	85	84	83	82	81	79	78	77	76	74	73	71	69	68
TDS removal [%]	91	90	89	88	87	86	84	83	82	81	79	76	73	72	71
Biogas generation [L.d^{-1}]	90	89	88	87	86	85	83	82	81	80	78	75	73	71	70
Biogas yield [L.g^{-1} COD]	04.06	07.02	08.71	10.50	10.42	11.21	12.03	12.06	12.11	12.06	12.63	12.62	12.61	12.62	12.61
Biomethane generation (L.d^{-1})	0.009	0.009	0.009	0.010	0.008	0.008	0.008	0.007	0.007	0.007	0.007	0.007	0.006	0.006	0.005
Biomethane yield (L.g^{-1} COD)	02.06	03.51	04.41	05.32	05.35	05.71	06.11	06.21	06.21	06.22	06.40	06.40	06.40	06.40	06.40
pH	0.004	0.004	0.005	0.005	0.004	0.004	0.004	0.004	0.004	0.003	0.004	0.004	0.003	0.003	0.002
VFA [mg.L^{-1} as CH$_3$COOH]	7.8	7.7	7.8	7.6	7.7	7.8	7.7	7.6	7.5	7.4	7.5	7.6	7.3	7.5	7.3
Alkalinity [mg.L^{-1} as CaCO]	94	90	83	79	75	72	69	66	61	57	55	52	49	44	37
VFA/Alkalinity ratio	887	884	881	876	870	864	860	856	852	849	842	838	830	824	790
	0.10	0.10	0.09	0.09	0.08	0.08	0.08	0.08	0.07	0.07	0.06	0.06	0.06	0.05	0.04

Table 5c: Operating Phase III: Varying OLR from 1.55 to 7.25 kg COD.m^{-3}.d^{-1} and keeping HRT constant at 5 d (R1).

HRT [d]					5					
OLR [g COD.m^{-3}·d^{-1}]	1.55	2.55	3.05	3.55	4.05	4.55	5.05	5.55	6.05	7.25
BOD removal [%]	80	77	75	71	69	66	64	62	59	55
COD removal [%)]	78	75	73	69	67	64	62	60	57	53
Lignin removal [%]	69	66	62	58	53	47	40	33	28	17
Phenol removal [%]	66	63	59	55	49	42	37	29	22	14
TSS removal [%]	77	74	72	68	66	63	61	59	56	53
TOS removal [%]	74	71	69	65	63	60	58	56	53	50
TDS removal [%]	79	76	74	70	68	65	63	62	58	53
Biogas generation [L.d^{-1}]	78	75	73	69	67	64	62	60	57	54
Biogas yield [L.g^{-1} COD]	0.387	0.535	0.549	0.639	0.729	0.819	0.909	0.999	0.907	1.087
Biomethane generation (L.d^{-1})	0.008	0.007	0.006	0.006	0.006	0.006	0.006	0.006	0.005	0.005
Biomethane yield (L.g^{-1} COD)	0.197	0.273	0.281	0.326	0.372	0.417	0.463	0.509	0.462	0.554
pH	0.004	0.004	0.004	0.003	0.003	0.003	0.003	0.002	0.002	0.002
VFA [mg.L^{-1} as CH$_3$COOH]	7.7	7.6	7.6	7.5	7.4	7.3	7.2	7.1	7.0	6.9
Alkalinity [mg.L^{-1} as CaCO]	84	81	78	74	71	67	62	59	52	48
VFA/Alkalinity ratio	878	870	860	845	796	784	764	748	724	712
	0.09	0.09	0.09	0.09	0.09	0.08	0.08	0.08	0.07	0.07

Table 6a: Operating Phase I: Varying HRT from 10 d to 110 d and keeping OLR constant at 3.25 kg COD.m^{-3}.d^{-1} (R2).

HRT [d]	10	20	30	40	50	60	70	80	90	100	110
OLR [g COD.m^{-3}·d$^{-1]}$						3.25					
BOD removal [%]	64	75	84	93	92	93	93	92	92	93	93
COD removal [%)]	61	73	81	91	90	91	91	90	90	91	91
Lignin removal [%]	37	49	65	82	81	82	82	81	81	82	82
Phenol removal [%]	34	47	62	80	79	80	80	79	79	80	80
TSS removal [%]	56	67	78	90	89	90	90	89	89	90	90
TOS removal [%]	53	63	74	87	86	87	87	86	86	87	87
TDS removal [%]	57	68	78	91	90	91	91	90	90	91	91
Biogas generation [L.d^{-1}]	57	69	80	91	90	91	91	90	90	91	91
Biogas yield [L.g^{-1} COD]	07.47	07.73	08.21	08.51	08.50	08.50	08.49	08.50	08.50	08.49	08.49
Biomethane generation (L.d^{-1})	0.007	0.007	0.008	0.008	0.008	0.008	0.008	0.008	0.008	0.008	0.008
Biomethane yield (L.g^{-1} COD)	03.81	03.93	04.17	04.33	04.31	04.32	04.31	04.32	04.32	04.31	04.31
pH	0.003	0.003	0.004	0.004	0.004	0.004	0.004	0.004	0.004	0.004	0.004
VFA [mg.L^{-1} as CH$_3$COOH]	7.7	7.8	7.7	7.6	7.5	7.4	7.3	7.2	7.2	7.1	7.0
Alkalinity [mg.L^{-1} as CaCO]	89	84	80	75	73	68	61	55	49	45	42
VFA/Alkalinity ratio	897	884	880	865	854	832	798	785	765	754	736
	0.10	0.09	0.09	0.08	0.08	0.08	0.07	0.07	0.06	0.06	0.06

Table 6b: Operating Phase II: Varying OLR from 1.50 to 7.32 kg COD.m^{-3}.d^{-1} and HRT from 10 d to 150 d (R2).

HRT [d]	10	20	30	40	50	60	70	80	90	100	110	120	130	140	150
OLR [g COD.m^{-3}·d$^{-1]}$	1.50	2.50	3.25	3.75	4.25	4.75	5.25	5.50	5.75	6.00	6.25	6.50	6.75	7.00	7.32
BOD removal [%]	91	90	89	88	86	84	82	81	80	79	77	75	74	72	70
COD removal [%)]	89	88	87	86	85	83	81	80	79	77	76	74	73	71	69
Lignin removal [%]	80	78	76	74	72	70	68	67	66	64	62	59	57	55	51
Phenol removal [%]	76	74	72	70	68	67	65	64	62	60	58	56	55	53	49
TSS removal [%]	88	87	86	85	84	83	81	80	79	78	76	74	72	70	69
TOS removal [%]	85	84	83	82	81	80	78	77	76	75	73	72	70	68	67
TDS removal [%]	90	89	88	87	86	85	83	82	81	80	78	75	72	71	70
Biogas generation [L.d^{-1}]	89	88	87	86	85	84	82	81	80	79	77	74	72	70	69
Biogas yield [L.g^{-1} COD]	04.06	07.02	08.72	10.51	10.41	11.21	12.02	12.06	12.11	12.06	12.62	12.61	12.60	12.61	12.60
Biomethane generation (L.d^{-1})	0.009	0.009	0.009	0.010	0.008	0.008	0.008	0.007	0.007	0.007	0.007	0.007	0.006	0.005	0.005
Biomethane yield (L.g^{-1} COD)	02.06	03.51	04.41	05.31	05.31	05.71	06.11	06.21	06.21	06.21	06.41	06.40	06.39	06.40	06.39
pH	0.004	0.004	0.005	0.005	0.004	0.004	0.004	0.004	0.004	0.003	0.004	0.004	0.003	0.003	0.003
VFA [mg.L^{-1} as CH$_3$COOH]	7.9	7.8	7.9	7.8	7.7	7.9	7.7	7.6	7.5	7.4	7.5	7.4	7.6	7.5	7.4
Alkalinity [mg.L^{-1} as CaCO]	98	95	85	81	78	75	72	69	63	59	56	54	51	45	39
VFA/Alkalinity ratio	890	886	883	879	872	865	863	858	855	850	844	840	834	828	795
	0.11	0.11	0.09	0.09	0.09	0.08	0.08	0.08	0.08	0.07	0.07	0.06	0.06	0.05	0.05

Table 6c: Operating Phase III: Varying OLR from 1.55 to 7.25 kg COD.m^{-3}.d^{-1} and keeping HRT constant at 5 d (R2).

HRT [d]					5					
OLR [g COD.m^{-3}.d^{-1}]	1.55	2.55	3.05	3.55	4.05	4.55	5.05	5.55	6.05	7.25
BOD removal [%]	79	76	74	70	68	65	63	61	58	54
COD removal [%)]	77	74	72	68	66	63	61	59	56	52
Lignin removal [%]	67	64	60	55	52	45	38	29	24	15
Phenol removal [%]	64	61	57	54	45	40	35	26	19	11
TSS removal [%]	76	73	71	67	65	62	60	58	55	52
TOS removal [%]	73	70	68	64	62	59	57	55	52	49
TDS removal [%]	78	75	73	69	67	64	62	61	57	52
Biogas generation [L.d^{-1}]	77	74	72	68	66	63	61	59	56	53
Biogas yield [L.g^{-1} COD]	0.383	0.607	0.697	0.773	0.847	0.860	0.903	0.940	0.963	1.013
Biomethane generation (L.d^{-1})	0.008	0.008	0.008	0.007	0.007	0.006	0.006	0.006	0.005	0.004
Biomethane yield (L.g^{-1} COD)	0.195	0.309	0.353	0.393	0.430	0.437	0.460	0.477	0.490	0.517
pH	0.004	0.004	0.004	0.004	0.003	0.003	0.003	0.003	0.003	0.002
VFA [mg.L^{-1} as CH$_3$COOH]	7.8	7.7	7.7	7.6	7.5	7.4	7.3	7.2	7.1	7.0
Alkalinity [mg.L^{-1} as CaCO]	88	85	80	77	73	69	65	61	55	51
VFA/Alkalinity ratio	884	875	866	850	798	786	767	754	729	716
	0.10	0.10	0.09	0.09	0.09	0.09	0.08	0.08	0.07	0.07

of RMWW in ASCR- R1 and R2. The pH of the substrate and inoculum mix in both reactors was regularly monitored. As shown in Fig. 5a, pH values in reactors R1 and R2 were 7.7 and 7.8, respectively, at an HRT of 20 d in OP I, and they gradually diminished in both reactors with the increase in HRT. Similarly, Fig. 5b and 5c illustrate the pH range of OP II and OP III, respectively. In OP II, the highest pH values in reactors R1 and R2 were 7.8 and 7.9, respectively, which were achieved under three conditions- an HRT of 10 d and OLR of 1.50 kg COD.m^{-3}.d^{-1}, HRT of 30 d and OLR of 3.25 kg COD.m^{-3}.d^{-1}, and HRT of 60 d and OLR of 4.75 kg COD.m^{-3}.d^{-1}. In OP III, the highest values of pH in reactors

R1 and R2 were 7.7 and 7.8, respectively, at an OLR of 1.55 kg COD.m^{-3}.d^{-1}, and they gradually diminished with the increasing OLR in both reactors.

The analysis of VFA variation was done in three operating phases based on increase and decrease in feed concentration; the results are depicted in Fig. 6a, 6b, and 6c. During acetogenic conditions, VFA and alcohols are converted into acetic acid by H$_2$-utilizing homo-acetogens and H$_2$+CO$_2$ by H$_2$-producing acetogens, which are ultimately converted to methane and CO$_2$ gas by acetoclastic and CO$_2$-reducing methanogens respectively. As a result, pH is not lowered below 6.5 throughout the digestion process in
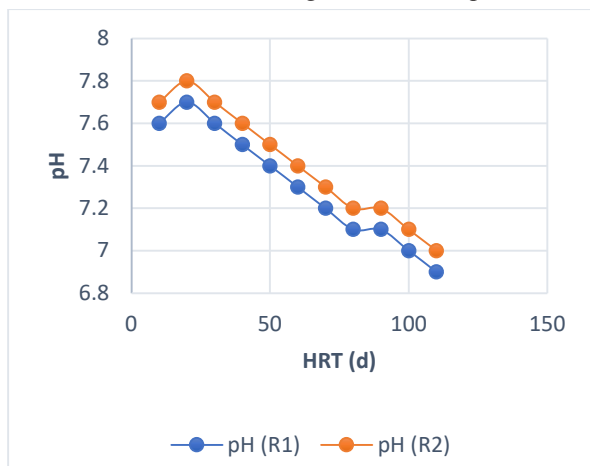
Fig. 5a: pH variation with HRT in OP I.
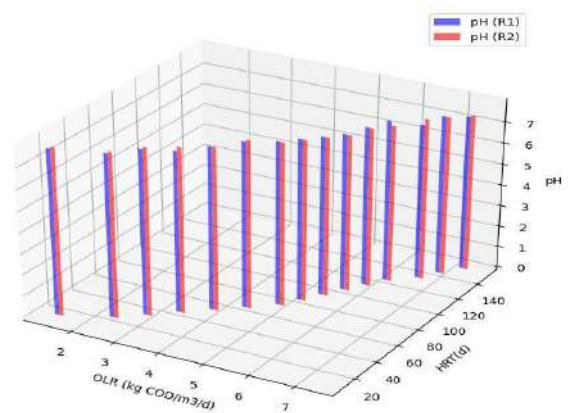
Fig. 5b: pH variation with varying HRT and OLR in OP II.
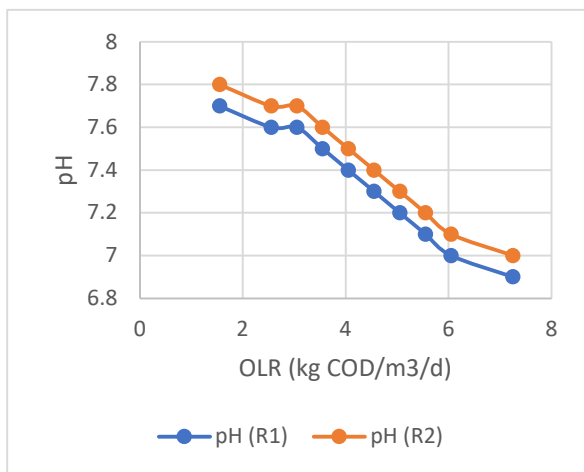
Fig. 5c: pH variation with OLR in OP III.
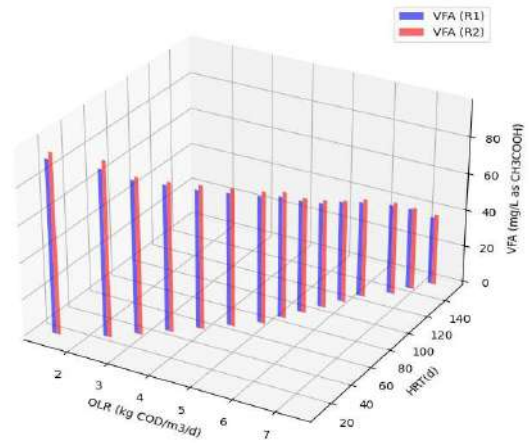
Fig. 6b: VFA variation with varying OLR and HRT in OP II.
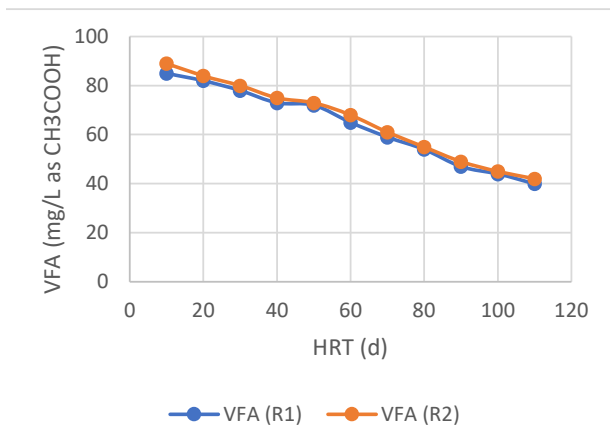
Fig. 6a: VFA variation with HRT in OP I.
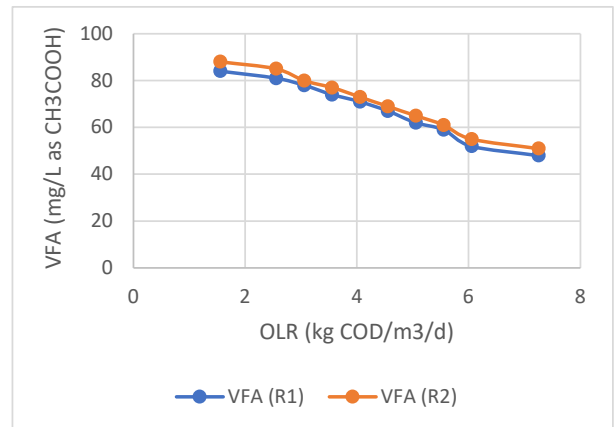
Fig. 6c: VFA variation with OLR in OP III.

any operating phase. The analysis of alkalinity variation was done in three operating phases, and the results are depicted in Fig. 7a, 7b, and 7c. The alkalinity of the RMWW was in the range of 712-897 mg.L^{-1} as CaCO$_3$ in the two reactors-R1 and R2. The alkalinity of RMWW in reactor R1 ranged from 734-894, 790-887, and 712-878 mg.L^{-1} as CaCO$_3$ in operating phases I, II, and III, respectively. Similarly, the alkalinity of RMWW in reactor R2 ranged from 736-897, 795-890, and 716-884 mg.L^{-1} as CaCO$_3$ in operating phases I, II, and III, respectively. Thus, the alkalinity of RMWW in both reactors did not fall below 712 mg.L^{-1} as CaCO$_3$ due to the conversion of VFA into CH$_4$ and CO$_2$.

Pollutant Reduction Efficiencies of ASCR- R1 and R2

BOD reduction efficiency: The BOD reduction efficiencies of the bioreactors R1 and R2 in operating phases I, II, and III are depicted in Fig. 8a, 8b, and 8c, respectively. Fig. 8a

shows that at an HRT of 40 d, the BOD removal efficiencies of reactors R1 and R2 were 94% and 93%, respectively, in OP I when OLR was kept constant at 3.25 kg COD.m^{-3}.d^{-1}. In this phase, the BOD reduction efficiencies of the two reactors went on increasing from an HRT of 10 d up to 40 d, and at 40 d the maximum removal efficiencies of both reactors were observed. After 40 d up to 110 d, the BOD removal efficiencies of both reactors remained nearly stationary. Fig. 8b shows that the highest BOD removal efficiencies achieved in reactors R1 and R2 were 92% and 91%, respectively, at an OLR of 1.50 kg COD.m^{-3}.d^{-1} and HRT of 10 d in OP II. Similarly, in OP III, the highest BOD removal efficiencies attained in reactors R1 and R2 were 80% and 79%, respectively, at the OLR of 1.55 kg COD.m^{-3}.d^{-1} and constant HRT of 5 d, as illustrated in Fig. 8c. In this phase, BOD removal efficiencies were decreased as the OLR was increased from 1.55 kg COD.m^{-3}.d^{-1}. Thus,
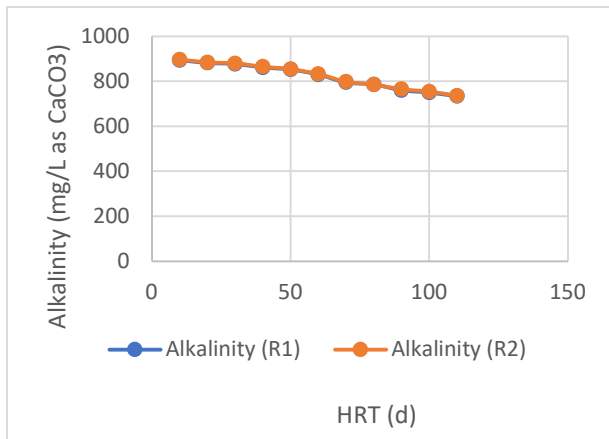
Fig. 7a: Alkalinity variation with HRT in OP I
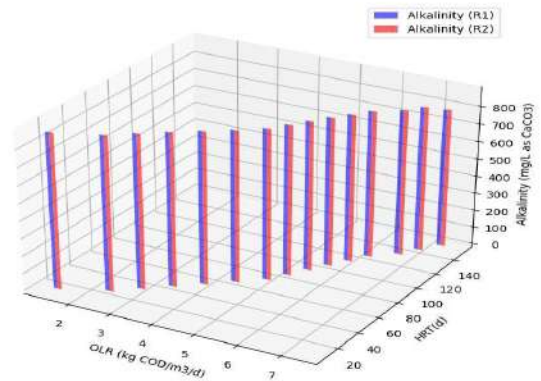
Fig. 7b: Alkalinity variation with varying OLR and HRT in OP II.
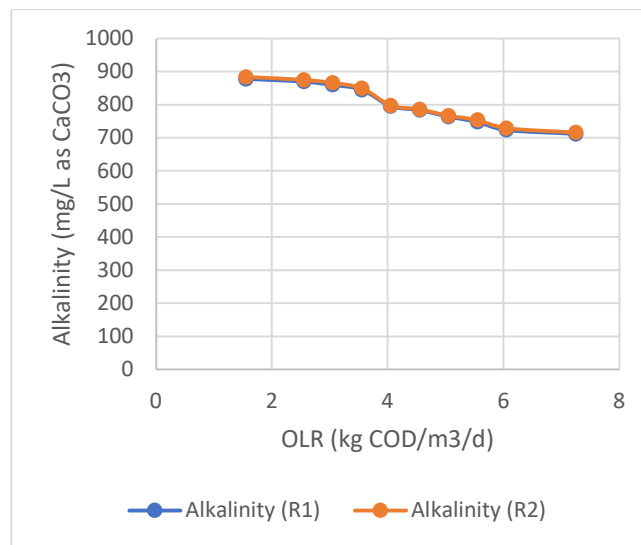
Fig. 7c: Alkalinity variation with OLR in OP III.

the highest BOD reduction in both reactors was noticed at a higher HRT and lower OLR.

COD reduction efficiency: The COD reduction efficiencies of the reactors R1 and R2 in OP I, OP II, and OP III are shown in Fig. 9a, 9b, and 9c, respectively. The highest COD removal efficiencies obtained in reactors R1 and R2 were 92% and 91%, respectively, in OP I at an HRT of 40 d and constant OLR of 3.25 kg $COD.m^{-3}.d^{-1}$, as shown in Fig. 9a. The COD removal efficiencies of both reactors remained almost stationary after 40 d up to 110 d in OP I. Fig. 9b shows that the highest COD reduction efficiencies achieved in reactors R1 and R2 were 90% and 89%, respectively, in OP II at an OLR of 1.50 kg $COD.m^{-3}.d^{-1}$ and HRT of 10 d. Similarly, in OP III, the highest COD reduction efficiencies attained in reactors R1 and R2 were 78% and 77%, respectively, at

an OLR of 1.55 kg $COD/m^3/d$ and constant HRT of 5 d as shown in Fig. 9c. In this phase, COD removal efficiencies were decreased as the OLR was enhanced from 1.55 kg $COD.m^{-3}.d^{-1}$. Thus, the highest COD reduction in both reactors was noticed at a higher HRT and lower OLR.

Lignin reduction efficiency: The lignin reduction efficiencies of the reactors R1 and R2 in OP I, OP II, and OP III are shown in Fig. 10a, 10b, and 10c, respectively. Fig. 10a shows that at an HRT of 40 d and constant OLR of 3.25 kg COD.m-3.d-1, the highest lignin removal efficiencies obtained in reactors R1 and R2 were 84% and 82%, respectively, in OP I; the lignin removal efficiencies of both reactors remained almost stationary after 40 d up to 110 d. Fig. 10b shows that the highest lignin removal efficiencies obtained in reactors R1 and R2 were 82% and
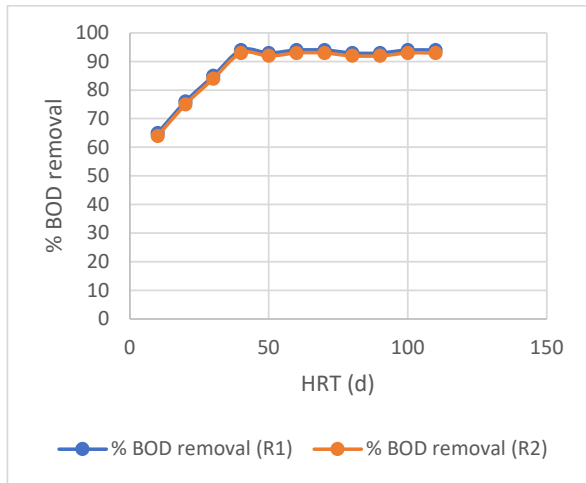
Fig. 8a: Variation of % BOD removal with HRT in OP I.
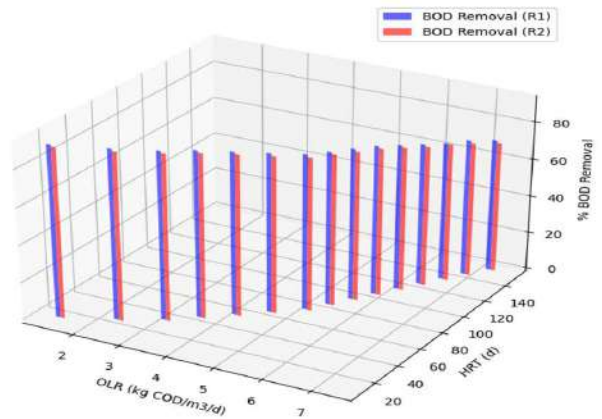
Fig. 8b: Variation of % BOD removal with varying OLR and HRT in OP II.
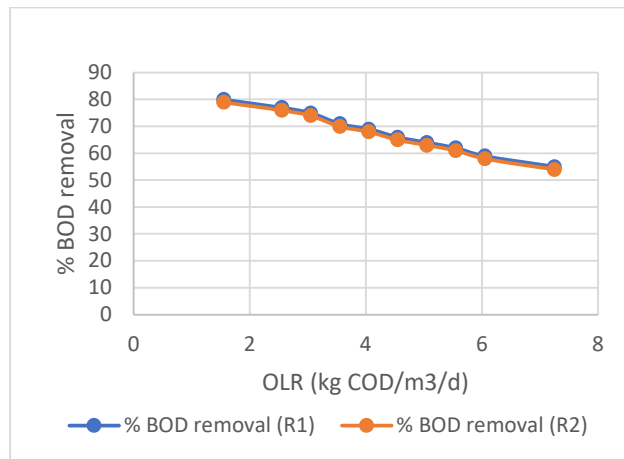
Fig. 8c: Variation of % BOD removal with OLR in OP III.

80%, respectively, in OP II at an OLR of 1.50 kg COD.m-3.d-1 and HRT of 10 d. Similarly, in OP III, the highest lignin removal efficiencies achieved in reactors R1 and R2 were 69% and 67%, respectively, at an OLR of 1.55 kg COD.m-3.d-1 and constant HRT of 5 d as shown in Fig. 10c. In this phase, the lignin removal efficiencies were decreased as the OLR was enhanced from 1.55 kg COD.m-3.d-1. Thus, the highest lignin reduction in both reactors was observed at a higher HRT and lower OLR.

Phenol reduction efficiency: The phenol reduction efficiencies of the reactors R1 and R2 in OP I, OP II, and OP III are shown in Fig. 11a, 11b, and 11c, respectively. As shown in Fig. 11a, the highest phenol removal efficiencies obtained in OP I in reactors R1 and R2 were 82% and 80%, respectively, at an HRT of 40 d and constant OLR of 3.25 kg COD.m^{-3}.d^{-1}; the phenol removal efficiencies of both reactors
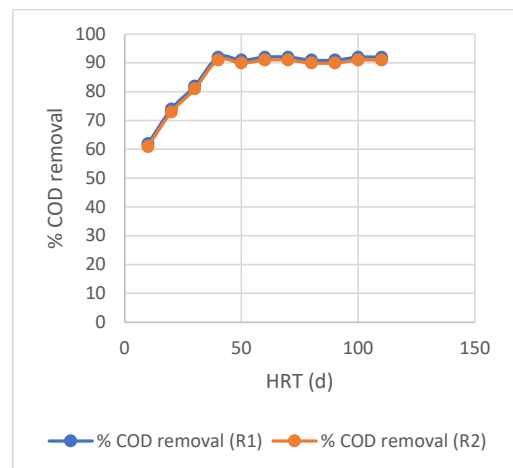
Fig. 9a: Variation of % COD removal with HRT in OP I.
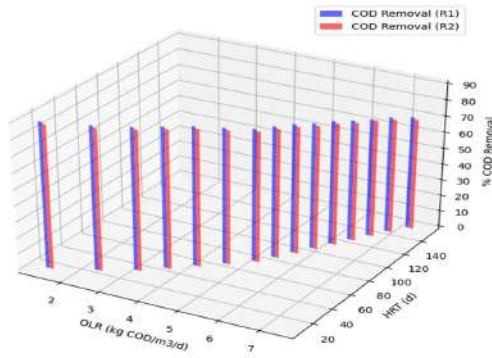
Fig. 9b: Variation of % COD removal with varying OLR and HRT in OP II.
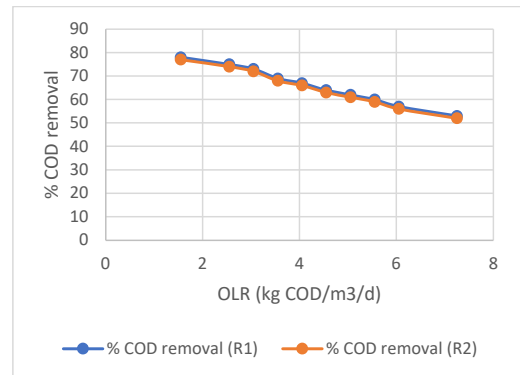
Fig. 9c: Variation of % COD removal with OLR in OP III.
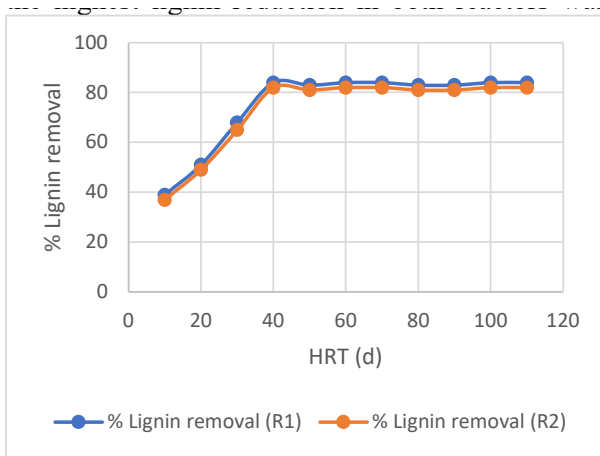
Fig. 10a: Variation of % Lignin removal with HRT in OP I.
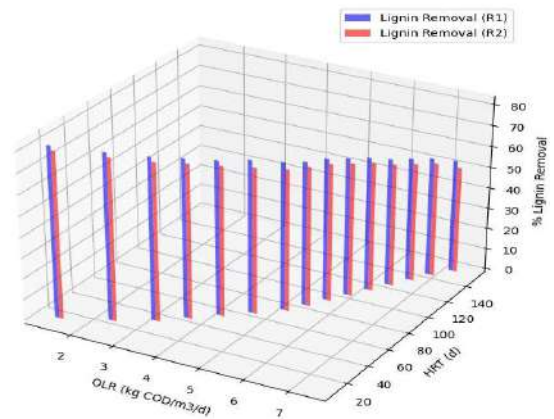
Fig. 10b: Variation of % Lignin removal with varying OLR and HRT in OP II.
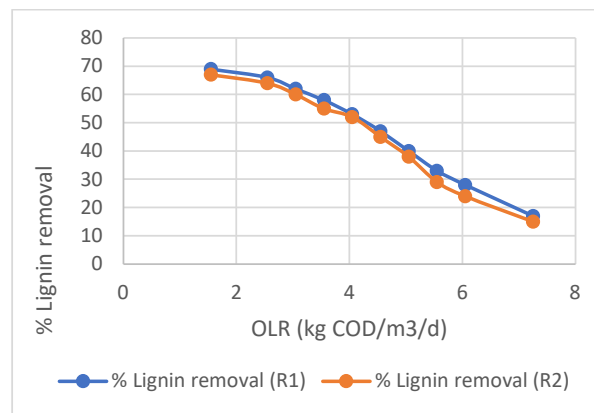
Fig. 10c: Variation of % Lignin removal with OLR in OP III.

remained almost stationary after 40 d up to 110 d. Fig. 11b shows that the highest phenol removal efficiencies obtained in reactors R1 and R2 were 80% and 76%, respectively, in OP II at an OLR of 1.50 kg COD.m^{-3}.d^{-1} and HRT of 10 d. Similarly, in OP III, the highest phenol removal efficiencies achieved in reactors R1 and R2 were 66% and 64%, respectively, at an OLR of 1.55 kg COD.m^{-3}.d^{-1} and constant HRT of 5 d, as shown in Fig. 11c. In this phase,

the phenol removal efficiencies were decreased as the OLR was increased from 1.55 kg $COD.m^{-3}.d^{-1}$. Thus, the highest phenol reduction in both reactors was observed at a higher HRT and lower OLR.

On observing the graphs plotted in Fig. 8, 9, 10, and 11 depicting the BOD, COD, lignin, and phenol removal efficiencies, respectively, in the three operating phases at different OLR and HRT conditions, it can be concluded that the highest pollutant reduction efficiencies of both reactors R1 and R2 occurred at a lower OLR and higher HRT. The pollutant removal efficiency of R1 was only slightly more than that of R2, but the alkali pretreatment of R1 by NaOH was considerably costlier than that of R2 by $Ca(OH)_2$. The highest BOD, COD, lignin, and phenol removal efficiencies of R1 were 94%, 92%, 84%, and 82%, respectively, whereas those of R2 were 93%, 91%, 82%, and 80% respectively. The BOD and COD contents of effluents from reactors R1 and R2 were 223 $mg.L^{-1}$ and 434 $mg.L^{-1}$ as well as 261 $mg.L^{-1}$ and 488 $mg.L^{-1,}$ respectively, at their highest pollutant removal efficiencies. Thus, BOD and COD contents of the effluents

from both reactors complied with the effluents discharge standards for safe disposal into public sewers (BOD= 350 $mg.L^{-1}$, COD- Not defined) as per the Environmental (Protection) Rules, 1986, Govt. of India, New Delhi. Furthermore, the effluents from both reactors may be used for irrigating crops after minor physicochemical treatment like electrocoagulation or adsorption on chitosan (Choudhary et al. 2015, Thirugnanasambandham et al. 2013, Kandagatla et al. 2023) complying with the effluent discharge standards (BOD= 100 $mg.L^{-1}$, COD= 250 $mg.L^{-1}$) for irrigation. The significant removal of the two xenobiotic compounds lignin and phenol from RMWW by the two reactors R1 and R2 was feasible due to the presence of lignin and phenol removing bacterial species in the cow dung fed BGPS (inoculum) as well as the bioremediation of the substrate with the white rot fungi (*Phanerochaete chrysosporium*).

Costa et al. (2017) worked on the bioremediation of lignin present in synthetic wastewater as well as industrial paper and pulp mill wastewater (PPMWW) by mycoremediation with white rot fungi viz., *Phanerochaete chrysosporium*
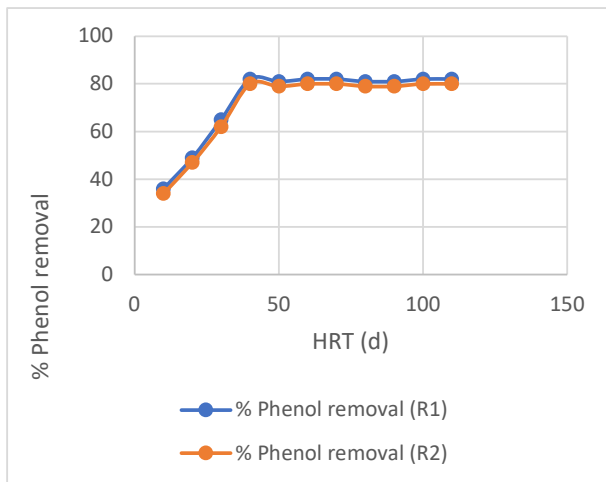
Fig. 11a: Variation of % Phenol removal with HRT in OP I.
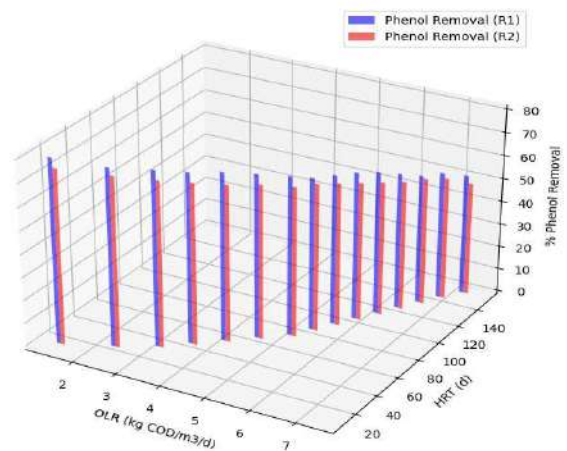
Fig. 11b: Variation of % phenol removal with varying OLR and HRT in OP II.
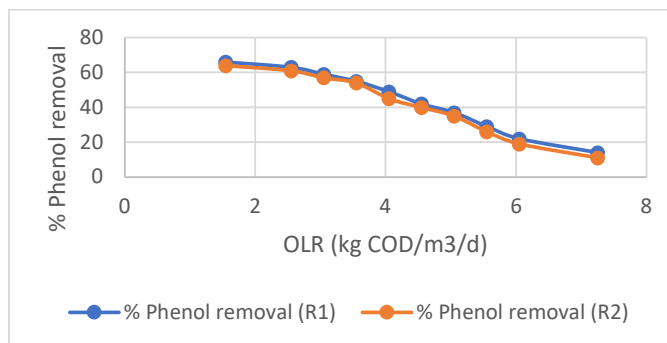
Fig. 11c: Variation of % Phenol removal with OLR in OP III.

and *Bjerkandera adusta*. The researchers concluded that *P. chrysosporium* and *B. adusta* removed 74% and 97% of lignin from the synthetic wastewater, whereas both fungal strains removed 100% of lignin from the PPMWW in 8 to 10 days. Ahmadi et al. (2006) studied the bioremediation of phenol removal from olive mill wastewater (OMWW) with white rot fungi (*Phanerochaete chrysosporium*). The researchers diluted the OMWW with the solution of mineral salt blended with ammonium sulfate, glucose, and yeast. The fungi thrived in the diluted OMWW and removed 90% of phenol from the OMWW.

Kumar et al. (2022) studied the biodegradation of paper and pulp mill wastewater (PPMWW) to remove lignin using the bacterial strain *Bacillus* sp. The researchers concluded that *Bacillus* sp. removed 89% of lignin and 40% of color at 1000 mg.L^{-1} lignin in an HRT of 3 days. Singh et al. (2022) studied the biodegradation of paper and pulp mill sludge (PPMS) to remove lignin by the bacterial strain *Bacillus* sp. The researchers found that *Bacillus* sp. removed 84% of lignin in an HRT of 14 days. Haq and Kalamdhad (2023) studied the bioremediation of paper and pulp mill wastewater (PPMWW) by the bacterial strain *Pseudomonas* sp. The researchers found that the *Pseudomonas* sp. removed 65.6% of lignin, 85.7% of color, and 98.4% of phenol from the wastewater in an HRT of 6 days. De Angelis et al. (2013) worked on lignin removal from industrial wastewater by *Enterobacter* sp. in anaerobic conditions. The researchers found that the microbial strain removed 56% of lignin from the wastewater in an HRT of 48 h. Yadav et al. (2022) studied the microbial degradation of lignin and phenol. The researchers found that the bacterial strains *Bacillus* sp., *Pseudomonas* sp., *Actinomycetes* sp. and *Streptomycetes* sp. can biodegrade lignin and dihydroxyl phenol from industrial wastewater.

Reddy et al. (2017) studied the in-situ biodegradation of phenol from phenol-laden contaminated wastewater using *Bacillus* sp. The researchers found that the bacterial sp. removed 84% of phenol from the contaminated wastewater in an HRT of 6 days. Ke et al. (2018) carried out an investigation into the bioremediation of phenol from phenol-laden synthetic wastewater using *Bacillus* sp. The researchers concluded that the microbial sp. removed 87.2% and 100% of phenol in an HRT of 12 h and 24 h, respectively, from the synthetic wastewater. Diksha et al. 2023 studied the phenol-rich sewage by *Bacillus* sp. at 1250 mg.L^{-1} phenol. The researchers concluded that the bacterium removed 83.9% of phenol from the sewage in an HRT of 13 days. Song et al. (2009) studied the biodegradation of phenol and Cr (VI) by *Pseudomonas* sp. in a reactor in the mineral liquid medium. They found that the microbial strain removed 70.5% of phenol and 83.2% of Cr (VI) from the liquid medium.

Mahgoub et al. (2023) studied the biodegradation of phenolic wastewater by *Pseudomonas* sp. in a mineral salt medium. They found that the bacterium removed 74.68% of phenol at 1.0 g.L^{-1} in an HRT of 3 days and tolerated high phenol contents up to 2.0 g.L^{-1}. Stoilova et al. 2006 investigated the biodegradation of high amounts of phenol in a synthetic phenol solution with the help of the filamentous fungal strain *Aspergillus* sp. The findings revealed that 85% of phenol was degraded in an HRT of 6 days. El-Din 2023 studied the biodegradation of phenol from a synthetic phenol solution by the marine fungal strain *Aspergillus* sp. The study revealed that 88% of phenol was reduced from the synthetic solution in an HRT of 168 h at 31°C temperature.

Sharma and Singh (2015) carried out a morpho-biochemical analysis of the cow dung. The test results revealed that the bacteria present in cow dung belonged to *Bacillus* sp., *Pseudomonas* sp., *Salmonella* sp., etc. The biochemical tests to characterize the microorganisms present in cow dung aimed at bio-remediating the potent xenobiotic compound benzene were carried out by Godambe and Fulekar (2016). The researchers selected 10 well-isolated bacterial colonies for testing. The test results revealed that the microorganisms present in cow dung belonged to *Basilus* sp., *Pseudomonas* sp., *Enterobacter* sp., etc. A microbial investigation to determine the bacterial diversity existing in cow dung was conducted by Munshi et al. (2018). The results revealed that the microorganisms present in cow dung predominantly belonged to *Basilus* sp., *Pseudomonas* sp., *Salmonella* sp., etc. The microorganisms present in cow dung were studied by Devi et al. (2023). The researcher found that the cow dung inhabited plentiful microbial diversity comprising enormous bacterial, fungal, and protozoan species such as *Bacillus* sp., *Pseudomonas* sp. and *Aspergillus* sp. etc.

Microbial Analysis of the Anaerobic Sludge from the Lab-scale Bioreactors

The microbial analysis of the anaerobic sludge from the lab-scale bioreactors was performed in the Department of Biotechnology, Pandit Ravishankar Shukla University, Raipur, Chhattisgarh, India. The analytical reports revealed that the digestate comprised the bacterial strains *Bacillus* sp., *Pseudomonas* sp., *Enterobacter* sp., *Actinomycetes* sp. and *Streptomycetes* sp. as well as the fungal strain *Aspergillus* sp., which confirms the significant removal of lignin and phenol. The evidence of microbial species present in anaerobic sludge is shown in Fig. 12, 13 and 14.

Analyses of Biogas Generation and Biomethane Yield in Three Different Operating Phases

The biogas generations from anaerobic digestion of RMWW

Bacillus sp.
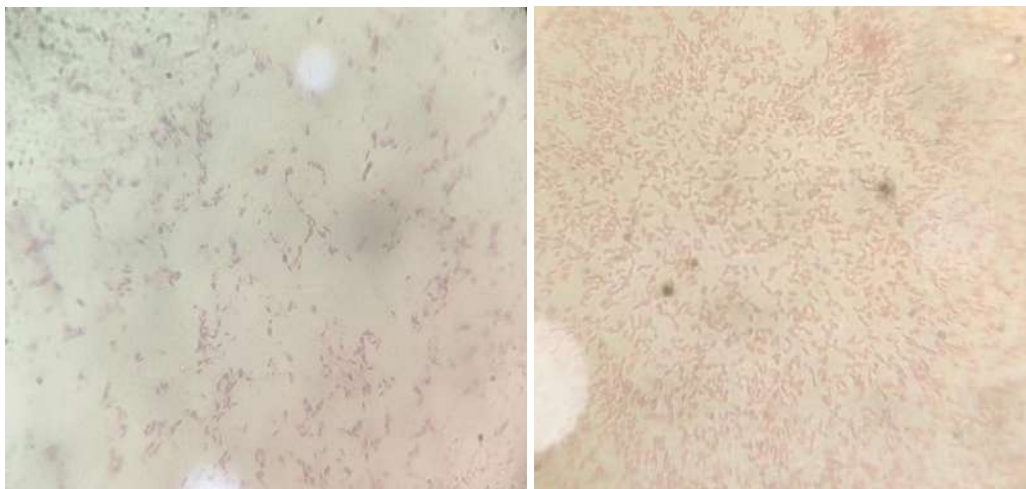
Gram +ve *Bacillus* sp.   Gram -ve *Bacillus* sp.

Pseudomonas sp.
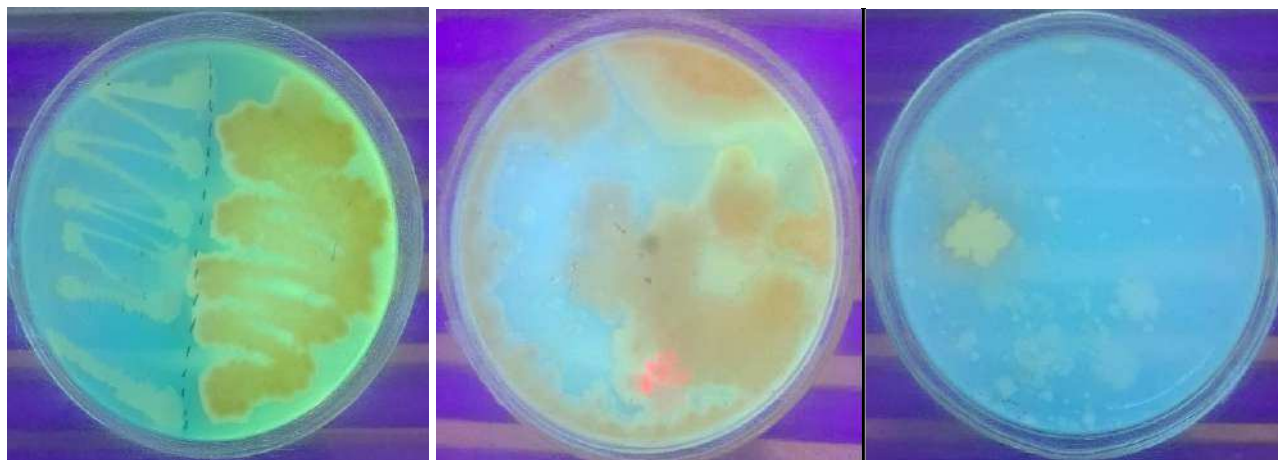
Pseudomonas fluorescens sp. Culture on King's medium emits fluorescence under UV light.

Fig. 12: Evidence of *Bacillus* sp. and *Pseudomonas* sp.

in ASCR- R1 and R2 under different OLR and HRT conditions are given in Tables 5a, 5b, 5c, 6a, 6b, and 6c, respectively. After 16 days of the reactors' stabilization and 4 days of the arrival of uniform and steady biogas generation from the reactors after initial fluctuations, the biogas produced was monitored daily. The cumulative sum of the biogas generated from both reactors was separately calculated every 10 days, shown in the tables mentioned earlier against each HRT. In Operating Phase I (OP I), the HRT was varied from 10 d to 110 d, and OLR was kept constant at 3.25 kg COD.m^{-3}.d^{-1}; the highest biogas generation was visualized after an HRT of 40 d. After hydraulic retention of 40 d, the biogas generated from both reactors were nearly stationary throughout 110 d, which is illustrated by the above-cited tables. In OP II, the HRT was changed from 10 d to 150 d, and q the OLR was changed from 1.50 to 7.32 kg COD.m^{-3}.d^{-1}; the highest generation of biogas was visualized at an HRT of 110 d and an OLR of 6.25 kg COD.m^{-3}.d^{-1}. In OP III, the OLR was changed from 1.55 to 7.25 kg COD.m^{-3}.d^{-1}, and HRT was kept constant at 5 d for each loading rate; the highest biogas

Enterobacter sp.

Gram-negative, rod-shaped. Culture grows under facultative anaerobic conditions.
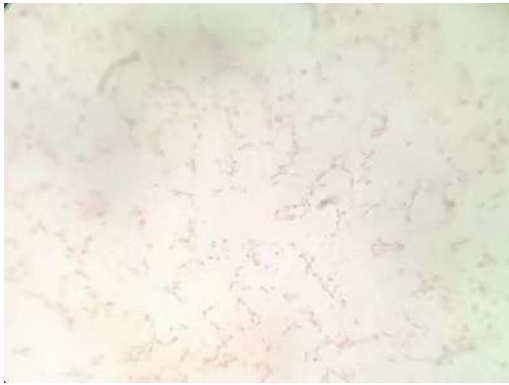
Gram -ve *Bacillus* sp.

Aspergillus sp.
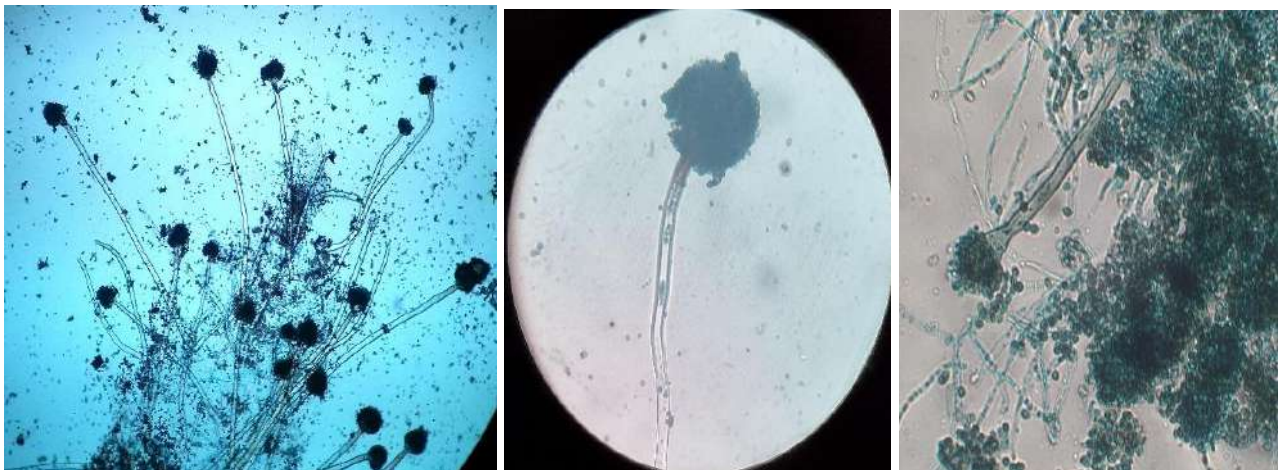
Aspergillus niger   *Aspergillus* sp.

Fig. 13: Evidence of *Enterobacter* sp. and *Aspergillus* sp.

generation was visualized at an OLR of 7.25 kg COD.m^{-3}.d^{-1}. These results manifested that the maximum biogas generation from reactors- R1 and R2 was obtained at an enhanced OLR and HRT. The highest biogas generation from both reactors in different operating phases is shown in Fig. 15.

Biomethane yield is another paramount parameter for assessing the bioreactor's performance. The maximum biomethane yield in operating phases I, II, and III from the anaerobic semi-continuous reactors- R1 and R2 are shown in Fig. 16. The biomethane yield ranged from 0.002-0.005 L.g^{-1} COD in both reactors throughout the operation process. The results indicate that the biomethane yield depends on OLR conditions. A low OLR value ushered in low organic contents in the substrate of the reactors, which ultimately ushered in low biomethane yield. On the contrary, too high OLR resulted in an improper food-to-microorganisms (F/M)

Actinomycetes sp.

Gram +ve *Bacillus* sp.

Streptomyces sp.
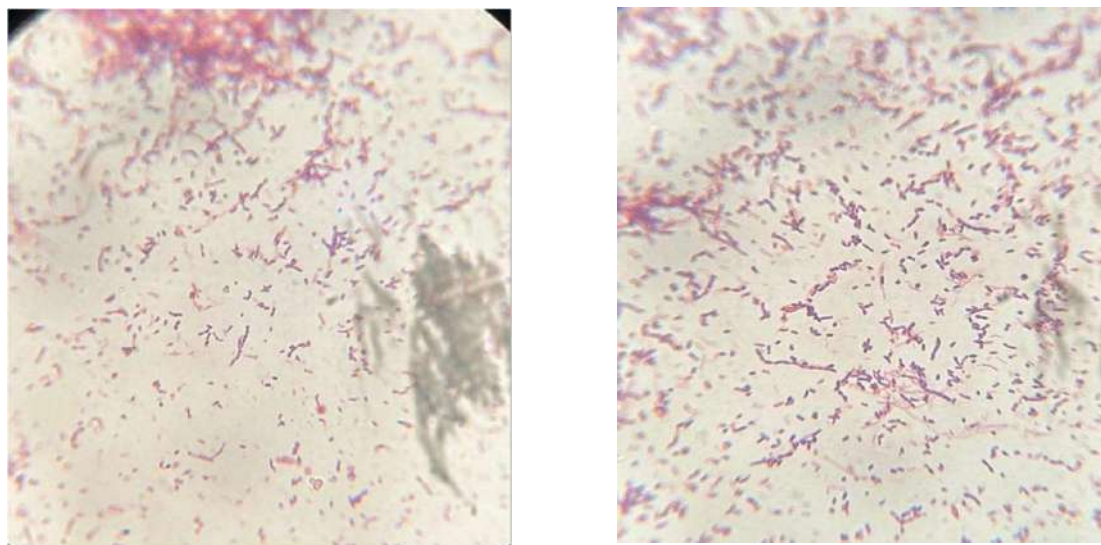
Streptomyces sp.   Gram +ve *Bacillus* sp.

Fig. 14: Evidence of *Actinomycetes* sp. and *Streptomyces* sp.

ratio, which also resulted in a low biomethane yield. Thus, an optimum OLR is suitable for attaining higher biomethane yield. The maximum biomethane yield (0.005 L.g^{-1} COD) achieved in OP II in both reactors was the highest among all three operating phases, as shown in Fig. 16.

Analyses of the Digestates from Bioreactors- R1 and R2

After the completion of the biological treatment of the RMWW in ASCR- R1 and R2 in the three operating phases I, II, and III, the digestates from both reactors were evacuated.
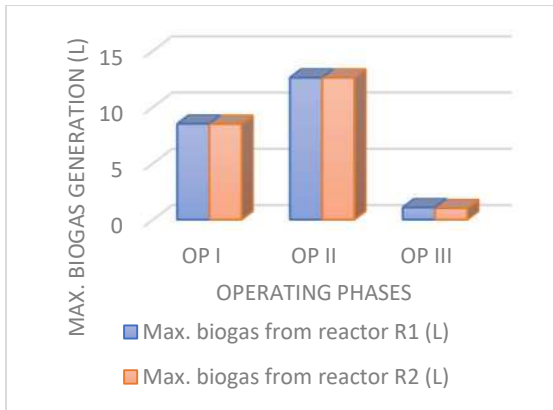
Fig. 15: Maximum biogas generation in operating phases I, II, and III.
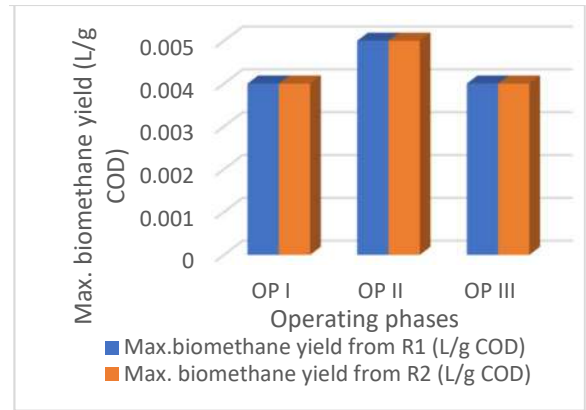
Fig. 16: Maximum biomethane yield in operating phases I, II, and III.

Small quantities of the digestates from both reactors were taken out for analysis. The analyte digestates were dried in the lab oven at 103°C-105°C so that the mechanically occluded water present in the digestates was almost driven out. The dried analyte digestates were properly desiccated in the desiccator. Eventually, the dried and desiccated digestates from reactors R1 and R2, as shown in Fig. 17 and 18, were analyzed by Scanning Electron Microscope with Energy-Dispersive X-ray Spectroscope (SEM/EDX) in the Department of Metallurgical and Materials Engineering (SEM Lab), NIT Raipur, Chhattisgarh, India. As per the SEM/EDX reports, digestate from the bioreactor R1

(BRD-1) and the digestate from the bioreactor R2 (BRD-2) both contain the macronutrients viz., N, P, K, Ca, Mg, Al, Na, and micronutrients viz., Fe, Zn, Cu, Mn, Cl, C, O, etc., essential for the plant growth. The analytical reports of SEM/EDX of BRD-1 and BRD-2 are shown in Fig. 19a, 19b, and 20a, 20b, respectively.

The digestate samples BRD-1 and BRD-2 were also sent to the Department of Soil Science and Agricultural Chemistry, Indira Gandhi Krishi Vishwavidyalaya (IGKVV) Raipur, Chhattisgarh for quantitative analyses of the essential macro and micronutrients present in the samples. As per the chemical analysis report of IGKVV Raipur, both BRD-

Table 7: Analytical report of digestates from bioreactors- R1 & R2 i.e., BRD-1 & BRD-2.

Essential plant nutrients (macro/micro)	Nitrogen (N)	Phosphorus (P)	Potassium (K)	Zinc (Zn)	Copper (Cu)	Manganese (Mn)	Iron (Fe)
BRD-1 [in g.kg^{-1} i.e., ppm]	14,500	2,600	12,900	23	6	47	104
BRD-2 [in g.kg^{-1} i.e., ppm)	14,900	2,300	11,400	19	7	43	107

Fig. 17: Oven-dried and crushed BRD-1.

Fig. 18: Oven-dried and crushed BRD- 2.

Fig. 19a: SEM/EDX image of BRD-1.
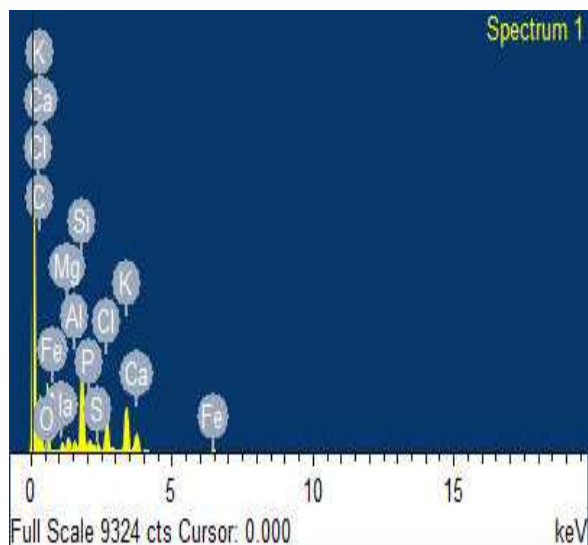
Fig. 19b: SEM/EDX spectrum of BRD-1.
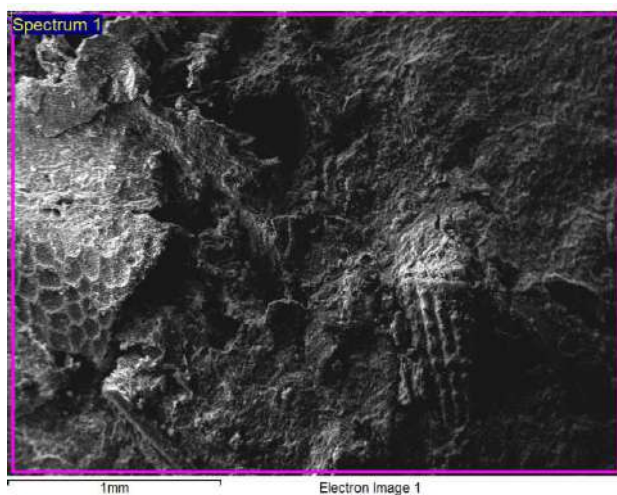
Fig. 20a: SEM/EDX image of BRD-2.
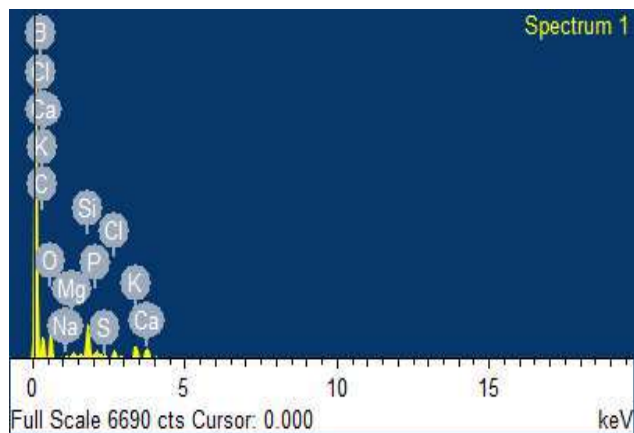
Fig. 20b: SEM/EDX spectrum of BRD-2.

1 and BRD-2 contain appropriate amounts of macro and micronutrients essential for plant growth, which are shown in Table 7. As a result, digestates of the reactors dealing with the biological anaerobic treatment of the rice mill wastewater may be used as biofertilizers for crops and as soil conditioners since they contain oxygen also according to the SEM/EDX reports.

CONCLUSIONS

The study proposed biological anaerobic treatment of rice mill wastewater, which significantly removed the pollutants and produced biomethane (CH_4). The highest pollutant removal efficiencies were observed in both reactors at an HRT of 40 d and onward in OP I. The highest BOD, COD, lignin, and phenol removal percentages achieved in reactors R1 and R2 were 94%, 92%, 84%, 82%, 93%, 91%, 82%, and 80%, respectively. The highest biogas generation was achieved at an HRT of 110 d and OLR of 6.25 kg $COD.m^{-3}.d^{-1}$ in both reactors in OP I. The highest biomethane yield was achieved in both reactors at an OLR of 3.25 kg $COD.m^{-3}.d^{-1}$ and an HRT of 30 d in OP II. The alkali pretreatment of RMWW by $Ca(OH)_2$ in bioreactor R2 gave almost a similar pollutant removal efficiency as NaOH pretreatment. Hence, alkali pretreatment of RMWW by $Ca(OH)_2$ may be recommended in rice mills because it is cheaper than NaOH. The pollutant removal, biogas yield, and biomethane yield were analyzed under varying conditions of HRT and OLR. A long HRT and low OLR conditions

provided the maximum pollutant removal efficiency and biomethane yield. The reactor digestates were rich in macro and micronutrients essential for plant growth.

ACKNOWLEDGEMENT

REFERENCES

Agrawal, A.V., Chaudhari, P.K. and Ghosh, P., 2023. Effect of microwave treatment on maximizing biogas yield for anaerobic co-digestion of fruit and vegetable waste and anaerobic sludge. *Biomass Conversion and Biorefinery*, 84, pp. 1-13.

Ahmadi, M., Vahabzadeh, F., Bonakdarpour, B., Mehranian, M. and Mofarrah, E., 2006. Phenolic removal in olive oil mill wastewater using loofah-immobilized *Phanerochaete chrysosporium*. *World Journal of Microbiology and Biotechnology*, 22, pp.119-127.

Alderson, M.P., Santos, A.B.D. and Filho, C.R.M., 2015. Reliability analysis of low-cost, full-scale domestic wastewater treatment plants for reuse in aquaculture and agriculture. *Ecological Engineering*, 82, pp.6-14.

Annamalai, N. and Johnson, A., 2023. Analysis and forecasting of area under cultivation of rice in India: Univariate time series approach. *SN Computer Science*, 4(2), p.193.

Aralkar, S., Kshirsagar, R., Lande, V. and Agarkar, B., 2023. Exploring the nutritive sweetener liquid jaggery: Physicochemical characteristics and its application. *The Pharma Innovation Journal*, SP-12(12), pp.388-391.

Choudhary, M., Majumder, S. and Neogi, S., 2015. Studies on the treatment of rice mill effluent by electrocoagulation. *Separation Science and Technology*, 50(4), pp.505-511.

Chen, Y., Zhao, Z., Zou, H., Yang, H., Sun, T., Li, M. and Gu, L., 2019. Digestive performance of sludge with different crop straws in mesophilic anaerobic digestion. *Bioresource Technology*, 289, p.121595.

Central Pollution Control Board, 2008. Comprehensive Industry Document on Pulse, Wheat, and Rice Mills. Ministry of Environment, Forest, and Climate Change, Govt. of India Report, New Delhi, p.7

Costa, S., Dedola, D.G., Pellizzari, S., Blo, R., Rugiero, I., Pedrini, P. and Tamburini, E., 2017. Lignin biodegradation in pulp-and-paper mill wastewater by selected white rot fungi. *Water*, 9(12), p.935.

Devi, L.O., Gautam, P.K. and Sharma, I., 2023. Screening and identification of bacteria and fungus present in cow dung. *Journal of Survey in Fisheries Sciences*, 10(3), pp.111-119.

Dhanasekar, S. and Sasivarman, B., 2016. Evaluation of anaerobic digestor for treating paper mill wastewater. *Indian Journal of Science and Technology*, 9(23), pp.1-6.

Diksha, Kumar, R., Kumar, S., Kumari, A. and Panwar, A., 2023. Biodegradation of phenol-rich sewage water using indigenous bacterial consortium: A laboratory-to-plant scale study. *International Journal of Environmental Science and Technology*, pp.1-16.

De Angelis, K.M., Sharma, D., Varney, R., Simmons, B., Isern, N.G., Markillie, L.M. and Robinson, E.W., 2013. Evidence supporting dissimilatory and assimilatory lignin degradation in *Enterobacter lignolyticus* SCF1. *Frontiers in Microbiology*, 4, p.280.

Duan, Y., Yang, J., Song, Y., Chen, F., Li, X., Awasthi, M.K. and Zhang, L., 2021. Clean technology for biochar and organic waste recycling and utilization in apple orchards. *Chemosphere*, 274, p.129914.

El-Din, E., 2023. Tracking of phenol bioremediation by two marine eco-friendly Aspergillus terreus MHG30 (ON649683) and A. terreus MHG60 (ON649704) strains at optimum conditions. *Egyptian Journal of Aquatic Biology and Fisheries*, 27(4), pp. 579-595.

Giri, D. and Satyanarayan, S. 2015. Treatment of parboiled rice manufacturing wastewater using anaerobic fixed film fixed bed reactor packed with special media. *Int J Plant, Anim Environ Sci*, 5, pp. 87-93.

Godambe, T. and Fulekar, M.H., 2016. Cow dung bacteria offer an effective bioremediation for hydrocarbon-benzene. *International Journal of Biotech Trends and Technology*, 6(3), pp.13-22.

Haq, I. and Kalamdhad, A.S., 2023. Enhanced biodegradation of toxic pollutants from paper industry wastewater using *Pseudomonas sp*. immobilized in composite biocarriers and its toxicity evaluation. *Bioresource Technology Reports*, p.101674.

Hu, C., Yan, B., Wang, K.J. and Xiao, X.M., 2018. Modeling the performance of an anaerobic digestion reactor by the anaerobic digestion system model (ADSM). *Journal of Environmental Chemical Engineering*, 6(2), pp.2095-2104.

Hongwei, Y., Zhanpeng, J., Shaoqi, S. and Tang, W.Z., 2002. INT–dehydrogenase activity test for assessing anaerobic biodegradability of organic compounds. *Ecotoxicology and Environmental Safety*, 53(3), pp.416-421.

Kandagatla, N., Kunnoth, B., Sridhar, P., Tyagi, V., Rao, P.V. and Tyagi, R.D., 2023. Rice mill wastewater management in the era of circular economy. *Journal of Environmental Management*, 348, p.119248.

Kalantzis, D., Daskaloudis, I., Lacoere, T., Stasinakis, A.S., Lekkas, D.F., De Vrieze, J. and Fountoulakis, M.S., 2023. Granular activated carbon stimulates biogas production in pilot-scale anaerobic digester treating agro-industrial wastewater. *Bioresource Technology*, 376, p.128908.

Ke, Q., Zhang, Y., Wu, X., Su, X., Wang, Y., Lin, H. and Chen, J., 2018. Sustainable biodegradation of phenol by immobilized *Bacillus sp*. SAS19 with porous carbonaceous gels as carriers. *Journal of Environmental Management*, 222, pp.185-189.

Kesharwani, N. and Bajpai, S., 2020. Batch anaerobic co-digestion of food waste and sludge: A multi-criteria decision modeling (MCDM) approach. *SN Applied Sciences*, 2, pp.1-11.

Khan, S., Ahmad, R., Phulpoto, I.A., Kashif, M. and Shen, P., 2022. Effect of rice winery wastewater as a co-substrate to enhance anaerobic digestion of molasses for methane production. *Bioresource Technology Reports*, 18, p.101062.

Kumar, R., Singh, A., Maurya, A., Yadav, P., Yadav, A., Chowdhary, P. and Raj, A., 2022. Effective bioremediation of pulp and paper mill wastewater using *Bacillus cereus* as a possible kraft lignin-degrading bacterium. *Bioresource Technology*, 352, p.127076.

Kumar, S. and Deswal, S., 2021. A review of current techniques used in India for rice mill wastewater treatment and emerging techniques with valuable by-products. *Environmental Science and Pollution Research*, 28, pp.7652-7668.

Li, N., He, L., Lu, Y.Z., Zeng, R.J. and Sheng, G.P., 2017. The robust performance of a novel anaerobic biofilm membrane bioreactor with mesh filter and carbon fiber (ABMBR) for low to high-strength wastewater treatment. *Chemical Engineering Journal*, 313, pp.56-64.

Liu, X., Khalid, H., Amin, F.R., Ma, X., Li, X., Chen, C. and Liu, G., 2018. Effects of hydraulic retention time on anaerobic digestion performance of food waste to produce methane as a biofuel. *Environmental Technology & Innovation*, 11, pp.348–357.

Lourenco, V.A., Nadaleti, W.C., Vieira, B.M. and Chua, H., 2021. Methane production test of the anaerobic sludge from rice parboiling industries with the addition of biodiesel glycerol from rice bran oil in Brazil. *Renewable and Sustainable Energy Reviews*, 149, p.111331.

Mahgoub, S.A., Qattan, S.Y., Salem, S.S., Abdelbasit, H.M., Raafat, M., Ashkan, M.F. and Abd El-Fattah, H.I., 2023. Characterization and

biodegradation of phenol by *Pseudomonas aeruginosa* and *Klebsiella variicola* strains isolated from sewage sludge and their effect on soybean seeds germination. *Molecules*, 28(3), p.1203.

Mao, C., Feng, Y., Wang, X. and Ren, G., 2015. Review on research achievements of biogas from anaerobic digestion. *Renewable and Sustainable Energy Reviews*, 45, pp.540-555.

Masih, J.C., Mehta, S., Malik, K., Sindhu, S. and Anand, R.C., 2019. Enhancement of biogas production from cattle dung using additive. *Journal of Entomology and Zoology Studies*, 7(1), pp.1625-1630.

Munshi, S.K., Roy, J. and Noor, R., 2018. Microbiological investigation and determination of the antimicrobial potential of cow dung samples. *Stamford Journal of Microbiology*, 8(1), pp.34-37.

Naik, G.P., Poonia, A.K. and Chaudhari, P.K., 2022. Maximization of biogas by minimal microwave and alkaline pretreatment of rice straw. *Biomass Conversion and Biorefinery*, 75, pp.1-14.

Nain, K.S., Gupta, A. and Bedi, M., 2015. Performance evaluation of effluent treatment plant for rice industry: A case study of Aggarwal Agro-industry Ambala, Haryana. *Journal of Engineering Science and Innovative Technology (IJESIT)*, 4(5), pp.177–184.

Pradhan, A. and Sahu, S.K., 2004. Process details and effluent characteristics of a rice mill in the Sambalpur district of Orissa. *Journal of Industrial Pollution Control*, 20(1), pp.111-124.

Paddy Outlook - March 2023. USDA's Global rice production estimate in 2022/23. Available at: https://pjtsau.edu.in/files/AgriMkt/2023/March/Paddy-March-2023.pdf. (accessed on 23-12-2024)

Raychaudhuri, A., Sahoo, R.N. and Behera, M., 2023. Sequential anaerobic-aerobic treatment of rice mill wastewater and simultaneous power generation in microbial fuel cell. *Environmental Technology*, 44(21), pp.3176-3182.

Raychaudhuri, A. and Behera, M., 2020. Comparative evaluation of methanogenesis suppression methods in microbial fuel cell during rice mill wastewater treatment. *Environmental Technology & Innovation*, 17, p.100509.

Reddy, M.V., Yajima, Y., Choi, D. and Chang, Y.C., 2017. Biodegradation of toxic organic compounds using a newly isolated *Bacillus sp.* CYR2. *Biotechnology and Bioprocess Engineering*, 22, pp.339-346.

Saini, J.K., Saini, A. and Lohchab, R.K., 2016. Rice mill wastewater treatment by up-flow anaerobic sludge blanket reactor. *International Journal of Plant, Animal and Environmental Sciences*, 6, pp.128–134.

Sharma, B. and Singh, M., 2015. Isolation and characterization of bacteria from cow dung of desi cow breed on different morpho-biochemical parameters in Dehradun, Uttarakhand, India. *International Journal of Advanced Pharmacy, Biology and Chemistry*, 4(2), pp.276-281.

Sharifi-Rad, J., Painuli, S., Sener, B., Kılıç, M., Kumar, N.V., Semwal, P. and Calina, D., 2023. Revisiting the nutraceutical profile, chemical composition, and health benefits of jaggery: Updates from recent decade. *e Food*, 4(2), p.e75.

Singh, A., Kumar, R., Maurya, A., Chowdhary, P. and Raj, A., 2022. Isolation of functional ligninolytic Bacillus aryabhattai from paper mill sludge and its lignin degradation potential. *Biotechnology Reports*, 35, p.e00755.

Song, H., Liu, Y., Xu, W., Zeng, G., Aibibu, N., Xu, L. and Chen, B., 2009. Simultaneous Cr (VI) reduction and phenol degradation in pure cultures of *Pseudomonas aeruginosa* CCTCC AB91095. *Bioresource Technology*, 100(21), pp.5079-5084.

Stoilova, I., Krastanov, A., Stanchev, V., Daniel, D., Gerginova, M. and Alexieva, Z., 2006. Biodegradation of high amounts of phenol, catechol, 2, 4-dichlorophenol, and 2, 6-dimethoxyphenol by *Aspergillus awamori* cells. *Enzyme and Microbial Technology*, 39(5), pp.1036-1041.

Thirugnanasambandham, K., Sivakumar, V. and Maran, J.P., 2013. Application of chitosan as an adsorbent to treat rice mill wastewater: Mechanism, modeling, and optimization. *Carbohydrate Polymers*, 97(2), pp.451-457.

Tsegaye, D. and Leta, S., 2022. Optimization of operating parameters for biogas production using two-phase bench-scale anaerobic digestion of slaughterhouse wastewater: Focus on methanogenic step. *Bioresources and Bioprocessing*, 9(1), p.125.

Varshney, C.K., 2012. All India Rice Exporters Association Event. Available online at: (accessed 20.08.2023). http://www.airea.net/Events-Rice.

Veluchamy, C. and Kalamdhad, A.S., 2017. Influence of pretreatment techniques on anaerobic digestion of pulp and paper mill sludge: A review. *Bioresource Technology*, 245, pp.1206–1219.

Weng, C.K., Ismail, N. and Ahmad, A., 2014. Application of partial-mixed semi-continuous anaerobic reactor for treating palm oil mill effluent (POME) under mesophilic condition. *Iranica Journal of Energy and Environment*, 5, pp.209–217.

Xin, L., Guo, Z., Xiao, X., Xu, W., Geng, R. and Wang, W., 2018. Feasibility of anaerobic digestion for contaminated rice straw inoculated with waste activated sludge. *Bioresource Technology*, 266, pp.45–50.

Yadav, V.K., Gupta, N., Kumar, P., Dashti, M.G., Tirth, V., Khan, S.H. and Jeon, B.H., 2022. Recent advances in synthesis and degradation of lignin and lignin nanoparticles and their emerging applications in nanotechnology. *Materials*, 15(3), p.953.

Yuan, X., Wang, M., Park, C., Sahu, A.K. and Ergas, S.J., 2012. Microalgae growth using high-strength wastewater followed by anaerobic co-digestion. *Water Environment Research*, 84(5), pp. 396–404.

Yusrin, N.A., Nugroho, A. and Darmansyah, D., 2024. Analysis of rice's massive importing impact on poverty alleviation in Indonesia based on micro, macro, political, and international economics. In *Proceedings of the International Conference on Accounting and Finance*, pp.655-668.

Synergistic Impact of Sonophotocatalytic Degradation of Acephate Over Ag@CeO$_2$ Nanocomposite Catalysts

N. A. Deshmukh[1], P. D. Jolhe[2], S. Raut-Jadhav[3], S. P. Mardikar[4†] and M. P. Deosarkar[1]

[1]Department of Chemical Engineering, Sinhgad College of Engineering, Vadgaon, Pune, Maharashtra 411041, India

[2]Department of Biotechnology, Sinhgad College of Engineering, Vadgaon, Pune, Maharashtra 411041, India

[3]Department of Chemical Engineering, Bharati Vidyapeeth (Deemed to be University) College of Engineering, Dhankawadi, Pune 411043, India

[4]Smt. R.S College, Sant Gadge Baba Amravati University, Amravati, Maharashtra 444705, India

†Corresponding author: S. P. Mardikar; manik.deosarkar@vit.edu

ABSTRACT

Noble metal decorated metal oxide composites have proved to have Surface plasmon resonance (SPR) as a notable approach for efficient light absorption. Herein present work, a new sonochemical method is proposed for in-situ synthesis of noble metal-based CeO$_2$ composites for the sonophotocatalytic degradation of commercial Acephate solution. Pristine CeO$_2$ and Ag@CeO$_2$ with different Ag contents viz. 4, 6 and 8 wt. % were successfully synthesized by a facile in-situ sonochemical approach. The as-synthesized CeO$_2$ and Ag@CeO$_2$ nanocomposites were characterized by various physicochemical characterization techniques, including XRD, FTIR, UV-Vis spectroscopy, BET, and FESEM-EDS. Further, these CeO$_2$ and Ag@CeO$_2$ nanocomposites were employed for photocatalytic, sonocatalytic, and sonophotocatalytic degradation of commercial Acephate solution. Experimental results revealed that the photocatalytic and sonocatalytic processes follow a pseudo-first-order model, whereas the sonophotocatalytic process had a more substantial rate constant compared to the photocatalytic and sonocatalytic one. Further, the kinetics of the study were examined by the Langmuir-Hinshelwood model. Overall, the sonophotocatalytic degradation involving as-synthesized Ag@CeO$_2$ with 6 wt. % Ag content has shown to be the most effective method for the effective degradation of a commercial acephate solution.

INTRODUCTION

Organophosphorus pesticides (OPPs) are a class of substances that are often found in surface and groundwater from agro-industrial processes. OPPs are toxic and can bioaccumulate. Due to their hydrophobic and non-volatile nature, they are degraded mainly in the area of interface of cavitation bubbles. Acephate (AP) is a commercially available and water-soluble pesticide belonging to the phosphoramidothioate group of OPP insecticides that attaches to and inhibits the enzyme acetylcholinesterase (AChE) in blood and tissues of the nervous system. This results in an accumulation of the neurotransmitter acetylcholine, which repeatedly activates cholinergic receptors, causing weakness, miosis, and fasciculation of muscle, all of which can be fatal (Mota et al. 2023). Farmers rely on the use of acephate for crop protection because of its readily available and easily degradable nature, as well as its relatively high solubility (790 g.L^{-1}) (Raj et al. 2023). Acephate ($C_4H_{10}NO_3PS$) is a common foliar OPP. Acephate is well known for its anticholinesterase properties in insects and mammals. When plant-eating insects bite or suck plants with acephate, it attacks the insect's nervous system and kills it. However, acephate has high to severe acute oral toxicity or moderate inhalation toxicity for mammals (Singh et al. 2023). It harms the nervous system and respiratory tract, as well as causing eye and gastrointestinal disorders in people.

Fights insects on contact and stomach movement. As an organophosphate insecticide, acephate is readily soluble in water and absorbed by plants, helping to control insect predation. The environment is severely harmed by acephate toxicity, which impacts both target and non-target organisms. As with any pesticide, the proper application and adherence to recommended usage guidelines are essential to minimize adverse effects on non-target organisms and the ecosystem (Paunescu et al. 2022). Pesticides can occur as pollutants in water sources, and their toxicity, carcinogenicity, and mutagenicity can have adverse effects on human health or cause aesthetic problems such as taste and odor (Goswami et al. 2021).

Therefore, the effective methods for residual removal of acephate and its metabolites in the environment is an important research focus for environmental remediation. A literature survey shows that several researchers have employed different physicochemical/ biological methods for acephate degradation. For instance, A research employed microbial consortium for acephate degradation. The results demonstrated the potential of microbial consortium ZQ01 to degrade acephate in water as well as soil environments with a different and complementary acephate degradation pathway (Lin et al. 2022). In another report, a Sr/TiO$_2$-PCFM-based photocatalyst was employed for the photocatalytic degradation of acephate. The effects and mechanism of acephate photodegradation were investigated (Liu et al. 2019). In a work, green MCM-41/CO$_3$O$_4$ was synthesized from rice husk and peach leaves and utilized this photocatalyst for acephate removal. The results demonstrated 100% removal for 50 mg.L^{-1} of acephate within 40 min (AbuKhadra et al. 2020).

In recent years, there has been a focus on researching advanced oxidation processes (AOPs) to effectively break down harmful organic pollutants in water. Among the various AOPs commonly used ultrasound-mediated wastewater treatment has emerged as one of the most effective technologies (Berlan et al. 1994, Gogate, 2002). According to the first report on the effects of ultrasound irradiation on water in 1989, ultrasound irradiation generates cavities which, upon implosion, effectively degrade water using enormously reactive hydrogen (H$^\bullet$) and hydroxyl radicals (OH$^\bullet$) (Suslick 1989). Sonophotocatalysis uses ultrasonic irradiation to activate photocatalysis. Pollutants are degraded by sonophotocatalysis in two separate ways, namely mechanically and chemically. The mechanical properties of the ultrasound lead to consequences like surface cleaning, particle size reduction, and enhanced mass transfer. Cavitation is the result of tiny bubbles forming in a liquid during an acoustic wave's rarefaction cycle and then

violently collapsing during the wave's compression cycle. The chemical reaction that ultrasonic waves cause is what causes this phenomenon. One illustration of these effects is the dissociation of water into radicals. Pesticides are currently being photochemically treated on a commercial scale. However, not enough studies have been done on using sonophotocatalysis to treat wastewater that has been contaminated with acephate (Park 2009, Meshram et al. 2010).

Nowadays, the high surface-to-volume ratio and relatively small size of nanomaterials are attracting attention, and several technological applications are not feasible when related to bulk materials of the same chemical composition. By manipulating shape and size at the nanometer scale, materials with innovative applications can be designed and created. Nanomaterials have an extensive range of applications, including catalysis, sensors, antimicrobials, luminescent materials, and others, due to their exceptional physical, chemical, and optical features. The design and synthesis of NPs with specifically tailored structural features is a very difficult task in the field of nanoscience and nanotechnology. As a result, suitable synthetic methods are created to guarantee a consistent supply of these NPs in sufficient quantity (Abbasi et al. 2023). CeO$_2$ exhibits exceptional catalytic properties because of the reversible Ce^{3+}/Ce^{4+} couples and its high oxygen storage capacity with plenty of oxygen vacancies (V$_o$). These factors make CeO$_2$ an effective photocatalyst, and photo corrosion resistance. Only the UV can be absorbed by CeO$_2$, a semiconductor with a wide bandgap of about 2.8–3.1 eV. As such, there are restrictions on the application of CeO$_2$. A variety of techniques, including element doping, coupled semiconductors, solid-solution creation, noble metal deposition, and surface photosensitization, have been employed to increase the amount of visible light in CeO$_2$ (Ma et al. 2019, Meshram et al. 2017). It is well established that the practical use of CeO$_2$ is severely limited by its wide bandgap and frail absorption of visible light. Several researchers have preferentially chosen the modification of CeO$_2$ with noble metal (e.g., Au and Ag) nanoparticles to enhance its photoactivity. The enhanced photoactivity of novel metal-modified CeO$_2$ composites can be attributed to the extended light response range caused by to localized surface Plasmon resonance of novel metal nanoparticles (Vijaya et al. 2017, Nicoletti et al. 2013). Under visible light illumination, the novel metal-modified CeO$_2$ composites, direct photoinduced electron transfers from metal surfaces to the CeO$_2$ conduction band occur in anticipation of the Fermi level equilibrium. Reacting with dissolved O$_2$, the migrated e- may produce O$_2$$^{\bullet-}$ and other reactive radicals. The recombination of e$^-$-h$^+$ pairs was successfully

inhibited during photoreaction, improving the composite's photocatalytic performances (Zhou et al. 2012).

To find a practical means of improving the effectiveness of organic pollutants' ultrasonic-based degradation., herein we utilized the CeO$_2$ and Ag@CeO$_2$ coupled ultrasonic irradiation method. The goal of this study was to investigate the degradation of a commercial acephate solution by employing sonocatalysis, photocatalysis, and their combination, known as sonophotocatalysis. The focus was on understanding how key operating parameters influence degradation kinetics.

MATERIALS AND METHODS

For the experiment, the commercial formulation of acephate was purchased from Ravindra Agrochemicals, Pune. (Make: Tata Asataf 75% SP; Chemical name: O, S-dimethyl acetyl phosphoramidothioate; Molecular formula: C$_4$H$_{10}$NO$_3$PS, Molecular weight: 183.16 g.mol^{-1} and melting point 93°C white in color). Cerous nitrate hexahydrate [Ce(NO$_3$)$_3$.6H$_2$O] (purity 99%), Urea [NH$_2$.CO.NH$_2$] (99%), Tri-Sodium Citrate Dihydrate [Na$_3$C$_6$H$_5$O$_7$.2H$_2$O] was obtained from Vijay Chemicals Pune and was used as received. Distilled water was used throughout the experiment. A stock solution of acephate was prepared with a concentration of 1.5 g.L^{-1}; later, with proper dilution, various solutions with initial concentration were prepared for the actual experimental run.

Preparation of CeO$_2$ and Ag@CeO$_2$ Nanocomposites

In a typical synthesis process, a solution of 100 mL distilled water and 50 mL ethanol, 2.10 g citric acid, and 2.173 g cerous nitrate was added, and the solution was stirred for 15 min to make a homogeneous solution. This solution was treated as solution A. Further, this solution was heated to 60^{0}C, and to this solution, 100 ml aqueous solution of urea was added within 30 min under ultrasonic irradiation. After the complete addition of the urea solution, the resultant reaction mixture was ultrasonically treated for a further 3 h when the white precipitation was observed. Subsequently, the suspension mixture was centrifuged at 3000 rpm for 30 min. The collected products were washed with double distilled water and ethanol to eliminate impurities. The solid powder was then dried in a hot air oven at 80^{0}C for 24 hours. For the synthesis of Ag@CeO$_2$ samples, a certain amount of AgNO$_3$ along with cerous nitrate was taken during the preparation of Solution A, and the above process was repeated as is. The resulting CeO$_2$ and Ag@CeO$_2$ samples with different Ag contents (4, 6, and 8%) were labeled as PC, AC01, AC02, and AC03, respectively.

The chemical reaction taking place during synthesis is described below:-

Characterization

The products were analyzed for phase purity utilizing an automated X-ray powder diffractometer (XRD, PANalytical

$$H_2N\text{-}CO\text{-}NH_2 \; + \; H_2O \quad \xrightarrow{\text{mixing}} \quad NH_4^+ \; + \; OCN^-$$

Urea   Distilled water   Ammonium   Cyanate   ---------------(Solution A)

$$Ce(NO_3)_3.\,6H_2O \; + \; OH^- \; + \; 2H^+ \quad \xrightarrow{\text{mixing}} \quad Ce^{3+} + 3NO_3^- \; + 6H_2O$$

Cerium nitrate Hexahydrate   Ethanol   Citric acid

$$OCN^- \; + \; OH^- \; + \; 2H^+ \; + \; H_2O \quad \xrightarrow{\text{mixing}} \quad NH_3 \; + \; CO_3^{2-}$$

Ethanol   Citric acid   Distilled Water   Ammonia   Carbonate ion

----

$$2[Ce^{3+}] \; + \; 3\,CO_3^{2-} \quad \xrightarrow{\text{Sonication}} \quad CeO_2(CO_3).H_2O \; + \; CO_2 \; + \; (n\text{-}1)\,H_2O$$

Cerium nitrate   Carbonate ion   Complex Compound

$$Ce^{3+} + 3\,H_2O \quad \xrightarrow{\text{Sonication}} \quad Ce(OH)_3 + 3H^{3+}$$

Cerium Oxide

$$Ce(OH)_3 + OH^- + H_2O \quad \xrightarrow{\text{Washing}} \quad CeO_2$$

Empyrean) with Cu Ka radiation source (k = 0.15406 nm). The surface morphology, particle size, and composition of the photocatalysts were investigated using a Fourier scanning electron microscope (FE-SEM, HITACHI S4800 combined with EDX). BET-specific surface areas of the samples were determined using Brunauer Emmett Teller (BET) surface area analyzer (NOVA 2200e Quantachrome, USA) using nitrogen as a purge gas. The UV-Vis absorption spectra were measured using a UV–Vis spectrophotometer (UV-1800 Shimadzu), (Bruker Alpha-II) FTIR spectrophotometer was used for spectra measurement.

Photocatalytic, Sonocatalytic and Sonophotocatalytic Activity

In the present study, the degradation of Acephate as a model pesticide pollutant was investigated in the presence of pristine CeO_2 and $Ag@CeO_2$ composites through photocatalysis, sonocatalysis separately, and simultaneously viz. Sonophotocatalysis. The experimental setup used in this work is schematically illustrated in Fig. 1. The experimental setup manufactured by Johnson Plastosonic Pvt. Ltd., India, includes a 20 kHz low-frequency ultrasonic processor and 500 W power a quartz reactor with two UV tubes (8 W each), a temperature indicator, a wooden shield, and a cooling jacket with a capacity of 250 mL. During experiments based on sonocatalytic and sonophotocatalytic processes, the 13 mm ultrasonic probe tip was submerged in a 2 cm-deep acephate aqueous solution except for the photocatalytic process. The reactor's reaction temperature was maintained at 30±2°C by circulating cold water through a cooling jacket. To make sure that dangerous UV rays were blocked, a wooden cabinet was used. During all the experiments, the temperature and volume of the solution were held constant at 30±2°C and 250 mL, respectively. The pH of the solution was adjusted to the appropriate amount by adding 0.1 N NaOH and 0.1 N HCL wherever necessary. An ultrasonic horn with a time scale of 6 s on and 4 s off was used to perform sonication for 60 minutes of treatment time. Better temperature control was achieved by using the ultrasonic horn's pulsed (on/off) mode, which extends the time for heat dispersion. During experimentation, a stock solution of 1.5 g.L^{-1} with a natural pH of 5.5 was prepared freshly to perform the experiments. The same concentration of solution is used throughout the experiment. For degradation studies of aqueous acephate solutions. The ultrasound power in ultrasonication was adjusted at 100 W. CeO_2 and $Ag@CeO_2$ catalysts were used in the present study. During degradation experiments the effect of pH, initial acephate concentration, and catalyst loading were investigated in ultrasound, UV environment, and in combined ultrasound plus UV environment. A 10 mL sample at a regulated interval of 10 min was taken to analyze the degradation progress. A sample was taken using a pipette at different time intervals, and the sample was then subjected to UV analysis after centrifuge. The % degradation was determined by using the following formula:

% Degradation = 100 × (C_0 - C)/C_0, where C_0 = initial concentration of acephate solution, C = concentration of acephate solution after ultrasound irradiation (Hannachi et al. 2023).

The analysis of the reproducibility of the data reported involved conducting tests at least twice and presenting the

Fig. 1: Schematic diagram of reactor used for acephate degradation.

mean in the discussion of the standard experimental errors, which were found to be 2%.

RESULTS AND DISCUSSION

Structural Characterization of Pristine CeO_2 and Ag@CeO_2 Composites

XRD analysis: Powder XRD analysis was used to examine the crystal structure, phase purity, and crystallite size of the as-synthesized pristine and Ag@CeO_2 composites. The XRD patterns of as-synthesized pristine and Ag@CeO_2 composites are shown in Fig. 2. The X-ray diffraction pattern of pure CeO_2 (sample PC) shown in Fig. 2 displays peaks at angles of 28.95, 33.18, 47.84, 56.65, 59.58, and 69.82, corresponding to the (1 1 1), (2 0 0), (2 2 0), (3 1 1), (2 2 2), and (4 0 0) planes of the face-centered cubic structure of CeO_2. These findings are consistent with existing literature (Sun et al. 2004). Further, for all Ag@CeO_2 samples viz. AC01, AC02, and AC03, The diffraction peaks of FCC CeO2 are visible along with additional peaks that appear at 38.14, 64.18, and 78.24 with (h k l) values of (1 1 1), (2 2 0), and (3 1 1) crystal planes of Ag NPs corresponding to face-centered cubic elemental silver (Ag^0) (Batool et al. 2019). Other than these, no additional impurity peaks were seen in the XRD spectra of the CeO_2 and Ag@CeO_2 samples, demonstrating the as-synthesized samples' purity. Additionally, the broad reflection peaks indicate that the crystal size is small, likely in the nanoscale range.

FTIR analysis: FTIR is a technique for obtaining a spectrum of infrared rays of absorption or emission from a solid, liquid, or gas. The FT-IR spectra of the Ag-modified CeO_2 and pristine CeO_2 are displayed in Fig. 3. A range of 500 to 4000 cm^{-1} was observed in the FT-IR spectra. The peaks are obtained due to the stretching of various chemical bonds within the cerium oxide (Fudala et al. 2022).

The standard Infrared position of different bond-vibrations provides information about the type and nature of the bond. The O-H bond stretching appears at 3362 cm^{-1}, the C-H bond stretching can be seen by the peak at 1546.68 cm^{-1}, the C-C bond stretching is represented by the peak at 1109.94 cm^{-1}, and the C-O bonding is located at 849 cm^{-1}. The O-H bond vibrations in the H_2O molecule and the Ce-O-Ce bond vibrations are primarily responsible for these stretching (Cam et al. 2022). Peak 3918 cm^{-1} corresponds to the stretching of the O-H bond; peak 2211 cm^{-1} shows the stretching of the C-H bond; peak 1121 cm^{-1} corresponds to the stretch of the C-C bond; and peak 853 cm^{-1} corresponds to the stretching of the C-O bond. This stretching is mostly caused by the vibrations of the O-H bonds in the H_2O molecule and the Ce-O-Ce bond. 627 cm^{-1} is attributed to Ag bonds (Mei et al. 2022) (Hannachi et al. 2023).

FESEM-EDX analysis: The morphological analysis of as-synthesized CeO_2 and Ag@CeO_2 composites was conducted using the FESEM technique, and the results are depicted in Fig. 4 (a-d).

The results reveal that pristine CeO_2 (sample PC) exhibits agglomerated nanoparticles-like morphology. However, distinct changes in the morphology can be observed for Ag-modified CeO_2 samples. For samples AC01, AC02, and AC03, the morphology varies from agglomerated nanoparticles to vesicular nanosheets with Ag nanoparticles decorated on these sheets. More detailed insights on the morphology of as-synthesized Ag@CeO_2 nanocomposites were obtained by analyzing a representative 6 wt.% Ag@

Fig. 2: XRD spectra of as-synthesized pristine and Ag@CeO_2 with different Ag contents.

Fig. 3: FT-IR spectra of as-synthesized pristine & Ag@CeO$_2$ with different Ag contents.

Fig. 4. (a-d): FESEM images of Pristine CeO$_2$ and Ag@CeO$_2$ nanocomposites.

CeO$_2$ sample (AC02) by EDS elemental mapping and the corresponding results are depicted in Fig. 4 (e-i). The results revealed that Ag^0 nanoparticles are evenly distributed over the vesicular morphology of CeO$_2$. The as-synthesized sample contains only Ce, Ag and O, which further represents the as-synthesized sample is free of any impurity, which further supports the XRD results.

Electronic Structure and Redox Properties

The surface area of as-synthesized pristine CeO$_2$ and a representative 6 wt. % Ag@CeO$_2$ composite were further characterized by N$_2$ adsorption-desorption isotherm and the pore size distribution analysis of Barret-Joyner-Halenda (BJH) was studied at 77 K, and the findings are shown in Fig. 5, the samples PC and AC02 both display a typical BET isotherm with a type-IV hysteresis loop, indicating that the AgCeO$_2$ composite is mesoporous in both pristine forms. Remarkably, Ag@CeO$_2$ composite material has a specific surface area of 81.25 m^2.g^{-1}, which is higher than that of as-synthesised pristine CeO$_2$ NPs (67.5 m^2.g^{-1}), which is very later to the previously published literature (Sun et al. 2004), which indicates that the introduction of Ag enhanced the surface area of CeO$_2$ particle. Consequently, the average pore diameter of the CeO$_2$ sample (PC) viz. 15.09 nm was reduced in the presence of Ag, and the pore diameter was 11 nm (Negi et al. 2018).

The UV-vis spectra of pure CeO$_2$ and Ag@CeO$_2$ with different Ag concentrations are depicted in Fig. 6 (a-d) and show well-resolved absorption bands with peaks at 310 and 412 nm.

Fig. 4. (e-i): EDS-elemental mapping of a representative 6 wt. % Ag@CeO₂ (AC02) sample.

Fig. 5: N₂ adsorption-desorption isotherm of pristine CeO₂ synthesized and a representative 6 wt. % Ag@CeO₂ composites.

These bands are ascribed to an O_2-Ce^{4+} charge transfer transition as well as an interband transition (Bechambi et al. 2015). It is important to note that the CeO₂ spectrum exhibits a weak band originating from the O_2-to-Ce^{3+} charge transfer transition. However, based only on UV-vis spectra, the presence of Ce^{3+} species cannot be ruled out due to the wide bandwidths and potential overlap with a band characteristic of an interband transition (Hannachi et al. 2023, Munirathnam et al. 2023).

TAUC'S PLOTS

Using Tauc's method, the band gap energy was calculated (Chahal et al. 2022, Mishra & Ahmaruzzaman 2021). According to Tauc's approach, the absorption coefficient α, which is dependent on energy, can be inferred using the following formula. The formula is $(\alpha h \nu)n = K (h\nu - Eg)$, where h stands for Planck's constant, ν for photon frequency, K stands for a constant, and Eg is band gap energy. Two types of components, n, are distinguished: ½ for indirect

Fig. 6(a-d): UV-visible absorption spectra of as-synthesized pristine CeO_2 and $Ag@CeO_2$ samples.

Fig. 7 (a – d): Tauc's plots of as-synthesized pristine CeO_2 and $Ag@CeO_2$ samples.

band gaps and 2 for direct band gaps. Many times, diffuse reflectance spectra are used to determine the band gap energy (Meng et al. 2017).

The absorption spectrum of pure CeO_2 and CeO_2 doped with $AgNO_3$ at different concentrations (a direct band-gap semiconductor) is plotted against photon energy in Fig. 6 (a-

d). The spectrum is equation-transformed. There is a strong linear increase in light absorption in semiconductor materials as energy increases. The band gap energy is predicted by the x-intercept of the linear fit of the Tauc plot (D'Angelo et al. 2014, Makuła et al. 2018).

Cerium oxide has a direct band gap, as can be seen from Fig. 7 (a-d), which indicates a continuous steep rise in the graph and supports the accuracy of the band gap estimate. As a result, the factor n is the right value of 2. It can also be stated that upon retracing the linear line k, the x-axis representing the energy band gap value, crosses the line at 2.70 eV to 3.2 eV for CeO$_2$ nanoparticles, 2.64 eV for AC01, 2.61 eV for AC02, and 2.53 eV for AC03. The value of cerium oxide and Ag@CeO$_2$ samples ranges from 2.5 eV to 3.2 Ev (Yang et al. 2022).

Photocatalytic, Sonocatalytic, and Sonophotocatalytic Activities

The photocatalytic, sonocatalytic, and sonophotocatalytic efficiencies of pure CeO$_2$ and Ag@CeO$_2$ were measured using acephate pesticide as the test contaminant in a series of experiments. The degradation profiles of the acephate pesticide under solar radiation, photocatalyzed by pristine

CeO$_2$ and Ag@CeO$_2$ with different Ag concentrations, are depicted in Fig. 8. There was very little reduction in the concentration of acephate pesticide even after 60 minutes of exposure to the photocatalyst. Furthermore, compared to CeO$_2$ and Ag@CeO$_2$ catalysts, 6 wt. % Ag@CeO$_2$ (sample AC02) nanocomposites exhibited best photocatalytic activity. Acephate pesticide had a photocatalytic removal efficiency of only 46.76% and 77.55% when no catalyst or pristine CeO$_2$ was used. Compared to pristine CeO$_2$, Ag-modified CeO$_2$ samples increased degradation efficiency of 82.55%, 85.75%, and 83.40% for AC01, AC02, and AC03, respectively. When the Ag content was increased further, the degradation efficiency declined once the highest value reached 85.75% for AC02. The incorporation of Ag into CeO$_2$ is pivotal to the Ag@CeO$_2$ composites' photocatalytic performance, as suggested by these results (Ahmad et al. 2014).

Photocatalytic, Sonocatalytic, and Sonophotocatalytic Apparent Reaction Rate Constant

Regarding the acephate concentration, Pseudo-first order kinetics were observed in eq.1 the photocatalytic degradation of acephate by Ag@CeO$_2$ nanocomposites under UV light:

Fig. 8: Photocatalytic, sonocatalytic, and sonophotocatalytic degradation of Acephate in the presence of as-synthesized pristine CeO$_2$ and Ag@CeO$_2$ composites (Samples PC, AC01, AC02, and AC03).

$$\ln\frac{C_0}{C} = k_{photo} * t \qquad ...(1)$$

Where K_{photo}, a fundamental kinetic parameter for a variety of photocatalysts, is the photocatalytic reaction rate constant, where C represents the bulk solution's concentration at the reaction time and $[C_0]$ is the initial concentration in the bulk solution (Daneshvar et al. 2007, Janos et al. 2014). The linear fitting of ln (C_0/C) vs. t could be used to determine the apparent reaction rate constants. The results of an investigation into the reaction rate constant for several catalysts are given in Fig. 9 (Konstantinou & Albanis 2004).

According to the findings, K_{photo} was enhanced by adding Ag at various concentrations. Due to the strong coupling of CeO_2 and Ag at different concentrations, the nanocomposites have a significant amount of photocatalytic activity (Saquib & Muneer 2003, Li et al. 2013).

Regression coefficients and the highest rate constant measured at Pristine CeO_2 and Ag@CeO_2 are listed in Table 1. The rate constant increased from 2.24 to 2.71 min^{-1} with a corresponding change in catalyst amount. An increase in the catalyst's accessible active sites causes a rise in cavitational activity, which explains the positive effects of solid loading that have been observed (Salerno et al. 2017).

An increase in the catalyst's concentration leads to a higher hydroxyl radical formation, which in turn increases the catalyst's active site and reaction rate. However, if more was added, the suspension would become more opaque, reducing the amount of light present throughout the solution as more pesticide molecules start to break down (Kinetic).

The process of photoexciting electrons from the valence band into the conduction band of a wide band gap semiconductor photocatalyst is known as photocatalysis. This results in the creation of a positive hole in the valence band (Ahmad et al. 2013, Li et al. 2008). To reduce or eliminate contaminating molecules, the as-formed charge carriers (holes and electrons) at the catalyst surface start redox processes in the adsorbed molecules before the exciton is destroyed. Pristine CeO_2 and CeO_2 doped with $AgNO_3$ at varying concentrations were used in a Langmuir-Hinshelwood kinetic model. It has been established that the Langmuir-Hinshelwood relationship holds for initial rates of deterioration. Use the following eq.2, which

Fig. 9: Photocatalytic, sonocatalytic, and sonophotocatalytic apparent reaction rate constant in the presence of as-synthesized pristine CeO_2 and Ag@CeO_2 composites (Samples PC, AC01, AC02, and AC03).

Table 1: Reaction rate constant, regression coefficient, and Langmuir-Hinshelwood constant for various photocatalysts.

Sample	K$_{obs}$	K$_{obs}$ *100 (min^{-1})	R^2	K$_{LH}$
PC	0.022	2.24	0.937	0.065
AC01	0.0290	2.90	0.952	0.0130
AC02	0.0298	2.98	0.954	0.0500
AC03	0.271	2.71	0.987	0.0453

is displayed in Table 2 and Table 3, to determine the Hinshelwood constant (Meng et al. 2017).

$$\frac{1}{kobs} = \frac{1}{k_c\,K_{LH}} + \frac{[c_0]}{k_c} \qquad …(2)$$

Regarding the degradation of pollutants in wastewater through photocatalysis, sonocatalysis is a promising substitute. The impact of ultrasonic radiation on the acephate degradation process by Pristine

CeO$_2$ and CeO$_2$ doped with AgNO$_3$ varying concentrations were investigated and illustrated in Fig. 8b

The degradation of acephate pesticide by ultrasound, PC, AC01, AC02, and AC03 nanocomposites without catalyst and other methods were compared. It is found that AC02 degrades acephate pesticide

the most under ultrasonic irradiation for 60 minutes (82.58%). In contrast, acephate pesticides degraded 45.68%, 74.52%, 80.13%, and 79.60% under ultrasonic irradiation alone, without catalyst, PC, and AC01. Regarding the concentration of acephate pesticide, the sonocatalytic degradation of the pesticide by the Ag@CeO$_2$ nanocomposites followed eq.3 pseudo-first-order kinetics.

$$\ln\frac{C_0}{C} = k_{sono} * t \qquad …(3)$$

Based on the various catalysts exposed to ultrasonic irradiation, the reaction rate constant for sonocatalysis (K$_{sono}$) was calculated and is displayed in Fig. 9b. The highest rate constant was measured at Pristine CeO$_2$ and Ag@CeO$_2$ at different Ag concentrations. Regression coefficients and the Hinshelwood constant are listed in Table 2, and the rate constant increased from 2.62 to 3.13 min^{-1}. The findings demonstrate that the addition of CeO$_2$ doped with AgNO$_3$ enhanced K$_{sono}$. When catalyst and PC were not present, the

degradation of acephate pesticide happened more slowly than when AC01, AC02, and AC03 nanocomposites were present.

Numerous articles have described the sonocatalytic degradation of acephate insecticides in the presence of various catalysts. Numerous articles have described the sonocatalytic degradation of acephate insecticides in the presence of various catalysts. Numerous articles have described the sonocatalytic degradation of acephate insecticides in the presence of various catalysts. The process requires OH$^-$ for pesticide oxidation, which can be elucidated by the widely recognized hot spots and sonoluminescence mechanism (Rad et al. 2023). The solution may initially experience hot spots because of heterogeneous bubble nucleation, which produces cavitation bubbles.

These hot spots may pyrolyze H$_2$O molecules, resulting in the production of OH$^-$. Moreover, photocatalysts are created during sonication when catalyst particles are activated by UV light-induced sonoluminescence. When sonolysis is used as a solvent inside collapsing cavitation bubbles at extremely high temperatures, organic compounds are typically broken down by sonochemical processes (Mosleh & Rahimi 2017). When using a catalyst, electron-hole pairs are formed by the combination of ultrasonic irradiation and the catalyst, in addition to causing sonolysis of water. Pesticides can be broken down by electron-hole pairs into CO$_2$, H$_2$O, and inorganic species by producing OH$^-$ radicals and superoxide anions O$_2$. Furthermore, because of the high charge separation efficiency made possible by PC's synergistic effect and the absence of a catalyst. The catalytic activity of CeO$_2$ doped with AgNO$_3$ nanocomposites is significantly improved when compared to that of PC. Acephate pesticide was degraded more efficiently by CeO$_2$ doped with AgNO$_3$ nanocomposites than by PC and without a catalyst. Because AgNO$_3$ accepts electrons from

Table 2: Langmuir-Hinshelwood constant, regression coefficient, and reaction rate constant for sonocatalytic degradation of different photocatalysts.

Sample	K$_{obs}$	K$_{obs}$ *100 (min^{-1})	R^2	K$_{LH}$
PC	0.026	2.62	0.971	0.064
AC01	0.03030	3.03	0.967	0.0477
AC02	0.0337	3.37	0.957	0.0544
AC03	0.0313	3.13	0.971	0.0432

CeO_2, it significantly lowers charge carrier recombination, which boosts catalytic activity (Mena et al. 2017).

Using simultaneous ultrasonic and UV irradiation, acephate degradation was achieved in subsequent studies. Nanocomposites containing Pristine CeO_2 and CeO_2 doped with $AgNO_3$ at varying concentrations were investigated. Fig. 8(C) illustrates the variations in the concentration of acephate pesticide over time at different loadings and initial concentrations (Co) during sonophotocatalysis.

The sonophotocatalytic removal efficiency of acephate pesticide without catalyst and CeO_2 was only 48.76% and 84.70%. By contrast, the introduction of Ag increased the degradation efficiency by 85.60%, 90.50%, and 89.10% for AC01, AC02, and AC03, respectively. The degradation efficiency decreased as the Ag content increased after

reaching a maximum value of 90.50 percent for AC02. These findings imply that a major factor influencing the sonophotocatalytic activity of $Ag@CeO_2$ composites is the optimum amount of Ag introduction.

Sonophotocatalysis also appears to have a pseudo-first-order kinetic expression in eq.4, similar to photocatalysis and sonocatalysis.

$$\ln\frac{c_0}{c} = k_{sonophoto} * t \qquad \ldots(4)$$

The apparent sonophotocatalysis response rate constants ($K_{sonophoto}$) as shown in Fig. 9c. Sonophotocatalytic degradation usually proceeds more quickly than individual process degradation under comparable operating conditions. With a corresponding change in catalyst quantity, the rate constant increased from 3.30 to 3.56 min^{-1}. Furthermore,

Table 3: Langmuir-Hinshelwood constant, regression coefficient, and reaction rate constant of sonophotocatalytic degradation of different photocatalysts.

Sample	K_{obs}	$K_{obs}*100$ (min^{-1})	R^2	K_{LH}
PC	0.033	3.30	0.974	0.0792
AC01	0.0327	3.278	0.970	0.0502
AC02	0.0381	3.82	0.988	0.0716
AC03	0.0356	3.56	0.9871	0.0599

Table 4. The hybrid system's synergy index and the different photocatalyst treatment techniques.

Sample	K_{sono} (min^{-1})	K_{photo} (min^{-1})	$K_{sonophoto}$ (min^{-1})	Synergy index
PC	2.24	2.62	3.3	1.83
AC01	2.9	3.03	3.278	1.47
AC02	2.98	3.37	3.82	2.16
AC03	2.71	3.13	3.56	1.92

Fig. 10: Recycle photocatalytic, sonocatalytic, and sonophotocatalytic degradation performance of AC02 nanocomposite.

it seems that the combination of ultrasound and UV irradiation works in concert with Pristine CeO$_2$ and Ag@CeO$_2$ nanocomposites at different concentrations because K$_{sonophoto}$ > K$_{photo}$ > K$_{sono}$, the sum of the rate constants for each individual process is less than the total reaction rate constant. Several factors contribute to the benefit of combining photocatalysis and sonolysis, such as (i) higher radical production in the reaction mixture when hydroxyl groups are present. (ii) enhanced organic mass transfer between the catalyst surface and the liquid phase, (iii) ultrasonic luminescence-induced catalyst excitation (Daneshvar et al. 2007), and (iv) Catalyst particle fragmentation caused by ultrasound increases catalytic activity. It can be demonstrated that, in similar experimental conditions, sonophotocatalytic degradation proceeds far more quickly than individual sono and photocatalytic degradation.

To evaluate the pesticide degradation process's viability using sonophotocatalysis, the synergistic index was determined by dividing the sonophotocatalytic rate constant by the sum of the rate constants for the photocatalysis and sonocatalysis processes in the Sono and UV (eq. 5).

$$\text{Synergistic Index} = \frac{Ksonophoto - (Ksono + Kphoto)}{Ksonophoto} \quad \text{...(5)}$$

The process appeared to increase efficiency based on synergistic effect values greater than one. The efficiency gains from various processes were evaluated, and the results showed that the hybrid system performs better than the individual processes (Table 4). This may have something to do with the way ultrasonic waves (cavitation phenomena) affect the disaggregation of photocatalyst particles. The interfacial surface area was renewed as a result of these processes, improving mass transfer (Ahmed & Mohamed 2023).

AC02 nanocomposite's stability as a catalyst under ultrasonic and solar radiation, as well as when both are used together, was also investigated (Fig. 10). After five cycles of degradation testing, the composite's photocatalytic and sonocatalytic activity did not significantly decrease, indicating that it was reasonably stable under the conditions used in this investigation (Ahmed & Mohamed 2023), (Talukdar et al. 2021).

CONCLUSION

The current study uses different types of CeO$_2$, such as Pristine CeO$_2$ and Ag-modified CeO$_2$, at different concentrations to demonstrate the effectiveness of sonocatalytic, photocatalytic, and sonophotocatalytic oxidation of acephate pesticide solution. A pH of 11 and an initial pesticide solution concentration of 10 ppm were found to be the ideal parameters for the various approaches based on UV and US irradiation. The studies, including catalysts in the sonophotocatalytic oxidation techniques, demonstrated the beneficial role that each catalyst played in the pesticide acephate's breakdown. The experimental results showed that, in photocatalysis, the removal efficiency decreased with increasing Ag content beyond 6%. Without a catalyst, the values were only 46.76% and 77.55%. For AC02, the maximum value was reached at 85.75%. When using sonocatalysis, AC02 has been shown to degrade acephate pesticide the most (82.58%). In contrast, when PC, AC01, AC03, and ultrasonic irradiation were used alone, the percentages of degradation were 45.68%, 74.52%, 80.13%, and 79.60%, respectively. Pristine CeO$_2$ and acephate pesticide had an 84.70% and 48.76% sonophotocatalytic removal efficiency, respectively, without catalyst. Once the AC02 value has reached its maximum of 90.50%. This may be brought on by more reactive radicals being produced and a greater electron-hole gap at the hetero-interface. Consequently, the pristine CeO$_2$ and Ag@CeO$_2$. Composites are excellent choices for application in a range of environmental difficulties. It has been demonstrated that the best technique for figuring out the percentage of degradation of a commercial acephate solution is to use 6 wt. % Ag@CeO$_2$ by using the sonophotocatalytic (hybrid) method. As compared to the recent literature survey hybrid method is the most efficient technique by using 6 wt. % Ag@CeO$_2$ reached 90.50 % for degradation of acephate. The highest degradation of acephate by 6 wt. % Ag@CeO$_2$ has been reported. Even after five regeneration cycles, the majority of OPPs still have removal efficiencies above 85%. Furthermore, by looking at potential sustainable management plans and corrective actions, we hope to highlight the contamination aspects of acephate, a newly discovered OPP that is commonly utilized in plantations.

REFERENCES

Abbasi, R., Shineh, G. and Mobaraki, M., 2023. Structural parameters of nanoparticles affecting their toxicity for biomedical applications: a review. *Journal of Nanoparticle Research*, 25(3), p.43.

AbuKhadra, M.R., Mohamed, A.S., El-Sherbeeny, A.M. and Elmeligy, M.A., 2020. Enhanced photocatalytic degradation of acephate pesticide over MCM-41/Co3O4 nanocomposite synthesized from rice husk silica gel and Peach leaves. *Journal of Hazardous Materials*, 389, p.122129.

Ahmad, M., Ahmed, E. and Hong, Z., 2014. Photocatalytic, sonocatalytic, and sonophotocatalytic degradation of Rhodamine B using ZnO/CNTs composites photocatalysts. *Ultrasonics Sonochemistry*, 21, pp.761–773.

Ahmad, M., Ahmed, E. and Zhang, Y., 2013. Preparation of highly efficient Al-doped ZnO photocatalyst by combustion synthesis. *Current Applied Physics*, 13, pp.697–704.

Ahmed, M.A. and Mohamed, A.A.J.I., 2023. Advances in ultrasound-assisted synthesis of photocatalysts and sonophotocatalytic processes: A review. *iScience*, 27, p.108583.

Batool, S., Hussain, Z. and Niazi, M.B.K., 2019. Biogenic synthesis of silver nanoparticles and evaluation of physical and antimicrobial properties of Ag/PVA/starch nanocomposites hydrogel membranes for wound dressing application. *Journal of Drug Delivery Science and Technology*, 52, pp.403–414.

Bechambi, O., Touati, A., Sayadi, S. and Najjar, W., 2015. Effect of cerium doping on the textural, structural and optical properties of zinc oxide: role of cerium and hydrogen peroxide to enhance the photocatalytic degradation of endocrine disrupting compounds. *Materials Science in Semiconductor Processing*, 39, pp.807–816.

Berlan, J., Trabelsi, F., Delmas, H., Wilhelm, A.M. and Petrignani, J.F., 1994. Oxidative degradation of phenol in aqueous media using ultrasound. *Ultrasonics Sonochemistry*, 1(2), pp.S97–S102.

Cam, T.S., Omarov, S.O., Chebanenko, M.I., Izotova, S.G. and Popkov, V.I., 2022. Recent progress in the synthesis of CeO2-based nanocatalysts towards efficient oxidation of CO. *Journal of Science: Advanced Materials and Devices*, 7(1), p.100399.

Chahal, S., Phor, L., Singh, S., Singh, A., Malik, J., Goel, P., Kumar, A., Kumar, S. and Kumar, P., 2022. An efficient and unique method for the growth of spindle-shaped Mg-doped cerium oxide nanorods for photodegradation of p-Nitrophenol. *Ceramics International*, 48(19), pp.28961–28968.

D'Angelo, A.M., Webster, N.A. and Chaffee, A.L., 2014. Characterisation of the phase-transformation behaviour of Ce2O(CO3)2·H2O clusters synthesised from Ce(NO3)3·6H2O and urea. *Powder Diffraction*, 29(S1), pp.S84–S88.

Daneshvar, N., Aber, S., Dorraji, M.S., Khataee, A.R. and Rasoulifard, M.H., 2007. Photocatalytic degradation of the insecticide diazinon in the presence of prepared nanocrystalline ZnO powders under irradiation of UV-C light. *Separation and Purification Technology*, 58(1), pp.91–98.

Fudala, A.S., Salih, W.M. and Alkazaz, F.F., 2022. Synthesis of different sizes of cerium oxide CeO2 nanoparticles by using different concentrations of precursor via sol-gel method. *Materials Today: Proceedings*, 49, pp.2786–2792.

Gogate, P.R., 2002. Cavitation: an auxiliary technique in wastewater treatment schemes. *Advances in Environmental Research*, 6(3), pp.335–358.

Goswami, J., Banjare, M.K., Banjare, R.K., Rai, J.K. and Rai, M.K., 2021. Extraction of acephate pesticide in environmental and agricultural samples by spectrophotometric method. *Journal of the Indian Chemical Society*, 98(9), p.100138.

Hannachi, E., Slimani, Y., Nawaz, M., Sivakumar, R., Trabelsi, Z., Vignesh, R., Akhtar, S., Almessiere, M.A., Baykal, A. and Yasin, G., 2023. Preparation of cerium and yttrium doped ZnO nanoparticles and tracking their structural, optical, and photocatalytic performances. *Journal of Rare Earths*, 41(5), pp.682–688.

Janos, P., Kuran, P., Kormunda, M., Stengl, V., Grygar, T.M., Dosek, M., Stastny, M., Ederer, J., Pilarova, V. and Vrtoch, L., 2014. Cerium dioxide is a new reactive sorbent for fast degradation of parathion methyl and some other organophosphates. *Journal of Rare Earths*, 32(4), pp.360–370.

Kinetic L-H., 2012. Expression for the Photocatalytic Degradation of Metanil Yellow Aqueous Solutions by ZnO Catalyst. *Chemical Sciences Journal*, (CSJ-85), pp.1–8.

Konstantinou, I.K. and Albanis, T.A., 2004. TiO2-assisted photocatalytic degradation of azo dyes in aqueous solution: kinetic and mechanistic investigations: a review. *Applied Catalysis B: Environmental*, 49(1), pp.1–14.

Li, M., Hong, Z., Fang, Y. and Huang, F., 2008. Synergistic effect of two surface complexes in enhancing visible-light photocatalytic activity of titanium dioxide. *Materials Research Bulletin*, 43(8–9), pp.2179–2186.

Li, S., Zhang, M., Gao, Y., Bao, B. and Wang, S., 2013. ZnO–Zn/CNT hybrid film as light-free nanocatalyst for degradation reaction. *Nano Energy*, 2(6), pp.1329–1336.

Lin, Z., Pang, S., Zhou, Z., Wu, X., Li, J., Huang, Y., Zhang, W., Lei, Q., Bhatt, P., Mishra, S. and Chen, S., 2022. Novel pathway of acephate degradation by the microbial consortium ZQ01 and its potential for environmental bioremediation. *Journal of Hazardous Materials*, 426, p.127841

Liu, Z., Zhang, Y., Kong, L., Liu, L., Luo, J., Liu, B., Zhou, Q., He, F., Xu, D. and Wu, Z., 2019. Preparation and preferential photocatalytic degradation of acephate by using the composite photocatalyst Sr/TiO2-PCFM. *Chemical Engineering Journal*, 374, pp.852–862.

Ma, R., Zhang, S., Wen, T., Gu, P., Li, L., Zhao, G., Niu, F., Huang, Q., Tang, Z. and Wang, X., 2019. A critical review on visible-light-response CeO2-based photocatalysts with enhanced photooxidation of organic pollutants. *Catalysis Today*, 335, pp.20–30.

Makuła, P., Pacia, M. and Macyk, W., 2018. How to correctly determine the band gap energy of modified semiconductor photocatalysts based on UV–Vis spectra. *The Journal of Physical Chemistry Letters*, 9(23), pp.6814–6817.

Mei, Y., Zhang, Y., Li, J., Deng, X., Yang, Y., Yang, Q., Jiang, B., Xin, B., Yao, T. and Wu, J., 2022. Synthesis of Co-doped CeO2 nanoflower: Enhanced adsorption and degradation performance toward tetracycline in Fenton-like reaction. *Journal of Alloys and Compounds*, 904, p.163879.

Mena, E., Rey, A., Rodríguez, E.M. and Beltrán, F.J., 2017. Nanostructured CeO2 as catalysts for different AOPs based on the application of ozone and simulated solar radiation. *Catalysis Today*, 280, pp.74–79.

Meng, F., Fan, Z., Zhang, C., Hu, Y., Guan, T. and Li, A., 2017. Morphology-controlled synthesis of CeO2 microstructures and their room temperature ferromagnetism. *Journal of Materials Science & Technology*, 33(5), pp.444–451.

Meshram, S.P., Tayade, D.T., Ingle, P.D., Jolhe, P.D., Diwate, B.B. and Biswas, S.B., 2010. Ultrasonic cavitation induced degradation of Congo red in aqueous solutions. *Chemical Engineering Research Bulletin*, 14(2), pp.119–123.

Meshram, S.P., Adhyapak, P.V., Pardeshi, S.K., Mulla, I.S. and Amalnerkar, D.P., 2017. Sonochemically generated cerium-doped ZnO nanorods for highly efficient photocatalytic dye degradation. *Powder Technology*, 318, pp.120–127.

Mishra, S.R. and Ahmaruzzaman, M., 2021. Cerium oxide and its nanocomposites: structure, synthesis, and wastewater treatment applications. *Materials Today Communications*, 28, p.102562.

Mosleh, S. and Rahimi, M.R., 2017. Intensification of abamectin pesticide degradation using the combination of ultrasonic cavitation and visible-light-driven photocatalytic process: synergistic effect and optimization study. *Ultrasonics Sonochemistry*, 35, pp.449–457.

Munirathnam, R., SM, R.F., Manjunatha, S., Manjunatha, H.C., Vidya, Y.S., Sridhar, K.N., Seenappa, L. and Krishnaveni, S., 2023. Tulsi mediated green synthesis of zinc-doped CeO2 for supercapacitor and display applications. *Journal of Science: Advanced Materials and Devices*, 8(2), p.100551.

Negi, K., Kumar, M., Singh, G., Chauhan, S. and Chauhan, M.S., 2018. Nanostructured CeO2 for selective-sensing and smart photocatalytic applications. *Ceramics International*, 44(13), pp.15281–15289.

Nicoletti, O., de La Peña, F., Leary, R.K., Holland, D.J., Ducati, C. and Midgley, P.A., 2013. Three-dimensional imaging of localized surface plasmon resonances of metal nanoparticles. *Nature*, 502(7469), pp.80–84.

Park, J.H., 2009. Photochemical degradation and toxicity reduction of methyl 1-[(butylamino) carbonyl]-1H-benzimidazol-2-ylcarbamate

in agricultural wastewater: Comparative study of photocatalysis and sonophotocatalysis. *Desalination*, 249(2), pp.480–485.

Rad, T.S., Yazici, E.S., Khataee, A., Gengec, E. and Kobya, M., 2023. Tuned CuCr layered double hydroxide/carbon-based nanocomposites inducing sonophotocatalytic degradation of dimethyl phthalate. *Ultrasonics Sonochemistry*, 95, p.106358.

Salerno, A., Pitault, I., Devers, T., Pelletier, J. and Briançon, S., 2017. Model-based optimization of parameters for degradation reaction of an organophosphorus pesticide, paraoxon, using CeO2 nanoparticles in water media. *Environmental Toxicology and Pharmacology*, 53, pp.18–28.

Saquib, M. and Muneer, M., 2003. Titanium dioxide mediated photocatalyzed degradation of a textile dye derivative, acid orange 8, in aqueous suspensions. *Desalination*, 155(3), pp.255–263.

Singh, A., Singh, A., Singh, A., Singh, P., Singh, V., Singh, Y., Tuli, H.S., Abdulabbas, H.S. and Chauhan, A., 2023. Chemistry, metabolism, and neurotoxicity of organophosphorus insecticides: A review. *Nature Environment & Pollution Technology*, 22(4), pp.1867–1880.

Sun, C., Li, H., Wang, Z., Chen, L. and Huang, X., 2004. Synthesis and characterization of polycrystalline CeO2 nanowires. *Chemistry Letters*, 33(6), pp.662–663.

Suslick, K.S., 1989. The chemical effects of ultrasound. *Scientific American*, 260(2), pp.80–87.

Talukdar, K., Saravanakumar, K., Kim, Y., Fayyaz, A., Kim, G., Yoon, Y. and Park, C.M., 2021. Rational construction of CeO2–ZrO2@ MoS2 hybrid nanoflowers for enhanced sonophotocatalytic degradation of naproxen: Mechanisms and degradation pathways. *Composites Part B: Engineering*, 215, p.108780.

Vijaya, J.J., Jayaprakash, N., Kombaiah, K., Kaviyarasu, K., Kennedy, L.J., Ramalingam, R.J., Al-Lohedan, H.A., Mansoor-Ali, V.M. and Maaza, M., 2017. Bioreduction potentials of dried root of *Zingiber officinale* for a simple green synthesis of silver nanoparticles: antibacterial studies. *Journal of Photochemistry and Photobiology B: Biology*, 177, pp.62–68.

Yang, D., Xu, Y., Pan, K., Yu, C., Wu, J., Li, M., Yang, F., Qu, Y. and Zhou, W., 2022. Engineering surface oxygen vacancy of mesoporous CeO2 nanosheets assembled microspheres for boosting solar-driven photocatalytic performance. *Chinese Chemical Letters*, 33(1), pp.378–384.

Zhou, X., Liu, G., Yu, J. and Fan, W., 2012. Surface plasmon resonance-mediated photocatalysis by noble metal-based composites under visible light. *Journal of Materials Chemistry*, 22(40), pp.21337–21354.

Original Research Paper https://doi.org/10.46488/NEPT.2025.v24i01.B4144 **Open Access Journal**

Forward Osmosis Process for Concentration of Treated Tannery Effluent

S. U. Sayyad[1,2†] ⓘ

[1]Department of Civil Engineering, Indian Institute of Technology, Roorkee, Uttarakhand-247667, India
[2]Civil and Environmental Engineering Department, Veermata Jijabai Technological Institute, Nathalal Parekh Marg, Matunga, Mumbai-400019, India
†Corresponding author: ssayyad@ce.iitr.ac.in, susayyad@ci.vjti.ac.in

ABSTRACT

Forward Osmosis is a suitable pretreatment process for reverse osmosis for secondary-treated sewage reuse and secondary-treated industrial effluents. In this study, the FO process is investigated for concentrating synthetic secondary treated tannery effluents using 24 g.L^{-1} and 38 g.L^{-1} of NaCl solution as draw solution. Results showed that 38 g.L^{-1} NaCl solution when used, provided higher flux and lower flux decline ratio as compared to 24 g.L^{-1} NaCl solution. The solute rejection by FO membrane was more in FO experiments using 38 g.L^{-1} NaCl solution as DS as compared to 24 g.L^{-1} NaCl solution. Contact angle, Fourier transform infrared spectroscopy, and scanning electronic microscopy tests on pristine and chemically cleaned membranes indicated the change in membrane structure and the presence of foulants on the membrane surface, indicating insufficient chemical cleaning. Findings signify implications on the concentration of DS and the cleaning method adopted for concentrating treated tannery effluent efficaciously using the FO process.

INTRODUCTION

Leather making involves preparing hides/skins for tanning through pre-tanning operation, preservation of skin proteins permanently by tanning, and improving aesthetic properties during post-tanning stages. About 30-40 m^3 of wastewater is generated per ton of raw material processed. A variety of chemicals used for leather processing include sodium and ammonium salts, lime, fat liquors, antibiotics, tannins, dyes, etc. (Kaul et al. 2013). A portion of process chemicals ends up in the wastewater, generating a considerable amount of pollution load. The effluent treatment practice utilizes a conventional treatment system consisting of physico-chemical processes followed by biological methods. The conventional treatment system can remove pollutants such as Biochemical Oxygen Demand (BOD), Chemical Oxygen Demand (COD), and suspended solids. Often, resource recovery and water reuse are practiced in the industry to reduce the strength and quantity of wastewater produced. Biological treatment methods are practiced in the industry to remove total dissolved organics from wastewater. Even after treatment, the treated tannery wastewaters contain some amount of organic, nitrogenous matter and a high amount of total dissolved solids (TDS) (Pophali & Dhodapkar 2011, Ramteke et al. 2010).

The constituents contributing to TDS in tannery effluents are calcium, ammonium, magnesium, sodium, chlorides, nitrates, and sulfates. Such a treated effluent containing high TDS is not suitable for process and non-process reuse applications in the industry (Zhao et al. 2022). The effluent must be discharged to surface water, where strict limits are laid for chlorides and TDS parameters. Further, disposal of treated tannery effluent, high in chlorides and TDS, is reported to affect the fertility of the soil and contaminate groundwater, making the soil unsuitable

for agriculture and the water unfit for utilization purposes (Bhardwaj et al. 2023). Currently, Reverse Osmosis (RO) has been employed in tanning industries and common effluent treatment plants treating high TDS wastewater coming from the tannery industries (Ranganathan & Kabadgi 2011).

Suthanthararajan et al. (2004) investigated a pilot-scale case study of secondary treated tannery wastewater containing residual organic impurities and high concentrations of TDS, which are not removed by conventional treatment methods. A pilot plant membrane system designed for a capacity of 1 $m^3.h^{-1}$, consisting of nano and reverse osmosis (RO) membrane units, supported by pre-treatment operations of pressure sand filter, photochemical oxidizer, activated carbon filter, water softener, acid control, anti-oxidant, anti-scaling and cartridge filter, was analyzed to further treat and reuse the tannery wastewater. The maximum TDS removal efficiency of the polyamide RO membrane was above 98%. The permeate recovery of about 78% was achieved. The water recovered from the membrane system had a very low TDS concentration and was reused for the wet finishing process in the tanneries. The rejected concentrate obtained from the operation was sent to solar evaporation pans. Comparing the pre-treatment units, it was reported that most of the removal was achieved in the nanofiltration unit. The pre-treatment before the nano filter had little effect on the removal of organic and inorganic matter. The softener present in the system required periodical regeneration. The oxidizer and activated carbon filter were able to remove only 5 to 20% COD present in the influent. The sand media and cartridge filter were able to remove the suspended solids completely.

To improve the feed water quality of the RO system, the secondary treated tannery wastewater is passed through either conventional RO pre-treatment steps or Microfiltration (MF)/Ultrafiltration (UF)/Nanofiltration (NF) membrane systems. Conventional pre-treatment processes to reverse osmosis treatment system consist of pH adjustment followed by a coagulation/flocculation process, disinfection, multimedia filtration, activated carbon filtration, and cartridge filtration (Jang et al. 2017, Pramanik et al. 2014, Sweity et al. 2013). In addition, membrane pre-treatment technologies like MF, UF, and NF are also practiced for Reverse Osmosis (Kim et al. 2002). All these methods increase the cost of the treatment and chemical usage.

In this context, Forward Osmosis (FO) may provide an effective alternative to pre-treatment to RO for treating the secondary tannery effluents. It is learned from the literature (Al-Zuhairi et al. 2015, Korenak et al. 2019, Thiruvenkatachari et al. 2016, Zaviska et al. 2015) that forward osmosis, when used as pre-treatment to RO, has the highest potential to reduce RO membrane fouling and

scaling. This increases the life of the membranes, requires less chemical cleaning of membranes, and causes less damage to membranes during cleaning in the RO process. TDS removal from Tannery effluents is currently being accomplished in industries by RO process but comes under a high cost because of scaling, fouling, and damage of RO membranes, as discussed. Limited research is available for treating/concentrating tannery effluents with an FO system (Pal et al. 2017). Moreover, the researchers have often used cross-flow FO module configuration, which is quite an energy-intensive option, and no research is available on other FO module configurations used for treating secondary treated tannery effluent. In this study, we have evaluated the performance of the compartment configuration FO system in concentrating synthetic secondary treated tannery effluent. The objective of this research is as follows: 1. To investigate the performance of the FO process in terms of water flux, flux decline ratio, concentration factor, and contaminant rejection using synthetic secondary treated tannery effluent as feed solution. 2. Investigation of the effect of concentration of sodium chloride as a DS on contaminant rejection. 3. To investigate the FO membrane characteristics using different analytical techniques such as water contact angle (WCA), FTIR, SEM, and SEM-EDX.

MATERIALS AND METHODS

FO Membranes and Membrane Orientation

Aquaporin-embedded FO flat sheet membranes from Aquaporin Asia, Singapore, were purchased. The membranes were soaked in fresh deionized water and kept at 4ºC. Once a week, deionized water (DI) was replaced with fresh water. The membranes were washed in deionized water for at least 1 hour at room temperature before use. All studies were carried out with the active layer of the membrane towards the feed solution (FS).

Feed Solutions and Draw Solutions

The feed solution is either deionized water (DIW) or secondary treated tannery effluent. Synthetic secondary treated tannery effluent (SSTTE) solution simulating secondary treated real tannery effluents were prepared using Tannic acid (185 $mg.L^{-1}$), Peptone (100 $mg.L^{-1}$ $mg.L^{-1}$), NH_4Cl (1600 $mg.L^{-1}$), $CaSO_4$ (510 $mg.L^{-1}$), $MgSO_4$ $7H_2O$ (410 $mg.L^{-1}$), NaCl (6500 $mg.L^{-1}$), KCl (55 $mg.L^{-1}$), KNO_3 (40 $mg.L^{-1}$), Na_2SO_4 (5100 $mg.L^{-1}$) and $K_2Cr_2O_7$ (11.5 $mg.L^{-1}$) (Panizza & Cerisola 2004, Sundarapandiyan et al. 2010, Costa et al. 2010). To avoid bacterial growth in the SSTTE during the experimental duration, the SSTTE was autoclaved and cooled, and a dose of 6 $mg.L^{-1}$ ampicillin solution was added. The pH of the solution was adjusted

Table 1: Characteristics of synthetic secondary treated tannery effluent.

Parameter	Unit	SSTTE
pH	unitless	7.2-7.39
TDS	mg.L^{-1}	14147-14479.1
COD	mg.L^{-1}	326-336.10
Chlorides	mg.L^{-1}	4884.12-5072.39
Sulfates	mg.L^{-1}	3861.78-4191.75
Nitrates	mg.L^{-1}	21-22
Phosphates	mg.L^{-1}	6
Sodium	mg.L^{-1}	4420.85-4599.04
Potassium	mg.L^{-1}	51.34-57.73
Calcium	mg.L^{-1}	149.61-155.1
Magnesium	mg.L^{-1}	41.24-43.99
Ammonium	mg.L^{-1}	515.71-526.73
Total Chromium	mg.L^{-1}	3.7-4.07

using a 12 N NaOH solution. The characteristics of synthetic secondary treated tannery effluent are presented in Table 1.

The draw solution consisted of sodium chloride solutions of concentrations 24 g.L^{-1} and 38 g.L^{-1}, respectively. The initial volume of the draw solution was 1000 mL for all experiments. The chemical reagents were purchased from S. D. Fine Chemical Ltd. and were of analytical grade. Ampicillin was purchased from HiMedia, Mumbai. A Millipore water purification system (Merck Millipore, 18.2 MΩ·cm at 25 ºC) provided deionized water (DIW), which was used for preparing the draw and feed solutions, rinsing the FO module at the end of the experiment and diluting samples for analysis.

Bench Scale Forward Osmosis Setup

Fig. 1a shows a schematic sketch of the bench size experimental setup used in this study, and Fig. 1b shows a photograph view of the experimental setup. The experiment was conducted in an air-conditioned room at 23 ± 1°C. This continuous flow apparatus is used to test the performance of the FO process under continuous feed solution supply and constant concentration draw solution conditions. The feed solution reservoir (1) supplies feed solution to the feed solution tank. To determine water flux owing to the FO process, the weight of the feed solution reservoir is monitored at time intervals. Weight was measured manually on a weight
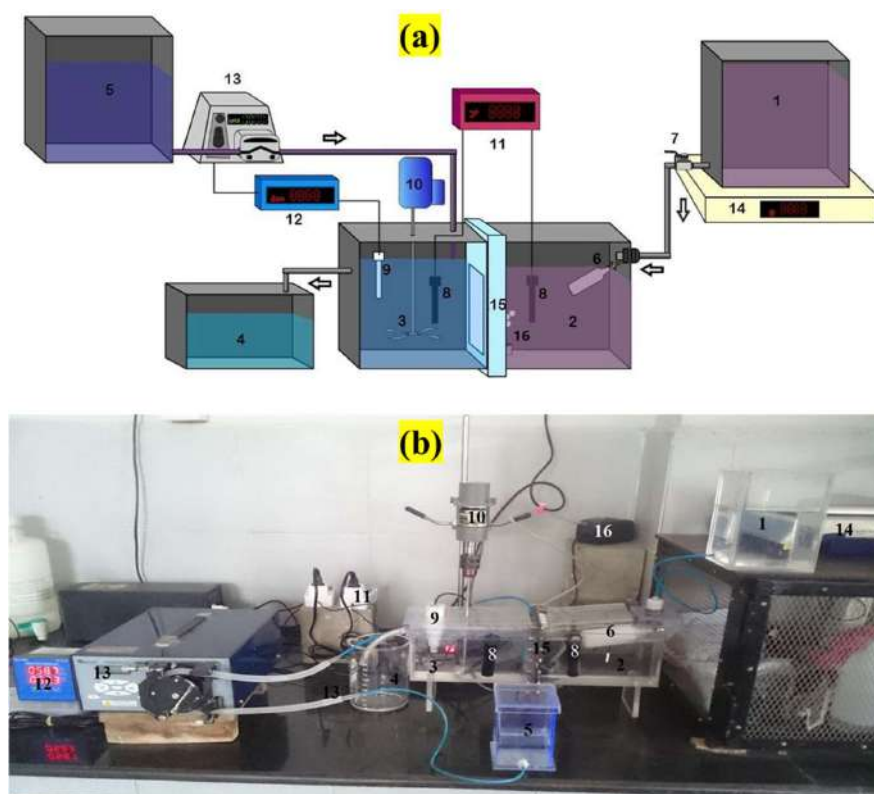
Fig. 1: Forward osmosis setup. a) Schematic diagram of the experimental setup, b) Photograph of the experimental setup. 1: Feed Solution Reservoir, 2: Feed Solution Tank, 3: Draw Solution Tank, 4: Separated Draw Solution Tank, 5: Concentrated Draw Solution Reservoir, 6: Float Valve 7: Flow Control Valve, 8: Heating Rods, 9: Conductivity Probe, 10: Stirrer, 11: Temperature Controller Unit, 12: Conductivity Controller Unit, 13: Peristaltic Pump, 14: Weigh Balance, 15: FO membrane Unit. 16: Aerator.

balance (14) (Citizen CTG, India). The aquaporin forward osmosis membrane vertically separates two acrylic tanks or compartments in this setup. The FO membrane is sealed to prevent leakage using a 3mm thick EPDM rubber sheet and 20 no's of 6 mm diameter stainless steel nuts and bolts. Out of the two compartments, the proper compartment (2) is of feed solution (which is deionized water/ wastewater), and the left compartment (3) is of draw solution, which is sodium chloride solution. The feed solution tank dimensions are 18.2cm length x 5.5cm width x 11cm height. The feed solution volume in the feed solution tank is maintained at 1 liter by providing a float valve (6) (MA052, Kerick, India) at the inlet of the feed solution tank. The effective membrane area is (8.5cm height x 4.0cm width) 34 cm^2. The feed solution faces the membrane's active layer. The volume of the feed solution is reduced while the volume of the draw solution is increased as pure water fluxes through the forward osmosis membrane. The float valve controls the rate at which feed solution is pumped into the feed solution tank from the feed solution reservoir.

The draw solution tank dimensions are 18.2cm × 5.5cm × 11cm. The draw solution volume used in the experiments is 1 L. The draw solution volume increases and dilutes due to pure water flux from the feed solution tank through the FO membrane. To collect and separate the increased draw solution volume, a 0.5mm diameter outlet port is provided to the draw solution tank at the height of 10 cm. The increased volume of the draw solution passes through the outlet port of the draw solution tank and gets collected in the separated draw solution tank (4). Thus, the draw solution volume in the draw solution tank is maintained constant. To maintain a constant concentration in the draw solution tank, a more concentrated draw solution (91.2 g.L^{-1} sodium chloride solution) is supplied to the draw solution tank from the concentrated draw solution reservoir (5) by a peristaltic pump (13) (Ravel, India) which is connected to a conductivity controller (12) (MSCD09, MicroSet, India). The increase in conductivity of the water in the feed solution tank due to reverse solute flux is measured by a conductivity meter (Inolab Cond720, WTW Germany). A temperature control unit controls the temperature of the two compartments separated by a membrane. The temperature control unit consists of 2 nos of heating rods (8) (MINI-THERM, Cobalt International, SC) and 2 nos of temperature controllers (11) (XK-W2001, Robocraze, India). Mixing is done in the draw solution tank with the help of an axial impeller connected to a laboratory stirrer (10) (RQG-121-D, Remi Elektrotechnik Ltd, India). Feed solution mixing was carried out by diffusing air with the help of an aerator (16) (Eheim, Germany). The forward osmosis setup is unique in one way: this setup does not utilize pumps for the circulation of feed solution and draw solution.

Forward Osmosis Experimental Procedure

For the feed solution as SSTTE, we used 24 and 38 g.L^{-1} of NaCl solution as the draw solution. All the experiments were conducted for 7 h. In all the experiments, aeration was done in the FS tank at a rate of 0.3 mL.min^{-1}, and mixing was done in the draw solution tank at a constant mixing rate of 75 RPM. For each experiment, a single membrane coupon is used. At the end of the experiment, the manufacturer-recommended procedure chemically cleaned the membrane coupon.

Calculation of Pure Water Flux, Flux Decline Ratio, Reverse Solute Flux, Concentration Factor, and Solute Rejection

The pure water flux J_w (LMH) was calculated using the equation (1) as given by (Dutta et al. 2022),

$$J_w = \Delta W/(\rho \times S_m \times \Delta t) \qquad \ldots(1)$$

Where ΔW is the weight (g) change of the feed solution over a specific time Δt (hours.), ρ is feed solution density (assumed 1.0 g.cm^{-3}), and S_m is the effective membrane surface area (m^2). Further, the flux decline ratio FDR (%) was calculated using equation (2) as given by (Mondal & De 2015).

$$FDR = 100 - [(J_{w,f}/J_{w,i}) \times 100] \qquad \ldots(2)$$

Where $J_{w,f}$ is the flux recorded at the end of the experiment, and $J_{w,i}$ is the initial recorded flux.

The concentration factor CF (%) was calculated as described by equation (3) as given by (Ortega-Bravo et al. 2016)

$$CF = 100 (C_{f,Final}/C_{f,Initial}) \qquad \ldots(3)$$

Where $C_{f,Final}$ is the final feed solution concentration (mg.L^{-1}) at the end of the experiment, and $C_{f,Initial}$ is the initial feed solution concentration (mg.L^{-1}).

Different ions in the feed solutions have been studied to determine their solute rejection factors. At the experiment's beginning and conclusion, the concentrations of ions in the draw and feed solutions were measured. Then, equation (4), as given by (Vital et al. 2018), was used to determine solute rejection SR (%).

$$SR = [(C_{f,Initial} - C_p)/C_{f,Initial}] \times 100 \qquad \ldots(4)$$

Where $C_{f,Initial}$ represents the initial concentration (mg.L^{-1}) of the ion on the feed side, and C_p is the concentration (mg.L^{-1}) of the ion on the permeate (draw side). Concentration (mg/L) on the permeate C_p is evaluated using equation (5) as given by (Vital et al. 2018)

$$C_p = (C_d \times V_d)/V_p \qquad \ldots(5)$$

Where C_d is the concentration (mg.L^{-1}) on the draw side, V_d is the volume (L) of the draw solution by the end of the experiment, and V_p is the volume (L) of water that permeates from the feed to the draw side.

Sampling and Analytical Methods

Feed solution (synthetic secondary treated tannery effluent) in the feed solution tank was collected before the start and after the completion of the experiment. Draw solution samples were collected at the end of the experiment for analysis. The feed solution samples were analyzed for COD, EC, Total Chromium, cations (Sodium, Ammonium, Potassium, Magnesium, and Calcium), and anions (Chlorides, Nitrates, Orthophosphates, and Sulphates). The draw solution samples were analyzed for Total Chromium, cations, and anions.

In brief, COD was determined (Aqualytic AL38SC) by a closed reflux colorimetric method according to Standard Methods for the Examination of Water and Wastewater. COD levels were determined by measuring the absorbance of the digested solution at 600nm on a Hach DR-6000 UV-visible spectrophotometer. Ion Chromatography determined cations (Sodium, Ammonium, Potassium, Magnesium, and Calcium) and anions (Chlorides and Sulphates) with chemical suppression of eluent conductivity (Metrohm, 850 Professional IC). Nitrate was measured as Nitrate-N by ultraviolet spectrophotometric screening method (APHA 4500). Phosphate was measured by the stannous chloride method (APHA 4500-P D). Further cation (Magnesium, Potassium, Total Chromium) concentrations in the DS were also analyzed using an inductively coupled plasma-optical emission spectrometer (ICP-OES, Agilent 700).

Membrane Characterization

At the NCNNUM laboratory in Mumbai, the Rame-hart contact angle instrument is used to measure the contact angle to quantify the hydrophobicity/hydrophilicity of virgin and chemically treated membranes. The membranes were air-dried at room temperature before contact angle measurements using the Sessile Drop Technique or Static Contact Angle measurements. The contact angles reported are the average of 7-9 measurements made with pure water droplets. The changes in the chemical structure of the samples were investigated using attenuated total reflection-Fourier transform infrared spectroscopy (ATR-FTIR, make: PerkinElmer (USA), L1600400 Spectrum TWO DTGS) at a resolution of 4 cm^{-1}. On samples of clean and chemically cleaned membranes, ATR/FTIR analysis was carried out. There are 20 scans with a wavelength range of 600-4000 cm^{-1} were used to examine the spectra. To achieve a similar close contact between the ATR crystal and sample surface, all samples were pressed down with the same amount of pressure. The FO membrane was examined using scanning electron microscopy (SEM) ((Carl Zeiss Model: Zeiss Gemini SEM) and energy-dispersive X-ray spectroscopy (EDX) (EDAX APEX). Surface and cross-sectional imaging were performed on clean membranes, and surface imaging was on chemically cleaned membranes. Coupons were dipped in liquid nitrogen and cut using a razor to show the membrane cross-section. Samples were sputtered with gold before SEM imaging to prevent charging of the non-conductive membrane surface.

RESULTS AND DISCUSSION

Water Flux and Flux Decline Ratio

Fig. 2 shows the change of flux as a function of time under FO mode using SSTTE as FS and 24 g.L^{-1} and 38 g.L^{-1} of NaCl solution as DS. When the DS concentration was 24 g.L^{-1} and 38 g.L^{-1} of NaCl solution, the initial flux values for SSTTE were 4.41 LMH and 7.44 LMH, respectively. Experiments with lower DS concentration have lower initial flux, while experiments with higher DS concentration have higher initial flux (Camilleri-Rumbau et al. 2019). However, with respect to time, the flux declines in experiments for DS concentrations of 24 g.L^{-1} and 38 g.L^{-1} NaCl solution. The first rapid decline in flux is mainly because of fouling, while further, the flux declines due to the combined effects of fouling, the concentration of FS, and the back diffusion of DS (Han et al. 2016). All this process is slower in lower DS concentration (24 g.L^{-1} of NaCl solution) experiments, while this is faster in higher DS concentration (38 g.L^{-1} of NaCl solution) experiments (Nguyen & Yoshikawa 2019). The flux values at the end of the experiment for SSTTE were 2.41 LMH and 5.44 LMH when the DS concentration was 24 g.L^{-1} and 38 g.L^{-1} of NaCl solution, respectively.

The flux decline ratio was calculated using equation (2). The initial flux decline ratio is low (5.21%) in lower DS concentration (24 g.L^{-1} of NaCl solution) experiments, whereas the initial flux decline ratio is more (9.14%) in higher DS concentration (38 g.L^{-1} of NaCl solution) experiments for FS as SSTTE (Morrow & Childress 2019). Fig. 3 shows that the flux decline ratio at the end of the experiment (7 hours) when using 24 g.L^{-1} and 38 g.L^{-1} NaCl solution as against SSTTE was 45.35% and 26.88%, respectively, whereas the average flux was 3.54 LMH and 6.175 LMH respectively. The flux decline ratio at the end of the experiment is more in the low DS concentration (24 g.L^{-1} of NaCl solution) experiment, whereas it is less in the high DS concentration (38 g.L^{-1} of NaCl solution) experiment. In hydraulic pressure-driven membrane processes, higher values of flux decline ratio indicate that the membrane has fouled more (Conidi et al. 2019). However, in FO processes where hydraulic pressure is not used, this may not be true. In the FO process, though, flux decline is slower in the low DS experiment than in the high DS experiment, but operating the
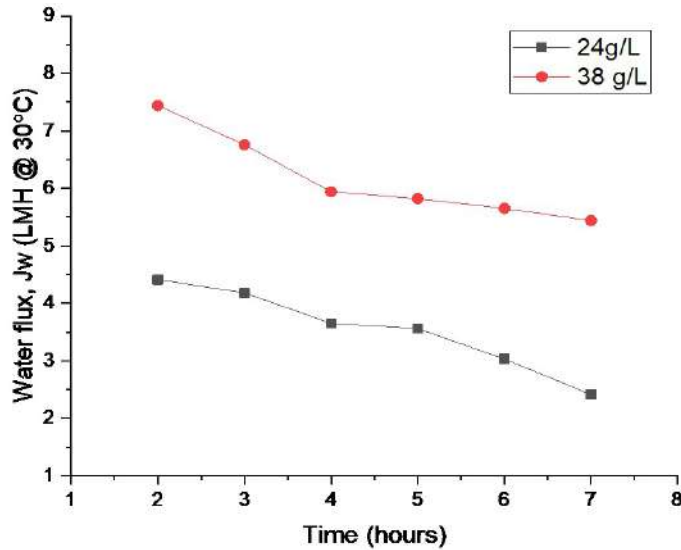
Fig. 2: Effect of draw solution concentration on pure water flux. FS is synthetic secondary treated tannery wastewater. DS concentration is 24 and 38 g.L^{-1} NaCl solution, respectively. DS concentration is kept constant throughout the experimental duration. All experiments are conducted at a constant temperature of 30°C. The membrane's active layer is facing towards the feed solution.
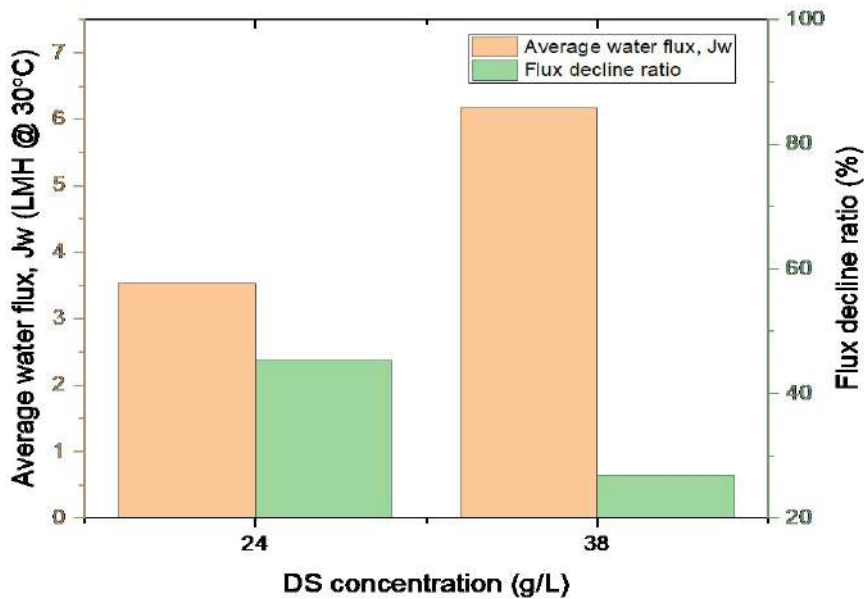
Fig. 3: Effect of draw solution concentration on average pure water flux and flux decline ratio. FS is synthetic secondary treated tannery wastewater. DS concentration is 24 and 38 g.L^{-1} NaCl solution, respectively. DS concentration is kept constant throughout the experimental duration. All experiments are conducted at a constant temperature of 30°C. The membrane's active layer is facing towards the feed solution.

FO process at low DS concentration has a greater impact on flux. A slight decrease in osmotic pressure gradient decreases the flux largely, especially at low DS concentrations, as compared to high DS concentrations, as the flux vs osmotic pressure curve is non-linear (Lay et al. 2012). The flux declines largely in low DS experiment as compared to high DS experiment because of fouling, then decrease in osmotic

pressure gradient due to concentration of FS, back diffusion of DS (RSF), and cake-enhanced osmotic pressure (CEOP) (Gao et al. 2018).

The low flux decline ratio (26.88%) in the experiment with SSTTE and 38 g.L^{-1} NaCl solution is mainly attributed to the high DS concentration in the DS tank (38 g.L^{-1} NaCl solution). At higher DS concentrations, flux is not impacted

by slight changes in the osmotic pressure gradient (Lay et al. 2012). Further the flux is also enhanced due to the novel FO module configuration used in this study. Mixing in the DS tank of the FO module configuration provides a uniform concentration of DS in the DS tank, while the configurations using pumps to circulate draw solution like the cross-flow configurations, plate and frame configuration, and hybrid dead-end cross-flow configuration, the concentration of draw solution at inlet and outlet are varying (Sagiv et al. 2014). Therefore, in these configurations, the entire effective area of the membrane will not be subjected to a uniform transmembrane pressure, resulting in a decreasing flux along the length of the membrane (Gruber et al. 2012).

Concentration Factor

Concentration factors (%) were calculated using equation (2.3). Concentration factors (CF) represent the percentage of the value of a specific parameter that increases or decreases due to the concentration process. When a parameter decreases, CF is presented as negative to emphasize that the parameter experienced a reduction. The greater the concentration gradient between FS and DS, the greater the FS concentration (Ortega-Bravo et al. 2016). Fig. 4 shows the concentration factors for Calcium, Magnesium, Potassium, Sodium, Ammonium, Electrical Conductivity (EC), Chlorides, Sulphates, Nitrates, Phosphates, COD and Total Chromium (Total Cr). Calcium concentration increased
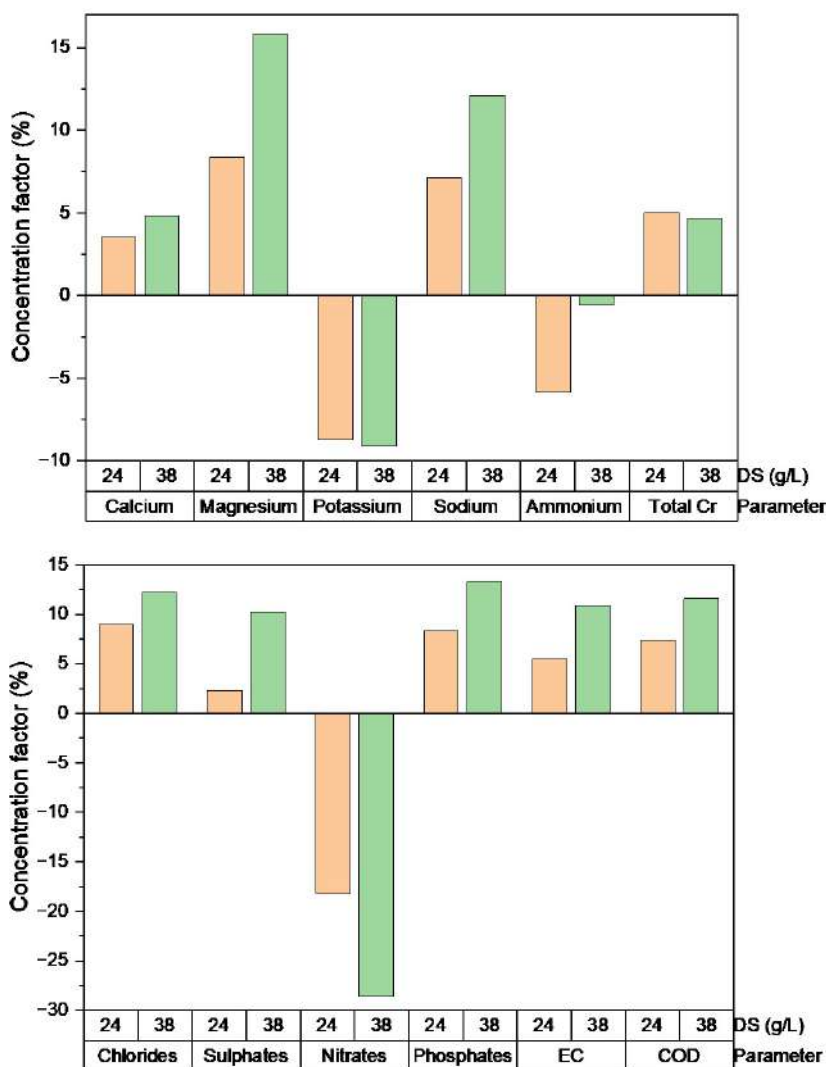
Fig. 4: Percentage change in concentration of FS parameters due to the Forward Osmosis process. FS is synthetic secondary treated tannery wastewater. DS concentration is 24 and 38 g.L^{-1} NaCl solution, respectively. DS concentration is kept constant throughout the experimental duration. All experiments are conducted at a constant temperature of 30 ºC. The membrane's active layer is facing toward the feed solution.

in SSTTE by 3.53% and 4.83% in experiments when DS was 24g.L^{-1} and 38 g.L^{-1} NaCl solution, respectively. When a mass balance was conducted, the experimental final concentration value differed from the theoretical values. The possible reason might be that calcium might have formed bonds with the negatively charged membrane surface and with other ions and precipitated on the membrane surface (Duong & Chung 2014). Magnesium concentration increased in SSTTE by 8.34% and 15.81% in experiments when DS was 24 g.L^{-1} and 38 g.L^{-1} NaCl solution, respectively. When a mass balance was conducted, the experimental final concentration value matched near the theoretical values. This verified that magnesium precipitation had not occurred on the membrane in 24 g.L^{-1} and 38 g.L^{-1} DS experiments. Magnesium has a high affinity towards Chlorides and Sulphates and must have formed a bond with Chlorides and Sulphates (Gao et al. 2018). Concentration factors for Potassium showed negative values of 8.73% and 9.10% in experiments when DS was 24g.L^{-1} and 38 g.L^{-1} NaCl solution, respectively. The possible reason might be the low hydrated radius of Potassium and the low capacity of the membrane to retain Potassium in the FS compartment, or it could be the transport of Potassium to DS due to the Donnan equilibrium effect. The Donnan equilibrium effect says that if an ion is having high affinity towards another ion than the one with which it is currently attached, then the ion will break the bond and join the bond with the ion with which it has high affinity. Sodium concentration increased in SSTTE by 7.12% and 12.1% in experiments when DS was 24g.L^{-1} and 38 g.L^{-1} NaCl solution respectively. When a mass balance was conducted the experimental final concentration value matched near to the theoretical values. Since FS contained a high concentration of sodium and the selected DS was also a NaCl solution so sodium flux from DS to FS was negligible. Likewise, Potassium the concentration factors for Ammonium showed negative values of 5.87% and 0.60% in experiments when DS was 24g.L^{-1} and 38 g.L^{-1} NaCl solution respectively. The possible reason might be the high diffusion coefficient, the low hydrated radius of ammonium, and the low capacity of the membrane to retain ammonium in the FS compartment, or could be the transport of ammonium to DS due to the Donnan equilibrium effect (Ortega-Bravo et al. 2016).

The total Chromium concentration factor in SSTTE is 5% and 4.67% for experiments when DS was 24 g.L^{-1} and 38 g.L^{-1} NaCl solution, respectively. This is because, in the case of higher DS concentration, the Total Chromium must have either been precipitated on the membrane or Total Chromium must have been transported to DS (Pham et al. 2021). Chloride concentration increased in SSTTE by 8.97% and 12.25% in experiments when DS was 24 g.L^{-1} and

38 g.L^{-1} NaCl solution, respectively. When a mass balance was conducted, the experimental final concentration value matched near the theoretical values. Sulfate concentration increased in SSTTE by 2.27% and 10.23% in experiments when DS was 24 g.L^{-1} and 38 g.L^{-1} NaCl solution, respectively. It is seen the concentration of Sulphates in the final FS is lower than the values obtained from the mass balance in experiments when DS was 24 g.L^{-1} and 38 g.L^{-1} NaCl solution. The possible reason might be the bonds formed with Calcium and Magnesium and precipitation on the membrane surface (Hancock et al. 2011, She et al. 2012). Concentration factors for Nitrates showed negative values of 18.18% and 28.57% in experiments when DS was 24 g.L^{-1} and 38 g.L^{-1} NaCl solution, respectively. The possible reason might be the high diffusion coefficient, the low hydrated radius of Nitrates, and the low capacity of the membrane to retain Nitrates in the FS compartment, or it could be the transport of nitrates to DS due to the Donnan equilibrium effect (Damirchi & Koyuncu 2021). Phosphate concentration increased in SSTTE by 8.33% and 13.33% in experiments when DS was 24 g.L^{-1} and 38 g.L^{-1} NaCl solution, respectively. When a mass balance was conducted, the experimental final concentration value matched near the theoretical values. The possible reason might be the large hydrated radius of negatively charged phosphate ions accumulated in the FS (Luo et al. 2018). For increasing DS concentration, the conductivity increase was high. When DS was 24 and 38 g.L^{-1} of NaCl solution, the SSTTE conductivity increased by 5.45% and 10.86%, respectively. Similarly, the COD increase in SSTTE was 7.36% and 11.57% when DS was 24 g.L^{-1} and 38 g.L^{-1} NaCl solution, respectively. This increase in concentration during the FO process is due to the addition of FS from the FS reservoir during the FO process (Hickenbottom et al. 2013).

Solute Rejection

The rejection of the ions under the FO system could be attributed to several reasons. (1) Because no pressure is applied in the FO process, the effect of convective flow on the ion transport is insignificant. (2) The Donnan equilibrium effect may also contribute to the high rejections under the FO process.

Fig. 5 showed the rejection of Total Chromium, Magnesium, Potassium, and Ammonium ions by the FO membrane when FS was SSTTE and DS was 24 g.L^{-1} and 38 g.L^{-1} of NaCl solution, respectively. ICPOES determined all the ions except ammonium. Chromium ions were rejected at 86.23% and 96.22% when DS was 24 g.L^{-1} and 38 g.L^{-1} of NaCl solution, respectively. The hydrated radius of chromium ion is 0.461 nm and, therefore, is well rejected
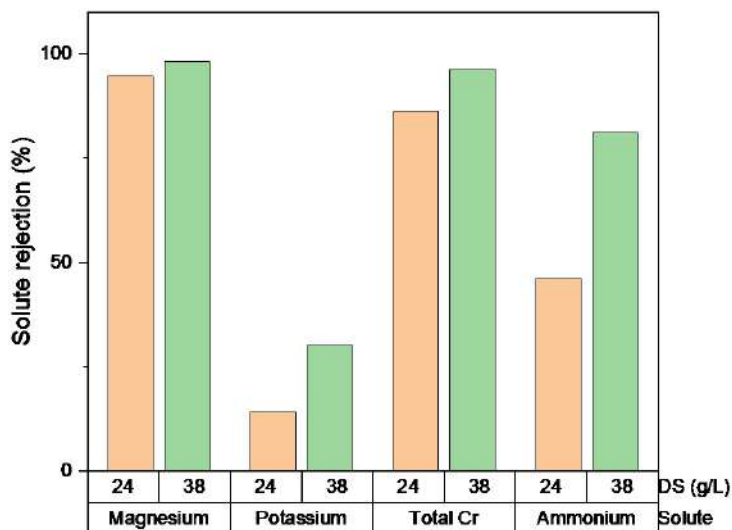
Fig. 5: Solute rejection by FO membrane. FS1 is synthetic secondary treated tannery wastewater with a concentration of 14 g.L^{-1}. DS concentration is 28 and 38 g.L^{-1} NaCl solution, respectively. DS concentration is kept constant throughout the experimental duration. All experiments are conducted at a constant temperature of 30 ºC. The membrane's active layer is facing towards the feed solution.

by the FO membrane (Pham et al. 2021). The rejection for Magnesium ion was 94.56% and 98.13% when DS was 24 g.L^{-1} and 38 g.L^{-1} of NaCl solution, respectively. Magnesium rejection was more significant at high DS concentrations. Magnesium is well rejected due to size exclusion because it is a divalent cation with a larger hydrated radius (0.428 nm) than the pore size of the FO membrane (Coday et al. 2015, Gao et al. 2018). The rejection of Potassium is 14.17 and 30.25% when DS was 24 g.L^{-1} and 38 g.L^{-1} of NaCl solution, respectively. The rejection of potassium was higher for higher DS concentrations. Furthermore, potassium, a monovalent ion with a low hydrated radius (0.331nm) and more excellent water permeability is less rejected by FO membranes irrespective of the FS concentration (Hancock et al. 2011, Roy et al. 2016). Likewise, in Potassium, the rejection of Ammonium was lower and was 46.15% and 81.16% when DS was 24 g.L^{-1} and 38 g.L^{-1} of NaCl solution, respectively. However, it is notable that the rejection of Potassium and Ammonium was higher when a 38 g.L^{-1} NaCl solution was used as DS as compared to a 24 g.L^{-1} NaCl solution.

Membrane Characterization

The pristine and chemically cleaned membrane was analyzed for contact angle, ATR-FTIR, SEM, and SEM EDX to determine if the membrane surface underwent modification due to the chemical cleaning. The chemical cleaning was done only on the active layer side of the membrane. The chemical cleaning was done using an alkaline-acid cleaning method. The alkaline solution would remove the organic

foulants on the membrane, and the acid solution would remove the inorganic constituents. Alkaline cleaning at 30ºC with 0.001 M NaOH solution (pH=11) for 30 min, followed by acid cleaning at 30 ºC with 0.01 M HNO$_3$ (pH = 2) for 30 min, was done to clean the membrane chemically.

Contact Angle

A surface is hydrophobic when its static water contact angle θ is >90° and is hydrophilic when θ is <90°. At 25°C, DI water was used as the probe liquid in a contact angle goniometer to assess the hydrophilicity of aquaporin membranes' active and support layers. The contact angle was recorded within 10 seconds of a small water droplet deposition on the flat membrane surface. The contact angle was measured from at least five random points to limit the influence of surface heterogeneity. The average value was then reported. The contact angle was measured for the new membrane and chemically cleaned membrane. The contact angle measurements for the active and support layers are given in Table 2.

Table 2: Contact angle values of pristine and chemically cleaned aquaporin forward osmosis membrane.

Membrane Layer	Contact angle		Reference
	Pristine FO membrane	Cleaned FO membrane	
Active layer	59.28±0.05º	52.66 ±0.05º	This study
Support layer	75.71º	58.91º	This study
Active layer	53º	---	(Omir et al. 2020)
Support layer	61º	---	

The contact angle values of the pristine membranes' active layer and support layer suggest that the active layer is more hydrophilic than the support layer. When the membrane was exposed to chemical cleaning, the contact angle of the active layer decreased from 59.28⁰ to 52.66⁰. No chemical cleaning of the support layer was done. However, the contact angle of the support layer changed from 75.71⁰ to 58.91⁰, making the support layer more hydrophilic. These results indicate that accumulating chemical cleaning agents on the membrane's surface increases membrane hydrophilicity. The increased hydrophilicity thus improves the flux performance of the membranes (Tasci et al. 2022).

Attenuated Total Reflectance-Fourier Transform Infrared Spectroscopy (ATR-FTIR)

ATR-FTIR spectra of a pristine and chemically cleaned aquaporin membrane's active layer were observed to identify any significant change in the chemical structure. Fig. 6a and Fig. 6b show the FTIR spectra of pristine and chemically cleaned membranes. Fig. 6a shows the FTIR

spectrum of the pristine membrane. The active layer of the pristine membrane is fully polyamide. FTIR spectrum showed characteristic peaks at 1656.99 cm^{-1}, 1577.79 cm^{-1}, and 1485.65 cm^{-1}, which suggested the selective layer of the aquaporin membrane was fully aromatic polyamide. Peaks at wave numbers 2854.41 cm^{-1} and 2925.01 cm^{-1} of the FTIR spectrum demonstrated the presence of the lipid tails of aquaporin protein. These peaks confirmed the incorporation of aquaporin proteins into the membrane-selective layer. The peak at 1743.34 cm^{-1} suggested the occurrence of the phosphate I band from the lipid bilayer of the aquaporin vesicles. The lipid tails of aquaporin protein were confirmed from peaks at wave numbers 2854.41 cm^{-1} and 2925.01 cm^{-1}. Fig. 6b shows the FTIR spectrum of the chemically cleaned membrane. After chemical cleaning, a significant change was observed in the FTIR spectrum at 3293.16 cm^{-1}, 1652.51 cm^{-1}, and 1372.93 cm^{-1}. This demonstrates that there must still be some foulants on the membrane (Khraisheh et al. 2020), or the chemicals used for cleaning the membrane must have changed the structure of the membrane (Li et al. 2017).
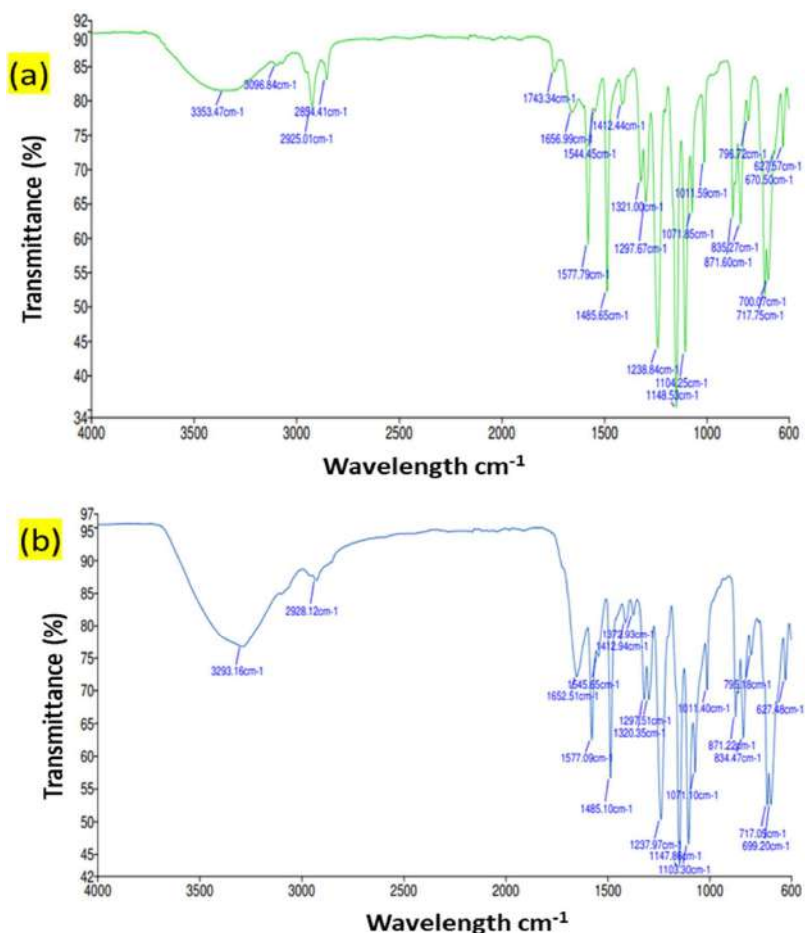
Fig. 6: FTIR spectrum of the a) pristine membrane and b) chemically cleaned membrane.
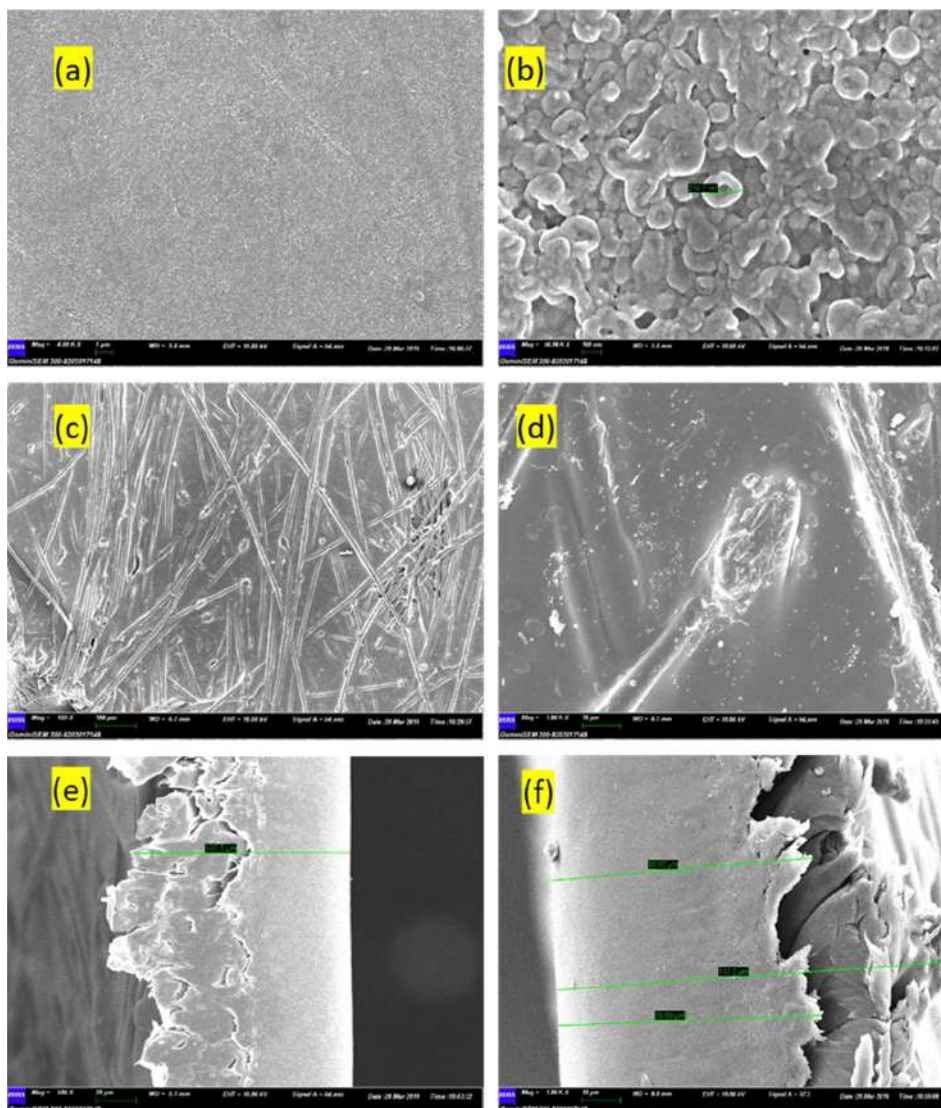
Fig. 7: SEM images of aquaporin-based forward osmosis pristine membrane at 10 kV a) active layer (AL) (magnification×4k) b) active layer (AL) with incorporated aquaporin vesicles(~210 nm) (magnification ×50k), c) support layer (SL) (magnification ×100), d) support layer (SL) (magnification×1k), e) cross-section (magnification×500), f) cross-section (magnification ×1k).

Scanning Electron Microscopy (SEM) and Energy Dispersive X-Ray Analysis (EDX)

Aquaporin vesicles with a round form were seen in the active membrane layer according to membrane cross-section morphology. Fig. 7 showed the existence of circular nodules with an estimated size of 100 nm at the membrane interface, comparable to the size of a proteoliposome containing aquaporin protein (Li et al. 2014). The aquaporin proteins were embedded in the active layer of AQP, which resulted in a porous structure for the active layer. All the membranes' cross-sections showed asymmetric structures, often resulting from the phase-inversion process.

Fig. 8 shows the SEM EDX analysis for the chemically cleaned membrane. To confirm that the foulant particles have been removed from the active layers of the aquaporin membrane, the active surfaces were characterized by SEM combined with EDX. The SEM images illustrated the adsorption of foulant particles on FO membranes after chemical cleaning. The EDX analysis confirms the presence of carbon (C), sulfur (S), and oxygen (O). However, this reveals the organic nature of the membranes to more extent. Traces of calcium (Ca) and magnesium (Mg) are seen throughout the examined membrane surfaces since the FS contained calcium and magnesium that must have been attached to the membrane surface and not removed after

Area 10

Smart Quant Results

Element	Weight %	Atomic %	Error %
C K	67.5	78.6	9
O K	16.1	14.1	11.2
NaK	0.5	0.3	13
MgK	0.3	0.2	9.6
S K	15.5	6.8	1.3
CaK	0.1	0	44.2

Selected Area 1

kV: 20	Mag: 2200	Takeoff: 8.2	Live Time(s): 20	Amp Time(μs): 3.84	Resolution:(eV) 128.2

467 Cnts   3.020 keV   Det: Element C2B
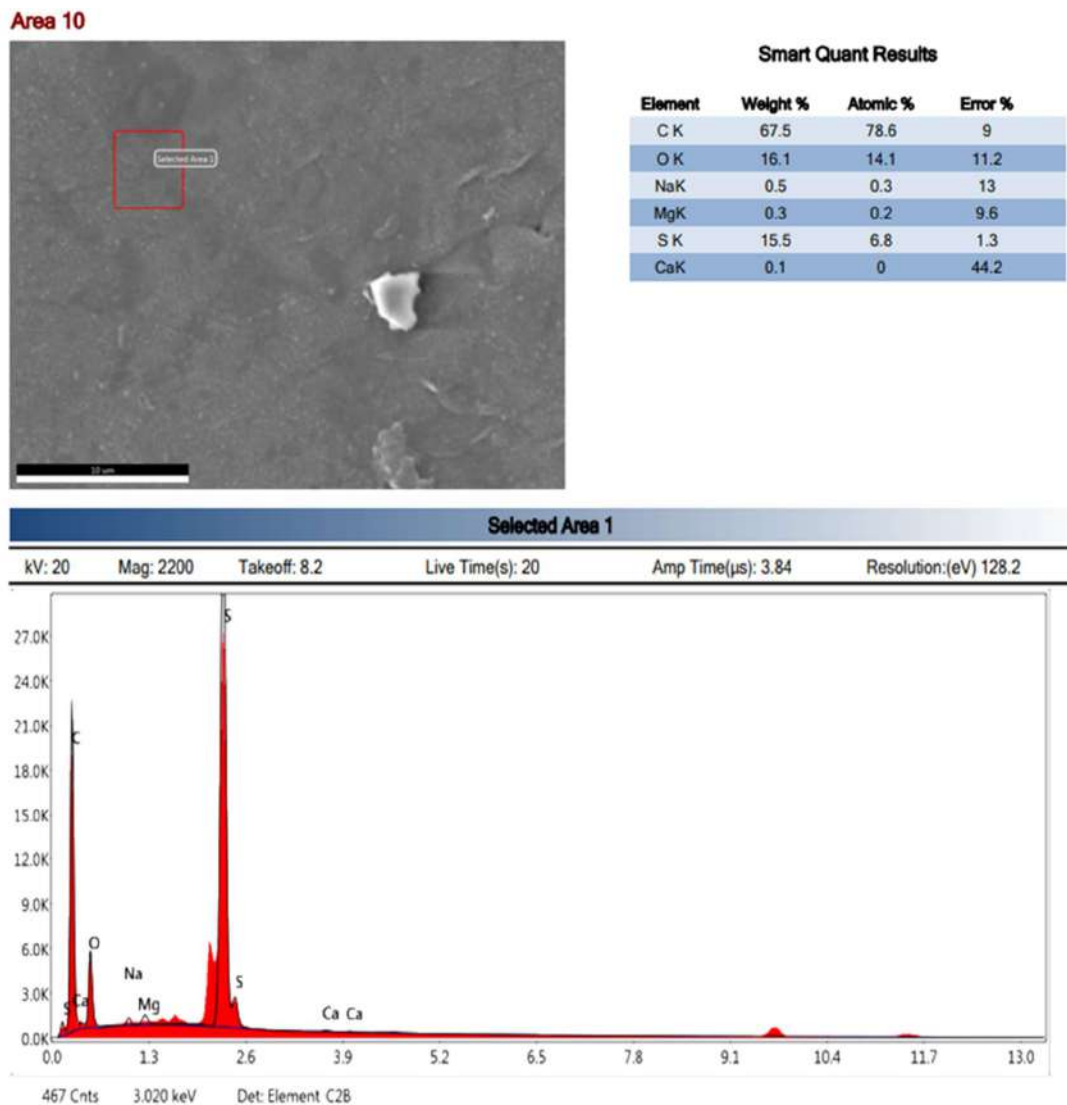
Fig. 8: SEM EDX spectra of the active layer of the chemically cleaned membrane.

chemical cleaning. The membrane's support layer possibly contained trapped sodium chloride, so a sodium peak was also found in the EDX analysis. This suggests the chemical cleaning method does not ensure 100% membrane cleaning.

CONCLUSIONS

A novel compartment configuration FO membrane system was built up for concentrating synthetic secondary treated tannery effluent. Membrane flux was affected by DS concentration. Experiments revealed higher fluxes and lower flux decline ratio for 38 g.L^{-1} NaCl solution as DS when compared with 24 g.L^{-1} NaCl solution, indicating its convenience for concentrating SSTTE. Concentration factors for ions like calcium, magnesium, sodium, chlorides, sulfates,

phosphates, and total chromium were positive, whereas ions like ammonium, potassium, and nitrates had negative concentration factors. Results indicated FO membrane had an excellent rejecting effect. Ions like magnesium and total chromium were largely rejected, whereas ions like ammonium and potassium were less rejected. Solute rejection was affected by DS concentration. Experiments with 24 g.L^{-1} NaCl solution as DS showed low rejection of ions as compared to experiments with 38 g.L^{-1} NaCl solution as DS. FO membrane had low fouling potential, with a fouling layer consisting of humic acid, protein, and polysaccharide. Fouled FO membrane was cleaned by chemical cleaning but still showed foulant deposits recommending more study on membrane cleaning procedures.

NOMENCLATURE

Description	Notation	Unit
Concentration of Draw Solution	C_d	$g.L^{-1}$
Concentration of Feed Solution	C_f	$g.L^{-1}$
Deionized Water	DIW	
Draw Solution	DS	
Effective Membrane Area	S_m	m^2
Feed Solution	FS	
Flux decline ratio	FDR	%
Forward Osmosis	FO	
Internal Concentration Polarization	ICP	
Pure Water Flux	J_w	LMH
Reverse Osmosis	RO	
Reverse Solute Flux	J_s	GMH
Sodium Chloride Solution	NaCl	$g.L^{-1}$
Thin Film Composite	TFC	
Density of Water	ρ	$kg.L^{-1}$
Temperature	T	°C
Concentration of ions on the permeate side	C_p	$mg.L^{-1}$
Volume of permeate from feed to draw side	V_p	L
Volume of DS at the end of the experiment	V_d	L
Concentration polarization	CP	
Concentration factor	CF	
Chemical Oxygen Demand	COD	$mg.L^{-1}$
Biochemical Oxygen Demand	BOD	$mg.L^{-1}$
Total Dissolved Solids	TDS	$mg.L^{-1}$
Synthetic secondary treated tannery effluent	SSTTE	
Solute rejection	SR	%

ACKNOWLEDGMENTS

REFERENCES

Al-Zuhairi, A., Merdaw, A.A., Al-Aibi, S., Hamdan, M., Nicoll, P., Monjezi, A.A., Al-ASwad, S., Mahood, H.B., Aryafar, M. and Sharif, A.O., 2015. Forward osmosis desalination from laboratory to market. *Water Supply*, 15(4), pp.834-844. https://doi.org/10.2166/ws.2015.038

Bhardwaj, A., Kumar, S. and Singh, D., 2023. Tannery effluent treatment and its environmental impact: A review of current practices and emerging technologies. *Water Quality Research Journal*, 58(2), pp.128-152. https://doi.org/10.2166/wqrj.2023.002

Camilleri-Rumbau, M.S., Soler-Cabezas, J.L., Christensen, K.V., Norddahl, B., Mendoza-Roca, J.A. and Vincent-Vela, M.C., 2019. Application of aquaporin-based forward osmosis membranes for processing of digestate liquid fractions. *Chemical Engineering Journal*, 371, pp.583-592. https://doi.org/10.1016/j.cej.2019.02.029

Coday, B.D., Almaraz, N. and Cath, T.Y., 2015. Forward osmosis desalination of oil and gas wastewater: Impacts of membrane selection and operating conditions on process performance. *Journal of Membrane Science*, 488, pp.40-55. https://doi.org/10.1016/j.memsci.2015.03.059

Conidi, C., Fucà, L., Drioli, E. and Cassano, A., 2019. A membrane-based process for the recovery of glycyrrhizin and phenolic compounds from licorice wastewaters. *Molecules*, 24(12), pp.2279. https://doi.org/10.3390/molecules24122279

Costa, C.R., Montilla, F., Morallón, E. and Olivi, P., 2010. Electrochemical oxidation of synthetic tannery wastewater in chloride-free aqueous media. *Journal of Hazardous Materials,* 180(1–3), pp.429-435. https://doi.org/10.1016/j.jhazmat.2010.04.048

Damirchi, M. and Koyuncu, I., 2021. Nutrient recovery from concentrated municipal wastewater by forward osmosis membrane and MgCl2 based draw solution. *Desalination and Water Treatment*, 211, pp.448-455. https://doi.org/10.5004/dwt.2021.26788

Duong, P.H.H. and Chung, T.-S., 2014. Application of thin film composite membranes with forward osmosis technology for the separation of emulsified oil–water. *Journal of Membrane Science*, 452, pp.117-126. https://doi.org/10.1016/j.memsci.2013.10.030

Dutta, S., Dave, P. and Nath, K., 2022. Choline chloride-glycerol (1:2 mol) as draw solution in forward osmosis for dewatering purposes. *Membrane and Water Treatment*, 13(2), pp.63-72. https://doi.org/10.12989/MWT.2022.13.2.063

Gao, Y., Fang, Z., Liang, P. and Huang, X., 2018. The direct concentration of municipal sewage by forward osmosis and membrane fouling behavior. *Bioresource Technology*, 247, pp.730-735. https://doi.org/10.1016/j.biortech.2017.09.145

Gruber, M.F., Johnson, C.J., Tang, C., Jensen, M.H., Yde, L. and Hélix-Nielsen, C., 2012. Validation and analysis of forward osmosis CFD model in complex 3D geometries. *Membranes*, 2(4), pp.764-782. https://doi.org/10.3390/membranes2040764

Han, G., Liang, C.-Z., Chung, T.-S., Weber, M., Staudt, C. and Maletzko, C., 2016. Combination of forward osmosis (FO) process with coagulation/flocculation (CF) for potential treatment of textile wastewater. *Water Research*, 91, pp.361-370. https://doi.org/10.1016/j.watres.2016.01.031

Hancock, N.T., Phillip, W.A., Elimelech, M. and Cath, T.Y., 2011. Bidirectional permeation of electrolytes in osmotically driven membrane processes. *Environmental Science & Technology*, 45(24), pp.10642-10651. https://doi.org/10.1021/es202608y

Hickenbottom, K.L., Hancock, N.T., Hutchings, N.R., Appleton, E.W., Beaudry, E.G., Xu, P. and Cath, T.Y., 2013. Forward osmosis treatment of drilling mud and fracturing wastewater from oil and gas operations. *Desalination*, 312, pp.60-66. https://doi.org/10.1016/j.desal.2012.05.037

Jang, A., Jung, J.-T., Kang, H., Kim, H.-S. and Kim, J.-O., 2017. Reuse of effluent discharged from tannery wastewater treatment plants by powdered activated carbon and ultrafiltration combined reverse osmosis system. *Journal of Water Reuse and Desalination*, 7(1), pp.97-102. https://doi.org/10.2166/wrd.2016.001

Kaul, S.N., Nandy, T., Szpyrkowicz, L., Gautam, A. and Khanna, D.R., 2013. Wastewater management with special reference to tanneries (Second Edition). Discovery Publishing House, New Delhi.

Khraisheh, M., Gulied, M. and AlMomani, F., 2020. Effect of membrane fouling on fertilizer-drawn forward osmosis desalination performance. *Membranes*, 10(9), pp.243. https://doi.org/10.3390/membranes10090243

Kim, S.L., Paul Chen, J. and Ting, Y.P., 2002. Study on feed pretreatment for membrane filtration of secondary effluent. *Separation and Purification Technology*, 29(2), pp.171-179. https://doi.org/10.1016/S1383-5866(02)00073-4

Korenak, J., Hélix-Nielsen, C., Bukšek, H. and Petrinić, I., 2019. Efficiency and economic feasibility of forward osmosis in textile wastewater treatment. *Journal of Cleaner Production*, 210, pp.1483-1495. https://doi.org/10.1016/j.jclepro.2018.11.130

Lay, W.C.L., Zhang, J., Tang, C., Wang, R., Liu, Y. and Fane, A.G., 2012. Factors affecting flux performance of forward osmosis systems. *Journal of Membrane Science*, 394–395, pp.151-168. https://doi.org/10.1016/j.memsci.2011.12.035

Li, P., Lim, S.S., Neo, J.G., Ong, R.C., Weber, M., Staudt, C., Widjojo, N., Maletzko, C. and Chung, T.S., 2014. Short and long-term performance of the thin-film composite forward osmosis (TFC-FO) hollow fiber membranes for oily wastewater purification. *Industrial & Engineering Chemistry Research*, 53(36), pp.14056-14064. https://doi.org/10.1021/ie502365p

Li, Z., Valladares Linares, R., Bucs, S., Fortunato, L., Hélix-Nielsen, C., Vrouwenvelder, J.S., Ghaffour, N., Leiknes, T. and Amy, G., 2017. Aquaporin based biomimetic membrane in forward osmosis: Chemical cleaning resistance and practical operation. *Desalination*, 420, pp.208-215. https://doi.org/10.1016/j.desal.2017.07.015

Luo, W., Xie, M., Song, X., Guo, W., Ngo, H.H., Zhou, J.L. and Nghiem, L.D., 2018. Biomimetic aquaporin membranes for osmotic membrane bioreactors: Membrane performance and contaminant removal. *Bioresource Technology*, 249, pp.62-68. https://doi.org/10.1016/j.biortech.2017.09.170

Mondal, M. and De, S., 2015. Characterization and antifouling properties of polyethylene glycol doped PAN–CAP blend membrane. *RSC Advances*, 5(49), pp.38948-38963. https://doi.org/10.1039/C5RA02889B

Morrow, C.P. and Childress, A.E., 2019. Evidence, determination, and implications of membrane-independent limiting flux in forward osmosis systems. *Environmental Science & Technology*, 53(8), pp.4380-4388. https://doi.org/10.1021/acs.est.8b05925

Nguyen, T.A. and Yoshikawa, S., 2019. Modeling and economic optimization of the membrane module for ultrafiltration of protein solution using a genetic algorithm. *Processes*, 8(1), p.4. https://doi.org/10.3390/pr8010004

Omir, A., Satayeva, A., Chinakulova, A., Kamal, A., Kim, J., Inglezakis, V.J. and Arkhangelsky, E., 2020. The behavior of aquaporin forward osmosis flat sheet membranes during the concentration of calcium-containing liquids. *Membranes*, 10(5), p.108. https://doi.org/10.3390/membranes10050108

Ortega-Bravo, J.C., Ruiz-Filippi, G., Donoso-Bravo, A., Reyes-Caniupán, I.E. and Jeison, D., 2016. Forward osmosis: Evaluation of thin-film-composite membrane for municipal sewage concentration. *Chemical Engineering Journal*, 306, pp.531-537. https://doi.org/10.1016/j.cej.2016.07.085

Pal, P., Chakrabortty, S., Nayak, J. and Senapati, S., 2017. A flux-enhancing forward osmosis–nanofiltration integrated treatment system for the tannery wastewater reclamation. *Environmental Science and Pollution Research*, 24(18), pp.15768-15780. https://doi.org/10.1007/s11356-017-9206-z

Panizza, M. and Cerisola, G., 2004. Electrochemical oxidation as a final treatment of synthetic tannery wastewater. *Environmental Science & Technology*, 38(20), pp.5470-5475. https://doi.org/10.1021/es049730n

Pham, M.T., Nishihama, S. and Yoshizuka, K., 2021. Removal of chromium from the water environment by forward osmosis system.

MATEC Web of Conferences, 333, p.04007. https://doi.org/10.1051/matecconf/202133304007

Pophali, G.R. and Dhodapkar, R.S., 2011. An overview of sustainability of common effluent treatment plant for clusters of tanneries. *Environment, Development and Sustainability*, 13(3), pp.493-506. https://doi.org/10.1007/s10668-010-9272-6

Pramanik, B.K., Roddick, F.A. and Fan, L., 2014. Effect of biologically activated carbon pre-treatment to control organic fouling in the microfiltration of biologically treated secondary effluent. *Water Research*, 63, pp.147-157. https://doi.org/10.1016/j.watres.2014.06.014

Ramteke, P.W., Awasthi, S., Srinath, T. and Joseph, B., 2010. Efficiency assessment of common effluent treatment plant (CETP) treating tannery effluents. *Environmental Monitoring and Assessment*, 169(1–4), pp.125-131. https://doi.org/10.1007/s10661-009-1156-6

Ranganathan, K. and Kabadgi, S.D., 2011. Studies on the feasibility of reverse osmosis (membrane) technology for the treatment of tannery wastewater. *Journal of Environmental Protection*, 02(01), pp.37-46. https://doi.org/10.4236/jep.2011.21004

Roy, D., Rahni, M., Pierre, P. and Yargeau, V., 2016. Forward osmosis for the concentration and reuse of process saline wastewater. *Chemical Engineering Journal*, 287, pp.277-284. https://doi.org/10.1016/j.cej.2015.11.012

Sagiv, A., Zhu, A., Christofides, P.D., Cohen, Y. and Semiat, R., 2014. Analysis of forward osmosis desalination via two-dimensional FEM model. *Journal of Membrane Science*, 464, pp.161-172. https://doi.org/10.1016/j.memsci.2014.04.001

She, Q., Jin, X., Li, Q. and Tang, C.Y., 2012. Relating reverse and forward solute diffusion to membrane fouling in osmotically driven membrane processes. *Water Research*, 46(7), pp.2478-2486. https://doi.org/10.1016/j.watres.2012.02.024

Sundarapandiyan, S., Chandrasekar, R., Ramanaiah, B., Krishnan, S. and Saravanan, P., 2010. Electrochemical oxidation and reuse of tannery saline wastewater. *Journal of Hazardous Materials*, 180(1–3), pp.197-203. https://doi.org/10.1016/j.jhazmat.2010.04.013

Suthanthararajan, R., Ravindranath, E., Chits, K., Umamaheswari, B., Ramesh, T. and Rajamam, S., 2004. Membrane application for recovery and reuse of water from treated tannery wastewater. *Desalination*, 164(2), pp.151-156. https://doi.org/10.1016/S0011-9164(04)00174-2

Sweity, A., Oren, Y., Ronen, Z. and Herzberg, M., 2013. The influence of antiscalants on biofouling of RO membranes in seawater desalination. *Water Research*, 47(10), pp.3389-3398. https://doi.org/10.1016/j.watres.2013.03.042

Tasci, R. O., Kaya, M. A. and Celebi, M., 2022. Hydrophilicity and flux properties improvement of high-performance polysulfone membranes via sulfonation and blending with Poly(lactic acid). *High-Performance Polymers*, 34(10), pp. 1115–1130. https://doi.org/10.1177/09540083221110031

Thiruvenkatachari, R., Francis, M., Cunnington, M. and Su, S., 2016. Application of integrated forward and reverse osmosis for coal mine wastewater desalination. *Separation and Purification Technology*, 163, pp. 181–188. https://doi.org/10.1016/j.seppur.2016.02.034

Vital, B., Bartacek, J., Ortega-Bravo, J. C. and Jeison, D., 2018. Treatment of acid mine drainage by forward osmosis: Heavy metal rejection and reverse flux of draw solution constituents. *Chemical Engineering Journal*, 332, pp. 85–91. https://doi.org/10.1016/j.cej.2017.09.034

Zaviska, F., Chun, Y., Heran, M. and Zou, L., 2015. Using FO as pre-treatment of RO for high scaling potential brackish water: Energy and performance optimization. *Journal of Membrane Science*, 492, pp. 430–438. https://doi.org/10.1016/j.memsci.2015.06.004

Zhao, J., Wu, Q., Tang, Y., Zhou, J. and Guo, H., 2022. Tannery wastewater treatment: Conventional and promising processes, an updated 20-year review. *Journal of Leather Science and Engineering*, 4(1), pp. 10. https://doi.org/10.1186/s42825-022-00082-7

Review Research Paper   https://doi.org/10.46488/NEPT.2025.v24i01.D1662   **Open Access Journal**

A Review on Extended Producer Responsibility Schemes for Packaging Waste Management and Research Gaps in the Field

T. T. Y. Anh[1,2]† (ID)**, S. Herat[1]** (ID) **and K. Prasad[2]** (ID)

[1]School of Engineering and Built Environment, Griffith University, Queensland 4111, Australia
[2]The University of Danang-University of Technology and Education, 48 Cao Thang St., Hai Chau Dist., Danang city, Vietnam
†Corresponding author: T.T.Y. Anh, thiyenanh.tran@griffithuni.edu.au

ABSTRACT

Recently, Extended Producer Responsibility (EPR) schemes have been considered as potential policies for solid waste management and many countries have applied them. Researchers, authorities, and producers need a comprehensive and up-to-date understanding of EPR. Therefore, this literature review aims to review the current research status of EPR implementation on packaging, to highlight actual experiences conducting EPR, and to find research gaps. Results indicate that during the last 5 years, there has been an increase in the amount of research on EPR in packaging and that packaging waste recycling under this scheme is the most considered activity. Additionally, the primary metrics used to assess the efficacy of EPRs are recycling and reducing packaging waste. According to the lessons learned, applying EPR to packaging should take stakeholder engagement, policy design, transparency, and incentive strategy into account. Additionally, knowing the economic effectiveness problems small- and medium-sized packaging companies face, the effectiveness of EPR methods on various materials and geographical areas, and the efficacy of monitoring methods are the main areas that need to be researched.

INTRODUCTION

A sustainable waste management policy framework known as Extended Producer Responsibility (EPR) is emerging as a potent organizational and economic instrument (Barbara et al. 2022, Septianingrum et al. 2023). Over the next twenty years, research on EPR is anticipated to increase as more scholars pay attention to these issues (Cai & Choi 2021). This scheme requires manufacturers to take responsibility for every phase of the life cycle of their products, from manufacturing to disposal. This initiative aims to encourage companies to minimize the harmful environmental effects of their packaging and goods by recycling, reusing, and efficiently disposing of them.

Packaging is essential for containment, protection, preservation, shipping, handling, and sales in today's product business (EPA 2023). However, most packaging items are single-use and become garbage after use, resulting in an extremely short product life cycle (Rubio et al. 2019). Therefore, its widespread usage raises substantial environmental issues regarding packaging waste (GIZ 2022, Oscar et al. 2022). In recent years, different nations have applied EPR frameworks to packaging waste management (Destyanto et al. 2019, Rubio et al. 2019). They have applied various EPR approaches in the field of packaging, ranging from stringent legislative requirements to voluntary industry-led programs, each with its aims, methods, and outcomes (Bakar & Mohamed 2023, Mayanti & Helo 2024, Morashti et al. 2022, Pruess & Garrett 2024, Rubio et al. 2019)

Previous studies on EPR performance in packaging have focused on various aspects such as cost-benefit analyses (Marques et al. 2014), effectiveness (Andreasi et al. 2020, Colelli et al. 2022, Löhle 2021, Massarutto 2014, Niza et al. 2014), policy effectiveness and trends (Lorang et al. 2022, Niza et al. 2014, Rubio et al. 2019), and the impact on different responsibility schemes (Arnaud 2015, Gupt & Sahay 2015, Harris et al. 2021, Kim 2012). Still, to the best of the authors' knowledge, no scoping review exists about EPR initiatives for packaging waste. Therefore, this review is conducted for several purposes. First, it seeks to identify and collect relevant literature on the effectiveness of EPR programs in packaging waste management. Second, the study intends to provide policymakers and industry stakeholders with lessons learned from real-life, evidence-based insights into the implementation of the EPR scheme in the packaging sector. Finally, the review will highlight research trends and gaps regarding packaging waste EPR schemes. These aims can be achieved by answering three questions, including "Is implementing the EPR schemes on packaging effective?", "What are the research trends and research gaps on the EPR programs in packaging?" and "What are the lessons learned from implementing EPR schemes on packaging worldwide?"

The article is divided into five sections. The introduction covers the study's goals and the research background. Next, the methodology section provides a detailed explanation of the methods used throughout the investigation. Then, the results section goes into the main findings from the literature review. Finally, the conclusion section summarises the analysis's key findings and suggests future research.

OVERVIEW OF EPR PROGRAMS ON PACKAGING

The European Union (EU) Directive 94/62/EC on Packaging and Packaging Waste, which was adopted by EU member states in 1994 (European Commission 1994), was one of the first reactions to enhance packaging waste management practices. This legislation represented the start of a large government response to the global issue of packaging waste, focusing on packaging waste in Europe. Since then, several political and economic instruments have been developed and geared toward solutions that necessitate increased producer leverage in dealing with problematic materials in the marketplace (Diggle & Walker 2022). Packaging materials (including beverage containers) make up approximately 17% of total EPR schemes globally, whereas waste from electrical and electronic equipment (WEEE) accounts for 35% of programs, tires account for 17%, and use oil, paint, chemicals, big appliances, and light bulbs account for 20% (Kaffine & O'Reilly 2013). By 2024, the application of the

EPR scheme in packaging has gained popularity in many places throughout the world. However, the specific status of EPR implementation varies greatly by jurisdiction, with some regions making tremendous progress while others are still in the planning and enforcement stages.

Europe

The implementation of EPR programs for packaging in Europe is the first of its kind in the global search for sustainable waste management practices. European nations have been at the forefront of adopting and refining EPR regulations for packaging materials due to their proactive dedication to environmental protection.

In the 1990s, the EU took strong legislative measures to manage and reduce packaging waste, and EPR was accepted as one of the primary policy tools within a comprehensive plan aimed at reducing landfill usage and recycling waste (Walter et al. 2019). With the adoption of EU Directive 94/62/EC on Packaging and Packaging Waste in 1994, the EU started legal measures towards improved recovery and diverting landfills of the rising amounts of domestic packaging trash that many European countries were disposing of annually (European Union 2020). The EU Directive 94/62/EC specifies current overall package recycling objectives of 55% until 2025, with a 25% by-weight plastic recycling target (European Commission). Many European countries that have implemented an EPR program for packaging have established plastic recycling rates that comply with or exceed the EU's current recycling objectives (Eurostat). New standards will demand at least 65% by weight of all packaging waste be recycled by December 31, 2025, with 50% targets varied by material for plastic recycling. Furthermore, by December 31, 2030, objectives will be raised to require that at least 70% by weight of all packaging waste be recycled, with a 55% recycling target for plastic. In 2019, Lithuania and Czechia had the largest plastics recycling rates in the EU, although presently, very little analysis is available on the administration and efficacy of these member states' programs. Meanwhile, companies in the Netherlands must obey the rules from the 2014 Packaging Management Decree. EPR covers to all packaging, and only producer responsibility organisation (PRO), 'Afvalfonds Verpakkingen', is responsible. Since the program's inception in 2008, the Netherlands has achieved considerable advances in EPR for packaging (European Environment Agency 2022).

America

Countries in North and South America have recognized the environmental impact of packaging waste, so they have integrated EPR frameworks into their waste management

strategies early on. From the 1970s, the United States was one of the early users of EPR for numerous materials, employing advanced-disposal fees for hazardous wastes, WEEE, and beverage containers. Oregon and Maine have currently established fee-based, obligatory EPR programs for packaging waste. In 2021, Oregon passed the Plastic Pollution and Recycling Modernisation Act, and Maine passed LD 1541, an "Act to support and improve municipal recycling programs and save taxpayer money" (Maine Department of Environmental Protection, Oregon Department of Environmental Quality). Additionally, Canada, at present, has five regional EPR programs implemented for packaging. Ontario was the first province to launch the program in 2004, followed by Québec in 2005, Manitoba in 2010, British Columbia in 2014, and Saskatchewan in 2016 (Diggle & Walker 2020). Harmonized EPR for packaging trash adoption in Canada has been identified as an essential phase for improved entire plastic waste management and a circular plastics economy (Canadian Council of Ministers of the Environment 2019, Diggle & Walker 2020). Moreover, Chile authorized a mandatory EPR program for packaging in June 2019 via the EPR Decree for Packaging (Prevent Waste Alliance 2021a). In addition, regarding Resolution No. 0191, Venezuela adopted an obligatory EPR program for packaging in 2020 (Gonzalez 2020).

Africa

The implementation of the EPR framework for packaging waste in African countries has had a variety of applications. As of May 2021, the South African Ministry of Forestry, Fisheries, and the Environment approved Section 18 of the National Waste Management Act for a national fee-based, mandatory EPR for packaging that covers paper, packaging, and some single-use (Arp et al. 2021, Geyer et al. 2017, Prevent Waste Alliance 2021b). In 2020, Kenya took significant steps, with the Ministry of Environment and Forestry enacting legislation to authorize fee-based, mandatory EPR schemes for packaging materials (WWF 2022). In 2014, the Nigerian government implemented optional EPR for products and packaging by establishing guidelines for EPR policy implementation through the National Environmental Standards and Regulations Enforcement Agency (Ajania & Kunlerea 2019). In Africa, continuous efforts are being made to apply EPR for packaging in the foreseeable future.

Asia

Currently, the state of EPR implementation for packaging differs across Asia. EPR programs for packaging materials are mandated in Taiwan, South Korea, Japan, and Vietnam. In 1998, Taiwan's Waste Disposal Act approved an EPR

program for packaging materials (Taiwan Environmental Protection Agency 2021). In 2003, South Korea began a program with the passage of the Act on Promoting Resource Saving and Recycling (Prevent Waste Alliance 2021c) that covers four packaging materials (paper packaging, glass bottles, metal cans, and plastic packaging) under this EPR program (Ministry of Environment 2010). In 1995, Japan's packaging EPR program began with the Act on the Promotion of Sorted Collection and Recycling of Containers and Packaging. During the first decade of the program's implementation, Japan's program was regarded as advantageous between 1997 and 2010; package recycling rates increased by 27% (OECD 2014).

Furthermore, in 2020, India established an EPR program via the Rules for Plastic Waste Management exclusively for plastic packaging materials, which it called the Uniform Framework of EPR (India Ministry of Environment 2020). India's EPR scheme has evolved from the voluntary proactiveness among its stakeholders (Pani & Pathak 2021). In the Philippines, recyclers and private-sector actors conduct several voluntary schemes (Johannes et al. 2021). Indonesia has an EPR framework for packaging under the Law of Solid Waste Management (2008), which is reinforced by Ministerial Regulation 81/2012. However, this framework has never been applied (Johnson 2022). Furthermore, since 2010, Australia has run a voluntary packaging industry program called the Australian Packaging Covenant, which seeks to improve the environmental effects of packaging materials. Signatories must follow an action plan and report yearly, although they are not subject to a mandated EPR program (Australian Packaging Covenant Organization 2017). From January 1, 2024, EPR in the field of packaging in Vietnam was adopted by Decree No. 08/2022/ND-CP. Each type of packaging that must be recycled will have a mandated recycling rate determined by the package's life cycle, disposal and collection rate, national recycling objectives, environmental protection standards, and socioeconomic factors (The Government of Vietnam 2022).

MATERIALS AND METHODS

The effectiveness of various monitoring systems for EPR scheme compliance in packaging is investigated in this study using qualitative and quantitative methods to meet the aforementioned goals. Moreover, this review protocol followed the Preferred Reporting Items for Systematic Reviews and Meta-Analyses (PRISMA) reporting standards (Liberati et al. 2009). To identify future research direction and trends in the fields of packaging waste management, a three-stage review technique was employed, comprising planning, searching, and reporting (Johnsen et al. 2017,

Tranfield et al. 2003). Details of the search method are described in the next section.

Stage 1: Planning

In the planning stage, the potential benefit of undertaking a systematic literature review on the EPR schemes within the packaging sector was identified in consideration of a) the growing number of countries that are planning or implementing EPR, b) the importance of packaging and the environmental impact of packaging waste, c) the hesitation of the government authorities on managing EPR for packaging sector throughout the implementation stage, d) the difficulties of gaining knowledge of the efficacy, and e) the research directions of EPR in the packaging context. Second, the PCC framework is applied to establish the fundamental analysis and research questions (Table 1) (Pollock et al. 2023). Finally, three research questions are defined to accomplish the paper's aims.

Stage 2: Searching

The search stage for a literature review involves an in-depth identification of relevant publications. A clear and organized review procedure was developed, including the search strategy, inclusion and exclusion criteria, and data extraction and synthesis process.

On March 26, 2024, a thorough online search was performed through Scopus and Web of Science using three keywords: "Extended Producer Responsibility", "EPR", and "packaging", to guarantee complete coverage of accessible literature. These databases use a consistent search syntax, made possible using Boolean operators (AND, OR) to link the keywords efficiently (see Table 2). The "TITLE-ABS-KEY" field was chosen for the term "packaging" in all databases to avoid limiting the sample size because it might not always appear in titles and abstracts, or it might appear as sources (food and beverage, pharmacy, agriculture, etc.) or material (carton, plastic, paper, etc.). This stage also strictly enforced inclusion and exclusion criteria (Mengist et al. 2020). The Preferred Reporting Items for Systematic Reviews and Meta-Analyses (PRISMA) criteria were used to screen the publications to evaluate their relevance to

Table 1: PCC framework elements of the paper.

PCC element	Feature in this review
Population	NA *
Concept	Extended Producer Responsibility schemes for packaging waste management
Context	Across the world

* Not applicable here because we examined EPR frameworks broadly, not a particular population or condition.

the study issue (Morashti et al. 2022). Only peer-reviewed papers published in English that focused on EPR programs in packaging were evaluated. Additionally, duplicate articles, inaccessible articles, and non-peer-review journals, i.e., conference proceedings, grey literature, and book chapters, were excluded. The titles and abstracts of the records were reviewed, and publications that did not fulfill the inclusion requirements were discarded (Saeed et al. 2019). The writer carefully reviewed the remaining publications' contents to remove irrelevant articles. The process of searching all manuscripts was conducted via Covidence software, and a final collection of 51 qualified articles was produced. Details of the search protocol for this review are shown in Fig. 1.

Stage 3: Reporting

Following the multi-step searching phase, Microsoft Excel was used to extract data, and the VOSviewer was chosen to develop networks, highlighting relationships among the studied data. This software helped to generate a map that shows publishing trends and the major subject areas with the greatest interest in the study topic. Because keyword data in Web of Science and Scopus is inconsistent, generating maps with this program requires a thesaurus file containing keywords with the same meaning (Eck & Waltman 2019). To illustrate this, keywords such as "Extended Producer

Table 2: The search queries conducted and the total number of articles.

Databases	Searching string and searching terms	No of articles
Scopus	(TITLE ("Extended Producer Responsibility") OR TITLE ("EPR"))	19,951
	(TITLE ("Extended Producer Responsibility") OR TITLE ("EPR") AND TITLE-ABS-KEY ("packaging"))	64
	(TITLE ("Extended Producer Responsibility") OR TITLE ("EPR") AND TITLE-ABS-KEY ("packaging")) AND (LIMIT-TO (LANGUAGE , "English")) AND (LIMIT-TO (DOCTYPE , "ar") OR LIMIT-TO (DOCTYPE , "re")) AND (LIMIT-TO (SRCTYPE , "j")) AND (LIMIT-TO (PUBSTAGE , "final"))	*44*
Web of Science	"Extended Producer Responsibility" (Title) or "EPR" (Title)	19,758
	"Extended Producer Responsibility" (Title) or "EPR" (Title) and "packaging" (*a*ll *fields*)	208
	"Extended Producer Responsibility" (Title) or "EPR" (Title) and "packaging" (* *exclude criteria*)	163
Sum		**207**

Note. Date of acquisition: March 26, 2024
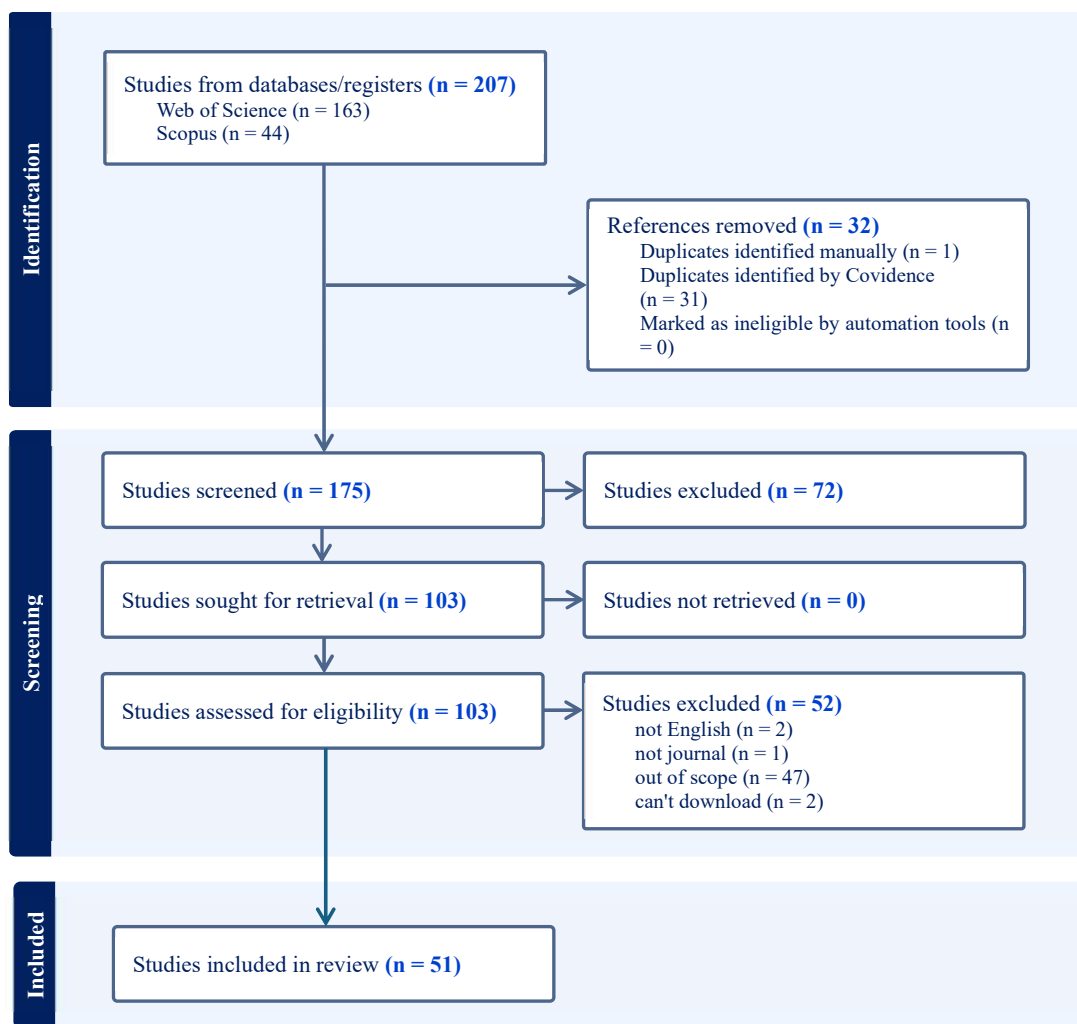
Fig. 1: The PRISMA flow chart showing the process of selecting articles.

Responsibility", "Extended Producer Responsibility (EPR)", and "responsibility" were combined into a single phrase, "Extended Producer Responsibility". The thesaurus summary is listed in Table 3.

The data were analyzed and organized into five categories: bibliometric and network analysis, literature analysis, lesson learned, and research gaps. The final report aims to contribute to the body of knowledge and practices on EPR schemes in packaging, offering valuable insights for improving solid waste management.

RESULTS AND DISCUSSION

Bibliometric and Network Analysis

The analysis of the 51 articles collected from Scopus and Web of Science indicates that, before 2000, no journal article

Table 3: Thesaurus of various keywords.

Keyword	Replaced by
Extended producer responsibility (EPR) EPR	Extended producer responsibility
European Union	Europe
Product packaging	Packaging
Plastic waste	Packaging waste
Economic aspect	Economics
Government regulation Environmental policy	Policy
Plastic	Plastics
Environmental management Waste management	Management
Priority journal	
Sustainability	Sustainable development
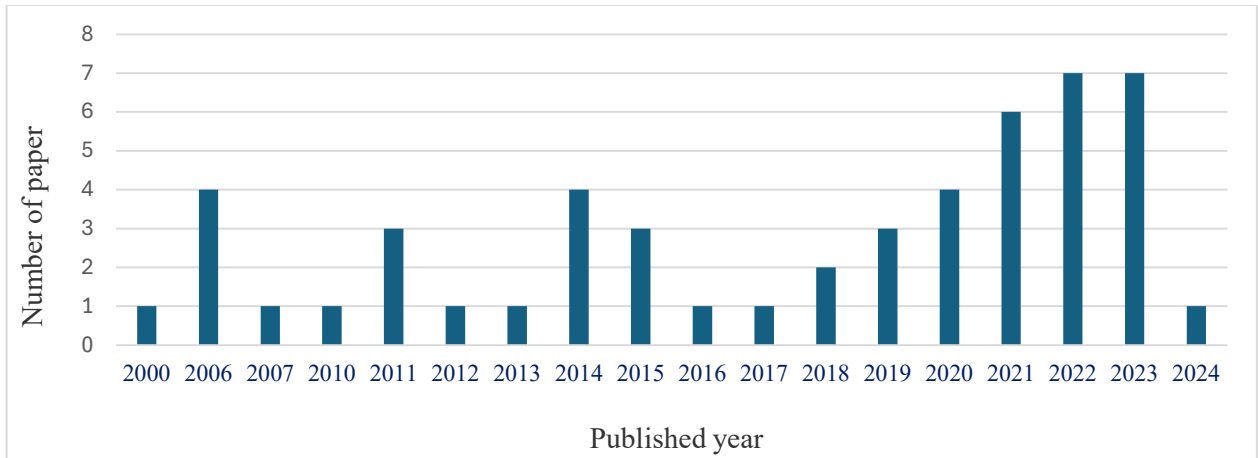
* Note: The total for articles published in 2024 has not been completed because the search period ended on March 26, 2024.

Fig. 2: Number of published papers annually.

could be found on the topic of EPR on packaging. Moreover, between 1991 and 2023, a small number of articles were published before 2018, as shown in Fig. 2, with 7 papers (14 %) published from 2000 to 2010 and 16 papers (31 %) published between 2011 and 2018. In line with trends in publications on "EPR on packaging", 28 papers (55%) articles that were gathered for examination in this study were published between 2019 and 2024, meaning the continuous rapid growth of packaging management under the EPR programs' research papers in recent years, because EPR and CE concepts have increased in significance since 2010.

The literature analysis also reveals the top journals with the largest number of articles, as follows: Waste Management and Research (8), Journal of Cleaner Production (7), Journal of Industrial Ecology (5), Waste Management (4), and Resources, Conservation and Recycling (3). Moreover, regarding publications published by the country, it is revealed that most publications are from Europe (10), Canada (4), China (3), and the United States (2). Few publications on "EPR on packaging" originated in developing nations compared to developed countries, namely Europe, where nations are leading EPR activities, such as Indonesia, Iran, India, etc.

This analysis only includes terms that appear at least four times. Of these terms (513), 40 fulfilled the criteria, which decreased to thirty-one after applying the thesaurus file. The frequency map of these terms is shown in Fig. 3. The thickness of the lines represents the strength of the relationship among the nodes (keywords), which was calculated using the number of papers in which the two keywords appeared together. The distance between nodes represents their relationship and the similarity of their themes, with shorter distances indicating tighter links. The most commonly recurring keyword is "Extended Producer

Responsibility" (n=38), which is essential to the map. Other frequent keywords include "management" (n=27), "recycling" (n=25), "packaging" (n=22), and "packaging waste" (n=15), among others. The map shows that plastic is the most common material and has generated more research interest than other materials in the packaging industry under EPR initiatives. This map also shows that recycling is mostly considered to promote solid waste management.

Fig. 4 depicts the time-series growth of the subjects in the examined 51 chosen papers published between 1991 and 2024. The articles' themes were restricted to "environmental planning", "cost-benefit analysis," and "landfill" by 2014. From 2016 to 2018, subjects have expanded to include "Extended Producer Responsibility", "management", "policy", and "Europe". However, in 2018, the issues that garnered the most interest are "circular economy", "sustainability", and "recycling". These challenges are expected to grow in the future since they have received media attention and are part of government policy. In contrast, waste treatment research has declined over time.

Regarding the research methodologies, there is a predominant focus on quantitative methods, which comprised 76% of the approaches employed. This means that statistical inference in this research field is widespread. In addition, qualitative methods were also found, to a lesser extent, with 4% of the approaches dedicated to in-depth exploration and understanding of actual case studies. A mixed-method approach was used in14% of the total in addressing complex research questions. These methodological approaches offer a clear picture of EPR frameworks in packaging.

Some Facts About the Effectiveness of EPR Scheme on Packaging
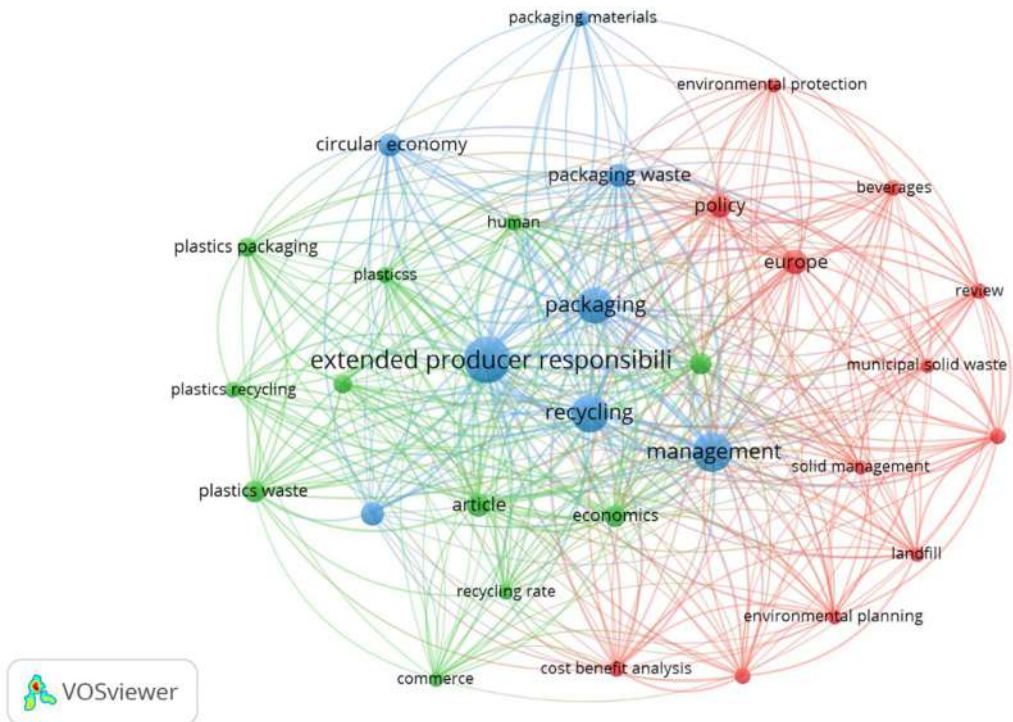
Fig. 3: Keywords Co-occurrence in 51 publications.
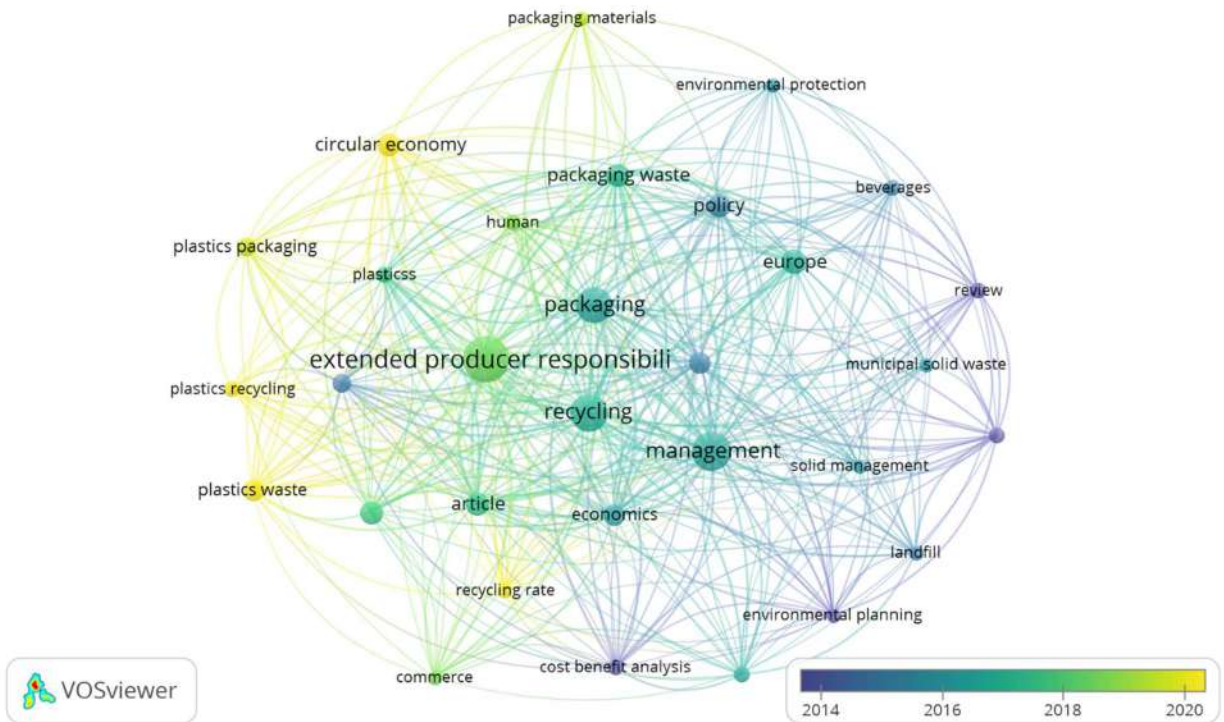
Fig. 4: Topics throughout the research period.

Understanding EPR's influence on waste management is critical for assessing its contribution to encouraging sustainable behaviors, lowering environmental damages, and creating a circular economy. This section analyses empirical data, case studies, and expert opinions to examine real-life cases and potential opportunities for implementing EPR programs in the context of packaging waste.

Waste Reduction and Recycling Rates

Overall, EPR for packaging has been effectively implemented across Europe in accordance with European Parliament and Council Directive 94/62/EC goals (Cahill et al. 2011). Germany and Austria have drastically decreased the total amount of packaging on the marketplace, used less material in packaging, and recycled more packaging. For example, between 1991 and 1997, Germany decreased packaging waste by 1.4 million tons (13%), encouraged by EPR legislation and industry cooperation. According to surveys of producers in Germany and Austria, implementing an obligatory EPR policy has been the critical driver of package optimization. (Quinn & Sinclair 2006). Furthermore, the economies of Portugal and Spain have been able to boost recycling and recovery rates over the years in the direction of the EU goals: a) achieving 100% of the area's coverage, b) growing the quantities of waste selectively collected, c) raising the public's understanding of the importance of recycling through constantly awareness campaigns for the individuals, d) supporting recycling of recyclable materials from the undifferentiated collection, and e) promoting recycling of recyclable materials (Niza et al. 2014, Rubio et al. 2019). An investigation of the EPR for plastic packaging waste in Spain, Italy, France, Germany, and Poland found that the EPR systems also helped enhance recycling rates. In addition, between 2006 and 2018, waste collection rates rose while employing the EPR system. EPR initiatives have demonstrated outstanding achievements in plastic packaging waste collection and recycling, meeting waste management expenses, and varied effectiveness, depending on each country's environment. (Lorang et al. 2022). The EU's recovery and recycling programs for food and beverage containers (and other packaging waste), such as the Belgian Fost Plus and German Green Dot System, reflect EPR's success. More than 130,000 enterprises currently participate in the Green Dot scheme, and the Green Dot emblem appears on 460 billion consumer items. Furthermore, approximately 14.7 million tonnes of used packaging trash was collected and repurposed by European organizations (Agamuthu & Visvanathan 2014).

In Canada, before the EPR program's adoption in 1989, beverage litter constituted 72% of the waste collected in the region, and by 2004, this was reduced to 7.5% (Ajania & Kunlerea 2019). Beverage container EPR programs have produced significant recovery rates, frequently surpassing 80% (McKerlie et al. 2006, Quinn & Sinclair 2006). However, a study by Harris et al. (2021) revealed that there was no decrease in shoreline pollution levels in British Columbia after implementing the EPR policy for packaging (Harris et al. 2021).

Except for Korea, the writers could not locate much information about waste reduction and recycling under EPR initiatives in Asian nations. Since implementing the EPR scheme in 2003, product recycling in Korea has steadily grown. Between 2003 and 2007, 6,069,000 tonnes of waste materials were recycled. In 2007, recycling rose by 32.3% compared to the period before the EPR system was adopted (Kim 2012). However, according to Kim & Mori (2015), the recycling rate in Korea between 2000 and 2011 decreased from 59% to 40%, respectively, and the recycling volume fell accordingly. The fundamental reason for this decline is that small and medium-sized producers are not subjected to mandatory recycling under the EPR program.

Eco-Design and Innovation in the Packaging Industry

EPR schemes motivate producers to consider environmental concerns in product design and promote consumer knowledge about the environmental effect of products, resulting in greater demand for eco-friendly products and packaging, thus inspiring producers to implement eco-design practices (Barbara et al. 2022, Schamber & Bon 2022, Susanna et al. 2017, Wiesmeth & Hackl 2011, Peng et al. 2020). However, unfortunately, excluding British Columbia, EPR has had much less of an impact on product innovation and ecological design (Massarutto 2014, Walls 2006). The producer responsibility system in British Columbia encouraged redesigns of 2-liter soft drink bottles because of glass breakage and recyclability difficulties. The shift to thinner plastic walls with molded ridges for structural support reflects the EPR program's goal of encouraging industry-wide transitions toward more sustainable packaging (McKerlie et al. 2006). By contrast, Røine & Lee (2008) showed that the majority of companies in Norway's plastic packaging sector do not prioritize environmental concerns, such as green goods and eco-design. While specific industrial organizations and Producer Responsibility Organisations promote eco-design, the reaction from businesses has been limited. Similarly, in India, under the EPR initiative, producers and users of plastic packaging have investigated innovative alternatives, such as bamboo for items such as straws, bowls, plates, and cutlery, with local trials. At the same time, the Indian government and stakeholders have experimented with various technologies such as incineration, use in road construction, and fuel oil conversion to add value to plastic waste management.

Nevertheless, these acts are infrequent, and the outcomes are not ideal (Pani & Pathak 2021). In addition, according to the mechanism test of Peng et al. (2020), the EPR system may promote companies that develop innovative green technology through government subsidies, but it has little effect on encouraging the development of green technology through corporate environmental responsibility. Similarly, the authors' heterogeneity research revealed that the EPR system promotes corporate green technology innovation more significantly in non-state-owned and non-high-tech businesses.

Public Awareness

Rubio et al. (2019) showed that conducting EPR policies favored waste awareness over time in Portugal and Spain. This is apparent in the population's growing understanding of the importance of recycling, which has been assisted by continuing awareness programs to encourage recycling recyclable goods from undifferentiated collections. In addition, the Green Dot program in Germany, including more than 130,000 companies and 460 billion consumer packages indicates the growth in public awareness of recovery and recycling waste. Similarly, the FostPlus initiative in Austria has been successful, with 95% of residents sorting their waste packaging for recycling (Agamuthu & Visvanathan 2014).

In conclusion, these international performance outcomes of EPR practices indicate the importance of EPR schemes in terms of the amount of packaging waste, recycling rates, public awareness, and eco-design. Unfortunately, information about stakeholder collaboration, financial effectiveness, energy savings, and job creation could not be obtained through the collected articles. Therefore, despite such apparent success, the effectiveness of the EPR frameworks could not be easily concluded from the preceding information. It can also be said that recycled and reduced rates of packaging waste are the primary and more manageable factors used for evaluating EPR effectiveness, and there is a lack of control and study on other efficiencies of EPR schemes. These gaps should be examined more in the foreseeable future by continuously evaluating and reviewing them in different databases, such as NGOs and government reports, conference proceedings, etc.

Lessons Learned on EPR Implementation for Packaging Around the World

The global examination of EPR programs for packaging brings valuable insights and lessons for policymakers, industry stakeholders, and environmental campaigners alike. As governments face the complex problems of controlling packaging waste and achieving sustainability goals, examining the experiences and achievements of EPR projects provides significant information for developing successful policies and strategies. In this review, numerous critical lessons have emerged from adopting EPR programs for packaging globally, shining a light on packaging waste management approaches.

Policy Design

The policy design for EPR adoption in packaging waste management is critical (Carola 2000). Specific targets, objectives, and processes in EPR regulations motivate action and stimulate the creation of waste management systems to achieve goals. In 2021, the research results of a case study in British Columbia revealed that there had been no improvement in pollution levels following the implementation of an inadequate EPR policy for packaging to minimize shoreline pollution, indicating the need for policy interventions (Harris et al. 2021). Lessons learned from the research findings of Park (2021) on the efficacy of the steel can packaging EPR program complement previous studies that show that a more severe EPR policy does not result in increased recycling. In other words, the government's approach of establishing high recycling rate objectives does not always result in higher recycling rates. As a result, governments should consider setting realistic goal recycling rates for manufacturers rather than presuming that high recycling targets will result in more recycling. In contrast, effective EPR policies have increased trash collection, recycling, and recovery performance for certain waste flows in Portugal and Russia (Liubarskaia & Putinceva 2021, Niza et al. 2014). Furthermore, it is important to develop EPR policies for packaging that are tailored to specific locations and packaging waste management systems. Tailoring policies to the local environment can result in more effective implementation and better outcomes. South Africa's experience with EPR in the packaging sectors demonstrates that obligatory, government-imposed laws (as in the plastic bag business) do not appear to be effective in driving recovery compared to voluntary industry initiatives (as in the can, glass, and PET industries) (Nahman 2010). In addition, when establishing EPR policies, it is essential to have a thorough understanding of specific sectors, market features, and product characteristics because no single type of EPR policy suits every business (Røine & Lee 2008). Finally, Harris et al. (2021) notably suggested that policy interventions need to incorporate comprehensive monitoring and evaluation systems to quantify the outcomes of pollution reduction initiatives directly.

Stakeholder Engagement

EPR initiatives require participation from stakeholders

such as producers, retailers, waste management companies, consumers, and government agencies to ensure success (Polzer et al. 2016). The participation of all essential stakeholders from the early stages of policy creation to implementation is critical to the efficacy of EPR (Mayers 2008). Several studies and real-world situations support this inclusive approach. By including all stakeholders in the entire procedure through the EPR framework, nations such as Korea have raised recycling rates, minimized waste, and provided economic advantages and job possibilities in the recycling business (Kim 2012). In Europe, the efficacy of EPR programs, notably in beverage carton management, has been attributed to collaboration between manufacturers and the concerned public, as well as governmental initiatives. Additionally, Cahill et al. (2011) found that benefits are more evident when local governments actively develop and implement national systems, use existing trash infrastructure, and establish defined responsibilities for producers and local governments. Lessons from India's EPR framework emphasize the significance of incorporating several stakeholders, including the informal sector, to guarantee buy-in, collaboration, and long-term viability (Pani & Pathak 2021).

Transparency and Accountability

Under the EPR scheme, successful waste management relies heavily on establishing precise regulations and guarantees of accountability and transparency in packaging waste collection, recycling, and handling (Mayers 2008). Building trust among stakeholders and guaranteeing the integrity of EPR schemes requires transparency in financial aspects, data reporting, and decision-making processes, as noted by Lifset et al. (2023). Joltreau (2022) also emphasized the need for effective monitoring and continuous evaluation systems to track progress, identify weaknesses, and guarantee that stakeholders fulfill their responsibilities. Robust data management systems are required to track product life cycles, waste generation, and recycling rates. More importantly, according to Quinn and Sinclair (2006), these initiatives need to be governed by the government.

Incentives Strategy

Developing incentive strategies for EPR implementation impacts EPR participation and waste management. According to Wiesmeth & Hackl (2011), incentive-compatible frameworks that promote environmentally friendly behaviors while penalizing noncompliance are vital for encouraging producer engagement and supporting sustainable practices. In addition, Sui et al. (2024) noted that dynamic subsidy policies influence producers' participation behavior. Specifically, providing economic incentives to producers can improve

the products' design and environmental impact (Kunz et al. 2018, Mayers 2008). The achievement of EPR schemes for beverage containers in Nova Scotia is an example of the value of incentivizing (Diggle & Walker 2020). However, Joltreau (2022) discovered that the EPR financial incentive did not trigger any consistent shifts in packaging materials. Therefore, Agamuthu & Visvanathan (2014) argue that it is prudent to establish government incentives to encourage the increasing use of recycled products as raw materials to create new ones. These insights underscore the importance of developing comprehensive and dynamic incentive strategies to drive meaningful change and progress in EPR implementation.

Excluding the above lessons, other experiences involving the existence of sustainable end markets and integration of an EPR with two bonus/penalty programs should be considered while implementing EPR in the packaging industry (Agamuthu & Visvanathan 2014, Arnaud 2015)

Research Gaps on EPR Scheme for Packaging

While research on packaging waste EPR schemes has brought significant insights, there are still several research gaps in current EPR systems that require further investigation. Following the literature review, some ideas emerged, as described following.

One notable shortcoming is a lack of understanding about the economic efficacy of the EPR scheme. Barbara et al. (2022) discovered that existing research has focused primarily on European nations and ignored the economic aspect. However, the experiences of the Netherlands, Italy, Austria, Spain, and France show that EPR can act as a financial mechanism promoting the transition to a circular economy, in particular in the realm of packaging. Therefore, there needs to be more research on how finances change or the cost-benefits of EPR deployment for both governments and producers in different economic contexts. It is also critical to investigate how EPR systems might affect consumer pricing. Economic assessments can assist governments and industry stakeholders in making decisions about building and managing EPR systems.

Moreover, a full awareness of the issues faced by small- and medium-sized packaging businesses conforming to EPR policies is critical for promoting inclusiveness and delivering equitable outcomes (Wiesmeth & Hackl 2012). They frequently confront specific challenges, such as limited financial resources, technical competence, and regulatory complexities, which could limit their ability to meet EPR standards. Researching these issues and designing tailored solutions to help them participate in EPR programs is critical. By tackling the specific needs and constraints of small and

medium-sized packaging enterprises, policymakers can ensure that EPR schemes on packaging are accessible and equitable for all stakeholders, ultimately improving the efficacy and longevity of packaging waste management attempts.

Furthermore, another area that requires attention is the limited knowledge of the recycling performance of EPR programs on packaging, with a primary focus on plastics and, to a lesser extent, steel or paper (Agamuthu & Visvanathan 2014, Diggle et al. 2023, Park 2021). This limited scope prevents a thorough knowledge of the efficacy of EPR methods over a wide range of packaging materials and geographic settings. Research should cover a broader spectrum of packaging materials, such as glass, aluminum, and other metals, to close this gap. Scholars can gain insight into the problems and possibilities associated with diverse material streams by examining the recycling success of EPR programs across various packaging materials in both developed and developing nations.

Finally, the design of EPR programs for packaging waste management is never independent of the monitoring systems (OECD 2016). Therefore, systems designed to monitor the amount of money generated from license fees, the companies registered, the technologies utilized to convert wastes, the quantity of packaging recovered, and so on need to be conducted. Monitoring methods are required for every system to work effectively (Mwanza & Mbohwa 2019). However, no articles describe monitoring methods or analysis of the contribution of monitoring ways to the success of EPR implementation. By examining monitoring technologies, researchers can identify the best methods and give policymakers and industry stakeholders with evidence-based insights into the efficacy and implications of various monitoring approaches for EPR compliance in the packaging sector.

Addressing these research gaps is necessary for expanding our understanding and improving the efficacy of EPR systems for packaging waste management. By encouraging more studies, EPR frameworks may considerably help worldwide efforts to move to a more circular and sustainable economy.

CONCLUSIONS

In conclusion, the EPR programs for packaging waste management have been thoroughly examined in this article, which has also provided an overview of the field's current research state and actual implementations across the globe and highlighted research needs. The findings have shown that the research on EPR in packaging has recently been investigated more, and this program's most thought-out activity is recycling waste. Additionally, some evidence about the effectiveness of EPR on packaging, involving

recycling and reducing packaging waste, eco-design, and public awareness, was found. Moreover, the lessons learned indicate that when implementing EPR in packaging, policies should consider stakeholder engagement, transparency tactics, and incentive approaches. Specific research gaps for future investigation have also been identified. These include analyzing the financial effectiveness of EPR systems for different stakeholders, looking into potential obstacles that small- and medium-sized businesses may face under the EPR scheme, and evaluating the efficacy of surveillance techniques on compliance from many stakeholders.

Academics, legislators, and industry professionals can find the study's conclusions useful as a reference because they could help comprehend or make decisions regarding EPR on packaging. However, there are certain limitations to this study as well. First, the sample size might be constrained because the data was taken from the Web of Science and Scopus databases and was limited to journal articles published in English. Second, it remains unclear whether EPR schemes are truly effective regarding packaging. Furthermore, the present study has not yet profoundly analyzed lessons learned for countries under specific conditions. These limitations will be tackled in future research with a deep analysis.

REFERENCES

Agamuthu, P. and Visvanathan, C., 2014. Extended producers' responsibility schemes for used beverage carton recycling. *Waste Management Research*, 32(1), pp.1–3. doi:10.1177/0734242X13517611.

Ajania, I.A. and Kunlerea, I.O., 2019. Implementation of the extended producer responsibility (EPR) policy in Nigeria: Towards sustainable business practice. *Nigerian Journal of Environment and Health*, 75, pp.44–56.

Andreasi, B., Susanna, B., Alessio, F., Giorgia, A. and F., T., 2020. Extended producer responsibility: How to unlock the environmental and economic potential of plastic packaging waste? *Resources, Conservation and Recycling*, 162, pp.105030. doi:10.1016/j.resconrec.2020.105030.

Arnaud, B., 2015. Extended producer responsibility and green marketing: An application to packaging. *Environmental and Resource Economics*, 67(2), pp.285–296. doi:10.1007/s10640-015-9986-x.

Arp, R., Kock, L.d. and Anben, P., 2021. Extended producer responsibility for plastic packaging in South Africa: A synthesis report on policy recommendations.

Australian Packaging Covenant Organization., 2017. *Australian Packaging Covenant*.

Bakar, K.A. and Mohamed, A.F., 2023. Analysis of consumer preferences and attitudes towards sustainable consumption of plastic beverage packaging in Malaysia. *IOP Conference Series: Earth and Environmental Science,* 16, p.23.

Barbara, S.T., Thier, A. and Hornicki, K., 2022. The concept of extended producer responsibility in the field of packaging industry and the energy sector in the light of the circular economy: The example of Poland. *Energies*, 15(23), pp.39060. doi:10.3390/en15239060.

Cahill, R., Grimes, S.M. and Wilson, D.C., 2011. Extended producer responsibility for packaging wastes and WEEE: A comparison of implementation and the role of local authorities across Europe. *Waste Management Research*, 29(5), pp.455–479. doi:10.1177/0734242X10379455.

Cai, Y.J. and Choi, T.M., 2021. Extended producer responsibility: A systematic review and innovative proposals for improving sustainability. *IEEE Transactions on Engineering Management*, 68(1), pp.272–288. doi:10.1109/tem.2019.2914341.

Canadian Council of Ministers of the Environment., 2019. *Canada-wide Action Plan on Zero Plastic Waste: Phase 1*.

Carola, H., 2000. Is extended producer responsibility effective? *Environmental Science & Technology,* 7(3), p.21.

Colelli, F.P., Croci, E., Bruno Pontoni, F. and Floriana Zanini, S., 2022. Assessment of the effectiveness and efficiency of packaging waste EPR schemes in Europe. *Waste Management*, 148, pp.61–70. doi:10.1016/j.wasman.2022.05.019.

Destyanto, A.R., Putu Swasti Kirana and Ardi, R., 2019. Model conceptualization of system dynamics for evaluating extended producer responsibility strategy in plastic waste management policy in Indonesia. *Waste Management Research*, 91, pp.612-626

Diggle, A. and Walker, T.R., 2020. Implementation of harmonized extended producer responsibility strategies to incentivize recovery of single-use plastic packaging waste in Canada. *Waste Management*, 110, pp.20–23. doi:10.1016/j.wasman.2020.05.013.

Diggle, A. and Walker, T.R., 2022. Environmental and economic impacts of mismanaged plastics and measures for mitigation. *Environments*, 9(2), p.65. doi:10.3390/environments9020015.

Diggle, A., Walker, T. R. and Adams, M., 2023. Examining potential business impacts from the implementation of an extended producer responsibility program for printed paper and packaging waste in Nova Scotia, Canada. *Circular Economy*, 2(2). https://doi.org/10.1016/j.cec.2023.100039

Eck, N. J. V. and Waltman, L., 2019. *VOSviewer Manual*.

EPA., 2023. Containers and Packaging: Product-Specific Data. Retrieved from https://www.epa.gov/facts-and-figures-about-materials-waste-and-recycling/containers-and-packaging-product-specific

European Commission., 1994. European Commission European Parliament and Council Directive 94/62/EC of 20 December 1994 on Packaging and Packaging Waste.

European Commission., Packaging waste. https://environment.ec.europa.eu/topics/waste-and-recycling/packaging-waste_en

European Environment Agency., 2022. Early warning assessment related to the 2025 targets for municipal waste and packaging waste.

European Union., 2020. Packaging and packaging waste. Retrieved from https://eur-lex.europa.eu/legal-content/EN/TXT/?uri=celex%3A31994L0062

Eurostat., *Recycling rate of packaging waste by type of packaging*. https://ec.europa.eu/eurostat/cache/metadata/en/cei_wm020_esmsip2.htm

Geyer, R., Jambeck, J. R. and Law, K. L., 2017. Production, use, and fate of all plastics ever made. *Science Advances*, 3(7), e1700782. https://doi.org/10.1126/sciadv.1700782

GIZ., 2022. *Assessing the role and impact of EPR in the prevention of marine plastic packaging litter*. Available at: https://www.giz.de/en/downloads/giz2022-en-epr-plastic-packaging-litter.pdf

Gonzalez, D. S., 2020. *Venezuela: New rules on the extended liability of producers, importers, and distributors of containers, paper packaging and wrapping, cardboard, plastic, disposable glass and tires*. Available at: https://insightplus.bakermckenzie.com/bm/consumer-goods-retail_1/venezuela-new-rules-on-the-extended-liability-of-producers-importers-and-distributors-of-containers-paper-packaging-and-wrapping-cardboard-plastic-disposable-glass-and-tires

Gupt, Y. and Sahay, S., 2015. Review of extended producer responsibility: A case study approach. *Waste Management Research*, 33(7), pp.595–611. https://doi.org/10.1177/0734242X15592275

Harris, L., Liboiron, M., Charron, L. and Mather, C., 2021. Using citizen science to evaluate extended producer responsibility policy to reduce marine plastic debris shows no reduction in pollution levels. *Marine Policy*, 123. https://doi.org/10.1016/j.marpol.2020.104319

India Ministry of Environment, F. a. C. C., 2020. *Guideline Document: Uniform Framework for Extended Producers Responsibility*.

Johannes, H. P., Kojima, M., Iwasaki, F. and Edita, E. P., 2021. Applying the extended producer responsibility towards plastic waste in Asian developing countries for reducing marine plastic debris. *Waste Management Research*, 39(5), pp.690–702. https://doi.org/10.1177/0734242X211013412

Johnsen, T. E., Miemczyk, J. and Howard, M., 2017. A systematic literature review of sustainable purchasing and supply research: Theoretical perspectives and opportunities for IMP-based research. *Industrial Marketing Management*, 61, pp.130–143. https://doi.org/10.1016/j.indmarman.2016.03.003

Johnson, A., 2022. *EPR and Policy Development in Indonesia, India, Thailand, Philippines, and Vietnam*. Springer.

Joltreau, E., 2022. Extended producer responsibility, packaging waste reduction, and eco-design. *Environmental and Resource Economics*, 83(3), pp.527–578. https://doi.org/10.1007/s10640-022-00696-9

Kaffine, D. and O'Reilly, P., 2013. What have we learned about extended producer responsibility in the past decade? A survey of the recent EPR economic literature. *Waste Management Research*, 11, pp.72-83

Kim, J.H., 2012. Extended producer responsibility (EPR) and job creation in Korea *Waste Management and the Environment VI*.

Kim, S. and Mori, A., 2015. Revisiting the extended producer responsibility program for metal packaging in South Korea. *Waste Manag*, 39, pp.314–320. https://doi.org/10.1016/j.wasman.2015.02.006

Kunz, N., Mayers, K. and Wassenhove, L.V.V., 2018. Stakeholder views on extended producer responsibility and the circular economy. https://www.oecd.org/environment/extended-producer-responsibility.htm

Liberati, A., Altman, D.G., Tetzlaff, J., Mulrow, C., Gotzsche, P.C., Ioannidis, J. P., Clarke, M., Devereaux, P.J., Kleijnen, J. and Moher, D., 2009. THE PRISMA statement for reporting systematic reviews and meta-analyses of studies that evaluate health care interventions: explanation and elaboration. *PLoS Medical*, 6(7), p.e1000100. https://doi.org/10.1371/journal.pmed.1000100

Lifset, R., Kalimo, H., Jukka, A., Kautto, P. and Miettinen, M., 2023. Restoring the incentives for eco-design in extended producer responsibility: The challenges for eco-modulation. *Waste Management Research*, 168, pp.189–201. https://doi.org/10.1016/j.wasman.2023.05.033

Liubarskaia, M. A. and Putinceva, N.A., 2021. The role of the secondary resource market in the development of the extended producer responsibility mechanism in Russia. *Conference Series: Earth and Environmental Science*, 11, p.16.

Löhle, S., Brinkmann, J., Wagner, J. and Le, H.A., 2021. *Assessment of extended producer responsibility (EPR) for plastic packaging waste in Viet Nam*. Available at : https://wwfint.awsassets.panda.org/downloads/20210208_epr_scheme_assessment_for_packaging_in_vn__final.pdf

Lorang, S., Yang, Z., Zhang, H., Lü, F. and He, P., 2022. Achievements and policy trends of extended producer responsibility for plastic packaging waste in Europe. *Waste Disposal & Sustainable Energy*, 4(2), pp.91–103. https://doi.org/10.1007/s42768-022-00098-z

Maine Department of Environmental Protection. Extended Producer Responsibility Program for Packaging. Available at: https://www.maine.gov/dep/waste/recycle/epr.html

Marques, R.C., da Cruz, N.F., Simões, P., Faria Ferreira, S., Pereira, M.C. and De Jaeger, S., 2014. Economic viability of packaging waste recycling systems: A comparison between Belgium and Portugal. *Resources, Conservation and Recycling*, 85, pp.22-33. https://doi.org/10.1016/j.resconrec.2013.12.015

Massarutto, A., 2014. The long and winding road to resource efficiency – An interdisciplinary perspective on extended producer responsibility. *Resources, Conservation and Recycling*, 85, pp.11-21. https://doi.org/10.1016/j.resconrec.2013.11.005

Mayanti, B. and Helo, P., 2024. Circular economy through waste reverse logistics under extended producer responsibility in

Finland. *Waste Management Research*, 42(1), pp.59-73. https://doi.org/10.1177/0734242X231168801

Mayers, C.K., 2008. Strategic, financial, and design implications of extended producer responsibility in Europe: A producer case study. *Journal of Industrial Ecology*, 11(3), pp.113-131. https://doi.org/10.1162/jiec.2007.1228

McKerlie, K., Knight, N. and Thorpe, B., 2006. Advancing extended producer responsibility in Canada. *Journal of Cleaner Production*, 14(6-7), pp.616-628. https://doi.org/10.1016/j.jclepro.2005.08.001

Mengist, W., Soromessa, T. and Legese, G., 2020. Ecosystem services research in mountainous regions: A systematic literature review on current knowledge and research gaps. *Science of The Total Environment*, 702, p.134581. https://doi.org/10.1016/j.scitotenv.2019.134581

Ministry of Environment, 2010. Korea Environmental Policy Bulletin: Extended Producer Responsibility.

Morashti, J., An, Y. and Jang, H., 2022. A systematic literature review of sustainable packaging in supply chain management. *Sustainability*, 14(9), p.65. https://doi.org/10.3390/su14094921

Mwanza, B. and Mbohwa, C., 2019. Strategies enhancing extended producer responsibility enforcement: A review.

Nahman, A., 2010. Extended producer responsibility for packaging waste in South Africa: Current approaches and lessons learned. *Resources, Conservation and Recycling*, 54(3), pp.155-162. https://doi.org/10.1016/j.resconrec.2009.07.006

Niza, S., Santos, E., Costa, I., Ribeiro, P. and Ferrão, P., 2014. Extended producer responsibility policy in Portugal: A strategy towards improving waste management performance. *Journal of Cleaner Production*, 64, pp.277-287. https://doi.org/10.1016/j.jclepro.2013.07.037

OECD, 2014. The State of Play on Extended Producer Responsibility (EPR): Opportunities and Challenges. Available at: https://www.oecd.org/environment/waste/Global%20Forum%20Tokyo%20Issues%20Paper%2030-5-2014.pdf

OECD, 2016. Extended Producer Responsibility: Updated Guidance for Efficient Waste Management. https://doi.org/10.1787/9789264256385-en

Oregon Department of Environmental Quality. Plastic Pollution and Recycling Modernization Act. Available at: https://www.oregon.gov/deq/recycling/Pages/Modernizing-Oregons-Recycling-System.aspx

Oscar, H., Catalina, C. and Carolina, M., 2022. Integrating ecodesign in food packaging solutions for EPR compliance in Chile: Knowledge transfer from theory to practice. *DRS2022: Bilbao*.

Pani, S.K. and Pathak, A.A., 2021. Managing plastic packaging waste in emerging economies: The case of EPR in India. *Journal of Environmental Management*, 288, p.112405. https://doi.org/10.1016/j.jenvman.2021.112405

Park, S., 2021. Assessing the recycling performance of extended producer responsibility (EPR) programs: A case study of the steel can packaging recycling system in South Korea. *Journal of the Air & Waste Management Association*, 71(5), pp.586-596. https://doi.org/10.1080/10962247.2020.1866120

Peng, Y., Yan, D., Sriram, V. and Song, S., 2020. Does extended producer responsibility improve eco-innovation: an empirical study of product take-back programs. *SSRN*, 15, pp.121-136. https://doi.org/https://doi.org/10.2139/ssrn.3687582

Pollock, D., Peters, M.D.J., Khalil, H., McInerney, P., Alexander, L., Tricco, A.C., Evans, C., de Moraes, E.B., Godfrey, C.M., Pieper, D., Saran, A., Stern, C. and Munn, Z., 2023. Recommendations for the extraction, analysis, and presentation of results in scoping reviews. *JBI Evidence Synthesis*, 21(3), pp.520-532. https://doi.org/10.11124/JBIES-22-00123

Polzer, M.A.J.P. and Persson, K.M., 2016. The importance of extended producer responsibility and the national policy of solid waste in Brazil.

International Journal of Environment and Waste Management, 18, pp.101–119. https://doi.org/10.1504/IJEWM.2016.080398

Prevent Waste Alliance, 2021a. Developing a legal framework for EPR in Chile.

Prevent Waste Alliance, 2021b. Development from a voluntary to a mandatory EPR scheme for packaging.

Prevent Waste Alliance, 2021c. The Republic of Korea's EPR System for Packaging: An Asian Role Model.

Pruess, J.T. and Garrett, R.D., 2024. Potential effectiveness of extended producer responsibility: An ex-ante policy impact analysis for plastic packaging waste in Belgium, France, and Germany. *SSRN*, 47(6), p.5103: https://doi.org/http://dx.doi.org/10.2139/ssrn.4715103

Quinn, L. and Sinclair, A. J., 2006. Policy challenges to implementing extended producer responsibility for packaging. *Canadian Public Administration/Administration Publique du Canada*, 49(1), pp.60-79. https://doi.org/10.1111/j.1754-7121.2006.tb02018.x

Røine, K. and Lee, C.Y., 2008. With a Little Help from EPR?: Technological change and innovation in the Norwegian plastic packaging and electronics sectors. *Journal of Industrial Ecology*, 10(1-2), pp.217-237. https://doi.org/10.1162/108819806775545448

Rubio, S., Ramos, T.R.P., Leitão, M.M.R. and Barbosa-Povoa, A.P., 2019. Effectiveness of extended producer responsibility policies implementation: The case of Portuguese and Spanish packaging waste systems. *Journal of Cleaner Production*, 210, pp.217-230. https://doi.org/10.1016/j.jclepro.2018.10.299

Saeed, P.S., Mura, P. and Wijesinghe, S.N.R., 2019. A systematic review of systematic reviews in tourism. *Journal of Hospitality and Tourism Management*, 39, pp.158-165. https://doi.org/10.1016/j.jhtm.2019.04.001

Schamber, P. and Bon, S., 2022. Extended producer responsibility (EPR) and packaging regulations in Argentina: reflections on the aspects associated with the blocking of the draft legislation initiatives. *Detritus*, 19, pp.18-27. https://doi.org/10.31025/2611-4135/2022.15195

Septianingrum, D., Mizuno, K. and Herdiansyah, H., 2023. Extended producer responsibility for waste management policy. *Jurnal Penelitian Pendidikan IPA*, 9(5), pp.2686-2692. https://doi.org/10.29303/jppipa.v9i5.3469

Sui, Y., Sun, Q. and Zhu, X., 2024. Optimizing express packaging recycling: A tripartite evolutionary game modeling government strategies under extended producer responsibility. *Environmental Technology & Innovation*, 33, p.351. https://doi.org/10.1016/j.eti.2023.103510

Susanna, E.W., Jean-Pierre, G., Pantzar, S.M., Janssens, C. and Brin, P., 2017. EPR in the EU Plastics Strategy and the Circular Economy: A focus on plastic packaging.

Taiwan Environmental Protection Agency, 2021. Recycling regulations in Taiwan and the 4-in-1 recycling program. Available at: https://www.epa.gov/sites/default/files/2014-05/documents/handout-1a-regulations.pdf

The Government of Vietnam, 2022. Decree No. 08/2022/ND-CP of Government on elaboration of several articles of the law on environmental protection.

Tranfield, D., Denyer, D. and Smart, P., 2003. Towards a Methodology for Developing Evidence-Informed Management Knowledge by Means of Systematic Review. *British Journal of Management*, 14(3), pp.207-222. https://doi.org/10.1111/1467-8551.00375

Walls, M., 2006. *Extended Producer Responsibility and Product Design: Economic Theory and Selected Case Studies*. https://dx.doi.org/10.2139/ssrn.901661

Walter, L. F., Saari, U., Fedoruk, M., Iital, A., Moora, H., Klöga, M. and Voronova, V., 2019. An overview of the problems posed by plastic products and the role of extended producer responsibility in Europe. *Journal of Cleaner Production*, 214, pp.550-558. https://doi.org/10.1016/j.jclepro.2018.12.256

Wiesmeth, H. and Hackl, D., 2011. How to successfully implement extended

producer responsibility: considerations from an economic point of view. *Waste Management Research*, 29(9), pp.891-901. https://doi.org/10.1177/0734242X11413333

Wiesmeth, H. and Hackl, D., 2012. Extended Producer Responsibility and the impact of various policy instruments: the example of packaging waste. *Environmental Economy, Policy and International Environmental Relations*, 6(2), p. 424.

WWF, 2022. Extended Producer Responsibility for single-use plastics and packaging waste streams: An assessment for Kenya. World Wide Fund for Nature.

Modeling Landslide Hazard in the Eastern Himalayan Mountain Region of the Papumpare District of Arunachal Pradesh, India Using Multicriteria Decision-Making (MCDM) and Geospatial Techniques

Tilling Riming [ID], **Praduyt Dey**† [ID]**, Santanu Kumar Patnaik** [ID] **and Manju Narzary** [ID]

Department of Geography, Rajiv Gandhi University, Itanagar, Arunachal Pradesh, India
†Corresponding author: Praduyt Dey; praduytd25@gmail.com

ABSTRACT

Landslides are significant natural hazards that cause damage to the environment, life, and properties, mainly in hilly terrain. This research was mostly focused on generating a landslide susceptibility zone map of Papumpare District, Arunachal Pradesh, and classifying the region from high susceptibility to least susceptibility using AHP modeling techniques considering the landslide causative factors. The Analytical Hierarchy Process (AHP) is a multicriteria decision-making model (MCDM) in which each parameter is compared based on its role in triggering a landslide. A total of eight parameters were selected based on the factors that could affect the most, like Slope, Rainfall, Drainage Density, Lineament Density, Geomorphology, Soil, Geology, and Land use/Land cover. These layers were prepared using ArcGIS 10.8 software and ERDAS IMAGINE 2014. Based on the output, the region was classified into five zones of landslide susceptibility classes. Of these, the high-very-high landslides are mostly amassed near the steep and disturbed slopes due to earth-cutting, especially for building or construction of roads. Validation was done using the ROC curve (73.2%) suggesting good performance of the model. The outcome of this work will provide information for proper landslide hazard management and will help in formulating suitable mitigation strategies in the future.

INTRODUCTION

Natural disasters are emerging as a huge threat to human life, property, and the environment. Landslides, a significant hazard, are more severe and frequent in the regions where topography is rugged and human settlements are sparse. Many natural factors such as earthquakes, heavy rainfall, river bank erosion by flood water, anthropogenic activities including development of infrastructures, deforestation, slope excavation causing slope failure, building townships in environmentally sensitive zones, etc, have also amplified the impact of disasters. Climate-induced disasters such as floods, landslides, and cyclones are increasing concerns among the community. These climate-induced disasters are projected to become more severe with region-specific intensification (IPCC 2021). Landslides serve as one of the most catastrophic geological hazards in the hilly regions. It is more frequent in high mountainous regions where cloudburst-induced extreme rainfall causes huge movement of debris down the slope (Kirschbaum et al. 2020). In recent years, landslide events have modified landforms, affected biodiversity, triggered various hazards like floods, earth-cutting, and alteration of river courses due to sedimentation, and damaged life and properties (Lombardo et al. 2020, Hao et al. 2023).

India's distinct climate and geodynamics make it susceptible to various naturally occurring disasters. Studies show that about 60% of its landmass is

susceptible to earthquakes of different magnitudes, about 8% to cyclone hazards, about 68% to drought, 12% to floods, and approximately 15% area is vulnerable to landslides. Nearly 14% of India's land area is landslide-prone, among which one-fifth falls under the northeastern region (Raju 2002). Almost the entire NE region is susceptible to landslides of various degrees due to its complex terrain conditions.

Landslide zonation maps formulated through geospatial technologies are crucial in disaster management and risk mitigation (Kanwal et al. 2016, Huan et al. 2023). According to Fell et al. (2007, 2008) and AGS (2000), landslide hazard zonation means the classification of terrain into different zones that are characterized based on the spatial and temporal probability of the phenomenon, including location, volume, and future prediction of landslide occurrence. The availability of high-resolution spatial data, geoinformatics, and fast-processing computers has automated landslide hazard/susceptibility mapping processes, minimizing fieldwork and delineating potential landslide-affected areas (Ilanloo 2011). In recent years, several techniques have been utilized for the identification and assessment of landslide susceptibility zones, including machine learning (ML) (Jhunjhunwalla et al. 2019, Merghadi et al. 2020),

logistic regression model (Hemasinghe et al. 2018, Shano et al. 2022), analytical hierarchy process (Das et al. 2022, Barman et al. 2024), frequency ratio (Yadav et al. 2023, Qazi et al. 2023). Many researchers have experimented with GIS using various causative factors to perform models for landslide hazards (Sarkar & Kanungo 2004, Hong et al. 2007, Kouli et al. 2010, Avtar et al. 2011, Othman et al. 2012, Devkota et al. 2013, Paulín et al. 2014, Ahmed 2015, Pareta & Pareta 2015, Younes Cárdenas and Mera 2016, Hadmoko et al. 2017, Stanley & Kirschbaum 2017, Mahdadi et al. 2018). This requires the identification of those areas that are or could be affected by landslides and the calibration of the chances of such landslides occurring within a specific period. Commenting on the eventuality of landslides through zonation mapping itself is a challenging task. The LHZ maps do not directly incorporate the magnitude and time before or after the occurrences. The methodology to develop a susceptibility map hinge on several elements, viz., the nature of the terrain, parameters to be considered, available data on slope, rainfall, seismicity, geology, soil, etc. The AHP techniques are very productive in identifying potential landslide zones as they depend on subjective knowledge and expert judgments and are constantly checked through
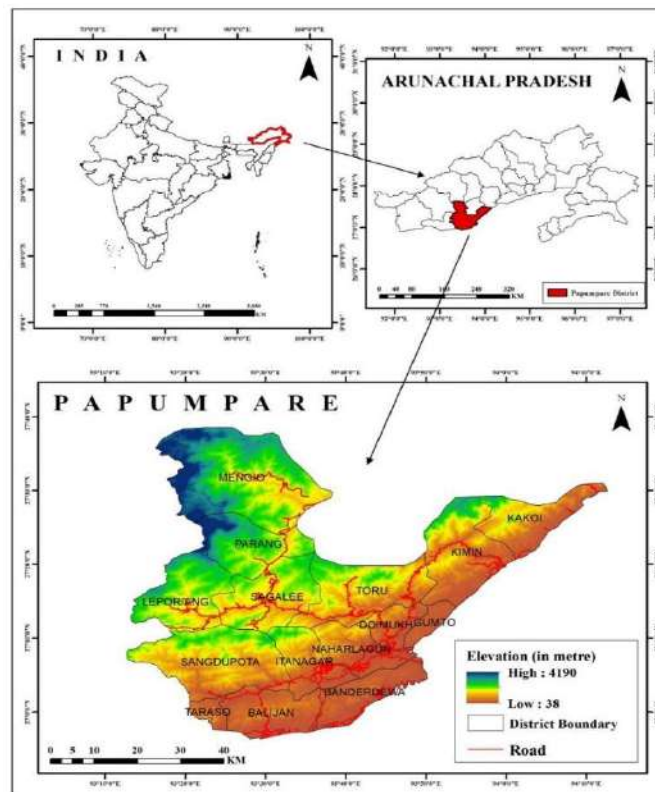
Fig. 1: Locational Map of the Papum Pare District, Arunachal Pradesh.

consistency measures (Veerappan et al. 2017, Ozioko & Igwe 2020). Thus, for minimizing the impact of landslides, the AHP-based susceptibility map becomes important since the area is classed between very low hazard to very high hazard zones based on different landslide hazard zones (Arora et al. 2004). Landslide hazard mapping offers knowledge that helps designers and engineers locate landslide-prone areas to implement effective mitigation measures.

Here in this study, the method used for preparing the zonation map of the Papumpare district is the GIS-based-Analytical Hierarchy Process (AHP), given by (Saaty 1980). AHP is an accepted multicriteria decision-making analysis method that has been widely applied to many decision-making systems. AHP technique integrated with the landslide hazard map makes it more reliable (Feizizadeh et al. 2014). This research attempts to produce information that can be useful for predicting the location of future landslides in the Papumpare district of Arunachal Pradesh which will help the planners and policymakers in the effective management of landslide hazards in the region.

STUDY AREA

The Papumpare district is situated in the southwestern part of Arunachal Pradesh, bordering Assam. The name Papumpare is procured from the rivers Papum and Pare, which flow through the district. Papumpare district lies between 93°12' E to 94°13' E Longitudes and 26°56' N to 27°35' N Latitudes (Fig. 1). The district covers a geographical area of 3462 sq.km in the lesser Himalayan zone. It is bounded by Lower Subansiri and Kurung Kumey districts in the north, East Kameng district in the west, and North Lakhimpur district of Assam in the east and south. Papumpare ranked 14th among the districts of Arunachal Pradesh in terms of area. The district is covered by thick forest which has sub-tropical, deciduous, and humid types of vegetation. Mostly, the low-lying regions and valleys are occupied by inhabitants. The Hill range approximately varies from 300 m to 2700 m above sea level. Itanagar, the state capital, is situated at an altitude of 440m above MSL.

MATERIALS AND METHODS

Data Sources

Several causative factors which are responsible for landslides were studied for this project. The study is solely based on the secondary data obtained from various sources (Table 1). The selected factors were slope, rainfall, drainage density, lineament density, geomorphology, soil type, geology, and land use/land cover. Various thematic layers were generated within ArcGIS software 10.8 to develop the LSZ map. A

Table 1: Database and its sources.

Data	Source
Cartosat-3, version 3 (1.12m resolution) DEM	Downloaded from NRSC-Bhuvan, https://bhuvan-app1.nrsc.gov.in/
CHIRPS Annual Rainfall data (0.05° resolution)	Downloaded from Climate Hazard Centre, UC Santa Barbara, https://data.chc.ucsb.edu/products/CHIRPS-2.0/
LULC from satellite image Landsat-8 OLI	Downloaded from the United States Geological Survey, http://earthexplorer.usgs.gov/
Lineament, Geology, Geomorphology	Downloaded from Geological Survey of India, https://bhukosh.gsi.gov.in/
Soil data	Downloaded from the Food and Agriculture Organization of the United Nations (FAO), https://www.fao.org/

topographical map of scale 1:50,000 from the Survey of India has been georeferenced. Cartosat-3, version 3 (1.12 m resolution) DEM was employed to develop slope and drainage density maps. For rainfall, the data were downloaded from the Climate Hazards Group InfraRed Precipitation with station data (CHIRPS 0.05° resolution). The spatial distribution of rainfall data for the study is estimated using the interpolation method (Kriging). LULC map was generated from Landsat-8 OLI by supervised classification in ERDAS IMAGINE 2014. The Geomorphology, Geology, and Lineament map of the study area was obtained from the Geological Survey of India. Soil data were collected from the Food and Agriculture Organization (FAO).

Application of AHP Techniques

The AHP (Saaty 1980) is a technique employed to determine the weight of different parameters. Relative ratings/scores were assigned to every parameter according to the level of influence, the literature review, and expert opinions. Each class of parameter was graded using Saaty's nine-point weighing scale (0-9), i.e., the pairwise comparison matrix (Table 2), where a high rating indicates a high influence on the occurrence of landslides. The final layout for the LHZ map was carried out by using weighted overlay analysis within the ArcGIS 10.8 software using each of the generated thematic layers.

According to Gorsevski et al. (2006), AHP is a hierarchical structure of a pairwise comparison matrix consisting of equal rows and columns. For formulating a comparison matrix, each parameter is rated against each one of the parameters by assigning a rate that is relatively more dominant. The scale ranges between 1 to 9 (Table 2). Thus, comparison matrices are pursued as input, and the relative weights are accorded as output. Fig. 2 shows the methodological framework adopted

Table 2: Weights for Pairwise comparison. Source: (Saaty 1990).

Scales	Intensity	Descriptions
1	Equally important	Both factors are important
3	Slightly important	One among others is slightly more effective than a certain factor
5	Quite important	One among others strongly tends to a certain factor
7	Extremely important	One among others is extremely dominant to a certain factor
9	Absolutely important	A factor has the highest possibility of tending to a certain factor

in delineating the landslide inventory map of Papumpare district, Arunachal Pradesh.

Computation of the Weights Assigned to Parameters

After assigning the pairwise comparison matrix (Table 3), the calculation was done. The comparison matrix in AHP consists of rows and columns; each row of the matrix is compared to the other, and each row indicates the relative significance between the two criteria. In this matrix, the rows follow the inverse of each criterion and its significance with others (Bera et al. 2019). Subsequently, the weights were

normalized (Table 4) to minimize the biases that exist in the weight assignment (Saravanan et al. 2021).

The calculation of the Consistency ratio (CR) validates the result and was coined to consider whether the comparison matrix is consistent or not (Kolat et al. 2012).

$$\text{Consistency Ratio (CR)} = \frac{CI}{RI}$$

$$CI = \frac{\lambda max - n}{n - 1}$$

Where, λ - eigenvalue and n - number of factors

To determine the Consistency Index, AHP compares it by Random index (RI), and the result is called Consistency Ratio, which can be defined as CR = CI/RI. The Random index (Table 5) is the randomly generated comparison matrix of order 1 to 10 obtained by approximating random indices (Saaty 1990). Table 3 shows the value of RI.

As per the values of CR, if CR is less than 0.10, the ratio indicates a sensible level of consistency for the given pairwise comparisons. Thus, if CR is greater than 0.10, then the ratio indicates inconsistent judgments. In certain cases, the assigned values for the given matrix should be reconsidered and re-evaluated.
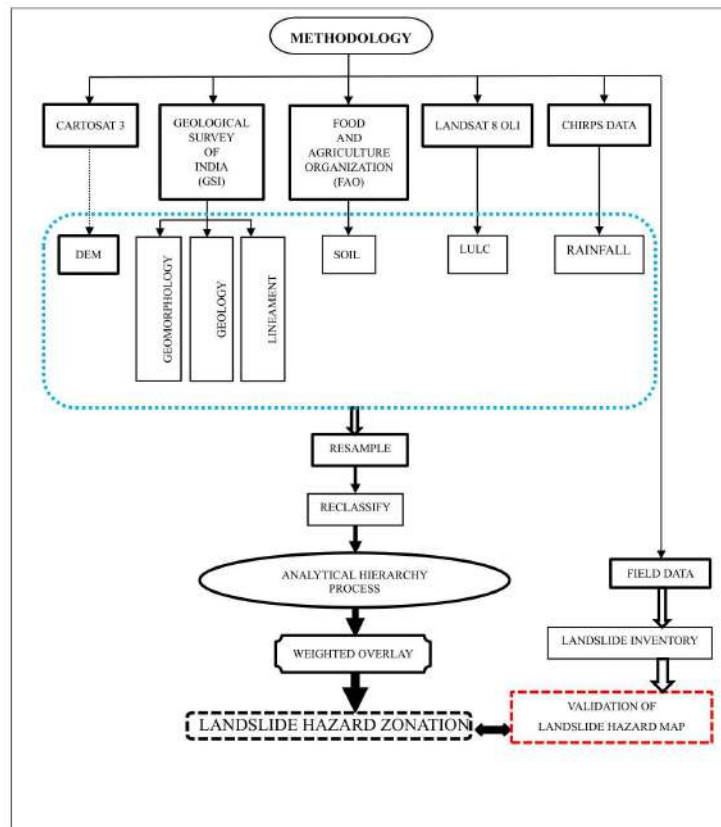
Fig. 2: Conceptual Framework.

Table 3: Pair-wise comparison matrix.

CRITERIA	SL	RF	DD	LD	GE	SO	G	LULC
Slope (SL)	1	2	3	3	4	5	6	7
Rainfall (RF)	0.5	1	2	4	5	5	6	7
Drainage density (DD)	0.33	0.5	1	2	3	4	6	6
Lineament density (LD)	0.33	0.25	0.5	1	3	4	6	6
Geomorphology	0.25	0.2	0.33	0.33	1	2	3	5
Soil	0.2	0.2	0.25	0.25	0.5	1	3	4
Geology (G)	0.17	0.17	0.17	0.17	0.33	0.33	1	3
LULC	0.14	0.14	0.17	0.17	0.2	0.25	0.33	1

Table 4: Standardized comparison matrix and calculation of criterion weights.

CRITERIA	SL	RF	DD	LD	GE	SO	G	LULC	Total Weight	Standardized Weight
Slope (SL)	0.34	0.45	0.40	0.27	0.23	0.23	0.19	0.18	2.31	0.29
Rainfall (RF)	0.17	0.22	0.27	0.37	0.29	0.23	0.19	0.18	1.93	0.24
Drainage density (DD)	0.11	0.11	0.13	0.18	0.18	0.19	0.19	0.15	1.25	0.16
Lineament density (LD)	0.11	0.06	0.07	0.09	0.18	0.19	0.19	0.15	1.03	0.13
Geomorphology	0.09	0.04	0.04	0.03	0.06	0.09	0.10	0.13	0.58	0.07
Soil	0.07	0.04	0.03	0.02	0.03	0.05	0.10	0.10	0.44	0.06
Geology (G)	0.06	0.04	0.02	0.02	0.02	0.02	0.03	0.08	0.28	0.03
LULC	0.05	0.03	0.02	0.02	0.01	0.01	0.01	0.03	0.18	0.02

Table 5: Random Index.

N	1	2	3	4	5	6	7	8	9	10
RI	0.0	0.0	0.58	0.90	1.12	1.24	1.32	1.41	1.45	1.49

Based on this study, the calculated overall value for the consistency ratio was 0.065, which shows that the comparisons of each factor/parameter indicate a reasonable consistency and that the weights (Table 6) were appropriate for the model.

Eigenvector λ = sum of consistency vector/ no. of parameters(N)

$$\lambda = 8.64$$

Consistency Index = 0.092

Consistency Ratio = 0.065

Table 6: Consistency Vector for each criterion.

CRITERIA	Weight	Consistency Vector
Slope	2.56	8.87
Rainfall	2.22	9.20
Drainage	1.41	9.03
Lineament	1.14	8.84
Geomorphology	0.61	8.45
Soil Type	0.46	8.32
Geology	0.28	8.10
LULC	0.18	8.33

RESULTS AND DISCUSSION

Slope

The slope plays a major role, as the degree of slope angle is considered the main causative factor used to generate the susceptibility in landslides. According to (Lee et al. 2004), as the degree of slope angle increases, shear stress in soil or overlying material increases as well. The slopes of the study area (Fig. 3) were classified into five categories such as steep (>50°), which cover 301.49 sq. km, and high (31°- 40°) covers 798.41 sq. km. Moderately high (21°- 30°) covers 1024.26 sq. km, gentle (11°- 20°) covers 897.96 sq. km, and rolling slopes (<10) which covers 497.57 sq. km. A steep slope with more mobilizing force may fail early (Anbalagan et al. 2015). In steeper slopes, due to gravity, the weight of the underlying material will be more compared to moderate slope, thus, the weights were allotted accordingly (Table 7).

Rainfall

Landslides triggered by rainfall are primarily caused by the build-up of pore water pressures in the ground (Sengupta et al. 2010). For the preparation of the rainfall distribution

map (Fig. 4), 10-year rainfall data were considered. The intensity of the annual average rainfall of the region ranges between 864 and 2884 mm. The rainfall map was divided into five categories, namely, 864-1268 mm, which covers 465.47 sq. km, 1268-1664 mm covers 708.40 sq. km, 1664-2012 mm covers 987.89 sq. km, 2012-2392 sq. km, and 2392-2884 mm which covers 591.84 sq. km. Higher intensity of rainfall was found in the eastern part of the region, and the northern region showed moderate-intensity rainfall (864-1664 mm). Intense rainfall during monsoon causes rainwater seepage, due to which the materials get saturated and loosened, this, in turn, causes slope failure. Higher rainfall zones were provided with high weights and vice-versa (Table 7).

Drainage Density

Drainage is an important factor that controls the landslide as its densities control the nature of the soil and its geotechnical properties (Pareta 2004). The function of infiltration is negatively correlated to drainage density. High-density values are indicative of lower infiltration rates and higher surface flow velocity. The lower the infiltration rate, the more favorable it is for runoff, thus indicating higher drainage density. The study area (Fig. 5) has been divided into five classes, namely, 0.01-0.22 km/sq.km, which covers a 438.62 sq.km area, 0.22-0.34 km/sq.km covers 828.2

sq.km, 0.34-0.44 km/sq.km covers 939.57 sq.km, 0.44-0.55 km/sq.km covers 818.31 sq.km and 0.55-0.78 km/sq.km covers 505.3 sq.km. High-density values, i.e., between 0.01-0.78 km/sq.km, are witnessed in whole parts of the region. The susceptibility of landslide zones is proportional to the function of drainage density due to its relation with surface runoff and permeability. The weights were allotted according to the dominance of drainage in different locations of the Papumpare district (Table 7).

Lineament Density

Lineament is a linear feature in a landscape that is an expression of an underlying geological structure, such as a fault. Lineament appears as a fault-aligned valley, fold-aligned hills, straight coastline, or union of these features. Lineament helps to surmise mineral prospects of a region, analyze structural deformation patterns/trends, identify geological boundaries, and surmise crustal structure and various subsurface phenomena in areas of unexposed lithology. Lineament and any planar structure are important factors for assessing the stability of slopes which destabilize the area as well as lead to the deterioration of rocks, which energize the weathering processes. The lineament density varies between 0 and 74.9 km/km square. Hence, the Lineament density (Fig. 6) has been classified upon natural
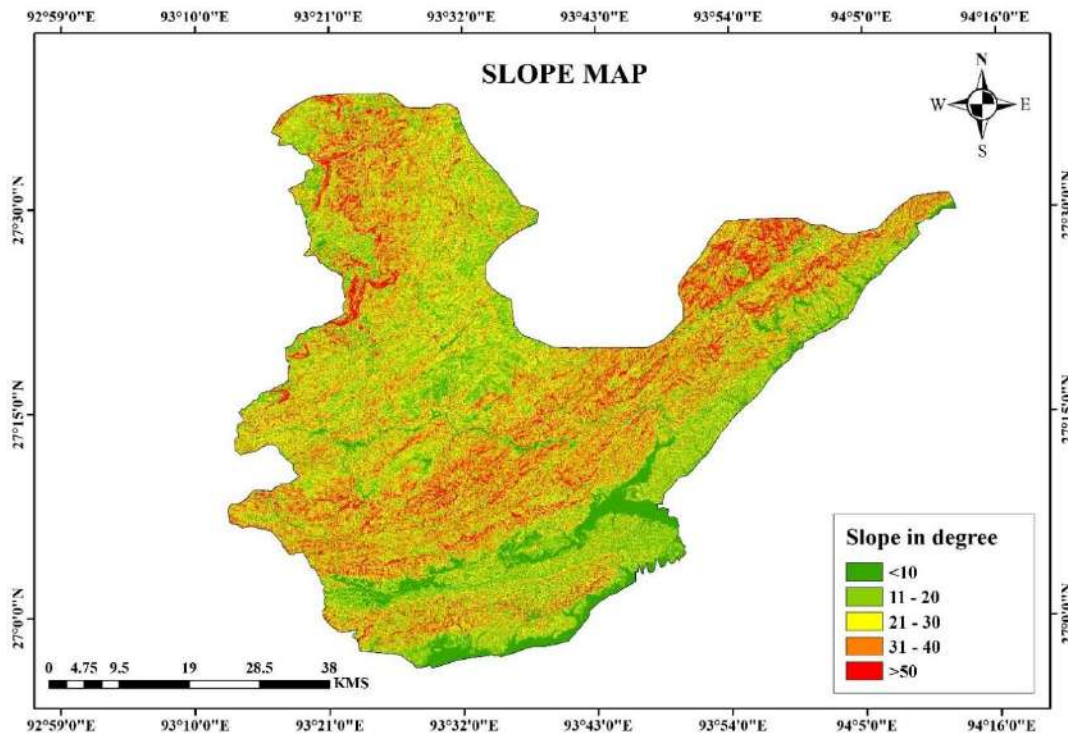
Fig. 3: Slope map.
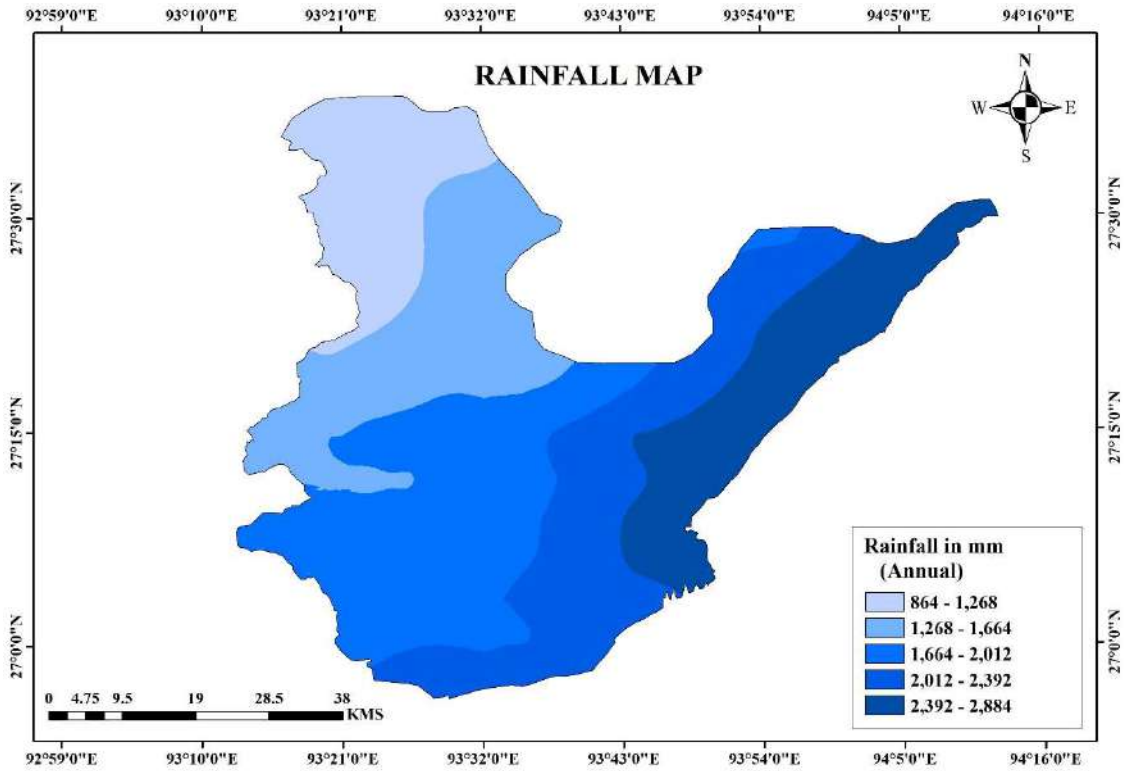
Fig. 4: Rainfall map.
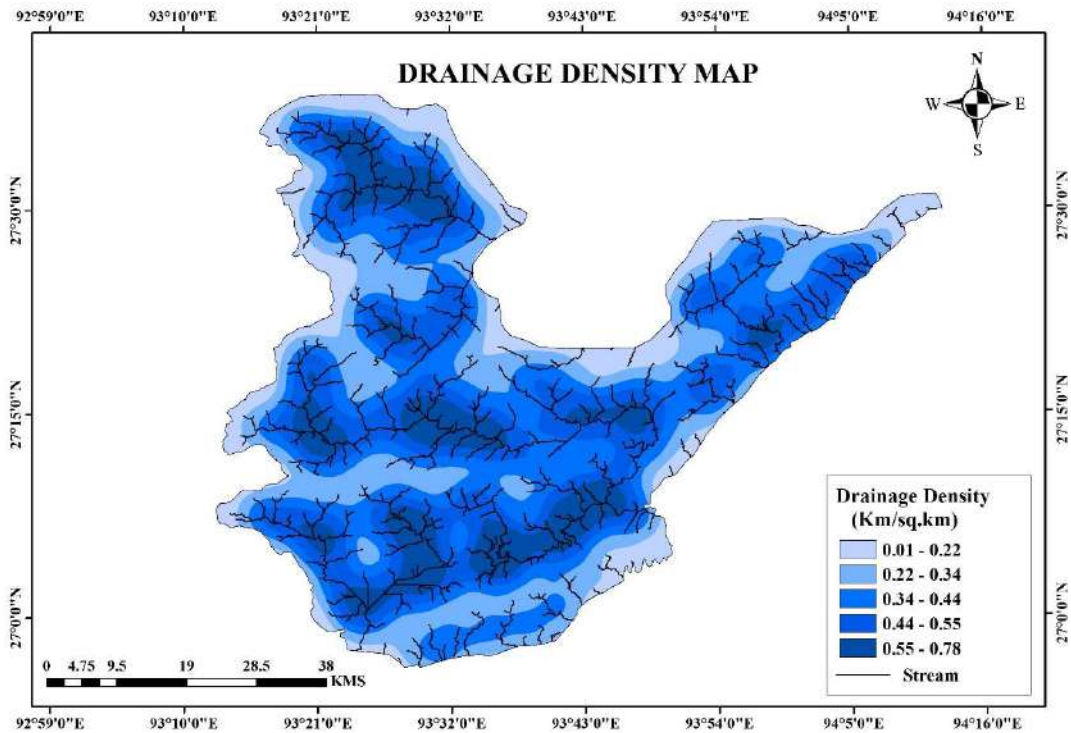
Fig. 5: Drainage Density map.

breaks into 5 classes such as class I (0-6.46 km/sq.km), class II (6.46-18.21 km/sq.km), class III (18.21-31.42 km/sq.km), class IV (31.42-42.04 km/sq.km), class V (49.04-74.9 km/sq.km). The regions with high lineament density values were provided with higher weights and vice-versa (Table 7).

Geomorphology

The geomorphologic map depicts important geomorphic units, landforms, and underlying geology to provide an understanding of the processes, lithology, structures, and geologic controls related to landslide susceptibility. The geomorphology of the region (Fig. 7) consists of a river, an alluvial/flood plain, highly/low dissected structural hills, a pediment/piedmont slope, and mass wasting. The region is mostly mountainous, forming a part of the eastern Himalayan ranges. The high/low dissected structural hills dominate the region with 3361.44 sq. km of areal coverage comprising 95.23% of the geographical area of the region, followed by alluvial/flood plain with 96.60 sq.km (2.73%), rivers occupying 49.83 sq.km (1.41%), pediment slope covering 21.53 sq.km (0.60%) and the rest are mass wasting products spread across 2.33 sq.km area (0.06%). The weights are ranks assigned to the geomorphological class, and sub-classes are depicted in Table 7.

Soil

Soil texture, soil depth, and soil erosion play an important role in assessing the stability of the soil and landslide susceptibility of the land. In the case of soil texture, the landslide occurrence probability value is higher in rocky and sandy loam and is lower in fine sandy loam, silt/gravelly silt loam, and loam (Lee et al. 2004). According to the generated soil map (Fig. 8), the region is mainly composed of three soil types: loamy soil (1516.33 sq.km areal coverage), fine loamy soil (1054.44 sq.km), and coarse loamy soil (959.18 sq.km). The study shows that lightweight soils like sandy and coarse loams are easy to detach as they need low organic matter content, leading to an inability to stable aggregates. Therefore, soil with a lot of sand, steep slopes, and intensive fall, which represent the most dominant factors of landslide, cause severe harm to the land, and thus, weights were provided accordingly (Table 7). Thus, the susceptibility of an area to landslide increases with the increase of soil erosion.

Geology

Lithology is one such factor that is oftentimes used for landslide susceptibility analysis in the hilly area
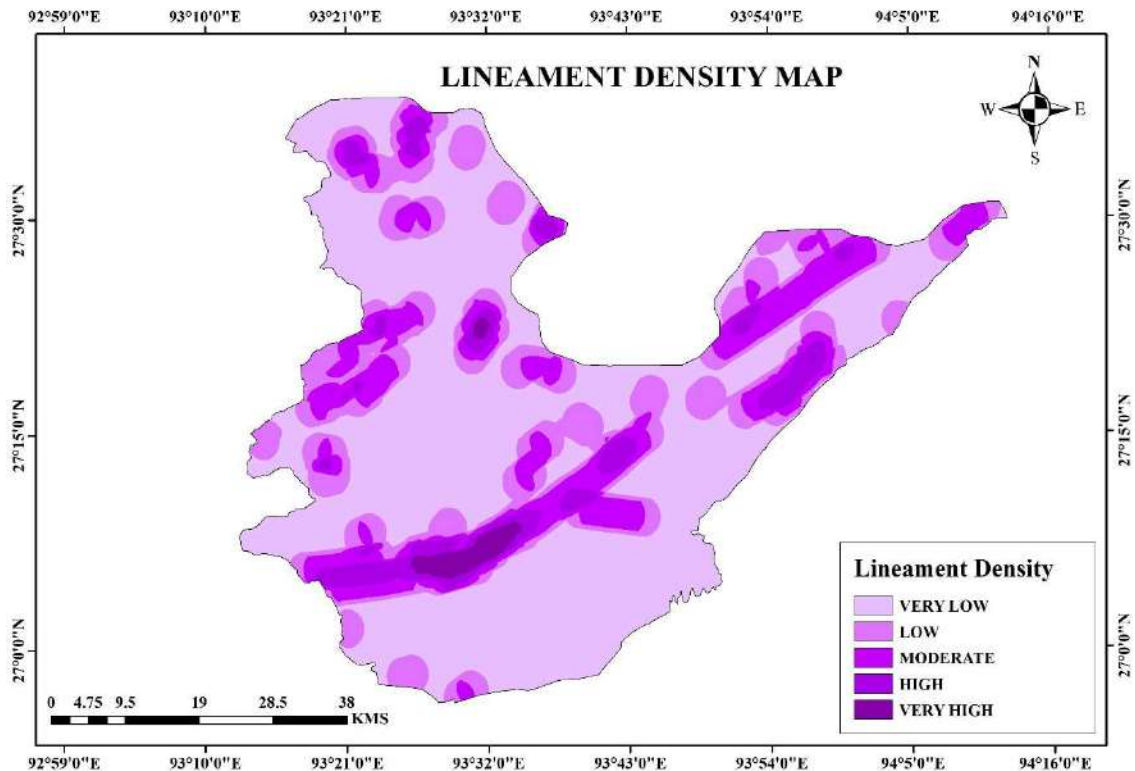
Fig. 6: Lineament Density map.
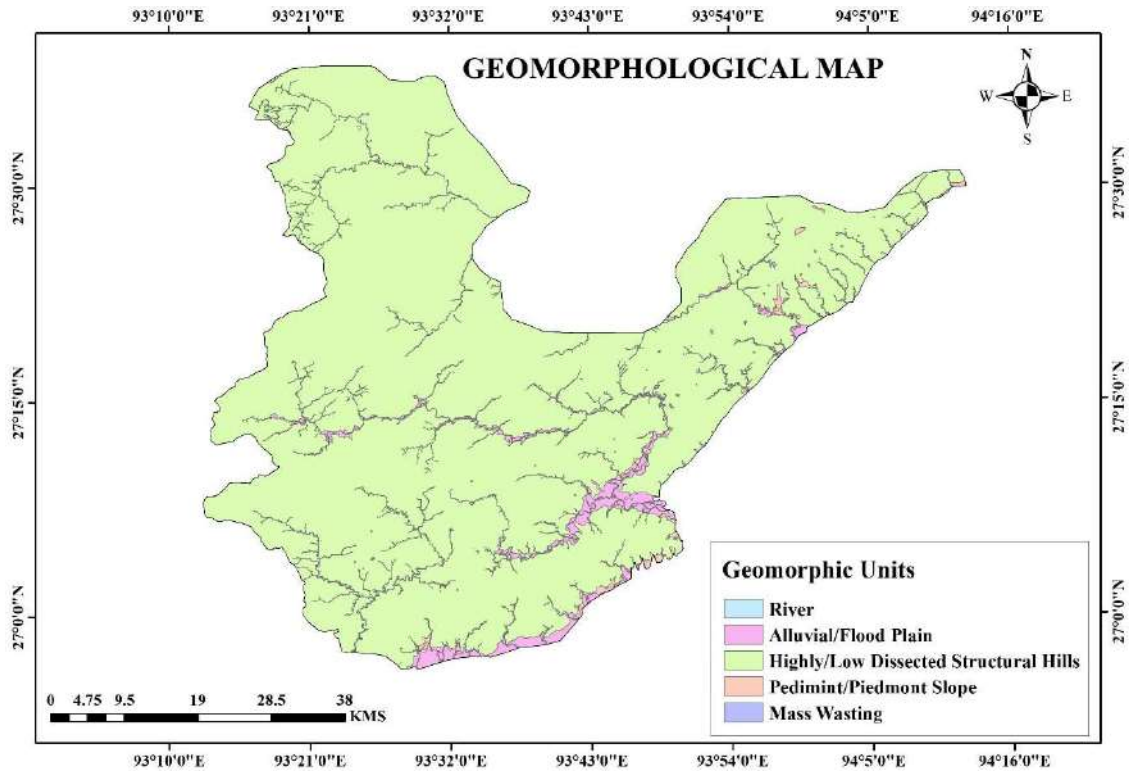
Fig. 7: Geomorphology.
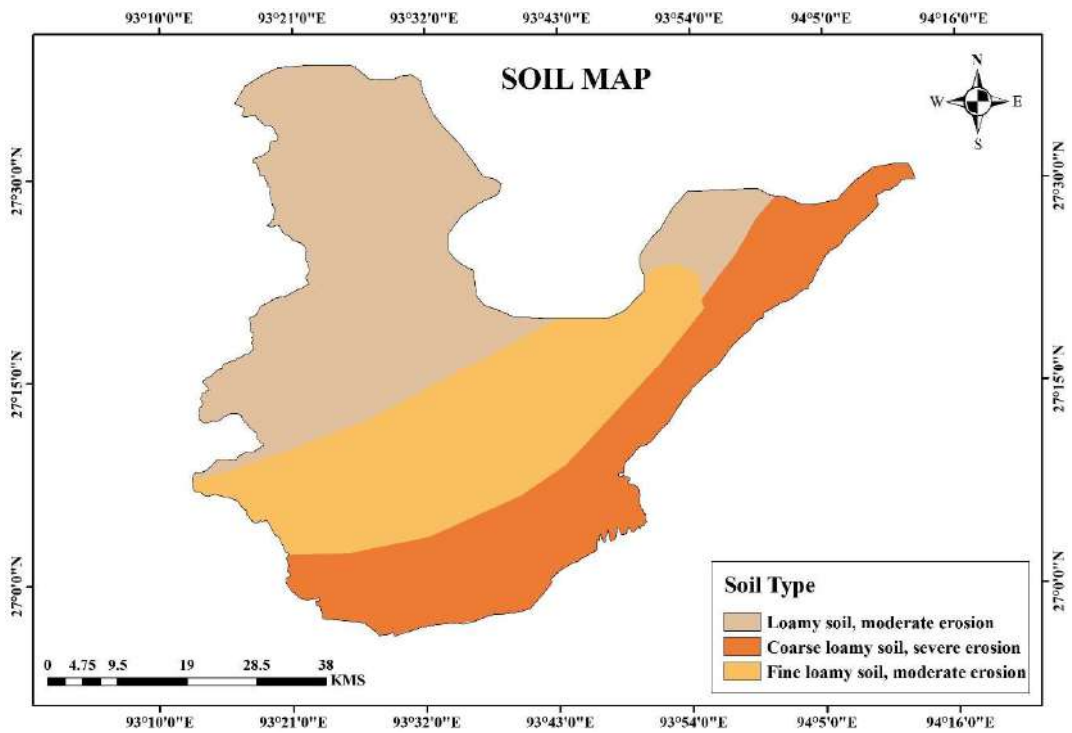
Fig. 8: Soil map.

(Althuwaynee et al. 2016). Landslides generally depend on the rock properties of the region because of the variance in strength and permeability of rocks. Due to heavy rainfall, weak or highly weathered or eroded rocks cause frequent landslides in different places around the world. In the study area (Fig. 9), the rocks that are the most dominant are the Siwalik group (59.28% area), followed by Undifferentiated Quaternary sediments (39.22% area), the Bomdila group (1.14% area) and the Lower Gondwana group (0.34% area). The region dominated by undifferentiated quaternary sediments was assigned the highest weight due to its unstable structure, and the Bomdila group was given the least weight as these rocks are comparatively older and more stable (Table 7).

Land-use/Land-cover

Alteration in land use/land cover is a crucial factor for landslide susceptibility models. Anthropogenic factors like the construction of buildings, roads, bridges, deforestation, etc., in the hilly regions also contribute to the event of landslides due to the instability of the slope. The LULC map (Fig 10) was prepared using Landsat 8 OLI satellite data. Five categories of land use/land cover were classified in the region, namely, dense forest (3385.23 sq.km), cropland (30.72 sq.km), sandbar (5.78 sq.km), rivers (10.02 sq.km),

and settlement (98.25 sq.km) were identified. In general, the region has a dense vegetation cover with thick evergreen forests, which are very less susceptible to landslides and, thus, were assigned the lowest weight. The weights assigned to each LULC sub-class are depicted in Table 7.

Landslide Hazard Zonation

The LSZ map was delineated by weighted overlay analysis which was performed in ArcGIS 10.8 software, with reference to the eight parameters cited above. The weighted values of each parameter (Table 7) indicate the impact of each parameter on another. Accordingly, the susceptibility map of the region contains five zones, based on the landslide susceptibility index such as "very low hazard, low hazard, moderate hazard, high hazard, and very high hazard" (Fig. 11). Table 8 signifies that 6.35% (223.55 sq. km) of the area falls under the very high zone, 26.29% (925.02 sq. km) has a high zone, 40.68% (1431.43 sq. km) in the moderate zone, 26.69% (938.24 sq. km) in low zone and only 0.003% (0.12 sq. km) has a very low potential for the occurrence of landslide. Most of the area falls under the moderate to high zone. The map demonstrates that the high to very high-landslide-hazard zone was concentrated in the following circles, i.e., Doimukh, Itanagar, Kakoi, Kimin,
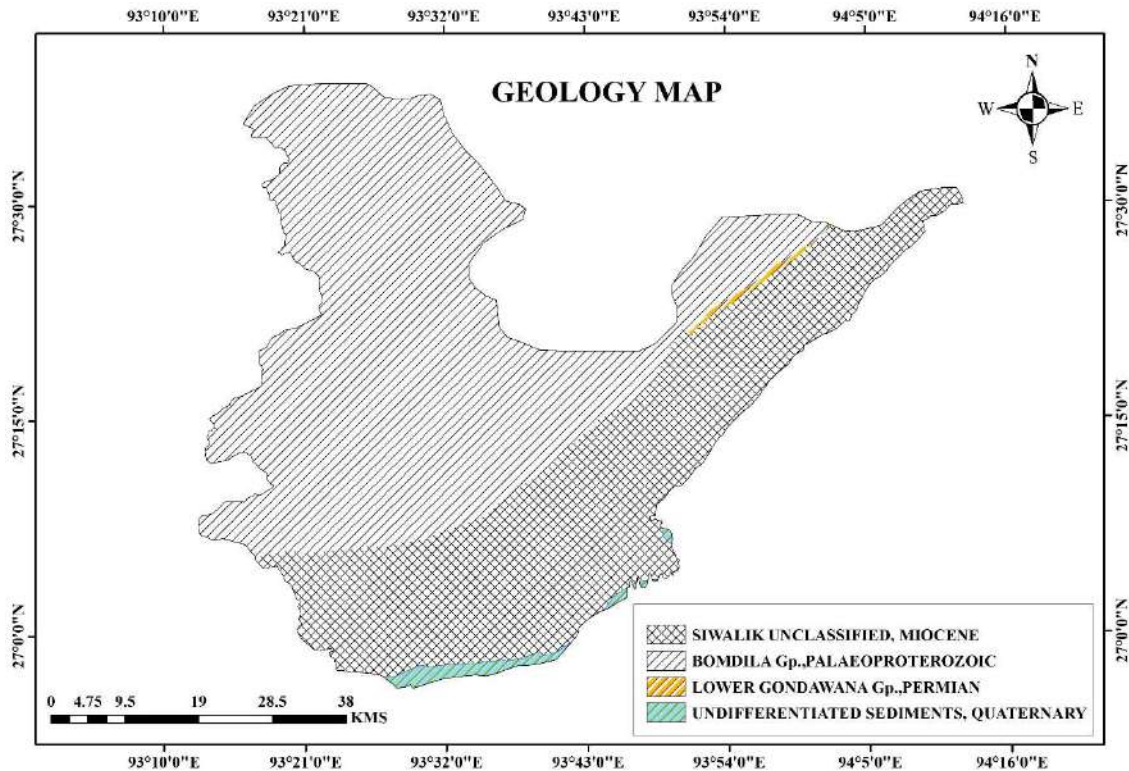
Fig. 9: Geology.
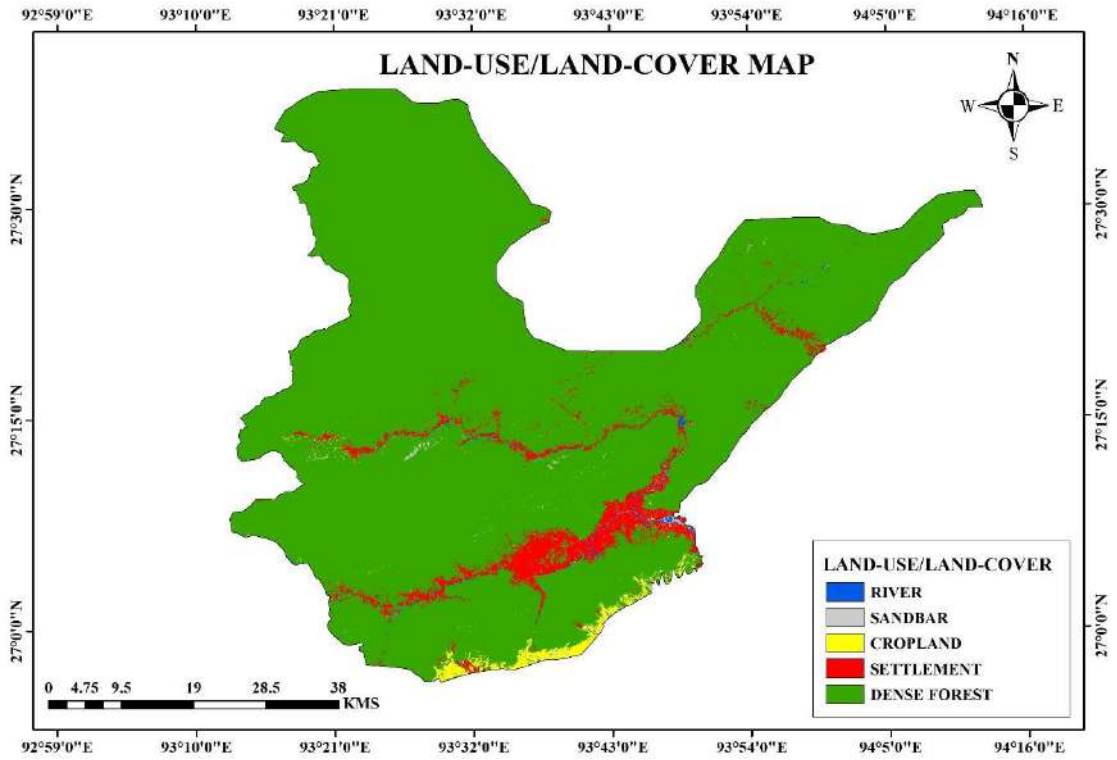
Fig. 10: Land use/Land cover map.
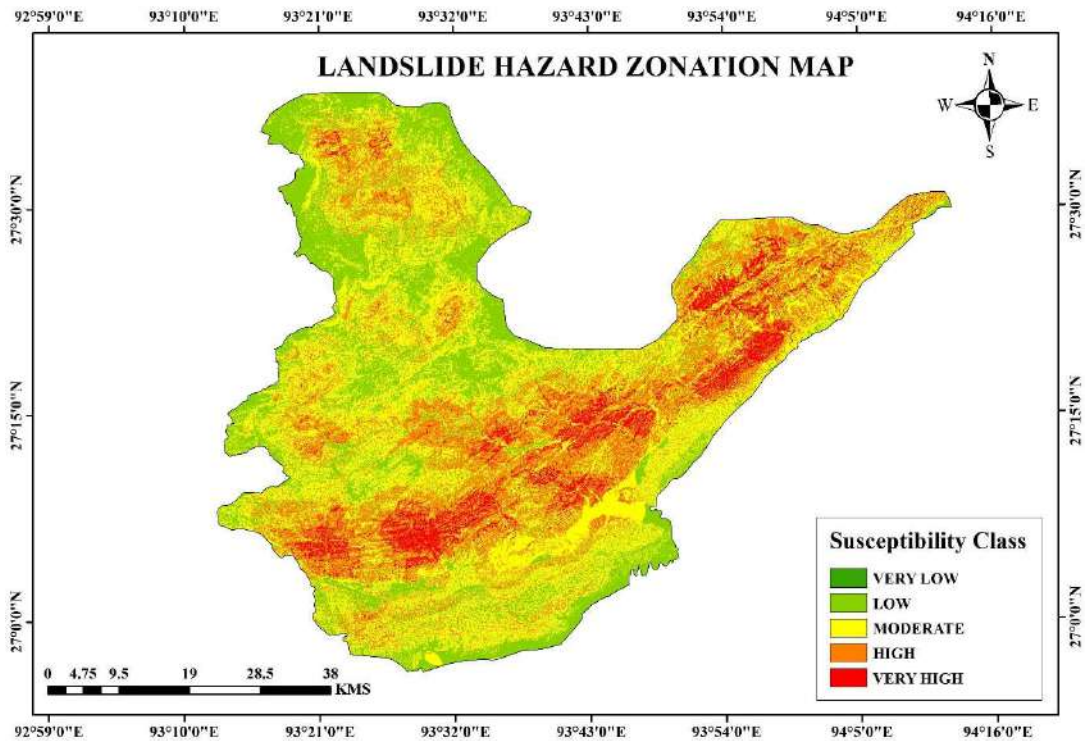
Fig. 11: LHZ map of the study area.

Table 7: Landslide hazard weights values and rating system of different thematic layers.

Factors	Classes	Weights	Rating	Consistency Ratio
Slope (in degree)	<10	0.29	1	0.017
	11-20		3	
	21-30		5	
	31-40		7	
	>50		9	
Rainfall (in mm)	864-1268	0.24	5	0.045
	1268-1664		6	
	1664-2012		7	
	2012-2392		8	
	2392-2884		9	
Drainage Density [Km. sq.km^{-1}]	0.01-0.22	0.16	1	0.016
	0.22-0.34		3	
	0.34-0.44		5	
	0.44-0.55		7	
	0.55-0.78		9	
Lineament Density [Km.sq.km^{-1}]	0-6.46	0.13	1	0.020
	6.46-18.21		3	
	18.21-31.42		5	
	31.42-42.04		7	
	49.04-74.9		9	
Geomorphology	River	0.07	3	0.039
	Alluvial/Floodplain		4	
	Highly/low dissected structural hills		5	
	Pedimont/Piedmont slope		6	
	Mass Wasting		7	
Soil	Loamy soil, moderate erosion	0.06	4	0.006
	Fine loamy soil, moderate erosion		5	
	Coarse loamy soil, severe erosion		6	
Geology	Siwalik unclassified, Miocene	0.03	6	0.086
	Bomdila Gp. Paleoproterozoic		4	
	Lower Gondwana Gp. Permian		5	
	Undifferentiated sediment, Quaternary		7	
LULC	River	0.02	8	0.053
	Sandbar		7	
	Cropland		6	
	Settlement		5	
	Dense Forest		4	

Naharlagun, Sangdupota, Toru, etc. Most of the concentrated hazard zones are seen near steep terrains and disturbed slopes because of earth-cutting for the construction of roads, buildings, etc. Areas that have low-hazard potential zones are largely concentrated in the southern part of the district, which are mostly low-lying regions. The delineated zonation map shows that the degree of landslide hazard decreases with increasing distance from drainage, lineament, and settlements.

Map Validation of LHZ Map with Field Data

Validation of the hazard zones is essential to confirm the precision rate of the landslide susceptibility map acquired based on the AHP model. In the current study, validation is done by using ROC (Receiver Operating Characteristic) as a

Table 8: Area of zones (Percentage).

Susceptibility zone	Area [km^2]	Area in Percentage [%]
Very Low zone	0.12	0.003
Low zone	938.24	26.69
Moderate zone	1431.43	40.68
High zone	925.02	26.29
Very High zone	223.55	6.35

tool for appraising the efficiency of landslide zonation. ROC curve is mostly used to show the correlation between True Positive Rate and False Positive Rate graphically (Althouse 2016). A landslide inventory map (Fig. 12) was prepared based on data collected from the Geological Survey of India
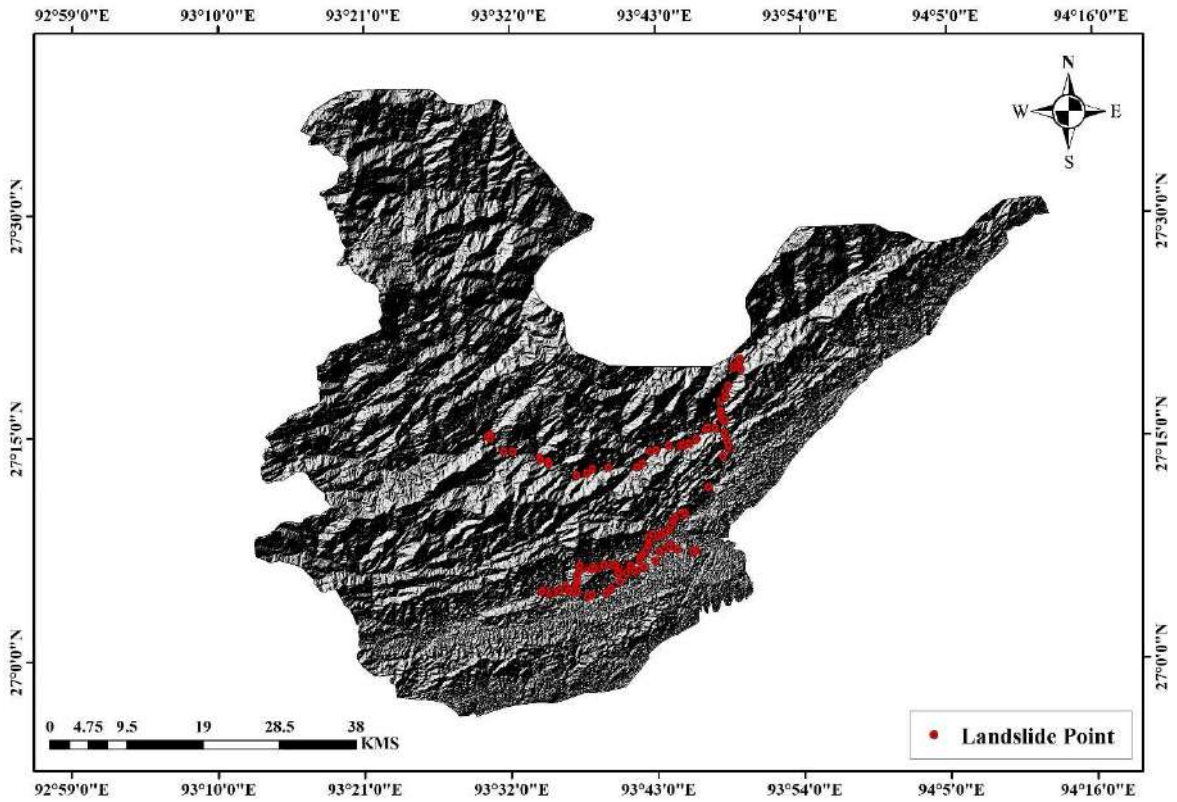
Fig. 12: Landslide inventory map.
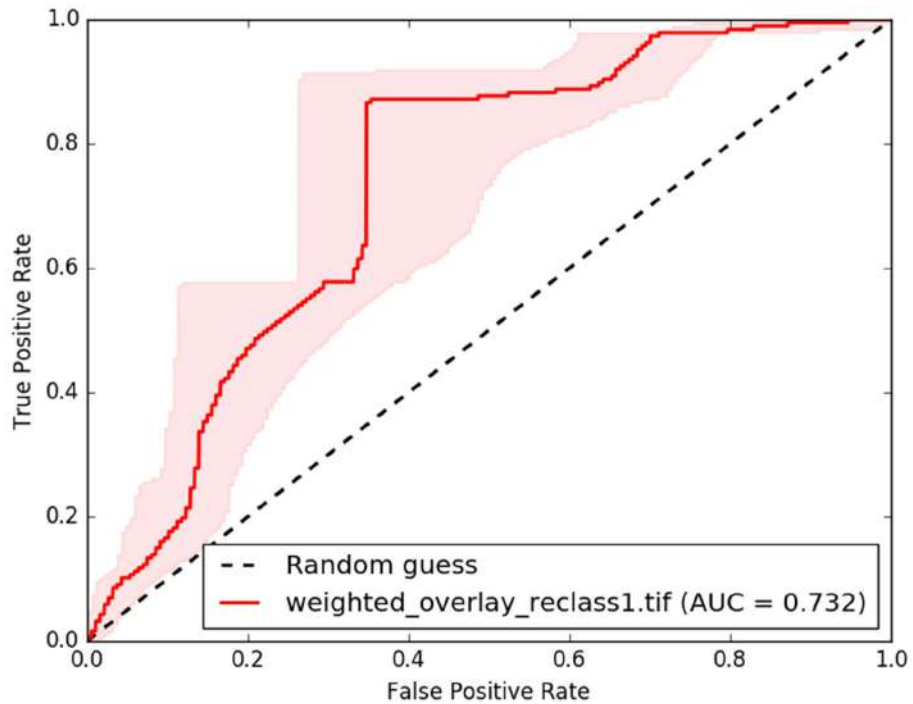
Fig. 13: ROC curve for Landslide zonation map derived from AHP.
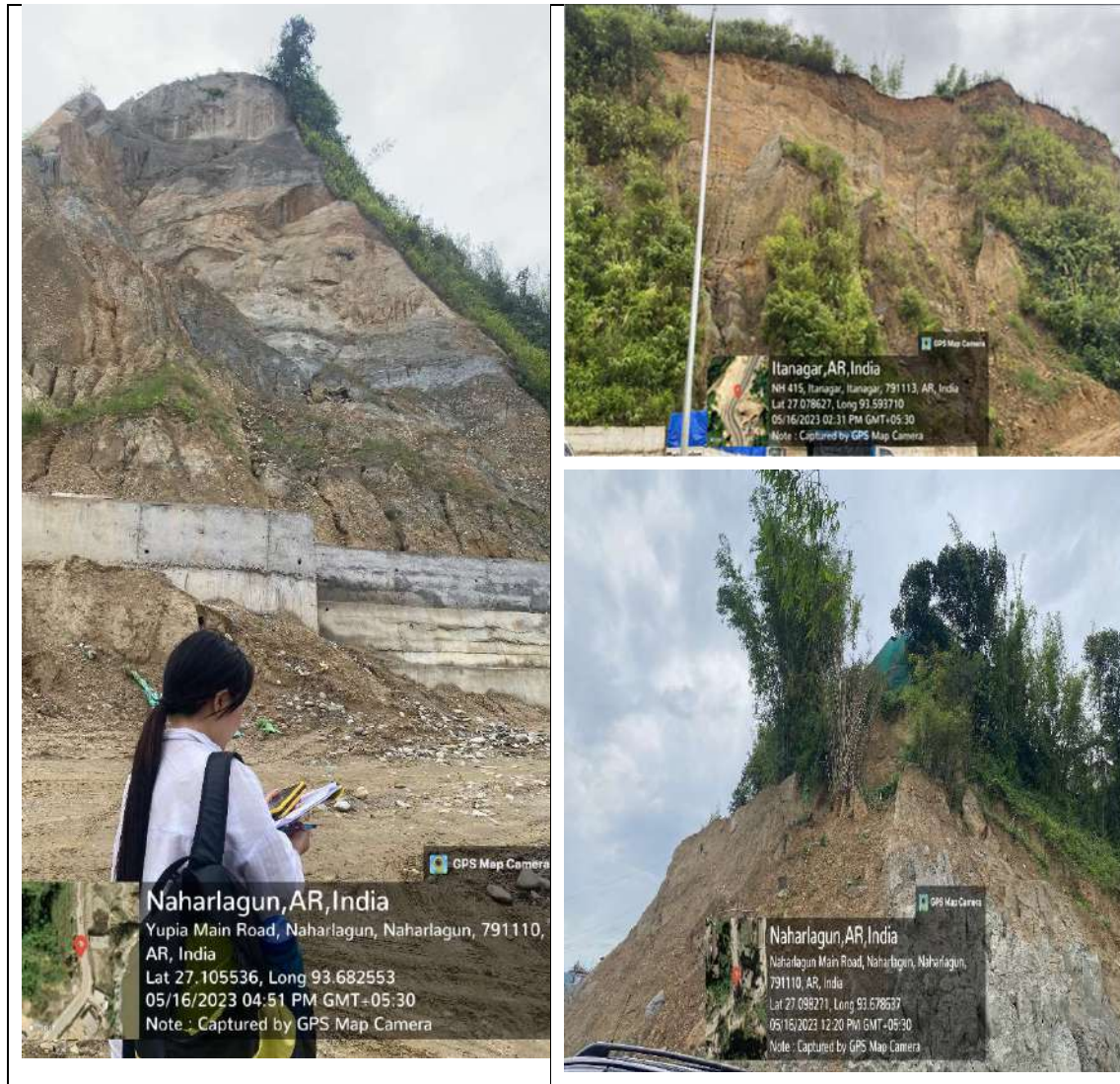
Fig. 14: Photographs of some selected landslide sites of the study area.

and field visits. A total of hundred landslide location points were collected using the GPS device during the field survey and Geological Survey of India and were analyzed with the LHZ map using ArcSDM tools. The value of the accuracy curve for the Area Under Curve (AUC) ranges between 0.5 to 1, and the prediction model based on the ROC curve and AHP generated a value of 0.73 or 73%, which quantifies that the prediction is good (Fig. 13). Fig. 14 shows images from the field visit identifying some active landslide zones in the Papumpare districts.

Limitations and Suggestions for Future Research

The landslide hazard zonation (LSZ) of the Papumpare district using GIS and AHP techniques provided significant results. However, the research has several limitations that should be acknowledged for building a base for future studies in the region. Some of the limitations include a lack of adequate landslide data, inaccessibility due to rugged terrain conditions and limited field validation, subjectivity in the AHP model, and lack of monitoring temporal change in different landslide triggering factors. Thus, future courses of research need to be guided by the integration of real-time data, consideration of other hazards associated with landslides, and the use of GIS-based machine learning (ML) and deep learning (DL) in landslide zone mapping.

CONCLUSIONS

Papumpare, the capital district of Arunachal Pradesh, is prone

to frequent landslide, which occurs every year mostly due to heavy downpours, seismic activity, and anthropogenic interference. During the monsoon season, the region faces difficulties caused by landslides, resulting in several issues like loss of life, damage of properties, and hindering social and economic progress. In the present research, potential landslide sites were identified by integrating AHP and geospatial technologies using eight landslide-triggering factors. The findings revealed that more than 70% (2,580 sq. km) of the region falls under moderate to very high landslide zones, and the rest of the region falls under low to very low landslide potential zones. The higher landslide susceptibility was witnessed in the areas affected by human intervention, higher rainfall, and geological vulnerability. The validation of the LSZ map was realized through field surveys and by generating a landslide inventory map and ROC-AUC curve with an accepted value of 0.73. The results suggest good landslide predictability. However, the improvement of the prediction accuracy of the delineated map can be further reformed by considering more factors. The resulting LHZ map of the Papumpare district can be a reliable repository of information supporting land-use planning and management of the terrain, helping to minimize the impact of landslides in the region.

REFERENCES

Ahmed, B., 2015. Landslide susceptibility mapping using multi-criteria evaluation techniques in Chittagong Metropolitan Area, Bangladesh. *Landslides*, 12, pp.1077–1095. https://doi.org/10.1007/s10346-014-0521-x

Althouse, A.D., 2016. Statistical graphics in action: Making better sense of the ROC curve. *International Journal of Cardiology*, 215, pp.9-10. http://dx.doi.org/10.1016/j.ijcard.2016.04.026

Althuwaynee, O.F., Pradhan, B. and Lee, S., 2016. A novel integrated model for assessing landslide susceptibility mapping using CHAID and AHP pair-wise comparison. *International Journal of Remote Sensing*, 37(5), pp.1190-1209. https://doi.org/10.1080/01431161.2016.1148282

Anbalagan, R., Kumar, R., Lakshmanan, K., Parida, S. and Neethu, S., 2015. Landslide hazard zonation mapping using frequency ratio and fuzzy logic approach: a case study of Lachung Valley, Sikkim. *Geoenvironmental Disasters*, 2(6), pp.1–17. https://doi.org/10.1186/s40677-014-0009-y

Arora, M.K., Das Gupta, A.S. and Gupta, R.P., 2004. An artificial neural network approach for landslide hazard zonation in the Bhagirathi (Ganga) Valley, Himalayas. *International Journal of Remote Sensing*, 25(3), pp.559–572. https://doi.org/10.1080/0143116031000156819

Australian Geomechanics Society (AGS), 2000. Landslide risk management concepts and guidelines. *Australian Geomechanics*, 35, pp.49–92.

Avtar, R., Singh, C.K., Singh, G., Verma, R.L., Mukherjee, S. and Sawada, H., 2011. Landslide susceptibility zonation study using remote sensing and GIS technology in the Ken-Betwa River Link area, India. *Bulletin of Engineering Geology and the Environment*, 70(4), pp.595–606. https://doi.org/10.1007/s10064-011-0368-5

Barman, J., Biswas, B. and Rao, K.S., 2024. Hybrid integration of analytical hierarchy process (AHP) and the multiobjective optimization on the basis of ratio analysis (MOORA) for landslide susceptibility zonation of Aizawl, India. *Natural Hazards*, 120, pp.8571–8596. https://doi.org/10.1007/s11069-024-06538-9

Bera, A., Mukhopadhyay, B.P. and Das, D., 2019. Landslide hazard zonation mapping using multi-criteria analysis with the help of GIS techniques: a case study from Eastern Himalayas, Namchi, South Sikkim. *Natural Hazards*, 96, pp.935–959. https://doi.org/10.1007/s11069-019-03580-w

Das, S., Sarkar, S. and Kanungo, D.P., 2022. GIS-based landslide susceptibility zonation mapping using the analytic hierarchy process (AHP) method in parts of Kalimpong Region of Darjeeling Himalaya. *Environmental Monitoring and Assessment*, 194, p.234. https://doi.org/10.1007/s10661-022-09851-7

Devkota, K.C., Regmi, A.D., Pourghasemi, H.R., Yoshida, K., Pradhan, B., Ryu, I.C., Dhital, M.R. and Althuwaynee, O.F., 2013. Landslide susceptibility mapping using certainty factor, index of entropy, and logistic regression models in GIS and their comparison at Mugling-Narayanghat road section in Nepal Himalaya. *Natural Hazards*, 65(1), pp.135–165. https://doi.org/10.1007/s11069-012-0347-6

Feizizadeh, B., Roodposhti, M.S., Jankowski, P. and Blaschke, T., 2014. A GIS-based extended fuzzy multi-criteria evaluation for landslide susceptibility mapping. *Computers & Geosciences*, 73, pp.208–221. https://doi.org/10.1016/j.cageo.2013.11.009

Fell, R., Corominas, J., Bonnard, C., Cascini, L., Leroi, E. and Savage, W.Z., 2008. Guidelines for landslide susceptibility, hazard and risk zoning for land use planning. *Engineering Geology*, 102(3-4), pp.85–98. https://doi.org/10.1016/j.enggeo.2008.03.022

Fell, R., Whitt, G., Miner, A. and Flentje, P.N., 2007. Guidelines for landslide susceptibility, hazard and risk zoning for land use planning. *Australian Geomechanics Journal*, 42(1), pp.13–36

Gorsevski, P.V., Jankowski, P. and Gessler, P.E., 2006. A heuristic approach for mapping landslide hazard by integrating fuzzy logic with analytic hierarchy process. *Control and Cybernetics*, 35, pp.121–146.

Hadmoko, D.S., Lavigne, F. and Samodra, G., 2017. Application of a semiquantitative and GIS-based statistical model to landslide susceptibility zonation in Kayangan Catchment, Java, Indonesia. *Natural Hazards*, 87, pp.437–468. https://doi.org/10.1007/s11069-017-2772-z

Hemasinghe, H., Rangali, R.S.S., Deshapriya, N.L. and Samarakoon, L., 2018. Landslide susceptibility mapping using logistic regression model (a case study in Badulla District, Sri Lanka). *Procedia Engineering*, 212, pp.1046–1053. https://doi.org/10.1016/j.proeng.2018.01.135

Hoa, P.V., Tuan, N.Q., Hong, P.V., Thao, G.T.P. and Binh, N.A., 2023. GIS-based modeling of landslide susceptibility zonation by integrating the frequency ratio and objective–subjective weighting approach: a case study in a tropical monsoon climate region. *Frontiers in Environmental Science*, 11, p.1175567. https://doi.org/10.3389/fenvs.2023.1175567

Hong, Y., Adler, R. and Hufman, G., 2007. Use of satellite remote sensing data in the mapping of global landslide susceptibility. *Natural Hazards*, 43, pp.245–256. https://doi.org/10.1007/s11069-006-9104-z

Huan, Y., Song, L. and Khan, U., 2023. Stacking ensemble of machine learning methods for landslide susceptibility mapping in Zhangjiajie City, Hunan Province, China. *Environmental Earth Sciences*, 82, p.35. https://doi.org/10.1007/s12665-022-10723-z

Ilanloo, M., 2011. A comparative study of fuzzy logic approach for landslide susceptibility mapping using GIS: An experience of Karaj dam basin in Iran. *Procedia-Social and Behavioral Sciences*, 19, pp.668–676. https://doi.org/10.1016/j.sbspro.2011.05.184

Intergovernmental Panel on Climate Change (IPCC), 2021. *Climate Change 2021: The Physical Science Basis*. [online] Available at: https://wmo.int/media/magazine-article/regional-trends-extreme-events-ipcc-2021-report [Accessed 26 June 2024]

Jhunjhunwalla, M., Gupta, S.K. and Shukla, D.P., 2019. Landslide Susceptibility Zonation (LSZ) Using Machine Learning Approach for DEM Derived Continuous Dataset. In: Santosh, K. and Hegadi, R. (eds) *Communications in Computer and Information Science*, vol. 1037, Springer, p.45. https://doi.org/10.1007/978-981-13-9187-3_45

Kanungo, D.P., Sharma, S. and Pain, A., 2014. Artificial Neural Network

(ANN) and Regression Tree (CART) applications for the indirect estimation of unsaturated soil shear strength parameters. *Frontiers of Earth Science*, 8, pp.439–456. https://doi.org/10.1007/s11707-014-0416-0

Kanwal, S., Atif, S. and Shafiq, M., 2016. GIS-based landslide susceptibility mapping of northern areas of Pakistan, a case study of Shigar and Shyok Basins. *Geomatics, Natural Hazards and Risk*. https://doi.org/10.1080/19475705.2016.1220023

Kirschbaum, D., Kapnick, S.B., Stanley, T. and Pascale, S., 2020. Changes in extreme precipitation and landslides over High Mountain Asia. *Geophysical Research Letters*, 47, e2019GL085347. https://doi.org/10.1029/2019GL085347

Kolat, C., Ulusay, R. and Suzen, M.L., 2012. Development of geotechnical micro zonation model for Yenisehir (Bursa, Turkey) located at a seismically active region. *Engineering Geology*, 127, pp.36–53. https://doi.org/10.1016/j.enggeo.2011.12.014

Kouli, M., Loupasakis, C. and Soupios, P., 2010. Landslide hazard zonation in high-risk areas of Rethymno Prefecture, Crete Island, Greece. *Natural Hazards*, 52, pp.599–621. https://doi.org/10.1007/s11069-009-9403-2

Lee, S., Choi, J. and Min, K., 2004. Probabilistic landslide hazard mapping using GIS and remote sensing data at Boun, Korea. *International Journal of Remote Sensing*, 25(11), pp.2037–2052. https://doi.org/10.1080/01431160310001618734

Lombardo, L., Tanyas, H. and Nicu, I.C., 2020. Spatial modeling of multi-hazard threat to cultural heritage sites. *Engineering Geology*, 277, p.105776. https://doi.org/10.1016/j.enggeo.2020.105776

Mahdadi, F., Boumezbeur, A., Hadji, R., et al., 2018. GIS-based landslide susceptibility assessment using statistical models: a case study from Souk Ahras province, N-E Algeria. *Arabian Journal of Geosciences*, 11, p.476. https://doi.org/10.1007/s12517-018-3770-5

Masson-Delmotte, V., Zhai, P., Pirani, A., Connors, S.L., Péan, C. and Berger, S., 2021. *Climate Change 2021: The Physical Science Basis*. Cambridge University Press https://dx.doi.org/10.1017/9781009157896

Merghadi, A., Yunus, A.P., Dou, J., Whiteley, J., Thai, Pham, B., Bui, D.T., Avtar, R. and Abderrahmane, B., 2020. Machine learning methods for landslide susceptibility studies: A comparative overview of algorithm performance. *Earth-Science Reviews*, 207, p.103225. https://doi.org/10.1016/j.earscirev.2020.103225

Othman, A.N., Naim, W.M. and Noraini, S., 2012. GIS-based multi-criteria decision making for landslide hazard zonation. *Procedia - Social and Behavioral Sciences*, 35, pp.595–602. https://doi.org/10.1016/j.sbspro.2012.02.126

Ozioko, O.H. and Igwe, O., 2020. GIS-based landslide susceptibility mapping using heuristic and bivariate statistical methods for Iva Valley and environs Southeast Nigeria. *Environmental Monitoring and Assessment*, 192, pp.1–19. https://doi.org/10.1007/s10661-019-7951-9

Pareta, K. and Pareta, U., 2015. Geomorphological interpretation through satellite imagery & DEM data. *American Journal of Geophysics Geochemistry Geosystems*, 1(2), pp.19–36.

Pareta, K., 2004. Hydro-geomorphology of Sagar district (MP): A study through remote sensing technique. In: Proceedings of XIX MP Young Scientist Congress, Madhya Pradesh Council of Science and Technology (MAPCOST), Bhopal.

Paulín, G.L., Bursik, M., Hubp, J.L., et al., 2014. A GIS method for landslide inventory and susceptibility mapping in the Río El Estado watershed, Pico de Orizaba volcano, Mexico. *Natural Hazards*, 71, pp.229–241. https://doi.org/10.1007/s11069-013-0911-8

Qazi, A., Singh, K. and Vishwakarma, D.K., 2023. GIS based landslide susceptibility zonation mapping using frequency ratio, information value, and weight of evidence: A case study in Kinnaur District HP, India. *Bulletin of Engineering Geology and the Environment*, 82, p.332. https://doi.org/10.1007/s10064-023-03344-8

Raju, M., 2002. Landslide hazard zonation for effective land management of mountainous terrain. In: *Arunachal Pradesh: Environmental Planning and Sustainable Development-Opportunities and Challenges*, Hepaticas Occasional Publication, (16), pp.439–443.

Saaty, T.L., 1980. *The Analytic Hierarchy Process*. McGrawhill, Juc. New York.

Saaty, T.L., 1990. How to make a decision: The analytic hierarchy process. *European Journal of Operational Research*, 48(1), pp.9–26. https://doi.org/10.1016/0377-2217(90)90057-I

Saravanan, S., Saranya, T., Abijith, D., Jacinth, J.J. and Singh, L., 2021. Delineation of groundwater potential zones for Arkavathi sub-watershed, Karnataka, India using remote sensing and GIS. *Environmental Challenges*, 5, p.100380. https://doi.org/10.1016/j.envc.2021.100380

Sarkar, S. and Kanungo, D.P., 2004. An integrated approach for landslide susceptibility mapping using remote sensing and GIS. *Photogrammetric Engineering & Remote Sensing*, 70(5), pp.617–625. http://dx.doi.org/10.14358/PERS.70.5.617

Shano, L., Raghuvanshi, T.K. and Meten, M., 2022. Landslide hazard zonation using logistic regression model: The case of Shafe and Baso catchments, Gamo Highland, Southern Ethiopia. *Geotechnique & Geology Engineering*, 40, pp.83–101. https://doi.org/10.1007/s10706-021-01873-1

Stanley, T. and Kirschbaum, D.B., 2017. A heuristic approach to global landslide susceptibility mapping. *Natural Hazards*, 87(1), pp.145–164. https://doi.org/10.1007/s11069-017-2757-y

Veerappan, R., Negi, A. and Siddan, A., 2017. Landslide susceptibility mapping and comparison using frequency ratio and analytical hierarchy process in part of NH-58, Uttarakhand, India. In: *Advancing Culture of Living with Landslides: Volume 2 Advances in Landslide Science* (pp. 1081–1091). Springer International Publishing. https://doi.org/10.1007/978-3-319-53498-5_123

Yadav, M., Pal, S.K., Singh, P.K. and Gupta, N., 2023. Landslide susceptibility zonation mapping using frequency ratio, information value model, and logistic regression model: A case study of Kohima District in Nagaland, India. In: Thambidurai, P. and Singh, T.N. (eds), *Landslides: Detection, Prediction, and Monitoring*. Springer, Cham. https://doi.org/10.1007/978-3-031-23859-8_17

Younes Cárdenas, N. and Erazo Mera, E., 2016. Landslide susceptibility analysis using remote sensing and GIS in the western Ecuadorian Andes. *Natural Hazards*, 81, pp.1829–1859. https://doi.org/10.1007/s11069-016-2157-8

Recent Advances and Prospects of Microbial Biosurfactant-Mediated Remediation of Engine Oil Pollution: A Comprehensive Review

Nafisa Mohammed Babayola[iD] **and Martins A. Adefisoye†**[iD]

Department of Microbiology, School of Science and Technology, Babcock University, Ilishan-Remo 121103, Nigeria
†Corresponding author: Martins A. Adefisoye; adefisoyem@babcock.edu.ng

ABSTRACT

A major global concern is the widespread environmental destruction caused by hydrocarbons, especially from the dumping of spent engine oil. Hydrocarbons are a major source of pollution in the environment and have an impact on agriculture, aquatic life, and soil fertility. The necessity of resolving this issue is highlighted by the detrimental impact on soil biocenosis and the potential conversion of soils into technogenic deserts. Due to high costs and polluting byproducts, the conventional approach of treating contaminated soil, sediment, and water is unsustainable. However, bioremediation, which makes use of biological agents like fungi and bacteria, appears to be a more practical and affordable solution. Microbial biosurfactants present a possible solution for environmental restoration due to their less harmful nature compared to chemical surfactants. This review highlights the green and sustainable nature of microbial biosurfactants while examining their advancements, biotechnological potentials, and future possibilities for bioremediation. The review also looks at the genetic basis and economic viability of biosurfactants for bioremediation applications. Furthermore, the review emphasizes the need for more studies in overcoming the challenges of large-scale application of biological surfactants for bioremediation of pollution and environmental restoration. As partners in nature, these bacteria aid in the breakdown of hydrocarbons, highlighting the need for industry and the environment to coexist sustainably. As biosurfactants are less harmful to the environment than chemical surfactants, they are more in line with the global trend toward sustainable methods and the use of natural processes for ecological restoration.

INTRODUCTION

The pollution of the environment by petroleum hydrocarbons and their products is an ongoing global challenge with its attendant problems (Venkatraman et al. 2024). Intentional or accidental disposal of spent engine oil into the soils and waterways is one of the most notable environmental problems (Shehu et al. 2023), almost as widespread as crude oil pollution in many developing countries (Emoyan et al. 2020). Hydrocarbons, their derivatives, and waste products, including spent engine oil, have been identified as significant contributors to the menace of environmental pollution (Ahmad 2022) and mainly emanate from the automobile industry, including auto mechanic workshops (Muze et al. 2020). Hydrocarbons are thought to be among the most hazardous environmental contaminants because of their extreme toxicity and widespread occurrence in the biosphere (Umar et al. 2021). Aquatic and marine plants and animals have not been spared from the effects of these activities, which have also led to the contamination of agricultural soils. Hydrocarbons and their by-products rank second in terms of their detrimental effects, right behind radioactivity (Waters et al. 2018). Due to its tremendous adsorbing surface area, the soil is particularly impacted because of its ability to store huge quantities of pollutants. The chemical composition, structure, and qualities of many soils have been significantly affected by hydrocarbon pollution, which in turn impairs soil fertility and agronomic value. This adverse situation has detrimental

effects on soil biocenosis (Sydorenko 2023). Oil spills have the potential to transform soils into typical technogenic deserts devoid of most biological life. Soils contaminated with hydrocarbons are unsuitable for agricultural purposes and can potentially contaminate ground and surface waters. Depending on the kind of soil, self-restoration can take a long time, 10 to 30 years or more (Liftshits et al. 2018).

The typical approach of treating contaminated soil, sediment, and water is proven to be unsustainable because of the huge cost and generation of contaminating byproducts (Da'ana et al. 2021). However, with the versatile capabilities of biological agents, such as bacteria, fungi, and other microorganisms or their enzymes, bioremediation has evolved as a sustainable, cost-effective, and natural method for restoring contaminated soil, surface water, and groundwater (Pande et al. 2020). To accelerate the breakdown and/or removal of inorganic and organic contaminants, microorganisms are cultivated in the presence of contaminated soil, sediment, or water samples. This is an emerging and rapidly growing green and sustainable biotechnological field (Kumar et al. 2018). For instance, a biomolecule by *Bacillus* sp. isolated from a water reservoir in Brazil had previously been studied by Korenblum and associates (Korenblum et al. 2012). Similarly, Joshi et al. (2016) synthesized, optimized, and characterized biosurfactant from a *Bacillus licheniformis* W16 strain isolated from soil samples collected near an oil well in Oman, while El-Sheshtawy et al. (2015) produced biological surfactant with *B. licheniformis* isolated from an Egyptian oil reservoir. These studies demonstrate the versatility of biosurfactant-producing bacteria, particularly *Bacillus* strains, from different geographic locations (Brazil, Oman, and Egypt). This geographic diversity highlights the adaptability of these microbes to varying environmental conditions associated with oil contamination. Their findings suggest that exploring microbial strains from different regions can provide insight into biosurfactant production and optimize their application for bioremediation in diverse ecosystems. In many developing such as Nigeria, there are a lot of oil-contaminated soils, and this has negative health, social, and economic effects since there is inadequate regulation of oil waste disposal, among other things (Adeola et al. 2022, Orisakwe 2021). This review seeks to synthesize information and discusses the advances, biotechnological potentials, and prospects of microbial biosurfactants as an important green and sustainable option for the bioremediation of spent engine oil-contaminated soils, the genetics of the biosurfactant-producing microbes and the economic viability of microbial biosurfactants for bioremediation processes.

MICROBIAL BIOSURFACTANTS AND THEIR PROPERTIES

Biosurfactants are biosurface-active agents which are produced by numerous microorganisms. Biosurfactants are exopolymeric substances (EPS) with amphipathic properties, produced outside of the cell or as part of cell membrane biomolecules by a variety of bacteria, fungi, and yeasts (Santos et al. 2016). The commonly used surfactants are chemically derived (Moldes et al. 2021), but their high persistence power, low degradation rate, and hazardous nature limit their applications (Alizadeh-Sani et al. 2018). Microbial (bio) surfactants hold numerous advantages over chemical surfactants, including greater selectivity, less toxicity, increased temperature tolerance, stability in pH change, and high salt tolerance (Sarubbo et al. 2022, Shekhar et al. 2015). Due to their numerous potential uses as wetting agents, emulsifiers, foaming agents, detergents, and dispersants, biosurfactants, which can be neutral or anionic, are becoming more and more valued in the commercial sector (Gaur et al. 2021). They can be used in many different industries, such as the food processing, cosmetics, petroleum, agricultural, and pharmaceutical sectors, so also in oil recovery, site management, and cleanup (Adetunji & Olaniran 2018, Araújo et al. 2019). Their potential as antiviral, antifungal, antibacterial, and anti-adhesive medicines against a variety of drug-resistant organisms has also been explored for a variety of biological uses (Alara & Alara 2024). Biosurfactants are high-efficiency molecules, they enhance the extraction of oil from the well (Enhanced Oil Recovery) and are frequently employed in hydrocarbon bioremediation research (Karlapudi et al. 2018).

CLASSIFICATION AND CHEMICAL NATURE OF BIOSURFACTANTS

The chemical composition and microbiological source are the main criteria for classifying biosurfactants. As depicted in (Fig. 1), microbial surfactants are categorized into high (including polymeric and particulate surfactants) and low (including phospholipids, lipopeptides, and glycolipids) molecular weight surfactants (Abo Elsoud 2021). Biosurfactants based on high molecular weight and low molecular weight include:

1. **Polymeric biosurfactants:** Lipomanan, alasan, liposan, and emulsan are among the most notable polymeric biosurfactants (Luft 2022). Nonetheless, at low concentrations, emulsan is thought to be an effective bioemulsifier for emulsifying hydrocarbon-water mixtures. The most -researched examples include emulsan and biodispersan, which are produced

by *Acinetobacter calcoaceticus* and contain a heteropolysaccharide moiety bonded covalently to fatty acids (Adetunji & Olaniran 2021). *Candida lipolytica* produces liposan, an emulsifier that is primarily composed of carbohydrates (83%) and proteins (17%). *Yarrowia lipolytica* also produces a similar type of glycoprotein complex (Shekhar et al. 2015).

2. **Glycolipids:** They contain lipids attached to a carbohydrate by a glycosidic bond. The carbohydrate moiety attached to aliphatic or hydroxy aliphatic acids through an ether or ester group makes up these widely researched and widely used biosurfactants (Saranraj et al. 2022). The carbohydrates domain consists of rhamnose, mannose, glucose, galactose, galactose sulfate, and glucuronic acid (Adetunji & Olaniran 2021). According to Chrzanowski et al. (2012), rhamnolipids, mannosyl erythritol lipids, trehalose lipids, cellobiolipids, and sophorolipids are the glycolipids that have been investigated the most**.**

3. **Phospholipids:** When cultured in n-alkane-rich conditions, bacteria create large amounts of phospholipid and fatty acid biosurfactants (Adetunji & Olaniran 2021). The length of the hydrocarbon chain is correlated with the amount of hydrophilic and lipophilic components in the surfactants (Aubry et al. 2020). The phosphatidyl ethanolamine-containing vesicles excreted by *Acinetobacter* sp. make micro-emulsions of alkane and water, while *Rhodococcus erythropolis* creates vesicles that lessen the interfacial tension of a hexadecane and water mixture (Karlapudi et al. 2018).

4. **Lipopeptides:** The most investigated lipopeptide is surfactin, which is synthesized by *Bacillus subtilis* ATCC 21332 (Chavarria-Quicaño et al. 2023). Lipopeptides consist of amino acids linked to the carboxyl and hydroxyl groups of a C_{14} acid via a lactone bond (Bhadra et al. 2023). It is considered the most potent biosurfactant with remarkable surface activity at low concentrations (Nadaf et al. 2021).

5. **Particulate biosurfactants:** A type of particulate biosurfactant that aids in microorganisms' absorption of alkanes is extracellular membrane vesicles by partitioning oil-water mixtures and forming micro-emulsions at the interface (Siddiqui et al. 2021). Vesicles made by *Acinetobacter* sp. are one example of this. They are composed of phospholipids, proteins, and lipopolysaccharides (Vijayakumar & Saravanan 2015).

BIOSURFACTANT PRODUCING MICROORGANISMS

Microorganisms have well been explored for biosurfactant production in diverse industries including food, medicine, cosmetics, agriculture, and environmental cleanup (Sunde & Borresen 2016). Compared to their chemical counterparts, biosurfactants provide several benefits, including reduced toxicity, biodegradability, and the possibility of producing them at a very cheap cost using renewable resources. According to reports, a large number of the microorganisms that produce biosurfactants are also capable of breaking down hydrocarbons (Singh et al. 2021). Nonetheless, research conducted in recent decades has demonstrated the impact of surfactants produced by microorganisms on increased oil recovery in addition to bioremediation (Gudina et al.
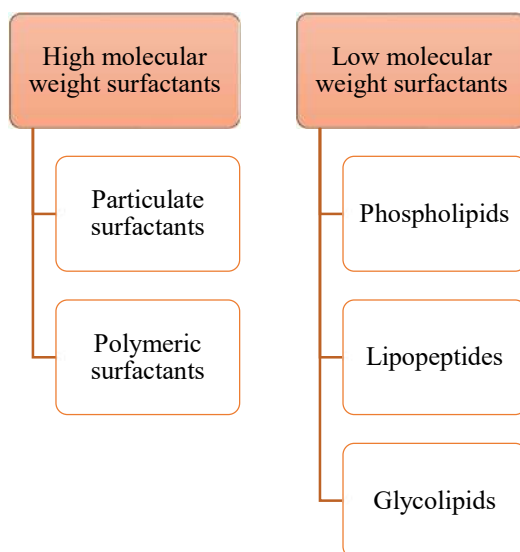
Fig. 1: Classification of biosurfactants based on molecular weight.

2018, Nikolova & Gutierrez 2021). Certain bacteria, such as *Achromobacter xylosoxidans* DN002 and *B. licheniformis*, possess the ability to degrade aromatic hydrocarbon fractions (Eskandari et al. 2017). Likewise, other bacteria, like *Dietzia* spp. and *Geobacillus thermodenitrifican*, are capable of degrading particular alkanes (Xu et al. 2018). The microorganisms capable of breaking down hydrocarbons often use them as sources of energy and carbon for their growth and reproduction (Ivshina et al. 2024). To relieve the hydrocarbon-induced physiological stress in the bulk microbiological environment, indigenous bacteria eventually break down or metabolize petroleum hydrocarbons (Siddiqui et al. 2021, Tripathi et al. 2022). For instance, in the study of Patil et al. (2012) on the breakdown of engine oil in polluted soil, the authors isolated and identified versatile hydrocarbon-degrading bacteria strains, including *Bacillus* species, *Acinetobacter* species, *Micrococci* species, *Pseudomonas* species, and *Streptomyces* species. *Bacillus licheniformis*, an effective hydrocarbon-degrading strain with resistance to high salinity, alkalinity, and temperature, was also identified by Liu et al. (2016) from soils polluted by oil in the vicinity of Tianjin, China's Dagang Oilfield. Even with their more complex structures, the strain that was observed was able to degrade both long-chain and short-chain alkanes.

Microorganisms produce a range of compounds, including biosurfactants, which enable the transport of carbon sources into their cells, even when they are intractable, such as hydrocarbons (Banerjee et al. 2024). Ionic surfactants are released by certain bacteria, and they help to emulsify the CxHy (hydrocarbon with x carbon atoms and y hydrogen atoms) material present in the growth media (Unaeze 2020). Some examples of this class of biosurfactants are sophorolipids, which are produced by multiple *Torulopsis* species, and rhamnolipids, which are produced by various *Pseudomonas* species (Kumar et al. 2021). By generating lipopolysaccharides or nonionic surfactants within their cell wall, certain other bacteria can modify the structure of their cell wall. *Rhodococcus erythropolis*, different *Mycobacterium* spp., and *Arthrobacter* spp. are examples of this category, and they generate nonionic trehalose corynomycolates (Sulochana et al. 2021). *Acinetobacter* spp. create lipopolysaccharides such as emulsan (Sen et al. 2021), and *Bacillus subtilis* produces lipoproteins like surfactin (Choi et al. 2021).

Yeasts, including *Candida*, *Rhodotorula*, and *Saccharomyces*, have also been investigated for their potential to produce biosurfactants (Adebayo et al. 2021). Depending on the strain and method used, producing biosurfactants from yeasts might be a profitable endeavor. Moreover, yeasts are simple to grow. Relatively few fungi are known to produce biosurfactants (Mohapatra et al. 2022). Fungi such as *Candida bombicola*, *C. lipolytica*, *C. ishiwadae*, *Aspergillus ustus*, and *Trichosporon ashii* are a few of the fungi that have been explored for biosurfactant production (Abdel-Azeem et al. 2021). *Starmerella bombicola* has been reported to synthesize a biosurfactant known as sophorolipids (Rawat et al. 2020). It is well known that several of these can make biosurfactants from inexpensive raw materials. The primary class of biosurfactants that these strains produce are called sophorolipids, or glycolipids (Prasad et al. 2021). When *Candida lipolytica* grows on n-alkanes, it creates lipopolysaccharides that are linked to the cell wall (Rivaldi et al. 2018).

THE GENETICS OF BIOSURFACTANT PRODUCTION

Microbial surfactants are encoded by arrays of genes, while numerous production routes, operons, and enzymes involved in the synthesis have been identified (Markande et al. 2021). The core synthetic genes for the production of bacillibactin, fengycin, and surfactin in *Bacillus* sp. XT-2, a novel facultative-halophilic long-chain hydrocarbon degrader, was elucidated by Wang et al. (2022). To demonstrate how genetic engineering of strains that produce biosurfactant can lead to the creation of an affordable bioremediation system, Wu et al. (2019) developed a systematic genetic engineering approach in which 53 genes of *Bacillus subtilis* 168 were altered to produce surfactin biosurfactant. Their investigation involved five main stages to optimize surfactin production. Initially, they combined the entire *sfp* gene into *B. subtilis* 168 to activate the biosurfactant biosynthesis. In an attempt to lessen competition in the second stage, 3.8 percent of the targeted strain's entire genome, which controls the polyketide synthase pathways and biofilm formation, was deleted. The third phase involves the possible overexpression of self-resistance-associated proteins, which improves the cell tolerance to the surfactin biosurfactant. The supply of precursor branched-chain fatty acids was boosted in the fourth phase by the engineering of the branched-chain fatty acid biosynthesis pathway. Ultimately, they redirected Acetyl-CoA from the process of cell growth to the manufacture of surfactin by improving the transcription of *srfA*. Furthermore, Zhu et al. (2021) reported that there are four Open reading frames (ORFs) governing the genetic regulation of lipopeptides. These ORFs in the *srfA* operon directs the synthesis of surfactin, including *srfAA*, *srfAB*, *srfAC*, and *srfAD*, which are multi-enzyme synthase complexes responsible for the synthesis of surfactin. The biosurfactant titer in this experiment reached a maximum value of 12.8 g/l, demonstrating the enormous potential of genetic engineering techniques and the crucial role that genome sequencing plays in creating an ideal biosurfactant-

base bioremediation system (Wu et al. 2019). Yasmin et al. (2022) in their study, reported that the major factor governing the biosynthesis of biosurfactants is the genetic makeup of the organisms producing these biosurfactants.

Some of the genes that have been reported to produce biosurfactants are depicted in (Table 1).

MICROBIAL SURFACTANTS FOR VARIOUS BIOTECHNOLOGICAL APPLICATIONS

Biosurfactants unique qualities and eco-friendliness make them useful in a variety of industries. They have been applied for different purposes in the following industries:

Oil Industry

According to Haider (2020), there was a 1.5% increase in global oil consumption in 2018 to 99.5 million barrels per day. It is anticipated that light and medium oils will become scarcer at the current rate of usage, increasing the need for heavy and extra-heavy oils (Sarubbo et al. 2022). In addition, it is anticipated that the world's oil supplies will run out in the next 40 to 45 years (Fenibo et al. 2019). According to Rawat et al. (2020) and Khademolhosseini et al. (2019), biosurfactants effectively mobilize immobile hydrocarbons by encouraging the decrease of surface tension between the oil and rock, this, in turn, lessens the capillary forces that impede the oil's passage through the rock pores.

Food Sector

The use of biosurfactants in food has gained attention recently due to consumers' growing interest in vegetarian and vegan food products, as well as sustainably produced components. (Hassoun et al. 2024). Some of these natural chemicals have low toxicity and can be utilized to improve formulations by changing their texture or viscosity and inhibiting the growth of some harmful microbes (Ribeiro et al. 2020). This increases food's shelf life, quality, and safety. Microorganisms utilized for biosurfactants in the food industry include *Saccharomyces cerevisiae*, *Meyerozyma guilliermondii*, *C. lipolytica*, *C. utilis*, *Starmerella bombicola*, and *Candida sphaerica* (Thraeib et al. 2022).

Detergent Industry

The detergent market encompasses personal care, household, and heavy industrial cleaning solutions. The most commonly used chemical surfactants are usually derived from petrochemicals. These often pose a significant risk to aquatic life (Chirani et al. 2021). Biosurfactants are increasingly emerging as a viable commercial substitute for these artificially produced surfactants (Celik et al. 2021). This circumstance has prompted a search for environmentally friendly goods, such as detergents that degrade efficiently through microbial breakdown and are made of straight-chain organic molecules (Farias et al. 2021). One of the main qualities of biosurfactants in this industry is their capacity to emulsify, which is essential for detergent activity. Other

Table 1: Some of the reported biosurfactant-producing genes.

Genes	
rhlA, *rhlB*, and *rhlC* genes	These genes are frequently identified in *Pseudomonas aeruginosa* and are involved in the formation of rhamnolipid biosurfactants (Shatilla et al. 2020). While *rhlB* and *rhlC* are involved in the production of the final rhamnolipid structure (Zhao et al. 2021), *rhlA* encodes the enzyme responsible for the synthesis of the precursor molecule (Wittgens et al. 2017).
Sophorolipid genes	Yeasts, especially *Candida bombicola*, produce sophorolipids, which are glycolipid biosurfactants (Qazi et al. 2022). *SL1*, *SL2*, and *SL3* are among the genes involved in sophorolipid production (Park et al. 2022). Enzymes involved in the synthesis of sophorose, the building block of sophorolipids, are encoded by these genes (Liu et al. 2020).
Alasan genes	Alasan genes encode a biosurfactant generated by *Acinetobacter species* (Saranraj et al. 2022). The production of alasan involves the *alsA* and *alsB* genes. According to Dabbagh et al. (2020), and *alsB* is involved in the precursor's transportation and acylation to create the final alasan molecule (Dabbagh et al. 2020).
Emulsan genes	*Acinetobacter calcoaceticus* produces the glycolipid biosurfactant emulsan (Pirog et al. 2021). The genes *emuC*, *emuD*, and *emuA* are involved in emulsan biosynthesis. These genes are in charge of the synthesis and assembly of emulsan on the surface of bacteria (Segovia et al. 2021).
Surfactin operon	*Bacillus subtilis* and other *Bacillus* species produce the lipopeptide biosurfactant surfactin, also known as the surfactin operon (Li et al. 2021). There are several genes in the surfactin operon, including *srfA*, *srfB*, *srfC*, *srfD*, and *srfE* (Kashif et al. 2022). The synthesis, transport, and regulation of surfactin production are carried out by these genes (Muller et al. 2021).
Mannosylerythritol lipids (MELs) genes	MELs are glycolipid biosurfactants produced by yeast-like fungi such as *Pseudozyma* spp. (Nouri et al. 2023). The biosynthesis of MELs involves several genes, including *MEL1*, *MEL2*, and *MEL3* (Perdomo et al. 2020). These genes encode enzymes responsible for the synthesis and modification of MELs (Yamamoto et al. 2022).

than this, others resembling commercial detergents may find application in the laundry and detergent industries (Drakontis & Amin 2020). By comparing a lipopeptide from *B. subtilis* SPB1 to commercial detergents, Bouassida et al. (2018) found that the latter was less effective in reducing stains from coffee and vegetable oil. Likewise, Fei et al. (2020) discovered that *B. subtilis* HSO121 surfactin has the same applications as chemical surfactants but also has the benefits of low toxicity and no irritation, as well as good wetting capacity and emulsifying activity, high compatibility, stability, biodegradability, and foaming capacity.

Cosmetic Industry

The development of products with more renewable and natural active ingredients is the global trend in the cosmetics business to reduce or eliminate the use of synthetic raw materials (Goyal & Jerold 2023). Besides affecting people and animals, chemical surfactants can impact soils and groundwater, harming the environment. The cosmetic industry can benefit from the properties of microbial biosurfactants, such as their antimicrobial, skin surface moisturizing, and low toxicity (Karnwal et al. 2023). These properties can potentially replace chemical surfactants in current pharmaceutical formulations for personal skincare and cosmetics.

Nanotechnology

In nanotechnology, biosurfactants are mostly used because of their ability to function as stabilizers and reducing agents, particularly for silver particles, which makes them useful for the creation of nanoparticles (Vecino et al. 2021). This is because there is a growing demand for "green" substitutes for the chemical processes currently in use (Duehnen et al. 2020). Therefore, biosurfactants represent a substitute that supports an effective, environmentally friendly procedure that requires no energy and doesn't include any hazardous substances (Joanna et al. 2018). With documented biological activity, certain microbes, like the bacterium *B. subtilis*, may synthesize gold and silver nanoparticles both intracellularly and extracellularly (Rane et al. 2017).

Agriculture

The adaptable characteristics of biosurfactants additionally render them suitable for use in agriculture, primarily as a substitute for synthetic surfactants in pesticide and agrochemical formulations (Gayathiri et al. 2022). This has encouraged the growth of "green chemistry" in this industry in response to the need to lessen or eliminate the harmful effects that excessive use of chemical compounds has on the environment and human health (Köhl et al. 2019).

BIOREMEDIATION STRATEGIES

Bioremediation techniques have advanced over the last 20 years, with the ultimate aim being the inexpensive and environmentally friendly restoration of damaged environments (Landa-Acuña et al. 2020). Different bioremediation approaches, as shown in (Fig. 2) have been developed and studied. However, no particular bioremediation strategy can be regarded as the most effective for restoring damaged habitats due to the nature and diversity of contaminants (Bala et al. 2022). Most issues about the biodegradation and bioremediation of polluting substances can be resolved by native microorganisms that are common in contaminated locations, provided that the environment is favorable to their growth and metabolism. (Verma & Jaiswal 2016). Among the main benefits of bioremediation over chemical and physical remediation techniques are its cost- and environmentally-friendly characteristics. Bioremediation strategies are generally classified as ex-situ and in-situ, as depicted in Fig. 2.

Ex-situ Bioremediation

Ex-situ bioremediation techniques involve removing pollutants from contaminated sites and moving them to another location for remediation (Butnariu & Butu 2020). Excavated contaminated soils are spread out on the ground and cleaned with natural microorganisms. The evaluation of ex-situ bioremediation techniques usually takes into account the cost of treatment, the kind and concentration of pollutants, the level of pollution, the location of the polluted site, and its geology (Azubike et al. 2016).

In-situ Bioremediation

When bioremediation is carried out at the original site of pollution, it is referred to as in situ bioremediation (Fragkou et al. 2021). The concept of in situ bioremediation is mostly utilized to address groundwater and soil contamination (Marcon et al. 2021). Since the process does not involve excavation, the soil structure is either a little disturbed or not at all (Zeng & Hausmann 2022). Since excavation processes do not incur additional costs, the desired cost of these methods should be lower than that of ex-situ bioremediation methods (Muhammad et al. 2024). The expense of developing and setting up some advanced equipment on the site to increase microbial activity during bioremediation, however, can be a major issue (Azubike et al. 2016).

APPLICATION OF BIOSURFACTANT-PRODUCING MICROORGANISMS FOR IN-SITU AND EX-SITU DEGRADATION OF HYDROCARBON AND ITS PRODUCTS
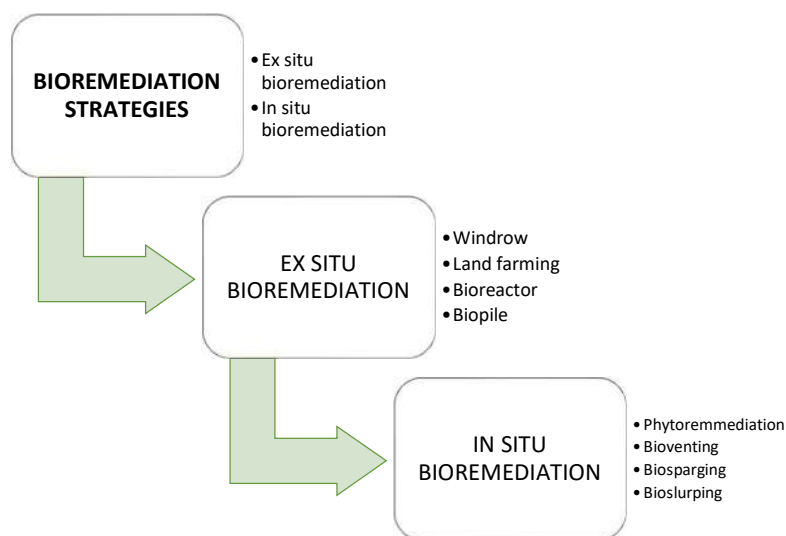
Fig. 2: Bioremediation strategies.

Some bacteria like *Dietzia* spp., *Oleispira antarctica*, *Pseudomonas* spp. (Ibrar et al. 2022), *Geobacillus thermodenitrifican* and *Bacillus licheniformis* can degrade aromatic or resinous hydrocarbon components. These bacteria use the hydrocarbons as energy and carbon sources for growth and reproduction, as well as to relieve physiological stress brought on by hydrocarbons in the microbial bulk environment; indigenous bacteria eventually break down or metabolize hydrocarbons (Kleindienst et al. 2015). Hydrocarbon-contaminated soil is cleaned up using a variety of recognized bacterial strains that function as effective biodegraders. Bioremediation is carried out by microorganisms, either indigenous or foreign (Jabbar et al. 2022). The availability of nutrients can increase the activity of native microorganisms, even as the introduction of exogenous bacteria to the contaminated site promotes bioremediation (Liu et al. 2020a). The most crucial stage in the biodegradation of hydrocarbons, according to Shi et al. (2019), is the formation of the interface between substrates and bacteria that break down petroleum. Presently, there are three methods to develop this interface:

1. In an aqueous solution, microbial organisms dissolve and absorb petroleum hydrocarbons (Ambaye et al. 2023).

2. Microbial cells directly absorb large hydrocarbon molecules. (Pandolfo et al. 2023).

3. Small hydrocarbon particles that are encapsulated, pseudo-soluble, or quasi-soluble interact with microbial cells for absorption (Ejaz et al. 2021).

Contrarily, bacterial cell hydrophobicity influences how well they attach to petroleum hydrocarbons (Kebede et al.

2021). Thus, for the bioremediation process to be more effective, the bacterial cells must be highly hydrophobic, which calls for the use of biosurfactants to facilitate the effective interaction of the bacteria with the petroleum hydrocarbons (Zahed et al. 2022). According to Chandra et al. (2013), in aerobic catabolism, the hydrocarbon skeleton appears to be modified by the addition of one or two hydroxyl groups. This seems to be the initial step in the process. The primary enzymatic response during the early intracellular breakdown of organic pollutants is the process of incorporating and activating oxygen (Mbachu 2020), oxygenase and peroxidase-catalyzed, making it an oxidative reaction (Cárdenas-Moreno et al. 2023, Chandra et al. 2013).

The addition of one oxygen atom and two hydroxyl groups to hydrocarbons, respectively, is catalyzed by monooxygenases and dioxygenases. Peripheral degradation pathways transform organic contaminants into metabolites of vital intermediate breakdown, like the tricarboxylic acid cycle (Fuentes et al. 2014). The major precursor metabolites include acetyl-CoA, succinate, and pyruvate, which are used in cell biomass synthesis (Kim et al. 2021) and gluconeogenesis to produce sugars required for subsequent biochemical activities involved in growth and development. (Scholtes & Giguère 2022). Therefore, by oxidizing these substrates, the bacterium can live in an environment with low nutrients (Wang et al. 2020). However, sulfate and nitrate function as terminal electron acceptors during anaerobic degradation (Su et al. 2023), which is carried out by coupling hydrocarbons to carbon dioxide (CO_2) or fumarate (Sah et al. 2022). However, the anaerobic degradation of petroleum hydrocarbons proceeds more slowly than aerobic microbial catabolism (Wartell et al. 2021).

There are only a few types of bacteria that can break down a broad range of hydrocarbons (Ławniczak et al. 2020). For example, *Dietzia* spp. DQ-12-45-1b uses n-alkanes (C_6-C_{40}) (Feknous et al. 2019) and other substances as its only carbon source, and *Achromobacter xylosoxidans* DN002 breaks down a range of monoaromatic and polyaromatic hydrocarbons (Gaur et al. 2022, Ma et al. 2015). However, only a small portion of petroleum hydrocarbon components can be metabolized by the majority of bacterial species, rendering others inaccessible (Varjani 2017, Xu et al. 2018). This is because various native bacterial species have unique catalytic enzymes (Xu et al. 2024). Hence, the cooperation of various functional bacteria is necessary to accomplish the effective bioremediation of petroleum hydrocarbon-contaminated soils (Dombrowski et al. 2016). Varjani et al. (2015) provided evidence to bolster the aforementioned claims when they stated that breaking down 3% v/v crude oil at a rate of 83.49% is the halotolerant Hydrocarbon Utilizing Bacterial Consortium (HUBC), composed of *Pseudomonas aeruginosa*, *Stenotrophomonas maltophilia*, and *Ochrobactrum* spp. (Siddiqui et al. 2021).

In a field study by Szulc et al. (2014) in the course of treating soil contaminated with diesel oil for 365 days, an 89% biodegradation efficiency by an artificial consortium made up of *Alcaligenes xylosoxidans*, *Aeromonas hydrophila*, *Pseudomonas fluorescens In*, *Gordonia* spp., *Rhodococcus In equi*, *Pseudomonas putida*, *Stenotrophomonas maltophilia*, and *Xanthomonas* spp. was confirmed (Szulc et al. 2014, Xu et al. 2018). These genes work in concert to achieve pollution purification because the bacterial consortium possesses a variety of catabolic genes (Gurav et al. 2017). As a result, the synergistic effects of a variety of catabolic genes within a bacterial consortium are advantageous in attaining the purification of contaminants (Albers et al. 2018). Due to the following factors, a bacterial consortium consisting of strains of *Mycobacterium*, *novosphingobium*, *Mycobacterium ochrobactrum* (Laothamteep et al. 2021), and a *Bacillus* strain demonstrated synergistic pyrene degradation (Zhang et al. 2022). Two *Mycobacterium* bacteria started the process of pyrene breakdown, whereas the *Bacillus* strain increased the bioavailability of pyrene by generating biosurfactants. Pyrene intermediates were successfully removed by *Mycobacterium ochrobactrum* and *Mycobacterium novosphingobium* (Wanapaisan et al. 2018). However, because of the complexity of the hydrocarbon components, it has been necessary to create a genetically modified bacteria or a minimally functional bacterial consortium for hydrocarbon bioremediation. (Dvorak et al. 2017).

Furthermore, two other issues that require resolution are the guard of the altered bacteria and the stability of the community (Xu et al. 2018). Therefore, the results mentioned above imply that using bacterial consortia could be a rational and efficient method for successfully removing petroleum hydrocarbons from polluted areas (Lara-Moreno et al. 2021). According to da Silva et al. (2021), the commercially manufactured biosurfactant derived from *Starmerella bombicola* significantly decreased water's surface tension, indicating both a strong emulsification and dispersal capacity for hydrophobic chemicals and a lack of toxicity in the investigated conditions (Hossain et al. 2021). In both static and kinetic testing, the designed biosurfactant demonstrated exceptional performance in eliminating motor oil (Gielnik 2019) and promoting the biodegradation of the contaminant in various soil types (da Silva et al. 2021). Another study reported by Almeida et al. (2021) where the potassium sorbate-containing biosurfactant from *Candida tropicalis* UCP0996 in petroleum products decontamination displayed stability and promoted a high motor oil emulsification rate (over 90%) at almost all tested conditions

CASE STUDIES

Extreme conditions can be stable for biosurfactants because of their high surface activity, capacity to emulsify, and resistance to high temperatures and salt concentrations (Bami et al. 2022). According to Durval et al. 2020 and Huang et al. 2020 Serratia marcescens ZCF25 and Bacillus cereus UCP 1615, two microorganisms isolated from oily sludge, produce extremely stable lipopeptide-type biosurfactants that lower surface tension and can remediate oil spills. Ambust et al. (2021) demonstrated that Pseudomonas spp. SA3 produced a biosurfactant that enhances agricultural crop growth in oil-contaminated soil, with emulsification and surface tension reduction capacities of 43% and 34.5 (milli Newton per meter) $mN\ m^{-1}$, respectively. Studies have shown that when Serratia spp. are cultivated in spent vegetable oil, they produce a biosurfactant that increases the solubility of various contaminants, including tetrachloroethylene (TCE), perchloroethylene (PCE), naphthalene, toluene, and phenanthrene. These samples were taken from a petroleum-contaminated site (Mulligan 2014). In their study of oil degradation in oil-polluted soil, Patil et al. (2012) found that possible hydrocarbon-degrading bacteria included *Bacillus* species, *Acinetobacter* species, *Micrococci* species, *Pseudomonas* species, and *Streptomyces* species. *Bacillus licheniformis*, an effective hydrocarbon-degrading strain resistant to high salinity, alkalinity, and temperature, was identified by Liu et al. (2016) from severely oil-contaminated soil near the Dagang Oilfield in Tianjin, China. The strain has been reported to break down both long-chain and short-chain alkanes, even with their more intricate structures (Liu et al. 2016). It also secretes emplastic at high temperatures,

which may be used as a surfactant to enhance the emulsifying action. Furthermore, Verma & colleagues, in 2006, evaluated the ability of three bacterial isolates from a contaminated site in Ankleshwar, India, to degrade oily sludge (Bahmani et al. 2020, Verma et al. 2006). Based on the gravimetric analysis, they found that *Acinetobacter* species, *Bacillus* species, and *Pseudomonas* species respectively degraded approximately 59%, 37%, and 35% of the oily sludge in five days at 30 °C (Swetha et al. 2020). Additionally, after five days, the *Bacillus* spp. were able to metabolize aromatics and components of oily sludge with a chain length of C12–C30 more effectively than the other two strains that had been found, according to the capillary gas chromatographic examination. Six naturally occurring oil-degrading bacterial species were identified by Jiji and Prabakaran (2020) as *Bacillus cereus, Pseudomonas aeruginosa, Bacillus subtilis, Pseudomonas* spp., *Bacillus* spp. and *Staphylococcus aureus* from soil contaminated with petroleum in Kerala, India's Changanassery, Kottayam district (Jiji & Prabakaran 2020). Thermophilic strains of *P. aeruginosa* and *B. subtilis* that are native to North-East India are effective in biodegrading crude petroleum oil (Bharathi 2019). Similarly, published literature indicates that the most significant hydrocarbon-degrading bacterial genera in polluted soils are *Variovorax, Bacillus, Achromobacter, Rhodococcus, Nocardioides, Nocardia, Pseudomonas, Sphingomonas, Arthrobacter,* and some other unculturable bacterial clones (Jiji & Prabakaran 2020). According to Karlapudi et al. in 2018, *P. aeruginosa* isolated from oil-polluted seawater can produce biosurfactants and, after 28 days of incubation, break down nonadecanes, hexadecanes, octadecanes, and heptadecanes (Karlapudi et al. 2018). Furthermore, *P. aeruginosa* was also reported to

efficiently decompose a variety of hydrocarbons, including virgin, tetradecane, and 2-methylnaphthalene (Li 2018). Furthermore, a great deal of research has been done on the capacity of many bacterial genera, including *Bacillus, Rhodococcus, Alcaligenes, Corynebacterium, Acinetobacter, and Pseudomonas,* to produce biosurfactants that lead to the effective breakdown of petroleum oil (Abbasian et al. 2016). *Acinetobacter haemolyticus* and the biosurfactant-producing strain *Pseudomonas* ML2 were introduced into soil polluted with hydrocarbons for a two-month incubation period to study the degradation of hydrocarbons. *Pseudomonas* ML2 and *Acinetobacter haemolyticus* were found to decrease hydrocarbon concentration by 11–71% and 39–71%, respectively (Karlapudi et al. 2018). According to a different study (Itrich et al. 2015), the oil degradation capacity of FinasolOSR-5 was increased when it was combined with trehalose-5, dicorynomycolates, a biosurfactant. This allowed for the complete elimination of volatile aromatic organic compounds from contaminated soil in a shorter time frame. These results demonstrated the amazing hydrocarbon-degrading capacity of bacterial cell-free biosurfactants (Karlapudi et al. 2018). From now on, the capacity of microorganisms to produce biosurfactants in conjunction with their capacity to bioremediate hydrocarbons might be utilized to accelerate the process of bioremediation in environments contaminated by hydrocarbons (Kebede et al. 2021). Some of the case studies on biosurfactant-producing microorganisms in bioremediation are shown in (Table 2).

LIMITATIONS OF MICROBIAL BIOSURFACTANT-MEDIATED REMEDIATION

Native bacteria are slow-growing and have low metabolic

Table 2: Case studies on biosurfactant-producing microorganisms in bioremediation.

Microorganisms	Category of Pollutant	Type of Biosurfactant	References
Serratia spp.	Hydrocarbon	Lipopeptide	Gidudu et al. (2020)
Paenibacillus spp. D9	Motor oil and diesel	Lipopeptide	Jimoh & Lin (2020)
P. aeruginosa	Crude oil	Rhamnolipids	Karlapudi et al. (2018)
Serratia spp.	Petroleum	Serrawettin	Sah et al. (2022)
Pseudomonas spp.	Oil	Rhamnolipids	Ambust et al. (2021)
B. cereus UCP 1615 and *S. marcescens* ZCF25	Oil	Lipopeptide	Durval et al. (2020)
B. stratospheric strain FLU	Motor oil	Lipopeptide	Nogueria Felix et al. (2019)
S. marcescens	Burned motor oil	Lipopeptide	Araújo et al. (2019)
Pseudomonas ML2	Hydrocarbon	Rhamnolipids	Karlapudi et al. (2018)
B. cereus, P. aeruginosa, B. subtilis and *S. aureus*	Petroleum	Lipopeptides, rhamnolipids and surfactin	Jiji and Prabakaran (2020)
Achromobacter spp. A-8	Petroleum	Not specified	Deng et al. (2020)
Wickerhamomyces anomalous	Crude oil	Lipopeptide	Souza et al. (2018)
Starmerella bombicola	Motor oil	Commercial biosurfactants	Da Silva et al. (2021)

activity because they are difficult to domesticate, which makes decontamination a laborious and ineffective process. Moreover, polycyclic aromatic hydrocarbons (PAHs) and alkanes with carbon chains that are longer and shorter (C_{10}, C_{20}–C_{40}) are difficult to break down (Paniagua-Michel & Banat 2024). Therefore, in the oil-contaminated site, hydrocarbon-degrading bacteria cannot remove all oil components. (Sun et al. 2022). However, hydrocarbon molecules are difficult to break down and stick to soil particles. As a result, one of the major issues limiting biodegradation in the environment is the minimal availability of oil contaminants to microbes (Sah et al. 2022). There is a need for researchers to employ a variety of tactics, including biostimulation techniques, which involve adding nutrients to promote microbial growth and activity, bioaugmentation, hydraulic control, genetic engineering of the microbe, and several other techniques to address these problems. The goal of these strategies is to increase the hydrocarbon's accessibility to microorganisms that break them down, which will help overcome the obstacles presented by local bacteria that develop slowly and their inability to break down particular hydrocarbon components.

FUTURE PROSPECTS

The economics of producing biosurfactants has been the subject of a great deal of research over the past 20 years, but achieving commercial success in comparison to synthetic alternatives still presents a difficulty (Rawat et al. 2020). There are still some areas that require research and a variety of approaches that can be used to boost the industrial production of these biomolecules. Production costs could be greatly decreased, for example, by producing biosurfactants in non-sterile environments. It is necessary to conduct more thorough research on the use of unprocessed and fortified waste substrates as well as the co-production of biosurfactants with other commercially viable products, particularly in large fermentation vessels. Future developments regarding the genes that produce biosurfactants have great potential to transform oil-contaminated site bioremediation techniques. Unlocking the complexities of these genes offers a way to improve the productivity and selectivity of biosurfactant synthesis, increasing their influence on environmental cleaning as our knowledge of microbial genetics expands. Investigating the genetic variety of bacteria that produce biosurfactants is one fascinating direction. The range of surfactant types that can be used for bioremediation can be increased by identifying and analyzing novel biosurfactant genes from various bacterial strains. This variability could be the key to creating customized solutions for particular kinds of oil contamination or environmental circumstances, enabling a more accurate and successful cleanup strategy.

CONCLUSIONS

In conclusion, the thorough investigation of the activities of biosurfactant-producing bacteria and their potential for bioremediation in oil-contaminated sites opens a promising new arena for environmental restoration. Investigating the activities of bacteria that produce biosurfactants and their potential for bioremediation at oil-contaminated locations throws up an exciting world of opportunities for hydrocarbon degradation. By delving into the complex methods these microbes use, this review has shed light on how they help lessen the ecological effects of contamination and oil spills. These fascinating microbes come out as nature's partners in restoring our ecosystems because they can break down hydrocarbons and improve oil solubility. Their elaborate relationship with pollutants demonstrates the fine equilibrium that exists in the microbial world and provides a glimmer of hope for a peaceful and sustainable cohabitation between industry and the environment. In addition, biosurfactants have greater advantages for the environment over chemical surfactants that are typically employed in oil-contaminated site remediation response because of their environmentally benign nature. Contrasting dramatically with the possible ecological impact connected with manufactured surfactants is the natural, biological process of microorganisms producing biosurfactants. This facet corresponds with the worldwide transition towards sustainable methodologies and emphasizes the need to utilize nature's inbuilt processes for ecological restoration.

REFERENCES

Abbasian, F., Lockington, R., Megharaj, M. and Naidu, R., 2016. A review on the genetics of aliphatic and aromatic hydrocarbon degradation. *Applied Biochemistry and Biotechnology*, 178, pp.224–250. doi: 10.1007/s12010-015-1881-y.

Abdel-Azeem, A.M., Yadav, A.N., Yadav, N. and Sharma, M. (eds), 2021. *Industrially Important Fungi for Sustainable Development: Volume 2: Bioprospecting for Biomolecules*. CRC Press, pp.299-346. doi: 10.1007/978-3-030-85603-8.

Abo Elsoud, M.M.A., 2021. *Microbial Biosurfactants*. Springer. Doi: 10.1007/978-981-15-6607-3_4.

Adebayo-Tayo, B.C., Ezejiofor, A.N., Akanni, G. and Adebiyi, O.F., 2021. Yeast derived biosurfactants: Characteristics, applications, and potential for environmental remediation. *Biotechnology Reports*, 29, p.e00593.

Adeola, A.O., Akingboye, A.S., Ore, O.T., Oluwajana, O.A., Adewole, A.H., Olawade, D.B. and Ogunyele, A.C., 2022. Crude oil exploration in Africa: socio-economic implications, environmental impacts, and mitigation strategies. *Environmental Systems and Decisions*, 42, pp.26-50. doi: 10.1007/s10669-021-09827-x.

Adetunji, A.I. and Olaniran, A.O., 2018. Treatment of lipid-rich wastewater using a mixture of free or immobilized bioemulsifier and hydrolytic enzymes from indigenous bacterial isolates. *Desalination and Water Treatment*, 132, pp.274-280.

Adetunji, A.I. and Olaniran, A.O., 2021. Production and potential biotechnological applications of microbial surfactants: An overview. *Saudi Journal of Biological Sciences*, 28(1), pp.669-679. doi: 10.1016/j.sjbs.2020.10.058.

Ahmad, I., 2022. Microalgae–bacteria consortia: A review on the degradation of polycyclic aromatic hydrocarbons (PAHs). *Arabian Journal for Science and Engineering*, 47(1), pp.19-43.

Alara, J.A. and Alara, O.R., 2024. Biosurfactants as potential and sustainable substitutes for synthetic drugs against antimicrobial resistance and drug adverse effects: a review. *Advances in Traditional Medicine (ADTM)*. doi: 10.1007/s13596-023-00734-x.

Albers, P., Weytjens, B., De Mot, R., Marchal, K. and Springael, D., 2018. Molecular processes underlying synergistic linuron mineralization in a triple‐species bacterial consortium biofilm revealed by differential transcriptomics. *MicrobiologyOpen*, 7(2), pe00559.

Alizadeh-Sani, M., Hamishehkar, H., Khezerlou, A., Azizi-Lalabadi, M., Azadi, Y., Nattagh-Eshtivani, E., Fasihi, M., Ghavami, A., Aynehchi, A. and Ehsani, A., 2018. Bioemulsifiers derived from microorganisms: Applications in the drug and food industry. *Advanced Pharmaceutical Bulletin*, 8, pp.191-199. doi: 10.15171/apb.2018.023.

Almeida, D.G., Soares da Silva, R.d.C.F., Meira, H.M., Brasileiro, P.P.F., Silva, E.J., Luna, J.M., Rufino, R.D. and Sarubbo, L.A., 2021. Production, characterization and commercial formulation of a biosurfactant from Candida tropicalis UCP0996 and its application in decontamination of petroleum pollutants. *Processes*, 9, p.885.

Ambaye, T.G., Vaccari, M., Franzetti, A., Prasad, S., Formicola, F., Rosatelli, A. and Rtimi, S., 2023. Microbial electrochemical bioremediation of petroleum hydrocarbons (PHCs) pollution: Recent advances and outlook. *Chemical Engineering Journal*, 452, p.139372.

Ambust, S., Das, A. and Kumar, R., 2021. Bioremediation of petroleum-contaminated soil through biosurfactant and Pseudomonas sp. SA3 amended design treatments. *Current Research in Microbial Sciences*, 2, p.100031. doi: 10.1016/j.crmicr.2021.100031.

Araújo, H.W.C., Andrade, R.F.S., Montero-Rodríguez, D., Rubio-Ribeaux, D., da Silva, C.A.A. and Campos-Takaki, G.M., 2019. Sustainable biosurfactant produced by Serratia marcescens UCP 1549 and its suitability for agricultural and marine bioremediation applications. *Microbial Cell Factories*, 18, p.2.

Aubry, J.M., Ontiveros, J.F., Salager, J.L. and Nardello-Rataj, V., 2020. Use of the normalized hydrophilic-lipophilic-deviation (HLDN) equation for determining the equivalent alkane carbon number (EACN) of oils and the preferred alkane carbon number (PACN) of nonionic surfactants by the fish-tail method (FTM). *Advances in Colloid and Interface Science*, 276, p.102099.

Azubuike, C.C., Chikere, C.B. and Okpokwasili, G.C., 2016. Bioremediation techniques – classification based on site of application: principles, advantages, limitations and prospects. *World Journal of Microbiology and Biotechnology*, 32, p.180. https://doi.org/10.1007/s11274-016-2137-x.

Bahmani, F., Honarvar, B., Estakhr, Z. and Kherameh, M.A.M., 2020. Kinetic study of oily sludge biodegradation under shaking conditions. *International Journal of Environment and Waste Management*, 26(4), pp.487-503.

Bala, S., Garg, D., Thirumalesh, B.V., Sharma, M., Sridhar, K., Inbaraj, B.S. and Tripathi, M., 2022. Recent strategies for bioremediation of emerging pollutants: a review for a green and sustainable environment. *Toxics*, 10(8), p.484.

Bami, M.S., Estabragh, M.A.R., Ohadi, M., Banat, I.M. and Dehghannoudeh, G., 2020. Biosurfactants aided bioremediation mechanisms: A mini-review. *Soil and Sediment Contamination*, doi: 10.1080/15320383.2021.2016603.

Banerjee, S., Gupta, N., Pramanik, K., Gope, M., GhoshThakur, R., Karmakar, A. and Balachandran, S., 2024. Microbes and microbial strategies in carcinogenic polycyclic aromatic hydrocarbons remediation: a systematic review. *Environmental Science and Pollution Research*, 31(2), pp.1811-1840.

Bhadra, S., Chettri, D. and Kumar Verma, A., 2023. Biosurfactants: Secondary metabolites involved in the process of bioremediation and biofilm removal. *Applied Biochemistry and Biotechnology*, 195(9), pp.5541-5567.

Bharathi, B., 2019. *Biodegradation of Crude Oil Contaminated Soil by Microbial Inoculants*. Lulu.com.

Bouassida, M., Fourati, N., Ghazala, I., Ellouze-Chaabouni, S. and Ghribi, D., 2018. Potential application of Bacillus subtilis SPB1 biosurfactants in laundry detergent formulations: Compatibility study with detergent ingredients and washing performance. *Engineering in Life Sciences*, 18, pp.70-77.

Butnariu, M. and Butu, A., 2020. Viability of in situ and ex-situ bioremediation approaches for degradation of noxious substances in stressed environs. In *Bioremediation and Biotechnology, Vol 4: Techniques for Noxious Substances Remediation*, pp.167-193.

Cárdenas-Moreno, Y., González-Bacerio, J., García Arellano, H. and del Monte-Martínez, A., 2023. Oxidoreductase enzymes: Characteristics, applications, and challenges as a biocatalyst. *Biotechnology and Applied Biochemistry*, 70(6), pp.2108-2135.

Çelik, A., Manga, E.B., Çabuk, A. and Banat, I.M., 2021. Biosurfactants› potential role in combating COVID19- and similar future microbial threats. *Applied Sciences*, 11(1), pp.1-16.

Chandra S., Sharma, R., Singh, K. and Sharma A., 2013. Application of bioremediation technology in the environment contaminated with petroleum hydrocarbon. *Ann Microbiol.* 63(2), pp. 417–431. doi: 10.1007/s13213-012-0543-3.

Chavarria-Quicaño, E., De la Torre-González, F. and González-Riojas, M., 2023. Nematicidal lipopeptides from Bacillus paralicheniformis and Bacillus subtilis: A comparative study. *Applied Microbiology and Biotechnology*, 107, pp.1537-1549. https://doi.org/10.1007/s00253-023-12391-w.

Chirani, M.R., Kowsari, E., Teymourian, T. and Ramakrishna, S., 2021. Environmental impact of increased soap consumption during COVID-19 pandemic: biodegradable soap production and sustainable packaging. *Science of the Total Environment*, 796.

Choi, S. K., Park, S. Y., Kim, R. and Lee, C. H. 2021. Bacillus subtilis as a platform for microbial production of biopolymers. *Frontiers in Bioengineering and Biotechnology*, 9, p. 656936.

Chrzanowski, L., Ławniczak, L. and Czaczyk, V., 2012. Why do microorganisms produce rhamnolipids? *World Journal of Microbiology and Biotechnology*, 28, pp.401-419.

da Silva, I.G.S., de Almeida, F.C.G., da Rocha e Silva, N.M.P., de Oliveira, J.T.R., Converti, A. and Sarubbo, L.A., 2021. Application of green surfactants in the remediation of soils contaminated by hydrocarbons. *Processes*, 9, p.1666. https://doi.org/10.3390/pr9091666.

Da'ana, D.A., Zouari, N., Ashfaq, M.Y., Abu-Dieyeh, M., Khraisheh, M., Hijji, Y.M. and Al-Ghouti, M.A., 2021. Removal of toxic elements and microbial contaminants from groundwater using low-cost treatment options. *Current Pollution Reports*, 7(3), pp.300-324.

Dabbagh, F., Parvizpour, S. and Teymouri, M.A., 2020. A comprehensive review on rhamnolipid biosurfactant produced by *Acinetobacter* species. *Journal of Biomedical Materials Research Part A*, 108(8), pp.1755-1772.

Deng, Z., Jiang, Y., Chen, K., Gao, F. and Liu, X., 2020. Petroleum depletion property and microbial community shift after bioremediation using Bacillus halotolerans T-04 and Bacillus cereus 1-1. *Frontiers in Microbiology*, 11, p.353.

Dombrowski, N., Donaho, J.A., Gutierrez, T., Seitz, K.W., Teske, A.P. and Baker, B.J., 2016. Reconstructing metabolic pathways of hydrocarbon-degrading bacteria from the Deepwater Horizon oil spill. *Nature Microbiology*, 1(7), pp.1-7. doi: 10.1038/nmicrobiol.2016.57.

Drakontis, C.E. and Amin, S., 2020. Biosurfactants: formulations, properties, and applications. *Current Opinion in Colloid & Interface Science*, 48, pp.77-90.

Duehnen, S., Betz, J., Kolek, M., Schmuch, R., Winter, M. and Placke, T., 2020. Toward green battery cells: Perspective on materials and technologies. *Small Methods*, 4(7), p.2000039.

Durval, I.J.B., Mendonça, A.H.R., Rocha, I.V., Luna, J.M., Rufino, R.D., Converti, A. and Sarubbo, L.A., 2020. Production, characterization, evaluation and toxicity assessment of a *Bacillus cereus* UCP 1615 biosurfactant for marine oil spills bioremediation. *Marine Pollution Bulletin*, 157, p.111357. doi: 10.1016/j.marpolbul.2020.111357.

Dvorak, P., Nikel, P.I., Damborský, J. and de Lorenzo, V., 2017. Bioremediation 3.0: engineering pollutant-removing bacteria in the times of systemic biology. *Biotechnology Advances*, 35(7), pp.845-866. doi: 10.1016/j.biotechadv.2017.08.001.

Ejaz, M., Zhao, B., Wang, X., Bashir, S., Haider, F.U., Aslam, Z. and Mustafa, A., 2021. Isolation and characterization of oil-degrading *Enterobacter* sp. from naturally hydrocarbon-contaminated soils and their potential use against the bioremediation of crude oil. *Applied Sciences*, 11(8), p.3504.

El-Sheshtawy, H.S., Aiad, I., Osman, M.E., Abo-ELnasr, A.A. and Kobisy, A.S., 2015. Production of biosurfactant from *Bacillus licheniformis* for microbial-enhanced oil recovery and inhibition of the growth of sulfate-reducing bacteria. *Egyptian Journal of Petroleum*, 24, pp.155-162.

Emoyan, O.O., Onocha, E.O. and Tesi, G.O., 2020. Concentration assessment and source evaluation of 16 priority polycyclic aromatic hydrocarbons in soils from selected vehicle-parks in southern Nigeria. *Science Africa*, 7, pp.1–13.

Eskandari, S., Hoodaji, M., Tahmourespour, A., Abdollahi, A., Mohammadian-Baghi, T., Eslamian, S. and Ostad-Ali-Askari, K., 2017. Bioremediation of polycyclic aromatic hydrocarbons by *Bacillus Licheniformis* ATHE9 and *Bacillus Mojavensis* ATHE13 as newly strains isolated from oil-contaminated soil. *Journal of Geography, Environment and Earth Science International*, 11, pp.1–11. doi: 10.9734/JGEESI/2017/35447.

Farias, C.B.B., Almeida, F.C.G., Silva, I.A., Souza, T.C., Meira, H.M.R., Silva, R.C.F.S., Luna, J.M., Santos, V.A., Converti, A., Banat, I.M. and Sarubbo, L.A., 2021. Production of green surfactants: market prospects. *Electronic Journal of Biotechnology*, 51, pp.28-39.

Fei, D., Zhou, G.W., Yu, Z.Q., Gang, H.Z., Liu, J.F., Yang, S.Z., Ye, R.Q. and Mu, B.Z., 2020. Low-toxic and nonirritant biosurfactant surfactin and its performances in detergent formulations. *Journal of Surfactants and Detergents*, 23, pp.109-118.

Feknous, N., Branes, Z., Batisson, I. and Amblard, C., 2019. Growth of indigenous bacteria *Vibrio alginolyticus* and *Dietzia* sp. isolated from the east coast of Algeria in the presence of monoaromatic hydrocarbons. *Environment Protection Engineering*, 45(3), p.1341.

Fenibo, E.O., ljoma, G.N., Selvarajan, R. and Chikere, C.B., 2019. Microbial surfactants: The next generation multifunctional biomolecules for applications in the petroleum industry and its associated environmental remediation. *Microorganisms*, 7, pp.1-29.

Fragkou, E., Antoniou, E., Daliakopoulos, I., Manios, T., Theodorakopoulou, M. and Kalogerakis, N., 2021. In situ aerobic bioremediation of sediments polluted with petroleum hydrocarbons: A critical review. *Journal of Marine Science and Engineering*, 9(9), p.1003.

Fuentes, S., Méndez, V., Aguila, P. and Seeger, M., 2014. Bioremediation of petroleum hydrocarbons: catabolic genes, microbial communities, and applications. *Applied Microbiology and Biotechnology*, 98(11), pp.4781–4794. doi: 10.1007/s00253-014-5684-9.

Gaur, V.K. and Manickam, N., 2021. Microbial biosurfactants: production and applications in circular bioeconomy. *Biomass, Biofuels, Biochemicals*, 16, pp.353-378.

Gaur, V.K., Tripathi, V. and Manickam, N., 2022. Bacterial-and fungal-mediated biodegradation of petroleum hydrocarbons in soil. *Development in Wastewater Treatment Research and Processes*, 72, pp.407-427. .

Gayathiri, E., Prakash, P., Karmegam, N., Varjani, S., Awasthi, M.K. and Ravindran, B., 2022. Biosurfactants: potential and eco-friendly material for sustainable agriculture and environmental safety: A review. *Agronomy*, 12(3), p.662.

Gidudu, B., Mudenda, E. and Chirwa, E.M., 2020. Biosurfactant produced by *Serrati* sp. and its application in bioremediation enhancement of oil sludge. *Chemical Engineering*, 79, pp.433–438. doi: 10.3303/CET2079073.

Gielnik, A., 2019. Digestate valorization for bioremediation of petroleum hydrocarbons contaminated soils. *Environmental Science and Pollution Research*, 61(7), pp.343-356

Goyal, N. and Jerold, F., 2023. Biocosmetics: technological advances and future outlook. *Environmental Science and Pollution Research*, 30(10), pp.25148-25169.

Gudiña, E.J., Fernandes, E.C., Rodrigues, A.I., Teixeira, J.A. and Rodrigues, L.R., 2016. Biosurfactant production by *Bacillus subtilis* using corn steep liquor as culture medium. *Frontiers in Microbiology*, 7, p.1343.

Gurav, R., Lyu, H., Ma, J., Tang, J., Liu, Q. and Zhang, H., 2017. Degradation of n-alkanes and PAHs from the heavy crude oil using salt-tolerant bacterial consortia and analysis of their catabolic genes. *Environmental Science and Pollution Research*, 24(12), pp.11392–11403. doi: 10.1007/s11356-017-8446-2.

Haider, W.H., 2020. Estimates of total oil & gas reserves in the world, future of oil and gas companies and SMART investments by E & P companies in renewable energy sources for future energy needs. *Int. Pet. Technol. Conf.*, IPTC, 10.2523.

Hassoun, A., Bekhit, A.E.D., Jambrak, A.R., Regenstein, J.M., Chemat, F., Morton, J.D. and Ueland, Ø., 2024. The fourth industrial revolution in the food industry—part II: Emerging food trends. *Critical Reviews in Food Science and Nutrition*, 64(2), pp.407-437.

Hossain, K.M.Z., Deeming, L. and Edler, K.J., 2021. Recent progress in Pickering emulsions stabilized by bioderived particles. *RSC Advances*, 11(62), pp.39027-39044.

Huang, Y., Zhou, H., Zheng, G., Li, Y., Xie, Q., You, S. and Zhang, C., 2020. Isolation and characterization of biosurfactant-producing *Serratia marcescens* ZCF25 from oil sludge and application to bioremediation. *Environmental Science and Pollution Research*, 27(22), pp.27762–27772. doi: 10.1007/s11356-020-09006-6.

Ibrar, M., Khan, S., Hasan, F. and Yang, X., 2022. Biosurfactants and chemotaxis interplay in microbial consortium-based hydrocarbon degradation. *Environmental Science and Pollution Research*, 29(17), pp.24391-24410.

Itrich, N.R., McDonough, K.M., Van Ginkel, C.G., Bisinger, E.C., LePage, J.N., Schaefer, E.C., Menzies, J.Z., Casteel, K.D. and Federle, T.W., 2015. Widespread microbial adaptation to l-glutamate-N, N-diacetate (L-GLDA) following its market introduction in a consumer cleaning product. *Environmental Science and Technology*, 49(22), pp.13314–13321. doi: 10.1021/acs.est.5b03649.

Ivshina, I.B., Kuyukina, M.S. and Krivoruchko, A.V., 2024. Extremotolerant *Rhodococcus* as an important resource for environmental biotechnology. *Actinomycetes in Marine and Extreme Environments*, 142, pp.209-246.

Jabbar, N.M., Alardhi, S.M., Mohammed, A.K., Salih, I.K. and Albayati, T.M., 2022. Challenges in the implementation of bioremediation processes in petroleum-contaminated soils: A review. *Environmental Nanotechnology, Monitoring & Management*, 18, p100694.

Jiji, J. and Prabakaran, P., 2020. Isolation and identification of microorganisms from total petroleum hydrocarbon-contaminated soil sites. *Malaysian Journal of Soil Science*, 24, pp.107–119.

Jimoh, A.A. and Lin, J., 2020. Bioremediation of contaminated diesel and motor oil through the optimization of biosurfactant produced by *Paenibacillus* sp. D9 on waste canola oil. *Bioremediation Journal*, 24(1), pp.21–40. doi: 10.1080/10889868.2020.1721425.

Joanna, C., Marcin, L., Ewa, K. and Grazyna, P., 2018. A nonspecific synergistic effect of biogenic silver nanoparticles and biosurfactant towards environmental bacteria and fungi. *Ecotoxicology*, 27, pp.352-359.

Joshi, S.J., Al-Wahaibi, Y.M., Al-Bahry, S.N., Elshafie, A.E., Al-Bemani, A.S., Al-Bahri, A. and Al-Mandhari, M.S., 2016. Production,

characterization, and application of *Bacillus licheniformis* W16 biosurfactant in enhancing oil recovery. *Frontiers in Microbiology*, 7. doi: 10.3389/fmicb.2016.01853.

Karlapudi, A.P., Venkateswarulu, T.C., Tammineedi, J., Kanumuri, L., Ravuru, B.K., Ramu Dirisala, V. and Kodali, V.P., 2018. Role of biosurfactants in bioremediation of oil pollution-a review. *Petroleum*, 4(3), pp.241-249.

Karnwal, A., Shrivastava, S., Al-Tawaha, A.R.M.S., Kumar, G., Singh, R., Kumar, A. and Malik, T., 2023. Microbial biosurfactant as an alternate to chemical surfactants for application in cosmetics industries in personal and skin care products: A critical review. *BioMed Research International*.

Kashif, A., Rehman, R., Fuwad, A., Shahid, M.K., Dayarathne, H.N.P., Jamal, A. and Choi, Y., 2022. Current advances in the classification, production, properties and applications of microbial biosurfactants–A critical review. *Advances in Colloid and Interface Science*, 306, p.102718.

Kebede, G., Tafese, T., Abda, E.M., Kamaraj, M. and Assefa, F., 2021. Factors influencing the bacterial bioremediation of hydrocarbon contaminants in the soil: mechanisms and impacts. *Journal of Chemistry*, 71, pp.1-17.

Khademolhosseini, R., Jafari, A., Mousavi, S.M., Hajfarajollah, H., Noghabi, K.A. and Manteghian, M., 2019. Physicochemical characterization and optimization of glycolipid biosurfactant production by a native strain of *Pseudomonas aeruginosa* HAK01 and its performance evaluation for the MEOR process. *RSC Advances*, 9, pp.7932-794.

Kim, Y., Lama, S., Agrawal, D., Kumar, V. and Park, S., 2021. Acetate as a potential feedstock for the production of value-added chemicals: Metabolism and applications. *Biotechnology Advances*, 49, p.107736.

Kleindienst, S., Paul, J.H. and Joye, S.B., 2015. Using dispersants after oil spills: impacts on the composition and activity of microbial communities. *Nature Reviews Microbiology*, 13(6), pp.388–396. doi: 10.1038/nrmicro3452.

Köhl, J., Kolnaar, R. and Ravensberg, W.J., 2019. Mode of action of microbial biological control agents against plant diseases: relevance beyond efficacy. *Frontiers in Plant Science*, 10, p.119.

Korenblum, E., DeAraujo, L.V., Guimarães, C.R., DeSouza, L.M., Sassaki, G., Abreu, F., Nitschke, M., Lins, U., Freire, D.M.G., Barreto-Bergter, E. and Seldin, L., 2012. Purification and characterization of a surfactin-like molecule produced by *Bacillus* sp. H2O-1 and its antagonistic effect against sulfate-reducing bacteria. *BMC Microbiology*, 12, p.252. doi: 10.1186/1471-2180-12-252.

Kumar, P.S. and Ngueagni, P.T., 2021. A review on new aspects of lipopeptide biosurfactant: Types, production, properties and its application in the bioremediation process. *Journal of Hazardous Materials*, 407, 124827.

Kumar, V., Shahi, S.K. and Singh, S., 2018. Bioremediation: An eco-sustainable approach for restoration of contaminated sites. In: Singh, J., Sharma, D., Kumar, G., Sharma, N. (eds) *Microbial Bioprospecting for Sustainable Development*. Springer. https://doi.org/10.1007/978-981-13-0053-0_6

Landa-Acuña, D., Acosta, R.A.S., Hualpa Cutipa, E., Vargas de la Cruz, C. and Luis Alaya, B., 2020. Bioremediation: A low-cost and clean-green technology for environmental management. *Microbial Bioremediation & Biodegradation*, 19, pp.153-171.

Laothamteep, N., Kawano, H., Vejarano, F., Suzuki-Minakuchi, C., Shintani, M., Nojiri, H. and Pinyakong, O., 2021. Effects of environmental factors and coexisting substrates on PAH degradation and transcriptomic responses of the defined bacterial consortium OPK. *Environmental Pollution*, 277, p.116769.

Lara-Moreno, A., Morillo, E., Merchán, F. and Villaverde, J., 2021. A comprehensive feasibility study of effectiveness and environmental impact of PAH bioremediation using an indigenous microbial degrader consortium and a novel strain *Stenotrophomonas maltophilia* CPHE1

isolated from industrially polluted soil. *Journal of Environmental Management*, 289, p.112512.

Ławniczak, Ł., Woźniak-Karczewska, M., Loibner, A.P., Heipieper, H.J. and Chrzanowski, Ł., 2020. Microbial degradation of hydrocarbons—basic principles for bioremediation: A review. *Molecules*, 25(4), p.856.

Li, H., 2018. *Biospectroscopy Diagnosis of Bacterial Interaction with Environmental Molecules*. Lancaster University.

Li, J.Y., Wang, L., Liu, Y.F., Zhou, L., Gang, H.Z., Liu, J.F. and Mu, B.Z., 2021. Microbial lipopeptide-producing strains and their metabolic roles under anaerobic conditions. *Microorganisms*, 9(10), p.2030.

Lifshits, S.K., Glyaznetsova, Y. and Chalaya, O.N., 2018. Self-regeneration of oil-contaminated soils in the Cryolithozone on the example of the territory of the former oil pipeline "Talakan-Vitim". In: Proceedings of the INTEREKSPO GEO-SIBIR, Novosibirsk, Russia, 23–27 April 2018; pp. 199– 206.

Liu, B., Ju, M., Liu, J., Wu, W. and Li, X., 2016a. Isolation, identification, and crude oil degradation characteristics of a high-temperature, hydrocarbon-degrading strain. *Marine Pollution Bulletin*, 106(1–2), pp.301–307. doi: 10.1016/j.marpolbul.2015.09.053.

Liu, B., Liu, J., Ju, M., Li, X. and Yu, Q., 2016b. Purification and characterization of biosurfactant produced by *Bacillus licheniformis* Y-1 and its application in remediation of petroleum-contaminated soil. *Marine Pollution Bulletin*, 107(1), pp.46–51. doi: 10.1016/j.marpolbul.2016.04.025.

Liu, H., Tan, X., Guo, J., Liang, X., Xie, Q. and Chen, S., 2020a. Bioremediation of oil-contaminated soil by a combination of soil conditioner and microorganisms. *Journal of Soils and Sediments*, 20, pp. 2121-2129.

Liu, J., Li, J., Gao, N., Zhang, X., Zhao, G. and Song, X., 2020b. Identification and characterization of a protein Bro1 essential for sophorolipids synthesis in *Starmerella bombicola*. *Journal of Industrial Microbiology and Biotechnology*, 47(4-5), pp.437-448.

Luft, L., 2022. Fungal polysaccharides as biosurfactants and bioemulsifiers. *Fungal Biopolymers and Biocomposites: Prospects and Avenues*, 819, pp.105-127.

Ma, Y.L., Lu, W., Wan, L.L. and Luo, N., 2015. Elucidation of fluoranthene degradative characteristics in a newly isolated *Achromobacter xylosoxidans* DN002. *Applied Biochemistry and Biotechnology*, 175(3), pp.1294–1305. doi: 10.1007/s12010-014-1347-7.

Marcon, L., Oliveras, J. and Puntes, V.F., 2021. In situ nanoremediation of soils and groundwaters from the nanoparticle's standpoint: A review. *Science of the Total Environment*, 791, 148324.

Markande, A.R., Patel, D. and Varjani, S., 2021. A review on biosurfactants: properties, applications and current developments. *Bioresource Technology*, 330, 124963.

Mbachu, A.E., Chukwura, E.I. and Mbachu, N.A., 2020. Role of microorganisms in the degradation of organic pollutants: A review. *Energy and Environmental Engineering*, 7(1), pp.1-11.

Mohapatra, D., Rath, S.K. and Mohapatra, P.K., 2022. Soil fungi for bioremediation of pesticide toxicants: A perspective. *Geomicrobiology Journal*, 39(3-5), pp.352-372.

Moldes, A.B., Rodríguez-López, L., Rincón-Fontán, M., López-Prieto, A., Vecino, X. and Cruz, J.M., 2021. Synthetic and bio-derived surfactants versus microbial biosurfactants in the cosmetic industry: An overview. *International Journal of Molecular Sciences*, 22(5), p. 2371.

Muhammad, M., Batool, S., Hivare, V., Li, W.J., Waheed, A. and Sinha, D., 2024. Bioremediation techniques—classification, principles, advantages, limitations, and prospects. *Microbiome-Assisted Bioremediation*, 213, pp.1-23.

Müller, J., Heermann, R., Fuchs, T.M. and Blank, K., 2021. The surfactin synthetase operon srfA-srfE from *Bacillus subtilis* ATCC 6633: In-depth characterization and redesign of the module organization. *MicrobiologyOpen*, 10(1), p.e1169.

Mulligan, C.N., 2014. *Biosurfactants: Research Trends and Applications*, Springer, p.231.

Muze, N.E., Opara, A.I., Ibe, F.C. and Njoku, O.C., 2020. Assessment of the geo-environmental effects of activities of auto-mechanic workshops at Alaoji Aba and Elekahia Port Harcourt, Niger Delta, Nigeria. *Environmental Analysis, Health and Toxicology*, 35(2). https://doi.org/10.5620/eaht.e2020005

Nadaf, S.J., Kumbar, V.M., Torvi, A.I., Hoskeri, J.H. and Shettar, A.K., 2021. Antioxidant Biosurfactants. In: Inamuddin, Ahamed, M.I., Prasad, R. (eds) *Microbial Biosurfactants*. Environmental and Microbial Biotechnology, Springer, pp.87-128.. https://doi.org/10.1007/978-981-15-6607-3_3.

Nikolova, C. and Gutierrez, T., 2021. Biosurfactants and Their Applications in the Oil and Gas Industry: Current State of Knowledge and Future Perspectives. *Frontiers in Bioengineering and Biotechnology*, 9, p.626639. Pubmed ID 33659240. doi: 10.3389/fbioe.2021.626639.

Nogueira Felix, A.K., Martins, J.J.L., Lima Almeida, J.G., Giro, M.E.A., Cavalcante, K.F., Maciel Melo, V.M., Loiola Pessoa, O.D., Ponte Rocha, M.V., Rocha Barros Gonçalves, L., de Santiago, S. and Aguiar R., 2019. Purification and characterization of a biosurfactant produced by Bacillus subtilis in cashew apple juice and its application in the remediation of oil-contaminated soil. *Colloids Surf B Biointerfaces*. 1(175), pp. 256–263. doi: 10.1016/j.colsurfb.2018.11.062.

Nouri, H., Moghimi, H. and Lashani, E., 2023. *Multifunctional Microbial Biosurfactants*. Springer Nature, pp.87-128.

Orisakwe, O.E., 2021. Crude oil and public health issues in Niger Delta, Nigeria: Much ado about the inevitable. *Environmental Research*, 194, p.110725. doi: 10.1016/j.envres.2021.110725.

Pande, V., Pandey, S.C. and Sati, D., 2020. Bioremediation: an emerging effective approach towards environment restoration. *Environmental Sustainability*, 3, pp.91–103. https://doi.org/10.1007/s42398-020-00099-w.

Pandolfo, E., Barra Caracciolo, A. and Rolando, L., 2023. Recent advances in bacterial degradation of hydrocarbons. *Water*, 15(2), p.375.

Paniagua-Michel, J. and Banat, I.M., 2024. Unravelling Diatoms' Potential for the Bioremediation of Oil Hydrocarbons in Marine Environments. *Clean Technologies*, 6(1), pp.93-115.

Park, I., Oh, S., Nam, H., Celi, P. and Lillehoj, H.S., 2022. Antimicrobial activity of sophorolipids against *Eimeria maxima* and *Clostridium perfringens*, and their effect on growth performance and gut health in necrotic enteritis. *Poultry Science*, 101(4), p.101731.

Patil, T.D., Pawar, S., Kamble, P.N. and Thakare, S.V., 2012. Bioremediation of complex hydrocarbons using microbial consortium isolated from diesel oil polluted soil. *Der Chemica Sinica*, 3(4), pp.953–958.

Perdomo, J., Quintana, C., González, I., Hernández, I., Rubio, S., Loro, J.F. and Quintana, J., 2020. Melatonin Induces Melanogenesis in Human SK-MEL-1 Melanoma Cells Involving Glycogen Synthase Kinase-3 and Reactive Oxygen Species. *International Journal of Molecular Sciences*, 21(14), p.4970.

Pirog, T.P., Lutsai, D.A. and Muchnyk, F.V., 2021. Biotechnological potential of the *Acinetobacter* genus bacteria. *Microbiological Journal/Mikrobiolohichnyi Zhurnal*, 83(3), pp.616-623.

Prasad, R.V., Kumar, R.A., Sharma, D., Sharma, A. and Nagarajan, S., 2021. Sophorolipids and rhamnolipids as a biosurfactant: Synthesis and applications. *Green Sustainable Process for Chemical and Environmental Engineering and Science*, 15(31), pp.423-472.

Qazi, M.A., Wang, Q. and Dai, Z., 2022. Sophorolipids bioproduction in the yeast *Starmerella bombicola*: current trends and perspectives. *Bioresource Technology*, 346, p.126593.

Rane, A.N., Baikar, V.V., Kumar, D.V.R. and Deopurkar, R.L., 2017. Agro-industrial wastes for production of biosurfactant by *Bacillus subtilis* AN 88 and its application in the synthesis of silver and gold nanoparticles. *Frontiers in Microbiology*, 8, pp.1-12.

Rawat, G., Dhasmana, A. and Kumar, V., 2020. Biosurfactants: the next generation biomolecules for diverse applications. *Environmental Sustainability*, 3, pp.353-369. doi: 10.1007/s42398-020-00128-8.

Ribeiro, B.G., Guerra, J.M.C. and Sarubbo, L.A., 2020. Biosurfactants: production and application prospects in the food industry. *Biotechnol. Prog.*, 36(5), p.e3030

Rivaldi, J.D., Vessoni Penna, T.C. and Dussán, K.J., 2018. Production of glycolipids and cell-bound lipopolysaccharides by *Candida lipolytica* growing on n-alkanes. *AMB Express*, 8(1), p.68.

Sah, D., Rai, J.P.N., Ghosh, A. and Chakraborty, M., 2022. A review on biosurfactant producing bacteria for remediation of petroleum contaminated soils. *3 Biotech*, 12(9), p.218. https://doi.org/10.1007/s13205-022-03277-1.

Santos, D.K.F., Rufino, R.D., Luna, J.M., Santos, V.A. and Sarubbo, L.A., 2016. Biosurfactants: multifunctional biomolecules of the 21st century. *International Journal of Molecular Sciences*, 17, p.1-31.

Sarubbo, L.A., Maria da Gloria, C.S., Durval, I.J.B., Bezerra, K.G.O., Ribeiro, B.G., Silva, I.A. and Banat, I.M., 2022. Biosurfactants: Production, properties, applications, trends, and general perspectives. *Biochemical Engineering Journal*, 181, p.108377.

Scholtes, C. and Giguère, V., 2022. Transcriptional control of energy metabolism by nuclear receptors. *Nature Reviews Molecular Cell Biology*, 23(11), pp.750-770.

Sen, B., Joshi, S. G. and Upreti, R. K., 2021. Bacterial lipopolysaccharides: Pathogenesis, structural diversity, and role in immune modulation. *Trends in Microbiology*, 29(11), pp. 946-961.

Segovia, V., Reyes, A. and Rivera, G., 2021. Production of rhamnolipids by the *Thermoanaerobacter* sp. CM-CNRG TB177 strain isolated from an oil well in Mexico. *Applied Microbiology and Biotechnology*, 105, pp.5833–5844. https://doi.org/10.1007/s00253-021-11468-8.

Shatilla, F., Diallo, M.M., Şahar, U., Ozdemir, G. and Yalçın, H.T., 2020. The effect of carbon, nitrogen and iron ions on mono-rhamnolipid production and rhamnolipid synthesis gene expression by Pseudomonas aeruginosa ATCC 15442. *Archives of Microbiology*, 202, pp.1407- 1417.

Shehu, P., Azi, B., Zakka, S.D., Tanimu, A., Akanbi-Lawal, N. and Yakubu, A., 2023. Effect of mishandling and vending of used engine oil on the environment, health and urban planning in Kaduna Metropolis: A call to action for a paradigm shift. *Urban Planning and Construction*, 1(1), pp.9-25.

Shekhar, S., Sundaramanickam, A. and Balasubramanian, T., 2015. Biosurfactant producing microbes and their potential applications: A review. *Critical Reviews in Environmental Science and Technology*, 45, pp.1522–1554.

Shi, K., Xue, J., Xiao, X., Qiao, Y., Wu, Y. and Gao, Y., 2019. Mechanism of degrading petroleum hydrocarbons by compound marine petroleum-degrading bacteria: surface adsorption, cell uptake, and biodegradation. *Energy & Fuels*, 33(11), pp.11373–11379. doi: 10.1021/acs.energyfuels.9b02306.

Siddiqui, Z., Anas, M., Khatoon, K. and Malik, A., 2021. Biosurfactant-producing bacteria as potent scavengers of petroleum hydrocarbons. In: Lone, S.A., Malik, A. (eds) *Microbiomes and the Global Climate Change*. Springer, Singapore. https://doi.org/10.1007/978-981-33-4508-9_17.

Souza, K.S.T., Gudina, E.J., Schwan, R.F., Rodrigues, L.R., Dias, D.R. and Teixeira, J.A., 2018. Improvement of biosurfactant production by *Wickerhamomyces anomalous* CCMA 0358 and its potential application in bioremediation. *Journal of Hazardous Materials*, 346, pp.152–158. doi: 10.1016/j.jhazmat.2017.12.021.

Su, X., Sun, F., Zhang, J., Xing, D., Li, X., Song, Z. and Li, A., 2023. Characterization and shifting of microbial community to denitrification for anaerobic sulfamethoxazole biodegradation with different electron acceptors. *Journal of Cleaner Production*, 387, p.135870.

Sulochana, S. B., Ramalakshmi, S., Nagarajan, S. and Gnanamani, A.,

2021. Microbial surfactants: Recent approaches and prospects in biotechnology. *Frontiers in Microbiology*, 11, 606612.

Sun, S., Su, Y., Chen, S., Cui, W., Zhao, C. and Liu, Q., 2022. Bioremediation of oil-contaminated soil: exploring the potential of endogenous hydrocarbon degrader *Enterobacter* sp. SAVR S-1. *Applied Soil Ecology*, 173, p.104387.

Sunde, E. P. and Børresen, T. 2016. Biotechnological production of biosurfactants and their applications. In *Microbial Biosurfactants*, pp. 217-236.

Swetha, S., Elakiya, V. P., Ammonica, B. K., Valli, N. C. and Prakash, P., 2020. Degradation of crude oil using the indigenous isolate Bacillus sp SEA18. *Journal of Environmental Management*.

Sydorenko, A., 2023. Biocenotic influence of the great cormorant (Phalacrocorax carbo L.) in the Azov-Black Sea region of Ukraine. *IOP Conference Series: Earth and Environmental Science*, 1254(1), p.012013.

Szulc, A., Ambrożewicz, D., Sydow, M., Ławniczak, Ł., Piotrowska-Cyplik, A., Marecik, R. and Chrzanowski, Ł., 2014. The influence of bioaugmentation and biosurfactant addition on bioremediation efficiency of diesel-oil contaminated soil: feasibility during field studies. *Journal of Environmental Management*, 132, pp.121–128. doi: 10.1016/j.jenvman.2013.11.006.

Thraeib, J. Z., Altemimi, A. B., Jabbar Abd Al-Manhel, A., Abedelmaksoud, T. G., El-Maksoud, A. A. A., Madankar, C. S. and Cacciola, F., 2022. Production and characterization of a bioemulsifier derived from microorganisms with potential application in the food industry. *Life*, 12(6), p.924.

Tripathi, S., Chandra, R., Purchase, D., Bilal, M., Mythili, R. and Yadav, S., 2022. Quorum sensing-a promising tool for degradation of industrial waste containing persistent organic pollutants. *Environmental Pollution*, 292, pp.118342.

Umar, H.A., Abdul Khanan, M.F., Ogbonnaya, C., Shiru, M.S., Ahmad, A. and Baba, A.I., 2021. Environmental and socioeconomic impacts of pipeline transport interdiction in Niger Delta Nigeria. *Heliyon*, 7, p.e06999. doi: 10.1016/j.heliyon.2021.e06999.

Unaeze, C.H., 2020. Application of biosurfactants in environmental remediation.

Varjani, S.J., 2017. Microbial degradation of petroleum hydrocarbons. *Bioresource Technology*, 223, pp.277–286. doi: 10.1016/j.biortech.2016.10.037.

Varjani, S.J., Rana, D.P., Jain, A.K., Bateja, S. and Upasani, V.N., 2015. Synergistic ex-situ biodegradation of crude oil by halotolerant bacterial consortium of indigenous strains isolated from onshore sites of Gujarat, India. *International Biodeterioration & Biodegradation*, 103, pp.116–124. doi: 10.1016/j.ibiod.2015.03.030.

Vecino, X., Rodríguez-López, L., Rincón-Fontán, M., Cruz, J.M. and Moldes, A.B., 2021. Nanomaterials synthesized by biosurfactants. In *Comprehensive Analytical Chemistry*, 94, pp.267-301. Elsevier.

Venkatraman, G., Giribabu, N., Mohan, P.S., Muttiah, B., Govindarajan, V., Alagiri, M. and Karsani, S.A., 2024. Environmental impact and human health effects of polycyclic aromatic hydrocarbons and remedial strategies: A detailed review. *Chemosphere*, 54, p.141227.

Verma, J.P. and Jaiswal, D.K., 2016. Book review: advances in biodegradation and bioremediation of industrial waste. *Frontiers in Microbiology*, 6, pp.1–2. doi: 10.3389/fmicb.2015.01555.

Verma, S., Bhargava, R. and Pruthi, V., 2006. Oily sludge degradation by bacteria from Ankleshwar, India. *International Biodeterioration & Biodegradation*, 57(4), pp.207–213. doi: 10.1016/j.ibiod.2006.02.004.

Vijayakumar, S. and Saravanan, V., 2015. Biosurfactants: types, sources and applications. *Research Journal of Microbiology*, 10, pp.181-192.

Wanapaisan, P., Laothamteep, N., Vejarano, F., Chakraborty, J., Shintani, M. and Muangchinda, C., 2018. Synergistic degradation of pyrene by five culturable bacteria in a mangrove sediment-derived bacterial consortium. *Journal of Hazardous Materials*, 342, pp.561–570. doi: 10.1016/j.jhazmat.2017.08.062.

Wang, J., Li, G., Yin, H. and An, T., 2020. Bacterial response mechanism during biofilm growth on different metal material substrates: EPS characteristics, oxidative stress and molecular regulatory network analysis. *Environmental Research*, 185, p.109451.

Wang, X.T., Liu, B., Li, X.Z., Lin, W., Li, D.A. and Dong, H., 2022. Biosurfactants produced by novel facultative-halophilic Bacillus sp. XT-2 with biodegradation of long chain n-alkane and the application for enhancing waxy oil recovery. *Energy*, 240, p.122802. doi: 10.1016/j.energy.2021.122802.

Wartell, B., Boufadel, M. and Rodriguez-Freire, L., 2021. An effort to understand and improve the anaerobic biodegradation of petroleum hydrocarbons: A literature review. *International Biodeterioration & Biodegradation*, 157, p.105156.

Waters, C.N., Zalasiewicz, J., Summerhayes, C., Fairchild, I.J., Rose, N.L., Loader, N.J., Shotyk, W., Cearreta, A., Head, M.J., Syvitski, J.P.M., Williams, M., Wagreich, M., Barnosky, A.D., Zhisheng, A., Leinfelder, R., Jeandel, C., Gatuszka, A., Sul, J.A.I.D., Gradstein, F.M. and Edgeworth, M., 2018. Global Boundary Stratotype Section and Point (GSSP) for the Anthropocene Series: Where and how to look for potential candidates. *Earth-Science Reviews*, 178, pp.379–429.

Wittgens, A., Kovacic, F. and Müller, M.M., 2017. Novel insights into biosynthesis and uptake of rhamnolipids and their precursors. *Applied Microbiology and Biotechnology*, 101, pp.2865–2878. doi: 10.1007/s00253-016-8041-3.

Wu, Q., Zhi, Y. and Xu, Y. 2019. Systematically engineering the biosynthesis of a green biosurfactant surfactin by *Bacillus subtilis* 168. *Metab Engineering*, 52, pp.87–97. doi:10.1016/j.ymben.2018.10.004.

Xu, W., Wu, Y., Gu, W., Du, D., Lin, Y. and Zhu, C. 2024. Atomic-level design of metalloenzyme-like active pockets in metal-organic frameworks for bioinspired catalysis. *Chemical Society Reviews*, 63, p.340. doi:10.1039/D4CS00340K.

Xu, X., Liu, W., Tian, S., Wang, W., Qi, Q., Jiang, P., Gao, X., Li, F., Li, H. and Yu, H. 2018. Petroleum hydrocarbon-degrading bacteria for the remediation of oil pollution under aerobic conditions: A perspective analysis. *Front Microbiology*, 9, p.2885. doi:10.3389/fmicb.2018.02885.

Yamamoto, S., Tsukahara, M., Yoshida, S., Matsushita, T. and Saito, T. 2022. Genetic and biochemical analysis of mannosyl erythritol lipid biosynthesis genes in *Pseudozyma*. *Bioscience, Biotechnology, Biochemistry*, 86(7), pp.1374-1384. doi:10.1080/09168451.2022.2075403.

Yasmin, A., Aslam, F. and Fariq, A. 2022. Genetic evidence of biosurfactant production in two *Bacillus subtilis* strains, MB415 and MB418, isolated from oil-contaminated soil. *Frontier Bioengineering, Biotechnology*, 10, p.1-12. doi:10.3389/fbioe.2022.849451.

Zahed, M.A., Matinvafa, M.A., Azari, A. and Mohajeri, L., 2022. Biosurfactant, a green and effective solution for bioremediation of petroleum hydrocarbons in the aquatic environment. *Discover Water*, 2(1), p.5.

Zeng, N. and Hausmann, H. 2022. Wood Vault: remove atmospheric CO2 with trees, store wood for carbon sequestration for now and as biomass, bioenergy and carbon reserve for the future. *Carbon Balance and Management.*, 17(1):2. doi:10.1186/s13021-022-00243-1.

Zhang, T. and Zhang, H. 2022. Microbial consortia are needed to degrade soil pollutants. *Microorganisms*, 10(2), p.261. doi:10.3390/microorganisms10020261.

Zhao, F., Wang, Q., Zhang, Y. and Lei, L. 2021. Anaerobic biosynthesis of rhamnolipids by *Pseudomonas aeruginosa*: performance, mechanism and its application potential for enhanced oil recovery. *Microbial Cell Factories*, 20(1), pp.1-12. doi:10.1186/s12934-021-01669-1.

Zhu Z., Zhang B., Cai Q., Cao Y., Ling J., Lee K. and Chen, B., 2021. A critical review on the environmental application of lipopeptide micelles. *Bioresour. Tech.*, 339, p. 125602. doi: 10.1016/j.biortech.2021.125602

Adsorptive Remediation of Dyes Through A Novel Approach from Nanotechnology: A Comprehensive Review

Sadia Shakoor[1]†, M. Shahnawaz Khan[2] and M. Ehtisham Khan[3]

[1]Bradford Training Institute for Engineers, Aligarh-202 001, U.P., India
[2]International College of Engineering and Management, Department of Fire Safety Engineering/Management, Muscat, PO Box 2511, Sultanate of Oman
[3]Department of Chemical Engineering Technology, College of Applied Industrial Technology, Jazan University, Jazan-45971, Kingdom of Saudi Arabia
†Corresponding author: Sadia Shakoor; sadia.shakoor67@gmail.com

ABSTRACT

Due to rapid industrial growth and the increased economic status of people, water sources across the globe are being significantly polluted with a wide array of effluents. Industrial, agronomic, and customary activities have led to the repeated infestation of water by discarded materials. Consequently, there is an urgent need for advanced technologies to effectively eradicate these impurities from wastewater. Among the various methods established for wastewater remediation, the adsorption process has gained remarkable significance due to its efficiency and effectiveness. The use of nano adsorbents (NADs) represents an emerging solution to these environmental issues. NADs possess exceptional physical and chemical characteristics, which enhance their applicability compared to traditional adsorbents. Their advanced grade, prominence, and excellence in various arenas make them a superior choice for wastewater treatment. Recent explorations have shown that NADs, such as carbon nanotubes, graphene, and metal and metal oxide nano adsorbents, have a pronounced and favorable impact on wastewater treatment. The focus of this review article is to provide current data and insights into the use of NADs for wastewater remediation. It aims to highlight the benefits of these novel materials and to discuss the potential areas for further improvement in this field. By exploring the latest advancements and applications of NADs, this review seeks to contribute to the ongoing efforts to address the critical issue of water pollution and to promote sustainable water management practices.

INTRODUCTION

Rapid industrialization, together with innovation in science and technology, upgrades the standard of living, opening out towards viable economic growth and worldwide hustle (Xu et al. 2018, Nayyar 2021). The penalty of such rapid growth is an environment convoyed by considerable pollution issues (Rasheed et al. 2020). Water contamination is a severe concern that the world is facing nowadays (Afroz et al. 2014). At present, the world is facing the problem of scarcity of clean drinking water because of inadequate clean water resources (Afroz et al. 2014). Worsening of the water quality alongside the unceasing reduction in the accessibility of clean drinking water is due to the enhanced usage of water in industrial, domestic, and agronomic zones (Pimentel et al. 2004, Goel 2006). Industrial runoff encompasses many precarious and virulent pollutants severely affecting the ecosystem (McGlade et al. 2020, Sharma et al. 2021). An extensive array of waste is generated from these industries which are ultimately discharged into the water resources and, henceforth, modifying the characteristics and aesthetics of water (Gardetti & Torres 2017, Loucks & Van Beek 2017). Amongst the numerous wastes originating in

these industries, colored stuff predominantly, the dyes are the supreme released contaminant (Tahir et al. 2021). To boost the aesthetics of the goods, dyes are far and wide exploited by a lot of industries such as food, textile, rubber, automobiles, cosmetics, printing and photographic sectors, pharmaceuticals, etc. (Gázquez et al. 2014, Tahir et al. 2021). As soon as the dye-laden effluents from such industries enter the water resources, it is now untimely and occasionally challenging to treat because of the complex structure and non-biodegradable character of dyes (Dhakate et al. 2020). Textile industries use dyes on a large scale. Commercially, about 0.1 million dyes are accessible globally, and around 7.0×105 metric tons of dyes are manufactured annually (Bharathi & Ramesh, 2013, Cockerham et al. 2022). The total dye input in textile industries is higher than 104 tons annually, and approximately 10-15% of dyes are released back into water (Husain 2006, Singh & Arora 2011). Dyes can be mutagenic, cancer-causing, and potential allergen. Therefore, the adulteration of dyes in water can be menacing for flora and fauna as well as humans (Khan et al. 2017b Ramesh & Muthuraman 2018).

IMPACT OF DYES ON LIFE

Dyes, as pollutants, are a serious disconcertment for civilization as their intricate assemblies and non-biodegradable nature make them damaging to life (Kahlon et al. 2018). They are a precarious category of organic pollutants that are being discharged into water resources directly or indirectly (Kahlon et al. 2018). They disturb the ecosystem and are mostly carcinogenic, mutagenic, and teratogenic and also have damaging effects on the excretory,

respiratory, reproductive as well as central nervous systems (Duruibe et al. 2007, Hashimi et al. 2020). They spoil the aesthetics of water bodies and curb the sunlight perforation in water, thereby affecting the aquatic flora and fauna.

Dyes are commonly classified into different categories and sub-categories (Fig. 1) on the basis of their source, well-established dye structure (nature of chromophore group), and the mode of their application (compatibility of the dye-fiber type) (Routoula 2019, Velusamy et al. 2021). Amongst the numerous classes, azo dyes are a prevalent assembly of colorants comprising almost half of all the accessible dyes used in the industries. Azo dyes are characterized by –N=N– bond where one nitrogen atom is bonded to an aromatic group (naphthalene or benzene rings) (Bafana et al. 2011, Ajmal et al. 2014, Dassanayake et al. 2021).

Furthermore, they possess amphoteric character because of the auxiliary functional groups such as carboxyl (–COOH), hydroxyl (–OH), amino (–NH_2), or sulfoxyl (O=S=O). These dyes may act as anionic, cationic, or non-ionic based on the pH of the surrounding medium. Classification and characteristics of azo dyes are outlined in Table 1.

Acidic dyes express damaging effects on the eyes, respiratory system, melanoma, and mutagenicity in humans (Hammam et al. 2015). Basic dyes have a noxious nature, leading to allergic complications, skin annoyance, mutations (skin carcinoma), escalation of heartbeat, moreover a rise in the prevalence of trauma, vomiting, cyanosis, icterus, tetraplegia, and tissue mortification (Afreen et al. 2018, Elgarahy et al. 2021). The amine group in these dyes is the key entity behind their toxicity (Khan et al. 2016, 2017a, 2018, Vishnu et al. 2021). Henceforth, dye remediation
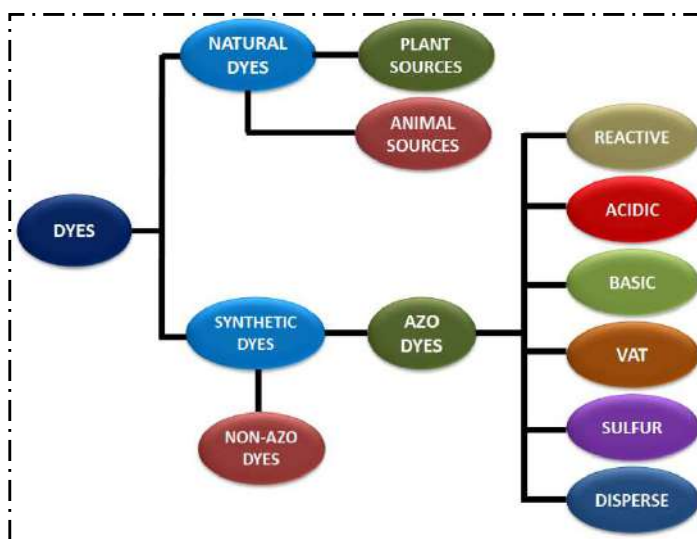
Fig. 1: Classification of dyes based on chemical composition.

Table 1: Classification of azo dyes.

Class	Solubility Characteristic	Fiber	Fixation %	Pollutant
Reactive	• Water-soluble • Anionic	• Cotton • Cellulosic • Wool	60-90	Colour, salt, alkali, unfixed dye, surfactants, defoamer, diluents
Acidic	• Water-soluble • Anionic	• Cotton • Nylon • Wool • Acrylic • Protein	80-93	Colour; organic acids; unfixed dye
Basic	• Water-soluble • cationic • Applied in acidic dye baths	• Protein • Cellulosic • Nylon • Polyester • Acrylic	97-98	Not available
Vat	• Water-insoluble • Chemically complex	• Cotton • cellulosic • Wool	60-70	Color, alkali, oxidizing, and reducing agents
Sulfur	• Water-insoluble • Non-ionic	• Cotton • Cellulosic	60-70	Color, alkali, oxidizing and reducing agents, unfixed dye
Disperse	• Water-insoluble • Non-ionic	• Acrylic • Modacrylic • Nylon • Polyester	80-92	Color, organic acids, carriers, leveling agents, diluents phosphates, defoamers, lubricants, dispersants

Table 2: Pros and cons of dye-removal techniques.

Methods	Pros	Cons
Physical (Sedimentation, filtration, floatation, coagulation, reverse osmosis, solvent extraction, adsorption)	• Good removal of a wide variety of dyes • regeneration- no adsorbent loss, • effective oxidation at the lab scale, • economically feasible	• expensive • concentrated and high sludge formation • not effective for all dyes
Chemical (neutralization, reduction, oxidation, catalysis, ion exchange, electrolysis)	• simplicity of application • Fenton's reagent is a suitable chemical means • Ozone can be applied in its gaseous state and does not increase the volume of wastewater and sludge. • No chemical consumption and no sludge buildup	• The reagent needs to be activated by some means • Sludge formation • Formation of by-products • Relatively high flow rates cause a direct decrease in dye removal
Biological (stabilization, aerated lagoons, trickling filters, activated sludge, fungal treatment, flocculation, anaerobic digestion)	• Allows azo and other water-soluble dyes to be decolorized • Certain dyes have a particular affinity for binding with microbial species • Decolorized in 24 to 30 hours	• Under aerobic conditions, azo dyes are not readily metabolized • Not effective for all dyes • Anaerobic breakdown yields methane and hydrogen sulfide

from wastewater before its discharge into the water sources is a serious environmental perturbation in the present hour (Madima et al. 2020, Arora et al. 2021).

WATER MANAGEMENT TECHNOLOGIES

Physical techniques (sedimentation, filtration, floatation, coagulation, reverse osmosis, solvent extraction, and adsorption), chemical techniques (neutralization, reduction, oxidation, catalysis, ion exchange, and electrolysis), and biological techniques (stabilization, aerated lagoons, trickling filters, activated sludge, fungal treatment, flocculation and anaerobic digestion) are employed for the confiscation of dyes from wastewater (Gunatilake 2015, Carolin et al. 2017, Wu et al. 2017, Yadav et al. 2021) Such techniques are steadfast and display specific outcomes. However, on the other hand, they also have some limits like lesser efficacy, greater investment, generation of too much sludge, and high maintenance charges, making them unbefitting for economical practice.

All of these methods have their pros and cons, such as high operational /energy expenses, generation of huge expanses of sludge, and production of detrimental byproducts (Table 2).

Still, from the above-mentioned techniques for wastewater remediation, the adsorption route is the most tempting method due to its easy functioning, high efficacy, easiness, cost-efficiency, and persistence (Wu et al. 2017). Moreover, in the majority of explorations, the process is reversible, and henceforth, the adsorbents can be without difficulty recycled recurrently, making the overall adsorption process more cost-effective. Additionally, the accessibility of an immense choice of adsorbents to befit precise requisite makes it more adaptable (Creamer & Gao 2016, Wu et al. 2017). Owing to the diverse benefits aforementioned, the adsorption method has acknowledged consideration all around the environment adoring society (Liu et al. 2016).

Adsorption is the adhering of a particle superficially to a surface. The particle might be a gas, liquid, or solid (atom, molecule, or ion), and the surface might be a liquid or solid. The binding between the particle and the surface is either chemical or physical (Liu et al. 2016, Ijaz & Zafar 2021). The substances offering the surface are the adsorbents, while the entity that is attached to the surface is the adsorbate (Li et al. 2009, Farrukh et al. 2013, Dutta et al. 2019).

Adsorbate particles are associated with adsorbent via two kinds of forces, viz. physical and chemical, in the processes named physisorption and chemisorption. Physisorption is caused by feeble attractive forces amid adsorbate-adsorbent molecules, while chemisorption occurs through the formation of a strong chemical bond (Jelmy et al. 2021). An adsorbent is considered effective; constraints like surface area, porous nature, adsorption capacity, and mechanical strength ought to be extremely high alongside the viability of supplementary features like cost-efficiency, untroubled renewal, persistence, and selectiveness (Jelmy et al. 2021). A diagrammatic illustration of the elimination of dyes from wastewater using adsorption is displayed in Fig. 2. Several factors, namely, adsorbate/adsorbent interaction, surface area (adsorbent), adsorbent/adsorbate proportion, particle size (adsorbent), temperature, pH, contact time, etc.,

are calculated as they are accountable for the elimination rates of dyes (Gupta 2009, Banerjee et al. 2015, Mashkoor & Nasar 2020). Detailed investigations of such optimized factors are considered to be useful in the remediation of dyes efficiently and for the progress of commercial-scale wastewater treatment processes (Karimifard & Moghaddam 2018, Islam et al. 2019). Amongst the diversity of adsorbents available, activated carbon is the utmost chosen adsorbent for the confiscation of dyes owing to its outstanding adsorption capability (Ahmad et al. 2021). However, extensive application of activated carbon is constrained as it is costly (Whitacre et al. 2012, Ahmad et al. 2021). A variety of non-conventional economical adsorbent materials have been investigated by various researchers for the remediation of dyes (Crini 2006, Rafatullah et al. 2010, Dawood & Sen 2014). These encompass agricultural wastes industrial waste products, clay materials, zeolites, siliceous materials, biosorbents, biomass and others (cyclodextrin, starch, cotton), Artocarpus heterophyllus peel, Allium sativum peel, hazelnut shell, pineapple stem, longan shell, consumed tea leaves zeolite, corncobs and so on (Bouzaida & Rammah 2002, Crini & Morcellet 2002, O'mahony et al. 2002, Özacar & Şengil 2002, Crini 2003, Delval et al. 2003, Walker et al. 2003, Allen et al. 2004, Wong et al. 2004, Aksu & Tezer 2005, Hameed 2009). Consequently, the considerations have been encouraged to discover more economical and proficient replacements of activated carbon. Innate components, agronomic and industrialized trashes and bio-sorbents can be the most credible replacements (Whitacre et al. 2012).

Also, the non-conventional adsorbents displayed diversified conclusions, with several cases exhibiting high removal efficiencies as compared to the activated carbons (Gupta et al. 2013, Vieira et al. 2020).

But, the investigations for innovative and futuristic adsorbents with high dye removal efficiencies with excellent regenerability are a crucial part of current research in the water treatment field. Currently, nanoparticles (NPs) are
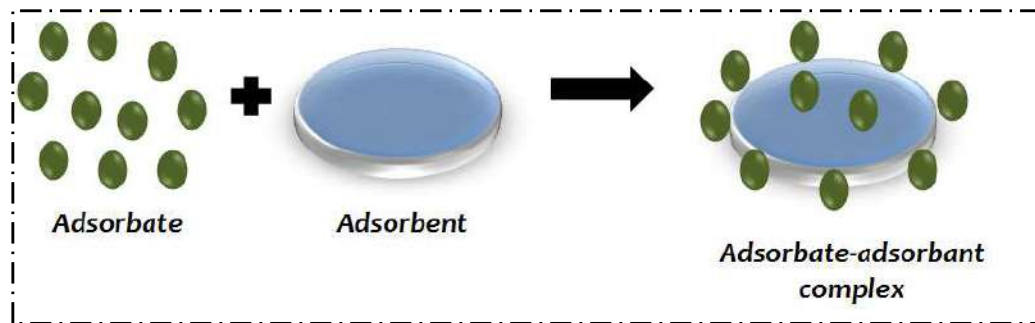
Fig. 2: Schematic representation of the Adsorption process.

being exploited for the decontamination of wastewater. These anticipated NPs are being made with distinctive assets like enormous surface area/volume ratio and surface characteristics to tackle noxious contaminants.

IMPLEMENTATION OF NANOTECHNOLOGY IN DYES REMOVAL

Nanotechnology presents a new arena of science offering a significant part in wastewater treatment (Nasrollahzadeh et al. 201, Thangadurai et al. 2020, Shakoor et al. 2023). The word 'Nano' is extracted from the Greek term 'Nanos', meaning dwarf or exceptionally tiny. Nanoparticle size covers the 1-100 nm range and is distributed in all media (gaseous, liquid, solid). Such characteristics make them the most desirable materials for an extensive array of uses (Gangadhar et al. 2012). NPs may be categorized as inorganic, polymeric, solid lipids, liposomes, nano-crystal, nanotubes, and dendrimers (Biswas et al. 2014, Ansari et al. 2020). NPs are synthesized via physical, chemical, or biological techniques (Jameel et al. 2020). The chemical technique is significant since it requires little duration for the preparation of a variety of NPs (Ju-Nam & Lead 2008). Polymeric NPs are synthesized via the polymerization of several monomer units like methacrylic acid, acrylic esters, methacrylic, and so on (Martin et al. 2021). Synthesis of inorganic NPs might be done in the manifestation of polymers like polylactic acid and polyglycolic acid etc. (Xue et al. 2019). Presently, chemical techniques, viz., dispersion of pre-formed polymers, polymerization of monomeric units, and coacervation of hydrophilic polymers, are practically aiming for the synthesis of diverse polymeric NPs (Xue et al. 2019). Metal/metal oxide NPs might be synthesized via different physical methods, namely, evaporation-condensation, sol-gel technique, solvothermal method, chemical reduction, laser ablation, etc. Amongst several methodologies, the biological one is exceedingly effective owing to its environmentally friendly approach. This category of NPs includes those synthesized using plants, fungi, yeast, bacteria, viruses, proteins, enzymes etc., (Saratale et al. 2018, Salem & Fouda 2021).

Numerous nanomaterials have been synthesized and used for the sequestration of impurities existing in wastewater (Ata et al. 2019, Mustapha et al. 2020). They have remarkably high surface area-volume ratio, micro- or mesoporous structure, high adsorption capability, cost-efficiency, and regenerability (Chang et al. 2019). These nano-adsorbents (NADs) perforate deeply, act quickly, and possess outstanding pollutant-binding capability (Chang et al. 2019). NADs might be shaped into nanowires, nanotubes, nanofilms, and nanoparticles. In wastewater

management, several practically viable and effective NADs are recognized as having characteristic features for successful decontamination of wastewater (Sharma et al. 2009, Harja & Ciobanu 2020, Janani et al. 2022). Outstanding removal efficiencies of NADs have been published in the literature regarding the confiscation of dyes from wastewater (Ahmed et al. 2020, Essekri et al. 2021, Ansari et al. 2023, Afridi et al. 2023). NADs can be classified into different categories based on their application in adsorption techniques, namely, magnetic, nanostructured mixed oxides, and metallic/metallic oxides (Ahmadi et al. 2017). In addition to these, nanotubes, nanosheets, and carbon/silicon/polymer nanoparticles are a few NADs utilized for the adsorptive removal of dyes from wastewater (Ahmadi et al. 2017).

Wastewater treatment methods using nanotechnology are hopeful approaches to overcome the key hurdles in water treatment technologies.

NANO-ENGINEERED ADSORBENT

Prerequisites for an efficient adsorbent are the constraints like higher surface area, highly favorable porosity, greater absorptivity, and eminent mechanical strength, as well as supplementary features like cost-efficiency, easy regenerability, viability, and selectivity (Mahfoudhi & Boufi 2017). Numerous adsorbents are being used for wastewater treatment, which mainly include those obtained from agronomic, domestic, and industrialized wastes, polymeric materials, and organic as well as inorganic substances (Mahfoudhi & Boufi 2017). However, the adsorbents obtained from such sources have low absorptivity (Mahfoudhi & Boufi 2017). Hence, it has become essential to discover more innovative, operative, and excellent adsorbents for wastewater treatment (Tara et al. 2020). The cost and physiognomies like particle size, homogeneous size organization, shape, crystal framework, composition, purity, stabilization, and reproducibility make the NPs appropriate for utilization in various fields like sensors, biomedical applications, and, in particular, in water treatment. The utilization of NADs in wastewater treatment opens up a new arena for the application of nanotechnology (Tara et al. 2020).

The most extensively studied NADs for wastewater treatment are carbon nanotubes (CNTs), graphene and metal oxides such as Fe_3O_4, MnO_2, CO_3O_4, TiO_2, MgO, ZnO, etc (Luo et al. 2010, Apul et al. 2013, Abas et al. 2014, Khan et al. 2016, 2015, Zare et al. 2015a, Mohammad et al. 2019, Mohammad et al. 2021a,b). They might be prepared in diverse morphological arrangements. Hereby, this review aims to update on the recent advancements in dye remediation from wastewater using NPs as efficient adsorbents along with the viewpoints in this part of the exploration.

CARBON-BASED NANOMATERIALS

Recently, NPs based on carbon, namely, graphene, fullerenes, and carbon nanotubes, have attracted noteworthy attention owing to their superlative assets, predominantly vast surface area, porosity, thermal and mechanical strengths, and removal efficacy (Bhatnagar & Minocha 2006 Mauter & Elimelech 2008, Shakoor & Nasar 2017, 2018a, Varghese et al. 2019, Shahbazi et al. 2020).

Carbon Nanotubes (CNTs)

Sumio Iijima, a Japanese physicist, discovered CNTs in the arc evaporation method (Ajayan et al. 1993). Apart from the arc evaporation method, several other methods, namely, laser ablation, flame synthesis, chemical vapor deposition, and electrolysis, have been described for the synthesis of CNTs (Terrones 2003, Farhat & Scott 2006, Nayeri & Jafari 2024). It is worth mentioning that arc evaporation, chemical vapor deposition, and laser ablation procedures are widely used for the synthesis of CNTs (Farhat & Scott 2006). The CNTs comprise graphene/graphite sheets that wind up in a tube shape having a diameter in the nanometer range and length in the micrometer range. The ends of CNTs are capped with a hemisphere of the fullerene-like entity. The hollow-tiered structures of CNTs offer a high surface area as well as high porosity. This unique assembly of CNTs possesses mechanical strength, electronic as well as thermal stability. They might be metallic or semiconducting depending upon the class of chiral characteristics (chiral angle between carbon hexagons and tube axis) (Aqel et al. 2012, Gusain et al. 2020).

CNTs have been substantially applied for the remediation of dyes in wastewater treatment as a result of their high absorptivity for dyes(Gusain et al. 2020, Thakur et al. 2024).

CNTs are classified into single-walled CNTs and multi-walled CNTs (Fig. 3). Single-walled CNTs are comprised of single graphene sheets that wind up in a cylinder whereas multi-walled CNTs are made of coaxial piling of graphene sheets to form of a cylinder with the adjoining sheets being adhered by weak van der Waals forces with an interspacing of approximately 0.34 nanometers (Aqel et al. 2012).

Multi-walled CNTs have been exploited for the adsorptive elimination of single dye systems such as Congo red (Zare et al. 2015b), methyl orange (Yao et al. 2011), blue 116 (Vuono et al. 2017), red 159 (Vuono et al. 2017) and yellow 81 (Vuono et al. 2017), maxilon blue (Alkaim et al. 2015), reactive blue 4 (Machado et al. 2012), reactive red M-2BE (Machado et al. 2011), direct blue 53 (Prola et al. 2013), ponceau 4R (Ferreira et al. 2017), allura red (Ferreira et al. 2017), etc. The adsorption behavior of multi-walled CNTs on cationic-anionic binary dye systems was also studied (Ma et al. 2018). Multi-walled CNTs were utilized for adsorptive remediation studies of acid red 183 and methylene blue in an aqueous solution. It was observed that multi-walled CNTs possess higher adsorptive attraction towards methylene blue as compared to acid red 183 in single as well as dual-dye systems (Ma et al. 2018).

The maximum adsorption capacity in the case of mono-dye set-up was obtained to be 59.7 for methylene blue (cationic) and 45.2 $mg.g^{-1}$ for acid red 183 (anionic).

(a) Single-walled carbon nanotubes   (b) Multi-walled carbon nanotubes
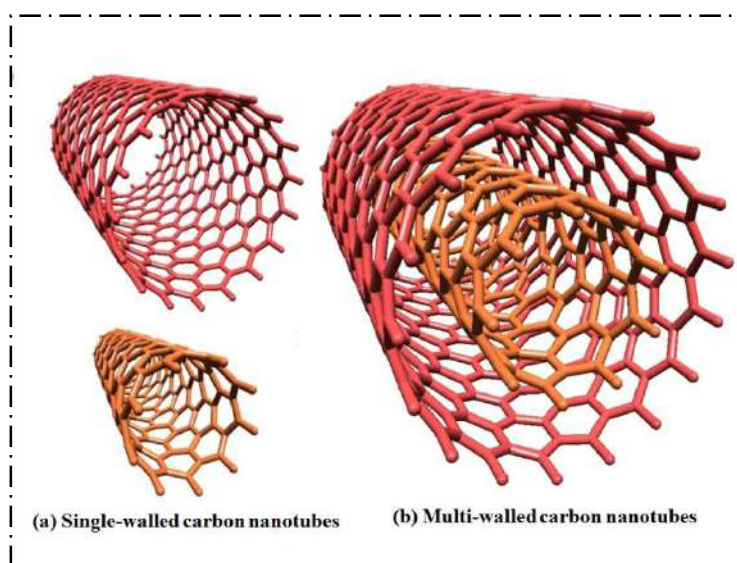
Fig. 3: Schematic representation of single-walled and multi-walled CNTs.

For dual-dye set-up, keeping the concentration of acid red 183 constant (20 mg/L), an increase in adsorptive removal of both the dyes was observed with the increase in methylene blue concentration, suggesting a synergistic effect. On the other hand, by maintaining a constant methylene blue concentration (10 mg/L), adsorptive removal of methylene blue was found to be reduced with increasing acid red 183 concentrations, while acid red 183 exhibits a rising inclination in adsorption capacity (Wang et al. 2012, Shakoor & Nasar 2016).

Functional modifications of CNTs have been commenced for the introduction of different functional groups, thereby providing fresh adsorption sites (Wang et al. 2012). Many research explorations have confirmed the enhanced elimination of dyes from wastewater by modified CNTs using various functional groups. Such functional modifications lead to the reduction in the accumulation of CNTs, escalation of adsorption, durability, selectiveness, and affinity for pollutants in wastewater (Gupta et al. 2013, Gupta & Saleh, 2013). Amongst the various functionalization methods, oxidation is the simplest mode for the introduction of –OH and C=O groups to the walls of CNTs. Multi-walled CNTs obtained after oxidation were more efficient for the elimination of methyl red (MR) and bromothymol blue (BB) in water (Ghaedi & Kokhdan 2012, Sadegh et al. 2017). An adsorption capacity of 41.63 $mg.g^{-1}$ was reported by Yao et al. for the elimination of MB on CNTs at 333 K (Yao et al. 2010). Similar experiments were executed by Shahryari et al. (Shahryari et al. 2010) on multi-walled CNTs with high surface area (280 m^2 g^{-1}) in comparison to the CNTs (160 m^2 g^{-1}) investigated by Yao et al. An adsorption capacity of 132.6 $mg.g^{-1}$ at 310 K was observed for MB dye. The adsorption capacities are also influenced by the experimental constraints and kinds of adsorbents. Relative adsorption capacities of orange II dye from aqueous solution by the utilization of multi-walled CNTs and carbon nanofibers adsorbents were calculated in batch experimentations by Rodríguez et al. (Rodríguez et al. 2010). It was observed that the adsorptive elimination of anionic orange II on multi-walled CNT (77.83 $mg.g^{-1}$) was a little higher than carbon nanofiber (66.12 $mg.g^{-1}$).

CNT-impregnated chitosan hydrogel (CS/CNT) beads were synthesized to investigate the elimination of Congo red dye. CS/CNT beads revealed a higher maximum adsorption capacity (450.4 $mg.g^{-1}$) as compared to the chitosan without impregnation (200 $mg.g^{-1}$, Langmuir isotherm model) (Chatterjee et al. 2010). A unique type of CS/CNT beads was synthesized by (Chatterjee et al. 2011) by treating multi-walled CNTs with sodium dodecyl sulfate to upgrade mechanical characteristics (Chatterjee et al. 2011). These unique CS/CNT beads revealed a maximum adsorption capacity of 375.94 $mg.g^{-1}$ for Congo red dye (Chatterjee et al. 2011). It is worthy of mentioning that CNTs might be consequently generated on a macroscale by different methodologies to reduce the production cost thereby increasing their subsequent consumption in environmental safeguard administration. Utilization of CNTs in wastewater treatment is anticipated to be a revolution in upcoming research (Hussain et al. 2024).

Graphene

Graphene comprises one or more layers of carbon atoms adhered by weak Van der Waal forces and p–p stacking associations with a distinctive 2D assembly and tremendous mechanical, thermal, and electrical characteristics (Shahryari-ghoshekandi & Sadegh 2014, Rajabi et al. 2019). Several studies were conducted employing graphene and graphene oxide for the elimination of dyes from wastewater. For modification of the physico-chemical properties, reduced graphene oxide (rGONSs) and graphene oxide nanosheets (GONSs) were prepared by incorporating them in composite fragments. rGONSs, as well as GONSs layers, have large aspect ratios with huge electronic surfaces providing powerful intermolecular forces amongst the adsorbate molecules (Denis & Iribarne 2012). Owing to the exposed layered arrangement, rGONSs show significantly accelerated adsorption kinetics as compared to the CNTs (Ji et al. 2013, Yu et al. 2014).

Amongst the various carbon-based nanomaterials (Activated carbons, single-walled CNTs, and multi-walled CNTs), rGONSs showed enhanced absorptivity of two synthetic organic compounds (phenanthrene and biphenyl) in an aqueous medium (Thakur & Kandasubramanian 2019). Also, rGONSs are comparatively low-priced compared to single-walled CNTs. rGONSs were employed for the elimination of cationic red X-GRL (Li et al. 2011c), methylene blue (Li et al. 2011°, Yang et al. 2011), methyl orange (Li et al. 2011b), Congo red (Li et al. 2011b) from aqueous solutions. The maximum adsorption capacities for p-toluenesulfonic acid, 1-naphthalenesulfonic acid, and methylene blue on GNS goes to 1430, 1460, and 1520 mg.g-1 at 303 K, respectively, highest amongst all nanomaterials calculated so far (Wu et al. 2011). The abundance of functional groups with oxygen superficially on graphene oxide nanosheets was described as executing an essential part of the adsorption process. Relative to activated carbons and CNTs, graphene oxides and graphene nanosheets exhibit a stronger adsorption affinity for dyes in wastewater.

Metal Oxide-Based Nanomaterials

Nanomaterials based on metal/metal oxides are a class of inorganic nanomaterials extensively utilized to confiscate

dyes from wastewater. Metal oxides have negligible environmental effects, little solubility, and do not contribute to secondary pollution. Nowadays, zero-valent iron, iron oxides/hydroxides (Fe_3O_4), titanium oxide (TiO_2), zinc oxide (ZnO), and copper oxide (CuO) nanoparticles as well as in its composites form have been employed as adsorbent for the confiscation of dyes from wastewater (Khan et al. 2019b, 2019a). In recent times, zero-valent iron was synthesized by Rahman et al. (Rahman et al. 2014) with a borohydride chemical reduction method and is being employed for the elimination of azo dyes from wastewater. (Arabi et al. 2013) carried out kinetic and thermodynamic investigations for eliminating vat green dye from wastewater using zero-valent iron NADs. Diverse methodologies, namely, oxidation, reduction, disproportionation, hydrolysis, sol-gel, high-pressure hydrothermal, and co-precipitation, have been employed to synthesize iron oxide nanoparticles (Lu et al. 2006, Teja & Koh, 2009, Layek et al. 2010). Iron oxide and zero-valent iron composite NADS have also been synthesized and exploited for the elimination of precarious toxic pollutants from wastewater (catalytic and magnetic character of such NADs exhibited greater efficiency for dye confiscation). Iron being the most prevalent element in the earth crust and triviality of its resources and ease of production makes ferric oxides an economical adsorbent for dye adsorption**.**

Novel magnetic Fe_3O_4@CNADs were synthesized and employed for the confiscation of methylene blue and Congo red (Zhang & Kong 2011). The maximum adsorption capacity was found to be 44.38 and 11.22 $mg.g^{-1}$ for methylene blue and Congo red, respectively. Improvements in the iron oxides and zero-valent iron nanoparticles were also made by mingling such particles with different organic and/or inorganic constituents.

An adsorbent with a size in the nano range having an enormous surface area might proficiently confiscate dyes. However, the consumed nanoparticles are hard to isolate afterward, and continuing exposure might cause toxicity altogether. By utilizing magnetic iron oxide nanoparticles, such difficulties can be overcome. Nevertheless, additional efforts are desired to make the procedure extra efficient and innovative. The maximum adsorption capacity of magnetic zero-valent iron nanoparticles prepared by the coprecipitation method and loading on Arabic gum was found to be 14 $mg.g^{-1}$ for methylene blue dye (Alzahrani 2014). A novel bi-metallic Fe-Zn nanoparticle prepared by co-precipitation technique has been employed for the confiscation of malachite green and Congo red from wastewater by Gautam et al. (Gautam et al. 2015).The maximum adsorption capacity of the adsorbent was found to be 21.74 $mg.g^{-1}$ for malachite green and 28.56

$mg.g^{-1}$ for Congo red. The polypyrrole-coated magnetic Fe_3O_4 nanoparticle (PPy@Fe_3O_4) was also utilized as an adsorbent to eliminate synthetic textile dye RB19. The maximum adsorption capacity of PPy@Fe_3O_4 for RB19 was observed to be 112.4 $mg.g^{-1}$ (Shanehsaz et al., 2015). L-arginine-functionalized Fe_3O_4 magnetic nanoparticles (Fe_3O_4@L-arginine) were synthesized, and the removal efficiency for Reactive Blue 19 was observed to be 96.3% under optimum conditions. The adsorption mechanism obeyed pseudo-second-order kinetics and Freundlich isotherm (Dalvand et al. 2016).

Apart from iron, other metal-based nanoparticles and their composites have also been synthesized and exploited for dye remediation, showing tremendous removal efficiency for various types of dyes. Cupric oxide (CuO) nanoparticles synthesized by numerous procedures were employed for the removal of various dyes such as MO, MB, crystal violet (CV), CR, trypan blue (TB), etc. (Mustafa et al. 2013, Mekewi et al. 2016, Sasikala et al. 2016, Taufik & Saleh 2017, Shakoor & Nasar 2018b, 2019).

Mustafa et al. (Mustafa et al. 2013) synthesized the cupric oxide (CuO) nanoparticles using the precipitation method and employed it for the adsorptive studies on MB dye, accomplishing a removal efficiency of 88.9%. Similarly, Mekewi et al.(Mekewi et al. 2016) synthesized CuO nanoparticles and chemically activated them with montmorillonite clay, and used them for the removal of MB dye from an aqueous solution.

Sol-gel method was adopted to synthesize the iron (II, III) oxide/zinc (II) oxide/copper (II) oxide (Fe_3O_4/ZnO/CuO) nano-composites. The Fe_3O_4/ZnO/CuO nanocomposites with different amounts of CuO nanoparticles were used for photocatalytic degradation of MB dye under UV/vis light and ultrasound arrangement. Faster degradation of MB was observed using a higher quantity of CuO in visible light and also with a lower quantity of CuO in UV light (Taufik & Saleh 2017). Adsorptive studies were carried out on cerium-loaded CuO NPs by Sasikala et al. (Sasikala et al. 2016) for the remediation of azo dyes such as MO and TB in UV radiation. Silver nanoparticles-loaded AC was used as an adsorbent by Karimi et al. (Ghaedi et al. 2013) for the elimination of MO dye. In their study, it was observed that an increase in the pH of the dye solution was accompanied by enhanced adsorption of MO. The removal efficiency increased from 67.3 to 98.8%, with a rise in pH from 2 to 5. Mady et al. (Mady et al. 2017) prepared Ag-$ZnFe_2O_4$@ reduced graphene oxide (rGO) nanocomposites by a one-pot microwave-assisted self-assembly technique. The Ag-$ZnFe_2O_4$@rGO nanocomposites thus obtained with a 15.2 weight percentage of rGO exhibited brilliant

adsorption characteristics and high photocatalytic activity for the elimination of degradation of rhodamine B (RhB), MB, and MO dyes. The Ag-ZnFe$_2$O$_4$@rGO nanocomposite can be recovered straightforwardly with a simple magnet and can be used five times with no substantial reduction in its photocatalytic activity. The Ag-ZnFe$_2$O$_4$@rGO nanocomposite catalyst can also be employed for the confiscation of hard-to-degrade unwanted constituents because of its high proficiency in both UV and visible light and its excellent regenerability.

Yang et al. (2016)synthesized novel silver-containing vanadate semiconductor nanorod (Ag$_2$ZnV$_4$O$_{12}$ nanorod) was prepared using the sol-gel process, and the photocatalysis was explored by photodegradation of RhB dye excited by the light wavelength higher than 420 nm.

Ni-doped ZnO nanoparticles were synthesized by a simple low-precipitation method at low temperatures and were exploited for the degradation of anionic Fast Green (FG) and cationic Victoria Blue (VB) dyes (Saharan et al. 2015), synergistic influence of Ni-doped ZnO nanoparticles and ultrasonication leads to practically complete mineralization of both FG and VB dyes in merely 5 minutes of contact time in the manifestation of light. The recovered nanoparticles were utilized yet again to degrade the same dyes recurrently under ultrasonic irradiation. The sonodegradation efficiency for FG and VB was found to be 96% and 94%, respectively, in the first 2 cycles. After that, only a slight decrease in the catalytic efficiency was observed. Cobalt ferrite (CoFe2O4) nanoparticles prepared and functionalized with an amine (-NH2) group were employed for the adsorption studies on Direct Green6 (DG6), Direct Red 80 (DR80), and Acid Blue 92 (AB92) dyes. The amine group was introduced to enhance the adsorption activity of the CoFe2O4 nanoparticles. The adsorption was quite fast, and adsorption equilibrium was attained in about 15 minutes. Experimental outcomes indicate that the system obeys the Langmuir adsorption isotherm model equation and fits better than the other equations (Yavari et al. 2016).

A thin-film TiO$_2$-coated nano-structured template was synthesized by metal-assisted wet etching of Si. This was used as a substrate for the deposition of a 10 nm thick film of TiO$_2$ by atomic layer deposition.is studied by dye degradation in water. The photocatalytic efficacy of this nanostructured template was evaluated by the degradation of two dyes in aqueous solution, namely, MB and MO (Scuderi et al. 2014).

The nanostructured TiO$_2$ revealed that the photo-degradation reaction rate is approximately 3 (for MB) and 12 times (for MO) as compared to the rate of TiO$_2$ flat film (Scuderi et al. 2014). New photoactive composites, Cu2O/TiO2 nanoparticles in novel inorganic geopolymer matrix

altered by cetyltrimethylammonium bromide (CTAB), were synthesized to efficiently confiscate MB dye from aqueous solution. The mechanism of the removal of dye involves a combination of adsorption (under dark conditions) and photodegradation (under UV radiation). MB adsorption in the dark obeys pseudo-second-order kinetics and is best described by Freundlich-Langmuir isotherms. The adsorptive behavior of the CTAB-modified geopolymer-centered composites is far superior to the ones based on unmodified geopolymer hosts. The most effective composite is the one containing 5-weight percent Cu2O/TiO2 in a CTAB-modified geopolymer host. These composites set up a new class of materials with outstanding potential in environmental protection applications (Falah et al. 2016).

Glutaraldehyde cross-linked magnetic chitosan nanoparticles (GMCNs) not only exhibited outstanding adsorptive behavior for food dyes but also exhibited small cytotoxicity. Adsorption features of FD&C Blue 1 and D & C Yellow 5 in aqueous solutions by GMCNs were carried out. The adsorption mechanism was better depicted by the pseudo-second-order kinetics and the Langmuir adsorption isotherm model. Maximum adsorption capacities of GMCNs at pH 3.0 and 298K were found to be 475.6 and 292.1 mg.g^{-1} for FD&C Blue 1 and D&C Yellow 5, respectively. Thermodynamic studies demonstrated that the reactions were spontaneous and exothermic (Zhou et al. 2014).

DISADVANTAGE OF NANO ADSORBENT MATERIALS

NADs play a vital part in elucidating ecological concerns like the decontamination of wastewater due to their incredible physiochemical properties. At the same time, certain shortcomings can be acknowledged while utilizing NADs in wastewater treatment (Yaqoob et al. 2020). One key shortcoming is the probable ecotoxicity of the remaining nanomaterial in water, which might cause secondary toxic impacts and possibly hurt humans, animals, and other life forms (Wang et al. 2019, Zhu et al. 2019, Sardar et al. 2021). Another major shortcoming is the utilization of large amounts of NADs in the procedure to accomplish a realistic treatment period, thereby leading to the wastage of little prospective activity. Studies have been carried out to isolate powdery leftovers of the water treatment procedures by application of membranes which in turn enhance the price of the overall procedure. Some studies have conveyed the detrimental effects of nanomaterials because of the addition of materials in water for its decontamination. For example, chlorination of water to get rid of pathogens present in it leads to the formation of cancer-causing by-products. Furthermore,

owing to the small size of nanoparticles, they can enter the lymph and blood via the epithelial and endothelial barriers and travel further into the brain, heart, liver, and other organs of human beings (Pandey et al. 2023). Hence, future studies are required with a focus on advanced comprehension and refinement in the utilization of NADs in water treatment.

CONCLUSIONS

Amidst the variety of wastewater treatment techniques available to date, the adsorption technique is the utmost proficient and long-established one. The adsorption technique can exterminate organic as well as inorganic pollutants without creating any by-products or noxious intermediary substances. Consequently, it has an extensive pertinence in eradicating contaminants from a water resource. In recent times, NADs have been used in the adsorption process due to their exceptional assets. Thus, NADs are considered next-generation adsorbents and execute very well in restraining pollutants from wastewater. Various NADs can be utilized, like nanometals and their oxides and carbon nanotubes, because of the unique assets like a large surface expanse, stability, etc. However, there are still some shortcomings that limit the promotion of these materials. These shortcomings include the cost-effectiveness of the method, ecological apprehensions, and practical challenges like scaling up to the industrial level and system setup. Additionally, there are a few other challenges linked to the size of these materials, where the separation of nano adsorbents from water is a grave concern. Also, the availability of large quantities of nano adsorbents with low costs for water treatment destinations can be a serious issue for commercial procedures. Furthermore, preventing the release of used nanomaterials into the environment is a serious challenge because they accumulate for long periods.

In the future, novel studies can be performed with these materials in order to advance their applications in wastewater remediation, along with more investigations regarding the limitations of NADs.

ACKNOWLEDGEMENTS

REFERENCES

Abas, Z., Kim, H.S., Zhai, L., Kim, J. and Kim, J.H., 2014. Possibility of cellulose-based electro-active paper energy scavenging transducer. *Journal of Nanoscience and Nanotechnology*, 14, pp.7458-7462.

Afreen, S., Omar, R.A., Talreja, N., Chauhan, D. and Ashfaq, M., 2018. Carbon-based-nanostructured materials for energy and environmental remediation applications. In: *Approaches in Bioremediation*. Springer, pp.369-392.

Afridi, S.K., Umar, K., Parveen, T. and Razali, M.R., 2023. Nanocomposites in the degradation of organic pollutants. In: *Nanocomposites- Advanced Materials for Energy and Environmental Aspects*. Woodhead Publishing, Elsevier, pp.321-348.

Afroz, R., Masud, M.M., Akhtar, R. and Duasa, J.B., 2014. Water pollution: Challenges and future direction for water resource management policies in Malaysia. *Environmental Urban Asia*, 5, pp.63-81.

Ahmad, K., Ashfaq, M. and Nawaz, H., 2021. Removal of decidedly lethal metal arsenic from water using metal organic frameworks: a critical review. *Reviews in Inorganic Chemistry,* 16, pp.9-12.

Ahmadi, M., Elmongy, H., Madrakian, T., Abdel-Rehim, M., 2017. Nanomaterials as sorbents for sample preparation in bioanalysis: A review. *Analytica Chimica Acta*, 958, pp.1-21.

Ahmed, M., Mashkoor, F. and Nasar, A., 2020. Development, characterization, and utilization of magnetized orange peel waste as a novel adsorbent for the confiscation of crystal violet dye from aqueous solution. *Groundwater for Sustainable Development*, 10, p.100322.

Ajayan, P., Ebbesen, T., Ichihashi, T., Iijima, S., Tanigaki, K. and Hiura, H., 1993. Opening carbon nanotubes with oxygen and implications for filling. *Nature*, 362, pp.522-525.

Ajmal, A., Majeed, I., Malik, R.N., Idriss, H. and Nadeem, M.A., 2014. Principles and mechanisms of photocatalytic dye degradation on TiO$_2$ based photocatalysts: A comparative overview. *RSC Advances*, 4, pp.37003-37026.

Aksu, Z. and Tezer, S., 2005. Biosorption of reactive dyes on the green alga Chlorella vulgaris. *Process Biochemistry*, 40, pp.1347-1361.

Alkaim, A.F., Sadik, Z., Mahdi, D.K., Alshrefi, S.M., Al-Sammarraie, A.M., Alamgir, F.M., Singh, P.M. and Aljeboree, A.M., 2015. Preparation, structure and adsorption properties of synthesized multiwall carbon nanotubes for highly effective removal of maxilon blue dye. *Korean Journal of Chemical Engineering*, 32, pp.2456-2462.

Allen, S., McKay, G. and Porter, J.F., 2004. Adsorption isotherm models for basic dye adsorption by peat in single and binary component systems. *Journal of Colloid and Interface Science*, 280, pp.322-333.

Alzahrani, E., 2014. Gum Arabic-coated magnetic nanoparticles for methylene blue removal. *International Journal of Innovative Research in Science, Engineering and Technology*, 3, pp.15118-15129.

Ansari, M.A., Chung, I.-M., Rajakumar, G., Alzohairy, M.A., Alomary, M.N., Thiruvengadam, M., Pottoo, F.H. and Ahmad, N., 2020. Current nanoparticle approaches in nose to brain drug delivery and anticancer therapy – a review. *Current Pharmaceutical Design*, 26, pp.1128-1137.

Ansari, M.A.H., Khan, M.E., Mohammad, A., Baig, M.T., Chaudhary, A. and Tauqeer, M., 2023. Application of nanocomposites in wastewater treatment. In: *Nanocomposites – Advanced Materials for Energy and Environmental Aspects*. Woodhead Publishing, Elsevier, pp.297-320.

Apul, O.G., Wang, Q., Zhou, Y. and Karanfil, T., 2013. Adsorption of aromatic organic contaminants by graphene nanosheets: Comparison with carbon nanotubes and activated carbon. *Water Research*, 47, pp.1648-1654.

Aqel, A., Abou El-Nour, K.M., Ammar, R.A. and Al-Warthan, A., 2012. Carbon nanotubes, science and technology part (I) structure, synthesis and characterization. *Arabian Journal of Chemistry*, 5, pp.1-23.

Arabi, S., Sohrabi, M.R. and Khosravi, M., 2013. Adsorption kinetics and thermodynamics of vat dye onto nano zero-valent iron. *Indian Journal of Chemical Technology*, 20, pp.173-179.

Arora, K., Kaur, P., Kumar, P., Singh, A., Patel, S.K.S., Li, X., Yang, Y.H., Bhatia, S.K. and Kulshrestha, S., 2021. Valorization of wastewater resources into biofuel and value-added products using a microalgal system. *Frontiers in Energy Research*, 9, 119.

Ata, S., Tabassum, A., Bibi, I., Majid, F., Sultan, M., Ghafoor, S., Bhatti, M.A., Qureshi, N. and Iqbal, M., 2019. Lead remediation using

smart materials: A review. *Zeitschrift für Physikalische Chemie*, 233, pp.1377-1409.

Bafana, A., Devi, S.S. and Chakrabarti, T., 2011. Azo dyes: past, present, and the future. *Environmental Reviews*, 19, pp.350-371.

Banerjee, S., Gautam, R.K., Jaiswal, A., Chattopadhyaya, M.C. and Sharma, Y.C., 2015. Rapid scavenging of methylene blue dye from a liquid phase by adsorption on alumina nanoparticles. *RSC Advances*, 5, pp.14425-14440.

Bharathi, K. and Ramesh, S., 2013. Removal of dyes using agricultural waste as low-cost adsorbents: a review. *Applied Water Science*, 3, pp.773-790.

Bhatnagar, A. and Minocha, A., 2006. Conventional and non-conventional adsorbents for removal of pollutants from water – A review. *International Journal of Chemical Technology*, 13, pp.203-217.

iswas, A.K., Islam, M.R., Choudhury, Z.S., Mostafa, A. and Kadir, M.F., 2014. Nanotechnology-based approaches in cancer therapeutics. *Advances in Natural Sciences: Nanoscience and Nanotechnology*, 5, p.043001.

Bouzaida, I. and Rammah, M., 2002. Adsorption of acid dyes on treated cotton in a continuous system. *Materials Science and Engineering*, 21, pp.151-155.

Carolin, C.F., Kumar, P.S., Saravanan, A., Joshiba, G.J. and Naushad, M., 2017. Efficient techniques for the removal of toxic heavy metals from the aquatic environment: A review. *Journal of Environmental Chemical Engineering*, 5, pp.2782-2799.

Chang, B., Shi, W., Yin, H., Zhang, S. and Yang, B., 2019. Poplar catkin-derived self-templated synthesis of N-doped hierarchical porous carbon microtubes for effective CO_2 capture. *Chemical Engineering Journal*, 358, pp.1507-1518.

Chatterjee, S., Chatterjee, T., Lim, S.-R. and Woo, S.H., 2011. Effect of the addition mode of carbon nanotubes for the production of chitosan hydrogel core-shell beads on adsorption of Congo red from aqueous solution. *Bioresource Technology*, 102, pp.4402-4409.

Chatterjee, S., Lee, M.W. and Woo, S.H., 2010. Adsorption of Congo red by chitosan hydrogel beads impregnated with carbon nanotubes. *Bioresource Technology*, 101, pp.1800-1806.

Cockerham, C., Caruthers, A., McCloud, J., Fortner, L.M., Youn, S. and McBride, S.P., 2022. Azo-dye-functionalized polycarbonate membranes for textile dye and nitrate ion removal. *Micromachines*, 13, p.577.

Creamer, A.E. and Gao, B., 2016. Carbon-based adsorbents for postcombustion CO_2 capture: a critical review. *Environmental Science and Technology*, 50, pp.7276-7289.

Crini, G., 2003. Studies on adsorption of dyes on beta-cyclodextrin polymer. *Bioresource Technology*, 90, pp.193-198.

Crini, G., 2006. Non-conventional low-cost adsorbents for dye removal: a review. *Bioresource Technology*, 97, pp.1061-1085.

Crini, G. and Morcellet, M., 2002. Synthesis and applications of adsorbents containing cyclodextrins. *Journal of Separation Science*, 25, pp.789-813.

Dalvand, A., Nabizadeh, R., Ganjali, M.R., Khoobi, M., Nazmara, S. and Mahvi, A.H., 2016. Modeling of Reactive Blue 19 azo dye removal from colored textile wastewater using L-arginine-functionalized Fe_3O_4 nanoparticles: Optimization, reusability, kinetic and equilibrium studies. *Journal of Magnetism and Magnetic Materials*, 404, pp.179-189.

Dassanayake, R.S., Acharya, S. and Abidi, N., 2021. Recent advances in biopolymer-based dye removal technologies. *Molecules*, 26, p.4697.

Dawood, S. and Sen, T., 2014. Review on dye removal from its aqueous solution into alternative cost-effective and non-conventional adsorbents. *Journal of Chemical Processing Engineering*, 1, pp.1-11.

Delval, F., Crini, G., Vebrel, J., Knorr, M., Sauvin, G. and Conte, E., 2003. Starch-modified filters are used for the removal of dyes from wastewater. *Macromolecular Symposia*, Wiley, pp.165-172.

Denis, P.A. and Iribarne, F., 2012. A First‐Principles Study on the Interaction between Alkyl Radicals and Graphene. *Chemistry – European Journal*, 18, pp.7568-7574.

Dhakate, S.R., Singh, B.P., Gupta, B.K., Subhedar, K.M., Srivastava, S.K., Saravanan, M., Saini, P., Kumar, S., Prathap, P. and Kumari, S., 2020. Advanced materials for strategic and societal applications. *Metrology for Inclusive Growth of India*, Springer, pp.811-879.

Duruibe, J.O., Ogwuegbu, M. and Egwurugwu, J., 2007. Heavy metal pollution and human biotoxic effects. *International Journal of Physical Sciences*, 2, pp.112-118.

Dutta, T., Kim, T., Vellingiri, K., Tsang, D.C., Shon, J., Kim, K.-H. and Kumar, S., 2019. Recycling and regeneration of carbonaceous and porous materials through thermal or solvent treatment. *Chemical Engineering Journal*, 364, pp.514-529.

Elgarahy, A., Elwakeel, K., Mohammad, S. and Elshoubaky, G., 2021. A critical review of biosorption of dyes, heavy metals, and metalloids from wastewater as an efficient and green process. *Cleaner Engineering and Technology*, 4, p.100209.

Essekri, A., Hsini, A., Naciri, Y., Laabd, M., Ajmal, Z., El Ouardi, M., Ait Addi, A. and Albourine, A., 2021. Novel citric acid-functionalized brown algae with a high removal efficiency of crystal violet dye from colored wastewaters: insights into equilibrium, adsorption mechanism, and reusability. *International Journal of Phytoremediation*, 23, pp.336-346.

Falah, M., MacKenzie, K.J., Knibbe, R., Page, S.J. and Hanna, J.V., 2016. New composites of nanoparticle Cu (I) oxide and titania in a novel inorganic polymer (geopolymer) matrix for destruction of dyes and hazardous organic pollutants. *Journal of Hazardous Materials*, 318, pp.772-782.

Farhat, S. and Scott, C.D., 2006. Review of the arc process modeling for fullerene and nanotube production. *Journal of Nanoscience and Nanotechnology*, 6, pp.1189-1210.

Farrukh, A., Akram, A., Ghaffar, A., Hanif, S., Hamid, A., Duran, H. and Yameen, B., 2013. Design of polymer-brush-grafted magnetic nanoparticles for highly efficient water remediation. *ACS Applied Materials & Interfaces*, 5, pp.3784-3793.

Ferreira, G.M.D., Ferreira, G.M.D., Hespanhol, M.C., de Paula Rezende, J., dos Santos Pires, A.C., Gurgel, L.V.A. and da Silva, L.H.M., 2017. Adsorption of red azo dyes on multi-walled carbon nanotubes and activated carbon: A thermodynamic study. *Colloids and Surfaces A: Physicochemical and Engineering Aspects*, 529, pp. 531-540.

Gangadhar, G., Maheshwari, U. and Gupta, S., 2012. Application of nanomaterials for the removal of pollutants from effluent streams. *Nanoscience and Nanotechnology Asia*, 2, pp.140-150.

Gardetti, M.A. and Torres, A.L., 2013. Sustainability in fashion and textiles: values, design, production and consumption. *Routledge, Greenleaf Publishing*, p.403.

Gautam, R.K., Rawat, V., Banerjee, S., Sanroman, M.A., Soni, S., Singh, S.K. and Chattopadhyaya, M.C., 2015. Synthesis of bimetallic Fe–Zn nanoparticles and their application towards adsorptive removal of carcinogenic dye malachite green and Congo red in water. *Journal of Molecular Liquids*, 212, pp.227-236.

Gázquez, M.J., Bolívar, J.P., García-Tenorio García-Balmaseda, R. and Vaca, F., 2014. A review of the production cycle of titanium dioxide pigment. *Materials Science and Applications*, 5, pp.441-458.

Ghaedi, M., Karimi, F., Barazesh, B., Sahraei, R. and Daneshfar, A., 2013. Removal of Reactive Orange 12 from aqueous solutions by adsorption on tin sulfide nanoparticle loaded on activated carbon. *Journal of Industrial and Engineering Chemistry*, 19, pp.756-763.

Ghaedi, M. and Kokhdan, S.N., 2012. Oxidized multiwalled carbon nanotubes for the removal of methyl red (MR): kinetics and equilibrium study. *Desalination and Water Treatment*, 49, pp.317-325.

Goel, P., 2006. Water pollution: causes, effects, and control. *New Age International*, p.418.

Gunatilake, S., 2015. Methods of removing heavy metals from industrial wastewater. *Methods*, 1, p.14.

Gupta, V., 2009. Application of low-cost adsorbents for dye removal – a review. *Journal of Environmental Management*, 90, pp.2313-2342.

Gupta, V.K., Kumar, R., Nayak, A., Saleh, T.A. and Barakat, M., 2013. Adsorptive removal of dyes from aqueous solution onto carbon nanotubes: a review. *Advances in Colloid and Interface Science*, 193, pp.24-34.

Gupta, V.K. and Saleh, T.A., 2013. Sorption of pollutants by porous carbon, carbon nanotubes and fullerene – an overview. *Environmental Science and Pollution Research*, 20, pp.2828-2843.

Gusain, R., Kumar, N. and Ray, S.S., 2020. Recent advances in carbon nanomaterial-based adsorbents for water purification. *Coordination Chemistry Reviews*, 405, p.213111.

Hameed, B., 2009. Removal of cationic dye from aqueous solution using jackfruit peel as non-conventional low-cost adsorbent. *Journal of Hazardous Materials*, 162, pp.344-350.

Hammam, A., Zaki, M.S., Yousef, R.A. and Fawzi, O., 2015. Toxicity, mutagenicity, and carcinogenicity of phenols and phenolic compounds on humans and living organisms [A Review]. *Advances in Environmental Biology*, 9, pp.38-49.

Harja, M. and Ciobanu, G., 2020. Eco-friendly nano-adsorbents for pollutant removal from wastewater. *Handbook of Nanomaterials and Nanocomposites for Energy and Environmental Applications*, pp.1-22.

Hashimi, M.H., Hashimi, R. and Ryan, Q., 2020. Toxic effects of pesticides on humans, plants, animals, pollinators, and beneficial organisms. *Asian Plant Research Journal*, 5, pp.37-47.

Husain, Q., 2006. Potential applications of the oxidoreductive enzymes in the decolorization and detoxification of textile and other synthetic dyes from polluted water: A review. *Critical Reviews in Biotechnology*, 26, pp.201-221.

Hussain, M., Hussaini, S.S., Shariq, M., AlMasoud, N., AlZaidy, G.A., Hassan, K.F., Ali, S.K., Azooz, R.E., Siddiqui, M.A. and Seku, K., 2024. Frankincense-based functionalized multiwalled carbon nanotubes with iron oxide composites for efficient removal of crystal violet: Kinetic and equilibrium analysis. *ACS Omega*, 9, pp.11459-11470.

Ijaz, M. and Zafar, M., 2021. Titanium dioxide nanostructures as efficient photocatalysts: Progress, challenges, and perspective. *International Journal of Energy Research*, 45, pp.3569-3589.

Islam, M.A., Ali, I., Karim, S.A., Firoz, M.S.H., Chowdhury, A.-N., Morton, D.W. and Angove, M.J., 2019. Removal of dye from polluted water using novel nano manganese oxide-based materials. *Journal of Water Process Engineering*, 32, p.100911.

Jameel, M.S., Aziz, A.A. and Dheyab, M.A., 2020. Comparative analysis of platinum nanoparticles synthesized using sonochemical-assisted and conventional green methods. *Nano-Structures & Nano-Objects*, 23, p.100484.

Janani, R., Gurunathan, B., Sivakumar, K., Varjani, S., Ngo, H.H. and Gnansounou, E., 2022. Advancements in heavy metals removal from effluents employing nano-adsorbents: Way towards cleaner production. *Environmental Research*, 203, p.111815.

Jelmy, E., Thomas, N., Mathew, D.T., Louis, J., Padmanabhan, N.T., Kumaravel, V., John, H. and Pillai, S.C., 2021. Impact of structure, doping and defect-engineering in 2D materials on CO_2 capture and conversion. *Reaction Chemistry & Engineering*, 6, pp.1701-1738.

Ji, L., Chen, W., Xu, Z., Zheng, S. and Zhu, D., 2013. Graphene nanosheets and graphite oxide as promising adsorbents for removal of organic contaminants from aqueous solution. *Journal of Environmental Quality*, 42, pp.191-198.

Ju-Nam, Y. and Lead, J.R., 2008. Manufactured nanoparticles: an overview of their chemistry, interactions and potential environmental implications. *Science of the Total Environment*, 400, pp.396-414.

Kahlon, S.K., Sharma, G., Julka, J., Kumar, A., Sharma, S. and Stadler, F.J., 2018. Impact of heavy metals and nanoparticles on aquatic biota. *Environmental Chemistry Letters*, 16, pp.919-946.

Karimifard, S. and Moghaddam, M.R.A., 2018. Application of response surface methodology in physicochemical removal of dyes from wastewater: a critical review. *Science of the Total Environment*, 640, pp.772-797.

Khan, M.E., Han, T.H., Khan, M.M., Karim, M.R. and Cho, M.H., 2018. Environmentally sustainable fabrication of Ag@ g-C_3N_4 nanostructures and their multifunctional efficacy as antibacterial agents and photocatalysts. *ACS Applied Nano Materials*, 1, pp.2912-2922.

Khan, M.E., Khan, M.M. and Cho, M.H., 2016. CdS-graphene nanocomposite for efficient visible-light-driven photocatalytic and photoelectrochemical applications. *Journal of Colloid and Interface Science*, 482, pp.221-232.

Khan, M.E., Khan, M.M. and Cho, M.H., 2017a. Ce^{3+}-ion, surface oxygen vacancy, and visible-light-induced photocatalytic dye degradation and photo capacitive performance of CeO_2-graphene nanostructures. *Scientific Reports*, 7, pp.1-17.

Khan, M.M., Saadah, N.H., Khan, M.E., Harunsani, M.H., Tan, A.L. and Cho, M.H., 2019a. Phytogenic synthesis of band gap-narrowed ZnO nanoparticles using the bulb extract of *Costus woodsonii*. *Bionanoscience*, 9, pp.334-344.

Khan, M.M., Saadah, N.H., Khan, M.E., Harunsani, M.H., Tan, A.L. and Cho, M.H., 2019b. Potentials of *Costus woodsonii* leaf extract in producing narrow band gap ZnO nanoparticles. *Materials Science in Semiconductor Processing*, 91, pp.194-200.

Khan, M.S., Abdelhamid, H.N. and Wu, H.F., 2015. Near-infrared (NIR) laser-mediated surface activation of graphene oxide nanoflakes for efficient antibacterial, antifungal, and wound healing treatment. *Colloids and Surfaces B: Biointerfaces*, 127, pp.281-291.

Khan, M.S., Gedda, G., Gopal, J. and Wu, H.F., 2014. Probing the cytotoxicity of CdS–MPA and CdSe–MUA QDs on the bacterial pathogen *Staphylococcus aureus* using MALDI-MS. *Analytical Methods*, 6, pp.5304-5313.

Khan, M.S., Talib, A., Pandey, S., Bhaisare, M.L., Gedda, G. and Wu, H.-F., 2017b. Folic Acid navigated Silver Selenide nanoparticles for photo-thermal ablation of cancer cells. *Colloids and Surfaces B: Biointerfaces*, 159, pp.564-570.

Layek, S., Pandey, A., Pandey, A. and Verma, H., 2010. Synthesis of γ–Fe_2O_3 nanoparticles with crystallographic and magnetic texture. *International Journal of Engineering Science and Technology*, 2, pp.33-39.

Li, B., Cao, H. and Yin, G., 2011a. Mg (OH)2@ reduced graphene oxide composite for removal of dyes from water. *Journal of Materials Chemistry*, 21, pp.13765-13768.

Li, J.-R., Kuppler, R.J. and Zhou, H.-C., 2009. Selective gas adsorption and separation in metal-organic frameworks. *Chemical Society Reviews*, 38, pp.1477-1504.

Li, N., Zheng, M., Chang, X., Ji, G., Lu, H., Xue, L., Pan, L. and Cao, J., 2011b. Preparation of magnetic $CoFe_2O_4$ functionalized graphene sheets via a facile hydrothermal method and their adsorption properties. *Journal of Solid State Chemistry*, 184, pp.953-958.

Li, Y., Liu, T., Du, Q., Sun, J., Xia, Y., Wang, Z., Zhang, W., Wang, K., Zhu, H. and Wu, D., 2011c. Adsorption of cationic red X-GRL from aqueous solutions by graphene: equilibrium, kinetics, and thermodynamics study. *Chemical and Biochemical Engineering Quarterly*, 25, pp.483-491.

Liu, L., Chen, C., Yang, S., Xie, H., Gong, M. and Xu, X., 2016. Fabrication of superhydrophilic–underwater superoleophobic inorganic anti-corrosive membranes for high-efficiency oil/water separation. *Physical Chemistry Chemical Physics*, 18, pp.1317-1325.

Loucks, D.P. and Van Beek, E., 2017. *Water resource systems planning and management: An introduction to methods, models, and applications*. Springer Nature, pp.624.

Lu, J., Yang, S., Ng, K.M., Su, C.H., Yeh, C.S., Wu, Y.N. and Shieh, D.-B., 2006. Solid-state synthesis of monocrystalline iron oxide nanoparticle based ferrofluid suitable for magnetic resonance imaging contrast application. *Nanotechnology*, 17, pp.5812.

Luo, T., Cui, J., Hu, S., Huang, Y. and Jing, C., 2010. Arsenic removal and recovery from copper smelting wastewater using TiO_2. *Environmental Science and Technology*, 44, pp.9094-9098.

Ma, J., Ma, Y. and Yu, F., 2018. A novel one-pot route for large-scale synthesis of novel magnetic CNTs/Fe@ C hybrids and their applications for binary dye removal. *ACS Sustainable Chemistry and Engineering*, 6, pp.8178-8191.

Machado, F.M., Bergmann, C.P., Fernandes, T.H., Lima, E.C., Royer, B., Calvete, T. and Fagan, S.B., 2011. Adsorption of Reactive Red M-2BE dye from water solutions by multi-walled carbon nanotubes and activated carbon. *Journal of Hazardous Materials*, 192, pp.1122-1131.

Machado, F.M., Bergmann, C.P., Lima, E.C., Royer, B., de Souza, F.E., Jauris, I.M., Calvete, T. and Fagan, S.B., 2012. Adsorption of Reactive Blue 4 dye from water solutions by carbon nanotubes: experiment and theory. *Physical Chemistry Chemical Physics*, 14, pp.11139-11153.

Madima, N., Mishra, S., Inamuddin, I. and Mishra, A., 2020. Carbon-based nanomaterials for remediation of organic and inorganic pollutants from wastewater: A review. *Environmental Chemistry Letters*, 18, pp.1169-1191.

Mady, A.H., Baynosa, M.L., Tuma, D. and Shim, J.-J., 2017. Facile microwave-assisted green synthesis of $Ag-ZnFe_2O_4$@ rGO nanocomposites for efficient removal of organic dyes under UV- and visible-light irradiation. *Applied Catalysis B: Environmental*, 203, pp.416-427.

Mahfoudhi, N. and Boufi, S., 2017. Nanocellulose as a novel nanostructured adsorbent for environmental remediation: A review. *Cellulose*, 24, pp.1171-1197.

Martin, J., Desfoux, A., Martinez, J., Amblard, M., Mehdi, A., Vezenkov, L. and Subra, G., 2021. Bottom-up strategies for the synthesis of peptide-based polymers. *Progress in Polymer Science*, 115, p.101377.

Mashkoor, F. and Nasar, A., 2020. Magnetized *Tectona grandis* sawdust as a novel adsorbent: Preparation, characterization, and utilization for the removal of methylene blue from aqueous solution. *Cellulose*, 27, pp.2613-2635.

Mauter, M.S. and Elimelech, M., 2008. Environmental applications of carbon-based nanomaterials. *Environmental Science and Technology*, 42, pp.5843-5859.

McGlade, J., Landrigan, P., Stegeman, J., Fleming, L., Allemand, D., Anderson, D., Backer, L., Brucker-Davis, F., Chevalier, N. and Corra, L., 2020. Human health and ocean pollution. *Annals of Global Health*, 86, p.651.

Mekewi, M., Darwish, A., Amin, M., Eshaq, G. and Bourazan, H., 2016. Copper nanoparticles supported onto montmorillonite clays as an efficient catalyst for methylene blue dye degradation. *Egyptian Journal of Petroleum*, 25, pp.269-279.

Mohammad, A., Khan, M.E., Cho, M.H. and Yoon, T., 2021a. Adsorption promoted visible-light-induced photocatalytic degradation of antibiotic tetracycline by tin oxide/cerium oxide nanocomposite. *Applied Surface Science*, 565, p.150.

Mohammad, A., Khan, M.E., Cho, M.H. and Yoon, T., 2021b. Fabrication of binary SnO_2/TiO_2 nanocomposites under a sonication-assisted approach: Tuning of band-gap and water depollution applications under visible light irradiation. *Ceramics International*, 47, pp.15073-15081.

Mohammad, A., Khan, M.E., Karim, M.R. and Cho, M.H., 2019. Synergistically effective and highly visible light-responsive $SnO_2-g-C_3N_4$ nanostructures for improved photocatalytic and photoelectrochemical performance. *Applied Surface Science*, 495, p.1432.

Mustafa, G., Tahir, H., Sultan, M. and Akhtar, N., 2013. Synthesis and characterization of cupric oxide (CuO) nanoparticles and their

application for the removal of dyes. *African Journal of Biotechnology*, 12, pp.6650-6660.

Mustapha, S., Ndamitso, M., Abdulkareem, A., Tijani, J., Shuaib, D., Ajala, A. and Mohammed, A., 2020. Application of TiO_2 and ZnO nanoparticles immobilized on clay in wastewater treatment: A review. *Applied Water Science*, 10, pp.1-36.

Nasrollahzadeh, M., Sajadi, S.M., Sajjadi, M. and Issaabadi, Z., 2019. Applications of nanotechnology in daily life. *Interface Science and Technology*, 28, pp.113-143.

Nayeri, D. and Jafari, A., 2024. A review on the recent development of carbon nanotubes (CNTs) application for polymeric mixed-matrix membranes: Synthesis, performance, and future challenges. *Journal of Inorganic and Organometallic Polymers*, 17, pp.1-31.

Nayyar, D., 2021. Industrialization in developing Asia since 1970: Why technology, learning, and innovation matter. *Innovation and Development*, 11, pp.365-385.

O'Mahony, T., Guibal, E. and Tobin, J., 2002. Reactive dye biosorption by *Rhizopus arrhizus* biomass. *Enzyme and Microbial Technology*, 31, pp.456-463.

Özacar, M. and Şengil, İ.A., 2002. Adsorption of acid dyes from aqueous solutions by calcined alunite and granular activated carbon. *Adsorption*, 8, pp.301-308.

Pandey, P., Khan, F., Agarwal, S. and Singh, M., 2023. Nano adsorbents in wastewater treatment: A new paradigm in wastewater management. *Letters in Applied Bionanoscience*, 12, pp.1-17.

Pimentel, D., Berger, B., Filiberto, D., Newton, M., Wolfe, B., Karabinakis, E., Clark, S., Poon, E., Abbett, E. and Nandagopal, S., 2004. Water resources: Agricultural and environmental issues. *BioScience*, 54, pp.909-918.

Prola, L.D., Machado, F.M., Bergmann, C.P., de Souza, F.E., Gally, C.R., Lima, E.C., Adebayo, M.A., Dias, S.L. and Calvete, T., 2013. Adsorption of Direct Blue 53 dye from aqueous solutions by multi-walled carbon nanotubes and activated carbon. *Journal of Environmental Management*, 130, pp.166-175.

Rafatullah, M., Sulaiman, O., Hashim, R. and Ahmad, A., 2010. Adsorption of methylene blue on low-cost adsorbents: A review. *Journal of Hazardous Materials*, 177, pp.70-80.

Rahman, N., Abedin, Z. and Hossain, M.A., 2014. Rapid degradation of azo dyes using nano-scale zero-valent iron. *American Journal of Environmental Science*, 10, p.157.

Rajabi, M., Mahanpoor, K. and Moradi, O., 2019. Preparation of PMMA/GO and PMMA/GO-Fe_3O_4 nanocomposites for malachite green dye adsorption: Kinetic and thermodynamic studies. *Composites Part B: Engineering*, 167, pp.544-555.

Ramesh, M. and Muthuraman, A., 2018. *Natural and Artificial Flavouring Agents and Food Dyes*. Elsevier, pp.1-28.

Rasheed, T., Shafi, S., Bilal, M., Hussain, T., Sher, F. and Rizwan, K., 2020. Surfactants-based remediation as an effective approach for removal of environmental pollutants-A review. *Journal of Molecular Liquids*, 318, p.113960.

Rodríguez, A., Ovejero, G., Sotelo, J., Mestanza, M. and García, J., 2010. Adsorption of dyes on carbon nanomaterials from aqueous solutions. *Journal of Environmental Science and Health, Part A*, 45, pp.1642-1653.

Routoula, E., 2019. Understanding peroxidase immobilization on bioinspired silicas and application of the biocatalyst for dye removal. *University of Sheffield*, 11, p.1.

Sadegh, H., Ali, G.A., Gupta, V.K., Makhlouf, A.S.H., Shahryari-Ghoshekandi, R., Nadagouda, M.N., Sillanpää, M. and Megiel, E., 2017. The role of nanomaterials as effective adsorbents and their applications in wastewater treatment. *Journal of Nanostructure in Chemistry*, 7, pp.1-14.

Saharan, P., Chaudhary, G.R., Lata, S., Mehta, S. and Mor, S., 2015. Ultra-fast and effective treatment of dyes from water with the synergistic

effect of Ni-doped ZnO nanoparticles and ultrasonication. *Ultrasonics Sonochemistry*, 22, pp.317-325.

Salem, S.S. and Fouda, A., 2021. Green synthesis of metallic nanoparticles and their prospective biotechnological applications: an overview. *Biological Trace Element Research*, 199, pp.344-370.

Saratale, R.G., Karuppusamy, I., Saratale, G.D., Pugazhendhi, A., Kumar, G., Park, Y., Ghodake, G.S., Bharagava, R.N., Banu, J.R. and Shin, H.S., 2018. A comprehensive review on green nanomaterials using biological systems: Recent perception and their future applications. *Colloids and Surfaces B: Biointerfaces*, 170, pp.20-35.

Sardar, M., Manna, M., Maharana, M. and Sen, S., 2021. *Green Adsorbents to Remove Metals, Dyes and Boron from Polluted Water*, Springer, pp.377-403.

Sasikala, R., Karthikeyan, K., Easwaramoorthy, D., Bilal, I.M. and Rani, S.K., 2016. Photocatalytic degradation of trypan blue and methyl orange azo dyes by cerium-loaded CuO nanoparticles. *Environmental Nanotechnology, Monitoring & Management*, 6, pp.45-53.

Scuderi, V., Impellizzeri, G., Romano, L., Scuderi, M., Nicotra, G., Bergum, K., Irrera, A., Svensson, B.G. and Privitera, V., 2014. TiO$_2$-coated nanostructures for dye photo-degradation in water. *Nanoscale Research Letters*, 9, pp.1-7.

Shahbazi, D., Mousavi, S., Nayeri, D., 2020. Low-cost activated carbon: characterization, decolorization, modeling, optimization and kinetics. *International Journal of Environmental Science and Technology*, 17, pp.3935-3946.

Shahryari-Ghoshekandi, R. and Sadegh, H., 2014. Kinetic study of the adsorption of synthetic dyes on graphene surfaces. *Jordan Journal of Chemistry*, 9, pp.267-278.

Shahryari, Z., Goharrizi, A.S. and Azadi, M., 2010. Experimental study of methylene blue adsorption from aqueous solutions onto carbon nanotubes. *International Journal of Water Resources and Environmental Engineering*, 2, pp.016-028.

Shakoor, S., Khan, M.S. and Khan, M.E., 2023. *Nanocomposites- Advanced Materials for Energy and Environmental Aspects*. Elsevier, pp.662.

Shakoor, S. and Nasar, A., 2016. Removal of methylene blue dye from artificially contaminated water using citrus limetta peel waste as a very low cost adsorbent. *Journal of the Taiwan Institute of Chemical Engineers*, 66, pp.154-163.

Shakoor, S. and Nasar, A., 2017. Adsorptive treatment of hazardous methylene blue dye from artificially contaminated water using cucumis sativus peel waste as a low-cost adsorbent. *Groundwater for Sustainable Development*, 5, pp.152-159.

Shakoor, S. and Nasar, A., 2018a. Adsorptive decontamination of synthetic wastewater containing crystal violet dye by employing Terminalia arjuna sawdust waste. *Groundwater for Sustainable Development*, 7, pp.30-38.

Shakoor, S. and Nasar, A., 2018b. Utilization of Punica granatum peel as an eco-friendly biosorbent for the removal of methylene blue dye from aqueous solution. *Journal of Applied Biotechnology & Bioengineering*, 5, pp.242-249.

Shakoor, S. and Nasar, A., 2019. Utilization of Cucumis sativus peels as an eco-friendly biosorbent for the confiscation of crystal violet dye from artificially contaminated wastewater. *Analytical Chemistry Letters*, 9, pp.1-19.

Shanehsaz, M., Seidi, S., Ghorbani, Y., Shoja, S.M.R. and Rouhani, S., 2015. Polypyrrole-coated magnetic nanoparticles as an efficient adsorbent for RB19 synthetic textile dye: Removal and kinetic study. *Spectrochimica Acta Part A: Molecular and Biomolecular Spectroscopy*, 149, pp.481-486.

Sharma, J., Goutam, J., Dhuriya, Y.K. and Sharma, D., 2021. *Microbial Rejuvenation of Polluted Environments*, Springer, pp.1-31.

Sharma, Y.C., Srivastava, V., Singh, V., Kaul, S. and Weng, C., 2009. Nano-adsorbents for the removal of metallic pollutants from water and wastewater. *Environmental Technology*, 30, pp.583-609.

Singh, K. and Arora, S., 2011. Removal of synthetic textile dyes from wastewaters: a critical review on present treatment technologies. *Critical Reviews in Environmental Science and Technology*, 41, pp.807-878. Tahir, M.B., Tufail, S., Ahmad, A., Rafique, M., Iqbal, T., Abrar, M., Nawaz, T., Khan, M.Y. and Ijaz, M., 2021. Semiconductor nanomaterials for the detoxification of dyes in real wastewater under visible-light photocatalysis. *International Journal of Environmental Analytical Chemistry*, 101(11), pp.1735-1749.

Tara, N., Siddiqui, S.I., Rathi, G., Chaudhry, S.A. and Asiri, A.M., 2020. Nano-engineered adsorbent for the removal of dyes from water: A review. *Current Analytical Chemistry*, 16(1), pp.14-40.

Taufik, A. and Saleh, R., 2017. Synthesis of iron (II, III) oxide/zinc oxide/copper (II) oxide (Fe$_3$O$_4$/ZnO/CuO) nanocomposites and their photosonocatalytic property for organic dye removal. *Journal of Colloid and Interface Science*, 491, pp.27-36.

Teja, A.S. and Koh, P.Y., 2009. Synthesis, properties, and applications of magnetic iron oxide nanoparticles. *Progress in Crystal Growth and Characterization of Materials*, 55(1), pp.22-45.

Terrones, M., 2003. Science and technology of the twenty-first century: synthesis, properties, and applications of carbon nanotubes. *Annual Review of Materials Research*, 33, pp.419-501.

Thakur, K. and Kandasubramanian, B., 2019. Graphene and graphene oxide-based composites for removal of organic pollutants: A review. *Journal of Chemical and Engineering Data*, 64(5), pp.833-867.

Thakur, A., Kumar, A. and Singh, A., 2024. Adsorptive removal of heavy metals, dyes, and pharmaceuticals: Carbon-based nanomaterials in focus. *Carbon: The International Journal of the Science and Technology of Carbon*, 217, pp.118621.

Thangadurai, D., Sangeetha, J., Prasad, R., 2020. Nanotechnology for food, agriculture, and environment. *Springer Nature*, pp.1-180.

Varghese, A.G., Paul, S.A. and Latha, M., 2019. Remediation of heavy metals and dyes from wastewater using cellulose-based adsorbents. *Environmental Chemistry Letters*, 17(4), pp.867-877.

Velusamy, S., Roy, A., Sundaram, S. and Kumar Mallick, T., 2021. A review on heavy metal ions and containing dyes removal through graphene oxide-based adsorption strategies for textile wastewater treatment. *The Chemical Record*, 21(5), pp.1570-1610.

Vieira, W.T., de Farias, M.B., Spaolonzi, M.P., da Silva, M.G.C. and Vieira, M.G.A., 2020. Removal of endocrine disruptors in waters by adsorption, membrane filtration, and biodegradation. A review. *Environmental Chemistry Letters*, 18(3), pp.1113-1143.

Vishnu, D., Dhandapani, B., Kannappan Panchamoorthy, G., Vo, D.V.N. and Ramakrishnan, S.R., 2021. Comparison of surface-engineered superparamagnetic nanosorbents with low-cost adsorbents of cellulose, zeolites, and biochar for the removal of organic and inorganic pollutants: A review. *Environmental Chemistry Letters*, 19(5), pp.3181-3208.

Vuono, D., Catizzone, E., Aloise, A., Policicchio, A., Agostino, R.G., Migliori, M. and Giordano, G., 2017. Study of adsorption behavior of multi-walled carbon nanotubes towards dyes applied in textile applications. *Advanced Science Letters*, 23(5), pp.5851-5854.

Walker, G., Hansen, L., Hanna, J.A. and Allen, S., 2003. Kinetics of reactive dye adsorption onto dolomitic sorbents. *Water Research*, 37(9), pp.2081-2089.

Wang, S., Ng, C.W., Wang, W., Li, Q. and Hao, Z., 2012. Synergistic and competitive adsorption of organic dyes on multi-walled carbon nanotubes. *Chemical Engineering Journal*, 197, pp.34-40.

Wang, X., Yin, R., Zeng, L. and Zhu, M., 2019. A review of graphene-based nanomaterials for removal of antibiotics from aqueous environments. *Environmental Pollution*, 253, pp.100-110.

Whitacre, J., Wiley, T., Shanbhag, S., Wenzhuo, Y., Mohamed, A., Chun, S., Weber, E., Blackwood, D., Lynch-Bell, E. and Gulakowski, J., 2012. An aqueous electrolyte, sodium ion functional, large format energy storage device for stationary applications. *Journal of Power Sources*, 213, pp.255-264.

Wong, Y., Szeto, Y., Cheung, W. and McKay, G., 2004. Adsorption of acid dyes on chitosan—equilibrium isotherm analyses. *Process Biochemistry*, 39(5), pp.695-704.

Wu, P., Jiang, L.Y., He, Z. and Song, Y., 2017. Treatment of metallurgical industry wastewater for organic contaminant removal in China: status, challenges, and perspectives. *Environmental Science: Water Research and Technology*, 3(6), pp.1015-1031.

Wu, T., Cai, X., Tan, S., Li, H., Liu, J. and Yang, W., 2011. Adsorption characteristics of acrylonitrile, p-toluenesulfonic acid, 1-naphthalenesulfonic acid, and methyl blue on graphene in aqueous solutions. *Chemical Engineering Journal*, 173(1), pp.144-149.

Xu, M., David, J.M. and Kim, S.H., 2018. The fourth industrial revolution: Opportunities and challenges. *International Journal of Financial Research*, 9(2), pp.90-95.

Xue, Y., Hong, X., Gao, J., Shen, R. and Ye, Z., 2019. Preparation and biological characterization of the mixture of poly (lactic-co-glycolic acid)/chitosan/Ag nanoparticles for periodontal tissue engineering. *International Journal of Nanomedicine*, 14, pp.483.

Yadav, M., Singh, G. and Jadeja, R., 2021. Physical and Chemical Methods for Heavy Metal Removal. *Pollutants and Water Management: Resources, Strategies and Scarcity*, 15, pp.377-397.

Yang, L., Wan, Y., Huang, Y., Weng, H., Qin, L. and Seo, H.J., 2016. Synthesis, surface, and optical properties of $Ag_2ZnV_4O_{12}$ nanoparticles for efficient photocatalytic water splitting. *Journal of Applied Physics*, 120(10), pp.103304.

Yao, Y., Bing, H., Feifei, X. and Xiaofeng, C., 2011. Equilibrium and kinetic studies of methyl orange adsorption on multiwalled carbon nanotubes. *Chemical Engineering Journal*, 170, pp.82-89.

Yao, Y., Xu, F., Chen, M., Xu, Z. and Zhu, Z., 2010. Adsorption of cationic methyl violet and methylene blue dyes onto carbon nanotubes. *2010 IEEE 5th International Conference on Nano/Micro Engineered and Molecular Systems*, IEEE, 54 pp.1083-1087.

Yaqoob, A.A., Parveen, T., Umar, K. and Mohamad Ibrahim, M.N., 2020. Role of nanomaterials in the treatment of wastewater: a review. *Water*, 12, pp.495.

Yavari, S., Mahmodi, N.M., Teymouri, P., Shahmoradi, B. and Maleki, A., 2016. Cobalt ferrite nanoparticles: preparation, characterization and anionic dye removal capability. *Journal of Taiwan Institute of Chemical Engineers*, 59, pp.320-329.

Yu, J.-G., Zhao, X.-H., Yang, H., Chen, X.-H., Yang, Q., Yu, L.-Y., Jiang, J.H. and Chen, X.Q., 2014. Aqueous adsorption and removal of organic contaminants by carbon nanotubes. *Science of the Total Environment*, 482, pp.241-251.

Zare, K., Gupta, V.K., Moradi, O., Makhlouf, A.S.H., Sillanpää, M., Nadagouda, M.N., Sadegh, H., Shahryari-Ghoshekandi, R., Pal, A. and Wang, Z.-J., 2015a. A comparative study on the basis of adsorption capacity between CNTs and activated carbon as adsorbents for removal of noxious synthetic dyes:65u a review. *Journal of Nanostructure in Chemistry*, 5, pp.227-236.

Zare, K., Sadegh, H., Shahryari-Ghoshekandi, R., Maazinejad, B., Ali, V., Tyagi, I., Agarwal, S. and Gupta, V.K., 2015b. Enhanced removal of toxic Congo red dye using multiwalled carbon nanotubes: kinetic, equilibrium studies and its comparison with other adsorbents. *Journal of Molecular Liquids*, 212, pp.266-271.

Zhang, Z. and Kong, J., 2011. Novel magnetic Fe_3O_4@C nanoparticles as adsorbents for removal of organic dyes from aqueous solution. *Journal of Hazardous Materials*, 193, pp.325-329.

Zhou, Z., Lin, S., Yue, T. and Lee, T.C., 2014. Adsorption of food dyes from aqueous solution by glutaraldehyde cross-linked magnetic chitosan nanoparticles. *Journal of Food Engineering*, 126, pp.133-141.

Zhu, Y., Wu, J., Chen, M., Liu, X., Xiong, Y., Wang, Y., Feng, T., Kang, S. and Wang, X., 2019. Recent advances in the biotoxicity of metal oxide nanoparticles: Impacts on plants, animals and microorganisms. *Chemosphere*, 237, pp.124403.

Phytochemistry of *Aloe vera*: A Catalyst for Environment-Friendly Diverse Nanoparticles with Sustained Biomedical Benefits

S. Yadav[iD], A. Khan[iD] and J. G. Sharma†

Department of Biotechnology, Delhi Technological University, Delhi-110042, India
†Corresponding author: J. G. Sharma; sharmajaigopal@dce.ac.in

ABSTRACT

Nanotechnology has become one of the most active fields in the research area and is getting more attention toward nanoparticle synthesis. Green synthesis methods using various plants, fungi, bacteria, and algae were used to synthesize nanoparticles with proper requirements and maintain sterile conditions to get the desired products. *Aloe vera*, a bio-medicinal plant, contains a wide range of phytochemicals such as phenolic, hydroxyl groups, alkaloids, polyols, polysaccharides, etc, which act as reducing and capping agents with high efficiency. This review revealed that aloe vera-derived nanoparticles are safe, stable, cost-effective, and eco-friendly, and they also possess significant applications for drug targeting, disease resistance, tissue engineering, wound healing, anticancer, antibacterial, and cosmetic industries. Synthesized metal nanoparticles are characterized through UV-visible spectroscopy, X-ray diffraction, scanning electron and transmission electron microscopy, photoluminescence, and the Well-diffusion method. It is highly interesting to note that aloe vera-mediated silver and zinc nanoparticles possess high potency against multi-drug resistant pathogens. Here, anticancer, antioxidant, anti-inflammatory, and photocatalytic activity separately showed by aloe vera peel, gel, and leaf, along with possible challenging situations faced during plant extract-based nanoparticle synthesis, are highlighted. Additionally, the introduction of GMOs is subjected to play an important role in advancing green methods. However, more research is required to estimate the dose's safety, degradation, and synergistic mechanism inside the human body for better use of the green method for the treatment of microbial infections.

INTRODUCTION

With the reasons for the advances in science and technology research, nanotechnology has become 1 of the most active fields in every research area. They are significantly used in electronic devices and are seeking attention for the synthesis of nanoparticles. Nanoparticles are characterized as of nano or minuscule dimensions as they lie within a range between 1-100 nanometres and possess a large surface-volume ratio and high reactivity with their ideal synthesis route. Nanoparticles display unique properties like magnetic, optical, electrical, chemical, and other various biological properties (Zharov et al. 2005). Top-down & bottom-up approaches synthesize nanoparticles with the involvement of physical and chemical methods for the synthesis of NPs. Chemical synthesis occurs through methods including co-precipitation, sol-gel, hydrothermal, etc. Methods require excessive energy with the release of toxic, carcinogenic by-products (Ying et al. 2022). At present, green chemistry approaches are being used to develop nanoparticles using Phyto-fabrication of plant extracts (precursor) and microbes (Koratala et al. 2023).

An ecologically friendly way to form a stable and novel nanoparticle with the requirement of little energy and chemicals and also eliminating fewer wastes is pointed as "green synthesis". This method is more advantageous as natural sources, nontoxic, and cost-effective (Behravan et al. 2019). Plant extracts, which contain

components like alkaloids, polyphenols, vitamins, and steroids, act as reducing and capping agents and result in the formation of stable metal nanoparticles (Sargazi et al. 2022). Metal NPs produced by plant extracts or green methods are more stable. Phenolic groups in plant extracts have a higher capacity to reduce the metal ions for nanoparticle synthesis in comparison to fungi and bacteria. Plants are getting more attention in synthesizing metal nanoparticles like Cu, Au, Ag, Zn, CO, etc. They exhibit a high composition of biomolecules like proteins, enzymes, flavonoids, and terpenoids. These phytochemicals have great medicinal value and act as reducing and stabilizing agents (Akbar et al. 2020). The extent of metal ions reduction to synthesize specific metal NPs directly depends on the type and concentration of phytoconstituent present in plant extracts (Iravani 2011). With the use of NPs, Antibiotic-resistant bacteria exhibit increased antibacterial activity. The green route reduces the risk of contamination and helps to maintain the cell structure. Plant-mediated nanoparticles have various antimicrobial, anti-inflammatory, drug delivery anticancer, antioxidant, etc properties (Muthu et al. 2021). Its biological production recycles the expensive metals such as gold and silver in the waste stream. With the increment in alkaline conditions, metal ions will get reduced to attain a petite size of the nanoparticle, whereas, with the increment in temperature, there is an increment in the absorption spectra (profound effect), which results in the rapid formation of nanoparticles (Song et al. 2009). Due to the reason of having nano size and the high surface-volume ratio of nanoparticles, they have great application in agricultural fields in the formation of pesticides and fertilizers to resist damage to crops from diseases, drug delivery, and diagnosis in tissue engineering (Altammar 2023). Several different types of nanoparticles varying in size and shape are synthesized with their biological applications. Using biological methods like plant extracts, bacteria, fungi, and other pathogens, green synthesis has emerged as an ideal option over conventional methods for NP synthesis (Behravan et al. 2019).

From ancient times medicinal plants have been seeking more attention in the fields of medicinal drugs and disease treatment. Active components in natural sources play a vital therapeutic role in health benefits. Various plants such as *Medicago sativa*, *A. indica*, *Aloe vera*, *Tamarind*, *Alfa Alfa*, *Hydrilla* sp., *Mangifera indica*, *Cassia fistula*, *Piper betel*, and many more medicinal plants have been used for metal NP's synthesis. Among various plants, aloe vera is proposed to be chosen for metal nanoparticles due to its cheap, eco-friendly, non-toxic nature and numerous therapeutic properties as anticancer, anti-inflammation, antioxidant, antifungal, etc. *Aloe barbadensis* Miller, commonly called aloe vera, is the oldest plant species with the highest medicinal

properties ever known. Aloe vera is one of the most common succulent xerophyte plants of the family *Liliaceae* and is grown in hot and dry climates in India, Japan, and China (Baruah et al. 2016). Aloe plants can grow up to a height of 60-120cm. It can survive as below as 40°C temperature and freezing (Grindlay & Reynolds 1986). This green plant has a high water-storing capacity in leaves to survive in harsh conditions. Aloe leaves are covered with a thick epithelium layer containing colorless, viscous, and bitter gel with parenchymatous cells. Among 420 kinds of *Aloe* species, *Aloe vera* is one of the most effective and active plants with medicinal properties, commercially used (Ahlawat & Khatkar 2011). Several researchers have attempted to identify the active component responsible for the medicinal properties of aloe vera in wound healing in case of burns and inflammation (Rao Kandregula et al. 2015). It contains 200 active components, including enzymes, minerals, polysaccharides, and amino acids, present in different layers or parts of the aloe leaf. Some chemical compounds include anthraquinones, glycoside sterols, lipids, etc. (Gao et al. 2019). These chemical components have different advantages as antiviral, anti-inflammatory, antidiabetic, antioxidative, and anticancer properties. It is widely used in products related to the pharmaceutical, food, and cosmetics industries. Thus, this review provides a detailed analysis of aloe vera-mediated synthesis of nanoparticles (Table 1) through ongoing research related to it with their potential antibacterial, anticancer, and photodegradation applications for a safe future by eco-friendly or green approach.

How is a Flora-Derived Green Synthesis of Metal Nanoparticles Utilized in Comparison to Conventional Methods?

The trend of synthesis of safe, novel, and less harmful nanoparticles is exploited all over. Different methods like physical, chemical, and biosynthesis methods are used for the synthesis of nanoparticles. Despite using physio-chemical methods for producing metal nanoparticles, green synthesis approaches are now exploited in the research sector due to their eco-friendly nature and several clinical and nutraceutical properties. Physical methods for synthesis require high energy and release harmful chemicals and waste products. Chemical methods face many problems, like using toxic and expensive solvents (Kundu et al. 2014) and heating the chemicals at high temp, with low pressure, which leads to increased risk to human health and surroundings (Li et al. 2011). These methods decline the biological applications and desired mass production. To overcome this problem, the global market transitioned towards environment-friendly methods. Different green methods or biological systems are used for nanoparticle synthesis. Biosynthesis methods

are quite safe, Harmless, and novel approaches, including plants and microorganisms for medicinal applications (Rabiee et al. 2020). Microbial systems are cost-effective and nontoxic for the environment, including bacteria, fungi, algae, yeast, etc, for nano-size particles. These work to reduce and stabilize the particular metal nanoparticle (Gericke Mariekie & Pinches Anthony 2006). Among these biological systems, fungi have better quality in production due to low expenses for downstream processing, highly efficient for extracellular enzymes used for large mass production, good metal reduction, and utilization of biomass (Sarkar et al. 2014). It is quite challenging for researchers because of the complexity of toxic metals for the synthesis of nanoscale materials. Microbes-mediated nanoparticles are not completely viable to form the desired product, they require a proper sterile condition and high maintenance. No control for nanoparticle size, structure, and time for microbial screening are some major drawbacks of microbial systems for nanoparticle synthesis (Kundu et al. 2014). Researchers investigated to reveal that plant parts and their extracts are the most ideal and cost-effective, nontoxic method of nanoparticle synthesis with deficient maintenance of requirements in the system. Plant extracts contain numerous active phytocomponents like flavonoids, amino acids, minerals, enzymes, polysaccharides (Gao et al. 2019), polyols, and polyphenols (Ovais et al. 2018). Phytochemicals in plant extracts act as stabilizing agents as compared to microbial systems for nanoparticle synthesis to reduce toxic heavy metals. Any parts like the root, stem, leaf, or flower of a plant containing phytochemicals can be used for synthesizing various nanoparticles like gold,

silver, copper, zinc, etc (Iravani 2011). Plant-mediated nanoparticle synthesis is cheap, accelerated, and doesn't require specific conditions and screening of microbial cultures as microbial systems do, and was easily synthesized in a controlled condition at room temperature (Rajakumar et al. 2012) with quite stirring and heating (Acharyulu et al. 2014). This is done by simply mixing the reducing agents present in plant extracts in an aqueous solution of the respective metal of the nanoparticle to be synthesized (Fig. 1). Synthesis of nanomaterial comprises three phases: (a) activation phase; metal ion gets reduced, (b) growth phase; aggregation of small particles to form large nanoparticles via Ostwald ripening, (c) termination phase; concluded the shape of a nanoparticle. The formation of nanoparticles is characterized by a visual change in the color of the solution or by UV-Vis Spectroscopy. Finally, nanoparticles are collected by washing before drying at low temperatures. The capacity of certain metal ions to get reduced depends on the presence and concentration of specific functional groups such as hydroxyl, phenol, aldehyde, ketones, carboxylic acid, and amines, as well as phytochemicals like polyols, polyphenols, and enzymes present in plant extract (Iravani 2011). Plant-mediated synthesis of nanoparticles is stable for getting higher yield, which makes it a highly preferred method over other biosynthesis methods. Plant-extracted nanoparticles have various diagnostic and therapeutic applications in biotechnology. Several nanomaterials synthesized by this method have unique properties. Ex- Gold and silver nanoparticles synthesized by plant extracts have anti-microbial, anticancer, and antiviral properties. Whereas Zinc oxide nanoparticles are efficient for the production of
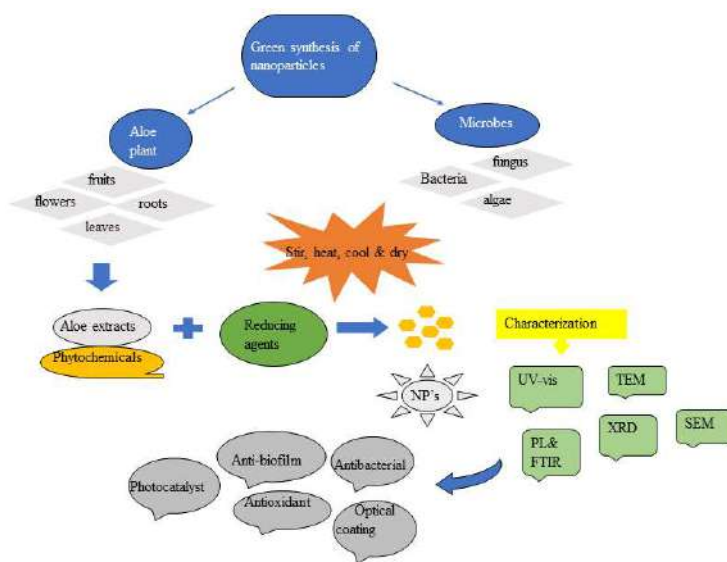
Fig. 1: Plant-facilitated NP synthesis with its biomedical applications.

cosmetic products and for coating purposes (Mittal et al. 2013). Therefore, plant extracts proposed an efficient method for fast, safe, convenient, and stable way of nanoparticle synthesis.

An Overview of the Plant, *Aloe barbadensis* Miller (Aloe vera)

The scientific name of Aloe vera is *Aloe barbadensis* Miller, commonly called 'Gwar path' or simply 'Aloe vera'. It is a green shrub that belongs to the family Liliaceae. It is a xerophytic, succulent plant that grows in dry and hot climates. Triangular leaves of aloe vera are enveloped with a thick epidermis layer and cuticles at the edges. Thick, fleshy leaves contain a bitter and viscous gel with parenchymatous cells. High water-holding capacity makes them able to survive in variable temperatures (Grindlay & Reynolds 1986). It is widely known for its healing and medicinal applications in burns, inflammation, gastric problems, stress, cosmetics, and many more. It contains 200 biologically active aloe components such as proteins, carbohydrates, acemannan, polyphenols, anthraquinones, etc (Talukdar et al. 2023). These secondary metabolites in gel provide anticancer, antidiabetic, antioxidant, antimicrobial, and anti-fungal benefits. Aloe vera consists of three layers. A thick outermost layer or rind produces proteins and carbohydrates. The middle layer contains yellow bitter latex rich in anthraquinones and glycosides (Baruah et al. 2016). The innermost layer contains mainly 98 percent water, and the rest are vitamins, sterols, and glucomannans (Chelu et al. 2023).

It has a unique, fast mechanism to heal damaged tissue by its active secondary metabolites. Mannose-6-phosphate (Hashemi et al. 2015), gibberellin, acemannan (Jettanacheawchankit et al. 2009a), saponin (Baruah et al. 2016), and polysaccharides (Tabandeh et al. 2014) are responsible for repairing damaged tissues. Wound healing is done by activating collagen production to increase blood supply in damaged areas. Also, it induces re-epithelialization by the proliferation of fibroblasts. Some constituents like lupeol (Das et al. 2011), aloe resin Es (Das et al. 2011), bradykinesia, alkaline phosphatase, peroxidase, cinnamic acid (Das et al. 2011), aloin, and aloe emodin, have anti-inflammatory properties. They act by blocking their nitric oxide synthase and cyclooxygenase pathway at the site of infection. Aloe vera extracts have an anticancer effect in lymphoma cells, and murine T-cell lymphoma in a dose-dependent manner was reported. Anthraquinones, emodin, aloin, and acemannan show active anticancer effects by inhibiting tumor growth and promoting apoptosis (Pradhan 2023). Aloe-emodin has antimicrobial properties and inhibits biofilm formation in microbes like *Mycobacterium*

tuberculosis, Staphylococcus aureus, and *Enterococcus* (Xiang et al. 2017). By reducing oxidative stress, lowering blood glucose levels, increasing insulin levels, and improving islets in the pancreas, aloe polysaccharides (Kim et al. 2018) and aloe-emodin (Alshatwi & Subash-Babu 2016) act as antidiabetic agents by inhibiting apoptosis and oxidative stress signaling. Aloe vera extracts can improve skin health by promoting collagen formation in fibroblast cells and maintaining skin hydration. Aloe sterols (Misawa et al. 2008), acemannan (Jettanacheawchankit al. 2009b), aloesin (Wu et al. 2012), and aloin (Jettanacheawchankit et al. 2009b) are active components useful in treating hyperpigmentation, pimples, wrinkles, and other skin-related problems that are yet investigated. Acemannan is the most active phytochemical in reducing oral ulcers, gum diseases like gingivitis and plaque, and neurodegenerative diseases. Processing methods of these compounds can change the concentration of their laxative property. Aloe vera extracts can create toxic effects like kidney issues, allergies, and abdomen pain in some cases if taken in high concentration without prescription. Aloin is mainly responsible for allergy reactions (Fujii 2003). To avoid any toxic effects, a safe dose is necessary for benefits. Aloe extracts are assessed to prevent the generation of ROS and also increase the release of Ca^{2+} ions inside cells to treat neurodegenerative disorders such as Parkinson's, Amyotrophic lateral sclerosis, Alzheimer's, and Huntington's diseases. Researchers found aloe vera wastes to be used as fertilizer, biofuels, drug delivery systems, and in the pharma industry. Evaluating all of the therapeutic properties of this plant, it is a crucial element in green nanoparticle synthesis with various pharmacological effects.

Diverse Forms of Aloe vera-Facilitated Nanoparticles

Aloe vera-derived Ag-nanoparticles: Aloe vera is significantly used for silver nanoparticle synthesis (Ag NPs). Silver nanoparticles gained the most attention for their different properties and applications in various fields of study. Plant extracts containing phytoconstituents are helpful in the reduction of silver ions to form safe, non-toxic, and enhanced therapeutic effects of AV-Ag NPs. Various crucial parameters affecting Ag NP synthesis are pH, the concentration of reducing agent and aloe extracts, and temp. pH can change the size and morphology of NPs (basic pH elevates the synthesis of NPs) (Singh & Dhaliwal 2019). Concentration and reaction time should be optimum for reducing silver ions to form nanoparticles (Devaraj et al. 2013).

Arshad et al. (2022) synthesized AV-Ag NPs against multi-drug resistant pathogens and observed NP synthesis by simply mixing silver nitrate solution and aloe extract solution in 4-6 hrs of incubation at 65°C. Characterization of particles

is done by UV-visible spectroscopy, X-ray diffraction, and scanning electron microscopy, resulting in spherical shape nanoparticles in the range of 30-80nm (Arshad et al. 2022).

Begum et al. (2020) demonstrated the synthesis of AV-Ag NPs to measure antibacterial activity against gram-positive and gram-negative bacteria by disc diffusion method. Synthesis of AV-Ag NPs was carried out by taking a 5:95 ratio of aloe vera extract to silver nitrate solution at optimum pH 8 for a day. Characterization of synthesized NPs by SEM shows spherical particles with a size of 20-24 nm (Begum et al. 2020).

Begum & Mahboob (2019) evaluated the antioxidant properties of aloe extracts and aloe-mediated silver nanoparticles in vitro and in vivo studies. A preliminary identification test was conducted to detect the presence and antioxidant properties of phytochemicals present in the aloe extracts for the synthesis of AV-Ag NPs. AV-Ag NP synthesis was confirmed by UV-vis spectroscopy. A reddish-brown color of the solution was observed due to the excitation of surface plasmon resonance of synthesized silver nanoparticles in the reaction mixture. It resulted in the synthesis of spherical shape AV-Ag NPs with maximum absorption at 400 nm and size in the range of 20 to 24 nm. In Vitro, the antioxidant property was determined by some methods like lipid peroxidation inhibition (LPOI), DPPH, i.e.,1,1-Diphenyl-2-picrylhydrazyl, and reducing power assay based on the concentration of aloe vera extract and AV-Ag NPs. It resulted in high LPOI in aloe vera extract, high DPPH activity, and reduced power activity in AV-Ag NPs. On the other hand, an in vivo study of AV-Ag NPs was performed in rats for 28 days (10 mg.kg^{-1} of body weight). It showed the reno-protective effect by reducing the level of MDA and increasing in level of catalase, SOD, and GSH level. Antioxidant potential and nontoxic effect of AV-Ag NPs based on their conc., size, and exposure period were estimated by this study (Begum & Mahboob 2019).

Nalini & Kay (2020) synthesized spherical AV-Ag NPs, which were 12-40 nm in size measured by SEM and at a temperature of 32°C. They analyzed the antimicrobial properties of these synthesized AV-Ag NPs on cotton fabric against the bacteria E. coli and Staphylococcus aureus. The analysis was carried out in the Well diffusion method and streak plate method to measure the zone of inhibition, with an absorbance at 420 nm, and resulted in bactericidal effects.

Mohamed & El-Masry (2020) prepared AV-Ag NPs with exposure to sunlight to increase the reducing efficiency. NPs were characterized through TEM, FTIS (Fourier transform infrared spectroscopy), and dynamic light scattering. Formation of colloidal spherical AV-Ag NPs, with size in the range of 94 nm, absorption peak noted at 400 nm. The

resulting AV-Ag NPs have significantly high antibacterial effects to stop the growth of Gram-positive *Staphylococcus aureus*, Gram-negative *Pseudomonas aeruginosa*, and yeast (*Candida albicans*). Besides, it has high therapeutic or anticancer effects on breast cancer cells (Mohamed & El-Masry 2020).

Vélez et al. (2018) synthesized silver nanoparticles using aqueous and ethanolic extracts of aloe vera as reducing agents. High-resolution TEM was used to identify nanoparticle Sizes and was found to be 2-7 nm by aqueous extracts and 3-14 nm by ethanolic extracts. Researchers reported that even a small concentration of aqueous and ethanolic aloe extracts mediated silver nanoparticles show results for effective removal of harmful mercury detected by atomic absorption spectroscopy and antibacterial activity for mesophilic pathogen *Kocuria variants* (Vélez et al. 2018).

Dinesh et al. (2015) showed that a very low dose of AV-Ag NPs is required to show a mosquitocidal effect against *Anopheles stephensi* and to stop the growth of *Bacillus subtilis* and *Salmonella typhi* in water. They used SEM, XRD, and FTIR techniques for the characterization of synthesized AV-Ag NPs (Dinesh et al. 2015).

Basak et al. (2018) produced spherical aloe-mediated Ag NPs. Evidence of exp. Conclude anticancer activity against MCF-7 and T47D (breast cancer cells) and antimicrobial properties against bacterial species (Basak et al. 2018). In this study, an experiment was performed to compare the antibacterial properties of *Aloe vera*, *Portulaca oleracea*, and *Cynodon dactylon*, mediated silver nanoparticles through the disc diffusion method, which calculates their MIC (minimum inhibitory concentration) values. Size and shape were determined by technique, SEM, and UV-vis Spectroscopy. They found that aloe vera-mediated NPs exhibit high bactericidal 50μg/mL concentration against various species of bacteria (Abalkhil et al. 2017).

A group of Researchers experimented on 30 male mice weighing between 50 to 70 g. They aim to determine the efficiency of recovering epithelial cells on ulcers due to irradiation. Mice were classified into five groups and exposed to harmful radiation, which resulted in the induction of ulcers in each mouse. After irradiation, the first group received no treatment to function as a control, whereas the Second group was ulcer-induced but no treatment was received for it. The third group was treated with aloe extracts, the fourth group was treated with Ag NPs, and the fifth group was treated with a combination of both, i.e., AV-Ag NPs, respectively. The team identified that AV-Ag NPs treated mice have elevated collagen synthesis due to an increase in IL-10 level when compared to individual AV and Ag NPs. This restoration efficiency of epithelial tissues helps in reducing the adverse

effects of inflammatory reactions and re-epithelialization in case of ulcer formation (El-Batal & Ahmed 2018).

Aloe vera-derived Au-nanoparticles: Gold is effectively being used in the synthesis of nanoparticles due to its high physical, chemical, electric, thermal, and optical properties and exhibits great applications in electronic devices, biomedicines, drug delivery, and sensing devices. Various shapes of gold nanoparticles were synthesized, like spherical, triangles, etc, based on the concentration of aloe extracts used for agglomeration.

Nalini & Kay (2020) synthesized spherical AV-AuNPs (aloe-mediated gold nanoparticles) below 15 nm in size and at a temperature of 34°C measured by SEM after 16 hrs of incubation. They identified the antimicrobial properties of synthesized AV-AuNPs on cotton fabric against E. coli and Staphylococcus aureus. The test was carried out in the Well diffusion method and streak plate method and exhibited an absorbance of 530 nm (Nalini SP & K 2020).

In a study conducted by (Malik et al. 2023) where, they synthesized gold nanoparticles using Aloe vera, *Gymnema sylvestre*, and honey. They aimed to study the toxicity of gold nanoparticles. When chloroauric acid ($HAuCl_4.3H_2O$) was mixed with aloe extracts, it led to a change in color of the mixture from brownish to purple then it was centrifuged at around 150 rpm in a dark room. Characterization of synthesized AuNPs via XRD, UV-vis, FTIR, and SEM. They discovered (AV-AuNPs) of size 30-45 nm, and an absorbance peak was noted at 540 nm. The yield and absorbance of gold NPs directly depend on the elevation of temperature. Furthermore, they examine the cytotoxic effects of AuNPs by conjugating them with anticancer drugs to treat MCF-7 and MDA-MB231 breast cells (Malik et al. 2023).

Chandran et al. (2006) reported the biological synthesis of gold nanotriangles and spherical-shaped silver nanoparticles using aloe vera extracts. When they mixed the chloroauric acid solution and aloe extracts it resulted in a brownish-red color solution after 5 h of incubation. The presence of crystalline gold nanotriangles was detected with size ranges between 50-350 nm and was confirmed by UV- -vis -NIR absorption spectroscopy. It exhibits two absorption bands. TEM analyses that MTP (multiple twinned particles) of varying shapes direct the formation of crystalline gold triangular nanoparticles. Strong NIR absorption is widely used to treat cancer and in optical coating (Chandran et al. 2006).

Aloe vera-derived CuO-nanoparticles: Due to the unique properties of copper oxide nanoparticles, they are highly used in the synthesis of gas sensors and resistant materials. Multiple applications of copper oxide nanoparticles synthesized by varying concentrations of aloe extracts exhibit antibacterial, antifungal, and antifouling activities. From all works of literature, copper has higher antibacterial properties as compared to Ag, Au, and Zn metals.

A study of the synthesis of CuO NPs was carried out by (Narayanan et al. 2023) and his team using aloe extract. 5 g of aloe leaf was mixed with 200 ml of distilled water, heated, cooled, and filtered out. 0.56 g copper acetate monohydrate dissolved in distilled water with magnetic stirring to make a solution. When aloe extract is added to copper sulfate solution, the solution turns out to be green from blue. Brown precipitates of copper oxide particles appeared—characterization of synthesized spherical CuO nanoparticles through UV-vis, FTIR, SEM, and TEM. More than 80 percent of the efficiency of photocatalytic properties of AV-Cu NPs was reported by researchers (Narayanan et al. 2023).

This study aimed to determine the electrocatalyst activity of copper-cobalt oxide-based electrodes on Ni-substrate. In this hydrothermal process, aloe vera extracts are used as surfactants to induce the growth of NPs. Copper & and cobalt oxide-based electrocatalysts exhibit applications in oxygen-evolving processes. In this exp (Sarkar et al. 2023), Ni substrate was prepared by first treating it with acetone, followed by a bath in HCl, distilled water, and ethanol, and drying at the end. On the other side, an aloe vera extract sol. was also prepared by boiling, stirring, and cooling. The reaction was conducted in different mineral mediums (HCl, CA, DEA, NaOH, and H_2NCONH_2) containing an equal ratio of both copper & and cobalt metal oxide on the Ni-substrate. The solution was heated at 130°C, cooled at RT, and dried to separate the catalysts from the Ni substrate. Characterization was successfully carried out by XRD, EDS (energy dispersive spectrum), Field Emission SEM, and testing oxygen evolving performance. This study showed that an acidic mineral medium influences the growth of copper oxide, whereas basic minerals promote the growth of cobalt oxide. Besides this, aloe vera-based metal oxide with urea mineral medium is anticipated to have high electro-catalytic potential on Ni-substrate (Sarkar et al. 2023).

Rehman & Shahid Minhas (2021) experimented by mixing 6 g of copper nitrate solution and aloe extracts at 120°C by stirring for 7 h. Finally, after several hours, black-colored precipitates appeared, confirming 60 nm spherical-shaped CuO NPs. These synthesized nanoparticles are characterized by SEM and XRD. The potency of CuO NPs was discovered to kill MCF-7 cell lines of breast cancer (Rehman & Shahid Minhas 2021).

Researchers successfully synthesize CuO NPs using aloe extracts and copper chloride or copper sulfate as precursors and changing the type and quantity of copper precursor

results in the formation of rod, spherical, and platelet-like shapes of pure copper oxide nanoparticles varying in size from 9-23 nm. Rod and platelet-shaped CuO NPs have high resistance to bacteria due to their increased surface area compared to spherical-shaped particles analyzed by (Tavakoli et al. 2019).

Kumar et al. (2015) studied the synthesis of copper oxide nanoparticles using 5 mL of aloe vera extracts added to 10 mM of copper nitrate. The mixture was heated at 120°C on vigorous magnetic stirring for a day, resulting in a dark red color. Finally, a black ppt of CuO NPs appeared with a size of 22 nm obtained by XRD and TEM techniques. They found efficient antibacterial activity against fish pathogens like *Aeromonas hydrophila*, *Flavobacterium branchiophilum*, and *Pseudomonas fluorescens*, causing infection in fishes. The bactericidal effects of synthesized nanoparticles were analyzed via the micro-dilution broth technique (Kumar et al. 2015).

Gunalan et al. (2012) reported the synthesis of monodisperse copper oxide nanoparticles by chemical and biological methods. They dissolve copper sulfate and aloe extract solution by continuing magnetic stirring of the mixture. Keeping the mixture under vigorous stirring for 7 hrs at 130°C, a black precipitated solution of copper oxide was observed. After two times centrifugation of the mixture at 3500 rpm, the crushed dry product was collected for its optical property analysis. Maximum particles were observed to be 20 nm, and characterization of CuO NPs was done via UV-vis, photoluminescence, XRD, and SEM (Gunalan et al. 2012).

Aloe vera-derived ZnO-nanoparticles: Zinc oxide has low toxic effects and is under-listed as GRAS (Generally Recognised as Safe) by the US Food and Drug Administration. It has many applications in cosmetics, plastic, paints, pharmacy, and microelectronic devices and is widely used to synthesize efficient nanoparticles against pathogens. At present, further research is going on zinc oxide nanoparticles which are highly used due to their high efficiency as an antimicrobial agent.

To compare inhibitory effects against *Klebsiella pneumonia* isolated from patient samples, Hammood et al. (2022) compared zinc oxide nanoparticles synthesized by aloe vera with chemically synthesized zinc nanoparticles. In this study, 1 mM of ZnO solution was mixed in 10 mL of aloe extracts keeping it for around 30-35 min on a magnetic stirrer, maintaining a neutral pH. The resulting White ZnO nanoparticles underwent centrifugation at 1000 rpm for nearly 10 min before drying and characterization—maximum absorption between 360 to 380 nm depicted by UV-vis spectrum. Scanning electron microscope indicates spherical-shaped Zn nanoparticles of 20 to 40 nm. Other properties of particles were studied via atomic force microscopy, X-ray diffraction, and infrared spectroscopy. This study identified that aloe-mediated zinc nanoparticles exhibit greater inhibition against *K. pneumonia* as compared to commercially prepared zinc nanoparticles (Hammood et al. 2022).

Khatana et al. (2021) synthesized aloe-mediated zinc oxide nanoparticles to examine their antibacterial properties
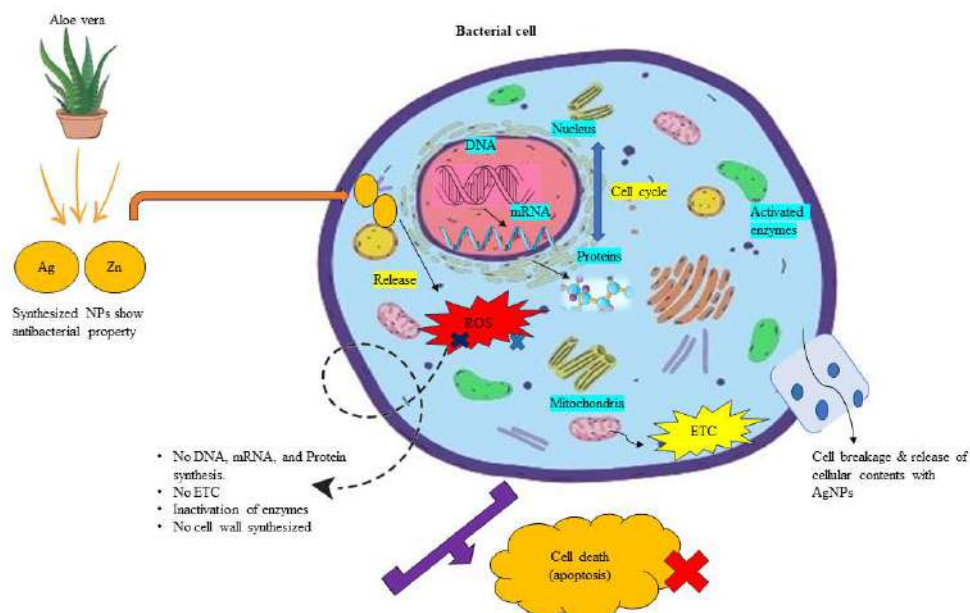
Fig. 2: Role of aloe vera-derived silver and zinc NPs (antibacterial activity).

against different bacterial strains. 100 g of aloe leaves were washed, chopped, and boiled in 100 ml of distilled water and filtered to get a fresh aloe solution. 0.50 g zinc acetate solution was dissolved in freshly prepared aloe extracts solution to 12 pH, and colored zinc oxide nanoparticles were formed. L-ascorbic acid and other components are responsible for ZnO NP synthesis. A flower-like shaped Zn O NP was observed under SEM, showing 0.126 nm of interplanar space. Studied results show high antibacterial efficiency (Fig. 2) against *S. aureus*, *E. coli*, and *Pseudomonas aeruginosa* (Khatana et al. 2021).

Zinc oxide-nanocomposites (ZnO-BAV, ZnO-WAV, and ZnO-N) were prepared using dried powder of black and white aloe vera and dried powder of Terminalia arjuna nuts by Dar et al. to explore their antibacterial efficiency. At the start of this study, 5 g of dried plant contents of both plants were taken separately in 100 mL of distilled water. Stir each solution at nearly 100 rpm on a hot plate maintaining its temperature at 70°C for 15 min. On the other side, prepare a solution of zinc acetate by adding 2.9 g in 50 ml of distilled water at room temperature for one hour. After preparing both solutions, mix 50 mL of aloe extract in zinc acetate solution and leave at 100 rpm on an orbital shaker for at least 3 hours. After all this procedure researchers centrifuged yellow ZnO nanocomposites settled at the bottom and dried them at 80°C. Synthesized ZnO-nanocomposites were characterized by UV-visible, SEM, and FTIR techniques, respectively. SEM revealed the morphology of ZnO-BAV (zinc oxide-black Aloe vera) appeared as fibrous-wired of size 27-71 nm, ZnO-WAV (zinc oxide-white aloe vera) as octahedral of size 29-75 nm, and ZnO-N (zinc oxide-nuts) as scattered particles of size 32-83 nm. The disc diffusion method showed a larger zone of inhibition by ZnO-BAV when tested *against E. coli* and *B. stabilis*. ZnO-WAV and Zno-N both showed efficient antimicrobial properties only against E. coli. However, no response showed against *B. stabilis* (Dar et al. 2021).

Sharma et al. (2020) successfully conducted a study on the antimicrobial and photodegradation of dye depending on different sizes and shapes of zinc oxide nanoparticles synthesized. The procedure involved the preparation of zinc acetate dihydrate, Zn $(CH_3CO_2)_2 \cdot 2H_2O$ solution, and aloe leaves were washed, chopped, boiled, and filtered to extract aloe juice. With continued stirring, dropwise addition of aloe extract to different concentrations of 5, 10, and 50 mmol. kg^{-1} of zinc acetate solution at 70°C with pH 11.5. After regular heating for 4 hours, yellow-whitish-colored zinc oxide nanoparticles were synthesized, collected, and dried. UV-visible spectrum analyzes the optical properties of AV-ZnO NPs between 200 to 800 nm with a sharp absorption peak around 370 nm, and the band gap was calculated to be 3.4 eV. SEM, TEM, or EDS (SEM-energy dispersive X-ray spectroscopy) examined the size and shape of ZnO NPs at varying concentrations of Zn $(CH_3CO_2)_2 \cdot 2H_2O$. They obtained hexagonal NPs with a size of 63 nm at 5 mmol.kg^{-1}, spherical and hexagonal NPs with a size of 60 to 180 nm at 10 mmol.kg^{-1}, and cuboidal or rod-shaped nanoparticles with a size of 40 to 45 nm at 50 mmol.kg^{-1}. It has been noticed that 50 mg of the catalytic load is enough for degrading dye for spherical and hexagonal shape nanoparticles. However, there is an increase in degradation efficiency that led to an increase in the concentration of catalytic load for cuboid-shaped zinc oxide nanoparticles. Results also show that synthesized ZnO NPs are effective against pathogens such as *S. aureus, B. subtilis,* and *E. coli* (Sharma et al. 2020).

Aloe peel extract was used by Chaudhary et al. (2019) to synthesize zinc-oxide nanoparticles to depict its efficiency against bacterial and fungal pathogens. Synthesized Zinc oxide nanoparticles were hexagonally confirmed by TEM and with a size range between 50-220 nm UV-vis spectra. Hydroxyl, amine, aromatic, and carbonate groups are responsible for ZnO NP synthesis tested through FTIR. This study results in ZnO NPs having efficient bactericidal and antifungal effects against E. coli and A. niger (Chaudhary et al. 2019). Another similar study on aloe vera peel was performed to form nanovesicles for analyzing active healing mechanisms. Researchers discovered the anti-inflammatory effects of aloe vera peel-mediated nanovesicles (NV's) in macrophages and keratinocytes in case of burn wounds. Synthesized NV's prevent stimulation, contraction, and differentiation of both myofibroblast and fibroblast cells *in vitro* (Ramírez et al. 2024).

Ali et al. (2016) with the help of a simple, safe, and eco-friendly 1-pot biosynthesis method to synthesize Aloe vera functionalized zinc oxide NPs (AV-ZnO NPs) using aloe vera leaf extracts and zinc sulfate. They synthesized these AV-ZnO nanoparticles by heating at 60°C for three hours and with pH-8. It's a simple procedure of synthesis of NPs that doesn't require much temperature, pressure, or any toxic chemical. Characterization of NPs by XRD, SEM, UV-visible spectrum, and SEM-EDX was done to analyze nanoparticles within a range of 13 to 18 nm. The results of this experiment showed that aloe vera functionalized ZnO-NPs (AV-ZnONPs) used as nano antibiotics exhibit great antibacterial and anti-biofilm effects against S. aureus, a gram-positive, and E. coli, a gram-negative bacterium (Ali et al. 2016).

A group of researchers synthesized ZnO nanoparticles by using 60 mL of aloe vera leaf extracts and 5 g of zinc nitrate, a precursor. The mixture was collected in a ceramic crucible and heated at 400°C for two hours in a furnace. The resulting

light-yellow particles were collected, dried, and ground in powder form. ZnO nanoparticles were characterized by a UV-vis spectrum with an absorption peak of 360 nm. SEM and XRD analyze oval zinc oxide nanoparticles with a size range between 70 and 74 nm. It has been found that increasing the concentration of zinc-oxide-nanoparticles resulted in an increment in the growth, hydrogen peroxide, and lipid peroxidation contents of soybean(Hashemi et al. 2016).

Synthesis of ZnO NPs by utilizing precursor (zinc nitrate), cold and hot aloe leaf extracts (biosynthetic process), and sodium hydroxide used for a chemical method to estimate and compare their antibacterial efficiency against various strains of bacteria. Characterization of ZnO-AVH (hot aloe extract), ZnO-AVC (cold aloe extract), and ZnO-C (chemical) through X-RD, SEM, and calculating MIC values. SEM images assessed the morphology of nanoparticles: rod shape of ZnO-AVH &ZnO-AVC and spherical shape: ZnO-C. ZnO-AVC and ZnO-C resulted in small particle size as compared to ZnO-AVH and significantly showed high anti-bacterial effects against strains such as *Bacillus subtilis, Staphylococcus aureus, Pseudomonas aeruginosa,* and *Escherichia coli* (Laxshmi et al. 2012).

In this study, Sangeetha et al. (2011) reported the synthesis of AV-ZnO NPs and compared it to the ZnO-NPs synthesized by chemical method. They examined the morphology and optical properties of both methods. For the chemical method, zinc oxide NPs were produced with the dissolution of zinc nitrate in a sodium hydroxide (NaOH) solution. It formed white precipitates of nanoparticles after ten minutes of centrifugation at 3000 rpm and was dried. On the other hand, side, zinc nitrate was added in different concentrations of aloe leaf and aloe gel solution, and yellow-whitish precipitates appeared in the case of aloe-mediated nanoparticles. They centrifuged it two times at 4500 rpm for 10 to 15 min before drying at 80°C. Characterization of NPs by UV-visible spectra, TEM, and XRD analyze their average size. Aloe leaf (34 nm), aloe gel (35 nm), and approximately 60 nm of average size were analyzed by the chemical process. FTIR predicted the functional group responsible for Zn-NPs formation. Researchers highlighted that aloe-mediated NPs have many applications in the industrial field (Sangeetha et al. 2011).

Aloe vera-derived indium oxide nanoparticles: A semiconductor, indium oxide has a variety of applications in LED (light emitting diodes), solar cells, gas sensors, nanotubes, nanowires, and nanoparticles, etc. indium oxide has the property of great transparency for visible lights and strongly interacts with toxic gas molecules on any surface. Indium oxide nanoparticles are synthesized by chemical methods but they can also be synthesized by green methods by using cost-effective, eco-friendly, non-time-consuming aloe vera extracts.

Synthesis of indium oxide (In_2O_3) nanoparticles was discussed by (Maensiri et al. 2008) using indium acetylacetonate, a precursor, and prepared aloe extracts by boiling. This was prepared by directly dissolving indium acetylacetonate in aloe vera solution by constant stirring and drying at 60°C. calcination of dried indium oxide nanoparticles (In_2O_3 NPs) in box furnaces at different temperatures (400°C, 500°C, and 600°C) for at least two hours. Characterization of calcinated nanoparticles was done through XRD, PL, and TEM. Strong PL was shown by In_2O_3 nanoparticles because of the generation of oxygen vacancy during calcination. TEM discovered cubic In_2O_3 NPs with an average size of 5 to 50 nm depending on calcinated temperature Phokha et al. 2008).

Aloe vera-derived titanium dioxide nanoparticles: Titanium dioxide nanoparticles (TiO_2 NPs) are inflammable, white colored, nontoxic, with surface-reactivity, high thermal stability, and photocatalyst. These are highly used in cosmetic products, drug delivery, implants, and bioimaging. These are considered as effective bactericidal agents against a range of pathogens.

Ahmed et al. (2023) synthesized aloe-mediated titanium dioxide (AV-TiO_2) nanoparticles. They synthesized TiO_2 NPs by simply dissolving titanium isopropoxide (TTIP) as a precursor in a drop-by-drop manner in different concentrations of aloe extract solution (10 mL, 20 mL, and 30 mL) with continued vigorous stirring for two hours. Samples were washed with ethanol and distilled water and dried before their calcination at 450°C. XRD, FTIR, and RAMAN techniques confirmed a small optical band gap and high photocatalytic property of green synthesized spherical TiO_2 when compared to chemically or water-synthesized titanium dioxide nanoparticles. This study showed that aloe vera-mediated titanium dioxide nanoparticles with dose-dependent exhibit high radio-sensitization activity (Ahmed et al. 2023).

Hanafy et al. (2020) focused on the synthesis and characterization of titanium dioxide nanoparticles using aloe vera extract at varied pH (acidic, neutral, and basic) levels. TiO_2NPs involved a procedure, the addition of aloe extract solution drop by drop to titanium tetrachloride ($TiCl_4$) solution at (RT) room temperature. Finally, the mixture was then maintained at three varying pHs with the help of ammonium hydroxide and hydrochloric acid. White suspended nanoparticles were washed and followed by drying at 500°C. Spherical-shaped TiO_2 nanoparticles were characterized through XRD, UV-visible, and TEM. Maximum absorption of TiO_2 NPs under acidic, neutral,

Table 1: A concise summary of parameters for aloe vera-facilitated various nanoparticles.

Type of nanoparticle synthesized	Precursor or reducing agent	Incubation at (temperature)	Morphology and dimensions (in nanoscale)	Estimated property	References
Ag	Silver nitrate soln.	65$°C$	Spherical 30-80 nm	Antimicrobial	(Arshad et al. 2022)
Ag	Silver nitrate sol.	N/A	Spherical 20-24 nm	Antibacterial	(Begum et al. 2020)
Ag	Silver nitrate sol.	RT	Spherical 20-24 nm	Antioxidant	(Begum & Mahboob 2019)
Ag	Silver nitrate sol.	32$°C$	Spherical 12-40 nm	Antibacterial	(Nalini & Kay 2020)
Ag	Silver nitrate sol.	Sunlight exposure	Colloidal-spherical 94 nm	Antibacterial, Anticancer	(Mohamed & El-Masry 2020)
Ag	Silver nitrate sol.	57-80$°C$	2-24 nm	Antibacterial, Elimination of mercury	(Vélez et al. 2018)
Ag	Silver nitrate sol.	N/A	Spherical, cubic 30-57 nm	Mosquitocidal effects	(Dinesh et al. 2015)
Ag	Silver nitrate sol.	N/A	Spherical 10-30 nm	Anticancer	(Basak et al. 2018)
Ag	Silver nitrate and polyvinylpyrrolidone (PVP)	N/A	Spherical 10-17 nm	Anti-inflammatory, Re-epithelialization	(El-Batal & Ahmed 2018)
Au	Chloroauric acid	34$°C$	Spherical Below 15nm	Antimicrobial	(Nalini & Kay 2020)
Au	Chloroauric acid	30-50$°C$	Spherical 30-45 nm	Against Cytotoxic effects	(Malik et al. 2023)
Au	Chloroauric acid	N/A	Triangles 50-350 nm	Anticancer, optical coating	(Chandran et al. 2006)
CuO	Copper acetate monohydrate	N/A	Spherical	Photocatalyst	(Narayanan et al. 2023)
CuO	Copper nitrate sol.	120$°C$	Spherical 60 nm	Anticancer	(Rehman & Shahid Minhas 2021)
CuO	Copper chloride or copper sulfate	N/A	Rod, spherical, platelet. 9-23 nm	Antibacterial	(Tavakoli et al. 2019)
CuO	Copper nitrate sol.	120$°C$	22 nm	Antibacterial	(Kumar et al. 2015)
CuO	Copper sulfate	130$°C$	20 nm	Optical property	(Gunalan et al. 2012)
Zn	Zinc oxide	N/A	Spherical 20-40 nm	Antibacterial (Klebsiella pneumonia)	(Hammood et al. 2022)
ZnO	Zinc acetate sol.	N/A	Flower-like 0.126 nm	Antibacterial	(Khatana et al. 2021)
ZnO	Zinc acetate	RT	Fibrous, octahedral 27-75 nm	Antimicrobial	(Dar et al. 2021)
ZnO	Zinc acetate dihydrate	70$°C$	Hexagonal and spherical 60-180 nm, Cuboid and rod shape 40-45 nm	Antimicrobial Photocatalyst	(Sharma et al. 2020)
ZnO	Zinc sulfate and sodium hydroxide	N/A	Hexagonal 50-220 nm	Antibacterial Antifungal	(Chaudhary et al. 2019)
ZnO	Zinc sulfate	N/A	13-18 nm	Antibacterial Anti-biofilm	(Ali et al. 2016)
In₂O₃	Indium acetylacetonate	400-600$°C$	Cubic 5-50 nm	Optical property	(Maensiri et al. 2008)

Table Cont....

Type of nanoparticle synthesized	Precursor or reducing agent	Incubation at (temperature)	Morphology and dimensions (in nanoscale)	Estimated property	References
TiO₂	Titanium isopropoxide	450°C	Spherical	Photocatalyst, Radio-sensitizer	(Ahmed et al. 2023)
TiO₂	Titanium tetrachloride	N/A	Spherical 13-22 nm	N/A	(Hanafy et al. 2020)
TiO₂	Titanium oxyhydroxide	N/A	80-90 nm	Photocatalyst	(Nithya et al. 2013)
NiO	Nickel nitrate hexahydrate	300-500°C	Cubic crystals	Antibacterial Antifungal	(Ahmad et al. 2022)
CeO₂	Cerium nitrate hexahydrate	600°C	Spherical 42-50 nm	Antibacterial Antifungal	(Shetty et al. 2022)
CeO₂	Cerium nitrate sol.	N/A	Irregular 13-15 nm	Antibacterial Photocatalyst	(N et al. 2021)
CeO₂	Cerium nitrate hexahydrate	600°C	Spherical, With a diameter of 63.6 nm	Optical property	(Kanneganti et al. 2014)

and basic pH was examined to be 318, 326, and 320 nm, respectively. The average size of TiO₂ NPs was estimated to be 22.86±0.85, 15.83±0.902, and 13.3±0.68 nm. The researchers pointed out that for the formation of small-sized, pure, and crystalline forms of TiO₂, basic pH would be preferred (Hanafy et al. 2020).

The biosynthesis of titanium dioxide NPs was successfully carried out to study and analyze their photocatalytic properties for Rh B dye (Rhodamine B dye). A mixture was prepared by adding titanium oxyhydroxide to aloe vera gel extracts and was stirred for a day. The light green appearance of the solution indicates the synthesis of TiO₂ nanoparticles. Particles were then dried at 120°C. AFM (atomic force microscopy) confirmed the average size of 80 to 90 nm of titanium dioxide nanoparticles. When the photocatalytic efficiency was tested for Rh B dye, it showed that TiO₂ synthesized by aloe vera had high efficiency (41%) of decolorization for dye, whereas chemically synthesized TiO₂ showed less efficiency with 24% (Nithya et al. 2013).

Aloe vera-derived nickel oxide nanoparticles: Nickel oxide nanoparticles possess ideal catalytic, magnetic, biocompatible, antifungal, and antibacterial properties. They are highly used in solar cell batteries, fuel cells, gas sensors, and various biomedical areas.

An experiment was performed by Ahmad et al. (2022) to synthesize nickel oxide nanoparticles using nontoxic, cost-effective, and eco-friendly aloe vera leaves. In this procedure, Ni $(NO_3)2 \cdot 6H_2O$ was added to the aloe vera extract solution and continued stirring on a hot plate for nearly one hour, from 72°C to 80°C. The collected samples of nickel oxide nanoparticles were washed three times with deionized water and then dried at 80°C. After doing this finally, dried particles were collected in a ceramic crucible and kept at 300°C, 400°C, and 500°C for 1-2 h. XRD characterization estimated that pure and stable cubic crystals of NiO are

obtained at 500°C, and if temperature exceeds 500°C to 600°C then the crystallinity of NiO NPs declined. The results revealed that NiO NPs annealed at 500°C exhibited high antibacterial activity against both gram-positive and gram-negative strains of pathogens and had less antifungal activity (Ahmad et al. 2022).

Aloe vera-derived cerium oxide nanoparticles: Cerium oxide NPs have a range of applications in nano-pharmacy, solar cells, fuel cells, gas sensors, and other polishing objects. CeO₂ is considered an intelligent photosensitizer, helpful in detecting and targeting cancer.

Shetty et al. (2022) synthesized cerium oxide nanoparticles by "low-temperature combustion process" by mixing 4.3 g of cerium nitrate hexahydrate (Ce $(NO_3)_2$ $6H_2O$) to 9 to 10 ml of aloe vera gel solution acting as fuel. Keep the homogenized solution in a furnace at 600°C, which led to yellow dried particles of CeO₂ nanoparticles. SEM and TEM showed the spherical CeO₂ nanoparticles of size about 42 to 50 nm with crystalline structure depicted through the PXRD (powder X-ray diffraction) technique. The author estimated higher antibacterial properties (MIC-2 to 5 μg.mL^{-1}) in order of *S. aureus > E. aerogenes > E. coli* by agar diffusion assay. Whereas antifungal effects (MIC-15 μg.mL^{-1}) are shown in order of *A flavus > A. clavatus > A. niger* (Shetty et al. 2022).

Present experimentation analyses the effectiveness of photodegradation and bactericidal properties of CeO₂-NPs. Purushotham et al. (2021) mixed cerium nitrate to aloe gel extract solution on a magnetic stirrer resulting in the synthesis of cerium oxide NPs. PXRD and UV-vis spectroscopy obtained irregular shapes of particles with sizes of about 13 to 15 nm. The increasing order of antibacterial properties was estimated as P. aeruginosa > E. coli > K. pneumonia. Up to 97% degradation of Indigo Carmine was recorded with UV radiation in one hour. 85% to 89% degradation showed with Blue 4 dye in one hour thirty minutes.

Kanneganti et al. (2014) Reported the same as earlier: synthesized cerium oxide nanoparticles by forming a homogenized mixture of cerium nitrate hexahydrate solution and aloe vera gel broth solution. Calcinate particles for two hours to obtain a fine, pure, and dried powder of particles at around 600°C. Resulted particles were characterized through XRD, FTIR, SEM, and TEM analyzers, and the size of cerium oxide NPs was determined as spherical with an average diameter of 63.6 nm through dynamic scattering assay (Kanneganti et al. 2014).

CHALLENGES AND UPCOMING PROSPECTS

Nanotechnology has enormous benefits through nanoparticle synthesis due to the reasons of their targeted drug delivery, reduced toxic effects, high biocompatibility, and safety. Aloe-assisted NPs are modified by conjugation, functionalization, and control of size to enhance their biomedical applications. Here, in this review article, the roles and the various biological benefits of aloe vera-mediated nanoparticles are highlighted. Some challenging situations are faced with plant extracts during dry or hot climates, as there is a reduction in phytochemicals due to the shedding of leaves. This led to low productivity and no control over shape & size. In the future, the demand for products that are aloe-based silver and zinc NPs is expected to elevate. Also, nowadays, Aloe vera-based Ag NPs are highly used for edible product packaging. So, there's a proper need for assessment of the quality, degradation, and other PK (pharmacokinetic) mechanisms inside the human body. Furthermore, the introduction of GMOs for enhancement in proteins, molecules, and other enzymes will be the key future in green synthesis.

CONCLUSIONS

This review article summarizes a quick study of several nanoparticles, such as silver, gold, zinc oxide, copper oxide, indium oxide, titanium dioxide, nickel oxide, and cerium oxide. Production of these metals or metal oxide nanoparticles using *Aloe vera* extract follows a green method. This one-step process is fast, simple, safe, non-hazardous, low-cost, high-yield approach. Synthesized AV-MNPs (Aloe vera mediated metal nanoparticles) concluded with various biomedical properties, including antifungal, antibacterial, anti-inflammatory, anticancer, antidiabetic, and antioxidant. AV-MNPs are characterized by multiple techniques such as UV-visible spectroscopy, scanning and transmission electron microscopy, X-ray diffraction, photoluminescence, and Fourier transform IR spectroscopy. The average size of nanoparticles synthesized varies with the quantity of aloe vera extract used at different temperatures, deduced by cited references. The conclusion from this review highly prefers

to use of aloe-mediated nanoparticles, mostly silver and zinc, against bactericidal effects. It also prohibits using too much dose of AV-MNPs as it may cause harmful issues. More research is needed to better understand its safety and clinical use. Besides this, long-time stability, and overcoming barriers to improve the delivery of aloe-mediated NPs to targeted sites must be addressed for further research in this area. There is much research literature available on silver, zinc, and nanoparticles, but insufficient works of literature are available on gold, nickel, cerium, and indium nanoparticles synthesized by the aloe vera plant. So, more focus should be required on less explored aloe-mediated nanoparticles and the reason for their restriction towards using their application must be analyzed. In addition to this, there is also a need to investigate the synergistic potency of aloe vera towards various diseases and other microbial infection treatments.

ACKNOWLEDGEMENT

REFERENCES

Abalkhil, T.A., Alharbi, S.A., Salmen, S.H. and Wainwright, M., 2017. Bactericidal activity of biosynthesized silver nanoparticles against human pathogenic bacteria. *Biotechnology and Biotechnological Equipment*, 31(2), pp.411–417. doi.org/10.1080/13102818.2016.12 67594.

Acharyulu, N.P.S., Dubey, R.S., Swaminadham, V., Kollu, P., Kalyani, R.L. and Pammi, S.V.N., 2014. Green synthesis of CuO nanoparticles using *Phyllanthus Amarus* leaf extract and their antibacterial activity against multidrug-resistant bacteria. *IJERT*, 164, pp. 3415-3510

Ahlawat, K.S. and Khatkar, B.S., 2011. Processing, food applications and safety of aloe vera products: a review. *Journal of Food Science and Technology*, *48*, pp.525-533. doi.org/10.1007/s13197-011-0229-z.

Ahmad, B., Khan, M.I., Naeem, M.A., Alhodaib, A., Fatima, M., Amami, M., Al-Abbad, E.A., Kausar, A., et al., 2022. Green synthesis of NiO nanoparticles using *Aloe vera* gel extract and evaluation of antimicrobial activity. *Materials Chemistry and Physics*, 288. doi.org/10.1016/j. matchemphys.2022.126363.

Ahmed, N.K., Abbady, A., Elhassan, Y.A. and Said, A.H., 2023. Green synthesized titanium dioxide nanoparticles from *Aloe vera* extract as a promising candidate for radiosensitization applications. *BioNanoScience*, 13(2), pp.730–743. doi.org/10.1007/s12668-023-01085-2.

Akbar, S., Tauseef, I., Subhan, F., Sultana, N., Khan, I., Ahmed, U. and Haleem, K.S., 2020. doi.org/10.1080/24701556.2019.1711121.

Ali, K., Dwivedi, S., Azam, A., Saquib, Q., Al-Said, M.S., Alkhedhairy, A.A. and Musarrat, J., 2016. *Aloe vera* extract functionalized zinc oxide nanoparticles as nano antibiotics against multi-drug resistant clinical bacterial isolates. *Journal of Colloid and Interface Science*, 472, pp.145–156. doi.org/10.1016/j.jcis.2016.03.021.

Alshatwi, A.A. and Subash-Babu, P., 2016. Aloe-emodin protects RIN-5F (Pancreatic β-cell) cells from glucotoxicity via regulation of pro-inflammatory cytokine and downregulation of Bax and caspase 3. *Biomolecules and Therapeutics*, 24(1), pp.49–56. doi.org/10.4062/biomolther.2015.056.

Altammar, K.A., 2023. A review on nanoparticles: characteristics, synthesis, applications, and challenges. *Frontiers in microbiology*, 14, p.1155622. doi.org/10.3389/fmicb.2023.1155622.

Arshad, H., Saleem, M., Pasha, U. and Sadaf, S., 2022. Synthesis of *Aloe vera*-conjugated silver nanoparticles for use against multidrug-resistant microorganisms. *Electronic Journal of Biotechnology*, 55, pp.55–64. doi.org/10.1016/j.ejbt.2021.11.003.

Baruah, A., Bordoloi, M. and Baruah, H.P.D., 2016. Aloe vera: A multipurpose industrial crop. *Industrial Crops and Products*, 94, pp.951-963.

Basak, P., Majumder, R., Jasu, A., Paul, S. and Biswas, S., 2018. Potential therapeutic activity of bio-synthesized silver nanoparticles as anticancer and antimicrobial agent. *IOP Conference Series: Materials Science and Engineering*, 10, p.1202. doi.org/10.1088/1757-899X/410/1/012020.

Begum, Q. and Mahboob, T., 2019. Evaluation of antioxidant activity of biologically synthesized silver nanoparticles using Aloe vera. *Int J Bio l Biotech*, 16, pp.641-653.

Begum, Q., Kalam, M., Kamal, M. and Mahboob, T., 2020. Biosynthesis, characterization, and antibacterial activity of silver nanoparticles derived from *Aloe barbadensis Miller* leaf extract. *IJB*, 145, p.2383. doi.org/10.30498/IJB.2020.145075.2383.

Behravan, M., Hossein Panahi, A., Naghizadeh, A., Ziaee, M., Mahdavi, R. and Mirzapour, A., 2019. Facile green synthesis of silver nanoparticles using *Berberis vulgaris* leaf and root aqueous extract and its antibacterial activity. *International Journal of Biological Macromolecules*, 124, pp.148–154. doi.org/10.1016/j.ijbiomac.2018.11.101.

Chandran, S.P., Chaudhary, M., Pasricha, R., Ahmad, A. and Sastry, M., 2006. Synthesis of gold nanotriangles and silver nanoparticles using *Aloe vera* plant extract. *Biotechnology Progress*, 22(2), pp.577–583. doi.org/10.1021/bp0501423.

Chaudhary, A., Kumar, N., Kumar, R. and Salar, R.K., 2019. Antimicrobial activity of zinc oxide nanoparticles synthesized from *Aloe vera* peel extract. *SN Applied Sciences*, 1(1), p.144. doi.org/10.1007/s42452-018-0144-2.

Chelu, M., Musuc, A.M., Popa, M. and Calderon Moreno, J., 2023. Aloe vera-based hydrogels for wound healing: Properties and therapeutic effects. *Gels*, 9(7), p.539. doi.org/10.3390/gels9070539.

Dar, A., Rehman, R., Zaheer, W., Shafique, U. and Anwar, J., 2021. Synthesis and characterization of ZnO-nanocomposites by utilizing *Aloe vera* leaf gel and extract of *Terminalia arjuna* nuts and exploring their antibacterial potency. *Journal of Chemistry*, 20, pp.889-894. doi.org/10.1155/2021/9448894.

Das, S., Mishra, B., Gill, K., Ashraf, M.S., Singh, A.K., Sinha, M., Sharma, S. and Xess, I., 2011. Isolation and characterization of a novel protein with anti-fungal and anti-inflammatory properties from *Aloe vera* leaf gel. *International Journal of Biological Macromolecules*, 48(1), pp.38–43. doi.org/10.1016/j.ijbiomac.2010.09.010.

Gericke, M. and Pinches, A., 2006. Microbial production of gold nanoparticles. *Gold Bulletin*, 39(1), pp.22-28.

Grindlay, D. and Reynolds, T., 1986. The Aloe vera phenomenon: a review of the properties and modern uses of the leaf parenchyma gel. *Journal of Ethnopharmacology*, 16(2-3), pp.117-151.

Gunalan, S., Sivaraj, R. and Venckatesh, R., 2012. Aloe barbadensis Miller mediated green synthesis of mono-disperse copper oxide nanoparticles: Optical properties. *Spectrochimica Acta - Part A: Molecular and Biomolecular Spectroscopy*, 97, pp.1140–1144. doi:10.1016/j.saa.2012.07.096.

Hammood, I.A., Nijris, O.N. and Alwan, L.H., 2022. Comparing the effect of zinc oxide nanoparticles biosynthesized by Aloe barbadensis and chemically manufactured on *Klebsiella pneumoniae* isolated from the inflamed middle ear. *International Journal of Health Sciences*, (June, 14), pp.14976–14988. doi:10.53730/ijhs.v6ns2.8964.

Hanafy, M.S., Fadeel, D.A.A., Elywa, M.A. and Kelany, N.A., 2020. Green synthesis and characterization of TiO2 nanoparticles using aloe vera extract at different pH values. *Scientific Journal of King Faisal University*, 21(1), pp.103–110. doi:10.37575/b/sci/2020.

Hashemi, S., Asrar, Z., Pourseyedi, S. and Nadernejad, N., 2016. Plant-mediated synthesis of zinc oxide nanoparticles and their effect on growth, lipid peroxidation, and hydrogen peroxide contents in soybean. *Indian Journal of Plant Physiology*, 21(3), pp.312–317. doi:10.1007/s40502-016-0242-3.

Hashemi, S.A., Madani, S.A. and Abediankenari, S., 2015. The review on properties of Aloe vera in healing of cutaneous wounds. *BioMed Research International*, 2015(1), p.714216.. doi:10.1155/2015/714216.

Iravani, S., 2011. Green synthesis of metal nanoparticles using plants. *Green Chemistry*, 13(10), pp.2638–2650. doi:10.1039/c1gc15386b.

Jettanacheawchankit, S., Sasithanasate, S., Sangvanich, P., Banlunara, W. and Thunyakitpisal, P., 2009a. Acemannan stimulates gingival fibroblast proliferation; expressions of keratinocyte growth factor-1, vascular endothelial growth factor, and type I collagen; and wound healing. *Journal of Pharmacological Sciences*, 109(4), pp.525–531. doi:10.1254/jphs.08204FP.

Jettanacheawchankit, S., Sasithanasate, S., Sangvanich, P., Banlunara, W. and Thunyakitpisal, P., 2009b. Acemannan stimulates gingival fibroblast proliferation; expressions of keratinocyte growth factor-1, vascular endothelial growth factor, and type I collagen; and wound healing. *Journal of Pharmacological Sciences*, 109(4), pp.525–531. doi:10.1254/jphs.08204FP.

Kanneganti, A., Venkateswara Rao, K., Sai Priya, G., Anil Kumar, K., Venkateswara Rao, K. and Bykkam, S., 2014. Bio-Synthesis of Cerium Oxide Nanoparticles using Aloe Barbadensis Miller Gel. *International Journal of Scientific and Research Publications*, 4(6). Pp.641-652

Khatana, C., Kumar, A., Alruways, M.W., Khan, N., Thakur, N., Kumar, D. and Kumari, A., 2021. Antibacterial potential of zinc oxide nanoparticles synthesized using Aloe vera (L.) Burm.f.: A green approach to combat drug resistance. *Journal of Pure and Applied Microbiology*, 15(4), pp.1907-1914. doi:10.22207/JPAM.15.4.12.

Kim, K., Chung, M.H., Park, S., Cha, J., Baek, J.H., Lee, S.Y. and Choi, S.Y., 2018. ER stress attenuation by Aloe-derived polysaccharides in the protection of pancreatic β-cells from free fatty acid-induced lipotoxicity. *Biochemical and Biophysical Research Communications*, 500(3), pp.797-803. doi:10.1016/j.bbrc.2018.04.162.

Koratala, A., Chandra, N.C., Rabiei, Y., Rezvani, Z. and Neshat, S., 2023. Aloe vera applications and Aloe vera-based nanomaterials. *Journal of Renal Endocrinology*, 9, p.e22063. doi:10.34172/jre.2023.22063.

Kumar, P.P.N.V., Shameem, U., Kollu, P., Kalyani, R.L. and Pammi, S.V.N., 2015. Green synthesis of copper oxide nanoparticles using aloe vera leaf extract and its antibacterial activity against fish bacterial pathogens. *BioNanoScience*, 5(3), pp.135–139. doi:10.1007/s12668-015-0171-z.

Kundu, D., Hazra, C., Chatterjee, A., Chaudhari, A. and Mishra, S., 2014. Extracellular biosynthesis of zinc oxide nanoparticles using *Rhodococcus pyridinivorans* NT2: Multifunctional textile finishing, biosafety evaluation and in vitro drug delivery in colon carcinoma. *Journal of Photochemistry and Photobiology B: Biology*, 140, pp.194–204. doi:10.1016/j.jphotobiol.2014.08.001.

Lakshmi, V., Jeeva, R., Sharath, M.N., Chandraprabha, E., Neelufar, H.A. and Patra, M., 2012. Synthesis, characterization, and evaluation of antimicrobial activity of zinc oxide nanoparticles. *Journal of Biochemical Technology*, 3(5), pp.51–54.

Li, X., Xu, H., Chen, Z.S. and Chen, G., 2011. Biosynthesis of

nanoparticles by microorganisms and their applications. *Journal of nanomaterials*, *2011*(1), p.270974. doi:10.1155/2011/270974.

Maensiri, S., Laokul, P., Klinkaewnarong, J., Phokha, S., Promarak, V. and Seraphin, S., 2008. Indium oxide (In2O3) nanoparticles using Aloe vera plant extract: Synthesis and optical properties. *J Optoelectron Adv Mater*, *10*(3), pp.161-165.

Malik, S., Niazi, M., Khan, M., Rauff, B., Anwar, S., Amin, F. and Hanif, R., 2023. Cytotoxicity study of gold nanoparticle synthesis using aloe vera, honey, and gymnema sylvestre leaf extract. *ACS Omega*, 8(7), pp.6325–6336. doi:10.1021/acsomega.2c06491.

Misawa, E., Tanaka, M., Nomaguchi, K., Yamada, M., Toida, T., Takase, M., Iwatsuki, K. and Kawada, T., 2008. Administration of phytosterols isolated from Aloe vera gel reduces visceral fat mass and improves hyperglycemia in Zucker diabetic fatty (ZDF) rats. *Obesity Research and Clinical Practice*, 2(4), pp.239–245. doi:10.1016/j.orcp.2008.06.002.

Mittal, A.K., Chisti, Y. and Banerjee, U.C., 2013. Synthesis of metallic nanoparticles using plant extracts. *Biotechnology advances*, *31*(2), pp.346-356. doi:10.1016/j.biotechadv.2013.01.003.

Mohamed, N. and El-Masry, H.M., 2020. Aloe Vera gel extract and sunlight-mediated synthesis of silver nanoparticles with highly effective antibacterial and anticancer activity. *Journal of Nanoanalysis*, 7(1), pp.73–82. doi:10.22034/jna.2020.1884807.1176.

Muthu, K., Rini, S., Nagasundari, S.M. and Akilandaeaswari, B., 2021. Photocatalytic reduction and antioxidant potential of green synthesized silver nanoparticles from Catharanthus roseus flower extract. *Inorganic and Nano-Metal Chemistry*, 51(4), pp.579–589. doi:10.1080/24701556.2020.1799404.

Nalini, S.P. and Kay, V., 2020. Green synthesis of silver and gold nanoparticles using aloe vera gel and determining its antimicrobial properties on nanoparticle-impregnated cotton fabric. *Journal of Nanotechnology Research*, 02(03). doi:10.26502/jnr.2688-85210015.

Narayanan, M., Natarajan, R.K., Sekar, D.J.G., Paramasivan, R., Srinivasan, B., Ahmad, Z. and Khan, F.S., 2023. Enriched biological activity of copper oxide nanoparticles derived from Aloe vera extract. *Biomass Conversion and Biorefinery,* 23, p.4589. doi:10.1007/s13399-023-04589-9.

Nithya, A., Rokesh, K. and Jothivenkatachalam, K., 2013. Biosynthesis, characterization and application of titanium dioxide nanoparticles. *Nano Vis*, *3*(3), pp.169-174.

Ovais, M., Khalil, A.T., Islam, N.U., Ahmad, I., Ayaz, M., Saravanan, M., Shinwari, Z.K. and Mukherjee, S., 2018. *Applied Microbiology and Biotechnology*, 18, p.146. doi:10.1007/s00253-018-9146-7.

Pradhan, B., 2023. Phytochemistry, pharmacology, and toxicity of *aloe vera*: a versatile plant with extensive therapeutic potential. *Plant Archives*, 23(2), p.056. doi:10.51470/PLANTARCHIVES.2023.v23.no2.056.

Purushotham, B., Surendra, B.S., TR, S.S. and Prashantha, S.C., 2021. Eco-friendly synthesis of CeO2 NPs using Aloe barbadensis Mill extract: Its biological and photocatalytic activities for industrial dye treatment applications. *Journal of Photochemistry and Photobiology*, 7, p.100038. doi:10.1016/j.jpap.2021.100038.

Rabiee, N., Bagherzadeh, M., Kiani, M. and Ghadiri, A.M., 2020. *Rosmarinus officinalis* directed palladium nanoparticle synthesis: Investigation of potential antibacterial, antifungal, and Mizoroki-Heck catalytic activities. *Advanced Powder Technology*, 31(4), pp.1402–1411. doi:10.1016/j.apt.2020.01.024.

Rajakumar, G., Rahuman, A.A., Roopan, S.M., Khanna, V.G., Elango, G., Kamaraj, C., Zahir, A.A. and Velayutham, K., 2012. Fungus-mediated biosynthesis and characterization of TiO2 nanoparticles and their activity against pathogenic bacteria. *Spectrochimica Acta - Part A: Molecular and Biomolecular Spectroscopy*, 91, pp.23–29. doi:10.1016/j.saa.2012.01.011.

Ramírez, O., Pomareda, F., Olivares, B., Huang, Y.L., Zavala, G., Carrasco-Rojas, J., Álvarez, S., Leiva-Sabadini, C., et al., 2024. *Aloe vera* peel-derived nanovesicles display anti-inflammatory properties and prevent myofibroblast differentiation. *Phytomedicine*, 122. doi:10.1016/j.phymed.2023.155108.

Rao Kandregula, G., Ganapathi Rao, K., Ashok, C., Venkateswara Rao, K., Shilpa Chakra, C. and Tambur, P., 2015. Green Synthesis of TiO₂ Nanoparticles Using *Aloe vera* Extract. Available from: https://www.researchgate.net/publication/282502800.

Rehman, A. and Minhas, A.S., 2021. Green Route Synthesis of Copper Oxide Nanoparticles Against MCF-7 Cell Line (Breast Cancer). *NUST Journal of Natural Sciences*, 6(1).

Sangeetha, G., Rajeshwari, S. and Venckatesh, R., 2011. Green synthesis of zinc oxide nanoparticles by *Aloe barbadensis miller* leaf extract: Structure and optical properties. *Materials Research Bulletin*, 46(12), pp.2560–2566. doi:10.1016/j.materresbull.2011.07.046.

Sargazi, S., Laraib, U., Er, S., Rahdar, A., Hassanisaadi, M., Zafar, M.N., Díez-Pascual, A.M. and Bilal, M., 2022. *Nanomaterials*, 12, pp.1102. doi:10.3390/nano12071102.

Sarkar, D.K., Selvanathan, V., Mottakin, M., Islam, M.A., Almohamadi, H., Alharthi, N.H. and Akhtaruzzaman, M., 2023. Phytochemicals assisted green synthesis of copper oxide/cobalt oxide as an efficient electrocatalyst for oxygen evolution reaction. *International Journal of Hydrogen Energy,* 7, pp.042. doi:10.1016/j.ijhydene.2023.07.042.

Sharma, S., Kumar, K., Thakur, N., Chauhan, S. and Chauhan, M. S. 2020. The effect of shape and size of ZnO nanoparticles on their antimicrobial and photocatalytic activities: A green approach. *Bulletin of Materials Science*, 43(1), pp.1-11. doi.org/10.1007/s12034-019-1986-y.

Shetty, A. N., S., K., Desai, K. K. and Patil, S. C. 2022. Green combustion synthesis of CeO2 nanostructure using Aloe vera (L.) Burm f. leaf gel and their structural, optical, and antimicrobial applications. *BioNanoScience*, 12(3), pp.757-765. doi:10.1007/s12668-022-01001-0.

Singh, J.,and Dhaliwal, A. S. 2019. Novel green synthesis and characterization of the antioxidant activity of silver nanoparticles prepared from *Nepeta leucophylla* root extract. *Analytical Letters*, 52(2), pp.213–230. doi.org/10.1080/00032719.2018.1454936.

Song, J. Y., Jang, H. K.,and Kim, B. S. 2009. Biological synthesis of gold nanoparticles using Magnolia kobus and Diopyros kaki leaf extracts. *Process Biochemistry*, 44(10), pp.1133–1138. doi.org/10.1016/j.procbio.2009.06.005.

Tabandeh, M. R., Oryan, A. and Mohammadalipour, A. 2014. Polysaccharides of Aloe vera induce MMP-3 and TIMP-2 gene expression during the skin wound repair of rats. *International Journal of Biological Macromolecules*, 65, pp.424–430. doi.org/10.1016/j.ijbiomac.2014.01.055.

Talukdar, D., Talukdar, P., Luwang, A.D., Sarma, K., Deka, D., Sharma, D. and Das, B. 2023. Phytochemical and nutrient composition of Aloe vera (Aloe barbadensis Miller) in an agro-climatic condition of Mizoram, India. *Asian Journal of Dairy and Food Research*, 17, pp.1-11. doi.org/10.18805/ajdfr.dr-2047.

Tavakoli, S., Kharaziha, M. and Ahmadi, S. 2019. Green synthesis and morphology dependent antibacterial activity of copper oxide nanoparticles. *Journal of Nanostructure*, 9(1), pp.163–171. doi.org/10.22052/JNS.2019.01.018.

Vélez, E., Campillo, G., Morales, G., Hincapié, C., Osorio, J.,and Arnache, O. 2018. Silver nanoparticles obtained by aqueous or ethanolic Aloe vera extracts: an assessment of the antibacterial activity and mercury removal capability. *Journal of Nanomaterials*, 28, pp.1-11. doi.org/10.1155/2018/7215210.

Wu, X., Yin, S., Zhong, J., Ding, W., Wan, J. and Xie, Z. 2012. Mushroom tyrosinase inhibitors from Aloe barbadensis Miller.

Fitoterapia, 83(8), pp.1706-1711. doi.org/10.1016/j.fitote.2012.09.028.

Xiang, H., Cao, F., Ming, D., Zheng, Y., Dong, X., Zhong, X., Mu, D. and Li, B., 2017. Aloe-emodin inhibits Staphylococcus aureus biofilms and extracellular protein production at the initial adhesion stage of biofilm development. *Applied Microbiology and Biotechnology*, 101(17), pp.6671–6681. doi.org/10.1007/s00253-017-8403-5.

Ying, S., Guan, Z., Ofoegbu, P. C., Clubb, P., Rico, C., He, F. and Hong, J. 2022. doi.org/10.1016/j.eti.2022.102336.

Zharov, V.P., Kim, J. W., Curiel, D. T. and Everts, M. 2005. Self-assembling nanoclusters in living systems: application for integrated photothermal nanodiagnostics and nanotherapy. *Nanomedicine: Nanotechnology, Biology, and Medicine*, 1(4), pp.326-345. doi.org/10.1016/j.nano.2005.10.006.

Review Research Paper   https://doi.org/10.46488/NEPT.2025.v24i01.D1684   **Open Access Journal**

A Review on Soil Metal Contamination and its Environmental Implications

Sadaf Hanif[1†], Shaukat Ali[1,2], Asif Hanif Chaudhry[3], Nosheen Sial[4], Aqsa Marium[1] and Tariq Mehmood[1]

[1]Department of Chemistry, Superior University, Lahore, Pakistan
[2]Building Research Station, Communication and Works, Lahore, Pakistan
[3]Geological Survey of Pakistan, Lahore, Pakistan
[4]Government Graduate College for Women, Gulberg, Lahore, Pakistan
†Corresponding author: Sadaf Hanif; sadafzara2407@gmail.com

ABSTRACT

The rapid increase in heavy metal accumulation within soil ecosystems has become a significant concern due to various anthropogenic activities such as industrial processes, agricultural practices, and urbanization. These activities have led to elevated levels of heavy metals like lead, cadmium, mercury, and arsenic in the soil, which, when surpassing permissible limits, pose severe toxicological risks to both human health and plant life. Once heavy metals are introduced into the soil, they can be readily absorbed by plants, subsequently entering the food chain and affecting the metabolic activities of humans and animals consuming these contaminated plants. Although trace amounts of heavy metals are naturally present in the soil, their concentration beyond safe thresholds can lead to deleterious effects, including disruption of enzymatic functions, damage to cellular structures, and interference with essential biological processes. Studies have highlighted that children living in urban and industrial areas are particularly vulnerable to heavy metal exposure, which can result in cognitive impairments, developmental delays, and various other health issues. Furthermore, long-term exposure to these metals can lead to chronic diseases such as cancer, kidney dysfunction, and cardiovascular disorders. Given the escalating threat posed by soil metal contamination, it is imperative to implement stringent management practices aimed at maintaining soil chemistry within safe limits. These practices may include the remediation of contaminated sites, the adoption of sustainable agricultural methods, regular monitoring of soil quality, and the use of phytoremediation techniques to mitigate the impact of heavy metals. Ensuring the safe production of food requires a comprehensive understanding of soil dynamics and the integration of innovative strategies to prevent and control heavy metal pollution. Consequently, addressing this environmental challenge is crucial for safeguarding public health, preserving ecological balance, and promoting sustainable development.

INTRODUCTION

Pollution means the addition of harmful things to the environment. These harmful chemical agents destroy the ecosystem and affect living and non-living creatures. The addition of these chemicals alters the composition of soil.

Soil pollution is not confined to a specific place. It is a global issue nowadays; sustainable development Goals and Millennium development goals by the United Nations are focused on the restoration of soil, focused nowadays on mitigating the heavy metals from soil. The heavy metals present in the soil are damaging the soil's natural environment. Around the world, the focus has been on the detection and removal of heavy metal contamination to ensure food security and zero hunger.

HEAVY METALS PRESENT IN SOIL

The presence of heavy metals in soil can have significant effects on various industries, such as agriculture and archaeology. Deshmukh et al. (2019) emphasized the importance of heavy metal levels in soil for determining irrigation requirements,

crop selection, and fertilizer usage to achieve maximum yield. In a separate study, Qiu et al. (2019) examined the impact of heavy metals on buried cultural artifacts in soil, highlighting the importance of analyzing the spatial distribution and form of heavy metals to understand their effects on historical objects. Additionally, Zhang et al. (2020) discussed the challenges of soil contaminated with both heavy metals and pesticides, emphasizing the necessity for effective remediation strategies and assessment methods. In a recent study by Petruzzelli et al. (2020), they delved into the availability and accessibility of heavy metals in soil, underscoring the significance of examining these aspects to gauge potential risks to humans and the environment. Surprisingly, Besra & Mishra (2020) looked into the effectiveness of myco-remediation in soaking up heavy metals from polluted agricultural soil, proposing that mushrooms could serve as a valuable weapon in combating heavy metal contamination. Moreover, Longhi et al. (2022) debated the emergence of resistance to heavy metals in microorganisms that are exposed to soil, underlining the necessity of addressing the tolerance of bacteria towards heavy metals. Additionally, Deng et al. (2023) pinpointed the factors that govern the dispersion of heavy metals in agricultural soils. It is important to recognize that the quality of soil plays a key role in the levels of heavy metals present. Despite the findings that soil pH and organic matter do not have a significant impact, other soil characteristics are considered to be major factors in the distribution of heavy metals. The research available stresses the significance of recognizing and addressing the presence of heavy metals in soil within a variety of fields, including agriculture, environmental science, and archaeology. Several studies have investigated various aspects of heavy metal pollution in the soil, underlining the necessity for effective remediation plans and assessment techniques to reduce the potential dangers linked with heavy metal contamination.

The purpose of the study was to evaluate the factors affecting metal mobility in soil, identify potentially harmful elements for human health, assess metal accumulation in horticultural crops, and examine the toxicity of naturally occurring chromium in soils and water. The analysis showed high levels of heavy metals, such as chromium and nickel, in vegetables, indicating a transfer of metals from soil to plants. Soil environmental properties are complex, making remediation and treatment difficult and costly. A study by Mandal et al. (2020) discusses progress and future opportunities in biochar composites. Application and reflection in the soil environment are crucial. Sustainable materials such as biomaterials, biochar, and composites offer a practical solution for remediation. The focus is on soil remediation, specifically the removal of heavy metals using biochar-based composites. Moghal et al. (2020) conducted

studies on immobilizing heavy metals and enhancing the geotechnical properties of cohesive soils using the EICP technique. They explored the swelling and permeability characteristics of two native Indian cohesive soils (Black and Red). Experiments were conducted to study the sorption and desorption of heavy metals (Cd, Ni, and Pb) on these soils to understand their response.

The study by Tun et al. (2020) aimed to analyze the levels of toxic heavy metals in the soil of small-scale gold mining sites in Myanmar. The findings revealed elevated concentrations of heavy metals in the soil at these mining locations. The daily intake of metals was found to be below 1, indicating that they were within safe limits for consumption. However, Ahmad et al. (2021) reported higher enrichment concentrations of metals, suggesting that metals were also present in soil and fodder samples near roadsides. Natural zeolite, while containing high impurities, has a limited capacity to stabilize heavy metals in soil due to its single mechanism of heavy metal stabilization. The capacity of soil to stabilize heavy metals is limited. In their study, Ma et al. (2022) aimed to investigate zeolite modification technologies, understand how polymetallic contaminated soil is stabilized, and assess the effectiveness of MZEO for stabilization. Hyperaccumulators release transporters that help move heavy metals from soil to different parts of plants. Yaashikaa et al. (2022) explore the harmful effects of heavy metals on the environment and various phytoremediation methods for transporting and collecting heavy metals from polluted soil. Currently, research on heavy metals in city soil lacks spatial correlation analyses for different heavy metals. Current research on soil heavy metals in cities lacks spatial correlation analysis between different heavy metals and a relative assessment of ecological and health risks. Li et al. (2019) provide technical support for preventing and controlling urban heavy metal pollution. Meanwhile, Atta et al. (2023) study the accumulation of heavy metals in soils, vegetables, and crop plants irrigated with wastewater. They conduct a health risk assessment of heavy metals in Dera Ghazi Khan, Punjab, Pakistan. An investigation is carried out to determine metal concentrations in wastewater, soil, and various plant species. The average values of heavy metals in soil samples fall within the WHO/FAO safe limit, although levels of Cr and Pb stand out were the most frequent (100%) among the metals. The mustard (*Brassica juncea* L.) plant is a well-known and widely accepted hyper-accumulator of heavy metals.

IMPORTANCE OF SOIL QUALITY

The quality of the soil is extremely important for maintaining both agricultural productivity and environmental health. Good quality soil can improve crop yields and make them

more resistant to changes in the climate, resulting in higher overall crop production. To assess soil quality, various factors such as pH levels, organic carbon content, nitrogen levels, phosphorus and potassium levels, and micronutrient levels need to be analyzed. Research has demonstrated that soil quality is affected differently by various types of land use, with agriculture generally producing better quality soil than plantation land. Methods like principal component analysis and assessing common soil parameters can help in the evaluation of soil quality and in determining how to manage and improve it. Soil quality is extremely important for a variety of ecosystems, including agricultural, forest, and disrupted ecosystems like reclaimed mine soils. Studies have indicated that adding organic matter to mine soils may not always lead to long-term improvements in soil quality. In agricultural systems, soil organic carbon (SOC) is known to be vital for maintaining soil health, preserving soil and water quality, and influencing nutrient, water, and biological processes. Developing soil quality indicators is crucial for assessing soil degradation and restoration, as seen in forest soils in southeastern Spain. According to Zornoza et al. (2007), the nitrogen content and bioavailability of litter are key factors in shaping microbial communities in soil ecosystems. In a study conducted in Southern Italy, Muscolo et al. (2014) emphasized the importance of identifying biochemical markers as early signs of changes in soil quality. Additionally, research has shown the significance of the connection between soil organic matter fractions and microbial metabolic diversity in forest ecosystems (Esperschütz et al. 2012). According to research by Tian et al. (2015), the relationship between the quality of litter, soil characteristics, and microbial communities plays a significant role in the priming effect, ultimately impacting the breakdown of organic matter in the soil, as discussed by Fanin et al. (2020). To assess soil quality in controlled experimental environments known as mesocosms, it is necessary to examine a range of chemical, biological, and combined indicators to gauge levels of mineral buildup, potential ecological threats, activity of soil organisms, fertility, and the overall health of the soil. According to a study by Napoletano et al. (2021), cover crops have been proven to enhance soil quality and protect the environment. They do this by reducing nutrient loss, improving soil moisture levels, and increasing organic matter in the soil. Another study by Ogilvie et al. (2021) highlights the significance of interactions between plant roots and soil in cover crop systems.
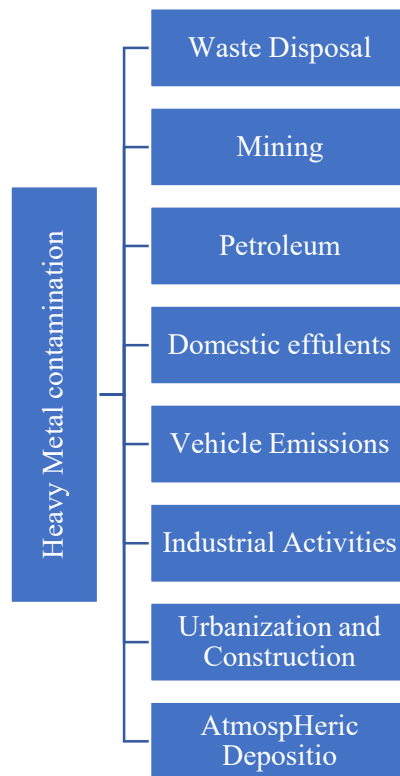
Fig. 1: The sources of heavy metal accumulation in soil matter.

SOURCES OF SOIL CONTAMINATION

Soil contamination with heavy metals has many sources: industrial effluents, sewage untreated water, mining activities, anthropogenic activities, agronomic practices, domestic effluents,

Soil metal contamination can come from a variety of sources and can have lasting effects on soil microbial properties (Fig. 1). A study conducted by Chander et al. (2001) in Lower Saxony, Germany, looked at soils contaminated with sewage sludge, sediment, and debris from mining and factory operations. They observed that the ratio of biomass C to soil C decreased in the order of sludge > sediment > debris contamination, corresponding to the increasing presence of heavy metals. In China, Wang et al. (2003) investigated soil contamination and the uptake of heavy metals by plants in polluted areas, underscoring the impact of heavy metal contamination on plant health. Möller et al. (2004) studied the issue of urban soil pollution in Damascus, Syria. They highlighted the dangers of heavy metal build-up in humans and livestock from directly consuming soil or breathing in dust. Krishna et al. (2008) looked at soil contamination in the Manali Industrial Area in Chennai, Southern India. Sollitto et al. (2010) investigated heavy metal pollution in the Zagreb Region in Northwest Croatia using advanced geostatistics methods. Chandrasekaran et al. (2014) analyzed the levels of heavy metals in the soils of Yelagiri Hills, Tamilnadu, India, investigating both human-made and natural sources. Meanwhile, Zhao et al. (2014) studied soil contamination in China and ways to address it, and Hou et al. (2020) looked at metal pollution in agricultural soils and how bioremediation can promote food safety and sustainability. Additionally, Qin et al. (2020) conducted a detailed examination of heavy metal pollution in Chinese agricultural soils, exploring sources like pesticides, fertilizers, vehicle emissions, coal combustion, sewage irrigation, and mining.

Soil pollution is the addition of harmful agents into the soil; these alter the composition of the soil, which changes the reaction of soil towards something like a change in the pH at low pH. Some elements become toxic, and some element's activity is disturbed due to the change in the pH. Elements show maximum activity at a specific pH. Plant growth is affected by the pH of the soil. The nutrient cycle of the soil is disturbed by the addition of foreign elements. Every element has its side effects when it exceeds its limit. At a certain pH, the leachability of contaminants increases. The World Health Organization has given the range of soil pH between 6 and 7.5.

With time the world is going toward rapid urbanization and advanced agricultural practices. With this advancement in techniques, more and more chemicals are being used that are posing harmful effects on the soil environment. When excess amounts of fertilizers are used, concentrations of heavy metals and other toxic metals are increasing with negative effects on flora and fauna. The ecosystem is destroyed due to such activities. The metals are required in trace amounts to operate in the best manner, but due to the addition of external factors, they are increasing day by day, which is leading to the lethal stage. Heavy metals are present in the earth's biosphere. These metals are lead, mercury, arsenic, and copper; these metals are present in the natural soil in trace quantities. The main source of these elements in the soil is the weathering of materials over time and the accumulation of these heavy metals in the soil. With time, these metals accumulate in the soil, and day by day, the quantity of these metals is increasing, due to which crops and humans are being affected.

IMPACTS ON PLANT GROWTH AND AGRICULTURAL PRODUCTIVITY

The phototoxic effects related to heavy metals are also observed in different studies. According to Nachana'a Timothy et al. (2019), heavy metal accumulation has causing direct effect on plants, and it may change the activity cycle of plants by changing the enzyme activity, affecting plant growth, and directly changing the soil quality. Rojczyk-Gołebiewska et al. (2013) studied the Krebs cycle activity and its effects on the plant concluded that some metals like iron and, manganese, and zinc could affect the activity of the Krebs cycle by inhibiting or promoting some specific enzymes of the cycle. Therefore, it directly affects the energy production of plant cells. The medicinal plants consumed with heavy metal accumulation had even more adverse effects.

Finck (1980) studied the accumulation of zinc and copper-like metals in the soil due to the use of town waste for the fertilization of the soil. Deficiency of heavy metal indeed causes damage to the plant, but it is also not beneficial for the plants to accumulate the heavy metals more than the standard. As far as the agro system is concerned, the fertilizers used increase the productivity of the fruits, but once the heavy metal concentration is increased, its management is difficult. A controlled environment is important for plant growth and human safety.

In animals, bioaccumulation is also causing serious health issues. When the animals eat grass or consume polluted water, heavy metals accumulate in their tissues. When humans consume these animals in the form of meat, these metals enter the human body and affect different organs of the body. For example, in humans, the quantity of Pb lead, even in trace amounts, can retard the growth.

ANTHROPOGENIC ACTIVITIES

Anthropogenic activities are responsible for this heavy metals' accumulation (Tilwankar et al. 2018). Some heavy metals play an important part in the physiological activities of humans as well as plants. The geography of the environment also participates in heavy metal deposition. Some areas are enriched with minerals and metals. It is beneficial until it is at the permissible level of heavy metals Environment protection agencies are fully focused on controlling the heavy metal balance in soil. The environment due to rapid industrialization, the accumulation is increasing robustly (Ali et al. 2015, Karim et al. 2015) reported that due to the growing population, the demand for food is also increasing, as well as more land is required for housing. The cultivating land is reducing day-by-day urbanization. With the growing need for food and less agriculture, such activities are used to enhance the quantity of crops, but unfortunately, the quality of the soil and crop yields are decreasing. The addition of fertilizers, pesticides, sewage water irrigation, and municipal waste disposal GIS is used for getting the source of pollutants. (Buck et al. 1995) found that the excess use of fertilizers causes the deposition of heavy metal accumulation; the study was for cadmium and zinc. It was observed that this accumulation was because of ion exchange, and it also reduces the pH of the soil.

Pesticides

Pesticides are also the cause of soil pollution. Although these are used for the plant's well-being, it has so many worse effects on the soil. Pesticides can damage the plant in different ways. A study reported that it can cause chlorosis, disturb the photosynthesis cycle, and plant leaf pigmentation. It can change the enzyme of the plant. The toxic elements present in pesticides when washed off with rain or while watering the fields, these elements get mixed with soil and constitute a soil component. These elements leech down over time and disturb the nature of the soil. In advanced agricultural practices, the farmers are using pesticides for pest control in excess amounts. These practices are safe for plants, but when it comes to soil, it is harmful to the soil environment. A study in 2007 (Komatsuzaki & Ohta 2007) was conducted on wheat that resulted from the dramatic increase in heavy metals that were due to excessive use of fertilizers and pesticides. Pesticides' toxic content leaches down and gets mixed with the underground water. That underground water is then used for different purposes.

By the passage of time, many studies have shown the heavy metal accumulation in the crop of wheat. Lead and cadmium are the most focused metals for the wheat crop as per their effects. Wang et al. (2011) studied the wheat of Northwest China and concluded that the roots of the wheat plant contain more Cadmium in the plant as compared to the shoot. Ma et al. (2019a) worked on the different zones of soil with higher and lower deposition of heavy metals from the atmosphere and further calculated the results of lead. Afterward, Ma et al. (2019b) worked on the mechanism of lead uptake due to the environmental deposition of heavy metal lead in the wheat crop; this study gave the understanding of the lead uptake from the soil to plant as it is directly related to food security and human health as well.

Petroleum

Petroleum effluents, called sludge of petroleum products, when mixed with the soil, contain many toxic metals as well as other polluting agents. The impact of heavy metal pollution from petroleum activities is a growing concern in various regions of the world. Rusai et al. (2020) conducted a study in Romania to assess the pollution levels of heavy metals and total petroleum hydrocarbons (TPH) in soil and vegetation near oil pipelines and oil wells. The results showed that the concentrations of heavy metals and TPH exceeded the limits, indicating the extent of pollution in the area. Mokarram et al. (2020) focused on the assessment of the water quality of river water in southern Iran, especially the Khor River, due to industrial wastewater. In this study, the water quality index and heavy metal assessment index were used to determine the pollution level at different stations along the river, highlighting the impact of heavy metal pollution on water quality. In a comprehensive review by Priyadarshanee & Das (2020), the potential of metal-resistant bacteria in the biosorption and removal of hazardous heavy metals in wastewater treatment was discussed. This review highlighted the different mechanisms by which bacterial biomass binds different metal ions and highlighted the importance of environmental parameters in the metal removal process. Zheng et al. (2020) conducted a human health risk assessment in the Pearl River Delta urban agglomeration in China, focusing on heavy metal contamination of soil and food crops. This study systematically evaluated the risks associated with heavy metals such as Cd, Cr, Pb, Hg, and As and provided insights into the spatial risk patterns of heavy metal contamination in soils and crops. Yan et al. (2020) discussed phytoremediation as a promising approach for revegetation of heavy metal-contaminated areas and highlighted the mechanisms by which plants absorb, transport, and detoxify heavy metals in contaminated soils. In a study by Li et al. (2020), the effects of co-contamination of heavy metals and TPH on soil bacterial communities were investigated. This study focused on the changes in microbiota in soil contaminated with heavy metals and TPH and revealed the responses of soil microorganisms to

different types of pollution. Overall, the reviewed literature highlights the significant impact of heavy metal pollution from petroleum activities on soil, water, and vegetation in different regions. Research highlights the need for effective remediation strategies and risk assessments to reduce the negative impacts of heavy metal contamination on human health and the environment.

Mining Activities

Mining activities and the expansion of industrial areas are causes of pollution globally. Carbon emission, as well as the effluents of industries, when they enter into the natural water untreated, is destroying the marine ecosystem. Well, when it comes to other sources of water, the heavy metals present in the water leech down and become part of the groundwater table. This polluted groundwater Is then used for irrigating the fields. These heavy metals move into the different parts of the plant. The heavy metals present in the soil are now part of our food chain. Marine food also contains Heavy metal accumulation in their bodies. When these are consumed cause different damages to Human health (Meena 2021). Lead (Pb), Mercury (Hg), cadmium (Cd), nickel (Ni), and arsenic (As) are the most lethal ones. Heavy metals are present in the soil environment naturally, but a little change in its composition can cause serious health effects. The heavy metals do not affect alone. They combine with other elements, either organic or inorganic forms, forming chelates, microfibers, microplastics, and others. The specific forms are more toxic, like dimethyl mercury, which is more toxic in inorganic form.

Root vegetables are used worldwide for their health benefits, like carrots, radishes, parsley, and beetroots (Knez et al. 2022). These are now at risk of eating. These vegetables are consumed widely for their antioxidant properties. Heavy metal contamination is also observed, but microplastic addition is more dangerous. The fragments of fibers deposit into the plant from the soil directly. Entering into the plant system, this fiber travels into other parts of the plants, like fruits and leaves. The consumption of these plastic fibers poses serious health risks. The research was conducted BY (Chary et al. 2008) at Musi River. It was observed that (Zn) zinc chromium, copper and mercury, nickel, and lead were detected in leafy and non-leafy parts of plants. Cattle milk was also analyzed in the results the heavy metals concentration was increased in the urine and blood of individuals due to the consumption of these plants and vegetables as well the cattle milk. The heavy metal addition in soil not only destroys the plant it is also not favorable for soil. These heavy metals accumulate in the parts of plants' roots and shoots as well as in the fruits that we consume. The amount of heavy metals is tolerant to the body up to some extent; when it crosses the lethal dose, it becomes hazardous to human health. The amount of zinc, chromium, and lead was higher in leafy vegetables like spinach and roots.

In medicinal plants, the accumulation of heavy metals is even more alarming. Now, the world is moving again to herbal medicines. The plants have been used for medicinal purposes since the world came into being. Plants are used to treat almost every disease. Studies were conducted at Pretoria to check the amount of heavy metal deposition in the plants that were used to treat cancer. Samples of different places were collected and analyzed. Inductive coupled plasma (ICP-MS) Spectroscopy was used to analyze the quantity of heavy metals. The results showed that all the metals were within the permissible level. As the amount of heavy metal is continuously increasing, prolonged use will create critical issues. In a study conducted to check the heavy metal concentration in vegetables, two vegetables, cabbage and carrots, were selected. Their concentrations were measured, and in the results, all the metals were in high concentration except nickel.

ENVIRONMENTAL IMPACTS

Effects on Soil Microorganisms

Microorganisms are crucial for maintaining the balance in soil ecosystems through nutrient cycling and decomposition processes. However, prolonged exposure to heavy metals can negatively impact these microorganisms. This can result in reduced diversity, activity, and biomass of microbial populations, as well as changes in their composition. Moreover, heavy metals can disrupt important microbial functions like nitrogen fixation and carbon mineralization, causing imbalances in nutrient levels and soil fertility by Sharma et al. (2020). As a consequence, plant productivity may decrease, and overall ecosystem health could be compromised. It is essential to assess the impact of heavy metal accumulation on soil microorganisms.

The addition of heavy metals is increasing day by day due to anthropogenic activities. We are ingesting these heavy metals by different means. Food security is the

Table 1: The amount of metals that are permissible according to WHO and FAO.

Element	The permissible amount of heavy metals(mg/kg)
Cd	0.2
Pb	0.3
Ni	67.9
Fe	425.5
Cu	73.3
Zn	99.4

most concerning agenda. According to Islam et al. (2007), heavy metals are accumulating in the soil, destroying the soil's natural environment; due to anthropogenic activities, bioaccumulation is alarming in the food chain, and human activities like the use of detergents, mining, effluents of industries, vehicle exhaust are the main causes of heavy metal deposition in the soil. The plants uptake the heavy metals from the soil and transport them into the leaves or fruits. Consumption of these vegetables and fruits is causing serious health issues in human life. Belhaj et al. (2016) studied the effect of sewage-irrigated sunflower plants and then compared it to the untread plants and saw a great difference in the heavy metal concentration of chromium, copper, zinc, and nickel. Hu et al. (2018) studied the soil of Southeast China for the study of identification of heavy metals and finding its sources. Heavy metal concentration was noticed after the application of fertilizers to the soil. Moreover, Rai et al. (2019) in the study stated that cadmium and lead present in the soil accumulate in the soil of rice fields. It was also observed that an increase in pH caused the immobilization of heavy metals.

Contamination of Surface Water and Groundwater

Ghosh et al. (2012) in a study revealed that for a long-term application of sewage, untreated water used for agriculture causes heavy metals to transfer into the crops and vegetables further, this study shows that effluents of heavy metals are most important to remove from the water before using it as an agricultural watering. Additionally, Alghobar et al. (2017) reported the heavy metal accumulation in tomatoes irrigated with sewage water in a city of India named Mysore. Xue et al. (2019) studied the heavy metals present in the crops of wheat and maize. This study was conducted in comparison to groundwater and sewage water irrigation. This study gave a special focus on mitigating untreated water of sewage.

In food soil stabilization the accumulation of heavy metals is disturbing the metabolic system of humans as well as directly affecting the mortality rate. Ingestion of heavy metals is causing serious health effects. Soil pollution with heavy metals in China is worse (Yang et al. 2018). This study is a comparison of areas of China from industry and agriculture. Cadmium, lead, and arsenic were more serious in Southeast China more severe than in Northwest China. Children are more affected than adults and old people. As a result, toxic heavy metals transfer into the plant tissues; this accumulation of metals in the plant can have adverse effects on plants as well as humans who eat them. This study showed the effect of heavy metals on the growth of maize plants. The heavy metals cadmium and chromium were observed. Cd was the most toxic. Atomic absorption spectroscopy (AAS) was used for the analysis of samples. It was observed that the affected plants had stunted growth. In another experiment, two heavy metals were added and combined to check the activities that resulted in more adverse. The two metals together were also observed to check the impact. It
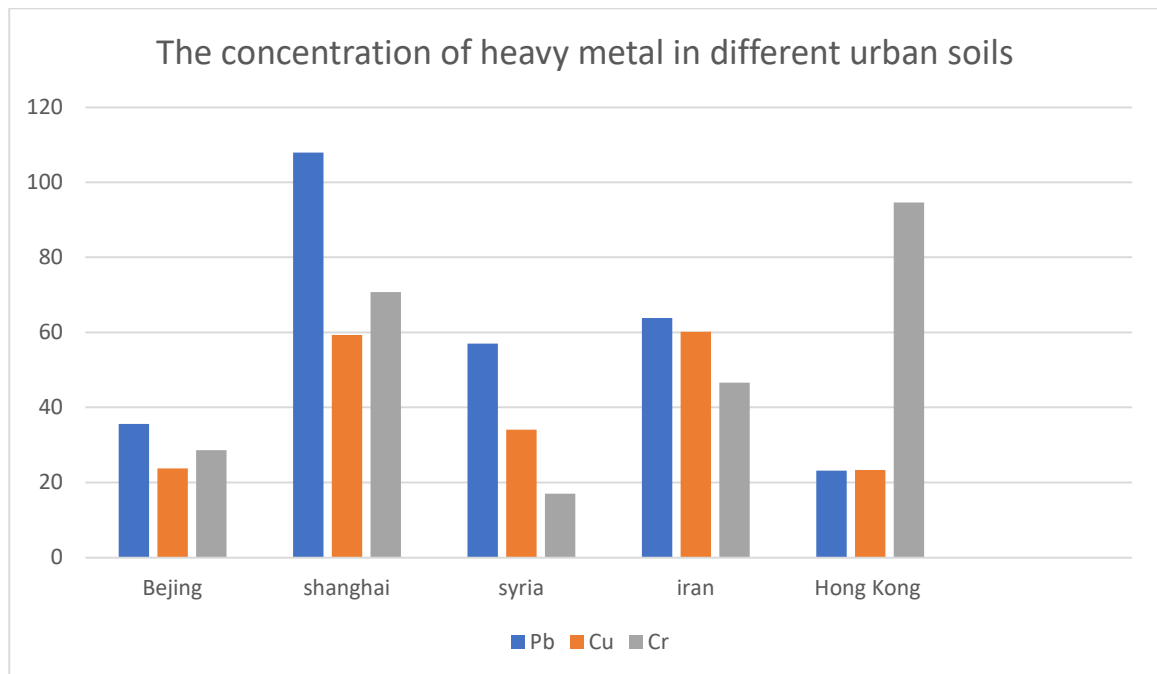
Fig. 2: The concentration of heavy metals in different urban soils.

gave even worse results. The effect observed was that seed protein also decreased.

In another study, the effect of heavy metal accumulation was observed in animal milk. The grazing cattle of river swans consume the vegetation, and the milk produced from that animal is consumed by the population living there (Perveen et al. 2017). Two data sets were analyzed for the heavy metal accumulation from the Swan River. Data A was an upstream area of the Swan River. Data B was downstream of the river swan. Samples of milk were collected from different areas around the Swan River. For the analysis of heavy metal accumulation atomic absorption Spectroscopy was used. After the quantification of data sets it showed that the concentration of heavy metals in the milk is greater in data set B. Zinc metal had the highest concentration, and the lowest was Ni and Pb. In another study (Muhammad et al. 2019), two areas of Baluchistan were selected to check the contamination of heavy metals. This study was conducted to compare Zhou and Lorelei for heavy metal contamination. For checking the contamination Atomic Absorption Spectroscopy was used. The results showed that the concentration of iron was greatest, and Cd was least concentrated in the Zhob area. Fig. 2 shows the concentration of heavy metals in different soils. According to Afzal et al. (2014), the study was conducted to determine the heavy metal accumulation in the soil as well as groundwater. It is reported that the heavy metals iron, nickel, chromium, cadmium, manganese, and zinc were analyzed, and all of them were high, but chromium was the most concentrated, 0.82-2.25 mg.L^{-1}

Heavy metal accumulation is not only confined to soil. Its main source is water that irrigates the fields; the water coming to irrigate the fields is mixed with the effluents of industries that contain loads of heavy metals in the water. This polluted water does not only contain heavy metals but also other more dangerous elements but, in this study, we are focused only on the heavy metals and their effects on plants and human health. Most of the areas are irrigating the fields with the sewage water merged with polluted water from industries. The farmers are not aware of this matter and how this will affect the health of people who consume this unhealthy food. Cereals are the most consuming foods like maize and wheat is most cultivated. A study revealed the amount of lead in wheat; this lead was out of the permissible level of metal (Table 1). The water we drink is also not fit to drink; the air we breathe in also contains the particles that are coming from the vehicle exhaust, the heavy metals are also present in the air. Heavy metals are essential for plants and animals in a permissible amount. Guo et al. (2018) were conducted to check the lead, Arsenic, and Mercury in the wheat; in the results, Cadmium was more in the wheat as compared to lead, and the concentration of metals was most in the roots as compared to the stem and leaf.

After that, according to Asif et al. (2020) study conducted at a well-known industrial area, Hattar, it was observed that all the effluents were directly drained into the waters. It was seen that due to the shortage of water for agriculture, this water is used. This untreated water that is drained into the natural waters from the industries contains an excess of heavy metals. A study reported that two million tons of water is disposed of into natural waters per day. It is destroying the marine aquatic system.

Resources of soil pollution are very diverse. The ecosystem is disturbed by the heavy metal accumulation in the soil due to anthropogenic activities. Sewage-irrigated food that contains heavy metals enters the food chain directly or indirectly. Directly, it enters the body through breathing activity and dermal touch; indirect ways are eating contaminated food and drinking contaminated water. Another study for resource checking was conducted in Kasur, Punjab, Pakistan; the common source of the heavy metal was the leather industry of Kasur, Pakistan (Malik et al. 2010). The study was conducted in Islamabad, Pakistan for the determination of heavy metal accumulation in the soil. The samples were analyzed to check the movement of heavy metals from soil, stem, and roots. The grass species showed the highest concentration of Zn.

EFFECTS ON HUMAN HEALTH

The presence of heavy metals in soil is a serious concern for human health as they can potentially enter the human food chain (Kasraei 1996). The rapid growth of industries, cities, and farming has resulted in an increase in heavy metal pollution in soil, sparking worries about how the metals are spread, their levels in different areas, and their impact on human health (Krishna et al. 2004). Research has found that heavy metal contamination in soil not only harms human health but also has negative effects on agriculture (Jing et al. 2007). Using natural materials like olive husk and cow manure has been studied as a way to decrease the availability of heavy metals in polluted soil. Emphasizing the importance of sustainable farming practices, a study by Clemente et al. (2007) highlighted the need for implementing methods that promote environmental health. Other research conducted by Chopra et al. (2009) has delved into strategies for managing heavy metal pollution in agricultural land to prevent harm to human well-being. Findings from various studies have shown that heightened levels of heavy metals in soil, particularly lead and chromium, can potentially endanger the health of individuals living in industrial and

residential areas. Concerns have been raised specifically regarding the health of children. In a study by Olawoyin et al. (2012), the risks of heavy metal exposure in such regions were underscored. Furthermore, assessments on heavy metal accumulation in crops grown in soil irrigated with treated wastewater have further magnified the urgency of examining the potential health hazards associated with heavy metal exposure. According to a study by Qureshi et al. (2016), the issue of heavy metal contamination in soil, particularly in northern Telangana, India, is a significant concern. Recent research, like the one conducted by Adimalla et al. (2018), has focused on assessing the distribution, contamination levels, and potential health risks associated with heavy metals in surface soils in this region. Additionally, studies have explored phytoremediation mechanisms as a potential way to remove heavy metals from contaminated soil, underscoring the importance of understanding how heavy metals impact human health. Overall, the literature emphasizes the importance of continuous research and the development of effective management strategies to address the impact of heavy metals in soil on human health.

Reports that heavy metals enter into the human body by directly drinking polluted water or indirectly through the food chain, but HM are a source of oxidative source for cells (Lawal et al. 2021). This study showed human health effects. The consumption of metals above the permissible level is causing lung cancer, cerebral palsy, mental retardation, and even gastrointestinal issues. Some of the metals cause genetic disorders, and the DNA by Adduct Formation was observed in this study. The cattle that stray eat from the dumping sites and consume the polluted things that contain heavy metals, too. Eating the meat of these cattle can add HM to the human metabolism (Su et al. 2014). Heavy metals are reported to be the most polluting soil in terms of heavy metals. Mulching is also a source of pollution.

Disruption of Soil Structure and Nutrient Cycling

The addition of heavy metals is disrupting the nutrient cycle. The enzymes of the system are disturbed by the activity of heavy metals. Cd is a heavy metal that affects metabolism in a way that a person becomes calcium deficient. Cd is announced as the 6th most toxic heavy metal.

If we talk about lead (Pd), it can cause damage to the digestive tract. Nickel is the heavy metal that is most lethal. It can even cause tumors in the human body. Waseem et al. (2014) stated that lead intake is causing the high level of lead in the blood. It is reported that it is a reason for hypertension in the population. Constables of Karachi city are more affected than in Islamabad, as in Islamabad, there is less exhaust from vehicles. The school children of

Lahore had effects of Cd, which directly led to the disease of osteotoxic. The metal deposition on soil has direct effects on human health. Metal particles are entering into the human body through the respiratory system through dust particles. It causes breathing disorders as it directly enters the lungs. Heavy metals are entering into the body with dermal contact. It is posing serious allergies and skin irritations.

Analytical Methods for Detection and Monitoring

The removal of heavy metals from the soil is a major environmental issue that requires effective analytical methods. Researchers have proposed various techniques for this purpose. Goltz et al. (1994) discussed using soil vapor extraction (SVE) to eliminate volatile organic compounds from the vadose zone. Buck et al. (1995) recommended physical extraction methods like magnetic separation or aqueous biphasic processes to remove challenging phases such as uranium metaphosphate from soils. Carabias-Martínez et al. (2005) emphasized the use of pressurized liquid extraction (PLE) to extract environmental pollutants from soil samples. In addition, analytical methods like near-infrared reflectance spectroscopy (NIRS) have been studied for predicting different soil properties. In a study by Chang et al. (2001), it was mentioned that soil roughness can affect soil organic carbon assessment when using field spectrometry. Similarly, Denis et al. (2014) also highlighted this impact. Another study by Russell et al. (2016) introduced a fast fluorescence-based technique for screening hydrocarbon contaminants in soil and water samples. These methods are aimed at providing efficient and reliable ways to analyze and eliminate contaminants from soil. Overall, the review of the literature indicates that a combination of analytical methods like SVE, PLE, NIRS, and fluorescence screening can be used effectively to remove heavy metals and other pollutants from soil. More research and innovation in this field are crucial to addressing environmental concerns related to soil pollution.

Getting rid of heavy metals from the soil is a major issue for the environment, and it requires special techniques to do it properly. Qu et al. (2019) looked at how soil minerals, organic matter, and heavy metals interact, underscoring the need to understand how reactions at interfaces can help immobilize them. Chang et al. (2019) introduced a new method called circulation-enhanced electrokinetic (CEEK) using EDTA to remove lead from polluted soil, showing how keeping the pH neutral can help get rid of heavy metals. In a study conducted by Li et al. (2019), investigated a newly discovered bacterium that can both absorb and oxidize Mn (II) to remove heavy metals from the soil. This research points to the promising potential of using microbial-based

methods for soil remediation. Another study by Gnanasundar et al. (2020) delved into the use of electrokinetic and phytoremediation to address inorganic contaminants in the soil. They emphasized the effectiveness of processes like electro-osmosis, electro-migration, and electrophoresis in removing these pollutants. Lastly, a study by Wang et al. (2024) introduced an electro-spun nanofiber membrane treated with amines as a barrier material for remediating Cr (VI) contaminated soil. Their findings showcased the membrane's impressive adsorption capabilities and ability to be reused. In a recent study, Yang et al. (2022) introduced a new method for removing Cd and Cu from agricultural soil using a combination of organic acid solubilization and eluent drainage. This technique is both eco-friendly and effective for soil remediation. Additionally, Bhat et al. (2022) highlighted the potential of phytoremediation in removing heavy metals from soil. They specifically focused on using hyper-accumulator plant species that can tolerate high concentrations of heavy metal contaminants. Inobeme et al. (2023) talked about new developments in tools for measuring heavy metals, emphasizing the need for different methods to get precise results. The research indicates that a mix of advanced analytical tools, like microbial methods, electrokinetics, phytoremediation, and new materials, is crucial for effectively getting rid of heavy metals from soil.

Remediating techniques are also used like ion exchange, ultrafiltration, some membrane processes, and photocatalysis (Abarca 2020). These techniques were introduced, but nowadays, these are used by merging, giving better results. Soil restoration is most focused on researchers nowadays. Different techniques are used to remove heavy metals. It is believed that heavy metals can never be eradicated, but they can be reduced to some extent by using different techniques. Advanced techniques are applied nowadays. For example, soil stabilizers are used to fix the soil. Different kinds of siderophore metal complexes are used to remove metals from soil. This is an advanced technique combined with chelating agents (Hadia-e-Fatima 2018). Several strategies have been used for the remediation of heavy metals from soil. Path evaluation has been used to assess the adsorption of Cd, Cu, Ni, Pb, and Zn with the aid of using soil primarily based totally on elements which include soil pH, CEC, natural carbon content, and clay content. Electrodialytic remediation combines electrodialysis with the electromigration of ions in polluted soil to take away heavy metals (Hu et al. 2018). Phytoextraction, the usage of vegetation like *Brassica napus* and *Raphanus sativus*, has proven capacity for extracting heavy metals from infected soil (Mortvedt 1995). In situ, immobilization of metals has been highlighted as a promising answer for soil remediation that specializes in manipulating the bioavailability of heavy

Country	Cd	Hg	Pb
Austria	-15%	-36%	-51%
Belgium	-52%	-59%	-81%
Bulgaria	-75%	-59%	-65%
Croatia	-35%	-39%	-61%
Cyprus	-62%	-70%	-20%
Czechia	-27%	-38%	-62%
Denmark	-3%	-66%	-29%
Estonia	-11%	19%	-47%
Finland	-41%	-41%	-40%
France	-57%	-65%	-48%
Germany	11%	-52%	-33%
Greece	-83%	-69%	-84%
Hungary	1%	-42%	3%
Ireland	-30%	-31%	-32%
Italy	-49%	-50%	-36%
Latvia	-48%	9%	-98%
Lithuania	-1%	-10%	10%
Luxembourg	-33%	-62%	-36%
Malta	-92%	-81%	-16%
Netherlands	-77%	-54%	-84%
Poland	13%	-17%	0%
Portugal	-27%	-30%	-25%
Romania	-15%	-51%	-36%

○   Decrease as the comparison in 2005.

●   Increase as a comparison in 2005!

Fig. 3: Reduction percentage of heavy metals in comparison of 2021 with 2005.

metals through the usage of soil amendments (Derakhshan Nejad et al. 2018). Phytoremediation, which entails the usage of vegetation to ease up heavy metallic infected soil, has been identified as an environmentally sustainable technique

(Ashraf et al. 2019). Different remediation strategies, which include in situ immobilization, phytoremediation, and organic strategies, have been reviewed for eliminating heavy metals from soil (Dhaliwal et al. 2019). The multidisciplinary technique of phytoremediation entails soil chemistry, plant physiology, and plant-microbiology interactions to ease up heavy metallic infected soil (Shah et al. 2020). Fig.3 shows the reduction of heavy metals in 2021 as compared to 2005. Overall, that research displays diverse, powerful techniques for remediating heavy metals from soil.

CONCLUSIONS

The heavy metals present in the soil are causing serious health effects on humans directly or indirectly. These heavy metals present in soil enter the plant and then persist, entering the food chain. Every metal has different effects. Different studies showed that due to urbanization, industrialization, the addition of fertilizers, and new agricultural practices, environmental effects are the cause of the addition of heavy metals in the soil day by day. Different analytical techniques like SVE, PLE, and NIRS, are being used to determine the heavy metals. However, there is a dire need to focus on maintaining the soil chemistry for the safe production of crops and vegetables. We need to raise awareness among farmers for safe agricultural practices, and public awareness is also necessary for proper waste disposal.

REFERENCES

Abarca, R.R.M., Gaudio, M.T., Chakraborty, S. and Bhattacherjee, P., 2020. Metals toxic pollutants in the environment: anthropogenic and geological causes and remediation. In *Current Trends and Future Developments on (Bio-) Membranes* (pp. 124-109). Elsevier.

Adimalla, N. and Wang, H., 2018. Distribution, contamination, and health risk assessment of heavy metals in surface soils from northern Telangana, India. *Arabian Journal of Geosciences*, 11(21), p.684.

Afzal, M., Shabir, G., Iqbal, S., Mustafa, T., Khan, Q.M. and Khalid, Z.M., 2014. Assessment of heavy metal contamination in soil and groundwater at leather industrial area of Kasur, Pakistan. *CLEAN–Soil, Air, Water*, 42(8), pp.1133-1139.

Ahmad, K., Sana, N., Nazar, S., Khan, Z.I., Bashir, H., Nadeem, M., Akhter, P., Munir, M., Mahmoud, A.H., Mohammed, O.B. and Ashfaq, A., 2020. Assessment of lead and zinc profile from vehicle emission in roadside fodder plants. *Rev Chim*, 71(12), pp.115-130.

Alghobar, M.A. and Suresha, S., 2017. Evaluation of metal accumulation in soil and tomatoes irrigated with sewage water from Mysore city, Karnataka, India. *Journal of the Saudi Society of Agricultural Sciences*, 16(1), pp.49-59.

Ali, Z., Kazi, A.G., Malik, R.N., Naz, M., Khan, T., Hayat, A. and Kazi, A.M., 2015. Heavy metal built-up in agricultural soils of Pakistan: sources, ecological consequences, and possible remediation measures. *Heavy metal contamination of soils: Monitoring and remediation*, pp.23-42.

Ashraf, S., Ali, Q., Zahir, Z.A., Ashraf, S. and Asghar, H.N., 2019. Phytoremediation: Environmentally sustainable way for reclamation of heavy metal polluted soils. *Ecotoxicology and Environmental safety*, 174, pp.714-727.

Asif, M., Sharf, B. and Anwar, S., 2020. Effect of heavy metals emissions on ecosystem of Pakistan. *Indonesian Journal of Social and Environmental Issues (IJSEI)*, 1(3), pp.160-173.

Atta, M.I., Zehra, S.S., Dai, D.Q., Ali, H., Naveed, K., Ali, I., Sarwar, M., Ali, B., Iqbal, R., Bawazeer, S. and Abdel-Hameed, U.K., 2023. Amassing of heavy metals in soils, vegetables and crop plants irrigated with wastewater: Health risk assessment of heavy metals in Dera Ghazi Khan, Punjab, Pakistan. *Frontiers in Plant Science*, 13, p.1080635.

Belhaj, D., Elloumi, N., Jerbi, B., Zouari, M., Abdallah, F.B., Ayadi, H. and Kallel, M., 2016. Effects of sewage sludge fertilizer on heavy metal accumulation and consequent responses of sunflower (Helianthus annuus). *Environmental Science and Pollution Research*, 23, pp.20168-20177.

Besra, M.S. & Mishra, P.K. 2020. Mycoremediation of heavy metals present in contaminated agricultural soil. Dissertation, Vinoba Bhave University.

Bhat, S.A., Bashir, O., Haq, S.A.U., Amin, T., Rafiq, A., Ali, M., Américo-Pinheiro, J.H.P. and Sher, F., 2022. Phytoremediation of heavy metals in soil and water: An eco-friendly, sustainable and multidisciplinary approach. *Chemosphere*, 303, p.134788.

Buck, E.C., Brown, N.R. and Dietz, N.L., 1995. *Analytical electron microscopy characterization of Fernald soils*. Annual report, October 1993-September 1994 (No. ANL41/94-). Argonne National Lab.

Carabias-Martínez, R., Rodríguez-Gonzalo, E., Revilla-Ruiz, P. and Hernández-Méndez, J., 2005. Pressurized liquid extraction in the analysis of food and biological samples. *Journal of Chromatography A*, 1089(1-2), pp.1-17.

Chander, K., Dyckmans, J., Joergensen, R., Meyer, B. and Raubuch, M., 2001. Different sources of heavy metals and their long-term effects on soil microbial properties. *Biology and Fertility of Soils*, 34, pp.241-247.

Chandrasekaran, A., Ravisankar, R., Harikrishnan, N., Satapathy, K.K., Prasad, M.V.R. and Kanagasabapathy, K.V., 2015. Multivariate statistical analysis of heavy metal concentration in soils of Yelagiri Hills, Tamilnadu, India–Spectroscopical approach. *Spectrochimica Acta Part A: Molecular and Biomolecular Spectroscopy*, 137, pp.589-600.

Chang, C.W., Laird, D.A., Mausbach, M.J. and Hurburgh, C.R., 2001. Near-infrared reflectance spectroscopy–principal components regression analyses of soil properties. *Soil Science Society of America Journal*, 65(2), pp.480-490.

Chang, J.H., Dong, C.D., Huang, S.H. and Shen, S.Y., 2020. The study on lead desorption from the real-field contaminated soil by circulation-enhanced electrokinetics (CEEK) with EDTA. *Journal of Hazardous Materials*, 383, p.121194.

Chary, N.S., Kamala, C.T. and Raj, D.S.S., 2008. Assessing risk of heavy metals from consuming food grown on sewage irrigated soils and food chain transfer. *Ecotoxicology and Environmental Safety*, 69(3), pp.513-524.

Chopra, A.K., Pathak, C. and Prasad, G., 2009. Scenario of heavy metal contamination in agricultural soil and its management. *Journal of Applied and Natural Science*, 1(1), pp.99-108.

Clemente, R., Paredes, C. and Bernal, M.P., 2007. A field experiment investigating the effects of olive husk and cow manure on heavy metal availability in a contaminated calcareous soil from Murcia (Spain). *Agriculture, Ecosystems & Environment*, 118(1-4), pp.319-326.

Deng, W., Wang, F. and Liu, W., 2023. Identification of factors controlling heavy metals/metalloid distribution in agricultural soils using multi-source data. *Ecotoxicology and Environmental Safety*, 253, p.114689.

Denis, A., Stevens, A., Van Wesemael, B., Udelhoven, T. and Tychon, B., 2014. Soil organic carbon assessment by field and airborne spectrometry in bare croplands: Accounting for soil surface roughness. *Geoderma*, 226, pp.94-102.

Derakhshan Nejad, Z., Jung, M.C. and Kim, K.H., 2018. Remediation of soils contaminated with heavy metals with an emphasis on immobilization technology. *Environmental Geochemistry and Health*, 40, pp.927-953.

Dhaliwal, S.S., Singh, J., Taneja, P.K. and Mandal, A., 2020. Remediation techniques for removal of heavy metals from the soil contaminated through different sources: a review. *Environmental Science and Pollution Research*, 27(2), pp.1319-1333.

Esperschütz, J., Zimmermann, C., Dümig, A., Welzl, G., Buegger, F., Elmer, M., Munch, J.C. and Schloter, M., 2013. Dynamics of microbial communities during decomposition of litter from pioneering plants in initial soil ecosystems. *Biogeosciences*, 10(7), pp.5115-5124.

Fanin, N., Alavoine, G. and Bertrand, I., 2020. Temporal dynamics of litter quality, soil properties and microbial strategies as main drivers of the priming effect. *Geoderma*, 377, p.114576..

Finck, A., 1980. Limits of heavy metal nutrient fertilization. In *Agrochemicals in Soils* (pp. 368-363). Pergamon.

Ghosh, A.K., Bhatt, M.A. and Agrawal, H.P., 2012. Effect of long-term application of treated sewage water on heavy metal accumulation in vegetables grown in Northern India. *Environmental Monitoring and Assessment*, 184, pp.1025-1036.

Gnanasundar, V.M. and Raj, R.A., 2021. Remediation of inorganic contaminants in soil using electrokinetics, phytoremediation techniques. *Materials Today: Proceedings*, 45, pp.950-956.

Goltz, M.N. and Oxley, M.E., 1994. An analytical solution to equations describing rate-limited soil vapor extraction of contaminants in the vadose zone. *Water Resources Research*, 30(10), pp.2691-2698.

Guo, G., Lei, M., Wang, Y., Song, B. and Yang, J., 2018. Accumulation of As, Cd, and Pb in sixteen wheat cultivars grown in contaminated soils and associated health risk assessment. *International Journal of Environmental Research and Public Health*, 15(11), p.2601.

Hadia-e-Fatima, A.A., 2018. Heavy metal pollution–A mini review. *J Bacteriol. Mycol. Open Access*, 6(3), pp.179-181.

Hou, D., O'Connor, D., Igalavithana, A.D., Alessi, D.S., Luo, J., Tsang, D.C., Sparks, D.L., Yamauchi, Y., Rinklebe, J. and Ok, Y.S., 2020. Metal contamination and bioremediation of agricultural soils for food safety and sustainability. *Nature Reviews Earth & Environment*, 1(7), pp.366-381.

Hu, W., Wang, H., Dong, L., Huang, B., Borggaard, O.K., Hansen, H.C.B., He, Y. and Holm, P.E., 2018. Source identification of heavy metals in peri-urban agricultural soils of southeast China: An integrated approach. *Environmental Pollution*, 237, pp.650-661.

Inobeme, A., Mathew, J.T., Jatto, E., Inobeme, J., Adetunji, C.O., Muniratu, M., Onyeachu, B.I., Adekoya, M.A., Ajai, A.I., Mann, A. and Olori, E., 2023. Recent advances in instrumental techniques for heavy metal quantification. *Environmental Monitoring and Assessment*, 195(4), p.452.

Islam, E.U., Yang, X.E., He, Z.L. and Mahmood, Q., 2007. Assessing potential dietary toxicity of heavy metals in selected vegetables and food crops. *Journal of Zhejiang University Science B*, 8(1), pp.1-13.

Jing, Y.D., He, Z.L. and Yang, X.E., 2007. Role of soil rhizobacteria in phytoremediation of heavy metal contaminated soils. *Journal of Zhejiang University Science B*, 8(3), pp.192-207.

Karim, Z., Qureshi, B.A. and Mumtaz, M., 2015. Geochemical baseline determination and pollution assessment of heavy metals in urban soils of Karachi, Pakistan. *Ecological Indicators*, 48, pp.358-364.

Kasraei, R., Rodríguez-Barrueco, C. and Arroyo, M.I., 1996. The effect of Al and Mn on growth and mineral composition of *Casuarina equisetifolia* Forst. In *Fertilizers and Environment: Proceedings of the International Symposium "Fertilizers and Environment",* held in Salamanca, Spain, 26–29, September 1994 (pp. 75-81). Springer Netherlands.

Knez, E., Kadac-Czapska, K., Dmochowska-Ślęzak, K. and Grembecka, M., 2022. Root vegetables—Composition, health effects, and contaminants. *International journal of environmental research and public health*, 19(23), p.15531.

Komatsuzaki, M. and Ohta, H., 2007. *Soil management practices for sustainable agro-ecosystems,* Sustain. Sci., 2, pp. 103-120. Springer-Verlag.

Krishna, A.K. and Govil, P.K., 2004. Heavy metal contamination of soil around Pali industrial area, Rajasthan, India. *Environmental Geology*, 47, pp.38-44.

Krishna, A.K. and Govil, P.K., 2008. Assessment of heavy metal contamination in soils around Manali industrial area, Chennai, Southern India. *Environmental Geology*, 54, pp.1465-1472.

Lawal, K.K., Ekeleme, I.K., Onuigbo, C.M., Ikpeazu, V.O. and Obiekezie, S.O., 2021. A review on the public health implications of heavy metals. *World Journal of Advanced Research and Reviews*, 10(3), pp.255-265.

Li, D., Li, R., Ding, Z., Ruan, X., Luo, J., Chen, J., Zheng, J. and Tang, J., 2020. Discovery of a novel native bacterium of Providencia sp. with high biosorption and oxidation ability of manganese for bioleaching of heavy metal contaminated soils. *Chemosphere*, 241, p.125039.

Li, Q., You, P., Hu, Q., Leng, B., Wang, J., Chen, J., Wan, S., Wang, B., Yuan, C., Zhou, R. and Ouyang, K., 2020. Effects of co-contamination of heavy metals and total petroleum hydrocarbons on soil bacterial community and function network reconstitution. *Ecotoxicology and Environmental Safety*, 204, p.111083.

Longhi, C., Maurizi, L., Conte, A.L., Marazzato, M., Comanducci, A., Nicoletti, M. and Zagaglia, C., 2022. Extraintestinal pathogenic Escherichia coli: beta-lactam antibiotic and heavy metal resistance. *Antibiotics*, 11(3), p.328.

Ma, C., Liu, F., Hu, B., Wei, M., Zhao, J. and Zhang, H., 2019a. Quantitative analysis of lead sources in wheat tissue and grain under different lead atmospheric deposition areas. *Environmental Science and Pollution Research*, 26, pp.36710-36719.

Ma, C., Liu, F.Y., Hu, B., Wei, M.B., Zhao, J.H., Zhang, K. and Zhang, H.Z., 2019b. Direct evidence of lead contamination in wheat tissues from atmospheric deposition based on atmospheric deposition exposure contrast tests. *Ecotoxicology and Environmental Safety*, 185, p.109688.

Ma, C., Xie, P., Yang, J., Liu, F., Hu, H., Du, J., Zhang, K., Lin, L. and Zhang, H., 2022. Relative contribution of environmental medium and internal organs to lead accumulation of wheat grain. *Science of The Total Environment*, 818, p.151832.

Malik, R.N., Husain, S.Z. and Nazir, I., 2010. Heavy metal contamination and accumulation in soil and wild plant species from industrial area of Islamabad, Pakistan. *Pak J Bot*., 42(1), pp.291-301.

Mandal, S., Pu, S., Adhikari, S., Ma, H., Kim, D.H., Bai, Y. and Hou, D., 2021. Progress and future prospects in biochar composites: Application and reflection in the soil environment. *Critical Reviews in Environmental Science and Technology*, 51(3), pp.219-271.

Meena, O.P. 2021. Heavy metals toxicity and the environment protection. *Journal of Environmental Analytical Chemistry,* 8, pp. 1-4.

Moghal, A.A.B., Lateef, M.A., Abu Sayeed Mohammed, S., Ahmad, M., Usman, A.R. and Almajed, A., 2020. Heavy metal immobilization studies and enhancement in geotechnical properties of cohesive soils by EICP technique. *Applied Sciences*, 10(21), p.7568.

Mokarram, M., Saber, A. and Sheykhi, V., 2020. Effects of heavy metal contamination on river water quality due to release of industrial effluents. *Journal of Cleaner Production*, 277, p.123380.

Möller, A., Müller, H.W., Abdullah, A., Abdelgawad, G. and Utermann, J., 2005. Urban soil pollution in Damascus, Syria: concentrations and patterns of heavy metals in the soils of the Damascus Ghouta. *Geoderma*, 124(1-2), pp.63-71.

Mortvedt, J.J., 1995. Heavy metal contaminants in inorganic and organic fertilizers. *Fertilizer Research*, 43, pp.55-61.

Muhammad, S., Ullah, R. and Jadoon, I.A., 2019. Heavy metals contamination in soil and food and their evaluation for risk assessment in the Zhob and Loralai valleys, Baluchistan province, Pakistan. *Microchemical Journal*, 149, p.103971.

Muscolo, A., Panuccio, M.R., Mallamaci, C. and Sidari, M., 2014. Biological indicators to assess short-term soil quality changes in forest ecosystems. *Ecological Indicators*, 45, pp.416-423.

Nachana'a Timothy, E.T.W., 2019. Environmental pollution by heavy metal: an overview. *Chemistry*, 3(2), pp.72-82.

Napoletano, P., Colombo, C., Di Iorio, E., Memoli, V., Panico, S.C., Ruggiero, A.G., Santorufo, L., Maisto, G. and De Marco, A., 2021. Integrated approach for quality assessment of technosols in experimental mesocosms. *Sustainability*, 13(16), p.9101.

Ogilvie, C.M., Ashiq, W., Vasava, H.B. and Biswas, A., 2021. Quantifying root-soil interactions in cover crop systems: a review. *Agriculture*, 11(3), p.218.

Olawoyin, R., Oyewole, S.A. and Grayson, R.L., 2012. Potential risk effect from elevated levels of soil heavy metals on human health in the Niger Delta. *Ecotoxicology and Environmental Safety*, 85, pp.120-130.

Perveen, I., Raza, M.A., Sehar, S., Naz, I., Young, B. and Ahmed, S., 2017. Heavy metal contamination in water, soil, and milk of the industrial area adjacent to Swan River, Islamabad, Pakistan. *Human and Ecological Risk Assessment: An International Journal*, 23(7), pp.1564-1572.

Petruzzelli, G., Pedron, F. and Rosellini, I., 2020. Bioavailability and bioaccessibility in soil: a short review and a case study. *AIMS Environmental Science*, 7(2).

Priyadarshanee, M. and Das, S., 2021. Biosorption and removal of toxic heavy metals by metal tolerating bacteria for bioremediation of metal contamination: A comprehensive review. *Journal of Environmental Chemical Engineering*, 9(1), p.104686.

Qin, G., Niu, Z., Yu, J., Li, Z., Ma, J. and Xiang, P., 2021. Soil heavy metal pollution and food safety in China: Effects, sources and removing technology. *Chemosphere*, 267, p.129205.

Qiu, L., Zhuang, X., Huang, X., Liu, P. and Zhao, X., 2021. Study on heavy metals' influence on buried cultural relics in soil of an archaeological site. *Environmental Technology*, 42(12), pp.1955-1966.

Qu, C., Chen, W., Hu, X., Cai, P., Chen, C., Yu, X.Y. and Huang, Q., 2019. Heavy metal behaviour at mineral-organo interfaces: Mechanisms, modelling and influence factors. *Environment International*, 131, p.104995.

Qureshi, A.S., Hussain, M.I., Ismail, S. and Khan, Q.M., 2016. Evaluating heavy metal accumulation and potential health risks in vegetables irrigated with treated wastewater. *Chemosphere*, 163, pp.54-61.

Rai, P.K., Lee, S.S., Zhang, M., Tsang, Y.F. and Kim, K.H., 2019. Heavy metals in food crops: Health risks, fate, mechanisms, and management. *Environment International*, 125, pp.365-385.

Rojczyk-Gołębiewska, E. and Kucharzewski, M., 2013. Influence of chosen metals on the citric acid cycle. *Polski Merkuriusz Lekarski: Organ Polskiego Towarzystwa Lekarskiego*, 34(201), pp.175-178.

Rusai, L., Lazar, I., FACIU, E. and Kamari, A., 2020. Assessment of anthropogenic activity impact on the oil-field exploitations near Moinesti city, Bacau County, Romania. *Romanian Biotechnological Letters,* pp. 1143-1150.

Russell, A.L., Martin, D.P., Cuddy, M.F. and Bednar, A.J., 2016. A Rapid, Fluorescence-Based Field Screening Technique for Organic Species in Soil and Water Matrices. *Bulletin of Environmental Contamination and Toxicology*, 96, pp.773-778.

Shah, V. and Daverey, A., 2020. Phytoremediation: A multidisciplinary approach to clean up heavy metal contaminated soil. *Environmental Technology & Innovation*, 18, p.100774.

Sharma, A. and Nagpal, A.K., 2020. Contamination of vegetables with heavy metals across the globe: hampering food security goal. *Journal of Food Science and Technology*, 57, pp.391-403.

Sollitto, D., Romic, M., Castrignanò, A., Romic, D. and Bakic, H., 2010. Assessing heavy metal contamination in soils of the Zagreb region (Northwest Croatia) using multivariate geostatistics. *Catena*, 80(3), pp.182-194.

Su, C., 2014. A review on heavy metal contamination in the soil worldwide: Situation, impact and remediation techniques. *Environmental Skeptics and Critics*, 3(2), p.24.

Tian, J., McCormack, L., Wang, J., Guo, D., Wang, Q., Zhang, X., Yu, G., Blagodatskaya, E. and Kuzyakov, Y., 2015. Linkages between the soil organic matter fractions and the microbial metabolic functional diversity within a broad-leaved Korean pine forest. *European Journal of Soil Biology*, 66, pp.57-64.

Tilwankar, V.T., Swapnil Rai, S.R. and Bajpai, S.P., 2018. A review on contamination profile of heavy metals and its role in environment. *Plant Archives*, 18(2), pp. 1239-1247.

Tun, A.Z., Wongsasuluk, P. and Siriwong, W., 2020. Heavy metals in the soils of placer small-scale gold mining sites in Myanmar. *Journal of Health and Pollution*, 10(27), p.200911.

Wang, D., Wu, D., Wei, A., Gao, J., Pan, C., Mao, Z. and Feng, Q., 2024. Scalable, high flux of electrospun nanofibers membrane for rapid adsorption-reduction synergistic removal of Cr (VI) ions in wastewater. *Separation and Purification Technology*, 360, p.130747.

Wang, J., Yao, Z., Jiang, Y., Xi, B., Ni, S. and Zhang, L., 2021. Aminated electrospun nanofiber membrane as permeable reactive barrier material for effective in-situ Cr (VI) contaminated soil remediation. *Chemical Engineering Journal*, 406, p.126822.

Wang, Q.R., Cui, Y.S., Liu, X.M., Dong, Y.T. and Christie, P., 2003. Soil contamination and plant uptake of heavy metals at polluted sites in China. *Journal of Environmental Science and Health, Part A*, 38(5), pp.823-838.

Wang, Z.W., Nan, Z.R., Wang, S.L. and Zhao, Z.J., 2011. Accumulation and distribution of cadmium and lead in wheat (Triticum aestivum L.) grown in contaminated soils from the oasis, north-west China. *Journal of the Science of Food and Agriculture*, 91(2), pp.377-384.

Waseem, A., Arshad, J., Iqbal, F., Sajjad, A., Mehmood, Z. and Murtaza, G., 2014. Pollution status of Pakistan: a retrospective review on heavy metal contamination of water, soil, and vegetables. *BioMed research International*, 2014(1), p.813206.

Xue, P., Zhao, Q., Sun, H., Geng, L., Yang, Z. and Liu, W., 2019. Characteristics of heavy metals in soils and grains of wheat and maize from farmland irrigated with sewage. *Environmental Science and Pollution Research*, 26, pp.5554-5563.

Yaashikaa, P.R., Kumar, P.S., Jeevanantham, S. and Saravanan, R., 2022. A review on bioremediation approach for heavy metal detoxification and accumulation in plants. *Environmental Pollution*, 301, p.119035.

Yan, A., Wang, Y., Tan, S.N., Mohd Yusof, M.L., Ghosh, S. and Chen, Z., 2020. Phytoremediation: a promising approach for revegetation of heavy metal-polluted land. *Frontiers in Plant Science*, 11, p.359.

Yang, Q., Li, Z., Lu, X., Duan, Q., Huang, L. and Bi, J., 2018. A review of soil heavy metal pollution from industrial and agricultural regions in China: Pollution and risk assessment. *Science of the Total Environment*, 642, pp.690-700.

Yang, S., Li, Y., Si, S., Liu, G., Yun, H., Tu, C., Li, L. and Luo, Y., 2022. Feasibility of a combined solubilization and eluent drainage system to remove Cd and Cu from agricultural soil. *Science of the Total Environment*, 807, p.150733.

Yang, Y., Li, Y.L., Niu, S., Chen, W.P., Wang, T.Q. and Wang, M.E., 2022. Assessing the Lead Accumulation Risks of Wheat Grain by Developing a Source-Specific Accumulation Risk Assessment Model. *Huan Jing ke Xue= Huanjing Kexue*, 43(8), pp.4212-4218.

Zhang, H., Yuan, X., Xiong, T., Wang, H. and Jiang, L., 2020. Bioremediation of co-contaminated soil with heavy metals and pesticides: Influence factors, mechanisms and evaluation methods. *Chemical Engineering Journal*, 398, p.125657.

Zhao, F.J., Ma, Y., Zhu, Y.G., Tang, Z. and McGrath, S.P., 2015. Soil contamination in China: current status and mitigation strategies. *Environmental Science & Technology*, 49(2), pp. 750-759.

Zheng, S., Wang, Q., Yuan, Y. and Sun, W., 2020. Human health risk assessment of heavy metals in soil and food crops in the Pearl River Delta urban agglomeration of China. *Food Chemistry*, 316, p.126213.

Zornoza, R., Mataix-Solera, J., Guerrero, C., Arcenegui, V., Mayoral, A.M., Morales, J. and Mataix-Beneyto, J., 2007. Soil properties under natural forest in the Alicante Province of Spain. *Geoderma*, 142(3-4), pp.334-341.

Original Research Paper   https://doi.org/10.46488/NEPT.2025.v24i01.B4215   **Open Access Journal**

Analysis of CMIP6 Simulations in the Indian Summer Monsoon Period 1979-2014

Lakshmana Rao Vennapu[1†], Krishna Dora Babu Kotti[2], Sravani Alanka[3] and Pavan Krishnudu Badireddi[4]

[1]Department of Meteorology and Oceanography, Andhra University, Visakhapatnam, India

[2]Department of Geography, School of Distance Education, Andhra University, Visakhapatnam, India

[3]Flood Meteorological Office, Meteorological Center Hyderabad, IMD, India

[4]Ideal Institute of Technology, Kakinada, East Godavari, India

†Corresponding author: Lakshmana Rao Vennapu; lakshman.met@gmail.com

ABSTRACT

The monsoon system in India plays a pivotal role in shaping the country's climate. Recent studies have indicated that the increasing variability of monsoons is attributable to climate change, resulting in prolonged periods of drought and excessive rainfall. Understanding, analyzing, and forecasting monsoons is crucial for socioeconomic sustainability and communities' overall well-being. Climate forecasts, which project future Earth climates typically up to 2100, rely on models such as the Couple Model Intercomparison Project (CMIP). However, confidence in these forecasts remains low due to the limitations of global climate models, particularly in terms of capturing the intricacies of monsoon dynamics, notably from June to September. To address this issue, researchers have examined precipitation simulations under various future scenarios using both CMIP5 and the latest CMIP6 models. Evaluating the performance of these models from 1979 to 2014, particularly in simulating mean precipitation and temperature, has revealed improvements in multi-model ensembles (MME), highlighting advancements in monsoon characteristics. By comparing the CMIP5 and CMIP6 models, researchers have identified the most reliable models for climate downscaling research, which can provide more accurate predictions of regional climate changes, thereby offering valuable insights for enhancing climate modeling in the Indian subcontinent.

INTRODUCTION

Over the previous century, there have been notable alterations in the temporal and spatial distributions of worldwide precipitation, increasing both the frequency and intensity of natural calamities (Zhang et al. 2016). Human actions, such as the emission of greenhouse gases and modifications in land usage, have brought about a 1°C elevation in the global mean temperature since the pre-industrial era, inducing extreme weather, oceanic warming, acidification, and modifications in ecosystems, which are anticipated to endure throughout the 21st century. The mean global surface temperature grew by 0.99°C from 1850 to 1900 during the initial two decades of the 21st century (IPCC Report 2021). Alterations in land use and land cover (LULC) affect the physical characteristics of the Earth's surface, thereby regulating the transfer of moisture, kinetic energy, and heat into the atmosphere, consequently influencing localized or regional variations in surface temperatures (Bonan 2008).

India's economy is heavily dependent on the agricultural sector, where the Southwest Monsoon season contributes to 75% of its total rainfall. Fluctuations in monsoon precipitation have a significant impact on various aspects, such as agriculture, the economy, water availability, power production, and ecosystems. Analyzing these variations is crucial for minimizing negative consequences and

anticipating droughts and floods. Alterations in global climate patterns and rising global temperatures could influence the circulation of monsoons. Krishnan (2012) examined the response of the South Asian monsoon (SAM) system to global climate change. Their findings revealed a decline in the strength of the overturning boreal summer monsoon circulation and the southwesterly monsoon flow over the last five decades. This decline has been linked to a reduction in the number of days with moderate-to-heavy monsoon rainfall and upward vertical air movements. If this trend continues, it is projected that by the conclusion of the 21st century, there will be a diminished large-scale monsoon flow, weaker vertical air velocities will weaken, and orographic precipitation in the Western Ghats Mountains will decrease.

The unpredictability and irregularity of monsoons have led to substantial financial losses, damage to individuals and assets, and devastation of agricultural areas and the ecosystem in recent years, prompting concerns regarding food insecurity. Consequently, the prediction and comprehension of monsoon rainfall patterns have emerged as focal points for many Asian nations (Reuter et al. 2013).

Observations of the Indian summer monsoon in central India have revealed a declining trend in rainfall during the latter half of the 20th century (Ramanathan et al. 2005, Bollasina et al. 2011, Mishra et al. 2012, 2014, Jin & Wang 2017). The diminishing pattern of the Indian monsoon is linked to greenhouse gas-induced warming of the sea surface of the Indian Ocean, while simultaneous warming across the Indian subcontinent has been mitigated by aerosols and alterations in land cover (Deser et al. 2010).

Recent studies utilizing global coupled models generally agree that the Indian monsoon precipitation is projected to rise as a result of climate change throughout the 21st century (Chaturvedi et al. 2012, Menon et al. 2013, Lee & Wang 2014, Asharaf & Ahrens 2015, Mei et al. 2015, Sharmila et al. 2015). The sixth phase of the Coupled Model Intercomparison Project (CMIP6) has introduced enhanced global climate models (GCMs) that aim to overcome the limitations of CMIP5 by incorporating advanced physical algorithms. These updated models now incorporate "Shared Socioeconomic Pathways" (SSPs), aligning future radiative forcing scenarios with socioeconomic storylines (Song et al. 2020, Si et al. 2020). It is crucial to comprehend the advantages of the CMIP6 model over the CMIP5 model and assess their accuracy before using their climate predictions in decision-making and policy formulation. In the present work, we evaluate the performance of two generations of climate models, CMIP5 and CMIP6, by comparing their ability to simulate mean precipitation and temperature over the historical period from 1979 to 2014.

Our objective was also to analyze the improvements in the multi-model ensemble (MME) from CMIP6 for monsoon characteristics. Spatial and temporal, we studied the mean precipitation changes interannual and spatially in both generations of the models (CMPI 5 and CMIP 6). This study aimed to assess the enhancements in the CMIP6 MME of monsoon characteristics, focusing on mean precipitation. Apart from this, the study compares projections from seven CMIP5 models and eight CMIP6 models for various atmospheric parameters, such as precipitation, winds, and pressure, especially during the 36-year Southwest Monsoon period over 36 years (1979-2014), both spatially and temporally. Various statistical skill scores, such as Tylor and interannual variability scores, were used for both temporal and spatial analyses of the atmospheric parameters. We specifically compared the ensemble model mean precipitation patterns with the IMD-observed precipitation in the past and present. The major objective of this study was to evaluate the valuation of the performance of two generations of climate models: CMIP5 and CMIP6. For all models in the two generations, mean precipitation overestimated the observed interannual spatial variance.

MATERIALS AND METHODS

In the present study, the monthly data of 7 CMIP5 and 8 CMIP6 models were taken for a period of 36 years from 1979 to 2014 with a horizontal resolution of $2.50° × 2.50°$. For validation of the model simulations, the IMD gridded data were used for evaluation of atmospheric variables temperature and precipitation, while ECMWF reanalysis datasets were used to evaluate the Mean Sea Level Pressure (MSLP) and winds at 850 hPa. Gridded climate data for temperature and precipitation (Pai et al. 2014) is obtained from the India Meteorological Department (IMD). Gridded precipitation dataset from IMD is available at a much finer spatial resolution, i.e., $0.25° × 0.25°$ (Pai et al. 2014) for the period 1979-2014 are used for analysis. Precipitation data from Pai et al. 2014 is used for mapping observed precipitation bias over India for the period 1979-2014. IMD provides gridded temperature data at a resolution of $1° × 1°$ for the period 1951 to 2019. Recently, IMD has also introduced a new temperature data product at $0.5° × 0.5°$ resolution for the limited period of 1980-2019, which roughly translates into 50 Km in length and 50 km in width (Srivastava et al. 2009), which is used for observation.

ERA5 is the fifth generation of ECMWF atmospheric reanalysis of the global climate. ERA5 Climate reanalysis gives a numerical description of the recent climate, produced by combining models with observations. ERA5 combines vast amounts of historical observations into global

estimates using advanced modeling and data assimilation systems. ERA-Interim (Dee et al. 2011) monthly datasets are used for pressure at mean sea level and meridional and zonal winds during the June-September period of 1979-2014 with a spatial resolution of 1×1.CMIP-5 models and CMIP-6 models used for the study are given in Tables 1 and 2, respectively.

The Taylor diagram metric (Taylor 2001) was used to assess the overall performance of each model against the observational performance. Bias correction and panel plotting were performed to compare the model and observations. These were performed using GRADS and FERRET software. Recently, many studies have demonstrated that the Taylor diagram can be used to summarize the relative merits of a collection of different models (Taylor 2001). This study also estimated the required statistical scores for the observed and model data and displayed them using a Taylor diagram. This shows the relative skill of test fields simulated by different models to match the observation in terms of correlation, standard deviation, and centered root-mean-square differences. Ranking CMIP6 models based on their performance in simulating multiple variables over different timeframes is a challenging task because a GCM may show various degrees of accuracy for different variables

and timeframes. Taylor Score, root mean square error, and interannual variability scores in the spatial domain are estimated and displayed in bar diagrams.

RESULTS AND DISCUSSION

Several studies have highlighted the shortcomings of CMIP5 models in consistently overestimating or underestimating monsoon characteristics over South Asia and the Indian subcontinent, depending on different precipitation indices. This inconsistency reduces confidence in future projections. Over the past decade, various statistical and dynamic downscaling approaches (Kannan & Ghosh 2013, Salvi 2013) have been proposed to improve local-scale simulations. However, these approaches have not consistently resulted in significant improvements and sometimes even worse results (Sharma 2018).

Comparative Evaluation of Temperature in the CMIP5 and CMIP6 Models

Fig. 1 shows a Taylor diagram illustrating the ability of global climate models to simulate monthly mean precipitation during the Indian summer monsoon. Eight models were analyzed, with the blue contours representing the root

Table 1: List of CMIP5 models used for the study.

Model ID	Institute	Country	Horizontal resolution	Temporal resolution
GISS-E2-R	The National Aeronautics and Space Administration	USA	$2.50^0 \times 2.50^0$	1979-2014
MPI-ESM-LR	Max Plank Institute For Meteorology	GERMANY	$2.50^0 \times 2.50^0$	1979-2014
ACCESS-1-0	CSIRO Climate Science Centre	AUSTRALIA	$2.50^0 \times 2.50^0$	1979-2014
IPSL-CM5A-LR	Institute for Pierre-Simon Laplace	FRANCE	$2.50^0 \times 2.50^0$	1979-2014
NCAR-CESM2	National Center for Atmospheric Research	USA	$2.50^0 \times 2.50^0$	1979-2014
Had GEM-2-ES	Met Office Hadley Center	UK	$2.50^0 \times 2.50^0$	1979-2014
MIROC 5	University of Tokyo, National Institute for Environmental Studies, and Japan Agency for Marine-Earth Science and Technology (MIROC)	JAPAN	$2.50^0 \times 2.50^0$	1979-2014

Table 2: List of CMIP6 models used for the study.

Model ID	Institute	Country	Horizontal resolution	Temporal resolution
IITM-ESM	Indian Institute of Tropical Meteorology, Pune	INDIA	$2.50^0 \times 2.50^0$	1979-2014
GISS-E2.1-G	The National Aeronautics and Space Administration	USA	$2.50^0 \times 2.50^0$	1979-2014
MPI-ESM-1.2-HAM	Max Plank Institute For Meteorology	GERMANY	$2.50^0 \times 2.50^0$	1979-2014
ACCESS-CM2	CSIRO Climate Science Centre	AUSTRALIA	$2.50^0 \times 2.50^0$	1979-2014
IPSL-CM6A-LR	Institute for Pierre-Simon Laplace	FRANCE	$2.50^0 \times 2.50^0$	1979-2014
NCAR-CESM2	National Center for Atmospheric Research	USA	$2.50^0 \times 2.50^0$	1979-2014
Had GEM3-GC3.1	Met Office Hadley Center	UK	$2.50^0 \times 2.50^0$	1979-2014
MIROC 6	University of Tokyo	JAPAN	$2.50^0 \times 2.50^0$	1979-2014
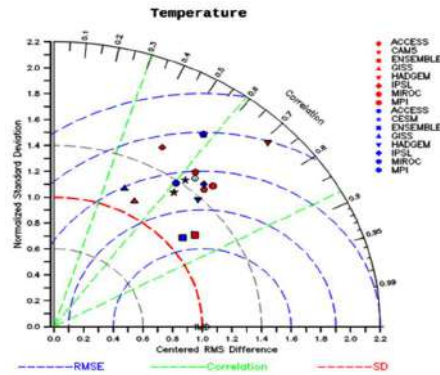
Fig. 1: Taylor diagram displaying a statistical comparison of fourteen CMIP model estimates of the monthly mean surface temperature with observations during the Indian summer monsoon.
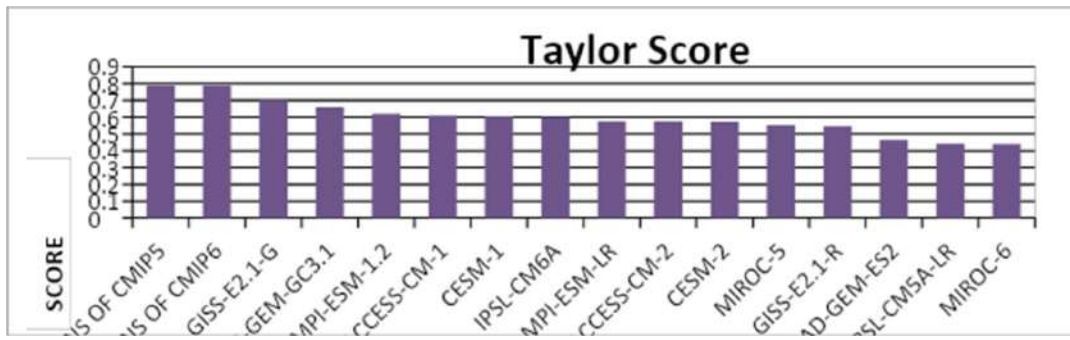
Fig. 2: Taylor score of 14 CMIP5 and CMIP6 models for monthly mean temperatures(1979-2014) compared with IMD temperature (X-axis).

mean square error and the radial distance from the origin representing the standard deviation. Models close to the observation point have high correlation and low RMS errors, whereas models directly at the observation point have the correct standard deviation.

All models overestimated the observed interannual spatial variance. The temperatures of GISS-E2.1-G (CMIP6), GISS-E2-R (CMIP5), and CESM-1 (CMIP5) were very close to the observations, whereas all other models were far from the observation values. Ensembles of both CMIP5 and CMIP6 models showed a high correlation with observations, which is a good representation for modeling. The Taylor Score shows the relative performance of the model. The score is relatively skillful and simulates both the amplitude and pattern of variability (RMSE and Correlation).

From Fig. 2 and Table 3, the Taylor score of GISS-E2.1-G, HAD-GEM-GC3.1, MPI-ESM-1.2 of the CMIP6 models, and ACCESS-CM1 and CESM1 of the CMIP5 models have the highest skill scores, while the other models have low skill scores. A key measure of a climate model's effectiveness is its ability to realistically simulate interannual variability. The Interannual Variability Skill (IVS) metric is used

Table 3: Table showing the skill scores of fourteen CMIP5 and CMIP6 models estimates of the monthly mean temperatures during the Indian summer monsoon.

MODEL	Taylor-score	Interannual Variability Score
ACCESS 1-0	0.3609	0.1114
CESM1-CAM5	0.2892	0.3247
ENS OF CMIP5	0.2052	3.985
GISS-E2-R	0.1442	3.539
HadGEM2-ES	0.3201	0.5404
IPSL-CM5A-LR	0.2399	1.126
MIROC-5	0.3434	0.0018
MPI-ESM-LR	0.2582	1.302
ACCESS-CM2	0.2428	1.322
CESM2-CAM6	0.3184	0.01962
ENS-CMIP5	0.2248	2.797
GISS-E2.1-G	0.338	0.04993
HadGEM3-GC3.1	0.3227	0.1932
IPSL-CM6A-LR	0.3114	0.562
MIROC-6	0.3082	0.1224
MPI-ESM-1.2-HAM	0.2453	1.203
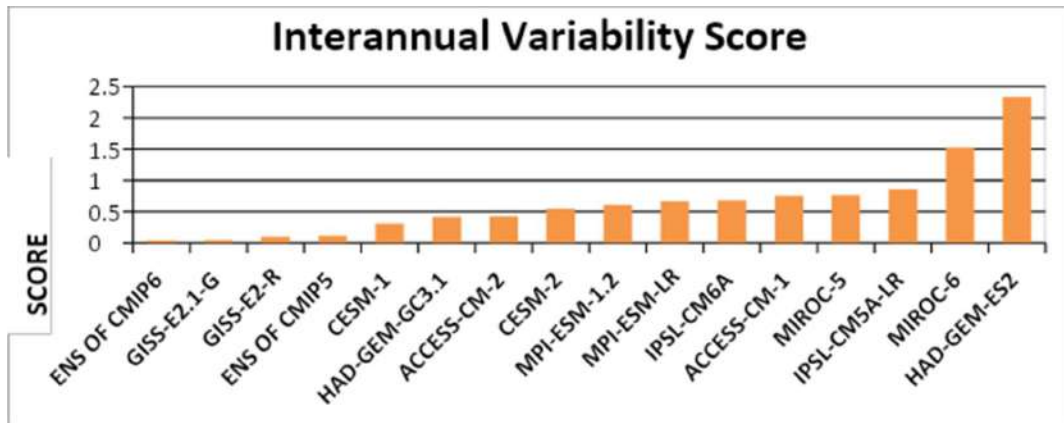
Fig. 3: Interannual variability score (IVS) of CMIP5 and CMIP6 models for monthly mean temperatures (1979-2014) compared with IMD temperature (X-axis).

to evaluate this performance. A smaller IVS value indicates that the model is better at capturing interannual variability.

In Fig. 3, the IVS for GISS-E2.1-G of the CMIP6 and GISS-E2-R models and the CESM1 of the CMIP5 models show the highest skill (low values) compared to the other models.

Comparative Evaluation of Precipitation in the CMIP5 and CMIP6 Models

In Fig. 4 and Table 4, the CMIP5 and CMIP6 models show low correlation values for precipitation compared to the temperatures (Fig. 1). Of all the models, the GISS-E2.1-G, CESM-2 of the CMIP6, and MIROC5 of the CMIP5 model

Table 4: Table showing skill scores of fourteen model estimates of the monthly mean precipitation during Indian summer monsoon.

MODELS	TS	IVS
ACCESS-CM-1	0.3609	0.1114
CESM-1	0.2892	0.3247
ENS-CMIP5	0.2052	3.985
GISS-E2.1-G	0.1442	3.539
HAD-GEM-ES2	0.3201	0.5404
IPSL-CM5A-LR	0.2399	1.126
MIROC-5	0.3434	0.001795
MPI-ESM-1.2	0.2582	1.302
ACCESS-CM-2	0.2428	1.322
CESM-2	0.3184	0.01962
ENS-CMIP6	0.2248	2.797
GISS-E2.1	0.338	0.04993
HAD-GEM-GC3.1	0.3227	0.1932
IPSL-CM6A	0.3114	0.562
MIROC-6	0.3082	0.1224
MPI-ESM-1.2	0.2453	1.203

simulations are coming closer to the observations, which indicates better performance compared to the other models.

In Fig. 5, the Taylor scores of ACCESS-CM-1, MIROC5 of CMIP5, and GISS-E2.1-G of the CMIP6 models are shown as having the highest skill (high values), while the rest of the models have low skill (low values). In Fig. 6, the Interannual Variability Score of MIROC5 of the CMIP5 models and GISS-E2.1-G CESM-2 of the CMIP6 models show high IVS skill scores (low values) compared with the rest of the models.

Evaluation of the CMIP6 Model Skill During the Indian Summer Monsoon

Evaluation of temperature in CMIP6 models: Fig. 7 shows the spatial distribution of temperature (0K) in the CMIP6 models compared to the IMD temperature during 1979-2014. From this Fig., it can be seen that the IITM-ESM,
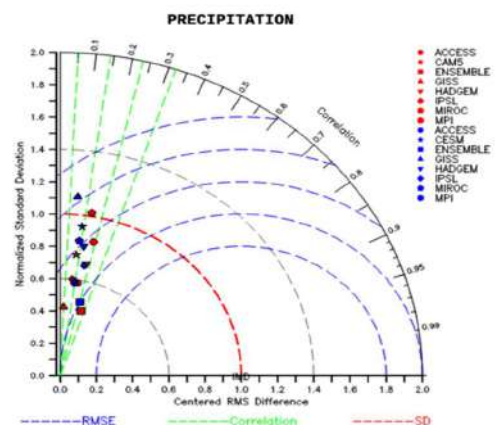
Fig. 4: Taylor diagram displaying a statistical comparison of CMIP5 and CMIP6 model estimates of the monthly mean precipitation with observations during the Indian summer monsoon.
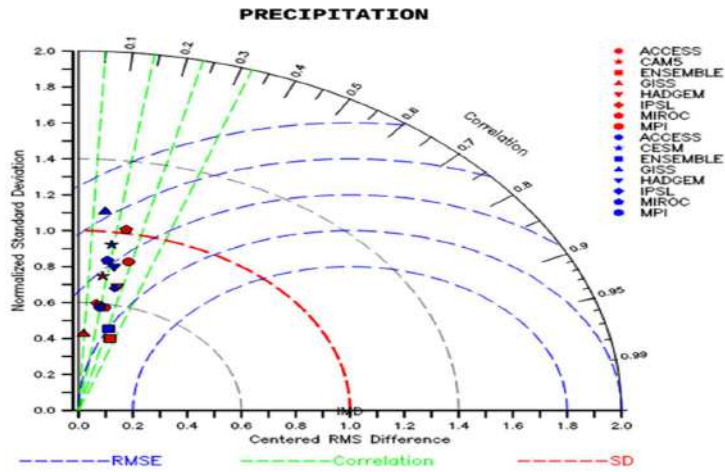
Fig. 5: Taylor scores of 14 CMIP5 and CMIP6 models for monthly mean precipitation (1979-2014) compared with IMD gridded rainfall (X-axis).
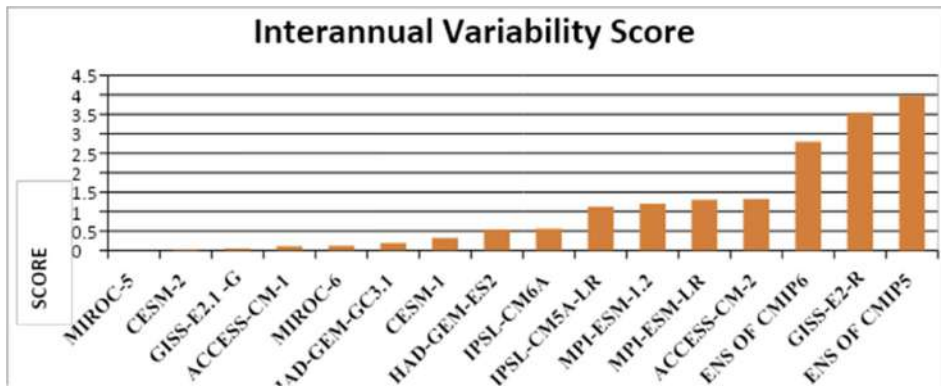
Fig. 6: Interannual variability score (IVS) of CMIP5 and CMIP6 models for monthly mean precipitation (1979-2014) compared with IMD gridded rainfall (X-axis).
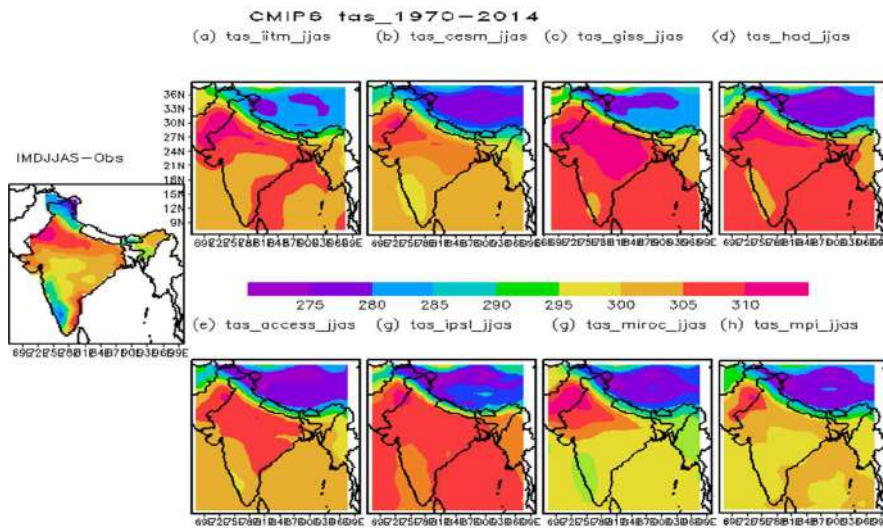
Fig. 7: Spatial distribution of temperature (0K) of 8 CMIP-6 models(a-h) compared to the IMD temperature during 1979-2014.
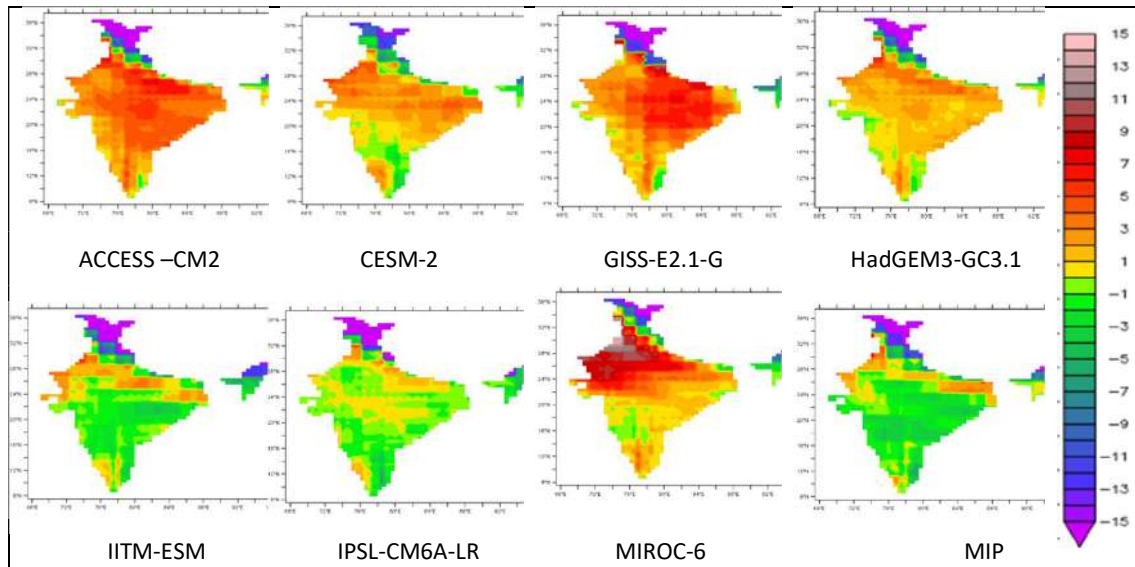
Fig. 8: Temperature biases from observation (IMD) and 8 CMIP-6 models.
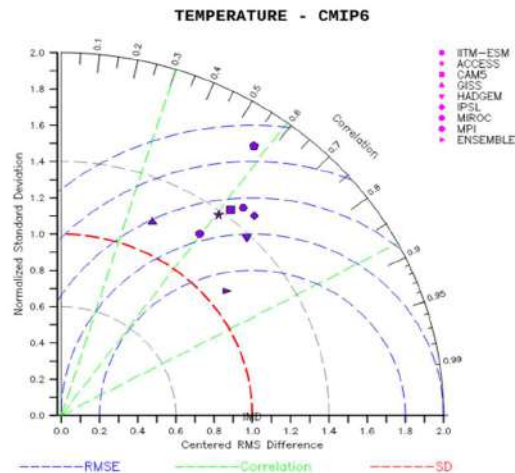
Fig. 9: Taylor diagram of monthly mean temperature variance (JJAS) for observation and 8 CMIP-6 models, the standard deviation is represented by radial distance from the origin, the correlation coefficient is represented by the azimuthal position, and the distance of the test field from observation represents centered root mean square deviation.

CESM-2, MIROC6, and MPI-ESM-LR models fare better than the other models in terms of temperature distribution. From bias plots of temperature (Fig. 8) models, ACCESS, CESM2, GISS-E2-G, and MIROC-6 models overestimated the temperature up to 5-70C, and IITM-ESM, IPSL-CM6A-LR, and MIP models underestimated the temperature up to 30°C. All the models are underestimating the temperature in Jammu and Kashmir, some parts of the northeastern state region, up to 150°C.

The IITM ESM model shows slightly low temperatures over central India and very low temperatures over the Jammu and Kashmir regions as compared with the models. In Fig.

9, the Taylor diagram of the monthly mean temperatures of the models shows that the GISS and IITM-ESM models are close to the observation, and the IITM-ESM and Had GEM models are strongly correlated with the model. The ensemble of the models has an excellent correlation with the observation.

Precipitation in CMIP6 Models: Fig. 10 shows the spatial distribution of precipitation (mm/day)of CMIP6 models compared to the IMD precipitation during 1979-2014. From this Fig., it can be seen that the IITM, CESM, GISS, MIROC, IPSL, MIROC, and MPI models fare better than the other models in terms of rainfall distribution.
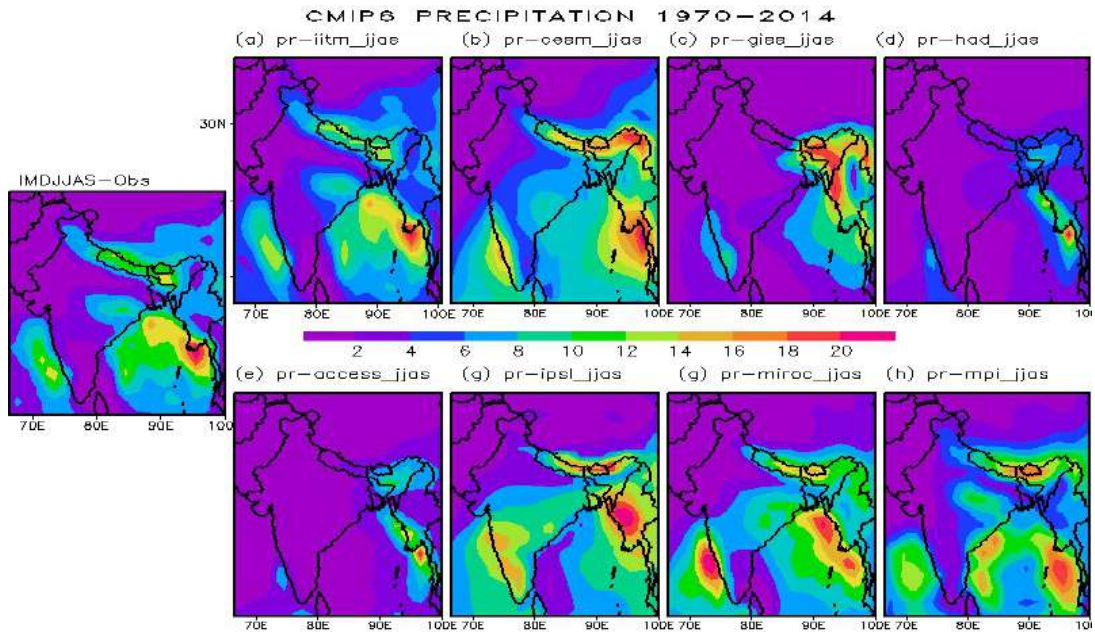
Fig. 10: Spatial distribution of precipitation of 8 CMIP-6 models(a-h) compared to the IMD precipitation during 1979-2014.
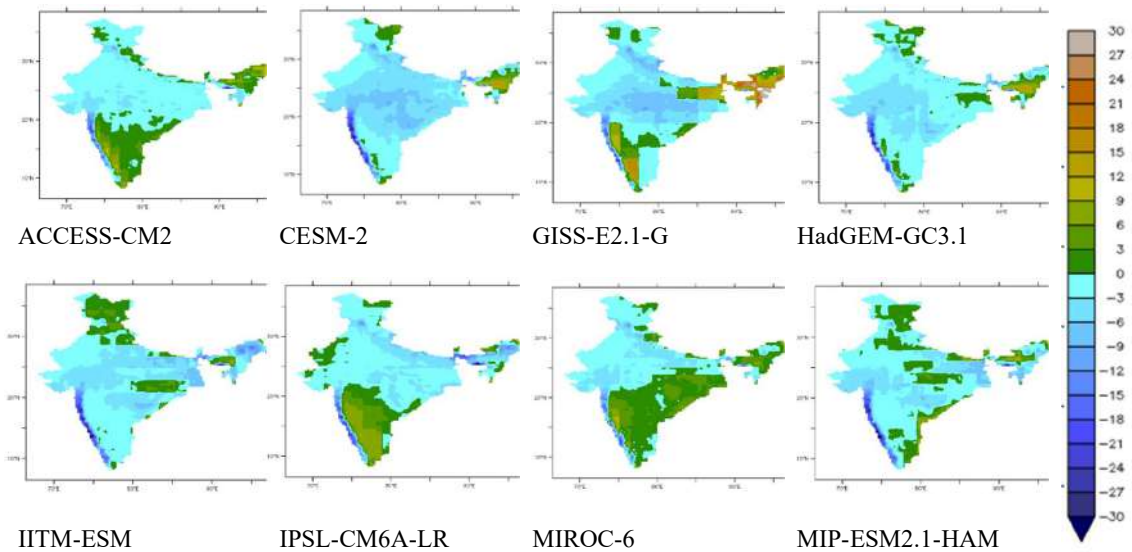
Fig. 11: Precipitation biases from observation (IMD) and 8 CMIP-6 models.

From the Bias plots (Fig. 11), CESM, HADGEM, IITM-ESM, and MPI models underestimate the precipitation up to 3-6mm/day, and ACCESS, GISS, IPSL, MIROC models are overestimating (0-3mm.day^{-1}) over the south peninsular parts of India. IITM model is slightly overestimating in the Jammu and Kashmir regions and underestimating in the western Ghats regions.

CMIP-6 models are simulating the precipitation with low(Positive and Negative) biases, which is a good indication in modeling. Fig. 12 shows the Taylor diagram of the monthly mean precipitation of models, shows that CESM and GISS models are close to the observation but have low correlation, and IITM-ESM shows a higher correlation than all other models.

Pressure at mean sea level in CMIP6 models: The models CESM, GISS, IPSL, and MIROC are performing good simulations when compared with the observation; models IITM, HAD, ACCESS, and MPI are not performing good
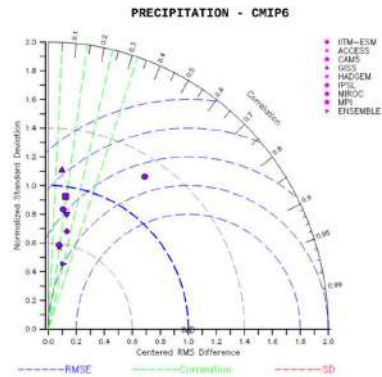
Fig. 12: Taylor diagram of monthly mean precipitation variance (JJAS) for observation(IMD) and 8 CMIP-6 models, the standard deviation is represented by radial distance from the origin, the correlation coefficient is represented by the azimuthal position and distance of the test field from observation represent centered root mean square deviation.
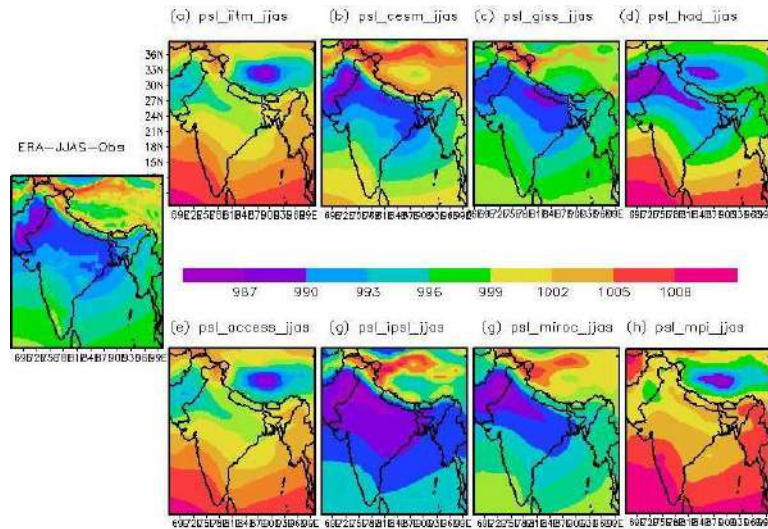
Fig. 13: Panel Plots of monthly means of pressure at mean sea level of observation and 8 CMIP-6 models (a-h).
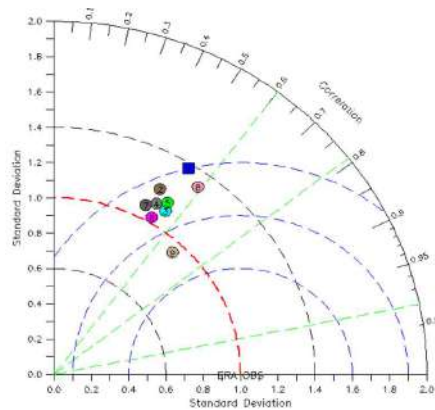
Fig. 14: Taylor diagram of monthly(JJAS)means of pressure at mean sea level (PSL) variance for observation(ERA)and 8 CMIP-6 models; standard deviation is represented by radial distance from the origin, the correlation coefficient is represented by the azimuthal position and distance of the test field from observation represent centered root mean square deviation.
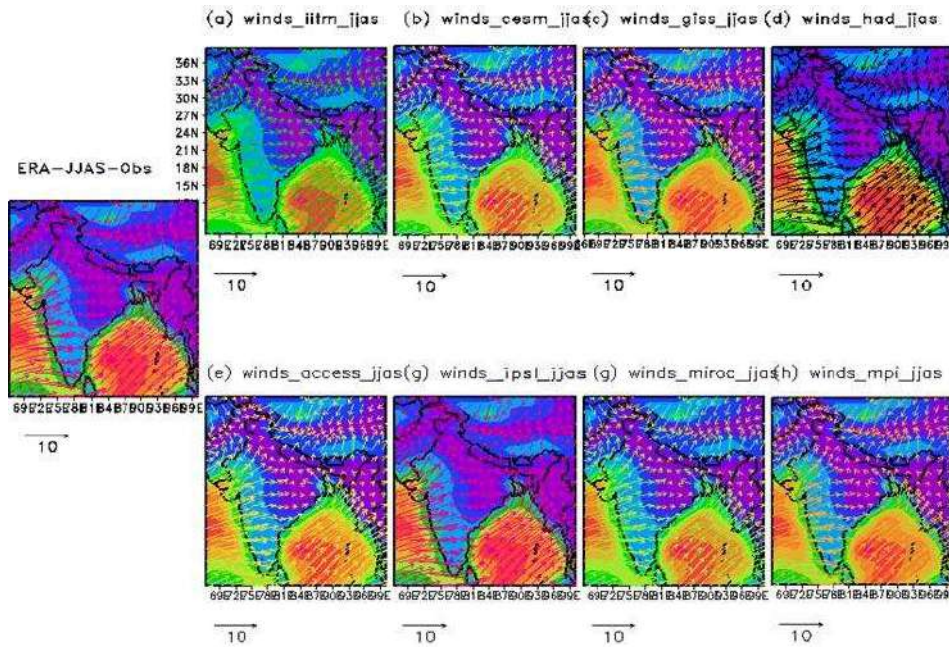
Fig. 15: Plots of Mean Zonal and Meridional winds of observation (ERA) and 8 CMIP-6 models.

U-WIND   **V-WIND**
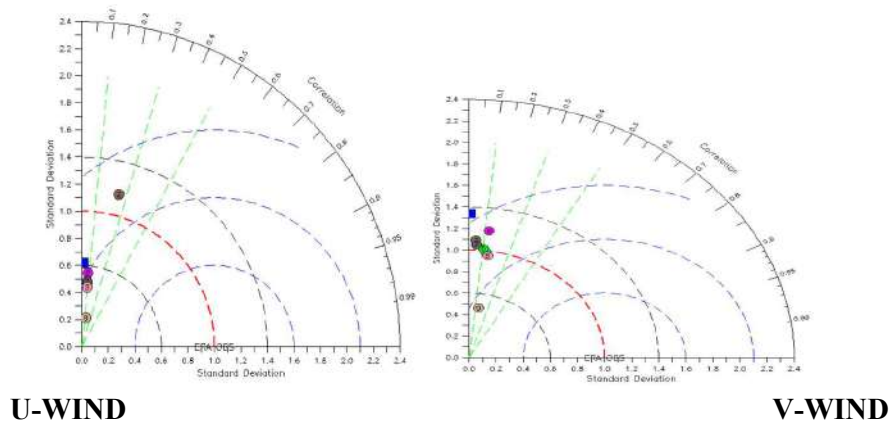
Fig. 16: Taylor diagram for a variance of (a) zonal wind and (b) meridional wind from 8 CMIP6 models.

simulations when compared with the observation obtained from ERA.

Fig. 14 shows the Taylor diagram of monthly mean pressure at mean sea level for the models, showing that CESM, GISS, IPSL, and MIROC are close to the observation.

Wind patterns in CMIP6 models, zonal and meridional: Fig. 15 shows that the models ACCESS, HAD, and IPSL perform better simulations compared with the observation taken from the ERA reanalysis. Figs. 16a & 16b shows the Taylor diagram of U Wind AND V Wind, which shows that all the models' correlation is very low. ACCESS is close to the observation in U-Wind, and ACCESS GISS

CESM MIROC MPI is very close to the observation in V-Wind.

CONCLUSION

The Indian summer monsoon was analyzed using coupled climatological models from 1979 to 2014. Data from the CMIP5 and CMIP6 model datasets, each containing seven models, were downloaded and studied. The IITM-ESM model was also compared with the CMIP-6 model. The main results showed that the CESM1 (CAM5), GISS-E2.1-G, and CMIP5 models showed low correlation values for precipitation and temperatures compared to observations.

The GISS-E2.1-G, CESM-2, and MIROC5 models showed better performance compared to the other models. The Taylor score of the ACCESS-CM-1, MIROC5, and GISS-E2.1-G models had the highest skill level, whereas the Interannual Variability Score of the MIROC5 and GISS-E2.1-G CESM-2 models had the highest IVS skill level. The IITM-ESM, CESM-2, MIROC6, and MPI-ESM-LR models outperformed the other models in terms of temperature distribution. However, the models ACCESS, CESM2, GISS-E2-G, and MIROC-6 overestimate temperatures up to 5-70 C and underestimate temperatures up to 30°C. The IITM ESM model revealed slightly low temperatures in central India and very low temperatures in the Jammu and Kashmir regions. The models performed better in simulations than in observation, with CESM, GISS, IPSL, and MIROC performing better than the IITM, HAD, ACCESS, and MPI models.

The wind patterns in the CMIP6 models were also close to the observations. We found that only a slight improvement occurred in the CMIP6 models but not substantial in the simulation of temperature and precipitation. Upon analyzing the CESM-2 model results, it was found that the model performs better simulations of temperature than the other CMIP-6 models. GISS-E2.1-G is the model that is performing better simulations of precipitation in CMIP6 models. CESM, GISS, IPSL, and MIROC models are performing better simulations of pressure at mean sea level pressure in CMIP-6 models. ACCESS model is performing better simulations of zonal and meridional winds.

The model showed a good response to temperature and precipitation simulations, although there are slight biases that need to be enhanced. However, most studies have focused on the simulation ability of the study region and have overlooked the influence of topography on model performance. The topography of Asia is complex and significant, making it unscientific to ignore regional differences and discuss model applicability. Both equal-weight and non-equal-weight methods were used to average multi-model ensembles and analyze individual models' performance in extreme precipitation regions.

Using the CMIP 6 multi-model ensembles downscaled to the scale at which the crop and livestock would be useful for adaptation planning and investment. Crop and livestock models were run on a site-specific basis to simulate the effects of climate change on relative yield distribution in the farm population. These models can be used to evaluate how system adaptation can alter the impacts of climate change. Changes in planting dates, fertilizer application rates, and irrigation use can be modified in crop models.

REFERENCES

Asharaf, S. and Ahrens, B., 2015. Indian summer monsoon rainfall processes in climate change scenarios. *Journal of Climate*, 28(13), pp.5414-5429

Bollasina, M., Ming, Y. and Ramaswamy, V., 2011. Anthropogenic Aerosols and the Weakening of the South Asian Summer Monsoon. *Journal of Climate*, 24(24), pp.6031-6046.

Bonan, G.B., 2008. Forests and climate change: Forcings, feedbacks, and the climate benefits of forests. *Science*, 320(5882), pp.1444-1449.

Chaturvedi, R.K., Joshi, J., Jayaraman, M., Bala, G. and Ravindranath, N.H., 2012. Multi-model climate change projections for India under representative concentration pathways. *Current Science*, 103(7), pp.791-802.

Deser, C., Alexander, M.A., Xie, S.P. and Phillips, A.S., 2010. Sea surface temperature variability: Patterns and mechanisms. *Annual Review of Marine Science*, 2(1), pp.115-143.

Intergovernmental Panel on Climate Change (IPCC), 2021. The Physical Science Basis. ISBN 978-92-9169-158-6.

Jin, Q. and Wang C., 2017. A revival of Indian summer monsoon rainfall since 2002. *Nature Climate Change*, 7(8), pp.587-594.

Kannan, S. and Ghosh, S., 2013. A Nonparametric Kernel Regression Model for Downscaling Multisite Daily Precipitation in the Mahanadi Basin. *Water Resources Research*, 49, pp.1360-1385.

Krishnan, R., 2012. Conserved features of intermediates in amyloid assembly determine their benign or toxic states. *Proceedings of the National Academy of Sciences of the United States of America*, 109(28), pp.11172-11177.

Lee, J.Y. and Wang, B., 2014. Future change of global monsoon precipitation in the CMIP5. *Climate Dynamics*, 42(1), pp.101-119.

Mei, W., Xie, S.-P., Primeau, F., McWilliams, J.C. and Pasquero, C., 2015. Northwestern Pacific typhoon intensity controlled by changes in ocean temperatures. *Nature Geoscience*, 8(2), pp.140-144.

Menon, A., Levermann, A., Schewe, J., Lehmann, J. and Frieler, K., 2013. Consistent increase in Indian monsoon rainfall and its variability across CMIP-5 models. *Earth System Dynamics*, 4(2), pp.287-300.

Mishra, V., Shah, R. and Thrasher, B., 2014. Soil moisture droughts under the retrospective and projected climate in India. *Journal of Hydrometeorology*, 15(6), pp.2267–2292.

Mishra, V., Smoliak, B.V., Lettenmaier, D.P. and Wallace, J.M., 2012. A prominent pattern of year-to-year variability in Indian Summer Monsoon Rainfall. *Proceedings of the National Academy of Sciences of the United States of America*, 109(19), pp.7213-7217.

Ramanathan, V., Chung, C., Kim, D., Bettge, T., Buja, L., Kiehl, J., Washington, W., Fu, Q., Sikka, D. and Wild, M., 2005. Atmospheric brown clouds: Impacts on South Asian climate and hydrological cycle. *Proceedings of the National Academy of Sciences*, 102, pp.5326–5333.

Reuter, M., Piller, W.E., Harzhauser, M. and Kroh, A., 2013. Cyclone trends constrain monsoon variability during late Oligocene sea level high stands (Kachchh Basin, NW India). *Climate of the Past*, 9(1), pp.1–15.

Salvi, A., 2013. High-resolution multisite daily rainfall projections in India with statistical downscaling for climate change impact assessment.

Sharma, A., Hamlet, A.F., Fernando, H.J.S., Catlett, C.E., Horton, D.E., Kotamarthi, V.R., Kristovich, D.A.R., Packman, A.I., Tank, J.L. and Wuebbles, D.J., 2018. The need for an integrated land☐lake☐atmosphere modeling system, exemplified by North America's Great Lakes region. *Earth's Future*, 6(10), pp.1366-1379.

Sharmila, S., Joseph, S., Sahai, A.K., Abhilash, S. and Chattopadhyay, R., 2015. Future projection of Indian summer monsoon variability under climate change scenario: an assessment from CMIP5 climate models. *Global and Planetary Change*, 124, pp.62–78.

Si, S., Bi, X.Q., Kong, X.H. and Hua, W., 2020. Analysis of the spatiotemporal distribution characteristics of major

greenhouse gases and aerosol emissions intensity in CMIP6 scenarios. *Climate and Environmental Research*, 25, pp.366–384.

Song, Y.J., Li, X.F., Bao, Y., Song, Z., Wei, M., Shu, Q. and Yang, X., 2020. FIO-ESM v2.0 Outputs for the CMIP6 Global Monsoons Model Intercomparison Project Experiments. *Advances in Atmospheric Sciences*, 37, pp.1045-1056.

Taylor, K.E., 2001. Summarizing multiple aspects of model performance in a single diagram. *Journal of geophysical research: atmospheres*, *106*(D7), pp.7183-7192.

Zhang, P., Zang, J. and Chen, M., 2016. Economic impacts of climate change on agriculture: the importance of additional climatic variables other than temperature and precipitation. *Journal of Environmental Economics and Management*, 83(4), pp.91-108.

A Review on Electrooxidation Treatment of Leachate: Strategies, New Developments, and Prospective Growth

R. Priyadarshini Rajesh[iD] **and M. P. Saravanakumar**†[iD]

Department of Environmental and Water Resources Engineering, School of Civil Engineering, Vellore Institute of Technology, Vellore-632 014 Tamil Nadu, India

†Corresponding author: M.P. Saravanakumar; mpsaravanakumar@vit.ac.in

ABSTRACT

Improper disposal of landfill leachate, a highly polluted wastewater, can harm living beings and the ecosystem. Of all the treatment technologies available, electrochemical techniques have the most advantages in terms of ease of use, affordability, and the ability to degrade various contaminants found in landfill leachate effectively. Though there are a sufficient number of research articles regarding the electrochemical treatment of leachate, it has many research gaps, such as a study on the mechanism of radicle generation, pollutant degradation, study on different electrodes with various pollutants concentrations, application of green catalysts, byproduct formation assessment, energy recovery, etc. This review article explores the applications of electrooxidation techniques for the treatment of landfill leachate. Key aspects discussed include the (i) fundamental concepts in electrochemical treatment and its mechanism, (ii) factors affecting the electrochemical treatment efficiency, (iii) the applicability of leachate treatment with different electrochemical methods, (iv) recent advances, (v) merits, and demerits and (vi) proposal of future scope and the studies needed. The integration of electrooxidation with other treatment processes and the challenges hindering widespread adoption are also addressed. Overall, electrooxidation demonstrates promise as an effective and sustainable method for managing landfill leachate. Consequently, this article directs chacurrent and future research efforts toward optimizing the leachate treatment through electrooxidation techniques.

INTRODUCTION

Uncontrolled increases in population and industrial production generate masses of solid trash, which is primarily dumped in landfills (Choden et al. 2022, Hadi 2023). In many nations, landfills are the principal technique for disposing of solid trash because it is inexpensive and simple (Gautam et al. 2019, Mohajeri et al. 2010, Mor & Ravindra 2023, Umar et al. 2010). Landfills produce leachate, which has a major impact on living beings and ecological health if improperly handled and disposed of (Baiju et al. 2018, Seibert et al. 2019c). It contains a high range of chemical oxygen demand (COD), ammonia, biochemical oxygen demand (BOD), metal ions, endocrine disruptors, antibiotics, pesticides, microplastics, xenobiotics, and refractory compounds which are carcinogenic and mutagenic even in small concentrations (Deng et al. 2020, Eggen et al. 2010, El-Saadony et al. 2023, Ghosh et al. 2017, Seibert et al. 2019c, Torretta et al. 2017). The contaminants in leachate also include chlorinated aliphatics, aromatic compounds, fatty acids, higher alkanes, phenolic compounds, polyaromatic hydrocarbons, nonylphenol ethoxy carboxylate acids, polychlorinated dibenzofurans, dibenzo-p-dioxins, polychlorinated phthalates, biphenyls, emerging pollutants from personal care product (PCP) & pharmaceutical industries and perfluorinated compounds, pollutants that primarily pertain to the 126 contaminants of priority designated by the US EPA (Eggen et al. 2010, Jin et al. 2022, Oturan et al. 2015). Additionally, it is also expected to

have a few unidentified and unanticipated contaminants (Ding et al. 2021). The leachate composition greatly varies with the type of landfill, precipitation, compaction method, waste composition, age, weather, and its contact with the environment. The strategy of treatment used is mostly influenced by the characteristics and chemical constituents of leachate (Khalil et al. 2018, Pieus Thanikkal & Pooppana Antony 2021, Samadder et al. 2017). For example, biological techniques help treat young leachates with a high BOD_5/COD ratio (Desireddy et al. 2020, Manasa & Mehta 2021). Because biological treatment is more dependable, easy to use, and economical, it is usually used to treat leachate that has high BOD_5 concentrations (del Amo et al. 2023, Ilmasari et al. 2022b, 2022a). However, leachates with a low BOD_5/COD ratio and a high concentration of hazardous components are considered suitable for physicochemical treatment techniques (Clemente et al. 2024, Kanmani & Dileepan 2023, Lei et al. 2023, Umar et al. 2010). So, the leachate pollutant characteristics are mostly signified by its presence of COD, BOD, and ammonia (Renou et al. 2008). The microbial distribution and its toxicity in leachate are rarely encountered (Deng & Englehardt 2006a).

Numerous approaches to leachate treatment have been documented, including leachate reuse, treating alongside household leachate, and utilizing physicochemical procedures like coagulation, adsorption, chemical oxidation, precipitation, air stripping, membrane process, and plasma technology (Deng et al. 2019, Kuang et al. 2023, Mathew & Saravanakumar 2023, Torretta et al. 2017). Various aerobic and anaerobic biological treatments are also reported as standalone, pre-treatment, and post-treatment (Li et al. 2023, Mishra et al. 2023, Seibert et al. 2019a, Yan et al. 2023). AOPs can convert non-biodegradable contaminants into harmless, biodegradable compounds (Mohajeri et al. 2010). Though several treatment methods are available, each method has disadvantages in terms of cost and efficiency. In the past twenty years, researchers have become interested in electrochemical oxidation due to its wide range of applications, low environmental impact, straightforward design and operation, ease of adjusting pressure, applied voltage and temperature, automation capabilities, breakdown of refractory organics, low sludge production, and complete mineralization (Deng et al. 2019, Mandal et al. 2017, Narenkumar et al. 2023). Electrochemical
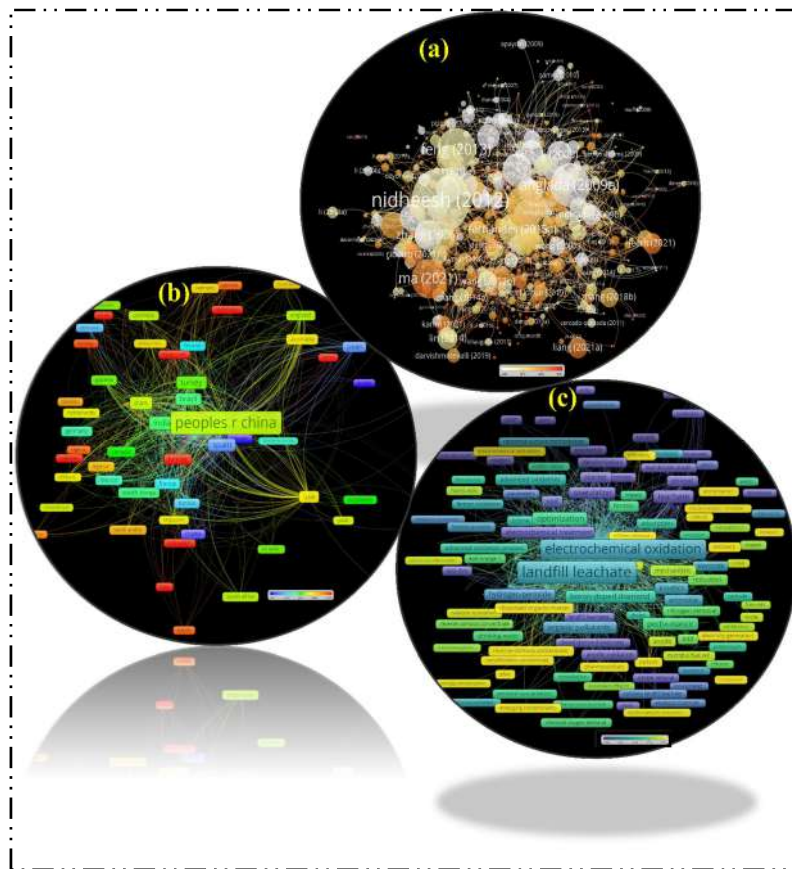
Fig. 1: Web of Science search result for keywords electrochemical oxidation and leachate Vos viewer's overlay visualization of (a) year-wise author citations, (b) country-wise number of publications, and (c) keyword co-occurrence searched on 31st March 2024.

oxidation techniques are well suited to treating wastewater with high salinity and conductivity (Alam et al. 2022). Because of this, the electro-oxidation (EO) process presents an alluring substitute for conventional treatment methods for wastewater with elevated amounts of pollutants (Wang et al. 2012). Electrochemical technologies have discovered a market where they may quickly gain the lead due to their benefits, particularly in the reduction of refractory materials (Liu et al. 2018, Martínez-Huitle et al. 2015). Lower valent compounds, like sulfide and ammonium, can be eliminated by electrochemical oxidation, which can also mineralize refractory organic materials, such as humic and fulvic-like compounds. Certain high-valent compounds, including nitrite and nitrate, can be eliminated by electrochemical reduction (Liu et al. 2023, Wang et al. 2020a, Zhang et al. 2021). Numerous electrochemical techniques, such as electro-Fenton aided with photocatalysis, electro-Fenton, peroxy coagulation with electro-Fenton, and electro-coagulation combined with EO, have shown good effectiveness in eliminating COD, ammonia, and suspended particles from landfill leachate. Fig. 1. represents the web of search results using the VOS viewer software using the keywords 'electrooxidation' and 'leachate'.

BASIC CONCEPTS

In actuality, there are two varieties of EO: indirect and direct oxidation as given by the equation (1) (Ding et al. 2021). EO preferentially transforms organic pollutants into biodegradable compounds using chemisorbed active oxygen and electrolytic combustion. Physisorbed •OH converts the organics completely into H2O, CO_2, and inorganic ions

(Priyadarshini Rajesh & Saravanakumar 2023). Electrodes that produce higher oxides, MO_{x+1} (i.e., chemisorbed dynamic oxygen), and electrodes that allow radicals to build up made up of •OH (i.e., physisorbed dynamic oxygen) on their outermost layer are utilized for the selective oxidation of organics by combustion (Martínez-Huitle et al. 2015).

(a) Direct oxidation: During direct oxidation, pollutants are generally adsorbed to the entire surface of the anode, and the anodic electron exchange mechanism degrades the contaminants. This event persists in one or more phases until the ultimate oxidation product, mostly CO_2, is generated (Martínez-Huitle et al. 2015). The other parallel process produces hydroxyl radicals, which is the breakdown of water ions favoring the COD removal, specifically aromatic substrates (Cabeza et al. 2007). Direct EO occurs at a lower current density, before O_2 evolution, at a slower reaction rate, and based on the anode's electrocatalytic activity. The formation of a coating (which consists of polymers) on the surface of the anode causes sluggish reaction kinetics, diffusion limitations, and a reduction in the electrode's catalytic efficiency when solutes are dissolved the disadvantages (Lee et al. 2022, Radjenovic & Sedlak 2015). Fig. 2 shows the overall mechanism of different electrochemical systems.

$$\text{Pollutants (P)} \rightarrow P_{oxi} + ne^- \qquad \dots(1)$$
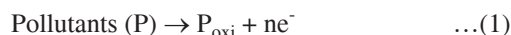
(b) Indirect oxidation: Through the formation of either chemisorbed active oxygen (oxygen in the matrix of an oxide of metal anode (MO)) or physisorbed active oxygen hydroxyl radical (•OH), indirect or assisted
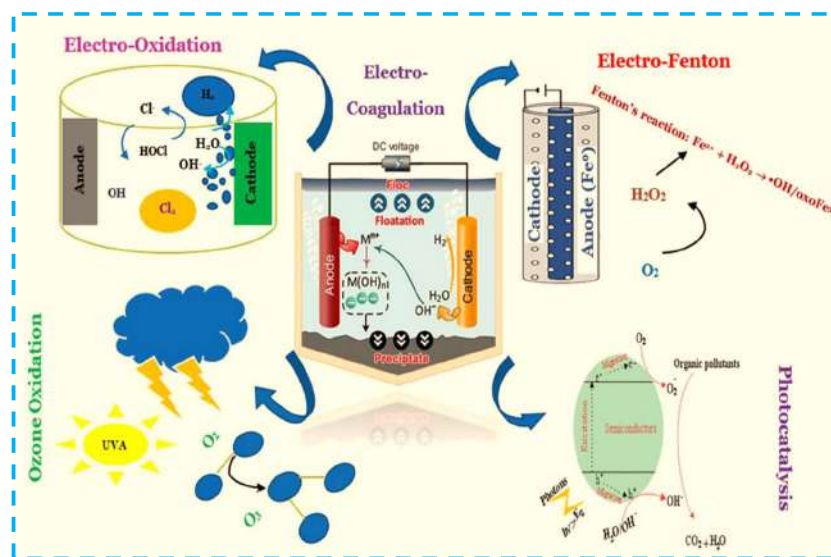
Fig. 2: Overall degrading mechanism of contaminants in various electrochemical systems. (Reprinted with permission from Hajalifard et al. 2023, Copyrights {2023}, Springer Nature)

oxidation takes place at the anode surface (Comninellis & Chen 2010). Removal of ammonium nitrogen is favored if indirect oxidation dominates (Cabeza et al. 2007). To oxidize contaminants through various pathways, powerful oxidants such as radicals of hydroxyls and reactive chlorine ions are first produced near the electrode layer before spreading into an entire solution as given by the equations (2), (3) and (4). Compared to hydroxyl radicals, chlorine ions are more accountable for the breakdown of ammonia (Zhang et al. 2021). The leachate's indirect oxidation of the chloride ions produces active chlorine (hypochlorous acid, gaseous chlorine, or hypochlorite) at the anode surface, which helps remove TOC (Radjenovic & Sedlak 2015).

$$2Cl^- \rightarrow 2e^- + Cl_2 \qquad \qquad \dots(2)$$

$$Cl_2 + H_2O \rightarrow H^+ + HOCl + Cl^- \qquad \dots(3)$$

$$R + HOCl \rightarrow H^+ + H_2O + CO_2 + Cl^- \qquad \dots(4)$$
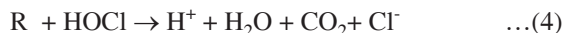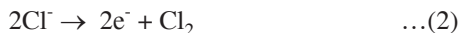
FACTORS AFFECTING ELECTROCHEMICAL OXIDATION

(a) **pH:** The pH influences the conductivity, solubility of the solution, structure, and morphology of the byproduct formed during the electrochemical process (Yasri et al. 2020). Alkaline pH favors ammonia removal. The quantities of chlorine radicals generation (Cl_2, HClO, and ClO^-) and the NH_4^+/NH_3 equilibria in leachate are determined by their pH. At pH greater than 10, the una bound NH_3 is mostly present, whereas, at pH less than 8, NH_4 ions are more common. It is demonstrated at pH less than 3, the presence of Cl_2 in leachate, at pH 8-3 for the presence of HClO, and at pH greater than 8 for the decay of protons into ClO^-. Studies confirm that the HClO-mediated chlorination of ammonia occurs at neutral or alkaline conditions ($6 < pH < 9$) was favorable (Zhang et al. 2021).

The solubility of humic substances differs with the pH. The organic matter precipitation decreases the DOC value at pH 3. It is possible to lower the 33% COD by merely acidifying the landfill leachate (Oturan et al. 2015). Organic pollutants' (either unprotonated or protonated) molecular structures can primarily be altered by pH levels, promoting an increase or decrease in the removal rates (Martínez-Huitle et al. 2015). The ubiquitous breakdown of oxidants is largely dependent on pH, as demonstrated by the fact that the reaction between hypochlorous acid and hypochlorite reaches its maximal pace at the neutral pH (Wu et al. 2014).

At very low pH values (pH<2), the highest decay of chlorine gas occurs. The electromigration process, which determines the efficacy of the EO process, is highly impacted by pH (but pH>2 to reduce chlorine loss) (Tomcsaâ Nyi et al. 1999). Increased pH promotes organic oxidation by •OH. Because of reasons like the proton consumption, The pH of the medium doesn't stay exactly constant throughout the EO reaction because of the reaction of hydrogen evolution occurring at the cathode and the reaction called oxygen evolution on the anode. The leachate solution, the diffusion of layers, and the electrodes' porous nature all have different local pH. A lower pH favors chlorine evolution for porous anodes (mostly metal oxide anodes) (Ghernaout et al. 2011). OER causes the solution to become locally acidified and move toward a more anodic potential. Therefore, it is possible to think about OER from a chloride solution as a self-retarding process (Martínez-Huitle et al. 2015).

Ding et al. (2021) found that in acidic circumstances, the electro-Fenton-like mechanism produced more •OH radicals owing to the production of HClO. However, basicity accelerated an undesirable process that converted hypochlorite (ClO^-) ions to chlorate ions, slowing the creation rate of •OH. The improved elimination of COD at acidic pH is mostly due to oxidation by ClO^-/HClO and •OH. However, elevating the pH to 9 increased precipitations in the electro-coagulation process.

Mohajeri et al. (2010) discovered that degradation occurs more slowly at pH 6, which may be due to the generation of fewer hydroxyl radicals than at acidic pH. Moreover, hydrogen peroxide degrades quickly to water and oxygen in basic solutions and is unstable above the pH of 5. Between pH 2 and pH 4, persistent hydroxyl radicals are produced, and this pH range has significant oxidizing potential. Additionally, degradation was reported to be reduced at pH levels below 2. This is because Fe^{2+} cannot degrade H_2O_2 to OH• at pH levels lower than 2. H_2O_2 captures one proton, converting it into $H_3O_2^+$, $H_3O_2^+$ is electrophilic, resulting in a slower rate of reaction between.

According to Wang et al. (2020b), the maximum TOC degradation effectiveness was achieved at the acidic pH. At an elevated pH, additional Fe^{3+} precipitates as $Fe(OH)_3$, possibly reducing the cathode's active areas for the production of H_2O_2. This resulted in a modest drop in TOC removal effectiveness at pH 4 and 5. Equation (6), which describes the reaction between the electro-generated H_2O_2 and the proton to make H_3O^{2+}, was observed when the pH was below three as given by the equation (5). Because H_3O^{2+} is persistent and electrophilic, it slows down the rate at which H_2O_2 and Fe^{2+} interact. Additional studies on the organic molecules' oxidation in leachate have found that Fenton reactions are inhibited at very acidic pH levels (Wang et al. 2012).

$$H_2O_2 + H^+ \rightarrow H_3O_2 \qquad \qquad \dots(5)$$

According to Fernades et al. (2017) DOC removal was less impacted by the initial pH in trials conducted at a pH of 5 than the COD removal, suggesting that pH affects the rating process of oxidation more significantly than mineralization. Once more, the generation of the highly unstable hydroxyl radical, which prefers oxidization to mineralization, has been accountable for this (Fernandes et al. 2017). Cossu et al. investigated how pH affected the EO treatment of leachate. From the experimental trials conducted at acidic and basic conditions, it is observed that the rate order constant increased slightly under acidic circumstances. The reason for this trend can be a drop in the amount of CO_3^{2-} and HCO_3^{3-} ions, which are always present within the leachate. Compared to organic molecules, ions such as these respond to •OH radicles more quickly, making it beneficial to remove carbonates from leachate (Cossu et al. 1998).

(b) Catalyst concentration: The use of catalysts like H_2O_2 and iron in the electrofenton process of leachate improves the degradation efficiency. The •OH radicle concentration changes with the addition of an external catalyst. For instance, in the electrofenton treatment of leachate, a boost in the direct addition of an iron concentration raises the •OH radicle concentration as given in equation (7) (Deng et al. 2021). A higher concentration of •OH radicles results from a rise in

H_2O_2 concentration, which also improves the organic compound removal efficiency as given in equation (8) (Priyadarshini Rajesh and Saravanakumar 2023). Similarly, the addition of peroxymonosulfate (PMS) salts in leachate increases the removal of the organics as well as decreases energy consumption by the production of sulfate and •OH radicles as given by equations (6), (7), (8) & (9) (Fernandes et al. 2021). Adding coagulants externally during the electro-coagulation technique increases pollutant removal efficiency. Choosing the optimized dosage of catalyst is highly important because the increase in catalyst dosage leads to adverse reactions like the formation of hydroxides with the salts in leachate with less formation of •OH radicles, thereby reducing the efficiency of pollutants removal (Wang et al. 2012).

$$Fe_3O_4 + 8H^+ \rightarrow Fe^{2+} + 2Fe^{2+} + 4H_2O \qquad …(6)$$

$$Fe^{2+} + H_2O_2 \rightarrow Fe^{3+} + •OH + OH^+ \qquad …(7)$$

$$SO_4^{2-} \rightarrow SO_4^{•-} + e^- \qquad …(8)$$

$$HSO_4^- + •OH \rightarrow SO_4^{•-} + H_2O \qquad …(9)$$
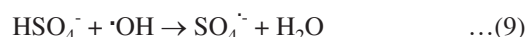
The electrode material with/without additional coatings can also be used as a catalyst for the electrooxidation reaction. (Tejera et al. 2021) used iron electrodes as catalysts which dissolution can act to improve COD removal. The results
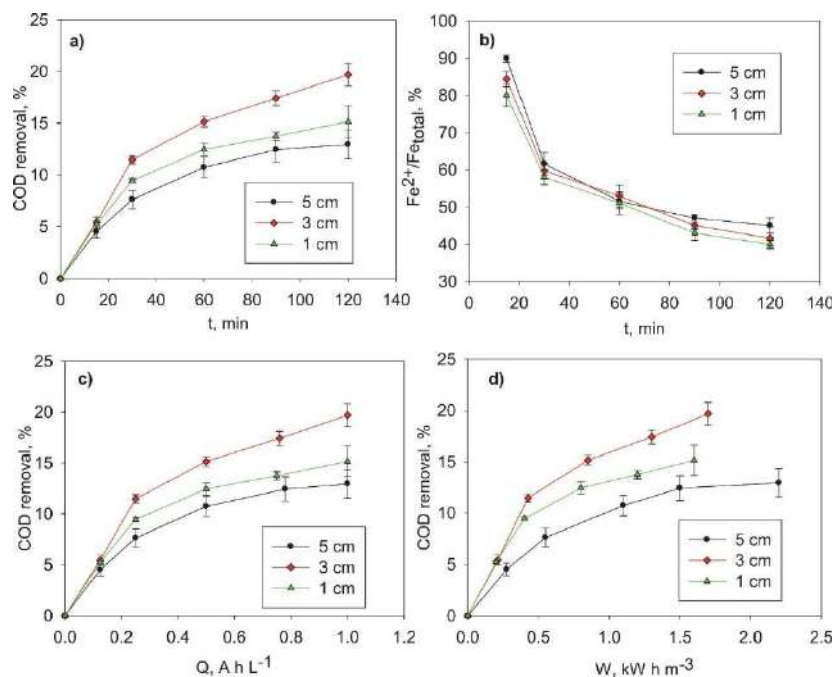
Fig. 3: EC performance applied to leachate considering (a) COD removal different electrode distances (current density, j = 5 mA cm^{-2}, pH =8.3, (b) iron species distribution, (c) COD removal with the applied charge, and (d) COD removal with power consumption. Reprinted with permission from (Tejera et al. 2021), Copyrights {2021}, Elsevier.
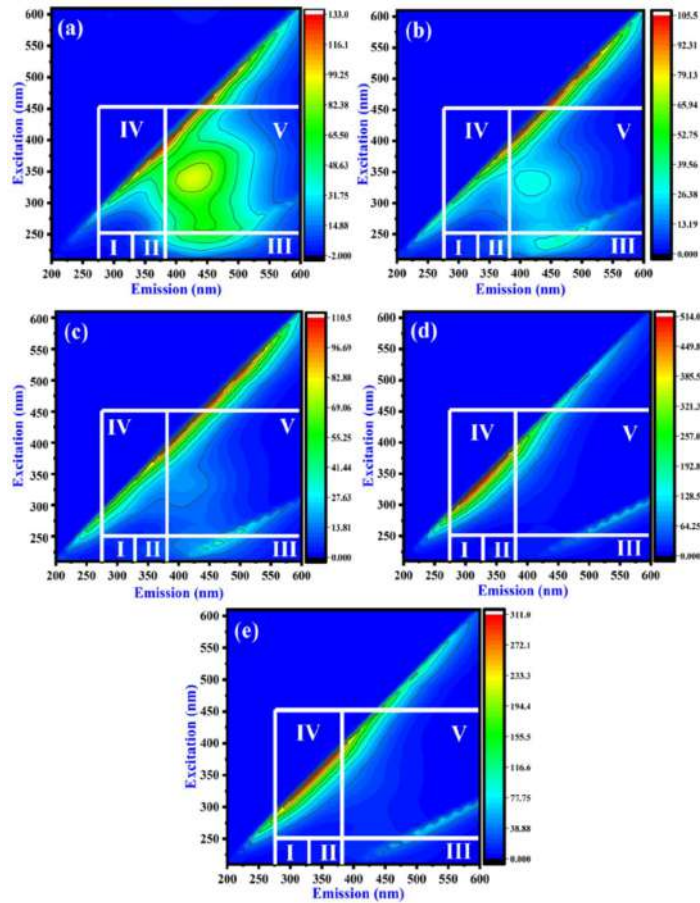
Fig. 4: 3D spectroscopy analysis of (a) raw leachate, and treated leachate under optimal conditions at different time intervals of (b) 10 minutes, (c) 20 minutes, (d) 30 minutes, and (e) 1 hour. Reprinted with permission from Priyadarshini Rajesh and Saravanakumar, 2023, Copyright (2023), Elsevier.

obtained for different conditions of change in the applied charge, distribution of iron species, and power consumption are given in Fig. 3.

(c) Retention time: For continuous performance, one essential aspect is the hydraulic time of retention (Millán et al. 2021). According to Musa & Idrus (2020), a reduced hydraulic retention time is associated with an increased treatment efficacy at a specific unit operating volume. In contrast, the treatment efficacy at the constant state dropped as the hydraulic retention duration decreased (Zhang et al. 2012a). Fig. 4 displays the dissolved organic matter (DOM) elimination process using three-dimensional excitation-emission fluorescence spectroscopy of leachate electro-Fenton treatment at various time intervals (10, 20, 30, and 60 minutes) (Priyadarshini Rajesh & Saravanakumar 2023). The increase in retention time leads to the reaction of degradation of organic compounds from the radicals generated. Hence, sufficient time for the degradation of organics time is important, and more retention time than needed elevates

the treatment cost. Hence, optimization of retention time is very crucial in EO treatment (GilPavas et al. 2020, Qiao & Xiong 2021, Wang et al. 2020c).

(d) Electrode surface area: Increased electrode area may result in the generation of more •OH radicals and give more contact area with the leachate (Dong et al. 2022, Salazar-Banda et al. 2021, Sher et al. 2020). Hence, optimizing the electrode surface area is very crucial (Brillas et al. 2009). The research of Wang et al. (2024a) indicates that in the early stages of electro-Fenton treatment, a small drop in the organics elimination rate was seen when the cathode surface was increased from $10~cm^2$ to $20~cm^2$. This was because when the source of power was switched on, greater amounts of iron would start to accumulate on the bigger cathode, which would reduce the amount of organic material removed during the first step of electro-Fenton treatment by iron flocculation. After the electro-Fenton treatment, the $20~cm^2$ cathode removed organics with an efficiency of 82% compared to 73% for the $10~cm^2$ cathode.

The carbon–PTFE cathode was the site of both H_2O_2 generation and Fe^{2+} recuperation. Therefore, increasing the cathode area also increases the rates of these processes. Thus, it was possible to develop more potent oxidants for oxidizing the pollutants in leachate by using a larger cathode. Therefore, increasing the cathode area might enhance the organics removal efficiency (Wang et al. 2012). An increase in the treatment's capital expenses is also implied by an increased surface area of electrodes to reactor volume proportion (Radjenovic & Sedlak 2015). Therefore, adjusting the electrode surface area is crucial for evaluating the EO reaction's efficiency (Asfaha et al. 2021, Ghanbarlou et al. 2020, Moradi et al. 2020).

(e) Effect of inter-electrode distance: Ohm's law states that when the inter-electrode distance decreases, current flow rises and cell resistance lowers (Yasri et al. 2020). Reducing the distance between electrodes can help eliminate the constraints on the pollutants' mass transit toward the surface of the electrodes and enhance their electrolytic reaction (Castro et al. 2022, Sanni et al. 2022, Sivaranjani et al. 2020). Yasri et al. tried to shorten the distance between the electrodes while maintaining a steady current to lower interelectrode resistance. However, this increased the issue of gas production and layer development across the electrodes, further decreasing the process efficiency (Yasri et al. 2020). Zhang et al. found that when the gap between the two electrodes was between 1.3 and 2.1 cm, the COD elimination rate was nearly constant. For a 1.3 cm gap, the COD removal effectiveness was 80.4%, and for a 2.1 cm gap, it was 80.8%. The COD elimination efficacy decreased with increasing or decreasing distance above this range. The COD elimination effectiveness was found to be 73.6% at a distance of 0.7 cm and 71.8% at a distance of 2.8 cm. The electro-regenerated ferrous ion at the anode is readily oxidized to ferric ion as given by the equation (10), when the electrodes are positioned too closely together, which lowers the efficiency of continuous Fenton reactions. The increased distance is attributed to the constrained movement of ferric ions toward the cathodes' exterior, in which ferrous ion regeneration occurs, is responsible for the increased distance. As a result, the hydroxyl radicals produced become ineffective in the reactivation of ferrous ions (Zhang et al. 2006). As a result, maximizing the distance between electrodes is crucial to the pollutants' overall rate of degradation.

$$Fe^{2+} \rightarrow Fe^{3+} + e^- \qquad \qquad \ldots(10)$$

(f) Current density: The current density could be expressed as the quantity of electrons that flow across the unit region of operational electrodes. Lower current density increases the treatment time to meet the permitted discharge limit standards, which increases the need for larger facilities and initial investments (Chowdhury et al. 2020, Shahedi et al. 2020). Increased application of current density wastes energy because fractional electrical energy influences the electrolyte and promotes undesirable reactions (He et al. 2022). So, tuning the current density is a crucial aspect of lowering operational expenses. Enhanced current density promotes both indirect and direct electrooxidation. A rise in current density enhances the OER (Fan et al. 2019). The density of current at which no accumulation of oxidizable matter on an anode surface is called limiting current density. If the current density has increased more than this, electrolysis efficiency decreases by the transfer of leachate molecules, such as O_2 at the anode and H_2 at the cathode. Many research works have been undertaken to establish a correlation between limiting current density and COD (Cabeza et al. 2007). Increased current density promotes indirect oxidation by hydroxyl radicals and electrolyte-derived oxidants (Zhuo et al. 2022). COD degradation increases exponentially with high current density (Khaleel et al. 2023). Decreased current density promotes direct oxidation, which removes ammonia more slowly (Meng et al. 2020a). Guan et al. found that ammonia elimination occurred at greater current densities via indirect oxidation via reactive chlorine produced near the anode. A subsequent increase in current density will lower the oxidation performance after the maximum current efficiency is reached due to the inhibition of ammonia circulation, the production of inactive chlorine byproducts, and the transpiration of gaseous chlorine (Zhang et al. 2021). According to Oturan et al. (2015) leachate #1 and leachate #2 are determined to have removed 85.5 and 83.8% of the total organic carbon after 18 hours of electro-Fenton at 500 mA. Leachate #1 and #2 are projected to have a somewhat higher TOC removal degree at 1000 mA, at 89 and 91%, respectively. This outcome shows that at the ideal current density, the removal efficiency was significantly higher (Oturan et al. 2015). Generally, the majority of the investigations are run in the galvanostatic mode. Current density is recorded in several investigations, while anodic potentials are published infrequently. These limited data constraints to study the impact of the current density at the anodes and potential adverse effects (Radjenovic & Sedlak 2015). To indicate the current efficiency, one can use the general current efficiency (GCE), instantaneous current efficiency (ICE), and/or electrochemical

oxidation index (EOI) (Muthuraman & Moon 2012). The ratio of the experimental to the theoretical total organic carbon (TOC) removal is known as the mineralization current efficiency or MCE. As the current increases, various oxidants such as persulfate, hydrogen peroxide, peroxophosphate, chlorine, and so on are formed. Other operational factors, such as temperature, dissolved O_2, inorganic ions, anode type, and pH all have an impact on oxidant generation. A high rate of flow and a small current density minimizes the formation of perchlorate and chlorate ions (Bergmann et al. 2009). Under controlled charge transfer, the majority of organic matter reaches the anodic surface area and consumes the •OH, which is the reason for the hindrance of perchlorate formation (Mousset et al. 2020, Radjenovic et al. 2020, Sharma et al. 2022). When the current density increases, the degrading activity becomes mass transport regulated, rendering the organic pollutants near the electrodes' vicinity insignificant. This makes it possible to produce elevated quantities of perchlorate (Luo et al. 2023, Stiber et al. 2021, Zhang et al. 2020). So, maintaining current at less than limiting current density can minimize the production of ClO_4^- making organic compounds react with the •OH radicle near the anode vicinity. The leachate treatment in conditions of lower pH, high concentrations of NaCl and high organic content, and higher current density with chloride formation will be favorable for efficient abatement (Leow et al. 2020, Luo et al. n.d., C. Wang et al. 2021a, 2021b). Current efficiency can be defined as the equation given below by the equation (11).

$$CE = VF\,(COD_0 - COD_t)\,/\,8It \qquad \ldots(11)$$

Where V *is* the volume of the electrolyte, COD_0 is the chemical oxygen demand at time zero, COD_t *is* the chemical oxygen demand at time t, *F is* the Faraday constant, and I is the current intensity (Zhang et al. 2006). Additionally, as the voltage range increases, the emergence of Fe^{2+}/Fe^{3+} and $HClO/ClO^-$ also increases concurrently (Ding et al. 2021). According to Wang et al. (2024b) (the generation of H_2O_2 increased when the density of current rose from 10 to 40 mA/cm^2. TOC removal effectiveness rose from 10 to 30 mA/cm^2 but then declined slightly when the current increased to 40 mA/cm^2. This suggests that at high current densities, the H_2O_2 generated in situ had not effectively transformed to form •OH radicals (Wang et al. 2012).

(g) **Reactor geometry:** There is no standard design for the electrochemical reactor. Achieving maximum effectiveness in the removal of organic contaminants is largely dependent on the configuration of electrocoagulation (EC) reactors (Cornejo et al. 2021,

Sandoval et al. 2022a). Various EO reactor designs have been used to incinerate organic contaminants, but they all need to meet certain operating requirements based on the properties of wastewater. Designing an EO reactor should consider many factors, such as lowering the ohmic drop, preventing the buildup of gas bubbles, and boosting mass transfer. Optimized by computational fluid dynamics (CFD) modeling. Before the analysis of experiments on the laboratory scale and later when the scaling up of pilot plants, numerical simulation was essential within the development and research of multiple electrochemical procedures because it tests various electrode shapes and materials and characterizes the methods' primary functional variables. Furthermore, CFD models have proven to be an invaluable tool in enhancing several current EO reactor designs that run inefficiently in many conventional procedures (Rivera et al. 2021, Sandoval et al. 2022b). The reactor geometry should ensure the leachate is exposed to uniform electrolysis in all directions and facilitate proper circulation of radicles so that the pollutants get degraded properly in both the batch and continuous systems (Yasri et al. 2020).

(h) **Chlorides and bromides concentration:** The EO treatment efficiency depends on the concentration of bromides and chlorides in leachate, which forms byproducts such as bromide ions, chlorate, chlorite, chlorine dioxide, hypochlorite, hypochlorous acid, perchlorate, chloramines, brominated and chlorinated organics (Martínez-Huitle et al. 2015, Radjenovic & Sedlak 2015). Numerous factors, including the sort of anode and the number of chloride ions in the electrolyte, affect the effectiveness of chlorine formation, pH, current, voltage, and other coexisting substances. If the chloride concentration decreases, it favors ammonium removal (Zhang et al. 2021).

The bromine and chlorine species generated near the anode vicinity also form poisonous organic bromine and chlorine byproducts during the treatment (Carvalho de Almeida et al. 2023, Leow et al. 2020, C. Wang et al. 2021b). The chloride radical (Cl-), also known as free chloride or active chloride, undertakes rapid addition, abstraction of hydrogen atoms, and immediate transfer of electrons interactions with aromatic compounds at second-order rate constants of 10^8 to 10^9 M^{-1}. If the chloride concentration is higher in leachate, chloride radicals are transformed into dichloride (Cl_2) anion radicals. Cl_2 generated degrades with organic molecules like Cl^- but at a slower magnitude of two to four orders (Radjenovic & Sedlak 2015). This is likely due to their engagement with both chemical and electrochemical reactions (Martínez-Huitle et al. 2015).

HOCl/OCl⁻ oxidizes the bromides, resulting in hypobromous acid. The HOBr produced is more reactionary than hypochlorous acid when exposed to certain organic molecules, like phenolic compounds. Bromide is a powerful scavenger of ·OH. Chlorate, perchlorate, and bromates are problematic carcinogens and mutagens (WHO 2018, Kurniawan et al. 2022, Xu et al. 2023). Reducing current density minimizes the formation of chloride ions, yet it further decreases the treatment's oxidation efficacy due to decreased formation of ·OH radicals and charge transfer limitations (Radjenovic & Sedlak 2015).

The pH concentration at the anode and in the whole solution affects the transformation of chlorides to chlorine, hypochlorite, and/or hypochlorous acid (Ghernaout et al. 2011, Meng et al. 2020b, Neodo et al. 2012). Thus, the organic material is oxidized by electrogenerated reactive chlorine shlep in conjunction with direct oxidation near the surface of the electrode, and the organic material is oxidized by chloro, hydroxyl, and oxychloride radicals, creating a complex system to predict the role of operating parameters for performance of the process (Kurban et al. 2024, Yang et al. 2013, Zhao et al. 2024). In an atmosphere of NaCl, Boudreau et al. noticed that sulfamethoxazole using BDD (boron-doped diamond) broke down quickly, producing some dangerous chlorine metabolites. Remarkably, the resultant byproducts separated into minerals following prolonged electrolysis, while they accumulated in the mixture following a comparison of chemical hydrochlorination with sodium hypochlorite (Boudreau et al. 2010).

The formation of active chlorine can be affected by both the chemical nature and the pH of the solution available near the anode (Luna-Trujillo et al. 2020). To obtain insight into this process, it is critical to realize that the chloride oxidation is accelerated at low pH and that porous anodes may display

significantly lower pH than in the rest of the solution (Ghernaout et al. 2011). A pH difference exists between the anode's surface and the entire solution as a result of OER around the anode acidifying the solution. Chloride oxidation can activate chlorine even in nonacidic solutions because porous anodes maintain a pH value that is extremely low in their porous nature and is mostly devoid of the overall pH (Wu et al. 2021, Yu et al. 2023). It's crucial to keep in mind that metal oxide anodes typically have a porous structure, which promotes chlorine development at nonacidic levels of pH (Scialdone et al. 2009).

It is noteworthy that there has been little research on the impact of the anode's nature on the synthesis of organochlorinated chemicals, and the available data do not permit a comprehensive understanding of this impact. Metal oxide anodes, especially RuO_2 and IrO_2, may effectively oxidize organics and huge amounts of Cl^-. They are typically suitable choices for the oxidation of organics because, for the active production of chlorine, they have elevated current efficiency, minimal production of perchlorate and chlorate, an elevated level of porosity, and long-term mechanical and chemical stability (Kim et al. 2002, Kraft 2008, Radjenovic et al. 2011, Song et al. 2023).

The formation of undesirable organochlorinated compounds, such as active chlorine, should be considered when deciding on an anode (He et al. 2022). Using nonactive anodes, like BDD, is more desirable due to the intermediacy of hydroxyl radicals (Durán et al. 2018, Hu et al. 2021, Medeiros De Araújo et al. 2014). However, among other things, choosing the right operating conditions (such as low current densities) is necessary to avert or at least lessen the generation of perchlorate. For example, because chloroacetic acid is highly resistant to active chlorine, BDD achieved much greater efficiency than metallic oxide anodes, even
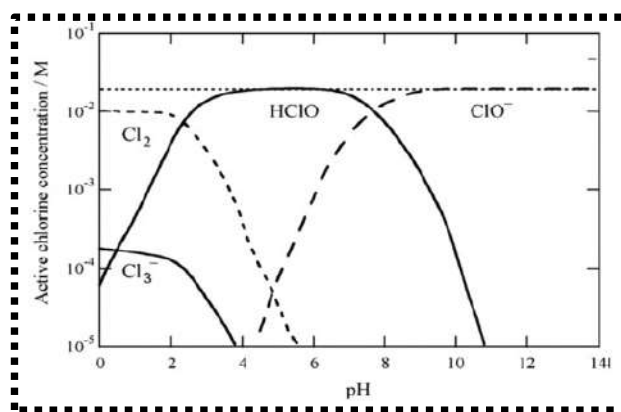
Fig. 5: Radicle production varies with pH and active chloride concentration obtained with permission from Martínez-Huitle et al. 2015, Copyright {2015}, American Chemical Society.
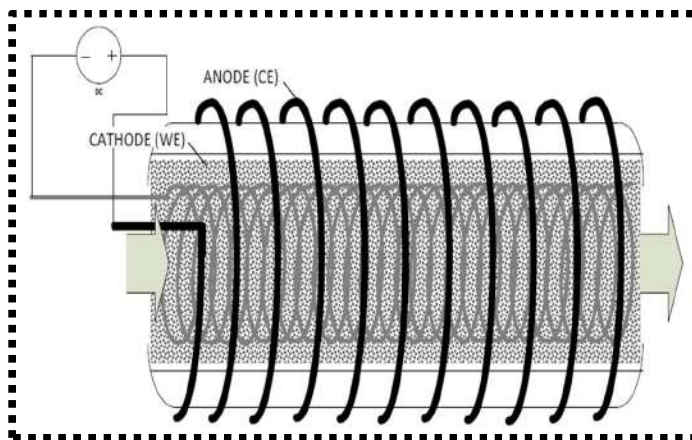
Fig. 6: The working electrode is a three-dimensional reactor made of metal-impregnated activated carbon and designed to treat low-conductivity drinking water. Reprinted with permission from Radjenovic and Sedlak, 2015, Copyright {2015}, American Chemical Society.

in the face of considerable chlorides (Scialdone et al. 2014).

The concentration of chloride drops because additional types of chlorine are formed throughout the tests, and their concentration rises with applied current density. After eight hours of testing, the amount of chloride fell from 11.1 to 8.3 g/L with the greatest rate of decay occurring at a given current density of 1.4 A and monitoring the nitrate quantity that developed during the tests Fig. 5, Since likewise increases the transmitted current intensity, it can be concluded that the best way to remove nitrogen is through the production of nitrogen gas, as the quantity of nitrate produced is far smaller than the proportion of nitrogen eliminated. The finding is supported by literature, which claims that at high chloride concentrations, the primary oxidation product is nitrogen gas production (Pérez et al. 2012). Even with the high chloride level, there was little nitrogen removed. Equation (12), which describes the side reaction between HOCl and ferrous ions, may be the cause of this. Hypochlorous acid will be consumed and unable to convert into ammonium nitrogen as a result (Gómez-Espinosa et al. 2017).

$$2Fe^{2+} + HOCl + H^+ \rightarrow 2Fe^{3+} + Cl^- + H_2O \qquad …(12)$$
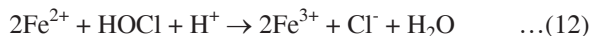
 (i) Pattern and orientation of the electrode: The pattern and orientation of the electrode decide the efficiency of the electrochemical treatment (Durán et al. 2018, Hu et al. 2021, Liu et al. 2022). For instance, tilted electrodes are found to be more effective than vertical electrodes. By enhancing mass transfer, optimizing the electrode's geometrical layout expands the contact area between the electrodes and contaminants. A revolving electrochemical reactor of multielectrode was created by Fan et al. (2019) that broke the bubble curtain formed, increased the mass transfer, decreased the resulting diffusion layer's thickness, encouraged forced

convection movement, increased the reaction area on the anode surface, reduced the ohmic resistance at anode due to bubbles formed and increases the reaction rate between the active radicals formed and wastewater. There has been a rise in the phenol decomposition rate from 58.8% to 84.3%. With an increase in the rotational speed of electrodes from 0 to 300 rpm within 100 minutes (Fan et al. 2019).

To get around the mass transfer restrictions in electrochemical systems, plate, and frame filter press reactors can be employed. In a typical flow-by mode, the direction of the current movement is perpendicular to the path of the electrolyte movement. As a result, there are significant limits on mass transmission at the surface of the electrode due to a thin, stationary boundary layer. Due to crossflow filtration, flow-through electrolytic reactors can somewhat mitigate this disadvantage by improving the pollutants' convective transfer to the surface of the electrode (Radjenovic & Sedlak 2015). Fig. 6 represents the three-dimensional reactor. In the case of the flow-through manner, porous three-dimensional electrodes can be used.

Granular and three-dimensional electrodes are used for coupled electrochemical oxidation and adsorption. Granules function as bipolar electrodes and encourage oxidation when they are loaded into a traditional frame reactor and two-dimensional plate with granular or particulate electrode materials like graphite or granular activated carbon (GAC) (Martínez-Huitle et al. 2015). Further research is essential on three-dimensional electrolytic reactors (Fig. 7) with carbon-based fillers since they may be appropriate for treating wastewater with significant potential for the generation of halogenated organic byproducts. Dyes were treated using carbon nanotube (CNT) filters aided with electrooxidation, which oxidized the dyes directly at the CNTs. Poor
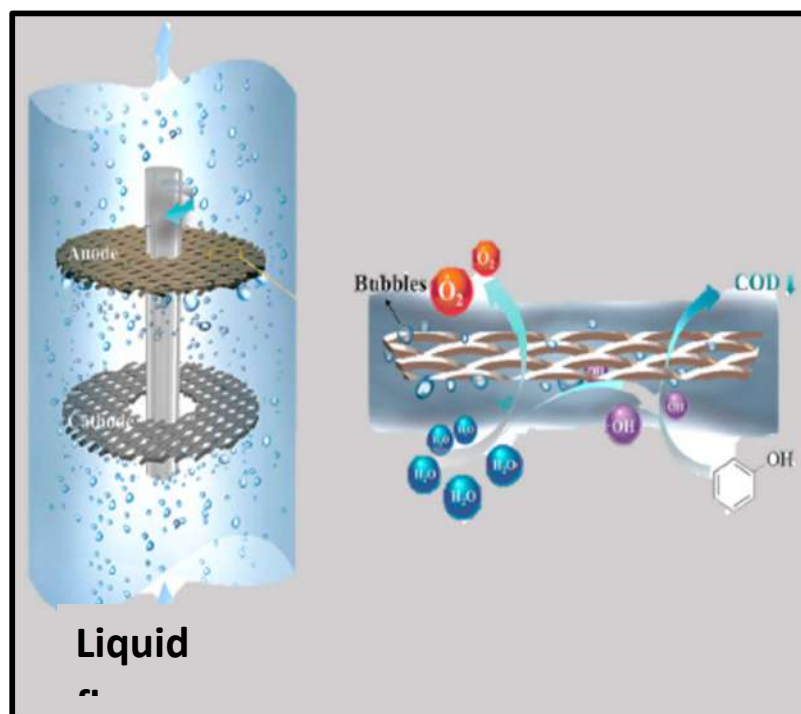
Fig. 7: A 3D rotating electrode schematic representation. Reprinted with permission from (Fan et al. 2019), Copyright {2019}, American Chemical Society.

performance can result from bed blockage, increased pressure in the back caused by the bubble formation, and deterioration of the carbon-based material when using porous electrodes in waste treatment. A crossflow electrochemical filtering device fitted with a porous Ebonex anode produced remarkable phenol removal through electrochemical oxidation and adsorption (Radjenovic & Sedlak 2015). Thus, the pattern and orientation of the electrode play a significant role in the EO's overall efficiency. In-depth studies in the future for variations with different patterns and orientations are necessary for better optimization.

(j) **Conductivity:** The wastewater with high conductivity of more than or equal to 2000 μmhocm^{-1} favors indirect oxidation predominantly (Martínez-Huitle & Ferro 2006, Yu et al. 2023, Zhou et al. 2011). Because of the existence of different inorganic and metal ions, the leachate conductivity is typically higher than this; hence, indirect oxidation is essential to the electrochemical treatment of leachate (Lin & Chang 2000, Palanivelu 2005, Ramprasad 2012). The voltage reduction in the electrolytic reactors grows with decreasing electrolyte conductivity. Na_2SO_4 or other supportive electrolytes have occasionally been used during wastewater treatment to boost conductivity and accelerate the transfer rate of electrons (Li et al. 2020, Liu et al. 2021, Shih et al. 2018). It prevents the electrolysis

process from producing hazardous and cancer-causing chlorinated species. Additionally, more SO_4^{2-} gathering would be adsorbed on the exterior of the electrode as a result of the extra electrolyte, reducing the electrode's active site count. So, it must be added at an optimized level if needed (Fan et al. 2019). It is typically necessary to add sodium sulfate or sodium chloride to achieve the desired conductivity value (Abdel-Fatah et al. 2021, Kerwick et al. 2005). It should be noted that adding chlorides causes Cl$^-$ Chlorine-mediated oxidation, and adding sulfates causes the production of persulfates at inactive anodes. In cases where the conductivity of wastewater is exceedingly inadequate, three main methods may be offered: (1) incorporating salts like $NaSO_4$ or NaCl to increase conductivity, which favors the process by generating Cl$^-$ or SO_4 ions (2) applying special microfluidic reactors, (3) using membrane filtration or another preconcentration procedure before the electrooxidation as a post-treatment. The presence of particulate matter is common in leachate, and its role in EO is rarely focused on in the literature (Martínez-Huitle et al. 2015).

(k) **Bubbles formed:** The formation of bubbles has multiple effects in the EO process. It occurs mainly in two ways: (i) Gas bubbles cling to nucleation sites and blanket the surface of the electrode, thereby reducing

the active surface area of the electrodes and increasing the electrolyte's resistance. (ii) momentum exchange happens due to micro-convection in the electrode's immediate proximity. The gaseous bubble stratum expands in proportion to the height of the anode. Liu et al. discovered that while the overall size of the gaseous bubble strata remains constant, the void fraction increases when the current density rises. This demonstrates that the velocity of the gas bubble is mostly independent of current density. A high rate of flow reduces the vacancy percentage near the anode surface by boosting the amount of gas production and shortening the time that gas bubbles stay in the area. The gas bubble's tremendous lateral velocity is due to its rapid gas release rate. As a result, the gas bubble layer gets thicker at a high lateral velocity. The hydraulic diameter reduces as the electrode gap rises which also causes the flow velocity to decrease. The rate of gas generation increases as the distance between the electrodes decreases. On the other hand, the void fraction rises, and the overall thickness of the gaseous bubble strata decreases as the space between the electrodes rises. Because of the diverse characteristics of the gas bubbles and the complicated arrangement of the gas bubble strata that form, the coefficient of mass transfer of an electrochemical cell has not been the topic of systematic investigation. This mass transfer distribution could majorly affect the reaction between the gas bubbles and electrochemical oxidation (Liu et al. 2018). The role of bubble formation in the influence of EO rate with leachate treatment has not been studied. Hence, there is a literature gap in the discussion.

(l) Type of electrode: Anodes are classified into two types: non-active and active depending on the strong and faint interaction of hydroxyl radicals (•OH) generated by electrolysis occurring on the electrode surface (Ma et al. 2023).

Active anodes such as IrO_2 and RuO_2 have a lower potential for O_2 generation and a lower ability to degrade recalcitrant organic compounds (Einaga 2022, Radjenovic & Sedlak 2015). The surface at active anodes may combine with •OH to generate a substance known as superoxide (MO) or higher oxide. $[MO + H^+ + e^- \rightarrow M(•OH)]$. This happens when the metal oxide anode can achieve inflated oxidation states greater than the typical potential for O_2 evolution. The MO/M redox pair mediates organic oxidation. $(MO + R \rightarrow M + RO)$ and participate in the chemical degradation of the higher oxide species to initiate the side of OER. $(MO \rightarrow M + 1/2O_2)$ (Ma et al. 2019, Martínez-Huitle et al. 2015).

Non-active anodes like PbO_2 and SnO_2 exhibit lesser electrochemical reactions for O_2 generation and elevated

efficacy in degrading organic compounds (Mandal et al. 2020, Radjenovic & Sedlak 2015). More focus has been placed on non-active electrodes to fully mineralize molecules of organic substances (Liu et al. 2018). Higher oxides cannot form in non-active electrodes, but hydroxyl radicals, also known as physisorbed active oxygen (•OH), enable organics to oxidize nonselectively until they completely decompose into CO_2. The reaction can be given by the equation (13).

$$aM(•OH) + R \rightarrow M + xH^+ + nH_2O + mCO_2 + ye^- \quad …(13)$$
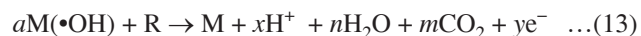
R is an organic molecule compound requiring a = (n + 2m) oxygen atoms to mineralize to carbon dioxide. R has m atoms of carbon and no heteroatoms. Reduced efficiency can arise from concurrent oxidation or dimerization of the beginning •OH in both types of anodes $[M(•OH) \rightarrow 2M + H2O_2]$ or $[M + 1/2O_2 + H^+ + e^-]$. The •OH dimerizes to H_2O_2 on the anode surface due to its reduced adsorption capacity. Accordingly, anodes with lower O_2 evolution overpotential—that is, anodes that are better OER catalysts, cause the organics to partially oxidize; anodes with higher O_2 evolution overpotential, that is, anodes that are worse OER catalysts—cause the organics to completely oxidize to CO_2, which makes it as an ideal suitable electrode for wastewater treatment such as the PbO_2 and BDD. The weaker M−•OH interaction is the reason behind the higher anode reactivity for organic oxidation (Martínez-Huitle et al. 2015).

The materials of anode favor the chlorine evolution reaction (CER), hydroxyl radical formation, and oxygen evolution reaction (Zhang et al. 2021). The ideal electrode material would be inexpensive, show mechanical, physicochemical, and electrolysis medium stability, and have minimal activity against side reactions with significant activity against organic oxidation (Martínez-Huitle et al. 2015). Fig. 8 shows the various radicle generation at variations of pH and different dopings with the electrodes.

The effectiveness of electrochemical treatment methods and the possibility of hazardous byproduct development are contingent on the selection of electrode material (Radjenovic & Sedlak 2015). Because of its high oxidation power and high oxygen overvoltage, the BDD electrode was thought to be the most effective anode among the other anodes utilized for the mineralization of wastewater. Several researchers have used BDD electrodes for the abatement of leachate (Oturan et al. 2015). The BDD property of high O_2 overpotential favoring direct oxidation makes them function well compared to anodes of metal oxide. The adsorption of weakly formed ·OH can explain the elevated contaminant removal efficiency of the anode made of BDD during the electrolysis with the organics as given by equation (14).

$$BDD + H_2O \rightarrow H^+ + BDD (·OH) + e^- \quad …(14)$$
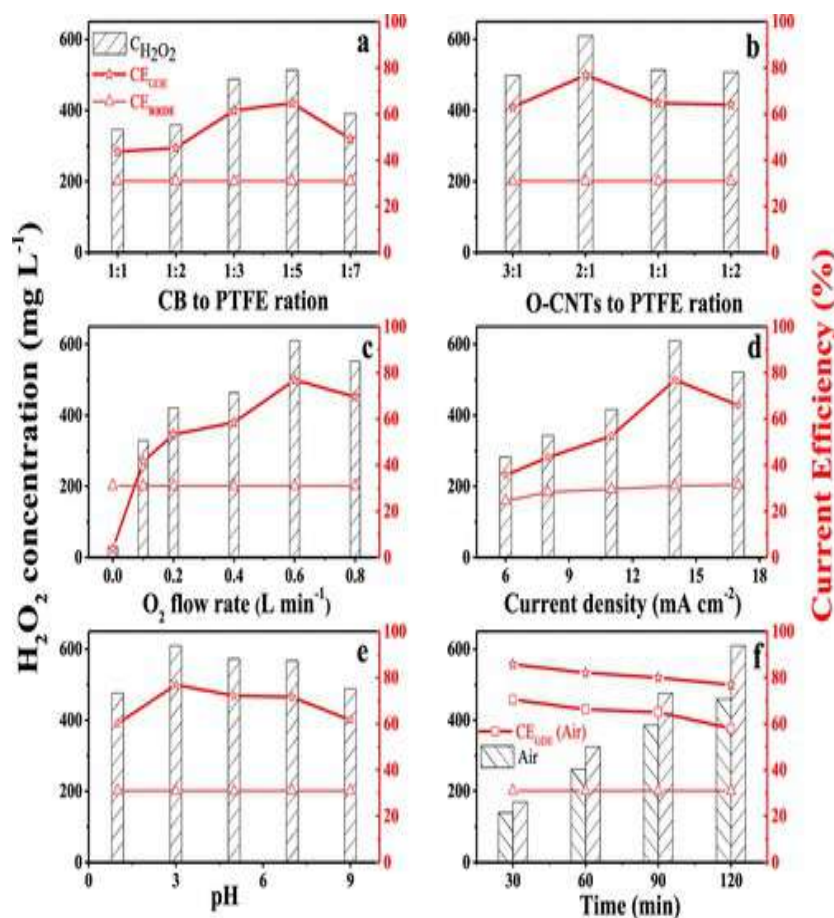
Fig. 8: Effects of (a) carbon black to PTFE ratio, (b) O-CNTs to PTFE ratio, (c) O_2 flow rate, (d) current density, and (e) pH on the yields of H_2O_2 and current efficiency of gas diffusion electrode (GDE). (f) Cumulative H_2O_2 concentration and current efficiency of GDE with different time durations of H_2O_2 generation. Conditions for (f): 0.1 mol L^{-1} Na_2SO_4, carbon black to PTFE ratio: 1:5, O-CNTs to PTFE ratio: 2:1, pH: 3, current density: 14 mA cm^{-2}, and O_2 flow rate: 0.6 L min^{-1}. Electrolysis time for (a–e) is 60 min and other conditions for (a–e) are similar to (f) except the one as variable. Reprinted with permission from (Wang et al. 2020c) Copyright {2020}, American Chemical Society.

The characteristics of the ·OH radicle formed in the BDD electrode are still not fully revealed due to the lack of spectroscopic evidence. A few authors came up with a theory that, due to the higher reactivity of ·OH radicles generated by BDD, the reactions of oxidation are constricted to an adsorbed film near the electrode vicinity (Kapałka et al. 2009). They reported that when BDD anodes were utilized for an electrochemical reaction for acetic acid in a concentrated solution with designated $^{18}O_2$, the involvement of molecules of oxygen in the chain radicle reactions was witnessed by the generation of $C^{18}O_2$ and $C^{16}O^{18}O$. The ·OH electrogenerated may induce the production of organic radicals (R·), which form organic peroxy radicals (ROO·) in the presence of O_2. The resultant peroxy radicals set off further chain reactions that accelerate the rate of organic compound electrooxidation in a non-Faradaic manner (Kapałka et al. 2008).

Along with the oxidizing of organics, the anodes of BDD can also produce H_2O_2, ozone, and ferrate ions. It can also generate peroxy dicarbonate ($C_2O_6^{2-}$), peroxy disulfate ($S_2O_8^{2-}$), and peroxy diphosphate a ($P_2O_8^{4-}$) with carbonate, sulfate, and ions of phosphate. In this, the peroxy disulfate formation occurs in two steps. (1) production of the sulfate radical (SO^{4-}) by either (1) recombining two SO_4^- radicals to give peroxy disulfate or (2) reacting of sulphuric acid or HSO_4 with the electrocatalytically generated •OH or through the sulfate ion's direct oxidation at the anode as given by the equations (15), (16), (17) and (18). (Radjenovic & Sedlak 2015).

$$SO_4^{2-} \rightarrow SO_4^{·-} + e^- \qquad \ldots(15)$$

$$·OH + HSO_4^- \rightarrow H_2O + SO_4^{·-} \qquad \ldots(16)$$

$$·OH + H_2SO^4 \rightarrow H_3O^+ + SO_4^{·-} \qquad \ldots(17)$$

$$SO_4^{·-} + SO_4^{·-} \rightarrow S_2O_8^{2-} \qquad \ldots(18)$$
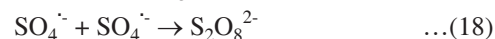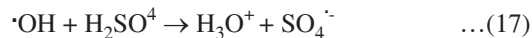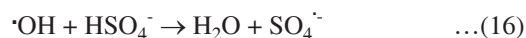
A good electrode is expected to have characteristics such as (1) enhanced chemical and physical stability, (2) persistent against corrosion, erosion, and passive layer formation, (2) possessing good conductivity, (3) selectivity, (4) increased catalytic reactions, (5) low cost and (6) high durability (Du et al. 2021). Various electrodes such as granular activated carbon, polypyrrole, activated carbon fiber (ACF), graphite, glassy carbon, massive Pt and platinized Ti, pure and doped-PbO_2 and mixed metal oxides (MMO) of Ir, Ru, Sn, Sb, Ta, and Ti have been experimented till now. Most of the studies have revealed that the greater efficiency was with the "nonactive anodes" like PbO_2 and BDD. Dimensionally stable anodes (DSA), SnO_2, graphite, PbO_2, and BDD reveal higher chemical resistance during electrolysis (Comninellis & Chen 2010).

Carbon electrodes are relatively economical in cost and with increased surface area (L. Xu et al. 2023). Hence are usually used for pollutant oxidation in 3D electrolytic reactors, including fluidized beds, packed beds, porous electrodes, carbon particles, etc., The application of high anodic potentials leads to lower durability due to surface corrosion (Deng et al. 2024). Creating more toxic Pb^{2+} as a secondary pollution is the major drawback in the case of PbO_2 anodes. The Ti/PbO_2 anodes are comparatively stable, and their stability and performance rely on the fabrication method (Shen & Zhang 2023). With identical properties, Ti/SnO_2 has been detected to have limited durability (Meng et al. 2023).

Pt anodes are most utilized in both synthesis and preparative electrolysis owing to their strong corrosion resistance regardless of powerful combative media (Lemeyonouin Aliou Guillaume et al. 2013, Stucki et al. 1991, Tröster et al. 2002). DSA constitutes a Ti stratum veneered with a slim conduction layer of MMO or metal oxide (Ir, Ru, Ta, Sn, Sb, and/or Ti) (Choi et al. 2023, Veerman et al. 2010, Wang et al. 2021a). From the time of this anode production, many researchers made attempts to develop novel coatings for use in electrochemical processes. Many research papers have proved that anodes of BDD make full mineralization of various contaminants such as ammonia, aniline, cyanide, drugs, dyes, hydrocarbons, pesticides, phenols, surfactants, etc. (Brinzila et al. 2012, Fabiańska et al. 2014, Pacheco et al. 2011, Polcaro et al. 2004, Song et al. 2021)

Experiments with different testing electrodes and the relative interaction with radicals of •OH with the organics proved the dual types of behavior (nonactive and active) of BDD in a few experiments (Fabiańska et al. 2014, Pacheco et al. 2011, Song et al. 2021). The frequent reduction of anode performance is due to rust and clogging (Candido &

Gomes 2011, Ken & Sinha 2021, Najafinejad et al. 2023, Saha et al. 2020). The electrode passivation, denoting the genesis inhibiting layer formed because of the polymer layer development or adsorption of byproduct in electrolysis occurs in the anodes. It can be reduced by operating in the galvanostatic mode (Martínez-Huitle et al. 2015).

(m) Temperature: Because the temperature rises, there is a larger mass transfer toward the anode because the medium viscosity decreases and increases in mineralization rate (Anglada et al. 2009, Palanivelu 2005, Ramprasad 2012). However, the thermal decomposition of a few oxidants may also occur at higher temperatures. When nonactive anodes are used at higher temperatures and flow rates, the degradation process intensifies and leads to decreased electrocoagulation and higher current efficiency. This was found in EO treatments undertaken at various temperatures in the absence of the formation of any extra oxidants except •OH (Rocha et al. 2012, Särkkä et al. 2015, Un et al. 2008). The EO process is usually preferred to work at ambient temperature as it requires less energy. Hence, an intense study should also be done for the parameter temperature to gain the highest oxidation ability in the electro-oxidation process (Martínez-Huitle et al. 2015, Özyurt et al. 2017, You et al. 2016). Temperature has a minimal effect on organic elimination when compared to other parameters, although having a positive impact on the effectiveness of treatment in Fenton-like procedures. Lower than 8.3 °C temperatures result in weaker early kinetics, which has an impact on the removal performance and reaction rate (Deng & Englehardt 2006b). However, because flocs become unstable at high temperatures, COD removal may be adversely affected by temperatures above 50°C. The most suitable temperature range is between 20°C and 30°C due to the much-improved treatment outcomes in this range. This is because excessively high or low temperatures negatively affect the effectiveness of processes. Hermosilla et al. found that raising the Fenton process's temperature from 25°C to 45°C somewhat enhanced the elimination of COD (Hermosilla et al. 2009). Several further investigations have found similar results for the Fenton process. The scientists discovered that COD removal increased with temperature, even while the proportion of COD removal reduced at temperatures above ambient. Even if the boost in COD elimination resulting from temperature rise is less significant than other factors, higher temperatures are good for organic oxidation (Umar et al. 2010).

(n) Dissolved oxygen: The electrolyte oxidation to O_2 is one of the reactions in the EO of contaminants, and it

intensely decreases the process efficacy and increases the operation costs. Reduction of dissolved oxygen can electrogenerate H_2O_2 as given by the equation (19), according to the cathode material. When Fe^{2+} cations come into contact with dissolved oxygen in acidic media, they oxidize incredibly slowly. However, in alkaline or neutral environments, Fe^{2+} is instantly changed into $Fe(OH)_2$, which is then swiftly oxidized to $Fe(OH)_3$ by dissolved oxygen (Bae et al. 2022, GilPavas et al. 2017, Ouarda et al. 2020).

$$2H^+ + O_2 + 2e^- \rightarrow H_2O_2 \qquad \text{…(19)}$$

Kapałka et al. have reported that dissolved oxygen (DO) may positively elevate the efficacy of the electro-oxidation process (Kapałka et al. 2009). The external aeration elevates the overall efficacy of the EO process (Priyadarshini Rajesh & Saravanakumar 2023). The role of DO is not deeply investigated, which has to be done in future studies for a better understanding of the prediction of the EO mechanism.

(o) Influence of suspended solids: The increased formation and precipitation of the wastewater's floc had a positive effect on the elimination of COD from the level of suspended matter. The initial concentrate had 500 mg/L of suspended solids. By centrifuging the mixture or introducing 1g/L of kaolin, the suspended solids concentrations ranging from 0 and 1500 mg/L were achieved. The elimination of COD without suspended particles was 41%, however, at 500 mg/L and 1500 mg/L, it was 61% and 71%, respectively, showing the beneficial impact of suspended materials on the EO-like process. Due to the low effectiveness of electro-coagulation, the EO and electro-Fenton-like process predominate contaminants removal in wastewater without suspended solids. Increased suspended solids improved electro-coagulation while slowing down the mass transfer of oxidants and pollutants, which reduced the effectiveness of the EO and electro-Fenton-like reactions for elimination. There were no discernible variations in the amount of ammonia removed between concentrations with either no suspended particles at all or 500 mg/L. This suggests that SS had minimal impact on the in-situ $HClO/ClO^-$ production as well. More suspended solids would, therefore, improve floc generation and precipitation via the electro-coagulation/electro-Fenton-like process but would hinder oxidants' mass transfer in the EF-like process, increasing the breakdown of COD and a negligible effect on ammonia removal (Ding et al. 2021).

BYPRODUCT ASSESSMENT

Thus, the different electrochemical treatments of leachate have been proven not only for removing organics in leachate but also for many emerging micropollutants like Bisphenol-A (Seibert et al. 2019a). This analysis was done
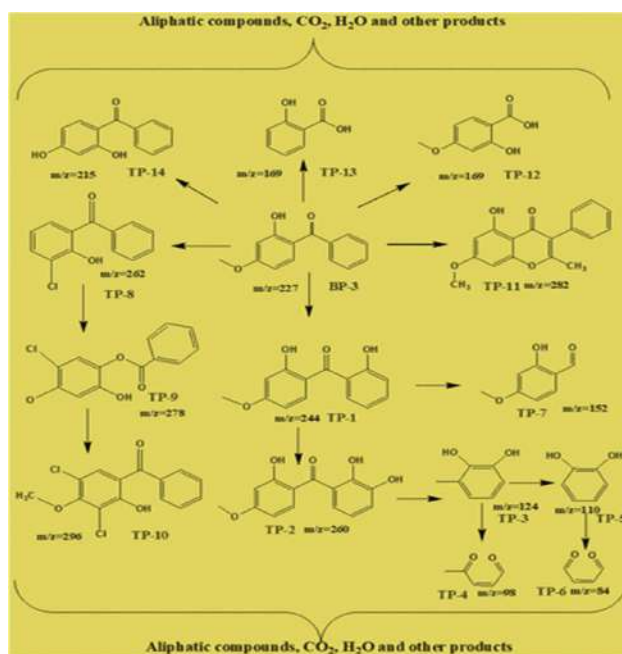
Fig. 9: A suggested pathway for the breaking down of bisphenol-3 utilizing ultrasound and electrocoagulation method. Reprinted with permission from (Patidar and Srivastava, 2023), Copyright {2023}, American Chemical Society.

by using advanced instruments like GC-MS, LC-MS, etc., This analysis is very important not only for assessing the removal of pollutants but also for the byproduct formation. The stabilized leachate was treated using photo-electro-Fenton in which the byproducts formed are less toxic than the parental compounds. Because sometimes the byproducts formed are more hazardous than the parent pollutant during the treatment. However, after some time, the byproducts may convert into another less toxic form during the electrochemical treatment. Hence, the way of byproduct formation, and its degradation pathway are also very important, which influence the determination of optical treatment time. Fig. 9 shows by-product formation in the electrocoagulation of bisphenol-3 degradation with ultrasound assistance. Additionally, the production of byproducts frequently results in a rise in the number of chemicals discovered after treatment, which validates that the degradation of pollutants due to increased molecular weight compounds in raw leachate cannot be detected by these instruments, but the degraded lower molecular weight byproducts can be detected (Seibert et al. 2019a).

The genotoxicity assay is also needed to double-ensure that the leachate has been treated to the desired level. Because only advanced instruments cannot detect all the pollutants accurately in both the raw leachate and raw leachate treated with an EO-EC system, the phytotoxicity of early seed growth was the focus of this investigation. Furthermore, a study was carried out on the unprocessed leachates and produced wastewaters, encompassing an analysis of any possible correlations between the phytotoxicity outcomes and the ICP-OES characterization. Fig. 10 depicts the germination tray used in the phytotoxicity experiments. The results of the phytotoxicity evaluations showed that the suggested treatment strategy reduced the phytotoxicity of the generated effluents. This result can be attributed to

changes in the organic matter's molecular configuration. The electrospray ionization techniques for molecular transformation analysis of dissolved organic matter are included in the recent advanced analysis of wastewater treatment. The 3D EEM analysis only shows the rough removal of humic compounds, fulvic-like compounds, soluble microbial byproducts, etc., with its intensity but not the CHNS compounds and byproducts formation in depth. Thus, advanced ionization spray instruments like FTICR-MS and ORBITRAP are essential for the in-depth analysis of the byproducts formed during the electro-oxidation treatment. Such analysis is not done often owing to the unavailability of the instrument or higher analysis costs. The result is often depicted as a van-Krevelen diagram. Fig. 11 shows the van Krevelen diagram of CHON and CHO of dissolved organic matter in leachate concentrate after Anaerobic/oxic biodegradation (a) and coagulation by $Fe_2(SO4)_3$ (b).

RECENT ADVANCES

Using three combinations of EO modes—monopulse (MP), double pulse (DP), and direct current (DC) Jiang et al. attempted to develop a kinetic framework for the breakdown of organic matter in leachate and transform a semicontinuous/batch reactor to a continuously operating tubular unit for catalytic ozonation of leachate using Fe^{2+}. To maintain a constant reaction volume throughout the experiments, the input of ozone, air, catalyst solution, and foam outflow were all controlled. It was successful in converting the semicontinuous/batch unit with a stream of recycle to operate in a continuous flow. This method increased the leachate's biodegradability significantly, demonstrating its efficacy as a pretreatment. The kinetics were studied for the utilization of a continually operating reactor for catalytic ozonation. Using data from experiments, a mathematical model of carbon

Fig. 10: A germination tray was employed in the phytotoxicity trials. Reprinted with permission from (Martínez-Cruz and Rojas-Valencia 2024), Copyright {2024}, MDPI.f
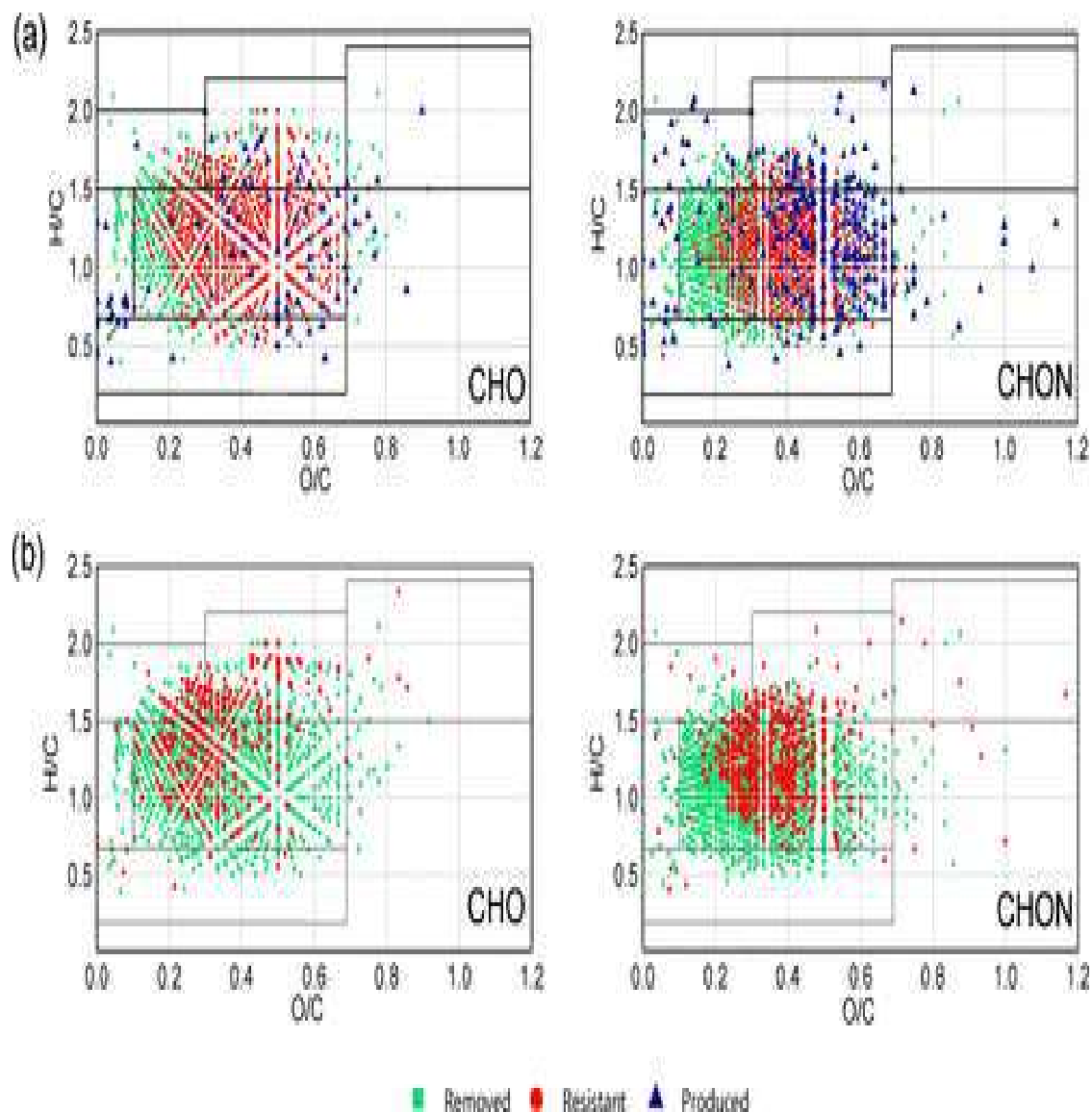
Fig. 11: Van Krevelen diagrams of DOM's CHO and CHON during (a) aerobic and oxic biodegradation in leachate concentration and coagulation by $Fe_2(SO4)_3$ (b) Points in red indicate raw leachate peaks that remained constant (resistant), points in blue indicate new peaks that emerged during biodegradation (generated), and points in green indicate raw leachate peaks that vanished following biodegradation or coagulation (removed). Reprinted with permission from (Yuan et al. 2017), Copyrights {2017}, American Chemical Society.

chain fractionization and decomposition was presented and assessed. The model demonstrated good predictability. The degradation reaction had an average value of 1×108 mol L^{-1} s^{-1} as a constant of kinetics under the circumstances of the current investigation. Apart from the breakdown of TOC, the model also forecasts the number of various chemicals in the solution and the progression of the chain length dispersion (humic and fulvic acids, for example), enabling models with varying degrees of confirmation. The radicals HO_3 and O_3^- are primarily responsible for deterioration, according to the model. For operation scaling, the model developed was able to forecast the reagent quantity and the parameters required to achieve a particular degree of degradation of organics. For instance, the proposed model may predict the amount of reagent and operational parameters needed to create a complete system for leachate abatement and attain a certain amount of TOC removal. On the anodes of a typical DC source oxidation process, there is often a formation of the oxide layer. This leads to higher energy consumption in addition to impeding

Table 1: A few recent advanced methods and materials in the electrochemical treatment of leachate.
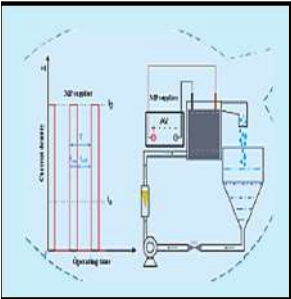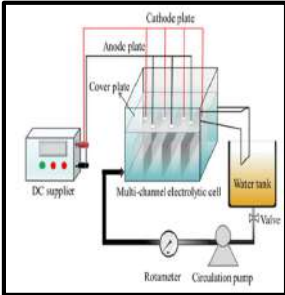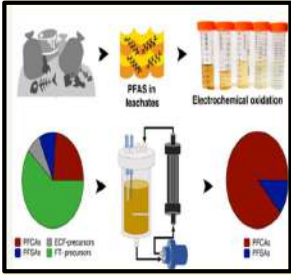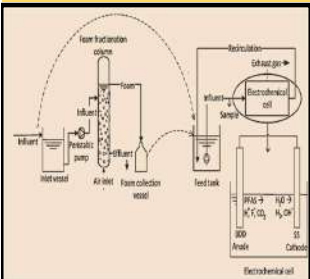
Diagram	Description	Advantages	Ref.
	Pulse Electrochemical Oxidation in a Multi-channel Flow Reactor	Compared to direct current EO, mono-pulse EO gave excellent removal of organics and Nitrogen	(Jiang et al. 2021)
	Multichannel flow reactor for Removal of Simultaneous Desalination and Recalcitrant Organics through electro-oxidation of Reverse Osmosis Leachate	Higher removal of COD (96%), Cl–(96%), and color (99%)	(Yan et al. 2021)
	Electrochemical Transformation Pathways of Perfluoroalkyl Acid (PFAA) in Treatment of Leachate	In-depth study for electrochemical degradation pathways in landfill leachates PFAA	(Maldonado et al. 2022)
	A Pilot-Scale Study on Fractionated Foam aided with Electrochemical Oxidation for leachate PFAS Treatment	Good removal in long-chain PFAS and organofluorine concentration	(Smith et al. 2023)
	A Bipolar Membrane-Integrated Electro chlorination Process	Higher production of HO• & ClO• radicles for higher ammonia removal	(Kuang et al. 2023)

Table Cont....

Diagram	Description	Advantages	Ref.
	Chlorine Reuse in UV/Electrochemical Oxidation of Leachate	Higher reduction of UV_{254} efficiency in less time and energy	(Sato et al. 2023)
	Simultaneous Recovery of NH_3–N and Removal of Heavy Metals from Manganese Residue Leachate Using an Electrodialysis System	87% removal of heavy metals and 95% recovery of NH_3–N	(Yi et al. 2023)
	Hybrid Fenton–Electrocatalytic Membrane Reactor–Biological Aerated Filter for Nanofiltration Retentate Leachate Treatment	The extremely high removal of COD (93%) and color (99%)	(Wang et al. 2024a)
	Electrocatalytic oxidation of landfill leachate coupling with hydrogen production	98% COD removal with 100 ml/min hydrogen production rate	(Wang et al. 2024b)

the anodic oxidation process on the anodes. Comparably, EO treated a biologically processed leachate utilizing power model sources (MP–EO), DC (DC–EO), and DP (DP–EO) in a multi-channel reactor (Jiang et al. 2021). Table 1 shows the publications of some recent studies.

RO concentration from the leachate abatement is extremely tough to cure because of its high concentration of resistant organic compounds, salt content, and color.

Utilizing RuO_2/IrO_2-coated titanium material (RuO_2/IrO_2-Ti) serving as the anodes, Yan et al. created a novel multichannel flow reactor created to use electrochemical oxidation to concurrently remove organics and desalinate from RO leachate concentrate. The electrode gaps in the reactor were set at 5 mm. The parameters of the process, like the superficial circulation velocity, current density, etc., affecting the average energy consumption and reducing efficacy of the COD were studied. The findings showed

that the removal efficiency of COD, color, and Cl⁻could increase to 96.5, 99.6%, and 96.7 respectively, after three hours of treatment. Thus, a new method for the simultaneous elimination of desalination and COD has been proposed with low energy consumption is very low. To process leachate RO concentrates, this work offers an alternate technology (Yan et al. 2021).

Many contaminants found in leachates are detrimental to the ecosystem and humans, notably per- and poly-fluoroalkyl substances (PFAS) studied by Maldonado et al. Previous literature only focuses on PFAS detection and its biodegradation in leachate, however, the use of oxidative techniques to remove perfluoroalkyl acid (PFAA) precursors from leachates is yet to be investigated. This study assessed the quantities of specific and dubious PFAS in leachate over time while they underwent electrochemical treatment. The leachate contained 19 different classes of 53 PFAS, according to LC-QToF studies. This is the first study to examine the treatment of landfill leachate for various PFAS types. The leachate's molar component included 7% precursors of electrochemical fluorination (ECF), 33% PFAAs, and 60% precursors of fluorotelomer (FT). Other research employing the total oxidizable precursor (TOP) assay identified other precursors that LC-QToF did not detect. Identifying known electrochemical decomposition routes was possible by looking at the transitional and final products generated during the electrochemical process. To summarize, the treatment resulted in the electrochemical conversion of precursors based on fluorotelomer and sulfonamide into perfluoroalkyl carboxylic acids (PFCAs). Furthermore, the findings of the electrochemical treatment revealed that short-chain PFAS, specifically PFBA and PFBS, dominated the concentrations. The degree to which PFBA and PFBS should be degraded influences the amount of and the energy required by the electrochemical method. This critical factor should not be overlooked in feasibility assessments. Furthermore, due to the complexity of leachates and the much higher concentrations of a variety of other substances containing PFAS, pretreatment techniques are required before the electrochemical treatment of PFAS in leachates to boost energy efficacy and shorten the duration of the electrochemical system. Although this study presented an overview of the consequences of electrochemical oxidation of PFAS in leachates, more research is needed to specifically oxidize PFAS and increase the practicality of electrochemical oxidation (Maldonado et al. 2022).

Water around the world contains pervasive manmade pollutants called per- and poly-fluoroalkyl substances (PFAS), which are very challenging to remove using standard water treatment methods. Smith et al. developed a workable treatment method that uses an EO phase to break down the per- and poly-fluoroalkyl substances (PFAS) and foam fractionation to separate them from landfill leachate and groundwater. The research integrated comprehensive characterization methods, such as PFAS total parameters, target, and toxicity assessment, with an upgraded experimental methodology. Furthermore, a recently created associated computational simulation effectively recreated the EO dynamics. Short and long-chain PFAS degraded up to 31 and 86%, respectively, whereas the intended treatment train's mean total PFAS degradation was 50%. By using bacterial bioluminescence bioassays and transthyretin binding, the therapy was able to reduce the water's harmful potency. Furthermore, the water's removable organofluorine content dropped by as much as 44%. When taken as a whole, these results enhance our comprehension of a viable and workable strategy for the on-site treatment of PFAS-contaminated water (Smith et al. 2023).

Although electrochemical oxidation is a useful technique for treating mature leachate, because ammonium is susceptible to oxidation by free chlorine (FC) or HO• at low pH values, it is not a very effective way to remove ammonium. To overcome this issue, Kuang et al. suggest a novel bipolar membrane electrochlorination (BPM-EC) technique. According to the results, the BPM-EC system outperformed divided and undivided reactors in monopolar membranes in terms of reduced byproduct generation, including nitrates and chloramines, improved Faradaic system performance, and lower energy usage. Mechanistic investigations showed that adding BPM helped to create alkaline conditions close to the anode, which in turn helped to produce FC and surface-bound HO•, which in turn encouraged the in situ creation of ClO•, a crucial species that is reactive and primarily responsible for speeding up ammonium oxidation and enabling selective nitrogen shift. The evaluation of batch and continuous flow settings to see how well BPM-EC performed in leachate treatment with different ammonium levels. This supports the enhancement of ClO• in the BPM-EC reactor, which catalyzes the ammonium conversion at acidic conditions. Importantly, the suggested BPM-EC method outperformed the typical undivided EC process in removing COD and ammonium from mature landfill leachate. A kinetic model incorporating the essential factors was created and correctly estimated the number of ideal BPM-EC reactors needed to remove all ammonium. The BPM-EC procedure is promising for treating ammonium-containing wastewater due to its effectiveness and reduced byproduct formation compared to EC methods that utilize divided or undivided cells via monopolar membranes and conventional chlorination procedures with chemical input. The capacity to accomplish total ammonium removal is

particularly desirable, given that little research on utilizing AOPs for leachate treatment has focused on ammonium removal owing to the sluggish reaction between ammonium and HO•. This is in contrast to findings on the combination of monopolar membranes and BPMs for isolation and ammonium recovery in extremely concentrated solutions. The author concepts a method of transformation rather than an exchange process, and it is ideal for processing medium-concentration ammonium containing leachate to eradicate nitrogen pollution. BPM-EC is predicted to be an economical, flexible, and green treatment facility for eliminating ammonium and TN (Kuang et al. 2023)

The leachate from landfills, with simultaneous treatment with city sewage, is still a common procedure in the handling of waste, particularly as it has a high ultraviolet absorption at 254 nm. While oxidation is a promising method for DOM degradation, leachate requires significant chemical dosing. An immediate and required option is electrochemical treatment using ultraviolet radiation (UV/EO), which produces chlorine radicals. However, extended UV/EO raises the problem of residual chlorine formation, resulting in toxic compound formation. Sato et al. modified UV/EO to recycle the residual chlorine, with partial replacement of processed leachate with untreated ones, lessening the UV_{254} of the following batch. The response surface methodology application improved the energy efficiency of the chlorine-reuse process, which involved changing the current and the Reynolds number. Sequentially adding a UV dichlorination unit eliminated formulas resistant to EO/UV, giving rise to an 81% decline in UV_{254}. This strategy enhances leachate abatement, especially in locations with existing cotreatment facilities, by demonstrating the reduced potential for genotoxicity and acute toxicity when discharged with municipal sewage at 3% v/v (Sato et al. 2023).

The issue of elevated NH_3-N and heavy metal concentrations in manganese residue leachate (MRL) requires immediate attention due to the potential impact on nearby ecosystems and potentially the ecological system. Yi et al. propose a unique electrodialysis technique for eliminating heavy metals from MRL and recovering NH_3-N using a titanium dioxide nanowire (TiO_2 NW) electrode. Assessing the ecological concerns associated with reusing recovered NH_3-N involves conducting plant growth tests and ecotoxicity investigations. The electrodialysis device that uses a proton membrane to divide the two chambers can remove heavy metals from MRL by 87%–97% while recovering NH_3–N from MRL by 95%. Plant development can be considerably aided by the recovery solution that is collected from the cathode chamber. The outcomes of the ecotoxicity study additionally show that by encouraging

Bacillus reproduction, the retrieved NH_3-N can enhance soil fertility by optimizing the composition of the soil microbial community. This research may offer fresh insight into the safe disposal and resource retrieval of MRLIn order to remove heavy metals from MRL, this work suggests a novel electrodialysis device with TiO_2 NW electrode and the recovery of NH_3-N. The devised technique is capable of eliminating heavy metals (such as lead, cadmium, chromium, etc.) and recovering more than 90% of NH_3-N from the leachate of manganese residue. The produced liquid nitrogen fertilizer appears to be environmentally benign based on the results of the ecotoxicity trial. By encouraging Bacillus reproduction, the recovered NH_3-N can enhance soil fertility by optimizing the composition of the soil microbial community. This research may offer fresh insight into the safe disposal and resource retrieval of MRL, leading to a sustainable green future (Yi et al. 2023).

Wang et al. (2024a) studied a combined biological aerated filter (BAF) and the Fenton processes to create a distinctive hybrid and unified approach relying on the fixed-bed electrocatalytic membrane reactor (FBER) for treating the NF retentate of leachate. The purpose of the FBER procedures and Fenton was to increase the degradation of the NF-concentrated leachate for the BAF process by breaking down the recalcitrant contaminants. With a beginning pH of 3, a molar $[H_2O_2]/[Fe^{2+}]$ ratio of 2/1, and an H_2O_2 dosing of 90 mmol L^{-1}, the Fenton technique removed 64.6% of the chemical oxygen demand (COD). The proportion of BOD_5 to COD rose from 0.05 to 0.38 at a voltage of 2 V and retention 10 min upon treatment with the FBER procedure, exhibiting strong degradation. Finally, during a 48-hour BAF treatment, the removal efficacy of COD and chroma reached 93 and 99% of NF in the retentate, respectively, meeting Chinese wastewater discharge regulations. Thus, the research proposes a highly successful hybrid technique to ease the NF retentate with an extraordinary COD elimination rate (>93%). It is possible to reduce the NF retentate chroma from 1600 to 8, which indicates a 99.5% color elimination performance. A plain carbon membrane-based sequential FBER method demonstrated a high rate of COD removal and outstanding biodegradability increase. This study exhibited the potential benefits of utilizing a comprehensive Fenton-FBER-BAF approach to treating other complicated types of industrial wastewater, such as NF retentate (Wang et al. 2024b).

Wang et al. (2020c) studied leachate treatment with simultaneous hydrogen generation. An integrated electrochemical water system was created involving the anodic electro-oxidation purification of the leachate through a waste incinerator facility in addition to the combined

Table 2: Comparison of different EO of leachate from various countries.

Landfill Site	Nature of leachate	Type of treatment	Percentage removal of pollutants	Type of electrode used	Reference
Wuhan, China	Raw leachate	Electro-Fenton	65% of COD	Ti/RuO_2-IrO_2	(Zhang et al. 2006)
Sivas, Turkey	Raw leachate	Electro-Fenton	72% COD, 87% PO_4-P, 90% color, and 26% NH_4-N	Cast iron	(Atmaca 2009)
Penang, Malaysia	Raw leachate	Electro-Fenton	95% color and 94% COD	Aluminum electrode	(Mohajeri et al. 2010)
Beijing, China	Nanofiltration concentrate of leachate	Electro-Fenton	TOC 82%, and total nitrogen 51%	Carbon–PTFE cathode, Pt anode	(Wang et al. 2012)
Wuhan, China	Raw leachate	Electro-Fenton	94% of COD	Ti/RuO2–IrO2–SnO2–TiO2 mesh anodes and Ti mesh cathodes	(Zhang et al. 2012b)
Penang, Malaysia	Raw leachate	Electro-Fenton	100% Coliform removal	Aluminum electrode	(Aziz et al. 2013)
Kochi, India	Raw leachate	Photo-electro-Fenton and membrane bioreactor	89% TSS, 83% COD, 71% BOD, 100% NH_4-N, 58% P, 92% 65% Sulphate, Sulphide and 65% Cl removal	Cast iron	(Nivya and Minimol Pieus 2016)
Portuguese	Reverse osmosis concentrates of leachate	Electro-Fenton	62% COD	Graphite cathode, BDD anode	(Fernandes et al. 2017)
Osona, Spain	Partial nitrification-anammox effluent of leachate	Microbial Electro-Fenton	62% COD	Stainless steel, wire mesh (cathode), rod (anode)	(Hassan et al. 2017)
Shanghai, China	Raw leachate	Electro-ozonation and sequential batch reactor	COD 64.8%, color 90%, and nickel 52%	Ti/RuO2–IrO2	(Mojiri et al. 2017)
Tamilnadu, India	Raw leachate	Electro-Fenton and biological treatment	97% COD	TiO_2/Ti anode and Graphite cathode	(Baiju et al. 2018)
Guangdong, China	Nanofiltration concentrate of leachate	Electro-Fenton	70% COD	Carbon-PTFE cathode and IrO_2-Ta_2O_5 anode	(Hu et al. 2018)
Weifang, China	Raw leachate	Persulfate based EC	72% COD	CuZn cathode and Iron anode	(Deng et al. 2021)
Abadan, Iran	Raw leachate	Combined EC/aeration, PMS/ZVI/UV, and EF	COD, ammonia, and TOC of 98, 94%, and 93% respectively.	Aluminum electrodes	(Khavari Kashani et al. 2023)
Vellore, India	Raw leachate	Electro-Fenton	TOC 79%, UV254 93%, COD 90%, and NH3-N 90%	Stainless steel	(Priyadarshini Rajesh and Saravanakumar 2023)
Not available	Bio-treated leachate	Persulfate EO & electrocoagulation	91, 80, and 39% for biogenic humic-like components C1, C2, and C3, respectively.	Graphite felt cathode and Iron anode	(Guan et al. 2023)
Centre of Iran	Raw leachate	Electro-ozonation with ZnO nano-granules as a catalyst	COD, BOD_5, TOC, $P-PO_4^{-3}$, NH_4^+-N, color, and turbidity were reduced to 90, 89, 89, 87, 89, 99, and 99%	Iron tubes	(Mehralian et al. 2024)
Suzhou, China	RO concentrate of leachate	EO	84% of humic acid	Cathode as Al and anode as Ti/Ti_4O_7	(Hu et al. 2024)

cathodic electrolysis method for producing hydrogen. Four kinds of electrolyzers were built with varied channels of flow and tested the impact of various factors of the paired reactions' electrolysis. The outcomes show that the pin-type electrolyzer performs better than the energy usage and degrading functioning of the other three electrolyzers. When the current is high At a flow velocity of 100 milliliters per minute and a density of 4000 A/m^2, the pin-type electrolyzer exhibits a minimal potential of 6 V, a COD removal rate of 98% for the leachate and the energy usage of 200 Wh. The creation of hydrogen through the electro-oxidation of leachate presents a viable pathway for the development of

novel hybrid electrocatalytic water treatment systems with energy recovery (Wang et al. 2024b).

MERITS AND DEMERITS

Electrochemical technology is an excellent way to remediate landfill leachate, with the removal of various types of pollutants like dissolved organic carbon, infective microbes, ammonia, etc., as shown in Table 2. It was also found to degrade many emerging pollutants like disinfection byproducts, EDC, pesticides, etc., It has many advantages like less space consumption, rapid treatment, and can be aided with automation for simple operation. Many times, primary or secondary treatment is not essential. Processes like simple electro-coagulation, electro-oxidation, etc., do not need any external addition of chemicals. Because in the electro-Fenton treatment of leachate, iron sludge may be generated with the external addition of iron salt, and H_2O_2 storage in the treatment plant is difficult during the addition as a catalyst. Hence, the persulfate-like non-polluting catalyst is preferred for the EO treatment (Xiao et al. 2020). The EO treatment of leachate has lower energy consumption than many other technologies (Priyadarshini Rajesh & Saravanakumar 2023). The downsides of electrochemical technology include the consumption of power. Green energy, like solar power, can be used as an alternative. The energy recovery in the form
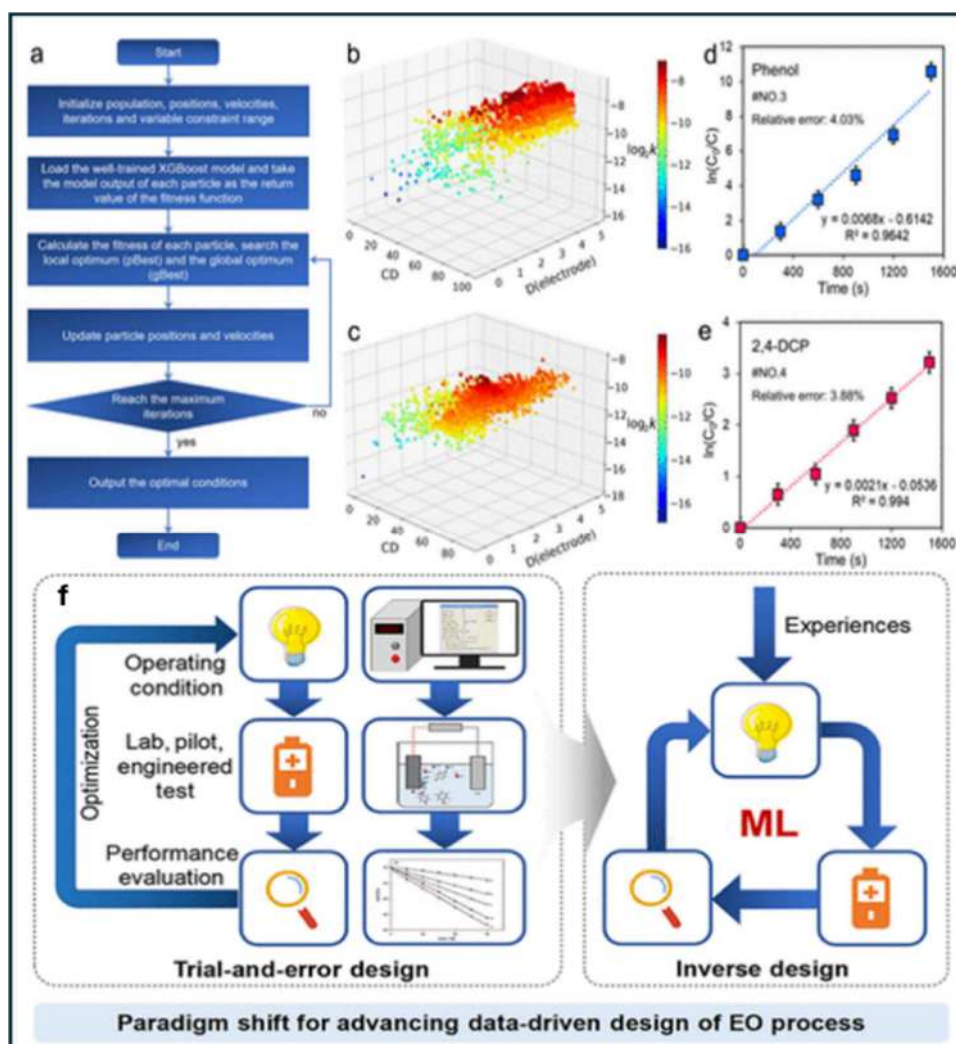
Fig. 12: (a) The PSO algorithm, which maximizes k for the electrochemical oxidation of (b) phenol and (c) 2,4-DCP, the experimental verification (kinetic plots) for the electrochemical oxidation of phenol, (e) 2,4-DCP under the optimized conditions derived from the ML framework for inverse design, and (f) paradigm shift for advancing data-driven design of EO process are the foundations of the schematic flowchart of inverse design. Reprinted with permission from {(Sun et al. 2023)}, Copyright {2023}, American Chemical Society.
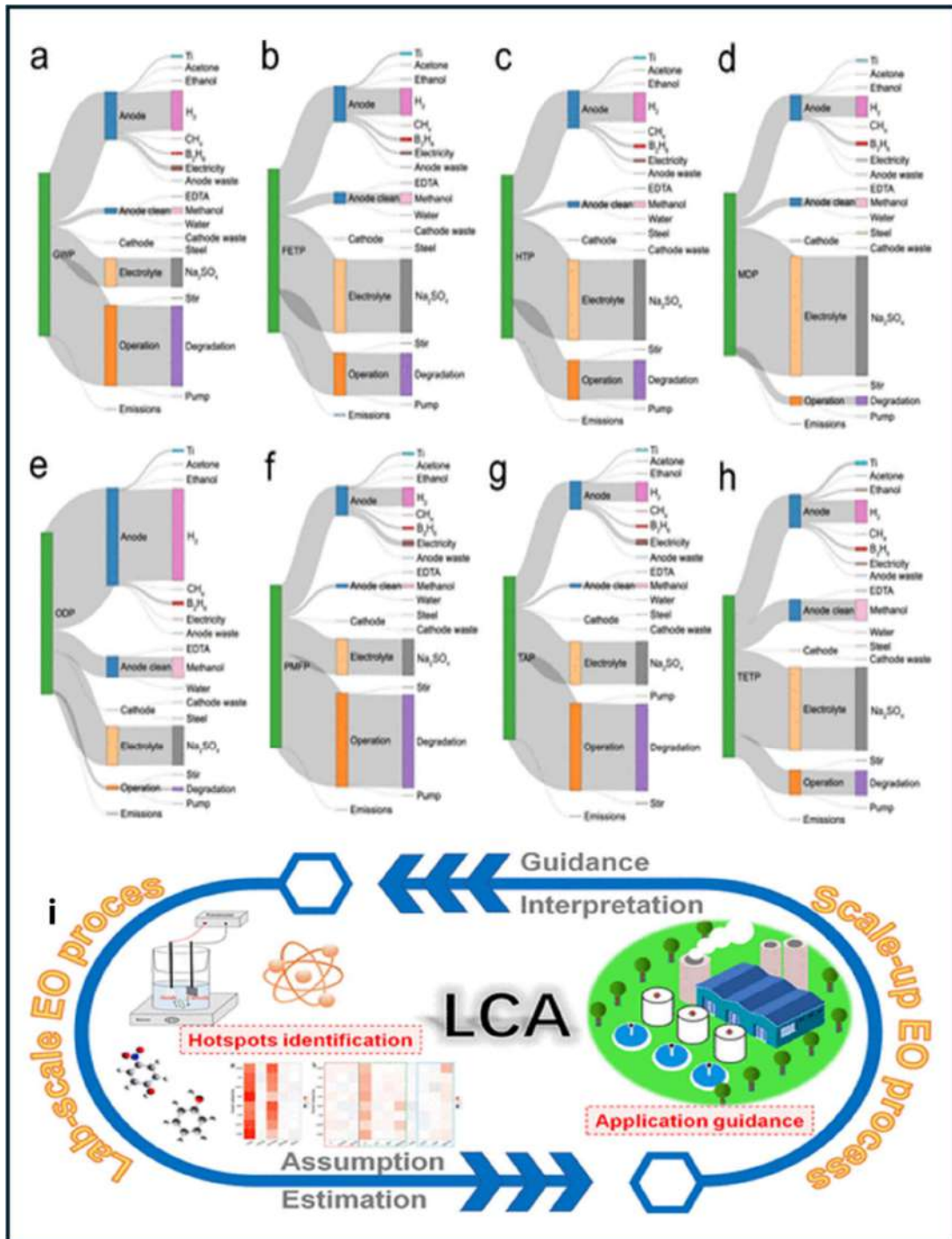
Fig. 13: (a-h) The flow diagram of the Life Cycle Assessment (LCA) and the Sankey diagram of the environmental consequences and primary contributors for the scale-up EO process. Reprinted with permission from {(Sun et al. 2023)}, Copyright {2023}, American Chemical Society.

of hydrogen gas, ammonia gas, chloride gas, etc., from the electrodes will also reduce the overall cost of the process. Using low-cost electrodes like iron or other cheap electrodes will also reduce the overall cost. The byproducts generated should be carefully monitored with proper retention time for degradation, as sometimes they may be higher in risk
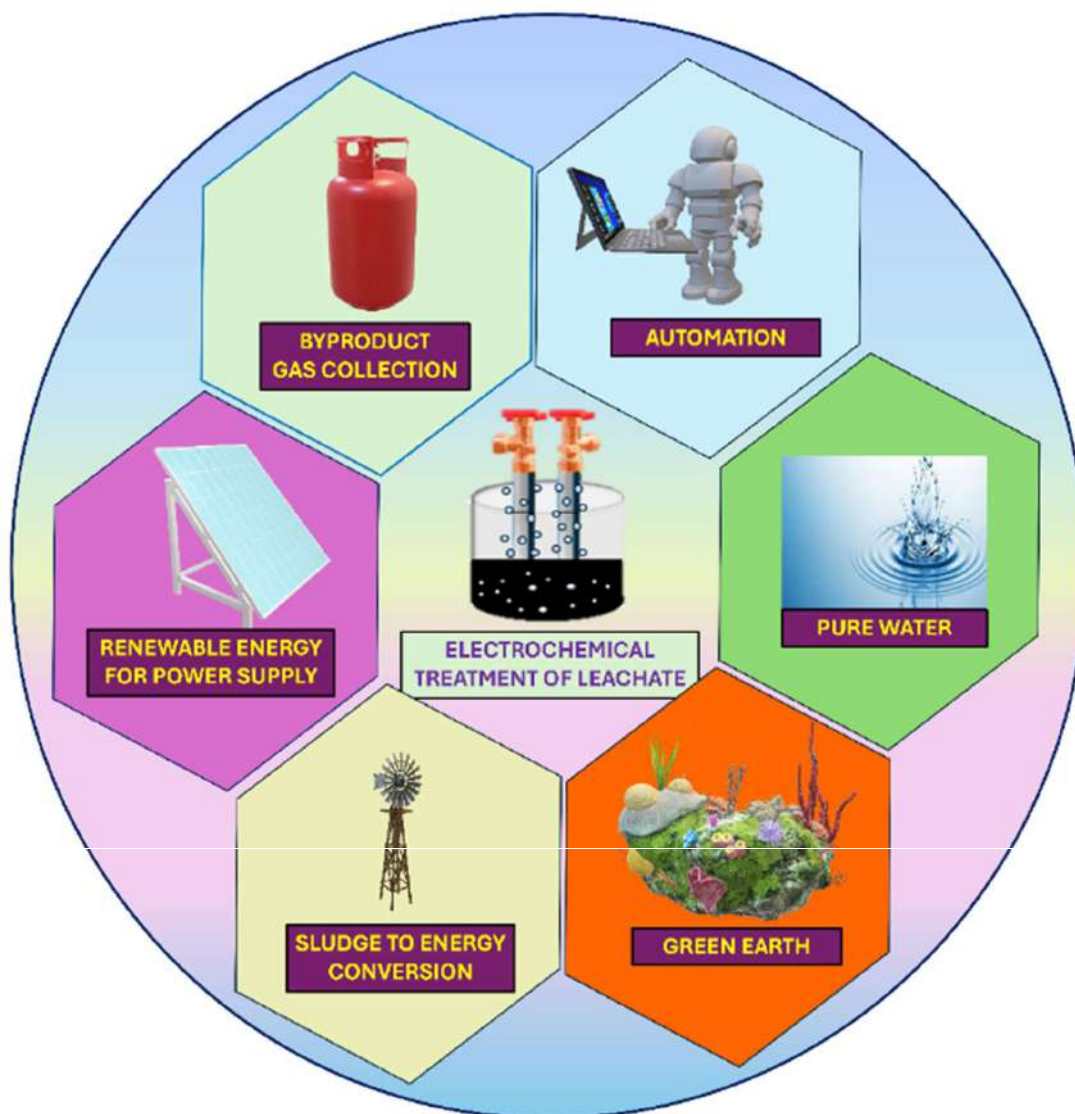
Fig. 14: Multiple benefits of electro-oxidation treatment of leachate for a better future.

than the basic pollutants. Hence, there is a huge research gap in mechanism and byproduct formation in the pollutant treatment of leachate, which in the future has to be filled.

FUTURE STUDIES

(a) **Machine learning:** The EO treatment of leachate could be studied with machine learning for better prediction, optimization, and automation in the future. Sun et al. present a machine learning (ML) basis for a target-driven inverse model of the electrochemical oxidation (EO) technique for water treatment. Based on retraining the data set associated with pollutant features and response ailments, the XGBoost model performed the best in terms of forecasting reaction rate (k), with Rext 2 of 0.84 and RMSEext of 0.79. Based on 315 data points gathered from the available literature, the contaminant quantity, current density, and gap energy (Egap) were determined to be the most important parameters for the inverse modeling of the EO operation.

Adding conditions for reaction as model input characteristics, for example, made additional details available and increased the sample size of the data set, both of which increased model accuracy. Shapley additive explanations (SHAP) were used to conduct feature significance analysis to identify data patterns and understand features. The ML-based inverse model for the EO technique was extended to a stochastic scenario to adjust to the ideal circumstances,
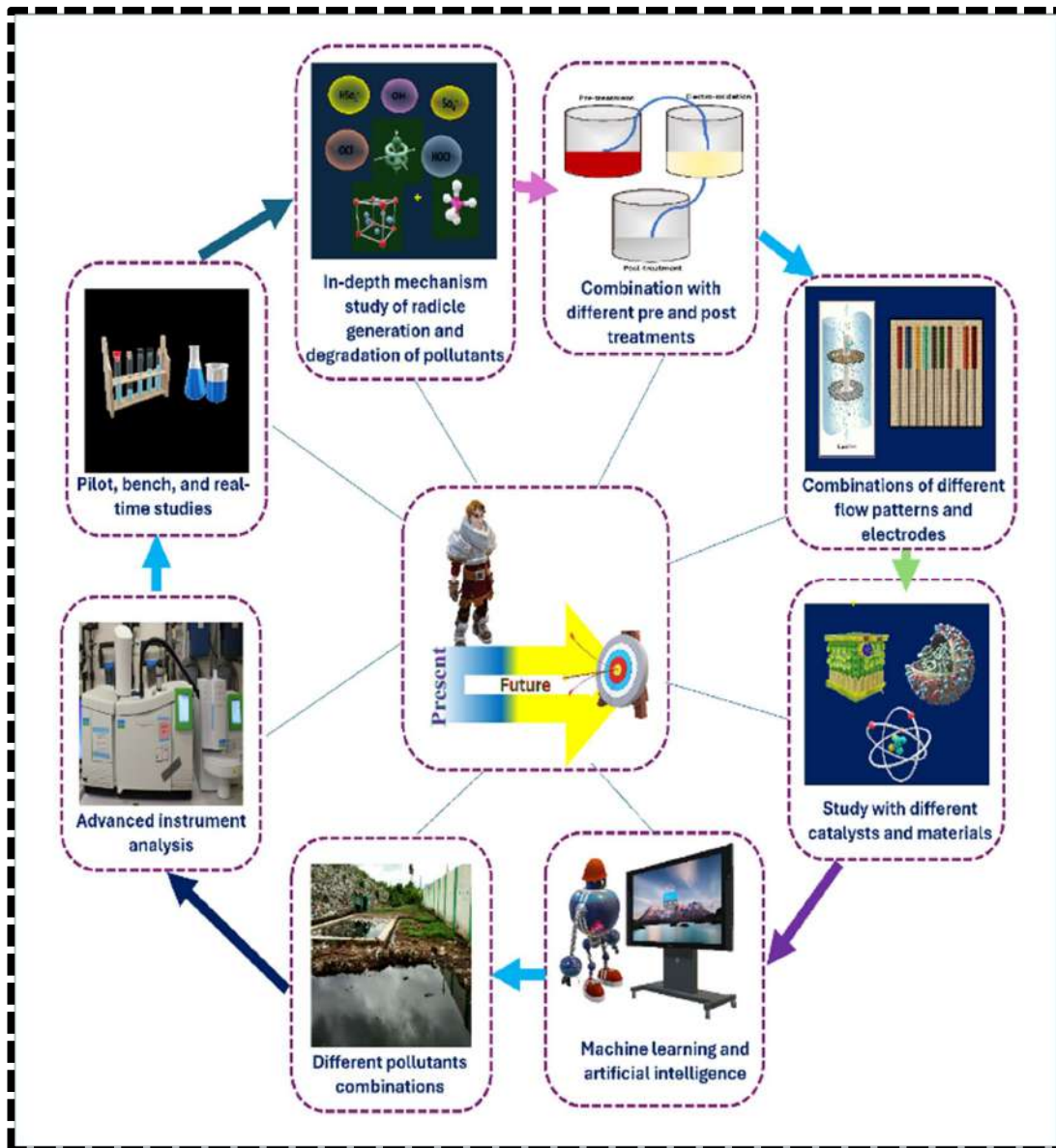
Fig. 15: Literature gap and future perspectives of EO for a sustainable environment.

using 2,4-dichlorophenol (2,4-DCP) and phenol as model pollutants of models. The resulting projected k values were near to the experimental k values after experimental validation, reflecting an absolute error of less than 5%. This investigation proposes a paradigm change from traditional experimentation and error to the data-driven mode for promoting EO procedure advancement through efficient, cost-effective, and environmentally conscious goal-driven tactics, making In the context of zero emissions and global carbon peaking, electrochemical water filtering more economical, efficient, environmentally benign, and time-consuming.

The study included a proof-of-concept demonstration of the machine learning framework for target-oriented inverse design of an EO process for water purification. Firstly, the determination of the important characteristics that influenced EO water treatment procedures (current density, contaminant level, gap energy, Egap) was studied and also supplied readers with open-source data that they could freely obtain. Second, a paradigm shift was demonstrated from the traditional trial-and-error approach to the data-driven inverse design framework for the electrochemical treatment process. Fig. 12, shows the ML overall design of EO.

Thirdly, the required information is obtained, and a suggested inverse design methodology is used to make process and design intensification more sustainable, dependable, and efficient across a range of water treatment processes. In the framework with global peaking of carbon and carbon neutrality, the data-based approach permits the least carbon emission and environmental impact during research and development (R&D) when weighed against experimental methods. Though this much is done, the authors overcome disadvantages, with usage for several considerations like the issue of overestimation arising from the fairly small number of data points used in model development due to the limitations in data availability. An expanded raw data set is necessary to create predictive models that are both sufficiently reliable and useful. Integrating tiny sets of information from different reactions involving oxidation through transferable knowledge may be a useful strategy because the EO process could share certain similarities in fundamentals. However, the ML models were limited to lab-scale situations because the data used in this study came from experimental testing that was already published in the literature. Collecting data at higher scales is necessary for scaling up design using ML models, but sadly, there are not many data points available. Furthermore, the forecasting inaccuracies of the models tied to the initial info collection deviance invariably affected the ML-based inverse design for the EO process. For instance, the original information collection's lacking information was filled in using the kNN technique, which may have introduced bias into the substitution of data and the actual values. More precise approaches, along with greater trustworthy data collection, can help minimize this problem in future efforts. The comprehensibility of the models in this investigation persists to be weak, as the main objective is to create prediction models with exceptional precision for inverse design. Acknowledging the balance that exists between the interpretability and accuracy of the models will remain crucial to comprehending the models' workings. Developing more accurately interpretable models or doing thorough post hoc interpretation of the models are, hence, extremely appealing. In tandem, these findings show that the idea of ML-based inverse design for the electrochemical treatment process is in its early stages, and extra work is required to improve the prospective application, understanding, and correctness of this method (Sun et al. 2023).

(b) Life cycle assessment: Although electrochemical oxidation (EO) is a reliable method for purifying water, the materials and energy used to prepare the electrodes and run the process may have an indirect negative impact on the environment. This study used prospective life cycle assessment (LCA) (Fig. 13) to quantitatively investigate the environmental effects of the new EO technique from laboratories to the workplace. By contrasting two common processes (adsorption and Fenton method) with three indicative anode materials (PbO_2, SnO_2, and boron-doped diamond), the environmental effects of EO technology were evaluated at the laboratory scale. This allowed for the verification of the EO process's rivalry and the identification of the critical elements leading to environmental hotspots. The life cycle inventory was then created when the scaling-up EO LCA was completed to provide direction for use in reality (Sun et al. 2022).

(c) Microplastic degradation studies: Because microplastics are becoming more and more common in the environment, they have become one of the most pervasive contaminants. Microplastics' hydrophobicity and intricate structure may require a lengthy period for them to degrade. The exquisite AOPs can produce hydroxyl (OH) radicals and reactive oxygen. By causing structural alterations that result in the formation of functional groups, including carbonyl, hydroxyl, and modified C-H groups, these radicals start the breakdown of plastic. Modifications in chemical structure provide a substitute to quicken microplastics' breakdown. The degradation of microplastics using the EO method has not been studied yet. Amelia et al. studied that by combining ozonation with hydrogen peroxide (H_2O_2), AOPs were able to modify the molecular nature of PE (polyethylene), microplastics. Using Fourier Transform Infrared (FTIR) analysis, the impact of the AOPs in samples of polyethylene microplastics was assessed. The findings indicate that the O-H and C=O bands are becoming more intense, while the C-H groups are becoming less intense. When applying both the ozonation and hydrogen peroxide methods under a flow rate of 3 $L.min^{-1}$ and pH 12, the maximum carbonyl index (CI) value was 1.33 (Amelia et al. 2021). Tan et al. used graphene oxide/zinc oxide (GO-ZnO) photocatalyst to study the application of photocatalysis in the degradation of LDPE (low-density polyethylene) microplastic with UV light irradiation. At 1000 ppm of GO-ZnO dosage, the amount of microplastic loss in mass from the preliminary investigation was the largest. In comparison to alkaline and acidic conditions, the photodegradation efficiency was largest at the pH 7 solution. Additionally, as the working temperature rose, so did the mass loss of microplastic (Tan et al. 2023). Thus, the combination of different oxidants with EO in the variation of influencing parameters like pH, voltage, etc., has to be studied in the future. Recent studies have also shown that boiling water

reduces microplastic consumption in drinking water (Yu et al. 2024). Hence, the temperature variation in the EO treatment of microplastics in leachate is also to be explored in the future.

An in-depth study with different electrodes, like 3d electrodes, porous electrodes, non-porous electrodes, rotating electrodes, carbonaceous electrodes, etc., with different cathodic and anodic combinations, is needed to bring out the best efficiency of the process. The combination of different additions of green catalysts, and complete byproducts assessment with advanced instruments like LCMS, FTICR-MS, etc., is crucial for ensuring the process's mechanism, efficiency, and safety. The combination with various primary and secondary treatments pre & post-treatment is also to be done. The mechanism for the generation of radicals at each time interval, various should be in detail. The role of aeration is also not studied in detail. Thus, there is a huge gap in determining the overall mechanism of the EO process. The sludge produced can be converted into useful products like biochar for a sustainable environment. Many investigations are done at a lab scale which has to be implemented to bench scale, pilot scale, and real-time. Similarly, there is a literature gap for many emerging pollutants in leachate for its degradation study in EO. The multiple benefits of EO are represented in Fig. 14. Fig. 15 represents the future studies needed for the EO treatment of leachate or any wastewater.

CONCLUSIONS

The EO treatment of leachate has several advantages compared to other methods. Future studies for the optimization of the process for different electrode combinations and integrated electrochemical processes with different green catalysts can reduce the overall cost and improve efficiency. Emerging pollutants like microplastics must be experimented with to know the degradation efficacy. The mechanism needs to be studied in-depth with byproducts assessment using advanced instruments. Green energy like solar energy, can be used for the power supply to reduce the overall cost of the process. The gas generated during the EO may be collected as a useful byproduct. Thus, the EO has several merits in the treatment of heavily polluted wastewater like stabilized leachate. The research gap for the treatment of various emerging pollutants and their combinations needs to be estimated. The life cycle assessment must be done compared with other methods to properly select a method of treatment and a sustainable environment. Thus, optimizing the mentioned suggestions and further study will make the EO technique for wastewater treatment one of the most efficient techniques in the future.

REFERENCES

Abdel-Fatah, M.A., Hawash, S.I. and Shaarawy, H.H., 2021. Cost-effective clean electrochemical preparation of ferric chloride and its applications. *Egypt Journal of Chemistry*, 64, pp.3841–3851. https://doi.org/10.21608/ejchem.2021.75921.3717

Alam, R., Khan, S.U., Usman, M., Asif, M. and Farooqi, I.H., 2022. A critical review on treatment of saline wastewater with emphasis on electrochemical-based approaches. *Process Safety and Environmental Protection*, 17, p.54. https://doi.org/10.1016/j.psep.2021.11.054

World Health Organization (WHO), 2018. *Alternative drinking-water disinfectants: bromine, iodine and silver*. World Health Organization.

Amelia, D., Fathul Karamah, E., Mahardika, M., Syafri, E., Mavinkere Rangappa, S., Siengchin, S. and Asrofi, M., 2021. Effect of advanced oxidation process for chemical structure changes of polyethylene microplastics. *Materials Today: Proceedings*, 17, pp.2501–2504. https://doi.org/10.1016/j.matpr.2021.10.438

Anglada, Á., Urtiaga, A. and Ortiz, I., 2009. Contributions of electrochemical oxidation to wastewater treatment: Fundamentals and review of applications. *Journal of Chemical Technology and Biotechnology*, 22, p.14. https://doi.org/10.1002/jctb.2214

Asfaha, Y.G., Tekile, A.K. and Zewge, F., 2021. Hybrid process of electrocoagulation and electrooxidation system for wastewater treatment: A review. *Clean Engineering and Technology*, 11, p.261. https://doi.org/10.1016/j.clet.2021.100261

Atmaca, E., 2009. Treatment of landfill leachate by using electro-Fenton method. *Journal of Hazardous Materials*, 163, pp.109–114. https://doi.org/10.1016/j.jhazmat.2008.06.067

Aziz, H.A., Othman, O.M. and Abu Amr, S.S., 2013. The performance of Electro-Fenton oxidation in the removal of coliform bacteria from landfill leachate. *Waste Management*, 33, pp.396–400. https://doi.org/10.1016/j.wasman.2012.10.016

Bae, Y., Crompton, N.M., Sharma, N., Yuan, Y., Catalano, J.G. and Giammar, D.E., 2022. Impact of dissolved oxygen and pH on the removal of selenium from water by iron electrocoagulation. *Water Resources*, 15, p.117

Baiju, A., Gandhimathi, R., Ramesh, S.T. and Nidheesh, P.V., 2018. Combined heterogeneous Electro-Fenton and biological process for the treatment of stabilized landfill leachate. *Journal of Environmental Management*, 210, pp.328–337. https://doi.org/10.1016/j.jenvman.2018.01.019

Bergmann, M.E.H., Rollin, J. and Iourtchouk, T., 2009. The occurrence of perchlorate during drinking water electrolysis using BDD anodes. *Electrochimica Acta*, 54, pp.2102–2107. https://doi.org/10.1016/j.electacta.2008.09.040

Boudreau, J., Bejan, D. and Bunce, N.J., 2010. Competition between electrochemical advanced oxidation and electrochemical hypochlorination of acetaminophen at boron-doped diamond and ruthenium dioxide-based anodes. *Canadian Journal of Chemistry*, 88, pp.418–425. https://doi.org/10.1139/V10-017

Brillas, E., Sirés, I. and Oturan, M.A., 2009. Electro-Fenton process and related electrochemical technologies based on Fenton's reaction chemistry. *Chemical Reviews*, 109, pp.6570–6631. https://doi.org/10.1021/cr900136g

Brinzila, C.I., Pacheco, M.J., Ciríaco, L., Ciobanu, R.C. and Lopes, A., 2012. Electrodegradation of tetracycline on BDD anode. *Chemical Engineering Journal*, 209, pp.54–61. https://doi.org/10.1016/j.cej.2012.07.112

Cabeza, A., Urtiaga, A.M. and Ortiz, I., 2007. Electrochemical treatment of landfill leachates using a boron-doped diamond anode. *Industrial & Engineering Chemistry Research*, 46, pp.1439–1446. https://doi.org/10.1021/ie061373x

Candido, L. and Gomes, J.A.C.P., 2011. Evaluation of anode materials for the electro-oxidation of ammonia and ammonium ions. *Materials Chemistry and Physics*, 129, pp.1146–1151. https://doi.org/10.1016/j.matchemphys.2011.05.080

Carvalho de Almeida, C., Ganiyu, S.O., Martínez-Huitle, C.A., dos Santos, E.V., Barrios Eguiluz, K.I. and Salazar-Banda, G.R., 2023. Unprecedented formation of reactive BrO– ions and their role as mediators for organic compounds degradation: The fate of bromide ions released during the anodic oxidation of Bromophenol blue dye. *Electrochemical Science Advances*, 3, p.225. https://doi.org/10.1002/elsa.202100225

Castro, J.A., López-Maldonado, J.T., Cárdenas, J., Orozco, G., Bustos, E. and Rivera, F.F., 2022. Design of an electrochemical flow reactor prototype to the electro-oxidation of amoxicillin in aqueous media using modified electrodes with transition metal oxides. *Journal of Environmental Chemical Engineering*, 10, p.114. https://doi.org/10.1016/j.jece.2022.107165

Choden, Y., Pelzang, K., Basnet, A.D.R. and Dahal, K.B., 2022. Modeling of leachate generation from landfill sites. *Nature Environment and Pollution Technology*, 21, pp.993–1002. https://doi.org/10.46488/NEPT.2022.v21i03.006

Choi, S., Choi, W. Il, Lee, J.S., Lee, C.H., Balamurugan, M., Schwarz, A.D., Choi, Z.S., Randriamahazaka, H. and Nam, K.T., 2023. A reflection on sustainable anode materials for electrochemical chloride oxidation. *Advanced Materials,* 10, p.429 https://doi.org/10.1002/adma.202300429

Chowdhury, M.F., Khandaker, S., Sarker, F., Islam, A., Rahman, M.T. and Awual, M.R., 2020. Current treatment technologies and mechanisms for removal of indigo carmine dyes from wastewater: A review. *Journal of Molecular Liquids,* 17, p.406. https://doi.org/10.1016/j.molliq.2020.114061

Clemente, E., Domingues, E., Quinta-Ferreira, R.M., Leitão, A. and Martins, R.C., 2024. Solar photo-Fenton and persulphate-based processes for landfill leachate treatment: A critical review. *Science of the Total Environment,* 16, p.471. https://doi.org/10.1016/j.scitotenv.2023.169471

Comninellis, C. and Chen, G., 2010. *Electrochemistry for the Environment.* Springer New York. https://doi.org/10.1007/978-0-387-68318-8

Cornejo, O.M., Murrieta, M.F., Castañeda, L.F. and Nava, J.L., 2021. Electrochemical reactors equipped with BDD electrodes: Geometrical aspects and applications in water treatment. *Current Opinion in Solid State and Materials Science*, 25, p.100935. https://doi.org/10.1016/j.cossms.2021.100935

Cossu, R., Polcaro, A.M., Lavagnolo, M.C., Mascia, M., Palmas, S. and Renoldi, F., 1998. Electrochemical treatment of landfill leachate: Oxidation at Ti/PbO2 and Ti/SnO2 anodes. *Environmental Science and Technology*, 32(12), pp.3570–3573. https://doi.org/10.1021/es971094o

del Amo, E.H., Poblete, R., Sánchez, O. and Maldonado, M.I., 2023. Biological treatment and microbial composition of landfill leachate using a composting process in an airlift bioreactor. *Journal of Cleaner Production*, 415, p.137748. https://doi.org/10.1016/j.jclepro.2023.137748

Deng, J., Lu, J., Yan, Q. and Pan, J., 2021. Basic research on chemical mechanical polishing of single-crystal SiC-Electro-Fenton: Reaction mechanism and modeling of hydroxyl radical generation using condition response modeling. *Journal of Environmental Chemical Engineering*, 9, p.104954. https://doi.org/10.1016/j.jece.2020.104954

Deng, Y., Chen, N., Feng, C., Chen, F., Wang, H., Kuang, P., Feng, Z., Liu, T., Gao, Y. and Hu, W., 2019. Treatment of organic wastewater containing nitrogen and chlorine by combinatorial electrochemical system: Taking biologically treated landfill leachate treatment as an example. *Chemical Engineering Journal*, 364, pp.349–360. https://doi.org/10.1016/j.cej.2019.01.176

Deng, Y., Chen, N., Hu, W., Wang, H., Kuang, P., Chen, F. and Feng, C., 2021. Treatment of old landfill leachate by persulfate enhanced electro-coagulation system: Improving organic matters removal and precipitates settling performance. *Chemical Engineering Journal*, 424, p.130262. https://doi.org/10.1016/j.cej.2021.130262

Deng, Y. and Englehardt, J.D., 2006a. Treatment of landfill leachate by the Fenton process. *Water Research*, 40(20), pp.3683–3694. https://doi.org/10.1016/j.watres.2006.08.009

Deng, Y. and Englehardt, J.D., 2006b. Treatment of landfill leachate by the Fenton process. *Water Research*, 40(20), pp.3683–3694. https://doi.org/10.1016/j.watres.2006.08.009

Deng, Y., Zhu, X., Chen, N., Feng, C., Wang, H., Kuang, P. and Hu, W., 2020. Review on electrochemical system for landfill leachate treatment: Performance, mechanism, application, shortcoming, and improvement scheme. *Science of the Total Environment*, 745, p.140768. https://doi.org/10.1016/j.scitotenv.2020.140768

Deng, Z., Xu, S., Liu, C., Zhang, X., Li, M. and Zhao, Z., 2024. Stability of dimensionally stable anode for chlorine evolution reaction. *Nano Research*, 17(2), pp.200–212. https://doi.org/10.1007/s12274-023-5965-7

Desireddy, S., P.C., S., R.L., M. and Mehta, A., 2020. Development of an up-flow anoxic nano-biotechnological reactor for simultaneous removal of ammonia and COD from low C/N secondary treated wastewater. *Journal of Water Process Engineering*, 36, p.101344. https://doi.org/10.1016/j.jwpe.2020.101344

Ding, J., Jiang, M., Zhao, G., Wei, L., Wang, S. and Zhao, Q., 2021. Treatment of leachate concentrate by electrocoagulation coupled with electro-Fenton-like process: Efficacy and mechanism. *Separation and Purification Technology*, 255, p.117668. https://doi.org/10.1016/j.seppur.2020.117668

Dong, F., Pang, Z., Yang, S., Lin, Q., Song, S., Li, C., Ma, X. and Nie, S., 2022. Improving wastewater treatment by triboelectric-photo/electric coupling effect. *ACS Nano,* I1, p.755. https://doi.org/10.1021/acsnano.1c10755

Du, X. and Oturan, M.A., 2021. Nanostructured electrodes for electrocatalytic advanced oxidation processes: From materials preparation to mechanisms understanding and wastewater treatment applications. *Applied Catalysis B: Environmental*, 23, p.332. https://doi.org/10.1016/j.apcatb.2021.120332

Durán, F.E., de Araújo, D.M., do Nascimento Brito, C., Santos, E.V., Ganiyu, S.O. and Martínez-Huitle, C.A., 2018. Electrochemical technology for the treatment of real washing machine effluent at pre-pilot plant scale by using active and non-active anodes. *Journal of Electroanalytical Chemistry*, 818, pp.216–222. https://doi.org/10.1016/j.jelechem.2018.04.029

Eggen, T., Moeder, M. and Arukwe, A., 2010. Municipal landfill leachates: A significant source for new and emerging pollutants. *Science of the Total Environment*, 408, pp.5147–5157. https://doi.org/10.1016/j.scitotenv.2010.07.049

Einaga, Y., 2022. Boron-doped diamond electrodes: Fundamentals for electrochemical applications. *Accounts of Chemical Research*, 55, pp.3605–3615. https://doi.org/10.1021/acs.accounts.2c00597

El-Saadony, M.T., Saad, A.M., El-Wafai, N.A., Abou-Aly, H.E., Salem, H.M., Soliman, S.M., Abd El-Mageed, T.A., Elrys, A.S., Selim, S., Abd El-Hack, M.E., Kappachery, S., El-Tarabily, K.A. and AbuQamar, S.F., 2023. Hazardous wastes and management strategies of landfill leachates: A comprehensive review. *Environmental Technology & Innovation*, 31, p.103150. https://doi.org/10.1016/j.eti.2023.103150

Fabiańska, A., Białk-Bielińska, A., Stepnowski, P., Stolte, S., Siedlecka, E.M. and 2014. Electrochemical degradation of sulfonamides at BDD electrode: Kinetics, reaction pathway and eco-toxicity evaluation.

Journal of Hazardous Materials, 280, pp.579–587. https://doi.org/10.1016/j.jhazmat.2014.08.050

Fan, T.X., Cai, Y., Chu, G.W., Luo, Y., Zhang, L.L. and Chen, J.F., 2019. A novel rotating multielectrodes reactor for electrochemical oxidation process intensification. *Industrial & Engineering Chemistry Research*, 58, pp.2396–2404. https://doi.org/10.1021/acs.iecr.8b05736

Fernandes, A., Labiadh, L., Ciríaco, L., Pacheco, M.J., Gadri, A., Ammar, S. and Lopes, A., 2017. Electro-Fenton oxidation of reverse osmosis concentrate from sanitary landfill leachate: Evaluation of operational parameters. *Chemosphere*, 184, pp.1223–1229. https://doi.org/10.1016/j.chemosphere.2017.06.088

Fernandes, A., Nunes, M.J., Rodrigues, A.S., Pacheco, M.J., Ciríaco, L. and Lopes, A., 2021. Electro-persulfate processes for the treatment of complex wastewater matrices: Present and future. *Molecules,* 61, p.821. https://doi.org/10.3390/molecules26164821

Gautam, P., Kumar, S. and Lokhandwala, S., 2019. Advanced oxidation processes for treatment of leachate from hazardous waste landfill: A critical review. *Journal of Cleaner Production*, 7, p.639. https://doi.org/10.1016/j.jclepro.2019.117639

Ghanbarlou, H., Nasernejad, B., Nikbakht Fini, M., Simonsen, M.E. and Muff, J., 2020. Synthesis of an iron-graphene based particle electrode for pesticide removal in three-dimensional heterogeneous electro-Fenton water treatment system. *Chemical Engineering Journal*, 25, p.395. https://doi.org/10.1016/j.cej.2020.125025

Ghernaout, D., Naceur, M.W. and Aouabed, A., 2011. On the dependence of chlorine by-products generated species formation of the electrode material and applied charge during electrochemical water treatment. *Desalination,* 12, p.74. https://doi.org/10.1016/j.desal.2011.01.010

Ghosh, P., Thakur, I.S. and Kaushik, A., 2017. Bioassays for toxicological risk assessment of landfill leachate: A review. *Ecotoxicology and Environmental Safety*, 141, pp.233–246. https://doi.org/10.1016/j.ecoenv.2017.03.023

GilPavas, E., Arbeláez-Castaño, P., Medina, J. and Acosta, D.A., 2017. Combined electrocoagulation and electro-oxidation of industrial textile wastewater treatment in a continuous multi-stage reactor. *Water Science and Technology*, 76, pp.2515–2525. https://doi.org/10.2166/wst.2017.415

GilPavas, E., Dobrosz-Gómez, I. and Gómez-García, M.Á., 2020. Efficient treatment for textile wastewater through sequential electrocoagulation, electrochemical oxidation and adsorption processes: Optimization and toxicity assessment. *Journal of Electroanalytical Chemistry*, 11, p.878. https://doi.org/10.1016/j.jelechem.2020.114578

Gómez-Espinosa, D., Cervantes-Aguilar, F.J., Río-García, J.C. Del, Villarreal-Barajas, T., Vázquez-Durán, A. and Méndez-Albores, A., 2017. Ameliorative effects of neutral electrolyzed water on growth performance, biochemical constituents, and histopathological changes in Turkey poults during aflatoxicosis. *Toxins (Basel)*, 9, p.116. https://doi.org/10.3390/toxins9030104

Guan, S., Ding, J., Zhao, Q., Liu, F., Gao, Q., Nadagouda, M.N., Al-Anazi, A. and 2023. Evaluation of persulfate enhanced electrocoagulation (EC/PS) for bio-treated landfill leachate: Organics transformation pathways and carbon flow quantitative analysis. *Chemical Engineering Journal*, 11, p.468. https://doi.org/10.1016/j.cej.2023.143698

Hadi, N.S., 2023. Leachate Characterization and Assessment of Soil Pollution Near Some Municipal Solid Waste Transfer Stations in Baghdad City. *Nature Environment and Pollution Technology*, 22, pp.2239–2247. https://doi.org/10.46488/NEPT.2023.v22i04.052

Hajalifard, Z., Mousazadeh, M., Khademi, S., Khademi, N., Jamadi, M.H. and Sillanpää, M., 2023. The efficacious of AOP-based processes in concert with electrocoagulation in abatement of CECs from water/wastewater. *Nature Partner Journals Clean Water,* 11, p.21-36. https://doi.org/10.1038/s41545-023-00239-9

Hassan, M., Pous, N., Xie, B., Colprim, J., Balaguer, M.D. and Puig, S., 2017. Employing Microbial Electrochemical Technology-driven electro-Fenton oxidation for the removal of recalcitrant organics from sanitary landfill leachate. *Bioresource Technology*, 243, pp.949–956. https://doi.org/10.1016/j.biortech.2017.07.042

He, Y., Zhao, D., Lin, H., Huang, H., Li, H. and Guo, Z., 2022. Design of diamond anodes in electrochemical degradation of organic pollutants. *Current Opinion in Electrochemistry,* 21, p.878. https://doi.org/10.1016/j.coelec.2021.100878

Hermosilla, D., Cortijo, M. and Huang, C.P., 2009. Optimizing the treatment of landfill leachate by conventional Fenton and photo-Fenton processes. *Science of the Total Environment*, 407, pp.3473–3481. https://doi.org/10.1016/j.scitotenv.2009.02.009

Hu, P., Li, H., Tan, Y., Adeleye, A.S. and Hao, T., 2024. Enhanced electrochemical treatment of humic acids and metal ions in leachate concentrate: Experimental and molecular mechanism investigations. *Journal of Hazardous Materials*, 4, p.462. https://doi.org/10.1016/j.jhazmat.2023.132774

Hu, Y., Lu, Y., Liu, G., Luo, H., Zhang, R. and Cai, X., 2018. Effect of the structure of stacked electro-Fenton reactor on treating nanofiltration concentrate of landfill leachate. *Chemosphere*, 202, pp.191–197. https://doi.org/10.1016/j.chemosphere.2018.03.103

Hu, Z., Cai, J., Song, G., Tian, Y. and Zhou, M., 2021. Anodic oxidation of organic pollutants: Anode fabrication, process hybrid and environmental applications. *Current Opinion in Electrochemistry,* 7, p.589. https://doi.org/10.1016/j.coelec.2020.100659

Ilmasari, D., Kamyab, H., Yuzir, A., Riyadi, F.A., Khademi, T., Al-Qaim, F.F., Kirpichnikova, I. and Krishnan, S., 2022a. A review of the biological treatment of leachate: Available technologies and future requirements for the circular economy implementation. *Biochemical Engineering Journal*, 187, p.1612. https://doi.org/10.1016/j.bej.2022.108605

Ilmasari, D., Sahabudin, E., Riyadi, F.A., Abdullah, N. and Yuzir, A., 2022b. Future trends and patterns in leachate biological treatment research from a bibliometric perspective. *Journal of Environmental Management*, 22, p.594. https://doi.org/10.1016/j.jenvman.2022.115594

Jiang, Z., Cheng, Z., Yan, C., Zhang, X., Tian, Y., Zhang, X. and Quan, X., 2021. Simultaneous removal of nitrogen and refractory organics from a biologically treated leachate by pulse electrochemical oxidation in a multi-channel flow reactor. *ACS Omega*, 6, pp.25539–25550. https://doi.org/10.1021/acsomega.1c03567

Jin, Q., Tao, D., Lu, Y., Sun, J., Lam, C.H., Su, G. and He, Y., 2022. New insight on occurrence of liquid crystal monomers: A class of emerging e-waste pollutants in municipal landfill leachate. *Journal of Hazardous Materials*, 423, p.127146. https://doi.org/10.1016/j.jhazmat.2021.127146

Kanmani, S. and Dileepan, A.G.B., 2023. Treatment of landfill leachate using photocatalytic based advanced oxidation process – a critical review. *Journal of Environmental Management*, 345. https://doi.org/10.1016/j.jenvman.2023.118794

Kapałka, A., Lanova, B., Baltruschat, H., Fóti, G. and Comninellis, C., 2008. Electrochemically induced mineralization of organics by molecular oxygen on boron-doped diamond electrode. *Electrochemistry Communications*, 10(7), pp. 1215–1218. https://doi.org/10.1016/j.elecom.2008.06.005

Kapałka, A., Fóti, G. and Comninellis, C., 2009. The importance of electrode material in environmental electrochemistry: Formation and reactivity of free hydroxyl radicals on boron-doped diamond electrodes. *Electrochimica Acta*, 54(7), pp. 2018–2023. https://doi.org/10.1016/j.electacta.2008.06.045

Ken, D.S. and Sinha, A., 2021. Dimensionally stable anode (Ti/RuO2) mediated electro-oxidation and multi-response optimization study for remediation of coke-oven wastewater. *Journal of Environmental Chemical Engineering*, 9(2), pp. 105025. https://doi.org/10.1016/j.jece.2021.105025

Kerwick, M.I., Reddy, S.M., Chamberlain, A.H.L. and Holt, D.M., 2005. Electrochemical disinfection: An environmentally acceptable method of drinking water disinfection?. *Electrochimica Acta*, 50(26), pp. 5270–5277. https://doi.org/10.1016/j.electacta.2005.02.074

Khaleel, G.F., Ismail, I. and Abbar, A.H., 2023. Application of solar photo-electro-Fenton technology to petroleum refinery wastewater degradation: Optimization of operational parameters. *Heliyon*, 9, p.21. https://doi.org/10.1016/j.heliyon.2023.e15062

Khalil, C., Al Hageh, C., Korfali, S. and Khnayzer, R.S., 2018. Municipal leachates health risks: Chemical and cytotoxicity assessment from regulated and unregulated municipal dumpsites in Lebanon. *Chemosphere*, 208, pp.1–13. https://doi.org/10.1016/j.chemosphere.2018.05.151

Khavari Kashani, M.R., Wang, Q., Khatebasreh, M., Li, X., Sheikh Asadi, A.M., Boczkaj, G. and Ghanbari, F., 2023. Sequential treatment of landfill leachate by electrocoagulation/aeration, PMS/ZVI/UV and electro-Fenton: Performance, biodegradability and toxicity studies. *Journal of Environmental Management*, 338, p.61. https://doi.org/10.1016/j.jenvman.2023.117781

Kim, K.-W., Lee, E.-H., Kim, J.-S., Shin, K.-H. and Jung, B.-I., 2002. Material and organic destruction characteristics of high temperature-sintered RuO[sub 2] and IrO[sub 2] electrodes. *Journal of The Electrochemical Society*, 149, pp.D187. https://doi.org/10.1149/1.1515280

Kraft, A., 2008. Electrochemical water disinfection: A short review. *Platinum Metals Review*, 41, p.789. https://doi.org/10.1595/147106708X329273

Kuang, W., Yan, Z., Chen, J., Ling, X., Zheng, W., Huang, W. and Feng, C., 2023. A bipolar membrane-integrated electrochlorination process for highly efficient ammonium removal in mature landfill leachate: The importance of ClO• generation. *Environmental Science and Technology*, 57, pp.18538–18549. https://doi.org/10.1021/acs.est.2c05735

Kurban, M., Zhang, Y., Wang, Y., Su, Z., Zhou, T., Zhou, C., Xie, C., Li, L., Li, J., Bai, J. and Zhou, B., 2024. Chlorine oxide radical: An emerging free radical for denitrification and pollutant degradation. *Journal of Environmental Chemical Engineering*, 12, p.630. https://doi.org/10.1016/j.jece.2024.112630

Kurniawan, S.B., Pambudi, D.S.A., Ahmad, M.M., Alfanda, B.D., Imron, M.F. and Abdullah, S.R.S., 2022. Ecological impacts of ballast water loading and discharge: Insight into the toxicity and accumulation of disinfection by-products. *Heliyon*, 6, p.89. https://doi.org/10.1016/j.heliyon.2022.e09107

Lee, K.M., Lee, H.J., Seo, J., Lee, T., Yoon, J., Kim, C. and Lee, C., 2022. Electrochemical oxidation processes for the treatment of organic pollutants in water: Performance evaluation using different figures of merit. *ACS ES&T Engineering*, 9, p.228. https://doi.org/10.1021/acsestengg.2c00228

Lei, Y., Hou, J., Fang, C., Tian, Y., Naidu, R., Zhang, J., Zhang, X., Zeng, Z., Cheng, Z., He, J., Tian, D., Deng, S. and Shen, F., 2023. Ultrasound-based advanced oxidation processes for landfill leachate treatment: Energy consumption, influences, mechanisms, and perspectives. *Ecotoxicology and Environmental Safety*, 11, pp.27-36. https://doi.org/10.1016/j.ecoenv.2023.115366

Lemeyonouin Aliou Guillaume, P., Ollo, K., Aliou Lemeyonouin Guillaume, P. and Konan Honoré, K., 2013. Electrochemical treatment of the wastewaters of abidjan on thermally prepared platinum modified metal oxides electrodes. *European Journal of Scientific Research*, 45, pp.123–130.

Leow, W.R., Lum, Y., Ozden, A., Wang, Y., Nam, D.H., Chen, B., Wicks, J., Zhuang, T.T., Li, F., Sinton, D. and Sargent, E.H., 2020. Chloride-mediated selective electrosynthesis of ethylene and propylene oxides at high current density. *Science (1979)*, 368, pp.1228–1233. https://doi.org/10.1126/science.aaz8459

Li, M., Zhang, Q., Sun, F., Cui, M.H., Liu, H. and Chen, C., 2023. The effect of microbial electrolysis cell coupled with anaerobic digestion for landfill leachate treatment. *Journal of Water Process Engineering*, 55, pp.104260. https://doi.org/10.1016/j.jwpe.2023.104260

Li, W., Liu, G., Miao, D., Li, Z., Chen, Y., Gao, X., Liu, T., Wei, Q., Ma, L., Zhou, K. and Yu, Z., 2020. Electrochemical oxidation of Reactive Blue 19 on boron-doped diamond anode with different supporting electrolyte. *Journal of Environmental Chemical Engineering*, 8, pp.103997. https://doi.org/10.1016/j.jece.2020.103997

Lin, S.H. and Chang, C.C., 2000. Treatment of landfill leachate by combined electro-Fenton oxidation and sequencing batch reactor method. *Water Research*, 34, pp.4243–4249. https://doi.org/10.1016/S0043-1354(00)00185-8

Liu, G., Zheng, F., Li, J., Zeng, G., Ye, Y., Larson, D.M., Yano, J., Crumlin, E.J., Ager, J.W., Wang, L. and Toma, F.M., 2021. Investigation and mitigation of degradation mechanisms in Cu2O photoelectrodes for CO2 reduction to ethylene. *Nature Energy*, 6, pp.1124–1132. https://doi.org/10.1038/s41560-021-00927-1

Liu, J., Ren, N., Qu, C., Lu, S., Xiang, Y. and Liang, D., 2022. Recent advances in the reactor design for industrial wastewater treatment by electro-oxidation process. *Water (Switzerland)*, 14, pp.3711. https://doi.org/10.3390/w14223711

Liu, L., Cai, W., Chen, Y. and Wang, Y., 2018. Fluid dynamics and mass transfer study of electrochemical oxidation by CFD prediction and experimental validation. *Industrial and Engineering Chemistry Research*, 57, pp.6498–6504. https://doi.org/10.1021/acs.iecr.7b04226

Liu, Z., Tao, Y., Zhang, Z., He, J., Yang, K. and Ma, J., 2023. Active chlorine mediated ammonia oxidation in an electrified SnO2–Sb filter: Reactivity, mechanisms and response to matrix effects. *Separation and Purification Technology*, 312, p.123369. https://doi.org/10.1016/j.seppur.2023.123369

Luna-Trujillo, M., Palma-Goyes, R., Vazquez-Arenas, J. and Manzo-Robledo, A., 2020. Formation of active chlorine species involving the higher oxide MOx+1 on active Ti/RuO2-IrO2 anodes: A DEMS analysis. *Journal of Electroanalytical Chemistry*, 878, p.114661. https://doi.org/10.1016/j.jelechem.2020.114661

Luo, Y., Zhang, Z., Chhowalla, M. and Liu, B., 2023. recent advances in design of electrocatalysts for high-current-density water splitting. *Electrocatalysis Journal*, 18, pp.123–135.

Ma, J., Trellu, C., Skolotneva, E., Oturan, N., Oturan, M.A. and Mareev, S., 2023. Investigating the reactivity of TiOx and BDD anodes for electro-oxidation of organic pollutants by experimental and modeling approaches. *Electrochimica Acta*, 439, pp.141513. https://doi.org/10.1016/j.electacta.2022.141513

Ma, Y., Guo, Z., Dong, X., Wang, Y. and Xia, Y., 2019. Organic Proton-Buffer Electrode to Separate Hydrogen and Oxygen Evolution in Acid Water Electrolysis. *Angewandte Chemie*, 131, pp.4670–4674. https://doi.org/10.1002/ange.201814625

Maldonado, V.Y., Schwichtenberg, T., Schmokel, C., Witt, S.E. and Field, J.A., 2022. Electrochemical transformations of perfluoroalkyl acid (PFAA) precursors and PFAAs in landfill leachates. *ACS Environmental Science and Technology Water*, 2, pp.624–634. https://doi.org/10.1021/acsestwater.1c00479

Manasa, R.L. and Mehta, A., 2021. Current perspectives of anoxic ammonia removal and blending of partial nitrifying and denitrifying bacteria for ammonia reduction in wastewater treatment. *Journal of Water Process Engineering*, 23, pp.102085. https://doi.org/10.1016/j.jwpe.2021.102085

Mandal, P., Dubey, B.K. and Gupta, A.K., 2017. Review on landfill leachate treatment by electrochemical oxidation: Drawbacks, challenges and future scope. *Waste Management*, 69, pp.250–273. https://doi.org/10.1016/j.wasman.2017.08.034

Mandal, P., Gupta, A.K. and Dubey, B.K., 2020. Role of inorganic anions on the performance of landfill leachate treatment by electrochemical oxidation using graphite/PbO2 electrode. *Journal of Water Process Engineering*, 33, pp.101119. https://doi.org/10.1016/j.jwpe.2019.101119

Martínez-Cruz, A. and Rojas-Valencia, M.N., 2024. Assessment of phytotoxicity in untreated and electrochemically treated leachates through the analysis of early seed growth and inductively coupled plasma-optical emission spectroscopy characterization. *horticulturae*, 10, pp.10067. https://doi.org/10.3390/horticulturae10010067

Martínez-Huitle, C.A. and Ferro, S., 2006. Electrochemical oxidation of organic pollutants for the wastewater treatment: Direct and indirect processes. *Chemical Society Reviews*, 35, pp.1324–1340. https://doi.org/10.1039/b517632h

Martínez-Huitle, C.A., Rodrigo, M.A., Sirés, I. and Scialdone, O., 2015. Single and Coupled Electrochemical Processes and Reactors for the Abatement of Organic Water Pollutants: A Critical Review. *Chemical Reviews*, 115(24), pp.13362–13407. https://doi.org/10.1021/acs.chemrev.5b00361

Mathew, A.T. and Saravanakumar, M.P., 2023. Removal of bisphenol A and methylene blue through persulfate activation by calcinated δ-MnO2 nanorods: effect of ultrasonic assistance and toxicity assessment. *Environmental Science and Pollution Research*, 30(14), pp.14497–14517. https://doi.org/10.1007/s11356-022-23146-x

Medeiros De Araújo, D., Cañizares, P., Martínez-Huitle, C.A. and Rodrigo, M.A., 2014. Electrochemical conversion/combustion of a model organic pollutant on BDD anode: Role of sp3/sp2 ratio. *Electrochemistry Communications*, 47, p.37–40. https://doi.org/10.1016/j.elecom.2014.07.017

Mehralian, M., Ehrampoush, M.H., Ebrahimi, A.A. and Dalvand, A., 2024. Electro-catalytic ozonation of contaminants in landfill leachate: Optimization by BBD, economic evaluation, mechanism, and reaction pathway. *Colloids and Surfaces A: Physicochemical and Engineering Aspects*, 68, pp.123–130. https://doi.org/10.1016/j.colsurfa.2024.133263

Meng, J., Geng, C., Wu, Y., Guan, Y., Gao, W., Jiang, W., Liang, J., Liu, S. and Wang, X., 2023. Comparing the electrochemical degradation of levofloxacin using the modified Ti/SnO2 electrode in different electrolytes. *Journal of Electroanalytical Chemistry*, 94, p.117633. https://doi.org/10.1016/j.jelechem.2023.117633

Meng, X., Khoso, S.A., Jiang, F., Zhang, Y., Yue, T., Gao, J., Lin, S., Liu, R., Gao, Z., Chen, P., Wang, L., Han, H., Tang, H., Sun, W., Hu, Y., 2020. Removal of chemical oxygen demand and ammonia nitrogen from lead smelting wastewater with high salts content using electrochemical oxidation combined with coagulation–flocculation treatment. *Separation and Purification Technology*, 45, pp.211–220. https://doi.org/10.1016/j.seppur.2019.116233

Millán, M., García-Orozco, V.M., Lobato, J., Fernández-Marchante, C.M., Roa-Morales, G., Linares-Hernández, I., Natividad, R. and Rodrigo, M.A., 2021. Toward more sustainable photovoltaic solar electrochemical oxidation treatments: Influence of hydraulic and electrical distribution. *Journal of Environmental Management*, 50, p.112064. https://doi.org/10.1016/j.jenvman.2021.112064

Mishra, S., Singh, V., Ormeci, B., Hussain, A., Cheng, L., Venkiteshwaran, K., 2023. Anaerobic–aerobic treatment of wastewater and leachate: A review of process integration, system design, performance and associated energy revenue. *Journal of Environmental Management*, 82, p.116898. https://doi.org/10.1016/j.jenvman.2022.116898

Mohajeri, S., Aziz, H.A., Isa, M.H., Zahed, M.A. and Adlan, M.N., 2010. Statistical optimization of process parameters for landfill leachate treatment using electro-Fenton technique. *Journal of Hazardous Materials*, 176(1-3), pp.749–758. https://doi.org/10.1016/j.jhazmat.2009.11.099

Mojiri, A., Ziyang, L., Hui, W., Ahmad, Z., Tajuddin, R.M., Abu Amr, S.S., Kindaichi, T., Aziz, H.A., Farraji, H., 2017. Concentrated landfill leachate treatment with a combined system including electro-ozonation and composite adsorbent augmented sequencing batch reactor process. *Process Safety and Environmental Protection*, 68, pp.253–262. https://doi.org/10.1016/j.psep.2017.07.013

Mor, S. and Ravindra, K., 2023. Municipal solid waste landfills in lower- and middle-income countries: Environmental impacts, challenges and sustainable management practices. *Process Safety and Environmental Protection*, 95, pp.510–530. https://doi.org/10.1016/j.psep.2023.04.014

Moradi, M., Vasseghian, Y., Khataee, A., Kobya, M., Arabzade, H. and Dragoi, E.N., 2020. Service life and stability of electrodes applied in electrochemical advanced oxidation processes: A comprehensive review. *Journal of Industrial and Engineering Chemistry*, 65, pp.144–155. https://doi.org/10.1016/j.jiec.2020.03.038

Mousset, E., Quackenbush, L., Schondek, C., Gerardin-Vergne, A., Pontvianne, S., Kmiotek, S., Pons, M.N., 2020. Effect of homogeneous Fenton combined with electron transfer on the fate of inorganic chlorinated species in synthetic and reclaimed municipal wastewater. *Electrochimica Acta*, 80, pp.282–291. https://doi.org/10.1016/j.electacta.2019.135608

Muthuraman, G. and Moon, I.S., 2012. A review on an electrochemically assisted-scrubbing process for environmental harmful pollutant's destruction. *Journal of Industrial and Engineering Chemistry*, 18(6), pp.1761–1768. https://doi.org/10.1016/j.jiec.2012.03.021

Najafinejad, M.S., Chianese, S., Fenti, A., Iovino, P. and Musmarra, D., 2023. Application of electrochemical oxidation for water and wastewater treatment: An overview. *Molecules*, 28(10), p.4208. https://doi.org/10.3390/molecules28104208

Narenkumar, J., Sathishkumar, K., Das, B., Rajasekar, A., Rajakrishnan, R., Rajamohan, R. and Malik, T., 2023. An integrated approach of bioleaching-enhanced electrokinetic remediation of heavy metals from municipal waste incineration fly ash using *Acidithiobacillus* spp. *Frontiers in Environmental Science*, 11, p.1273930. https://doi.org/10.3389/fenvs.2023.1273930

Neodo, S., Rosestolato, D., Ferro, S. and De Battisti, A., 2012. On the electrolysis of dilute chloride solutions: Influence of the electrode material on Faradaic efficiency for active chlorine, chlorate and perchlorate. *Electrochimica Acta*, 80, pp.282–291. https://doi.org/10.1016/j.electacta.2012.07.017

Nivya, T.K. and Minimol Pieus, T., 2016. Comparison of photo electrofenton process(pef) and combination of pef process and membrane bioreactor in the treatment of landfill leachate. *Procedia Technology*, 24, pp.224–231. https://doi.org/10.1016/j.protcy.2016.05.030

Oturan, N., Van Hullebusch, E.D., Zhang, H., Mazeas, L., Budzinski, H., Le Menach, K., Oturan, M.A., 2015. Occurrence and Removal of Organic Micropollutants in Landfill Leachates Treated by Electrochemical Advanced Oxidation Processes. Environ Sci Technol 49, 12187–12196. https://doi.org/10.1021/acs.est.5b02809

Ouarda, Y., Trellu, C., Lesage, G., Rivallin, M., Drogui, P. and Cretin, M., 2020. Electro-oxidation of secondary effluents from various wastewater plants for the removal of acetaminophen and dissolved organic matter. *Journal of Hazardous Materials*, 350, pp.123-130.

Özyurt, B., Camcıoğlu, Ş. and Hapoglu, H., 2017. A consecutive electrocoagulation and electro-oxidation treatment for pulp and paper mill wastewater. *Desalination and Water Treatment*, 93, pp.214-228. https://doi.org/10.5004/dwt.2017.21257

Pacheco, M.J., Santos, V., Ciríaco, L. and Lopes, A., 2011. Electrochemical degradation of aromatic amines on BDD electrodes. *Journal of Hazardous Materials*, 186, pp.1033-1041. https://doi.org/10.1016/j.jhazmat.2010.11.108

Palanivelu, K., 2005. Electrochemical treatment of landfill leachate. *Journal of Hazardous Materials*, 190, pp.1-6.

Patidar, R. and Srivastava, V.C., 2023. Ultrasound enhanced electro-Fenton mineralization of benzophenone: Kinetics and mechanistic analysis. *ACS ES and T Water*, 3, pp.1595-1609. https://doi.org/10.1021/acsestwater.2c00364

Pérez, G., Saiz, J., Ibañez, R., Urtiaga, A.M. and Ortiz, I., 2012. Assessment of the formation of inorganic oxidation by-products during the electrocatalytic treatment of ammonium from landfill

leachates. *Water Research*, 46, pp.2579-2590. https://doi.org/10.1016/j.watres.2012.02.015

Pieus Thanikkal, M. and Pooppana Antony, S., 2021. Integrated electro-Fenton and membrane bioreactor system for matured landfill leachate treatment. *Journal of Hazardous, Toxic, and Radioactive Waste*, 25(4), pp.04020058. https://doi.org/10.1061/(asce)hz.2153-5515.0000556

Polcaro, A.M., Mascia, M., Palmas, S. and Vacca, A., 2004. Electrochemical degradation of diuron and dichloroaniline at BDD electrode. *Electrochimica Acta*, 49, pp.649-656. https://doi.org/10.1016/j.electacta.2003.09.021

Priyadarshini Rajesh, R. and Saravanakumar, M.P., 2023. Leachate xenobiotics electrocatalytic degradation and simultaneous carbon quantum dots synthesis for anti-counterfeiting applications. *Inorganic Chemistry Communications*, 158, pp.111673. https://doi.org/10.1016/j.inoche.2023.111673

Qiao, J. and Xiong, Y., 2021. Electrochemical oxidation technology: A review of its application in high-efficiency treatment of wastewater containing persistent organic pollutants. *Journal of Water Process Engineering*. https://doi.org/10.1016/j.jwpe.2021.102308

Radjenovic, J., Bagastyo, A., Rozendal, R.A., Mu, Y., Keller, J. and Rabaey, K., 2011. Electrochemical oxidation of trace organic contaminants in reverse osmosis concentrate using RuO2/IrO2-coated titanium anodes. *Water Research*, 45, pp.1579-1586. https://doi.org/10.1016/j.watres.2010.11.035

Radjenovic, J., Duinslaeger, N., Avval, S.S. and Chaplin, B.P., 2020. Facing the challenge of poly- and perfluoroalkyl substances in water: Is electrochemical oxidation the answer? *Environmental Science and Technology*. https://doi.org/10.1021/acs.est.0c06212

Radjenovic, J. and Sedlak, D.L., 2015. Challenges and opportunities for electrochemical processes as next-generation technologies for the treatment of contaminated water. *Environmental Science and Technology*, 49, pp.11292-11302. https://doi.org/10.1021/acs.est.5b02414

Ramprasad, C., 2012. Electrochemical treatment of landfill leachate. *International Journal of Applied Science and Engineering Research*, 1, pp.7-12. https://doi.org/10.6088/ijaser.0020101006

Renou, S., Givaudan, J.G., Poulain, S., Dirassouyan, F. and Moulin, P., 2008. Landfill leachate treatment: Review and opportunity. *Journal of Hazardous Materials*, 41, p.651. https://doi.org/10.1016/j.jhazmat.2007.09.077

Rivera, F.F., Pérez, T., Castañeda, L.F. and Nava, J.L., 2021. Mathematical modeling and simulation of electrochemical reactors: A critical review. *Chemical Engineering Science*. https://doi.org/10.1016/j.ces.2021.116622

Rocha, J.H.B., Gomes, M.M.S., Fernandes, N.S., Da Silva, D.R. and Martínez-Huitle, C.A., 2012. Application of electrochemical oxidation as alternative treatment of produced water generated by Brazilian petrochemical industry. *Fuel Processing Technology*, 96, pp.80-87. https://doi.org/10.1016/j.fuproc.2011.12.011

Saha, J., Chakraborty, I. and Ghangrekar, M.M., 2020. A novel tin-chloride-zirconium oxide-kaolin composite coated carbon felt anode for electro-oxidation of surfactant from municipal wastewater. *Journal of Environmental Chemical Engineering*, 8, pp.104489. https://doi.org/10.1016/j.jece.2020.104489

Salazar-Banda, G.R., Santos, G. de O.S., Duarte Gonzaga, I.M., Dória, A.R. and Barrios Eguiluz, K.I., 2021. Developments in electrode materials for wastewater treatment. *Current Opinion in Electrochemistry*. https://doi.org/10.1016/j.coelec.2020.100663

Samadder, S.R., Prabhakar, R., Khan, D., Kishan, D. and Chauhan, M.S., 2017. Analysis of the contaminants released from municipal solid waste landfill site: A case study. *Science of the Total Environment*, 580, pp.593-601. https://doi.org/10.1016/j.scitotenv.2016.12.003

Sandoval, M.A., Calzadilla, W. and Salazar, R., 2022a. Influence of reactor design on the electrochemical oxidation and disinfection

of wastewaters using boron-doped diamond electrodes. *Current Opinion in Electrochemistry,* 65, p.7421. https://doi.org/10.1016/j.coelec.2022.100939

Sanni, I., Karimi Estahbanati, M.R., Carabin, A. and Drogui, P., 2022. Coupling electrocoagulation with electro-oxidation for COD and phosphorus removal from industrial container wash water. *Separation and Purification Technology*, 282, pp.119992. https://doi.org/10.1016/j.seppur.2021.119992

Särkkä, H., Bhatnagar, A. and Sillanpää, M., 2015. Recent developments of electro-oxidation in water treatment - A review. *Journal of Electroanalytical Chemistry*, 225, pp.115-123. https://doi.org/10.1016/j.jelechem.2015.06.016

Sato, Y., Guo, H., Xiang, Y., Goh, J., Luo, Y., Chen, G., Wang, J. and Chen, G., 2023. Chlorine Reuse in UV/Electrochemical Oxidation to Advance Sewage Cotreatment of Landfill Leachate. *ACS ES and T Water*, 3, pp.4123–4132. https://doi.org/10.1021/acsestwater.3c00514

Scialdone, O., Corrado, E., Galia, A. and Sirés, I., 2014. Electrochemical processes in macro and microfluidic cells for the abatement of chloroacetic acid from water. *Electrochimica Acta*, 132, pp.15–24. https://doi.org/10.1016/j.electacta.2014.03.127

Scialdone, O., Randazzo, S., Galia, A. and Silvestri, G., 2009. Electrochemical oxidation of organics in water: Role of operative parameters in the absence and in the presence of NaCl. *Water Research*, 43, pp.2260–2272. https://doi.org/10.1016/j.watres.2009.02.014

Seibert, D., Henrique Borba, F., Bueno, F., Inticher, J.J., Módenes, A.N., Espinoza-Quiñones, F.R. and Bergamasco, R., 2019a. Two-stage integrated system photo-electro-Fenton and biological oxidation process assessment of sanitary landfill leachate treatment: An intermediate products study. *Chemical Engineering Journal*, 372, pp.471–482. https://doi.org/10.1016/j.cej.2019.04.162

Seibert, D., Quesada, H., Bergamasco, R., Borba, F.H. and Pellenz, L., 2019b. Presence of endocrine disrupting chemicals in sanitary landfill leachate, its treatment and degradation by Fenton based processes: A review. *Process Safety and Environmental Protection*, 131, pp.255–267. https://doi.org/10.1016/j.psep.2019.09.022

Shahedi, A., Darban, A.K., Taghipour, F. and Jamshidi-Zanjani, A., 2020. A review on industrial wastewater treatment via electrocoagulation processes. *Current Opinion in Electrochemistry*. https://doi.org/10.1016/j.coelec.2020.05.009

Sharma, S., Shetti, N.P., Basu, S., Nadagouda, M.N. and Aminabhavi, T.M., 2022. Remediation of per- and polyfluoroalkyls (PFAS) via electrochemical methods. *Chemical Engineering Journal*. https://doi.org/10.1016/j.cej.2021.132895

Shen, H. and Zhang, W., 2023. Comparison of the electrochemical degradation of alizarin green (AG) by Ti/PbO2 electrode and Ti/IrO2+Ta2O5 electrode. https://doi.org/10.21203/rs.3.rs-2556667/v1

Sher, F., Hanif, K., Iqbal, S.Z. and Imran, M., 2020. Implications of advanced wastewater treatment: Electrocoagulation and electroflocculation of effluent discharged from a wastewater treatment plant. *Journal of Water Process Engineering*, 33. https://doi.org/10.1016/j.jwpe.2019.101101

Shih, Y.J., Huang, Y.H. and Huang, C.P., 2018. In-situ electrochemical formation of nickel oxyhydroxide (NiOOH) on metallic nickel foam electrode for the direct oxidation of ammonia in aqueous solution.

Sivaranjani, Gafoor, A., Ali, N., Kumar, S., Ramalakshmi, Begum, S. and Rahman, Z., 2020. Applicability and new trends of different electrode materials and its combinations in electro coagulation process: A brief review, in: *Materials Today: Proceedings*. Elsevier Ltd, pp.377–382. https://doi.org/10.1016/j.matpr.2020.05.379

Smith, S.J., Lauria, M., Ahrens, L., McCleaf, P., Hollman, P., Bjälkefur Seroka, S., Hamers, T., Arp, H.P.H. and Wiberg, K., 2023. Electrochemical Oxidation for Treatment of PFAS in Contaminated Water and Fractionated Foam─A Pilot-Scale Study. *ACS ES and T Water*, 3, pp.1201–1211. https://doi.org/10.1021/acsestwater.2c00660

Song, J., Yinhai, Y., Jia, Y., Wang, T., Wei, J., Wang, M., Zhou, S., Li,

Z., Hou, Y., Lei, L. and Yang, B., 2021. Improved NH3-N conversion efficiency to N2 activated by BDD substrate on NiCu electrocatalysis process. *Separation and Purification Technology*, 276, pp.119350. https://doi.org/10.1016/j.seppur.2021.119350

Song, X., Chen, X., Zhang, S. and Wu, D., 2023. Treatment of high chlorine-containing composting leachate biochemical effluent by Ti/RuO2-IrO2 anodic electrochemical oxidation: Optimization and evolution of pollutants. *Journal of Environmental Chemical Engineering*, 11, pp.109674. https://doi.org/10.1016/j.jece.2023.109674

Stiber, S., Balzer, H., Wierhake, A., Wirkert, F.J., Roth, J., Rost, U., Brodmann, M., Lee, J.K., Bazylak, A., Waiblinger, W., Gago, A.S. and Friedrich, K.A., 2021. Porous Transport Layers for Proton Exchange Membrane Electrolysis Under Extreme Conditions of Current Density, Temperature, and Pressure. *Advanced Energy Materials*, 11. https://doi.org/10.1002/aenm.202100630

Stucki, S., Kotz, R. and Carcer, B., 1991. Electrochemical wastewater treatment using high overvoltage anodes Part 11: Anode performance and applications.

Sun, Y., Bai, S., Wang, X., Ren, N. and You, S., 2023. Prospective Life Cycle Assessment for the Electrochemical Oxidation Wastewater Treatment Process: From Laboratory to Industrial Scale. *Environmental Science & Technology*. https://doi.org/10.1021/acs.est.2c04185

Sun, Y., Zhao, Z., Tong, H., Sun, B., Liu, Y., Ren, N. and You, S., 2023. Machine Learning Models for Inverse Design of the Electrochemical Oxidation Process for Water Purification. *Environmental Science & Technology*, 57, pp.17990–18000. https://doi.org/10.1021/acs.est.2c08771

Tan, S.Y., Chong, W.C., Sethupathi, S., Pang, Y.L., Sim, L.C. and Mahmoudi, E., 2023. Optimisation of aqueous phase low density polyethylene degradation by graphene oxide-zinc oxide photocatalysts. *Chemical Engineering Research and Design*, 190, pp.550–565. https://doi.org/10.1016/j.cherd.2022.12.045

Tejera, J., Hermosilla, D., Gascó, A., Miranda, R., Alonso, V., Negro, C., Blanco, Á., 2021. Treatment of mature landfill leachate by electrocoagulation followed by Fenton or UVA-LED photo-Fenton processes. *Journal of Taiwan Institute of Chemical Engineers*, 119, pp.33–44. https://doi.org/10.1016/j.jtice.2021.02.018

Tomcsaâ Nyi, L., De Battisti, A., Hirschberg, G., Varga, K. and Liszi, J., 1999. The study of the electrooxidation of chloride at RuO2/TiO2 electrode using CV and radiotracer techniques and evaluating by electrochemical kinetic simulation methods.

Torretta, V., Ferronato, N., Katsoyiannis, I.A., Tolkou, A.K. and Airoldi, M., 2017. Novel and conventional technologies for landfill leachates treatment: A review. *Sustainability (Switzerland)*, 9, pp.1009. https://doi.org/10.3390/su9010009

Tröster, I., Fryda, M., Herrmann, D., Schäfer, L., Hänni, W., Perret, A., Blaschke, M., Kraft, A. and Stadelmann, M., 2002. Electrochemical advanced oxidation process for water treatment using DiaChem® electrodes. *Diamond and Related Materials*, 11(4), pp.640–645. https://doi.org/10.1016/S0925-9635(01)00706-3

Umar, M., Aziz, H.A. and Yusoff, M.S., 2010. Trends in the use of Fenton, electro-Fenton and photo-Fenton for the treatment of landfill leachate. *Waste Management*, 30(5), pp.2113–2121. https://doi.org/10.1016/j.wasman.2010.07.003

Un, U.T., Altay, U., Koparal, A.S. and Ogutveren, U.B., 2008. Complete treatment of olive mill wastewaters by electrooxidation. *Chemical Engineering Journal*, 139(2), pp.445–452. https://doi.org/10.1016/j.cej.2007.08.009

Veerman, J., Saakes, M., Metz, S.J. and Harmsen, G.J., 2010. Reverse electrodialysis: Evaluation of suitable electrode systems. *Journal of Applied Electrochemistry*, 40(3), pp.1461–1474. https://doi.org/10.1007/s10800-010-0124-8

Wang, C., Zhu, M., Cao, Z., Zhu, P., Cao, Y., Xu, X., Xu, C. and Yin, Z., 2021a. Heterogeneous bimetallic sulfides based seawater electrolysis towards stable industrial-level large current density. *Applied Catalysis B: Environmental*, 291, pp.120071. https://doi.org/10.1016/j.apcatb.2021.120071

Wang, H., Yin, Z., Ding, J., Hui, H., He, B., Yin, Z. and Li, J., 2024a. Efficient hybrid process of fenton-electrocatalytic membrane reactor-biological aerated filter for the treatment of nanofiltration retentate from landfill leachate without concentrated liquor discharge. *Industrial & Engineering Chemistry Research*, 63(7), pp.2187–2195. https://doi.org/10.1021/acs.iecr.3c03984

Wang, J., Chen, R., Zhang, T., Wan, J., Cheng, X., Zhao, J. and Wang, X., 2020a. Technological Optimization for H2O2 Electrosynthesis and Economic Evaluation on Electro-Fenton for Treating Refractory Organic Wastewater. *Industrial & Engineering Chemistry Research*, 59(8), pp.10364–10372. https://doi.org/10.1021/acs.iecr.0c00742

Wang, J., Yao, J., Wang, L., Xue, Q., Hu, Z. and Pan, B., 2020b. Multivariate optimization of the pulse electrochemical oxidation for treating recalcitrant dye wastewater. *Separation and Purification Technology*, 230, pp.115851. https://doi.org/10.1016/j.seppur.2019.115851

Wang, Y., Li, X., Zhen, L., Zhang, H., Zhang, Y. and Wang, C., 2012. Electro-Fenton treatment of concentrates generated in nanofiltration of biologically pretreated landfill leachate. *Journal of Hazardous Materials*, 229–230, pp.115–121. https://doi.org/10.1016/j.jhazmat.2012.05.108

Wang, Y., Liu, Y., Wiley, D., Zhao, S. and Tang, Z., 2021b. Recent advances in electrocatalytic chloride oxidation for chlorine gas production. *Journal of Materials Chemistry A: Materials for Energy and Sustainability*, 9(10), pp.14392–14399. https://doi.org/10.1039/d1ta02745j

Wang, Y., Meng, G., Shan, M., Wang, D., Bai, Z., Zhou, X., Lv, Y., Bai, J. and Wang, C., 2020c. Treatment of high-ammonia-nitrogen landfill leachate nanofiltration concentrate using an Fe-loaded Ni-foam-based electro-Fenton cathode. *Journal of Environmental Chemical Engineering*, 8(1), pp.104243. https://doi.org/10.1016/j.jece.2020.104243

Wang, Y., Shan, G., Ma, K., Yang, L., Gao, L.Y., Zhang, M., Huo, X., Li, X., Zhang, J., Li, W. and Wang, Y., 2024b. Alkaline electrolyzer-improving electrocatalytic oxidation of landfill leachate coupling with hydrogen production. *International Journal of Hydrogen Energy*, 64(5), pp.926–934. https://doi.org/10.1016/j.ijhydene.2024.03.046

Wu, W., Huang, Z.H. and Lim, T.T., 2014. Recent development of mixed metal oxide anodes for electrochemical oxidation of organic pollutants in water. *Applied Catalysis A: General*, 482, pp.111–123. https://doi.org/10.1016/j.apcata.2014.04.035

Wu, Y., Ning, F., Wang, Z., Saad, A., Li, X. and Xia, D., 2021. 3D ordered macroporous copper nitride-titanium oxynitride as highly efficient electrocatalysts for universal-pH hydrogen evolution reaction. *Journal of Materials Chemistry A: Materials for Energy and Sustainability*, 9(15), pp.14392–14399. https://doi.org/10.1039/d1ta02457d

Xiao, P., An, L. and Wu, D., 2020. The use of carbon materials in persulfate-based advanced oxidation processes: A review. *Environmental Science: Water Research & Technology*, 35, pp.467–477. https://doi.org/10.1016/S1872-5805(20)60521-2

Xu, L., Li, W., Luo, J., Chen, L., He, K., Ma, D., Lv, S., Xing, D. and Xu, L., 2023. Carbon-based materials as highly efficient catalysts for the hydrogen evolution reaction in microbial electrolysis cells: Mechanisms, methods, and perspectives. *Chemical Engineering Journal*, 452, pp.144670. https://doi.org/10.1016/j.cej.2023.144670

Xu, Y., Mao, Z., Qu, R., Wang, J., Yu, J., Luo, X., Shi, M., Mao, X., Ding, J., Liu, B. and Xu, Y., 2023. Electrochemical hydrogenation of oxidized contaminants for water purification without supporting electrolyte. *Nature Water*, 1(2), pp.95–103. https://doi.org/10.1038/s44221-022-00002-3

Yan, C., Tian, Y., Cheng, Z., Wei, Z., Zhang, X. and Quan, X., 2021. Simultaneous desalination and removal of recalcitrant organics from

reverse osmosis leachate concentrate by electrochemical oxidation. *ACS Omega*, 6(5), pp.16049–16057. https://doi.org/10.1021/acsomega.1c01916

Yan, W., Wang, Y., Li, Y., Rong, C., Wang, D., Wang, C., Wang, Y., Yuen, Y.L., Wong, F.F., Chui, H.K., Li, Y.Y. and Zhang, T., 2023. Treatment of fresh leachate by anaerobic membrane bioreactor: On-site investigation, long-term performance and response of microbial community. *Bioresource Technology*, 383, pp.129243. https://doi.org/10.1016/j.biortech.2023.129243

Yang, X.J., Xu, X.M., Xu, J. and Han, Y.F., 2013. Iron oxychloride (FeOCl): An efficient Fenton-like catalyst for producing hydroxyl radicals in degradation of organic contaminants. *Journal of the American Chemical Society*, 135, pp.16058–16061. https://doi.org/10.1021/ja409130c

Yasri, N., Hu, J., Kibria, M.G. and Roberts, E.P.L., 2020. Electrocoagulation Separation Processes. *ACS Symposium Series*, 1348, pp.167–203. https://doi.org/10.1021/bk-2020-1348.ch006

Yi, Y., Feng, H., Wang, J., Tang, J., Wu, Y., Liang, X., Guo, Y. and Tang, L., 2023. Simultaneous recovery of NH3-N and removal of heavy metals from manganese residue leachate using an electrodialysis system. *ACS ES and T Water*, 3, pp.793–803. https://doi.org/10.1021/acsestwater.2c00580

You, S., Liu, B., Gao, Y., Wang, Y., Tang, C.Y., Huang, Y. and Ren, N., 2016. Monolithic porous Magnéli-phase Ti4O7 for electro-oxidation treatment of industrial wastewater. *Electrochimica Acta*, 214, pp.326–335. https://doi.org/10.1016/j.electacta.2016.08.037

Yu, W., Chen, Z., Fu, Y., Xiao, W., Dong, B., Chai, Y., Wu, Z. and Wang, L., 2023. Superb all-pH hydrogen evolution performances powered by ultralow Pt-decorated hierarchical Ni-Mo porous microcolumns. *Advanced Functional Materials*, 33. https://doi.org/10.1002/adfm.202210855

Yu, Z., Wang, J.J., Liu, L.Y., Li, Z. and Zeng, E.Y., 2024. Drinking boiled tap water reduces human intake of nanoplastics and microplastics. *Environmental Science & Technology Letters*, 11, pp.273–279. https://doi.org/10.1021/acs.estlett.4c00081

Yuan, Z., He, C., Shi, Q., Xu, C., Li, Z., Wang, C., Zhao, H. and Ni, J., 2017. Molecular insights into the transformation of dissolved organic matter in landfill leachate concentrate during biodegradation and coagulation processes using ESI FT-ICR MS. *Environmental Science & Technology*, 51, pp.8110–8118. https://doi.org/10.1021/acs.est.7b02194

Zhang, C., Luo, Y., Tan, J., Yu, Q., Yang, F., Zhang, Z., Yang, L., Cheng, H.M. and Liu, B., 2020. High-throughput production of cheap mineral-based two-dimensional electrocatalysts for high-current-density hydrogen evolution. *Nature Communications*, 11. https://doi.org/10.1038/s41467-020-17121-8

Zhang, G., Ruan, J. and Du, T., 2021. Recent advances on photocatalytic and electrochemical oxidation for ammonia treatment from water/wastewater. *ACS ES&T Engineering*, 1, pp.310–325. https://doi.org/10.1021/acsestengg.0c00186

Zhang, H., Ran, X. and Wu, X., 2012a. Electro-Fenton treatment of mature landfill leachate in a continuous flow reactor. *Journal of Hazardous Materials*, 241–242, pp.259–266. https://doi.org/10.1016/j.jhazmat.2012.09.040

Zhang, H., Ran, X. and Wu, X., 2012b. Electro-Fenton treatment of mature landfill leachate in a continuous flow reactor. *Journal of Hazardous Materials*, 241–242, pp.259–266. https://doi.org/10.1016/j.jhazmat.2012.09.040

Zhang, H., Zhang, D. and Zhou, J., 2006. Removal of COD from landfill leachate by electro-Fenton method. *Journal of Hazardous Materials*, 135, pp.106–111. https://doi.org/10.1016/j.jhazmat.2005.11.025

Zhao, C., Wu, Z., Lai, J., Liu, L., Li, H. and Wang, H., 2024. Efficient electrochemical oxidation of refractory organics in actual petrochemical reverse osmosis concentrates by Ti/SnO2-Sb mesh anode. *Process Safety and Environmental Protection*, 182, pp.1060–1071. https://doi.org/10.1016/j.psep.2023.12.067

Zhou, M., Liu, L., Jiao, Y., Wang, Q. and Tan, Q., 2011. Treatment of high-salinity reverse osmosis concentrate by electrochemical oxidation on BDD and DSA electrodes. *Desalination*, 277, pp.201–206. https://doi.org/10.1016/j.desal.2011.04.030

Zhuo, Q., Lu, J., Niu, J., Crittenden, J.C., Yu, G., Wang, S., Yang, B. and Chen, Z., 2022. Electrocatalytic oxidation processes for treatment of halogenated organic pollutants in aqueous solution: A critical review. *ACS ES and T Engineering*, 23, p.465. https://doi.org/10.1021/acsestengg.1c00465

Mechanism and Behavior of Phosphorus Adsorption from Water by Biochar Forms Derived from Macadamia Husks

Nguyen Van Phuong† [ORCID]

Institute of Science, Engineering and Environmental Management, Industrial University of Ho Chi Minh City, Vietnam
†Corresponding Author: Nguyen Van Phuong; nguyenvanphuong@iuh.edu.vn

ABSTRACT

High phosphate content in water causes eutrophication, leading to many risks to the aquatic environment and human health. This study used biochar derived from macadamia husks at the pyrolysis temperatures (300, 450, and 600℃) to remove P from water. Adsorption parameters such as initial pH, biochar dosage, initial P concentration, and adsorption time when biochar was exposed to the P solution were determined. The results show that pH 4 is optimal for P removal with biochar pyrolyzed at 300 and 450°C, while pH 6 gives biochar 600°C, biochar dosage 10 g.L^{-1}, concentration Initial P 25-200 mg.L^{-1} and adsorption time 40 minutes for 3 types of biochar. The maximum P adsorption capacity is 20.07, 20.03, and 20.03 mg.L^{-1} corresponding to 3 forms of biochar 300, 450, and 600°C. P adsorption data were consistent with the Freundlich isotherm model for all three biochar forms. The pseudo-second-order kinetic model was suitable for all three types of biochar, showing that the main adsorption mechanism is a surface chemical reaction. The study suggested that hydrogen bonding plays an important role in the adsorption of P onto biochar derived from macadamia husks. This study indicates that biochar derived from macadamia husks pyrolyzed at temperatures of 300, 450, and 600°C are all potentially effective and low-cost adsorbents for phosphate removal from water.

INTRODUCTION

Excess phosphorus (P) released into surface water can lead to eutrophication, disrupting the ecological balance. This can affect human health (Xu et al. 2022). Meanwhile, P is a non-renewable resource, so effectively recovering P will be a solution in the circular economy, which can prevent risks caused by excess P from water (Xu et al. 2022).

Various methods for P removal and recovery from wastewater have been explored, including biological methods, chemical precipitation, electrochemical methods, coagulation, membrane separation, and adsorption (Choi et al. 2019). Biological methods that rely mainly on the metabolism of certain microorganisms are considered promising (Xu et al. 2022). However, this method is only suitable for low P concentrations; the removal rate is usually low (30% to 40%) (Xu et al. 2022) and fluctuates according to operating conditions (Choi et al. 2019). Chemical methods can achieve the purpose of P removal (Xu et al. 2022). However, the cost is high, and the possibility of causing pollution due to sludge generation. Electrochemical processes are limited when wastewater contains many anionic compounds and the need to replace electrodes is often costly (Choi et al. 2019). The adsorption method is not only highly effective, simple to operate, and produces less sludge but can also be applied to treat wastewater with many different concentrations. Therefore, the adsorption method has attracted more and more attention worldwide (Xu et al. 2022).

There are many adsorbent materials, such as bentonite, zeolite, activated carbon, biochar, etc., used (Xu et al. 2022). Recently, the biochar-based adsorption

process has received more attention because of its effective adsorption capacity and low cost (Choi et al. 2019). Furthermore, it is possible to utilize the adsorbed product for agricultural production purposes.

The adsorption properties of biochar depend on the type of raw material, heating rate, pyrolysis temperature, and retention time (Luo et al. 2023). However, the P adsorption capacity of biochar is very different because phosphate anions are often repelled by some negatively charged surfaces of biochar, leading to very different P adsorption levels. Among 22 types of biochar derived from plants regarding the ability to adsorb P–PO_4, only 4 types of biochar were found to show the ability to adsorb P–PO_4 from water (Zhang et al. 2020).

The adsorption mechanism includes several interactions, such as physical adsorption, surface precipitation, complexation, electrostatic attraction, and ion exchange (Luo et al. 2023). SEM and TEM analysis determined the surface area and porosity of biochar; however, there is no correlation between biochar surface area and P adsorption capacity from water (Nobaharan et al. 2021). Therefore, exploring the P adsorption mechanism and behavior of biochar will improve the application efficiency of biochar from water P treatment.

Macadamia is an economically valuable crop that is grown around the world. Macadamia nut production produces a large amount of biomass residue, known as macadamia nut husks (Vu et al. 2023). In Dak Nong, Vietnam with about 1100 hectares, the yield is 1.5 tons of seeds/ha, and waste husks account for 75%. Currently, this waste source is mainly left to decompose naturally, which is highly wasteful. Biochar production is a trend in the circular economy in agriculture.

Therefore, studying the ability to adsorb P from water using biochar derived from macadamia husks pyrolyzed at different temperatures was investigated by determining different operating factors such as water pH, biochar dosage, initial P concentration, adsorption time as well as adsorption behavior and mechanism. The evaluation objective of the experiment is mainly based on P adsorption capacity but also considers the effectiveness of P treatment from water.

MATERIALS AND METHODS

Sampling Methods

The macadamia husk sample was taken in December 2023 from the Macadamia Nut Processing Company, DakNong Province, Vietnam. The husks were pre-dried, crushed to <5 mm, and dried in an oven (Shellab Drying Oven, USA) at 60°C for 24 hours.

Chemicals

Chemicals used in the study were of analytical purity: NaH_2PO_4, $K_2Cr_2O_7$, $SnCl_2$, $(NH_4)_6Mo_7O_{24}.4H_2O$ from Merck. EDTA, KCl, HCl, NH_4Cl, NaOH, HNO_3, NaOH, H_2O_2, H_2SO_4, $NaHCO_3$ from China.

Preparing Biochar

Biochar preparation was simulated according to a previous study (Phuong et al. 2021), in which processed macadamia husks were pyrolyzed in a Naberthem P330 furnace (Germany) at three temperatures: 300, 450, 600ºC (Bio 300, Bio 450, and Bio 600). The heating rate was 10°C.min^{-1}, the heat retention was 2 hours, and it cooled overnight in the furnace. The pyrolysis product was crushed through a 1 mm sieve and stored at 4°C. The biochar samples were then used to determine some of the surface properties of the biochar and used for further experiments.

Some biochar surface properties such as pH, pH_{pzc} (Tu. 2016), and total organic carbon (TOC) (Tan. 2011), P content in water were determined using the photometric method on SPECTROSCOPY, Model: GENESYS 10S UV-VIS, 6-/1-CELL, Brand: Thermo scientific/USA. A spectrophotometer FT/IR-4700 type A in 350-4000 cm^{-1} was used to determine the functional groups of biochar.

Experimental Design to Investigate Factors Affecting the Adsorption of Phosphorus

Initial pH: The experiment was performed in a 60 mL polypropylene tube by mixing 0.3 g of various types of biochar (Bio 300, Bio 450, and Bio 600) with 30 mL of 200 mg.L^{-1} P solution, initial pH values (2, 4, 6, and 8 were adjusted with HCl and NaOH). This mixture was shaken on a GFL 3015 circular shaker (Germany) at 350 rpm for 24 h. The pH was not adjusted during the experiments. The tubes were centrifuged at 4000 rpm for 15 min using a DLAB DM 0636 centrifuge and filtered through a 0.22 μm filter. The P content in the filtered solution was determined. Adsorption experiments were conducted at least three times.

Biochar dosage: The pH selected from the experiments of the initial pH section will be set to continue for experiments investigating biochar dosage (0.0; 0.10; 0.3; 0.5, 0.7; 1, 0 g) along with fixed conditions such as 30 mL of 200 mg.L^{-1} P solution, shaking speed of 350 rpm for 24 h.

Initial P concentration: The pH is selected from the experiments of the initial pH section, and the biochar dosage from the biochar dosage section will be set to continue for the experiments investigating the initial P concentration (0; 17, 25, 50, 100, 150 and 200 mg.L^{-1}) along with fixed conditions such as shaking speed of 350 rpm for 24 h.

Adsorption time: The pH is selected from the experiments of the initial pH section, and the biochar dosage from the biochar dosage section will be set to continue for the experiments to investigate the effect of adsorption time with the following conditions as P content of 200 mg.L^{-1}, and shaking speed of 350 rpm. Periodic patterns 20, 40, 80, and 160 minutes were removed (enough time to achieve equilibrium according to preliminary experiments). Analyze the P solution after filtration.

Evaluation of the adsorption behavior and mechanism includes evaluation of adsorption kinetics based on pseudo-first- and second-order kinetic models and equilibrium evaluation based on Langmuir and Freundlich adsorption models.

Data Analysis

Calculation

Adsorption capacity, mg/g: $q_i = \dfrac{(C_0 - C_i).V}{m}$ ...(1)

In which:

C_0 (mg.L^{-1}): initial concentration of P

C_i (mg.L^{-1}): P concentration of sample i in solution at equilibrium time

V (L): volume of P solution

m (g): mass of biochar sample

q_i (mg.g^{-1}): P adsorption capacity of sample i at equilibrium time.

K_L is the Langmuir adsorption constant (L.mg^{-1}).

Langmuir isotherm equation:

$$\frac{1}{q_i} = \frac{1}{K_L q_0}\frac{1}{C_i} + \frac{1}{q_0}$$ ...(2)

Freundlich isotherm equation:Hay:

$$q = y/m = K_F C^{\frac{1}{n_F}}$$ ...(3)

Hay:

$$Log q_i = \frac{1}{n_F} log C_i + log K_F$$ ...(4)

In which:

n_F: Freundlich isotherm constant, expressing P adsorption intensity.

K_F: Freundlich adsorption isotherm constant, expressing adsorption capacity.

Pseudo-first-order kinetic equation:

$$Ln(q_e - q_t) - Ln q_e = -k_1 t$$ ...(5)

or $$Ln(q_e - q_t) = -k_1 t + Ln q_e$$ ...(6)

Pseudo-second-order kinetic equation:

$$\frac{1}{q_t} = \frac{1}{t}\frac{1}{k_2 q_e^2} + \frac{1}{q_e}$$ ...(7)

Where:

q_e: P adsorption capacity at equilibrium (mg g^{-1})

q_t: P the adsorption capacity at time t (mg g^{-1})

k_1 (1 min^{-1}): constants of pseudo-first-order and pseudo-second-order kinetic

và k_2 (g mg^{-1} min^{-1}): constants of pseudo-first-order and pseudo-second-order kinetic

t (min): time adsorption.

Data Processing

Data was collected, calculated, and graphed based on software available in Excel 2016. Oneway ANOVA analysis on SPSS 23.

RESULTS AND DISCUSSION

Some Surface Properties of Biochar

Surface properties of biochar derived from Macadamia husk pyrolyzed at different temperatures include recovery efficiency (%H), pH, pHpzc, number of H$^+$ groups, cation exchange capacity (CEC), available phosphorus and ammonium nitrogen were determined and are presented in detail in Table 1. Biochar recovery efficiency (%H) in the study was 49.1; 32.0; 27.2% corresponds to pyrolysis temperatures of 300, 450 and 600°C. The results show that as the pyrolysis temperature increases, the biochar recovery efficiency decreases. This is explained by increasing the pyrolysis temperature, and the loss of volatile organic substances increases (Lehmann & Joseph 2015). Similar results were also found in the study by Li et al. (2024), with a recovery efficiency of 34.5% when pyrolysis of cotton (Gossypium sp. L.) straw at 500°C (Li et al. 2024). The results of analyzing the average recovery efficiency values of biochar samples (p<0.05) on SPSS 23 were statistically significant differences. This shows that each type of organic matter in the macadamia husk has been decomposed according to thermal fraction. Specifically, at the pyrolysis temperature of 300°C, only hemicellulose decomposes (220–315°C); at 450°C, cellulose decomposes, and at 600°C, lignin decomposes mainly (Huang et al. 2022).

The biochar pH value increased to 7.09, 8.06, and 8.04, respectively, for biochar samples Bio 300, Bio 450, and Bio 600. The difference in pH value in samples Bio 300 and Bio 450 is significantly different. This can explain why the hemicellulose in the macadamia husks component was well decomposed at a temperature of 300°C (Huang et al. 2022).

Table 1: Recovery efficiency and some surface chemical properties of biochar.

t ºC	% H	pH	pHpzc	%TOC
300	49.1[c]	7.09[a]	6.35[a]	41[b]
SD	0.3	0.11	0.14	2
450	32.0[b]	8.06[b]	7.87[b]	29[a]
SD	0.2	0.01	0.01	2
600	27.2[a]	8.04[b]	7.96[c]	30[a]
SD	0.1	0.06	0.11	2

A,b, and c in the same column indicate significant differences ($p<0.05$); SD: standard deviation; H%: biochar recovery efficiency; pHpzc: pH at the point of zero charges.

The pH values of Bio 450 and Bio 600 samples did not change significantly, possibly due to the decomposition of organic substances from 450 to 600 °C occurring at the same time as the formation of shorter-chain organic compounds (Huang et al. 2022).

The pHpzc value increased by 6.35, 6.87, and 7.96, respectively, with Bio 300, Bio 450, and Bio 600; the difference in pH values is statistically significant. The obtained results were smaller than those of biochar from coffee husks, according to previous research (Phuong et al. 2021). This can be explained by the difference in lignocellulosic material composition, which is common for materials containing lignocellulose.

TOC content tends to decrease with increasing pyrolysis temperature, Table 1. Specifically, TOC is 41, 29, and 30%, corresponding to pyrolysis temperatures of 300, 450, and 600°C. The research results were 26, 20, and 1% higher than materials from coffee husks (Phuong et al. 2021). This shows that the material origin affects the TOC content in biochar.

One-way ANOVA analysis showed that TOC content changes in biochar M450 and M600 were not significant, which may explain the slow destruction of organic matter such as lignin.

FTIR spectrum shows that the peaks at 3435 cm^{-1} belonging to –OH vibration, 1603 cm^{-1} for C=C, and C=O in the aromatic ring, and 1693 cm^{-1} for C=O in carboxyl group (Feng et al. 2021, Xiong et al. 2024). The strong, broad FTIR spectrum at wavelength 3414 cm^{-1} is mainly responsible for the stretching vibration of the hydroxyl group OH– (alcohol and phenolic). This shows that the –OH, –COOH groups can participate in electron exchange reactions (hydrogen bond formation) during the adsorption process (Xiong et al. 2024). The absorption peak ranges from 1600 to 1500 cm^{-1}, indicating the existence of an extended aromatic C=C ring. Therefore, the peak at 1603 cm^{-1} is considered to be the relaxation of the aromatic C=C ring. This intensity gradually decreases at the pyrolysis temperature of 450°C and is completely lost at 600°C. The research results are similar to Angın & Şensöz's research, which shows that aromatic rings disappear when the pyrolysis temperature increases (Angın & Şensöz 2014). At 1024 cm^{-1}, the sharp peak with moderate intensity illustrates the C–O–C stretching of ester groups in cellulose and hemicellulose (Kenchannavar & Surenjan 2022, Tomczyk et al. 2020). These peaks will also decrease or disappear with increasing pyrolysis temperature (Angın & Şensöz 2014). Fig. 1 shows that the peaks of the hydroxyl group and carbonyl group shift to 3030 cm^{-1} and decrease sharply in intensity when increasing the pyrolysis temperature. The decrease in the intensity of the bands described above shows that the acidic functional groups of the surface have decreased with increasing pyrolysis temperature (Angın & Şensöz 2014). The reduction or
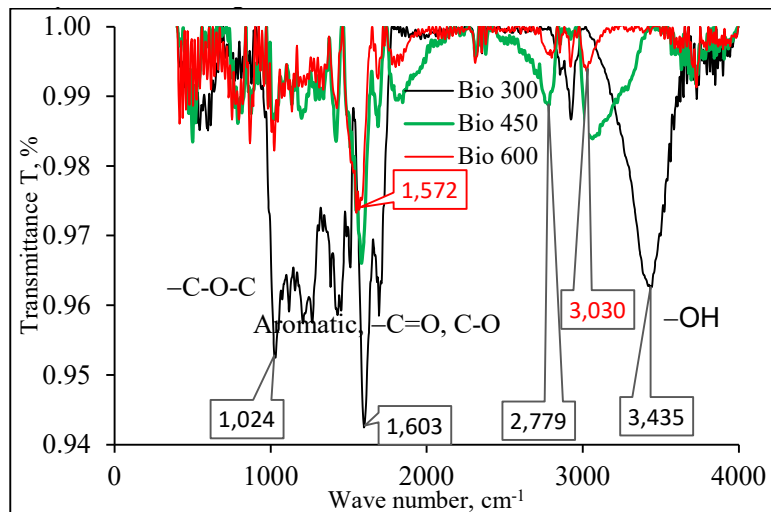
Fig. 1: FT-IR spectra of biochar forms.

disappearance of these peaks is related to the degradation and depolymerization of cellulose, hemicellulose, and lignin (Huang et al. 2022).

This can be explained by the fact that the pyrolysis of organic materials in the temperature range of 350–650°C cracked and formed new chemical bonds in the biomass, thereby forming new functional groups such as carboxyl, phenol, ether... (Tomczyk et al. 2020). These functional groups can form hydrogen bonds, greatly increasing the adsorption process of substances capable of forming hydrogen bonds or acting as electron donors or acceptors.

Factors Affecting the Adsorption of P from Water onto Biochar

Initial solution pH: The results of investigating the initial pH effect on the P adsorption capacity of biochar derived from macadamia nut husks prepared at different pyrolysis temperatures are presented in Fig. 2. For 300°C biochar, Fig. 2a shows that the adsorption capacity increased slightly from 18.44 to 18.45 mg g^{-1} when the initial pH was 2 and 4. As the initial pH increased to 6, the adsorption capacity decreased sharply to 16.7 mg g^{-1}, the decrease was statistically significant and maintained an insignificant change of 16.5 and 17.15 mg g^{-1} when the initial pH was 6 and 8 respectively.

Similarly, in the case of Bio 450, Fig. 2b shows that the adsorption capacity increased from 14.5 to 18.6 mg g^{-1}, this increase was significant when the initial pH of the solution increased from 2 to 4. Then, when increasing to pH 6, the adsorption capacity decreased significantly to 16.9 mg.g^{-1}. When the initial pH increased to 8, 10, the capacity increased again and maintained at 17.7 mg.g^{-1}.

For Bio 600, the adsorption capacity increased from 16.4 to 16.9 and 17.6 mg.g^{-1} when the initial pH of the solution was 2, 4, and 6, respectively. This increase is statistically significant. Then, when the initial pH increased to 8, the adsorption capacity decreased to 16.4 mg.g^{-1}, a significant decrease and negligible change at pH 10 (16.8 mg.g^{-1}), Fig. 2c.

This can be explained because, at different initial pH values, P can exist in different forms. Specifically, at pH 2, P exists mainly in the form of H_3PO_4 (pKa1= 2.12), so the P adsorption capacity at this pH is low. At pH 4-7, P exists mainly in the form of $H_2PO_4^-$ (pKa2=7.2) and will adsorb to the biochar surface through electrostatic bonds. Because the pHpzc of the three forms of biochar all have values > 6.3, when the solution pH is < 6.3, the positively charged biochar surface will create favorable conditions for adsorbing phosphorus anions based on the force of electrostatic bonding (Luo et al. 2023). At pH > 8, this pH value is higher than

the pHpzc of all three forms of biochar, then the biochar surface is negatively charged. The adsorption capacity of P anions decreases due to electrostatic repulsion (Nobaharan et al. 2021). Furthermore, as pH increases, OH$^-$ ions also increase, leading to competition for P anion adsorption sites on the biochar surface (Luo et al. 2023).

In the case of Bio 300, at pH 2, the P adsorption capacity is still higher than Bio 450 or Bio 600. This can be explained by the more diverse organic properties of Bio 300, such as containing lipids and cellulose, which causes it to dissociate less (Tomczyk et al. 2020).

When considering the P removal efficiency of biochar samples, Fig. 2d shows that at pH 4, the highest treatment efficiency is 92.8, 93.2, and 84.7%, corresponding to Bio 300, Bio 450, and Bio 600. Therefore, the study chose pH 4 for the next experiments when using Bio 300 and Bio 450, choosing pH 6 for Bio 600.

Biochar dosage: The results of investigating the effects of biochar dosage prepared at 300°C are presented in Fig. 3a. The results showed that the adsorption capacity decreased sharply when increasing the biochar content in the solution; the adsorption capacity decreased from 38.7 to 17.2; 7.6, and 5.4 mg.g^{-1} corresponds to biochar contents of 3, 10, 17, and 23 g.L^{-1}. This level decreased with statistical significance. While at dosages of 23 and 33 g.L^{-1}, the adsorption capacity did not change significantly.

With Bio 450°C presented in Fig. 3b, it shows that the adsorption capacity decreased by 41.8, 19.1, 10.4, 7.4, and 4.6 mg.g^{-1} corresponding to biochar dosages of 3, 10, 17, 23, and 33 g.L^{-1}. The reduction was significant at biochar dosages of 3, 10, 23 g.L^{-1}. Between 23 and 33 g.L^{-1}, the change in adsorption capacity was not statistically significant.

With Bio 600, the research results are presented in Fig. 3c. The results showed that the P adsorption capacity decreased by 41.2, 15.3, and 8.7 mg.g^{-1}, corresponding to biochar dosages of 3, 10, and 17 g.L^{-1}. This sequential decrease is statistically significant. P adsorption capacity at biochar dosages of 23 and 33 g.L^{-1} was not statistically significant.

Overall, the results of the study can be explained as increasing the adsorbent dosage leading to increased active sites and binding sites for phosphate ions on the surface of the biochar. This creates favorable conditions for phosphorus adsorption. However, the P removal efficiency does not increase and is stable when the adsorbent dosage is greater than 10 g.L^{-1}. This is explained by the fact that all experiments were conducted at the same initial P concentration (200 mg.L^{-1}). This condition is thought to be caused by the aggregation of biochar particles, reducing the

a. Bio 300

b. Bio 450

c. Bio 600

d. Treatment efficiency of 3 types of biochar
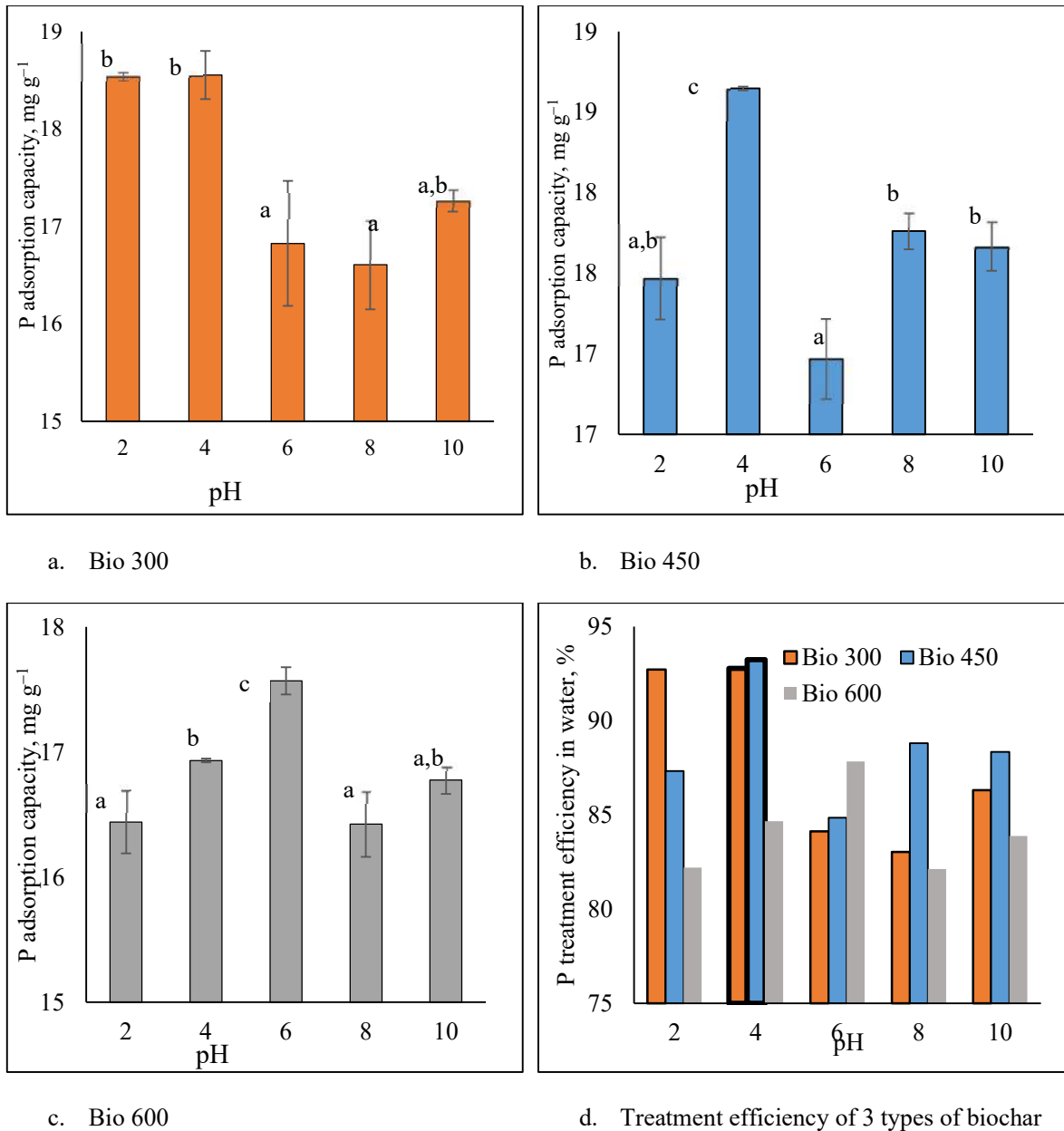
Fig. 2: Effect of pH on P adsorption capacity (mg.g^{-1}) of biochar at different pyrolysis temperatures. Different letters represent significant differences.

available surface area and leading to reduced P adsorption capacity (Luo et al. 2022).

The optimal dosage of biochar needs to be determined depending on the user's purpose. If the goal is to remove phosphate from wastewater, then more biochar is needed to remove it. If phosphorus adsorption with biochar is used as a fertilizer or to save costs, less biochar should be chosen. In this study, the adsorption capacity is based on consideration of treatment efficiency.

Experimental results showed that at pH 4, the P content is 200 mg.L^{-1}, so the biochar dosage should be 10 mg.L^{-1}. These parameters are used for further experiments.

Initial P concentrations: The results of investigating the effect of initial P concentrations (C_0) on the adsorption capacity of Bio 300 are presented in Fig. 4a. The results show that as C_0 increases, the adsorption capacity q also increases. Specifically, the P adsorption capacity increased by 0, 2.45; 4.84, 9.75, 14.19, and 18.56 mg.g^{-1}, corresponding to C_0

a. Bio 300

b. Bio 450

c. Bio 600

d. Treatment efficiency of 3 types of biochar
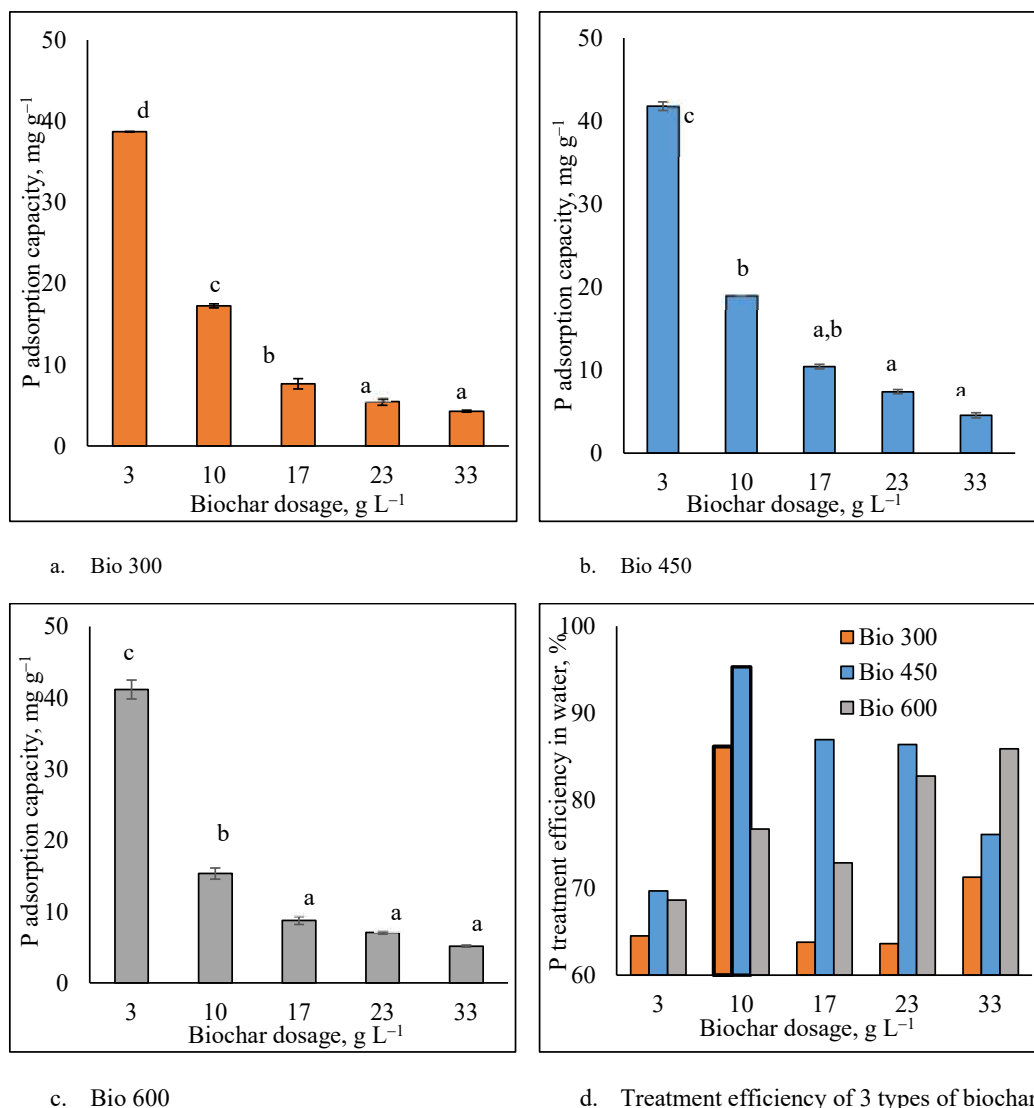
Fig. 3: Effect of biochar dosage and P adsorption capacity (mg g^{-1}) of biochar samples. Different letters represent significant differences.

concentrations of 0, 25, 50, 100, 150, and 200 mg.P.L^{-1}, respectively. The results of Oneway ANOVA analysis on SPSS 23 show that all values of P adsorption capacity are statistically significantly different. Research results show that the adsorption process continues under the current experimental conditions.

In the case of Bio 450, Fig. 4b, the research results show that the adsorption capacity increased from 0.00, 2.39, 4.83; 9.77, 14.48, and 18.65 mg.g^{-1} correspond to the initial C_0 values as in the Bio 300 experiment. Research results also show that the increase process is statistically significantly different in C_0 values in the experiment. The research results also show signs of saturated adsorption under current experimental conditions.

Similarly, for Bio 600, Fig. 4c shows that the adsorption capacity increases corresponding to the increase in initial concentration C_0. The adsorption capacity values increased significantly with the surveyed C_0 values. Specifically, the adsorption capacity increased by 0.00, 2.19, 4.03, 8.23, 13.03, and 17.66 mg.g^{-1} correspond to C_0 values of 0, 25, 50, 100, 150, and 200 mg L^{-1}, respectively. There was no sign of adsorption saturation under the experimental conditions.

Evaluation results of P treatment efficiency from water when conducting experiments under conditions such as pH 4 (or 6), biochar dosage 10 g.L^{-1}, and initial P content in the range of 25 to 200 mg.L^{-1} showed that P removal efficiency decreased with increasing pyrolysis temperature.

a.   Bio 300

b.   Bio 450

c.   Bio 600

d.   Treatment efficiency of 3 types of biochar
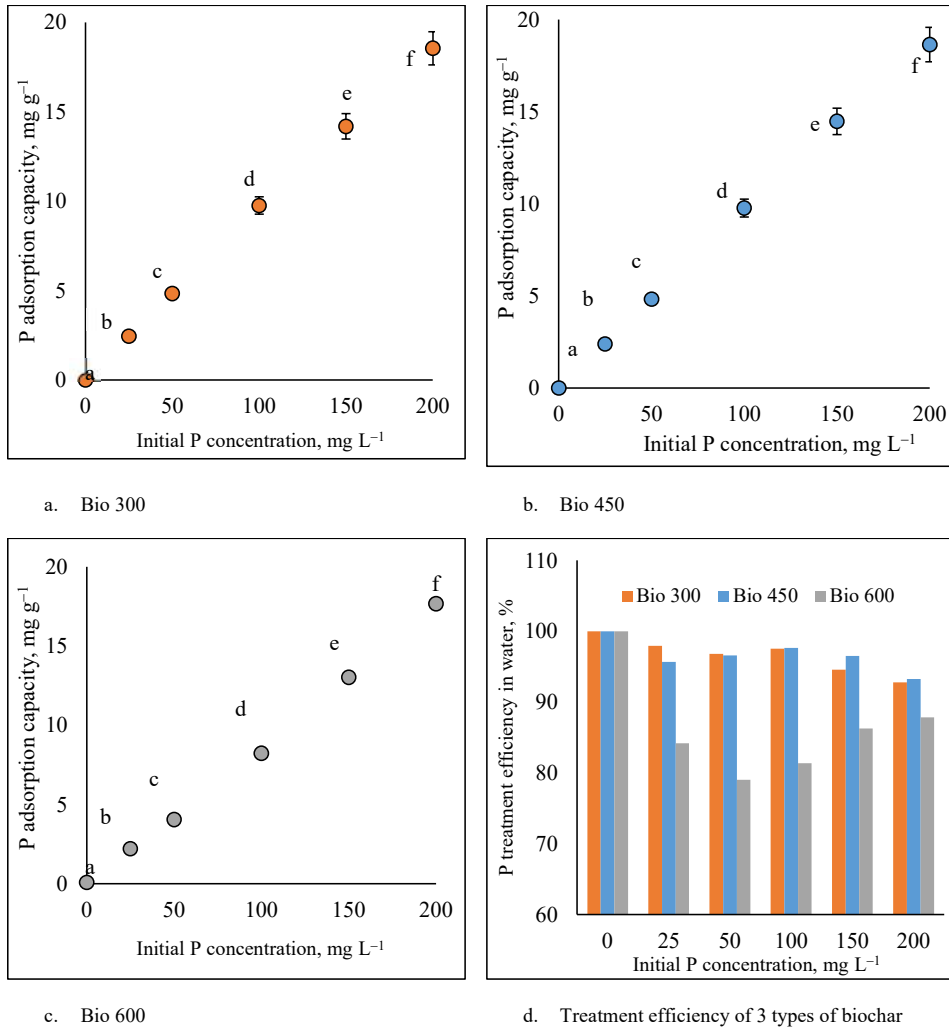
Fig. 4: Effect of initial P concentration and P adsorption capacity (mg g^{-1}) of biochar samples. Different letters represent significant differences.

Specifically, P treatment efficiency (%) fluctuated (98.0-92.8); (95.7-93.2); (84.2-87.8) corresponding to the Bio 300, Bio 450, and Bio 600 samples, respectively, Fig. 4c. This result is much larger than the results reported by Nobaharan et al. that peanut hull-derived biochar had a P removal efficiency of 61% at an initial P concentration of 5 mg.L^{-1} at pH 7, as well as with magnesium-modified corn biochar that only achieved a P removal efficiency of 90% at an initial P concentration of 84 mg.L^{-1}, pH 7.8 (Nobaharan et al. 2021).

The results show that the adsorption process has not reached the adsorption saturation state under experimental conditions. This can be explained in the form of an adsorption curve of this type, also known as a constant partition isotherm (Tan 2011). The adsorption process is characterized by a continuous distribution of the solute in the solution and the

adsorbent. This type of adsorption is common when new adsorption sites appear as soon as the solute is adsorbed from the solution (Tan 2011). Then, the newly formed hydrogen bonds continue to develop through the bridge P P–OH... O=P. This bond is stronger than the hydrogen bond of water (MacLeod & Rosei 2011).

Adsorption time: Investigation of the time factor on the P adsorption capacity of Bio 300 is presented in Fig. 5a. The results showed that the adsorption capacity increased rapidly at 19.98 mg.g^{-1} in 20 minutes. After that, the adsorption capacity continued to increase slightly from 20.04 to 20.06 mg.g^{-1} at 40 and 80 minutes, and the process increased insignificantly after 160 minutes, at which time it was considered to stop. This result is similar in Bio 450 and Bio 600 (Fig. 4b and Fig. 4c). Specifically, with Bio 450, after 20 min, the adsorption capacity was 19.92 mg.g^{-1}. After 40

a. Bio 300

b. Bio 450

c. Bio 600

d. Treatment efficiency of 3 types of biochar
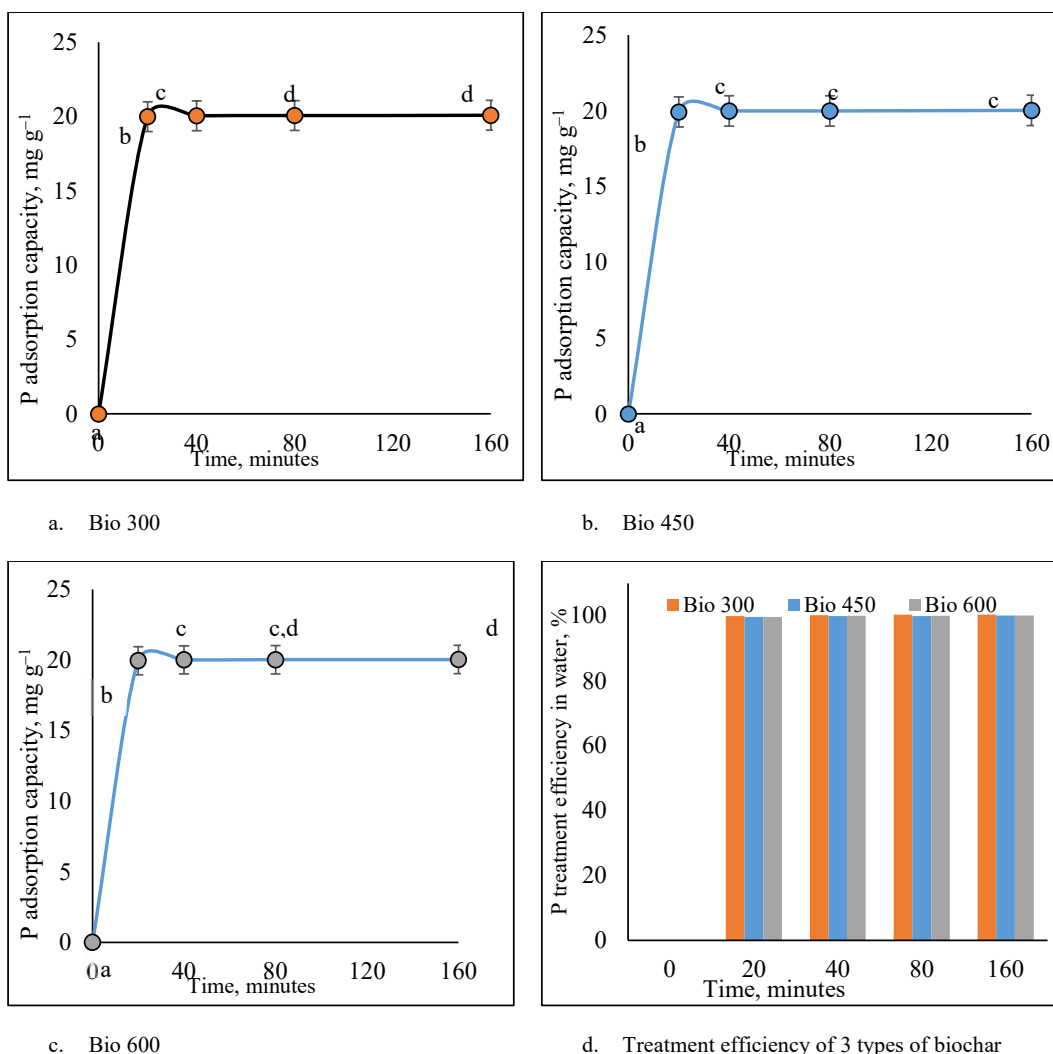
Fig. 5: Effect of time on P adsorption capacity (mg g^{-1}) of biochar samples. Different letters represent significant differences.

minutes, it was 19.98 mg g^{-1}, and it was considered to stop. With Bio 600, it is 19.94 and 20.00 mg g^{-1}.

Results from kinetic studies of P adsorption have shown that there are two stages in the P adsorption process on biochar. The chemical adsorption phase occurred rapidly and was followed by a surface diffusion control phase when the surface adsorption sites were saturated. (Nobaharan et al. 2021).

Experimental results showed that the time to reach the saturated adsorption state occurred in about 20 to 40 minutes for all 3 forms of biochar.

Adsorption Equilibrium

Further data modeling according to the Langmuir model shows that only Bio 300 is more suitable than other forms of biochar due to the large correlation coefficient R^2 (0.97) and the calculated maximum adsorption capacity value (q_0=19, 59 mg g^{-1}) is close to the experimental value (18.6 mg.g^{-1}), Table 2. The research results were higher than biochar derived from pine trees at a maximum of 13,898 mg g^{-1}; maize-straw is 8.809 mg g^{-1} (Zhao et al. 2017). This result shows that the phosphate adsorption process is monolayer adsorption (Feng et al. 2021). Meanwhile, the results of calculating q_0 and the experimental results of both Bio 450 and Bio 600 samples were very different, so the Langmuir model was not appropriate. Besides, when considering the Freundlich model, the 3 types of biochar were all suitable because R^2 was > 0.92. K_F were 4.06; 2.61; 0.41; and 1/ n_F is 0.61; 1.15; 1.10. The value $1/n_F$ was a function of the adsorption intensity during the adsorption process, and it represents heterogeneity (Feng et al. 2021)

Table 2: P adsorption equilibrium parameters.

Models	Pyrolysis temperature	Parameters		R^2	q(ex)
		q_0 [mg.g^{-1}]	K_L		
Langmuir	300°C	19.6	0.28	0.97	18.6
	450°C	-36.3	-0.06	0.91	18.6
	600°C	73.43	0.01	0.95	17.7
Freundlich		$1/n_F$	K_F		
	300°C	0.61	4.06	0.95	
	450°C	1.15	2.61	0.93	
	600°C	1.10	0.41	0.92	

q(ex): P adsorption capacity in the experiment

This finding indicates that during the P adsorption process of three types of biochar with multilayer layers, many heterogeneous surfaces appeared on the biochar surface, and the adsorption may be related to the interactions of chemical interaction between the adsorbent and adsorbent. An explanation of the research results was also found in Yi and Chen (2018).

P Adsorption Kinetics

Calculated data of kinetic parameters showed that the pseudo-second-order kinetic model (Table 3) is more suitable, with a correlation coefficient $R^2 > 0.97$ and the calculated adsorption capacity value (qe). Compared with the experimental adsorption value (qex), it is almost the same. Specifically, qe calculated from the second-order kinetic equation is 20.09, 20.03, and 20.04 mg.g^{-1}, very close to the experimental value (qex) for three types of biochar, Bio 300, Bio 450, and Bio 600, respectively, which are 20.07, 20.03 and 20.03 mg.g^{-1} (Table 3). Therefore, the P adsorption rate of the three types of biochar is controlled by the chemical adsorption mechanism, consistent with previous reports (Feng et al. 2021). Then, the kinetics of P adsorption is mainly due to chemical bonding or chemisorption involving electron sharing between phosphate ion species and biochar (Feng et al. 2021). The adsorption rate of the three types of biochar fluctuated insignificantly in the range of 0.444-0.525.

Table 3: Calculation results of kinetic parameters.

Models	Pyrolysis temperature	qe [mg.g^{-1}]	Kinetic constant	qex	R^2
Pseudo-first-order kinetic	300°C	0.10	$k_1=0.009$	20.07	0.74
	450°C	0.17	$k_1=0.005$	20.03	0.85
	600°C	0.09	$k_1=0.011$	20.03	0.87
Pseudo-second-order kinetic	300°C	20.09	$k_2=0.491$	20.07	0.98
	450°C	20.03	$k_2=0.444$	20.03	0.97
	600°C	20.04	$k_2=0.525$	20.03	0.98
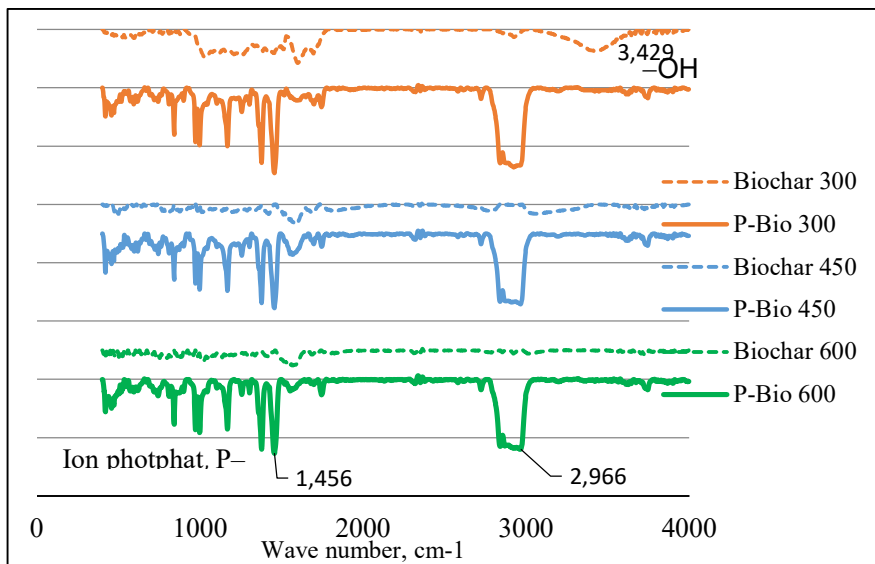
Fig. 6: FT-IR spectra of biochar samples before adsorption (Bio 300, Bio 450, and Bio 600) and after P adsorption (P-Bio 300; P-Bio 450 and P-Bio 600).

Fig. 6 shows the appearance of peaks of O–H groups of hydrogen bonds shifted to 2932 cm^{-1}, and this shows that biochar functional groups may have a role in the P adsorption process through the bridging. hydrogen P–OH...O=P (MacLeod & Rosei 2011). From FTIR spectrum analysis, the increase in peak intensity and shift of the spectrum peak showed that the adsorption may be due to interactions arising after adsorption. Meanwhile, functional groups OH and aromatic carbon can also play an important role in the P adsorption process (Kenchannavar & Surenjan 2022). Asymmetric P–O vibrations of the adsorbed $H_2PO_4^-$ and HPO_4^{2-} groups were also detected in the range of 900-1454 cm^{-1} and appeared in all 3 biochar samples after adsorption (MacLeod & Rosei 2011). The research findings have a basis for confirming that hydrogen bonding plays an important role in the adsorption process of phosphorus ions on the surface of biochar derived from macadamia husks.

Overall, the results of the study confirmed the potential of using biochar derived from macadamia shells (a locally available agricultural waste) at pyrolysis temperatures to remove (adsorb) P from water. The product of the adsorption process can not only be used as a soil conditioner (improving pH, providing organic carbon) but also as a fertilizer (providing P). The contribution of this solution to the circular economy in agriculture (using waste) is well-founded.

CONCLUSIONS

Biochar derived from macadamia husks was pyrolyzed at 300, 450, and 600. Characteristics of biochar forms were determined. The results showed that factors such as initial pH, biochar dosage, initial P concentration, and adsorption time affected the P adsorption capacity of three types of biochar. Besides, the phosphate adsorption capacity at pyrolysis temperatures of 300 and 450°C is higher than biochar pyrolysis at 600°C. Freundlich isotherm and pseudo-second-order kinetic models were found to be most suitable for phosphate adsorption onto biochar forms. This shows that chemisorption interactions occur on the biochar surface through the hydrogen bond bridge P=O...HO–P. Research has shown that biochar produced from macadamia husks can adsorb P from water and that biochar pyrolysis temperature has a non-significant impact on the adsorption capacity of biochar. The study was only conducted in the laboratory under controlled conditions. Therefore, when implemented in practice, additional studies are needed, such as adsorption in the presence of ions (such as ammonium, nitrate, and sulfate), and the particle size of the biochar should also be considered, then the potential risks can be assessed more accurately.

REFERENCES

Angın, D. and Şensöz, S., 2014. Effect of pyrolysis temperature on chemical and surface properties of biochar of rapeseed (*Brassica napus* L.). *International Journal of Phytoremediation*, 16(7-8), pp.684-693.

Choi, Y.K., Jang, H.M., Kan, E., Wallace, A.R. and Sun, W., 2019. Adsorption of phosphate in water on a novel calcium hydroxide-coated dairy manure-derived biochar. *Environmental Engineering Research*, 24(3), pp.434-442.

Feng, Y., Zhao, D., Qiu, S., He, Q., Luo, Y., Zhang, K., Shen, S. and Wang, F., 2021. Adsorption of phosphate in aqueous phase by biochar prepared from sheep manure and modified by oyster shells. *ACS Omega*, 6(48), pp.33046-33056.

Huang, X., Ren, J., Ran, J.-Y., Qin, C.L., Yang, Z.Q. and Cao, J.P., 2022. Recent advances in pyrolysis of cellulose to value-added chemicals. *Fuel Processing Technology*, 229, p.107175.

Kenchannavar, P. and Surenjan, A., 2022. Application of circular economy in wastewater treatment using biochar-based adsorbent derived from sewage sludge. *IOP Conference Series: Earth and Environmental Science*, 142, p.101242.

Lehmann, J. and Joseph, S., 2015. *Biochar for Environmental Management: Science, Technology and Implementation*. Routledge.

Li, Y., Zhao, B., Wang, L., Li, Y., Wang, T., Jia, Y. and Zhao, M., 2024. Competitive adsorption of Cd (II) and Zn (II) on biochar, loess, and biochar-loess mixture. *Nature Environment & Pollution Technology*, 23(1), p.65.

Luo, D., Wang, L., Nan, H., Cao, Y., Wang, H., Kumar, T.V. and Wang, C., 2022. Phosphorus adsorption by functionalized biochar: a review. *Environmental Chemistry Letters*, 7, pp.1-29.

Luo, D., Wang, L., Nan, H., Cao, Y., Wang, H., Kumar, T.V. and Wang, C., 2023. Phosphorus adsorption by functionalized biochar: a review. *Environmental Chemistry Letters*, 21(1), pp.497-524.

MacLeod, J. and Rosei, F., 2011. 3.02-Directed assembly of nanostructures. In: D.L. Andrews, G.D. Scholes and G.P. Wiederrecht, eds. *Comprehensive Nanoscience and Technology*. Academic Press.

Nobaharan, K., Bagheri Novair, S., Asgari Lajayer, B. and van Hullebusch, E.D., 2021. Phosphorus removal from wastewater: the potential use of biochar and the key controlling factors. *Water*, 13(4), p.517.

Phuong, N.V., Hoang, N.K., Luan, L.V. and Tan, L., 2021. Evaluation of NH_4^+ adsorption capacity in water of coffee husk-derived biochar at different pyrolysis temperatures. *International Journal of Agronomy*, 21, pp.1-9.

Tan, K.H., 2011. *Principles of Soil Chemistry*. Taylor and Francis Group, LLC.

Tomczyk, A., Sokołowska, Z. and Boguta, P., 2020. Biochar physicochemical properties: pyrolysis temperature and feedstock kind effects. *Reviews in Environmental Science and Bio/Technology*, 19(1), pp.191-215.

Tu, T., 2016. Physical and chemical characterization of biochar derived from rice husk. *Hue University Journal of Science*, 120, pp.233-247.

Vu, N.L., Nguyen, N.D., Tran-Nguyen, P.L., Nguyen, H.V., Dinh, T.M.T. and Nguyen, H.N., 2023. Evolution of properties of macadamia husk throughout gasification: hints for a zero-waste energy production system. *Biomass and Bioenergy*, 171, p.106735.

Xiong, M., Dai, G., Sun, R. and Zhao, Z., 2024. Passivation effect of corn vinasse biochar on heavy metal lead in paddy soil of Pb-Zn mining area. *Nature Environment & Pollution Technology*, 23(1).

Xu, Y., Liao, H., Zhang, J., Lu, H., He, X., Zhang, Y., Wu, Z., Wang, H. and Lu, M., 2022. A novel Ca-modified biochar for efficient recovery of phosphorus from aqueous solution and its application as a phosphorus biofertilizer. *Nanomaterials,* 12(16), p.2755.

Yi, M. and Chen, Y., 2018. Enhanced phosphate adsorption on Ca-Mg-loaded biochar derived from tobacco stems. *Water Science and Technology,* 78(11), pp.2427-2436.

Zhang, M., Song, G., Gelardi, D.L., Huang, L., Khan, E., Mašek, O., Parikh, S.J. and Ok, Y.S., 2020. Evaluating biochar and its modifications for the removal of ammonium, nitrate, and phosphate in water. *Water Research,* 186, p.116303.

Zhao, S., Wang, B., Gao, Q., Gao, Y. and Liu, S., 2017. Adsorption of phosphorus by different biochars. *Spectroscopy Letters,* 50(2), pp.73-80.

The Utility of Synthetic Biology in the Treatment of Industrial Wastewaters

Monica Joshi and Jai Gopal Sharma†

Department of Biotechnology, Delhi Technological University, Delhi-110042, India

†Corresponding author: Jai Gopal Sharma; sharmajaigopal@dce.ac.in

ABSTRACT

Effective treatment of industrial wastewater effluents before discharging them to the soil and water bodies has always been one of the paramount environmental concerns. The pollutants in untreated wastewater effluents have hazardous implications for human health and the ecosystem. Conventional physical and chemical processes of industrial wastewater treatment have many complications and they often fall short in the treatment of new and diverse varieties of pollutants. Several microbial strains in nature have shown their remediation property, but they possess limited efficiency in breaking down pollutants into non-toxic components. Synthetic biology is a perfect amalgam of two fields – biological science and engineering, and it has transformed our ways of understanding the functioning of complex biological systems. Researchers have reported that some engineered microbes can achieve remediation efficiency of up to 100% in specific pollutants such as heavy metals and hydrocarbons. For example, microbes like *Pseudomonas veronii* have been shown to reduce cadmium concentrations by up to 100%, and *Pseudomonas putida* has been shown to reduce phenol concentrations by 92%. Synthetic biology-based biosensors are also being developed for pollution monitoring and control of industrial wastewater. In this review, we discuss these advancements of synthetically engineered microorganisms in the treatment of industrial wastewater.

INTRODUCTION

Industries are the major driving force behind the growth and development of a country, but they also produce toxic effluents that are the leading cause of water and soil pollution (Saxena 2020). Effluents released from the manufacturing processes of petrochemical, textile, electroplating, pharmaceutical, and food industries constitute industrial wastewater (Nasr 2022). This effluent consists of a variety of organic and inorganic matter, dyes, and metal ions (chromium, cadmium, lead, copper, zinc, and nickel) (Nasr 2022). These contaminants cause the degradation of the natural biota of water, air, and soil by changing their physiochemical properties (Saravanan et al. 2023). Furthermore, untreated wastewater discharged into the river can cause several severe diseases like chronic dermatoses and skin cancer, lung infection, and eye irritation (Kesari et al. 2021). Hence, the wastewater discharged from these industries is the prominent cause of toxicity to human health and the environment (Singh et al. 2023). It has been reported that around 3-10 billion gallons of untreated wastewater is released into the environment, and an estimated 80 percent of wastewater is reused globally without any intervention of physical or chemical treatment (Saddique et al. 2023). The rise in the global population will also lead to the global rise of the concertation of discharged industrial wastewater. Untreated industrial wastewater pollutants contain harmful pollutants which, if entered into the water supply, would lead to deterioration of water quality (Jones et al. 2021) or, if entered into the food chain, would lead to severe allergies and other diseases. Hence, effective wastewater treatment processes are needed.

For the treatment of industrial wastewater, many chemical and physical techniques have been in application, like physical sedimentation, physical filtration, ozonation, chemical precipitation, adsorption, and ion exchange (Saravanan et al. 2021). However, they have many limitations, like high costs needed for optimum working and maintenance, low resource recovery from industrial wastewater, and utilization of high energy for the treatment processes to happen (Dutta et al. 2021, Yaashikaa et al. 2022). Biological methods that are utilized for the treatment of industrial wastewater are microbial remediation, aerobic treatment, anaerobic treatment, oxidation ponds, and activated sludge. These methodologies also have many limitations, such as the sludge disposable problem in the case of activated sludge methodology, the need for very large space to be successfully operational in the case of oxidation ponds, high capital cost, and odor nuisance in anaerobic treatment, cost expensive in aerobic treatment (Saravanan et al. 2021). Hence, we need a microbial wastewater system over a traditional wastewater system that would be green, sustainable (Sharma et al. 2023), and highly efficient. It has been long established that the intrinsic degradation property of microbes can be utilized in the degradation of environmental pollutants. This intrinsic property is applied in the bioremediation process where microbes, via their metabolic processes, degrade and convert the pollutants into less toxic substances. Despite this impressive ability of microbes, bioremediation has many limitations, like incomplete breakdown of organic pollutants, low efficiency of microbial remediation, and remediation process only effective for biodegradable contaminants (Jabbar et al. 2022). These limitations of microbial bioremediation processes can be improved by synthetic biology.

Using synthetic biology, we can modify metabolic pathways or/and create new metabolic pathways in new microbial cells that would be able to degrade not only biodegradable pollutants but also synthetic pollutants. The main synthetic pollutants occurring in the environment are pesticides, pharmaceuticals, polycyclic aromatic hydrocarbons (PAHs), phthalates, chlorinated phenol compounds, absorbable organic halides, and inorganic metal ions (Bhatt et al. 2021). Synthetic biology is a field that utilizes the principles of both biology and engineering field to create novel biological systems having modified or new functions. This is achieved by using molecular and computational tools that create the new genetic architecture of a microbe (Jiménez-Díaz et al. 2022). This new genetic architecture consists of a series of new components (gene promoters, transcription factors, enzymes, etc.) that together build new metabolic pathways with end products that could be studied and even re-build (Rylott & Bruce 2020). Hence,

in the field of environmental remediation, advances in synthetic biology led to the construction of microorganisms that can scavenge and biodegrade a variety of toxic wastes like aromatic compounds, pesticides, microplastics, greenhouse gases, etc (Thai et al. 2023).

The integration of the field of synthetic biology and remediation (synthetic bioremediation) using microbes for the treatment of industrial wastewater has shown immense advancements in recent times. Many engineered microbial strains have shown their capability to degrade contaminants. Recently, Tomijiro Hara et al., in their experiment, engineered an *E. coli* strain capable of degrading a variant of Polychlorinated biphenyls (organohalide pollutants) in a natural landscape at a level that is sufficient for clean-up of PCB pollution (Hara et al. 2021). Sharma et al. reported that the genetically engineered *Pseudomonas* strain shows an enhanced ability of metal remediation in aquatic and terrestrial ecosystems near the industrial sites of pulp and paper (Sharma et al. 2021). Enzyme engineering within the microorganisms not only speeds up the remediation process but also solves the key limitations of chemical treatments and minimizes over-reliance on them. Additionally, microorganisms, with the help of synthetic biology tools, are created that can function as biological sensors (Aminian-Dehkordi et al. 2023). These biological sensors help in the real-time monitoring of pollutant levels and, hence, are an effective technique for monitoring water quality (Aminian-Dehkordi et al. 2023).

Synthetic biology can also be used to study the microbiota of industrial wastewater treatment plants using tools such as metagenomics, metatranscriptomics, metaproteomics, and metabolomics. These tools can help identify the key genes, enzymes, pathways, and microorganisms involved in pollutant degradation and reveal the relationship between running parameters and the keystone microorganisms (Jiang et al. 2022). In the world of bioremediation, synthetic biology could be used to design biosensors, enzymes with unique activities towards persistent organic xenobiotics, organisms that are resistant to challenging environmental conditions, robust biopolymers, artificial storage organelles for toxic metals, and much more (Rylott & Bruce 2020). Here in this review, we present synthetic biology approaches applied in the treatment of industrial wastewater. We begin with describing important components used in bioengineering including chassis, genetic circuits, transcription factors, and gene editing tools. Then, we move to specific synthetic biology ways for the treatment of industrial wastewater, where we describe strategies like metabolic pathway modifications, enzyme engineering, and synthetic microbial consortia for pollutant degradation. Furthermore, we discuss

biosensors for the detection of pollutants in industrial wastewater. Finally, the role of biofilms in enhancing the efficiency of biodegradation is discussed.

SYNTHETIC BIOLOGY COMPONENTS USED IN BIOENGINEERING

Sometimes, the term engineering biology is used as an alternative to the term synthetic biology (Zhang et al. 2023). The ultimate goal of synthetic biology is to bioengineer microorganisms having specific functionalities (Kim et al. 2016a). This goal is achieved by following the iterative "design-build-test-learn" (DBTL) cycle (Kitano et al. 2023, Garner 2021). In the first stage, the design of a biological system with pre-defined functionalities is created, followed by the build step, where simulations of that system will be conducted (Garner 2021). Assessment of differences between the performances of the simulation and the actual biological system in a real-life situation is conducted (test stage), and new insights are driven from it (learn stage) (Garner 2021).

Chassis

Despite the advancements in microbes-assisted remediation, bioremediation when using native microbes is not able to effectively degrade calcitrant pollutants because of genetic instability in microbes (Yaashikaa et al. 2022) and minor fluctuations in environmental like changes in pH, temperature, etc., could interfere with their ability needed for the degradation of the pollutants (Singh et al. 2021). Synthetic biology can overcome these challenges by building microbial systems as chassis for the bioremediation of these pollutants. In synthetic biology, chassis is referred to as a genetically modified model cell (McCarty & Ledesma-Amaro 2019). In a chassis, computational and molecular tools are used to engineer the genetic circuits and metabolic pathways to express desired results (Kim et al. 2016b). Most commonly, chassis organisms used in synthetic biology are the bacteria *Escherichia coli* and *Bacillus subtilis* and the yeast *Saccharomyces cerevisiae* (Tang et al. 2020, Kim et al. 2016b). These organisms have properties that make them a suitable chassis. These organisms are characterized by fast growth, supported by a wide variety of molecular tools. This led to an easy understanding of synthetic biology circuits and metabolic pathways (Kim et al. 2016b). Chassis can be constructed in two ways: top-down approach and bottom-up approach (Chi et al. 2019).

Genetic Circuits

To get a desired expression from the host cell, it is important to achieve precise control of gene expression, which is achieved by using synthetic genetic circuits. Synthetic genetic circuits are made up of networks of multiple interconnected gene switches that regulate cellular function by controlling the initiation and termination of a target gene expression (Xie & Fussenegger 2018). The synthetic biology field is primarily based on the construction of genetic circuits that could work either independently within cells or together by combining with a cell's biological network (MacDonald & Deans 2016).

Transcription Factor

Transcription is a crucial process as it is the fundamental step in the molecular processes that determine cell behavior and health (MacDonald & Deans 2016). Gene expression in a cell is initiated by the transcription process (Tietze & Lale 2021). The promoter situated upstream region of the gene's coding sequence determines the rate of transcription in a cell (Eisenhut et al. 2024). Therefore, scientists often alter the promoter region to regulate the strength of gene expression (Eisenhut et al. 2024). Hence, the most important regulatory point in a genetic circuit is transcription (Bradley et al. 2016). Scientists are aiming for better control of the genetic circuits by studying transcriptional networks in the cell.

Moreover, they are looking for endogenous trigger systems that turn on genetic circuits. With the help of these endogenous trigger systems, they can fine-tune the genetic circuits to find disease, bio-engineer new cell functions, and program cells with the ability to make independent decisions (MacDonald & Deans 2016). Another aspect of transcriptional regulation that makes it crucial for synthetic biology applications is that transcriptional regulation paves the way for a cell to regulate its enzymatic levels and stoichiometry, thereby preventing harmful metabolite accumulation, underutilized enzymes and the formation of unnecessary macromolecular compounds (Engstrom & Pfleger 2017).

Transcription in cells is regulated by transcription factors that activate or repress promoter activities (Tietze & Lale 2021). Synthetically engineered transcription factors are composed of a binding domain that identifies and then binds to a specific target DNA sequence and an effector domain that can activate or inhibit transcription (Eisenhut et al. 2024). Using in-silico technology, synthetic transcription factors can be created. Synthetic transcription factors for the regulation of gene expression are derived from proteins like zinc fingers (ZFs), transcription activator-like effectors (TALEs), and clustered regularly interspaced short palindromic repeats associated protein (CRISPR-Cas) (Chen et al. 2022). Synthetic zinc fingers are constructed by combining several zinc protein domains, where each zinc finger protein is typically made of 30 amino acids that are organized in a ββα

motif. These engineered zinc fingers can identify 9-18 base pairs of specific DNA sequences, facilitating the targeting of desired sequences within the genome and thereby regulating gene expression (MacDonald & Deans 2016, Dai et al. 2018). On the other hand, TALEs are huge DNA-binding proteins having a size greater than 120 kilodaltons. These proteins have secretion signals on their N-termini end and nuclear localization signals on their C-termini end. The central helical domain region constitutes the bulk of these proteins as it is made of 15.5-19.5 near-perfect repeats of 34 amino acids and is responsible for the majority of DNA sequence-specific binding activity (Engstrom & Pfleger 2017). Recently, CRISPR-based tools have gained immense popularity for metabolism regulation, either independently or as part of a genetic circuit (Lv et al. 2022). CRISPRi (CRISPR-interference), a modification of CRISPR system, is used for sequence-specific transcriptional regulation. CRISPRi is made of two units – Cas9 endonuclease, which is catalytically inactive, and a single guide RNA (sgRNA), which precisely binds to targeted DNA at specific locations in the genome. Inactive Cas9, when targeted to promoter regions, acts as an RNA-guided repressor protein, which stops transcription by blocking polymerase movement through steric hindrance. With the help of this tool, multiple gene regulation can happen simultaneously by changing either the expression of Cas9 or the level of complementarity between the synthetic guide RNA (sgRNA) and the target sequence (Kent & Dixon 2020).

Gene Editing Tools

We can rationally engineer microbial cells at a global (genome) or local (gene) level by precisely modifying DNA sequences with the help of gene editing tools (Rafeeq et al. 2023). It has been shown in many types of research that genetically modified organisms are better at bioremediation processes than native microorganisms across various environments such as soil, groundwater, and activated sludge, exhibiting enhanced capabilities in degrading diverse organic pollutants as they show greater resistance to heavy metals, has greater substrate range, increase enzyme activity, and binding affinity (Haripriyan et al. 2022). The gene editing process involves the use of engineered enzymes (nucleases) that are able to create double-strand breaks in the DNA at desired locations. These double-strand breaks are then repaired by nonhomologous end joining (NHEJ) or homology-directed repair (HDR) (Barreiro & García-Estrada 2022). Key genetic tools employed for this are CRISPR-Cas, ZFN, and TALEN. Among these, CRISPR is the most effective and productive gene editing tool. CRISPR-Cas system has three main types – I, II, and III (Jaiswal et al. 2019). The Cas9 cleavage protein binds to the target sequence that is determined by the RNA guide molecules, which is the sequence after the protospacer adjacent motif (PAM) sequence in the genome. Following this, scientists can delete, correct, or insert genes into the break. Deletion occurs with the aid of non-homologous end-joining (NHEJ), and correction and insertion occur with the aid of homology-directed repair (HDR) (Gao et al. 2020). CRISPR-Cas system can modify the metabolic degradation pathway of specific pollutants in a microorganism by inserting or deleting the genes at multiple regions, thereby enhancing the bioremediation process (Ahmad et al. 2023). In a study, it was found that the biotransformation efficiency in *Bacillus licheniformis* reached a hundred percent after the deletion of the *yvmC* gene by employing the CRISPR-Cas9 technique (Rafeeq et al. 2023). When compared with the CRISPR-Cas system, both ZFN and TALEN cannot modify multiple genomic regions and can randomly bind to DNA sequences, leading to a much higher probability of off-target mutation (Jaiswal et al. 2019). The limitation of CRISPR-Cas is large Cas protein size leads to difficulty in cell delivery, the requirement of more whole genome data, and some chances of off-target mutation (Ranjbar & Malcata 2022). Hence, gene editing tools aim to achieve a better microbial bioremediation process by introducing diverse genes into the microbial cell to target specific pollutants (Hassan & Ganai 2023).

SYNTHETIC BIOLOGY WAYS FOR TREATMENT OF INDUSTRIAL WASTEWATERS

Microbial enzymes are responsible for the breakdown of toxic pollutants. There are four steps in the mechanism of microbial degradation of pollutants: 1. Microorganisms produce surfactants for the emulsion of pollutants; 2. The outer layer of the microorganism then adsorbs emulsified pollutants; 3. The adsorbed pollutant enters from the outer cell film layer to the cell layer via passive or active transport; 4. Upon entering the cell, the pollutant undergoes an enzymatic reaction with the corresponding enzymes to complete its degradation process (Yaashikaa et al. 2022).

In this new era of advancements in multi-omics techniques and genetic engineering, we can now select the most suitable microorganism host for the remediation process. Various tools based on genomic, proteomics, and metabolic data are employed to identify catabolic genes, novel pathways, or proteins involved in the biodegradation process so that we can engineer efficient metabolic degradation pathways for a target pollutant. Additional analysis of transcriptomic data can equip us with important information like cellular responses, post-exposure to toxic pollutants, and their influence on the metabolic state (Jiménez-Díaz et al.

2022). Synthetic biology synthesizes its components (gene promoters, transcription factors, enzymes, etc.) with the help of molecular tools and system biology, that together construct the metabolic degradation pathways with outputs that can be tested, reconstructed, and fine-tuned (Rylott & Bruce 2020).

CONSTRUCTION OF MODIFICATIONS IN METABOLIC DEGRADATION PATHWAYS

A series of general steps can be followed for the construction of modifications in metabolic degradation pathways: 1. Select your target pollutant and determine its physical and chemical properties; 2. Study the existing metabolic pathways in microorganisms that can degrade the target pollutants. Investigate the information of metabolites and enzymes that serve as the building blocks of the degradation pathway; 3. Select a suitable chassis based on multi-omics data analysis. Utilize molecular bio tools to introduce gene-encoding enzymes responsible for pollutant degradation into the chassis; 4. Optimize the synthetic metabolic degradation pathway. This can involve adjustments in the expression level of pathway genes and balancing metabolic flux. The pathway is shown in Fig. 1. For instance, *Pseudomonas sp*. *The B13* degradation pathway was modified, which led to increased efficiency in the degradation of methyl phenols and methyl benzoates (Ahmad et al. 2023). However, the process of screening the host for suitable enzymes that are capable of acting on the target pollutant is time-consuming. Additionally, conducting multiple biodegradation assays simultaneously in the laboratory poses significant challenges (Adetunji et al. 2023). Thanks to the advancements in computational techniques, in-silico bioremediation methods have emerged to cater to this problem. This in-silico approach relies on various scientific fields, including genomics, computational biology, proteomics, bioinformatics, molecular modeling, molecular dynamics simulation (MDS), and specialized algorithms for pathway prediction. Additionally, this approach also utilizes the dataset from several microbial databases. Furthermore, progress in sequencing technologies and bioinformatic algorithms has helped us in improving the

bioremediation efficiency as these advancements led us to the further in-depth analysis of genomic sequences, which helped us in finding the innate metabolic enzymes and pathways for bioremediation (Tran et al. 2021).

The EAWAG Biocatalysis/Biodegradation Database, which contains the EAWAG-BBD pathway prediction system, can be used for the in-silico construction of metabolic degradation pathways. This EAWAG biodegradation database contains comprehensive information on microbial biochemical catalysis reactions that include biodegradation pathways for various chemical compounds and their microbial enzymes. By accessing this database, users can predict the degradation pathway of the target pollutant (Singh et al. 2020). Kelly et al. proposed a mechanism based on computational methods to find a suitable enzyme candidate for the degradation of toxic personal care products present in wastewater that are not effectively eliminated by conventional wastewater treatment. Computational analysis was done to study the biodegradability of the specific pollutant, and a pathway prediction system was utilized to find the metabolic pathways and enzymes that would react with the pollutant. They were successfully able to identify the enzyme with a degradation rate 40 times higher than previously reported rates (Aukema et al. 2017).

In addition to the design of the degradation pathway, the choice of chassis is also very important. For this, several microbial cells have been considered over the years, but none of them satisfies all the desired characteristics that are required in an ideal microbial degrader host. *Pseudomonas Putida,* which is soil bacteria, has emerged as a potential host degrader as it fulfills many criteria for growing and surviving in adverse environmental conditions and the ability to degrade recalcitrant pollutants (Dvořák et al. 2017). With the help of next-generation sequencing and omics data analysis, we can study biochemical catalysis taking place inside the microbial host as well as between the microbial host and the contaminant environment (Yaashikaa et al. 2022). The incorporation of synthetic metabolic pathways into actual producer strain has been
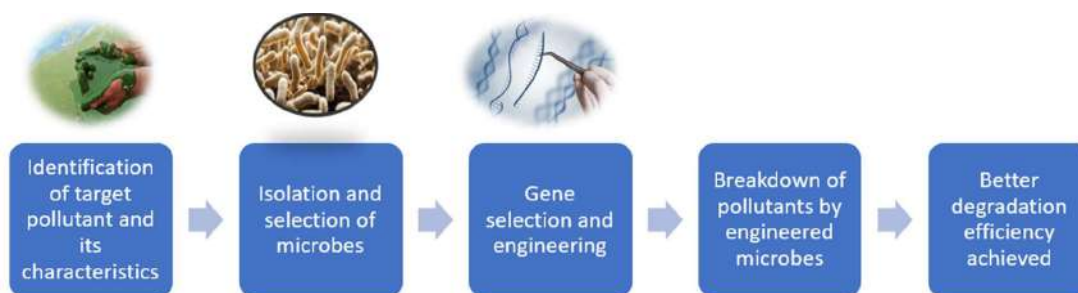
Fig. 1: Workflow of pollutant degradation using synthetic biology.

made easier by the new technological advancements in genetic engineering. DNA assembly tools, such as BioBrick assembly, Gibson assembly, Golden Gate assembly, ligase cycling reaction, single strand assembly, transformation-associated recombination (TAR) cloning, and uracil-specific excision reagent (USER) cloning, are examples. These tools have simplified the assembling process of multicomponent and large-sized gene clusters. DNA assembly tools have enabled the expression of assembled metabolic pathway genes using plasmids. Additionally, we can construct optimized metabolic pathway genes for expression in specific host strains (e.g., codon-optimized) using oligonucleotide and gene synthesis technologies (Choi et al. 2019). By engineering metabolic degradation pathways, we can prevent the production of toxic intermediates (Yaashikaa et al. 2022).

Enzyme Engineering

Over the past few decades, it has been reported that several bacterial species have the ability to produce enzymes. Many of these bacterial enzymes have shown their role in the mitigation or elimination of complex environmental pollutants (Singh et al. 2020). Enzymes are highly efficient biological catalysts, and they can transform toxic compounds into simpler, non-toxic compounds. Thereby, bacteria utilize these enzymes in their metabolic cycle for the effective removal of pollutants from the contaminant sites. Among the major classes of enzymes, oxidoreductases, and hydrolases are the classes that have been most extensively researched for their property of degrading toxic compounds into environmentally safer compounds. This is due to the fact that these enzyme classes possess high catalytic activity and the ability to target wide ranges of substrates, including xenobiotic pollutant compounds (Zhu et al. 2019). Over the past few years, researchers have been working on isolating microbial enzymes to use in biodegradation pathways instead of using the whole organism. This is because enzymes exhibit greater substrate specificity and a higher motility rate owing to their smaller size. However, we are still not able to fully utilize the potential of this technique because of some limitations like lower productivity, activity, and stability of enzymes, as they are very sensitive to the changing environmental factors, and that will have an adverse effect on their activity (Ahmad et al. 2023).

Also, for the enzymatic degradation of complex environmental pollutants like lignin in paper and pulp effluents, pesticides, aromatic hydrocarbons, and plastics, large quantities of enzymes need to be produced. However, these enzymes are produced in insufficient quantities (Aminian-Dehkordi et al. 2023). However, recently, some studies have shown how, by using recombinant DNA technology technique, we can produce large quantities of required enzymes. For example, according to a recent study, recombinant enzyme laccase was produced by various host organisms like bacteria, yeast, and filamentous fungi (Zhu et al. 2019). In another study, it has been shown that the production of recombinant hydrolases, such as lipases, carboxylesterases, and cutinases, has a high potential for pollutant remediation (Zhu et al. 2019). Furthermore, enzyme engineering can modify such properties in enzymes, making them have better catalytic activity and stability than native enzymes (Yang et al. 2021), so that they will be useful for onsite bioremediation of contaminated sites (Bhatt et al. 2021). Enzymatic properties of the rate-limiting enzymes of the important degradation pathways are extensively researched, and from that, important enzymatic data are analyzed (Yang et al. 2021).

The steps involved in enzyme engineering are as follows: 1. Protein engineering; 2. Modification of the enzyme; and 3. Screening of the modified enzyme (Bhatt et al. 2021). Protein engineering can be done in three ways – rational design (site-directed mutagenesis), random methods like random mutagenesis, and directed evolution. Rational design is a useful approach if we already know the structure and mechanism of the target protein. In a recent experiment, a novel fungal polyphenol oxidase was engineered by site-directed mutagenesis to produce different enzyme variants with increased catalytic activity and varying specificities for bioremediation of chlorophenols (Zhu et al. 2019). Another study reported that after the rational modification of the carboxylase enzyme, the biodegradation of a harmful phenol derivative was increased by forty percent, and the stereoselectivity property of that modified enzyme was increased by thirty-nine-fold (Aminian-Dehkordi et al. 2023). On the other hand, the directed evolution approach can yield enzymes having enhanced properties even in the absence of information regarding protein structure or catalytic mechanism (Zhu et al. 2019). For instance, using this approach, ligninolytic enzymes in fungi were modified with properties such as extreme pH resistance (Zhu et al. 2019).

Synthetic Microbial Consortia

Microbial cells rationally engineer their metabolic pathways by using metabolic engineering. The overall efficiency and functioning of these reconstructed pathways depend on various factors, including precursors, cofactor demands, and the optimal expression of pathway enzymes. However, sometimes, these reconstructed metabolic degradation pathways do not function as expected because of a metabolic burden on the microbial cell. To improve this limitation of metabolic burden in a cell, microbial co-cultures have been rationally designed to distribute the metabolic burden of complex and lengthy biosynthetic pathways across

different strains or species, thereby enhancing bio-production performance. This co-cultivation technique can successfully reduce the metabolic stress of engineered microbial cells caused by the overexpression of long and complicated metabolic pathways (Jawed et al. 2019).

When the population of two or more microbial species live together in a symbiotic relationship, this relationship is known as microbial consortia. The microbial consortia can perform complex metabolic processes that would be impossible for a single strain to do. A single strain of a microorganism is not able to produce different varieties of enzymes that are required for the complete degradation of the xenobiotic pollutants found in the environment. It has been observed that naturally occurring microbial consortia can degrade complex compounds but their degradation efficiency is less. They can degrade compounds like plastics, petroleum, antibiotics, azo dyes, and some pollutants found in sewage. We can enhance the degradation efficiency by constructing synthetic microbial consortia by adding new genetic materials and modules (Sharma & Shukla 2020).

The synthetic microbial consortia can be rationally constructed in two ways – top-down approach and bottom-up approach. The top-down approach involves a multi-omics study of microbial communities to understand the workings of the microbial system at the molecular level and then constructing novel communities based on this knowledge. Whereas the bottom-down approach involves rational engineering of microbial consortia based on genetic elements, modules, circuits, and metabolic pathways to obtain microbial consortia with improved efficiency, stability, and controllability. Considering the difficulty in making synthetically engineered cells, the bottom-up approach is mostly used for the construction of synthetic microbial consortia (Jia et al. 2016). Techniques that synthetic biology uses to engineer microbial cells can also be employed in engineering complex functions and behaviors of microorganisms in microbial consortia. This can be achieved by using tools such as intercellular signaling, exogenous inputs, and syntrophic interactions. All these tools, combined, can control factors like population level, task distribution, and spatial arrangements among the microorganisms in the microbial consortia (McCarty & Ledesma-Amaro 2019). In bioremediation, other than improved biodegradation efficiency, consortia also have other advantages like providing support for secondary applications of treated wastewater and the promotion of ecological sustainability (Sharma et al. 2023). In an experiment, the researcher created a consortium by combining the bio-surfactant producer *Rhodococcus erythropolis OSDS1* with petroleum hydrocarbon degraders *Serratia proteamaculans S1BD1, Alcaligenes sp. OPKDS2, Rhizobium sp. PNS1, and Pseudomonas sp. BSS9BS1*. This

consortium exhibited higher efficiency and a wider range of capabilities in degrading petroleum hydrocarbons as compared to a single strain (Gao et al. 2020). Leong et al., in their experiment, showed a pollutant removal efficiency of 94% from municipal wastewater using microbial consortia involving microalgae and bacteria (Gao et al. 2020). Despite many advantages of using synthetic microbial consortia, many limitations of this technique are also there. These limitations include a limited understanding of bacteria interaction patterns and mechanisms, difficulty in rational designing efficient and functional microbial communities, and determining the roles played by these communities in different areas (Gao et al. 2020).

Another important point that should be considered when creating synthetic microbial consortia is the appropriate selection of chassis strains. It should be determined whether the chassis strains with efficient catalytic abilities would be compatible to co-exist with other strains. For this, strains with low mutation rates, no production of toxic by-products, and levels of high tolerance should be selected. Additionally, proper division of labor should be followed while dividing long degradation pathways into several strains. While synthetic microbial consortia reduce the metabolic burden on cells, excessive segmentation of metabolic pathways will also lead to confusion and disrupt efficient mass transfer among strains in consortia. Recent studies have reported an increase in the efficiency of degradation of complex compounds by microbial consortia if the strains in consortia are assembled in an orderly spatiotemporal manner. Assembly of spatial-linked microbial consortia can even involve incompatible microbial strains. This has great potential in the bioremediation field (Cao et al. 2022).

SYNTHETIC BIOLOGY APPROACH FOR DETECTION OF POLLUTANTS

The choice of method for removal of pollutants in wastewater is based on the contamination level of pollutants in the wastewater (Razzak et al. 2022). Microbes can act as very capable sensors because of some inherent qualities. Their small size enables them to be a highly sensitive small-scale detector that can sense, integrate, and react dynamically to various environmental factors. Biosensors are defined as genetically engineered microbes or independent biological components that are engineered to sense environmental signals and convert them to detectable output for us. They can also report microbial interactions in complex environments. The biosensor consists of the following modular features: 1. Sensor module – detects specific environmental conditions as input signals; 2. Processing module – calculate the input signals; 3. Output module – generates signals that can be

detected and measured. An important characteristic that a biosensor must possess to effectively study ecological processes is the capability to survive and perform in a contaminant region without getting interfered with by environmental conditions like temperature, hydration, pH, and substrate levels (Del Valle et al. 2021).

Microbial whole-cell biosensors comprise a genetic component that functions as a sensor to detect an analyte or a toxin and a reporter protein that generates a measurable output signal. These microorganisms' genomes or plasmids are genetically incorporated with the genes that are necessary for cellular response to the target analyte or toxin with the reporter protein. CFE biosensors are also known as cell-free transcription/translation systems. As the name suggests, they function independently of cellular processes; they are the isolated genetic circuits in the environment that sense and respond to the changing environmental factors. CFE biosensors have many advantages like no risk of plasmid loss and genetic instability and no need for biocontainment upon deployment. Ethical issues of using living microbes as a sensor can be avoided by using CFE. However, there is a major disadvantage to employing cell-free biosensors; at the industrial level, CFE biosensors have a high cost of production and deployment. Furthermore, with the use of bioinformatics tools, we can identify synthetic pathways to convert indetectable molecules into detectable ligands, constructing modular CFE for a wide variety of applications. Biosensor systems have modular and engineerable genetic components, which makes them highly optimizable and portable systems (Aminian-Dehkordi et al. 2023). Nowadays, we can engineer biosensors that are able to detect multiple environmental contaminants by eliciting a distinct signal for each kind of contaminant. These kinds of biosensors hold more significance in real-life situations as environmental regions are not contaminated by only one type of pollutant. Rather, they are contaminated by a wide variety of pollutants with varying physical and chemical properties (Yaashikaa et al. 2022). Whether a biosensor is suitable or not for a real-life situation is assessed by the following criteria: specificity and sensitivity to the target contaminant, range of its operation in the environment, and dynamic range. Computational tools and machine learning tools have fastened the designing and development of more advanced novel biosensors (Yu et al. 2023).

BIOFILMS IN WASTEWATER TREATMENT

Biofilm is the term coined for aggregated microbial communities that are permanently bound to the outer surface of living or non-living systems present in the environment and are encased by the self-generated layer of extracellular polymeric substance. The following steps take place in the biofilm formation: microbiome bound to the surface of the living or non-living system, synthesis of extracellular polymeric substance (EPS) around the microbiome, microbial communication via signaling, and the transition of the microbiome into planktonic cells (Chattopadhyay et al. 2022). Biofilm formation is dependent on several factors: the optimum presence of nutrients and energy required for their growth, the right environmental parameters in terms of geochemistry, the existence of inhibitors, predator microorganisms that feed on biofilms, and the effect of hydrodynamics on the transport of solutes which leads to mechanical stress on biofilms (Garg et al. 2023). Biofilms can survive harsh environmental conditions like changes in pH, occurrence of toxic chemicals and free radicals, and depletion of nutrients. Biosurfactants present in the EPS layer are involved in the formation of biofilms. These biosurfactants take part in the bioremediation process of environmental pollutants (Chattopadhyay et al. 2022). In a biofilm, pollutants are more bioavailable to the degrading organisms and microorganisms show enhanced potential in degrading pollutants. Microbial metabolism is responsible for this, and enzymes of the metabolic pathway convert environmental pollutants into non-toxic compounds (Muhammad et al. 2020).

CONCLUSIONS

With the global rise in the number of industries in the near future, there will be a tremendous rise in the volume of discharged wastewater from the industries as well. Wastewater contains various untreated harmful toxic wastes, which, when discharged into the water and soil, cause serious harm to the environment and human health. Therefore, finding novel, effective ways for the treatment of wastewater is very important. Herein, we have discussed how synthetic biology can help revolutionize the field of bioremediation of recalcitrant pollutants found in wastewater by designing effective and sustainable biological systems. Now, we can bioengineer novel microorganisms to target specific categories of pollutants and, hence, enhance the efficiency of wastewater treatment processes. Nowadays, more recalcitrant pollutants are identified in industrial wastewater, which cannot be treated by conventional bioremediation practices. Synthetically bioengineered microorganisms can solve this problem.

Moreover, the use of bioengineered microorganisms in different wastewater treatment systems, like activated sludge reactors, makes these systems highly efficient. By integrating synthetic biology techniques and these treatment systems, scientists can improve efficiency and save energy and cost. They can also design specific wastewater treatment

systems to meet the specific needs of different industries. Metabolic pathways for the degradation of target pollutants can be completely re-engineered. However, the task of optimization is difficult. Enzymatic properties can also be remodified. Synthetic biology-based biosensors are used to detect pollutant levels and also study microbial interactions with pollutants in a complex environment. Synthetic microbial consortia surpasses the limitations of the synthetic bacterium in the bioremediation of pollutants. However, many challenges limit the application of synthetic biology in the treatment of industrial wastewater pollutants. Modified microorganisms are still not able to effectively target some pollutants. We are still not able to fully comprehend the interactions between the pollutants and the microorganisms in the environment nor the interactions of the microorganisms with each other in the complex environment. It's taking time for the researchers to identify novel enzymes for bioremediation. We need to apply computational approaches to identify novel enzymes and also make them robust by necessary optimization. Furthermore, transferring synthetic microbes from the lab to the environment also leads to ethical issues. Synthetically designed microbes can disrupt the biosphere by gene transfer to other bacteria. In conclusion, many studies have shown the utility of synthetic biology in the bioremediation of pollutants but still, we need more research studies to address the challenges to harness the full potential of synthetic biology in the treatment of industrial wastewaters.

ACKNOWLEDGMENT

REFERENCES

Adetunji, C.O., Morumda, D., Dauda, W.P., Abraham, P., Glen, E., Abraham, M.P., Ifechukwude, C.N., Adetunji, J.B., Kanmodi, K.K. and Nnyanzi, L.A., 2023. *In silico Approaches to Macromolecular Chemistry*, Elsevier, pp.479–501.. https://doi.org/10.1016/B978-0-323-90995-2.00003-5.

Ahmad, A., Mustafa, G., Rana, A. and Zia, A.R., 2023. Improvements in bioremediation agents and their modified strains in mediating environmental pollution. *Current Microbiology*, 80(6), p.208. https://doi.org/10.1007/s00284-023-03316-x.

Aminian-Dehkordi, J., Rahimi, S., Golzar-Ahmadi, M., Singh, A., Lopez, J., Ledesma-Amaro, R. and Mijakovic, I., 2023. Synthetic biology tools for environmental protection. *Biotechnology Advances*, 68, p.108239. https://doi.org/10.1016/j.biotechadv.2023.108239.

Aukema, K.G., Escalante, D.E., Maltby, M.M., Bera, A.K., Aksan, A. and Wackett, L.P., 2017. Identification of bioremediation potential: carbamazepine and other recalcitrant personal care products. *Environmental Science & Technology*, 51(2), pp.880–888. https://doi.org/10.1021/acs.est.6b04345.

Barreiro, C. and García-Estrada, C., 2022. *New Frontiers and Applications of Synthetic Biology*. Elsevier, pp.45–65. https://doi.org/10.1016/B978-0-12-824469-2.00012-9.

Bhatt, P., Gangola, S., Bhandari, G., Zhang, W., Maithani, D., Mishra, S. and Chen, S., 2021. New insights into the degradation of synthetic pollutants in contaminated environments. *Chemosphere*, 268, p.128827. https://doi.org/10.1016/j.chemosphere.2020.128827.

Bradley, R.W., Buck, M. and Wang, B., 2016. Tools and principles for microbial gene circuit engineering. *Journal of Molecular Biology*, 428(5), pp.862–888. https://doi.org/10.1016/j.jmb.2015.10.004.

Cao, Z., Yan, W., Ding, M. and Yuan, Y., 2022. Construction of microbial consortia for microbial degradation of complex compounds. *Frontiers in Bioengineering and Biotechnology*, 10. https://doi.org/10.3389/fbioe.2022.1051233.

Chattopadhyay, I, J, R.B., Usman, T.M.M. and Varjani, S., 2022. Exploring the role of microbial biofilm for industrial effluents treatment. *Bioengineered*, 13(3), pp.6420–6440. https://doi.org/10.1080/21655979.2022.2044250.

Chen, W.C.W., Gaidukov, L., Lai, Y., Wu, M.-R., Cao, J., Gutbrod, M.J., Choi, G.C.G., Utomo, R.P., Chen, Y.-C., Wroblewska, L., Kellis, M., Zhang, L., Weiss, R. and Lu, T.K., 2022. A synthetic transcription platform for programmable gene expression in mammalian cells. *Nature Communications*, 13(1), p.6167. https://doi.org/10.1038/s41467-022-33287-9.

Chi, H., Wang, X., Shao, Y., Qin, Y., Deng, Z., Wang, L. and Chen, S., 2019. Engineering and modification of microbial chassis for systems and synthetic biology. *Synthetic and Systems Biotechnology*, 4(1), pp.25–33. https://doi.org/10.1016/j.synbio.2018.12.001.

Choi, K.R., Jang, W.D., Yang, D., Cho, J.S., Park, D. and Lee, S.Y., 2019. Systems metabolic engineering strategies: Integrating systems and synthetic biology with metabolic engineering. *Trends in Biotechnology*, 37(8), pp.817–837. https://doi.org/10.1016/j.tibtech.2019.01.003.

Dai, Z., Zhang, S., Yang, Q., Zhang, W., Qian, X., Dong, W., Jiang, M. and Xin, F., 2018. Genetic tool development and systemic regulation in biosynthetic technology. *Biotechnology for Biofuels*, 11(1), p.152. https://doi.org/10.1186/s13068-018-1153-5.

Del Valle, I., Fulk, E.M., Kalvapalle, P., Silberg, J.J., Masiello, C.A. and Stadler, L.B., 2021. Translating new synthetic biology advances for biosensing into the earth and environmental sciences. *Frontiers in Microbiology*, 11, p.373. https://doi.org/10.3389/fmicb.2020.618373.

Dutta, D., Arya, S. and Kumar, S., 2021. Industrial wastewater treatment: Current trends, bottlenecks, and best practices. *Chemosphere*, 285, p.131245. https://doi.org/10.1016/j.chemosphere.2021.131245.

Dvořák, P., Nikel, P.I., Damborský, J. and de Lorenzo, V., 2017. Bioremediation 3.0: Engineering pollutant-removing bacteria in the times of systemic biology. *Biotechnology Advances*, 35(7), pp.845–866. https://doi.org/10.1016/j.biotechadv.2017.08.001.

Eisenhut, P., Marx, N., Borsi, G., Papež, M., Ruggeri, C., Baumann, M. and Borth, N., 2024. Manipulating gene expression levels in mammalian cell factories: An outline of synthetic molecular toolboxes to achieve multiplexed control. *New Biotechnology*, 79, pp.1–19. https://doi.org/10.1016/j.nbt.2023.11.003.

Engstrom, M.D. and Pfleger, B.F., 2017. Transcription control engineering and applications in synthetic biology. *Synthetic and Systems Biotechnology*, 2(3), pp.176–191. https://doi.org/10.1016/j.synbio.2017.09.003.

Gao, B., Sabnis, R., Costantini, T., Jinkerson, R. and Sun, Q., 2020. A peek in the micro-sized world: A review of design principles, engineering tools, and applications of the engineered microbial community. *Biochemical Society Transactions*, 48(2), pp.399–409. https://doi.org/10.1042/BST20190172.

Garg, E., Varma, A. and Smitha, M.S., 2023. *Modern Approaches in Waste Bioremediation*. Springer International Publishing, pp.365–375. https://doi.org/10.1007/978-3-031-24086-7_17.

Garner, K.L., 2021. Principles of synthetic biology. *Essays in Biochemistry*, 65(5), pp.791–811. https://doi.org/10.1042/EBC20200059.

Hara, T., Takatsuka, Y., Nakata, E. and Morii, T., 2021. Augmentation of an engineered bacterial strain potentially improves the cleanup of PCB water pollution. *Microbiology Spectrum*, 9(3). https://doi.org/10.1128/spectrum.01926-21

Haripriyan, U., Gopinath, K.P., Arun, J. and Govarthanan, M., 2022. Bioremediation of organic pollutants: A mini-review on current and critical strategies for wastewater treatment. *Archives of Microbiology*, 204(5), p.286. https://doi.org/10.1007/s00203-022-02907-9

Hassan, S. and Ganai, B.A., 2023. Deciphering the recent trends in pesticide bioremediation using genome editing and multi-omics approaches: A review. *World Journal of Microbiology and Biotechnology*, 39(6), p.151. https://doi.org/10.1007/s11274-023-03603-6

Jabbar, N.M., Alardhi, S.M., Mohammed, A.K., Salih, I.K. and Albayati, T.M., 2022. Challenges in the implementation of bioremediation processes in petroleum-contaminated soils: A review. *Environmental Nanotechnology, Monitoring and Management*, 18, p.694. https://doi.org/10.1016/j.enmm.2022.100694

Jaiswal, S., Singh, D.K. and Shukla, P., 2019. Gene editing and systems biology tools for pesticide bioremediation: A review. *Frontiers in Microbiology*, 10, p.87. https://doi.org/10.3389/fmicb.2019.00087

Jawed, K., Yazdani, S.S. and Koffas, M.A.G., 2019. Advances in the development and application of microbial consortia for metabolic engineering. *Metabolic Engineering Communications*, 9, e00095. https://doi.org/10.1016/j.mec.2019.e00095

Jia, X., Liu, C., Song, H., Ding, M., Du, J., Ma, Q. and Yuan, Y., 2016. Design, analysis, and application of synthetic microbial consortia. *Synthetic and Systems Biotechnology*, 1(2), pp.109–117. https://doi.org/10.1016/j.synbio.2016.02.001

Jiang, S., Tang, J., Rahimi, S., Mijakovic, I. and Wei, Y., 2022. Editorial: Efficient treatment of industrial wastewater with microbiome and synthetic biology. *Frontiers in Environmental Science*, 10, p.292. https://doi.org/10.3389/fenvs.2022.902926

Jiménez-Díaz, V., Pedroza-Rodríguez, A.M., Ramos-Monroy, O. and Castillo-Carvajal, L.C., 2022. Synthetic biology: A new era in hydrocarbon bioremediation. *Processes*, 10(4), p.471. https://doi.org/10.3390/pr10040712

Jones, E.R., van Vliet, M.T.H., Qadir, M. and Bierkens, M.F.P., 2021. Country-level and gridded estimates of wastewater production, collection, treatment, and reuse. *Earth System Science Data*, 13(2), pp.237–254. https://doi.org/10.5194/essd-13-237-2021

Kent, R. and Dixon, N., 2020. Contemporary tools for regulating gene expression in bacteria. *Trends in Biotechnology*, 38(3), pp.316–333. https://doi.org/10.1016/j.tibtech.2019.09.007

Kesari, K.K., Soni, R., Jamal, Q.M.S., Tripathi, P., Lal, J.A., Jha, N.K., Siddiqui, M.H., Kumar, P., Tripathi, V. and Ruokolainen, J., 2021. Wastewater treatment and reuse: A review of its applications and health implications. *Water, Air, and Soil Pollution*, 232(5). https://doi.org/10.1007/s11270-021-05154-8

Kim, J., Salvador, M., Saunders, E., González, J., Avignone-Rossa, C. and Jiménez, J.I., 2016a. Properties of alternative microbial hosts used in synthetic biology: Towards the design of a modular chassis. *Essays in Biochemistry*, 60(4), pp.303–313. https://doi.org/10.1042/EBC20160015

Kim, J., Salvador, M., Saunders, E., González, J., Avignone-Rossa, C. and Jiménez, J.I., 2016b. Properties of alternative microbial hosts used in synthetic biology: Towards the design of a modular chassis. *Essays in Biochemistry*, 60(4), pp.303–313. https://doi.org/10.1042/EBC20160015

Kitano, S., Lin, C., Foo, J.L. and Chang, M.W., 2023. Synthetic biology: Learning the way toward high-precision biological design. *PLOS Biology*, 21(4), e3002116. https://doi.org/10.1371/journal.pbio.3002116

Lv, X., Hueso-Gil, A., Bi, X., Wu, Y., Liu, Y., Liu, L. and Ledesma-Amaro, R., 2022. New synthetic biology tools for metabolic control. *Current Opinion in Biotechnology*, 76, p.102724. https://doi.org/10.1016/j.copbio.2022.102724

MacDonald, I.C. and Deans, T.L., 2016. Tools and applications in synthetic biology. *Advanced Drug Delivery Reviews*, 105, pp.20–34. https://doi.org/10.1016/j.addr.2016.08.008

McCarty, N.S. and Ledesma-Amaro, R., 2019. Synthetic biology tools to engineer microbial communities for biotechnology. *Trends in Biotechnology*, 37(2), pp.181–197. https://doi.org/10.1016/j.tibtech.2018.11.002

Muhammad, M.H., Idris, A.L., Fan, X., Guo, Y., Yu, Y., Jin, X., Qiu, J., Guan, X. and Huang, T., 2020. Beyond risk: Bacterial biofilms and their regulating approaches. *Frontiers in Microbiology*, 11. https://doi.org/10.3389/fmicb.2020.00928

Nasr, M., 2022. Aquatic pollution and wastewater treatment system. In *Algae and Aquatic Macrophytes in Cities: Bioremediation, Biomass, Biofuels, and Bioproducts*, pp.23–37. Elsevier. https://doi.org/10.1016/B978-0-12-824270-4.00006-7

Rafeeq, H., Afsheen, N., Rafique, S., Arshad, A., Intisar, M., Hussain, A., Bilal, M. and Iqbal, H.M.N., 2023. Genetically engineered microorganisms for environmental remediation. *Chemosphere*, 310. https://doi.org/10.1016/j.chemosphere.2022.136751

Ranjbar, S. and Malcata, F.X., 2022. Is genetic engineering a route to enhance microalgae-mediated bioremediation of heavy metal-containing effluents? *Molecules*, 27(5), p.1473. https://doi.org/10.3390/molecules27051473

Razzak, S.A., Faruque, M.O., Alsheikh, Z., Alsheikhmohamad, L., Alkuroud, D., Alfayez, A., Hossain, S.M.Z. and Hossain, M.M., 2022. A comprehensive review on conventional and biological-driven heavy metals removal from industrial wastewater. *Environmental Advances*, 7, p.100168. https://doi.org/10.1016/j.envadv.2022.100168

Rylott, E.L. and Bruce, N.C., 2020. How synthetic biology can help bioremediation. *Current Opinion in Chemical Biology*, 58, pp.86–95. https://doi.org/10.1016/j.cbpa.2020.07.004

Saddique, Z., Imran, M., Javaid, A., Latif, S., Kim, T.H., Janczarek, M., Bilal, M. and Jesionowski, T., 2023. Bio-fabricated bismuth-based materials for removal of emerging environmental contaminants from wastewater. *Environmental Research*, 229, p.115. https://doi.org/10.1016/j.envres.2023.115861

Saravanan, A., Kumar, P.S., Duc, P.A. and Rangasamy, G., 2023. Strategies for microbial bioremediation of environmental pollutants from industrial wastewater: A sustainable approach. *Chemosphere*, 313, p.7323. https://doi.org/10.1016/j.chemosphere.2022.137323

Saravanan, A., Senthil Kumar, P., Jeevanantham, S., Karishma, S., Tajsabreen, B., Yaashikaa, P.R. and Reshma, B., 2021. Effective water/wastewater treatment methodologies for toxic pollutants removal: Processes and applications towards sustainable development. *Chemosphere*, 280, p.595. https://doi.org/10.1016/j.chemosphere.2021.130595

Saxena, G., 2020. *Bioremediation of Industrial Waste for Environmental Safety*. Springer. https://doi.org/10.1007/978-981-13-1891-7

Sharma, B. and Shukla, P., 2020. Designing synthetic microbial communities for effectual bioremediation: A review. *Biocatalysis and Biotransformation*, 38(6), pp.405–414. https://doi.org/10.1080/10242422.2020.1813727

Sharma, M., Agarwal, S., Agarwal Malik, R., Kumar, G., Pal, D.B., Mandal, M., Sarkar, A., Bantun, F., Haque, S., Singh, P., Srivastava, N. and Gupta, V.K., 2023. Recent advances in microbial engineering approaches for wastewater treatment: A review. *Bioengineered*, 14(1), p.2184518. https://doi.org/10.1080/21655979.2023.2184518

Sharma, P., Pandey, A.K., Udayan, A. and Kumar, S., 2021. Role of microbial community and metal-binding proteins in phytoremediation of heavy metals from industrial wastewater. *Bioresource Technology*, 326, p.124750. https://doi.org/10.1016/j.biortech.2021.124750

Singh, A.K., Bilal, M., Iqbal, H.M.N. and Raj, A., 2021. Trends in predictive biodegradation for sustainable mitigation of environmental pollutants: Recent progress and future outlook. *Science of the Total Environment*, 770, p.561. https://doi.org/10.1016/j.scitotenv.2020.144561

Singh, A.K., Chowdhary, P. and Raj, A., 2020. *Microorganisms for Sustainable Environment and Health*. Elsevier, pp. 249–285. https://doi.org/10.1016/B978-0-12-819001-2.00013-9

Singh, B.J., Chakraborty, A. and Sehgal, R., 2023. A systematic review of industrial wastewater management: Evaluating challenges and enablers. *Journal of Environmental Management*, 348, p.119230. https://doi.org/10.1016/j.jenvman.2023.119230

Tang, T.-C., An, B., Huang, Y., Vasikaran, S., Wang, Y., Jiang, X., Lu, T.K. and Zhong, C., 2020. Materials designed by synthetic biology. *Nature Reviews Materials*, 6(4), pp.332–350. https://doi.org/10.1038/s41578-020-00265-w

Thai, T.D., Lim, W. and Na, D., 2023. Synthetic bacteria for the detection and bioremediation of heavy metals. *Frontiers in Bioengineering and Biotechnology*, 11, p. 868. https://doi.org/10.3389/fbioe.2023.1178680

Tietze, L. and Lale, R., 2021. Importance of the 5ʹ regulatory region to bacterial synthetic biology applications. *Microbial Biotechnology*, 14(6), pp.2291–2315. https://doi.org/10.1111/1751-7915.13868

Tran, K.M., Lee, H.M., Thai, T.D., Shen, J., Eyun, S.-il and Na, D., 2021. Synthetically engineered microbial scavengers for enhanced bioremediation. *Journal of Hazardous Materials*, 419, p.6516. https://doi.org/10.1016/j.jhazmat.2021.126516

Xie, M. and Fussenegger, M., 2018. Designing cell function: assembly of synthetic gene circuits for cell biology applications. *Nature Reviews Molecular Cell Biology*, 19(8), pp.507–525. https://doi.org/10.1038/s41580-018-0024-z

Yaashikaa, P.R., Devi, M.K. and Kumar, P.S., 2022. Engineering microbes for enhancing the degradation of environmental pollutants: A detailed review on synthetic biology. *Environmental Research*, 214, p.86. https://doi.org/10.1016/j.envres.2022.113868

Yang, Y., Zhang, Z.-W., Liu, R.-X., Ju, H.-Y., Bian, X.-K., Zhang, W.-Z., Zhang, C.-B., Yang, T., Guo, B., Xiao, C.-L., Bai, H. and Lu, W.-Y., 2021. Research progress in bioremediation of petroleum pollution. *Environmental Science and Pollution Research*, 28(34), pp.46877–46893. https://doi.org/10.1007/s11356-021-15310-6

Yu, W., Xu, X., Jin, K., Liu, Y., Li, J., Du, G., Lv, X. and Liu, L., 2023. Genetically encoded biosensors for microbial synthetic biology: From conceptual frameworks to practical applications. *Biotechnology Advances*, 62, p.108077. https://doi.org/10.1016/j.biotechadv.2022.108077

Zhang, X.-E., Liu, C., Dai, J., Yuan, Y., Gao, C., Feng, Y., Wu, B., Wei, P., You, C., Wang, X. and Si, T., 2023. Enabling technology and core theory of synthetic biology. *Science China Life Sciences*, 66(8), pp.1742–1785. https://doi.org/10.1007/s11427-022-2214-2

Zhu, B., Chen, Y. and Wei, N., 2019. Engineering Biocatalytic and Biosorptive Materials for Environmental Applications. *Trends in Biotechnology*, 37(6), pp.661–676. https://doi.org/10.1016/j.tibtech.2018.11.005

Original Research Paper   https://doi.org/10.46488/NEPT.2025.v24i01.D1700   **Open Access Journal**

Optimizing Community Health Center Effluent Treatment with Moving Bed Biofilm Reactor Technology Combined with Activated Carbon and Chlorine

Budirman[1,2], Muhammad Farid Samawi[2,5†], Fahruddin[3], Paulina Taba[4], Mahatma Lanuru[5] and Agus Bintara Birawida[6]

[1]Department of Environmental Health, Health Polytechnic of the Ministry of Health, Makassar, Indonesia
[2]Environmental Management Study Program, Postgraduate School, Hasanuddin University, Makassar, Indonesia
[3]Department of Biology, Faculty of Mathematics and Natural Sciences, Hasanuddin University, Makassar, Indonesia
[4]Department of Chemistry, Faculty of Mathematics and Natural Sciences, Hasanuddin University, Makassar, Indonesia
[5]Department of Marine Science, Faculty of Marine Science and Fisheries, Hasanuddin University, Makassar, Indonesia
[6]Department of Environmental Health, Faculty of Community Health, Hasanuddin University, Makassar, Indonesia
†Corresponding author: Muhammad Farid Samawi; faridsamawi@unhas.ac.id

ABSTRACT

Community Health Centers are small-scale hospitals that serve community medicine in Indonesia. These activities generate wastewater containing various contaminants, such as pathogens, chemicals, and nutrients, which can pollute the environment and endanger human health. So, efforts are needed to reduce their impact through wastewater treatment. This research applies an anaerobic-aerobic biofilter system with Moving Bed Biofilm Reactor (MBBR) technology combined with activated carbon and chlorine in treating wastewater. The treatments in the study were different service capacities and wastewater treatment, with three replicates in each treatment. The residence time of wastewater in the system is 4 h. The results showed that combining MBBR technology, activated carbon, and chlorine could reduce temperature, TSS, pH, BOD_5, COD, NH_3, and Coliform values in wastewater in three Community Health Center services. Thus, it can be concluded that the different services and wastewater treatment efforts, combined with MBBR, activated charcoal, and chlorine, have been proven to affect and improve the quality of wastewater from the Community Health Center to meet the effluent quality standards.

INTRODUCTION

Community health centers, as part of health facilities in Indonesia, play an important role in public health but also generate a lot of wastewater containing various contaminants such as pathogens, chemicals, and nutrients. Improper management of this wastewater can cause severe environmental pollution and pose a great risk to the surrounding community (López-Ramírez et al. 2024, Rahmi et al. 2024). These residues can affect soil microorganisms, disrupt ecological processes, and possibly contaminate crops in agriculture (Patel et al. 2019). Therefore, wastewater treatment is crucial in maintaining both environmental and public health, especially with limited resources and infrastructure (Capps 2019, Santos et al. 2020). Biological treatment of liquid waste using an aerobic, anaerobic biofilter system is being developed. One of the environmentally friendly wastewater treatment is by using bacteria that can be decomposers in the biodegradation process (Madan et al. 2022, Waqas et al. 2023)

Environmental considerations also underlie the development of biological wastewater treatment where the environmental impact is smaller than chemical treatment (Dutta & Bhattacharjee 2021, Liu et al. 2021). Many systems have been used for secondary wastewater effluent treatment, such as activated sludge systems,

trickling filters, Biodisc or Rotating Biological Contactors (RBC), oxidation ponds, and constructed wetlands. However, compliance with regulatory standards for effluent management often requires big costs and sophisticated technology. Therefore, there is an urgent need for practical and cost-effective wastewater treatment methods (Capps 2019, Saraswati et al. 2021, Waqas et al. 2023). We need effective and efficient wastewater treatment technology to overcome this problem (López-Ramírez et al. 2024, Yuan et al. 2019).

In sometimes cases, biological treatment is also unable to effectively treat wastewater due to the hazardous and biologically resistant components contained in the wastewater. Therefore, physicochemical processes can be one of the appropriate solutions to be combined (Valand et al. 2019, Zhang et al. 2024). Moving Bed Biofilm Reactor (MBBR) technology has been recognized as effective in treating wastewater with high organic matter content (di Biase et al. 2019, Santos et al. 2020). Moving Bed Biofilm Reactor (MBBR) utilizes moving media in the reactor to facilitate the growth of biofilms that play an important role in degrading organic matter present in wastewater. In addition, this technology also has advantages in terms of operational flexibility and ease of maintenance compared to conventional wastewater treatment systems (Eid et al. 2024, Ongena et al. 2023).

However, relying solely on the MBBR is insufficient to remove all contaminants in wastewater. Therefore, it is necessary to integrate additional technologies, such as activated carbon and chlorination, to improve treated water quality. Activated carbon can be an adsorbent (Sultana et al. 2022, Valand et al. 2019). Activated carbon is one of the materials with essential properties, namely adsorption (Chen et al. 2021). On the other hand, chlorine is necessary for disinfection, killing pathogens and microorganisms that may still be present after the primary treatment (He et al. 2022, Mulyati et al. 2022). In addition, combining chlorine pre-treatment with other methods, such as microalgae-based systems, has improved overall treatment efficiency by reducing pollutants such as detergents and phenols in wastewater (Hu et al. 2020).

Integrating an MBBR with activated carbon can significantly reduce high contaminant levels in wastewater treatment, especially in decentralized systems (Al Hosani et al. 2022). It shows the practical potential of implementing this technology in community health centers. MBBR systems have even been successfully used in various industries, including municipalities, paper mills, pharmaceuticals, and fish farms, demonstrating their versatility and effectiveness in treating different types of wastewater (Alizadeh et al.

2019). In addition, MBBR applications offer operational advantages by producing less sludge than traditional activated sludge processes, contributing to cost savings and operational efficiency (Suryawan et al. 2021).

Integration of MBBR with other treatment technologies, such as ozonation or membrane filtration, was also shown to improve overall treatment efficiency and reduce the environmental footprint of the wastewater treatment process (Alharthi et al. 2022, Banti et al. 2023, Dai et al. 2023, Tang et al. 2020) In addition, incorporating granular activated carbon coated on a carrier surface inside an MBBR has been shown to significantly increase the removal of chemical oxygen demand and total suspended solids, underscoring the positive impact this combination has on pollutant removal efficiencies (Nur Dhamirah & Aida Isma 2019). In line with this, another study found that chlorine effectively reduced antibiotic-resistant genes in wastewater during disinfection (He et al. 2022) and prevented nosocomial infections in healthcare facilities (Duvernay et al. 2020). This paper informs efforts to reduce the impact of small-scale hospital wastewater on the environment through wastewater treatment using MBBR combined with activated charcoal and chlorine.

MATERIALS AND METHODS

The research is an experimental study of a wastewater treatment system combining Moving Bed Biofilm Reactor (MBBR) biofilter technology with activated carbon and chlorine. The parameters observed are physical parameters, including temperature and total suspension solid; chemical parameters, including pH, BOD_5, COD, and NH_3; and biological parameters, which are coliform. Effluent samples were collected from wastewater discharged by inpatient facilities at the Community Health Center. The treatments tested were service and effluent treatment with three replications of each observation at each location. The types of services were Service-1 community health centers serving an average of 84235 people/year, Service-2 community health centers serving an average of 122633 people/year, and Service-3 community health centers serving an average of 43934 people/year. Parameter measurements were taken before and after treatment and compared to the control without treatment. The residence time of wastewater in the system is four hours.

Samples taken at the specified service are analyzed at the environmental laboratory with proper handling following applicable standards. Then, the samples are tested using the test methods and standards shown in Table 1.

The materials used were the Kaldness model K1 Plus, activated carbon, and 90% chlorine solution. The activated

Table 1: Sample Analysis Method.

No.	Parameters	Source	Methods
1	NH_3	mg.L^{-1}	Spectrophotometer
2	TSS (Total Suspended Solids)	mg.L^{-1}	Gravimetry
3	Temperature	°C	Thermometer
4	pH (Degree of Acidity)	-	Potentiometry
5	Total Coliform	/100mL	MPN
6	BOD (Biological Oxygen Demand)	mg.L^{-1}	Titrimetric/ Potentiometry
7	COD (Chemical Oxygen Demand)	mg.L^{-1}	Spectrophotometer UV-VIS

carbon used in this study was characterized by a scanning electron microscope (SEM) to observe its surface morphology. SEM testing was carried out with a magnification of 5000x and 10000x to get a detailed picture of activated carbon's pore structure, which can be seen in Fig. 1.

Natural bacterial growth was carried out in the MBBR biofilter reactor containing Kaldness K1 Plus with the amount of media as much as 40% of the reactor volume (24 L of a total of 60 L reactor) (Fig. 2). After 21 days, a biofilm layer was formed on the MBBR media that supported the biodegradation process.

The wastewater treatment system uses four cylindrical plastic containers with a capacity of 60 L. The first container is used for settling wastewater, and the second container is an aerobic reactor processing container that uses MBBR technology. The third container contains activated carbon, which functions as an adsorbent media, and the third container is then connected to a chlorinator for disinfection. A picture of the applied wastewater treatment system is illustrated in Fig. 3.

The wastewater in this experiment came from three community health center services, which amounted to 35m^3. day^{-1}. The residence time used for wastewater treatment was calculated as follows (Cruz-Salomón et al. 2017).

Fig. 1: Surface morphology of (a) 5000x magnification activated carbon and (b) 10000x magnification activated carbon.

Fig. 2: Kaldnes Type K1 Plus.

Fig. 3: Model of wastewater treatment system.

$$\tau = \frac{Vreaktor\ P3}{Q} \qquad \ldots(1)$$

Description:

τ = Residence time

Vreactor = Reactor volume (in liters)

Q = Effluent flow rate into the reactor (in liters per day)

The parameter removal efficiency was calculated using the following formula (Dolatabadi & Ahmadzadeh 2019):

$$\text{Efficiency} = \frac{\overline{X}_{Before\ treatment} - \overline{X}_{After\ Treatment}}{X\ Before\ treatment}\ 100\% \qquad \ldots(2)$$

The data obtained were analyzed using tables and graphs, and the differences in service and processing treatments were tested with a two-way analysis of variance (Two-way ANOVA). Fig. 4 illustrates the abstract of this research.

RESULTS AND DISCUSSION

Wastewater Characteristics

The pre-treatment wastewater exhibited physical characteristics, including odor and a brownish turbid appearance. Laboratory analysis showed that temperature and pH values were within acceptable limits based on
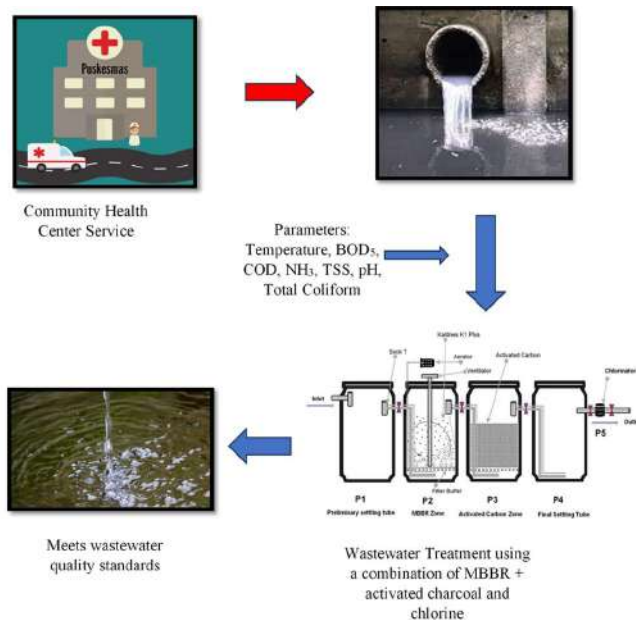
Fig. 4: Infographic abstract of the research.

Table 2: Characteristics of Community Health Center Wastewater in 2024.

No.	Parameters	Community Health Center			Unit	Maximum rate*
		Service 1	Service 2	Service 3		
1	Organic Material	211,72	432,92	195,92	mg.L^{-1}	
2	Temperature	28	29	29	^{o}C	<30
3	pH	7,64	7,45	7.63	-	6 - 9
4	BOD$_5$	112.1	224.1	249.6	mg.L^{-1}	30
5	COD	410	520	680	mg.L^{-1}	100
6	TSS	150	300	316	mg.L^{-1}	30
7	Ammonia	23,525	47,625	47.2	mg.L^{-1}	10
8	Total Coliform	24000	24000	24000	MPN.100mL^{-1}	3000

*Wastewater quality standard
Source: primary data

regulatory standards, while parameters such as BOD, ammonia, COD, and TSS exceeded quality standards. The initial characteristics of the wastewater effluent can be seen in Table 2.

Wastewater Parameters

Temperature: The results showed that the average temperature of untreated wastewater from Service-3 was 29°C, Service-2 was 29°C, and Service-3 was 28.7^{o}C. At the same time, the treated wastewater decreased to Service-1 of 28.6^{o}C, Service-2 of 28.3^{o}C, and Service-3 of 28.7^{o}C. The three wastewater sources have different temperature values and removal rates. The average temperature value of each treatment can be seen in Fig. 5.

Fig. 5 shows that the average wastewater temperature after treatment has decreased from 28.3-28.7°C. It shows that the wastewater treatment process causes a decrease in media temperature but not significantly. Temperature variations can impact microorganisms. Higher water temperatures can lead to decreased dissolved oxygen levels and increased oxygen consumption by microorganisms (Wang et al. 2023). These findings are consistent with the results reported by Lewar

et al. (2020), where the study showed that BOD and COD removal rates reached 83.96% and 84.02%, respectively, with the highest efficiency observed at 35°C (Lewar et al. 2020).

TSS (Total Suspended Solids): The suspended solids contained in the wastewater decreased with the treatment process. The average decrease in TSS content after treatment with MBBR biofilter technology is shown in Fig. 6.

Microorganisms are important in sewage treatment by utilizing organic pollutants as nutrients. They absorb dissolved organic pollutants through sorption, while organic particles adhere to their cell walls through adsorption. In addition, microorganisms produce enzymes that can break down these organic particles, facilitating the removal of dissolved and particulate organic pollutants from sewage (Snyder & Wyant 2013.). The results showed a significant reduction in the Total Suspended Solids (TSS) content in wastewater after treatment. For example, TSS levels in Service-1 wastewater decreased to an average of 8 mg.L^{-1}, marking a reduction of 142 mg.L^{-1}, with a combination of Moving Bed Biofilm Reactor (MBBR) and activated carbon biofilter technologies achieving 94% efficiency. Similar reductions also occurred in wastewater from Service-2 and
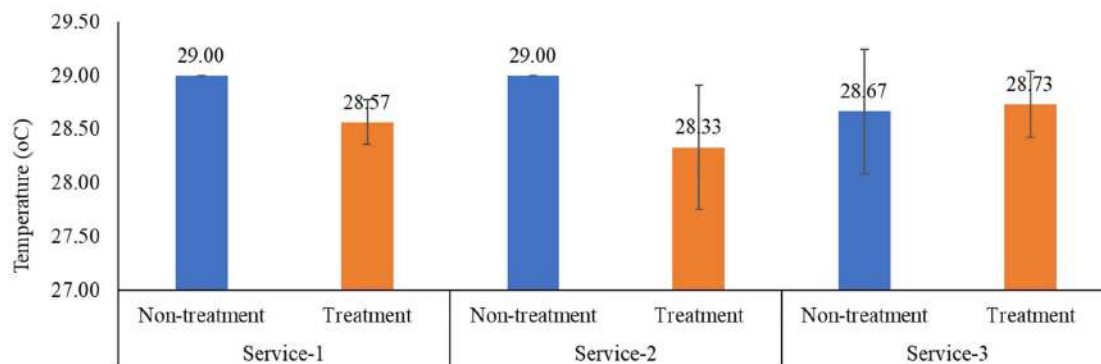
Fig. 5: Untreated and treated wastewater temperature values.
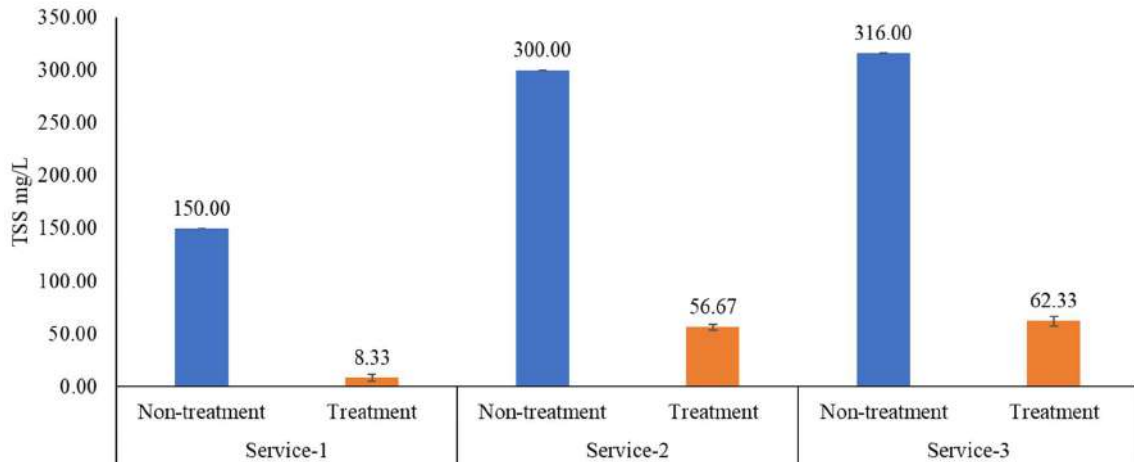
Fig. 6: TSS value of wastewater without and treatment process.

Service-3, where TSS levels decreased to 57 mg.L^{-1} and 62 mg.L^{-1}, with average reductions and efficiencies of 81% and 80% using MBBR combined with activated carbon and chlorine.

This finding aligns with research conducted by Nhut et al. (2019), who reported an SS removal efficiency of 91,8% in domestic wastewater using MBBR (Nhut et al. 2019). Integrating biofilters with activated carbon proved very important in reducing TSS levels in wastewater. The high surface area of activated carbon, facilitated by its porous structure, increases its adsorption capacity. These pores provide sufficient space for adsorbates to interact with activated carbon, thereby increasing the efficiency of the adsorption process. As a result, activated carbon integrated into MBBR biofilter technology effectively reduces the TSS content in the wastewater.

pH: The results showed that the pH value without wastewater treatment for Service-1 was 7.7, Service-2 was 7.5, and

Service-3 was 7.4. While the pH value after wastewater treatment decreased to Service-1 of 7.5, Service-2 of 7.3, and Service-3 of 6.9. The average pH value of each treatment can be seen in Fig. 7.

A decrease in pH can result from oxygen consumption during the decomposition of organic matter, leading to increased levels of CO_2, which in turn affects pH stability. In biological processes, pH plays a vital role in nitrification. The optimal pH conditions for nitrosomonas and nitrobacter bacteria range from 7.5 to 8.5 (Faust et al. 2024, Park et al. 2022). This is consistent with the statement that the ideal acidity (pH) for the growth of autotrophic ammonia-oxidizing bacteria is in the range of 7.5 to 8.5 (Albina et al. 2019).

BOD_5 (Biochemical Oxygen Demand): The BOD_5 content of the wastewater after treatment decreased significantly. Fig. 8 shows the average BOD_5 content in all treatments.

Fig. 8 shows that the average BOD_5 decreased significantly after treatment. The BOD_5 values of wastewater
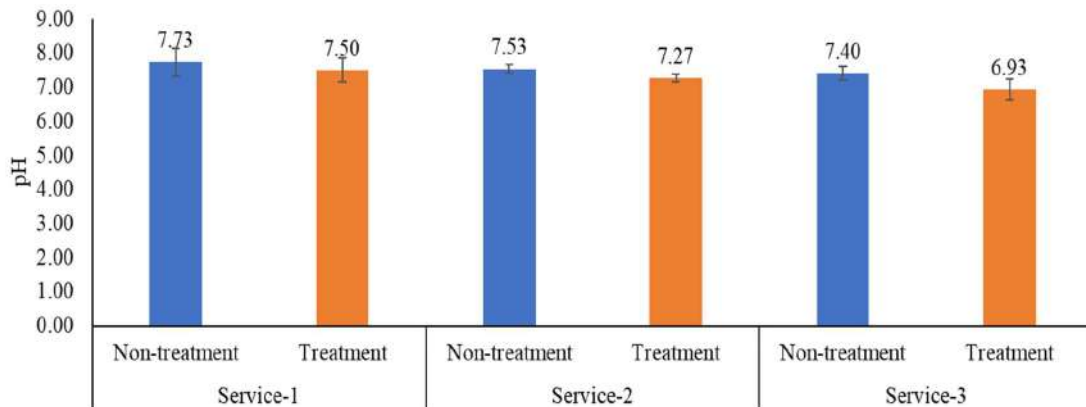
Fig. 7: Wastewater pH value without and treatment process.
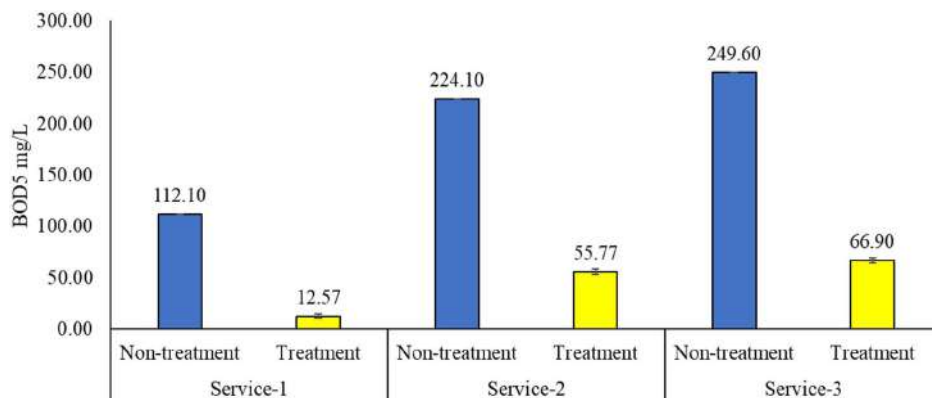
Fig. 8: BOD_5 values of wastewater without and treatment process.

from Service-1 decreased to 13 mg.L^{-1} on average, marking a reduction of 100 mg.L^{-1}, with the MBBR biofilter technology combined with activated carbon, achieving 89% efficiency. Similarly, wastewater from Service-2 decreased to an average of 56 mg.L^{-1}, with a reduction of 168 mg.L^{-1} and 75% efficiency using MBBR combined with activated carbon. The BOD value$_5$ from Service-3 showed an average decrease of 67 mg.L^{-1}, with a reduction of 183 mg.L^{-1}, and an efficiency of 73% using MBBR combined with activated carbon.

In comparison, research by Aniriani et al. (2022) on wastewater treatment in the Pondok Pesantren Mahasiswa IPAL of Lamongan Islamic University showed a reduction in BOD by 61.75%. (Aniriani et al. 2022). Another study by Osmani et al. (2021) reported a decrease in BOD of 91% (Osmani et al. 2021), and certainly, this study shows the level of BOD removal from health center wastewater using the MBBR method with Kaldness Media (K1 Plus) combined with activated carbon, can be said to be effective because it achieves optimal removal rates ranging from 73% to 89%.

COD: The results of measuring the COD content of wastewater in various treatments can be seen in Fig. 9.

Based on Fig. 9, it can be seen that the average COD content has decreased after treatment. Wastewater from Service-1 dropped to an average of 55 mg.L^{-1}, with a reduction of 355 mg.L^{-1}, achieving 87% efficiency using MBBR biofilter technology combined with activated carbon. Similarly, wastewater from Service-2 dropped to an average of 127 mg.L^{-1}, with a reduction of 393 mg.L^{-1} and 76% efficiency using MBBR combined with activated carbon. Service-3 showed a decrease to 188 mg.L^{-1} on average, with 492 mg.L^{-1} reduction and 72% efficiency using MBBR combined with activated carbon.

The results of Faggiano et al. (2023) showed that the chemical oxygen demand (COD) reached a maximum removal of 98.5% high removal efficiency. This study successfully reduced organic matter and nutrients from landfill leachate using an anaerobic-aerobic MBBR mobile media biofilm reactor and activated carbon adsorption integration (Faggiano et al. 2023). In a different study, the MBBR-MBR hybrid system developed by Yang and López-Grimau (2021) showed a COD removal efficiency of up to 93% when applied to wastewater from the textile sector in Spain, indicating the system's treatment is quite effective for industrial wastewater containing organic contaminants
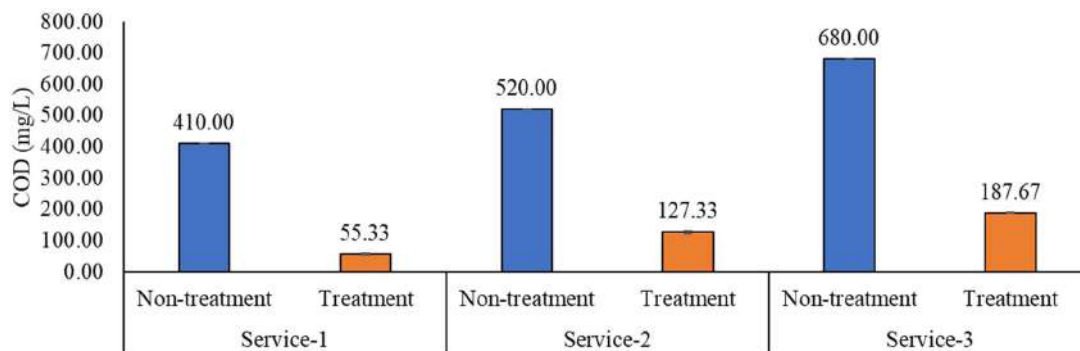
Fig. 9: COD values of wastewater without and treatment process.

(Yang & López-Grimau 2021). Nguyen Chuyen Thuan et al. (2024) found that granular activated carbon at a concentration of 20 g.L^{-1} for 60 minutes can achieve a COD removal effectiveness of 56.8% (Thuan et al. 2024). These results indicate that GAC is efficient in COD removal and has great potential for wastewater treatment that requires the management of complex organic contaminants. These results confirm the effective use of activated carbon as an additional treatment in wastewater treatment systems.

Kaldness medium (K1) provides a large surface area (~500 m^2.m^{-3}) suitable for the attachment of aerobic bacteria (Banti et al. 2023). The smaller media volume compared to the reactor water volume encourages random movement and turbulence among the media under aeration, enhancing their rotation and movement effectiveness and thereby improving treatment efficiency (Ramadina 2023).

NH$_3$: The measurement results of Free Ammonia levels in wastewater in various treatments can be seen in Fig. 10.

Based on the test results, the average NH$_3$ content decreased significantly to 0 mg/L in all wastewater source treatments. NH$_3$ levels after treatment reached 100% efficiency with MBBR biofilter technology combined with activated carbon. These results are consistent with research conducted by Said et al. (2018), who reported ammonia removal efficiencies of 94.05%, 93.42%, 89%, and 79.6% at various contact times (12 h, 8 h, 6 h, and 4 h) in an aeration tank with a sludge circulation ratio of 1.0 Q = 0 R. At ammonia loading of 0.106 to 0.302 kg.m^3.day^{-1}, ammonia removal efficiencies ranged from 95.54% to 83.01% (Said & Syabani 2018). This condition is due to the availability of sufficient oxygen in the aerobic reactor, facilitating proper degradation by Nitrosomonas and Nitrobacter bacteria. Ammonium converted into nitrate-nitrogen is further converted into N$_2$ gas, which is released into the atmosphere through denitrification. In comparison, research by Dewi

et al. (2019) using activated sludge achieved 94.70% effectiveness in reducing ammonia levels but required five days of treatment time (Dewi et al. 2019). Another study by Chávez et al. (2019) showed that activated carbon from coffee grounds is effective in absorbing ammonia liquid waste (Chávez et al. 2019). These findings underscore the effectiveness of MBBR biofilters combined with activated carbon in reducing ammonia content in the wastewater. Nonetheless, additional treatments such as activated carbon adsorption and ultraviolet light photolysis are still needed to optimize the treatment process of healthcare facility wastewater.

Total Coliforms: Fig. 11 shows the average total coliform content in wastewater at three service and treatment marks and processes. The untreated wastewater was 24,000/100 mL. The average Total Coliform content has decreased, i.e., wastewater from Service-1 decreased to 573/100 mL, marking a decrease of 23,427/100 mL with efficiency reaching 98%. Similarly, wastewater from Service-2 decreased to 610/100 mL on average, a reduction of 23,390/100 mL, with an efficiency of 97%, while Service-3 showed a decrease to 497/100 mL on average, a reduction of 23,503/100 mL, with an efficiency of 98%.

The results in Fig. 11 show that the effluent treatment effectively reduced coliform bacteria. Activated carbon has demonstrated its efficacy as an adsorbent for removing various contaminants from water, including harmful pathogens (Couso-Pérez et al. 2023). Activated carbon is known for its ability to adsorb organic substances, odor, taste, and other pollutants in water, thus improving water quality by reducing potentially harmful contaminants (Wysowska et al. 2021). The significant reduction of coliform bacteria in treated wastewater can also be attributed to chlorine's application in the reactor's final stage (Mulyati et al. 2022, Valentukeviciene et al. 2024)
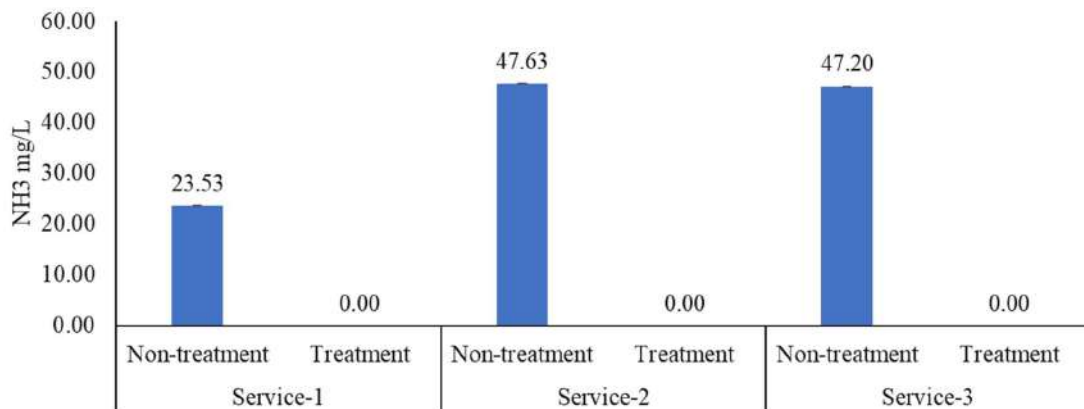
Fig. 10: Decrease in NH$_3$ wastewater without and treatment process.
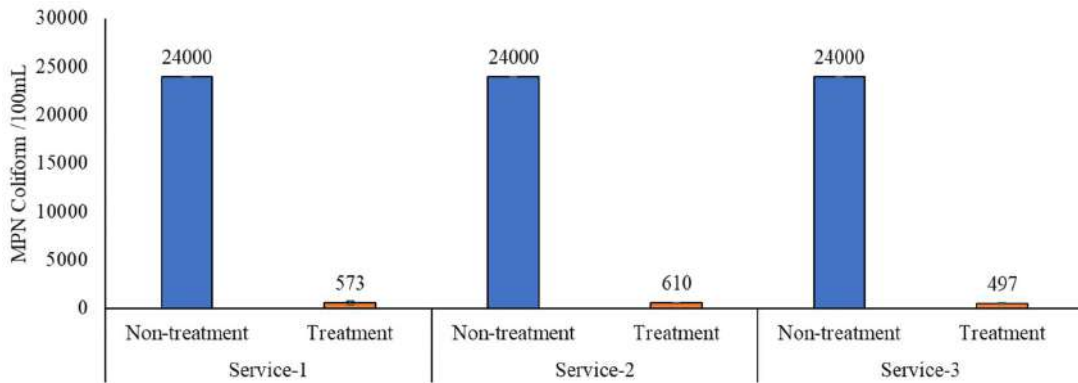
Fig. 11: Values of total coliform in wastewater without and with the treatment process.

Based on the ANOVA test results in Table 3, it can be explained that there are significant differences in several parameters between services and processing. The parameters tested include COD, BOD, TSS, Ammonia, Total Coliforms, pH, and temperature.

There is a significant effect between services on COD, BOD, NH_3, TSS, and pH concentrations, with a P-value <0.05. It indicates that the effluent conditions in each service are different and affect the treatment results. Various services may have variations in effluent composition, contaminant types, and other operational conditions that affect treatment effectiveness. However, there was no significant effect between services with temperature and total coliform, with p values > 0.05. It shows that the Service variation does not

Table 3: Two-way ANOVA test results between treatments.

Treatment	Dependent Variable	Type III Sum of Squares	df	Mean Square	F	Sig.
Services	COD	121771.444	2	60885.722	11070.131	0.000'
	BOD5	31114.534	2	15557.267	4663.294	0.000'
	NH_3	570.632	2	285.316	1.30563E+31	0.000'
	Coliform	10033.333	2	5016.667	0.568	0.581
	TSS	44102.778	2	22051.389	3227.033	0.000'
	pH	0.608	2	0.304	4.022	0.046
	Temperature	0.043	2	0.022	0.162	0.852
Processing	COD	768386.722	1	768386.722	139706.677	0.000'
	BOD5	101505.161	1	101505.161	30426.193	0.000'
	NH_3	7004.545	1	7004.545	3.20533E+32	0.000'
	Coliform	2472451200	1	2472451200	280076.284	0.000'
	TSS	203947.556	1	203947.556	29845.984	0.000'
	pH	0.467	1	0.467	6.184	0.029
	Temperature	0.534	1	0.534	3.988	0.069
Service * Processing	COD	15164.778	2	7582.389	1378.616	0
	BOD5	5928.268	2	2964.134	888.5	0
	NH_3	570.632	2	285.316	1.30563E+31	0
	Coliform	10033.333	2	5016.667	0.568	0.581
	TSS	11493.444	2	5746.722	840.984	0
	pH	0.048	2	0.024	0.316	0.735
	Temperature	0.421	2	0.211	1.573	0.247

Source: primary data

significantly affect these two parameters. Treatment using an MBBR biofilter combination of activated carbon and chlorine significantly affected all parameters except temperature, with a p-value < 0.05. It means that this treatment is effective in reducing the concentration of BOD, COD, NH_3, TSS, pH, and Total coliforms in wastewater. For temperature, there was no significant difference after treatment (P > 0.05), indicating that this treatment did not significantly affect the wastewater temperature. The MBBR process and using activated carbon and chlorine did not appear to result in significant temperature changes.

There was a significant interaction between service and treatment on COD, BOD, NH_3, and TSS concentrations with p values <0.05. It is shown that the treatment effect varies by service. There was no significant interaction between service and treatment on total coliform, pH, and temperature, with p values > 0.05. It means that the effect of the treatments on these parameters is not affected by the service. The decrease in coliform, pH, and temperature stability was more influenced by the treatment mechanism than service differences.

The purpose of the combination of activated carbon, chlorine, and Moving Bed Biofilm Reactor (MBBR) is to reduce TSS, NH_3, COD, and other wastewater quality indicators (Madan et al. 2022). This combination increases the overall treatment effectiveness and accelerates the decomposition of organic and chemical contaminants (Alharthi et al. 2022). MBBR has the advantage of biofilm formation, which is very important for the biodegradation of pollutants. In addition, activated carbon is a very effective adsorbent for removing organic chemicals that are difficult to degrade in biofilters (Chen et al. 2021). Chlorine is used as a disinfectant after treatment to reduce pathogenic bacteria as much as possible before the wastewater is released into the environment (He et al. 2022). Combining these three technologies will provide a more effective and efficient treatment solution by accelerating pollution degradation and guaranteeing that the produced wastewater meets higher quality standards faster (Ongena et al. 2023).

The research demonstrates that treating wastewater from community health clinics using MBBR, activated carbon, and chlorine is effective. Parameters of water quality, such as TSS, NH_3, COD, BOD, and coliforms, all improved significantly. The excellent removal efficiencies attained across various parameters show the system's capacity to efficiently manage a range of pollutants. However, customized techniques based on individual wastewater characteristics are necessary, as demonstrated by the interplay between various services and the treatment process. The system works well, but depending on the operating environment and the characteristics of the

service. Adjustments are thus necessary to achieve perfect performance.

It is essential to acknowledge that despite the study's noteworthy reduction in wastewater pollutant parameters, this research has several limitations. First off, the results of this research cannot be generalized to other healthcare facilities with distinct features since the study's parameters were restricted to three health centers with particular wastewater characteristics and service circumstances. The influence of external factors, such as unmeasured contaminants, was not fully considered, even though they may greatly impair system performance. Lastly, this research focused more on short-term outcomes than long-term effectiveness, which is crucial to guaranteeing the sustainable performance of this technology, given the potential for system degradation owing to biofilm accumulation or microbial resistance to chlorine.

CONCLUSIONS

The combination of Moving Bed Biofilm Reactor (MBBR) technology, activated carbon, and chlorine effectively improved wastewater quality from the community health center, such as TSS, pH, BOD5, COD, NH_3, and Coliforms. The significant reduction efficiency is 89% for BOD5, 87% for COD, 94% for TSS, 100% for NH_3, and 98% for MPN Coliform. This combined treatment system is effective for small-scale hospital effluents such as community health centers. It has excellent potential to be adapted in various other health facilities, especially in resource-constrained areas. To ensure more comprehensive and sustainable implementation, further research is needed to assess the stability and effectiveness of this technology under various operational conditions and address challenges such as potential system degradation and adjustment to variations in effluent characteristics. Therefore, this technology is highly prospective for widespread adoption in sustainable medical waste management.

ACKNOWLEDGEMENTS

REFERENCES

Al Hosani, N., Fathelrahman, E., Ahmed, H. and Rikab, E., 2022. Moving Bed Biofilm Reactor (MBBR) for decentralized grey water treatment: Technical, ecological and cost efficiency comparison for domestic applications. *Emirates Journal of Food and Agriculture*, 34(7), pp.1-12. https://doi.org/10.9755/ejfa.2022.v34.i7.2848.

Albina, P., Durban, N., Bertron, A., Albrecht, A., Robinet, J.-C. and Erable, B., 2019. Influence of hydrogen electron donor, alkaline pH, and high nitrate concentrations on microbial denitrification: A review. *International Journal of Molecular Sciences*, 20(51), pp.5163. https://doi.org/10.3390/ijms20205163.

Alharthi, M.S., Bamaga, O., Abulkhair, H., Organji, H., Shaiban, A., Macedonio, F., Criscuoli, A., Drioli, E., Wang, Z., Cui, Z., Jin, W. and Albeirutty, M., 2022. Evaluation of a hybrid moving bed biofilm membrane bioreactor and a direct contact membrane distillation system for purification of industrial wastewater. *Membranes*, 13(1), pp.16. https://doi.org/10.3390/membranes13010016.

Alizadeh, S., Abdul Rahim, A., Guo, B., Hawari, J., Ghoshal, S. and Comeau, Y., 2019. Impacts of the continuous inflow of low concentrations of silver nanoparticles on biological performance and microbial communities of aerobic heterotrophic wastewater biofilm. *Environmental Science & Technology*, 53(17), pp.9148–9159. https://doi.org/10.1021/acs.est.9b01214.

Aniriani, G.W., Putri, M.S.A. and Nengseh, T., 2022. Efektivitas penambahan moving bed biofilm reactor (MBBR) terhadap kualitas air limbah di instalasi pengolahan air limbah pondok pesantren mahasiswa Universitas Islam Lamongan. *Jurnal Ilmiah Sains*, 22(1), pp.67. https://doi.org/10.35799/jis.v22i1.35562.

Banti, D.C., Samaras, P., Kostopoulou, E., Tsioni, V. and Sfetsas, T., 2023. Improvement of MBBR-MBR performance by the addition of commercial and 3D-printed biocarriers. *Membranes*, 13(8), pp.690. https://doi.org/10.3390/membranes13080690.

Capps, K.A., 2019. Wastewater infrastructure and the ecology and management of freshwater systems. *Acta Limnologica Brasiliensia*, 31, pp.1-10. https://doi.org/10.1590/s2179-975x3719.

Chávez, R.P., Pizarro, E.C.C. and Galiano, Y.L., 2019. Landfill leachate treatment using activated carbon obtained from coffee waste. *Engenharia Sanitária e Ambiental*, 24(5), pp.833–842. https://doi.org/10.1590/s1413-41522019178655.

Chen, W., Luo, J., Du, X., Ding, L. and Zhang, W., 2021. Activated carbon-gravity driven biomimetic membrane (AC-GDBM) for organic micro-polluted water treatment. *Journal of Cleaner Production*, 317, pp.128224. https://doi.org/10.1016/j.jclepro.2021.128224.

Couso-Pérez, S., Abeledo-Lameiro, M.J., Vidal-Varela, A.I. and Gómez-Couso, H., 2023. Removal of the waterborne parasite *Cryptosporidium parvum* from drinking water using granular activated carbon. *Journal of Environmental Chemical Engineering*, 11, pp.111185. https://doi.org/10.1016/j.jece.2023.111185.

Cruz-Salomón, A., Ríos-Valdovinos, E., Pola-Albores, F., Lagunas-Rivera, S., Meza-Gordillo, R. and Ruíz-Valdiviezo, V., 2017. Evaluation of hydraulic retention time on treatment of coffee processing wastewater (CPWW) in EGSB bioreactor. *Sustainability*, 10(1), pp.83. https://doi.org/10.3390/su10010083.

Dai, W., Pang, J.-W., Ding, J., Wang, Y.Q., Zhang, L.Y., Ren, N.Q. and Yang, S.S., 2023. Study on the removal characteristics and degradation pathways of highly toxic and refractory organic pollutants in real pharmaceutical factory wastewater treated by a pilot-scale integrated process. *Frontiers in Microbiology*, 14, pp.1128233. https://doi.org/10.3389/fmicb.2023.1128233.

Dewi, W.T., Budiarsa Suyasa, I.W. and Rai, I.N., 2019. Pengaruh penambahan lumpur aktif pada biofilter anoksik-oksik dalam menurunkan kadar amonia air limbah rumah sakit. *ECOTROPHIC: Jurnal Ilmu Lingkungan (Journal of Environmental Science)*, 13(1), pp.49. https://doi.org/10.24843/EJES.2019.v13.i01.p06.

di Biase, A., Kowalski, M.S., Devlin, T.R. and Oleszkiewicz, J.A., 2019. Moving bed biofilm reactor technology in municipal wastewater treatment: A review. *Journal of Environmental Management*, 247, pp.849–866. https://doi.org/10.1016/j.jenvman.2019.06.053.

Dolatabadi, M. and Ahmadzadeh, S., 2019. A rapid and efficient removal approach for degradation of metformin in pharmaceutical wastewater using electro-Fenton process, optimization by response surface methodology. *Water Science and Technology*, 80, pp.685–694. https://doi.org/10.2166/wst.2019.312.

Dutta, S. and Bhattacharjee, J., 2021. A comparative study between physicochemical and biological methods for effective removal of a textile dye from wastewater. *Chemicals and Metals in Wastewater Treatment*, 1, pp.1–21. https://doi.org/10.1016/B978-0-323-85657-7.00003-1.

Duvernay, P.-G., de Laguiche, E., Campos Nogueira, R., Graz, B., Nana, L., Ouédraogo, W., Sauter, Y. and Sauvageat, E., 2020. Preventing nosocomial infections in resource-limited settings: An interventional approach in healthcare facilities in Burkina Faso. *Infection, Disease & Health*, 25, pp.186–193. https://doi.org/10.1016/j.idh.2020.04.003.

Eid, A., El-Sayed, A.-E., Ayoub, M. and El-Morsy, A., 2024. Optimizing the MBBR System and Integrating Nanoparticles to Improve Wastewater Treatment Efficiency. *Ecological Engineering & Environmental Technology*, 25, pp.218–229. https://doi.org/10.12912/27197050/176313.

Faggiano, A., Motta, O., Ricciardi, M., Cerrato, F., Garcia Junior, C.A., Fiorentino, A. and Proto, A., 2023. Integrated anaerobic-aerobic moving bed biofilm reactor and biochar adsorption for the efficient removal of organic matter and nutrients from Brazilian landfill leachate. *Sustainability*, 15, pp.13914. https://doi.org/10.3390/su151813914.

Faust, V., Vlaeminck, S.E., Ganigué, R. and Udert, K.M., 2024. Influence of pH on urine nitrification: Community shifts of ammonia-oxidizing bacteria and inhibition of nitrite-oxidizing bacteria. *ACS ES&T Engineering*, 4, pp.342–353. https://doi.org/10.1021/acsestengg.3c00320.

He, H., Choi, Y., Wu, S.J., Fang, X., Anderson, A.K., Liou, S.-Y., Roberts, M.C., Lee, Y. and Dodd, M.C., 2022. Application of nucleotide-based kinetic modeling approaches to predict antibiotic resistance gene degradation during UV- and chlorine-based wastewater disinfection processes: From bench- to full-scale. *Environmental Science & Technology*, 56, pp.15141–15155. https://doi.org/10.1021/acs.est.2c00567.

Hu, X., Meneses, Y.E. and Aly Hassan, A., 2020. Integration of sodium hypochlorite pretreatment with co-immobilized microalgae/bacteria treatment of meat processing wastewater. *Bioresource Technology*, 304, pp.122953. https://doi.org/10.1016/j.biortech.2020.122953.

Nur Dhamirah, S. J. and Aida Isma, M. I. 2019. The impact of granular activated carbon coated on the surface of Cosmo-ball in moving bed biofilm reactor. *Science Proceedings Series*, 1, pp.72–75. https://doi.org/10.31580/sps.v1i2.652.

Lewar, Y.S., Herawati, H. and Kahar, A., 2020. Pengaruh temperatur terhadap COD, BOD dan VFA pada pengolahan limbah cair pabrik kelapa sawit (LCPKS) dalam bioreaktor anaerobik. *Jurnal Chemurgy*, 4, pp.8. https://doi.org/10.30872/cmg.v4i2.4588.

Liu, W., Iordan, C.M., Cherubini, F., Hu, X. and Fu, D., 2021. Environmental impacts assessment of wastewater treatment and sludge disposal systems under two sewage discharge standards: A case study in Kunshan, China. *Journal of Cleaner Production*, 287, pp.125046. https://doi.org/10.1016/J.JCLEPRO.2020.125046.

López-Ramírez, M.A., Castellanos-Onorio, O.P., Lango-Reynoso, F., Castañeda-Chávez, M. del R., Montoya-Mendoza, J., Díaz-González, M. and Ortiz-Muñiz, B., 2024. Evaluation of an electrocoagulation process modified by Fenton reagent. *Nature Environment and Pollution Technology*, 23, pp.1007–1016. https://doi.org/10.46488/NEPT.2024.v23i02.034.

Madan, S., Madan, R. and Hussain, A., 2022. Advancement in biological wastewater treatment using hybrid moving bed biofilm reactor (MBBR): A review. *Applied Water Science*, 12, pp.141. https://doi.org/10.1007/s13201-022-01662-y.

Mulyati, S.A., Azizah, M., Srikandi, S., Maidaswar, M. and Atikah, N., 2022. The effectiveness of chlorine tablets in reducing coliform in

wastewater treatment plants. *Jurnal Sains Natural*, 12, pp.10. https://doi.org/10.31938/jsn.v12i1.340.

Nhut, H.T., Hung, N.T.Q., Sac, T.C., Bang, N.H.K., Quang Tri, T., Trung Hiep, N. and Minh Ky, N., 2019. Removal of nutrients and organic pollutants from domestic wastewater treatment by sponge-based moving bed biofilm reactor. *Environmental Engineering Research*, 25, pp.652–658. https://doi.org/10.4491/eer.2019.285.

Ongena, S., de Walle, A. Van, Mosquera-Romero, S., Driesen, N., Gutierrez, L. and Rabaey, K., 2023. Comparison of MBR and MBBR followed by UV or electrochemical disinfection for decentralized greywater treatment. *Water Research*, 235, pp.119818. https://doi.org/10.1016/j.watres.2023.119818.

Osmani, S.A., Rajpal, A. and Kazmi, A.A., 2021. Upgradation of conventional MBBR into aerobic/anoxic/aerobic configuration: A case study of carbon and nitrogen removal based sewage treatment plant. *Journal of Water Process Engineering*, 40, pp.101921. https://doi.org/10.1016/j.jwpe.2021.101921.

Park, S., Cho, K., Lee, T., Lee, E. and Bae, H., 2022. Improved insights into the adaptation and selection of Nitrosomonas spp. for partial nitritation under saline conditions based on specific oxygen uptake rates and next-generation sequencing. *Science of The Total Environment*, 822, pp.153644. https://doi.org/10.1016/j.scitotenv.2022.153644.

Patel, M., Kumar, R., Kishor, K., Mlsna, T., Pittman, C.U. and Mohan, D., 2019. Pharmaceuticals of emerging concern in aquatic systems: Chemistry, occurrence, effects, and removal methods. *Chemical Reviews*, 119, pp.3510–3673. https://doi.org/10.1021/acs.chemrev.8b00299.

Rahmi, R., Herniwanti, H. and Susanto, Y., 2024. The analysis of liquid medical waste management at the Bangkinang City Health Center. *Jurnal Kesehatan Tambusai*, 5, pp.615–626. https://doi.org/10.31004/jkt.v5i1.24648.

Ramadina, P.D.Z., 2023. Mengenal MBBR dengan aerasi nanobubble [WWW Document]. Available at: https://nanobubble.id/blog/mengenal-MBBR-dengan-teknologi-nanobubble.

Said, N.I. and Syabani, M.R., 2018. Penghilangan amoniak di dalam air limbah domestik dengan proses moving bed biofilm reactor (MBBR). *Jurnal Air Indonesia*, 7, p.239. https://doi.org/10.29122/jai.v7i1.2399.

Santos, A.D., Martins, R.C., Quinta-Ferreira, R.M. and Castro, L.M., 2020. Moving bed biofilm reactor (MBBR) for dairy wastewater treatment. *Energy Reports*, 6, pp.340–344. https://doi.org/10.1016/j.egyr.2020.11.158.

Saraswati, S.P., Diavid, G.H., Nisa, S.A., Amal, N. and Asriningtyas, V., 2021. Feasibility evaluation of wastewater treatment plant system: A case study of domestic wastewater system in Sleman Regency, Yogyakarta, Indonesia. *Journal of the Civil Engineering Forum,* 41, p.238.

Snyder, R. and Wyant, D., 2013. Activated sludge process control training manual for wastewater treatment plant operators. *Environments,* 15(2), pp.71-89

Sultana, M., Rownok, M.H., Sabrin, M., Rahaman, M.H. and Alam, S.M.N., 2022. A review on experimental chemically modified activated carbon to enhance dye and heavy metals adsorption. *Clean Engineering and Technology*, 6, pp.100382. https://doi.org/10.1016/j.clet.2021.100382.

Suryawan, I.W.K., Helmy, Q., Notodarmojo, S., Pratiwi, R. and Septiariva, I.Y., 2021. Textile dye Reactive Black 5 (RB5) bio-sorption with moving bed biofilm reactor and activated sludge. *Indonesian Journal of Environmental Management and Sustainability*, 5, p.71. https://doi.org/10.26554/ijems.2021.5.2.67-71.

Tang, K., Ooi, G., Spiliotopoulou, A., Kaarsholm, K., Sundmark, K., Florian, B., Kragelund, C., Bester, K. and Andersen, H., 2020. Removal of pharmaceuticals, toxicity, and natural fluorescence by ozonation in biologically pre-treated municipal wastewater, in comparison to subsequent polishing biofilm reactors. *Water (Basel)*, 12, pp.1059. https://doi.org/10.3390/w12041059.

Thuan, N.C., Phat, V.V., Thai Hang, T.T., Le Luu, T., Tripple, J. and Wagner, M., 2024. Treatment of seafood processing wastewater toward carbon neutrality: A comparison between coagulation/flocculation, chemical oxidation and absorbent methods. *Case Studies in Chemical and Environmental Engineering*, 10, pp.100792. https://doi.org/10.1016/j.cscee.2024.100792.

Valand, S.A., Shah, S.M., Singh, D.K. and Mundkar, S., 2019. Comparison of COD removal from textile wastewater by using activated carbon & activated lignite. *Plos One,* 16, pp.34-46

Valentukeviciene, M., Andriulaityte, I., Karczmarczyk, A. and Zurauskiene, R., 2024. Removal of residual chlorine from stormwater using low-cost adsorbents and phytoremediation. *Environments*, 11. https://doi.org/10.3390/environments11050101.

Wang, H., Xu, Y. and Chai, B., 2023. Effect of temperature on microorganisms and nitrogen removal in a multi-stage surface flow constructed wetland. *Water (Basel)*, 15, pp.1256. https://doi.org/10.3390/w15071256.

Waqas, S., Harun, N.Y., Sambudi, N.S., Bilad, M.R., Abioye, K.J., Ali, A. and Abdulrahman, A., 2023. A review of rotating biological contactors for wastewater treatment. *Water (Basel)*, 15, pp.1913. https://doi.org/10.3390/w15101913.

Wysowska, E., Wiewiórska, I. and Kicińska, A., 2021. The impact of different stages of the water treatment process on the number of selected bacteria. *Water Resources and Industry*, 26, pp.100167. https://doi.org/10.1016/j.wri.2021.100167.

Yang, X. and López-Grimau, V., 2021. Reduction of cost and environmental impact in the treatment of textile wastewater using a combined MBBR-MBR system. *Membranes (Basel)*, 11, pp.892. https://doi.org/10.3390/membranes11110892.

Yuan, Z., Olsson, G., Cardell-Oliver, R., van Schagen, K., Marchi, A., Deletic, A., Urich, C., Rauch, W., Liu, Y. and Jiang, G., 2019. Sweating the assets – The role of instrumentation, control, and automation in urban water systems. *Water Research*, 155, pp.381–402. https://doi.org/10.1016/j.watres.2019.02.034.

Zhang, L., Chen, Y., Zhang, H., Jin, Y., Shen, Z. and Duan, G., 2024. Application of membrane separation technology in electroplating wastewater treatment and resource recovery: A review. *Nature Environment and Pollution Technology*, 23, pp.649–665. https://doi.org/10.46488/NEPT.2024.v23i02.005.

An Experimental Investigation on Sustainable Concrete Made with Refractory Brick as a Substitute of Natural Fine Aggregate

Sanjeet Kumar ⓘ**, Md Asfaque Ansari†** ⓘ**, Lakshmi Kant** ⓘ **and Nitya Nand Jha** ⓘ

Department of Civil Engineering, Rashtrakavi Ramdhari Singh Dinkar College of Engineering, Begusarai, Bihar-851134, India

†Corresponding author: Md Asfaque Ansari; asfaqueansari.ce.dst@bihar.gov.in

ABSTRACT

In the face of the pressing global issue of waste management and the diminishing availability of natural resources, the management of non-biodegradable waste materials, including brick waste, poses significant challenges. Ineffective disposal practices not only create logistical obstacles but also pose health hazards. This study explores the potential of utilizing waste refractory bricks (RB) as a sustainable substitute for natural fine aggregates in concrete production. Various experimental investigations were conducted to evaluate the feasibility and performance of RB sand in concrete mixtures. Tests included assessments of fresh and hardened properties, such as slump values, compressive strength, tensile strength, flexural strength, and resistance to elevated temperatures. The research revealed that RB sand, when used as a partial replacement for fine aggregates, can significantly enhance the compressive strength of concrete, with optimal results observed at a 30% replacement level. Moreover, RB-based concrete exhibited improved split tensile strength compared to traditional concrete, particularly at replacement levels of 10% to 30%. Flexural strength also showed notable improvements, with the 40% replacement level demonstrating optimal performance. Additionally, the study investigated the effects of elevated temperatures on concrete specimens and found that RB-based sustainable concrete showed higher compressive strength retention compared to conventional concrete at a 30% replacement level. Furthermore, weight variation analysis indicated that RB-based concrete had a lower density compared to traditional concrete. Overall, the findings suggest that incorporating RB sand in concrete mixtures could offer a promising solution for sustainable construction practices, contributing to environmental conservation and human health preservation by reducing reliance on natural aggregates and minimizing adverse environmental impacts.

INTRODUCTION

Concrete stands as the primary structural material in building construction owing to its numerous advantages such as durability, integrity of strength, ease of molding and shaping in different types of frameworks as desired, and nonflammable characteristics (Aboutaleb et al. 2017, Kodur 2014, Krishna et al. 2019, Onyelowe et al. 2023). These qualities not only distinguish it as a widely preferred choice but also position it as an essential material in modern construction practices (Ansari & Roy 2023, Deti et al. 2024, Jureje et al. 2024). However, despite its extensive use and undeniable benefits, concrete cannot be considered an eco-friendly material due to its significant consumption of natural resources, exacerbating the shortage of these resources (Ansari & Roy 2023, Kaarthik & Maruthachalam 2021, Lokeshwari & Swamy 2011). Moreover, concrete structures, typically engineered and constructed for a minimum lifespan of 50 years, commonly deteriorate due to localized or widespread damage, particularly in scenarios like acid attacks. This deterioration presents considerable economic and social challenges for the replacement of a severely damaged structure (Nematzadeh et al. 2018). Waste management in the construction industry is

a pressing issue, particularly in major cities with limited landfill space.

In response to these challenges, recycling construction waste emerges as a rational approach, aligning with green construction principles to mitigate environmental pollution and reduce reliance on natural resources such as aggregates (both coarse and fine) and waste disposal (John & Parameswaran 2010, Khattab et al. 2021a, 2021b, 2021c, Paul et al. 2023, Vinay Kumar et al. 2018). Notably, the disposal of non-biodegradable waste, including brick waste, presents a formidable task, given its extended degradation period of over 4000 years (Baradaran-Nasiri & Nematzadeh 2017). Aggregates, constituting a significant portion (approximately 70 to 80%) of concrete volume, play a pivotal role in its composition, prompting extensive research into sustainable alternatives (Khattab & Hachemi 2020, Sambangi & Eluru 2022).

Refractory bricks (RB) represent a novel category of bricks distinguished by their unique chemical composition, which differs from conventional bricks (Deti et al. 2024, Khattab et al. 2021b). These bricks play a pivotal role in infrastructure development, offering resistance to temperature exposure and facilitating energy savings. Primarily employed in furnace linings for industries such as glass, ceramics, and cement production, refractory bricks are typically discarded after use, contributing to the generation of approximately 28 million metric tons of waste annually. Miserably, over 98% of these refractory materials are disposed of in landfills or dumped onto soil-based grounds.

However, waste refractory bricks offer a potentially innovative solution as an alternative aggregate, capable of replacing either partially or entirely natural fine aggregates in concrete production (Deti et al. 2024, Jureje et al. 2024, Khattab et al. 2021c). This approach not only contributes to sustainable building practices but also prioritizes the protection of human health and the environment while conserving natural aggregates, particularly coarse and fine materials. Despite these advantages, the utilization of RB waste as either a fine or coarse aggregate in the development of sustainable concrete has received minimal attention among researchers. Limited studies have been conducted on concrete incorporating RB waste, indicating a gap in current understanding and highlighting the need for further investigation (Khattab et al. 2021a, 2021b, 2021c, Sinha et al. 2023). Despite limited attention, previous studies have explored the feasibility of incorporating RB waste into concrete mixes, particularly as a fine aggregate replacement, demonstrating promising results in terms of mechanical properties and thermal stability (Ghosh & Samanta 2023, Saidi et al. 2015). However, comprehensive investigations into the physico-mechanical properties of

RB-based sustainable concrete, particularly under elevated temperatures, remain scarce.

This paper aims to fill this gap by conducting experimental research on the utilization of RB as a fine aggregate substitute in sustainable concrete. The study investigates both freshly mixed and hardened concrete properties, along with the effects of elevated temperatures, shedding light on the feasibility and performance of RB-based concrete as an eco-friendly construction material.

MATERIALS AND METHODS

Cement

This study utilized Portland Pozzolanic Cement (PPC) in accordance with IS 1489 (Part 1) to prepare conventional concrete. The physical properties of the PPC were determined in the laboratory and are detailed in Table 1. The initial and final setting times were found to be 45 minutes and 283 minutes, respectively.

Aggregates

Natural sand: Locally available river sand was used as a fine aggregate (FA) of Zone II type, conforming to IS 383 (2016), to make conventional concrete. The specific gravity of this sand was found to be 2.68. The physical properties of the sand were tabulated in Table 2. The particle size distribution curve of the sand is shown in Fig. 1.

Waste refractory bricks (RB sand): Waste refractory bricks were collected from the local area in the Begusarai

Table 1: Physical properties of cement.

Item	Properties
Cement type	PPC
Consistency [%]	34
Specific gravity	2.91
Initial setting time (minutes)	45
Final setting time (minutes)	283

Table 2: Physical properties of aggregates.

Item description	Properties		
	Natural fine aggregate	Waste refractory bricks	Coarse aggregate
Sizes [in mm]	0.075-4.75	0.075-4.75	10-20
Specific gravity	2.68	2.03	2.71
Apparent specific gravity	2.77	2.76	2.80
Fineness modulus [%]	2.55	3.15	5.78
Bulk Density [kg.m^{-3}]	1549	1539	1592
Water Absorption [%]	0.56	1.23	0.59
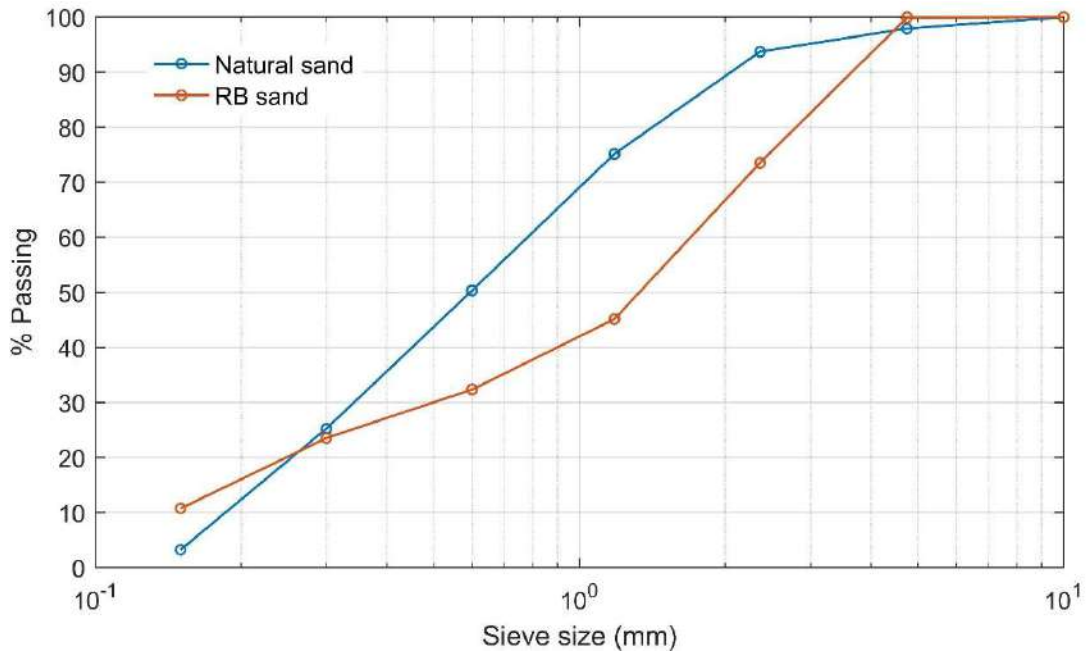
Fig. 1: Particle size distribution of fine aggregate.

Location Map of Study Area
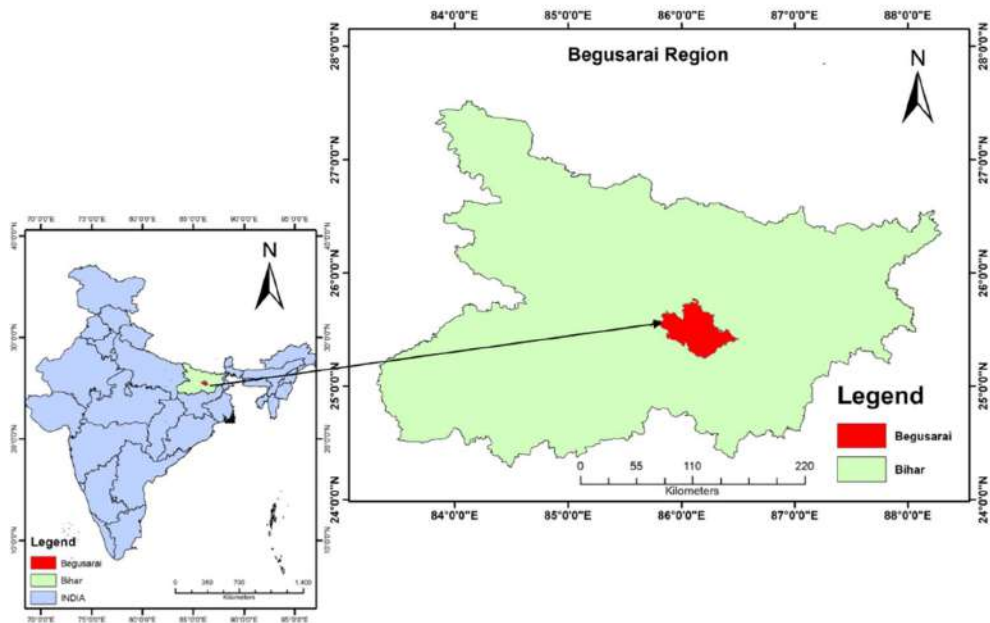
Fig. 2: RB waste collecting area map.

district of Bihar, India, as depicted in Fig. 2. These bricks were thoroughly cleaned and crushed using a manually operated rammer. The crushed RB waste was then dried properly, and sieve analysis was conducted to obtain different sizes of RB sand, which served as a fine aggregate replacement for natural sand. The entire process of preparing RB sand is illustrated in Fig. 3. Subsequently, the physical properties of RB sand were determined under laboratory conditions and are presented in Table 2. The maximum size of RB sand was taken as 4.75 mm. The
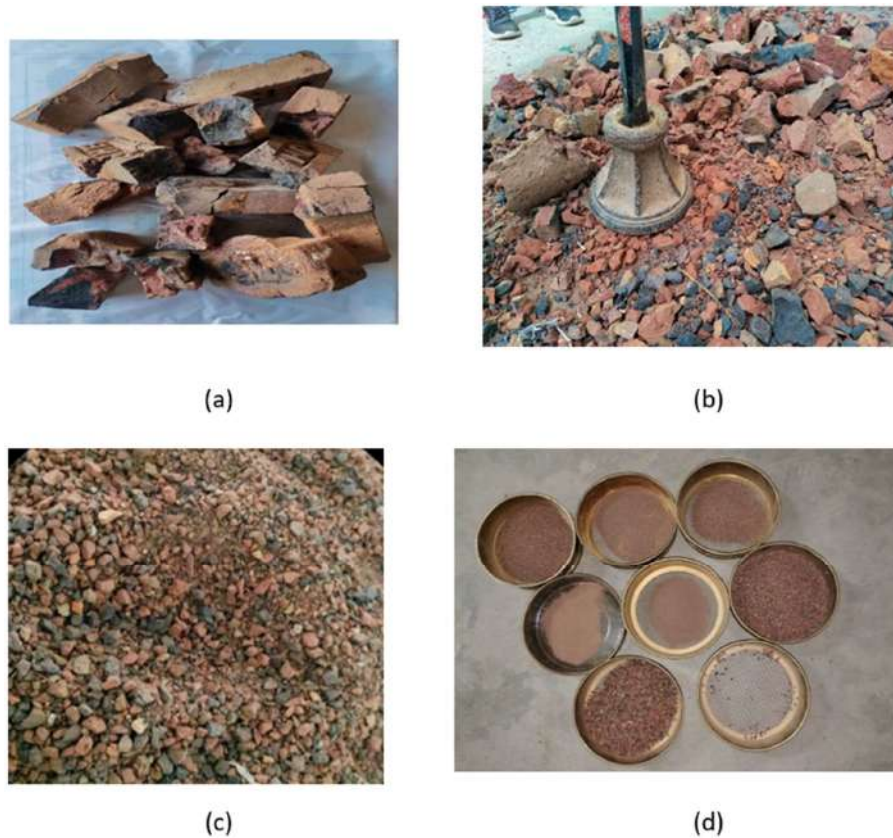
Fig. 3: Pictures of (a) RB waste (b) Breaking of RB waste (c) Crushed RB waste (d) RB sand.

particle size distribution curve of the RB sand is shown in Fig. 1.

Coarse aggregate: For this study, locally available coarse aggregate was utilized in the preparation of concrete materials. The size of this aggregate ranged from 10 mm to 20 mm. All aggregates employed in the experiments were maintained in SSD (saturated surface dry) conditions. Various physical properties of the aggregates were assessed in the laboratory and are detailed in Table 2. The photographic view of various types of aggregates used in this study is shown in Fig. 4.

Experimental Details

Mix proportion: For the current investigation, concrete mix designs of M30 grade were conducted, aiming for a slump of 100 mm as per the requirements outlined in IS 456 (2000) and IS 10262 (2019). The target design strength of the concrete was determined to be 38.5 MPa. The mix design proportions per cubic meter for different concrete mixtures are detailed in Table 3. The sample mixes labeled NC and RB30 correspond to normal concrete and concrete with refractory brick fine aggregate, respectively, with a 30% replacement of natural fine aggregate (FA).

Fig. 4: Pictures of (A) CA (10 mm) (B) CA (12.5 mm) (C) CA (20 mm) (D) FA (E) RB sand.

Table 3: Mix proportion of concrete.

Mix ID	Mix combination	Water [kg]	Cement [kg]	Ratio of W/C	Fine Aggregate [kg]		Coarse Aggregate [kg]			SP [%]
					FA	RB	10 [mm]	12.5 [mm]	20 [mm]	
NC	FA100%	148	344	0.43	715	0	370.5	494	370.5	1.00
RB10	FA90%+RB10%				641.5	71.5				1.05
RB20	FA80%+RB20%				572	143				1.10
RB30	FA70%+RB30%				500.5	214.5				1.15
RB40	FA60%+RB40%				429	286				1.20
RB50	FA50%+RB50%				357.5	357.5				1.25
RB70	FA30%+RB70%				214.5	500.5				1.30
RB100	FA0%+ RB100%				0	715				1.35

To achieve a consistent slump value, different percentages of Sika brand superplasticizer (Polycarboxylic Ether Polymer) with a density of 1.15 were employed in compliance with IS 9103 (1999). The mixing temperature was maintained at 25°C. Pure potable water, free from turbidity, was utilized for mixing purposes.

Casting and curing of specimens: Specimens of three types, namely cubes with standard dimensions of 150 × 150 × 150 mm, cylinders measuring 150 mm in diameter and 300 mm in height, and prisms with dimensions of 100 mm (breadth and depth) by 500 mm (length), were cast to evaluate the mechanical characteristics of sustainable concrete. The freshly mixed concrete was poured into the specimen molds in three layers. Immediately after each filling, the molds were placed on a vibrating table to ensure proper compaction and eliminate entrapped air, following the procedure recommended by Kaarthik and Maruthachalam (2021). After casting, the samples were allowed to harden for 24 hours before demolding. Subsequently, they were fully immersed in water for simultaneous curing for 28 days, as shown in Fig. 5. Following the 28-day curing period, the samples were removed from the water and allowed to air dry inside the material testing laboratory for 1 h before testing.

Testing of specimens: The slump values of various RB-mixed concrete mixtures were determined using a conventional slump cone apparatus in accordance with IS 1199 (1959), demonstrating their preferred workability. To maintain uniform slump values, a superplasticizer was added at different percentages, starting with 1.00% for control concrete and increasing by 0.05% at each replacement percentage level. After 28 days of curing, the mechanical properties of the samples, including the compressive strength of cube specimens, split tensile strength of cylinder specimens, flexural strength of prism specimens, and weight variation of all specimens, were assessed for RB-based fine aggregate concrete mixtures. The mean of three specimens was taken for each hardened concrete property.

Fig. 5: Photographic view of curing of specimens in curing tank.

Fig. 6: Compressive testing machine used in the test experiment.

The primary focus was on understanding the behavior of concrete in terms of its characteristic compressive strength. Various factors, such as size, shape, water-cement ratio, curing period, demolding technique, aggregate paste interfaces, use of admixtures, and application of stresses, influence concrete's compressive strength. Compressive strength testing was conducted on a computerized digital compression testing machine (CTM) with a capacity of 2000 kN, as shown in Fig. 6, following IS 516 (1959) standards.

Furthermore, considering that conventional concrete is weaker in tension compared to materials like steel, its split tensile strength is relatively low. Despite this, split tensile strength is crucial from an infrastructure damage perspective and requires careful investigation. Split tensile strength measurements were conducted after 28 days of curing following IS 5816 (1999) standards, using a 2000 kN computerized CTM at a uniform loading rate of 2 kN.sec^{-1}.

Flexural strength, or the ability of a material to resist bending deformation when subjected to an external load, was evaluated using prism specimens. The test was conducted using a three-point loading pattern at a rate of 2 kN.sec^{-1} on a 100 kN digital flexural testing machine, as shown in Fig. 7, following procedures outlined in IS 516 (1959).

Weight variation and elevated temperature: Before conducting tests for hardened properties, the weight of both conventional and RB-based sustainable concrete specimens was measured using a digital weighing balance machine with
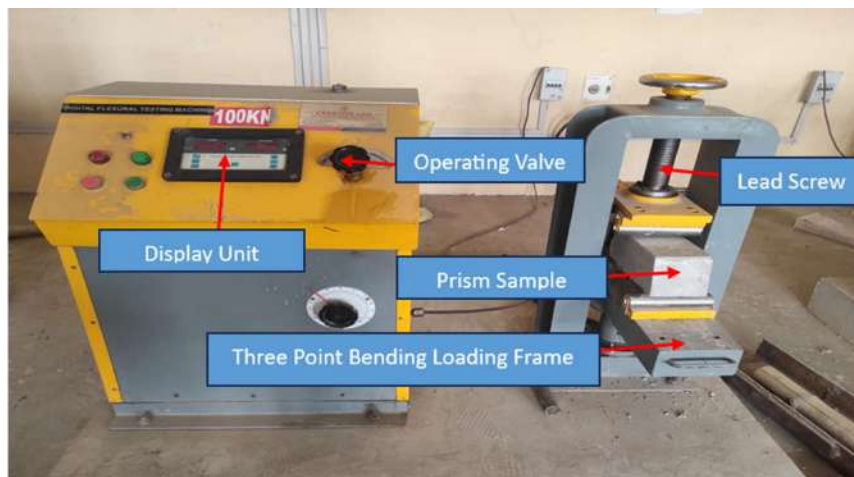
Fig. 7: Photographic view of flexural strength testing machine.
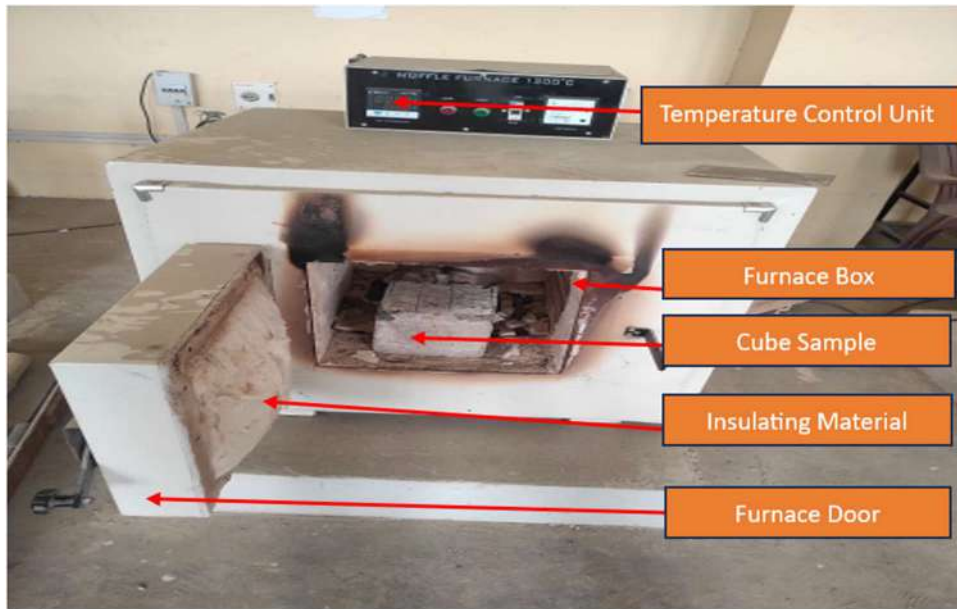
Fig. 8: Photographic view of the Muffle furnace used in this study.

a capacity of 500 ± 0.05 kg, following 28 days of curing for each specimen. This parameter is significant as it influences the self-weight of concrete, contributing to lightweight structures beneficial for practical applications (Sinha et al. 2023). Additionally, the percentage of weight variation was determined to assess any changes.

Subsequently, the cube specimen was removed from the curing water tank and allowed to air-dry for 1 h. Upon complete drying, it was subjected to elevated temperatures in a muffle furnace, as depicted in Fig. 8, with a machine capacity of 1200°C. The temperature was set to 600°C, half of the furnace's capacity, and maintained for 1 h to examine the effects of temperature on the concrete specimens, comparing them to both conventional and sustainable concrete compressive strengths.

RESULTS AND DISCUSSION

This study conducted experimental investigations to assess the feasibility of utilizing waste refractory bricks as a replacement for natural fine aggregates in concrete. Various percentages of RB bricks ranging from 10% to 100% were incorporated, and a series of laboratory tests, including compressive strength, tensile strength, and flexural strength, were performed. The results obtained from these tests were analyzed and discussed in detail in the subsequent sections.

Fresh Concrete Properties

The current study expected a concrete matrix mix with a targeted slump of 100 mm, a requirement successfully achieved with freshly mixed normal concrete recording a slump of 100 mm. Throughout the preparation process of RB-based sustainable concrete, a consistent value of 100 ± 2 mm was maintained, with a slight adjustment in the superplasticizer dose for each replacement to sustain the desired slump. The test results depicted in Fig. 9 demonstrate minimal variation in slump values across all percentages of RB sand compared to normal concrete mixes.

Influence of RB Sand Content on Compressive Strength of Concrete

The compressive strength analysis of concrete cubes, conducted after a 28-day curing period, aimed to assess the viability of RB sand as a substitute for natural fine aggregates under atmospheric conditions. Fig. 10 presents the compressive strength results obtained from experimental studies on various concrete mixtures at different replacement levels. The targeted strength of the concrete was 42.23 MPa, while the stipulated target strength was 38.25 MPa. Notably, specimens with a 10% substitution of fine aggregate with RB sand exhibited a 6.03% increase in compressive strength at 28 days. This improvement continued with higher replacement levels, with samples at 20% and 30% replacements showing increases of 11.03% and 14.23% in compressive strength, respectively. However, it was observed that higher percentages of RB sand resulted in decreased compressive strength, indicating an optimal replacement range.

In comparison to traditional concrete, the RB50 mix displayed a modest 3.4% increase in compressive strength.
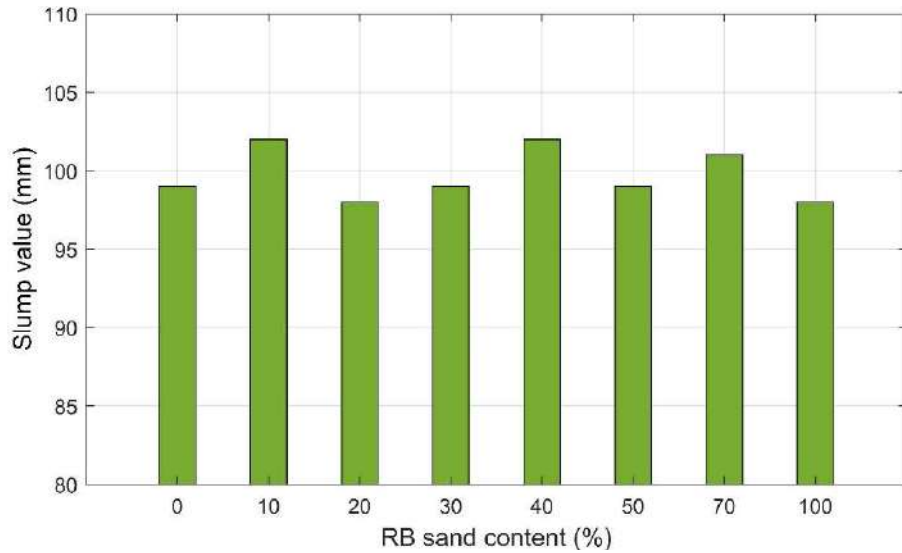
Fig. 9: Slump value of different concrete matrices with different RB sand content.
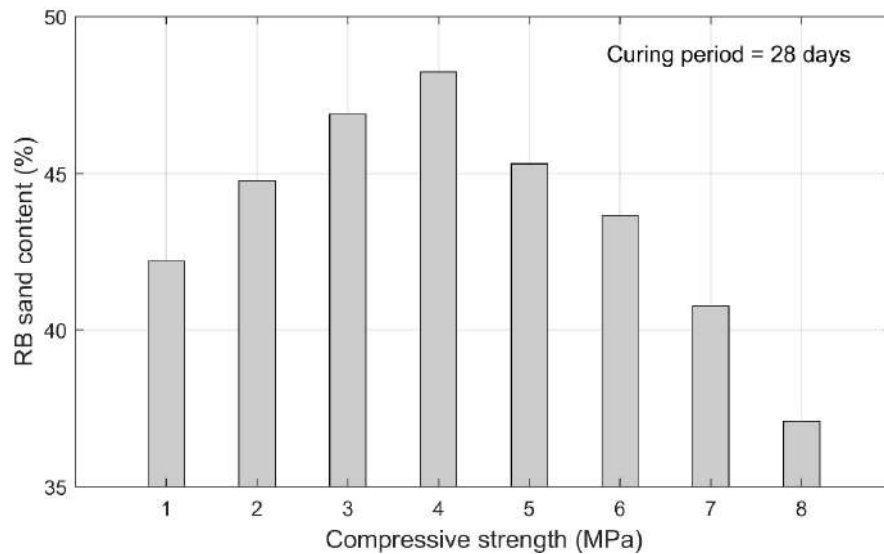
Fig. 10: Compressive strength of concrete specimen at various replacement levels of RB sand.

The particle size of RB sand played a crucial role, with larger particles potentially leading to higher permeability and reduced compressive strength. However, RB waste refractory bricks closely resembled natural sand sizes, facilitating better compaction and distribution of materials within the concrete matrix. Consequently, the smaller voids resulting from the inclusion of RB waste contributed to higher compressive strength. Overall, all replacement levels of concrete mixes achieved the targeted strength, with RB20 and RB30 mixes demonstrating the most significant improvements. Fig. 11 illustrates the partially eruptive failure pattern observed in cube samples. The compaction and distribution of materials,

aided by the smaller size of RB sand and improved binding between aggregates and cement, influenced the failure pattern, resulting in either eruptive or non-eruptive patterns in the cube specimens.

Influence of RB Sand Content on Split Tensile Strength of Concrete

The split tensile strength of concrete mixtures containing varying levels of RB sand content was evaluated using cylindrical concrete samples to investigate the influence of RB sand content on split tensile strength. As depicted in Fig. 12, the split tensile strength of conventional concrete
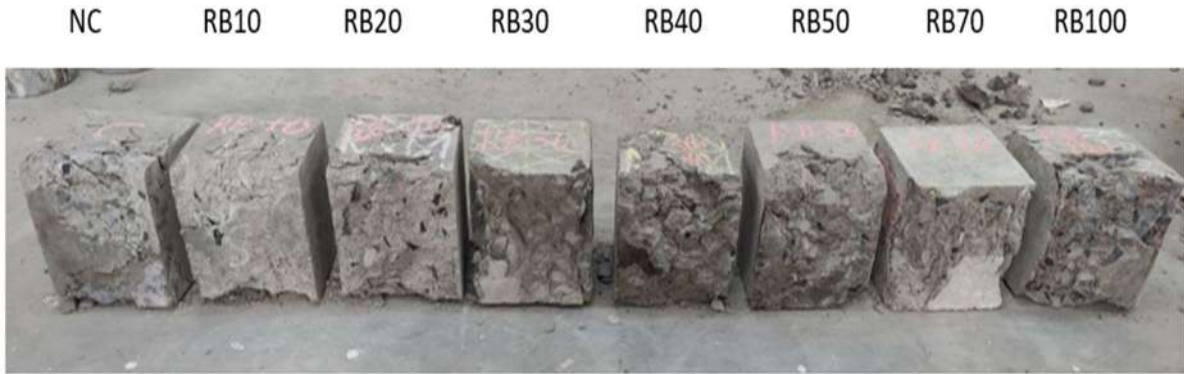
Fig. 11: Failure pattern of various cube samples at different RB sand content.
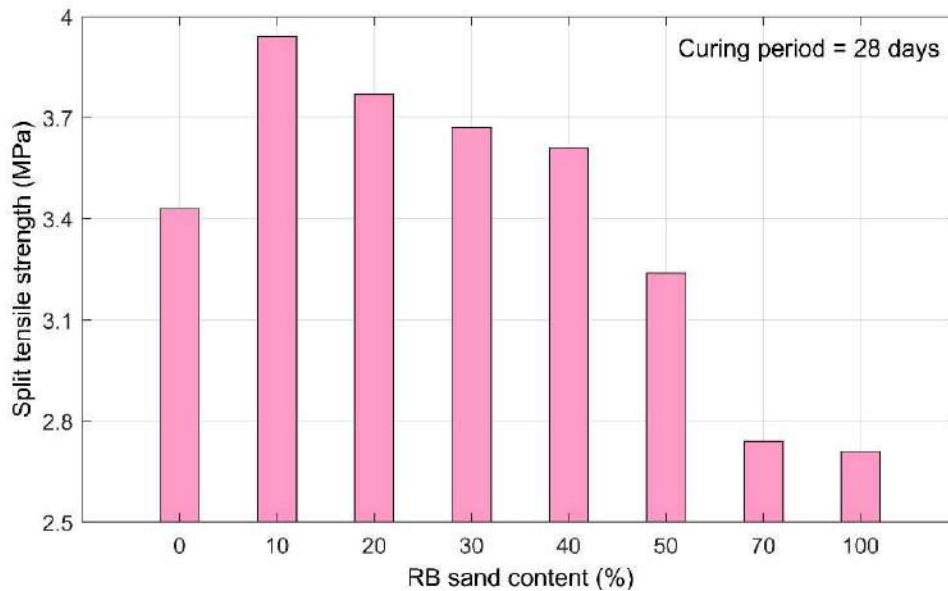
Fig. 12: Split tensile strength of concrete with various RB sand content.

(without RB sand) was found to be 3.46 MPa after 28 days of curing. Notably, concrete mixes with RB sand content of 10% and 20% exhibited strength recoveries of 15% and 10%, respectively, in comparison to conventional concrete. Furthermore, the sample with 30% RB sand content surpassed traditional concrete, achieving a split tensile strength of 7% higher. However, the remaining samples showed a decline in split tensile strength. This suggests that the substitution of RB sand ranging from 10% to 30% with fine aggregate led to an increase in split tensile strength. The observed improvement may be attributed to the pozzolanic behavior of cement. Conversely, the decline in strength could be attributed to increased water absorption of RB sand, crystal sizes, and texture, leading to poor bonding between cement pozzolanic behavior and the aggregate (Khattab & Hachemi 2020, Sinha et al. 2023). Fig. 13 illustrates the failure pattern

of the cylindrical specimens, revealing a split into two separate parts due to inadequate bonding among cement, RB sand, and coarse aggregate, with no observed eruptive-type failure during the testing of split tensile strength.

Effect of RB Sand Contents on Flexural Strength of Concrete

The flexural characteristics of both conventional concrete and concrete incorporating RB sand as a substitute for fine aggregates at various percentages were evaluated using prism samples after 28 days of curing. The flexural strength of traditional concrete, without any replacement of fine aggregate (FA), was measured at 6.91 MPa. Upon replacing fine aggregate with RB sand, specimens with replacements ranging from 10% to 70% exhibited higher bending strength compared to the conventional specimen. Interestingly, even

Fig. 13: Failure pattern of cylinder samples at different RB sand content.
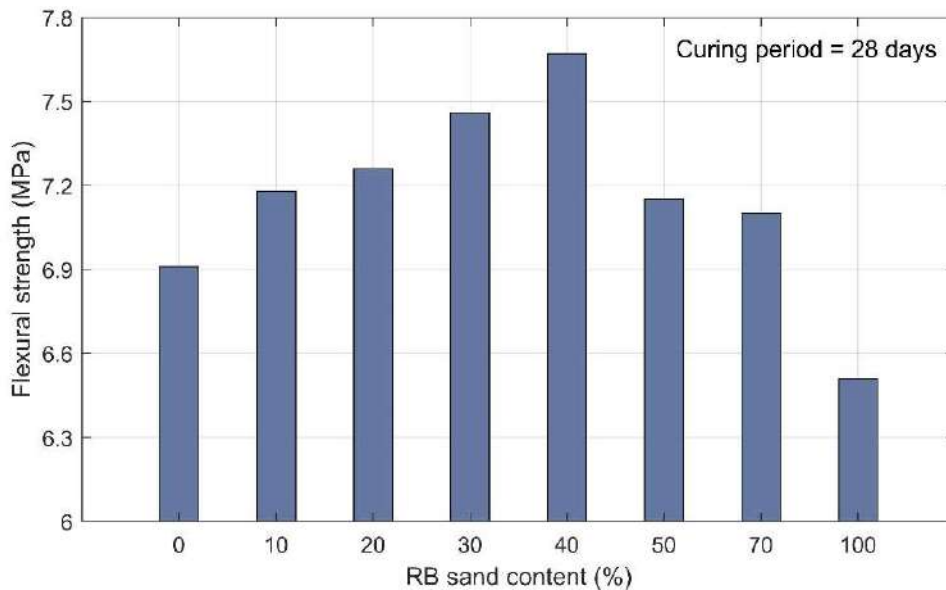
Fig. 14: Flexural strength of concrete specimen at various RB sand content.

the specimen with 100% replacement of fine aggregate showed only a minimal reduction in flexural strength relative to the normal concrete, as depicted in Fig. 14. The increase in flexural strength ranged from 2.8% to 11% compared to conventional concrete, with the optimum improvement observed at 7.67 MPa for the 40% RB sand replacement level. The increase in flexural strength with the increase in RB sand content could be attributed to the reduction in the weight of the mixture, speeding up the strength of the mortar due to the rapid pozzolanic reaction. The failure pattern of prism specimens after testing is shown in Fig. 15. A distinct flexural compression failure pattern is evident in this figure across all levels of RB sand content.

Effect of RB Sand Content on Weight Variation

The variation in weight was assessed for both hardened

conventional concrete samples and RB sand-based sustainable concrete samples with different replacement levels. Fig. 16 illustrates the weight variation of cube, cylinder, and prism samples. It was observed that as the replacement percentage increased, all sample types experienced a marginal decrease in weight. This suggests that the density of RB-sand is lower compared to traditional fine aggregate, as indicated by the fluctuations in weight.

Elevated Temperature Effects

After 28 days of curing, the cube specimen was kept in a muffle furnace for an hour at a constant temperature of 600°C and then cooled. Subsequently, compressive strength tests were conducted on the cubes. The compressive strength of normal concrete and RB sand content concrete before and after a fire is shown in Fig. 17. It can be noted from

Fig. 15: Failure pattern of prism sample at various RB sand content.
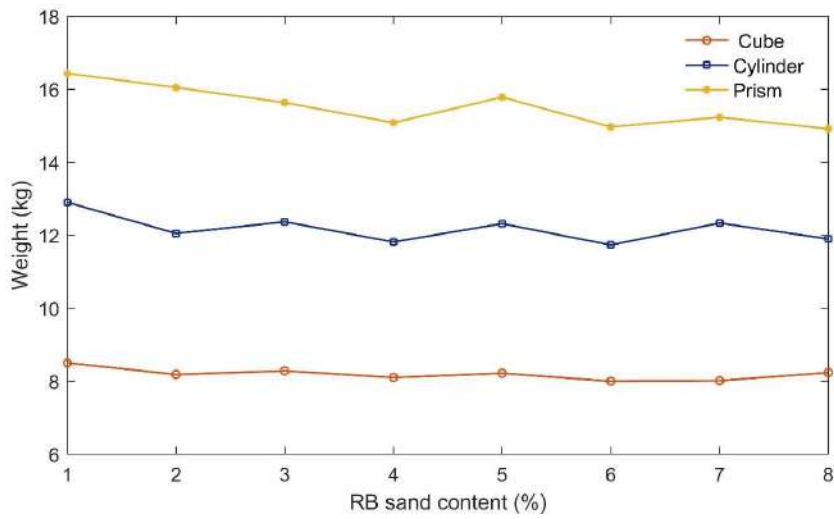
Fig. 16: Weight variation of concrete at various RB sand content.
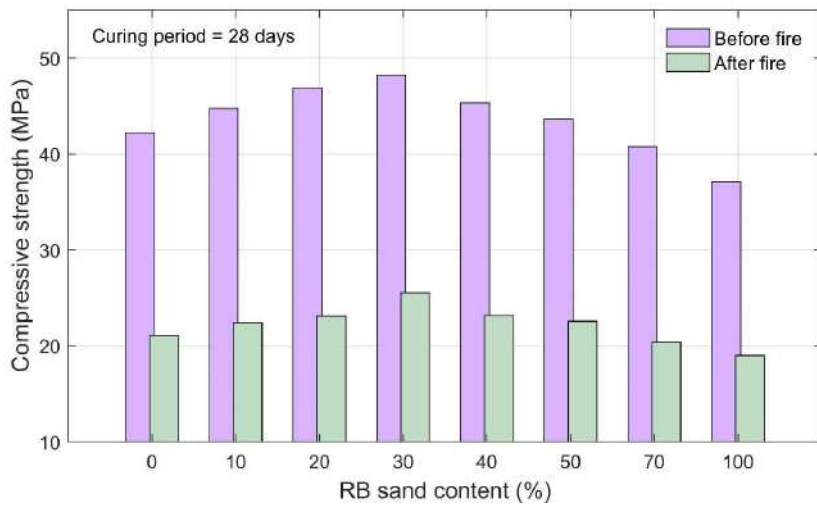
Fig. 17: Compressive strength of concrete sample before and after fire exposure.

this figure that the compressive strength of the control specimen after the temperature effects decreased by 50% as compared to the normal compressive strength test results of the control specimen. Additionally, the specimens with a 30% replacement of fine aggregate with RB sand exhibited the highest compressive strength compared to conventional concrete at elevated temperatures. However, beyond the 30% replacement level, all cube specimens showed a decrease in compressive strength.

CONCLUSIONS

This study investigates the feasibility of using RB sand as a sustainable alternative to fine aggregates in concrete mixtures. Through various experimental tests involving different percentages of RB sand content, the impact on compressive strength, tensile strength, flexural strength, temperature effects, and other relevant factors was examined. Based on the results and discussions presented, the following key conclusions can be drawn:

1. Fresh properties of the concrete matrix, such as slump values, remained consistent across all replacement levels of RB sand, indicating the feasibility of using RB sand as a fine aggregate substitute without compromising workability.

2. A significant increase in compressive strength was observed in sustainable concrete mixes with a 50% replacement of fine aggregate with RB sand after 28 days of curing, highlighting the potential of RB sand to enhance the mechanical properties of concrete.

3. Concrete mixes with 30% and 10% replacements of fine aggregate with RB sand exhibited the highest compressive strength and split tensile strength after 28 days, outperforming other mixes. These replacement levels showed superior performance compared to control mixes, while higher replacement levels resulted in a decrease in compressive strength.

4. Refractory brick-based sustainable concrete demonstrated a 50% decrease in compressive strength at elevated temperatures compared to normal control concrete. However, the 30% replacement level exhibited the highest compressive strength under elevated temperatures, indicating its potential for use in high-temperature environments.

5. The weight of cylinder, cube, and prism specimens decreased with increased replacement levels of RB sand, suggesting a lower density compared to control concrete.

Overall, the study highlights the potential of using RB sand as a substitute for natural fine aggregate in concrete production, particularly at replacement levels of 10% to 30%. This approach offers promising benefits in terms of enhancing mechanical properties, conserving natural resources, and reducing environmental impact, thereby supporting its inclusion in construction practices on a broader scale.

ACKNOWLEDGEMENT

REFERENCES

Aboutaleb, D., Safi, B., Chahour, K. and Belaid, A., 2017. Use of refractory bricks as sand replacement in self-compacting mortar. *Cogent Engineering*, 4(1), p.1360235. https://doi.org/10.1080/23311916.2017.1360235.

Ansari, M.A. and Roy, L.B., 2023. Effect of Geogrid Reinforcement on Shear Strength Characteristics of a Rubber-Sand Mixture under Undrained Triaxial Test. *Jordan Journal of Civil Engineering*, 17(2), p.01. https://doi.org/10.14525/JJCE.v17i2.01.

Baradaran-Nasiri, A. and Nematzadeh, M., 2017. The effect of elevated temperatures on the mechanical properties of concrete with fine recycled refractory brick aggregate and aluminate cement. *Construction and Building Materials*, 147, pp.865–875. https://doi.org/10.1016/j.conbuildmat.2017.04.138.

Deti, D., Tjaronge, M.W. and Caronge, M.A., 2024. Compressive loading and response time behavior of concrete containing refractory brick coarse aggregates. *Journal of Engineering and Applied Science*, 71(1), p.95. https://doi.org/10.1186/s44147-024-00433-7.

Ghosh, S. and Samanta, A.K., 2023. Utilization of recycled refractory brick as fine aggregate on various properties of sustainable concrete. *Materials Today: Proceedings,* 12, p.127. https://doi.org/10.1016/j.matpr.2023.03.712.

IS 10262. 2019. Concrete Mix Proportioning - Guidelines. *Bureau of Indian Standards*, pp. 1–44.

IS 1199. 1959. Methods of sampling and analysis of concrete. *Bureau of Indian Standards*, pp. 1–49.

IS 1489 (Part 1). 1991. Portland Pozzolana Cement-Specification. *Bureau of Indian Standards*, pp. 1–17.

IS 383. 2016. Coarse and fine aggregate for concrete - Specification. *Bureau of Indian Standards*, pp. 1–22.

IS 456. 2000. Plain and Reinforced Concrete. *Bureau of Indian Standards*, pp. 1–127.

IS 516. 1959. Methods of Tests for Strength of Concrete. *Bureau of Indian Standards*.

IS 5816. 1999. Splitting Tensile Strength of Concrete - Method of Test. *Bureau of Indian Standards*.

IS 9103. 1999. Concrete Admixtures - Specification. *Bureau of Indian Standards*.

John, J. and Parameswaran, P., 2010. Recycled Concrete Aggregate- A Substitute to Natural Coarse Aggregate. *Nature, Environment and Pollution Technology*, 9(2), pp.433-436.

Jureje, U., Tjaronge, M.W. and Caronge, M.A., 2024. Basic engineering properties of concrete with refractory brick as a coarse aggregate: compressive stress-time relationship assessment. *International Journal of Engineering*, 37(5), pp.931-940. https://doi: 10.5829/ije.2024.37.05b.11.

Kaarthik, M. and Maruthachalam, D., 2021. A sustainable approach to

characteristic strength of concrete using recycled fine aggregate. *Materials Today: Proceedings*, 45, pp.6377–6380. https://doi.org/10.1016/j.matpr.2020.11.058.

Khattab, M. and Hachemi, S., 2020. Performance of concrete made with recycled coarse aggregate from waste refractory brick. *Algerian Journal of Engineering Architecture and Urbanism*, 4(2), pp.79–94.

Khattab, M., Hachemi, S. and Al Ajlouni, M.F., 2021a. Evaluating the physical and mechanical properties of concrete prepared with recycled refractory brick aggregates after elevated temperatures' exposure. *Construction and Building Materials*, 311, p.125351. https://doi.org/10.1016/j.conbuildmat.2021.125351.

Khattab, M., Hachemi, S. and Al Ajlouni, M.F., 2021b. Recycled refractory brick as aggregate for eco-friendly concrete production. *Journal of Advanced Sciences and Engineering Technologies*, 4(1), pp.32–49. https://doi.org/10.32441/jaset.04.01.04.

Khattab, M., Hachemi, S. and Fawzi, M., 2021c. Use of recycled aggregate from waste refractory brick for the future of sustainable concrete. *Civil Engineering*, 30, pp.1–6.

Kodur, V., 2014. Properties of concrete at elevated temperatures. *ISRN Civil Engineering*, 2014, pp.1–15. https://doi.org/10.1155/2014/468510.

Krishna, D.A., Priyadarsini, R.S. and Narayanan, S., 2019. Effect of Elevated Temperatures on the Mechanical Properties of Concrete. *Procedia Structural Integrity*, 14, pp.384–394. https://doi.org/10.1016/j.prostr.2019.05.047.

Lokeshwari, M. and Swamy, C.N., 2011. Sustainable development through recycling of construction and demolition wastes in India. *Nature, Environment and Pollution Technology*, 10(1), pp.27-32.

Nematzadeh, M., Dashti, J. and Ganjavi, B., 2018. Optimizing compressive behavior of concrete containing fine recycled refractory brick aggregate

together with calcium aluminate cement and polyvinyl alcohol fibers exposed to an acidic environment. *Construction and Building Materials*, 164, pp.837–849. https://doi.org/10.1016/j.conbuildmat.2017.12.230.

Onyelowe, K.C., Gnananandarao, T., Jagan, J., Ahmad, J. and Ebid, A.M., 2023. Innovative predictive model for flexural strength of recycled aggregate concrete from multiple datasets. *Asian Journal of Civil Engineering*, 24(5), pp.1143–1152. https://doi.org/10.1007/s42107-022-00558-1.

Paul, S.C., Faruky, S.A.U., Babafemi, A.J. and Miah, M.J., 2023. Eco-friendly concrete with waste ceramic tile as a coarse aggregate: mechanical strength, durability, and microstructural properties. *Asian Journal of Civil Engineering*, 24(8), pp.3363–3373. https://doi.org/10.1007/s42107-023-00718-x.

Saidi, M., Safi, B., Bouali, K., Benmounah, A. and Samar, M., 2015. Improved behavior of mortars at a high temperature by using refractory brick wastes. *International Journal of Microstructure and Materials Properties*, 10(5/6), pp.366. https://doi.org/10.1504/IJMMP.2015.074992.

Sambangi, A. and Eluru, A., 2022. Role of copper slag on the improvement of strength, quality, and durability of high-strength self-compacting concrete: an industrial waste. *Asian Journal of Civil Engineering*, 23(6), pp.961–971. https://doi.org/10.1007/s42107-022-00466-4.

Sinha, S., Ghosh, S. and Samanta, A.K., 2023. Influence of waste refractory brick on the destructive and non-destructive properties of sustainable, eco-friendly concrete. *Materials Today: Proceedings*, 3, p.508. https://doi.org/10.1016/j.matpr.2023.03.508.

Vinay, K.B.M., Ananthan, H. and Balaji, K.V.A., 2018. Experimental studies on utilization of recycled coarse and fine aggregates in high-performance concrete mixes. *Alexandria Engineering Journal*, 57(3), pp.1749–1759. https://doi.org/10.1016/j.aej.2017.05.003.

Original Research Paper https://doi.org/10.46488/NEPT.2025.v24i01.B4212 **Open Access Journal**

Integrating Traditional Knowledge Systems for Wetland Conservation and Management: A Critical Analysis

Anushri Barman[1†] (ORCID), **Fulena Rajak**[1] **and Ramakar Jha**[2]

[1]Department of Architecture and Planning, National Institute of Technology Patna, Ashok Rajpath, Patna 800005, Bihar, India

[2]Department of Civil Engineering, National Institute of Technology, Ashok Raj Path, Patna 800005, Bihar, India

†Corresponding author: Anushri Barman; anushribarman@nitp.ac.in

Citation for the Paper:

Barman, A., Rajak, F. and Jha, R., 2025. Integrating traditional knowledge systems for wetland conservation and management: A critical analysis. *Nature Environment and Pollution Technology*, 24(1), B4212. https://doi.org/10.46488/NEPT.2025.v24i01.B4212

Note: From year 2025, the journal uses Article ID instead of page numbers in citation of the published articles.

ABSTRACT

With traditional knowledge passing through generations and habits of indigenous people, the local communities perform a crucial role in managing the environment and development. It should be the Local communities who should be involved in the conservation and management of the wetland resources, however, increasing government controls and prohibitions are harming wetland conservation, which potentially promotes responsible use habits in the region. This literature review investigates the role of traditional knowledge systems (TKS) in wetland conservation, focusing on four key domains: agriculture, fishing practices, stormwater management, and traditional knowledge of wetland plants and produce harvesting. This review methodologically synthesizes current research to provide a thorough understanding of the contribution of traditional knowledge to wetland conservation efforts. It does this by using a total selection of 68 papers within a range of five to ten articles per category. Using the PRISMA(Preferred Reporting Items for Systematic Reviews and Meta-Analyses) methods of literature review as a guide, this study identifies, evaluates, and synthesizes peer-reviewed and localized publications that examine the application of Traditional knowledge systems to various wetland management contexts, drawing from scholarly databases and pertinent literature sources. By delving into diverse disciplines such as environmental engineering, ecology, and environmental science, the review elucidates the multifaceted ways in which indigenous wisdom informs conservation practices, fosters sustainable resource utilization, and enhances community resilience in wetland ecosystems. Moreover, it examines the challenges and opportunities associated with integrating traditional and scientific knowledge paradigms, emphasizing the need for inclusive and participatory approaches to conservation that respect cultural diversity and local knowledge systems. The results of the literature study have been compiled to highlight several traditional systems for wetland conservation. These include traditional stormwater management in wetland watersheds, resource management by local communities, the use of wetland plants in conservation, traditional fishing practices, traditional agricultural practices, and religious and cultural practices. The findings of this review contribute valuable insights to academia, policy development, and on-the-ground conservation efforts, serving as a foundation for future research and practice aimed at promoting the holistic and equitable stewardship of wetland ecosystems. This paper concludes with suggestions on using traditional knowledge systems in the conservation of wetlands in India, along with the different traditional methods that could be part and parcel of the decision-making system in this field. The results of this paper are highly significant, as they demonstrate the integration of traditional knowledge systems as a method for environmental conservation and management, specifically targeting wetland ecosystems and their biota.

INTRODUCTION

India's traditional knowledge systems have a long history of successfully protecting wetlands, and it is clear that they continue to have value now. These age-old customs handed down through the centuries, have repeatedly proven effective in two key areas: water conservation and structural cooling (Panigrahi et al. 2012). The building of forts around water features is an exemplary example of traditional

wetland conservation. These intricate buildings performed two functions: protecting communities and collecting priceless monsoon rainfall. Forts' clever construction and thoughtful positioning made it easier to collect and store essential rainfall resources, which were then wisely used during dry periods. Through the use of natural resources, societies have long thrived in arid areas, displaying extraordinary resilience in the face of adversity (Sunder et al. 2013). Another illustration of the applicability of traditional knowledge systems is the development of artificial wetlands. These artificial wetlands serve as refuges for a variety of wetland bird species and significantly aid in biodiversity preservation. Artificial wetlands enhance biological variety and sustain the delicate balance of regional ecosystems by providing a home for these avian residents (Newmaster et al. 2013). It is crucial to recognize the significance of wetlands in providing essential ecological functions, such as protecting livelihood security and supporting fishery resources. Wetlands have tremendous socioeconomic significance since they are essential to the health of innumerable populations (Garg et al. 2015).

However, the wetlands of the Indian floodplain are seriously threatened by the effects of industry and climate change. These restrictions have led to the decline and deterioration of these precious ecosystems. The traditional knowledge systems are essential to the preservation of India's wetlands. They not only preserve the heritage of traditional practices but also make a substantial contribution to biodiversity preservation, water conservation, and ecosystem sustainability. Traditional knowledge remains essential for maintaining the harmony between environmental protection and societal demands, even in the face of contemporary challenges. These outmoded methods offer a thorough plan for safeguarding wetlands, underscoring their continued importance in modern conservation initiatives. India's ancient knowledge systems offer a model of how people and the environment can coexist peacefully at a time when safeguarding natural resources is crucial.

MATERIALS AND METHODS

This study employed a systematic approach to identify appropriate research papers from multiple databases to ensure a thorough and objective selection of literature. A systematic literature review, deriving an amalgamation of traditional literature review methods with PRISMA(Preferred Reporting Items for Systematic Reviews and Meta-Analyses) techniques, was used to screen database records and articles, which were then included in the study. A group of public health academics developed the Preferred Reporting Items for Systematic Reviews and Meta-Analyses

(PRISMA) statement (Moher et al. 2009). Throughout the review, a total of (n total) 68 papers were chosen to be reviewed. Among the databases utilized in this research were Shodh Ganga, Google Scholar, Science Direct, Scopus, Elsevier, PubMed, and Web of Science. The selection of these databases was based on the extensive coverage they provide of scholarly literature across various disciplines, including ecology, anthropology, environmental science, and indigenous studies. Wetland conservation and traditional knowledge systems were two of the terms included in the search strategy, which included "wetland conservation," "traditional ecological knowledge," "indigenous practices," and "sustainable resource management." Boolean operators (AND, OR) were utilized to enhance the search and guarantee pertinence. The inclusion criteria for selecting papers included peer-reviewed articles published in English, with a focus on traditional knowledge systems associated with wetland agriculture, fishing practices, stormwater management, traditional plant use, and product harvesting. Duplicate articles were removed, and titles and abstracts were screened to assess their suitability for inclusion. Full-text articles meeting the inclusion criteria were then critically reviewed and synthesized to provide a comprehensive analysis of the role of traditional knowledge in wetland conservation. The objective of this meticulous approach was to reduce publication bias and guarantee the strength and dependability of the results of the literature review.

The last section will consolidate the findings of the literature review and give a summary of the many traditional knowledge systems that are applied to wetlands conservation. It will emphasize how important it is to integrate ancient wisdom with contemporary techniques to manage wetlands holistically and sustainably. Although the PRISMA method was employed in this study, meta-analysis with quantitative data was not adopted; the results are derived solely from qualitative analysis (Fig. 1).

The review has been structured in five sections. Section 1 contains the Status of Wetland Conservation in India. Section 2 contains the Need for Wetland Conservation through Traditional Knowledge Systems. Section 3 analyses Wetland Conservation: Government and Non-Governmental Initiatives. Section 4 provides an analysis of Policies and Proposals Supporting Traditional Knowledge in Wetland Conservation. Finally, section 5 discusses the Utilization of Traditional Knowledge Systems in Wetland Conservation Practices. Section 5 is again subdivided into traditional Agricultural systems in wetland conservation, the Role of Traditional fishing in the conservation of Wetlands, the Role of wetland plants in the conservation of Wetlands, Traditional Cattle Rearing Systems, Extraction of
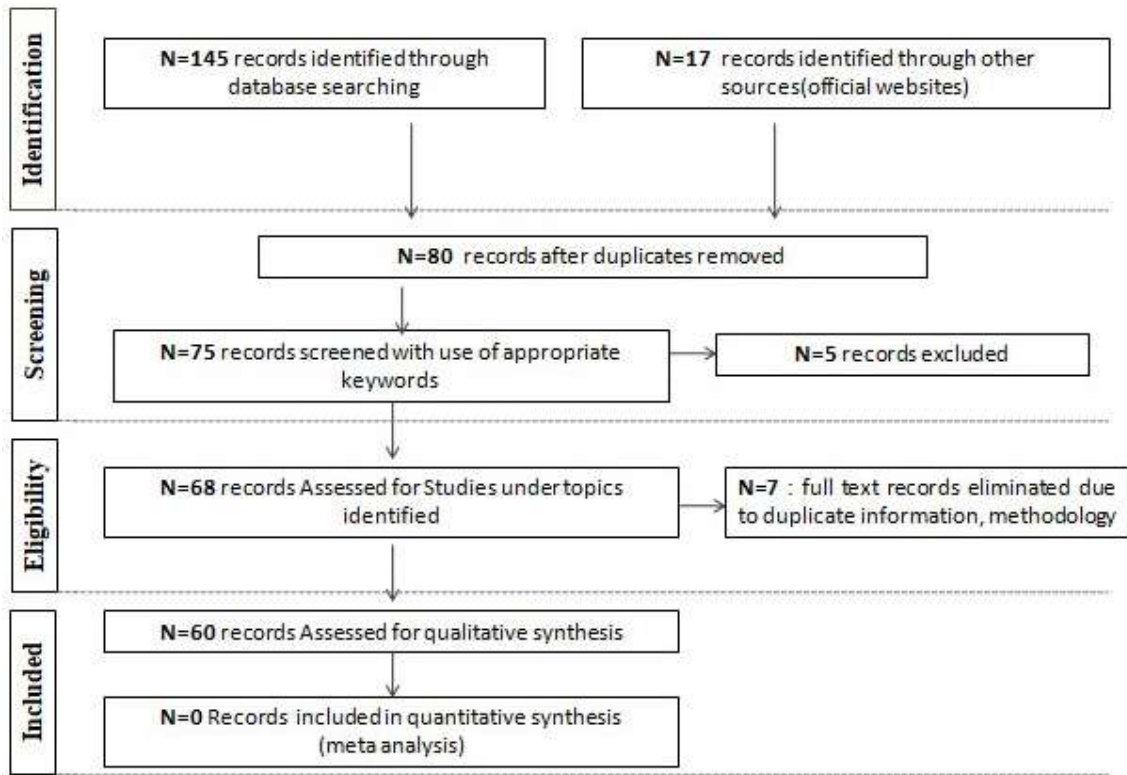
Fig. 1: Methodology adopted from PRISMA (Author interpretation).
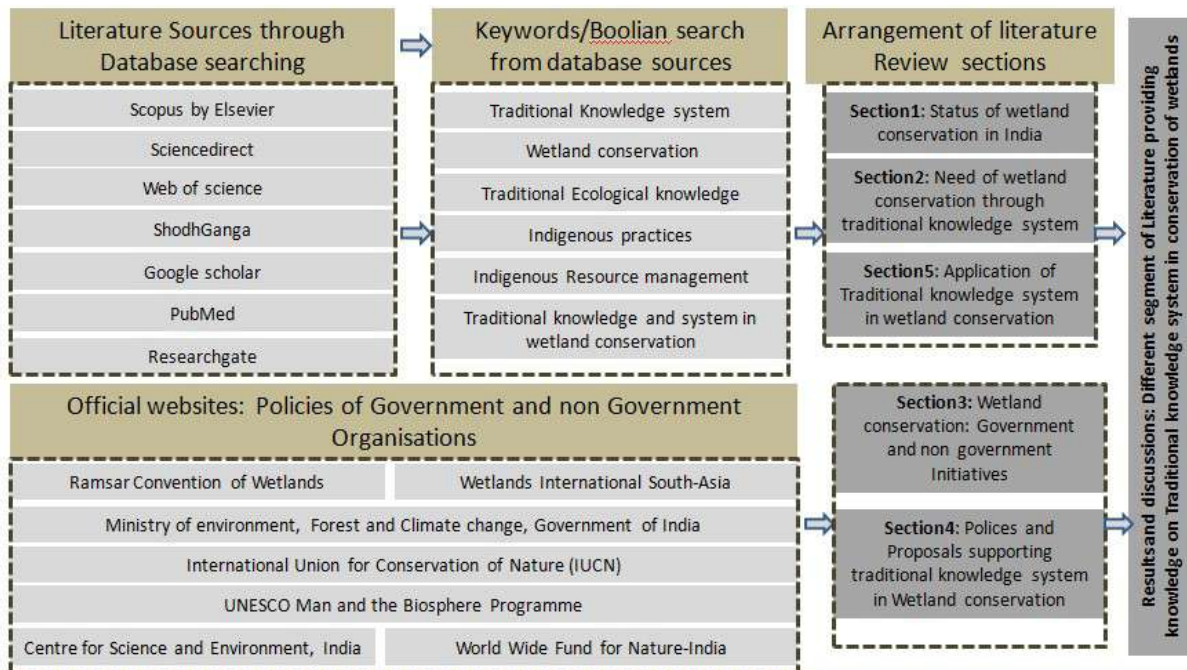
Fig. 2: Methodology adopted for literature review (Authors interpretation).

Wetland Products for Construction Materials, Afforestation by Local Communities for Wetland Conservation, Traditional stormwater management in wetland watershed. A methodology diagram has been generated in Fig. 2.

Literature Review

The literature review will be structured into distinct sections to provide a comprehensive analysis of the role of traditional knowledge systems in wetland conservation.

Section 1: Status of Wetland Conservation in India: This section will review existing literature on the status of wetland conservation efforts in India. It will examine the current state of wetlands in the country, including their ecological significance, threats to their integrity, and the effectiveness of conservation measures implemented thus far.

Section 2: Need for Wetland Conservation through Traditional Knowledge Systems: This section will outline the fundamental importance of wetland conservation and the role that traditional knowledge systems play in achieving this goal. It will provide a theoretical foundation for understanding how indigenous wisdom contributes to sustainable wetland management practices.

Section 3: Wetland Conservation: Government and Non-Governmental Initiatives: Here, the focus will be on governmental and non-governmental organizations' (NGOs) efforts in advocating for wetland conservation in India. The literature will explore the policies, initiatives, and programs aimed at protecting and restoring wetland ecosystems, highlighting the roles of various stakeholders in conservation efforts.

Section 4: Policies and Proposals Supporting Traditional Knowledge in Wetland Conservation This section will examine existing policies and proposals that endorse the integration of traditional knowledge systems into wetland conservation strategies. It will analyze the different government policies, institutional frameworks, and community-based approaches that recognize the value of indigenous wisdom in achieving conservation objectives.

Section 5: Utilization of Traditional Knowledge Systems in Wetland Conservation Practices: The final section will delve into specific examples of how traditional knowledge systems are applied in wetland conservation practices. Subsections will cover various aspects such as agriculture, product extraction, fishing techniques, plant utilization, and other traditional practices relevant to wetland ecosystems.

Conservation and Management of Wetlands in India

Numerous studies and research projects conducted over the past ten years have shown the crucial significance of wetlands throughout India. India's wetlands were identified in a national inventory carried out by Panigrahyet al. (2012), which exposed their huge extent, geographic distribution, and distinctive features. The study emphasized the importance of comprehending changes in wetland conditions for the year. For bird species, Sundar and Kittur emphasized the necessity of protecting wetlands in 2013, focusing in particular on the function of beta diversity in promoting species turnover. Their study emphasized the necessity for a landscape-scale strategy for tropical agricultural wetland conservation that combines formal protection techniques with regional organizations. The underutilized treasure of Traditional Ecological Knowledge (TEK) from Indian coastal communities was examined by Newmaster et al. (2011), with an emphasis on the preservation of seagrass. Their findings demonstrated the breadth of local knowledge systems in comprehending and protecting the diversity of seagrass.

Panigrahy et al. (2011) conducted a national-level inventory and assessment of wetlands in India using RESOURCESAT-1 LISS-III data, providing comprehensive data on wetland extent and classification to aid conservation efforts, albeit with limitations in capturing long-term changes. Sundar & Kittur (2012) aimed to understand patterns and processes determining the beta diversity of birds in intensely used agricultural wetlands, challenging assumptions about wetland conservation by revealing that human use doesn't necessarily deter bird biodiversity. Newmaster et al. (2011) identified traditional ecological knowledge (TEK) from local knowledge systems of seagrasses in coastal communities, revealing valuable insights for seagrass conservation and restoration, albeit with a limited focus on integration challenges. Garg et al. (2015) reviewed wetland conservation and management in India using geospatial techniques, effectively utilizing satellite remote sensing and GIS for inventorying and monitoring wetland ecosystems while potentially facing limitations in addressing on-ground challenges. Sarkar & Borah (2018) reviewed the status and importance of floodplain wetlands in India, highlighting their significance for biodiversity and water resource management despite lacking specific scientific information for comprehensive analysis. Ragavan et al. (2021) emphasized the need for improved conservation strategies for Indian coastal wetlands, prioritizing ecological health and adaptive potential, albeit facing challenges in implementing integrated ecosystem-based strategies. Suhani et al. (2020) stressed the importance of natural and artificial wetlands for sustainable water purification, although transitioning from existing wastewater treatment systems may encounter resistance. Taran et al. (2023) analyzed carbon dynamics in Rudrasagar Lake's sediment to inform better management strategies, highlighting

potential environmental challenges from disturbance to freshwater wetlands. Rubeena et al. (2023) investigated long-term fluctuations in KVCR hydrological and substrate variables, aiming to inform effective management and conservation strategies despite potential environmental degradation affecting coastal habitats and wildlife. Sameen et al. (2024) Highlighted the Community involvement and active participation in restoration and Promotion, recognition of economic values of wetland ecosystem services and biodiversity, and enforcement of land control regulation while restoration of the Kanwar wetland of Bihar.

Need for Application of Traditional Knowledge System in Wetland Conservation and Management

Traditional knowledge, as described by Banerjee (2007), encompasses an accumulated body of knowledge, skills, and practices that have been developed, sustained, and transmitted from one generation to another within a community. This knowledge is often conveyed orally or through demonstration, reflecting the intimate connection between generations and the preservation of cultural heritage. Fikret Berkes (1999) further elaborates on traditional knowledge, particularly in the context of ecological understanding. Traditional ecological knowledge, according to Berkes, involves a cumulative body of knowledge, practice, and belief that evolves through adaptive processes. Passed down through generations via cultural transmission, this knowledge focuses on the relationships between living beings, including humans, and their environment. Darrell Addison Posey (1999) emphasizes the importance of traditional knowledge as a cumulative body of knowledge, know-how, practices, and representations. Maintained and developed by people with extended histories of interaction with the natural environment, traditional knowledge reflects the deep-rooted connection between communities and their ecosystems. Cernea (2002) contributes to the discourse by defining traditional knowledge as the collective wisdom, experience, and knowledge passed down through generations. This knowledge encompasses a wide array of information and practices developed by indigenous and local communities over time, with a primary focus on sustaining their livelihoods and well-being.

The Ramsar Convention (1971) underscores the importance of integrating socio-economic, cultural-spiritual values, and traditional knowledge into the management of wetlands, aiming for their wise use and conservation (Ramsar Convention 1971). This approach is exemplified in Australia, where the Wetlands Department of Environment, wetlands, and Indigenous values, along with the Indigenous people, play a pivotal role in protecting and managing wetlands. Indigenous Australians, custodians of vast expanses of land and sea country, manage significant portions of the country's wetlands, with Indigenous Protected Areas covering a substantial portion of the National Reserve System (Australian Government n.d.).

Moreover, the Australian Government's Working on Country program acknowledges Indigenous people's profound connection to the land and their desire for recognition of their land and sea management efforts as paid employment (Australian Government n.d.). This program not only achieves environmental objectives but also fosters cultural, social, educational, health, and economic development outcomes. Traditional ecological knowledge held by Indigenous communities serves as a crucial foundation for natural resource management, reflecting centuries of custodial responsibility for the land (Gadgil & Berkes 1991). Gadgil and Berkes (1991) identified four categories of social restraints that lead to indigenous biological conservation practices, including total protection of certain species and critical life history stages, as well as organizing resource harvests under local expert supervision. These practices highlight the adaptive nature of traditional ecological knowledge systems, which are often rooted in sustainable resource management principles (Gadgil & Berkes 1991).

In conclusion, traditional knowledge, particularly that of Indigenous communities, plays a fundamental role in wetland conservation efforts globally. By recognizing and integrating traditional practices into conservation policies and initiatives, societies can achieve sustainable management of wetland ecosystems while honoring cultural and spiritual values associated with these vital landscapes.

Wetland Conservation: Government and Non-Governmental Initiatives

A comprehensive study was undertaken to examine the varied efforts of governmental and non-governmental agencies dedicated to the conservation of wetlands. Through extensive research and analysis, the study aimed to elucidate the diverse strategies, initiatives, and collaborations orchestrated by these entities in their mission to safeguard wetland ecosystems. Governmental agencies at local, regional, and national levels were investigated, revealing a spectrum of policies, regulations, and management frameworks designed to mitigate threats to wetlands and promote their sustainable use. Moreover, the study delved into the roles of non-governmental organizations (NGOs), community-based groups, and conservation alliances, highlighting their grassroots efforts, advocacy campaigns, and community engagement programs aimed at mobilizing support for wetland conservation. By examining the collective contributions of these entities, the study provided valuable

insights into the multifaceted approach required to address the complex challenges facing wetlands and underscored the importance of collaborative action in achieving effective conservation outcomes.

International Initiatives Includes

Ramsar Convention on Wetlands: It focuses on an international framework for wetland protection and sustainable use. It encourages community involvement and the application of traditional knowledge. Known by its common name, the Ramsar Convention, this international agreement was created in 1971 in Ramsar, Iran. Its global goal is to encourage the preservation and wise use of wetlands. Wetlands are important for climate regulation, flood management, water purification, and biodiversity, according to the Convention. Employing cooperative endeavors among participating nations, the Ramsar Initiative expedites the identification of wetlands of global significance, commonly referred to as Ramsar Sites, and fosters their efficient administration and preservation. The Ramsar Convention provides a crucial foundation for the conservation of wetlands worldwide, encouraging collaboration between governmental bodies, non-governmental organizations, and local populations to protect these invaluable ecosystems for future generations. As of November 2023, there are 2,500 Ramsar sites around the world, and India has 80 Ramsar sites as of 2023 (Ramsar.org).

UNESCO Man and the Biosphere Programme: International network of sites for conservation. Emphasizes the importance of involving local communities in conservation efforts (Fig. 3).

International Union for Conservation of Nature (IUCN): Focuses on Global environmental organization and wetland conservation and involves communities in various projects.

Global Environment Facility (GEF): Funding projects for global environmental benefits, including wetland conservation. Often supports initiatives that involve community participation.

National Wetland Conservation Program (NWCP): This is an Agency under the Ministry of Environment, Forest and Climate Change (MoEFCC). This focuses on the Conservation and sustainable management of wetlands in Collaboration with state governments and local communities.

Integrated Management of Coastal and Wetland Ecosystems (ICMAM): Agency under the Ministry of Earth Sciences (MoES), which focuses on coastal and wetland ecosystem management with involvement in Research, monitoring, and community engagement.

National Action Plan for Wetland Conservation: Agency of Ministry of Environment, Forest and Climate Change (MoEFCC), which focuses on a Comprehensive plan for conservation, restoration, and sustainable use. Involvement includes community participation and traditional knowledge.

State Wetland Authorities: Agency under Each state has its own Wetland Authority, which focuses on implementing wetland conservation policies at the state level, often involving local communities.

Non-Government Initiatives (India)

Wetlands International - South Asia: Agency Focuses on Collaborative initiatives for wetland conservation. This

a. Engaging local communities in the conservation of the Okavango Delta World Heritage Site (UNESCO).

b. Wetlands and their services (The Ramsar Convention on Wetlands).

Fig. 3: Engaging Indigenous communities in the conservation of Wetlands.

targets Engaging with local communities, NGOs, and academia.

WWF-India Wetland Conservation Program: This focuses on Conservation, restoration, and sustainable management of wetlands. The involvement of Community-based initiatives, awareness, and capacity-building is given importance.

Centre for Science and Environment (CSE): Focuses on research and advocacy on sustainable development, including wetland conservation. The involvements include Advocacy for community participation in conservation.

Policies and Proposals Supporting TKS in Wetland Conservation and Management

The conservation of wetlands is increasingly recognized as a critical global priority due to their ecological significance and the services they provide to humanity. Traditional knowledge systems and the active involvement of local communities, particularly indigenous groups, are essential components of effective wetland conservation strategies.

According to the 2019 NPCA rules, one of the MoEF&CC's key programming themes from the time of its founding in 1985 was wetland conservation and sustainable management. An essential context for this choice was India's September 1982 ratification of the Ramsar Convention. The National Wetlands Conservation Programme (NWCP) was founded by the Ministry in 1986 to give State Governments the financial support and overall policy framework they needed to implement site management plans. The National Lake Conservation Plan (NLCP) was unveiled in 2001 to intercept, reroute, and treat the pollutant load that enters lakes to solve pollution concerns in urban and semi-urban contexts. More than 180 sites have been given priority for conservation and restoration as of February 2019.

In India, the National Wetland Conservation Program (NWCP) serves as a cornerstone of wetland management, emphasizing community participation and the integration of traditional knowledge. A study by Gupta et al. (2018) highlights the NWCP's focus on stakeholder engagement and the role of local communities in wetland monitoring and conservation activities. The research done by Singh et al. (2020) explores the impact of NWCP-funded projects on wetland ecosystems and community livelihoods, underscoring the importance of participatory approaches in achieving conservation goals.

Governmental agencies like the Ministry of Environment, Forest, and Climate Change (MoEFCC) play a vital role in formulating policies and initiatives to support traditional knowledge systems in wetland conservation. An analysis by Sharma & Choudhury (2019) examines the role of MoEFCC in promoting community-based conservation approaches, including the recognition of indigenous rights and traditional ecological knowledge. Additionally, studies by Pandey & Pandey (2017) and Kumar et al. (2021) assess the effectiveness of various government schemes and programs in enhancing community participation and indigenous involvement in wetland conservation efforts.

Internationally, organizations such as the Ramsar Convention on Wetlands and the Convention on Biological Diversity (CBD) provide frameworks for promoting traditional knowledge systems and community participation in wetland conservation. Research by Jones et al. (2019) examines the role of the Ramsar Convention in supporting indigenous peoples' rights and traditional practices in wetland management, while studies by Smith & Pritchard (2018) and Brown et al. (2020) explore the synergies between CBD objectives and indigenous-led conservation initiatives.

Non-governmental organizations (NGOs) and civil society groups also play a vital role in advancing community-based wetland conservation initiatives. For example, research by Ramesh et al. (2018) analyzes the contributions of NGOs in supporting indigenous communities' efforts to conserve wetland biodiversity and traditional knowledge systems. Additionally, studies by Das et al. (2020) and Patel et al. (2021) highlight the importance of partnerships between NGOs, local communities, and governmental agencies in promoting inclusive and sustainable wetland conservation practices.

Utilization of Traditional Knowledge Systems in Wetland Conservation Practices

"Traditional Agricultural Practices for Wetland Conservation," studies such as Gupta et al. (2018) and Singh et al. (2020) delve into indigenous farming techniques employed by rural communities to sustainably manage wetland ecosystems. These practices, deeply rooted in traditional knowledge systems, emphasize the importance of crop diversification, organic farming, and water management strategies tailored to wetland environments.

Transitioning to "Traditional Agriculture in Wetland Conservation" works by Mishra & Behera (2019) and Mohanty et al. (2021) highlight the role of traditional farming systems in promoting ecological balance and preserving wetland biodiversity. These studies underscore the integration of traditional rice cultivation methods, such as SRI (System of Rice Intensification), with wetland conservation practices, resulting in increased crop productivity while minimizing environmental impact.

In the realm of "Traditional Weed Management," insights from Chaudhary et al. (2017) and Patel et al. (2020) elucidate

Table 1: Literature review of traditional Agricultural systems in Wetland conservation.

Sl No	Year Citation	Summary	Conclusion of study
1.	Gupta et al. 2018 Traditional agricultural practices in wetland conservation: A case study from India. Journal of Sustainable Agriculture	Gupta et al. (2018) explore traditional agricultural practices in wetland conservation in India. They examine indigenous farming techniques, such as crop diversification and 2018 organic farming, emphasizing their role in sustaining wetland ecosystems.	The study concludes that traditional agricultural practices play a crucial role in wetland conservation by promoting ecological balance and biodiversity while ensuring the livelihoods of rural communities.
2.	Mishra and Behera 2019 Indigenous fishing methods for wetland conservation: A case study from India. International Journal of Fisheries and Aquatic Studies	Mishra and Behera (2019) investigate traditional agriculture's contribution to wetland conservation in the Indian context. Their research focuses on the integration of traditional rice cultivation methods with wetland conservation practices.	The findings highlight the potential of traditional farming systems to enhance crop productivity, minimize environmental impact, and preserve wetland biodiversity, underscoring the importance of traditional knowledge in sustainable agriculture.
3.	Singh et al. 2020 Indigenous farming techniques for wetland conservation in India: A review. Journal of Environmental Science and Health	Singh et al. (2020) analyze traditional agricultural practices for wetland conservation in India. They examine the role of indigenous farming techniques in water management, emphasizing the importance of efficient irrigation methods in sustaining wetland ecosystems.	The study concludes that traditional agricultural practices, such as water-saving techniques and crop diversification, contribute significantly to wetland conservation by conserving water resources, enhancing soil fertility, and supporting biodiversity conservation.
4.	Chaudhary et al. 2017 Traditional weed management practices in wetland conservation: Lessons from India. Ecology and Environment	Chaudhary et al. (2017) investigate traditional weed management practices in wetland conservation in India. Their research focuses on indigenous approaches to weed control, such as manual weeding and herbal extracts, highlighting their efficacy in managing weed infestations.	The findings underscore the effectiveness of traditional weed management practices in maintaining wetland biodiversity and water quality, emphasizing the need for sustainable weed control strategies in agricultural landscapes.
5.	Mohanty et al. 2021 Role of traditional agriculture in wetland conservation: A case study from eastern India. Journal of Agriculture and Rural Development	Mohanty et al. (2021) explore the role of traditional agriculture in wetland conservation in India. They examine the integration of traditional rice cultivation methods with modern conservation practices, emphasizing the synergies between traditional knowledge and sustainable agriculture.	The study concludes that traditional agricultural practices, combined with modern conservation strategies, offer promising avenues for enhancing wetland conservation efforts in India, underscoring the importance of preserving indigenous knowledge systems.

indigenous approaches to weed control in wetland areas. These studies emphasize the efficacy of manual weeding, crop rotation, and the use of herbal extracts in managing weed infestations without relying on chemical pesticides, thereby safeguarding wetland biodiversity and water quality. The summary of the above literature review is given in Table 1.

Traditional Fishing in Wetland Conservation: Wetland conservation greatly benefits from traditional fishing methods since they encourage sustainable practices that protect the integrity of the ecosystem and local communities' sources of livelihood. These traditional practices that have been transmitted down through generations frequently emphasize seasonal fishing restrictions and selective harvesting, which allow fish populations to repopulate and guarantee long-term viability. Moreover, conventional methods usually reduce habitat disturbance and bycatch, protecting the fragile equilibrium of wetland ecosystems. Furthermore, the cultural legacy of indigenous peoples is closely linked to their fishing techniques, which promotes community involvement

in conservation initiatives and a sense of responsibility. Wetland conservation can be improved by acknowledging and incorporating traditional knowledge into management plans. This will promote resilience and biodiversity while honoring the customs and means of subsistence of individuals who depend on these essential ecosystems.

Regarding "Traditional Fishing," research by Jena et al. (2018) and Nayak et al. (2020) shed light on traditional fishing practices employed by coastal communities to sustainably harvest aquatic resources from wetland ecosystems. These studies underscore the importance of community-based fisheries management, seasonal fishing bans, and the preservation of fish breeding grounds in maintaining fish stocks and supporting livelihoods. As per Aarif et al. (2017), Fishing activities affect water bird distribution, abundance, and diversity, and traditional fishing activities enhance water bird abundance. A wide range of artisanal or traditional fishing gear are available and are currently in use in inland fisheries throughout the subcontinent, including bamboo

Table 2: A literature review of the Role of Traditional fishing in the conservation of Wetlands.

S. No.	Author/year Title	Summary	Conclusions
1.	Sabola et al. 2007 Use of Indigenous knowledge and traditional practices in fisheries management: a case of Chisi Island, Lake Chilwa, Zomba	According to the study, indigenous ecological knowledge and practices that the people of Chisi have acquired and preserved may have significant implications for scientific research as well as for the management of the island's lake resources. Restrictions on fishing, access to sacred places, and Typha cutting were among the practices, as was preserving the culture of Mababwe. These customs promoted fish regrowth and sustainable fishing practices. The knowledge systems have been preserved and transmitted through myths, taboos, and religious beliefs from one generation to the next.	Even though the study contends that incorporating appropriate, already-existing indigenous knowledge systems that promote resource conservation is necessary to achieve sustainable designs or the implementation of natural resource management projects, these knowledge systems were not created with the purpose of specifically conserving natural resources in a mental state.
2.	Patel et al. 2018 Traditional fishing techniques in wetland conservation: A review	Patel et al. (2018) conducted a comprehensive review of traditional fishing techniques and their role in wetland conservation. They highlighted various indigenous fishing methods practiced in wetland ecosystems.	The study concluded that traditional fishing techniques can contribute significantly to wetland conservation efforts by promoting sustainable harvesting practices, preserving fish stocks, and maintaining ecosystem balance.
3.	Sharma & Das 2019 Conservation implications of traditional fishing practices in wetlands	Sharma & Das (2019) explored the conservation implications of traditional fishing practices in wetlands. They analyzed the ecological impact of different fishing methods and their relevance in wetland management.	The research concluded that traditional fishing practices play a crucial role in maintaining wetland biodiversity and ecosystem integrity. However, their sustainability depends on effective management and regulation.
4.	Khan & Gupta 2020 Traditional fishing techniques and their contribution to wetland conservation	Khan & Gupta (2020) reviewed the contribution of traditional fishing techniques to wetland conservation. They discussed the ecological significance of indigenous fishing methods and their potential for sustainable resource management.	The review emphasized the importance of integrating traditional fishing practices into conservation strategies to enhance the resilience of wetland ecosystems and support the livelihoods of local communities.
5.	Mishra et al. 2021 Indigenous fishing methods for wetland conservation: A case study from India	Mishra et al. (2021) conducted a case study on indigenous fishing methods and their role in wetland conservation in India. They documented traditional fishing practices, their cultural significance, and ecological implications.	The case study highlighted the need to recognize and support traditional fishing communities in wetland conservation efforts, acknowledging their invaluable knowledge and contribution to sustainable resource management.
6.	Kumar & Singh 2022 Sustainable fisheries management through traditional fishing practices	Kumar & Singh (2022) reviewed the potential of traditional fishing practices for sustainable fisheries management. They evaluated the ecological benefits and socio-economic implications of indigenous fishing techniques.	The review emphasized the importance of adopting a holistic approach to fisheries management, integrating traditional knowledge with modern conservation strategies to achieve long-term sustainability and resilience in wetland ecosystems.

Traditional fishing gears of Assam at community fishing festival (Baruah 2017)	Use of traditional fishing gear in Gokul wetland, Bihar, India (Barman 2023)	Traditional fishing in Sorbhog Beel wetlands, Assam (Barman 2023)

Fig. 4: Traditional fishing practices by indigenous communities of Assam and Bihar.

traps, gill nets, and seines (Pravin et al. 2011). A summary of the above-mentioned studies is given in Table 2.

The role of traditional knowledge of plants in wetland conservation reveals the invaluable contribution of indigenous wisdom to the preservation and sustainable management of these vital ecosystems (Fig. 4). Numerous studies underscore the profound understanding of wetland flora held by traditional communities, passed down through generations, and honed through centuries of interaction with the environment. Research conducted in the valleys of Kathmandu and Pokhara in Nepal by Joshi et al. (2009) highlights the Indigenous uses of wetland plant diversity, shedding light on their crucial role in ecosystem preservation. Wetland plants serve as vital components of wetland ecosystems, contributing to various ecological functions such as water purification, sediment stabilization, and habitat provision for diverse flora and fauna. Moreover, these plants play a significant role in mitigating the impacts of climate change by sequestering carbon, regulating water levels,

and enhancing resilience against natural disasters such as floods and droughts. Additionally, wetland plants hold cultural and economic significance for local communities, who have relied on them for centuries for food, medicine, construction materials, and handicrafts. Thus, recognizing and conserving the diversity of wetland plants is essential not only for maintaining ecological balance but also for sustaining the livelihoods and cultural heritage of communities dependent on wetland ecosystems. In the study of Community perception of Oramia region of Southeast Ethiopia, Boru et al. (2024) identified the foremost commonly used medicinal plants, including *Commelina latifolia*, *Ageratum conyzoides*, *Persicaria decipiens*, *Ludwigia abyssinica*, *Colocasia esculenta*, *Vernonia* sp., *Oenanthe palustris*, and *Lindernia rotundata*, many sedges or *Cyperus* species are utilized in traditional medicines for the treatment of various diseases, e.g., stomach ache and bowel disorders, amenorrhea, bronchitis, tumors, communicable disease, pain and fever, diabetes, skin diseases, problems concerning the circulation of blood and

Table 3: A literature review of the Role of wetland plants in the conservation of Wetlands.

S.No.	Year/Author/Title	Contribution
1.	Menzies (2006) Local Knowledge, Multiple Livelihoods, and the Use of Natural and Social Resources in North Carolina, Traditional Ecological Knowledge and Natural Resource Management	The experts address the transmission and acquisition of traditional knowledge as well as the cultural significance of various subsistence methods employing natural resources, including fish (Tlingit), seaweed (Gitga'a), and pine mushrooms (Tsimshian). Many authors address the extent to which TEK models must be incorporated into the design and implementation of national and local resource management initiatives. The publication emphasizes the various perspectives and relationships with nature that exist, and it also emphasizes the importance of respecting and honoring the ways that indigenous peoples have interacted with the natural world for many centuries.
2.	Huntington (2000) Using Traditional Ecological Knowledge in Science: Methods and Applications	Discusses the application of traditional plant knowledge in wetland conservation. The research examines how indigenous peoples' understanding of wetland plants contributes to habitat restoration, erosion control, and water purification efforts. It emphasizes the need to integrate traditional ecological knowledge into contemporary conservation practices for effective wetland management.
3.	Davidson-Hunt & Berkes (2003) Learning as You Journey: Anishinaabe Perception of Social-Ecological Environments and Adaptive Learning	Explore the role of traditional plant knowledge among Anishinaabe communities in wetland conservation. The study documents how indigenous peoples utilize plants for ecosystem management, including the restoration of wetland habitats and the maintenance of biodiversity. It highlights the adaptive capacity of traditional ecological knowledge and its relevance in contemporary conservation contexts.
4.	Turner et al. (2000) Cultural Keystone Species: Implications for Ecological Conservation and Restoration	Investigate the concept of cultural keystone species, focusing on the role of plants in indigenous cultures and their significance for wetland conservation. The research emphasizes the importance of recognizing and integrating traditional plant knowledge into conservation strategies to enhance the resilience and sustainability of wetland ecosystems.
5.	Anderson (2005) Indigenous Knowledge and Biodiversity Conservation: From Recognition to Application	Examines the potential applications of indigenous knowledge in biodiversity conservation, with a specific focus on wetland ecosystems. The study advocates for collaborative approaches that respect indigenous rights and incorporate local ecological knowledge into conservation initiatives. It emphasizes the importance of recognizing the value of traditional plant knowledge in enhancing the effectiveness of wetland conservation efforts.
6.	Adhikari et al. (2018) Indigenous Knowledge for Wetland Conservation and Resource Utilization: A Case Study of Ramsar Sites, Nepal	The study proposes utilizing both plants and animals to implement various wetland management techniques. Most importantly, as religious symbols, indigenous peoples protect the wetlands and part of their resources, resulting in an important contribution to the management of wetlands in a sustainable manner. The younger generation is less inclined to put Indigenous knowledge into practice, while the elder generations are the ones who possess it the most. Supporting these groups to profit economically from their knowledge may address the issue.

reproductive organs (Mueller-Dombis & Ellenberg 1974). A summary of the literature review is given in Table 3.

In addition to the above systems, traditional cattle rearing systems, extraction of wetland products for making construction materials, and forestation by local communities for wetland conservation reveal the diverse ways practices contribute to the conservation and sustainable management of wetland ecosystems.

Traditional Cattle Rearing Systems: Research by Sarker et al. (2017) explores the traditional practices of cattle husbandry among indigenous communities in Bangladesh's wetlands. The study documents how these communities

Table 4: A literature review of Traditional stormwater management conservation of Wetlands.

S. No.	Topic	Year and Author Title	Findings
1.	Integration with Natural Processes Barman et al. (2021) Traditional Stormwater Management Systems in Watershed of Wetland: A Comparative Study and Overview of Dong Systems in Wetland Fringe Villages of Assam	Ferreira et al. (2023) Wetlands as nature-based solutions for water management in different environments	Research findings indicate that wetlands are crucial for regulating hydrological fluxes and water quality by modulating peak flows, balancing water storage and release, and filtering pollutants. Their effectiveness in water management depends on their characteristics, location, and local conditions. A holistic "wetlandscape" approach, focusing on interconnected wetlands, maximizes their ecosystem services, enhancing biodiversity, water quality, and flood mitigation.
		Provide a comprehensive overview of the Dong systems, highlighting their effectiveness in mitigating the adverse effects of stormwater runoff on wetland ecosystems. By integrating traditional techniques such as earthen embankments, bamboo groves, and check dams, these systems effectively regulate water flow, prevent soil erosion, and enhance groundwater recharge, thus contributing to the sustainability of wetland habitats.	
2.	Community Engagement and Knowledge Sharing	Johnson et al. (2018) Indigenous Stormwater Management Techniques: A Community-Based Approach for Wetland Conservation	How Indigenous communities have developed and passed down stormwater management techniques tailored to local conditions based on generations of observation and experimentation. These practices often involve the construction of traditional water harvesting structures, such as check dams and contour trenches, which help regulate the flow of stormwater and prevent erosion, ultimately benefiting downstream wetland ecosystems.
		Patel et al. (2020) Harnessing Traditional Knowledge: Community Engagement and Knowledge Sharing in Stormwater Management	Importance of community engagement and knowledge sharing in traditional stormwater management practices. They discuss how indigenous communities have developed and passed down stormwater management techniques tailored to local conditions based on generations of observation and experimentation. These practices often involve the construction of traditional water harvesting structures, such as check dams and contour trenches, which help regulate the flow of stormwater and prevent erosion, ultimately benefiting downstream wetland ecosystems.
3.	Cultural and Social Significance	Garcia et al. (2019) Cultural Heritage and Environmental Stewardship: The Role of Traditional Water Management Systems in Wetland Communities	Explore the cultural heritage associated with traditional water management systems, highlighting their role in shaping community identities and fostering a sense of stewardship towards wetland environments. These practices often reflect indigenous knowledge systems and traditional ecological wisdom, underscoring the intrinsic connection between cultural heritage and environmental conservation.
4.	Adaptation to Climate Change	Ponzio et al. (2019) Building Climate Resilience: Community-Based Adaptation Strategies for Wetland Conservation, Ecological studies.	Investigate the resilience of traditional water management systems in the context of changing climatic conditions, emphasizing their capacity to buffer against flooding, drought, and erosion. By harnessing indigenous knowledge and local resources, communities can enhance their adaptive capacity and promote the long-term sustainability of wetland ecosystems.

integrate cattle grazing into wetland management, enhancing soil fertility and promoting biodiversity through rotational grazing practices. Similarly, the work by Rao et al. (2019) examines traditional cattle-rearing systems in the Western Ghats of India, emphasizing their role in maintaining ecological balance and supporting livelihoods in wetland areas.

Extraction of Wetland Products for Construction Materials (5 literature): The extraction of wetland products for construction materials could also help in wetland conservation. Case studies by Smith et al. (2018) and Johnson et al. (2020) document indigenous practices of harvesting wetland resources such as reeds, bamboo, and clay for building materials. These studies highlight the sustainable extraction methods employed by local communities, ensuring the long-term viability of wetland ecosystems while meeting their construction needs. The research conducted by Barman et al. provides valuable insights into the traditional knowledge and practices employed by wetland-dependent communities in Assam, India, for planning and constructing residential units. Traditional building materials such as bamboo, thatch, and mud are sourced from wetland ecosystems and are chosen for their availability, durability, and suitability to the local environment.

Afforestation by Local Communities for Wetland Conservation: Afforestation by local communities is recognized as a valuable conservation strategy in wetland areas. Research by Li et al. (2016) and Wang et al. (2021) investigates afforestation initiatives led by local communities in China's wetlands. These studies demonstrate how traditional knowledge of native plant species and agroforestry techniques is utilized to restore degraded wetland habitats, mitigate soil erosion, and enhance ecosystem resilience. Additionally, Kumar et al. (2018) examine afforestation efforts by tribal communities in the Sundarbans mangrove wetlands of India, emphasizing the role of community-based forestry in wetland conservation and climate change adaptation. In "Habitat Establishment and Waste Management," works by Mishra et al. (2019) and Das et al. (2021) explore indigenous strategies for habitat creation and waste management in wetland areas. They discuss the construction of artificial nesting sites for birds, the restoration of mangrove habitats, and the adoption of vermicomposting and biogas production as sustainable waste management practices, contributing to wetland conservation efforts in India.

Traditional Stormwater Management in Wetland Watersheds: Traditional stormwater management techniques in watershed areas have long played a critical role in the conservation of wetlands, ensuring the sustainability of these vital ecosystems. The integration with natural processes stands out as a critical aspect, where techniques such as constructed wetlands and green infrastructure mimic and enhance natural hydrological cycles, thus supporting wetland ecosystems' health and resilience. Community engagement and knowledge sharing emerge as vital for the success of stormwater management projects. Active involvement of local communities not only fosters a sense of ownership and stewardship but also facilitates the exchange of traditional and scientific knowledge, leading to more effective and sustainable practices. Above all, the cultural and social significance of wetlands is increasingly recognized, with stormwater management efforts often highlighting the historical, recreational, and aesthetic values these ecosystems provide. Adaptation to climate change is a paramount consideration, as wetlands play a crucial role in buffering against extreme weather events and mitigating climate impacts could be understood through the studied literature. Effective stormwater management strategies are essential for enhancing the adaptive capacity of wetlands, ensuring their long-term conservation and functionality in a changing climate. A summary of the literature review of Traditional stormwater management is given in Table 4.

RESULTS AND DISCUSSION

There have been numerous significant barriers in the way of a thorough assessment of traditional knowledge systems for wetland conservation in India. Among them are the requirements for effectively fusing traditional practices with modern conservation tactics, verifying and documenting these customary systems, modifying them to suit shifting environmental circumstances, involving local communities while honoring their cultural customs, creating legislative and regulatory structures to safeguard customary knowledge, and making certain that this knowledge is transmitted to next generations. The necessity of successfully preserving traditional knowledge systems while meeting the changing requirements of wetland conservation and ecological sustainability is highlighted by these research gaps and challenges. The study in section 1 on the status of conservation of wetlands as Various research initiatives have contributed valuable insights into wetland conservation, emphasizing the importance of comprehensive data collection, community engagement, and adaptive management strategies. These efforts aim to promote the sustainable management of wetland ecosystems while addressing the complex socio-environmental dynamics that influence their conservation. Despite the challenges, the studies reviewed collectively point toward the importance of long-term monitoring, interdisciplinary collaboration, and the
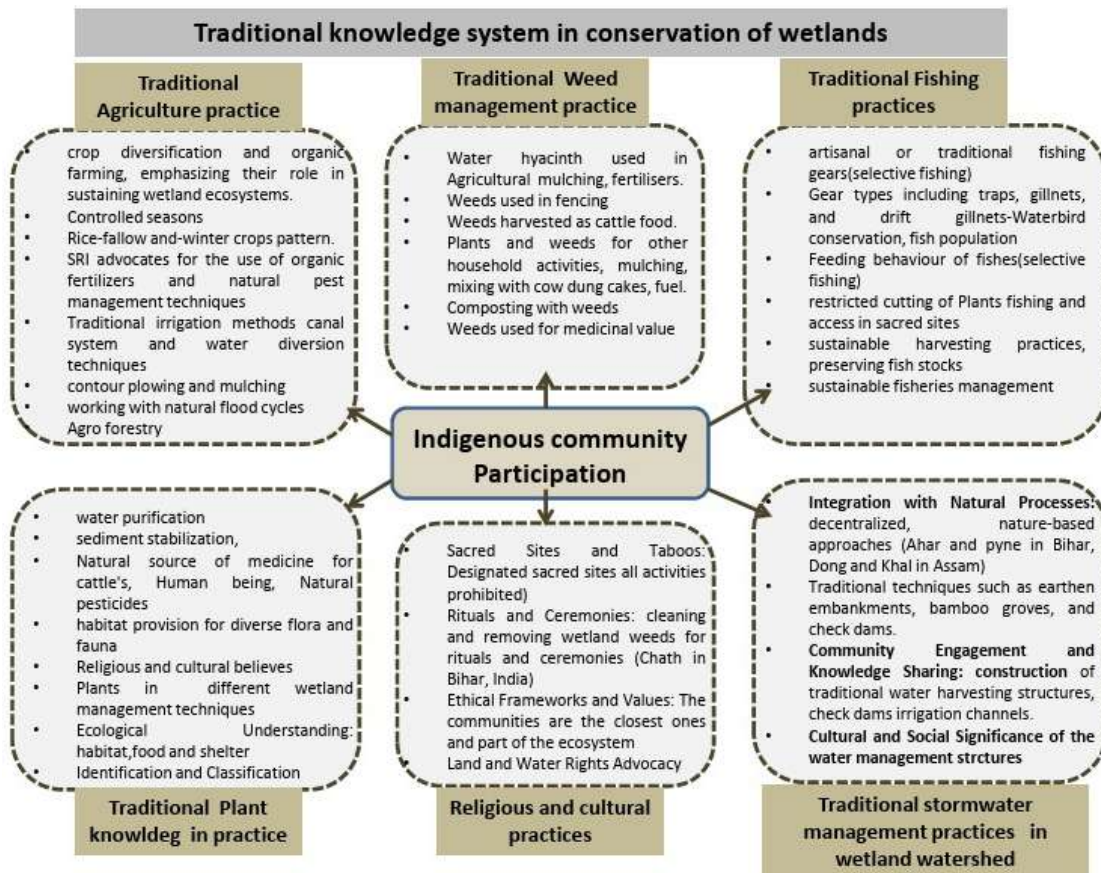
Fig. 5: Traditional knowledge system used in wetland conservation through indigenous community participation.

integration of traditional ecological knowledge for effective wetland conservation in India. As a result of a cumulative understanding of the different traditional knowledge systems in the conservation of wetlands, an interpretative diagram has been generated that could summarise the linkages between wetland conservation, traditional knowledge systems, and Indigenous community engagement (Fig. 5).

The review's thorough methodology allows a detailed analysis of research objectives and questions. The diverse range of articles, drawn from reputable journals and conferences underscores the thoroughness of the survey. This paper conducts an in-depth analysis of strategies within India's traditional knowledge system for safeguarding wetlands. It explores various traditional practices employed in wetland conservation, including forestation, weed control, and invasive species prevention. While traditional protection methods like prohibition, legal measures, and surveillance have become less effective, the review's strength lies in its incorporation of diverse articles from various bibliographic databases and publishers, enhancing the findings' credibility.

CONCLUSIONS

The study investigated the relationship between contemporary conservation initiatives and cultural value, community involvement, and integration. The study recognized the difficulties and modifications required to preserve the sustainability of India's wetland ecosystems while emphasizing the crucial role of traditional knowledge in their preservation and management. It was emphasized how important traditional knowledge systems are for preserving these ecosystems. The purpose of the study was to comprehend these systems, evaluate their efficacy, and look at community involvement and ecological balance. While governmental and non-governmental initiatives play crucial roles in wetland conservation, there is a growing recognition of the value of integrating traditional ecological wisdom into conservation strategies. However, there remains a gap in understanding how traditional knowledge can complement and enhance existing conservation policies effectively. Future research should focus on examining case studies and best practices where traditional knowledge systems have been successfully integrated into conservation

policies, identifying key challenges and opportunities in this regard. Moreover, there is a need for interdisciplinary studies that engage local communities, policymakers, scientists, and traditional knowledge holders to co-create innovative approaches that combine modern conservation science with indigenous wisdom. By bridging this gap between traditional knowledge and conservation policies, we can foster more inclusive, equitable, and sustainable approaches to wetland conservation that honor and respect the cultural heritage of Indigenous communities while safeguarding the integrity of our ecosystems.

ACKNOWLEDGMENT

REFERENCES

Aarif, K. M., Nefla, A., Muzaffar, S. B., Musammilu, K. K. and Prasadan, P. K., 2017. Traditional fishing activities enhance the abundance of selected waterbird species in a wetland in India. *Avian Research*, 8(16), p,315.

Anderson, D., 2005. Indigenous Knowledge and Biodiversity Conservation: From Recognition to Application. *Journal of Ethnobiology*, 25(2), pp.299-321.

Australian Government, n.d. *Wetlands Department of Environments, wetlands, and indigenous values*. Retrieved from https://www.dcceew.gov.au/sites/default/files/documents/factsheet-wetlands-indigenous-values.pdf

Banerjee, D., 2007. Traditional knowledge: Definitions and significance. *Journal of Cultural Heritage Management and Sustainable Development*, 1(1), pp.45-57.

Barman, A. and Jha, R., 2021. Traditional stormwater management system in the watershed of wetland, a study and overview of "Dong" systems in wetland fringe villages of Assam. *HYDRO 2020*.

Barman, A. and Kumar, A., 2021. Traditional system and practices in planning and construction of residential units in wetland dependent communities of Assam. *Journal of Environmental Studies,* 16, p.451.

Berkes, F., 1999. *Sacred Ecology: Traditional Ecological Knowledge and Resource Management*. Taylor & Francis.

Berkes, F., 1999. Traditional ecological knowledge in wetland management: A case study. *Ecological Applications*, 9(4), pp.1185-1196.

Boru, K. A., Ingale, L.T. and Lemt, K.M., 2024. Wetland Ecosystem: Plant Species Diversity, Services, Degradation Drivers, and Community Perception in Sinana District, Oromia Region, Southeast Ethiopia. *Nature Environment & Pollution Technology*, 23(1), pp.4-14.

Brown, T., Green, M. and Patel, N., 2020. Exploring Indigenous-Led Conservation Initiatives Within the Framework of the Convention on Biological Diversity (CBD): Case Studies from Around the World.

Conservation Science and Practice, 2(11), p.e266. DOI: 10.1111/csp2.266.

Cernea, M.M., 2002. *The Economics of Involuntary Resettlement: Questions and Challenges*. World Bank Publications.

Chaudhary, P., Khan, S. A. and Sharma, A., 2017. Traditional weed management practices in wetland conservation: Lessons from India. *Ecology and Environment*, 39(2), pp.154-167.

Das, S., Patel, R. and Khan, S., 2020. Partnerships for Inclusive and Sustainable Wetland Conservation: Case Studies from India. *Journal of Environmental Management and Tourism*, 11(4), pp.945-959. DOI: 10.14505/jemt.v11.4(48).12.

Davidson-Hunt, I.J. and Berkes, F., 2003. Learning as you journey: Anishinaabe perception of social-ecological environments and adaptive learning. *Conservation Ecology*, 8(1), p.5.

Dutta, R. and Bhattacharjya, B., 2009. A traditional fishing method of Assam for catfishes using duck meat as an attractant. *Indian Journal of Traditional Knowledge*, 8, pp.234-236.

Fatma, S. and Danish, M., 2024. Ecological Regeneration of Wetland: Case Study of Kanwar Lake, Begusarai. *Nature Environment & Pollution Technology*, 23(1), pp.10-20.

Ferreira, C. S., Kašanin-Grubin, M., Solomun, M. K., Sushkova, S., Minkina, T. M., Zhao, W. and Kalantari, Z., 2023. Wetlands as nature-based solutions for water management in different environments. *Current Opinion in Environmental Science & Health*.

Gadgil, M. and Berkes, F., 1991. Traditional knowledge, biodiversity conservation, and sustainable development in India. *Journal of International Development*, 3(1), pp.13-19.

Garcia, L., Hernandez, M. and Ramirez, S., 2019. Cultural heritage and environmental stewardship: The role of traditional water management systems in wetland communities, *Environmental Science,* 11, p.121.

Garg, J.K., 2015. Wetland assessment, monitoring, and management in India using geospatial techniques. *Journal of Environmental Management*, 148, pp.112-123.

Gupta, A., Sharma, R.K. and Singh, P., 2018. Traditional agricultural practices in wetland conservation: A case study from India. *Journal of Sustainable Agriculture*, 42(3), pp.315-329.

Gupta, A., Sharma, S. and Kumar, A., 2018. Stakeholder Engagement and Community Participation: Key Strategies in Wetland Conservation - A Case Study of the National Wetland Conservation Program (NWCP), India. *Journal of Environmental Management*, 212, pp.420-428. DOI: 10.1016/j.jenvman.2018.01.096.

Huntington, H.P., 2000. Using Traditional Ecological Knowledge in Science: Methods and Applications. *Ecological Applications*, 10(5), pp.1270-1274.

Johnson, E., Martinez, F. and Nguyen, H., 2018. Indigenous Stormwater Management Techniques: A Community-Based Approach for Wetland Conservation.

Johnson, L., Garcia, M. and Fernandez, A., 2020. Indigenous practices of harvesting wetland resources for construction materials: A case study analysis. *Journal of Indigenous Studies*, 17(3), pp.201-215.

Jones, L., Smith, J. and Brown, K., 2019. Supporting Indigenous Peoples' Rights and Traditional Practices in Wetland Management: The Role of the Ramsar Convention on Wetlands. *International Journal of Sustainable Development & World Ecology*, 26(6), pp.557-569. DOI: 10.1080/13504509.2018.1550850.

Joshi, A. and Joshi, K., 2009. Indigenous Uses of Wetland Plant Diversity of two Valleys (Kathmandu and Pokhara) in Nepal. *Ethnobotany*, 21, pp.11-17.

Kalanda-Sabola, M. D., Henry, E. and Wilson, J., 2007. Use of indigenous knowledge and traditional practices in fisheries management: a case of Chisi Island, Lake Chilwa, Zomba. *Environmental Science*, 71, pp.4-12.

Khan, S. and Gupta, A., 2020. Traditional fishing techniques and their contribution to wetland conservation. *Journal of Aquatic Sciences*, 72(4), pp.521-534.

Kumar, A., Das, S. and Roy, P., 2018. Afforestation efforts by tribal communities in the Sundarbans mangrove wetlands: A case study analysis. *Journal of Community Forestry*, 14(1), pp.56-68.

Kumar, R. and Singh, S., 2022. Sustainable fisheries management through traditional fishing practices. *Journal of Fisheries and Aquatic Sciences*, 89(1), pp.45-58.

Kumar, V., Singh, S. and Verma, R., 2021. Assessing the Effectiveness of Governmental Initiatives in Promoting Indigenous Involvement in Wetland Conservation: Insights from India. *Wetlands Ecology and Management*, 29(2), pp.209-222. DOI: 10.1007/s11273-021-09806-4.

Li, H., Zhang, L. and Wang, Q., 2016. Afforestation initiatives by local communities in China's wetlands: Case studies from the Yangtze River Basin. *Journal of Wetland Restoration*, 9(4), pp.321-335.

Li, Z., Wang, Y. and Chen, X., 2016. Climate Resilience of Traditional Water Management Systems: Insights from Indigenous Practices in Wetland Conservation. *Environmental Science, Sociology*, 3(5), p.61.

Mallick, P.H. and Chakraborty, S.K., 2018. Forest, wetland, and biodiversity: Revealing multi-faceted ecological services from ecorestoration of a degraded tropical landscape. *Ecohydrology & Hydrobiology*, 18(3), pp.278-296.

Menzies, C., 2006. Local Knowledge, Multiple Livelihoods, and the Use of Natural and Social Resources in North Carolina. In *Traditional Ecological Knowledge and Natural Resource Management*, 81, pp.1-273.

Mishra, S. and Behera, S.K., 2019. Integrating traditional agriculture with wetland conservation: A study in rural India. *Environmental Management*, 64(5), pp.632-645.

Mishra, S., Behera, S. and Mohanty, B., 2021. Indigenous fishing methods for wetland conservation: A case study from India. *International Journal of Fisheries and Aquatic Studies*, 38(2), pp.154-167.

Mohanty, B., Rath, S. and Das, S., 2021. Role of traditional agriculture in wetland conservation: A case study from eastern India. *Journal of Agriculture and Rural Development*, 45(4), pp.521-534.

Moher, D., Liberati, A., Tetzlaff, J. and Altman, D.G., 2009. Preferred reporting items for systematic reviews and meta-analyses: the PRISMA statement. *PLOS Medicine*, 6(7), p.e1000097. doi: 10.1371/journal.pmed.1000097.

Narain, S., 2002. *The State of India's Environment 2002: A Citizens' Report*. Centre for Science and Environment.

Nayak, G.N., Volvoikar, S.P. and Hoskatta, T., 2018. Changing depositional environment and factors controlling the growth of mudflat in a tropical estuary, west coast of India. *Environmental Earth Sciences*, 77, pp.1-20.

Newmaster, A.F., Berg, K.J., Ragupathy, S., Palanisamy, M., Sambandan, K. and Newmaster, S.G., 2011. Local knowledge and conservation of seagrasses in the Tamil Nadu State of India. *Journal of Ethnobiology and Ethnomedicine*, 7, pp.1-17.

Pandey, N. and Pandey, S., 2017. Government Schemes and Programs for Enhancing Community Participation in Wetland Conservation: A Case Study of India. *International Journal of Environmental Studies*, 74(5), pp.767-780. DOI: 10.1080/00207233.2017.1382809.

Panigrahy, S., Murthy, T.V.R., Patel, J.G. and Singh, T.S., 2012. Wetlands of India: inventory and assessment at 1: 50,000 scale using geospatial techniques. *Current Science*, pp.852-856.

Patel, A., Sharma, R. and Das, S., 2018. Traditional fishing techniques in wetland conservation: A review. *Journal of Aquatic Ecology*, 45(3), pp.321-335.

Patel, K., Gupta, M. and Singh, R., 2020. Harnessing Traditional Knowledge: Community Engagement and Knowledge Sharing in Stormwater Management.

Patel, N., Green, M. and Ramesh, K., 2021. Promoting Inclusive and Sustainable Wetland Conservation Practices Through Collaborative Partnerships: Lessons Learned from India. *Journal of Environmental Science and Management*, 24(1), pp.112-125. DOI: 10.35441/jesm.2021.24.1.12.

Ponzio, K., Osborne, T., Davies, G., LePage, B., Sundareshwar, P., Miller, S., Bochnak, A., Phelps, S., Guyette, M., Chowanski, K., Kunza, L., Pellechia, P., Gleason, R. and Sandvik, C., 2019. *Wetland Management and Restoration*. Springer, pp.1-10.

Posey, D.A., 1999. *Cultural and Spiritual Values of Biodiversity*. UNEP/Earthprint.

Ragavan, P., Kathiresan, K., Mohan, P.M., Ravichandran, K., Jayaraj, R.S.C. and Rana, T.S., 2021. Ensuring the adaptive potential of coastal wetlands of the need of the hour for sustainable management. *Wetlands Ecology and Management*, 29, pp.641-652.

Ramesh, K., Das, P. and Sharma, A., 2018. Contributions of Non-Governmental Organizations (NGOs) in Supporting Indigenous Communities' Efforts in Wetland Conservation: A Case Study in India. *Journal of Environmental Policy and Planning*, 20(6), pp.749-766. DOI: 10.1080/1523908X.2018.1428993.

Ramsar Convention, 1971. *Convention on Wetlands of International Importance especially as Waterfowl Habitat*. Ramsar Convention.

Rao, K.S., Reddy, N.S. and Kumar, P., 2019. Role of traditional cattle rearing systems in wetland conservation: A case study from the Western Ghats, India. *Journal of Wetland Ecology*, 8(2), pp.112-125.

Rubeena, K.A., Nefla, A., Aarif, K.M., AlMaarofi, S.S., Gijjappu, D.R. and Reshi, O.R., 2023. Alterations in hydrological variables and substrate qualities and its impacts on a critical conservation reserve in the southwest coast of India. *Marine Pollution Bulletin*, 186, p.114463.

Sarkar, U.K. and Borah, B.C., 2018. Flood plain wetland fisheries of India: with special reference to the impact of climate change. *Wetlands Ecology and Management*, 26, pp.1-15.

Sarker, S., Rahman, M.M. and Uddin, M.M., 2017. Traditional cattle rearing practices in wetlands: A case study in Bangladesh. *Journal of Wetland Management*, 12(3), pp.45-56.

Sharma, P. and Das, A.K., 2019. Conservation implications of traditional fishing practices in wetlands. *Journal of Environmental Management*, 55(6), pp.789-802.

Sharma, R. and Choudhury, A., 2019. Role of the Ministry of Environment, Forest, and Climate Change (MoEFCC) in Promoting Community-Based Wetland Conservation in India: A Policy Analysis. *Environmental Policy and Governance*, 29(4), pp.245-258. DOI: 10.1002/eet.1847.

Singh, A., Kumar, R. and Patel, S., 2020. Indigenous farming techniques for wetland conservation in India: A review. *Journal of Environmental Science and Health*, 55(9), pp.789-802.

Singh, R., Singh, S. and Kumar, M., 2020. Impact Assessment of National Wetland Conservation Program (NWCP) on wetland ecosystems and community livelihoods: A case study in India. *Ecological Engineering*, 144, p.105724. DOI: 10.1016/j.ecoleng.2019.105724.

Smith, A. and Pritchard, R., 2018. Synergies between convention on biological diversity (CBD) objectives and indigenous-led wetland conservation initiatives: A global perspective. *Biodiversity and Conservation*, 27(13), pp.3299-3315. DOI: 10.1007/s10531-018-1602-4.

Smith, J. A., Brown, R. B. and Patel, S., 2018. Sustainable extraction of wetland products for construction materials: Case studies from indigenous communities. *Journal of Sustainable Development*, 5(1), pp.78-91.

Suhani, I., Monika, Vaish, B., Singh, P. and Singh, R.P., 2020. Restoration, construction, and conservation of degrading wetlands: a step toward sustainable management practices. *Restoration of Wetland Ecosystem: A Trajectory Towards a Sustainable Environment*, 45, pp.1-16.

Sundar, K.G. and Kittur, S., 2013. Can wetlands maintained for human use also help conserve biodiversity? Landscape-scale patterns of bird use of wetlands in an agricultural landscape in north India. *Biological Conservation*, 168, pp.49-56.

Taran, M., Ahirwal, J., Deb, S. and Sahoo, U.K., 2023. Variability of carbon stored in inland freshwater wetlands in Northeast India. *Science of The Total Environment*, 859, p.160384.

Turner, N.J., Ignace, M.B. and Ignace, R., 2000. Cultural keystone species: Implications for ecological conservation and restoration. *Ecology and Society*, 4(1), p.1.

Wang, Y., Liu, C. and Chen, G., 2021. Community-led afforestation projects for wetland conservation: Insights from case studies in China. *Environmental Management*, 35(2), pp.189-202.

Yi, X., Peng, G., Liu, G., Ducharne, A., Ciais, P., Prigent, X., Li, X. and Tang, X., 2022. The trade-off between tree planting and wetland conservation in China. *Journal of Environmental Management*, 286, p.112218.

Environmental Impact of Al-Dalmaj Marsh Discharge Canal on the Main Outfall Drain River in the Eastern part of Al-Qadisiya City and Predicting the IQ-WQI with Sensitivity Analysis Using BLR

Zahraa Z. Al-Janabi[1†], Idrees A. A. Al-Bahathy[2], Jinan S. Al-Hassany[3], Rana R. Al-Ani[1], Ahmed Samir Naje[4] and Afrah A. Maktoof[5]

[1]Environmental Research Center, University of Technology, Baghdad, Iraq

[2]College of Engineering, AL-Qasim Green University, Babylon 51031, Iraq

[3]College of Science for Women, Biology Department, University of Baghdad, Baghdad, Iraq

[4]Soil Science and Water Resources Department, College of Agriculture, University of Al-Qadisiyah, Iraq

[5]Department of Biology, Collage of Science, University of Thi-Qar, Nasiriyah, Iraq

†Cressponding author: Zahraa Z. Al-Janabi; zahraahmedalmamory@yahoo.com

Citation for the Paper:

Al-Janabi, Z. Z., Al-Bahathy, I. A. A., Al-Hassany, J. S., Al-Ani, R. R., Naje, A. S. and Maktoof, A. A., 2025. Environmental impact of Al-Dalmaj marsh discharge canal on the main outfall drain river in the eastern part of Al-Qadisiya city and predicting the IQ-WQI with sensitivity analysis using BLR. *Nature Environment and Pollution Technology*, 24(1), D1661. https://doi.org/10.46488/NEPT.2025.v24i01.D1661.

Note: From year 2025, the journal uses Article ID instead of page numbers in citation of the published articles.

ABSTRACT

Monitoring water quality changes in any body of water is crucial as it directly relates to climate change. Evaluating the quality and quantity of fresh water for various uses is essential to maintaining safe water sources now and in the future. This study examined the water quality of the Main Outfall Drain River (MOD) in the eastern part of Al-Qadisiya Governorate at three sites over four seasons in 2023, using the Iraqi Water Quality Index (IQ-WQI). In most cases, the concentrations of dissolved oxygen (DO), biochemical oxygen demand (BOD5), and total dissolved solids (TDS) exceeded allowable limits for freshwater and aquatic life protection. The major contributing parameters to the river's low water quality were TDS, BOD5, turbidity, and DO. The use of the MOD for discharging agricultural effluents led to increased levels of TDS, BOD5, and turbidity. Temporal variation indicated that the summer season had the highest values compared to other seasons due to increased evaporation and low water discharge. Spatial variation showed the IQ-WQI of the sites in descending order from very poor water to unsuitable, with Site 3 having double the TDS concentrations compared to other sites. This increase may be attributed to the impact of the Al-Dalmag Marsh discharge canal, which comes into contact with the MOD at this site. Sensitivity analysis using backward linear regression was applied to predict the IQ-WQI and determine the most influential parameters on the IQ-WQI score. The test was conducted for two sets of water parameters (from the IQ-WQI calculation) and included 7 parameters for each freshwater and aquatic life use, obtaining different models.

INTRODUCTION

Water is among the numerous, plentiful natural resources that all living things, including humans, animals, plants, and other species, rely on. The increasing population, rising economic activity, and urbanization increase water demand. The environment around human life is in danger due to declining water levels, deteriorating water quality, and excessive surface water usage, considered the most significant water resource (Ingrao et al. 2023). Changes in the global water cycle, resulting from environmentally damaging and water-intensive human activities and climate change, significantly impact many nations' natural ecosystems and human health. Therefore, It is no longer appropriate to think of water as a renewable natural resource, given the patterns of water usage today (Wang & Liu 2023). The study of Ingrao et al. (2023) mentioned the following key issues that pertain to freshwater consumption with critical environmental and socioeconomic repercussions: (i)

the resource depletion, that is due to extraction surpassing regeneration over the long-term, with the risk that the resource may be unavailable for future generations; and - (ii) the rivalry for freshwater that arises when the availability of the resource is reduced for some users over a short time, leading to issues with the resource's appropriate distribution among a variety of users.

Surface water quality can be improved and preserved by utilizing various management strategies. One strategy to reduce pollution at its source is to use fewer chemicals and other contaminants. For example, on a national scale, the authorities can obligate industrial companies to implement green infrastructure practices like green roofs and rain gardens; for individual practices, homeowners can reduce the use of chemicals around their houses, like pesticides, fertilizer, etc., to reduce stormwater runoff. Still, the best solution to water pollution is to treat pollutants before they enter the surface water, which could be using sediment basins or artificial wetland treatment, among other techniques, to improve the water quality (Verma et al. 2020, Abed et al. 2021). Also, to avoid pollution disasters, it can use source management protocols, such as covering storage areas and reducing industrial effluent (Cheng et al. 2022).

In general, assessing water quality with a huge number of parameters is difficult to interpret, and the influence of these parameters on overall water quality is difficult to understand clearly. The process of estimating water quality is difficult, so a good judgment of the quality cannot be made depending on testing water parameters individually and for multiple samples (Syeed et al. 2023). Therefore, water quality analysis was subjected to several scientific techniques, like statistical evaluations and water quality indices WQI (Syeed et al. 2023). Chidiac et al. (2023) reviewed different indices applied worldwide with their mathematical combinations. They concluded there is no universal index that can be used by national agencies, users, or researchers, so the choice of the right index for any study will depend on the purpose of the water use and objectives; their study also illustrated the link between WQI and statistical analysis such as Pearson correlation and Principal component analysis to determine the interaction between the studied parameters.

WQI can be defended as a mathematical tool that can combine multiple values (water parameters) in an easy way to generate a single value or number that reflects the water quality status, and this method can be applied to different aquatic systems (lentic or lotic). Many local and international studies used several types of water quality indices like weighted index, Canadian water quality (CCME), etc. (Nong et al. 2020, Majeed & Nashaat 2022, Nguyen et al. 2022, Abed et al. 2023, Mohammed et al. 2022).

Backward Linear Regression (BLR) has been widely used in the past few years to handle a variety of environmental engineering issues, such as river water quality prediction modeling (Talukdar et al. 2023, Goodarzi et al. 2023). BLR models can be a very helpful tool to illustrate the change in water quality through time and sites and can reveal the most important parameters that affect water quality. It is an important resource, especially for developing forecast models using small sample sizes. Some researchers may find it tough to select a set of regressors for a model meeting all the necessary assumptions when using this method and when there are many alternative regressors. So, to test all possible permutations of regressors automatically using a brute-force method, the authors created an open-source Python software. Based on the user-specified assumptions (e.g., statistical significance of the estimates, multicollinearity, error normalcy, and homoscedasticity), the output shows the top linear regression models. Additional features of the script include the ability to choose linear regressions with user-specified regression coefficients (et al. 2023). In areas related to water research, artificial intelligence technology is a powerful and potentially multifunctional technique (Kouadri et al. 2021). The linear regression model is one of the first methods of statistical modeling.

However, in this study, sensitivity analysis based on Backward Linear Regression (BLR) was done to determine which water quality parameters influence the score of WQIs by observing an output variable's response concerning input variables' variations. Usually, the test is done by removing each parameter from the calculation of WQI and comparing the final results. The models can be evaluated using the correlation of coefficient (R^2), Sum Squares Error (SSE), and Root Means Square Error (RMSE) (Cheng et al. 2022). This research aims to evaluate the effect of the Dalmaj Marsh discharge canal on the Main Outfall Drain River. As well as it also aims to introduce the most important indices of water quality used at present to assess the quality of surface water for overall and aquatic life protection purposes, which is based on weight anthemic mean that provides the current and proper weight for each parameter according to its significant impact on the aquatic system, the model used is built for Iraqi water assessment using Delphi method to communicate with local and global experts in water quality indices for a consultation about the best and most important parameter that can use in building the index according to the nature of the Iraqi aquatic system and established weight to each parameter, the index called Iraqi Water Quality Index (Al-Janabi et al. 2023), also in this study a sensitivity analysis was conducted to predict the IQ-WQI and determine the most influential parameters on the IQ-WQI score for both uses.

MATERIALS AND METHODS

Study Area and Sampling

Main Outfall Drain is a river constructed and began to operate in 1992 with a 565 km length and is used to dump effluents from agricultural and industrial sources in the middle and southern lands of Iraq (Shahadha & Salih 2021). The study area was located on the Main Outfall Drain River section in the Eastern Al-Qadisiya Government. The samples were collected seasonally from winter to autumn 2023. Three sites were chosen; the first site was selected downstream of the supplying canal of Al-Dalmag marsh with water (Fig.1). The first one is located within Afak City, eastern Al-Qadisiya Government, on the mainstream of the Main Outfall Drain about 2 km downstream to a branching canal that supplies Al-Dalmag marsh with water (recharge canal) at 32.175715," N latitude and 45.335072" E longitude (32°17'57.15'' N) (45°33'50.72'' E). The second site is located at 32°06'10.76" N, 45°49'77.21" E, about 19 km downstream of the first site. The third site is situated near the bridge of the main street going to the Maysan Government in Al Bedair city (31°86'50.8" N and 45°63'84.3" E), about 24 km from the second site. This site is situated about 2 km downstream of the meeting of the discharge canal of Al-Dalmag Marsh with the Main Outfall Drain.

Table 1: The rates of water discharges of the main outfall drain river.

Sites	Winter	Spring	Summer	Autumn
Site1	4 m^3.s^{-1}	1 m^3.s^{-1}	0.6 m^3.s^{-1}	0.58 m^3.s^{-1}
Site2	3.13 m^3.s^{-1}	0.9 m^3.s^{-1}	0.53 m^3.s^{-1}	0.51 m^3.s^{-1}
Site3	1 m^3.s^{-1}	0.3 m^3.s^{-1}	0.51 m^3.s^{-1}	0.4 m^3.s^{-1}

Water discharge rates ranged from 1 m^3.s^{-1} in site 3 to 4 m^3.s^{-1} in site 1 in winter. On the other hand, in the Spring season, it ranged from 0.3 m^3.s^{-1} in site 3 to 1 m^3.s^{-1} in site 1. Site 3 was 0.51 m^3.s^{-1}, and site 1 was 0.6 m^3.s^{-1} in summer to 1 m^3.s^{-1} in site 1. Whereas it ranged from 0.4 m^3.s^{-1} in site 3 to 0.58 m^3.s^{-1} in site 1, as shown in Table 1 (The data obtained from Ministry of Water Resources and personal communication).

The samples were collected in a clean polyethylene bottle. Eight parameters were chosen to calculate the water quality index. Field measurements, including pH, water temperature (WT), and turbidity, were taken using a portable device. Experimental Measurements included biochemical oxygen demand (BOD$_5$), dissolved oxygen (DO), phosphate (PO$_4$), nitrate (NO$_3$), and total dissolved solids (TDS); all the mentioned parameters were determined according to APHA (APHA 2017) (Table 2).
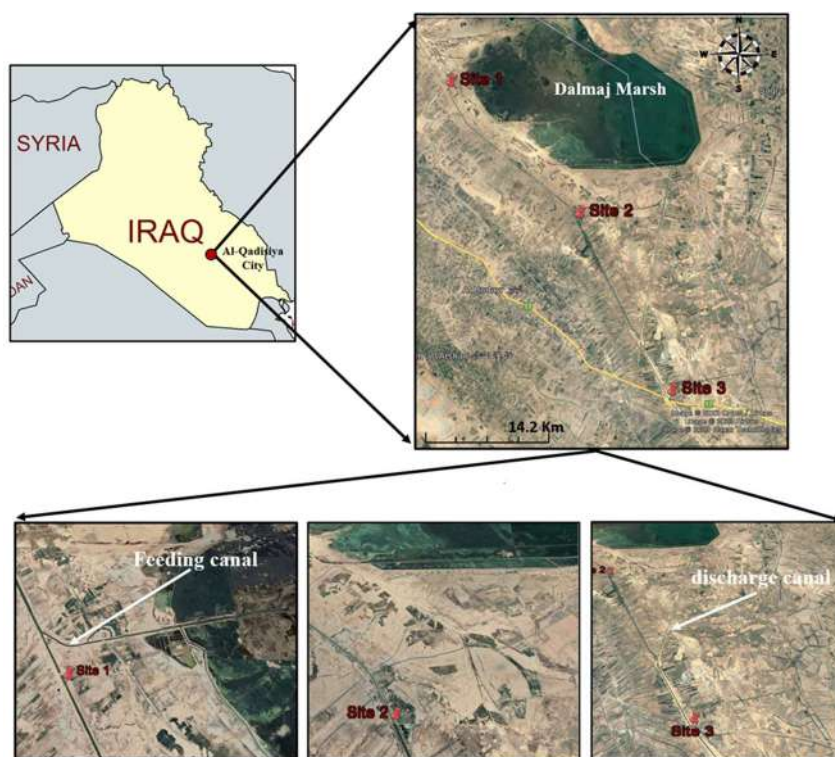
Fig. 1: Map showing the study area.

Table 2: Field and laboratory measurements (APHA 2017).

Parameters	Methods (APHA)	Instruments	Origin
pH	4500-H+ B	EC/Temperature/pH portable meter H19811	WTW, Germany
WT [C°]	WT 2550B		
Turbidity (NTU)	2130 B, Nephelometric method	Turbidity meter	Lovibond, Germany
BOD_5 [mg.L^{-1}]	5210 B, 5-Day BOD Test	Incubator/ JRAD	Memmert, Germany
DO [mg.L$^-$]	4500-OC-Azide modification	Titration	-
PO_4 [mg.L^{-1}]	4500-P C, Ascorbic Acid method	Spectrophotometer UV-1200	China
NO_3 [mg.L^{-1}]	4500-NO3-F, Colorimetric method	Multiparameter photometer/HI 83200	Romania
TDS [mg.L^{-1}]	2540-C, Total dissolved solids dried at 180ºC	Oven	Memmert, Germany

IQ-WQI Calculation

The IQ-WQI was calculated according to (Al-Janabi et al. 2023), which was done in four steps: step one, each parameter has assigned weights; step two, calculation of quality rating (Qi) for each parameter based on the concentration (observed value) of the ith parameter (Ci) divided by standard value of the nth parameter (Si) as shown in eq. 1 and 2; step 3, determination of sub-indices (SIi) by multiplying the final weight (Wi) of each parameter by its quality rating (eq. 2); step four, aggregation of each sub-indices to get the final index score using the additive (arithmetic) method (eq. 4). The Water quality rating is shown in Table 3.

$$Qi = \frac{C_i - C_{ideal}}{s_i - C_{ideal}} \times 100$$ (for DO and pH; Cideal for DO= 14.6; Cideal for pH=7)   …(1)

$$Qi = \frac{C_i}{s_i} \times 100$$ (for other parameters)   …(1)

$$SI_i = final\ wight \times Q_i$$ …(2)

$$IraqiWQI = \sum SI_i / Wi$$ …(3)

Statistical Comparison

The sensitivity study for IQ-WQI for both purposes, which is based on Backward Linear Regression (BLR) to ascertain which water quality parameter most affects the score of IQ-WQI, was carried out using Jeffreys Amazing Statistics Program (JASP) for statistical analysis based on the R programming language.

RESULTS AND DISCUSSION

Physicochemical Parameters

The physicochemical parameters (DO, BOD_5, pH, PO_4, NO_3, water temperature TDS, and Turbidity) were measured

to derive IQ- WQI. The ranges of parameters measured at three sites of the Main Outfall Drain are given in Table (4). No remarkable seasonal variation (Winter to autumn) was observed in the values of (pH, PO_4, NO_3, and water temperature that varied from (7.22-7.50) for pH, (0.05-0.1 mg.L^{-1}) for PO_4, (5.6- 11.7 mg.L^{-1}) for NO_3 in all sites, the values were well within the acceptable range of Iraqi standards for fresh water and for aquatic life protection.

The turbidity level varies from 31.82 to 39.47 mg.L^{-1}, and the mean concentrations were within the range for fresh water. At the same time, the turbidity values exceeded the recommended values for standard guidelines of aquatic life protection (5 NTU) (CMME 2001) in all sites.

In the majority of the cases, the DO, BOD_5, and TDS concentrations were higher than the allowable limit for Iraqi standards of fresh water and aquatic life protection, as well as turbidity for aquatic life protection. The ranges of these parameters were from (4.9- 5.6 mg.L^{-1}) for DO, (9.4 - 11.6 mg.L^{-1}) for BOD_5, (8008.2- 20636.8 mg.L^{-1}) for TDS, (31.8-39.4 NTU) for turbidity in all sites.

In the Assessment of Main Outfall Drain (MOD) using IQ-WQI, all study sites were ecologically unsuitable for freshwater and aquatic life protection with values > 100, except one value in site1 was 99.1 (very poor water quality) in winter because it falls within the range (70- 100) (Table 5).

The major contributing parameters to the river's very low water quality status were generally TDS, BOD5, turbidity, and DO (Table 4). It was used to discharge the agricultural effluents along about 565 km, thus leading to rising TDS, BOD5, and turbidity levels, as stated by Khuhawar et al. (2023), who studied the MOD River (Khuhawar et al. 2023). As well as the correlation of the high TDS concentrations with decreased levels of other parameters such as DO, as stated by Xu et al. (2019), who studied the Dan River basin

Table 3: Rating of the Water quality as per weight arithmetic water quality index method (Al-Janabi et al. 2023).

WQI Value	0-25	26-50	51-75	76-100	> 100
Rating of Water Quality	Excellent water quality	Good water quality	Poor water quality	Very Poor water quality	Unsuitable
	Blue	Green	Yellow	Orange	Red

Table 4: The results of physical-chemical parameters for the study sites.

Parameter	Observed mean Values			(Sn) for freshwater	(Wn) for freshwater	(Sn) For aquatic life protection	(Wn) for aquatic life protection
	St.1	St.2	St.3				
pH	7.225	7.25	7.5	7.50	0.0901	7.75	0.0901
WT[C°]	30.5	32.5	34.5	-	-	15	0.0926
Turbidity NTU	32.5	31.825	39.47	50.00	0.1150	5	0.1165
BOD_5 mg.L^{-1}	11.625	11.05	9.425	5.0	0.0901	-	-
DO mg.L^{-1}	5.2	4.91	5.65	5.00	0.4210	7.25	0.3986
PO_4 mg.L^{-1}	0.1552	0.0737	0.059	0.40	0.0947	0.1	0.0982
NO_3 mg.L^{-1}	7.089	5.685	11.70	15.00	0.096	15	0.0992
TDS mg.L^{-1}	8008.25	9841.125	20636.87	500.00	0.0931	500	0.1048
					$\Sigma Wn=0.1$		$\Sigma Wn= 1.0$

in China (Xu et al. 2019), where in nature, the relationship between DO and salts is opposite, an increase in salts will not allow atmospheric oxygen to dissolve in water.

IQ-WQI

Fig. (2) shows the temporal variation in IQ-WQI for Freshwater use and aquatic protection. The higher values of IQ-WQI were in the summer compared with other seasons. Meanwhile, the lower values were in winter in all sites. The reason may have been related to the higher levels of TDS and BOD_5 during the Summer season in all sites that coincided with low water discharges of the river, and vice versa in winter, as stated by Al-Zaidy (2021) who studied the same area for Main Outfall Drain in Al-Qadisiya Governorate.

Fig. 3 shows the spatial variation in IQ-WQI for Freshwater use and aquatic life protection. The higher values of IQ-WQI were in site 3 (lower quality). In contrast, the lower water quality index values were in site 1(higher quality). It was observed that Site 3 had double concentrations of TDS compared with S1 and S2, which may be due to being it was affected by water from the discharge canal of Al-Dalmag Marsh that met with the Main Outfall Drain in a site called the Waterfall Site about 2 km before Site 3, the fluxes of Al-Dalmag Marsh water contained higher content of TDS. The higher levels of TDS in Al-Dalmag Marsh water may related to the increasing evaporation rate and the low lentic water level of the marsh (Casamitjana et al. 2019) or may be due to the discharge of groundwater into the Main Outfall Drain River from the adjoining salt marsh (Al-Dalmag marsh) (Guimond & Tamborski 2021). In general, most of the sites during the winter season have low WQI values in comparison to other seasons, which can be related to increasing water discharges that can reduce the deterioration of water quality through the diluting of pollutants in water (Fan et al. 2022, Al-Janabi et al. 2024). As seen in Table 5, the only index value (99.11 bad water) at

site 1 during winter was different from the rest of the values, and if it is compared with the discharge value in the same season (Table 1), will find the discharge value (4 m^3.sec^{-1}) is higher than the rest of the seasons. This study's finding is close to that of Hussein et al. (2019) in their research on assessing the water quality of the Al-diwanaiah River, where they declared that the water severely threatens aquatic life but can be used for irrigation purposes only.

Sensitivity Analysis

The sensitivity analysis studies the response of the output results of the test to input parameter variation (Álvarez et al. 2018). To determine the parameter that most influences the water quality of the Al-Dalmaj and MOD, the study selected Backward Linear Regression (BLR) for freshwater and aquatic life protection index score. To evaluate the BLR model performance, the coefficient of determination (R2), Root Mean Square Error (RMSE), and Sum Square error (SSE) were used, where the use of these three criteria remarkably affected the fitness and residual measurement of the model in the prediction of WQI. The sensitivity test was done by eliminating one parameter from the calculation of IQ-WQI each time and comparing the outcome with the

Table 5: The results of IQ-WQI for freshwater use and aquatic life protection.

IQ-WQI value for Freshwater use			
Winter	Spring	Summer	Autumn
99.11	121.54	210.51	144.05
117.20	112.88	264.21	208.42
145.22	212.90	438.67	325.98

IQ-WQI value for the protection of aquatic life				
	Winter	Spring	Summer	Autumn
Site1	140.65	253.32	280.97	215.90
Site2	187.96	228.39	316.24	275.33
Site3	263.05	374.6	513.53	440.52
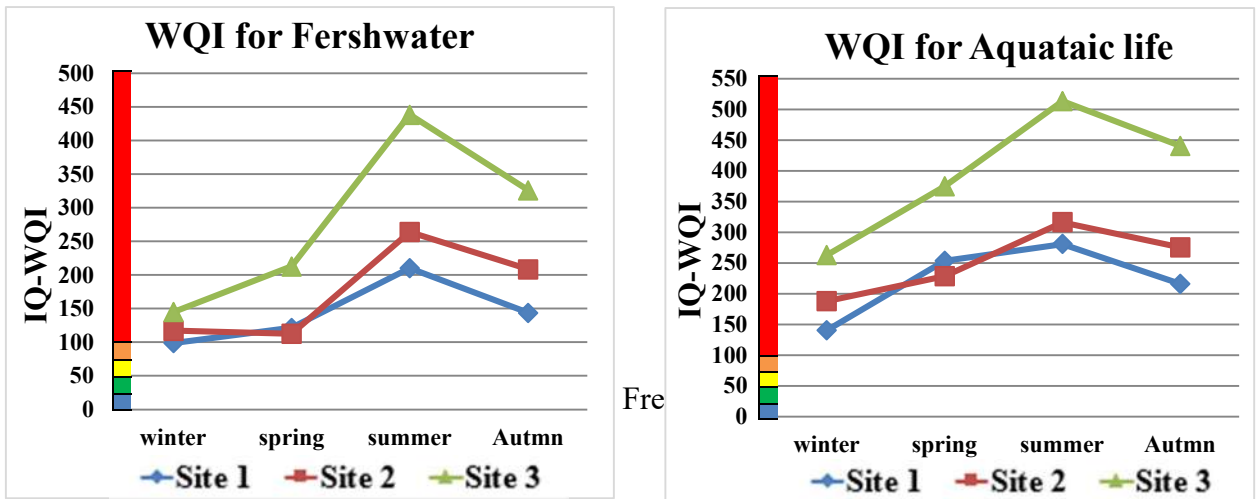
Fig. 2: Temporal variation in IQ-WQI for both Freshwater use and protection of aquatic life.
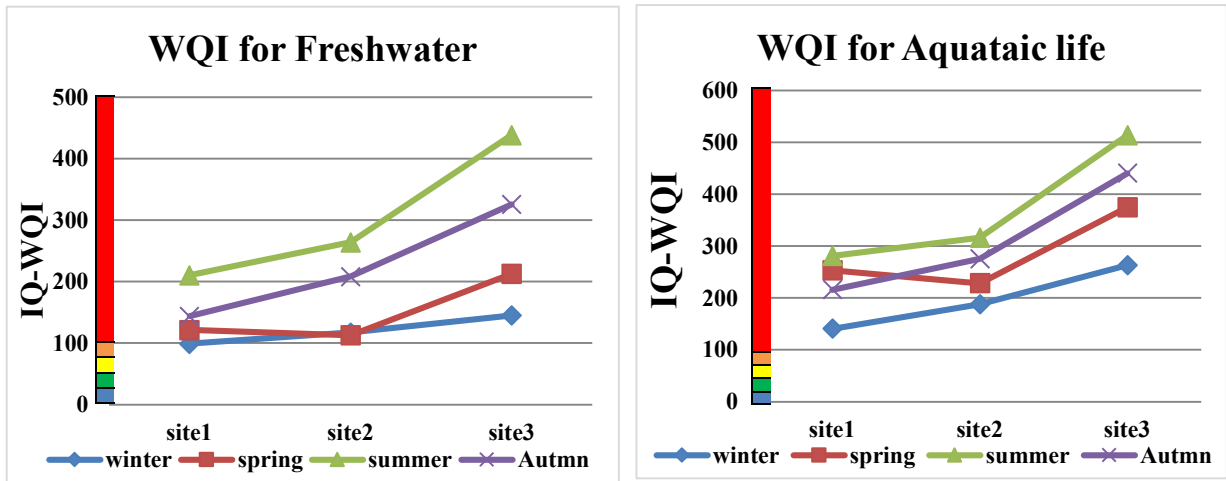
Fig. 3: Spatial variation in IQ-WQI for both freshwater use and protection of aquatic life.

original or reference results of IQ-WQI (reference IQ-WQI includes all parameters called IQ-WQI-Ref.). When the model has low R2 and high RMSE and SSE, it indicates an influencing parameter in calculating WQI; in contrast, if the model has High R2 and low RMSE and SSE, it indicates non-influencing parameters in the calculation. All data sets of this study (112 values) were subject to standardization before being used in the test to ensure a fair representation of all parameters in the IQ-WQI values.

The data set from the case study was chosen to describe this index's effectiveness and determine the most important parameters that must be present to calculate the index. 7 parameters from WQI calculation (DO, BOD_5, pH, PO_4, NO_3, TDS, Turbidity) were all selected as input and IQ-WQI as the output for BLR-IQ-WQI models.

BLR's first model, which represents the input parameters, called IQ-WQI-Ref, serves as a reference for the BLR model and includes all parameters used in calculating the index. Then, the assessing processes for the significance of the input parameters (IQ-WQI-Ref) were done by eliminating one parameter from the IQ-WQI-Ref (including seven parameters) for both uses (freshwater and aquatic life protection). Table 6 shows the performance of the BLR model that was evaluated using R2, RMSE, and SSE. The results of sensitivity analysis illustrated that the water quality index predicted by the BLR model brings reliable output, and the best-predicated model that contains the most effluence parameters on water quality for freshwater use is model number 4 and model 3 for aquatic life use, as shown in Table 5 where RMSE =11.347 and = 14.704, respectively.

Table 6: Sensitivity analysis for IQ-WQI model prediction (BLR-IQWQI) for freshwater use and aquatic life protection uses.

Model	Freshwater Use				Aquatic Life Protection Use			
	R	R²	Adjusted R²	RMSE	R	R²	Adjusted R²	RMSE
1	0.999	0.999	0.996	13.329	0.999	0.999	0.997	16.423
2	0.999	0.999	0.997	12.168	0.999	0.999	0.998	14.993
3	0.999	0.998	0.997	11.905	0.999	0.999	0.998	14.704
4	0.999	0.998	0.997	11.347	0.999	0.998	0.997	15.687

Table 7: Equations of sensitivity analysis for IQ-WQI prediction (BLR-IQ-WQI) for freshwater use.

Model Equation	Model Equation
BLR-IQ-WQI-Ref-model 1	$0.049 * DO + 0.220 * pH + 0.024 * BOD_5 + - 0.046 * PO_4 + - 0.00342 * NO_3 + 0.855 * TDS + - 0.133 * Turbidity$
BLR-IQ-WQI-model 2	$0.049 * DO + 0.220 * pH + 0.024 * BOD_5 + - 0.046 * PO_4 + 0.855 * TDS + - 0.133 * Turbidity$
BLR-IQ-WQI- model 3	$0.220 * pH + 0.024 * BOD_5 + - 0.024 * PO_4 + 0.864 * TDS + - 0.101 * Turbidity$
BLR-IQ-WQI- model 4	$0.208 * pH + 0.020 * BOD_5 + 0.878 * TDS + - 0.091 * Turbidity$

Table 8: Equations of sensitivity analysis for IQ-WQI prediction (BLR-IQWQI) for the protection of aquatic life.

Model Equation	Model Equation
BLR-IQ-WQI-Ref-model 1	$-0.080 * DO + 0.059 * pH + -0.00994 * WT + -0.059 * PO_4 + - 0.094 * NO_3 + 0.0998 * TDS + - 0.068 * Turbidity$
BLR-IQ-WQI-model 2	$-0.080 * DO + 0.059 * pH + - 0.059 * PO_4 + -0.093 * NO_3 + 0.996 * TDS + - 0.068 * Turbidity$
BLR-IQ-WQI- model 3	$-0.099 * DO + 0.053 * pH + 0.855 * + -0.125 * NO_3 + 1.055 * TDS + - 0.101 * Turbidity$
BLR-IQ-WQI- model 4	$-0.147 * DO + 0.049 * pH + 0.946 * TDS + - 0.134 * Turbidity$

Equations of sensitivity analysis for IQ-WQI prediction (BLR-IQ-WQI) for both uses are given in Tables 7 and 8.

The most significant and influential parameters on IQ-WQI for freshwater uses are pH, BOD, TDS, and Turbidity. Al Yousif & Chabuk (2023) reviewed several studies that indicated the importance of these parameters in the evaluation of water quality for surface water using different types of indices and pointed out that developing countries have recently increased their efforts to focus evaluate the water quality of rivers because it's the primary source of water for different uses (Al Yousif & Chabuk 2023). Nowadays, water resource management and water resource protection are often used interchangeably in practice, and water resource protection focuses on measures put in place, such as the control and prevention of water pollution. Furthermore, water resources management emphasizes enabling institutional roles, regulating and policy the environment, and management instruments as prerequisites to deploying water resources to support economic and social development while ensuring resource sustainability (Makanda et al. 2022).

For aquatic life protection, the most important parameters that influence IQ-WQI are DO, pH, PO_4, NO_3, TDS, and Turbidity, where this model contains the most parameters that encourage and support the growth of aquatic life, which can called the limited factors (DO, PO_4, NO_3) for algae which consider the base of the food chain (Indraswari & Adharini 2022, Bourgougnon et al. 2021).

CONCLUSIONS

The WQI approach used in the study to evaluate sites' water quality was helpful. Turbidity levels were within the range for fresh water. Meanwhile, the turbidity values exceeded the recommended values for standard guidelines of aquatic life protection (5 NTU) in all sites.

In most cases, the DO, BOD_5, and TDS concentrations were higher than the allowable limit for Iraqi freshwater standards and aquatic life protection standards. The major contributing parameters to the river's very low water quality status were generally TDS, BOD_5, turbidity, and DO. Since it was used to discharge the agricultural effluents along about 565 km, this led to rising TDS, BOD_5, and turbidity levels. The temporal variation in IQ-WQI for Freshwater use and aquatic life protection showed that the higher values were in the summer compared with other seasons. The reason may be related to the higher levels of TDS and BOD_5 in the Summer season in all sites that coincided with low water discharges of the river, and vice versa in winter. The spatial variation showed that IQ-WQI was in descending order by very poor water, which was unsuitable. Site 3 has double concentrations of TDS compared with other sites may be due to it being affected by the water of the discharge canal for Al-Dalmag Marsh that meets with the Main Outfall Drain in a site called the Waterfall Site about 2km before Site 3; thus, it was exposed to fluxes of Al-Dalmag Marsh water with higher content of TDS. Using sensitivity analysis

can show the most important parameters that can affect the water quality Characteristics, as well as using Backward Linear Regression (BLR) based on artificial intelligence techniques to predict the values of WQI, which can facilitate the calculations of indices accurately.

REFERENCES

Abed, I.F., Nashaat, M.R. and Mirza, N.N.A., 2023. Assessment of the water quality of the mollusa community in the Janabi River-Hayy City of Wasit Province by using Canadian water quality index. *International Journal of Environmental Research and Education*, 3(1), pp.57–68. doi:10.61186/injoere.3.1.57.

Abed, N.A., Al Kindi, Y.G. and Hussain, A.T., 2021. Assessment of the water quality index of the Tigris River between the University of Baghdad and the Diyala River. *Engineering and Technology Journal*, 39(3A), pp.512–519. doi:10.30684/etj.v39i3A.1392.

Al Yousif, M.A. and Chabuk, A., 2023. Assessment water quality indices of surface water for drinking and irrigation applications: A comparison review. *Journal of Ecological Engineering*, 24(5), pp.40–55. doi:10.12911/22998993/161194.

Al-Janabi, Z.Z., Al-Obaidy, A.M.J. and Hassan, F.M., 2023. A novel water quality index for Iraqi surface water. *Baghdad Science Journal*, 20(6), pp.2395–2413. doi:10.21123/bsj.2023.9348.

Al-Janabi, Z.Z., Hassan, F.M. and Al-Obaidy, A.H.M.J., 2024. Overall index of pollution (OIP) for Tigris River, Baghdad City, Iraq. *Iraqi Journal of Agricultural Sciences*, 55(2), pp.905–916. doi:10.36103/gqq14f43.

Álvarez, O., Muñoz, E., Maureira-Carsalade, N., Roco-Videla, Á., 2021. A sensitivity analysis approach for assessing the effect of design parameters in reducing seismic demand of base-isolated storage racks. *Applied Sciences*, 11(23), p.11553. doi:10.3390/app112311553.

Al-Zaidy, K.J., 2021, April. Study of some Reproductive Characteristics of Cyprinus Carpio (L., 1758) from Main Outfall Drain in Al-Qadisiyah City, Iraq. In *IOP Conference Series: Earth and Environmental Science*, 735(1), p. 012075).

APHA, 2017. *Standard Methods for the Examination of Water and Wastewater*. American Public Health Association, p.1796.

Bourgougnon, N., Burlot, A.S. and Jacquin, A.G., 2021. Algae for global sustainability? *Advances in Botanical Research*, 100, pp. 145–212. doi:10.1016/bs.abr.2021.01.003.

Casamitjana, X., Menció, A., Quintana, X.D., Soler, D., Compte, J., Martinoy, M. and Pascual, J., 2019. Modeling the salinity fluctuations in salt marsh lagoons. *Journal of Hydrology*, 575, pp.1178–1187. doi:10.1016/j.jhydrol.2019.06.018.

Cheng, C., Zhang, F., Shi, J. and Te, H., 2022. What is the relationship between land use and surface water quality? A review and prospects from remote sensing perspective. *Environmental Science and Pollution Research*, 29, pp.56887–56907. doi:10.1007/s11356-022-21348-x.

Chidiac, S., El Najjar, P., Ouaini, N., El Rayess, Y. and El Azzi, D., 2023. A comprehensive review of water quality indices (WQIs): history, models, attempts, and perspectives. *Reviews in Environmental Science and Bio/Technology*, 22(2), pp.349–395. doi:10.1007/s11157-023-09650-7.

Fan, S., Tinglin, H., Nan, L., Kai, L., Gang, W., Yang, L. and Haihan, Z., 2022. Effects of flood discharge on the water quality of a drinking water reservoir in China: characteristics and management strategies. *Journal of Environmental Management*, 314, p.115072. doi:10.1016/j.jenvman.2022.115072.

Fernandes, A.C.P., Fonseca, A.R., Pacheco, F.A.L., Sanches Fernandes, L.F., 2023. Water quality predictions through linear regression: a brute force algorithm approach. *MethodsX*, 10, p.102153. doi:10.1016/j.mex.2023.102153.

Goodarzi, M.R., Niknam, A.R.R., Barzkar, A., Niazkar, M. and Mehrjerdi, Y.Z., 2023. Water quality index estimations using machine learning algorithms: a case study of Yazd-Ardakan plain, Iran. *Water*, 15(1876), pp.1–24. doi:10.3390/w15101876.

Guimond, J. and Tamborski, J., 2021. Salt marsh hydrogeology: A review. *Water*, 13(4), pp.543. doi:10.3390/w13040543.

Hussein, K., Al-Bayati, S. and Al-Bakri, S.A.A., 2019. Assessing water quality for Al-Diwaniyah River, Iraq, using GIS technique. *Engineering and Technology Journal*, 37(7A), pp.256–264. doi:10.30684/etj.37.7A.6.

Indraswari, N. and Adharini, R.I., 2022. Reducing nitrate and phosphate concentrations in shrimp wastewater aquaculture using *Gelidium corneum*. *Ecological Engineering and Environmental Technology*, 23(5), pp.137–144. doi:10.12912/27197050/151880.

Ingrao, C., Strippoli, R., Lagioia, G. and Huisingh, D., 2023. Water scarcity in agriculture: An overview of causes, impacts, and approaches for reducing the risks. *Heliyon*, 9(8), p.e18507. doi:10.1016/j.heliyon.2023.e18507.

Khuhawar, M.Y., Lanjwani, M.F. and Jahangir, T.M., 2023. Assessment of variation in water quality at Right Bank Outfall Drain, including Manchar Lake, Sindh, Pakistan. *International Journal of Environmental Analytical Chemistry*, 103(16), pp.4598–4620. doi:10.1080/03067319.2021.1929948.

Kouadri, S., Elbeltagi, A., Islam, A.R.T. and Kateb, S., 2021. Performance of machine learning methods in predicting water quality index based on irregular data set: application on Illizi region (Algerian southeast). *Applied Water Science*, 11(190), pp.1–20. doi:10.1007/s13201-021-01528-9.

Majeed, O.S. and Nashaat, M.R., 2022. Physicochemical parameters of river water and their relation to zooplankton: A review. *IOP Conference Series: Earth and Environmental Science*, 1120(012040), pp. 1–20. doi:10.1088/1755-1315/1120/1/012040.

Makanda, K., Nzama, S. and Kanyerere, T., 2022. Assessing the role of water resources protection practice for sustainable water resources management: A review. *Water (Switzerland)*, 14(3153), pp.1–20. doi:10.3390/w14193153.

Mohammed, I., Al-Khalaf, S.K.H., Alwan, H.H. and Naje, A.S., 2022. Environmental assessment of Karbala water treatment plant using water quality index (WQI). *Materials Today: Proceedings*, 60, pp.1554-1560.

Nguyen, T.G., Phan, K.A. and Huynh, T.H.N., 2022. Application of integrated-weight water quality index in groundwater quality evaluation. *Civil Engineering Journal*, 8(11), pp.2661–2674. doi:10.28991/CEJ-2022-08-11-020.

Nong, X., Shao, D., Zhong, H. and Liang, J., 2020. Evaluation of water quality in the south-to-north water diversion project of China using the water quality index (WQI) method. *Water Research*, 178(115781), pp.1–15. doi:10.1016/j.watres.2020.115781.

Shahadha, S.S. and Salih, R.M., 2021. Assessment of the water suitability of the main outfall drain river for irrigation purposes in Iraq: Case study. *Iraqi Journal of Soil Sciences*, 1(21), pp.146–153. Available at: https://www.iasj.net/iasj/pdf/c8a2962a1ccd0c41.

Syeed, M.M., Hossain, S., Karim, R., Faisal, M., Hasan, M. and Hayat, R., 2023. Surface water quality profiling using the water quality index, pollution index and statistical methods: A critical review. *Environmental Sustainability Indicators*, 18(100247), pp.1–23. doi:10.1016/j.indic.2023.100247.

Talukdar, S., Ahmed, S., Naikoo, M.W., Rahman, A., Ningthoujam, S., Bera, S., Ramana, G.V. and Mallik, S., 2023. Predicting lake water quality index with sensitivity-uncertainty analysis using deep learning algorithms. *Journal of Cleaner Production*, 406, pp.136885. doi:10.1016/j.jclepro.2023.136885.

Verma, I., Setia, S., Berwal, P., Goel, R. and Singh, V., 2020. Analysis of the behavior of stiffened and unstiffened steel plate shear walls with enhanced performance. *IOP Conference Series: Materials Science and Engineering*, 804(012035), pp.1–13. doi:10.1088/1757-899X/804/1/012035.

Wang, X. and Liu, L., 2023. The impacts of climate change on the hydrological cycle and water resource management. *Water*, 15(13), pp.2342. doi:10.3390/w15132342.

Xu, G., Li, P., Lu, K., Tantai, Z., Zhang, J., Ren, Z., Wang, X., Yu, K., Shi, P. and Cheng, Y., 2019. Seasonal changes in water quality and its main influencing factors in the Dan river basin. *Catena*, 173, pp.131–140. doi:10.1016/j.catena.2018.10.014.

Characterization of Multiple Heavy Metal Resistant *Bacillus cereus* IEI-01 Isolated from Industrial Effluent and its *In Vitro* Bioremediation Potential

Pooja Dua[1], Abhishek Chauhan[2]† [ID], Anuj Ranjan[2] [ID], Jayati Arora[1], Hardeep Singh Tuli[3], Seema Ramniwas[4], Ritu Chauhan[5] [ID], Moyad Shahwan[6,7], Amita G. Dimri[8] and Tanu Jindal[2]

[1]Amity Institute of Environmental Science, Amity University, Noida, Uttar Pradesh, India

[2]Amity Institute of Environmental Toxicology, Safety and Management, Amity University, Noida, Uttar Pradesh, India

[3]Department of Biotechnology, Maharishi Markandeshwar (Deemed to be University), Mullana, Ambala 12 133207, Haryana, India

[4]University Centre for Research & Development, University Institute of Pharmaceutical Sciences, Chandigarh University, Gharuan, Mohali, Punjab, India

[5]Department of Biotechnology, Graphic Era Deemed to be University, Dehradun 248002, Uttarakhand, India

[6]Department of Clinical Sciences, College of Pharmacy and Health Sciences, Ajman University, Ajman 346, United Arab Emirates

[7]Centre of Medical and Bio-Allied Health Sciences Research, Ajman University, Ajman 346, United Arab Emirates

[8]Microbiology Laboratory, Sriram Institute for Industrial Research, 19 University Road, Delhi, India

†Corresponding author: Abhishek Chauhan; akchauhan@amity.edu

ABSTRACT

Heavy metal (HM) pollution has been a significant issue for the environment and public health. Unmonitored industrial effluents are a major source of HM pollution. However, metallotolerant bacteria thriving in such environments could be potentially useful for bioremediation purposes. In this study, *Bacillus cereus* IEI-01 was isolated from water samples of Badshahpur Lake, Gurugram, showcasing resilience to HM exposure and thriving under optimal conditions at 37°C and pH 7.0. Morphological and biochemical characterization showed its Gram-positive rod shape and metabolic versatility, including glucose fermentation and nitrate reduction capabilities. Molecular analysis further affirmed its close relation to the *Bacillus cereus* strain. Dynamic bacterial growth patterns were observed, with typical sigmoidal curves indicating significant growth over 72 h. When exposed to various HMs, the strain IEI-01 exhibited differential tolerance and promoting patterns, with cadmium (Cd) and lead (Pb) compared to other metals. Over 72 h, the strain exhibited substantial removal rates ranging from 60.64% to 87.43% for Cd and 41.87% to 52.62% for Pb. The concentration-dependent bio-removal efficiency of IEI-01 in Cd-spiked cultures displayed a declining trend with increasing concentrations, with removal rates ranging from 80.23% to 60.72% over the same period. These findings highlight the potential of *Bacillus cereus* IEI-01 for HM bioremediation, particularly at lower concentrations. Its efficacy in removing Cd and Pb from contaminated environments suggests promising applications in environmental cleanup efforts.

INTRODUCTION

Heavy metal pollution is a significant environmental issue arising from various industrial activities, including mining, metallurgy, chemical manufacturing, and waste disposal. These activities discharge substantial amounts of toxic metals such as lead (Pb), cadmium (Cd), chromium (Cr), and mercury (Hg) into natural ecosystems, posing severe risks to human health and the environment (Bhakta et al. 2014). Heavy metals are persistent contaminants that do not degrade naturally, leading to bioaccumulation in food chains and prolonged ecological and ecotoxicological impact (Ali & Rehman 2014, Das et al. 2016). Traditional methods for HM removal, such as chemical precipitation, ion exchange, and adsorption, are often expensive, inefficient for low-concentration contaminants, and can produce secondary pollution. In this context, bioremediation, using microorganisms to detoxify or immobilize HMs, has emerged as a promising,

eco-friendly alternative. Various bacteria, including those from the *Bacillus* genus, have shown considerable potential in bioremediation due to their metabolic versatility and ability to thrive in harsh conditions (Shakoori et al. 2010, Bestawy et al. 2013). *Bacillus cereus* has been widely studied for its resilience in environments contaminated with HMs. This resilience is largely attributed to its unique metabolic pathways and resistance mechanisms, which include biosorption, bioaccumulation, and biotransformation of HMs (Afzal 2023). *Bacillus cereus* strains have been isolated from various contaminated sites, including industrial effluents, where they exhibit capabilities to reduce, oxidize, or otherwise mitigate HM toxicity (Patra et al. 2010, Kelany et al. 2023). The ability of *Bacillus cereus* to form endospores further enhances its survival in extreme conditions, making it a suitable candidate for bioremediation applications (Monga et al. 2022). Shakoori et al. (2010b) isolated and characterized arsenic (As) -reducing bacteria from industrial effluents, demonstrating their potential in bioremediation. Similarly, Kour et al. (2019) explored zinc biosorption in *Bacillus* strains, providing insights into their metal tolerance mechanisms. The identification of specific genes and proteins involved in metal resistance, such as those encoding for metal efflux pumps and metal-binding proteins, is crucial for developing genetically engineered strains with enhanced bioremediation capabilities (Afzal et al. 2017, Kumari et al. 2021a). The ability of *Bacillus cereus* to tolerate and potentially remediate various HMs makes it a reliable microorganism for bioremediation (Kalsoom et al. 2021). Previous research by Al Azad et al. (2020) has shown that *Bacillus cereus* strains from different environments, including milk and soil, possess significant bioremediation properties. However, strains isolated from industrial effluents are particularly interesting due to their exposure to high concentrations of HMs, which could have induced unique adaptive mechanisms (Begum & Aundhati 2016).

Bioremediation efficiency *in vitro* is assessed by evaluating the bacterium's ability to reduce, sequester, or transform HMs in controlled conditions. Zahoor & Rehman (2009) isolated Cr (VI)-reducing bacteria capable of converting toxic Cr to less harmful forms. Similar studies have shown that *Bacillus cereus* can significantly reduce the concentrations of various metals, making them less bioavailable and toxic (Sharma et al. 2021, Ameen et al. 2020). Saduzzaman et al. (2023) also found that DAS1 exhibited optimal growth and 85% Cr(VI) remediation at pH 8, with immobilized bacteria increasing reduction efficiency to 90.4%. When combined with DAS2, the mixed culture achieved complete Cr(VI) removal using the X3Y2Z1 experiment design.

This study aims to screen and identify HM-tolerant *Bacillus cereus* and its potential for bioremediation of metals. The biochemical characterization of *Bacillus cereus* includes an array of tests to determine its metabolic capabilities and resistance to HMs. Furthermore, molecular techniques, 16s RNA gene sequencing were employed to identify specific strains of the microorganisms.

MATERIALS AND METHODS

Sample Collection and Premilinary Isolation

Samples were collected in March 2023 from Badshahpur Lake in Gurugram, India, located at latitude 28.39 and longitude 77.0466318. The samples were collected in sterilized 250 mL amber-color acid-washed polyethylene bottles from ten different locations within the lake to ensure a representative sample of the water quality. To isolate *Bacillus cereus*, the water samples underwent primary culture preparation on Mannitol-egg yolk-polymyxin agar (MYP) medium, which is selective for *B. cereus*. The cultures were incubated at 37°C for 24 to 72 h, starting from the 9th step of serial dilution of the water sample to ensure optimal growth conditions and isolate the desired bacteria. The samples underwent seven consecutive contamination-free subcultures following the initial incubation to obtain pure isolates. This rigorous subculturing process was essential to eliminate non-target microorganisms and achieve a pure culture of *B. cereus*. Finally, eight single colonies, each displaying distinct morphological characteristics, were selected from the final pure culture plate. These colonies were selected for further biochemical and molecular characterization to assess their potential for HM bioremediation.

Screening of Heavy Metal Resistant Bacteria

Screening of HM-resistant bacteria was conducted following the method previously described by Kumari et al. (2021a). Briefly, several isolated bacterial strains were tested for their ability to resist HMs by observing their growth on LB agar plates enriched with a mixture of 10 mg.L^{-1} concentrations of Cd, Cu, Pb, Cr, As, and Hg over two days. *Bacillus* isolate IEI-01, which exhibited significant growth, was selected as the most promising strain for further analysis (Desoky et al. 2020).

Morphological Characterization of Bacteria

The morphological characterization of *Bacillus* isolates involved examining their size, shape, motility, and staining properties. Bacterial smears were prepared, air-dried, heat-fixed, and stained with crystal violet or methylene blue to assess cell size and shape under a light microscope at 1000x

magnification. Motility was evaluated by inoculating a semi-solid agar medium with the isolates and observing the spread of growth from the stab line after incubating at 37°C for 24 to 48 h. Gram staining determined the bacteria's Gram-positive nature by retaining the crystal violet dye. Capsular staining identified the presence of a clear halo around cells, indicating a positive capsule, while spore staining revealed spore formers by retaining malachite green within the spores, contrasting with red-stained vegetative cells. Additionally, colony morphology on solid agar plates was observed for shape, texture, elevation, margin, size, and transparency, providing further insight into the isolates' characteristics. The colonies were typically rod-shaped, rough in texture, raised with irregular margins, measured 4-6 μm in size, opaque, and confirmed as spore-forming and Gram-positive (Chauhan & Jindal 2020)

Biochemical Characterization

To biochemically characterize *Bacillus* isolates, pink colonies were initially picked from MYP agar plates, streaked onto nutrient agar, and incubated at 37°C for 24 h to obtain pure cultures. Several biochemical tests were conducted on these cultures. Gram staining confirmed the isolates as Gram-positive rods. Glucose fermentation tests were performed to assess acid production. The Voges-Proskauer test was conducted to detect acetoin production from glucose fermentation. Methyl Red testing was carried out to determine stable acid production. The Citrate Utilization test was performed to assess citrate utilization. Indole production was examined using Kovac's reagent. The Oxidase test was conducted to detect cytochrome c oxidase activity. The catalase test was performed to determine the presence of the catalase enzyme. The nitrate reduction test was conducted to assess nitrate reduction to nitrite. Finally, the starch hydrolysis test was performed to determine starch degradation (Chauhan & Jindal 2020)

Molecular Characterization Using 16S rRNA Gene Sequencing

DNA isolation: Molecular characterization of our bacterial isolate began with the extraction of DNA. Samples were homogenized with extraction buffer and processed through phenol-chloroform extraction. Following centrifugation, the aqueous phase was collected, and DNA was precipitated using sodium acetate and isopropanol. The DNA was then washed with ethanol, air-dried, and dissolved in TE buffer, with RNA removal achieved using RNAse A. The extracted DNA was quantified using spectrophotometry, and purity was assessed by calculating the OD 260/280 ratio, aiming for values between 1.8 and 2.0 (Arora et al. 2024)

PCR amplification and sequencing: A fragment of the 16S rRNA gene was amplified using universal primers 27F and 1492R. The PCR amplicon was purified to remove contaminants and resolved on an agarose gel. Forward and reverse DNA sequencing was performed using an ABI 3730×l Genetic Analyzer with the BDT v3.1 Cycle sequencing kit. A consensus sequence was generated from the forward and reverse sequence data using alignment software.

Phylogenetic tree construction: The genetic sequences were identified using NCBI's BLAST software, comparing them to the closest relatives based on maximum identity scores. The top ten sequences were aligned using Clustal W, and a phylogenetic tree was constructed using the neighbor-joining algorithm in MEGA 10 software. The stability of the tree clades was determined through a 1000-replication bootstrap analysis, which involved creating pseudo-alignments by resampling the original alignment to generate a majority consensus tree. This tree displayed the percentage of times specific groups appeared on each side of a branch across 100 bootstrap replicates.

Optimizing Growth Conditions for *Bacillus* Sp. IEI-01: Temperature and pH Effects

To determine the optimal growth conditions for *Bacillus cereus* strain IEI-01, the methods described by Sheer et al. (2021) were employed, focusing on temperature and pH. For temperature optimization, LB-broth was prepared in sets and autoclaved, then inoculated with an overnight log phase culture of the isolate. These sets were incubated at 25°C, 37°C, and 45°C on a shaker for 24 h. The growth was measured by recording the optical density (OD) at 600 nm UV/vis spectrophotometer. For pH optimization, LB broth was adjusted to different pH levels (5.0, 7.0, 9.0) and similarly inoculated and incubated at 37°C on a shaker for 24 h. Post-incubation, the OD at 600 nm was measured to assess bacterial growth across the pH spectrum.

Impact of Heavy Metals on the Growth of *Bacillus cereus* Strain IEI-01

To investigate the effect of various HMs on the growth of *Bacillus cereus* strain IEI-01, OD at 600 nm was monitored over 72 days using LB broth. The metals examined included Cd, Cu, Pb, Cr, As, and Hg. Growth measurements were taken at specific intervals, 0, 12, 24, 48, and 72 days.

Evaluation of Bioremoval Efficiency of Heavy Metals by Bacterial Strains in LB Broth

LB broth (100 mL) in a 250 mL flask was individually spiked with 10 mg.L^{-1} of HMs Cd, Cu, Pb, Cr, As, and Hg and then inoculated with 50 μL of an overnight bacterial culture of $(2 \times 10^7$ CFU.mL$^{-1})$. Metal concentrations in these spiked
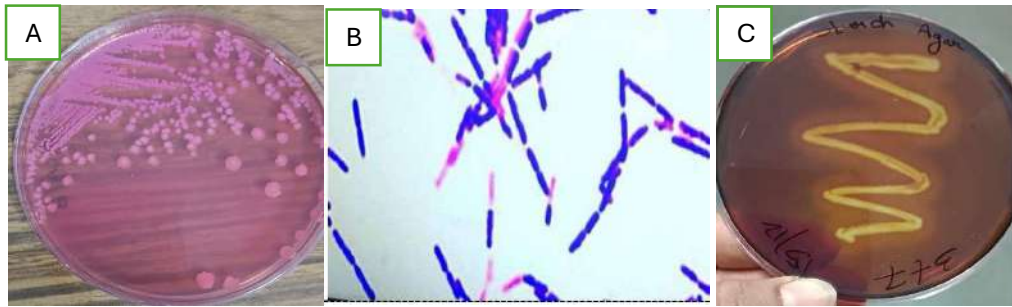
Fig. 1: Morphological and biochemical characteristics of *Bacillus* isolate IEI-01, showing (A) pink-colored colonies on MYP agar, (B) Gram-positive rod shape, and (C) starch hydrolysis on starch agar.

cultures were measured at specified intervals (0, 12, 24, 48, 72 h) using an ICP-OES. Samples were centrifuged at 3500 rpm for 30 min, and the supernatant was filtered through a 0.25 μm filter before ICP-OES analysis. The bioremoval of metal ions by the bacteria was calculated by determining the difference between the initial and final concentrations of HMs in the media (Radhika et al. 2006). The bio-removal percentage (BR%) and the metal ion removal rate (RR) by the strain were calculated using the following equations (Kumari et al. 2021b):

$$BR\,(\%) = \left\{\frac{C_0 - C_t}{C_0}\right\} \times 100$$

C_0 and C_t are metal ion concentrations at the time 0 min and at time interval t, respectively.

Methodology for Concentration-Dependent Bioremoval Efficiency of *Bacillus cereus* IEI-01 in Cadmium-Spiked Cultures

The concentration-dependent bioremoval efficiency of *Bacillus cereus* IEI-01 in Cd-spiked cultures was investigated over a 72-h incubation period. Initially, cultures of *Bacillus cereus* IEI-01 were prepared in LB broth and incubated overnight to reach the log phase. Cd solutions of varying concentrations ranging from 0.1 mg.L^{-1} to 5 mg.L^{-1} were then prepared by diluting a Cd stock solution in sterile water. Sampling was conducted at 12 h intervals over 72 h, and the Cd concentration in the culture supernatant was determined using ICP-OES. Bioremoval efficiency was calculated as described in the previous section.

RESULTS AND DISCUSSION

Bacillus isolate IEI-01 was successfully isolated from water samples collected from Badshahpur Lake, Gurugram, using selective MYP agar and rigorous subculturing. The strain demonstrated strong resistance to HMs, showing growth on LB agar plates containing 10 mg.L^{-1} of Cd, Cu, Pb, Cr, As,

and Hg. Further testing revealed that *Bacillus cereus* IEI-01 thrives optimally at a temperature of 37°C and a pH of 7.0, indicating its potential for effective HM bioremediation in contaminated environments.

Morphological and Biochemical Characterization Results

The HM-tolerant *Bacillus* sp., IEI-01, was identified as Gram-positive rods with metabolic versatility, as it could ferment glucose and produce acetoin, demonstrated by positive Voges-Proskauer tests. Additionally, the strain reduced nitrate to nitrite, as evidenced by positive nitrate reduction tests. Morphologically, IEI-01 formed rough,

Table 1: Morphological and Biochemical Characteristics of *Bacillus cereus*.

Characteristic	*Bacillus* isolate IEI-01
Morphological Characteristics	
Shape	Rod
Texture	Rough
Motility	Positive
Elevation	Raised
Margin	Irregular
Size	4-6 μm
Transparency	Opaque
Gram's Staining	Gram-positive
Capsular Staining	Positive
Spore Staining	Spore former
Biochemical Characteristics	
Methyl Red Reaction	Negative
Citrate	Positive
Indole Production	Negative
Voges–Proskauer Reaction	Positive
Oxidase Test	Negative
Catalase Test	Positive
Nitrate Test	Positive
Starch Hydrolysis	Positive

opaque, rod-shaped colonies with irregular margins and raised elevations, measuring 4-6 μm. Pink-colored colonies on MYP agar suggested mannitol fermentation, while clear zones around colonies on starch agar indicated starch hydrolysis. IEI-01 exhibited positive reactions for citrate utilization, catalase activity, and starch hydrolysis but tested negative for methyl red and oxidase. These findings highlight the potential of strain IEI-01 in bioremediation applications, attributed to its metabolic capabilities and resilience in HM environments. Fig. 1 illustrates these traits, highlighting pink colonies on MYP agar, Gram-positive rod-shaped cells, and starch hydrolysis on starch agar. Table 1 provides the morphological and biochemical characteristics of *Bacillus cereus*.

Molecular Characterization Results

Molecular characterization was carried out by performing 16S rRNA gene sequencing. For the amplification of 16S rRNA sequences, universal primers, 27F (5'-AGAGTTTGATCMTGGCTCAG-3') and 1492R (5'-TACGGYTACCTTGTTACGACTT-3'), were used. From the IEI-01 strain, the DNA extraction process yielded 133 ng of genetic material. On performing the NCBI BlastN analysis of the strains, their respective closest relatives could be identified. The genetic makeup of IEI-01 exhibited a striking 100% similarity to that of *Bacillus cereus* strain VC6, followed by a 99.71% similarity with *Bacillus cereus* strain SP4. This high level of genetic similarity can be indicative of common ancestry or shared genetic traits among these bacterial strains. The 16S rRNA phylogenetic tree of IEI-01 showing its relation with nearest neighbors can be seen in Fig. 2.

Bacterial Growth of *Bacillus cereus* IEI-01

In an optimal environment free from HM stress, *Bacillus cereus* IEI-01 exhibited typical bacterial growth characterized by a sigmoidal growth curve over 72 h. The absorbance values measured at OD600 showed an initial lag phase with an absorbance of 0.05 at 0 h, followed by exponential growth reaching an absorbance of 0.32 at 12 h. Subsequently, the growth rate peaked at 24 h with an absorbance of 1.21, indicating the onset of the stationary phase. By 48 and 72 h, the absorbance values slightly decreased to 1.19 and 1.01, respectively, suggesting stabilization of the bacterial population. This growth pattern illustrates the significant and typical growth behavior of *Bacillus cereus* IEI-01 in favorable conditions (Fig. 3).

Growth Dynamics of *Bacillus cereus* IEI-01 in the Presence of Various Heavy Metals
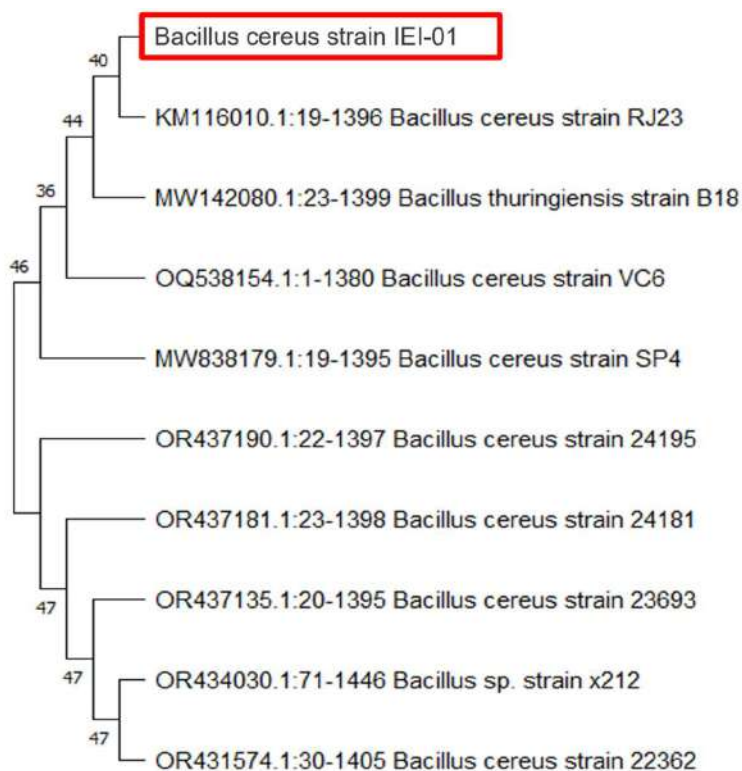
Fig. 2: A phylogenetic tree depicting the close relationship of *Bacillus cereus* IEI-01 with its nearest neighbors.
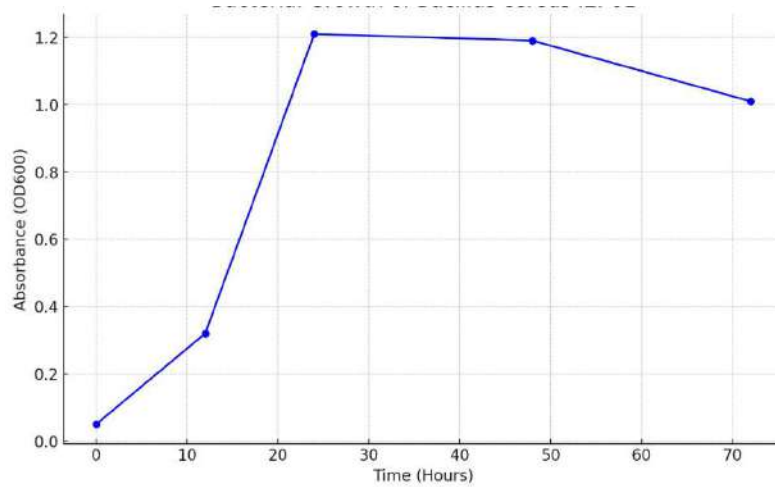
Fig. 3: Growth curve of *Bacillus cereus* IEI-01 under optimal environmental conditions. The graph shows absorbance (OD600) measurements taken at various time points (0, 12, 24, 48, and 72 h), illustrating the characteristic sigmoidal growth pattern of the bacterial culture.

The growth curves of *Bacillus cereus* strain IEI-01 in the presence of various HMs, measured by absorbance at OD600, reveal distinct patterns of bacterial growth over a 72-h incubation period. At the initial time point (0 h), all samples, including those with Cd, Cu, Pb, Cr, As, and Hg, exhibited low absorbance values between 0.04 and 0.06, indicating minimal initial growth. Over the first 12 h, significant growth was observed in the presence of Cd (0.37), Pb (0.34), and Cr (0.29), whereas Cu, As, and Hg showed lower growth rates with absorbance values below 0.25. By 24 h, the absorbance values peaked for most metals, with Cd (1.28), Pb (1.26), and Cr (1.20) supporting the highest bacterial growth. Cu, As, and Hg resulted in moderate growth with absorbance values ranging from 0.78 to 0.87. After 48 h, a slight decline in growth was noted for all metals except for a small increase in the presence of Cu (0.90). By 72 h, the overall absorbance decreased for most conditions, with Cd maintaining the highest absorbance (1.22), followed by Pb
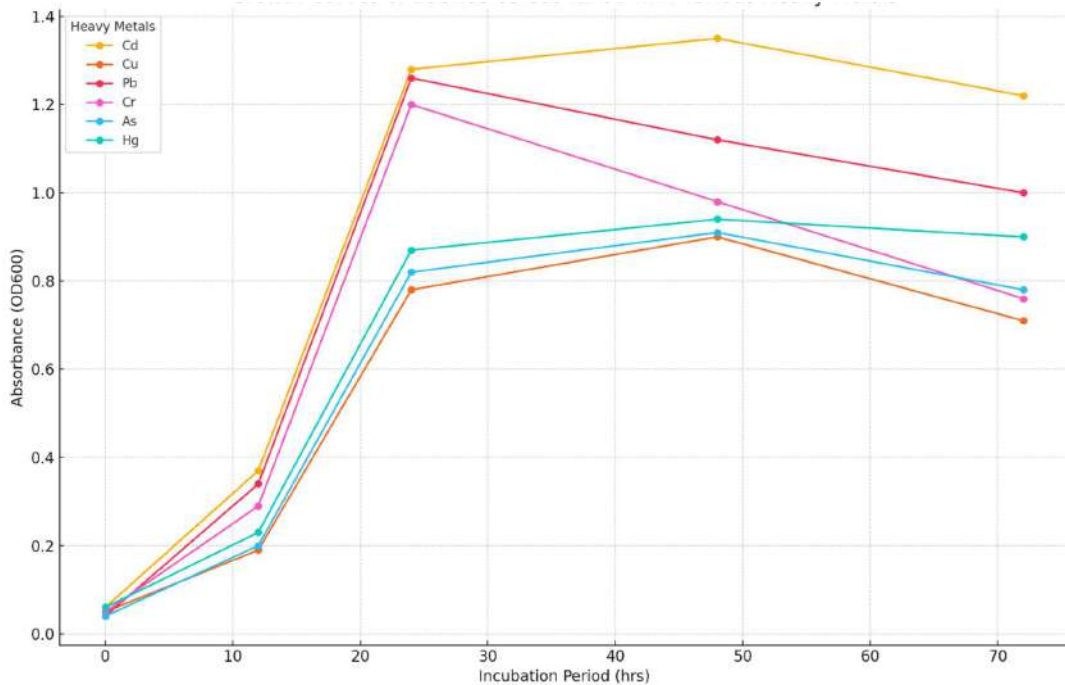
Fig. 4: Growth curves of *Bacillus cereus* IEI-01 with various HMs.

(1.00) and hg (0.90). The data indicate that *Bacillus cereus* IEI-01 exhibits differential tolerance and growth dynamics when exposed to various HMs, with Cd and Pb showing the most significant growth stimulation over time (Fig. 4).

Heavy Metal Bioremoval Efficiency of *Bacillus cereus* IEI-01 Over Time

The bio-removal capacity of *Bacillus cereus* IEI-01 for different HMs, expressed as Bioremoval (BR%) over a 72-hour incubation period, demonstrates varied efficiencies. At 12 h, Cd removal is the most effective at 58.41±2.3%, while Cu exhibits the lowest removal efficiency at 16.2±1.9%. Pb and Cr show moderate bioremoval capacities of 40.63±1.3% and 31.62±1.1%, respectively, whereas As and Hg are removed at 20.34±2.2% and 28.49±1.8%. By 24 h, the bio-removal of Cd significantly increases to 72.42±1.9%, making it the highest among all metals, while Hg also sees a notable rise to 37.52±2.1%. Pb maintains a steady removal rate (41.87±2.4%), whereas Cu, Cr, and As exhibit slight increases, reaching 19.52±0.6%, 38.83±1.4%, and 21.22±2.9%, respectively. After 48 h, the efficiency of Pb removal peaks at 52.62±2.1%, while Cd decreases slightly to 65.53±2.1%. Hg and As removal capacities improve to 32.82±1.4% and 24.52±2.4%, respectively, but Cu and Cr show minor declines to 17.43±1.1% and 34.34±1.8%. At 72 h, Cd's bioremoval decreases to 61.43±1.3%, but it remains the highest among the tested metals. The removal efficiencies for the other metals generally decline, with

Cu dropping to 11.32±1.6% and mercury to 26.52±2.2%, indicating a gradual decrease in bioremoval capacity over time for most metals. This data highlights *Bacillus cereus* IEI-01's strong potential for removing Cd and Pb from contaminated environments, with varying efficiencies for other metals (Fig. 5).

Concentration-Dependent Bioremoval Efficiency of *Bacillus cereus* IEI-01 in Cadmium-Spiked Cultures

The bio-removal efficiency of *Bacillus cereus* IEI-01 in Cd spiked cultures shows a concentration-dependent variation over a 72-h incubation period. At 12 h, the highest bio-removal capacity is observed at the lowest Cd concentration of 0.1 mg.L^{-1}, with $80.23 \pm 2.4\%$ removal. As the concentration increases, the bio-removal efficiency decreases, with $71.62 \pm 2.1\%$ at 0.5 mg.L^{-1}, $65.62 \pm 2.1\%$ at 1 m.L^{-1}, $64.62 \pm 2.3\%$ at 2.5 mg.L^{-1}, and $60.64 \pm 1.3\%$ at 5 mg.L^{-1}. By 24 h, the bio-removal rates improve across all concentrations, reaching $87.43 \pm 1.9\%$ for 0.1 mg.L^{-1} and maintaining high removal rates for higher concentrations: $80.82 \pm 1.9\%$ at 0.5 mg.L^{-1}, $78.82 \pm 1.7\%$ at 1 mg.L^{-1}, $69.25 \pm 1.2\%$ at 2.5 mg.L^{-1}, and $70.12 \pm 1.9\%$ at 5 mg.L^{-1}. At 48 h, the removal efficiency slightly decreases for lower concentrations, with $86.62 \pm 1.1\%$ for 0.1 mg.L^{-1} and $72.83 \pm 2.0\%$ for 0.5 mg.L^{-1}, while showing a steady performance for higher concentrations: $70.45 \pm 1.3\%$ at 1 mg.L^{-1}, $70.86 \pm 1.6\%$ at 2.5 mg.L^{-1}, and an increase to $74.89 \pm 2.1\%$ at 5 mg.L^{-1}. By 72 h, the bio-removal efficiency generally
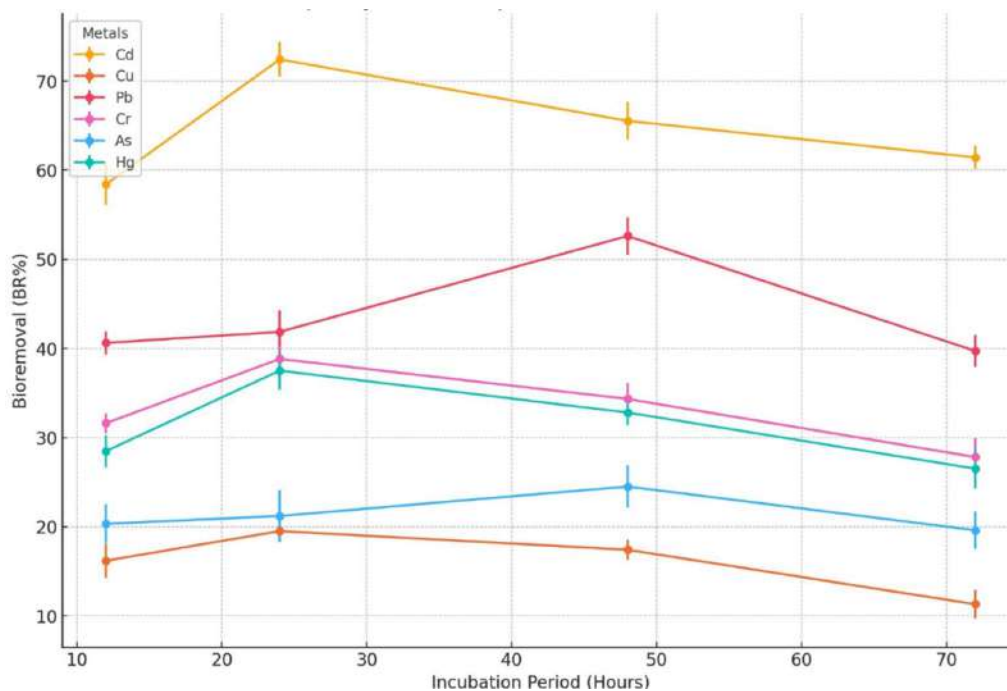
Fig. 5. Time-dependent heavy metal removal efficiency of *Bacillus cereus* IEI-01.
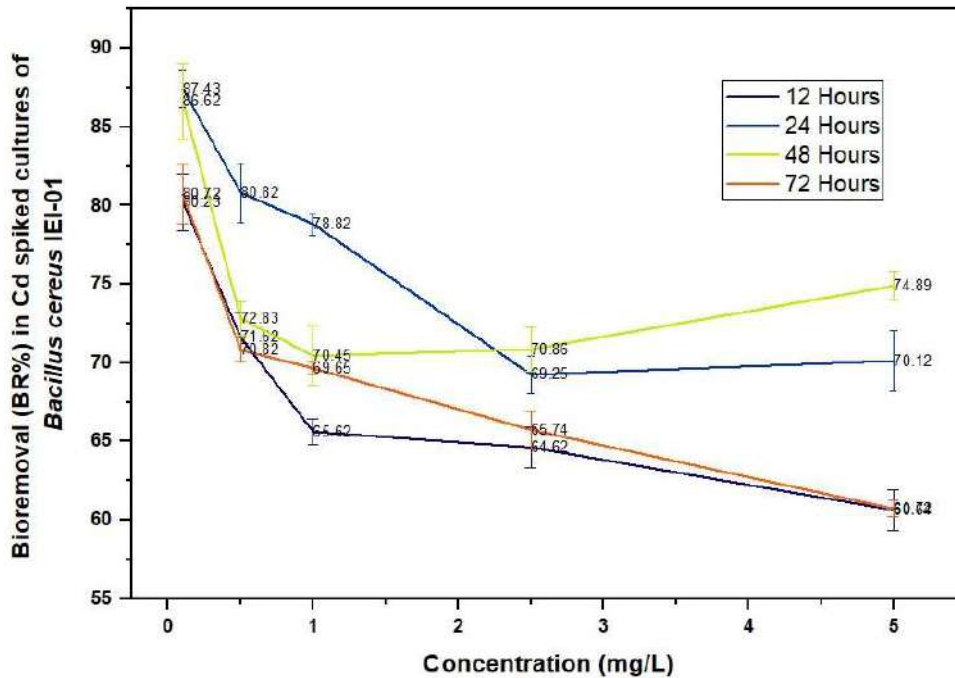
Fig. 6. Bioremoval capacity (BR%) of *Bacillus cereus* IEI-01 in cadmium (Cd) spiked cultures over 12, 24, 48, and 72 h across various Cd concentrations (0.1, 0.5, 1, 2.5, 5 mg.L^{-1}). Error bars represent the standard deviation.

declines but remains substantial, with 80.72 ± 2.0% at 0.1 mg.L^{-1} and decreasing as the concentration increases: 70.82 ± 2.1% at 0.5 mg.L^{-1}, 69.65 ± 1.4% at 1 mg.L^{-1}, 65.74 ± 3.2% at 2.5 mg.L^{-1}, and 60.72 ± 2.5% at 5 mg.L^{-1}. This data indicates that *Bacillus cereus* IEI-01 is highly effective at removing Cd from cultures, particularly at lower concentrations, with significant, albeit reduced, efficiency at higher Cd concentrations over time (Fig. 6).

DISCUSSION

Our study highlights *Bacillus cereus* IEI-01, a Gram-positive, rod-shaped bacterium isolated from Badshahpur Lake in Gurugram, which exhibits significant tolerance and bioremediation capabilities for various heavy metals (HMs). Identified through morphological and biochemical characterizations and confirmed via 16S rRNA sequencing, this strain is closely related to other *Bacillus cereus* strains, indicating shared resilient traits. Under optimal conditions, *Bacillus cereus* IEI-01 displayed a typical bacterial growth pattern, with heavy metals like Cd and Pb significantly stimulating its growth, while Hg and Cu resulted in moderate growth responses. Over 72 h, the strain demonstrated high bio-removal efficiencies, with cadmium showing the highest rate at 72.42% within 24 h, followed by notable but lesser rates for Pb and Hg and the lowest for Cu. The strain's ability to remove Cd was particularly impressive, achieving up to

87.43% removal at lower concentrations (0.1 mg.L^{-1}) within 24 h, though efficiency decreased with higher concentrations. Despite this decrease, significant removal capabilities were maintained even at higher concentrations (5 mg.L^{-1}). This finding suggests IEI-01's potential for application in HM bioremediation in contaminated environments.

Comparatively, Rengarajan et al. (2024) demonstrated the bioremediation potential of biochar and *Bacillus cereus* in treating HM-polluted mine surroundings. While our study focused on the bacterial strain's metal tolerance, Rengarajan et al. evaluated the combined effectiveness of biochar and bacteria. Both studies highlight the importance of integrated approaches for efficient metal removal. Furthermore, Maumela et al. (2024) investigated Pb bioremediation using a *Bacillus* sp. strain MHSD_36 isolated from *Solanum nigrum*. Our findings align with theirs in demonstrating the metal tolerance and bioremediation potential of Bacillus strains, albeit with variations in the targeted metals and specific bacterial strains. Harun et al. (2024) explored the bioremediation potential of *Paenebacillus* sp. and *Bacillus* sp. in lead-contaminated environments. While our study focused on *Bacillus cereus* IEI-01, their work underscores the broader applicability of bacterial remediation approaches across various HM contaminants. Moreover, Gupta et al. (2024) and Anusha et al. (2024) investigated Cr (VI) and multi-metal bioremediation, respectively,

showcasing diverse bacterial strains' versatility in metal removal. Although targeting different metals and bacterial strains, their findings complement ours by highlighting the collective contribution of bacterial remediation approaches to mitigating metal pollution.

In another study by Abo-Amer et al. (2014), *Azotobacter chroococcum's* role in HM bioremediation was examined, demonstrating the potential of diverse bacterial genera in environmental cleanup efforts. Similarly, Jahan et al. (2016) isolated and characterized *Bacillus thuringiensis* and *Bacillus pumilus* for Cr bioremediation, highlighting the importance of species-specific bacterial strains in metal detoxification processes. Raja et al. (2009) isolated HM-resistant bacteria from sewage water, illustrating the widespread distribution of metal-tolerant microorganisms in diverse environments. Their findings contribute to the understanding of microbial communities' potential role in mitigating metal pollution. Furthermore, Elahi et al. (2019) isolated and characterized *Microbacterium testaceum* B-HS2 from tannery effluent, emphasizing the importance of studying bacterial strains from specific industrial contexts for targeted bioremediation strategies. Additionally, Irawati et al. (2012) investigated copper-resistant bacteria from industrial wastewater, showcasing the relevance of studying microbial communities in anthropogenically impacted environments for pollution management. Nwagwu et al. (2017) isolated HM-tolerant bacteria from the Panteka stream in Nigeria, emphasizing the global relevance of studying bacterial bioremediation potentials in diverse ecosystems.

The study emphasizes *Bacillus cereus* IEI-01's metal resistance and bioremediation potential. The comparison with other studies underscores the broader spectrum of bacterial strains and metals targeted in HM remediation efforts. These findings collectively contribute to advancing our understanding of microbial-mediated approaches in environmental remediation.

CONCLUSIONS

In this study, *Bacillus cereus* IEI-01 was isolated from Badshahpur Lake in Gurugram and exhibited significant tolerance and bioremediation capabilities for various HMs. Morphological and biochemical characterizations identified it as a Gram-positive, rod-shaped bacterium with versatile metabolic abilities, such as glucose fermentation and nitrate reduction. Molecular analysis through 16S rRNA sequencing confirmed its close relationship to other *Bacillus cereus* strains, suggesting shared resilient traits. *Bacillus cereus* IEI-01 showed a typical bacterial growth pattern in optimal conditions and displayed distinct growth responses when exposed to HMs like Cd, Pb, and Cr). Cd and Pb significantly

stimulated its growth, while Hg and Cu resulted in moderate growth. Over 72 h, the strain demonstrated high bio-removal efficiencies, particularly for Cd, which reached 72.42% at 24 h. Pb and Hg also exhibited considerable bio-removal rates, though less than Cd, while Cu removal was the lowest. When tested for Cd removal across different concentrations, *Bacillus cereus* IEI-01 achieved up to 87.43% removal at lower concentrations (0.1 mg.L^{-1}) within 24 h, though efficiency decreased as Cd concentrations increased. Despite this, the strain maintained significant removal capabilities even at higher concentrations (5 mg.L^{-1}), indicating its potential for diverse applications in contaminated environments. These findings suggest that *Bacillus cereus* IEI-01 is a promising candidate for bioremediation, particularly effective in environments contaminated with Cd and Pb. Future studies should explore its application in real-world scenarios, potentially combining it with other remediation techniques to enhance its effectiveness.

ACKNOWLEDGMENTS

REFERENCES

Abo-Amer, A.E., Abu-Gharbia, M.A., Soltan, E.S.M. and Abd El-Raheem, W.M., 2014. Isolation and molecular characterization of heavy metal-resistant *Azotobacter chroococcum* from agricultural soil and their potential application in bioremediation. *Geomicrobiology Journal*, 31(7), pp.551-561.

Afzal, A.M., 2023. In-vitro evaluation of heavy metal tolerance and biosorptive potential of two native strains of *Bacillus cereus* against nickel and cobalt. *Annals of Clinical Medical Case Report*, 12(5), pp.1-11.

Afzal, A.M., Rasool, M.H., Waseem, M. and Aslam, B., 2017. Assessment of heavy metal tolerance and biosorption potential of *Klebsiella variicola* isolated from industrial effluents. *Amb Express*, 7, pp.1-9.

Al Azad, S., Farjana, M., Mazumder, B., Abdullah-Al-Mamun, M. and Haque, A.I., 2020. Molecular identification of a *Bacillus cereus* strain from Murrah buffalo milk showed in vitro bioremediation properties on selective heavy metals. *Journal of Advanced Veterinary and Animal Research*, 7(1), pp.62.

Ali, A. and Rehman, A., 2014. Uptake of mercury by a bacterium, *Pseudomonas sp. AN29*, isolated from industrial effluents and its potential use in wastewater treatment. *Iranian Journal of Science and Technology*, 38(A3), pp.231.

Ameen, F.A., Hamdan, A.M. and El-Naggar, M.Y., 2020. Assessment of the heavy metal bioremediation efficiency of the novel marine lactic acid bacterium, Lactobacillus plantarum MF042018. *Scientific Reports*, 10(1), pp.314.

Anusha, P., Natarajan, D., Rengarajan, S., Alfarraj, S. and Kandasamy, S., 2024. An assessment of metal absorption competence of indigenous metal-tolerant bacterial species in vitro study. *Environmental Research*, 251, pp.118700.

Arora, J., Ranjan, A., Chauhan, A., Rajput, V.D., Sushkova, S., Prazdnova, E.V. and Prasad, R., 2024. A novel study on anionic

surfactant degradation potential of psychrophilic and psychrotolerant *Pseudomonas spp*. identified from surfactant-contaminated river water. *Applied Biochemistry and Biotechnology*, 196(5), pp.2612-2629.

Begum, S.S. and Aundhati, A., 2016. Heavy metals tolerance and in vitro bioremediation potential in *Pseudomonas spp. r2*. *International Journal of Pharma, Chemistry, and Biological Science*, 6, pp.159-166.

Bestawy, E.E., Helmy, S., Hussien, H., Fahmy, M. and Amer, R., 2013. Bioremediation of heavy metal-contaminated effluent using optimized activated sludge bacteria. *Applied Water Science*, 3, pp.181-192.

Bhakta, J.N., Munekage, Y., Ohnishi, K., Jana, B.B. and Balcazar, J.L., 2014. Isolation and characterization of cadmium-and arsenic-absorbing bacteria for bioremediation. *Water, Air, & Soil Pollution*, 225, pp.1-10.

Chauhan, A. and Jindal, T., 2020. *Microbiological Methods for Environment, Food, and Pharmaceutical Analysis*. Springer Nature.

Das, S., Dash, H.R. and Chakraborty, J., 2016. Genetic basis and importance of metal-resistant genes in bacteria for bioremediation of contaminated environments with toxic metal pollutants. *Applied Microbiology and Biotechnology*, 100, pp.2967-2984.

Desoky, E.S.M., Merwad, A.R.M., Semida, W.M., Ibrahim, S.A., El-Saadony, M.T. and Rady, M.M., 2020. Heavy metals-resistant bacteria (HM-RB): Potential bioremediators of heavy metals-stressed *Spinacia oleracea* plant. *Ecotoxicology and Environmental Safety*, 198, pp.110685.

Elahi, A., Ajaz, M., Rehman, A., Vuilleumier, S., Khan, Z. and Hussain, S.Z., 2019. Isolation, characterization, and multiple heavy metal-resistant and hexavalent chromium-reducing *Microbacterium testaceum* B-HS2 from tannery effluent. *Journal of King Saud University-Science*, 31(4), pp.1437-1444.

Gupta, A., Gond, S.K. and Mishra, V.K., 2024. Isolation and characterization of hexavalent chromium-tolerant endophytic bacteria inhabiting *Solanum virginicum* L. roots: A study on potential for chromium bioremediation and plant growth promotion. *Journal of Hazardous Materials Letters*, 100114.

Harun, F.A., Yakasai, H.M., Jagaba, A.H., Usman, S., Umar, H.A. and Shukor, M.Y., 2024. Bioremediation potential of *Bacillus sp*. and *Paenibacillus sp*. novel lead-resistant isolates: Identification, characterization, and optimization studies. *The Microbe*, 100087.

Irawati, W., Yuwono, T., Soedarsono, J. and Hartiko, H., 2012. Molecular and physiological characterization of copper-resistant bacteria isolated from activated sludge in an industrial wastewater treatment plant in Rungkut-Surabaya, Indonesia. *Microbiology Indonesia*, 6(3), pp.3.

Jahan, N., Idrees, M., Zahid, M., Ali, N. and Hussain, M., 2016. Molecular identification and characterization of heavy metal-resistant bacteria and their role in bioremediation of chromium. *British Microbiology Research Journal*, 13(6), pp.1-11.

Kalsoom, M., Batool, A., Din, G., Din, S.U., Jamil, J., Hasan, F. and Shah, A.A., 2021. Isolation and screening of chromium-resistant bacteria from industrial waste for bioremediation purposes. *Brazilian Journal of Biology*, 83, pp.e242536.

Kelany, M.S., El-Sawy, M.A., El-Gendy, A.R. and Beltagy, E.A., 2023. Bioremediation of industrial wastewater heavy metals using solo and consortium *Enterobacter spp*. *Environmental Monitoring and Assessment*, 195(11), pp.1357.

Kour, R., Jain, D., Bhojiya, A.A., Sukhwal, A., Sanadhya, S., Saheewala, H. and Mohanty, S.R., 2019. Zinc biosorption, biochemical and molecular characterization of plant growth-promoting zinc-tolerant bacteria. *3 Biotech*, 9, pp.1-17.

Kumari, N., Chandrasekharan, N.V. and Wijayarathna, C.D., 2021a. Characterization of a multi-metal resistant *Bacillus cereus* strain TWSL_5 and its bioremediation potential for Cr, Pb, Zn, and Fe. *American Journal of Environmental Science*, 17(1), pp.49-62.

Kumari, W.M.N.H., Thiruchittampalam, S., Weerasinghe, M.S.S., Chandrasekharan, N.V. and Wijayarathna, C.D., 2021b. Characterization

of a *Bacillus megaterium* strain with metal bioremediation potential and in silico discovery of novel cadmium binding motifs in the regulator, CadC. *Applied Microbiology and Biotechnology*, 105(6), pp.2573-2586.

Maumela, P., Magida, S. and Serepa-Dlamini, M.H., 2024. Bioremediation of Pb contaminated water using a novel *Bacillus sp*. strain MHSD_36 isolated from *Solanum nigrum*. *PLOS ONE*, 19(4), e0302460.

Monga, A., Fulke, A.B., Gaud, A., Sharma, A., Ram, A. and Dasgupta, D., 2022. Isolation and identification of novel chromium tolerant bacterial strains from a heavy metal polluted urban creek: An assessment of bioremediation efficiency and flocculant production. *Thalassas: An International Journal of Marine Sciences*, 38(2), pp.1233-1244.

Nwagwu, E.C., Yilwa, V.M., Egbe, N.E. and Onwumere, G.B., 2017. Isolation and characterization of heavy metal tolerant bacteria from Panteka stream, Kaduna, Nigeria and their potential for bioremediation. *African Journal of Biotechnology*, 16(1), pp.32-40.

Patra, R.C., Malik, S., Beer, M., Megharaj, M. and Naidu, R., 2010. Molecular characterization of chromium (VI) reducing potential in Gram-positive bacteria isolated from contaminated sites. *Soil Biology and Biochemistry*, 42(10), pp.1857-1863.

Raja, C.E., Selvam, G.S. and Omine, K.I.Y.O.S.H.I., 2009. Isolation, identification, and characterization of heavy metal-resistant bacteria from sewage. *Geoenvironment,* 17, pp.205-211.

Rengarajan, S., Deepa, S., Natarajan, D., Pandian, A., Al-Ansari, M.M., Oza, G. and Sharma, A., 2024. Bioremediation potential of biochar and metal tolerant *Bacillus cereus* on heavy metal polluted mine surrounding pond and assessed cytotoxicity and phytotoxicity attributes of treated water on Brine shrimp larvae and Paddy seedling. *Journal of the Taiwan Institute of Chemical Engineers*, 415, p.105330.

Saduzzaman, M., Mini, K., Shardendu, S. and Ahmad, S.R., 2023. Evaluation of Cr (VI) Reducing Capability of *Bacillus licheniformis* DAS1 Using a Multifactor Experimental Approach. *Nature Environment and Pollution Technology*, 22(4), pp.1821-1831.

Shakoori, F.R., Tabassum, S., Rehman, A. and Shakoori, A.R., 2010b. Isolation and characterization of Cr6+ reducing bacteria and their potential use in bioremediation of chromium containing wastewater. *Pakistan Journal of Zoology*, 42(6), p.331.

Sharma, B. and Shukla, P., 2021. A comparative analysis of heavy metal bioaccumulation and functional gene annotation towards multiple metal resistant potential by *Ochrobactrum intermedium* BPS-20 and *Ochrobactrum ciceri* BPS-26. *Bioresource Technology*, 320, p.124330.

Shylla, L., Barik, S.K. and Joshi, S.R., 2021. Characterization and bioremediation potential of native heavy-metal tolerant bacteria isolated from rat-hole coal mine environment. *Archives of Microbiology*, 203(8), pp.2379-2392.

Tahir, U., Zameer, M., Ali, Q., Rafique, A., Ali, S.M., Arif, M.U. and Ali, D., 2023. Toxicity assessment of heavy metal (Pb) and its bioremediation by potential bacterial isolates. *Environmental Monitoring and Assessment*, 195(9), 1047.

Tariq, M., Waseem, M., Rasool, M.H., Zahoor, M.A. and Hussain, I., 2019. Isolation and molecular characterization of the indigenous *Staphylococcus aureus* strain K1 with the ability to reduce hexavalent chromium for its application in bioremediation of metal-contaminated sites. *Peer Journal*, 7, p.e7726.

Yadav, M., Manderia, S., Singh, S. and Deva, M., 2022. Isolation and characterization of polyvinyl chloride (PVC) degrading bacteria from polluted sites of Gwalior City, MP, India. *Nature Environment & Pollution Technology*, 21(1), p.614.

Zahoor, A. and Rehman, A., 2009. Isolation of Cr (VI) reducing bacteria from industrial effluents and their potential use in bioremediation of chromium containing wastewater. *Journal of Environmental Sciences*, 21(6), pp.814-820.

Original Research Paper   doi   https://doi.org/10.46488/NEPT.2025.v24i01.B4142   **Open Access Journal**

Unveiling Microplastic Ignorance: A Study on Knowledge and Awareness Among Pune's Urban Population – A Mixed Method Approach

Manisha Mistry† and S. G. Joshi

Symbiosis College of Nursing, Symbiosis International University, Maharashtra, Pune, India
†Corresponding author: Manisha Mistry; manishamistry@scon.edu.in

ABSTRACT

Microplastic pollution has become a global concern with potentially severe environmental and health implications. This research explores the level of knowledge and awareness about microplastics among the urban population of Pune, a busy city in India. A mixed-methods approach was employed using a sequential explanatory design. In the first phase, qualitative data were gathered through semi-structured interviews with 18 participants selected via purposive sampling. In the second phase, quantitative data were collected from 100 participants using a survey and convenience sampling. By combining insights from surveys, interviews, and existing literature, the study analyzed the extent to which residents of Pune are informed about microplastic pollution and their willingness to take action. The findings highlight the need for increased awareness campaigns and educational initiatives to address the growing microplastic problem in urban areas. The study concludes that plastics have become an integral part of our lives, necessitating robust mechanisms to eliminate them from daily use.

INTRODUCTION

Microplastics, those minuscule plastic particles measuring less than 5mm, have become pervasive in ecosystems globally, presenting a formidable environmental challenge (Thacharodi et al. 2023). Their origin is diverse, stemming from the breakdown of larger plastic items, industrial processes, and even personal care products (Ghosh et al. 2023). This ubiquity, however, is not without consequences, as microplastics pose significant threats to ecosystems, wildlife, and potentially human health, as highlighted by Blackburn and Green (2022).

Even in urban landscapes like Pune, the microplastic crisis has found a foothold. The combination of high population density, industrial activities, and prevalent lifestyle patterns significantly contributes to microplastic pollution in such urban areas (Mondal et al. 2023). Understanding the extent of awareness and knowledge about microplastics among the residents of selected urban areas in Pune becomes crucial in formulating strategies to combat this pervasive issue.

Larger plastic items, products of our convenience-driven lifestyles, succumb to the relentless forces of degradation, fragmenting into minuscule particles that persist in the environment (Li et al. 2023). Industrial processes, the backbone of modern economies, release these particles into the air and water, further disseminating them across vast landscapes (Prasittisopin et al. 2023). Even seemingly benign personal care products, laden with microplastics for texture and exfoliation, contribute to this environmental drama, adding to the complexity of the issue (Gomez-Gonzalez et al. 2023).

These minute invaders, invisible to the naked eye, traverse ecosystems with alarming ease, finding their way into terrestrial and aquatic realms alike (Surendran

et al. 2023). As they infiltrate these environments, they pose a potent threat to the delicate balance that sustains diverse ecosystems. From the depths of oceans to the heart of urban landscapes, microplastics have become unwelcome guests, disrupting natural processes and threatening the biodiversity that depends on them (Thacharodi et al. 2023).

Wildlife, from the tiniest organisms to majestic creatures, faces unforeseen challenges as microplastics become intertwined with their habitats (Sarkar et al. 2023). Moreover, as microplastics traverse the trophic levels, they become an inadvertent part of the human food chain (Al Mamun et al. 2023). Recent research has begun shedding light on the potential implications for human health, introducing a new dimension to the microplastic crisis. As these particles make their way into the food we consume, questions about the long-term consequences on human well-being and health are becoming increasingly urgent (Sun & Wang 2023).

This exploration into the microplastic conundrum seeks not only to unravel the complexities of its genesis and dispersion but also to underscore the urgency of collective action (Ghosh et al. 2023). It is a call to arms to address this silent threat that has permeated the very essence of our interconnected world. Through a deeper understanding of microplastics, their sources, and their far-reaching consequences, we can pave the way for informed strategies and collaborative efforts to mitigate their impact on ecosystems, wildlife, and human health. The journey into the heart of the microplastic challenge is not just an exploration; it is an imperative step toward safeguarding the delicate equilibrium that sustains life on our planet (Sharma et al. 2023).

The first step in addressing the microplastic challenge in urban areas is understanding the level of awareness among residents (Wani et al. 2023). Many may not be fully cognizant of the implications of microplastic pollution, assuming it to be a distant concern. This lack of awareness may stem from a limited understanding of the sources and consequences of microplastics (Ghosh et al. 2023). Consequently, educational initiatives are paramount to enlighten the public about the pervasive nature of these particles and their detrimental effects on the environment (Araújo et al. 2023).

Building awareness could involve implementing educational campaigns through various mediums, such as workshops, community events, and online platforms (Dittmann et al. 2023). Collaborating with schools, universities, and local community organizations can be instrumental in disseminating information about microplastics. Workshops can delve into the sources, impact, and potential solutions to microplastic pollution (Danopoulos et al. 2023). Furthermore, educational materials, such as

brochures and videos, can be distributed to reinforce the knowledge gained during these sessions (López 2023).

However, awareness alone may not suffice. Concrete strategies are needed to combat microplastic pollution actively (Tian et al. 2023). One effective approach involves reducing the sources of microplastics in urban areas. This could involve tighter regulations on industrial discharges, promoting the use of eco-friendly materials in manufacturing processes, and encouraging the development of sustainable alternatives to common products that contribute to microplastic pollution. Additionally, waste management practices play a crucial role in mitigating microplastic pollution (Hettiarachchi & Meegoda 2023). Enhancing recycling facilities, implementing strict waste disposal regulations, and encouraging responsible consumer behavior are essential steps. Municipal authorities can work towards implementing efficient waste collection systems and promoting the segregation of plastic waste at its source (Subashini et al. 2023).

Need for the study

Global environmental challenge: Microplastics, originating from diverse sources such as the breakdown of larger plastic items, industrial processes, and personal care products, have become ubiquitous in ecosystems globally. Their presence poses significant threats to ecosystems, wildlife, and potentially human health (Klingelhöfer et al. 2020).

Urban Contribution: Urban landscapes, exemplified by cities like Pune, face a heightened microplastic crisis due to factors such as high population density, industrial activities, and prevalent lifestyle patterns. Understanding the extent of awareness among urban residents is crucial in formulating effective strategies to combat this issue (Sugiura et al. 2021).

Consequences of microplastics: Larger plastic items break down into minuscule particles that persist in the environment. These particles, released into the air and water through industrial processes, infiltrate ecosystems with alarming ease, disrupting natural processes and threatening biodiversity (Van Tran et al. 2023).

Wildlife and human impact: Microplastics pose challenges to wildlife as they become intertwined with habitats and enter the human food chain. Recent research suggests potential implications for human health, raising urgent questions about the long-term consequences of microplastic consumption (Gündogdu et al. 2023).

Studying the level of knowledge among urban populations regarding microplastics is imperative due to the profound environmental impact of these minuscule plastic particles. Microplastics, measuring less than 5mm, have become

pervasive in urban ecosystems, stemming from various sources such as the breakdown of larger plastic items, industrial processes, and personal care products. The concentration of these particles is exacerbated in urban areas due to high population density, industrial activities, and prevalent lifestyle patterns.

Understanding the knowledge levels of urban residents is crucial for several reasons. Firstly, awareness acts as a catalyst for informed decision-making. Many individuals may not comprehend the implications of microplastic pollution, assuming it to be a distant concern. This lack of awareness may hinder collective efforts to address the issue. Secondly, informed citizens are more likely to actively participate in mitigation strategies. By understanding the sources and consequences of microplastics, urban dwellers can contribute to reducing their environmental footprint.

Moreover, as microplastics infiltrate ecosystems and the food chain, studying urban knowledge levels becomes a key component in addressing potential health risks for the population. In essence, studying the level of knowledge among urban people regarding microplastics is essential for fostering a sense of responsibility, promoting informed decision-making, and mobilizing collective action to combat the pervasive environmental challenge posed by these microscopic pollutants.

MATERIALS AND METHODS

Sequential Explanatory Design

To assess the knowledge and awareness of microplastics among urban residents of Pune, a structured questionnaire was designed. The survey contained multiple-choice questions, Likert scale statements, and open-ended questions, covering topics such as the definition of microplastics, sources, effects on the environment, and personal behaviors related to plastic use.

Sample Selection

Residents of three diverse urban areas in Pune were selected as the study population: Shivajinagar and Pimpri-Chinchwad. For the first phase (qualitative), the purposive sampling technique (sampling till saturation) was used to select 18 samples. In the second phase (quantitative), Convenience sampling was used to select 100 samples.

Data Collection

In the first phase, a semi-structured questionnaire was used to collect data from 18 samples, and the survey was administered to 100 participants from various age groups, professions, and educational backgrounds. The participants

Table 1: Demographic data of the participants (Phase 1).

n=18

S.No.	Demographic variables (Phase 1)	f	%
Age (Yr)			
a	18-24	0	0
b	25-34	4	22
c	35-44	8	44
d	45-54	4	22
e	55-64	2	11
f	65 and over	0	0
Gender			
a	Male	12	67
b	Female	6	33
Education Level			
a	Profession or honors	1	6
b	Graduate	8	44
c	Intermediate or diploma	6	33
d	High school certificate	3	17
e	Middle school certificate	0	0
f	Primary school certificate	0	0
g	Illiterate	0	0
Occupation			
a	Professionals	9	50
b	Technicians & Associate Professionals	1	6
c	Clerks	0	0
d	Skilled Workers and Shop & Market Sales Workers	3	17
e	Craft & Related Trade Workers	0	0
f	Plant & Machine Operators and Assemblers	0	0
g	Elementary Occupation	0	0
h	Unemployed	5	28
Household Income			
a	≥ 20482	1	6
b	10,241-20,481	4	22
c	7681-10,240	5	28
d	5120-7680	6	33
e	3072-5119	2	11
f	1034-3071	0	0
g	≤ 1033	0	0
Marital Status			
a	Single	1	6
b	Married	15	83
c	Divorced	1	6
d	Widowed	1	6

S.No.	Demographic variables (Phase 1)	f	%
Number of Household Members			
a	1	0	0
b	2	4	22
c	3	9	50
d	4	4	22
e	5 or more	1	6
Length of Residence in Urban Area			
a	Less than 1 year	0	0
b	1-5 years	1	6
c	6-10 years	12	67
d	11-15 years	3	17
e	16-20 years	2	11
f	Over 20 years		
Access to Information Sources (Can have more than one response)			
a	Internet access at home	14	78
b	Smartphone	18	100
c	Regularly watch TV	11	61
d	Read newspapers/magazines	6	33
e	None of the above	0	0
Do you have Environmental Awareness?			
a	Yes	18	100
b	No	0	0
c	Never	0	0

were approached in public spaces, parks, and residential neighborhoods. Additionally, interviews with key informants, such as environmentalists and educators, were conducted to gain deeper insights into the issue. The demographic data of the participants is presented in Tables 1 and 2.

RESULTS

Qualitative Analysis

Qualitative analysis was done using thematic analysis, where we identified recurring themes based on the responses provided by 15 participants to the four questions concerning microplastics and their potential impact on health and the environment.

Question 1: Explain how microplastics can enter the human body and potentially affect health.

Themes:

Ingestion as the primary route: The majority of participants emphasized that microplastics can enter the human body primarily through ingestion. They highlighted that consumption of contaminated food and water is the main

pathway for exposure. This theme underlines a common understanding among participants about the ingestion route.

Inhalation and skin contact: Some participants mentioned lesser-known pathways, such as inhalation of airborne microplastics and skin contact, but these were less frequently discussed. The theme of inhalation and skin contact highlighted participants' awareness of alternative routes of exposure.

Health concerns: Many participants expressed concerns about the potential health effects of microplastic ingestion. Themes included worries about digestive system issues, inflammation, and the possibility of microplastics carrying harmful chemicals. This theme reflected the participants' recognition of the potential risks associated with microplastics.

Question 2: Describe the impact of microplastic pollution on marine ecosystems and its indirect effects on human health.

Themes:

Marine ecosystem impact: A prevalent theme in participants' responses was their understanding of the detrimental effects of microplastics on marine ecosystems. They emphasized the ingestion of microplastics by marine life, bioaccumulation, entanglement, and disruptions in the marine food chain as primary impacts.

Transfer to human health: Participants consistently recognized the indirect effects on human health through the consumption of contaminated seafood. This theme highlighted participants' understanding of the potential transfer of toxins from marine organisms to human consumers.

Connectedness of ecosystems: Some participants highlighted the interconnectedness of marine and human health, emphasizing the importance of protecting the oceans to safeguard human well-being. This theme revealed participants' awareness of the broader ecological consequences of microplastic pollution.

Question 3: Suggest practical steps individuals can take to reduce their exposure to microplastics in their daily lives.

Themes:

Avoid single-use plastics: The most common theme in participants' responses was the recommendation to avoid single-use plastics. Participants emphasized reducing plastic waste through responsible consumption, indicating a strong emphasis on individual actions.

Choose microplastic-free products: Many participants suggested choosing products labeled as "microplastic-free" or "microbead-free" to minimize exposure. This theme underscored the role of informed consumer choices in reducing exposure.

Eco-friendly habits: Several participants advocated for eco-friendly habits, including recycling, using reusable containers and bags, and supporting policies that reduce plastic pollution. This theme reflected participants' recognition of the broader behavioral changes needed to address microplastic pollution.

Question 4: Explain the challenges associated with measuring the exact health impacts of microplastics on humans, considering their prevalence in the environment.

Themes:

Complex causality: Participants consistently acknowledged the complexity of establishing direct causality between microplastic exposure and health impacts. They recognized that various confounding factors make it challenging to attribute health issues solely to microplastics.

Tracing origins and long-term effects: Some participants highlighted the difficulty in tracing the origins of microplastics and assessing their long-term effects on human health. They emphasized the need for long-term studies. This theme demonstrated participants' awareness of the intricacies of studying microplastic health impacts.

Table 2: Demographic data of the participants (Phase 2).

n=100

S.No.	Demographic variables (Phase 2)	f	%
Age (Yr):			
a	18-24	12	12
b	25-34	32	32
c	35-44	13	13
d	45-54	32	32
e	55-64	6	6
f	65 and over	5	5
Gender:			
a	Male	26	26
b	Female	74	74
Education Level:			
a	Profession or honors	6	6
b	Graduate	18	18
c	Intermediate or diploma	15	15
d	High school certificate	12	12
e	Middle school certificate	33	33
f	Primary school certificate	14	14
g	Illiterate	2	2
Occupation:			
a	Professionals	9	9
b	Technicians & Associate Professionals	6	6

Table Cont....

S.No.	Demographic variables (Phase 2)	f	%
c	Clerks	4	4
d	Skilled Workers and Shop & Market Sales Workers	19	19
e	Craft & Related Trade Workers	21	21
f	Plant & Machine Operators and Assemblers	17	17
g	Elementary Occupation	9	9
h	Unemployed	15	15
Household Income:			
a	≥ 20482	15	15
b	10,241-20,481	12	12
c	7681-10,240	37	37
d	5120-7680	25	25
e	3072-5119	9	9
f	1034-3071	2	2
g	≤ 1033	0	0
Marital Status:			
a	Single	14	14
b	Married	78	78
c	Divorced	0	0
d	Widowed	8	8
Number of Household Members:			
a	1	12	12
b	2	45	45
c	3	21	21
d	4	9	9
e	5 or more	13	13
Length of Residence in Urban Area:			
a	Less than 1 year	2	2
b	1-5 years	19	19
c	6-10 years	32	32
d	11-15 years	26	26
e	16-20 years	9	9
f	Over 20 years	12	12
Access to Information Sources (Can have more than one response)			
a	Internet access at home	61	61
b	Smartphone	80	80
c	Regularly watch TV	56	56
d	Read newspapers/magazines	43	43
e	None of the above	0	0
Do you have Environmental Awareness:			
a	Yes	100	100
b	No	0	0
c	Never	0	0

Research rigor and collaboration: There was a consensus on the importance of rigorous scientific research and the standardization of analysis methods to address challenges in measuring health impacts. Participants also recognized the need for interdisciplinary collaboration. This theme highlighted the participants' understanding of the need for a comprehensive and well-coordinated scientific approach.

Outcome

The thematic qualitative analysis of participants' responses to the four questions on microplastics revealed clear and recurring themes. Participants displayed a solid understanding of how microplastics can enter the human body and the potential health effects. They also recognized the impact of microplastic pollution on marine ecosystems and understood the practical steps individuals can take to reduce exposure. Moreover, participants acknowledged the complexity of studying health impacts and the need for rigorous research and collaboration.

This analysis underscores the importance of informed individual actions and rigorous scientific research in addressing the challenges posed by microplastic pollution. Participants' responses reflect a general awareness of the

Table 3: Knowledge level of participants regarding microplastics (Phase 2).

n=100

Section	Items	f	%
I	**Understanding Microplastics:**		
1.	What are microplastics?	23	23
2.	What are some potential sources of microplastics in the environment?	27	27
3.	Which type of microplastic is typically more harmful to marine life due to its smaller size and ease of ingestion?	25	25
4.	In which of the following products can microplastics be commonly found?	34	34
5.	How can individuals reduce their exposure to microplastics in their daily lives?	45	45
6.	What is one potential risk of microplastic contamination in seafood?	19	19
7.	What is one way to minimize the release of microplastics from synthetic clothing during washing?	20	20
II	**Health Concerns and Effects:**		
1.	How do microplastics primarily enter our bodies?	33	33
2.	What health concerns are associated with the ingestion of microplastics?	27	27
3.	How can individuals reduce their exposure to microplastics from personal care products?	50	50
4.	What are some potential health concerns associated with the ingestion of microplastics?	14	14
5.	How can individuals reduce their exposure to products containing microplastics?	40	40
III	**Common Sources and Products:**		
1.	Which of the following is NOT a common source of microplastic pollution in the environment?	52	52
2.	In addition to personal care products, where else can microplastics be found in our daily lives?	49	49
3.	Which of the following personal care products may contain microplastics?	59	59
4.	What is one potential health concern associated with the ingestion of microplastics?	43	43
5.	What precautionary steps can individuals take to reduce their exposure to products containing microplastics?	58	58
IV	**Regulatory and Research Bodies:**		
1.	Which organization plays a significant role in researching and regulating microplastic pollution?	28	28
2.	What role can individuals play in reducing the release of microplastics into the environment?	18	18
3.	What is one-way individuals can reduce their exposure to microplastics from personal care products?	25	25
4.	How can microplastics be removed from water sources and the environment?	27	27
V	**Public Awareness and Education:**		
1.	How can individuals reduce their exposure to microplastics in their daily lives?	71	71
2.	What are some potential health concerns associated with the ingestion of microplastics?	46	46
3.	How can individuals reduce their exposure to microplastics from personal care products?	52	52
4.	What is one way to minimize the release of microplastics from synthetic clothing during washing?	19	19
VI	**True or False Statements:**		
1.	Microplastics are only found in the ocean and not in freshwater sources.	57	57
2.	Inhaling airborne microplastics poses no potential health risks to humans.	38	38
3.	Microplastics in seafood cannot be transferred to humans who consume them	40	40
4.	Synthetic clothing does not contribute to the release of microplastics into the environment during washing	59	59
5.	Microplastics are easily biodegradable and do not persist in the environment for long periods.	50	50
6.	Microplastics are only a concern for marine ecosystems and do not affect terrestrial environments	67	67
7.	Microplastics are only a concern for marine ecosystems and have no impact on human health	52	52
8.	Microplastics are easily biodegradable and do not persist in the environment for long periods	59	59

multifaceted nature of this issue and the interconnectedness of environmental and human health.

Quantitative Analysis

The semi-structured questionnaire was divided into 6 sections viz: Understanding Microplastics, Health Concerns and Effects, Common Sources and Products, Regulatory and Research Bodies, Public Awareness and Education (Table 3).

Understanding microplastics: The responses from participants in the urban area of Pune to questions about microplastics reflect a notable level of awareness and concern about environmental issues. Regarding the fundamental question of "What are microplastics?" 23% of participants responded, indicating a basic understanding of the concept. The question on potential sources of microplastics saw a slightly higher engagement, with 27% of participants offering insights into environmental origins. Notably, 25% of participants demonstrated awareness of the specific types of microplastics that pose greater harm to marine life due to their smaller size and ease of ingestion. A substantial 34% of respondents recognized the common products where microplastics are found, indicating a heightened awareness of their prevalence in everyday items. The question on individual actions to reduce exposure to microplastics garnered the highest response rate, with 45% of participants contributing, showcasing a keen interest in adopting practices to minimize personal impact. The potential risk of microplastic contamination in seafood saw responses from 19% of participants, suggesting a moderate level of concern for the impact on the food chain. Lastly, 20% of participants provided insights into minimizing the release of microplastics from synthetic clothing during washing, reflecting a reasonable level of awareness about preventive measures. Overall, the responses suggest a moderate level of environmental awareness among urban participants in Pune regarding microplastics and a willingness to engage in practices that contribute to reducing their environmental footprint.

Health concerns and effects: The responses from participants in the urban area of Pune to questions regarding the entry of microplastics into our bodies and associated health concerns reveal a significant level of awareness and concern. A notable 33% of participants provided insights into how microplastics primarily enter our bodies, indicating a heightened awareness of the pathways of exposure. When asked about health concerns associated with the ingestion of microplastics, 27% of participants demonstrated knowledge of the potential risks, showing a commendable understanding of the implications for human health. A particularly high engagement was observed in the question about reducing

exposure to microplastics from personal care products, with 50% of participants providing responses suggesting a strong interest in adopting practices that minimize exposure through daily routines. However, for potential health concerns associated with microplastic ingestion, the response rate was comparatively lower at 14%, indicating a need for increased awareness of this specific aspect. The question on reducing exposure to products containing microplastics saw a substantial 40% participation, highlighting a significant level of awareness and interest in adopting measures to minimize the use of such products. Overall, the responses reflect a commendable level of understanding among urban participants in Pune regarding the pathways of exposure, health concerns, and proactive measures to mitigate the impact of microplastics on personal well-being.

Common sources and products: The responses from participants in the urban area of Pune to questions about microplastic sources, their presence in daily life, health concerns, and preventive measures indicate a commendable level of awareness. A significant 52% of participants correctly identified which option is NOT a common source of microplastic pollution, showcasing a strong understanding of potential environmental contributors. The question about the presence of microplastics in daily life, beyond personal care products, saw a notable 49% engagement, indicating a broad awareness of the diverse sources of microplastics in our surroundings. A high 59% of participants accurately identified personal care products that may contain microplastics, reflecting a keen awareness of specific items contributing to environmental pollution. When asked about potential health concerns associated with microplastic ingestion, 43% of participants provided insights, highlighting a noteworthy understanding of the potential risks to human health. The question on precautionary steps to reduce exposure to products containing microplastics witnessed an impressive 58% participation, showcasing a proactive attitude among participants in adopting measures to minimize personal impact. Overall, the responses suggest a robust level of knowledge and awareness among urban participants in Pune regarding the sources, presence, health implications, and preventive strategies related to microplastics in the environment.

Regulatory and research bodies: The responses from participants in the urban area of Pune to questions related to microplastic research, regulation, individual responsibilities, and environmental remediation reflect a varying degree of awareness. About 28% of participants correctly identified an organization playing a significant role in researching and regulating microplastic pollution, indicating a moderate level of awareness regarding entities engaged in addressing

this environmental concern. The question about the role individuals can play in reducing the release of microplastics into the environment saw an 18% participation rate, suggesting that there may be room for increased awareness and understanding of personal responsibilities in mitigating microplastic pollution. Inquiring about ways individuals can reduce their exposure to microplastics from personal care products garnered a 25% response rate, highlighting a moderate interest in adopting practices to minimize personal impact. Finally, the question on the removal of microplastics from water sources and the environment saw a 27% participation rate, indicating a fair level of awareness regarding potential methods for mitigating the presence of microplastics in ecosystems. Overall, the responses suggest a weaker understanding in the context of microplastic research, individual roles, and environmental remediation.

Public awareness and education: The responses from participants in the urban area of Pune to questions addressing microplastic exposure and associated health concerns reveal a strong awareness among the community. A substantial 71% of participants provided insights into how individuals can reduce their exposure to microplastics in their daily lives, indicating a high level of interest and understanding in adopting practices that mitigate personal impact. However, the question on minimizing the release of microplastics from synthetic clothing during washing had a lower response rate of 19%, suggesting a potential area for increased awareness and education on specific preventive measures. Overall, the responses reflect a commendable level of awareness and a proactive attitude among urban participants in Pune regarding strategies to reduce personal exposure to microplastics and an understanding of the associated health concerns. The responses from participants in the urban area of Pune to the true/false questions on microplastics indicate a varied level of understanding and awareness. The majority, 57%, correctly recognized that microplastics are not exclusive to the ocean and can also be found in freshwater sources, demonstrating a solid understanding of the ubiquitous nature of microplastic pollution. However, a significant 38% believed that inhaling airborne microplastics poses no potential health risks, suggesting a potential area for increased awareness regarding the potential health implications of airborne microplastics. Regarding synthetic clothing and microplastics released during washing, a substantial 59% incorrectly believed that synthetic clothing does not contribute to environmental microplastic pollution, suggesting a misconception in this specific area. Finally, 67% of participants incorrectly believed that microplastics are only a concern for marine ecosystems and do not affect terrestrial environments, while 52% incorrectly thought that microplastics have no impact on human health, highlighting areas for improved

education on the broader implications of microplastics across ecosystems and human health. Overall, the responses suggest a need for targeted awareness campaigns to address specific misconceptions and enhance understanding regarding microplastics and their multifaceted impact.

DISCUSSION

The findings from our study reveal a significant level of awareness and understanding of microplastic pollution among Pune's urban population. Notably, 34% of respondents demonstrated good awareness by recognizing common products where microplastics are frequently found. This level of awareness mirrors the findings of Rahman et al. (2023), who observed similar awareness levels in their study. Additionally, the question addressing individual actions to reduce exposure to microplastics received the highest response rate, with 45% of participants actively contributing ideas. This trend aligns with the study by McMullen et al. (2023), where participants also showed a high level of engagement in reducing their microplastic exposure.

Our findings also concur with those of Thornton Hampton et al. (2022), indicating a commendable understanding of the potential health risks associated with the ingestion of microplastics, with 27% of participants demonstrating knowledge in this area. This understanding is crucial in driving public health initiatives and policy changes to mitigate the adverse effects of microplastic consumption. Furthermore, 52% of participants correctly identified an option that is not a common source of microplastic pollution. This highlights a robust understanding of potential environmental contributors among the surveyed population. A similar observation was made in the study conducted by Kneel et al. (2023). Moreover, an impressive 71% of participants provided insightful responses regarding how individuals can reduce their daily exposure to microplastics. This indicates both a high level of interest and a comprehensive understanding of practical measures to mitigate personal impact. The study by Wu et al. (2023) also found that participants exhibited an extraordinary understanding of plastic pollution and its effects on health.

These findings underscore the importance of continued awareness campaigns and educational initiatives to further enhance the public's understanding of microplastic pollution and encourage proactive measures to reduce its impact. By fostering a well-informed populace, we can better address the growing microplastic problem in urban areas and implement effective strategies for sustainable living.

CONCLUSION

The survey results underscore a concerning gap in the understanding of microplastics among Pune's urban

population. While participants were familiar with the term, their knowledge about the sources and consequences of microplastic pollution was notably limited. This revelation indicates a critical need for targeted educational programs to dispel misconceptions and enhance awareness about the intricate nature of microplastics.

Particularly troubling is the lack of awareness regarding microplastics originating from personal care products, which are extensively used by urban residents. This oversight is significant as personal care products contribute substantially to microplastic pollution. Raising awareness about the presence of microplastics in these commonly used items becomes imperative to mitigate their release into the environment. Educational initiatives should, therefore, specifically address the overlooked aspect of personal care products to bridge this awareness gap.

Furthermore, the research highlights a disconcerting inconsistency between knowledge and behavior among urban residents. While there is a recognition of microplastic pollution, this awareness often fails to translate into responsible actions. This disparity emphasizes the complexity of behavioral change and underscores the need for more comprehensive efforts to promote environmentally responsible practices. Strategies should encompass reducing single-use plastic consumption and improving recycling habits.

The overall findings illuminate a larger challenge-limited knowledge and awareness persist despite the evident presence of microplastic pollution in the urban surroundings of Pune. This knowledge-behavior gap accentuates the urgency for extensive awareness campaigns and educational initiatives. These efforts should not only aim to clarify misconceptions about microplastics but also emphasize the adoption of responsible practices and the reduction of microplastic sources.

In conclusion, addressing the microplastic crisis in urban areas like Pune requires a multifaceted approach. Comprehensive awareness campaigns and educational initiatives are essential to close the knowledge gap, correct misconceptions, and instigate behavioral change. By taking significant steps in these directions, urban communities can actively contribute to combating the microplastic crisis, thereby safeguarding the environment and public health.

RECOMMENDATIONS

Public Awareness Campaigns

Local authorities, environmental organizations, and educational institutions should collaborate to launch public awareness campaigns focusing on microplastic pollution. These campaigns can include workshops, seminars, and informational materials targeting residents of urban areas like Pune.

Integration into Educational Curriculum

Microplastic education should be integrated into the school curriculum to ensure that children are educated about this issue from a young age. This will help create a future generation that is more aware and responsible.

Regulation of Personal Care Products

Government bodies should regulate the use of microplastics in personal care products, ensuring that manufacturers disclose the presence of such particles in their products. Simultaneously, consumers should be educated about choosing micro-plastic-free alternatives.

Recycling and Plastic Reduction Initiatives

Encouraging residents to reduce their plastic consumption and adopt sustainable waste disposal practices is critical. Local authorities should implement recycling programs and incentivize responsible plastic use through policies and incentives.

REFERENCES

Al Mamun, A., Prasetya, T.A.E. and Ahmad, M., 2023. Microplastics in human food chains: Food becoming a threat to health safety. *Science of The Total Environment*, 858, p.159834.

Araújo, J.L., Morais, C. and Paiva, J.C., 2023. Students' attitudes towards the environment and marine litter in the context of a coastal water quality educational citizen science project. *Australian Journal of Environmental Education*, 39(4), pp.522-535.

Blackburn, K. and Green, D., 2022. The potential effects of microplastics on human health: What is known and what is unknown. *Ambio*, 51(3), pp.518-530.

Danopoulos, E., Stanton, T., Ma, Y., Horton, A.A., Chen, Q., Levermore, J.M. and Nel, H.A., 2023. Insights into technical challenges in the field of microplastic pollution through the lens of early career researchers (ECRs) and a proposed pathway forward. *Frontiers in Earth Science*, 11, p.1271547.

Dittmann, S., Kiessling, T., Mederake, L., Hinzmann, M., Knoblauch, D., Böhm-Beck, M. and Thiel, M., 2023. Sharing communication insights of the citizen science program Plastic Pirates-best practices from 7 years of engaging schoolchildren and teachers in plastic pollution research. *Frontiers in Environmental Science*, 11.

Ghosh, S., Sinha, J.K., Ghosh, S., Vashisth, K., Han, S. and Bhaskar, R., 2023. Microplastics as an emerging threat to the global environment and human health. *Sustainability*, 15(14), p.10821.

Gomez-Gonzalez, M.A., Da Silva-Ferreira, T., Clark, N., Clough, R., Quinn, P.D. and Parker, J.E., 2023. Toward understanding the environmental risks of combined microplastics/nanomaterials exposures: Unveiling ZnO transformations after adsorption onto polystyrene microplastics in environmental solutions. *Global Challenges*, 7(8), p.2300036.

Gündogdu, S., Rathod, N., Hassoun, A., Jamroz, E., Kulawik, P., Gokbulut, C. and Özogul, F., 2023. The impact of nano/micro-plastics toxicity on seafood quality and human health: facts and gaps. *Critical Reviews in Food Science and Nutrition*, 63(23), pp.6445-6463.

Hettiarachchi, L. and Meegoda, A., 2023. Microplastic pollution prevention: the need for robust policy interventions to close the loopholes in current waste management practices. *International Journal Of Environmental Research and Public Health*, 20(14), p.6434.

Klingelhöfer, D., Braun, M., Quarcoo, D., Brüggmann, D. and Groneberg, D.A., 2020. Research landscape of a global environmental challenge: microplastics. *Water Research*, 170, p.115358.

Kneel, S., Stephens, C.G., Rolston, A. and Linnane, S., 2023. Examining awareness, attitudes and behaviours of stakeholders in Irish Fishing towards plastic. *Resources, Environment and Sustainability*, 14, p.100131.

Li, Q., Yuan, M., Chen, Y., Jin, X., Shangguan, J., Cui, J. and Wang, Y., 2023. The neglected potential source of microplastics from daily necessities: A study on protective mobile phone cases. *Journal of Hazardous Materials*, 441, p.129911.

López, A., 2023. Seeing microplastic clouds: Using ecomedia literacy for digital technology in environmental education. *The Journal of Environmental Education*, 54(1), pp.46-57.

McMullen, K., Tirapé, A., Calle, P., Vandenberg, J., Alvarado-Cadena, O., Ota, Y. and Alava, J.J., 2023. Marine litter and social inequities entangle Ecuadorian mangrove communities: Perceptions of plastic pollution and well-being concerns in Puerto Hondo and Isla Santay, Ecuador. *Marine Policy*, 157, p.105857.

Mondal, S., Das, P., Mondal, A., Paul, S., Pandey, J.K. and Das, T.K., eds., 2023. *Remediation of Plastic and Microplastic Waste*. CRC Press.

Hettiarachchi, L. and Meegoda, A., 2023. Microplastic pollution prevention: the need for robust policy interventions to close the loopholes in current waste management practices. *International Journal of Environmental Research and Public Health*, 20(14), p.6434

Prasittisopin, L., Ferdous, W. and Kamchoom, V., 2023. Microplastics in construction and built environment. *Developments in the Built Environment*, 178, p.100188.

Rahman, N., Shozib, S.H., Akter, Y., Islam, A.R.T., Islam, S., Sohel, S. and Malafaia, G., 2023. Microplastic as an invisible threat to the coral reefs: Sources, toxicity mechanisms, policy intervention, and the way forward. *Journal of Hazardous Materials*, p.131522.

Sarkar, S., Diab, H. and Thompson, J., 2023. Microplastic pollution: Chemical characterization and impact on wildlife. *International Journal of Environmental Research and Public Health*, 20(3), p.1745.

Sharma, S., Sharma, V. and Chatterjee, S., 2023. Contribution of plastic and microplastic to global climate change and their conjoining impacts on the environment-A review. *Science of The Total Environment*, 875, p.162627.

Subashini, M.M. and Vignesh, R.S., 2023. Thermoplastic waste segregation classification system using deep learning techniques. *Multimedia Tools and Applications*, 18(6), pp.1-17.

Sugiura, M., Takada, H., Takada, N., Mizukawa, K., Tsuyuki, S. and Furumai, H., 2021. Microplastics in urban wastewater and estuarine water: Importance of street runoff. *Environmental Monitoring and Contaminants Research*, 1, pp.54-65.

Sun, A. and Wang, W.X., 2023. Human Exposure to Microplastics and Its Associated Health Risks. *Environment & Health*, 1(3), pp.139-149.

Surendran, U., Jayakumar, M., Raja, P., Gopinath, G. and Chellam, P.V., 2023. Microplastics in terrestrial ecosystem: Sources and migration in soil environment. *Chemosphere*, 976, p.137946.

Thacharodi, A., Meenatchi, R., Hassan, S., Hussain, N., Bhat, M.A., Arockiaraj, J. and Pugazhendhi, A., 2023. Microplastics in the environment: a critical overview on its fate, toxicity, implications, management, and bioremediation strategies. *Journal of Environmental Management*, 349, p.119433.

Thornton Hampton, L.M., Bouwmeester, H., Brander, S.M., Coffin, S., Cole, M., Hermabessiere, L. and Weisberg, S.B., 2022. Research recommendations to better understand the potential health impacts of microplastics on humans and aquatic ecosystems. *Microplastics and Nanoplastics*, 2(1), p.18.

Tian, W., Song, P., Zhang, H., Duan, X., Wei, Y., Wang, H. and Wang, S., 2023. Microplastic materials in the environment: Problem and strategical solutions. *Progress in Materials Science*, 132, p.101035.

Van Tran, T., Jalil, A.A., Nguyen, T.M., Nguyen, T.T.T., Nabgan, W. and Nguyen, D.T.C., 2023. A review of the occurrence, analytical methods, and impact of microplastics in the environment. *Environmental Toxicology and Pharmacology*, 79, p.104248.

Wani, A.K., Akhtar, N., Naqash, N., Rahayu, F., Djajadi, D., Chopra, C. and Américo-Pinheiro, J.H.P., 2023. Discovering untapped microbial communities through metagenomics for microplastic remediation: recent advances, challenges, and way forward. *Environmental Science and Pollution Research*, 11, pp.1-24.

Wu, J., Chen, H., Xu, J., Rahman, M.S.U., Li, S., Wang, J. and Liu, Y., 2024. The lull before microplastics pollution outbreaks: Some implications for human health and control strategies. *Nano Today*, 54, p.102062.

Deep Learning for Soil Nutrient Prediction and Strategic Crop Recommendations: An Analytic Perspective

P. Latha and P. Kumaresan† (ORCID)

School of Computer Science Engineering and Information Systems (SCORE), Vellore Institute of Technology, Vellore-632014, Tamilnadu, India

†Corresponding author: P. Kumaresan; pkumaresan@vit.ac.in

ABSTRACT

Agriculture has been a vital sector for the majority of people, especially in countries like India. However, the increasing need for food production has led to intensive farming practices that have resulted in the deterioration of soil quality. This deterioration in soil quality poses significant challenges to both agricultural productivity and environmental sustainability. To address these challenges, advanced soil nutrient prediction systems that utilize machine learning and deep learning techniques are being developed. These advanced soil nutrient prediction systems utilize various sources of data, such as soil parameters, plant diseases, pests, fertilizer usage, and changes in weather patterns. By mapping and analyzing these data sources, machine learning algorithms can accurately predict the distribution of soil nutrients and other properties essential for precise agricultural practices. A previous study compared machine learning algorithms like SVM and Random Forest with deep learning algorithms CNN and LSTM for predicting crop yields. The most appropriate model is a significant challenge, but several studies have evaluated recommendation system models using deep machine learning techniques. Deep learning models attain accuracy above 90%, while many ML models achieve rates between 90% and 93%. Furthermore, the research seeks to propose specific crop suggestions grounded in soil nutrients for precision agriculture to enhance crop productivity.

INTRODUCTION

The nutrients originate from the mineral component of the soil. Macronutrients, including oxygen, magnesium, nitrogen, oxygen, calcium, carbon, potassium, hydrogen, sulfur, and phosphorus, along with micronutrients like molybdenum, iron, boron, copper, manganese, zinc, and chlorine, are vital elements for crop growth. Minerals exist in the soil based on the pH indicators. Tobiszewski & Vakh (2023) analyzed one of the most essential elements for farming is soil. Regular soil analysis is the foundation of a valuable farming strategy for regulating soil quality. This technique aims to determine the precise amount of nutrients or other chemical, physical, and biological soil qualities. Keshavarzi et al. (2022) examined Soil nutrients, both micronutrients and macronutrients, which should be at optimum levels for agricultural production. Chana et al. (2023) suggested that crops require a favorable ratio of soil nutrients and weather conditions to grow well. Fertilizers assist in achieving high yields. Schut and Reymann (2023) have determined that the RC-KP model is a new approach that accurately predicts the short-term and long-term effects of fertilizers in crop rotations for nitrogen, phosphorus, and potassium. Khan et al. (2022) proposed the main challenge in creating a real-time and context-aware fertilizer recommendation system lies in the complexity of accurately mapping soil fertility in real-time. Kashyap & Kumar (2021) emphasized the importance of maintaining adequate soil moisture levels to support various biophysical processes. It includes seed germination, plant growth,

nutrient cycling, and the preservation of soil biodiversity. Keesstra et al. (2016) conducted a study to explore the significance of soil moisture in the hydrological cycle, which plays a crucial role in regulating runoff levels, vegetation production, and evapotranspiration. It also directly affects agricultural drought, uncertainty in crop yields, and food security conditions. Chandra et al. (2023) examined Soil fertility not only enhances vegetation restoration but also promotes the development of a carbon-neutral ecosystem. It is a crucial factor for plant nutrition and plays a vital role in maximizing crop productivity. Elbasiouny et al. (2022) proposed Climatic conditions have an impact on both plant productivity and soil nutrition. In their study, Sharma et al. (2021) discussed how the depletion of essential macro and micronutrients in soils occurs as a result of erosion, which is detrimental to plant growth, leading to decreased fertility with increasing soil depth. The availability of nutrients is influenced by several factors, including pH, organic matter content, temperature, and soil moisture. In recent decades, there have been significant advancements in AI, leading to the development of various Machine Learning methods such as RF, SVM, and ANN (Ahmad et al. 2010). These methods offer new possibilities for retrieving soil moisture from satellite data. Babalola et al. (2023) presented soil surface texture has an impact on different soil properties and water-holding capacities these classifications do not accurately represent the challenges found in real-world conditions. To address this issue, the author suggests using a CNN model to classify soil images taken under Uncontrolled Field Conditions. Durai & Shamili (2022) suggested DL and ML algorithms play a crucial role in agriculture. They

are primarily used to recommend crops based on weather parameters, suggest nutrient requirements, and determine the Degree Days. Kouadio et al. (2018) proposed an Extreme Learning Machine model that utilizes both MLR and RF to analyze soil fertility properties and produce a precise estimation of Robusta coffee yield. Kumar et al. (2023) employed a DL model called Deep Capsule Autoencoder with SoftMax Regression to predict the growth of crops such as sugarcane, rice, and wheat.

Deep learning algorithms suggest crops to farmers by gathering and processing the dataset, eliminating missing and duplicate data before training. Soil fertility plays a crucial role in vegetation regeneration and creating a carbon-neutral ecosystem. Fig. 1 shows crop recommendation system architecture for the qualities of the soil are determined based on its pH, macronutrients, micronutrients, climate, and geography. Using various input parameters with SVM, k-NN, RF, and Ensemble Techniques helps identify suitable crops for agriculture-fit soil. To select the most appropriate algorithm for crop recommendation, deep learning models utilize performance metrics such as F1 and accuracy scores. Machine Learning models serve as decision-support tools for predicting suitable crops in precision farming. The research aims to investigate soil nutrients in different soil types to help farmers choose the right crop for their land. ML and DL models will focus on examining primary soil nutrients, surveying minerals and fertilizers usage, predicting soil properties, identifying degradation of soil fertility, overviewing current issues in nutrient systems development, and finding suitable algorithms for crop recommendation.
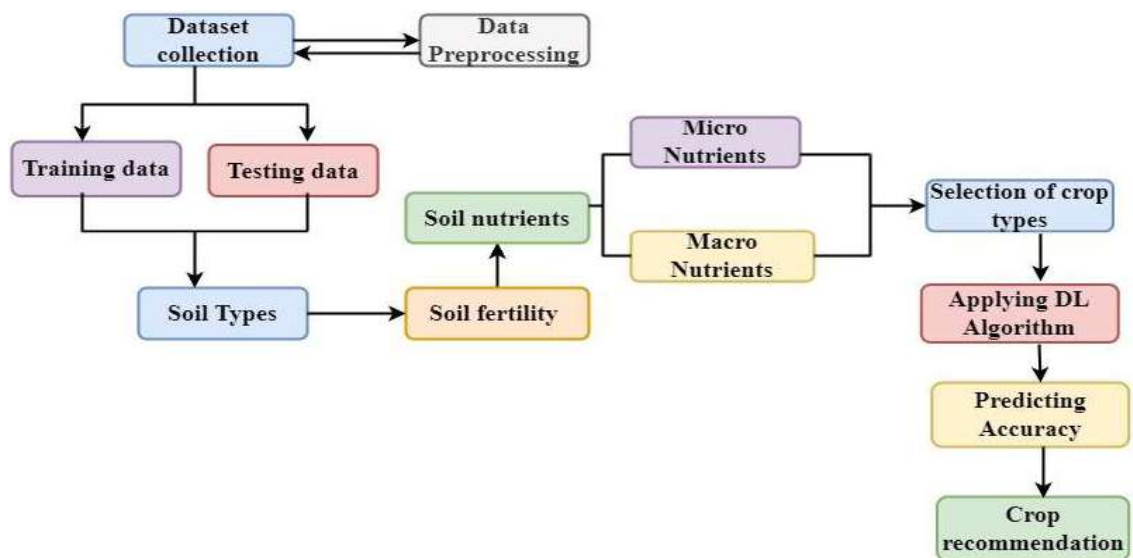
Fig. 1: Crop recommendation system architecture.

Structured Literature Review

Publications were selected using a search idiom to choose from scholarly literature. Various sources, including Elsevier, Springer Nature, Scopus, Google Scholar, IEEE Access, and MDPI, were utilized. After careful screening, 93 articles meeting PRISMA criteria for systematic reviews and meta-analyses were preferred. Fig. 2 illustrates the detailed flowchart of the systematic literature survey on publication analysis using the Prisma model.

Ahmed et al. (2021) improved the genetic algorithm and proposed nutrient recommendations based on time-series sensor data that are widely used in agricultural fertilizers to support healthy crop growth and promote optimal crop development through efficient root nutrition N, P, K. Lee et al. (2019) used deep learning to diagnose crop disease from crop leaf photos, the research suggests a self-predictable crop yield platform to forecast a farm's yearly production. A crop yield prediction module uses environmental data and disease information from the Crop Disease Diagnosis Module. Soil information was predicted by Kumara Perumal et al. (2022) using soil data, which included quantitative properties such as CEC, OC, and pH, as well as qualitative properties like order, suborder, and great group. The generated digital soil maps help farmers increase productivity by maximizing nutrient use and maintaining the agricultural ecosystem's sustainability. Dash et al. (2021) proposed ML algorithms such as SVM and DT, are used to distinguish the crop type and micronutrients for crop prediction. The soil pH, temperature, humidity, sunlight, and Rainfall influence the environmental factors and Crop growth. Gupta et al. (2022) examined farmers can precisely estimate crop yields throughout the growing season since it allows them to predict market prices and limits crop losses. The farmers are assisted through AI technology in making informed decisions about suggested crops to grow on their land. According to Gosai et al. (2021), several models, including Logistic Regression, Support Vector Machine, Naive Bayes, Decision Tree, Random Forest, and XGboost, have been suggested for cultivating multiple Indian crops. Sensors for measuring pH, temperature, humidity, NPK nutrients, soil moisture, and appropriate crop forecasts were created by Jejurkar Siddhi et al. (2021). Also decreases the risk of soil decay. Kimetu et al. (2008) used Artificial Intelligence to predict the soil properties offering suitable crop production. Fertilizers in agriculture are used for farm profitability and environmental
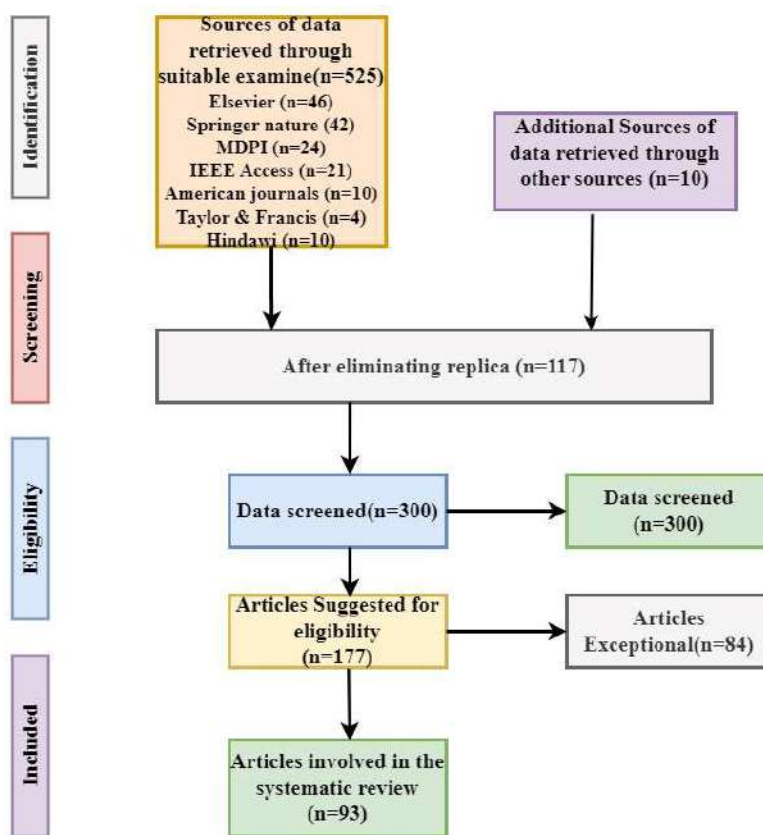
Fig. 2: Prisma Model.

protection. It computes complex nutrient deficiency and crop growth with the progress of soil fertility. Lacasta et al. (2018) found pests in crops that reduce crop yields without endangering human or environmental survival; as a result, governments have developed appropriate products and protocols of use. Finding pests and the right treatments is made easier by the established suggestion system. Principal component analysis and Sentinel 2 imagery were utilized by Singha et al. (2023) to forecast soil nutrients through Partial Least-Squares Regression and Support vector Machines Regression models, to optimize laboratory expenses. Amudha & Brindha (2022) explored the application of machine learning and deep learning techniques in identifying plant diseases and infections in various crops. The proposed model demonstrates strong computational performance and reduces processing time during the learning process. Archana & Kumar (2023) analyzed various deep learning algorithms, such as RNN, CNN, MLP, and LSTM, to predict crop yields in the agricultural sector. The CNN method proves to be highly effective in object detection and image classification, while the LSTM can capture complex and nonlinear relationships within the data. Both CNN and LSTM are valuable tools for accurately estimating agricultural yields. Sudhakar & Priya (2023) used computer vision technologies to improve crop health and productivity. These technologies were used to assess crop nutrient levels and identify any deficiencies. Techniques such as remote sensing, machine learning, and deep learning were employed to identify nutrient deficiencies in the crops.

Analysis of Soil Composition and Characteristics

Prakash et al. (2017) examined the soil dataset that was efficiently classified by utilizing classification algorithms such as ANN and SVM. These algorithms focused on various soil conditions, including fertility, depth, acidity, alkalinity, electrical conductivity, organic carbon, nitrogen, phosphorus, potassium, water-holding capacity, and porosity. John et al. (2020) highlighted the importance of analyzing SOC as an essential indicator of soil quality and fertility. They emphasized the need to understand its spatial distribution and the factors that influence it to achieve efficient and sustainable soil nutrient management using ANN, SVM, Cubist regression, RF, and MLR. Suchithra & Pai (2020) analyzed soil fertility on a village-by-village basis to identify and address nutrient deficiencies in soil, such as potassium, boron, organic carbon, and phosphorus. Senapaty et al. (2023) designed an IoT SNA- CR crop recommendation model for soil nutrient classification, minimized the use of fertilizers, and maximized productivity. Chandrappa et al. (2023) proposed statistical ML models, such as SVR, LR, and LSTM, to predict soil moisture data in multi-depth, using

seasonal and non-seasonal.

Assessment of Soil Fertility: Macronutrients and Micronutrients

Kaya & Basayigit (2022) stated that agricultural production relies on plants receiving the optimal amount of nutrients. These nutrients can be classified into macronutrients and micronutrients. Table 1 is used to differentiate ML and DL algorithm and their performance metrics using feature selection and utilization of different data sets.

Crop Recommendation Framework

The comparative analysis of supervised learning methods, including SVM, DT, GNB, and Xgboost, models was conducted by Lad et al. (2022) to enhance agricultural productivity and provide crop suggestions using soil attributes. Thilakarathne et al. (2022) Developed a cloud-based crop recommendation platform for assisting farmers in crop selection using various ML algorithms such as SVM, KNN, RF, XGBoost, and DT. Wankhade & Raut (2024) proposed a novel model called Efficient Deep Learning with Attention Mechanism Model, which aims to predict crop yields accurately using soil moisture and texture. BSFFS is used for extracting the features of a Bi-LSTM. Global Attention Mechanism is employed to predict the crop. Hossain et al. (2023) utilized a machine-learning approach to suggest appropriate crops by analyzing the levels of N, P, K, temperature, pH, humidity, and rainfall. They employed various algorithms, including DT, RFR, LR, K-NN, NN, SVM, and XGBoost. Kusuma Sri et al. (2023) suggested stacking LR, SVM, and NB algorithms into Gaussian Naive Bayes to select the most suitable crop based on soil nutrients and weather conditions. Gao et al. (2023) used RF and SVM to classify crops and optimize crop fields using Landsat 8 multispectral bands. Deshmukh et al. (2022) suggested machine learning techniques were used to recommend the top three crops based on soil and weather conditions. The goal of this research was to enhance soil quality, promote better crop growth, and assist farmers in reducing financial losses while increasing productivity. Varshitha & Choudhary (2022) analyzed to help farmers predict the most suitable crop for their soil using deep learning techniques, IoT elements, and deep neural networks. Predicting soil fertility and determining the suitable crops for meeting nutritional requirements includes soil factors, pH, organic carbon content, and NPK. Elavarasan & Vincent (2020) created a Q-learning network to predict crop yield using input parameters and reinforcement learning with parametric features and a threshold. Manjula & Djodiltachoumy (2022) used Gated Recurrent Units for crop-recommended prediction in evaluating trained and tested data to forecast crop production. In their study, Venkata

Table 1: Methods of soil fertility and crop optimization using machine and deep learning techniques.

S. No.	Title/Author	Soil/Crop recommendation / Feature Selection/Method ML/DL	Limitations of the existing system	Dataset	Performance Metrics
1.	Reshma and Aravindhar (2022)	analyze soil nutrients/Soil fertility/MLP, SVM, and DT	Overfitting and Underfitting, Need for Hybrid Models.	Southernmost region of Tamil Nadu.	Accuracies 94%.
2.	He et al. (2007)	To calculate pH level and soil nutrients/N, P, K, OM, and pH / NIR spectroscopy and PCA/PLS	it is not effective for predicting phosphorus (P) and potassium (K) levels.	From the field, 165 soil samples were collected.	Correlation Coefficient: 0.93 for N, 0.93 for OM, and 0.91 for pH.
3.	Wang et al. (2015)	To predict macronutrient contents, pH value, and organic matter content/N, P, K, OM and pH/VIS/NIR, PCR, MPA FT-NIR	Poor Prediction for Certain Nutrients, Volatilization Issues.	Longkang Farm, Bengbu City	Using VIS/NIR spectrometer predicting OM and pH values better.
4.	Arisandy et al. (2022)	Soil micronutrients/N, P, K/RF, GB, DNN, PLS	preprocessing methods and spectrometer differences can significantly affect the results.	Spectroscopic data was obtained from 54 datasets.	Accuracy 91.88%
5.	Peng et al. (2019)	Soil nutrients/TN, TP, TK/ PLSR, BPNN, and GA-BPNN	To improve the estimation accuracy of soil nutrient contents.	Guangdong, China	RRMSE value of 20.37%
6.	Swapna et al. (2020)	soil nutrients and pH values. / pH, OC, EC, NPK, Cu, Fe Mn, Mg S, Br/PCA, Regression analysis techniques	Insufficient amounts of any one micronutrient in the soil can restrict and interfere with a plant's ability to grow	agricultural department.	In comparison to other soil nutrients in this area, N and K were naturally high.
7.	Sirsat et al. (2018)	Soil nutrients and fertility/OC, P2O5, Fe, Mn, Zn./Regression methods SVR, RF, PLS, bagging and boosting.	It is critical to improve the quality of the soil and maintain appropriate levels of various nutrients.	Marathwada region	Accuracy 97.63%
8.	Escorcia-Gutierrez et al. (2022)	Designed Soil nutrients/P, K, OC, and B/DL, GRU, DBN, Bi-LSTM,	an effective tool is needed to determine the right amount of soil nutrients based on crop requirements and fertility levels.	Samples from individual farmers.	Accuracy 0.9497
9.	Nyakuri et al. 2022)	Soil on Climatic conditions/pH, EC, N, Cu, Fe/IoT architecture	to enhance the agriculture activities to satisfy the need to increase farm productivity	Real-time data	Accuracy 0.963
10.	Ma et al. (2022)	Soil nutrients/Soil properties (e.g., pH, total nitrogen, soc)/ DT, RF, SVM, and NN	intercropping is known to improve soil nutrients and crop productivity, and microbes mediate the effects on belowground processes.	Soil ecosystem multifunctionality.	Phosphorus 87% and 16%
11.	Ahado et al. (2023)	Forest soil/P, K, Ca, Mg, Cu, F and Pb/MLAs, SGB -RK, and CUB_RK	soil problems are caused by the composition of and the presence or absence of particular materials. This will reduce agricultural land productivity.	An auxiliary	Cubist_ RK
12.	Blesslin Sheeba et al. (2022)	Micronutrients in soil/B, OC, K, P, and pH./Extreme learning method (ELM)	the need for more advanced and accurate systems to manage soil quality and crop production effectively.	Mulberry cultivation districts	K-3-5%, N-80%, and S-75%.
13.	Thapa et al. (2021)	Micronutrients/Fe, B, Mn, Zn, Cu, Mo, Cl, and Ni/Soil and foliar applications, SOM	To explore the potential for using micronutrients, we reviewed the literature evaluating the effect of micronutrients on soybean production	Not Defined	Fe - 1.91
14.	Dasgupta et al. (2023)	Soil micronutrient/Zn and Fe/ Hybrid ensemble model	investigate the potential of micronutrients to evaluate their effect on soybean production.	Not Defined	R2: Zn, Fe .0.52,0.63

Naresh & Kullayamma (2024) introduced an innovative deep-learning approach that utilizes the Concurrent Excited Gated Recurrent Unit and Deep Learning to automatically recommend crops based on soil, fertilizers, and climatic conditions. Ezhilarasi & Rekha (2022) focused on increasing farmers' profit through crop recommendations in towns and villages, using fuzzy ant clustering and association rule mining for crops.

MATERIALS AND METHODS

Advanced Machine Learning Classifiers for Soil Nutrient Analysis and Crop Recommendation Systems

The Supervised and unsupervised learning techniques encompass a variety of methods, such as decision tree classifiers, Bayesian classifiers, artificial neural networks, nearest neighbor classifiers, random forests, and support vector machines for uncovering patterns being studied. Additionally, ML models, including DT, KNN, and multivariate logistic regression have been introduced for forecasting the annual crop yields in certain West African countries with promising accuracy. Finally, a system was proposed to predict crop yields and recommend fertilizer using random forest and logistic regression algorithms (Jagtap et al. 2022, Cedric et al. 2022, Devan et al. 2023).

Fig. 3 shows crop prediction performed using innumerable machine learning algorithms. Several studies have proposed various machine learning algorithms for crop prediction, including Decision Trees, Multiple Linear Regression, Neural networks, XGBoost, SVM, KNN, and Naïve Bayes. The authors proposed crop recommendations based on some variables, including rainfall, temperature, humidity, N, P, and K. Also, they analyzed soil moisture using Soil Moisture Active Passive brightness temperature and performed crop

recommendations utilizing the Internet of Things technology, along with the Message Queuing Telemetry Transport protocol and Random Forest algorithm.

These models achieved high accuracy rates in predicting rainfall, suitable crops, and soil classification. Additionally, ensemble models such as XGBoost and LightGBM were found to outperform others with an impressive 99.32% accuracy (Mahendra et al. 2020, Patil et al. 2020, Yange et al. 2020, Rahman et al. 2018, Raja et al. 2022, Padmapriya & Sasilatha 2023, Kumar et al. 2023, Tong et al. 2020, Rao et al. 2022, Dey et al. 2024, Nti et al. 2023).

Deep Learning Approaches for Enhanced Soil Nutrient Detection and Crop Recommendation Models

An Artificial Neural Network is a network of interconnected layers of nodes or neurons that mimics the neural architecture of the human brain. After processing input, these nodes train themselves to modify the connection strengths (weights) to gain knowledge from the data. This enables the network to recognize patterns, predict outcomes, and handle various machine learning and artificial intelligence tasks. Studies have shown that using the ANN approach aligned with deep learning architecture outperforms other methods in identifying crops most likely to thrive in fertile soil and forecasting crop yields with high accuracy. When it comes to classifying soil and determining agricultural yield, a variety of ML techniques are utilized, including ANN, MLP, RF NB, SVM, and LR (Yadav et al. 2021, Gopal & Bhargavi 2019). A convolutional neural network is a powerful tool for image recognition because it excels at recognizing patterns, but it requires vast amounts of labeled data. ML techniques developed by Nevavuori et al. (2019) rely on yield mapping equipment not widely used among farmers. Convolutional Neural Networks have shown promising results in image
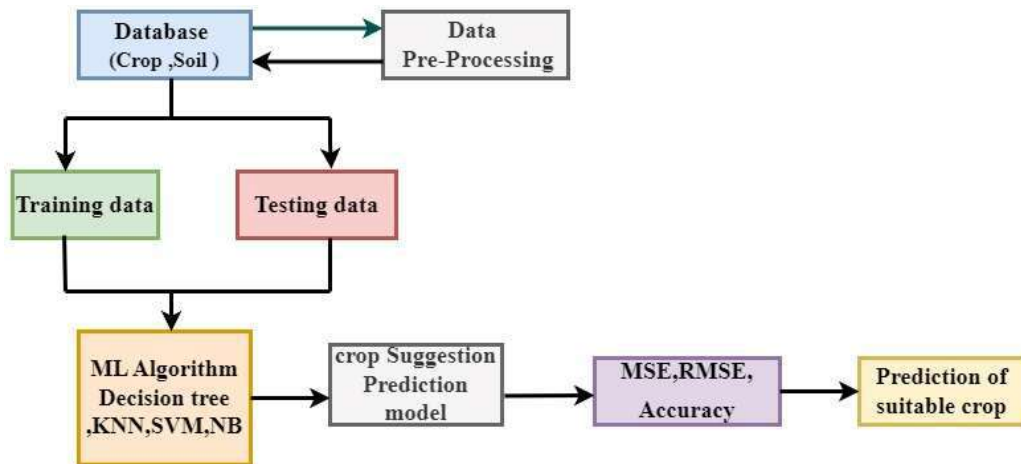
Fig. 3: Crop prediction using innumerable Machine Learning algorithms.

classification but present challenges in building crop yield forecast models, as highlighted by Xu et al. (2022). Laser-induced breakdown spectroscopy encounters reduced accuracy and stability in spectrum analysis due to soil heterogeneity; addressing this issue led to the utilization of non-pre-processed LIBS spectra for predicting soil type using CNN. A deep neural network consists of several layers positioned between the input and output layers. It shares common components such as neurons, synapses, weights, biases, and functions with other types of neural networks. This type of network can be trained like other machine learning algorithms. A special approach using deep neural networks is suggested for Predicting future crop yields by using historical yield data and greenhouse environmental information such as temperature, humidity, radiation, and CO_2 concentration (Gong et al. 2021). Recurrent neural networks belong to one of the two primary categories of artificial neural networks, distinguished by how information is transmitted between their layers. The term "convolutional neural network" describes networks with a finite impulse response, while "recurrent neural network" encompasses those with an infinite impulse response. Both types of networks exhibit temporal dynamic behavior. Sun et al. (2020) developed the Long Short-Term Memory, a widely utilized recurrent neural network architecture in Deep Learning. LSTM is known for its effectiveness in capturing long-term dependencies and is particularly well-suited for sequence prediction. Suebsombut et al. (2021) proposed an LSTM model to predict soil moisture values based on data from multiple sensors, while Kim et al. (2022) applied an LSTM model to reduce noise in agricultural sensors within a large-scale aquaponics system compared to traditional filtering approaches like Kalman and moving average filters. A densely interconnected network consists of multiple layers and utilizes combinations of neurons to transform input dimensions into the desired dimension. This allows outputs from certain neurons to serve as inputs for other neurons. Several studies have recommended using multilayer perceptron neural networks for data mining in agriculture, with the use of sigmoid and hyperbolic tangent activation functions being common. Techniques like machine learning have been suggested for crop recommendation to increase yield and quality while assisting farmers in selecting suitable crops for cultivation. These approaches outperform various algorithms, including instance-based learning with parameter k, Multi-Layer Perceptron, reduced error pruning tree, and C4.5 decision tree. Bhojani et al. (2020) and Garg and Alam (2023) proposed transfer learning refers to the utilization of a pre-trained model for a different task, which is particularly beneficial when the new task shares similarities with the original task or has limited data available. Cai et al. (2021) developed a soil nutrient extraction model by utilizing transfer learning and near-infrared spectroscopy as a response to the limitations of traditional models.

Evaluation Metrics for Assessing Soil Fertility and Crop Recommendation Systems

To predict crop yield, epochs are utilized to train the data and validate it when adjusting the base model and adding layers. Increasing the number of epochs leads to a reduction in loss details, indicating that the model is learning more as the epochs progress. The mean absolute error (MAE) determines the average magnitude of prediction errors, providing the average deviation between the expected and actual values for each forecast point. Mean absolute percentage error (MAPE), Mean squared error (MSE), and root mean squared error (RMSE) are error metrics used to assess prediction accuracy. Root absolute error (RAE) and Relative root mean squared error (RRMSE) can help farmers make decisions that increase crop yield. The RF algorithm has the lowest classification error when using RAE and RRMSE to evaluate the error measure. Crop yield is predicted to increase significantly by utilizing multi-sensor data for crop advice (Elbasi et al. 2023).

The terms "accuracy," "precision," and "recall" metrics are used to evaluate performance, including those used for crop recommendation systems. Here's what each term implies in this context:

- Accuracy: This refers to the percentage of accurate results (including both true positives and true negatives) out of all the cases that have been examined. For crop recommendations, it measures how frequently the model correctly predicts the right crop for given conditions.

- Precision: This metric represents the proportion of true positive predictions in the subset that the model predicted as positive. In crop recommendation, it is the ability of the model to only recommend a crop when it is indeed suitable.

- Recall: Recall refers to the percentage of true positives that the model correctly identifies. Sensitivity, often used interchangeably with recall, indicates the model's ability to identify all suitable conditions for a particular crop accurately.

- F1-Score: F1 = $2 \times \dfrac{Precision \times Recall}{Precision + Recall}$

- Sensitivity = $\dfrac{TP}{TP + FN}$

- Specificity = $\dfrac{TN}{TN + FP}$

For crop recommendation systems, these metrics are essential for accurately identifying and suggesting crops based on soil type, weather conditions, water availability, etc. They determine the effectiveness of providing reliable agricultural advice to farmers. Analyzing these metrics involves confusion matrices from classification reports or direct calculations using true positives, true negatives, false positives, and false negatives of test results.

Soil fertility index and soil pH content are critical for soil health management in agricultural research. They assess the ability of soil to provide essential nutrients to crops and measure acidity or alkalinity, which significantly affects nutrient availability and microbial activity. Analysis of variance is used to test if variations in soil management affect these factors, comparing mean levels across different practices. This information informs targeted recommendations for addressing nutrient deficiencies and advising on crop selection and fertilization plans tailored to optimize crop yield based on local conditions. Comprehensive soil testing coupled with knowledge of best management practices is essential for accurate recommendations (Jia et al. 2023, Aziz 2016, Gobbo et al. 2022).

RESULTS AND DISCUSSION

Optimized Proposed Model for Soil Fertility and Crop Recommendation Systems

Penghui et al. (2020) introduced a new hybrid model called an adaptive neuro-fuzzy inference system with mutational Salp Swarm and Grasshopper optimization algorithms, which incorporates optimization methods. They compared seven different models with the classic ANFIS model, showing that the ANFIS-MSG is particularly effective for forecasting soil temperature from a univariate air temperature scenario. Dinh et al. (2021) developed an SVM-based ML model to predict soil erosion using the L-SHADE-PWI approach, which optimizes SVM parameters through machine learning and metaheuristic optimization methods. Gopi & Karthikeyan (2024) suggested using DL and ML techniques to enhance crop productivity and predict yields. They proposed the RFOERNN-CRYP design, which combines Red Fox Optimization with Ensemble Recurrent Neural Network, along with LSTM, bidirectional LSTM, and GRU models. Choudhury et al. (2024) proposed a method to enhance prediction accuracy by integrating various classifiers based on KNN, DT, SVM, and LR into ensemble techniques using the Moth Flame Optimization algorithm for recommending crops. Shamshirband et al. (2020) demonstrated significant improvements in modeling soil temperature using SVM or MLP hybridized with Firefly optimization algorithm compared to standalone MLP or SVM models due to its effectiveness.

From the Survey, Fig. 4 shows the Crop recommendation and prediction for Agriculture using the Deep Learning Model. The crop recommendation System considers soil type, crop type, temperature, humidity, precipitation, and macro and micronutrient levels to recommend suitable crops for specific land. The proposed model uses deep learning algorithms for feature extraction and crop recommendation. The system involves three phases: The first phase - The dataset collection includes nitrogen (N), phosphorus (P), potassium (K), soil pH value, humidity, temperature, and rainfall parameters. Our goal is to help farmers choose the
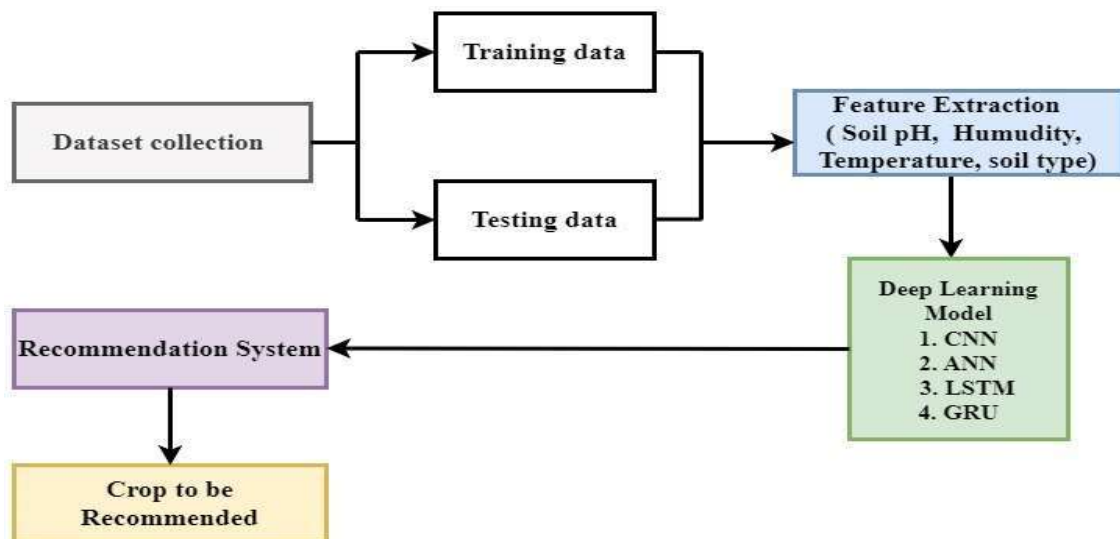
Fig. 4: Crop recommendation and prediction for Agriculture using the Deep Learning Model.

most suitable crops based on their unique circumstances and environment. We will achieve this by predicting which crops are well-suited to the factors that affect crop growth. The second phase focused on predicting soil nutrients to increase production. Different deep learning algorithms, including LSTM, CNN, ANN, and GRU, were utilized for this purpose. These algorithms helped suggest the most appropriate crop for a particular farm and predict crop yields. By considering the changes in environmental factors, this approach aimed to improve the accuracy of soil nutrient prediction and crop recommendations. Finally, in the third phase, the most suitable crop recommendation is based on using neural networks that are outperformed in the context of soil nutrient prediction and also in suitability of the crop. The referred data set is a publicly available Kaggle dataset.

The proposed model aims to improve soil nutrient prediction and crop recommendation by investigating intercropping systems, soil problems, soil nutrient deficiency, and preprocessing methods described in the limitation of the existing system in Table 1. These limitations will be significantly achieved by implementing deep learning algorithms such as ANN, CNN, LSTM, and GRU. These models will be trained with the feature selection process and analyze the various environmental factors to predict soil nutrients, recommend suitable crops, and help farmers achieve the expected yield as the best outcomes.

Interpretation of Crop Recommendation System Survey Outcome

This section examined the use of machine learning and deep learning techniques to estimate soil nutrients, analyze soil fertility, and suggest suitable crops for optimizing farmers' economic growth. Fig. 5 shows the survey analysis chart using several optimization and hybrid algorithms. In total, 93 papers were surveyed, with approximately 50 focusing on machine learning, 33 on deep learning, and 10 on optimization. Various machine learning techniques, including linear regression, random forest regression, k-nearest neighbors, support vector machines, decision trees, neural networks, and extreme gradient boosting, are recommended for crop prediction and classification in different agricultural scenarios. Regression techniques, including neural networks, deep learning, boosting lasso ridge regression, and Bayesian models, were employed to predict soil fertility and nutrient levels. Deep learning algorithms like LSTM, CNN, GRU, Bi-LSTM, DNN, SOM, RBM, DBN, GAN, RBFN MLP, and RNN were utilized to identify crop diseases from pictures of crop leaves. The GA-BPNN method was employed for mapping and estimating soil nutrients using hyperspectral techniques. For pH classification and prediction analysis, GRU, DBN, and Bi-LSTM were used, while LSTM, SVR, and LR predicted soil moisture. PCA was recommended with models such as RF, GD, DNN, and PLS applied for predicting soil minerals. LSTM, GRU, and CNN outperformed the others, resulting in high crop classification accuracy. The study aimed to test different machine learning and deep learning models to improve the accuracy of predictions. Different optimization and hybridization algorithms were utilized for tasks such as soil erosion prediction, soil temperature estimation, drought risk monitoring, crop recommendation, and crop yield estimation. Various evaluation factors were
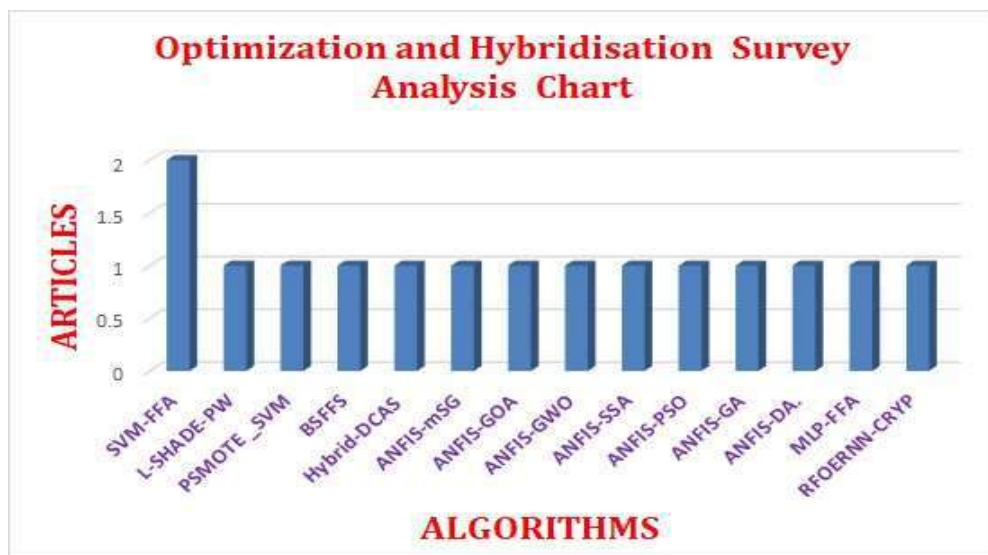
Fig. 5: Survey analysis chart.

utilized to assess the performance of different models, including precision and recall scores calculated separately for each crop type. Research publications utilized various activation functions for feature extraction and emphasized the potential of combining machine learning and deep learning techniques to optimize solutions. Extensive research on smart agriculture and intelligent soil nutrient prediction is essential for enhancing knowledge, improving prediction methods, and overcoming challenges faced by modern farmers in maximizing crop productivity.

CONCLUSIONS

In conclusion, the integration of deep learning and machine learning models into soil nutrient analysis and crop recommendation systems represents a significant advancement in precision agriculture. These models can analyze complex datasets, identify patterns, and provide accurate predictions based on a range of soil parameters, including fertility indices, pH levels, and nutrient content. The precise modeling of soil-plant interactions can be achieved through the implementation of deep learning architectures like Convolutional Neural Networks and machine learning algorithms such as Random Forests and Support Vector Machines. Advantages include improved accuracy in recommendations, real-time predictions for crop suitability and fertilization requirements, cost-effectiveness through automation, customization to regional data, and early warning systems for nutrient deficiencies. Challenges remain in terms of extensive high-quality datasets for model training/validation, interpretability of model predictions, and integrating these technologies into existing agricultural practices. Continued research is essential to refine these models further for global food security and sustainable farming practices.

REFERENCES

Ahado, S. K., Agyeman, P. C., Borůvka, L., Kamianske, R. and Nwogu, C., 2023. Using geostatistics and machine learning models to analyze the influence of soil nutrients and terrain attributes on lead prediction in forest soils. *Modeling Earth Systems and Environment*, 16, pp.1–14.

Ahmad, S., Kalra, A. and Stephen, H., 2010. Estimating soil moisture using remote sensing data: A machine learning approach. *Advances in Water Resources*, 33, pp.69–80.

Ahmed, U., Lin, J.C.W., Srivastava, G. and Djenouri, Y., 2021. A nutrient recommendation system for soil fertilization based on evolutionary computation. *Computers and Electronics in Agriculture*, 189, p.106407.

Amudha, M. and Brindha, K., 2022. Multi Techniques for Agricultural Image Disease Classification and Detection: A Review. *Nature Environment & Pollution Technology*, 21, pp.11-21.

Archana, S. and Kumar, P. S., 2023. A Survey on Deep Learning Based Crop Yield Prediction. *Nature Environment & Pollution Technology*, 22(2), p.434.

Arisandy, Y.P., Seminar, K.B., Purwanto, Y.A. and Hidayat, Y., 2022. Processing near-infrared spectroscopy signal to calculate soil macronutrient: A comparison of some machine learning approaches. *Creative Communication and Innovative Technology (ICCIT)*, 112, pp.1–9.

Aziz, M., 2016. Determine the pH of soil by using a neural network based on the soil's color. *International Journal of Advanced Research in Computer Science and Software Engineering*, 6(11), pp.51-54.

Babalola, E.O., Asad, M.H. and Bais, A., 2023. Soil surface texture classification using RGB images acquired under uncontrolled field conditions. *IEEE Access,* 415, pp.615.

Bhojani, S.H. and Bhatt, N., 2020. Wheat crop yield prediction using new activation functions in the neural network. *Neural Computing and Applications*, 32(17), pp.13941–13951.

Blesslin Sheeba, T., Anand, L.D., Manohar, G., Selvan, S., Wilfred, C.B., Muthukumar, K. and Asfaw, B.T., 2022. A machine learning algorithm for soil analysis and classification of micronutrients in IoT-enabled automated farms. *Journal of Nanomaterials*, 20, p.22.

Cai, H.T., Liu, J., Chen, J.Y., Zhou, K.H., Pi, J. and Xia, L. R., 2021. Soil nutrient information extraction model based on transfer learning and near-infrared spectroscopy. *Alexandria Engineering Journal*, 60(3), pp.2741–2746.

Cedric, L.S., 2022. Crops yield prediction based on machine learning models: Case of West African countries. *Smart Agriculture Technology*, 2, p.100049.

Chana, A.M., Batchakui, B. and Nges, B.B., 2023. Real-time crop prediction based on soil fertility and weather forecast using IoT and a machine learning algorithm. *Agricultural Sciences*, 14(5), pp.645–664.

Chandra, H., Pawar, P.M., Elakkiya, R., Tamizharasan, P.S., Muthalagu, R. and Panthakkan, A., 2023. Explainable AI for Soil Fertility Prediction. *IEEE Access,* 14, p.612.

Chandrappa, V.Y., Ray, B., Ashwatha, N. and Shrestha, P., 2023. Spatiotemporal modeling to predict soil moisture for sustainable smart irrigation. *Internet of Things*, 21, p.100671.

Choudhury, S.S., Pandharbale, P.B., Mohanty, S. N. and Jagadev, A. K., 2024. An acquisition-based optimized crop recommendation system with a machine learning algorithm. *EAI Endorsed Transactions on Scalable Information Systems*, 11(1), p.411.

Dasgupta, S., Debnath, S., Das, A., Biswas, A., Weindorf, D.C., Li, B. and Chakraborty, S., 2023. Developing regional soil micronutrient management strategies through ensemble learning-based digital soil mapping. *Geoderma*, 433, p.116457.

Dash, R., Dash, D. K. and Biswal, G. C., 2021. Classification of crops based on macronutrients and weather data using machine learning techniques. *Results in Engineering*, 9, p.100203.

Deshmukh, M., Jai, A., Joshi, O. and Shedge, R., 2022. Farming assistance for soil fertility improvement and crop prediction using XGBoost. *ITM Web of Conferences*, 44, p.03022.

Devan, K.P.K., Swetha, B., Uma Sruthi, P. and Varshini, S., 2023. Crop yield prediction and fertilizer recommendation system using hybrid machine learning algorithms. *Communication Systems and Network Technologies*, 54 pp.171-175.

Dey, B., Ferdous, J. and Ahmed, R., 2024. Machine learning-based recommendation of agricultural and horticultural crop farming in India under the regime of NPK, soil pH, and three climatic variables. *Heliyon*, 10(3), p.e04045.

Dinh, T.V., Nguyen, H., Tran, X.L. and Hoang, N.D., 2021. Predicting rainfall-induced soil erosion based on a hybridization of adaptive differential evolution and support vector machine classification. *Mathematical Problems in Engineering*, 2021, p.4153456.

Durai, S.K.S. and Shamili, M.D., 2022. Smart farming using machine learning and deep learning techniques. *Decision Analytics Journal*, 3, p.100041.

Elavarasan, D. and Vincent, P. D., 2020. Crop yield prediction using deep reinforcement learning model for sustainable agrarian applications. *IEEE Access*, 8, p.86886.

Elbasi, E., Zaki, C., Topcu, A.E., Abdelbaki, W., Zreikat, A.I., Cina, E. and Saker, L., 2023. Crop prediction model using machine learning algorithms. *Applied Sciences*, 13(16), p.9288.

Elbasiouny, H., El-Ramady, H., Elbehiry, F., Rajput, V.D., Minkina, T. and Mandzhieva, S., 2022. Plant nutrition under climate change and soil carbon sequestration. *Sustainability*, 14(2), p.914.

Escorcia-Gutierrez, J., Gamarra, M., Soto-Diaz, R., Pérez, M., Madera, N. and Mansour, R.F., 2022. Intelligent agricultural modeling of soil nutrients and pH classification using ensemble deep learning techniques. *Agriculture*, 12(7), p.977.

Ezhilarasi, T.P. and Rekha, K. S., 2022. Improved fuzzy ant colony optimization to recommend cultivation in Tamil Nadu, India. *Acta Geophysical*, 70(6), pp.2873-2887.

Gao, Z., Guo, D., Ryu, D. and Western, A.W., 2023. Training sample selection for robust multi-year within-season crop classification using machine learning. *Computers and Electronics in Agriculture*, 210, p.107927.

Garg, D. and Alam, M., 2023. An effective crop recommendation method using machine learning techniques. *International Journal of Advanced Technology and Engineering Exploration*, 10(102), p.498.

Gobbo, S., De Antoni Migliorati, M., Ferrise, R., Morari, F., Furlan, L. and Sartori, L., 2022. Evaluation of different crop model-based approaches for variable rate nitrogen fertilization in winter wheat. *Precision Agriculture*, 23(6), pp.1922-1948.

Gong, L., Yu, M., Jiang, S., Cutsuridis, V. and Pearson, S., 2021. Deep learning-based prediction on greenhouse crop yield combined TCN and RNN. *Sensors*, 21(13), p.4537.

Gopal, P.M. and Bhargavi, R., 2019. A novel approach for efficient crop yield prediction. *Computers and Electronics in Agriculture*, 165, p.104968.

Gopi, P.S.S. and Karthikeyan, M., 2024. Red fox optimization with ensemble recurrent neural network for crop recommendation and yield prediction model. *Multimedia Tools and Applications*, 83(5), pp.13159-13179.

Gosai, D., Raval, C., Nayak, R., Jayswal, H. and Patel, A., 2021. Crop recommendation system using machine learning. *International Journal of Scientific Research in Computer Science, Engineering and Information Technology*, 7(3), pp.558-569.

Gupta, S., Geetha, A., Sankaran, K.S., Zamani, A.S., Ritonga, M. and Raj, R., 2022. Machine learning and feature selection-enabled framework for accurate crop yield prediction. *Journal of Food Quality*, 2022, pp.1-7.

He, Y., Huang, M., García, A., Hernández, A. and Song, H., 2007. Prediction of soil macronutrient content using near-infrared spectroscopy. *Computers and Electronics in Agriculture*, 58(2), pp.144-153.

Hossain, M.D., Kashem, M.A. and Mustary, S., 2023. IoT-based smart soil fertilizer monitoring and m-based crop recommendation system. In: *2023 International Conference on Electrical, Computer and Communication Engineering (ECCE)*, IEEE, pp.1-6.

Jagtap, S.T., Phasinam, K., Kassanuk, T., Jha, S.S., Ghosh, T. and Thakar, C.M., 2022. Towards application of various machine learning techniques in agriculture. *Materials Today: Proceedings*, 51, pp.793-797.

Jejurkar, S.S., Meghna, S.B. and Wavhal, D.N., 2021. Crop prediction and disease detection using machine learning. *International Journal of Computer Science and Mobile Computing*, 10(2), pp.68-71.

Jia, X., Fang, Y., Hu, B., Yu, B. and Zhou, Y., 2023. Development of soil fertility index using machine learning and visible-near-infrared spectroscopy. *Land*, 12(12), p.2155.

John, K., Abraham Isong, I., Michael Kebonye, N., Okon Ayito, E., Chapman Agyeman, P. and Marcus Afu, S., 2020. Using machine learning algorithms to estimate soil organic carbon variability with environmental variables and soil nutrient indicators in an alluvial soil. *Land*, 9(12), p.487.

Kashyap, B. and Kumar, R., 2021. Sensing methodologies in agriculture for soil moisture and nutrient monitoring. *IEEE Access*, 9, pp.14095-14121.

Kaya, F. and Başayiğit, L., 2022. Spatial prediction and digital mapping of soil texture classes in a floodplain using multinomial logistic regression. *Intelligent and Fuzzy Techniques for Emerging Conditions and Digital Transformation: Proceedings of the INFUS 2021 Conference*, Volume 2, Springer International Publishing, pp.463-473.

Keesstra, S.D., Bouma, J., Wallinga, J., Tittonell, P., Smith, P., Cerdà, A., Montanarella, L., Quinton, J.N., Pachepsky, Y. and van der Putten, W.H., 2016. The significance of soils and soil science towards the realization of the United Nations Sustainable Development Goals. *SOIL*, 2, pp.111-128.

Keshavarzi, A., Kaya, F., Kaplan, G. and Başayiğit, L., 2022. Land cover classification in an arid landscape of Iran using Landsat 8 OLI science products: Performance assessment of machine learning algorithms. *Geoinformation*, 11, pp.175-179.

Khan, A.A., Faheem, M., Bashir, R.N., Wechtaisong, C. and Abbas, M.Z., 2022. Internet of Things (IoT) assisted context-aware fertilizer recommendation. *IEEE Access*, 10, pp.129505-129519.

Kim, J., Yu, B. and O'Hara, S., 2022. LSTM filter for smart agriculture. *Procedia Computer Science*, 210, pp.289-294.

Kimetu, J., Lehmann, J., Ngoze, S., Mugendi, D., Kinyangi, J., Riha, S.V., Louis R., John and Pell, A., 2008. Reversibility of soil productivity declines with organic matter of differing quality along a degradation gradient. *Ecosystems*, 17, p.81.

Kouadio, L., Deo, R.C., Byrareddy, V., Adamowski, J.F. and Mushtaq, S., 2018. Artificial intelligence approach for the prediction of Robusta coffee yield using soil fertility properties. *Computers and Electronics in Agriculture*, 155, pp.324-338.

Kumar, R., Gupta, M. and Singh, U., 2023. Precision agriculture crop recommendation system using KNN algorithm. *International Conference on IoT, Communication and Automation Technology (ICICAT)*, 61, pp.1-6.

Kumara Perumal, R., Pazhanivelan, S., Geethalakshmi, V., Nivas Raj, M., Muthu Manickam, D. and Kalia Perumal, R., 2022. Comparison of machine learning-based prediction of qualitative and quantitative digital soil-mapping approaches for Eastern Districts of Tamil Nadu, India. *Land*, 11(12), p.2279.

Kusuma Sri, B., Srilakshmi, V., Satyavada, S. and Kiran, G.U., 2023. Crop recommendation application using ensemble classifiers, *IEEE Access*, 8, pp.1-7.

Lacasta, J., Lopez-Pellicer, F.J., Espejo-García, B., Nogueras-Iso, J. and Zarazaga-Soria, F.J., 2018. Agricultural recommendation system for crop protection. *Computers and Electronics in Agriculture*, 152, pp.82-89.

Lad, A.M., Bharathi, K.M., Saravanan, B.A. and Karthik, R., 2022. Factors affecting agriculture and estimation of crop yield using supervised learning algorithms. *Materials Today: Proceedings*, 62, pp.4629-4634.

Lee, S., Jeong, Y., Son, S. and Lee, B., 2019. A self-predictable crop yield platform (SCYP) based on crop diseases using deep learning. *Sustainability*, 11(13), p.3637.

Ma, H., Zhou, J., Ge, J., Nie, J., Zhao, J., Xue, Z., et al., 2022. Intercropping improves soil ecosystem multifunctionality through enhanced available nutrients but depends on regional factors. *Plant and Soil*, 480(1), pp.71-84.

Mahendra, N., Vishwakarma, D., Nischitha, K., Ashwini, and Manjuraju, M.R., 2020. Crop prediction using machine learning approaches. *International Journal of Engineering Research & Technology (IJERT)*, 9(8), p.465.

Manjula, E. and Djodiltachoumy, S., 2022. Efficient prediction of recommended crop variety through soil nutrients using a deep learning algorithm. *Journal of Postharvest Technology*, 10(2), pp.66-80.

Nevavuori, P., Narra, N. and Lipping, T., 2019. Crop yield prediction with deep convolutional neural networks. *Computers and Electronics in Agriculture*, 163, p.104859.

Nti, I.K., Zaman, A., Nyarko-Boateng, O., Adekoya, A.F. and Keyeremeh, F., 2023. A predictive analytics model for crop suitability and

productivity with tree-based ensemble learning. *Decision Analytics Journal*, 8, p.100311.

Nyakuri, J.P., Bizimana, J., Bigirabagabo, A., Kalisa, J.B., Gafirita, J., Munyaneza, M.A. and Nzemerimana, J.P., 2022. IoT and AI-based smart soil quality assessment for data-driven irrigation and fertilization. *American Journal of Computing and Engineering*, 5(2), pp.1-14.

Padmapriya, J. and Sasilatha, T., 2023. Deep learning-based multi-labelled soil classification and empirical estimation toward sustainable agriculture. *Engineering Applications of Artificial Intelligence*, 119, p.105690.

Patil, D., Badarpura, S., Jain, A. and Gupta, A., 2020. Rainfall prediction using linear approach and neural networks and crop recommendation based on decision tree. *International Journal of Engineering Research & Technology (IJERT)*.

Peng, Y., Zhao, L., Hu, Y., Wang, G., Wang, L. and Liu, Z., 2019. Prediction of soil nutrient contents using visible and near-infrared reflectance spectroscopy. *ISPRS International Journal of Geo-Information*, 8(10), p.437.

Penghui, L., Ewees, A.A., Beyaztas, B.H., Qi, C., Salih, S.Q., Al-Ansari, N., et al., 2020. Metaheuristic optimization algorithms hybridized with artificial intelligence model for soil temperature prediction: Novel model. *IEEE Access*, 8, pp.51884-51904.

Prakash, M., Karthika, S. and Ramanani, S., 2017. An analysis for classification of soil data in data mining using R. *International Journal of Control Theory and Applications*, 10(2), pp.91-98.

Rahman, S.A.Z., Mitra, K.C. and Islam, S.M., 2018. Soil classification using machine learning methods and crop suggestion based on soil series. In *2018 21st International Conference of Computer and Information Technology (ICCIT)* (pp.1-4). IEEE.

Raja, S.P., Sawicka, B., Stamenkovic, Z. and Mariammal, G., 2022. Crop prediction is based on characteristics of the agricultural environment using various feature selection techniques and classifiers. *IEEE Access*, 10, pp.23625-23641.

Rao, M.S., Singh, A., Reddy, N.S. and Acharya, D.U., 2022. Crop prediction using machine learning. In *Journal of Physics: Conference Series* (Vol.2161, No.1, p.012033). IOP Publishing.

Reshma, S.J. and Aravindhar, D.J., 2022. A systematic approach to classifying soil and crop nutrients using machine learning algorithms. *International Journal of Intelligent Systems and Applications in Engineering*, 10(2s), pp.174-179.

Schut, A.G. and Reymann, W., 2023. Towards a better understanding of soil nutrient dynamics and P and K uptake. *Plant and Soil*, 492(1), pp.687-707.

Senapaty, M.K., Ray, A. and Padhy, N., 2023. IoT-enabled soil nutrient analysis and crop recommendation model for precision agriculture. *Computers*, 12(3), p.61.

Shamshirband, S., Esmaeilbeiki, F., Zarehaghi, D., Neyshabouri, M., Samadianfard, S., Ghorbani, M.A., et al., 2020. Comparative analysis of hybrid models of firefly optimization algorithm with support vector machines and multilayer perceptron for predicting soil temperature at different depths. *Engineering Applications of Computational Fluid Mechanics*, 14(1), pp.939-953.

Sharma, H., Sehgal, S.K., Dhaliwal, S.S. and Sharma, V., 2021. Monitoring and assessment of soil quality based on micronutrients and physicochemical characteristics in semi-arid sub-mountainous Shiwalik ranges of lower Himalayas, India. *Environmental Monitoring and Assessment*, 193(10), p.639.

Singha, C., Swain, K.C., Sahoo, S. and Govind, A., 2023. Prediction of soil nutrients through PLSR and SVMR models by VIs-NIR reflectance spectroscopy. *The Egyptian Journal of Remote Sensing and Space Sciences*, 26(4), pp.901-918.

Sirsat, M.S., Cernadas, E., Fernández-Delgado, M. and Barro, S., 2018. Automatic prediction of village-wise soil fertility for several nutrients in India using a wide range of regression methods. *Computers and Electronics in Agriculture*, 154, pp.120-133.

Suchithra, M.S. and Pai, M.L., 2020. Improving the prediction accuracy of soil nutrient classification by optimizing extreme learning machine parameters. *Information Processing in Agriculture*, 7(1), pp.72-82.

Sudhakar, M. and Priya, R.M., 2023. Computer Vision-Based Machine Learning and Deep Learning Approaches for Identification of Nutrient Deficiency in Crops: A Survey. *Nature Environment & Pollution Technology*, 22(3).

Suebsombut, P., Sekhari, A., Sureephong, P., Belhi, A. and Bouras, A., 2021. Field data forecasting using LSTM and Bi-LSTM approaches. *Applied Sciences*, 11(24), p.11820.

Sun, J., Lai, Z., Di, L., Sun, Z., Tao, J. and Shen, Y., 2020. Multilevel deep learning network for county-level corn yield estimation in the US Corn Belt. *IEEE Journal of Selected Topics in Applied Earth Observations and Remote Sensing*, 13, pp.5048-5060.

Swapna, B., Manivannan, S. and Nandhinidevi, R., 2020. Prediction of soil reaction (pH) and soil nutrients using multivariate statistical techniques for agricultural crop and soil management. *International Journal of Advanced Science and Technology*, 29(7s), pp.1900-1912.

Thapa, S., Bhandari, A., Ghimire, R., Xue, Q., Kidwaro, F., Ghatrehsamani, S., et al., 2021. Managing micronutrients for improving soil fertility, health, and soybean yield. *Sustainability*, 13(21), p.11766.

Thilakarathne, N.N., Bakar, M.S.A., Abas, P.E. and Yassin, H., 2022. A cloud-enabled crop recommendation platform for machine learning-driven precision farming. *Sensors*, 22(16), p.6299.

Tobiszewski, M. and Vakh, C., 2023. Analytical applications of smartphones for agricultural soil analysis. *Analytical and Bioanalytical Chemistry*, 415(18), pp.3703-3715.

Tong, C., Wang, H., Magagi, R., Goïta, K., Zhu, L., Yang, M. and Deng, J., 2020. Soil moisture retrievals by combining passive microwave and optical data. *Remote Sensing*, 12(19), p.3173.

Varshitha, D.N. and Choudhary, S., 2022. An artificial intelligence solution for crop recommendation. *Indonesian Journal of Electrical Engineering and Computer Science*, 25(3), pp.1688-1695.

Venkata Naresh, M. and Kullayamma, I., 2024. Deep learning-based concurrent excited gated recurrent unit for crop recommendation based on soil and climatic conditions. *Multimedia Tools and Applications*, 18, pp.1-30.

Wang, Y., Huang, T., Liu, J., Lin, Z., Li, S., Wang, R. and Ge, Y., 2015. Soil pH value, organic matter, and macronutrient content prediction using optical diffuse reflectance spectroscopy. *Computers and Electronics in Agriculture*, 111, pp.69-77.

Wankhade, S.R. and Raut, A.B., 2024. Development of a model for estimation of soil parameters using deep learning. *International Journal of Information Technology*, 11, pp.1-17.

Xu, X., Ma, F., Zhou, J. and Du, C., 2022. Applying convolutional neural networks (CNN) for end-to-end soil analysis based on laser-induced breakdown spectroscopy (LIBS) with less spectral preprocessing. *Computers and Electronics in Agriculture*, 199, p.107171.

Yadav, J., Chopra, S. and Vijayalakshmi, M., 2021. Soil analysis and crop fertility prediction using machine learning. *Machine Learning*, 8(3), p.2351.

Yange, T.S., Egbunu, C.O., Rufai, M.A., Onyekwere, O., Abdulrahman, A.A. and Abdulkadri, I., 2020. Using prescriptive analytics for the determination of optimal crop yield. *International Journal of Data Science and Analysis (IJDSA)*, 6(3), pp.72-82.

Penta Helix Collaboration Model Involving Reserve Component Personnel in Disaster Resilience in Malang Regency

D. Muktiyanto† (iD)**, S. Widagdo, M. Istiqomah and R. Parmawati**

Department of Doctoral Program in Resilience Studies, Postgraduate School, Brawijaya University, Malang, Indonesia
†Corresponding author: D. Muktiyanto; didikmuktiyanto@student.ub.ac.id

ABSTRACT

This study aims to analyze the Penta helix collaboration model for involving reserve component personnel in disaster resilience in Malang Regency. A qualitative approach was used with an in-depth interview method involving nine informants from various Penta helix actors, namely academia, business, the community, government, and the Media. The main findings indicate that the Penta helix collaboration model has the potential to enhance disaster resilience in Malang Regency. Its strengths lie in inclusive participation, transparency, clear leadership, and the commitment of stakeholders. However, there are still weaknesses, such as a lack of coordination, limited resources, and suboptimal role understanding that hinder the involvement of reserve component personnel. Each actor makes significant contributions: academics provide knowledge, businesses aid in logistics, communities engage in mitigation and emergency response, the government formulates policies, and the media disseminates information. Major challenges include a lack of coordination, limited resources, miscoordination, bureaucracy, insufficient training, and unclear legal frameworks. Improvement efforts include strengthening coordination, increasing resource capacity, clarifying roles, developing guidelines, and enhancing training. In conclusion, the Penta helix collaboration model in Malang Regency has great potential but requires improvements to enhance its effectiveness, providing insights for stakeholders to strengthen disaster resilience in the region.

INTRODUCTION

Indonesia is an archipelagic country with a total area of 5,193,250 square kilometers, covering both land and sea (Rahayu et al. 2024). The land area of Indonesia spans 1,919,440 square kilometers and consists of 17,508 islands (Anggadwita et al. 2015, Riwanto 2017), with a coastline stretching 3,977 miles and a vast ocean area of approximately 3,273,810 square kilometers (Kusumajanti et al. 2020). Indonesia holds a strategic position in the Asian region. Geographically, the Indonesian archipelago is dominated by tropical rainforests and lies at the convergence of three tectonic plates: the Indo-Australian Plate to the south, the Eurasian Plate to the west, and the Pacific Plate to the east. The boundaries between these plates form a series of volcanic mountain chains surrounding the Pacific Ocean known as the Pacific Ring of Fire (Wibowo & Sembri 2016), resulting in 127 active volcanic mountains across the country, making it one of the most volcanically active regions in the world (Hamna et al. 2024).

In addition to its captivating natural wealth, Indonesia is also known as one of the countries vulnerable to serious natural disasters, which can threaten the lives of its population (Wesnawa & Christiawan 2014). Recognizing this, since the Brundtland report was published in 1987, disaster risk reduction (DRR) has been acknowledged as a key strategy for achieving sustainable development (Imperiale & Vanclay 2021). DRR aims to minimize the negative impacts of natural disasters, thereby protecting the lives and property of communities (Imperiale & Vanclay

2024). By integrating DRR into development plans and collaborating to build community resilience, Indonesia can move towards a safer and more sustainable future. These efforts will not only protect lives and property but also support inclusive economic and social development.

One of the most frequent actual threats in Indonesia is the threat of disasters. Indonesia has a very high vulnerability to various disasters, such as earthquakes, tsunamis, floods, landslides, tornadoes, disease outbreaks, droughts, and volcanic eruptions (Alfajri et al. 2019). According to data from the National Disaster Management Agency (BNPB) on June 12, 2024, there were 891 disaster events in Indonesia throughout the year 2024, with 98.77% of them being hydrometeorological disasters and 1.23% being geological disasters (BNPB 2024). This reflects Indonesia's vulnerability to various types of natural disasters and highlights the importance of mitigation measures to reduce the impact of disasters in the future.

In the context of Malang Regency, East Java, it is classified as high risk in the national disaster risk class based on the 2021 National Disaster Vulnerability Index (IRBN) released by the National Disaster Management Agency (BNPB) with a score of 146.98 (BNPB 2021). The Malang Regency Regional Disaster Management Agency (BPBD) has extended the Emergency Response Alert Status for Hydrometeorological Disasters until the end of April 2024 and has mapped disaster-prone areas. The Head of the Emergency and Logistics Division of BPBD stated that this mapping is based on disaster risk assessments and previous incident data. Areas prone to strong winds include Karangploso, Dau, Singosari, Lawang, Pakis, Jabung, Tajinan, Poncokusumo, Bululawang, Gondanglegi, Sumberpucung, and Kepanjen. For landslides, vulnerable areas include Pujon, Ngantang, Kasembon, Karangploso, Dau, Singosari, Lawang, Poncokusumo, Tumpang, Ampelgading, Tirtoyudo, Dampit, Sumbermanjing Wetan, Wagir, Kromengan, Ngajum, and Wonosari. Flood-prone areas include Pujon, Ngantang, Kasembon, Karangploso, Dau, Singosari, Lawang, Pakis, Poncokusumo, Ampelgading, Tirtoyudo, Dampit, Sumbermanjing Wetan, Gedangan, Kalipare, and Wagir (Syamsuddin 2024). This indicates significant disaster risk potential in these areas, necessitating strategic measures to mitigate their impact.

Disaster resilience efforts in Malang also involve the local community, as proposed by Sudarmanto et al. (2020). This community played a significant role during the eruption of Mount Kelud by mobilizing, preparing, and evacuating people in Disaster-Prone Areas (DPA). Additionally, Rozikin et al. (2023) proposed the Family Disaster Resilience Program (Keluarga Tangguh Bencana - Katana). Therefore, reserve components should be involved in disaster management,

especially in Pentahelix collaborations, to enhance the effectiveness and evaluation of disaster resilience in Malang.

Disaster resilience is a concept that has recently been used in disaster discussions worldwide. With the increasing frequency and intensity of disasters globally, disaster resilience has pressed for the expansion of efforts to reduce disasters by building disaster resilience at the global, national, and local levels. The UN General Guidelines on Assisting Building Resilient Communities (2020) emphasize that resilience assessments provide the basis for building resilience as a precondition for achieving inclusive and sustainable development, peace, and prosperity for all while also highlighting its benefits and relevance to the economy (Hussain et al. 2023).

The Indonesian government has taken steps to strengthen the national defense system by establishing a national reserve component through Law Number 23 of 2019 concerning the management of national resources for state defense. Article 1, paragraph 9 of the law defines the reserve component (*Reserved components*) as a national resource that has been prepared to be activated through mobilization, to strengthen and enlarge the strength and capabilities of the main components (Indonesian National Armed Forces) (Indrawan & Efriza 2018). The concept of national resources in Law Number 23 of 2019 refers to several components, namely citizens/human resources, natural resources, artificial resources, as well as facilities and infrastructure (Hidayat 2022, Roringkon et al. 2022). Reserve component personnel have the potential to assist in various aspects of disaster management, such as evacuation, search and rescue, logistics distribution, and post-disaster rehabilitation.

The Penta helix collaborative approach in disaster management is crucial in facing complex disaster risks. By involving various stakeholders, including the government, non-governmental organizations, the private sector, and the community (pentahelix), effective cooperation in disaster response is expected to be achieved (Djuyandi & Hendradjaja 2021, Syamsunasir et al. 2023). The pentahelix collaboration in engaging reserve component personnel aims to enhance preparedness, expedite response, mitigate disaster impacts, and strengthen disaster resilience in the area. Therefore, analyzing the practices of pentahelix collaborative disaster management in engaging reserve component personnel is essential to understanding the effectiveness and challenges of disaster mitigation at the local level.

MATERIALS AND METHODS

Research Approach

This research utilizes a qualitative research method with a

case study approach. The case study approach was chosen because this research aims to understand and analyze in depth how to build collaboration with the five Penta helix stakeholders in the process of engaging reserve component personnel for disaster resilience in the Malang Regency.

Research Location

The research was conducted at various locations in Malang Regency, East Java, including the office of the Regional Disaster Management Agency (*BPBD*) of Malang Regency in Wonorejo, Kodim 0818/Malang in Blimbing, Brawijaya University in *Lowokwaru*, PT. Pindad Turen in Turen, the Humanitarian Network of East Java in Kepanjen, Radar Malang in Mojolangu, and disaster-prone villages in Malang Regency. *BPBD* and *Kodim* 0818/Malang were the main focus for obtaining information related to disaster management and the role of reserve component personnel. Meanwhile, Brawijaya University, PT. Pindad Turen and the Humanitarian Network of East Java provided academic support, logistics, and community information. Radar Malang was expected to provide information and education through the mass Media. The research also involved disaster-prone villages to understand the experiences of the community and their needs related to disaster management.

Data Sources

The research on "Collaboration Model Involving Reserve Component Personnel in Disaster Resilience in Malang Regency" utilizes various data sources to obtain comprehensive and accurate information. The informants involved include the Head of the Regional Disaster Management Agency (*BPBD*) of Malang Regency, relevant staff from *BPBD* of Malang Regency, research staff of Disaster Management/Bravo (Brawijaya Volcanology) at Brawijaya University, Human Resource Development (HRD) staff of PT. Pindad in Turen, Malang, the chairman of volunteers of the Humanitarian Network of East Java, HRD staff of Radar Malang, reserve component personnel of Kodam V/Brawijaya, and personnel of *BPBD* of Malang Regency. There were a total of nine (9) informants selected as research samples who were considered qualified and most knowledgeable about the research topic.

Additionally, documents such as Law Number 23 of 2019 concerning the Management of National Resources for State Defense, the National Disaster Management Plan (*RNPB*), the Regional Disaster Management Plan (*RPBD*) of Malang Regency, Reports on the Involvement of Reserve Component Personnel by the Regional Disaster Management Agency (*BPBD*) of Malang Regency, and research reports and publications related to the involvement of Reserve Component Personnel in Disaster Management will serve as primary data sources.

Data Collection Techniques

Informants: The informants in the research are as follows: *First*, the Regency Military Commander (*Dandim*) of 0818/Malang Regency, the Head of the Regional Disaster Management Agency (*BPBD*) of Malang Regency, relevant staff from government agencies, disaster research staff from *Bravo* (Brawijaya Volcanology) at Brawijaya University, HRD staff from PT. Pindad Turen, Malang, the chairman of the volunteer network "*Jaringan Kemanusiaan*" East Java, and HRD staff from Radar Malang. *Second*, personnel from the Regional Disaster Management Agency (*BPBD*) of Malang Regency and reserve personnel from *Kodam* V/ Brawijaya.

In-depth interview: The interview will be conducted in a structured manner based on interview guidelines that will be prepared beforehand.

Document study: Collecting secondary data through mass Media clips, government archives, regulations, books, journals, images and photos, and others.

Focus group discussion *(FGD):* FGD is conducted independently with each relevant party to explore the strengths and weaknesses of ongoing facts with concepts created from the interpretations of the relevant parties.

Data Analysis

Data analysis is conducted in several stages. First, content analysis is performed on the interview results, document studies, and FGDs to identify the main themes and patterns emerging from the collected data. The second stage is thematic analysis, where data is categorized based on emerging themes, and relationships between existing themes are identified. This process helps in understanding the deeper context related to the research topic. Furthermore, data triangulation is conducted, which involves comparing data obtained from various sources to ensure the validity and reliability of the data used in the research. By conducting data triangulation, it can be ensured that the data used is an accurate representation of the phenomenon under study; thus, the resulting analysis can be trusted and has high reliability.

RESULTS AND DISCUSSION

Research Location Description

Malang Regency is located between 112º17'10.9" to 122º57'00.00" East Longitude and 7º44'55.11" to 8º26'35.45"

South Latitude. Its area is approximately 3,347.8 km2, making it the second largest after Banyuwangi Regency in East Java. More than 50 percent of its area is agricultural land, including rice fields, gardens, and plantations. The average temperature ranges from 19ºC to 27ºC, making it a cool area sought after as a place for living and relaxation. Malang Regency is surrounded by six regencies and the Indonesian Ocean. Its boundaries include Pasuruan Regency, Probolinggo, Lumajang, the Indonesian Ocean, and Blitar Regency, as well as bordering Kediri Regency and Mojokerto Regency. Consisting of mountains and peaks, Malang Regency has a topography that supports vast forest potential and serves as a water source through agricultural irrigation rivers. Some famous mountains in this area are Mount Semeru (3,676 meters), Mount Kelud (1,731 meters), Mount Welirang (3,156 meters), and Mount Arjuno (3,339 meters). Its average elevation is 524 meters above sea level (BPBD 2020).

Penta helix Collaboration

The Penta helix collaboration involving reserve component personnel in disaster resilience in the Regency involves five main actors.

Academia

Table 1 summarizes the roles and contributions of academia as reserve components in disaster resilience in Malang

Table 1: Academia as reserve component personnel in disaster resilience.

Aspect	Description	Note
Disaster Management Resources (DMR)	Faculty and students through community service and CBL (community-based learning).	Interview on Friday, January 12, 2024, at the Bravo GRC Office, Brawijaya University, Malang.
	Educators across interdisciplinary fields between faculties and external parties.	
	Faculties of Mathematics and Natural Sciences, Engineering, Social and Political Sciences, Medicine, Informatics, Agriculture, Fisheries, Law, and Social Sciences.	
Support for Disaster Management Activities (DMA)	Support from the university and collaboration with other universities through MoUs.	
Challenges in Disaster Management Collaboration (DMA)	Complex coordination with relevant agencies and institutions for activity permits.	
	Activities need to align with the strategic plans and needs of the relevant agencies.	
Views on Involving Reserved Components Personnel	Enhancing the effectiveness and efficiency of work units, especially in emergency response.	
	Necessary involvement, particularly in post-disaster management.	
	Collaboration schemes among academia, the military, volunteers, and other stakeholders need to be designed.	
Conflict in Collaboration	So far, there have been no significant conflicts.	
Regulations Related to Disaster Management (DM)	The Universitas Brawijaya 2021–2025 Strategic Plan on Disaster and Environmental Affairs aligns with disaster management regulations.	
Disaster Management Collaboration Forum (DMCF)	The Disaster Management Forum (DMF) is formed as a study or research group, such as the BRAVO GRC and *PSKK* (Center for Earth and Disaster Studies).	
Inclusive Participation	All parties involved in the collaboration participate inclusively.	
Transparency	Collaboration among stakeholders is transparent.	
Leadership	The chairperson of the study group/center for disaster studies at Brawijaya University, which deals with disaster management issues, is considered most suitable to lead the collaboration.	
Trust	Each stakeholder should be able to build trust in the collaboration with all involved parties.	
Information Transparency	Face-to-face dialogues are crucial for gaining understanding and agreement regarding the scope and extent of work from each party involved in the collaboration.	
Commitment of Brawijaya University	Brawijaya University has a high commitment to collaborating on disaster management.	
Enhancing Pentahelix Collaboration	Shared understanding based on the Pentahelix model implemented in regular meetings involving all stakeholders.	
	All components or stakeholders are involved, ensuring alignment of perceptions.	
Coordination System Involving Reserved components	The coordination system involving *Reserved components* in disaster management is crucial.	

Source: primary data processed (year 2024).

Regency. Through research and development, support for disaster management activities, and coordination and collaboration with various stakeholders, academia can provide significant contributions to enhancing disaster resilience.

Business

Business actors play a crucial role in enhancing disaster resilience through various forms of contribution and collaboration. One of the companies actively involved in these efforts is PT Pindad (Table 2). The company provides assistance through its Corporate Social Responsibility (CSR) program to support disaster management. Additionally, PT Pindad also has several reserve component personnel who may be increased in the future and support humanitarian aid for disasters from various parties.

Community

Community actors play a vital role in enhancing disaster resilience by utilizing local potential and providing direct assistance in the field. One example is the Jaring Kemanusiaan Jawa Timur (JKJT) community, which has

field influencer teams consisting of 25 members per team to assist in disaster-affected areas (Table 3). JKJT focuses on empowering the potential of communities in disaster-prone areas and receives support from various parties for disaster management activities.

Government

The government, through the Malang Regency Regional Disaster Management Agency (BPBD), has a crucial role in strengthening disaster resilience by utilizing sufficient resources but requires strengthening in the field. Malang Regency BPBD and Kodim 0818/Malang Regency work together to provide support in collaborative disaster management, which is quite good despite facing challenges such as data accuracy, technical aspects of aid distribution, shortage of workers, vehicles, and public understanding of disasters (Table 4).

Media

The role of the media as supporting personnel in enhancing disaster resilience is explored in Table 5. The media, especially Radar Malang, has coverage teams

Table 2: Business (PT. Pindad) as reserve component personnel in disaster resilience.

Aspect	Description	Note
Role of PT Pindad	Providing assistance in the form of CSR for disaster management.	Interview on Thursday, January 11th, 2024, at PT Pindad's office in Malang.
	Having 8 *Reserved components* personnel and the possibility of increasing in the future.	
	Supporting humanitarian assistance for disasters from various parties.	
Challenges in Collaboration	Distribution of aid during disaster emergency response is still complicated.	
	Further training is needed for *Reserved components* personnel.	
	A legal framework is needed for the involvement of Reserved components personnel.	
View the Pentahelix Collaboration	PT Pindad has not been involved in formal collaboration forums.	
	Inclusive participation is achieved by carrying out the tasks and responsibilities of each stakeholder.	
	There is transparency in the collaboration.	
View on Leadership and Trust	*BNPB/BPBD* is considered the most suitable to lead the collaboration	
	Stakeholders can build trust, but adjustments are needed for disaster management conditions.	
View on Transparency	Face-to-face dialogue is considered key to transparency.	
	PT Pindad has never been invited to face-to-face dialogue.	
PT Pindad's Commitment	PT Pindad is committed to supporting every humanitarian activity, including disaster management and national resilience.	
Enhancing Pentahelix Collaboration	A better understanding of the goals and definition of the problem is needed.	
	Training for *Reserved components* personnel and education for stakeholders and the community are required.	
	Intermediate results are needed to assess activity achievements, create a more effective and efficient coordination system, and serve as parameters for the effectiveness of *Reserved components* personnel involvement.	

Source: primary data processed (year 2024).

Table 3: Interview Results from the *Jaring Kemanusiaan Jawa Timur (JKJT)* Community (Community Element) as Reserve Component Personnel in Disaster Resilience.

Aspect	Description	Note
Resources of JKJT	The field influencer team consists of 25 members per team to assist on the ground.	The interview was conducted on Friday, January 10th, 2024, at the *JKJT* Headquarters in Malang.
	Empowering the potential of the community in disaster-affected areas.	
Support for DMA Activities	Support from various parties is quite good.	
	Quick and uncomplicated coordination is needed for disaster victims' assistance.	
Challenges in DMA Collaboration	Miscoordination, complicated bureaucracy, and suboptimal distribution of aid.	
Perspective on the Involvement of Reserved Components Personnel	Personnel from Reserved components can be involved, but they need preparation and training.	
Perspective on Conflict	Conflict arises due to complicated bureaucracy, whereas the situation on the ground requires speed.	
Regulations Related to DMA	Law Number 24 of 2007 concerning Disaster Management.	
DMA Collaboration Forum	Focus Group Discussions (FGDs) are organized periodically by *BPBD*.	
Inclusive Participation	All involved parties participate inclusively and work together to assist disaster victims.	
Transparency	Reports and transparency regarding aid distribution are communicated to volunteers and joint teams in the field.	
Leadership	*BNPB/BPBD* is considered the most suitable to lead the collaboration.	
Trust	Trust can be well established, but job clusters are needed to avoid blaming each other and streamline disaster management.	
Information Transparency	Dialogue is the key to understanding roles and rights of support in collaboration, as well as to enhancing responsibility and humanitarian principles.	
Commitment of *JKJT*	*JKJT* is committed to upholding humanity, strengthening national resilience, and assisting as many disaster victims as possible.	
Improvement of Pentahelix Collaboration	Sharpening the collective understanding of the goals, problem definitions, and values to be achieved by creating job clusters.	
	Tracking the achievements of DMA activities through interim results for future evaluation and improvement.	
	Involving Reserved components in collaboration by clarifying its basic norms and legal foundations.	

Source: primary data processed (year 2024).

in disaster areas ready to support disaster management activities. Support from various parties within the media institution is highly beneficial for disaster management collaboration.

Pentahelix Collaboration Model for Involving Reserve Component Personnel in Disaster Resilience in Malang Regency

The pentahelix collaboration model offers a comprehensive approach to involving reserve component personnel in disaster resilience in Malang Regency. Based on research findings related to the Penta helix collaboration model in disaster management in Malang Regency, several important aspects are discussed, including:

Effectiveness of the Penta helix Collaboration Model

The Penta helix collaboration model in Malang Regency has

several strengths and weaknesses that need to be considered to enhance its effectiveness in improving disaster resilience.

The efforts to address the weaknesses, as shown in Table 6, regarding the effectiveness of the Pentahelix Collaboration Model in involving reserve component personnel in disaster resilience can be carried out in several ways, including:

a. Strengthening coordination and communication among actors

   Strengthening coordination and communication among actors through more effective collaborative forums. According to Martin et al. (2016), poor inter-organizational partnerships are barriers to successful disaster response. Therefore, coordination and communication among actors can be enhanced by facilitating strong bonding capacities among members, enabling efficient bridges to the entire

Table 4: Interview Results with the Government as Reserves for Disaster Resilience.

Aspect	Description	Note
Resources	The Regional Disaster Management Agency (*BPBD*) of Malang Regency has sufficient resources but still requires reinforcement in the field (*BPBD* Malang Regency).	• Interview on Monday, January 8, 2024, at the Office of the Regional Disaster Management Agency (*BPBD*) of Malang Regency.
	The Regency Military Command (*Kodim*) 0818/Malang Regency has 431 Babinsa personnel distributed across all Regencys (*Kodim* 0818/Malang Regency).	
Support for Disaster Management Activities	Support from various parties in disaster management collaboration is quite good. (*BPBD* of Malang Regency, *Kodim 0818/* Malang Regency).	
Challenges in Disaster Management Collaboration	The accuracy of data and technical aspects of aid distribution, the lack of manpower and transport vehicles, and the community's mindset about disasters (*BPBD* of Malang Regency).	
	The dynamic conditions in the field, especially during aid distribution (Kodim 0818/ Malang Regency).	• Interview on Tuesday, January 9, 2024, at the Office of the Regency Military Command (*Kodim*) of Malang Regency.
Perspectives on the Involvement of Reserve Personnel	The involvement of Reserved components personnel can help strengthen disaster resilience in Malang Regency (*BPBD* of Malang Regency, Kodim 0818/ Malang Regency).	
	Training and disaster management education are needed for Reserved components personnel (*BPBD* of Malang Regency).	
	A clear legal framework is needed regarding the involvement of Reserved components personnel in disaster management (*Kodim* 0818/Kab. Malang).	
Perspectives on Conflict in Collaboration	Conflicts that occur during the disaster management collaboration process tend to be minimal (*BPBD* of Malang Regency, Kodim 0818/ Malang Regency)	
	Conflicts usually arise due to a lack of personnel to assist in aid distribution (*BPBD* of Malang Regency).	
Regulations Related to Disaster Management	Law Number 24 of 2007 concerning Disaster Management (*BPBD* of Malang Regency, *Kodim* 0818/ Malang Regency)	
	Law Number 34 of 2004 concerning the Indonesian National Defense Forces (*Kodim* 0818/ Malang Regency).	
Collaboration Forums for Disaster Management	Focus Group Discussions (FGD) are organized periodically by the Regional Disaster Management Agency (BPBD) (*BPBD* of Malang Regency).	
	Periodic disaster management forums are held by the BPBD of Malang Regency (Kodim 0818/ Malang Regency).	
Inclusive Participation in Collaboration	All parties involved participate inclusively and work hand in hand in assisting disaster victims (*BPBD* of Malang Regency, Kodim 0818/ Malang Regency)	
Transparency in collaboration	Transparency in the collaboration process among stakeholders in Malang Regency is working well (*Kodim* 0818/ Malang Regency).	
	Budget utilization reports and information related to disaster management activities are provided to ensure transparency (*BPBD* of Malang Regency).	
Leadership in Collaboration	BNPB/BPBD is considered the most appropriate entity to lead the collaboration (*BPBD* of Malang Regency, Kodim 0818/ Malang Regency)	
Trust in Collaboration	Trust can be built effectively throughout the collaboration process (*BPBD* of Malang Regency, Kodim 0818/ Malang Regency)	
	Adaptation and training for *Reserved components* personnel are needed to foster better trust (*Kodim* 0818/ Malang Regency).	
Information Transparency in Collaboration	Regular face-to-face dialogues are conducted to ensure information transparency (*Kodim* 0818/ Malang Regency).	
	There is a need for inherent coordination regarding the command functions and tasks of Reserved component personnel in the field (*Kodim* 0818/ Malang Regency).	
Government Stakeholders' Commitment	Commitment to strengthen national resilience through collaboration in disaster management (*BPBD* of Malang Regency, *Kodim* 0818/ Malang Regency).	
	Commitment to assist the people, especially during disaster events (*Kodim* 0818/ Malang Regency).	

Source: primary data processed (year 2024).

Table 5: Interview Results with Media (*Radar Malang*) as Auxiliary Personnel in Disaster Resilience.

Aspect	Description	Note
Resources	The media has reporting teams in disaster areas ready to support disaster management activities.	Interview on Tuesday, January 9, 2024, at the Editorial Office of Radar Malang.
Support for Disaster Management Activities	Support from various parties within the media institution is highly beneficial for disaster management collaboration.	
Challenges in Disaster Management Collaboration	The limited supporting facilities for disaster management activities, considering the vast area of Malang Regency and the high number of communities vulnerable to disasters.	
Perspectives on the Involvement of Reserved Components Personnel	Involvement of Reserved components personnel is necessary as they are part of the national defense system and have the potential to strengthen national resilience through disaster management.	
	Clear regulations are needed regarding the involvement of Reserved components personnel in disaster management.	
Perspectives on Conflict in Collaboration	During the disaster management collaboration process, there have been no significant conflicts.	
Regulations Related to Disaster Management	Law Number 24 of 2007 concerning Disaster Management.	
Collaboration Forum for Disaster Management	Inclusive forums already exist, but the media has not been involved yet.	
Inclusive Participation in Collaboration	All parties involved in disaster management collaboration participate inclusively in the process.	
Transparency in collaboration	Transparency in the collaboration process among stakeholders in disaster management is already in place, with important aspects such as the disclosure of budget expenditure reports for disaster management activities.	
Leadership in Collaboration	BNPB/BPBD is deemed the most suitable party to lead disaster management collaboration.	
Trust in Collaboration	Trust can be built well within the collaboration process, and the involvement of Reserved components can strengthen this trust.	
Openness of Information in Collaboration	Face-to-face dialogue becomes crucial for understanding the openness of information regarding disasters and disaster management.	
	This dialogue also needs to involve Reserved components personnel if they are involved in disaster management.	
Commitment of Media Stakeholders	The commitment of the media is to continue supporting and promoting disaster management collaboration to be more effective and help educate the public about disaster mitigation.	
Understanding the Goals of Collaboration	Stakeholders have a sufficient understanding of the objectives of disaster management collaboration. This understanding should also be possessed by *Reserved component* personnel if they are involved.	
Measurement of Collaboration Achievement	Interim results are crucial to assessing the extent of achievement in disaster management collaboration. These interim results also serve as benchmarks for Reserved components personnel if they are involved.	

Source: primary data processed (year 2024).

Table 6: Strengths and Weaknesses of the Pentahelix Collaboration Model.

Strengths	Weaknesses
Inclusive participation from various actors, including academia, businesses, communities, government, and the Media	Lack of coordination and communication among actors
Transparency in the collaboration process and budget utilization	Limited resources in the field.
Clear leadership from *BNPB* and *BPBD*	inadequate understanding of the roles and responsibilities of each actor.
Commitment from stakeholders to strengthen disaster resilience	Suboptimal involvement of Reserved components personnel.

Source: primary data processed (year 2024).

network that enhance information processing and advocacy for member needs (Wiechman et al. 2024).

b. Enhancing resource capacity

Enhancing resource capacity in the field through training and the provision of adequate equipment. This is in line with Gundran et al.'s (2023) opinion that to improve disaster training, it is necessary to introduce various topics and scenarios, as well as implement modern technology.

c. Clarifying the roles and responsibilities of actors

Clarifying the roles and responsibilities of each actor in the collaboration document. According to Sentanu et al. (2021), the five actors in the Penta Helix concept should walk hand in hand and cooperate well, both as written in official documents such as job descriptions (tupoksi) and practically in the implementation of programs and activities.

d. Developing guidelines and regulations

Clear guidelines and regulations regarding the participation of Reserved components personnel in disaster management efforts need to be developed. The existence of military reserve components is a strategic step by the government to enhance national defense against threats in line with the strategic environmental dynamics in the 21st century. Therefore, military reserve components need to have a strong constitutional basis in accordance with the mandate of the National Defense Law (Roringkon & Saputro 2021), especially in carrying out their roles in disaster management.

By addressing the weaknesses and implementing the suggestions above, it is hoped that the pentahelix collaboration model in Malang Regency can become an effective model for enhancing disaster resilience in the region. As highlighted by Kurniadi et al. (2023), the synergistic effect of the pentahelix can enhance community resilience, meaning that the pentahelix collaboration model involving reserve component personnel can contribute to disaster resilience.

Contribution of Each Actor

The Penta helix collaboration model in Malang Regency involves five main actors: academia, business, community, government, and Media. Each actor has unique roles, resources, and constraints in contributing to disaster management.

a. Academia

The contribution of academia as reserve component personnel to disaster resilience includes:

- Providing knowledge and concepts for developing effective and sustainable disaster management programs.
- Conducting research and community service to help enhance disaster resilience in Malang Regency.
- Offering training and education to the community on disaster mitigation.

b. Business

The contribution of businesses, such as PT. Pindad, as reserve component personnel in disaster resilience, involves three main points:

- Providing CSR assistance to support disaster management activities.
- Assisting in the distribution of aid and logistics.
- Providing training and education to employees on disaster response.

c. Community

The contribution of community actors, such as volunteers from the East Java Humanitarian Network, as reserve component personnel in disaster resilience includes:

- Actively participating in mitigation, emergency response, and post-disaster rehabilitation activities.
- Providing assistance and support to disaster victims.
- Raising awareness among the community about the importance of disaster preparedness.

d. Government

The contribution of government actors, including the Directorate General of Defense Potential of the Ministry of Defense of the Republic of Indonesia (*Ditjen Pothan Kemhan* RI), the Regional Disaster Management Agency (*BPBD*) of Malang Regency, and the Regency Military Command (*Kodim*) of Malang Regency, as reserve component personnel in disaster resilience, includes:

- Formulating policies, regulations, and coordination to ensure the effectiveness of disaster management programs.
- Providing resources and infrastructure necessary for disaster management activities.
- Leading and coordinating collaboration among actors in disaster management.

e. Media

The contribution of media actors, such as Radar Malang, as reserve component personnel in disaster resilience includes:

- Disseminating information and education to the public about disaster risks, prevention measures, and emergency response.
- Assisting in raising public awareness about the importance of disaster preparedness.
- Monitoring and reporting on the development of disaster situations to the public.

The Penta helix collaboration in Malang Regency requires active contributions from all involved parties. By understanding the roles, resources, challenges, and obstacles of each actor, this collaboration can become an effective model for enhancing disaster resilience in the region (Subagyo et al. 2022).

Challenges and Barriers to Collaboration

The Penta helix collaboration model in Malang Regency, despite having considerable potential, still faces several challenges and barriers that need to be overcome to achieve optimal effectiveness. These challenges and barriers can be categorized into several aspects, namely:

a. Lack of coordination and communication among actors.
b. Limited resources in the field.
c. Lack of understanding of the roles and responsibilities of each actor.
d. Suboptimal involvement of Reserved components personnel.
e. Miscoordination and complex bureaucracy in aid distribution.
f. Insufficient training and education for Reserved components personnel and the community.
g. Lack of a clear legal framework regarding the involvement of Reserved components personnel.

The challenges and obstacles faced in the Penta helix collaboration in Malang Regency indicate that there is still ample room for improvement for this collaboration to achieve optimal effectiveness (Prajanti et al. 2023). Efforts to address these challenges and barriers need to be undertaken continuously and involve all relevant parties. By overcoming the existing challenges and barriers, it is hoped that the Penta helix collaboration in Malang Regency can become an effective model for enhancing disaster resilience in the region.

Efforts to Enhance Collaboration

Based on the analysis of the challenges and obstacles faced, here are several efforts that can be undertaken to enhance the effectiveness of Penta helix collaboration in Malang Regency:

a. Strengthen coordination and communication among actors through more effective collaborative forums.
b. Enhance resource capacity in the field through training and the provision of adequate equipment.
c. Clarify the roles and responsibilities of each actor in collaboration documents.
d. Develop clear guidelines and regulations regarding the involvement of Reserved components personnel in disaster management.
e. Increase training and education for Reserved components personnel and the community.
f. Build an effective and efficient coordination system involving Reserved components personnel.
g. Create job clusters to clarify the tasks and responsibilities of each actor.
h. Involve Reserved components personnel in face-to-face dialogues to enhance information transparency.
i. Measure the achievements of collaborative activities through interim outcomes for evaluation and future improvement.

Improving the effectiveness of pentahelix collaboration in Malang Regency requires comprehensive and sustainable efforts. These efforts need to focus on aspects such as coordination and communication, resource capacity, roles and responsibilities, guidelines and regulations, as well as training and education (Khorram-Manesh et al. 2016, Nugraha et al. 2023). By addressing the challenges and obstacles, it is hoped that Penta helix collaboration in Malang Regency can become an effective model for enhancing disaster resilience in the region.

The analysis of stakeholder engagement in the Penta helix for disaster resilience in Malang Regency covers three main stages: before, during, and after disasters. Before a disaster, academics conduct research to understand risks and develop mitigation strategies, as well as organize training and provide research-based policy inputs. The business sector contributes through CSR programs, employee training, and participation in collaboration forums. Communities are active in education, forming volunteer groups, and mapping local resources. The government develops regulations and policies, allocates budgets, and builds disaster-resistant infrastructure. Media plays a role in awareness campaigns, public education, and disaster risk monitoring.

During a disaster, academics provide technical support, conduct rapid disaster impact assessments, and help develop emergency response systems. The business sector provides logistical support, assists in aid distribution, and opens facilities to support emergency operations. Communities

carry out emergency response actions, provide social assistance, and manage evacuation centers. The government leads and coordinates all emergency response activities through the BPBD, provides emergency assistance, and maintains security in affected areas. The media provides up-to-date information, disseminates emergency response education, and reports urgent needs in the field.

After a disaster, academics evaluate disaster impacts, develop recovery programs, and provide technical assistance for community rehabilitation. The business sector supports reconstruction, aids economic recovery, and collaborates with the government and NGOs on rehabilitation projects. Communities engage in rehabilitation, provide psychosocial support, and enhance disaster preparedness capacity for the future. The government leads infrastructure reconstruction, provides financial aid, and improves policies based on experience. The media documents recovery efforts, disseminates information on the recovery process, and advocates for better policies and increased disaster response capacity. With active engagement from all stakeholders, disaster resilience in Malang Regency is expected to be enhanced at every stage.

Through active and collaborative engagement of all stakeholders via the Penta helix model, disaster resilience in Malang Regency is expected to be enhanced from pre-disaster to post-disaster stages. Sudarmanto et al. (2020) and Rozikin et al. (2023) indicate that the level of stakeholder engagement in community-based disaster resilience projects is crucial for the successful implementation of disaster management programs. Thus, this study provides an overview of the pentahelix collaboration model in disaster management in Malang Regency, identifying strengths, weaknesses, opportunities, and challenges. The findings of this research can serve as a basis for stakeholders in efforts to enhance collaboration effectiveness and strengthen disaster resilience at the local level.

CONCLUSIONS

The Penta helix collaboration model for engaging reserve component personnel in disaster resilience in Malang Regency offers a comprehensive approach. The analysis of this model demonstrates strengths in inclusive participation from various actors and transparency in the collaboration process. However, there are several weaknesses, such as a lack of coordination and communication among actors and limitations in resources in the field. To enhance its effectiveness, steps such as strengthening coordination, increasing resource capacity, and clarifying the roles of each actor are necessary. Every actor, ranging from academia, business, the community, the government, and

the media, plays a crucial role in this collaboration model. However, challenges include insufficient coordination and communication, resource limitations, and a lack of understanding of actor roles. To address these, efforts to strengthen coordination, enhance capacity, and clarify the roles of each actor are needed.

Several recommendations have been identified to enhance this collaboration, such as strengthening coordination and communication among actors, enhancing training and education, and developing clear guidelines and regulations regarding the involvement of reserve component personnel. With the implementation of these recommendations, it is hoped that the Penta helix collaboration model can become more effective and make a significant contribution to disaster management in Malang Regency.

ACKNOWLEDGMENT

REFERENCES

Alfajri, A., Setiawan, A. and Wahyudi, H., 2019. Synergy of regional defense spatial planning in facing non-military threats in Indonesia. *Global Strategies*, 13(1), pp.103-122. https://doi.org/10.20473/jgs.13.1.2019.103-122

Anggadwita, G., Mulyaningsih, H.D., Ramadani, V. and Arwiyah, M.Y., 2015. Women entrepreneurship in Islamic perspective: A driver for social change. *International Journal of Business and Globalisation*, 15(3), pp.389-404. https://doi.org/10.1504/IJBG.2015.071914

BNPB, 2021. IRBI; Indonesian disaster risk index. *Center for Data, Information, and Communication of the National Disaster Management Agency*.

BNPB, 2024. Summary of Disasters in 2024. Retrieved from https://gis.bnpb.go.id/arcgis/apps/sites/#/public/pages/bencana-besar-tahun-2024

BPBD, 2020. *Book of Output and Discussion Training Materials and Disaster Mitigation, Sharpness of Disaster Management Analysis by the Humanitarian Network, East Java*. BPBD.

Djuyandi, Y. and Hendradjaja, D., 2021. Military operation other than war (MOOTW): Military and civilian synergy to support the Citarum River revitalization program. *Turkish Journal of Computer and Mathematics Education (TURCOMAT)*, 12(7), pp.2122-2129.

Gundran, C.P.D., Lam, H.Y., Tuazon, A.C.A., Cleofas, J.V., Garcia, F.B. and Puli, T.E.M., 2023. Simulation training needs assessment for disaster preparedness and disaster response among selected agencies in the National Capital Region, Philippines. *International Journal of Disaster Risk Reduction*, 94, pp.103824. https://doi.org/10.1016/j.ijdrr.2023.103824

Hamna, H., Hidayat, S., BK, M.K.U., Rahmawati, K.R., Rivani, R., Nurmasayu, A. and Yago, R., 2024. Utilization of waste paper as teaching media for volcano eruption simulation in improving student knowledge. *Journal of Community Service and Empowerment*, 5(1), pp.73-84. https://doi.org/10.22219/jcse.v5i1.31122

Hidayat, F., 2022. The urgency of the civil servant recruitment policy in the reserve component. *Government Policy Journal*, 72, pp.29-38. https://doi.org/10.33701/jkp.v5i1.2217

Hussain, M., Tayyab, M., Ullah, K., Ullah, S., Rahman, Z.U., Zhang, J. and Al-Shaibah, B., 2023. Development of a new integrated flood resilience model using machine learning with GIS-based multi-criteria decision analysis. *Urban Climate*, 50, pp.101589. https://doi.org/10.1016/j.uclim.2023.101589

Imperiale, A. and Vanclay, F., 2021a. Conceptualizing community resilience and the social dimensions of risk to overcome barriers to disaster risk reduction and sustainable development. *Sustainable Development*, 29(5), pp.891–905. https://doi.org/10.1002/sd.2182

Imperiale, A.J. and Vanclay, F., 2024. Re⬚designing social impact assessment to enhance community resilience for disaster risk reduction, climate action and sustainable development. *Sustainable Development*, 32(2), pp.1571-1587. https://doi.org/10.1002/sd.2690

Indrawan, R.M.J. and Efriza, E., 2018. Membangun komponen cadangan berbasis kemampuan bela negara sebagai kekuatan pertahanan Indonesia menghadapi ancaman nir-militer. *Jurnal Pertahanan dan Bela Negara*, 8(2), pp.21-40. https://doi.org/10.33172/jpbh.v8i2.395

Khorram-Manesh, A., Lupesco, O., Friedl, T., Arnim, G., Kaptan, K., Djalali, A.R. and James, J., 2016. Education in disaster management: what do we offer and what do we need? Proposing a new global program. *Disaster Medicine and Public Health Preparedness*, 10(6), pp.854-873. https://doi.org/10.1017/dmp.2016.88

Kurniadi, A., Syamsunasir, S. and Widana, I.D.K.K., 2023. Pentahelix synergy in post-tsunami disaster recovery to support community resilience in facing disaster in Pandeglang Regency. *Technium Social Sciences Journal*, 42(1), pp.133–147. https://doi.org/10.47577/tssj.v42i1.8624

Kusumajanti, K., Widiastuti, N.P.E. and Kamaluddin, A., 2020. Strategies and role of local government in improving the competitiveness of traditional fishermen in Pandeglang, Banten. *Ekspresi dan Persepsi: Jurnal Ilmu Komunikasi*, 3(1), pp.12-21. https://doi.org/10.33822/.v3i1.1360

Martin, E., Nolte, I. and Vitolo, E., 2016. The four Cs of disaster partnering: Communication, cooperation, coordination, and collaboration. *Disasters*, 40(4), pp.621-643. https://doi.org/10.1111/disa.12173

Nugraha, Y.K. and Sumaryatiningsih, S., 2023. The Pentahelix model: Strengthening innovation potential and fostering science and education integration. *Journal of Islamic Education*, 8(1), pp.540-554.

Prajanti, S.D.W., Daud, D., Amin, S. and Adzim, F., 2023. A sustainable creative economy development model using a penta-helix approach based on local wisdom in Magelang City, Indonesia. *Vision for Sustainability*, 20, pp.239-275. https://doi.org/10.13135/2384-8677/7917

Rahayu, R.K., Damayanti, R. and Mahardika, M.G., 2024. Conceptualizing maritime-based decentralization toward better public service in the archipelagic region. *Jurnal Wacana Politik*, 9(1), p.941. https://doi.org/10.24198/jwp.v8i1.50941

Riwanto, A., 2017. Legal policy strategy for ocean governance to become the pivot of maritime world for establishing Indonesia's welfare. *Advanced Science Letters*, 23(10), pp.10016-10017. https://doi.org/10.1166/asl.2017.10372

Roringkon, D.L. and Saputro, G.E., 2021. Reservation component management to strengthen state defense to face threats. *Turkish Online Journal of Qualitative Inquiry*, 12(6), p.21.

Roringkon, D.L., Sarjito, A. and Saragih, H.J., 2022. Readiness of the capacity for the management of the land component reserve to strengthen the main components of the Indonesian National Army (TNI). *Manajemen Pertahanan: Jurnal Pemikiran dan Penelitian Manajemen Pertahanan*, 8(1), p.64.

Rozikin, P.M., Utami, W. and Kumalasari, K., 2023. Mosque-based disaster-resistant family improvement training in Sukopuro village, Malang Regency. *Asian Journal of Community Services*, 2(7), pp.573-578. https://doi.org/10.55927/ajcs.v2i7.5057

Sentanu, I.G.E.P.S., Galih, A.P. and Wismanu, R.E., 2021. The role of stakeholder. *International Journal on Public and Business Administration,* 31(7), pp.427-434. https://doi.org/10.2991/aebmr.k.210928.080

Subagyo, A., Handoko, R. and Wahyudi, H., 2022. Pentahelix policy management paradigm as a model for disaster management in Bojonegoro Regency East Java. *International Journal of Entrepreneurship and Business Development*, 5(4). https://doi.org/10.29138/ijebd.v5i4.1906

Sudarmanto, S., Paripurno, E.T. and Wahyuni, P., 2020. *The Role of Jangkar Kelud Community on Building Community Resilience Around Kelud Volcano, in Blitar, Kediri and Malang Regency, East Java Province, Indonesia*. AIP Publishing. https://doi.org/10.1063/5.0013231

Syamsuddin, M. 2024. BPBD Malang Regency maps disaster-prone areas. *Radio Republik Indonesia Journal*, 16, pp.11-21

Syamsunasir, M., Kurniadi, A. and Widana, I.D.K., 2023. Pentahelix synergy in post-tsunami disaster recovery to support community resilience in facing disaster in Pandeglang Regency. *Technium Society Science Journal*, 42, p.133. https://doi.org/10.47577/tssj.v42i1.8624

UN General Guidelines on Assisting Building Resilient Communities 2020. United Nations. Available at https://unsdg.un.org/sites/default/files/2021-09/UN-Resilience-Guidance-Final-Sept.pdf

Wesnawa, I.G.A. and Christiawan, P.I., 2014. *Geography of Disasters*. Graha Ilmu.

Wibowo, N.B. and Sembri, J.N., 2016. Analisis peak ground acceleration (PGA) dan intensitas gempabumi berdasarkan data gempabumi terasa tahun 1981-2014 di Kabupaten Bantul Yogyakarta. *Indonesian Journal of Applied Physics*, 6(01), pp.65. https://doi.org/10.13057/ijap.v6i01.1804

Wiechman, A., Alonso Vicario, S. and Koebele, E.A., 2024. The role of intermediate collaborative forums in polycentric environmental governance. *Journal of Public Administration Research and Theory*, 34(2), pp.196-210. https://doi.org/10.1093/jopart/muad017

Identification of *ars*B Genes in Metal Tolerant Bacterial Strains Isolated from Red Mud Pond of Utkal Alumina, Odisha, India

S. Panigrahi[1] (ID) **and D. P. Panigrahi[2]†**

[1]P.G. Department of Botany, Utkal University, Vani Vihar, Bhubaneswar-751004, Odisha, India
[2]P.G. Department of Botany, Government College Koraput, Dist. Koraput-764021, Odisha, India
†Corresponding author: D. P. Panigrahi; durga.panigrahi@gmail.com

ABSTRACT

Exploration of microbial flora in red mud ponds is a topic of economic importance. In this study, we report two bacterial strains isolated from red mud ponds of Utkal Alumina, Odisha India. These strains were identified to be *Brevundimonas* sp. and *Pseudomonas* sp. through 16S rDNA analysis which showed more than 99% similarities with their respective clades. The LD_{50} values showed metal resistance to As, Cr, Cu, and Pb in a range of 2-8 mM. Both the strains showed a high tolerance towards arsenic and lead but a low tolerance towards chromium and copper salts. The bioaccumulation of copper was found to be the maximum and that of arsenic was the minimum. To find out the underlying genetic mechanism of the metal tolerance, a degenerate PCR approach was made to find out the genes responsible for the metal efflux or transformation. Two putative *ars*B genes could be identified from these two strains. Phylogenetic analysis of deduced amino acid sequences showed similarities with the amino acid sequences of *ars*B genes of *Pseudomonas* strains and formed monophyletic clades with their *ars*B proteins. These strains thus harbor potential genetic mechanisms for metal tolerance. Determination of whole operons and their cloning is the future aspect of the study. Moreover, these bacterial strains have a high potential to accumulate copper and can be used in studies related to biomining of copper.

INTRODUCTION

Various macro and micro elements are necessary for the structural and functional maintenance of cells. Among elements, heavy metals are also important for the functioning of some enzymes. Heavy metals are those elements that have a density that exceeds $5g/cm^3$ (Ferguson 1990). Heavy metals are ubiquitously present on the earth's crust. Heavy metals like Ni, Mo, Fe, Zn, and Cu are essential in trace amounts, but Hg, Pb, As and Cr are not essentially required (WHO 1996). Moreover, these are included in carcinogen level 1 compounds. The sources of heavy metals are both natural and anthropogenic. Naturally, these elements come to the earth's surface through weathering and volcanic eruptions (Nriagu 1989, Bhattacharjee & Rosen 2007). Anthropogenic activities such as the use of agrochemicals, e-waste disposal, and rapid industrialization significantly contribute to heavy metal contaminations in the environment (Järup 2003). This increase in the level of heavy metal contamination has proportionally raised the toxicity level. The important heavy metals of concern are arsenic, cadmium, and chromium, which have been included in carcinogen level 1 (Beyersmann & Hartwig 2008). These heavy metals get circulated in the biosphere through the food chain (Morton & Dunnette 1994). These heavy metals are toxic in low concentrations. Their toxicity mainly affects the activities of vital enzymes. Organisms develop vivid mechanisms of resistance (Tchounwou et al. 2012). Many bacteria successfully inhabit the contaminated sites and develop tolerance or resistance mechanisms. Bacteria harbor many types of

genes to resist the toxicity of heavy metals which include, i. production of intracellular resistance ii. exporting to outside through an efflux system, iii) reduction to low toxic forms iv. Extracellular absorption and v. extracellular detoxification. Naturally, these bacteria develop many genetic systems to accomplish the detoxification task (Ianeva 2009, Bazzi et al. 2020).

Mines are depositories of heavy metals and thus become hotspots for resistant microbial diversity. Aluminium extraction in bauxite mines releases red mud or bauxite residue as waste which contains highly toxic heavy metals. The highly alkaline extraction process of alumina from bauxite through Bayer's process concentrates the heavy metals which are released along with red mud (Santini et al. 2915). The microbial diversity in bauxite residue, though low, possesses heavy metal resistance. These microbes which may be alkaliphilic or alkali tolerant portray various types of toxic metal resistance mechanisms. These mechanisms may be different from neutral contaminated sites (Trevors et al.1985, Hao et al. 2021).

In this study, heavy metal resistance in two Gram-negative bacteria is reported which were isolated from bauxite residues of Utkal Alumina, Odisha India. This alumina extraction company is one of the biggest alumina extraction companies in the world and produces 1.5 metric tons of alumina per year. Odisha contributes 71% of India's total aluminum production (Indian Bureau of Mines 2022). In these mines, bauxite residues are stored in large impervious ponds isolated from the external environment. Microbial study has not been reported from this red mud pond. The objectives of the present research are i.) isolation of heavy metal-resistant bacteria from the site and ii.) investigation of their resistance characteristics.

MATERIALS AND METHODS

Sample Collection

The red mud samples, from 15-20 cm depth, were collected from the red mud pond of Utkal Alumina situated in the Rayagada district of the state of Odisha, India (19.1831° N, 83.0269° E). They were kept in clean and sterile Polypropylene bags under ice packs.

Sample chemical analysis: The red mud samples were put in clean Petri dishes and dried in the oven at 70°C for 24 hours to determine the dry weight and moisture content. Sample pH was measured by suspending the samples in deionized water in a 1:2 (w/v) ratio. Elemental analysis was done following (Carrasco et al. 2005). Briefly, 1 gm dried sample was digested with 10 mL of nitric acid (65%) and 2 mL of H_2O_2 on a hotplate at 120°C. The digested samples were diluted up

to 100 mL by adding Mili 'Q' water and filtered through a 0.22-micron syringe filter. Heavy metal concentration in the soil was determined by Inductively Coupled Plasma-Optical Emission Spectrometry (ICP-OES, Perkin Elmer) facility present in Odisha University of Agriculture and Technology, Bhubaneswar, India.

Isolation of Bacterial strains: One gram of red mud was suspended in 100 mL of normal saline and diluted down to 10^{-6} dilutions. One ml from the last dilution was spread on Nutrient Agar (NA) medium (0.5% Tryptone, 0.3% Yeast Extract, 0.5 % NaCl, 1.6% Agar Powder) and incubated at 32°C. Colonies were observed for 3 days in 24 hours. Single colonies were streaked onto the NA medium several times to obtain pure cultures. Liquid culture of individual bacterial isolates was made in Nutrient Broth (0.5% Tryptone, 0.3% Yeast Extract, and 0.5 % NaCl).

Morphological and Biochemical Characterization of the Isolates

Gram staining, different carbon and nitrogen source utilization, catalase test, oxidase test, amylase, nitrate reduction test, H_2S production test, and methyl red test were done following Aneja (2009).

Heavy Metal Sensitivity Test

Heavy metal sensitivity test was performed by calculating Lethal Dose (LD_{50}). Heavy metals used in this study were Copper (as $CuSO_4.5H_2O$), Chromium (as Potassium dichromate; $K_2Cr_2O_7$), Arsenic (as sodium arsenate $Na_2HAsO_4. 7H_2O$), and lead (as lead acetate). The stock solutions of these heavy metals were prepared by dissolving the appropriate weight of the salts in Mili 'Q' water to get a 200 mM final concentration. The pH of the solutions was maintained at 7.

The LD_{50} values were calculated by growing the isolates in an NB medium supplemented with various concentrations of heavy metals (El-Deeb & Al-Sheri 2005). The percentages of bacterial growth under different heavy metal stress conditions were calculated with respect to the control set. The LD_{50} value was calculated from the linear graph obtained by plotting the percentages of bacterial growth against various metal concentrations.

Isolation of Genomic DNA and PCR Amplification of Target Sequences

Genomic DNA, from bacterial samples, was extracted using the guanidinium thiocyanate method following Cooper (2007). Quantification of DNA was done spectrophotometrically by recording absorbency at 260 nM and quality was checked by running 5μL of sample

Table 1: Primers used in the study.

Primer Name	Sequence	Desired band in bp	Reference
d*ars* C F d*ars* C R	5' -ATGACCGTCACCATHTAYCAYAAYC-3' 5' -CGACCGCCTCGCCRTCYTCYTT-3'	400	Sá Pereira et al. 2007
darsB F darsB R	5'-GGTGTGGAACATCGTCTGGAAYGCNAC-3' 5'-CAGGCCGTACACCACCAGRTACATNCC-3'	1000	Achour et al. 2007
dchrA F dchrA R	5'-CGAACAGCGCTTCCTGCAYGCNYTNAA-3' 5'-CGACGACGGCGGCNGTDATNGC-3'	960	Sá Pereira et al. 2009
dcoprunF dcoprunR	5'-GGSASDTACTGGTRBCAC-3' 5'-TGNGHCATCATSGTRTCRTT-3'	1000	Almitra et al. 2012
27 F 1492 R	5' AGAGTTTGATCMTGGCTCAG3' 5' TACGGYTACCTTGTTACGACTT3'	1500	Wilson et al.1990

through 2% agarose gel electrophoresis (Sambrook & Russel 2001).

Molecular identification of the bacterial samples was done by amplifying the 16S rDNA sequence. PCR reaction mixture (50 μL) consisted of 25μl of PCR Master mix (Aura Biotech, India), 0.4μM of primers each (27F and 1492R, Table 1), 50 ng template DNA, and water (remaining amount). The PCR reaction was performed in a thermocycler (Prima-96, HIMEDIA, Mumbai, India) with the following program: initial denaturation at 95°C for 3min., 30 cycles of denaturation at 95°C for 45 sec., annealing at 48°C for 1.30 min., elongation at 72°C for 1min., and a final extension at 72°C for 7 min. The PCR product was separated by electrophoresis using 2% agarose gel containing 1:10000 SYBR safe stain (HiSYBR Safe, HiMedia, Mumbai) for visualization.

Heavy metal-resistant genes were amplified using degenerate primers. The primers used in this study are given in Table 1. The 50 μL PCR mixture consisted of 25 μL of 2x PCR master mix (Aura Biotech, Chennai, India, 0.5 μM primers (forward and reverse each), 50 ng template DNA, and water (remaining amount). The PCR reaction was run using the following program, denaturation at 95°C for 2 min, 30 cycles of denaturation at 95°C for 45 sec, annealing at 44°C for 1 minute, elongation at 72°C for 1 minute, and a final extension at 72°C for 5min. The PCR products were separated by electrophoresis using a 2% agarose gel containing SYBR-safe DNA stain for visualization. The desired bands were cut and eluted using a DNA gel extraction kit (Genei, Bengaluru, India). The eluted DNA was again used as a template and reamplified using the same primers and PCR conditions.

DNA Sequencing and Bioinformatics Analysis

The desired bands were cut and purified through a Gel extraction kit (Genei, India). The purified samples were sequenced through a sequencing service provided by BioServe India Pvt. Ltd., India.

The 16 S rDNA sequences were received in .ab1 file format from the sequencing service. The obtained files,were checked in the Bio Edit version 7.2.5 software (Hall 1999). The sequences with low-quality peaks from both ends were trimmed. The residual sequences were subjected to BLASTN (Altschul et al. 1997) to find the most similar sequences which were subjected to multiple alignments using clustal W algorithms (Thompson et al. 1994). The alignment file was subjected to phylogenetic analysis in MEGA XI software (Tamura et al. 2021). The evolutionary distance matrix was calculated using the distance model (Jukes & Cantor 1969). The evolutionary tree was constructed using the neighbor-joining method (Saitou & Nei 1987) with bootstrap analysis based on 1000 resamplings.

Heavy metal resistance genes such as *chr*A, *coprun*F, *ars*C, and *ars*B genes were amplified using degenerate primers. The *ars*B gene sequences, obtained from sequencing service, were subjected to analysis through the Blast-X program (http://www.ncbi.nlm.nih.gov/BLAST). The protein sequences of the *ars*B gene were derived from the ORF Finder provided by NCBI (www.ncbi.nih.nlm.gov/ORFFINDER). The longest + sense ORF was chosen and subjected to the Blast X program to find similar proteins. The closest proteins and the query protein obtained from the ORF finder were chosen and subjected to multiple alignments by the MUSCLE algorithm (Edgar 2004). The distance matrix was calculated using the p-distance method. The Phylogenetic tree was done using the neighbor-joining method (Saitou & Nei 1987) with a bootstrap analysis based on 1000 resamplings using MEGA XI software (Tamura et al. 2021). Sequences obtained for other genes were also processed as mentioned.

Metal Uptake Assay

The metal bioaccumulation was assayed following a modified method of Carrasco et al. 2005. Each bacterial strain was grown in NB medium at 32°C to an absorbance (A_{620}) of 0.8. The sterile heavy metal stock solution was added to the growing culture to a final concentration of 100μM and

allowed for a further 12h. An aliquot of two mL of bacterial culture was taken, centrifuged and the pellet was washed with 1ml of mili 'Q' water to remove the excess medium. The residual pellet was dried and digested with 0.3 mL of concentrated HNO_3 at room temperature overnight. The mixture was incubated at 70°C for 30 min., cooled, and diluted up to 10 mL with mili 'Q' water. The heavy metal concentration was measured by ICP-OES, Perkin Elmer (OUAT, Bhubaneswar, India).

Statistical Data Analysis

Statistical analysis of all data was done using Microsoft Excel 2010. All the values are presented as mean ± standard deviation of three replicates. The significance difference between the means was calculated by the One Way Anova Test.

RESULTS AND DISCUSSION

The red mud samples were collected from the red mud pond of Utkal Alumina. The pH of the red mud samples was found to be 11.3±0.8. The water content was measured to be 74.87 ± 0.58 %. Concentrations of heavy metals chromium, copper, lead, and arsenic were found to be 234 mg/kg, 47.95mg/kg, 16.95mg/kg, and 8.35mg/kg, respectively.

Mines are natural depositories of heavy metals. Processing in Bauxite mines, copper mines, and gold mines releases heavy metals into the environment (Fashola et al. 2016, Kumari et al. 2015, Grafe et al. 2010) Red mud is the waste product obtained after alumina extraction from bauxite. This is highly alkaline and contains many heavy metals. The presence of Vanadium (1270 ppm) Chromium (615 ppm), and Arsenic (35 ppm) in substantial amounts

have been reported in red mud samples of alumina refinery processing, Daring Range, Western Australia (Grafe et al. 2010). Cr (36.6 ppm), As (3.76 ppm), Cu (24.1 ppm), and Pb (less than 0.038 ppm) have been reported in Indonesian red mud samples (Damayanti & Khareunnisa 2016). X-ray Absorption Spectroscopic analysis of red mud of Ajka bauxite mines, in Hungary, revealed the presence of arsenic in the form of arsenate at high alkaline pH (Lockwood et al. 2014)**.** The present study also reports a similar range of heavy metals in the red mud.

Bacterial Strain Isolation and Identification

Bacterial strains were isolated from the red mud samples by plating serially diluted samples on the NA medium. Colonies were observed on the plates in 24-48 hours after inoculation. Five different types of bacterial colonies could be distinguished and cultured further on the same medium. Out of five bacterial strains two bacterial strains were chosen for further studies based on their heavy metal tolerance ability (Fig. 1). The result of biochemical analysis is shown in Table 2. Both the strains could utilize

Fig. 1: Bacterial strains Brevundimonas sp. strain OURIIP3 (orange) and Pseudomonas sp. strain OURIIPT8 (white) isolated from red mud pond samples

Table 2: Characteristics of the bacteria.

Characteristics	Result	
	Brevundimonas sp. OURIIP3	*Pseudomonas* sp.OURIIP T8
Colony Characters	Round, small, convex. entire, smooth, opaque and orange	Round, small, convex. Entire, smooth and translucent
Gram reaction	Gram -ve	Gram -ve
Cell shape	Rod-shaped	Rod-shaped
Motility	+ve	+ve
Carbon source utilization		
+ve	Glucose, Dextrose, Fructose, Sucrose, Maltose, Mannitol, Starch Galactose, Lactose	Glucose, Dextrose, Fructose, Sucrose, Maltose, Mannitol, Starch
-ve	Citrate, Arabinose	Citrate, Arabinose, Lactose, Galactose
Nitrogen source utilization		
+ve	Lysine, Ornithine, Urea, Nitrate, Indole	Lysine, Ornithine, Urea, Nitrate, Indole
Other Biochemical tests		
+ve	Oxidase, Catalase, Methyl red, H_2S production, SIM	Oxidase, Catalase, Methyl red, H_2S production, SIM
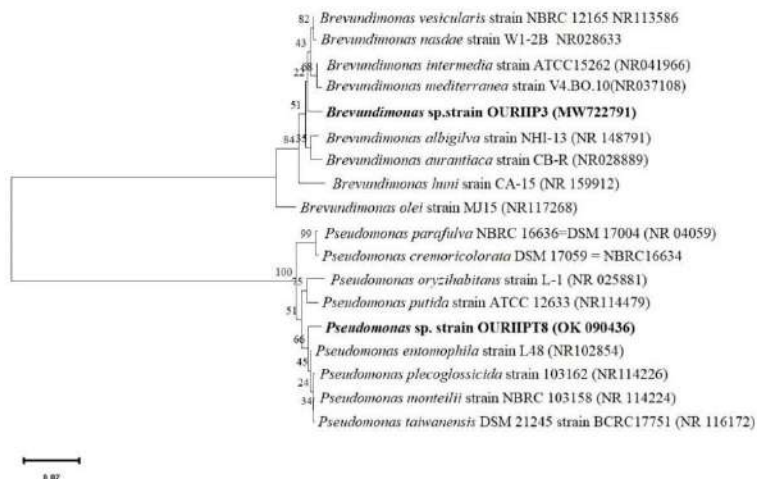
Fig. 2: Phylogenetic analysis of 16S rRNA genes of *Brevundimonas* sp. strain OURIIP3 and *Pseudomonas* sp. strain OURIIPT8. The distance matrix was calculated using the Jukes and Cantor model. The Phylogenetic tree was constructed using the neighbour joining method with a bootstrap analysis based on 1000 resamplings.

various carbohydrate and nitrogen sources provided in the culture but differ in utilization of Galactose and Lactose. Molecular analysis through 16S rDNA study revealed two different clades (Fig. 2). The isolate that formed a clade with *Brevundimonas* spp. showed a maximum 99.54% similarity with *B. vesicularis* NBRC12165 (accession No. NR113586). The isolate was named *Brevundimonas* sp. strain OURIIP3. Another isolate that formed a different clade with strains belongs to *Pseudomonas* sp. The isolate showed a maximum 99.01% similarity with *Pseudomonas plecoglossicida strain* 103162. The isolate was thus named *Pseudomonas* sp. strain OURIIPT8.

The harsh conditions like high alkalinity, temperature, and heavy metal toxicity, impact the growth of living organisms and make the red mud nearly barren. Very few microorganisms grow and adapt to the conditions. Studies of isolation of bacterial strains have not been studied extensively. However, Gram-positive bacterial strains generally outweigh in occurrence in such extreme conditions (Zampieri et al. 2019). One Gram-ve bacteria *Pseudomonas alcaliphila*, and nine Gram +ve bacteria belonging to genera *Bacillus*, *Agromyces*, *Chungangia*, *Kokuria*, *Microbacterium*, *Planococcus*, and *Salinococcus*, from red mud pond samples of National Aluminium Company Limited (NALCO) Damnjodi, Odisha, India (Krishna et al. 2014). Those bacteria are mostly alkali-tolerant than alkaliphilic. Isolation of 150 bacterial colonies belonging to *Bacillus*, *Lactobacillus*, and *Leuconostoc* genera, after the addition of glucose to the red mud samples, has been reported (Hamdy & Williams 2001). In the present study, out of five strains 2 strains were Gram -ve and the other 3 were Gram +ve bacterial isolates. The presence of heavy metals forces the strains to develop heavy metal tolerance and resistance in due course of time (Lottermoser 2010). Earlier the *Brevundimonas* sp. OURIIP3 strain has been reported to be an orange pigment-producing bacterium isolated from red mud samples of Utkal Alumina (Panigrahi & Panigrahi 2023).

Heavy Metal Tolerance Test and LD$_{50}$ Determination

The strains were grown in nutrient broth containing various concentrations of heavy metals to study the heavy metal tolerance. The result is presented in Fig. 3. The strain *Brevundimonas* sp. OURIIP3 showed an LD$_{50}$ value of 5.93mM, 6.64mM, 3.18mM, and 2.49mM for As, Pb, Cr, and Cu, respectively. *Pseudomonas* strain showed an LD$_{50}$ value of 8.19mM, 7.82mM, 5.43mM, and 4.71mM, respectively for As, Pb, Cr, and Cu. *Pseudomonas* sp. OURIIPT8 is more tolerant to different heavy metals than *Brevundimonas* sp. strain OURIIP3. Overall, the strains show a high tolerance to arsenic and the least tolerance to copper.

Phylogenetics of Putative Genes Through Degenerate PCR Approach

The presence of metal resistance genes was detected through PCR amplification using degenerate primers. Four degenerate primers were used for the identification of arsenic, chromium, and copper resistance genes. Desired bands of approximately 400 bp for *ars*C and 1kb each for *ars*B, *chr*B, and *cop*A could be amplified (Fig. 4). Sequencing of the amplified products and bioinformatics analysis was done. Only *ars*B sequences from both the isolates matched with other *ars*B sequences in Blast X analysis. Other sequences did not match with their corresponding genes. The *ars*B sequences were further
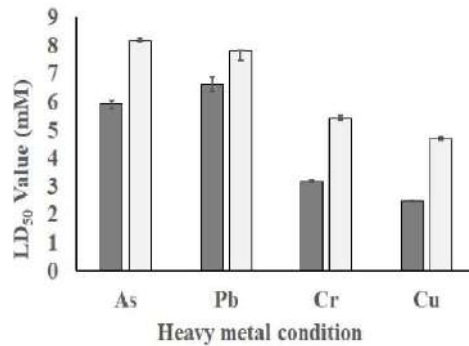
Fig. 3: Resistance of bacterial strains *Brevundimonas* sp. strain OURIIP3 and *Pseudomonas* sp. strain OURIIPT8 to different heavy metals by measuring Lethal Dose (LD50) values of As, Pb, Cr, and Cu shown by the strains in liquid culture
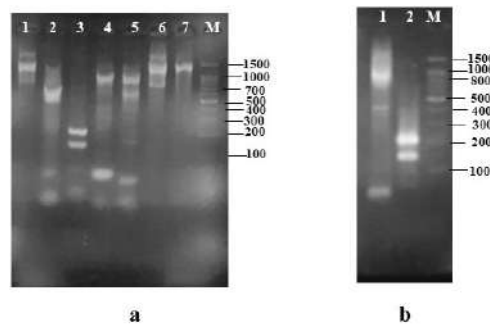
Fig. 4: Amplification of heavy metal resistant genes from genomic DNA isolated from *Pseudomonas* sp. strain OURIIPT8 and *Brevundimonas* sp. strain OURIIP3.**(a)** Lane 1, 2, 3, 4 amplification product of *ars*B, *chr*B, *ars*C and *cop*A, respectively from *Pseudomonas* sp. strain OURIIPT8; Lane 5, 6, 7 amplification product of *chr*B, *ars*B *cop*A, respectively from *Brevundimonas* sp. strain OURIIP3, L: DNA Ladder (100bp); **(b)** Lane 1 and 2 amplification product of *ars*B and *ars*C, respectively from *Brevundimonas* sp. strain OURIIP3.

subjected to find Open Reading Frames (ORFs) using NCBI ORF Finder. The sequence obtained from *Brevundimonas* sp. OURIIP3 (NCBI Acc. No. ON243663) could display 15 potential ORFs. The + sense ORF 8 with start at position 3 and end at position 698 showed similarities to arsenic transport proteins. The ORF was submitted to NCBI under the accession number ON243663. The deduced amino acid sequence from the ORF showed 95.45% similarities with the arsenic transporter protein of *Pseudomonas reactans*. Phylogenetically, the amino acid sequence formed a clade with the arsenic transporter gene of *Pseudomonas putida* strain with a bootstrap value of 71 (Fig. 5). Similarly, the full sequence (769 nucleotides) obtained from *Pseudomonas* sp. OURIIPT8 showed 23 ORFs. The ORF 10 with start at 90 and stop at 575 nucleotide position (NCBI Accession No. ON243664) was subjected to Blast X. The deduced amino acid sequences showed maximum similarity of 72.54% with arsenic transporter of *Pseudomonas putida*. Phylogenetically, the sequence formed a clade with arsenic transporter proteins of various species of *Pseudomonas* with a bootstrap value of 84 (Fig. 5).

Mine wastes such as red mud are unwanted by-products left after the extraction of aluminum through Bayer's process. Every industrially developed country adds mine wastes to the environment and thus faces the menace of heavy metal contamination (Hudson et al. 2011). Very few microorganisms colonize and inhabit the area and develop tolerance to high concentrations of heavy metals. These microbes harbor many operons to combat the heavy metal concentration (Newsome & Falagán 2021). Arsenic is a ubiquitous pollutant. Though it is a metalloid, its cytotoxicity resembles heavy metals. Bacteria have *ars* operons for arsenic resistance. The *ars*B is a gene that effluxs arsenite from the cell and *ars*C converts arsenate to arsenite. The simple *ars* operon is a three gene operon, *ars*RBC operon, found in *E. coli* (Carlin et al. 1995), *Pseudomonas aeruginosa* (Cai et al. 1998) and P. *fluorescens* (Prithivirajsingh 2001). In this study, the *ars*B gene could be amplified and sequenced. The sequences from *Brevundimonas* sp. OURIIP3 and *Pseudomonas* sp. strain OURIIPT8 are similar to *Pseudomonas reactans* and *Pseudomonas putida*, respectively. The similarities in sequences may be due to horizontal gene transfer. A high

Fig. 5: Phylogenetic analysis of deduced amino acid sequences of *ars*B genes from *Brevundimonas* sp. strain OURIIP3 and *Pseudomonas* sp. strain OURIIPT8. The distance matrix was calculated using the p-distance method. The Phylogenetic tree was constructed using the neighbor-joining method with a bootstrap analysis based on 1000 resamplings
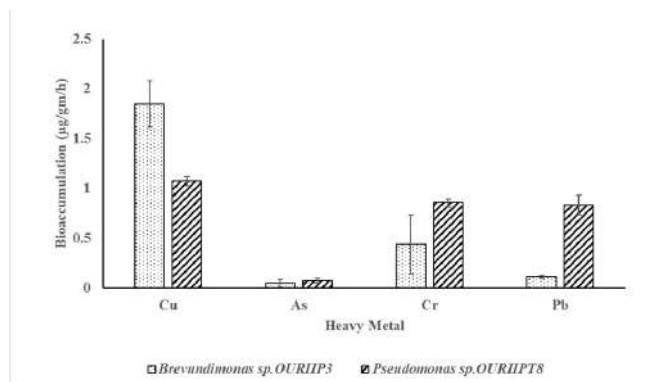
Fig. 6: Bioaccumulation of heavy metals by *Brevundimonas* sp. strain OURIIP3 and *Pseudomonas* sp. strain OURIIPT8.

As-tolerant *Brevundimonas aurantiaca* PFAB1 has been isolated from a hot spring in West Bengal, India (Banerjee et al. 2021). Soto et al., have reported *Brevundimonas* sp. B10 from Puchuncavi Valley, Central Chile, showed tolerance to arsenate up to 6000 mgL^{-1}.

The draft genome sequence of the *Brevundimonas* sp. B10 indicates the presence of two *ars* operons; one *ars* RBCH type and another *ars*RCH(ACR3) type. This suggests the presence of a vivid arsenic resistance mechanism in *Brevundimonas*. The *ars*B gene is widespread in the Pseudomonads as evident from NCBI database search. More than 29000 *ars*B entries can be found in the NCBI database. Many authors have also reported metal resistance by *Pseudomonas* spp. Raza et al. (2006) have isolated and characterized a multi-metal resistant (Cd, Cr, Ni, Pb) *Pseudomonas* sp. from industrial effluents of an oil mill. Pallanivel et al. 2020 have isolated *Pseudomonas stutzeri* LA3 strain from copper mines and

reported 50% bioaccumulations of copper at 50 mg l^{-1} of concentration. Naz et al. 2016 reported a *Pseudomonas* sp., isolated from the sugar industry, that can reduce 37% lead, 29% copper, and 32% chromium from the medium. Kumari et al. 2015 reported the isolation of six groups of bacteria belonging to *Bacillus*, *Pseudomonas*, *Acidothiobacillus*, and *Kocuria* sp. from acidic copper mines in China which showed metal resistances to six heavy metals such as Cu, Cr, Pb, Cd, Sb, and Ni. Altimira et al. 2012 (23) have reported 92 bacterial isolates from copper-polluted sites of Central Chile and found 6 highly tolerant isolates belonging to the genera *Sphingomonas*, *Stenotrophomonas,* and *Arthrobacter* show high resistance to copper. They have also reported the presence of the *cop*A gene in plasmids. It is thus evident that multi-resistant bacterial strains develop many mechanisms towards heavy metals and contribute to the cycling of the elements. The detection of *ars*B genes in the present study

indicates the presence of a functional arsenic efflux system in the bacterial strains. It also explains the high resistance of these strains to arsenic. The *cop*A and *chr*B genes could not be detected with the present degenerate primer sets. The operons can be detected by designing new degenerate primers.

Metal Uptake by Strains

Metal uptake assay was performed to study the amount of particular heavy metal accumulated by the strains. The results of bioaccumulation of heavy metals, presented as µg/gm/hr, are shown in Fig. 6. Copper accumulation was the highest in all three strains as compared to other metals. The strain *Pseudomonas* sp. OURIIPT8 shows more As, Cr, and Pb accumulation per hour. The *Brevundimonas* strain OURIIP3 accumulates the least amount of arsenic. The least amount of arsenic bioaccumulation may be attributed to the presence of an active arsenic efflux system in the strains.

CONCLUSION

In this study, the isolation of two multi-metal resistant bacteria belonging to the genera *Pseudomonas* and *Brevundimonas* is reported. They show resistance to Cr, Cu, As, and Pb. Both the strains show the presence of putative *ars*B genes and the functioning of an effective arsenic efflux system which results in high arsenic resistance and less bioaccumulation of arsenic inside them. Copper accumulation is more in all the strains than other metals. These results indicate that the strains can be used in bioremediation studies.

ACKNOWLEDGEMENTS

REFERENCES

Altimira, F., Yáñez, C., Bravo, G., González, M., Rojas, L.A. and Seeger, M., 2012. Characterization of copper-resistant bacteria and bacterial communities from copper-polluted agricultural soils of central Chile. *BMC Microbiology*, 12, p.193. https://doi.org/10.1186/1471-2180-12-193

Altschul, S.F., Madden, T.L., Schäffer, A.A., Zhang, J., Zhang, Z., Miller, W. and Lipman, D.J., 1997. Gapped BLAST and PSI-BLAST: a new generation of protein database search programs. *Nucleic Acids Research*, 25, pp.3389-3402.

Aneja, K., 2009. *Experiments in Microbiology, Plant Pathology, and Biotechnology*. New Delhi: New Age International (P) LTD., pp.245-295.

Banerjee, A., Sarkar, S., Gorai, S., Kabiraj, A. and Bandopadhyay, R., 2021. High arsenic tolerance in Brevundimonas aurantiaca PFAB1 from an arsenic-rich Indian hot spring. *Electronic Journal of Biotechnology*, 53, pp.1-7.

Bazzi, W., Abou F., Antoine G., Nasser, A., Haraoui, L.P., Dewachi, O., Abou-Sitta, G., Nguyen, V.K., Abara, A., Karah, N., Landecker, H., Knapp, C., McEvoy, M. M., Zaman, M. H. and Higgins, P. G., Matar and Ghassan, M. 2020. Heavy metal toxicity in armed conflicts potentiates AMR in *A. baumannii* by electing for antibiotic and heavy metal co-resistance mechanisms. *Frontiers in Microbiology*, 11, p.68. doi: 10.3389/fmicb.2020.00068

Beyersmann, D. and Hartwig, A., 2008. Carcinogenic metal compounds: recent insight into molecular and cellular mechanisms. *Archives of Toxicology*, 82(8), pp.493-512.

Bhattacharjee, H. and Rosen, B.P., 2007. Arsenic metabolism in prokaryotic and eukaryotic microbes. *Microbiology Monographs*, 6, pp.371-406.

Cai, J., Salmon, K. and DuBow, M.S., 1998. A chromosomal ars operon homologue of *Pseudomonas aeruginosa* confers increased resistance to arsenic and antimony in *Escherichia coli*. *Microbiology*, 144, pp.2705-2713. doi: 10.1099/00221287-144-10-2705

Carlin, A., Shi, W., Dey, S. and Rosen, B.P., 1995. The ars operon of *Escherichia coli* confers arsenical and antimonial resistance. *Journal of Bacteriology*, 177, pp.981-986. doi: 10.1128/jb.177.4.981-986.1995

Carrasco, A., Armario, P., Pajuelom, E., Burgosm, A., Caviedes, L.R., Chamber, A.M. and Palomares, A., 2005. Isolation and characterization of symbiotically effective Rhizobium resistant to arsenic and heavy metals after the toxic spills at the Aznalcòllar pyrite mines. *Journal of Soil Biology and Biochemistry*, 37, pp.1131-1140.

Cooper, J., 2007. Early interactions between legumes and rhizobia: disclosing complexity in a molecular dialogue. *Journal of Applied Microbiology*, 103, pp.1355-1365.

Damayanti, R. and Khareunnisa, H., 2016. Composition and Characteristics of Red mud: A case study on Tayan Bauxite residue from Alumina Processing plant at West Kalimantan. *Indonesian Mining Journal*, 19(3), pp.179-190.

Edgar, R.C., 2004. MUSCLE: multiple sequence alignment with high accuracy and high throughput. *Nucleic Acids Research*, 32(5), pp.1792-1797. doi: 10.1093/nar/gkh340

El-Deeb, S. and Al-Sheri, F., 2005. Role of some chemical compounds on the detoxification of *Rhizobium leguminosarum* biovar *viciae* by some heavy metals. *Pakistan Journal of Biological Sciences*, 8(12), pp.1693-1698.

Fashola, M.O., Ngole-Jeme, V.M. and Babalola, O.O., 2016. Heavy Metal Pollution from Gold Mines: Environmental Effects and Bacterial Strategies for Resistance. *International Journal of Environmental Research and Public Health*, 13(11), p.1047. doi: 10.3390/ijerph13111047

Ferguson, J.E., 1990. *The Heavy Elements, In: Chemistry, Environmental Impact and Health Effects*. Oxford: Pergamon Press., pp.211-212.

Grafe, M., Landers, M., Tappero, R., Klauber, C., Hutomo, G., Bee, G., Grabsch, A., Austin, P. and Davies, I., 2010. Chemistry of trace and heavy metals in bauxite residues (bauxite residue) from Western Australia. In: Gilkes, R. and Prakongkep, N. (eds.) *19th World Congress of Soil Science, Soil Solutions for a Changing World*. Brisbane, Australia: International Union of Soil Sciences, pp.39-42.

Hall, T.A., 1999. BioEdit: a user-friendly biological sequence alignment editor and analysis program for Windows 95/98/NT. *Nucleic Acids Symposium Series*, 41, pp.95-98.

Hamdy, M.K. and Williams, F.S., 2001. Bacterial amelioration of bauxite residue waste of industrial alumina plants. *Journal of Industrial Microbiology and Biotechnology*, 27, pp.228-233.

Hao, X., Zhu, J., Rensing, C., Liu, Y., Gao, S., Chen, W., Huang, Q. and Liu, Y.R., 2021. Recent advances in exploring the heavy metal (loid) resistant microbiome. *Computational and structural biotechnology journal*, 19, pp.94-109.

Hudson-Edwards, K.A., Jamieson, H.E. and Lottermoser, B.G., 2011. Mine wastes: Past, present, future. *Elements*, 7, pp.375-380. https://doi.org/10.2113/gselements.7.6.375

Ianeva, O.D., 2009. Mechanisms of bacteria resistance to heavy metals. *Microbiological Journal*, 71(6), pp.54-65.

Indian Bureau of Mines, 2022. Indian mineral industry & national economy. In: *Indian Minerals Year Book 2020- Part I*.

Järup, L., 2003. Hazards of heavy metal contamination. *British Medical Bulletin*, 68, pp.167-182.

Jukes, T. and Cantor, C.R., 1969. Evolution of protein molecules in mammalian protein metabolism. In: Munro, H.N. (ed.) *New York, Academic Press*, pp.21-132.

Krishna, P., Basu, A. and Reddy, M., 2014. Bacterial diversity of extremely alkaline bauxite residue site of alumina industrial plant using culturable bacteria and residue 16S rRNA gene clones. *Extremophiles*, 18(4), pp.665-676.

Kumari, D., Pan, X., Achal, V., Zhang, D., Al-Misned, F.A. and Mortuza, M.G., 2015. Multiple metal resistant bacteria and fungi from acidic copper mine tailings of Xinjing, China. *Environmental Earth Sciences*, 74(4), pp.3113-3121.

Lockwood, C.L., Mortimer, R.J.G., Stewart, D.I., Mayes, W.M., Peacock, C.L., Polya, D.A., Lythgoe, P.R., Lehoux, A.P, Gruiz,K. and Burke, I.T, 2014. Mobilisation of arsenic from bauxite residue (red mud) affected soils: effect of pH and redox conditions. *Applied Geochemistry*, 51, pp.268-277.

Lottermoser, B., 2010. *Mine wastes: Characterization, treatment and environmental impacts* (3rd ed.). Springer-Verlag.

Morton, W.E. and Dunnette, D.A., 1994. Health effects of environmental arsenic. In: Nriagu, J.O., ed. *Arsenic in the Environment Part II: Human Health and Ecosystem Effects*. New York: John Wiley & Sons, Inc., pp.17-34.

Naz, T., Khan, M.D., Ahmed, I., Rehman, S.U., Rha, E.S., Malook, I. and Jamil, M., 2016. Biosorption of heavy metals by *Pseudomonas* species isolated from sugar industry. *Toxicology and Industrial Health*, 32(9), pp.1619-1627. doi: 10.1177/0748233715569900.

Newsome, L. and Falagán, C., 2021. The Microbiology of Metal Mine Waste: Bioremediation Applications and Implications for Planetary Health. *GeoHealth*, 5(10), p.e2020GH000380. https://doi.org/10.1029/2020

Nriagu, J.O., 1989. A global assessment of natural sources of atmospheric trace metals. *Nature*, 338, pp.47-49.

Pallanivel, T.M., Sivakumar, N., Al-Ansari, A. and Victor, R., 2020. Bioremediation of copper by active cells of *Pseudomonas stutzeri* LA3 isolated from an abandoned copper mine soil. *Journal of Environmental Management*, 253, 109706.

Panigrahi, S. and Panigrahi, D.P., 2023. Characterization of a pigmented *Brevundimonas* sp. Isolated from red mud pond samples of a bauxite mine. *Journal of Environmental Biology*, 44, pp.359-366. https://doi.org/10.22438/jeb/44/3/MRN-5023.

Prithivirajsingh, S., Mishra, S.K. and Mahadevan, A., 2001. Detection and analysis of chromosomal arsenic resistance in *Pseudomonas fluorescens* strain MSP3. *Biochemical and Biophysical Research Communications*, 280, pp.1393-1401. doi: 10.1006/bbrc.2001.4287.

Raza, C.E., Anbazhagan, K. and Selvam, G.S., 2006. Isolation and Characterization of a metal-resistant *Pseudomonas aeruginosa* strain. *World Journal of Microbiology and Biotechnology*, 22, pp.577-585. https://doi.org/10.1007/s11274-005-9074-4.

Rojas, L.A., Yánez, C., González, M., Lobos, S., Smalla, K. and Seeger, M., 2011. Characterization of the metabolically modified heavy metal resistant *Cupriavidus metallidurans* strain MSR33 generated for mercury bioremediation. *PLOS One*, 14, e17555.

Saitou, N. and Nei, M., 1987. The neighbour-joining method: a new method for reconstructing phylogenetic trees. *Molecular Biology and Evolution*, 4, pp.406-425.

Sambrook, J. and Russel, D.W., 2001. *Molecular cloning - A laboratory Manual*. 3rd ed. Cold Spring Harbor, NY: Cold Spring Harbor Laboratory Press.

Santini, T.C., Kerr, J.L. and Warren, L.A., 2015. Microbially-driven strategies for bioremediation of bauxite residue. *Journal of Hazardous Materials*, 293, pp.131-157.

Sá-Pereira, P., Rodrigues, M., Videira e Castro, I. and Simões, F., 2007. Identification of an arsenic resistance mechanism in rhizobial strains. *World Journal of Microbiology and Biotechnology*, 23, pp.1351-1356.

Soto, J., Charles, T.C., Lynch, M.D., Larama, G., Herrera, H. and Arriagada, C., 2021. Genome sequence of Brevundimonas sp., an arsenic resistant soil bacterium. *Diversity*, 13(8), p.344. doi: 10.3390/d13080344.

Tamura, K., Stecher, G. and Kumar, S., 2021. MEGA 11: Molecular Evolutionary Genetics Analysis Version 11. *Molecular Biology and Evolution*, 38(7), pp.3022-3027. https://doi.org/10.1093/molbev/msab120.

Tchounwou, P.B., Yedjou, C.G., Patolla, A.K. and Sutton, D.J., 2012. Heavy metals toxicity and the environment. *EXS Supplementum*, 101, pp.133-164. doi: 10.1007/978-3-7643-8340-4_6.

Thompson, J.D., Higgins, D.G. and Gibson, T.J., 1994. CLUSTAL W: improving the sensitivity of progressive multiple sequence alignment through sequence weighting, position-specific gap penalties and weight matrix choice. *Nucleic Acids Research*, 22(22), pp.4673-4680. doi:10.1093/nar/22.22.4673.

Trevors, J.T., Oddie, K.M. and Belliveau, B.H., 1985. Metal Resistance in Bacteria. *FEMS Microbiology Letters*, 32, pp.39-54.

Wilson, K.H., Blatchington, R.B. and Green, R.C., 1990. Amplification of bacterial 16S ribosomal DNA with polymerase chain reaction. *Journal of Clinical Microbiology*, 28(9), pp.1942-1946.

World Health Organization, International Atomic Energy Agency & Food and Agriculture Organization of the United Nations, 1996. *Trace elements in human nutrition and health*. Geneva: World Health Organization. https://apps.who.int/iris/handle/10665/37931.

Zampieri, B.D., Nogueira, E.W., Quaglio, O.A. and Gunther, B., 2019. Overview of Known Alkaliphilic Bacteria from Bauxite Residue. *Journal of Mining and Mechanical Engineering*, 1(2), pp.41-50.

Assessment of ^{40}K and Heavy Metal Levels in Euphrates River of Al-Qadisiyah Governorate

S. K. Ibrahiem[1,2†] and H. A. Walli[1]

[1]Department of Environment, College of Science, University of Al-Qadisiyah, Diwaniyah, Iraq

[2]Ministry of Environment, Middle Euphrates Department, Al-Qadisiyah Environment Directorate, Diwaniyah, Iraq

†Corresponding author: S. K. Ibrahiem; Sci.env.mas22.10@qu.edu.iq

ABSTRACT

The objective of the current research is to measure the specific activity of ^{40}K and heavy metals in the water samples collected from the Al-Diwaniyah River in Al-Qadisiyah Governorate, Iraq. The activity of ^{40}K in water samples was ascertained using High Purity Germanium Spectrometer (HPGe) detector technology, which is based on a high-resolution gamma spectrometry system, and by using an atomic absorption spectrometer (A.A.S.) to determine the heavy metals of Ni, Cd and Pb, as well as measure some of the physical properties of water samples. The results indicated the concentration of ^{40}K in the water was presented in different concentrations. The lowest value was 2.6±0.5 Bq/L Al-Muhanawiyah, while the highest value was in Al-Diwaniyah center 24.6± 4.0Bq/L. On the other hand, the highest results of Pb, Cd and Ni have been 0.1247, 0.0652 and 0.157 ppm, respectively. While, the results of physics properties were from 7.05 to 8.3 for total dissolved solids (T.D.S.) values were from 2100 to 756.6 mg/L, electrical conductivity values were between 1140 and 3500 µs/cm, and turbidity values were between 7.0 and 54.5. Based on the results, the concentrations of the ^{40}K and heavy metals indicated that the results are almost slight compared to internationally accepted values.

INTRODUCTION

Water is a vital resource that nature has given to people and all other living things. However, due to human usage of pollutants, clean water is becoming increasingly scarce in many regions of the world (Usharani et al. 2010). Water serves as a vehicle via which radionuclides are transported and interact with many troposphere compartments. Soils, sediments, crustal rocks, biota, and even air constantly exchange radioactive elements with water (Mas et al. 2006). There are two sources that can contribute to increased radioactivity concentrations in water: anthropogenic radiation and natural radiation (Aswood et al. 2020). The long-lived radionuclides ^{238}U, ^{235}U, ^{232}Th, and ^{226}Ra, as well as the single ^{40}K, have been present since the Earth's formation. They are found in trace amounts in both nature and the human environment, the exposure to natural radiation being more significant than that of industrial radioactive sources (Aswood et al. 2022, UNSCEAR 2014). As a result, they account for the vast majority of human exposure to radiation from natural terrestrial sources, and there will be a risk for both cancer and non-cancerous diseases (Salih et al. 2019). Around the world, nuclear technology is being more widely used, and radionuclides are being used more often in industry, agriculture, medicine, and other atomic and radiological applications. This would be coupled with an increase in accidents, which would raise the possibility of human ionizing radiation exposure from the outside and radionuclide contamination of internal organs (Aswood et al. 2019). Several factors, such as the river basin's geological makeup, atmospheric inputs, industrial, agricultural, and urban activity, as well as the heavy metal present in water resources and rainfall amounts, all contribute

to the degradation of river water quality (Kareem & Shekha 2016). Many health hazards have been linked to exposure to high levels of heavy metals, including lead, copper, nickel, zinc, cadmium, and others, which is a reflection of both natural and human influences working together (Alhous et al. 2020). Therefore, information on the possible chemical and radiological danger of ingestion and cutaneous absorption may be obtained by measuring the quantities of heavy metals and radionuclides in water. The environment contains both heavy metals and radioactive elements, although the amounts of each vary depending on the geologic formation (Kadhim et al. 2020, Li et al. 2020).

As a result, radionuclides can exist as molten minerals, dust, or particles in water. They enter the body by inhalation or digestion. They emit internal radiation when they come into contact with the body (Salih & Aswood 2024). These water sources have higher levels of natural radioactivity due to sedimentation, dissolution, and transport. Furthermore, dust and other particles in water raise the concentration of heavy elements and radioactivity, primarily when water naturally transports radioactive materials over the surface of the Earth (Salman et al. 2020).

However, this transport process is affected by factors in the physical of the water, such as the constant change in pH, temperature, turbidity, dissolved solids content, etc. (Rahim 2020). Therefore, the purpose of this study was to determine radionuclides, including ^{40}K, and measure some heavy metals in surface water that were collected from the Euphrates River in the Governorate of Al-Qadisiyah.

MATERIALS AND METHODS

Study Area

Al-Qadisiyah Governorate is one of the Governorates of the Middle Euphrates region. It is located south of the capital, Baghdad, and away about 193 km. The study area site between latitudes 31.6858 -32.0451ºN and longitudes 45.0099- 44.7411ºE as shown in Fig. 1. It has a total area of 8,153m^2, which constitutes 1.9 % of the total area of Iraq, and the population was estimated to be 1,320,000 people, which constitutes about 2.73 % of the total population of Iraq. The Diwaniyah River passed through agricultural, commercial lands and industrial factories close to the river.

Sample Collection

The sampling spots were located using the Global Positioning device (G.P.S.), as shown in Table 1 coordinates for latitude and longitude. Additionally, twelve samples were collected from the surface water of the Euphrates River in Al-
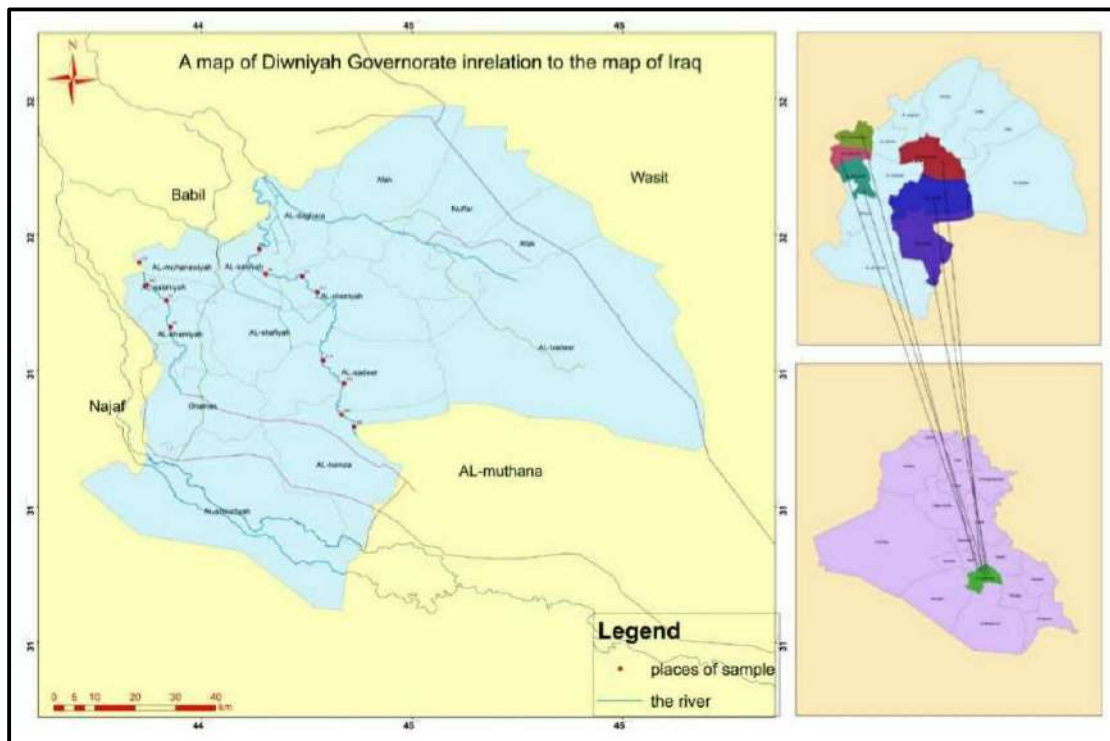
Fig. 1: The map of the study area.

Table 1: Water samples from Al-Diwaniyah River.

Sample codes	Regions	Location	Latitude (x)	Longitude (y)
S 1	Al-Siniyah	Al-jadwal	44.7411	32.0451
S 2		Omaltahab	44.7971	32.0321
S3	Al-Diwaniyah	Abu alfadhil	44.9077	32.0022
S 4		Sadr alyosfiyah	44.9232	31.9842
S 5	Al-shamiyah	Kasabatalshamiyah	44.5935	31.9658
S 6		AL-ain	44.5928	31.9181
S 7	Al-muhanawiyah	Aljajanalgharby	44.5334	32.0491
S 8		AL-kazaliyh	44.5711	31.9823
S 9	Al-sideer	AL-dahaya	44.9644	31.8022
S10		AL-milaha	44.9878	31.7809
S11	Al Hamza Al Sharqi	AL-shofa	45.0099	31.6858
S12		Azezallah	44.9712	31.7268

Qadisiyah governorate, Iraq, to measure the concentrations of radionuclides as well. Twelve samples of water were collected to measure physical and chemical properties.

Experimental Methods

The samples of surface water were collected from 12 different locations along the Euphrates River in Al- Qadisiyah governorate during 5 months (8-12) in 2023. The radionuclide concentrations were collected using a container volume of one liter made of polyethylene. A pure germanium reagent, HPGe (GC4020), was used to measure the radionuclide concentrations. The reagent used in the analysis is of the type (PNP). It has a separation ability of up to 2.0 keV at energy (1332 keV) peer back (^{60}CO). It was operated by using liquid nitrogen within a Dewar container to reach a temperature of (-176). To minimize the radiation background, layers of lead coated in copper were placed around the detector, making a thick shield that measured 10 cm.

This system operates using the program (Genie 2000) to determine the peaks, their energies, and the net area beneath each peak by analyzing the observed spectra. It is manufactured by the company (Canberra) (Riyadh & Al-Hamzawi 2023). Therefore, this system was chosen as the effective measurement technique. It is the most popular due to its desirable qualities, such as its high density (5.3 g/cm^3), which makes it have a high ability to stop nuclear radiation in a small way. Thorium ^{232}Th activity was measured through its daughters ^{212}Pb and ^{228}Ac with energy 583.1 and 911.1 keV, respectively. Radium^{226}Ra activity was measured through its daughters ^{214}Bi ^{214}Pb with energy 609.3 and 351.9 keV, respectively. Potassium ^{40}K activity was measured at single energy 1460.8 keV, as well as 12 measured Ni, Cd, and Pb content was also determined using Atomic Absorption Spectrophotometer A.A.S. Model

A.A. - 7000, Company SHIMADZU, Origin Japan (Rice et al. 2012). T he physical properties of water measured by pH meter were used to measure the pH Model SD300pH, Company Lovibond, Origin Germany. A conductivity (E.C.) meter Model Cond 7110, Company W.T.W., Origin Germany, was used to measure the total dissolved solids in water (mg/L) and electrical conductivity (µS/cm). Turbid meter, Model 2020wi, Company LaMotte, Origin U.S.A., and mg/L units were used to express the results.

Calculations

Specific Activity of Radionuclides

To estimate the radionuclides' particular activity (As) determined by equation 1 (Chougaonkar et al., 2004).

$$As = Cn/\varepsilon \times I\gamma \times t \times m \qquad \text{…(1)}$$

When the activity is in Bq/L, Cn is the total sub-peak count rate per second, ε: Efficiency, Iγ: gamma-ray emission intensity per energy, t: time (s),m: mass of the specimen (kg).According to equation (2), parameters such as radium equivalent activity (Ra$_{eq}$) is used to calculate the radiological hazards associated with exposure to radiation ^{226}Ra, ^{232}Th, and ^{40}K in water (Zorer 2019).

$$Raeq = C_{Ra}x\ 1.43 + C_{Th}x\ 0.07 + C_{K40} \qquad \text{…(2)}$$

The radium risks, such as radium equivalent (Ra$_{eq}$), these indicators are used to obtain total activity (^{226}Ra, ^{232}Th, and ^{40}K) Bq/L in water and the risk assessment of materials containing.

Absorbed dose rates (D$_R$)are determined using the following method (3) (Alaboodi et al. 2023).

$$D_R = C_{Ra} \times 0.461 + C_{Th} \times 0.623 + C_{K40} \times 0.041 \qquad \text{…(3)}$$

Additionally, an equation was used to determine the external hazard index (Hex), and the parameter's value

cannot be greater than the acceptable level's limit of unity (Heldal et al. 2021).

$$H_{ex} = \frac{C_{Ra}}{370} + \frac{C_{Th}}{259} + \frac{C_K}{4810} \leq 1 \qquad \ldots(4)$$

Heavy Metals in Water

The concentrations of heavy elements were calculated from the calibration curve and according to the equations mentioned (Hnamte 2013) in:

Heavy elements dissolved in water, then:

$$E_{Con.} = \frac{A \times B}{C} \times 1000 \qquad \ldots(5)$$

$E_{Con.}$: Water's dissolved element concentration (µg/L).

A: The element's concentration (mg/L).

B: The filtered sample's final volume (ml).

C: The filtered sample's initial volume (ml).

Statistical Analysis

Microsoft Office Excel 2013 and Graph Pad Prism 9.2.0 were used to gather, analyze, and present the data. Numbers were used to represent categorical data, while mean Standard Error Mean was used to convey numerical data. An unpaired one-way ANOVA was used to compare the mean values across the different groups for variables that were regularly distributed. When the P-value was less than 0.05, it was deemed significant.

RESULTS AND DISCUSSION

Specific Activity

Using HPGe gamma spectroscopy, the activity and amounts of naturally occurring radionuclides (^{226}Ra, ^{232}Th, and ^{40}K) in each of the water samples were ascertained. We assessed the activity concentration in unit Bq/L.

Table 2 shows the concentrations of radionuclides in all the drawn water samples that appeared. The naturally occurring radionuclide ^{40}K activity concentrations are in water only, and no results are displayed for other radionuclides. According to this table, the activity concentration of Potassium ^{40}K was measured with a maximum value of 24.6± 4 Bq/L in the S4 Al-Diwaniyah River. The minimum concentration 2.6±0.5, in S8 Al-muhanawiyah river, as tabulated in Table 2. The findings reveal that the natural radionuclide activity concentrations in the water samples are within the allowed limits. To ascertain the radiation threat from naturally occurring radioactivity associated with the water, the radiological parameters were evaluated, and the resulting values were compared with globally accepted safety limits.

Table 3 shows the external hazard indicators (H_{ex}), gamma dose rates ($D_R.$), and radium equivalent activity (Raeq) were sampled to (0.182 Bq/L) found in the (S8) sample. All of the (Re_{aq}) readings in the examined samples were discovered to be below the 370 Bq/L standard limits. Table 4 shows The (S4) sample's absorbed gamma dose rate ($D_R.$) varied from 1.009 nGy/h. The mean value of 0.7341 nGy/h of the rate of absorbed dose in the studied area is slightly more than the global limit of 55 nGy/h (Elewee & Aswood 2022). Regarding the external hazard index (Hex), the indicators' values ranged from 0.0051 Bq/L in the sample from S4andS7 to0.0005 Bq/L in sample S8, with an average value of 0.0037 Bq/L, which is somewhat less than the allowable limit $H_{ex} \leq 1$ (Heldal et al. 2021).

This indicates that the study's water samples will not harm the population as seen in Table 4. To discussion about the presence of radionuclides, the ^{40}K alone without other nuclides in water slightly varied from one site to another in the Euphrates river sampling in the Governorate of Al-Qadisiyah due to river water flow and dilution and lack of bioaccumulation led to a lack the concentration of radionuclides in the water being low or slight compared in the aqueous sediment based on the physical, chemical, and geochemical characteristics of the aquatic environment (Fallah et al. 2019). ^{40}K is more prevalent than the other isotopes in the samples under study due to its high rock abundance and abundance of heavy metals. This could be the result of runoff during the rainy season, which washes potassium fertilizers and stream forms into the river (Hamza et al. 2019). The external hazard indexes were within allowable levels, indicating that there are no significant radiation health concerns for those who use the water in their daily lives.

Concentration of Heavy Metals

Table 5 shows that the concentrations of heavy metals in water, such as lead, amounted to (0.1247-0.0002) parts per million, where the highest value was in sample 7 in Al-Mahnawiyah and the lowest value in sample 8 in Al-Salihiyah, while the values of cadmium ranged between (0.0652-00) parts per million, where the highest value was recorded in sample 11 in Al-Hamzah and the lowest value in sample 1 in Al-Suniya. Nickel concentrations ranged between (0.1571-0.0) parts per million, where the highest value was in sample 4 in Diwaniyah and the lowest value in sample 9 in Al-Sudair, as well as in sample 11 in Al-Hamzah was 0.0. The poor solubility of heavy metals in river water is due to their tendency to adsorb on suspended particles (Ahmed et al. 2021).

Table 6 shows the results that showed that the pH levels ranged between (7.05 - 8.3), where river water is

Table 2: Specific activity of ^{40}K in Euphrates River water samples.

Sample codes	Study area	^{40}K
S 1	Al-Siniyah(Al-jadwal)	14.4 ±1.4
S 2	Al-Siniyah(omaltahab)	17.2± 4
S3	Al-Diwaniyah(Abu alfadhil)	24±2
S 4	Al-Diwaniyah(Sadr alyosfiyah)	24.6± 4
S 5	Al-shamiyah(Kasabatalshamiyah)	18±1.3
S 6	Al-shamiyah(AL-ain)	14.9±1.5
S 7	Al-muhanawiyah(aljajanalgharby)	24.5± 4
S 8	Al-muhanawiyah(AL-kazaliyh)	2.6±0.5
S 9	Al-sideer(AL-dahaya)	19.7±1
S10	Al-sideer(AL-milaha)	17.9±3.3
S11	Al Hamza Al Sharqi(AL-shofa)	19.1±3
S12	Al Hamza Al Sharqi(Azezallah)	16.4±3

Table 3: Radioactive risks associated with water samples from the Euphrates River of Al-Diwaniyah Governorate.

Sample code	Raeq (Bq/L)	D.R. (nGy/h)	Hex
S1	1.008	0.590	0.0030
S2	1.204	0.705	0.0036
S3	1.68	0.984	0.0050
S4	1.722	1.009	0.0051
S5	1.26	0.738	0.0040
S6	1.043	0.611	0.0031
S7	1.715	1.005	0.0051
S8	0.182	0.17	0.0005
S9	1.379	0.808	0.0041
S10	1.253	0.734	0.0040
S11	1.337	0.783	0.0040
S12	1.148	0.672	0.0034
Mean ± SD	1.2440	0.7341	0.0037
global limits	370	55	⸦ 1

considered slightly alkaline. Table 7 shows that the highest value was in sample 8 in Al Mahnawiyah with an average of 7.97, and the lowest value of 7.225 was in sample 9 in Al Sudair. Electrical conductivity recorded values that ranged between (1140-3500) micro Siemens/cm, and the highest value was in sample 7 in Al-Mahanawiya at 3402, and the lowest value was 1201 in sample 4 in Al-Diwaniyah, while the values of total dissolved solids in water ranged between 2100-746 mg/L. The highest value was in sample 7 in Al-Mahanawiyah, and the lowest value was in sample 1 in Al-Suniyah, and the turbidity ranged between (54.5 - 7.0) NTU. The highest value in the sample was in Al-Diwaniyah, and the lowest value in the sample was 5 in Al-Shamiya. Furthermore, the alkalinity of river water accelerates the adsorption process and reduces the solubility of heavy metals (Al-Asadi et al. 2020). Elevated levels of lead in river water are likely attributable to increased gasoline use, agricultural runoff, and the discharge of untreated pollutants into the river.

Table 4: Radioactive risks associated with water samples from the Euphrates River of Al-Diwaniyah Governorate.

Radioactive risks	Number of values	Minimum	Maximum	Mean	Std. Error of Mean	Global Limits
Raeq (Bq/kg)	12	0.1820	1.7220	1.2440	0.1201	370
DR (nGy/h)	12	0.1700	1.0090	0.7341	0.0662	55
Hex	12	0.0005	0.0051	0.0037	0.0004	< 1

Table 5: Heavy metals examined in water samples of Al-Districts of Al-Diwaniyah Governorate.

Sequence	Names of rivers	Parameter		
		Pb (ppm)	Cd (ppm)	Ni (ppm)
S1	Al-Siniyah	0.0003	0.0	0.0032
S2	Al-Siniyah	0.0005	0.0024	0.0002
S3	Al-Diwaniyah	0.0051	0.0015	0.0509
S4	Al-Diwaniyah	0.0070	0.0007	0.1571
S5	AL-Shaamiyah	0.0004	0.0030	0.0001
S6	AL-Shaamiyah	0.1235	0.0046	0.0562
S 7	AL-Muhnawiyah	0.1247	0.0561	0.0031
S8	AL-Muhnawiyah	0.0002	0.0003	0.0002
S 9	AL-Seedir	0.0733	0.0314	0.0
S10	AL-Seedir	0.0061	0.0013	0.0252
S11	AL-Hamza	0.1012	0.0652	0.0
S12	AL-Hamza	0.0012	0.0001	0.0023

Table 6: Physical properties to taken water samples of AL-Diwaniyah River.

Sequence	Names of rivers	Parameter			
		P.H.	ECMs\cm	T.D.S.Mg\l	Turb.NTU
S1	Al-Siniyah	7.11	1243	746	10.60
S2	Al-Siniyah	7.8	1360	1092	28
S3	Al-Diwaniyah	7.54	1261	756.6	26.1
S4	Al-Diwaniyah	7.29	1140	812	39.6
S5	AL-Shaamiyah	7.12	1386	831.6	7.0
S6	AL-Shaamiyah	8.21	1322	793	14.6
S7	AL-Muhnawiyah	7.64	3500	2100	11.91
S8	AL-Muhnawiyah/AL-Salahiyah	8.3	1304	782.4	11.7
S9	AL-Seedir	7.05	1320	792	19.2
S10	AL-Seedir	7.4	1407	1110	23.6
S11	AL-Hamza	7.46	1304	786	11.1
S12	AL-Hamza	7.31	1198	938	54.5

The pH

An excellent measure of the extent of pollution and water quality is the pH of the aquatic systems. The pH values in the S8 AL-Muhnawiyah district's river (AL-Salahiyah) ranged from 8.3 to 7.05, with the AL-Seedir district having the lowest pH value. These findings indicated that the water samples' pH was relatively alkaline. A decrease in pH makes heavy metals more soluble and become more toxic. In contrast, an increase in pH leads to their precipitation in sediments as in pH values to AL-Muhnawiyah river in Table 7 & Fig. 2 (Thirumala 2012).

Table 7: A comparison of the pH values in the water of Al-Qadisiyah Governorate.

Names of places	Number of values	Minimum	Maximum	Mean	Std. Error of Mean	P value
Al-Siniyah	5	7.11	7.8	7.455	0.345	0.6346 ns
Al-Diwaniyah	5	7.29	7.54	7.415	0.125	
AL-Shaamiyah	5	7.12	8.21	7.665	0.545	
AL-Muhnawiyah	5	7.64	8.3	7.97	0.33	
AL-Seedir	5	7.05	7.4	7.225	0.175	
AL-Hamza	5	7.31	7.46	7.385	0.075	

ns: no significant p-value >0.05; *significant p-value ≤0.05; **significant p-value ≤0.001; ***significant p-value ≤0.0001.; **** significant p-value <0.0001.
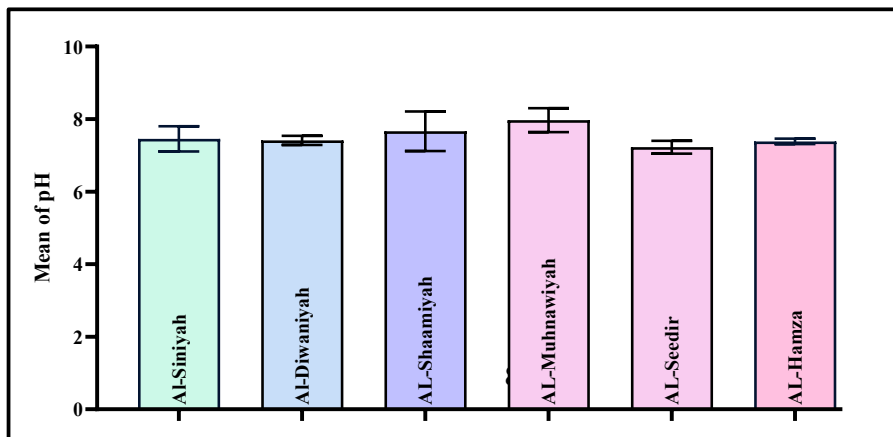
Fig. 2: Study locations' pH values.

The Turbidity

Table 8 and Fig. 3, presented the turbidity ranged between (54.5-7.0) NTU; the highest value in the sample was 12 in Al-Hamzah, and the lowest value in the sample was 5 in Al-Shamiya. The results of the study indicated that the high turbidity values may be due to the presence of particles and suspended materials in the water, which consist of clay, silt, sand, organic and inorganic materials, as well as various human activities, which lead to an increase in turbidity and its association with heavy metals (Laghari et al. 2018).

Total Dissolved Solids (T.D.S)

Table 9 and Fig. 4 presented the T.D.S. levels ranging from 746 mg/L in the S1 Al-Siniyah River to 2100 mg/L in the S7 AL-Muhnawiyah River, which had the highest value. According to the present total dissolved solids levels, AL-

Table 8: A comparison of the Turbidity test in the water of Al-Qadisiyah Governorate.

Names of places	Number of values	Minimum	Maximum	Mean	Std. Error of Mean	P value
Al-Siniyah	5	10.6	28	18.23	2.514	<0.0001 ****
Al-Diwaniyah	5	26.1	39.6	32.67	1.917	
AL-Shaamiyah	5	7	14.6	10.66	1.048	
AL-Muhnawiyah	5	11.7	11.91	11.81	0.105	
AL-Seedir	5	19.2	23.6	21.47	0.6998	
AL-Hamza	5	11.1	54.5	32.05	4.289	

ns: no significant p-value >0.05; *significant p-value ≤0.05; **significant p-value ≤0.001; ***significant p-value ≤0.0001.; **** significant p-value <0.0001.
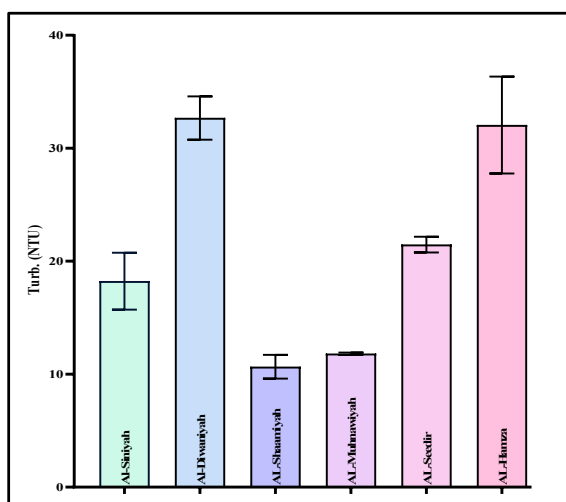
Fig. 3: Study locations' Turbidity values.

Table 9: A comparison of the T.D.S. test in the water of Al-Qadisiyah Governorate.

Names of places	Number of values	Minimum	Maximum	Mean	Std. Error of Mean	P value
Al-Siniyah	5	746	1092	919	173	0.0032 **
Al-Diwaniyah	5	756.6	812	784.3	27.7	
AL-Shaamiyah	5	793	831.6	812.3	19.3	
AL-Muhnawiyah	5	1782	2100	1941	158.8	
AL-Seedir	5	792	1110	951	159	
AL-Hamza	5	786	938	862	76	

ns: no significant p-value >0.05; *significant p-value ≤0.05; **significant p-value ≤0.001; ***significant p-value ≤0.0001.; **** significant p-value <0.0001.

Muhnawiyah is one of the study's salty sites. Fertilizers, high temperatures, and domestic sewage are the causes of the high concentration of total dissolved solids in the water (Laghari et al. 2018).

Conductivity of Electricity

Table 10 and Fig. 5, explain the capacity of a solution to conduct electric current is known as electrical conductivity, and it is influenced by temperature, ion valency, and concentration. According to the electrical conductivity data, AL-Diwaniyah had the lowest value at 1140 μs/cm, and S7 AL-Muhnawiyah had the greatest value at 3500 μs/cm. The current investigation yielded extremely high findings because it is closely correlated with both high temperature and the concentration of dissolved substances (T.D.S.) in water(Abowei 2010). Leaving waste during irrigation and
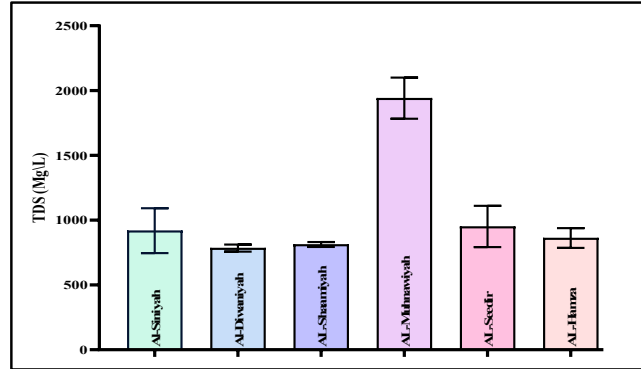
Fig. 4: The research locations' total dissolved solids values (mg/L).

Table 10: A comparison of the electrical conductivity test in the water of Al-Qadisiyah Governorate.

Names of places	Number of values	Minimum	Maximum	Mean	Std. Error of Mean	P value
Al-Siniyah	5	1243	1360	1302	58.5	<0.0001 ****
Al-Diwaniyah	5	1140	1261	1201	60.5	
AL-Shaamiyah	5	1322	1386	1354	32	
AL-Muhnawiyah	5	3304	3500	3402	98	
AL-Seedir	5	1320	1407	1364	43.5	
AL-Hamza	5	1198	1304	1251	53	

ns: no significant p-value >0.05; *significant p-value ≤ 0.05; **significant p-value ≤ 0.001; ***significant p-value ≤ 0.0001.; **** significant p-value <0.0001.
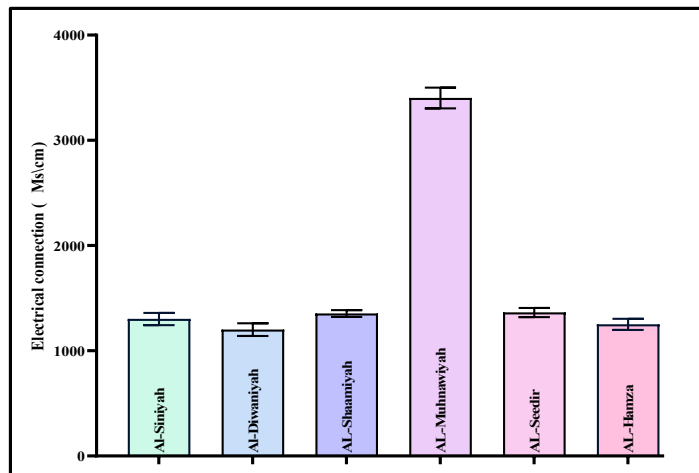

Fig. 5: Shows the research locations' electrical conductivity values (μs/cm).

river cleaning operations for long periods on the sides of the rivers, facilitates the return of large quantities of salts cumulatively, in addition to irregular fertilization operations in the soil, which add a percentage of salts to the soil that accumulate as a result of the phenomenon of continuous evaporation from the surface of the soil, and when watered and washed, the percentage of these salts returns to the streams. The river increases the values of conductivity and salinity together.

CONCLUSIONS

The radioactivity in water samples was collected from six regions of the Euphrates River in Al-Qadisiyah, Iraq, using pure germanium HPGe. The highest activity concentration of ^{40}K was 24.6 Bq/L, radium equivalent activity was 1.722 Bq/L as well as, and the absorbed dose was 1.00 nGy/h. The activity concentrations of ^{226}Ra and ^{232}Th were not found in the study area. The results of the radioactive test of ^{40}K are within permissible limits. On the other hand, the study demonstrated the concentrations of radionuclides and concentrations of heavy metals in water do not provide sufficient evidence of the occurrence of chemical and radioactive pollution due to their low concentration. The role of the competent authorities in protecting the river environment and preventing the dumping of pollutants into them is being activated by building units to treat liquid pollutant waste. The ongoing observation of the quality of the water to document any changes and minimize adverse effects on aquatic ecosystems, such as fertilizers and types of pesticides used in agriculture and overfishing in rivers.

ACKNOWLEDGEMENT

REFERENCES

Abdul Rahim, K.S., Zainuddin, Z., Idris, M.I., Priharti, W. and Aswood, M.S., 2020. Determination of the radiological risk from the natural radioactivity in irrigation at selected areas of Peninsular Malaysia. *Sains Malaysiana*, 49(6), pp.1439-1450.

Abowei, J.F.N., 2010. Salinity, dissolved oxygen, pH and surface water temperature conditions in Nkoro River, Niger Delta, Nigeria. *Advance Journal of Food Science and Technology*, 2(1), pp.36-40.

Ahmed, A.S.S., Hossain, M.B., Babu, S.M.O.F., Rahman, M.M. and Sarker, M.S.I., 2021. Human health risk assessment of heavy metals in water from the subtropical river, Gomti, Bangladesh. *Environmental Nanotechnology, Monitoring & Management*, 15, p.100416.

Alaboodi, A.S., Alslami, S.A., Kadhim, S.A., Alhous, S.F. and Khafaji, Q.S.A., 2023. Cancer risk as a result of annual consumption rate of selected samples from the Euphrates river in Iraq. *AIP Conference Proceedings*, 2977(1).

Al-Asadi, S.A.R., Al-Qurnawi, W.S., Al Hawash, A.B., Ghalib, H.B. and Alkhlifa, N.-H.A., 2020. Water quality and impacting factors on heavy metals levels in Shatt Al-Arab River, Basra, Iraq. *Applied Water Science*, 10(5), pp.1-15.

Alhous, S.F., Kadhim, S.A., Alkufi, A.A. and Kadhim, B.A., 2020. Measuring the level of Radioactive contamination of selected samples of Sugar and Salt available in the local markets in Najaf governorate/ Iraq. *IOP Conference Series: Materials Science and Engineering*, 928(7), p.072097.

Aswood, M.S., Alhous, S.F. and Abdulridha, S.A., 2022. Life time cancer risk evaluation due to inhalation of radon gas in dwellings of Al-Diwaniyah Governorate, Iraq. *Nature Environment and Pollution Technology*, 21(1), pp.331-337.

Aswood, M.S., Almusawi, M.S., Mahdi, N.K.W. and Showard, A.F., 2020. Evaluation of committed effective dose of Radon gas in drinking water in Al-Qadisiyah province, Iraq. *Periódico Tchê Química*, 17(36).

Aswood, M.S., Salih, A.A. and Al Musawi, M.S.A., 2019. Long-lived gamma-ray measurement in soil samples collected from city central of Al-Diwaniyah, Iraq. *Journal of Physics: Conference Series*, 1234(1), p.012003.

Chougaonkar, M.P., Eappen, K.P., Ramachandran, T.V., Shetty, P.G., Mayya, Y.S., Sadasivan, S. and Raj, V.V., 2004. Profiles of doses to the population living in the high background radiation areas in Kerala, India. *Journal of Environmental Radioactivity*, 71(3), pp.275-297.

Elewee, A.A. and Aswood, M.S., 2022. Estimation of Indoor Radon Concentration in Some Houses in Al-Shatra District, Dhi-Qar Governorate, Iraq. *Nature Environment and Pollution Technology*, 21(4), pp.1747-1752.

Fallah, M., Jahangiri, S., Janadeleh, H. and Kameli, M.A., 2019. Distribution and risk assessment of radionuclides in river sediments along the Arvand River, Iran. *Microchemical Journal*, 146, pp.1090-1094.

Hamza, Z.M., Kadhim, S.A. and Hussein, H.H., 2019. Assessment the norms for agricultural soils in Ghammas town, Iraq.

Heldal, H.E., Helvik, L., Haanes, H., Volynkin, A., Jensen, H. and Lepland, A., 2021. Distribution of natural and anthropogenic radionuclides in sediments from the Vefsnfjord, Norway. *Marine Pollution Bulletin*, 172, p.112822.

Hnamte, V., 2013. Economics of Public Water Distribution in Mizoram, A Case Study of Aizawl Water Supply Scheme. *Mizoram University*.

Kadhim, A.Y., Al-Ataya, K.H. and Aswood, M.S., 2020. Distribution of Radon Concentration in Farmland Soil Samples in Al-Shamiyah City, Al-Qadisiyah, Iraq. *Journal of Physics: Conference Series*, 1591(1), p.012089.

Kareem, M.A. and Shekha, Y.A., 2016. Evaluation of water quality for Greater Zab River by principal component analysis/factor analysis. *Iraqi Journal of Science*, pp.2650-2663.

Laghari, A.N., Walasai, G., Jatoi, A.R., Shaikh, F.A. and Siyal, Z.A., 2018. Performance analysis of water filtration units for reduction of pH, Turbidity, Solids and Electricity Conductivity. *Engineering, Technology & Applied Science Research*, 8(4), pp.3209-3212.

Li, K., Cui, S., Zhang, F., Hough, R., Fu, Q., Zhang, Z., Gao, S. and An, L., 2020. Concentrations, possible sources and health risk of heavy metals in multi-media environment of the Songhua River, China. *International Journal of Environmental Research and Public Health*, 17(5), p.1766.

Mas, J.L., García-León, M., García-Tenorio, R. and Bolívar, J.P., 2006. Radionuclide concentrations in water. In: *Radionuclide concentrations in food and the Environment*, pp.59-112. CRC Press.

Rice, E.W., Bridgewater, L. and Association, A.P.H., 2012. *Standard methods for the examination of water and wastewater* (Vol. 10). American Public Health Association, Washington, DC.

Riyadh, M. and Al-Hamzawi, A.A., 2023. Natural radionuclides and radiological hazards in sediment samples of the Euphrates River in Al Diwaniyah governorate, Iraq. *International Journal of Radiation Research*, 21(1), pp.159-162.

Salih, N. and Aswood, M., 2024. Measuring the radioactivity concentration of 40K, 226Ra, 232Th with PH, conductivity and radiological risk in tap water. *International Journal of Environmental Analytical Chemistry*, pp.1-21.

Salih, N.F., Aswood, M.S. and Hamzawi, A.A., 2019. Effect of porosity on evaluation of radon concentration in soil samples collected from Sulaymania governorate, Iraq. *Journal of Physics: Conference Series*, 1234(1), p.012024.

Salman, A.Y., Kadhim, S.A., Alaboodi, A.S. and Alhous, S.F., 2020. Study the contamination of Radioactivity levels of 226Ra, 232Th and 40K in (water) Iraq and their potential radiological risk to human population. *IOP Conference Series: Materials Science and Engineering*, 928(7), p.072008.

Thirumala, S., 2012. Physico-chemical characteristics of Tungabhadra River basin, a freshwater wetland in Harihara Karnataka, India. *Journal of Applied Technology in Environmental Sanitation*, 2(3).

UNSCEAR, 2014. Report of the United Nations Scientific Committee on the Effects of Atomic Radiation 2014: Sixty-first Session (21-25 July 2014).

Usharani, K., Umarani, K., Ayyasamy, P.M., Shanthi, K. and Lakshmanaperumalsamy, P., 2010. Physico-chemical and bacteriological characteristics of Noyyal River and groundwater quality of Perur, India. *Journal of Applied Sciences and Environmental Management*, 14(2).

Zorer, Ö.S., 2019. Evaluations of environmental hazard parameters of natural and some artificial radionuclides in river water and sediments. *Microchemical Journal*, 145, pp.762-766.

Original Research Paper | doi https://doi.org/10.46488/NEPT.2025.v24i01.B4194 | **Open Access Journal**

Use of Geopolymerized Fly Ash with GGBS as a Barrier for Waste Containment Facilities

S. S. S. Saranya† (ID) **and S. N. Maya Naik**

Department of Civil Engineering, BMS College of Engineering, Bengaluru, India
†Corresponding author: S. S. S. Saranya; saranyasagiri8@gmail.com

ABSTRACT

The present paper reports the results of experimental investigations performed to examine the feasibility of using fly ash (FA) and ground-granulated blast furnace slag (GGBS) geopolymers as barrier materials for waste containment facilities. The alkaline geopolymer is a blend of FA and GGBS with sodium hydroxide in concentrations varying from 1 to 5. The important properties of most barrier materials include strength and hydraulic conductivity. While FA can develop compressive strength through pozzolanic reactions, polymerized FA develops tensile strength. For the construction of barriers for landfills with higher heights, tensile strength assumes importance. To further improve the strength, FA can be amended with GGBS. Results indicate that the FA-GGBS mixture in the ratio of 40:60, when cured, exhibited higher strength at any molar concentration. Further, the hydraulic conductivity of the material, which is predominant for barriers in waste containment facilities, is studied. To examine the impact of the presence of heavy metals in the leachates, batch adsorption studies were executed on a 40% FA- 60% GGBS mixture. Leachate with nickel and lead were adapted for their retention within the barrier. It has been observed that the geopolymerized FA and GGBS can retain ionic metals. The retention capacity of heavy metals is due to their precipitation in the voids of the barrier material enabling further reduction in the hydraulic conductivity making geopolymer a sustainable barrier material.

INTRODUCTION

Landfilling is the widely followed approach for solid waste disposal. Leachate generated from these landfills is becoming a major threat to the surrounding environment (Ganjian et al. 2004a). To protect the adjacent sites from groundwater contamination, landfill liners were proposed in the past. Many conventional barrier materials used for facilities releasing leachates with ionic contaminants, such as heavy metals, increase their hydraulic conductivity.

Strength characteristics and the retention capacity of contaminants are the two primary parameters to be analyzed in a landfill design (Deka & Sreedeep 2016). Barriers play a very important role in the operation of any landfill.

Generally, attention is paid to either reducing the permeability of the liner or immobilizing contaminants, but the strength properties have not yet been examined (Shankar & Phanikumar 2012). In landfills with greater heights, a higher settlement and slope failure are expected (Sheng et al. 2021). Engineered landfills are designed aiming for enhanced strength and better performance by retaining contaminants in the liner system (Herrmann et al. 2010). In recent years, research has especially centered on the utilization of industrial by-products in waste containment facilities (Devarangadi & Shankar 2020).

Conventional mortar with polymerized FA with alkali is used to partly replace different amounts of sand in mortar and is extensively studied to minimize the environmental effects of disposal FA besides the environmental issue of extensive

mining of river sand. Industrial by-products such as FA and GGBS, when added together as a mixture, resulting in good strength due to hydration, forming cementitious compounds (Yawale & Patankar 2023). Polymerization of these components by alkali activation can further enhance the bonding effect of these materials (Wattez et al. 2021). Unlike Portland cement, where water is formed by hydration, geopolymerization eliminates water (Wilińska & Pacewska 2018). A further advantage is that this polymerization occurs at room temperature. Geo-polymerization does not form calcium silicate hydrates like those present in cement but develops strength by polycondensation of alumina and silica precursors at high concentrations of alkali (Qaidi et al. 2022).

Apart from strength, permeability is the major factor that affects the long-term performance of a liner (Ganjian et al. 2004). Landfill liners should be less permeable and are essential in waste disposal systems to control the flow of leachate and the migration of contaminants into the surrounding environment (Fall et al. 2010). In general, a clay liner following compaction should possess a permeability of 1×10^{-9} m/s or less (Cossu & Garbo 2018).

The primary aim of this study is to generate a barrier system with good strength in both compression and tension by using polymerized FA with GGBS mixtures, besides satisfying the liner requirements for hydraulic conductivity.

MATERIALS AND METHODS

Materials

The present investigation utilizes FA and GGBS as source materials, with sodium hydroxide (NaOH) pellets as an alkali activator. The FA utilized in the present investigation is procured from the Raichur thermal power plant in Karnataka, India. The percentage of lime (CaO) in FA used in this research is less than 2 and is categorized as Class F (Mishra & Ravindra 2015). The physical properties of the FA and GGBS used are provided in Table 1.

GGBS and sodium hydroxide used in the present research are procured from local distributors in Bangalore, Karnataka, India. The chemical compositions of FA and GGBS are outlined in Table 2.

It is seen from grain size analysis that the particles of FA are within the limits of fine sand and silt, while almost all the particles of GGBS are silt-sized.

Surface texture plays a crucial part in achieving density even with the same compactive effort (Hu et al. 2018). Hence, the microstructural properties were assessed by scanning electron microscopy (SEM) (Mukri et al. 2018).

Table 1: Physical properties of FA and GGBS.

Properties	FA	GGBS
Color	Grey	Whitish
Specific Gravity	2.14	2.80
Specific surface area(m^2/kg)	339.00	480.00
Liquid Limit (%)	27 .00	30.00
Sand size (%) (4.75 - 0.075 mm)	58.55	25.51
Silt size (%) (0.075 - 0.002mm)	39.82	70.49
Clay size (%) (<0.002mm)	0.63	4.00
Optimum Moisture Content (%)	15.60	22.70
Maximum Dry Density (kN/m^3)	14.00	15.90

Table 2: Chemical composition of FA and GGBS.

Constituent	Proportion by Weight (%)	
	FA	GGBS
Al_2O_3	39.64	20.85
SiO_2	50.44	32.81
Fe_2O_3	4.18	0.36
CaO	1.26	35.51

Fig. 1 illustrates the microscopic images of FA and GGBS. From the SEM image, it is observed that FA particles are hollow cenospheres, whereas GGBS particles are angular with clear edges.

Experimental Program

The specified work investigates the impacts of FA-GGBS-based geopolymers concerning the geotechnical properties of landfill liners. The experimental program is categorized as material collection, casting, and curing, followed by laboratory testing and data evaluation. A set of trials was performed on FA-GGBS mixtures to figure out the optimum FA-GGBS ratio and the required amount of alkali for effective liner requirements. The paper discusses mixtures with 20%, 40%, 60%, and 80% FA blended with GGBS after activating with alkali for synthesizing into geopolymers. The alkali concentration is varied from 1 to 5 Molar (M).

The compaction characteristics of various FA-GGBS mixtures are determined using the minicompaction test apparatus (Sharma & Sivapullaiah 2016).

Specimens with standard size (3.8 cm × 7.6 cm) were cast with respect to their maximum dry density (MDD) and optimum moisture content (OMC) for unconfined compressive strength (UCS) in a manner that the same impact energy is maintained for every sample (Palmer 2000). The mixtures were prepared on a dry-weight basis by adding the requisite quantity of water. Then the extruded samples were sealed in airtight bags, and the effect of time was
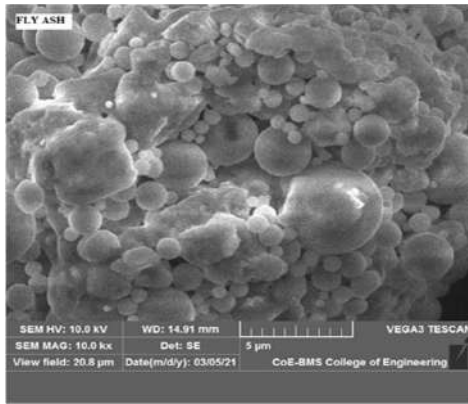
(a) Fly Ash
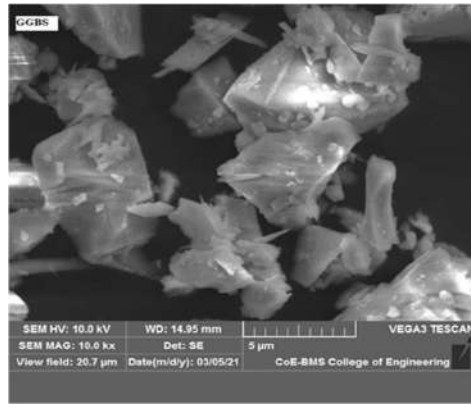
(b) GGBS

Fig. 1: SEM pictures of FA and GGBS.

investigated by curing the samples for 3, 14, and 28 days in a desiccator while maintaining 100% relative humidity at room temperature. The influence of alkali on FA-GGBS mixtures has been examined using unconfined compressive strength (UCS) as per IS 2720 (Part 10) standards.

Specimens with 100 mm in diameter and 200 mm in height were cast under molar concentrations of 1 to 5 to determine the tensile strength. The stiffness or tensile strength is studied by testing the specimens using a digital compression testing machine as per IS 5816 (1999) standards (Bellum et al. 2019).

Cubic specimens of 100 mm in size are cast and cured for 28 days to determine the permeability. The casted specimens were permeated with water and tested in terms of penetration depth as per IS 516-Part 2-Sec1 (Ibrahim & Issa 2016).

Batch equilibrium tests have been undertaken on a polymerized 40% FA and 60% GGBS mixture. 50 ppm each of lead (Pb) and nickel (Ni) solutions were prepared and used as leachate in the present study. 10 grams of adsorbent collected from the tested UCS samples were added to 100 mL of heavy metal solution and kept in a rotary shaker, maintaining a contact time of 8 hours. Later, the samples were filtered and tested for the presence of metal contaminants through atomic absorption spectroscopy.

A representative sample from the tested UCS specimens was collected and the morphology of the compounds was analyzed through microstructural studies.

RESULTS AND DISCUSSION

Compaction Characteristics

In this section, the compaction characteristics of FA blended with various percentages of GGBS were determined. The compaction curves are as shown in Fig. 2 and the optimum moisture content (OMC) and maximum dry density (MDD) are noted and presented in Table 3.

It is noticed from Fig. 2 that a rise in the percentage of GGBS, and MDD has increased whereas OMC is not following any particular trend. The enhancement in MDD is owing to the particle size, as it is seen from grain size analysis that GGBS is finer with more silt-sized particles. These finer particles fill the spaces left in the FA particles, following a dense mix, thereby increasing MDD.

UCS of FA-GGBS Mixtures Cured for Various Periods

UCS of FA and GGBS mixtures after various curing periods are presented in Fig. 3. Blending FA with GGBS will twin effect the strength both by improving the ratios of reactive silica and lime for the production of cementitious composites and by improving the silica-alumina ratio for effective polymerization with alkali (Sasui et al. 2019).

It is observed that the strength of FA-GGBS mixtures increases with the curing period. Cementitious compounds such as calcium silicate hydrate (CSH) formed are noticed over curing because of the pozzolanic reactions that are time-dependent.

Table 3: Compaction characteristics of FA-GGBS mixtures.

GGBS - FA (%)	OMC (%)	MDD (kN/m^3)
0:100	15.6	14.0
20:80	18.1	14.4
40:60	20.5	14.7
60:40	20.3	15.2
80:20	20.5	15.5
100:0	22.7	15.9
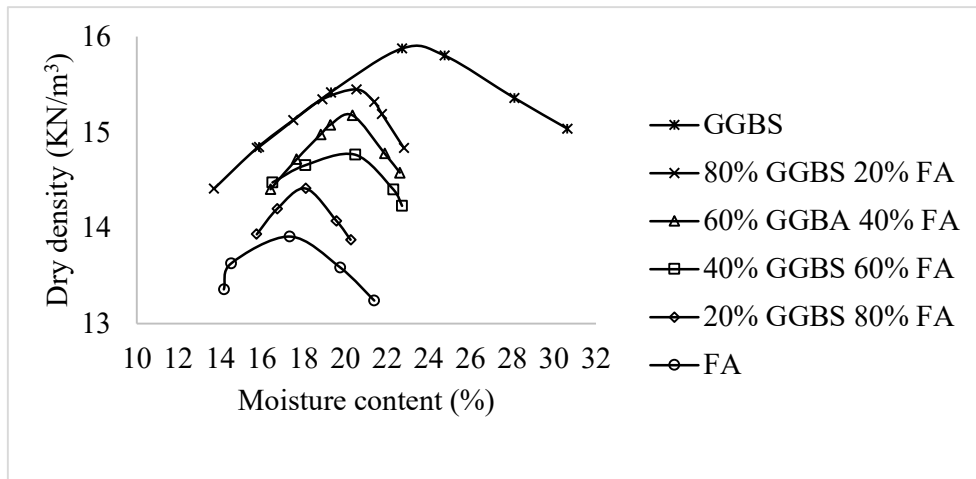
Fig. 2: Compaction curves of various FA-GGBS mixes.
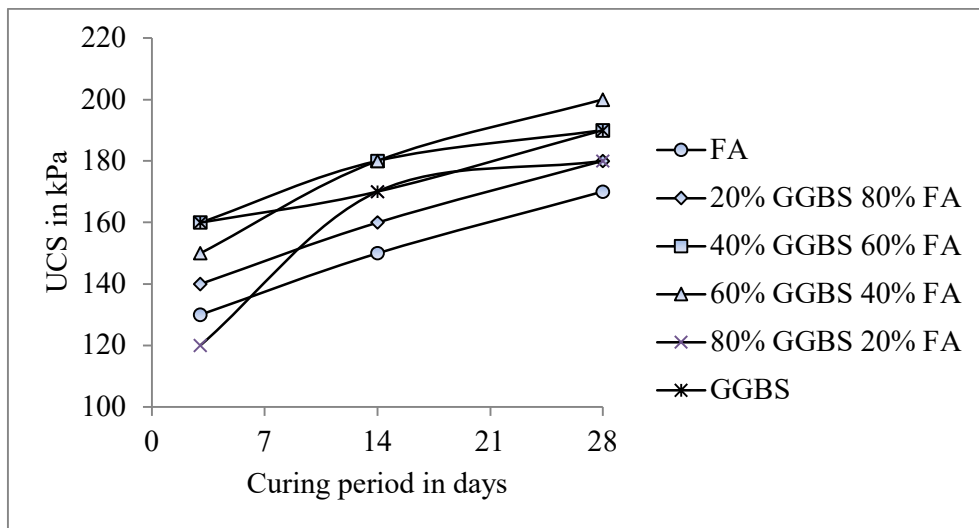
Fig. 3: Variation in UCS on FA and GGBS mixtures with curing period.

The escalation in strength of these mixtures is almost linear for FA with GGBS up to 60%. But for FA with 80% GGBS, the strength boosts steeply between 7 to 14 days and remains constant beyond 14 days. For GGBS alone, a marginal strength is noticed with curing. The increase in strength is because of the reactive silica and lime in FA/GGBS that undergoes pozzolanic reactions. It was noticed that FA with 60% GGBS showed the highest strength, which means the mixture of 40% FA and 60% GGBS has enough lime and silica essential to promote the pozzolanic reaction (Singh 2018). This may be attributed to the optimum ratio of lime and reactive silica in the combined mixture of FA and GGBS. For mixtures with higher GGBS, the rise in strength with curing is less, implying that the pozzolanic reactions are not proceeding owing to one of the constituents, i.e.,

reactive silica or lime, which is not in the right proportion. This justifies using mixtures rather than either of them.

The reaction of sodium hydroxide on FA-GGBS mixtures followed by a 28-day curing period is shown in Fig. 4. Pozzolanic reactions proceed finer in the existence of alkali due in account to better solubility of silica from FA and/or GGBS. Apart from better pozzolanic activity, sodium hydroxide is an alkaline activator that helps to form inorganic polymers which increase in association with the alkali concentration.

Fig. 4 portrays that at a subsequent curing of 28 days; a clear trend is evident in all FA and GGBS mixtures and at all alkali concentrations. A gradual increase in UCS is observed for the mixture with 60% GGBS. Beyond 60%
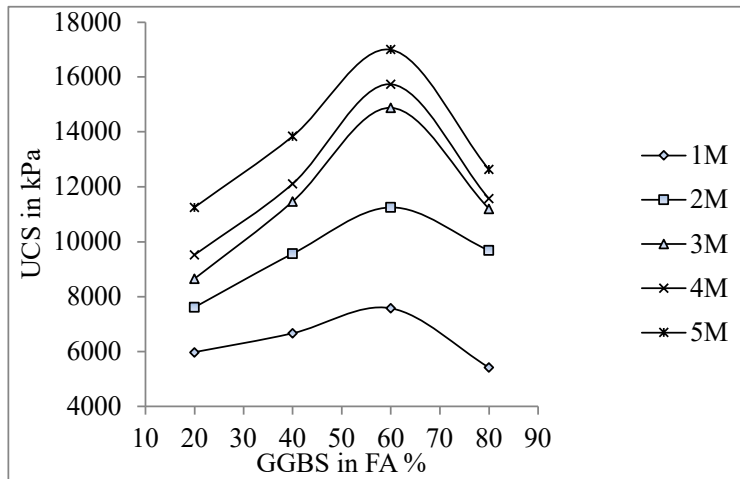
Fig. 4: Effect of alkali concentration on UCS of FA and GGBS mixtures after 28 days of curing.

GGBS, UCS is reduced with any concentration of alkali. The maximum strength is obtained at about 60% of GGBS at 28 days of curing at any concentration of alkali, but the optimum alkali concentration can be considered as 3M. The reduction in strength at a higher GGBS percent is larger for mixtures with increased concentrations.

Blending FA with GGBS can enhance the properties required to use them as a component of a landfill liner. Enhanced production of cementitious compounds by reactions amidst lime and reactive silica available in them, apart from their production by hydration reactions of GGBS and FA, is noticed. The number of cementitious compounds formed can increase with alkali concentration, and the participation of sodium in the formation of these compounds enhances the hydration reaction by forming cementitious compounds such as CSH gels over an increased curing time (Thakur et al. 2022). The extent of these compounds

formed can be advantageous when lime and reactive silica are together in the required proportion, and this can be evaluated by calculating the strength of various FA and GGBS combinations cured for various ages and with different concentrations of alkali. The mechanism becomes clearer if the variation in tensile strength influenced by these parameters is compared.

Tensile Strength of FA-GGBS Mixture

The optimized FA-GGBS mixture, which gave the highest compressive strength, is considered for tensile strength analysis. The tensile strength of a mixture of 40% FA and 60% GGBS with respect to alkali concentration at 28 days of curing is determined. Polymerization of silica in FA with alkali can be more advantageous in the development of tensile strength. Fig. 5 shows that the tensile strength progressively increases with an increase in the alkali
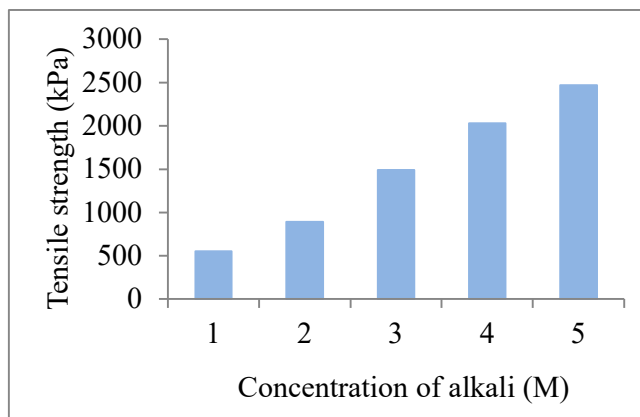
Fig. 5: Variation in tensile strength of 60% GGBS 40% FA mixture after 28 days of curing with alkali concentration.
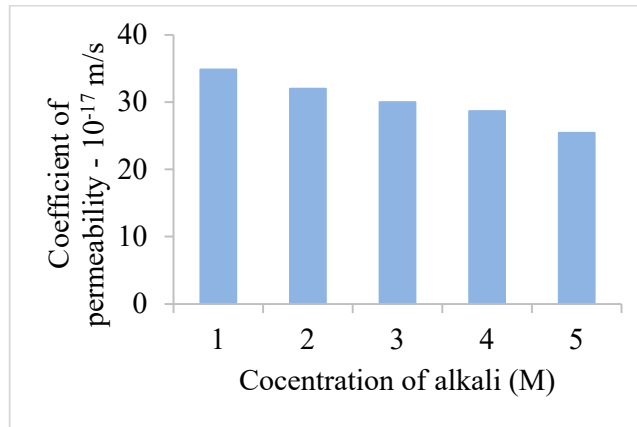
Fig. 6: Effect of permeability for optimized FA-GGBS mixture cured for 28 days.

concentration over a curing period of 28 days. This may be because of the polymerization of FA and GGBS with sodium-based alkaline activators.

In general, for cementitious materials, when the compressive strength increases, the tensile strength fails to increase proportionally, or rather, it may decrease as well. It is good to see that both compressive strength and tensile strength are increasing. The steep increase in tensile strength compared to UCS confirms the polymerization of FA and/ or GGBS. Unlike cementation by pozzolanic compounds, which substantially enhance the unconfined compressive strength (UCS), polymerization can increase tensile strength.

A closure examination of Fig. 4 and 5 reveals that the percent increase in tensile strength is higher than the corresponding increase in compressive strength at any curing period.

Permeability of FA-GGBS Mixture with Varying Alkali Concentration

Fig. 6 shows the permeability of an optimized mix of 40% FA and 60% GGBS with varying concentrations of alkali from 1 to 5 molar cured for 28 days. It is observed that a rise in the alkali concentration reduces the permeability. Geo-polymerization of reactive silica obtainable in fly ash in the presence of alkali, which confirms a significant lowering of permeability with alkali concentration, can be a reason. However, the role of more cementitious compounds in the reaction of reactive silica with lime over-curing cannot be ignored.

Batch Adsorption Studies

Batch adsorption tests were performed using an optimized FA-GGBS mixture as an adsorbent to a synthetic solution prepared in a laboratory at a known initial concentration of 100 ppm. Lead (Pb) and nickel (Ni) were the selected heavy metals for these studies. 10 grams of adsorbent are added to 100 ml of synthetic solution and kept in a rotary shaker, maintaining a contact time of 8 hours. Later, the collected solutions were filtered and tested for heavy metals through atomic absorption spectroscopy (AAS), as shown in Table 4.

Batch experiments were performed to evaluate the sorption capacity and retention of selected heavy metals (Pb and Ni). The concentration of Ni was below the detectable limit (BDL) at all alkali concentrations of 1-4 molar except 5 molars, whereas for Pb, a gradual abatement of the residual ions is observed, and at 5 molars the existence of Pb ions is below the detectable level. The solubility products of nickel and lead hydroxides are in the range of 10^{-13} and 10^{-20} mol/L (Scholz & Kahlert 2015). Thus, nickel is more strongly precipitated and retained at any given concentration. Theoretically, the retention can increase with a rise in the concentration of alkali. However, in the range of concentrations of 1 to 5 M alkali solution used, the differences can be very small. Lead precipitation shows some sensitivity to the alkali concentration and decreases over an increase in the concentration of alkali and can become completely precipitated at 5 molar alkali concentration. The precipitated hydroxide can redissolve if the alkali concentration is greatly increased. Thus, Ni precipitation decreases at higher concentrations of 5M alkali, and a small amount appears in soluble form. Despite all, both metals are retained to a great extent. This confirms the retention of Pb

Table 4: Heavy metal analysis.

Concentration of alkali	Nickle (Ni), mg/L	Lead (Pb), mg/L
1M	BDL	1.11
2M	BDL	0.60
3M	BDL	0.42
4M	BDL	0.34
5M	0.70	BDL
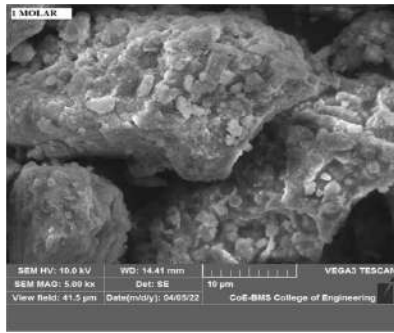
(a) 1 Molar
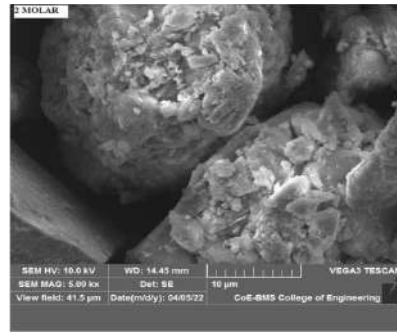
(b) 2 Molar
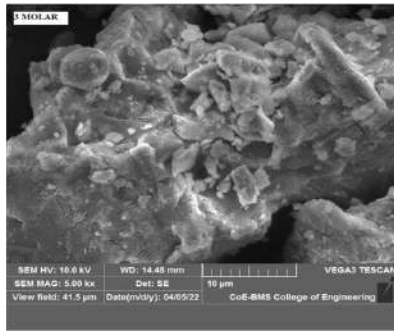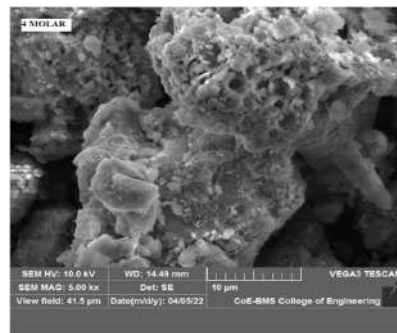
(c) 3 Molar   (d) 4 Molar
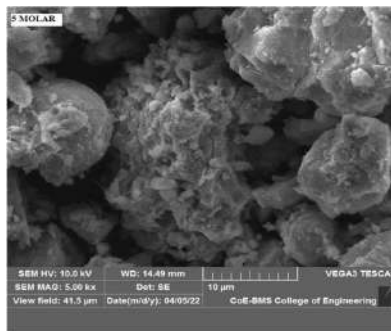
(e) 5 Molar

Fig. 7: SEM images of 60% GGBS and 40% FA mixture with different alkali concentrations after curing for 28 days.

and Ni in the developed barrier material, predominantly by precipitation.

Micro Structural Investigations

An attempt is made to support the above explanations for variations in UCS and tensile strength with varying GGBS content and alkali concentration. An observation on SEM images of various molars at 28 days of curing on the optimized mix shows that at low concentrations of alkali, the gel formation of FA-GGBS mixtures is less, and spherical and clear-edge shaped particles are observed, whereas, at higher molarity, major percent of FA and GGBS particles react and result in gel formation. The new mineralogical formation is maximum for 60% GGBS and 40% FA

at 28 days of curing with higher molarity, as exhibited in Fig. 7.

CONCLUSIONS

Based on the detailed experimental studies conducted on polymerized FA-GGBS with alkali and curing for 28 days for its possible application in the construction of barrier systems in waste containment systems, the following findings are drawn:

- The maximum dry density (MDD) of FA increased with the incorporation of GGBS but the optimum moisture content (OMC) decreased. Generally, it is presumed that higher MDD is preferred, as it generally indicates higher strength and lower settlements.

- Curing the FA-GGBS mixture increases its strength with the length of the curing time. Among all the mixtures, the mixture with 60% GGBS and 40% FA showed the highest strength after curing for 28 days. This has been attributed to the optimal utilization of reactive silica and lime present in FA-GGBS mixtures.

- While the concentration of alkali increases, the UCS increases for all mixtures, which is also the maximum for FA with 60% GGBS.

- The tensile strength of the mixture with 60% GGBS and 40% FA increased by alkali activation using sodium hydroxide due to the polymerization of FA in the existence of alkali.

- The permeability of the barrier material is much lower than the minimum permeability recommended for liners of waste disposal facilities. Permeability declines when the concentration of alkali enhances and the reason behind this is the effective formation of geopolymers.

- Relatively, the rise in tensile of the FA-GGBS mixture is greater than in UCS, this trend becomes particularly vivid at higher concentrations of alkali.

- A substantial decrease in the hydraulic conductivity confirms the predominant effect of polymerization in FA-GGBS mixtures with alkali solutions.

- The formation of cementitious compounds to bind the particles of FA and GGBS to increase the unconfined compressive strength and the polymerization of FA in the presence of sodium hydroxide to enhance tensile strength are qualitatively in tune with the changes observed in both forms of strength and permeability, as indicated from detailed microstructural studies through SEM.

- Batch equilibrium studies revealed effective retention of ionic metal contaminants by precipitation at high alkaline conditions prevailing in the barrier system.

- The studies established the feasibility of FA-GGBS admixture polymerized with alkali as a potential material in barrier systems for waste containment facilities, making it a more sustainable barrier material than conventional natural soil barriers.

REFERENCES

Bellum, R.R., Muniraj, K. and Madduru, S.R.C., 2019. Empirical relationships on mechanical properties of Class-F fly ash and GGBS based geopolymer concrete. *Annales De Chimie, Science Des Matériaux/Annales De Chimie*, 43(3), pp.189–197. https://doi.org/10.18280/acsm.430308.

Cossu, R. and Garbo, F., 2018. Landfill covers. In: *Elsevier eBooks*, pp.649–676.

Deka, A. and Sreedeep, S., 2016. Contaminant retention characteristics of fly ash–bentonite mixes. *Waste Management & Research*, 35(1), pp.40–46. https://doi.org/10.1177/0734242x16670002.

Devarangadi, M. and Shankar, U.M., 2020. Correlation studies on geotechnical properties of various industrial byproducts generated from thermal power plants, iron and steel industries as liners in a landfill- a detailed review. *Journal of Cleaner Production*, 261, 121207. https://doi.org/10.1016/j.jclepro.2020.121207.

Fall, M., Célestin, J. and Sen, H., 2010. Potential use of densified polymer-paste fill mixture as waste containment barrier materials. *Waste Management*, 30(12), pp.2570–2578. https://doi.org/10.1016/j.wasman.2010.07.016.

Ganjian, E., Claisse, P.A., Tyrer, M. and Atkinson, A., 2004a. Selection of cementitious mixes as a barrier for landfill leachate containment. *Journal of Materials in Civil Engineering*, 16(5), pp.477–486.

Ganjian, E., Claisse, P.A., Tyrer, M. and Atkinson, A., 2004b. Preliminary investigations into the use of secondary waste minerals as a novel cementitious landfill liner. *Construction & Building Materials*, 18(9), pp.689–699. https://doi.org/10.1016/j.conbuildmat.2004.04.020.

Herrmann, I., Andreas, L., Diener, S. and Lind, L., 2010. Steel slag used in landfill cover liners: laboratory and field tests. *Waste Management & Research*, 28(12), pp.1114–1121. https://doi.org/10.1177/0734242x10365095.

Hu, W., Nie, Q., Huang, B., Shu, X. and He, Q., 2018. Mechanical and microstructural characterization of geopolymers derived from red mud and fly ashes. *Journal of Cleaner Production*, 186, pp.799–806. https://doi.org/10.1016/j.jclepro.2018.03.086.

Ibrahim, M.A. and Issa, M.A., 2016. Evaluation of chloride and water penetration in concrete with cement containing limestone and IPA. *Construction & Building Materials*, 129, pp.278–288. https://doi.org/10.1016/j.conbuildmat.2016.10.085.

Mishra, A.K. and Ravindra, V., 2015. On the Utilization of Fly Ash and Cement Mixtures as a Landfill Liner Material. *International Journal of Geosynthetics and Ground Engineering*, 1(2). https://doi.org/10.1007/s40891-015-0019-1.

Mukri, M., Zainuddin, A.N., Abdullah, N.A. and Ibrahim, N., 2018. Performance of different percentage on nano-kaolin as additives in soil liner application. *Materials Today: Proceedings*, 5(10), pp.21604–21611. https://doi.org/10.1016/j.matpr.2018.07.009.

Palmer, B.A., 2000. Liners for waste containment constructed with class F and C fly ashes. *Journal of Hazardous Materials*, 76(2–3), pp.193–216.

Qaidi, S., Najm, H.M., Abed, S.M., Ahmed, H.U., Dughaishi, H.A., Lawati, J.A., Sabri, M.M.S., Alkhatib, F. and Milad, A., 2022. Fly Ash-Based Geopolymer Composites: A Review of the Compressive strength and Microstructure analysis. *Materials*, 15(20), 7098. https://doi.org/10.3390/ma15207098.

Sasui, S., Kim, G., Nam, J., Koyama, T. and Chansomsak, S., 2019. Strength and microstructure of Class-C fly ash and GGBS blend geopolymer

activated in NaOH & NaOH + Na2SiO3. *Materials*, 13(1), 59. https://doi.org/10.3390/ma13010059.

Scholz, F. and Kahlert, H., 2015. The calculation of the solubility of metal hydroxides, oxide-hydroxides, and oxides, and their visualisation in logarithmic diagrams. *ChemTexts*, 1(1). https://doi.org/10.1007/s40828-015-0006-0.

Shankar, M.U. and Phanikumar, B.R., 2012. Correlation studies on index properties of fly ash-stabilised expansive clay liners. *Geomechanics and Geoengineering*, 7(4), pp.283–291. https://doi.org/10.1080/17486025.2011.631036.

Sharma, A.K. and Sivapullaiah, P.V., 2016. Strength development in fly ash and slag mixtures with lime. *Proceedings of the Institution of Civil Engineers*. *Ground Improvement*, 169(3), pp.194–205. https://doi.org/10.1680/jgrim.14.00024.

Shen, H., Ren, Y., Huang, M., Zhang, Z. and Lan, J., 2021. Vertical expansion stability of an existing landfill: A case study of a landfill in Xi'an, China. *Advances in Civil Engineering*, 2021, pp.1–14. https://doi.org/10.1155/2021/5574238.

Singh, N., 2018. Fly Ash-Based Geopolymer Binder: a future

construction material. *Minerals*, 8(7), 299. https://doi.org/10.3390/min8070299.

Thakur, G., Singh, Y.P., Gehlot, A., Prakash, C., Saxena, K.K., Pramanik, A., Basak, A. and Shankar, S., 2022. Development of GGBS-Based Geopolymer Concrete Incorporated with Polypropylene Fibers as Sustainable Materials. *Sustainability*, 14(17), 10639. https://doi.org/10.3390/su141710639.

Wattez, T., Patapy, C., Frouin, L., Waligora, J. and Cyr, M., 2021. Interactions between alkali-activated ground granulated blast furnace slag and organic matter in soil stabilization/solidification. *Transportation Geotechnics*, 26, 100412. https://doi.org/10.1016/j.trgeo.2020.100412.

Wilińska, I. and Pacewska, B., 2018. Influence of selected activating methods on hydration processes of mixtures containing high and very high amount of fly ash. *Journal of Thermal Analysis and Calorimetry*, 133(1), pp.823–843. https://doi.org/10.1007/s10973-017-6915-y.

Yawale, A.D. and Patankar, S.V., 2023. Performance of GGBS and SBA in compressed stabilized earth blocks. In: *Composites Science and Technology*, pp.257–267. https://doi.org/10.1007/978-981-19-8979-7_21.

Identification and Functional Annotation of *Echium plantagineum* Metallothioneins for Reduction in Heavy Metals in Soil Using Molecular Docking

Y. S. Rasheed[1†], M. S. AL-Janaby[2] and M. H. Abbas[2]

[1]Department of Biology, College of Science, University of Anbar, Iraq

[2]Department of Biotechnology, College of Science, University of Anbar, Iraq

†Corresponding author: Yousry Sadoon Rasheed; yousry.rasheed@uoanbar.edu.iq

ABSTRACT

Heavy metal contamination in soil poses a significant environmental challenge globally, affecting agricultural productivity and human health. Phytoremediation, using plants to extract and detoxify heavy metals, presents a promising solution. This study investigates the novel potential of *Echium plantagineum*, a metal-tolerant species, in phytostabilization and phytoremediation and explores the role of metallothioneins in heavy metal reduction. A comprehensive literature review identified known metallothioneins involved in heavy metal reduction across various plant species. Moreover, genome annotation and gene prediction of *Echium plantagineum* were performed, predicting a total of 39,520 proteins. This comprehensive protein list facilitates the identification of metallothioneins or other metal-related proteins with potential functional roles in heavy metal tolerance, suggesting new targets to improve the effectiveness of phytoremediation. The sequences of these proteins were utilized to construct a protein BLAST database, against which known metallothioneins protein sequences from other plant species were subjected to BLAST searches, resulting in 41 top hits. Subsequent 3D modeling, structural analysis, protein-metal virtual screening, and functional annotation of the proteins revealed novel high affinities of Ctr copper transporter, zinc/iron permease, and nicotianamine synthase proteins with nickel, zinc, and zinc ion, suggesting their unexplored roles in the uptake of aforementioned ligands. Notably, this study identifies novel metallothioneins proteins in *Echium plantagineum*, highlighting their role in metal tolerance and phytoremediation.

INTRODUCTION

Heavy metals are naturally occurring elements found in the crust of the earth, and some of them are essential for biological processes. However, human activities introduce these metals into aquatic environments (Al-Khashman 2004). The primary sources of heavy metals are industrial activities like mining, foundries, and smelters, as well as diffuse sources such as pipes, products, and the combustion of by-products. These metals can also come from traffic and other human activities (Guvenç et al. 2003). Heavy metals such as copper (Cu), iron (Fe), manganese (Mn), zinc (Zn), cadmium (Cd), arsenic (As), nickel (Ni), cobalt (Co), lead (Pb), aluminum (Al), and mercury (Hg) contamination threatens soil ecosystems, agricultural productivity, and global human health (Rashid et al. 2023).

For instance, Cu and Zn are commonly used in industrial and agricultural applications, while Cd is often found in industrial waste and fertilizers. Metal contamination can result from mining activities and arsenic pesticides, while Pb comes from paints and vehicle emissions (Zaccone et al. 2010). Fe and Mn originate from industrial activities and natural watering processes, whereas Ni and Co may stem from industrial emissions and mining activities (Santana et al. 2020). Coal

combustion and mining are primary sources of Hg pollution, whereas Al causes environmental pollution through soil and water (Shinzato & Hypolito 2016, Streets et al. 2018).

The vague information on potential functions, structures, and properties of plant metallothioneins has resulted in sequence diversity (Freisinger 2009). Metallothioneins belong to the small, cystine-rich family and perform critical functions in regulating metal ions in plants. Similarly, these proteins act as metal chelators to maintain metal homeostasis through metal ion binding (Chatterjee et al. 2020, Joshi et al. 2016, Sharma et al. 2016).

Metallothioneins play a homeostatic role by preventing the accumulation of heavy metals through detoxification (Yaashikaa et al. 2022). Additionally, environmental factors such as oxidative stress and metal exposure to plant tissues are responsible for the higher expression of plant metallothionein genes, indicating their crucial role in metal tolerance (Ahn et al. 2012).

Due to their crucial role in heavy metal detoxification from soil, there is a dire need for the identification, characterization, and functional annotation of novel metallothioneins in plant species. Purple viper's bugloss, or *Echium plantagineum*, is a plant species with a high tolerance to contaminants in polluted soils. (Latini et al. 2022). *Echium plantagineum* tissues aid in soil decontamination by absorbing heavy metals and may have phytoremediation potential due to increased uptake of contaminants and soil microbes (Midhat et al. 2019, Skoneczny et al. 2019, Zine et al. 2020).

A search of the literature revealed no previous studies regarding the presence and role of metallothioneins as hyperaccumulators in Echium plantagineum, even though it exhibits potential regarding phytostabilization. These metallothioneins may be essential for the absorption of heavy metals in soil.

To fill this gap, here we identify, characterize and functionally annotate novel metallothioneins in the model plant, Echium plantagineum. Since hyperaccumulator genes have never been subject of addressing, to analyze the tolerance mechanisms of this plant against various heavy metal ions (Cu, Fe, Mn, Zn, Cd, As, Ni, Co, Pb, Mo, Ca, Fe+2, Fe+3, Mn+2, Zn+2, Al, Hg, and Cr) sequence homology has been used in this study. Moreover, the functional roles and interactions of these metallothioneins highlight the use of Echium plantagineum in heavy metal tolerance. These new metallothionein_genes could serve as transgenes to promote phytoremediation in hyperaccumulating plants.

MATERIALS AND METHODS

An extensive literature review was conducted using Google Scholar and PubMed databases to identify the metallothionein genes across various hyperaccumulator plant species involved in heavy metal reduction in soil. The literature review was performed using both subject terms and free words such as phytoremediation, metal absorption, metal transport, sequestration, soil detoxification, heavy metals, genes, proteins, hyperaccumulators, plants, and metallothioneins.

Sequences and Genomic Annotation Data Retrieval

A genome annotation data file and protein sequences of the literature-identified genes were retrieved from the National Center for Biotechnology Information (NCBI) (Anon n.d.-a) and the UniProt database (Anon n.d.-c). Moreover, the *Arabidopsis thaliana* species was chosen to predict the genes from the genome FASTA file through the AUGUSTUS tool (Stanke 2003), resulting in a General Gesture Format (GFF3) file with predicted genes and their genomic coordinates. NCBI is a repository of biological information and data (Sayers et al. 2021, Pruitt & Sherry 2021), while UniProt is a vast database of annotation data and protein sequences. Similarly, the AUGUSTUS tool is a popular gene prediction software (Keller et al. 2011).

The BLAST Sequence Analysis of *Echium plantagineum*

The BLAST sequence analysis was performed to find homologous genes using protein sequence similarities. BLAST+ package was used to make a protein database for predicted Echium plantagineum proteins. To perform searching of BLAST database, the proteins identified from literature to be involved in metal uptake in other plant species were used as your query. The "blastp" command was then used with additional parameters, which included a maximum of 1 alignment and an e-value cutoff of 1e-30. The E-value is a representation of the quality of the alignment and is defined as the expected number of alignments with the score of S within one database search. The default value is 10, but increasing it increases the number of chance matches and makes the search more strict. For protein-based homology search, the threshold is normally set at $E \leq 1e-5$ with lower values revealing clearer homology with values from 1e-25 (Choudhuri 2014). KinG was run with (-E 1e-30), this is a very low E-value threshold, meaning that it only returns the most significant hits, so this is good for applications like finding homologous proteins, or functional annotation. Also, restricting alignments to one essentially ensures that only the best match for each query sequence is displayed; the highest scoring hit per protein is known. The end results were then

arranged in table format, while hit identifiers were stored separately in a text file. Additionally, it was used to retrieve top hits from the protein database utilizing the "blastdbcmd" command tool of the NCBI BLAST+ (Anon 2021). This study has retrieved homologs of metal uptake-associated proteins from the Echium plantagineum species.Structural Prediction of Homologs and Functional Annotation

The next step involved predicting the 3D structures of the identified protein sequences. This was accomplished by utilizing Omegafold, a well-known 3D modeling tool for its accuracy in *ab initio* protein structure prediction (Wu et al. 2022). OmegaFold can handle protein sequences as long as 4096 residues when running on an NVIDIA A100 Graphics card with 80 GB of memory (Anon n.d.-b). However, due to limitations in computational resources, sequences larger in length (>1500 amino acids) were predicted through SWISS-MODEL (Waterhouse et al. 2018), a widely used homology modeling tool that leverages experimentally resolved homologous protein structures as templates. To functionally annotate the novel proteins, BLAST web-based search against other plant organisms was performed, whereas if no homologous sequences were found, InterPro database searching was performed to identify protein family or domain based on sequence search. InterPro is an extensive repository of protein families, superfamilies, and domains (Paysan-Lafosse et al. 2023).

Ligand Retrieval and Virtual Screening

Structures of ligands (Cu, Fe, Mn, Zn, Cd, As, Ni, Co, Pb, Mo, Ca, Fe^{+2}, Fe^{+3}, Mn^{+2}, Zn^{+2}, Al, Hg, and Cr) were retrieved from the PubChem database (PubChem n.d.), a chemical repository (Burley et al. 2023). The canonical SMILES for each ligand were retrieved and converted into *pdb.file* format through the *rdkit* library in Python. RDkit

Table 1: The metallothionein genes and their metal uptake in their respective species.

Genes	Organism/Genus	Metals
PgIREG1	*Psychotria gabriellae*	Ni
AtNRAMP1, MATE, FRD3	Arabidopsis	Mn, Fe, AI
AhZIP6, HMA4, NAS2	*Arabidopsis halleri*	Cd, Zn
COPT1, COPT5, AtMTP8, AtZIP1, AtMTP1, AtABCC3, AtVIT1, AtZIP1, AtCAX3, TpNRAMP5, IRT1, NRAMP1, PvACR3, AtZIP2, COPT1, CMT1, AtPIC1, HMA1, PAA1, YSL4, YSL6, PAA2, HMA8, PAM71, FRO3, MOT1, AtATM3, AtNRAMP6, RAN1, AtIRT2, AtECA3, MTP11, PAM71, ZTP29, AtIRT1, HMA2, HMA3, HMA4, AtHMA2, AtHMA4, AtABCC1, AtABBC2, AtPCR2, AtYSL1, AtYSL3, HMA4, NAS2	*Arabidopsis thaliana*	Mn, Zn, Cd, Fe, Co, As, Cu, Mo, Pb, Ca, Hg
BcIRT1, BcABCC1, BcABCC2	*Brassica chinensis*	Cd
NRAMP, BnMTP3	*Brassica napus*	Zn, Mn, Cd, Pb
CsMTP8.2	*Camellia sinensis*	Fe, Mn, Zn
bHLH, C2H2, ERF, bZIP, GRAS, MYB	*Cunninghamia lanceolata*	Al
ALS1, ART1, STOP, STAR1, STAR2, ALS3, FtFRDL1, FtFRDL2, MTPC2, PCSL, PCS	*Fagopyrum tataricum*	Al
PbMTP8.1	*Pyrus*	Mn
GmHMA8, GmHMA3, GmZIP1	*Glycine max*	Cd, Cu
HvHMA1, HvIRT1, HvZIP3, HvZIP5, HvZIP5	Hordeum vulgare	Zn, Cu, Fe^{+2}, Fe^{+3}, Mn^{+2}, Zn^{+2}
SOD, GST, IRT, CDFs, WRKY, ERFs, POD	*Medicago sativa*	Pb
MtVTL4, MtVTL8, TaVTL2, TaVTL3	*Medicago truncatula*	Fe, Co
NtMTP2, MTP1, AhNRAMP1, NtPIC1	Nicotiana tabacum	Co, Ni, Mn, Zn, Fe
IREG2	*Noccaea japonica*	Ni
OsHMA3, OsMTP1, OsABCC1, OsLCT1, OsHMA2, OsZIP3, OsZIP1, OsHMA5, OsNRAMP1, ARG1, MIT, OsIRT1, OsZIP4, OsNRAMP5, MAPK, YSL	*Oryza sativa*	Cd, Zn, As, Cu, Co, Ni, Fe, Mn, Cr, Fe^{+2}, Fe^{+3}, Mn^{+2}, Zn^{+2}
SaHMA3	*Sedum alfredii Hance*	Cd
SpHMA3	*Sedum plumbizincicola*	Cd
TaCT1	*Triticum aestivum*	Cu
ZmFDR4, ZmmCHAA1, ZmZLP1, YSL, ZmNAS4, ZmNAS2, ZmNAS9	*Zea mays*	Fe, Mn, Zn, Pb

Table 2: The genes of different species aligned with the gene sequences of the Echium database.

Species	Genes	Identifiers (*Echium plantagineum*)
Arabidopsis thaliana	YSL6	g10948
Arabidopsis thaliana	YSL1	g11126
Oryza sativa	IRT1	g11754
Arabidopsis thaliana	CAX3	g12062
Arabidopsis thaliana	ABCB25	g13956
Arabidopsis thaliana	HMA1	g14577
Brassica napus	RING-type E3 ubiquitin transferase	g14584
Cunninghamia lanceolata	MYB1	g14711
Oryza sativa	HMA5	g15210
Arabidopsis thaliana	COPT1	g18528
Arabidopsis thaliana	ABCC1	g18885
Arabidopsis thaliana	MTP11	g19065
Oryza sativa	ZIP1	g20449
Arabidopsis thaliana	CMT1	g21210
Arabidopsis thaliana	ZTP29	g21375
Oryza sativa	OsNramp5	g21607
Arabidopsis thaliana	DTX43	g22946
Arabidopsis thaliana	ABCC3	g24041
Oryza sativa	ZIP3	g24118
Arabidopsis thaliana	MTPC3	g25342
Arabidopsis thaliana	TIC21	g27043
Oryza sativa	MTP1	g28609
Arabidopsis thaliana	NRAMP1	g31075
Arabidopsis thaliana	HMA2	g33157
Arabidopsis thaliana	MTP1	g33971
Arabidopsis thaliana	DTX42	g34339
Oryza sativa	ARG1	g346
Arabidopsis thaliana	NAS2	g35440
Triticum aestivum	CT1-5B	g3625
Arabidopsis thaliana	PAA2	g36529
Arabidopsis thaliana	ECA3	g38544
Arabidopsis thaliana	PAM71	g38741
Arabidopsis thaliana	COPT5	g4534
Arabidopsis thaliana	MOT1	g4715
Medicago sativa	WRKY33	g4892
Oryza sativa	ZIP4	g4949
Arabidopsis thaliana	PCR2	g539
Arabidopsis thaliana	VIT1	g560
Arabidopsis thaliana	FRO3	g5731
Arabidopsis thaliana	PAA1	g7401
Arabidopsis thaliana	RAN1	g78

library is extensively utilized for molecular representation, substructure searching, and property prediction (Kunnakkattu

et al. 2023). The virtual screening of the shortlisted proteins against heavy metals was performed using the GNINA tool, which utilizes an ensemble of convolutional neural networks (CNNs) as a scoring function (McNutt et al. 2021). Grid box coordinates were specified to guide the GINNA tool during molecular docking, facilitating the interaction analysis between proteins and heavy metal compounds. Moreover, the top complexes for each ligand were characterized by the best binding affinity scores. Additionally, PyMOL (The PyMOL Molecular Graphics System, Version 2.0 Schrödinger, LLC) facilitated the visualization of the docked complexes (Yuan et al. 2017). The top 3 proteins were shortlisted for each ligand.

RESULTS AND DISCUSSION

An extensive literature review was performed to identify the genes involved in the metal uptake in different species. A total of 129 genes were identified that are involved in the metal uptake in 19 different species and two genera (*Arabidopsis* and *Pyrus*). Furthermore, the literature review revealed different species involved in the uptake of different metals, such as Cu, Fe, Mn, Zn, Cd, As, Ni, Co, Pb, Mo, Ca, Fe^{+2}, Fe^{+3}, Mn^{+2}, Zn^{+2}, AI, Hg, and Cr. The metallothionein genes and their metal uptake in their respective species are mentioned in Table 1.

Genomic Annotation Data for *Echium plantagineum*, Sequence Retrieval, and Sequence Alignment Through BLAST

The GFF3 files of *Echium plantagineum* were not available on the NCBI, Ensembl Plants, and Phytozome databases as the genomic annotation of this plant has not been done previously; therefore, genome sequences file of *Echium plantagineum* in FASTA format was retrieved from the NCBI and used in the AUGUSTUS tool for gene prediction of *Echium plantagineum*. AUGUSTUS predicted a total of 39,520 protein sequences given the *Echium plantagineum* genome FASTA file, while *Arabidopsis* was used as a model organism for the prediction.

Furthermore, the protein sequences of the identified genes from the literature review were retrieved using the UniProt database. A total of 70 sequences were retrieved out of 129 genes in different species from the UniProt database due to the unavailability of specific protein sequences. The literature-retrieved protein sequences were searched against the BLAST database for *Echium plantagineum*. The database search through BLAST resulted in 41 hits. The identifiers and gene names of aligned sequences are mentioned in Table 2.

3D Structure Prediction of Homologous Sequences

OmegaFold and SWISS-MODEL were used for the 3D

protein structure prediction of the 41 aligned sequences, while 24 structures were predicted using OmegaFold and 17 with SWISS-MODEL. The proteins such as g19065, g24041, g33157, g4949, and g27043, which were predicted using SWISS-MODEL, did not show full coverage with the templates, and their partial structures were retrieved after modeling. The protein structures predicted through SWISS-MODEL and OmegaFold are mentioned in Table 3.

Functional Annotation of the Homologous Sequences

The 41 predicted gene structures of *Echium plantagineum* underwent analysis using web-based servers such as BLAST and InterPro to identify their respective gene or protein domain/family names. Among these, 21 gene names were successfully identified through BLAST searches, whereas sequences that did not yield matches via BLAST, an InterPro sequence search was conducted, leading to the identification of 20 protein family/domain names for these sequences. The gene and protein family/domain names are mentioned in Table 4.

Retrieval of the Ligands and Virtual Screening

The ligands (metals) identified through the literature review were retrieved using the PubChem database. A total of 18 ligands, including Cu, Fe, Mn, Zn, Cd, As, Ni, Co, Pb, Mo, Ca, Fe^{+2}, Fe^{+3}, Mn^{+2}, Zn^{+2}, Al, Hg, and Cr, were retrieved in SMILES format and converted to pdb format. The ligands, their PubChem IDs, and SMILES are mentioned in Table 5.

Table 3: The protein sequences predicted using SWISS-MODEL, showing sequence coverage and sequence identity.

Proteins	Sequence Length	Coverage	Sequence Identity
g10948	646	4-646	82.06%
g11126	664	3-664	75.64%
g15210	989	1-989	75.94%
g19065	1239	839-1238	86.62%
g24041	1907	13-1329	70.99%
g33157	1078	7-691	70.45%
g36529	928	17-927	72.94%
g38544	959	1-959	84.15%
g4949	1146	130-666	11.38%
g7401	958	1-957	71.31%
g18885	1640	1-1639	73.70%
g13956	827	3-827	75.20%
g14584	839	1-839	70.11%
g21210	878	91-868	53.77%
g14577	762	1-760	72.16%
g27043	743	4-555	78.68%
g5731	647	1-647	70.70%

Table 4: The gene and protein family/domain names of the predicted structures.

BLAST Search	
Predicted Genes Identifiers	Identified Gene Names
g10948	HvYS1
g11126	HvYS1
g13956	ABCB25
g14577	PAA1
g14584	UBC core domain-containing protein
g14711	WER
g15210	AHA2
g18885	ABCB25
g21210	MET2A
g21607	101781512
g24041	ABCB19
g31075	101781512
g33157	HMA4
g346	ARGAH1
g3625	STP10
g36529	PAA2
g38544	AHA2
g38741	DIR6
g4892	WRKY4
g7401	PAA1
g78	RABF2B
InterPro Sequence Search	
Predicted Genes Identifiers	Identified Protein Family/Domains
g33971	Cation efflux protein
g35440	Nicotianamine synthase
g12062	Calcium/proton exchanger
g27043	Na(+)/H(+) antiporter NhaD-like
g539	PLAC8 motif-containing protein
g18528	Ctr copper transporter
g4949	Meiosis specific protein Spo22/ZIP4/TEX11
g560	Ccc1 family
g21375	Zinc/iron permease
g28609	Cation efflux protein
g34339	Multi-antimicrobial extrusion protein
g4715	Molybdate transporter 1/2
g4534	Ctr copper transporter
g25342	Cation efflux protein
g20449	Zinc/iron permease
g19065	Cation efflux protein
g24118	Zinc/iron permease
g5731	Cytochrome b245, heavy chain
g11754	Zinc/iron permease
g22946	Multi-antimicrobial extrusion protein

The virtual screening of the 41 predicted protein structures with 18 ligands was performed using the molecular docking tool Gnina. It resulted in 738 dockings with various binding affinities ranging from -1.05 kcal/mol to -1.91 kcal/mol. The top 5 best binding affinities were shown by the same protein, HvYS1, with Fe, Hg, Mo, As, and Mn, all showing the binding affinities of -1.91 kcal/mol. Notably, the Ctr copper transporter (g4534), Zinc/iron permease (g21375), and Nicotianamine synthase (g35440) proteins were shortlisted based on their specific interactions with the ligands Ni, Zn, and Zn^{+2}, with affinity scores of -1.7, -1.68, and -1.67, respectively. However, the remaining proteins did not exhibit any interaction with any of the nine poses of ligands. The interacting proteins, their corresponding ligands, and the affinity scores are listed in Table 6. Additionally, the zoomed view of the interacting proteins screened against the Ni, Zn, and Zn^{+2} ligands is illustrated in Fig. 1.

Protein-ligand interaction analysis was performed to gain insights into the interacting residues that contribute to the binding of shortlisted interacting proteins with Ni, Zn, and Zn^{+2}. The nicotianamine synthase protein exhibited binding interactions with Ni, Zn, and Zn^{+2} at the same residues: 181A (ALA), 179A (HIS), and 153A (ASP). Similarly, the zinc/iron permease exhibited binding at residues 52A (ALA), 53A (HIS), 47A (SER), and 50A (ASP) with all three ligands. Lastly, the Ctr copper transporter protein interacted with Ni at residues 20A (THR), 11A (VAL), and 9A (ARG).

Table 5: The ligands, PubChem IDs and SMILES.

Ligands	PubChem IDs	SMILES
Cu	23978	[Cu]
Fe	23925	[Fe]
Mn	23930	[Mn]
Zn	23994	[Zn]
Cd	23973	[Cd]
As	5359596	[As]
Ni	935	[Ni]
Co	104730	[Co]
Pb	5352425	[Pb]
Mo	23932	[Mo]
Ca	5460341	[Ca]
Fe^{+2}	27284	[Fe+2]
Fe^{+3}	29936	[Fe+3]
Mn^{+2}	27854	[Mn+2]
Zn^{+2}	32051	[Zn+2]
Al	5359268	[Al]
Hg	23931	[Hg]
Cr	23976	[Cr]

Table 6: Binding affinities of interacting proteins against Ni, Zn, and Zn^{+2}.

Ligand	Protein	Affinity
Ni	Ctr copper transporter (g4534)	-1.7
	Zinc/iron permease (g21375)	-1.68
	Nicotianamine synthase (g35440)	-1.67
Zn	Ctr copper transporter	-1.7
	Zinc/iron permease	-1.68
	Nicotianamine synthase	-1.67
Zn+2	Ctr copper transporter	-1.7
	Zinc/iron permease	-1.68
	Nicotianamine synthase	-1.67

Moreover, the Ctr copper transporter protein also displayed interactions with Zn and Zn^{+2} at residues 100A (ALA), 101A (VAL), 105A (ASN), 104A (TYR), and 103A (SER). The protein-ligand interactions are illustrated in Fig. 2.

Protein Domain Analysis and Functional Annotation

The shortlisted proteins were then functionally annotated through InterPro. It was observed that the g4534 protein has a Ctr copper transporter domain from 1-131 residues, whereas the g21375 protein has a Zinc/iron permease domain spanning 11-253. Contrary to this, it was observed that in the g35440 protein, almost the entirety of the protein length is covered by the Nicotianamine synthase domain. The domains are illustrated in Fig. 3. Furthermore, the functional annotation through Gene Ontology revealed key functional aspects of these proteins, such as the metal ion transmembrane transporter activity of g21375 protein, indicating a metal ion transport functionality of the protein, Fig. 3. This means that the protein is capable of transporting metal ions across cell membranes. In plants, metal ion transporters play crucial roles in regulating the uptake, distribution, and storage of essential metal ions such as iron, zinc, manganese, and copper. These transporters are essential for maintaining metal ion homeostasis and ensuring that plants supply these nutrients adequately without experiencing toxicity from excess metal ions.

Moreover, the g35440 protein has nicotianamine synthase activity. Nictioanamine is involved in plant metal detoxification processes, particularly in the chelation (binding) of heavy metals such as nickel, cadmium, and zinc. Plants can take up heavy metals from the soil, either through their roots or other mechanisms, and high concentrations of these metals can be toxic to the plant. Nictioanamine synthase activity allows the plant to produce nictioanamine, which can bind to heavy metals and form stable complexes, reducing their toxicity and facilitating their sequestration or removal from the plant's tissues. Contrary to this, the g4534 protein

Nickel (Ni)

(a) g4534-Ni

(b) g21375-Ni

(c) g35440-Ni

Zinc (Zn)

(d) g4534-Zn

(e) g21375-Zn

(f) g35440-Zn

Zinc (II) ion (Zn+2)

(g) g4534-Zn+2

(h) g21375-Zn+2

(i) g35440-Zn+2
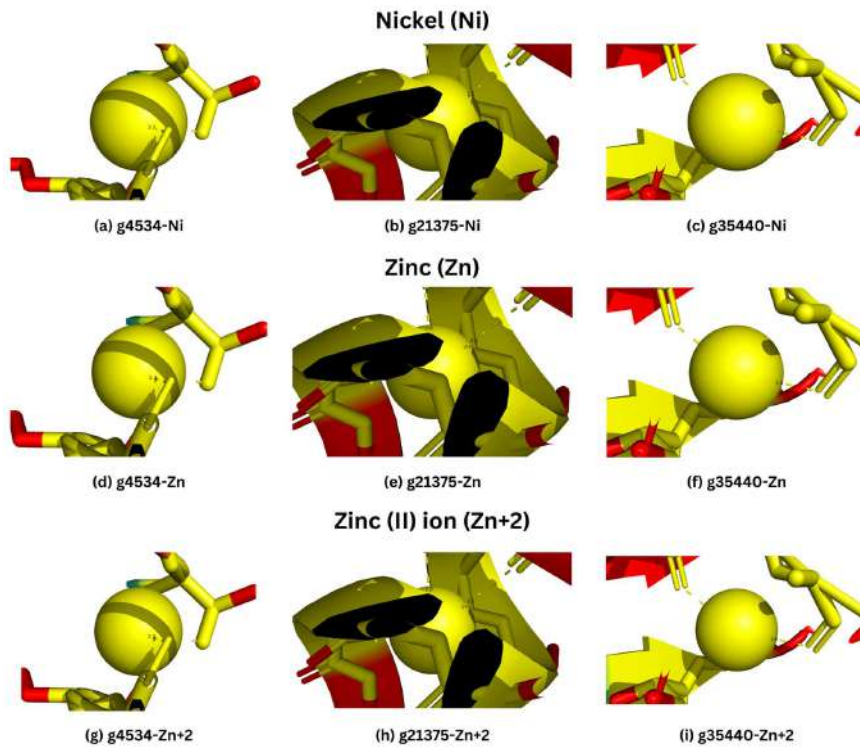
Fig. 1: The zoomed view illustration of interacting protein structures screened against Ni, Zn, and Zn^{+2}.

Nickel (Ni)

(a) g4534-Ni

(b) g21375-Ni

(c) g35440-Ni

Zinc (Zn)

(d) g4534-Zn

(e) g21375-Zn

(f) g35440-Zn

Zinc (II) ion (Zn+2)

(g) g4534-Zn+2

(h) g21375-Zn+2

(i) g35440-Zn+2
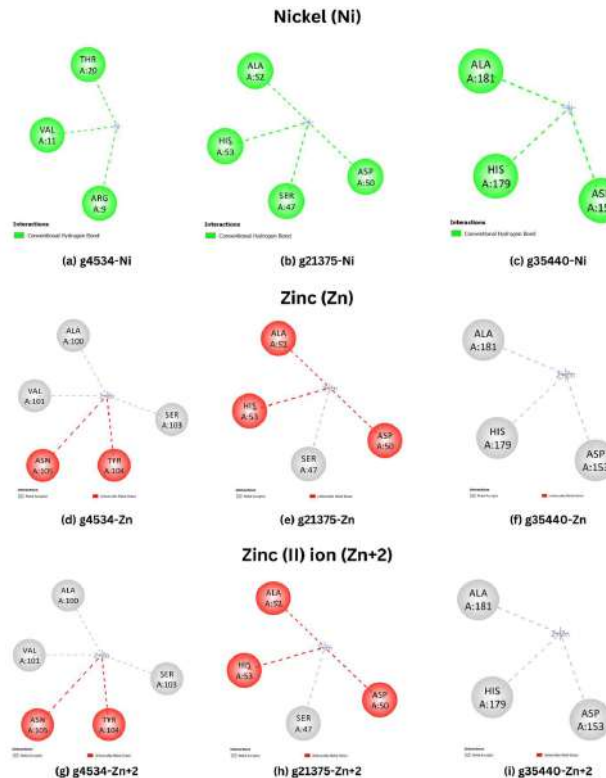
Fig. 2: 2D illustration of interactions of shortlisted interacting proteins with Ni, Zn, and Zn^{+2}.
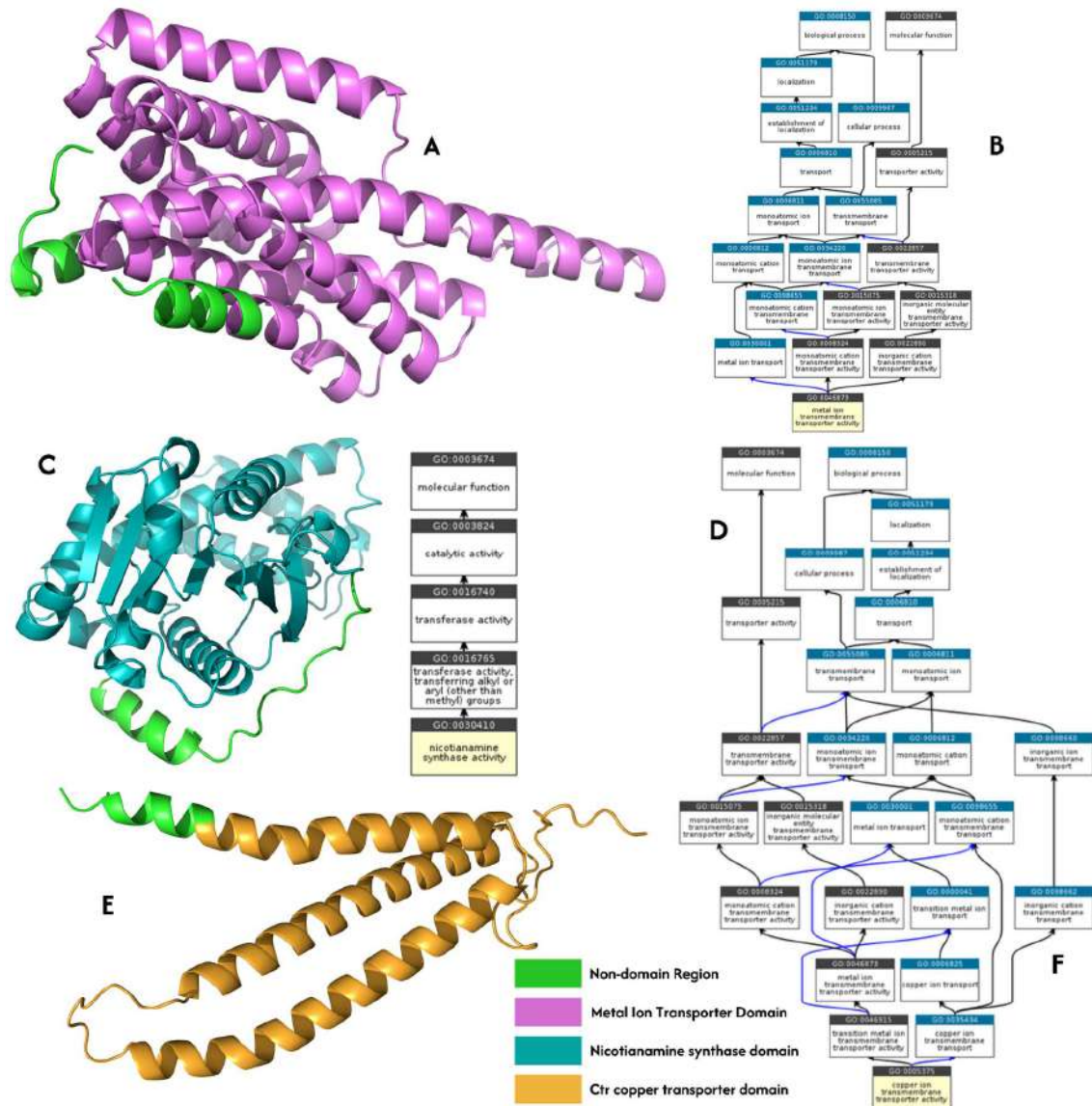
Fig. 3: Illustration of the identified domains with potential phytoremediation role and GO functions. (A) g21375 protein with its metal ion transporter domain (B) GO biological process and molecular functions of g21375 protein (C) g35440 protein with its nicotianamine synthase domain (D) GO biological process and molecular functions of g35440 protein (E) g4534 protein with its Ctr copper ion domain (F) GO biological process and molecular functions of g4534 protein.

has a Ctr copper transmembrane transporter activity. This protein is capable of transporting copper ions across cell membranes. In plants, copper is an essential micronutrient, but excessive copper can be toxic. Copper transporters, like the one encoded by the g4534 gene, play a crucial role in maintaining copper homeostasis by regulating the uptake, distribution, and storage of copper ions within the plant.

Discussion

Soil heavy metal contamination has emerged as a global environmental challenge, drawing significant public attention due to worries about the safety of agricultural products. Heavy metals encompass metallic elements and metalloids known for their potential biological harm, including cadmium, mercury, arsenic, lead, and chromium (Mitra et al. 2022). Understanding the metabolic responses and adaptations of plants to toxic metal exposure is critical for advancing phytoremediation efforts in contaminated areas (Alsafran et al. 2022).

Phytoremediation has emerged as a promising alternative

to traditional methods due to its cost-effectiveness, environmental friendliness, and aesthetic appeal. Thus far, approximately 500 plant species have been identified as hyperaccumulators of one or more metals, harnessing their natural extraction abilities (Li et al. 2019). However, further exploration is necessary, integrating biotechnological strategies with comprehensive multidisciplinary research to enhance plant tolerance and reduce the accumulation of toxic metals in soil.

Therefore, a comprehensive literature review was conducted to identify metallothioneins across diverse plant species (*Psychotria gabriellae, Arabidopsis halleri, Brassica chinensis, Camellia sinensis, Cunninghamia lanceolata, Fagopyrum tataricum, Pyrus, Hordeum vulgare, Medicago truncatula, Nicotiana tabacum, Noccaea japonica, Sedum alfredii,* and *Sedum plumbizincicola*) involved in the reduction of heavy metals, such as Ni, Mn/Mn^{+2}, Fe/Fe^{+2}/Fe^{+3}, Al, Cd, Zn/Zn^{+2}, Co, As, Cu, Mo, Pb, Ca, Hg, Cr in soil (Angulo-Bejarano et al. 2021, Jan & Parray 2016, Jogawat et al. 2021).

Notably, *Echium plantagineum*, a metal-tolerant species exhibiting a notably high Bioconcentration Factor (BCF) and low Translocation Factor (TF), holds the potential for phytostabilization purposes (El Berkaoui et al. 2021). Despite the promising potential of *Echium plantagineum* for phytostabilization, no previous study has investigated the presence or role of metallothioneins in this species, which could potentially be involved in the uptake of heavy metals from the soil.

However, the *Echium plantagineum* does not have enough proteome and genome resources available on public databases, a major limitation in identifying metallothioneins or metal uptake-related proteins from this plant. Consequently, this study highlights the novelty and significance of investigating the metallothioneins of *Echium plantagineum* by predicting the genes and proteins from the entire genome, resulting in 39,520 predicted protein sequences. However, *Arabidopsis thaliana* was used as the reference genome due to its fully sequenced genome and its regulatory mechanisms in genomics, transcriptomics, and proteomics comparable to other plant species (Di Silvestre et al. 2018). These predicted protein sequences were systematically compiled to construct a protein database. This database was subsequently employed for BLAST search against the 70 protein sequences of 129 genes identified from the literature review across different plant species, resulting in 41 top hits.

Moreover, the 41 protein structures of these top hits were subsequently predicted and subjected to screening against 15 ligands, identifying only Ctr copper transporter, zinc/iron permease, and nicotianamine synthase proteins exhibiting high affinity and interactions with Ni, Zn, and Zn+2 ligands.

Copper homeostasis is maintained (absorption, transportation, and growth) by the copper transporter family (COPT/Ctr) in plants (Nayeri et al. 2023, Wang et al. 2021). However, functional characterization of these copper transporter protein-encoding COPT genes has only been conducted in Arabidopsis and Oryza sativa (Wang et al. 2018). Therefore, here we show that the COPT/Ctr copper transporter protein has an unprecedented high affinity toward Ni, Zn, and Zn + 2 ligands of which this protein may have other essential applications apart from the classical copper transporter protein.

Metal ion transport in the body often involves future zip family, such as zinc/iron permease, which mainly mediate transition metal ions influx, including both zinc and iron. Besides Zn+2, ZIP transporters are also known to mediate the transport of several other transition metal cations, such as Mn+2, Fe+2, Cd+2, and Ni+2 (Ajeesh Krishna et al. 2020, Zhao & Zhou 2020). Increased Zn uptake (relative to non-hyperaccumulator species), and increased expression of some members of the ZIP family of transporters in Zn hyperaccumulators (Thlaspi caerulescens and Arabidopsis halleri) positively co-relate with increased Zn accumulation (Yan et al. 2020). The lack of citations regarding the zinc/iron permease role inside this hyperaccumulator means that this study is unrivalled and provides evidence that this transporter was also involved in Ni, Zn and Zn+2 uptake in this species of plant known as Echium plantagineum.Furthermore, nicotianamine (NA) serves as a primary metal chelator in plants and is synthesized catalytically by nicotianamine synthase. Nicotianamine synthase genes have been identified in various plant species, including *Oryza sativa, Zea mays, Hordeum vulgare, Triticum aestivum, Arabidopsis thaliana, Arabidopsis halleri, Solanum lycopersicum, Noccaea caerulescens*, and *Malus xiaojinensis*. Studies have demonstrated that overexpression of nicotianamine synthase in transgenic plants increases NA concentration, consequently elevating metal concentration. Specifically, the nicotianamine synthase gene from *N. caerulescens* enhances nickel accumulation in transgenic *Arabidopsis thaliana*, indicating its potential for improving divalent metal ion content and uptake, particularly in contaminated soil (Chen et al. 2019). Thus, the nicotianamine synthase can reduce the heavy metal toxicity from the contaminated soils (Nozoye 2018). Additionally, this study reveals that the nicotianamine synthase protein has a novel high affinity with ligands Ni, Zn, and Zn^{+2}, highlighting potential roles in phytoremediation.

Conclusively, this study identified the role of *Echium plantagineum* in heavy metal stress in contaminated soils.

Metallothioneins essential for heavy metal reduction were identified through a comprehensive literature review and BLAST search. Key proteins such as Ctr copper transporter, zinc/iron permease, and nicotianamine synthase were found to have novel high affinities with Ni, Zn, and Zn+2 metal ions, indicating their role in metal uptake and transport. This study underscores the functional annotation of metallothioneins of *Echium plantagineum* for reduction in heavy metals in soil, paving the way for future research and environmental applications.

CONCLUSIONS

In conclusion, the intricate interplay between *Echium plantagineum* and the heavy metal stress in contaminated soils was identified in this study. Metallothioneins essential for heavy metal reduction in various plant species were identified through a literature review, and BLAST was searched against plant gene sequences, identifying 41 top hits. Notably, screening these hits against ligands revealed novel high affinities of key proteins such as Ctr copper transporter, zinc/iron permease, and nicotianamine synthase with Ni, Zn, and Zn^{+2}, implying their role in metal uptake and transport. Hence, this study identified for the first time the functional annotation of the metallothioneins in the *Echium plantagineum* involved in reducing heavy metals from the soil, paving the way for future research and environmental applications.

REFERENCES

Ahn, Y.O., Kim, S.H., Lee, J., Kim, H., Lee, H.-S. and Kwak, S.S., 2012. Three Brassica rapa metallothionein genes are differentially regulated under various stress conditions. *Molecular Biology Reports*, 39(3), pp.2059–2067. doi: 10.1007/s11033-011-0953-5.

Ajeesh Krishna, T.P.A., Maharajan, T., Roch, G.V., Ignacimuthu, S. and Ceasar, S.A., 2020. Structure, function, regulation, and phylogenetic relationship of ZIP family transporters of plants. *Frontiers in Plant Science*, 11, p.662. doi: 10.3389/fpls.2020.00662.

Al-Khashman, O.A., 2004. Heavy metal distribution in dust, street dust and soils from the workplace in Karak Industrial Estate, Jordan. *Atmospheric Environment*, 38(39), pp.6803–6812. doi: 10.1016/j.atmosenv.2004.09.011.

Alsafran, M., Usman, K., Ahmed, B., Rizwan, M., Saleem, M.H. and Al Jabri, H., 2022. Understanding the phytoremediation mechanisms of potentially toxic elements: A proteomic overview of recent advances. *Frontiers in Plant Science*, 13, p.881242. doi: 10.3389/fpls.2022.881242.

Angulo-Bejarano, P.I., Puente-Rivera, J. and Cruz-Ortega, R., 2021. Metal and metalloid toxicity in plants: An overview on molecular aspects. *Plants*, 10(4), p.635. doi: 10.3390/plants10040635.

Anon, 2021. Extracting data from BLAST databases with Blastdbcmd. in *BLAST® Command Line Applications User Manual* [online]. National Center for Biotechnology Information (US). Available at https://www.ncbi.nlm.nih.gov/sites/books/NBK569853/

Anon, n.d.-a. National Center for Biotechnology Information. Retrieved June 25, 2024. from: https://www.ncbi.nlm.nih.gov/.

Anon, n.d.-b. OmegaFold/README.md at main · HeliXonProtein/OmegaFold. GitHub. Retrieved June 25, 2024, from https://github.com/HeliXonProtein/OmegaFold/blob/main/README.md.

Anon, n.d.-c. UniProt. Retrieved June 25, 2024, from https://www.uniprot.org/.

Burley, S.K., Bhikadiya, C., Bi, C., Bittrich, S., Chao, H., Chen, L., Craig, P.A., Crichlow, G.V., Dalenberg, K., Duarte, J.M., Dutta, S., Fayazi, M., Feng, Z., Flatt, J.W., Ganesan, S., Ghosh, S., Goodsell, D.S., Green, R.K., Guranovic, V., Henry, J., Hudson, B.P., Khokhriakov, I., Lawson, C.L., Liang, Y., Lowe, R., Peisach, E., Persikova, I., Piehl, D.W., Rose, Y., Sali, A., Segura, J., Sekharan, M., Shao, C., Vallat, B., Voigt, M., Webb, B., Westbrook, J.D., Whetstone, S., Young, J.Y., Zalevsky, A. and Zardecki, C., 2023. RCSB Protein Data Bank (RCSB.org): Delivery of experimentally determined PDB structures alongside one million computed structure models of proteins from artificial intelligence/machine learning. *Nucleic Acids Research*, 51(D1), pp.D488–D508. doi: 10.1093/nar/gkac1077.

Chatterjee, S., Kumari, S., Rath, S., Priyadarshanee, M. and Das, S., 2020. Diversity, structure, and regulation of microbial metallothionein: Metal resistance and possible applications in sequestration of toxic metals. *Metallomics*, 12(11), pp.1637–1655. Doi: 10.1039/d0mt00140f.

Chen, S., Zhang, M., Feng, Y., Sahito, Z.A., Tian, S. and Yang, X., 2019. Nicotianamine synthase gene 1 from the hyperaccumulator *Sedum alfredii* hance is associated with Cd/Zn Tolerance and Accumulation in Plants. *Plant and Soil*, 443(1), pp.413–427. doi: 10.1007/s11104-019-04233-4.

Choudhuri, S., 2014. *Bioinformatics for Beginners*. Academic Press, pp. 133–155.

Di Silvestre, D., Bergamaschi, A., Bellini, E. and Mauri, P.L., 2018. Large-scale proteomic data and network-based systems biology approaches to explore the plant world. *Proteomes*, 6(2), p.27. doi: 10.3390/proteomes6020027.

El Berkaoui, M., El Adnani, M., Hakkou, R., Ouhammou, A., Bendaou, N. and Smouni, A., 2021. Phytostabilization of phosphate mine wastes used as a store-and-release cover to control acid mine drainage in a semiarid climate. *Plants*, 10(5), p.900. doi: 10.3390/plants10050900.

Freisinger, E., 2009. Metallothioneins in Plants. In *Metallothioneins and Related Chelators* (pp. 107-153). RCB Publishing

Guvenç, N., Alagha, O. and Tuncel, G., 2003. Investigation of soil multi-element composition in Antalya, Turkey. *Environment International*, 29(5), pp.631–640. doi: 10.1016/S0160-4120(03)00046-1.

Jan, S. and Parray, J.A., 2016. *Heavy Metal Uptake in Plants*. Springer, pp.1-18.

Jogawat, A., Yadav, B., Chhaya, and Narayan, O.P., 2021. Metal Transporters in Organelles and Their Roles in Heavy Metal Transportation and Sequestration Mechanisms in Plants. *Physiologia Plantarum*, 173(1), pp.259–275. doi: 10.1111/ppl.13370.

Joshi, R., Pareek, A. and Singla-Pareek, S.L., 2016. *Plant Metal Interaction*. Elsevier, pp. 239–261.

Keller, O., Kollmar, M., Stanke, M. and Waack, S., 2011. A novel hybrid gene prediction method employing protein multiple sequence alignments. *Bioinformatics*, 27(6), pp.757–763. doi: 10.1093/bioinformatics/btr010.

Kunnakkattu, I.R., Choudhary, P., Pravda, L., Nadzirin, N., Smart, O.S., Yuan, Q., Anyango, S., Nair, S., Varadi, M. and Velankar, S., 2023. PDBe CCDUtils: An RDKit-based toolkit for handling and analyzing small molecules in the protein data bank. *Journal of Cheminformatics*, 15(1), p.117. doi: 10.1186/s13321-023-00786-w.

Latini, A., Papagni, I., Gatti, L., De Rossi, P., Campiotti, A., Giagnacovo, G., Mirabile Gattia, D. and Mariani, S., 2022. Echium vulgare and Echium plantagineum: A comparative study to evaluate their inclusion in Mediterranean urban green roofs. *Sustainability*, 14(15), p.9581. doi: 10.3390/su14159581.

Li, C., Zhou, K., Qin, W., Tian, C., Qi, M., Yan, X. and Han, W., 2019. A review on heavy metals contamination in soil: Effects, sources, and remediation techniques. *Soil and Sediment*

Contamination: An International Journal, 28(4), pp.380–394. doi: 10.1080/15320383.2019.1592108.

McNutt, A.T., Francoeur, P., Aggarwal, R., Masuda, T., Meli, R., Ragoza, M., Sunseri, J. and Koes, D.R., 2021. GNINA 1.0: Molecular docking with deep learning. *Journal of Cheminformatics*, 13(1), p.43. doi: 10.1186/s13321-021-00522-2.

Midhat, L., Ouazzani, N., Hejjaj, A., Ouhammou, A. and Mandi, L., 2019. Accumulation of heavy metals in metallophytes from three mining sites (Southern Centre Morocco) and evaluation of their phytoremediation potential. *Ecotoxicology and Environmental Safety*, 169, pp.150–160. doi: 10.1016/j.ecoenv.2018.11.009.

Mitra, S., Chakraborty, A.J., Tareq, A.M., Bin Emran, T., Nainu, F., Khusro, A., Idris, A.M., Khandaker, M.U., Osman, H., Alhumaydhi, F.A. and Simal-Gandara, J., 2022. Impact of heavy metals on the environment and human health: Novel therapeutic insights to counter the toxicity. *Journal of King Saud University - Science*, 34(3), p.101865. doi: 10.1016/j.jksus.2022.101865.

Nayeri, N., Li, P., Górecki, K., Lindkvist-Petersson, K. and Gourdon, P., 2023. Principles to recover copper-conducting CTR proteins for the purpose of structural and functional studies. *Protein Expression and Purification*, 203, p.106213. doi: 10.1016/j.pep.2022.106213.

Nozoye, T., 2018. The nicotianamine synthase gene is a useful candidate for improving the nutritional qualities and Fe-deficiency tolerance of various crops. *Frontiers in Plant Science*, 9. doi: 10.3389/fpls.2018.00340.

Paysan-Lafosse, T., Blum, M., Chuguransky, S., Grego, T., Lázaro Pinto, B., Salazar, G.A., Bileschi, M.L., Bork, P., Bridge, A., Colwell, L., Gough, J., Haft, D.H., Letunić, I., Marchler-Bauer, A., Mi, H., Natale, D.A., Orengo, C.A., Pandurangan, A.P., Rivoire, C., Sigrist, C.J.A., Sillitoe, I., Thanki, N., Thomas, P.D., Tosatto, S.C.E., Wu, C.H. and Bateman, A., 2023. InterPro in 2022. *Nucleic Acids Research*, 51(D1), pp.D418–D427. doi: 10.1093/nar/gkac993.

PubChem, n.d. PubChem. Retrieved June 25, 2024 from https://pubchem.ncbi.nlm.nih.gov/).

Rashid, A., Schutte, B.J., Ulery, A., Deyholos, M.K., Sanogo, S., Lehnhoff, E.A. and Beck, L., 2023. Heavy metal contamination in agricultural soil: Environmental pollutants affecting crop health. *Agronomy*, 13(6), p.1521. doi: 10.3390/agronomy13061521.

Santana, C.S., Montalván Olivares, D.M., Silva, V.H.C., Luzardo, F.H.M., Velasco, F.G. and de Jesus, R.M., 2020. Assessment of water resources pollution associated with mining activity in a semi-arid region. *Journal of Environmental Management*, 273, p.111148. doi: 10.1016/j.jenvman.2020.111148.

Sayers, E.W., Bolton, E.E., Brister, J.R., Canese, K., Chan, J., Comeau, D.C., Connor, R., Funk, K., Kelly, C., Kim, S., Madej, T., Marchler-Bauer, A., Lanczycki, C., Lathrop, S., Lu, Z., Thibaud-Nissen, F., Murphy, T., Phan, L., Skripchenko, Y., Tse, T., Wang, J., Williams, R., Trawick, B.W., Pruitt, K.D. and Sherry, S.T., 2021. Database resources of the National Center for Biotechnology Information. *Nucleic Acids Research*, 50(D1), pp.D20–D26. doi: 10.1093/nar/gkab1112.

Sharma, R., Bhardwaj, R., Handa, N., Gautam, V., Kohli, S.K., Bali, S., Kaur, P., Thukral, A.K., Arora, S., Ohri, P. and Vig, A.P., 2016. *Plant Metal Interaction*. Elsevier, pp. 263–283.

Shinzato, M.C. and Hypolito, R., 2016. Effect of disposal of aluminum recycling waste in soil and water bodies. *Environmental Earth Sciences*, 75(7), p.628. doi: 10.1007/s12665-016-5438-3.

Skoneczny, D., Zhu, X., Weston, P.A., Gurr, G.M., Callaway, R.M. and Weston, L.A., 2019. Production of pyrrolizidine alkaloids and shikonins in *Echium plantagineum* L. in response to various plant stressors. *Pest Management Science*, 75(9), pp.2530–2541. doi: 10.1002/ps.5540.

Stanke, M., 2003. The AUGUSTUS Gene Prediction Tool. Retrieved June 25, 2024, from https://bioinf.uni-greifswald.de/augustus/

Streets, D.G., Lu, Z., Levin, L., ter Schure, A.F.H. and Sunderland, E.M., 2018. Historical releases of mercury to air, land, and water from coal combustion. *Science of The Total Environment*, 615, pp.131–140. doi: 10.1016/j.scitotenv.2017.09.207.

Wang, H., Du, H., Li, H., Huang, Y., Ding, J., Liu, C., Wang, N., Lan, H. and Zhang, S., 2018. Identification and functional characterization of the ZmCOPT copper transporter family in maize. *PLOS ONE*, 13(7), p.e0199081. Doi: 10.1371/journal.pone.0199081.

Wang, Q., Wei, N., Jin, X., Min, X., Ma, Y. and Liu, W., 2021. Molecular characterization of the COPT/Ctr-type copper transporter family under heavy metal stress in alfalfa. *International Journal of Biological Macromolecules*, 181, pp.644–652. doi: 10.1016/j.ijbiomac.2021.03.173.

Waterhouse, A., Bertoni, M., Bienert, S., Studer, G., Tauriello, G., Gumienny, R., Heer, F.T., de Beer, T.A.P., Rempfer, C., Bordoli, L., Lepore, R. and Schwede, T., 2018. SWISS-MODEL: Homology modeling of protein structures and complexes. *Nucleic Acids Research*, 46(W1), pp.W296–W303. doi: 10.1093/nar/gky427.

Wu, R., Ding, F., Wang, R., Shen, R., Zhang, X., Luo, S., Su, C., Wu, Z., Xie, Q., Berger, B., Ma, J. and Peng, J., 2022. High-resolution de novo structure prediction from primary sequence. 2022.07.21.500999.

Yaashikaa, P.R., Senthil Kumar, P., Jeevanantham, S. and Saravanan, R., 2022. A review on bioremediation approach for heavy metal detoxification and accumulation in plants. *Environmental Pollution*, 301, p.119035. doi: 10.1016/j.envpol.2022.119035.

Yan, A., Wang, Y., Tan, S.N., Ghosh, S. and Chen, Z., 2020. Phytoremediation: A promising approach for revegetation of heavy metal-polluted land. *Frontiers in Plant Science*, 11, p.359. doi: 10.3389/fpls.2020.00359.

Yuan, S., Chan, H. and Hu, Z., 2017. Using PyMOL as a platform for computational drug design. *Wiley Interdisciplinary Reviews: Computational Molecular Science*, 7, p.e1298. Doi: 10.1002/wcms.1298.

Zaccone, C., Di Caterina, R., Rotunno, T. and Quinto, M., 2010. Soil–farming system – food – health: Effect of conventional and organic fertilizers on heavy metal (Cd, Cr, Cu, Ni, Pb, Zn) content in semolina samples. *Soil and Tillage Research*, 107(2), pp.97–105. doi: 10.1016/j.still.2010.02.004.

Zhao, M. and Zhou, B., 2020. A distinctive sequence motif in the fourth transmembrane domain confers ZIP13 iron function in *Drosophila melanogaster*. *Biochimica et Biophysica Acta (BBA) - Molecular Cell Research*, 1867(2), p.118607. doi: 10.1016/j.bbamcr.2019.118607.

Zine, H., Midhat, L., Hakkou, R., El Adnani, M. and Ouhammou, A., 2020. Guidelines for a phytomanagement plan by the phytostabilization of mining wastes. *Scientific African*, 10, p.e00654. doi: 10.1016/j.sciaf.2020.e00654.

Original Research Paper   https://doi.org/10.46488/NEPT.2025.v24i01.B4183   **Open Access Journal**

Exploring the Water Crisis and Viability of Unregulated Groundwater in India: An Analysis

Aditi Nidhi and J. Lakshmi Charan†

School of Law, Mahindra University, Hyderabad, India

†Corresponding author: J. Lakshmi Charan; lakshmicharan038@gmail.com

ABSTRACT

Water conservation and management are significant features of ancient Indian Vedic culture. However, India's rapid industrialization, globalization, and urbanization have posed a serious threat to this practice. Many metropolitan cities and other cities will likely have groundwater depletion in the near future. As per the 'United Nations University - Institute for Environment and Human Security (UNU-EHS)' report titled "The 2023 Interconnected Disaster Risks Report", India is close to reaching its tipping point of groundwater depletion. It also highlighted that 27 of 31 major global aquifers are depleting faster than they can be replenished. A combination of factors, including climate change, private land ownership, mechanical pumping, etc., led to the depletion of groundwater and water scarcity for farming and other purposes. Additionally, NITI Aayog and the Central Water Commission have released several reports that highlighted the plight of the country's aquifers. India's groundwater resources are not only a potential source for agricultural, domestic, and industrial needs in the country but also a threat to its sustainable development and equitable distribution. At present, there is no central law on the groundwater regulation. Although the Model Groundwater (Sustainable Management) Bill 2017 is an affirmative step, its effectiveness depends on implementation by state governments, the establishment of robust local institutions, and removing political incentives from groundwater management. Until now, landowners have enjoyed monopolistic access to groundwater due to common laws that recognize uncontrolled rights over the resources. These restrictions have perpetuated gross inequities in accessing groundwater, which makes a remarkable shift from previous laws. This paper evaluates India's existing groundwater laws to achieve sustainability, equity, and the effective execution of water rights. It also delves into the lacunae in the existing laws and suggestive measures to control the challenges of groundwater in India.

INTRODUCTION

Groundwater depletion is a major environmental concern across the globe, particularly in India. The Earth's surface is covered by 60% water, and the human body is composed of about 70% water. India has 16% of the global population, but the nation possesses only 4% of the world's freshwater resources (Pandey 2023). As a result, India is facing water scarcity and increasing groundwater extraction over the past few decades. India heavily relies on groundwater resources, which is evident from the fact that the country relies on 80% of its rural drinking water, 50% of its urban drinking water, and nearly two-thirds of its irrigation requirements (Saha & Ray 2018). Since the 1960s, the Indian government has emphasized technology transfer initiatives like the "Green Revolution" as a key strategy to ensure food security, which has led to increased demand for groundwater resources in agriculture. It is found that rapid rural electrification, along with advanced pump technologies, increases the borewells to meet the water demands. It is also estimated that borewells have increased from 1 million to 20 million, making India the world's largest consumer of groundwater resources (Bekele Shiferaw 2021).

Water is a vital component for various life processes, and it is employed in several developmental activities. However, water is a non-renewable energy source due to its limited availability over a few centuries. Such water scarcity is primarily due to groundwater depletion driven by agricultural activities and climate change. India extracts 260 cubic meters annually, which accounts for 25% of the total global groundwater extraction (TPCI 2021). The Central Ground Water Board (CGWB), Government of India, estimates that 60% of the total irrigated area is attributed to groundwater irrigation, and 85% of the rural drinking water supply relies on it. It is also estimated that the water availability for agricultural purposes in the Indus, Ganges, and Brahmaputra River basins is expected to decline. This water decline could potentially impact the food self-sufficiency of 63 million people (approx.) (Wang et al. 2023). A recent report estimates that the rate of groundwater depletion in India from 2041 to 2080 will be three times the current rate due to the effects of global warming (Bhanja et al. 2017).

As the country's temperature increases, it will lead to an accelerated withdrawal of groundwater, thereby contributing to faster depletion. Groundwater is located beneath the land subsidence and fissures consisting of soil, sand, and rock. This water is stored within and gradually moves through the geological formations of soil, sand, and rock, which are known as aquifers. The diminishing levels of groundwater in various parts of the country can be attributed to continual extraction, driven by increasing demand for freshwater due to various factors such as unpredictable rainfall patterns, increase in population growth, rapid industrialization, and urban expansion. Consequently, there is an urgent need to address this situation. It is essential to address the root causes of the man-made crisis of water demands before exploring the potential solutions.

When the country witnesses a gradual increase in temperature, people will extract more underground water, leading to a faster depletion of it. Groundwater refers to the water present beneath the earth's surface in the cracks and spaces made up of rock, sand, and soil. This water is stored and gradually flows through geological formations of soil, sand, and rock, called aquifers. In different regions of the country, the groundwater levels have declined due to the continuous withdrawal of water. Such withdrawal is necessitated by increasing demand for freshwater for various purposes, population growth, industrialization, urbanization etc. Consequently, there is an urgent need to address this situation. However, before exploring potential solutions, it is crucial to understand the underlying causes of this human-induced crisis.

HISTORY OF GROUND WATER IN INDIA: A STATISTICAL ANALYSIS

The historical development of groundwater is a scientific practice that reached its peak in the Indian Himalayan kingdom before the 17th century. In Vedic scriptures, groundwater was praised as springs that bestowed health, happiness, and peace on the community. In India, the history of groundwater can be broadly classified into three periods (Angelakis et al. 2016), namely Pre-historic and Historic, the British period (1818 to 1947 AD), and the post-Independence period (Kumar et al. 2005). During these periods, the use of groundwater in various rock types was associated with the religious and cultural aspects of society. India comprises 15% of the global population, but the country possesses 6% of the world's water resources and 2.5% of the world's land (Kumar et al. 2005). Ground water is one of the most common resources accessible to all and anyone is allowed to drill a well and extract as much water as needed. Indian thinkers like Manu had interests in exploring the means of rainwater storage and identifying groundwater sources. Ancient texts such as Brihat Samhita and Arthasastra depict the Earth's interior as an intricate network of water channels, dividing it into multiple streams at different levels that support diverse plant life. The ancient sages' texts suggest that groundwater resources can be explored in areas with limited surface water, which would support our economy.

India's groundwater usage has witnessed a substantial increase from 70 km³ in 1940 to approximately 290 km³ in the present day (Mukherjee 2019). It is estimated that India extracts 253 billion cubic meters (BCM) of water per year. According to the Twelfth Five Year Plan (2012-2017) (Boruah & Naz 2020), there are 28 million groundwater irrigation systems in India. In addition to being overused, groundwater is being contaminated, which puts the water table at serious risk. It has been observed that almost 70% of all districts in our country have issues related to groundwater quality. The severity of India's groundwater crisis is evident through the reports from different parts of the country (Bhanja et al. 2017). It calls for need and mitigation both in the fields and in the policy of our country. After Independence, when there was large-scale introduction of mechanized pumping was introduced, which led to a dramatic increase in groundwater extraction in the country (Fischer et al. 2022).

The red flags over underground water depletion can be analyzed from the Fig. 1. (Sandrp 2017)

Fig. 1 shows the data per capita availability of groundwater in the country over the years. The rate at which the groundwater is declining in metropolitan areas shows that if current trends continue, in 20 years, about 60% of
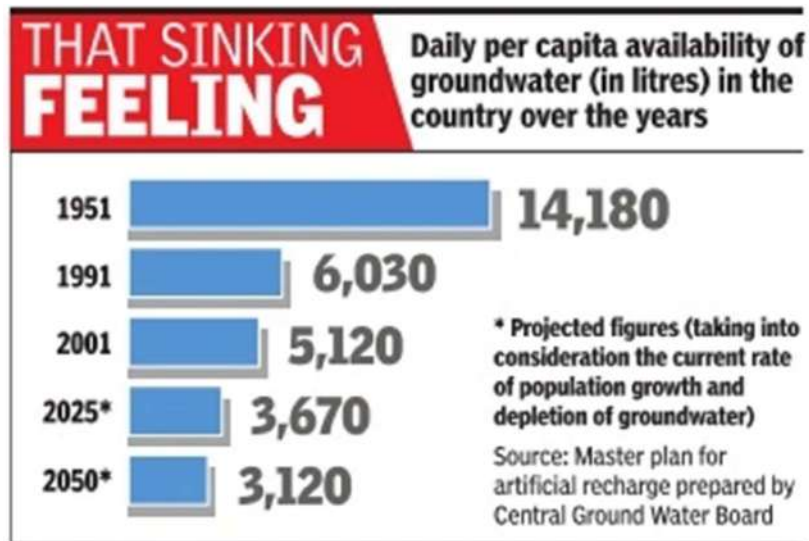
Fig. 1: Source: Central Ground Water Board.
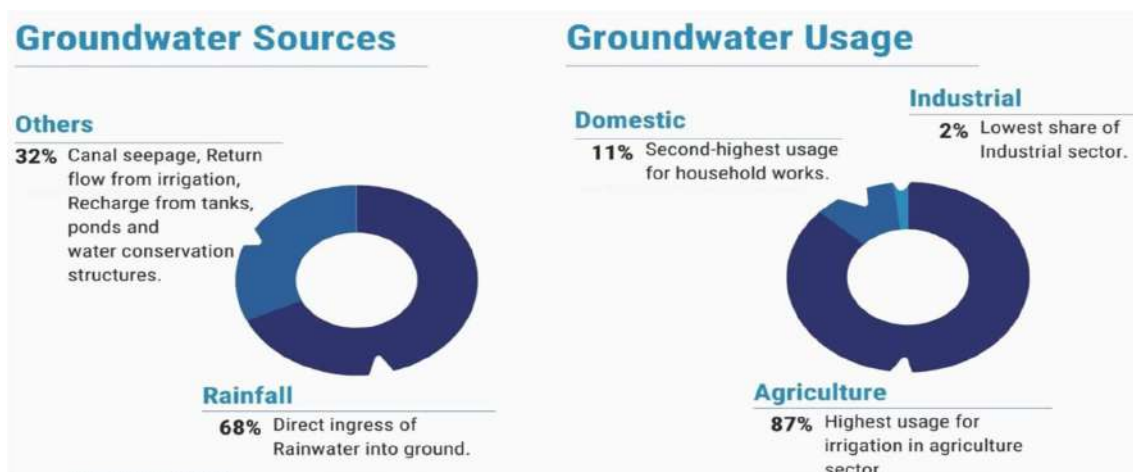
Fig. 2: Source: Ministry of Jal Shakti.

all India's aquifers will be in a critical condition (Gandhi & Namboodiri 2009).

In India, the 'Dynamic Ground Water Resource Assessment Report, 2022' released by the Ministry of Jal Shakti reported that the annual groundwater recharge is recorded at 437.60 billion Cubic Meters (BCM) (Koshy 2022). Such groundwater extraction has reached its lowest point since 2004, standing at 239.16 BCM compared to the 231 BCM recorded. In India, groundwater is predominantly used for irrigation purposes at '208.49 BCM', followed by domestic purposes at '27.05 BCM' and industrial usage at '3.64 BCM' (Mukherjee 2022). Fig. 2 shows the percentage of water in groundwater sources and its usage.

As per the CAG Report - 2021, the extraction of groundwater has risen from 58% to 63% between 2004 and 2017, surpassing the rate at which groundwater is being replenished (Comptroller and Auditor General of India 2021). According to the Central Ground Water Board (CGWB), around 17% of groundwater blocks are being over-exploited, meaning that the pace at which water is being extracted is higher than the rate at which the aquifer is being replenished. Furthermore, 5% and 14% of blocks are classified as crucial and semi-critical, respectively (Bekele Shiferaw 2021). The groundwater resources in India are in a precarious state in three key regions: the southern peninsular region, the western region and the north-western territory. The Dynamic Groundwater Resource Assessment Report -
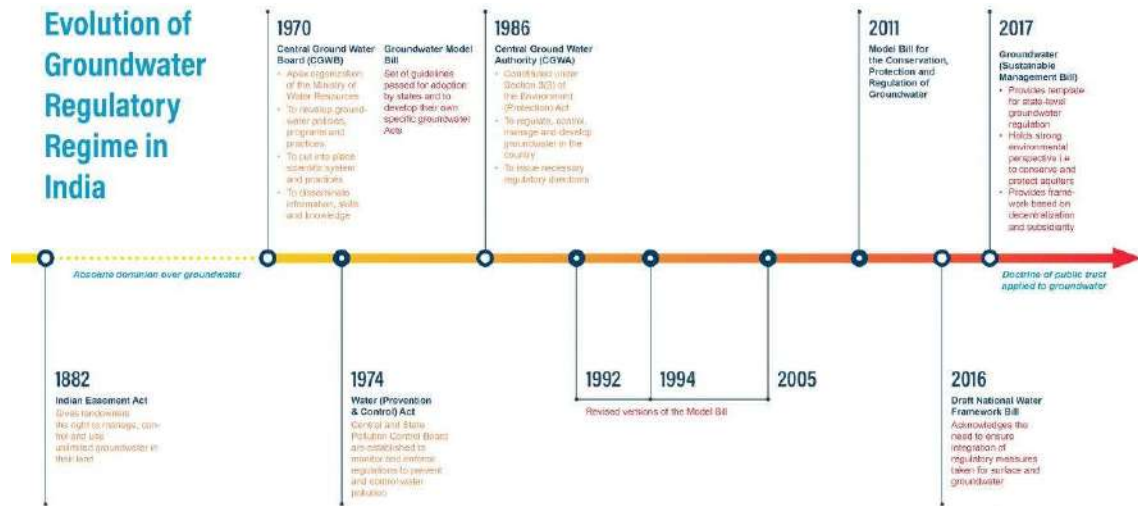
Source: Sindhuja Janakiraman and Purnanjali Chandra (WRI INDIA 2022)

Fig. 3: Development of India's Groundwater Regulatory System.

2022 states that the number of groundwater units classified as "overexploited" has reduced by 3 percent, while the number of units classified as safe has increased by 4 percent compared to 2017. There has been a general enhancement in the groundwater conditions across 909 units. India uses more groundwater than the United States and China combined, accounting for 25% of the world's extracted groundwater. Currently, over 70% of India's water supply for agriculture comes from groundwater (Bhattarai et al. 2021).

REGULATION OF GROUNDWATER IN INDIA: CHALLENGES AHEAD

Groundwater resources are vital to human existence, as they provide a significant proportion of the world's potable water (Food and Agriculture Organization of the United Nations, 2012). Nonetheless, the indiscriminate application of groundwater has given rise to a multitude of concerns. Numerous scientific studies demonstrate that if groundwater extraction persists at an alarming rate, the resource will eventually be depleted (Singh & Singh 2002). Some of the problems pertaining to groundwater are over-extraction, climate change, legal laxity, insufficient monitoring, poor management, etc. In India, monitoring and managing groundwater resources will be critical to ensure their sustainability and availability for future generations. The evolution of the groundwater regulatory regime in India can be traced since ancient times, and it reflects that there exist several challenges to the preservation of groundwater in India. As shown in Fig. 3 illustrates multiple revised versions in Indian legislation aimed at asserting absolute dominion over groundwater, but it remains in its infancy state.

The factors can be studied in detail as given below to see the menace of the problem.

Rising population: The growing urban population not only increases the demand for water but also amplifies challenges associated with waste and contaminated water management. The surge in urban population intensifies the burden of water and waste management. One of the most significant consumers of groundwater is India, which accounts for around 25 percent of the total global withdrawal (Water Crisis in India: The World's Largest Groundwater User, 2022). In India, 48% of urban water resources rely on groundwater (Kulkarni et al. 2015). As the population increases, the proportion of individuals lacking access to clean water is expected to rise.

Unplanned urbanization: Unplanned Urbanization leads to depletion of groundwater resources. Unplanned urbanization activities, such as the expansion of built-up and paved areas, have resulted in the loss of water infiltration into the ground. The absence of green cover reduces evapotranspiration, while an increase in surface runoff leads to urban flooding and a decrease in groundwater recharge. An investigation carried out in the United States revealed that each 1% rise in the impermeable surface area results in a 3.3% escalation in the intensity of urban flooding (Gies 2024). Urban sprawl alters the groundwater cycle by transforming the natural environment, watershed, and flow direction. This could lead to a substantial decline or increase in groundwater levels, diminished well productivity, and a deterioration in water quality.

Climate change: The impacts of climate change, such as irregular rainfall patterns, significantly disrupt the ability

of groundwater to replenish, which poses a substantial risk to both the quantity and quality of available groundwater. The most recent assessment reports from the Central Ground Water Board (CGWB) indicate that numerous places are being excessively exploited, with a majority of them being classified as critical or semi-critical. India is the greatest consumer of groundwater in the world, using an estimated 230 cubic kilometers per year, which accounts for more than 25% of the total global usage, as stated in the 2012 World Bank Report (Saha & Ray 2018). It provides approximately 80% of the water used for domestic purposes and 45% of the water used for irrigation in total. If the current rate of over-extraction persists, it could result in around 60% of India's aquifers becoming critical and pose a threat to over 80% of the country's drinking water within the next two decades (Boretti & Rosa 2019). This has a significant effect on the fair, sustainable, and environmentally clean availability of water resources, therefore limiting the utilization of the 'right to water' for both present and future generations (Nidhi 2023).

Legal laxity: Many bodies are involved in groundwater control, which results in fragmented regulation and the lack of an "integrated and comprehensive" regulatory approach. In addition, the lack of legal regulations governing the extraction of groundwater has led to over-exploitation. Indian Easements Act of 1882, determines the groundwater rights associated with the land. As a result, a large section of the society is excluded from the right to groundwater and does not have the right to land. In addition, the lack of comprehensive data on groundwater resources makes it difficult to formulate clear guidelines for the proper management of groundwater.

Groundwater pollution: Groundwater aquifers become contaminated as a result of the infiltration and seepage of various substances such as road runoff, industrial waste, landfill sites, and micro-pollutants. Groundwater pollution is primarily responsible for nitrate, arsenic, fluoride, etc. The excessive utilization of groundwater and the growing prevalence of privately owned bore wells to meet the water demand and supply result in the lowering of the water table, land sinking, infiltration of salty water, and contamination of the underground water source. These phenomena have significantly depleted groundwater resources. The major stressors include a lack of interest and stakeholders' awareness, the unclear role of regulatory bodies, and the absence of a monitoring and planning system.

GROUNDWATER GOVERNANCE AND LAWS RELATING TO GROUNDWATER

Landowners have the right to access and control resources beneath the land, including groundwater resources. This right originated from the English Law, which was incorporated under the 'Indian Easements Act of 1882' (Wahi 2022). In the 1960s, the proliferation of mechanized pumps had significantly escalated groundwater consumption leading to a sharp decline in water tables. This phenomenon spurred an increasing demand for groundwater law reforms. The Indian government realized the imperative need for a legal framework to regulate groundwater. It introduced several initiatives (viz., laws and policies) to regulate groundwater resources. In 1970, the Central Government proposed to adopt a Model Bill for the regulation of groundwater, which underwent multiple revisions (1992, 1996, and 2005) (Cullet 2012). Recently, the Indian Government adopted the Groundwater (Sustainable Management) Bill, 2017 to better suit our needs (Mukherji 2020).

In 1987, India adopted its first National Water Policy (NWP), recognizing water as a prime natural resource and a precious national asset (Wahi 2022). This policy prioritizes drinking water for both humans and animals. It advocates for the integrated and coordinated development of surface and groundwater, accompanied by regulations to limit groundwater exploitation. Although, India has a groundwater policy, still, the country faces challenges related to groundwater management due to policy deficiencies. Hence, NWP has been modified but mostly, it retained the same. The revised policy reinforced the need for regulating groundwater resources in order to prevent over-exploitation, ensuring groundwater usage is within recharge limits. However, the revised policy remained merely suggestive, and lacks a clear approach for groundwater management. Furthermore, the Ministry of Water Resources issued a new National Water Policy in 2012 to meet the challenges in the water sector (Rathee & Mishra 2021). Under the principle of public trust, this policy acknowledged groundwater management as a shared resource by the state. The goal of this policy was to accomplish both food security and sustainable groundwater management responsibilities. The NWP, 2012 addresses issues relating to the management of water resources, planning water scarcity, etc, providing new guidelines for states to adopt. It is noteworthy that the states have the autonomy to adopt these guidelines (Pandit & Biswas 2019).

In 1997, the Central Ground Water Authority (CGWA) was constituted to regulate, manage, and develop groundwater (Rishikesh Singh Faujdar 2015). This authority has been constituted following the directives of the Supreme Court in *M.C Mehta v. Union of India* (1987 SCR (1) 819). In this case, the Supreme Court issued directives that the Central Government under the 'Ministry of Environment and Forest

(MoEF)' shall constitute 'The Central Ground Water Board as an Authority under section 3(3) of the 'Environment (Protection) Act, 1986'. However, the 'Ministry of Environment and Forests (MoEF)' has decided to designate the Central Ground Water Board, an existing scientific and technical body under the Ministry of Water Resources, as 'Central Ground Water Authority' under Section 3(3) of the 'Environment (Protection) Act, 1986'. Its main functions are critical/over-exploited regions identified to provide suitable measures for the regulation and development of groundwater. The CGWA has formulated guidelines setting parameters for assessing proposals relating to withdrawal groundwater that have been revised over time.

In 2017, the Indian Government introduced the Groundwater (Sustainable Management) Bill in line with the national water policy guidelines. This bill acknowledges groundwater as a fundamental right and a public trust (Pandit & Biswas 2019). The Bill also expands on the decentralization mandate and aims to provide local bodies with regulatory authority over groundwater resources. The proposed framework aims to increase groundwater resources by incorporating groundwater security plans and significant local involvement. Therefore, the groundwater will be used responsively and people and the state will play an active role in using groundwater and safeguarding it for present and future generations. The new bill acknowledges the incorporation of protective principles, such as the precautionary principle, which were missing from the water policy. It also suggests that the groundwater should be protected at the aquifer level. The 'Central Ground Water Board (CGWB)' is implementing the 'National Aquifer Mapping and Management Program (NAQUIM)' to aid groundwater sustainability.

The Central Government has issued updated regulations governing groundwater use. The amended standards require no-objection certificates (NOCs) for existing industries, commercial units, and major housing societies and ban new industry and mining projects in over-exploited zones. However, domestic consumers, including armed forces, farmers, and micro and small enterprises withdrawing up to 10 cubic meters of water per day, are exempted from the requirement of a 'no objection certificate (NOC)' from the 'Central Ground Water Board (CGWB)'. The Uttar Pradesh Cabinet, led by Chief Minister Yogi Adityanath, adopted the Ground Water Act on February 11, 2020. It is considered a progressive step in regulating groundwater to raise the state's declining groundwater levels. Hence, there is a need for all the states to reform their groundwater law because inaction increases existing inequalities in access to groundwater. It's high time for the State to act as a public trustee of groundwater to make sure that groundwater is protected,

conserved, regulated, and properly managed.

The government has undertaken various initiatives shedding light on the concerning depletion of groundwater resources. The National Project on Aquifer Management (NAQUIM) and Atal Bhujal Yojana (ABY) have both been initiated to promote participatory groundwater management. The primary objective of the Atal Bhujal Yojana is to promote a shift in behavior by providing incentives. NAQUIM aims to create a detailed map of underground water sources to support well-informed decision-making. The Jal Jeevan Mission focuses on providing safe drinking water to rural households. The India-Groundwater Resource Estimation System (IN-GRES) is designed to facilitate annual assessments of groundwater levels. The Jal Shakti Abhiyan aims to promote rainwater harvesting and raise awareness through extensive campaigns (National Compilation on Dynamic Ground Water Resources of India 2023). Furthermore, the government implemented the Integrated Water Resource Management framework and the recommendations of the Mihir Shah Committee in an effort to enhance groundwater governance and utilization.

In the first place, Mihir Shah Committee Recommendations (Kumar 2018) should be implemented as follows: (a) There is a need to restructure the existing water commissions to form a new National Water Commission for collective management of ground and surface water; (b) The National Water Commission shall set up 8 divisions for a comprehensive water management approach. These 8 divisions include the Urban and Industrial Water Division, Water Security Division, River Rejuvenation Division, Irrigation Reform Division, Aquifer Mapping and Participatory Ground Water Management Division, Water Data Management and Transparency Division, Water Quality Division, and Knowledge Management and Capacity Building Division; (c) There is a need for participatory groundwater management, recognizing groundwater as a common pool resource for constant check on the groundwater extraction. Corrective measures like setting drilling depth requirements, and promoting crop patterns that avoid excessive withdrawal of resources are to be implemented.

Moreover, it is essential to prioritize the implementation of an integrated water resource management framework for groundwater planning and management. It encourages the planned use and administration of land and water resources. Furthermore, it is crucial to embrace water-sensitive urban architecture and planning. By controlling surface water, groundwater, and precipitation for water supply and demand, it aids in the management of the water cycle. There is a pressing need to implement a blue-green infrastructure approach. The gap in groundwater management can be filled

by increasing public awareness and engagement, as well as by fostering trust between communities and formal water sector agencies. It is necessary to conduct a policy review in the agricultural sector. The cropping system ought to be following the agroecology of the area. The abolition of agricultural subsidies on energy is something that should be done. These strategies aid in optimizing the utilization of groundwater in agricultural practices (Talat 2021).

NEED FOR DECENTRALIZATION FOR GROUNDWATER

India is experiencing a severe water crisis which requires urgent measures to address it (David 2024). Although the water crisis is often discussed, related laws and policies are least discussed. It is imperative to discuss the laws due to the rapid depletion of water tables, and it may exceed replenishment. The current legislation regarding groundwater employs a centralized 'command-and-control' strategy, where state-level authorities are responsible for regulating groundwater. However, such regulation is inadvisable for various legal reasons. Due to the diffuse nature of groundwater usage, a centralized system and agency using a command-and-control model would find it difficult to regulate the millions of extraction units that a state may have. It is very difficult to regulate groundwater, especially in regions/areas where groundwater is the primary water source. In many regions, regulating its use without interest among users could lead to outright opposition and non-compliance.

The Indian Constitution envisioned a 'participative' and 'decentralized structure' for the management of natural resources. In India, regulation of groundwater regulation is governed under these principles. Water law reforms of surface water have been implementing the ideas of decentralization and participation over several decades. It is recommended to advocate for the decentralization of authority to local governing entities, such as village panchayats and municipalities. Article 243G of the Constitution of India pertains to the delegation of authority and accountability to panchayats. It states that the "legislature of a State may, by law, endow the panchayats with such powers and authority ...." It is also witnessed that some states have implemented decentralization, which failed groundwater regulation. Kerala is renowned for its successful decentralization implementation in this regard. However, Kerala adopted the 'Kerala (Regulation and Control) Act, 2002' for a centralized regulation of groundwater.

Several recent legislative changes—particularly those targeted at encouraging investment and development—tend to flout the Indian Constitution's decentralization idea. The centralization of groundwater regulation is contrary to the basic principles of legal reforms on surface water resources. These water law reforms recognize decentralization and participation as fundamental principles. Hence, water law reforms show the co-existence of centralization and decentralization. The water law reforms require proper justification for the centralization of resources. However, it is found that there are no proper justifications for adopting a centralized command and control approach for groundwater resources. Additionally, it is found that the decentralization of water has existed for a long time, along with the cultural and ethnic pluralism of Indian society. The water ecology in India relies predominantly on rainfall, which exhibits a high degree of temporal variability and is distributed across many regions (Kumar et al. 2005). Hence, any endeavor to modify the groundwater legal system in India should be founded on the principle of subsidiarity (Koonan 2022). Implementing such a measure would demonstrate adherence to the notion of decentralization. It also provides abundant opportunities to address the concepts, customs, knowledge, and local requirements.

CONCLUSION

India's population accounts for approximately 16 percent of the global population, while the country possesses only four percent of the world's freshwater resources. Not only this, India is among the water-stressed nations in the world as a result of shifting weather patterns, recurrent droughts, and an excessive reliance on groundwater supplies. A United Nations assessment states that by 2050, India is predicted to experience acute water scarcity. It is crucial that the government swiftly conducts periodic analyses of groundwater sources in order to prevent the contamination of groundwater resources. The periodic evaluation can be calculated by considering elements such as the formation of new industries, the digging of new bore wells, effluents from industries, and other factors that contribute to groundwater contamination. The ideologies of the "Slow-Down Movement" and "Minimalistic Theory (Minimalism)" have been developed to promote sustainable development and efficient water utilization. Minimalism theory involves intentionally living and carefully analyzing the repercussions of one's activities. By embracing minimalism, individuals can effectively decrease their ecological footprints and prevent excessive consumerism from depleting the Earth's resources. Therefore, adopting minimalism is the sole approach to water conservation, which is crucial for achieving sustainable development.

REFERENCES

Angelakis, A.N., Voudouris, K. and Mariolakos, I., 2016. Groundwater utilization through the centuries focused on the Hellenic civilizations. *Hydrogeology Journal*, 24(5), pp.1311–1324. https://doi.org/10.1007/s10040-016-1392-0

Bekele Shiferaw, 2021. Addressing groundwater depletion: Lessons from India, the world's largest user of groundwater. Retrieved from https://ieg.worldbankgroup.org/blog/addressing-groundwater-depletion-lessons-india-worlds-largest-user-of-groundwater

Bhanja, S.N., Mukherjee, A., Rodell, M., Wada, Y., Chattopadhyay, S., Velicogna, I., Kishore, P. and Famiglietti, J.S., 2017. Groundwater rejuvenation in parts of India influenced by water-policy change implementation. *Scientific Reports (Nature Publishing Group)*, 7(1), p.7058. https://doi.org/10.1038/s41598-017-07058-2

Bhattarai, N., Pollack, A., Lobell, D.B., Fishman, R., Singh, B., Dar, A., Jain, M., 2021. The impact of groundwater depletion on agricultural production in India. *Environmental Research Letters*, 16(8), 085003. https://doi.org/10.1088/1748-9326/ac10de

Boretti, A. and Rosa, L., 2019. Reassessing the projections of the World Water Development Report. *NPJ Clean Water*, 2(1), p.39. https://doi.org/10.1038/s41545-019-0039-9

Boruah, J. and Naz, F., 2020. Groundwater Management under Indian Legal Framework. *Social Science Research Network*. https://doi.org/10.2139/ssrn.3794717

Comptroller and Auditor General of India, 2021. Report of the Comptroller and Auditor General of India on Ground Water Management and Regulation. In Union Government Ministry of Jal Shakti Department of Water Resources, River Development and Ganga Rejuvenation [Report]. Retrieved from https://cag.gov.in/webroot/uploads/download_audit_report/2021/Report%20No.%209%20of%202021_GWMR_English-061c19df1d9dff7.23091105.pdf

Cullet, P., 2012. The Groundwater Model Bill - Rethinking regulation for the primary source of water. *Economic & Political Weekly*, XLVII(45), p.1204.

David, S., 2024. Water resource management in India: problems and prospects. *Indian Journal of Public Administration*, 122, p.1823. https://doi.org/10.1177/00195561231221823

Fischer, C., Aubron, C., Trouve, A., Sekhar, M., Ruiz, L., 2022. Groundwater irrigation reduces overall poverty but increases socioeconomic vulnerability in a semiarid region of southern India. *Scientific Reports*, 12(1), p.12814. https://doi.org/10.1038/s41598-022-12814-0

Food and Agriculture Organization of the United Nations, 2012. Coping with water scarcity: An Action Framework for Agriculture and Food Security (Report No. 38). Retrieved from https://www.fao.org/3/i3015e/i3015e.pdf

Gandhi, V.P. and Namboodiri, N.V., 2009. Groundwater irrigation in India: gains, costs, and risks. *IIMA Research and Publications*, 8(3), p.219.

Gautam, R., 2022. Groundwater resource availability and its exploitation in India: A geographical study. *International Journal in Management and Social Science*, 10(10), pp.31–52.

Gies, E., 2024. Expanding paved areas has an outsize effect on urban flooding. *Scientific American*, 16, pp.121-136

Koonan, S., 2022. Revamping the Groundwater Legal Regime in India: Towards Ensuring Equity and Sustainability. *Socio-Legal Review*, 12(2), pp.45–73. https://doi.org/10.55496/YRUX4355

Koshy, J., 2022. Level of groundwater extraction lowest in 18 years, finds study. *The Hindu*. https://www.thehindu.com/sci-tech/energy-and-environment/level-of-groundwater-extraction-lowest-in-18-years-finds-study/article66116836.ece

Kulkarni, H., Shah, M. and Shankar, P., 2015. Shaping the contours of groundwater governance in India. *Journal of Hydrology: Regional Studies*, 4, pp.172–192. https://doi.org/10.1016/j.ejrh.2014.11.004

Kumar, M.D., 2018. *A Critique of Mihir Shah Committee (2016) Report on Water Reforms in India*. Elsevier, pp.83–97. https://doi.org/10.1016/b978-0-12-814903-4.00005-1

Kumar, R., Singh, R. and Sharma, K., 2005. Water resources of India.

Current Science, 89(5), pp.794–811. http://www.iisc.ernet.in/currsci/sep102005/794.pdf

Mukherjee, A., 2019. Changing groundwater landscape of India: implications to drinking water, food security, socio-economy and public health. *Proceedings of the Indian National Science Academy. Part A, Physical Sciences*, 43, p.497. https://doi.org/10.16943/ptinsa/2019/49708

Mukherjee, S., 2022. India's Groundwater Extraction Stage at 60% in 2022, Says Report. *Business Standard*. Retrieved from https://www.business-standard.com/article/specials/india-s-groundwater-extraction-stage-at-over-60-in-2022-says-report-122111001443_1.html

Mukherji, A., 2020. Sustainable groundwater management in India needs a Water-Energy-Food Nexus approach. *Applied Economic Perspectives and Policy*, 44(1), pp.394–410. https://doi.org/10.1002/aepp.13123

National Compilation on Dynamic Ground Water Resources of India, 2023. *Department of Water Resources, River Development and Ganga Rejuvenation, India*. Retrieved from https://jalshakti-dowr.gov.in/document/national-compilation-on-dynamic-ground-water-resources-of-india-2023/

Nidhi, A., 2023. Katowice climate package: Analysis, assessment, and outlook. *Nature, Environment and Pollution Technology*, 22(3), pp.1537–1545. https://doi.org/10.46488/nept.2023.v22i03.039

Pandey, P.C., 2023. India has 16% of the global population but only 4% of total water resources, resulting in water scarcity in many regions. *Climate Scorecard*, 16, pp.11-18.

Pandit, C. and Biswas, A.K., 2019. India's National Water Policy: 'feel good' document, nothing more. *International Journal of Water Resources Development*, 35(6), pp.1015–1028. https://doi.org/10.1080/07900627.2019.1576509

Rathee, R.K. and Mishra, S.K., 2021. Water policies in India: A critical review. *Indian Journal of Science and Technology*, 14(47), pp.3456–3466. https://doi.org/10.17485/ijst/v14i47.1828

Faujdar, R.S., 2015. Groundwater laws and policies in India: an assessment. *International Research Journal of Commerce Arts and Science*, 6(11), pp.1–13.

Saha, D. and Ray, R.K., 2018. *Groundwater Resources of India: Potential, Challenges and Management*. Springer, pp.19–42. https://doi.org/10.1007/978-3-319-75115-3_2

Sandrp, V., 2017. Groundwater 2016: India's Water Lifeline Continues to Bleed. Retrieved from https://sandrp.in/2017/02/09/ground-water-2016-indias-water-lifeline-continues-to-bleed/

Singh, D.K. and Singh, A.K., 2002. Groundwater situation in India: problems and perspective. *International Journal of Water Resources Development*, 18(4), pp.563–580. https://doi.org/10.1080/0790062022000017400

Talat, N., 2021. Urban water-supply management: indirect issues of climate change leading to water scarcity scenarios in developing and underdeveloped nations. In *Water conservation in the era of global climate change* (pp. 71-47). Elsevier. https://doi.org/10.1016/b978-0-12-820200-5.00009-9

Trade Promotion Council of India (TPCI), 2021. India's Depleting Groundwater: Time for Some Quick Action. *India Business and Trade*. Retrieved from https://www.tpci.in/indiabusinesstrade/blogs/indias-depleting-groundwater-time-for-some-quick-action/

Wahi, N., 2022. The evolution of the right to water in India. *Water*, 14(3), p.398. https://doi.org/10.3390/w14030398

Wang, J., Wei, J., Shan, W. and Zhao, J., 2023. Modeling the water-energy-food-environment nexus and transboundary cooperation opportunity in the Brahmaputra River Basin. *Journal of Hydrology. Regional Studies*, 49, p.101497. https://doi.org/10.1016/j.ejrh.2023.101497

WRI INDIA, 2022. Groundwater Regulation: The Challenge to Make the Invisible in India Retrieved from https://wri-india.org/blog/groundwater-regulation-challenge-make-invisible-visible-india.

Original Research Paper

Open Access Journal

Utilization of *Leiotrametes menziesii* BRB 73 for Decolorization of Commercial Direct Dyes Mixture with Different Culture Conditions

I. Apriani[1,2], D. H. Y. Yanto[3] , P. L. Hariani[4†] , H. Widjajanti[5] and O. D Nurhayat[3]

[1]Doctoral Program, Faculty of Mathematics and Natural Science, Universitas Sriwijaya. Palembang 30139, Indonesia

[2]Department of Biology, Faculty of Science and Technology, Universitas Islam Negeri Raden Fatah Palembang, South Sumatera, Indonesia

[3]Research Center for Applied Microbiology, National Research and Innovation Agency (BRIN). Cibinong 16911, Indonesia

[4]Department of Chemistry, Faculty of Mathematics and Natural Sciences, Universitas Sriwijaya, Palembang 30139, Indonesia

[5]Department of Biology, Faculty of Mathematics and Natural Sciences, Universitas Sriwijaya, Palembang 30139, Indonesia

†Corresponding author: P. L. Hariani: puji_lukitowati@mipa.unsri.ac.id

ABSTRACT

Mycoremediation is classified as an inexpensive, environmentally friendly, and effective technique to reduce wastewater. *Leiotrametes menziesii* BRB 73 was one of the White Rot Fungi (WRF) that has the potential to degrade dyes. Suitable environmental conditions can optimize dye decolorization results. This study aims to investigate optimal environmental conditions such as time incubation, concentration of dyes, pH, $CuSO_4$, and glucose concentration against decolorization of a mixture of direct dyes and enzyme activity (laccase and MnP). The mixture of commercial direct dyes used contains direct turquoise (DT), direct orange (DO), and direct yellow (DY) dyes. Decolorization was measured using a spectrophotometer at 400-700 nm. Laccase and MnP assay using ABTS and 2.6 DMP as substrate, respectively. The highest decolorization by *Leiotrametes menziesii* BRB 73 was produced at 54.3% at 96 hours and increased to 67% at a dye concentration of 500 mg.L^{-1}. Meanwhile, the highest laccase and MnP activities were 215 U.L^{-1} and 39 U.L^{-1}, respectively. pH range was quite wide, ranging from pH 5.5-9, supported by stable MnP activity from pH 3-7. $CuSO_4$ inducers were not required for the decolorization of these dyes. Decolorization was optimal at the addition of 1% glucose, while enzyme activities were 0.5% glucose. Decolorization of dyes by *Leiotrametes menziesii* BRB 73 was indicated through degradation pathways involving laccase and MnP enzymes. This isolate has a high tolerance to dye concentrations, a wide pH range, and low carbon requirements. Thus, it was recommended as a mycoremediation agent.

INTRODUCTION

Synthetic dyes are widely used in the textile industry, with more than 10,000 different dyes and pigments (Singh et al. 2023). The release of dyes into the environment causes a negative impact on water quality because it lowers the dissolved oxygen concentration and makes it difficult for light to penetrate the water, thus adversely affecting aquatic organisms (Ali et al. 2022). In addition, it can cause toxicity, carcinogenetic, and mutagenetic (Asgher et al. 2020).

Many chemicals (Fenton's reagent, ozonation, oxidation process, etc.) and physical methods (coagulation, adsorption, membrane filtration, flocculation, etc.) for removing dyes are available (Monga et al. 2022, Sudhaparimala & Usha 2022, Vinotha & Leema Rose 2023). However, these methods have their disadvantages which are: selective over types of dyes, low efficiency, sludge production, sometimes high cost, and generation of toxic by-products (Monga et al. 2022). Biodegradation by fungi is a relatively environmentally friendly, cost-effective, and effective method (Akhtar & Mannan 2020). Recently, White Rot Fungi (WRF) has

become a concern in handling dyes in the environment. This fungus has promising extracellular enzymes for degradation due to its wide substrate specificity and mild catalysis conditions such as laccase and manganese peroxidase (Dao et al. 2021, Ridtibud et al. 2024) (Table 1). The enzymes have good prospects in the degradation of dyes generated from textile industry waste (Kumar & Chandra 2020). WRF that produces these enzymes promises to degrade dyes effectively (Zafar et al. 2022), such as *Rigidoporus* sp. FMD21(Dao et al. 2021), *Coriolus versicolor, Pleurotus ostreatus* (Afiya et al. 2019), and *Trametes polyzona* (Pérez-Cadena et al. 2020), *Leiotrametes menziesii* (BRB 73) (Apriani et al. 2024).

Laccase and MnP are ligninolytic enzymes which are classified into two, namely phenol oxidase (laccase), and heme peroxidase (MnP) (Suryadi et al. 2022). Laccase (benzenediol: oxygen oxidoreductase; EC1.10.3.2) is a group of copper-containing polyphenol oxidases, which utilize molecular oxygen as the final electron acceptor (Bittencourt et al. 2023). Laccases can mediate coupling reactions that form the basis for dye removal (Kyomuhimbo & Brink 2023). This enzyme is capable of oxidizing various substrates such as ortho and para diphenols, phenolic acids, aromatic amines, methoxy-substituted phenols, and several other compounds (Herath et al. 2024). Thus, it makes laccase able to decolorize synthetic dyes of a wide spectrum of dyes such as RBBR, acid orange, direct green, direct blue, reactive red, malachite etc. (Kyomuhimbo & Brink 2023).

Manganese peroxidase (MnP, or Mn (II): H_2O_2 oxidoreductase, EC 1.11.1.13) is an extracellular glycoprotein containing heme as a prosthetic group (Suryadi et al. 2022). It catalyzes the oxidation of Mn^{2+} to Mn^{3+} in a multistep process (Herath et al. 2024). Furthermore, Mn^{3+} acts as a mediator in the process of oxidation for some phenolic and non-phenolic compounds (Kumar & Chandra 2020). It can catalyze the oxidation of a large spectrum of phenolic compounds, including toxic dye pollutants (Bilal et al. 2019).

Both laccase and MnP produced by WRF play a major role in the degradation of synthetic dyes (Bankole et al. 2018). However, fungal growth, extracellular enzyme production, and dye decolorization are determined by environmental factors such as pH, mediators, dyes, and carbon concentrations (Rajhans et al. 2021). Each WRF has different optimal environmental conditions, so this study needs to be carried out to determine the optimal conditions of *Leiotrametes menziesii* BRB 73 in the decolorization of mixtures of commercial direct dyes. In this study, we investigated the effect of various environmental conditions, such as time incubation, concentration of dyes, pH, $CuSO_4$, and glucose concentration for decolorization of mixture direct dyes by BRB 73. In addition, the relationship between environmental condition and enzymatic activities (Laccase and MnP).

MATERIALS AND METHODS

Culture Condition and Maintenance

Leiotrametes menziesii BRB 73 obtained from the culture collection of the Research Center for Applied Microbiology, BRIN was maintained and grown on a solid medium of malt extract agar (MEA). Isolate was cultivated on MEA at $25\pm3^{o}C$ for 7 days before treatment. Three plugs of isolate were grown in MGP broth containing, malt (20 $g.L^{-1}$), glucose (20 $g.L^{-1}$), and peptone (1 $g.L^{-1}$) at $25\pm3^{o}C$ (room temperature) for 7 days. A corkborer (diameter 0.5 cm) was used to form the plug. Cultures were added a mixture of commercial direct dyes (direct turquoise=DT, direct orange=DO, and direct yellow=DY) up to a concentration of 100 $mg.L^{-1}$. The supernatant of fungal cultures was centrifuged at 10.000 rpm at room temperature for 10 minutes within 96 after incubation for decolorization assay (Alam et

Table 1: Decolorization of direct dyes by White Rot Fungi.

WRF	Dyes	% decolorization	Enzyme	Reference
Trametes versicolor	Direct Green 6 Direct Blue 15 Direct Orange 26 Direct black 38 Direct Yellow 12	DG6: 76% DB15: 98% DO26: 92% DB38: 85% DY12: 70% (50 $mg.L^{-1}$ of dyes within 3 days of incubation)	Laccase	Pazarlioglu et al. 2010
Pleurotus flabellatus	Direct Blue 14 (DB14)	90.39% decolorization of 20 mg/L dyes for 6 hours incubation	Crude enzyme (MnP and Laccase)	Singh et al. 2013
Coriolopsis sp. Strain arf5	Direct Blue 71 (C.I. 34140)	40 to 90% of 200 $mg.L^{-1}$ DB71 within 5 days	Laccase	Cheng et al. 2016
Trametes hirsuta EDN084	Direct Blue 71	85%	Laccase	Chaurasia & Bharati 2019
Ganoderma lucidum EN2	Direct Red 5B (DR5B)	40.34% to 95.16% of 175 $mg.L^{-1}$ DR5B within 48 h		Sun et al. 2023)

al. 2021). Meanwhile, the supernatant was directly used for enzyme activities assay.

Optimation of Culture Conditions

To investigate cultural conditions, the experiment cultured isolates for 96 hours with different dye concentrations (100, 200, 300, 400 and 500 mg.L^{-1}) (Omar 2016). pH effect was monitored in the acidic to alkaline range, including pH 3, 3.5, 4, 4.5, 6, 6.5, 7, 7.5, 8, 8.5, and 9. Culture conditions were regulated using NaCl and NaOH (Colla et al. 2020). Copper sulfate ($CuSO_4$) (0, 1, 2, 3, 4, 5 mM) was added to the medium to determine their impact on decolorization and enzyme activities (Afreen et al. 2018, Zhu et al. 2016). Concentrations of glucose added in culture were 0, 0.5%, 1%, 2%, 3%, 4%, 5% and 10% (Alhomaidi et al. 2023). All experimental units were repeated 3 times.

Decolorization Assay

Percent decolorization was calculated after 96 hours of incubation using a TECAN infinite 200 pro microplate reader (Switzerland) (interval 400-700 nm). It was calculated according to formula: D = 100 [(A0-A1)/A0], where D is decolorization (%). A0 is initial absorbance. A1 is absorbance after decolorization (Anita et al. 2021).

Laccase Activity Assay

Laccase activity was measured using a TECAN infinite 200 pro microplate reader (Switzerland) at 420 nm for 60 s. ABTS was used as a substrate at room temperature. The assay mixture contained 250 μL of ABTS 2 mM, 50 μL of culture filtrate, and 200 μL of acetate buffer 0,1 M (pH.4.5). Laccase activity (U mL^{-1}) with molar absorptivity ($\mathcal{E}$) of 36,000 M^{-1} cm^{-1} was calculated according to formula Alam et al. (2021):

$$\text{Laccase activity } (U.\,mL^{-1}) = \frac{(Abs.(t) - Abs(0)) \; x \; Vtotal \; mixture \; (mL) \; x \; 10^3}{\mathcal{E} \, x \, V.enzyme \; (ml) \; x \; t \; x \; d} \quad ...(1)$$

Abs. (0) = the initial absorbance Abs. (t) = the final absorbance

10^3 = correction factor (μmol/mol) d = length of the cell

t = reaction time (1 min)

Manganese Peroxidase Activity Assay

Manganese peroxidase (MnP) activity was measured using a TECAN infinite 200 pro microplate reader (Switzerland) at 470 nm for 60 s. The assay mixture contained 100 μL culture filtrate, 12.5 μL 2,6 DMP 20 mM, 175 μL malonic buffer 50 mM (pH 4.5), 12.5 μL $MnSO_4$ 20 mM, 30 μL H_2O_2 2 mM. MnP activity (U mL^{-1}) was calculated according to the formula (Anita et al. 2021):

$$\text{MnP activity } (U.\,mL^{-1}) = \frac{(Abs.(t) - Abs(0)) \times Vtotal \; mixture \; (mL) \times 10^3}{\mathcal{E} \times V.enzyme \; (ml) \times t \times d} \quad ...(2)$$
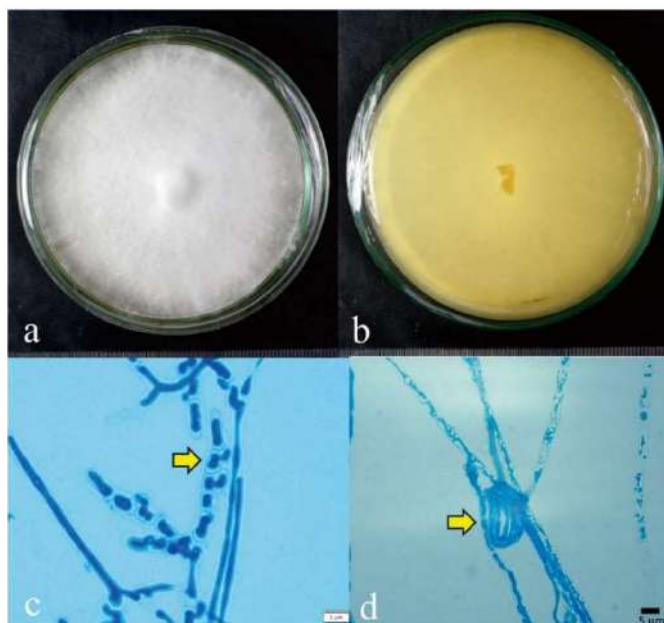
Fig. 1: Microscopic feature characteristic of *Leiotrametes menziesiii* BRB 73 after 5 days post inoculation; a) Mycelium of *L. menziesii* BRB 73 showed to be white, and flattened, (b) with a yellowish color mycelium on the reverse side, (c) The hyphae were thick-walled, hyaline, with clamp connection which width of the hypha varied from 1.77-3.56 μm, (d) and coil hyphae.

Abs. (0) = the initial absorbance Abs. (t) = the final absorbance

10^3 = correction factor (μmol/mol) (Ɛ) = 46,600 $M^{-1} cm^{-1}$

t = reaction time (1 min)   d = length of the cell

RESULTS AND DISCUSSION

Leiotrametes menziesii BRB 73 was a potential White Rot Fungus (WRF) that has not been widely reported for the decolorization of a mixture of direct dyes. *Leiotrametes menziesii* can be found in various host plants including *Acacia* sp, *Arthocarpus altilis*, *Cocos nucifera*, *Horsfieldia* sp., *Mangifera indica*, *Morinda citrifolia*, *Rhizopora* sp., and other plants (Park et al. 2021). This fungus has white hyphae, a degree of growth rate of 11.71 mm/day within 5-7 days on MEA media at 27± 2°C (Fig. 1). It produces lignocellulolytic enzymes consisting of laccase and MnP (Alexandropoulou et al. 2017). Moreover, different fungi have different environmental conditions in the decolorization of dyes. The data obtained showed that environmental conditions have an impact on the ability of fungi to remove dyes.

Time Incubation

Incubation time determines the rate of fungi to decolorize the dyes shown in Fig. 2 and Table 2. The highest decolorization by BRB 73 occurred at the final observations, which showed that this fungus had not yet reached the stationary phase. So, it was indicated that optimal incubation had not been obtained. This occurs in *Aspergillus niger* where decolorization of various synthetic dyes occurs after 96 hours (4 days) of incubation (Omar 2016).However, other cases showed that decolorization of Congo red by *Aspergillus*

Table 2: Effect time on decolorization of 200 mg.L^{-1} mixture of commercial direct dyes and enzyme production.

Time	Decolorization (%)	Laccase activity (U.mL^{-1})	MnP activity (U.mL^{-1})
24	6.2 ± 0.3	0.0 ± 0.0	0.8 ± 0.2
48	13.8 ± 0.9	50.4 ± 2.3	7.4 ± 1.3
72	23.3 ± 2.8	123.4 ± 4.8	20.5 ± 0.5
96	54.3 ± 0.6	164.4 ± 2.5	30.2 ± 4.0

quadrilineatus occurred after 72 hours of incubation (Yusuf et al. 2023).

Increased decolorization occurs until final incubation (96 H), which was followed by increased enzyme activity (laccase and MnP) (Table 2). It was proved that laccase and MnP play a major role in dye decolorization. Fungi produce enzymes that have similar abilities such as *P. prosopidis* (Bankole et al. 2018). Some White Rot Fungi degrade dyes into simple products by involving ligninolytic extracellular enzymes such as laccase and MnP to mineralize the dyes (Chaturvedi 2019). The mechanism involves the reaction of hydroxylation, demethylation, and cleavage ring (Shindhal et al. 2021).

Effects Of Environment Conditions on The Percentage of Decolorization and Biomass by BRB 73

Dyes concentration in this study ranged from 100-500 mg.L^{-1}. Fig. 3 shows that a high dye concentration results in increased dye removal, which ranges from 53-67%. Biomass has increased, although not significantly ranging from 0.12-0.13 g. Thus, it was found that BRB 73 can tolerate the highest concentration of commercial direct dyes. The dye concentration of 500 mg.L^{-1} showed no
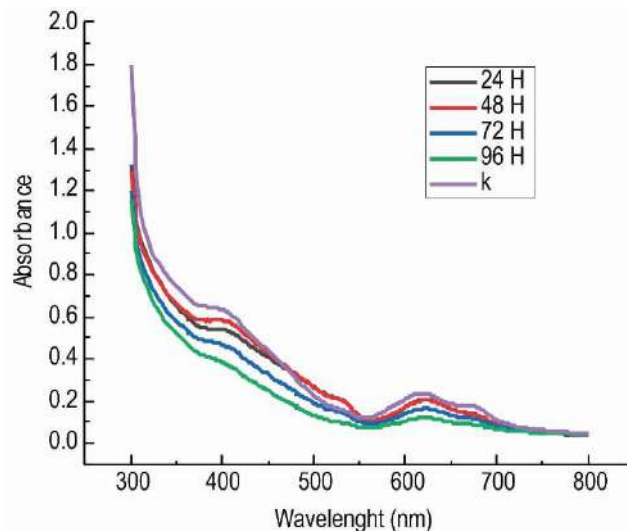
Fig. 2: Decolorization of commercial mixture dyes (200 mg.L^{-1}) by BRB 73 at various incubation times.
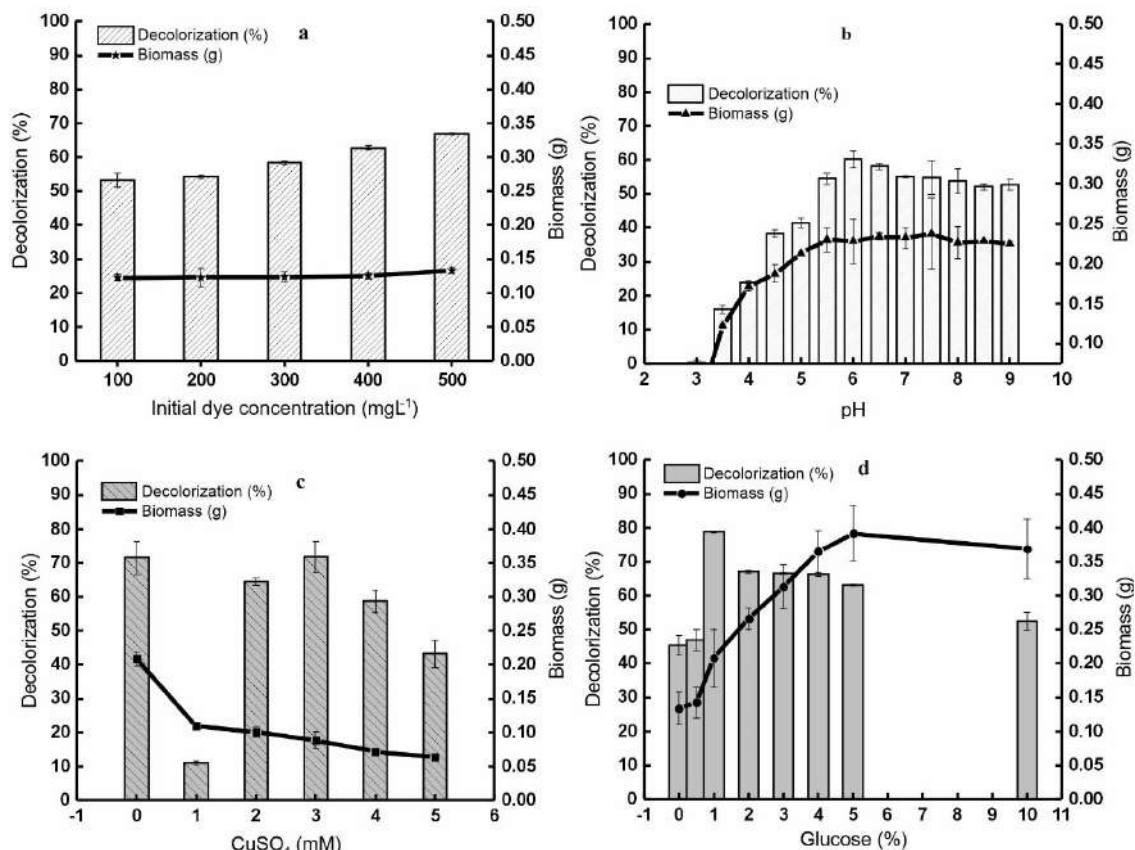
Fig. 3: Impact of environmental condition on dye decolorization and biomass by *Leiotrametes menziesii* BRB 73. dye concentration (a), pH (b), $CuSO_4$ (c), Glucose (d).

toxic symptoms, which was supported by stable biomass (Fig. 3a). Thus, it was indicated that BRB 73 was effective in commercial dye removal because it has a high tolerance to commercial direct dyes. In contrast to other studies, which showed that increased concentration leads to a decrease in the percentage of decolorization, such as *Ceriporia lacerate* (Wang et al. 2017), *Coriolus versicolor* and *Pleurotus ostreatus* (Afiya et al. 2019). The increased number of dye molecules causes fungal stress that inhibits fungal growth because the amount of enzymes produced to degrade dyes decreases (He et al. 2018).

Fungal growth is influenced by pH, generally, fungi grow at low pH which ranges from pH 4-5 (Sen et al. 2016). Each fungal species has a different favorable pH range, as shown in a study of seven *Lentinus* strains by Kalaw et al. (2021). Fig. 3B shows that mycelium growth increases from pH 3 to pH 5.5 Then, it becomes stable from pH 5.5 to pH 9. It can be indicated that this fungus has growth in a wide pH range. Other fungi that have a wide pH range are *G. lucidum* (Subedi et al. 2021), and *Lentinus swartzii* (Dulay et al. 2021). The graphic profiles of the percentage of decolorization and

biomass were similar. However, the highest decolorization at pH 6 was 60%. The optimum fungus at pH 6 in the absorption of Remazol Red RB Textile dyes was *Saccharomyces cerevisiae* (Sukarta et al. 2021). Decolorization decreases although not significantly when the alkaline value of the solution increases at pH 9 to 52%. In contrast to the research of Yusuf et al. (2023),the decrease in the percentage of congo red decolorization was drastic by *Aspergillus quadrilineatus*, with optimum decolorization at pH 5 was above 70% but drops dramatically at pH 7 to below 50%.

Inducers in dye decolorization were widely studied, including the copper sulfate group known to increase the production of laccase enzymes in WRF (Jaramillo et al. 2017) and increase dye degradation (Jiménez et al. 2019). Fig. 3C shows the impact of $CuSO_4$ inducers on fungal growth and dye decolorization. Increased inducer concentration resulted in stunted growth of BRB 73, which was indicated by decreased biomass, from 0.2 g to 0.06 g. It showed that high concentrations of $CuSO_4$ were toxic to fungi. According to Jiménez et al. (2019),the toxicity of heavy metals to microorganisms depends on concentration. It was
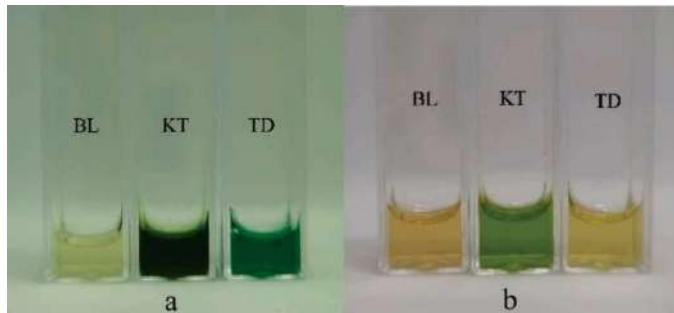
Fig. 4: Decolorization mixture of commercial direct dyes by BRB 73; a) 500 mg.L^{-1}; b) 100 mg.L^{-1} mixture dyes with added 1% glucose (optimum condition); BL (MGP medium), KT (before treatment), TD (after treatment).

observed that $CuSO_4$ concentrations between 0.1 and 1 mM did not inhibit growth. However, $CuSO_4$ concentrations higher than 1 mmol/L inhibit the growth of *P. ostreatus* mycelium (ACCC 52857) (Zhu et al. 2016). Meanwhile, the decolorization curve shows an unequal profile. The percentage of decolorization, both untreated and treated (3 mM), was 71.4% and 71.8%, respectively. It was indicated that $CuSO_4$ was not required as an inducer of BRB 73 in liquid cultures for the decolorization of these commercial dyes.

Glucose was utilized WRF in culture as a carbon source, evident from an increase in biomass from 0.132 g to 0.39 g (Fig. 3D). However, the addition of 10% of glucose resulted in a decrease in biomass to 0.37 g. Dye decolorization was optimal at a glucose concentration of 1%, which was 79%. Rajhans et al. (2021) recommend 1% glucose as the optimum concentration in the decolorization of azo dyes (Fig. 4). The decolorization profile curve showed a decrease while the glucose concentration increased. Similar study results occur in *Ganoderma multistipitatum*, increased glucose concentration can decrease dye decolorization (Alhomaidi et al. 2023). Due to high glucose concentrations, WRF mycelium prefers glucose degradation rather than complex molecular dyes (Senthilkumar et al. 2014). Fungi chose a simple carbon source that was utilized first (Hamad et al. 2014).

The Effect of Environmental Conditions on Laccase Activity

In this study, laccase plays a role in dye degradation, as seen from the increase in the activity of this enzyme according to the increase in the percentage of decolorization (Fig. 5A). Laccase increased from 154 U.L^{-1} to 215 U.L^{-1} indicates the presence of high dye concentrations capable of encouraging the production of laccase enzymes, as occurs in *T. versicolor* (Vel et al. 2020). Laccases are extracellular oxidoreductase enzymes reported by Bittencourt et al. (2023) to play a role in the decolorization of synthetic dyes. According to Castillo et al. 2023), laccases produced by fungi are more attractive

for bioremediation applications because these enzymes are not specific to the substrate and have a high potential for oxidation of a diverse range of pollutants, such as synthetic dyes. Degradation by enzymes produced by fungi is better than bacteria or algae (Sen et al. 2023). Laccase activity has not reached the highest values indicated by an increase in the percentage of decolorization. According to Vel et al. (2020) enzymes that reach the highest values show decolorization in the exponential or early stationary phase.

pH has a significant impact on the levels of laccase enzyme produced. The difference in contrast in laccase activity between Fig. 5A and 5B, shows that the addition of NaOH and HCl has an impact on decreasing laccase activity. It suggests that laccase was intolerant to the compound. According to Coria-Oriundo et al. (2021) laccase that was not stable in a wide pH range, intolerant to organic compounds, and high salts cannot be recommended on an industry scale. The highest laccase activity at pH 6 was 13 U.L^{-1} (Fig. 5B). Suryadi et al. (2022) reported that excessive laccase production by fungi was between pH 4.5 and 6. *O. canarii* shows maximal laccase activity at pH 4.5–5.5 (Lark et al. 2019).

$CuSO_4$ was presented in the culture medium as a mediator to increase laccase production by inducing laccase gene transcription (Dur et al. 2022). However, the presence of $CuSO_4$ in the culture medium decreases laccase activity by BRB 73, so it was indicated that the presence of $CuSO_4$ did not contribute to laccase production (Fig. 5C). It happens because the type of metal inducer and the concentration used are indicated not yet suitable for this WRF, similar facts occur in *Aspergillus flavus* with a concentration of 5 mM-10 mM (Liu et al. 2020). Laccase production by *Pleurotus ostreatus* MTCC 142 can be increased by the addition of Cu^{2+} (Das et al. 2016), while mediators for *M. arundinis* were HBA and HBT (Mendes et al. 2022). The optimum concentration of $CuSO_4$ for *A.maxima* was 0.1-3.0 mM (Kumar & Chandra 2020), while for *T. Versicolor* was 0.1 and 1 mM (Jaramillo et al. 2017).
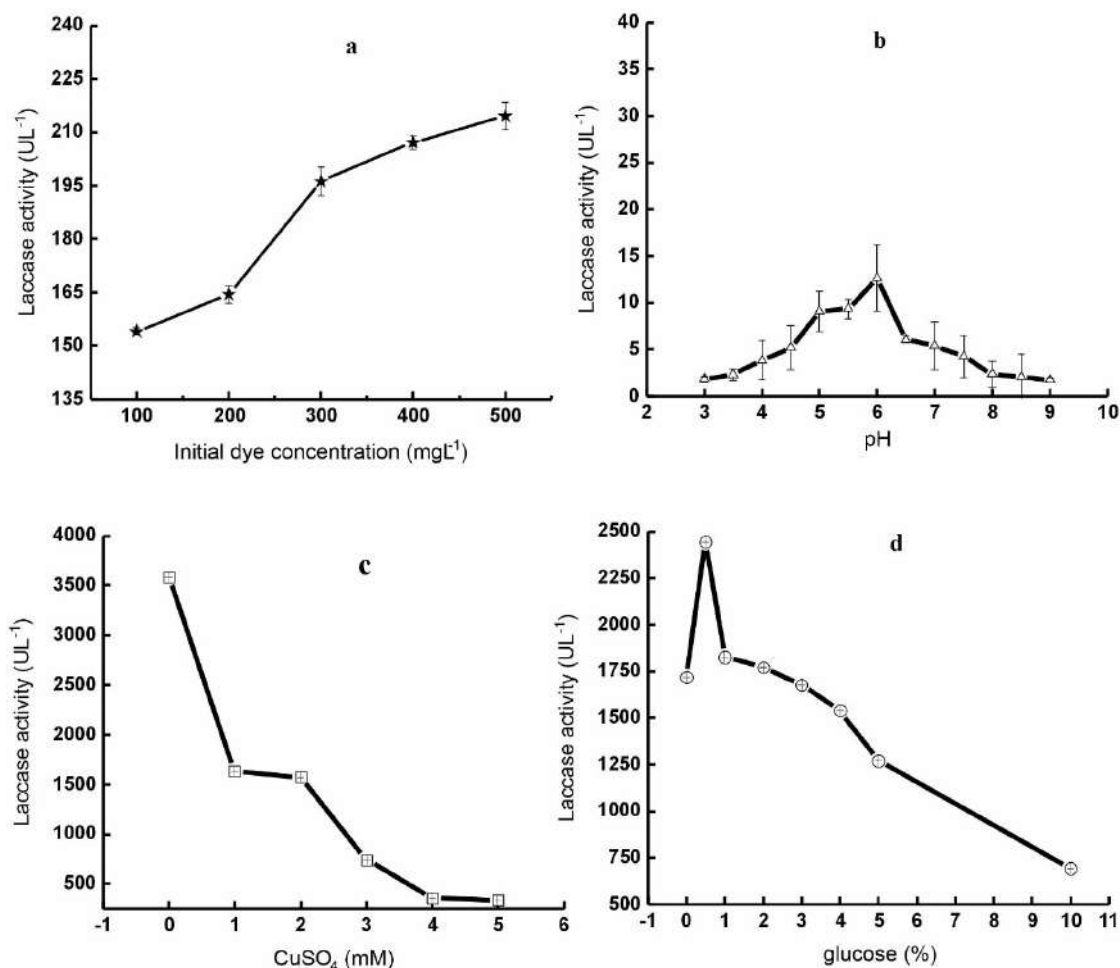
Fig. 5: Impact of environmental conditions on laccase activity by *Leiotrametes menziesii* BRB 73; (a) dye concentration, (b) pH, (c) CuSO$_4$, (d) glucose.

The curve profile between Figs. 5D and 2D have similarities. However, a glucose concentration of 0.5% stimulated the highest laccase production, which was 2444 U.L^{-1}. It was verified that a low concentration of glucose stimulates high laccase production (Daniel et al. 2018). The lowest laccase activity was at 10% glucose addition, which was 691 U.L^{-1}. High glucose concentrations result in both decreased laccase activity and decolorization. Suppression of laccase synthesis due to high concentrations also occurs in *Tramentes pubescens* (Alhomaidi et al. 2023).

In this study, the nutrients (nitrogen and glucose) of BRB 73 were insufficient so CuSO$_4$ added to the medium did not affect laccase activity. According to Duran-Sequeda et al. (2022), copper was involved in the induction of laccase if the conditions of the nutrient source (nitrogen and glucose) were sufficient. This nutrient affects the regulation of the laccase gene. In *P. ostreatus,* this condition can express transporter genes (CTRs) to uptake copper from the environment, resulting in an increase in laccase activity up to 20 times.

The Effect of Environmental Conditions on MnP Activity

Enzyme MnP was produced by BRB 73 during direct commercial synthetic dye decolorization. Their activities were much lower than laccase. However, this enzyme profile also shows improvement (Figs. 6A & 6B). MnP Activities at dye concentrations of 100 mg.L^{-1} and 500 mg.L^{-1} were 16 U.L^{-1} and 39 U.L^{-1}, respectively. It indicates that decolorization involves the MnP enzyme as well. According to Amaro Bittencourt et al. (2023), MnP produced by *Tramentes* sp. 48424 demonstrates high dye decolorization capability. Fungi can produce more than one enzyme in the decolorization process, such as laccase (Lac), manganese peroxidase (MnP), and lignin peroxidase (LiP) (Noman et al. 2020). All three enzymes were detected in RB5 decolorization by *P. chrysosporium* ATCC 24725
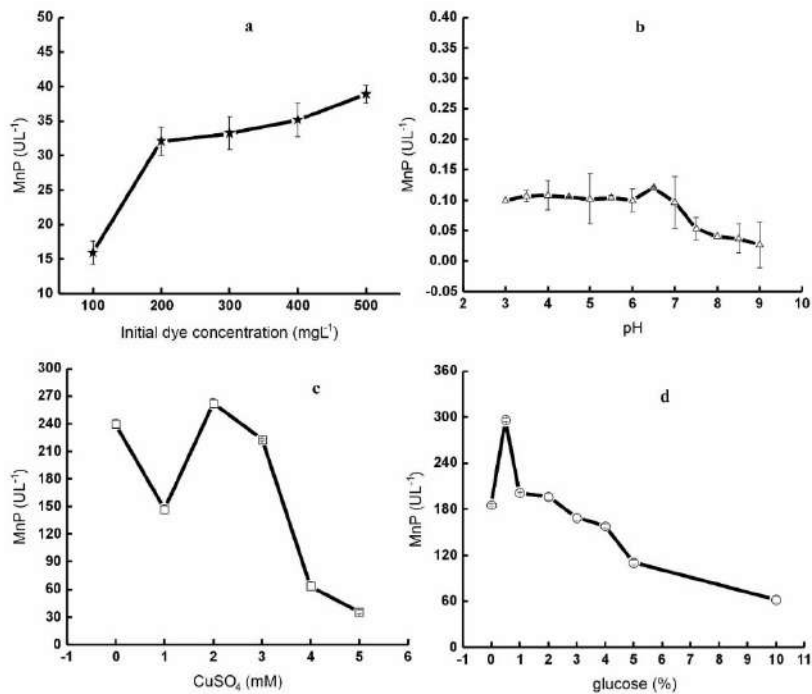
Fig. 6: Impact of environmental conditions on MnP activity by *Leiotrametes menziesii* BRB 73; (a) dye concentration, (b) pH, (c) CuSO$_4$, (d) glucose.

(Permpornsakul et al. 2016). *Trichoderma tomentosum* was indicated to involve two enzymes, namely manganese peroxidase and lignin peroxidase in decolorizing acid red 3 (He et al. 2018). The combination of various enzymes can significantly improve the biodegradation of textile dyes. However, the combination of enzymes depends on the type of dye, chemical structure, and microbes involved (Das et al. 2023).

pH affects enzyme production, as occurs in laccase production. MnP activity showed a stable value ranging from pH 3 to 7, which was 0.1 U.L^{-1}. Stability of MnP by *Echinodontium taxodii* 2538 at pH range 2-6 (Kong et al. 2016). The optimum pH of WRF for producing MnP was different, for example, *Clitopilus scyphoides* and *Cerrena unicolor* BBP6, which were 5.2 and 4.5, respectively (Rao et al. 2019). However, MnP decreased to 0.03 U.L^{-1} at pH 9. The overall data showed that the production of both enzymes, laccase and MnP, were lower than in other treatments (Figs. 5 & 6). Nevertheless, however, it was not affected by decolorization values ranging from 50-60%.

The impact of increasing CuSO$_4$ concentration causes a decrease in MnP activity (Fig. 6C). MnP activity was highest in additions of 2 mM, which was 262 U.L^{-1}. Whereas, the lowest MnP activity was 35 U.L^{-1} (5 mM of CuSO$_4$). Each WRF species requires a different concentration of CuSO$_4$ inducers to obtain optimum enzyme activity and decolorization (Laksmi et al. 2021).

MnP production decreases with the addition of glucose (Fig. 6D). The lowest glucose concentration (0.5%) was able to produce the highest MnP enzymes, which was 296 U.L^{-1}. Stress culture conditions can increase the MnP enzyme (Yuan et al. 2022). Meanwhile, the lowest activity was 62 U.L^{-1} at a concentration of 10% glucose. Other research information, shows that the type of carbon source affects the activity of MnP such as *P.ostreatus* which produces higher MnP using carbon sources from xylan (Daniel et al. 2018). Other fungi such as *Trichoderma harzianum* prefer sucrose over other carbon sources (Kumar & Arora 2022). Even without the addition of glucose, the presence of MnP was detected, which was 185 U.L^{-1}. However, the percentage of decolorization was 45%. In contrast, *M. palmivorus* VE111 produces high MnP at high glucose concentrations (30 g.L^{-1}), which was 59 U.L^{-1} (Daniel et al. 2018).

CONCLUSIONS

Leiotrametes menziesii BRB 73 has potential as a dye decolorization agent. It decolorized 54.3% of commercial direct dyes within 96 hours. Whereas, it was tolerance to dyes concentration exceeding 500 mg.L^{-1} which was supported by stable mycelium growth, increased laccase, and MnP enzyme activity. The decolorization pH range was quite wide, ranging from pH 5.5-9, supported by stable MnP activity from pH 3-7. However, the optimal condition of the laccase enzyme

was at pH 6. CuSO$_4$ inducers were not required by BRB 73 so it was necessary to study other types of inducers. Decolorization was optimal at the addition of 1% glucose, while enzyme activity was optimal at the addition of 0.5% glucose. This WRF produces extracellular enzymes including laccase and MnP during the decolorization process under various environmental conditions, which were indicated to play a major role in dyes degradation. Thus, it was recommended as a mycoremediation agent.

REFFERENCES

Afiya, H., Ahmet, E.E. and Shah, M.M., 2019. Enzymatic decolorization of Remazol Brilliant Blue Royal (RB 19) textile dye by White Rot Fungi. *Journal of Applied and Advanced Research*, 4(1), pp.11-15.

Afreen, S., Anwer, R., Singh, R.K. and Fatma, T., 2018. Extracellular laccase production and its optimization from *Arthrospira maxima* catalyzed decolorization of synthetic dyes. *Saudi Journal of Biological Sciences*, 25, pp.1446-1453.

Akhtar, N. and Mannan, M.A., 2020. Mycoremediation: Expunging environmental pollutants. *Biotechnology Reports*, 26, p.e00452.

Alam, R., Ardiati, F.C., Solihat, N.N., Alam, M.B., Lee, S.H., Yanto, D.H.Y., Watanabe, T. and Kim, S., 2020. Biodegradation and metabolic pathway of anthraquinone dyes by *Trametes hirsuta* D7 immobilized in light expanded clay aggregate and cytotoxicity assessment. *Journal of Hazardous Materials*, 405, p.124176.

Alexandropoulou, M., Antonopoulou, G., Fragkou, E., Ntaikou, I. and Lyberatos, G., 2017. Fungal pretreatment of willow sawdust and its combination with alkaline treatment for enhancing biogas production. *Journal of Environmental Management*, 203, pp.704-713.

Alhomaidi, E.A., Umar, A., Alsharari, S.S. and Alyahya, S., 2023. Evaluation of Lacc134 oxidoreductase of *Ganoderma multistipitatum* in detoxification of dye wastewater under different nutritional conditions. *Microbiological Research*, 14, pp.1398-1412.

Ali, S.S., Umar, A., Alsharari, S.S. and Alyahya, S., 2023. Evaluation of Lacc134 oxidoreductase of *Ganoderma multistipitatum* in detoxification of dye wastewater under different nutritional conditions. *Microbiological Research*, 14, pp.1398-1412.

Anita, S.H., Ningsih, F., Heri, D. and Yanto, D.H.Y., 2021. Biodecolorization of Remazol Brilliant Blue – R dye by Tropical White-Rot Fungi and their enzymes in the presence of guaiacol. *Jurnal Riset Kimia*, 12, pp.94-101.

Apriani, I., Yanto, D.H.Y., Hariani, P.L., Widjajanti, H. and Nurhayat, O.D., 2024. Potential of White Rot Fungi from Berbak-Sembilang National Park, Indonesia for decolorization and detoxification commercial Direct Dyes. *Trend in Sciences*, 21(6), pp.1-12.

Asgher, M., Muzammil, M., Ahmad, S., Khalid, N. and Bilal, M., 2020. Environmentally friendly color stripping of solar golden yellow R dyed cotton fabric by ligninolytic consortia from *Ganoderma lucidum* IBL-05. *Case Studies in Chemical and Environmental Engineering*, 2, p.100031.

Bankole, P.O., Adeyinka, A., Folashade, O., Vinayak, V. and Prabhu, S., 2018. Biodegradation and detoxification of Scarlet RR dye by a newly isolated filamentous fungus, *Peyronellaea prosopidis*. *Sustainable Environment Research*, 28, pp.214-222.

Bilal, M., Adeel, M., Rasheed, T., Zhao, Y. and Iqbal, M.N., 2019. Emerging contaminants of high concern and their enzyme-assisted biodegradation – A review. *Environment International*, 124, pp.336-353.

Bittencourt, G.A., Vandenberghe, L.P. de S., Martínez-Burgos, W.J., Valladares-Diestra, K.K., Murawski de Mello, A.F., Maske, B.L., Brar, S.K., Varjani, S., de Melo Pereira, G.V. and Soccol, C.R., 2023. Emerging contaminants bioremediation by enzyme and nanozyme-based processes – A review. *iScience*, 26(6), pp.1-19.

Castillo-M., L.A., Ramírez-G, C.A., Martínez-C, A., Reyes-G, J.R.,

Sánchez-O, E.M., Ibarra-V, J.R., Jiménez-J, R., Cuevas-V, G.M., Navarrete-M, A., Sandoval-A, O.A. and Gómez-R, C., 2023. Mathematical modeling for operative improvement of the decoloration of Acid Red 27 by a novel microbial consortium of *Trametes versicolor* and *Pseudomonas putida*: A multivariate sensitivity analysis. *Heliyon*, 9(11), p.e21793.

Chaturvedi, S., 2019. Azo Dyes Decolorization using White Rot Fungi. *Research & Reviews: Journal of Microbiology and Biotechnology*, 8(2), pp.9-19.

Chaurasia, P.K. and Bharati, S.L., 2019. Recent Myco-dye decolorization studies (Mini-review). *Journal of Biotechnology and Bioengineering*, 3(4), pp.27-31.

Cheng, W.N., Sim, H.K., Ahmad, S.A., Syed, M.A., Shukor, M.Y. and Yusof, M.T., 2016. Characterization of an azo-dye-degrading White Rot Fungus isolated from Malaysia. *Mycosphere*, 7(5), pp.560-569.

Colla, I.M., de Oliveira Filho, O.B.Q., de Freitas, J.D.S., Bertéli, M.B.D., Linde, G.A., Do Valle, J.S. and Colauto, N.B., 2020. Mycelial biomass cultivation of *Lentinus crinitus*. *Bioscience Journal*, 36(6), pp.2238-2246.

Coria-Oriundo, L.L., Battaglini, F. and Wirth, S.A., 2021. Efficient decolorization of recalcitrant dyes at neutral/alkaline pH by a new bacterial laccase-mediator system. *Ecotoxicology and Environmental Safety*, 217, p.112237.

Daniel, W., Schneider, H., Claudete, R., Mendonça, S., Gonçalves, F., Siqueira, D., José, A., Dillon, P. and Camassola, M., 2018. High level production of laccases and peroxidases from the newly isolated White-Rot Basidiomycete *Marasmiellus palmivorus* VE111 in a stirred-tank bioreactor in response to different carbon and nitrogen sources. *Process Biochemistry*, 69, pp.1-11.

Dao, A.T.N., Smits, M., Dang, H.T.C., Brouwer, A. and de Boer, T.E., 2021. Elucidating fungal *Rigidoporus* species FMD21 lignin-modifying enzyme genes and 2,3,7,8-tetrachlorodibenzo-p-dioxin degradation by laccase isozymes. *Enzyme and Microbial Technology*, 147, p.281-288.

Das, A., Bhattacharya, S., Panchanan, G., Navya, B.S. and Nambiar, P., 2016. Production, characterization and Congo red dye decolourizing efficiency of a laccase from *Pleurotus ostreatus* MTCC 142 cultivated on co-substrates of paddy straw and corn husk. *Journal of Genetic Engineering & Biotechnology*, 14(2), pp.281-288.

Das, S., Cherwoo, L. and Singh, R., 2023. Decoding dye degradation: Microbial remediation of textile industry effluents. *Biotechnology Notes*, 4, pp.64-76.

Dulay, R.M.R., Cabrera, E.C., Kalaw, S.P. and Reyes, R.G., 2021. Optimization of culture conditions for mycelial growth and fruiting body production of naturally-occurring Philippine mushroom *Lentinus swartzii* Berk. *Journal of Applied Biology and Biotechnology*, 9(3), pp.17–25.

Duran, D., Suspes, D., Maestre, E., Alfaro, M., Perez, G. and Pisabarro, A.G., 2022. Effect of Nutritional Factors and Copper on the Regulation of Laccase Enzyme Production in *Pleurotus ostreatus*. *Journal of Fungi*, 8, pp.1–21.

Rao, G.R., Ravichandran, A., Kandalam, G., Kumar, S.A., Swaraj, S. and Sridha, M., 2019. Enhanced production of manganese peroxidase from *Clitopilus scyphoides* employing statistical optimization for application in improving crop residue digestibility by ruminants. *Journal of Dairy, Veterinary & Animal Research*, 8(5), pp.190–203.

Hamad, H.O., Alma, M.H., Ismael, H.M. and Eri, A.G.O.C., 2014. The effect of some sugars on the growth of *Aspergillus niger*. *KSU Journal of Natural Sciences*, 17, pp.7–11.

He, X., Song, C., Li, Y., Wang, N., Xu, L., Han, X. and Wei, D., 2018. Efficient degradation of azo dyes by a newly isolated fungus *Trichoderma tomentosum* under non-sterile conditions. *Ecotoxicology and Environmental Safety*, 150, pp.232–239.

Herath, I.S., Udayanga, D., Jayasanka, D.J. and Hewawasam, C., 2024. Textile dye decolorization by white rot fungi – A review. *Bioresource Technology Reports*, 25, p.101687.

Iark, D., Buzzo, A.J.D., Garcia, J.A.A., Gesser, V., Vieira, C., Carvalho, R., Corrêa, G. and Peralta, R.A., 2019. Enzymatic degradation and detoxification of azo dye Congo red by a new laccase from *Oudemansiella canarii*. *Bioresource Technology*, 289, p.121655.

Jaramillo, A.C., Cobas, M., Hormaza, A. and Sanromán, M.Á., 2017. Degradation of adsorbed azo dye by solid-state fermentation: Improvement of culture conditions, a kinetic study, and rotating drum bioreactor performance. *Water, Air, & Soil Pollution*, 228, pp.205–219.

Jiménez, S., Velásquez, C., Mejía, F., Arias, M. and Hormaza, A., 2019. Comparative studies of pure cultures and a consortium of white-rot fungi to degrade a binary mixture of dyes by solid-state fermentation and performance at different scales. *International Biodeterioration & Biodegradation*, 145, p.104772.

Kalaw, S.P., Dulay, R.M.R., Damaso, E.J., Ramos, J.C., Del Rosario, M.A.G., Abon, M.D., De Leon, A.M., Undan, J.R. and Reyes, R.G., 2021. Optimization of mycelial culture conditions and fructification of *Lentinus* species using rice straw and sawdust based substrates. *Studies in Fungi*, 6(1), pp.519–530.

Kong, W., Chen, H., Lyu, S., Ma, F., Yu, H. and Zhang, X., 2016. Characterization of a novel manganese peroxidase from white-rot fungus *Echinodontium taxodii* 2538, and its use for the degradation of lignin-related compounds. *Process Biochemistry*, 51(11), pp.1776–1783.

Kumar, A. and Arora, P.K., 2022. Biotechnological applications of manganese peroxidases for sustainable management. *Frontiers in Environmental Science*, 10, pp.1–11.

Kumar, A. and Chandra, R., 2020. Ligninolytic enzymes and its mechanisms for degradation of lignocellulosic waste in environment. *Heliyon*, 6(2), p.e03170.

Kyomuhimbo, H.D. and Brink, H.G., 2023. Applications and immobilization strategies of the copper-centred laccase enzyme: a review. *Heliyon*, 9(2), p.e13156.

Laksmi, F.A., Agustriana, E., Nuryana, I., Rachmayati, R., Perwitasari, U. and Andriani, A., 2021. Removal of textile dye, RBBR, via decolorization by *Trametes hirsuta* AA-017. *Biosaintifika*, 13, pp.319–327.

Liu, S., Tsai, S., Guo, P. and Lin, C., 2020. Inducing laccase activity in white rot fungi using copper ions and improving the efficiency of azo dye treatment with electricity generation using microbial fuel cells. *Chemosphere*, 243, p.125304.

Mendes, N., Paula, D., Brugnari, T., Windson, C., Haminiuk, I. and Maria, G., 2022. Biotechnological potential of fungi from a mangrove ecosystem: Enzymes, salt tolerance and decolorization of a real textile effluent. *Microbiological Research*, 254, p.126899.

Monga, D., Kaur, P. and Singh, B., 2022. Microbe mediated remediation of dyes, explosive waste and polyaromatic hydrocarbons, pesticides and pharmaceuticals. *Current Research in Microbial Sciences*, 3, p.100092.

Noman, E., Talip, B.A., Al-Gheethi, A., Mohamed, R. and Nagao, H., 2020. Decolourisation of dyes in greywater by mycoremediation and mycosorption process of fungi from peatland; primary study. *Materials Today: Proceedings*, 31, pp.23–30.

Omar, S.A., 2016. Decolorization of different textile dyes by isolated *Aspergillus niger*. *Journal of Environmental Science and Technology*, 9(1), pp.149–156.

Park, M.S., Yoo, S., Cho, Y., Park, K.H., Kim, N.K., Lee, H.S. and Lim, Y.W., 2021. Investigation of the fungal diversity of the Federated States of Micronesia and the construction of an updated fungal inventory. *Mycobiology*, 49(6), pp.551–558.

Pazarlioglu, N.K., Akkaya, A., Akdogan, H.A. and Gungor, B., 2010. Biodegradation of Direct Blue 15 by free and immobilized *Trametes versicolor*. *Water Environment Research*, 82(7), pp.579–585.

Pérez-Cadena, R., García-Esquivel, Y., Castañeda-Cisneros, Y.E., Serna-Díaz, M.G., Ramírez-Vargas, M.R., Muro-Urista, C.R. and Téllez-Jurado, A., 2020. Biological decolorization of Amaranth dye with *Trametes polyzona* in an airlift reactor under three airflow regimes. *Heliyon*, 6(12), p.e05857.

Permpornsakul, P., Prasongsuk, S., Lotrakul, P., Eveleigh, D.E., Kobayashi, D.Y., Imai, T. and Punnapayak, H., 2016. Biological treatment of Reactive Black 5 by resupinate white rot fungus *Phanerochaete sordida* PBU 0057. *Polish Journal of Environmental Studies*, 25(3), pp.1167–1176.

Rajhans, G., Barik, A., Sen, S.K. and Raut, S., 2021. Degradation of dyes by fungi: an insight into mycoremediation. *BioTechnologia (Poznan)*, 102, pp.445–455.

Ridtibud, S., Suwannasai, N., Sawasdee, A., Champreda, V., Phosri, C., Sarp, S., Pisutpaisal, N. and Boonyawanich, S., 2024. Selection of white-rot fungi for decolorization of palm oil mill effluent and evaluation of biodegradation and biosorption processes. *Nature Environment and Pollution Technology*, 23(1), pp.235–243.

Sen, S.K., Raut, S., Bandyopadhyay, P. and Raut, S., 2016. Fungal decolouration and degradation of azo dyes: A review. *Fungal Biology Reviews*, 30(3), pp.112–133.

Sen, S.K., Raut, S. and Raut, S., 2023. Mycoremediation of anthraquinone dyes from textile industries: a mini-review. *Biotechnologia*, 104(1), pp.85–91.

Senthilkumar, S., Perumalsamy, M. and Prabhu, H.J., 2014. Decolourization potential of white-rot fungus *Phanerochaete chrysosporium* on synthetic dye bath effluent containing Amido black 10B. *Journal of Saudi Chemical Society*, 18(6), pp.845–853.

Shindhal, T., Rakholiya, P., Varjani, S., Pandey, A., Hao, H., Guo, W., Ng, H.Y. and Taherzadeh, M.J., 2021. A critical review on advances in the practices and perspectives for the treatment of dye industry wastewater. *Bioengineered*, 12(1), pp.70-78.

Singh, A.K., Iqbal, H.M.N., Cardullo, N., Muccilli, V., Fernández-Lucas, J., Schmidt, J.E., Jesionowski, T. and Bilal, M., 2023. Structural insights, biocatalytic characteristics, and application prospects of lignin-modifying enzymes for sustainable biotechnology. *International Journal of Biological Macromolecules*, 242(3), p.124968.

Singh, M.P., Vishwakarma, S.K. and Srivastava, A.K., 2013. Bioremediation of direct blue 14 and extracellular ligninolytic enzyme production by White Rot Fungi: *Pleurotus* Spp. *BioMed Research International*, 2013, pp.2–5.

Subedi, K., Basnet, B.B., Panday, R., Neupane, M. and Tripathi, G.R., 2021. Optimization of growth conditions and biological activities of Nepalese *Ganoderma lucidum* Strain Philippine. *Advances in Pharmacological and Pharmaceutical Sciences*, 2021, pp.1–7.

Sudhaparimala, S. and Usha, R., 2022. Tuning of carbon microspheres and graphene structures with hetero atoms for organic dye degradation and heavy metal remediation - influence of fructose as a precursor. *Nature Environment and Pollution Technology*, 21(2), pp.469–480.

Sukarta, I.N., Ayuni, N.P.S. and Sastrawidana, I.D.K., 2021. Utilization of khamir (*Saccharomyces cerevisiae*) as adsorbent of remazol red rb textile dyes. *Ecological Engineering & Environmental Technology*, 22(1), pp.117–123.

Sun, S., Liu, P. and Ullah, M., 2023. Efficient azo dye biodecolorization system using lignin-Co-cultured White-Rot Fungus. *Journal of Fungi*, 9(1).

Suryadi, H., Judono, J.J., Putri, M.R., Eclessia, A.D., Ulhaq, J.M., Agustina, D.N. and Sumiati, T., 2022. Biodelignification of lignocellulose using ligninolytic enzymes from White-Rot Fungi. *Heliyon*, 8(2), p.e08865.

Vel, C., Mejía-Ot, F. and Hormaza-Anaguano, A., 2020. Evaluation of several white-rot fungi for the decolorization of a binary mixture of anionic dyes and characterization of the residual biomass as potential organic soil amendment. *Journal of Environmental Management*, 254, p.109805.

Vinotha, S. and Rose, A.L., 2023. Comparative advanced oxidation decolorization of the triphenylmethane dye with dimethyl dioxirane and hydrogen peroxide. *Nature Environment and Pollution Technology*, 22(2), pp.803–815.

Wang, N., Chu, Y., Wu, F., Zhao, Z. and Xu, X., 2017. Decolorization and degradation of Congo red by a newly isolated white rot fungus, *Ceriporia lacerata*, from decayed mulberry branches. *International Biodeterioration & Biodegradation*, 117, pp.236–244.

Yanto, D.H.Y., Guntoro, M.A., Nurhayat, O.D., Anita, S.H., Oktaviani, M., Ramadhan, K.P., Pradipta, M.F. and Watanabe, T., 2021. Biodegradation and biodetoxification of batik dye wastewater by laccase from *Trametes hirsuta* EDN 082 immobilised on light expanded clay aggregate. *3 Biotech*, 11(5), pp.1–13.

Yuan, H., Li, J., Pan, L., Li, X., Yuan, Y., Zhong, Q. and Wu, X., 2022. Ecotoxicology and environmental safety particulate toxicity of metal-organic framework UiO-66 to white rot fungus *Phanerochaete chrysosporium*. *Ecotoxicology and Environmental Safety*, 247, p.114275.

Yusuf, F., Yakasai, H.M., Usman, S., Muhammad, J.B., Yaú, M., Jagaba, A.H. and Shukor, M.Y., 2023. Dyes-decolorizing potential of fungi strain BUK_BCH_BTE1 locally isolated from textile industry effluents: characterization and LC-MS analysis of the metabolites. *Case Studies in Chemical and Environmental Engineering*, 8, p.100453.

Zafar, S., Bukhari, D.A. and Rehman, A., 2022. Azo dyes degradation by microorganisms – An efficient and sustainable approach. *Saudi Journal of Biological Sciences*, 29(12), p.103437.

Zhu, C., Bao, G. and Huang, S., 2016. Optimization of laccase production in the white-rot fungus *Pleurotus ostreatus* (ACCC 52857) induced through yeast extract and copper. *Biotechnology and Biotechnological Equipment*, 30(2), pp.270–276.

Odor Emissions from Municipal Solid Waste Open Dumps Constituting Health Problems Due to their Composition, Ecological Impacts and Potential Health Risks

S. Srinivasan[1][†] iD **and R. Divahar**[2] iD

[1]Department of Civil Engineering, Aarupadai Veedu Institute of Technology, Vinayaka Missions Research Foundation, Salem, Tamil Nadu, India

[2]Civil Engineering, Aaarupadai Veedu Institute of Technology, VMRF, Chennai, Tamil Nadu, India

†Corresponding author: S. Srinivasan: srinivasan.civil@avit.ac.in

ABSTRACT

The presence of Hydrogen sulfide, Methane, Volatile Organic Compounds (VOCs), and other odorous compounds in the ambient air is the root cause of the offensive odor emitting from the MSW dumping yard. Composition features and health risks associated with odor emissions concentrations in MSW dumping yards. This paper aims to provide an overview of research on health problems due to their composition, ecological impacts, and potential health risks of volatile organic compounds (VOCs) and to examine the relationship between VOC exposure and chronic illnesses in humans and the environment. In this study, a comprehensive investigation of VOC odor emission from an urban MSW dumping site has been performed. The VOC odor sample was analyzed using the GC-MS technique. The maximum VOCs concentration reported is due to tert - butylbenzene at $1.41 \mu g.m^{-3}$ and the minimum is due to *Sec*-butylbenzene at $0.07 \mu g.m^{-3}$. Scientific databases, including Google Scholar, California Office of Environmental Health Hazard Assessment (OEHHA), and US EPA (Integrated Risk Information System (IRIS), were searched extensively using a bibliographic technique, in addition to a case study on MSW dumping yard workers. The findings of epidemiologic and experimental research, the emission of odors as a result of volatile organic compounds (VOCs) can cause a variety of non-cancerous health effects that are linked to abnormal functioning of the body's vital organs, including the nervous and coronary, and pulmonary systems. It can also have minimal impact on the environment by causing global warming and ozone layer depletion. The odor emissions from the dumpsite pose both carcinogenic and noncarcinogenic risks to the health of the individuals participating in the dumping yard. As a result of these results, it is important to manage odor emissions (VOCs) during composting and take steps to reduce their negative effects on the environment and public health.

INTRODUCTION

The annual production of solid waste (SW) dumping yards is rising due to residents' expansion, urbanization, and worldwide economic development. The World Bank estimates that 2.24 billion tonnes of MSW were created in 2020 and that in a world where nothing changes, 3.88 billion tonnes might have been produced by the year 2050 (Jayasinghe et al. 2023, The World Bank 2023), which will pose great challenges for governments. Odor complaints from locals have increased in recent years, according to many neighborhood organizations. These complaints are typically related to the dumping of municipal solid waste. Commercial and residential waste in a solid or semi-solid state that is produced in a municipal or notified area is referred to as municipal solid waste (MoEF 2022). One of the key concerns is the short- and long-term gaseous emissions that are connected to dangers to human health and the environment, even though MSW dumping sites can be managed or uncontrolled and the type of waste that is disposed of varies from one

country to others (EPA 1997, Young & Parker 1983). All waste management practices, including those at recycling facilities, transfer stations, composting services, and landfills, have the potential to lead to a variety of amenity complaints, such as air and odor emissions. Concerned neighbors are concerned about the odor, which has emerged as the most common complaint in recent years. Mixer of solid waste that can be classified as biodegradable (48.65%), recyclable (37.26%), residual (13.25%), and hazardous (0.84%) characterization of the waste generated at the Ifugao State University Potia Campus. Due to the overall composition of waste on the university campus formation of odor emissions takes place via biological and chemical composition, temperature, and wind speed, which are all the primary causes (Latugan 2024). Odors are a common and unavoidable consequence of the chemical and biological processes that occur when waste breaks down, and they have long been connected to waste disposal methods (Dlamini 2019). Both in landfills and composting yards, organic wastes undergo aerobic and anaerobic processes of decomposition, which are linked to common odors (US-EPA). There are three main types of organic volatility pollutants there are 1) Very volatile organic compounds, 2) Volatile Organic Compounds, and semi-volatile organic compounds. In the GC-MS analysis of collected samples, extremely few samples correspond with the VVOC groups of Methyl Chloride, chloromethane, and chloroform. At very low concentrations, these contaminants show high toxicity, so they are the most causing harm (David & Niculescu 2021). Odor complaints resulting from various household and commercial operations have become more frequent in recent years, especially with connection to waste management facilities and specifically MSW dumping yards. Both organic and inorganic compounds can have odor emissions, such as methane, volatile organic compounds (VOCs), ammonia, hydrogen sulfide, and sulfur-reduced compounds are the typical components of MSW odors (Cai et al. 2007). A dumping yard's odor emissions are typically low concentrations and evenly distributed, unlike industrial emissions (Mahin 2001). People can feel anxious after long-term exposure to such an environment (Jin-Feng Wang & Hu 2012). Determining the ambient concentration of VOCs in urban areas has received increased attention over the past decade due to the open dumping of MSW and the impact of VOCs on human health (IARC 2007). The environment is impacted by volatile organic compounds (VOCs) in addition to human health. When oxidants arise, volatile organic compounds (VOCs) are important. In the troposphere zone, for example, ozone and peroxyacetyl nitrate. In the MSW disposal yard, the majority of odor emission tests are conducted. The most notable odor molecules generated during the biodegradation process are

hydrogen sulfide, methyl mercaptan, and methyl sulfide (Wenjing et al. 2015). Odor emissions from the MSW dumping yard create a serious threat to the health of those who work with MSW and the occupants of the surrounding residential areas. They also have an impact on the day-to-day lives of the residents, primarily because of the weather. A modest increase in odor production affects the surrounding area (Liu & Zheng 2020). As per the IARC (2012) study, Groups 1 and 3 are categorized as carcinogenic disorders that primarily impact human health by causing harm to the lymphatic system, central nervous system, and reproductive system. (Demirel et al. 2014). VOCs have been identified as one of the main contributors to odor emissions in the MSW dumping yard. The objective of this paper is to give an in-depth understanding of all the information available regarding the impacts of volatile organic compounds (VOCs) on the environment and public health.

The present experimental study aims to discover the various combinations of odor compounds, their monitored concentrations in the MSW dumping yard, and the health effects that the presence of volatile organic compounds (VOCs) in the MSW dumping yard has on both humans and the environment. The research also attempts to discover the specific compounds, their concentrations, and the health effects that result from their composition. The main objective of this research was:

- To identify the different odor compounds (VOCs) in the MSW dumping yard.

- To provide an overview of research on health impacts due to their composition and ecological impacts.

- To determine the potential health risks of VOCs and to examine the relationship between VOC exposure and chronic illnesses.

Significance of Odor Emission

There have been several attempts to handle MSW segregation, but treating the solid waste in the dumping yard is still not being addressed comprehensively, as is disposing of MSW in the open dumps. It is one of the main reasons for emitting odor emissions from the open dumps as well as in the garbage bins. Both rural and urban areas are still observed gathering all kinds of waste (Ahluwalia & Patel 2018). VOCs are the main odor-emitting compounds in the MSW dumping yard. The main VOC families are sulfur compounds, terpenes, halogenated aromatic hydrocarbons, alkanes, alkenes, and oxygenated compounds. In our monitoring and analyses of VOCs from the MSW dumping yard, five different VOC families are present in the observed samples (Saral et al. 2009, Liu & Zheng 2020). Fikri (2024) has discussed gaseous pollutant formations, their potential health effects, and
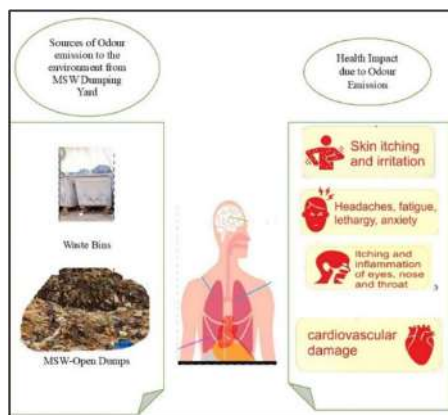
Fig. 1: Routes of MSW dumping yard-released odor compounds into the environment and their harmful effects on human health.

Fig. 2: (a) BDX II Abatement Air Sampler.

Fig. 2: (b) ADT PROBE.

clinical coding to identify gaseous pollutants like methane, carbon dioxide, and non-methane organic compounds at the Piyungan Landfill using the landGEM model. Eventually, there have been issues with odor emissions in both rural and urban regions that have not been successfully managed for the disposal of waste until the present day. Hence, this paper also discusses whether the odor emissions from MSW open dumps constitute health problems due to their composition, ecological impacts, and potential health risks shown in Fig.1

MATERIALS AND METHODS

Field-Based Investigation

Using an ADT probe and a BDX II abatement air sampler for the field-based investigation (shown in Figs. 2a and 2b), it was analyzed with a GC-MS Agilent 6890 N series instrument in the laboratory. The investigation was carried out at an MSW dumping yard adjacent to the one where different kinds of odor were gathered. The ADT probe was used to continuously monitor air quality monitoring inside the MSW over the complete disposal of fresh waste in the dumping yard in the pre-monsoon season of 2023. To track the geographic and seasonal variations in odor in the ambient air, samples are gathered while taking into account the local climatic conditions. Three different locations in the dumping yard were used to collect the samples. The samples were collected and then sent directly to the laboratory for analysis. Air samples containing these compounds will be collected at different distances from the MSW solid waste dumping yard because odors can be observed in ambient air. With a flow rate of 0.5–3.0 LPM, ambient air containing the odor-causing compounds will be collected in the ADT Sampling Probe utilizing a BDX II Abatement Air Sampler pump. The portable BDX II Abatement Air Sampler has an electrical flow control adjustment incorporated right into the

device. The battery pack is rechargeable. VOC samples were obtained using an ADT Probe that works with 9.1cm tubes that are either electronically labeled or untagged. After the sample has been taken, the tube's mouth will be carefully sealed off and labeled with the location, date, and time of the sample. The laboratory will get this sampling tube to find out the odor concentration.

Using GC/MS to Identify the Target VOCs

A gas chromatograph (GC) is used to assess the odor of volatile organic compounds (VOCs). The concentrations were measured using an Agilent 6890 N series GC (Gas Chromatograph system), which included a single Flame Ionization Detector (FID) column. There is one 100 psi EPC Splitless Injection Port used to inject the sample at the designated temperature. An autosampler, 6890 control electronics, 6890 injectors, a Pentium computer, and a 17-inch flat-panel monitor are all included in the GC. ADT probes are used at three sampling locations to take air samples. The solid waste dumping yard's three different locations are where the samples were taken. The ambient air collected from the landfill underwent an analysis of several VOC chemicals. Figs. 3, 4, and 5 depict VOC concentrations according to the solid waste.

RESULTS AND DISCUSSION

VOCs Impact and Concentration from MSW Dumping Yard

It was also found that alkanes, aromatic compounds, chlorofluorocarbons, halogenated compounds, and halogenated aromatic hydrocarbons had been identified, but only in the gaseous samples that were taken from the MSW

dumping yard (Rosa et al. 2005). The most common problems with VOCs are their various direct and indirect effects on people and the environment, Such as the detrimental effects of toxic substances on the environment and the community. An investigation of VOC generation (odor emissions) in MSW dumping yard site. The following information on odor emission concentrations and their health effects provides more information on the three various locations in the MSW dumping yard.

Composition and Chemical Concentration at Station-1

In MSW dumping yards, there are six different types of odor compounds. Fig. 3 shows the six volatile organic compounds, which are part of the aromatic compounds group of volatile organic compounds, were detected at sampling station 1. As a result of the selected temperature program, the peaks appear to separate more precisely. A 1.41 $\mu g.m^{-3}$ t-butylbenzene maximum concentration and a Sec butylbenzene 0.07 $\mu g.m^{-3}$ minimum concentration were found at MSW dumping yard station 1 (Kumarathilaka & Jayawardhana 2016). Two of the Very volatile organic compounds (VVOCs) that are most frequently discovered in landfill dumping yards are *m & p* -xylenes and toluene. According to a study in the

pre-monsoon season of 2023, toluene concentrations were 0.195 $\mu g.m^{-3}$, whereas m & p -xylenes concentrations ranged between 0.25 $\mu g.m^{-3}$ (Christensen et al. 1994). O-xylenes and ethylbenzene concentrations ranged between 0.12 and 0.18 $\mu g.m^{-3}$. There was a lower percentage of aromatic hydrocarbons in the other three sampling sites, but they were responsible for 93.7% of the carcinogenic risk associated with odorous chemicals released from MSW dumping grounds (Scaglia et al. 2011). The majority of the BTEX (benzene, toluene, ethylbenzene, and xylene) are discharged from the MSW dumping yard.

BTEX emitted into the environment from MSW dumping yards creates problems for public health and the environment. Toluene is a colorless liquid, and its family of VVOCs can severely harm neurological systems (David & Niculescu 2021).

Composition and Chemical Concentration at Station-2

A total of six odor compounds in landfill dumping yards are shown in Fig. 4. There are six volatile compounds in sampling station 2, of which four belong to the aromatic group, methyl chloride belongs to the halogenated group, and methyl ethyl ketone belongs to the chlorofluorocarbon
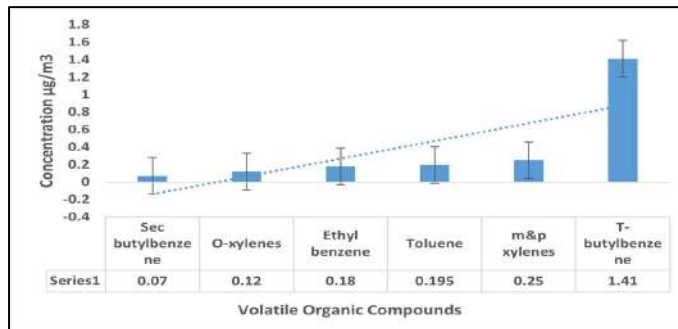
Fig. 3: MSW Dumping yard station-1.
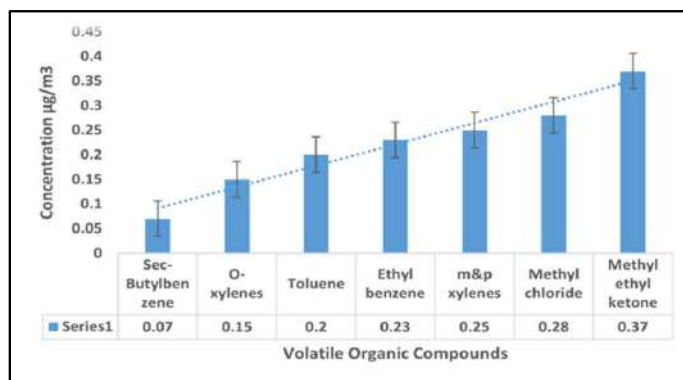
Fig. 4: MSW Dumping yard station-2.

group of Semi volatile organic compounds. As a result of the selected temperature program, the peaks appear to separate more precisely. A 0.37 μg.m^{-3} methyl ethyl ketone high concentration and a Sec butylbenzene 0.07 μg.m^{-3} low concentration were found at MSW dumping yard station-2 (Kumarathilaka & Jayawardhana 2016). Compared to VOCs, semi-volatile organic compounds. have a greater molecular weight and boiling point. In the MSW disposal yards, the toxicity from broken building debris, e-waste used furniture, and furnishings as additives can cause serious issues.

Methyl chloride is a colorless, explosive, and toxic chemical compound. Depending on the amount and duration of exposure, methyl chloride exposure can cause a variety of side effects, from fatigue and sickness to seizures and unconsciousness. Methyl chloride is also one of the dangerous pollutants that come under the VVOCs (Williams & Koppmann 2007). CFC-related occupational health risks in MSW dumping yards are moderately toxic, but their breakdown products are more dangerous (Hohener et al. 2003).

Composition and Chemical Concentration at Station-3

A total of five odor compounds in landfill dumping yards are shown in Fig. 5. There are five volatile compounds in the sampling station- 3 n-butylbenzene and benzene belong to the aromatic compound group, trichlorofluoromethane, chlorobenzene, and trichloroethane belong to the halogenated

compounds of VOCs. As a result of the selected temperature program, the peaks appear to separate more precisely. A 1.02 μg.m^{-3} benzene high concentration and a trichloroethylene 0.11 μg.m^{-3} low concentration were found at MSW dumping yard station-3 (Kumarathilaka & Jayawardhana 2016).

Long-term skin contact with volatile organic compounds (VOCs) at municipal solid waste (MSW) dumping yards can cause skin irritation. Occupational health risks from VOCs include the potential for cancer through inhalation (Liu et al., 2014). Inhalation is the primary exposure method, with aromatic compounds significantly impacting human health. This includes causing allergic reactions, asthma, and impaired lung function (Pan et al., 2023).

Comparison and Composition of Odor Compounds at Dumping Sites

Throughout monitoring, 18 odor compounds were detected in landfill dumping yards. A comparison and composition of odor compounds at dumping sites is shown in Fig. 6. Based on the temperature program selected, few odor compounds repeat in three stations, but the peaks appear to separate more precisely in all three stations. We analyzed odor samples using GC-MS. According to the analysis, the maximum number of odors reported is due to *T*-butylbenzene at 1.41 μg.m$^{-3,}$ and the minimum amount is due to *Sec*-butylbenzene at 0.07 μg.m^{-3}. Certain compounds found in the MSW dumping yard, such as *sec*-butylbenzene and *tert*-
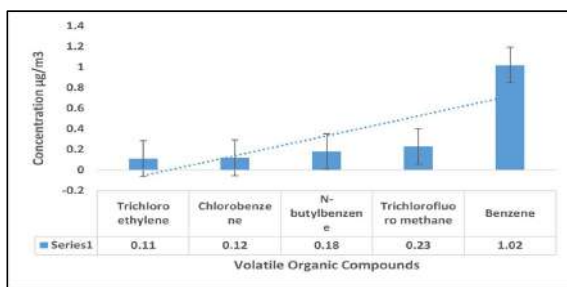
Fig. 5: MSW Dumping yard at station-3.
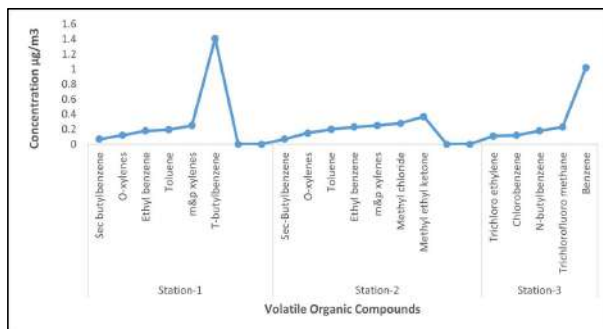
Fig. 6: Comparison and composition of odor compounds.

butylbenzene, can be inhaled or ingested. They are known to cause irritation to the skin, eyes, and respiratory tract. They may also result in lung aspiration (OEHHA 2024b).

Offensive Odors Due to Composition and Chemical Concentrations at Dumping Sites

Small amounts of odor compounds (methane, hydrogen sulfide, Volatile organic compounds, alkylbenzenes, mercaptans, benzene, toluene, and other aromatic hydrocarbons) in landfill dumping yards contribute to odors (Young & Parker 1983).

There is a wide range of odors associated with landfill dumping yard odor compounds, ranging from mildly pleasant to unpleasant and severe. Concentrations are influenced by the kinds of microorganisms found in the waste, as well as by the waste's age, composition, stage of decomposition, and pace of fermentation. Most smelly trace chemicals are considered to be hazards to the environment and workers' health (Young & Parker 1984, Young & Heasman 1985). The wind speed, humidity, and temperature levels in the surrounding air all have a significant impact on the spread of odors from the waste-dumping yard boundaries.

Formation of Odor Emissions (VOCs) and the Impact That They Have on The Environment and Humans

The term "VOCs" refers to organic compounds. VOCs are generated in the MSW dumping yard when various stages of waste and its type both compostable and non-compostable waste -are combined. Depending on the waste and surrounding temperature, VOCs are quickly emitted from the MSW dumping yard under normal pressure. Odor emissions, or volatile organic compounds, have a direct impact on the outdoor environment, cause nuisances to the surrounding area, and have an indirect and direct impact on human health. The detrimental effects of VOCs on the environment and people were the primary subject of discussion in this chapter.

These are the five primary phases in the MSW dumping yard that promote the discharge of odors during the odor emission process. The five phases are as follows: i) the MSW dump yard's size; ii) the landfill cover soil (biodegradation processes will be initiated based on waste type, age, and soil conditions); iii) the atmosphere's ambient temperature; iv) air permeation and oxidizing conditions; and v) biological and chemical activities (Randazzo et al. 2022). Fig. 7 shows the allergy symptoms due to inhalation of Odors at MSW Dumping Yard workers and nearby residents.

Inhaling volatile organic compounds from MSW dumping yards is the main way that humans are exposed to them. People can get a variety of health consequences as a result, such as mild respiratory diseases such as coughs, wheezes, allergies, and asthma (Su et al. 2012). The current study analyzed the impacts of each volatile organic compound (VOC) compound on the environment and MSW dumping yard personnel, as well as the different concentrations and pathways that VOCs emitted from these sites.

Benzene compound: A family of aromatic compounds includes benzene. The primary method of exposure from the MSW dumping yard is inhalation and is non-cariogenic. Health effects due to inhaling benzene from MSW dumping yards are possible to get decreased lymphocyte count (IRIS 2024). Symptoms of infected lymphocytes in human beings like fever, cough, runny nose, nutritional deficiencies, and also autoimmune diseases (NIH 2024). Symptoms due to inhalation of benzene at MSW Dumping Yard are shown in Fig. 1.

Chlorobenzene and ethylbenzene compounds: Chlorobenzene and ethylbenzene are from a family of aromatic compounds. Oral exposure is the main route of exposure from the MSW dumping yard; chlorobenzene
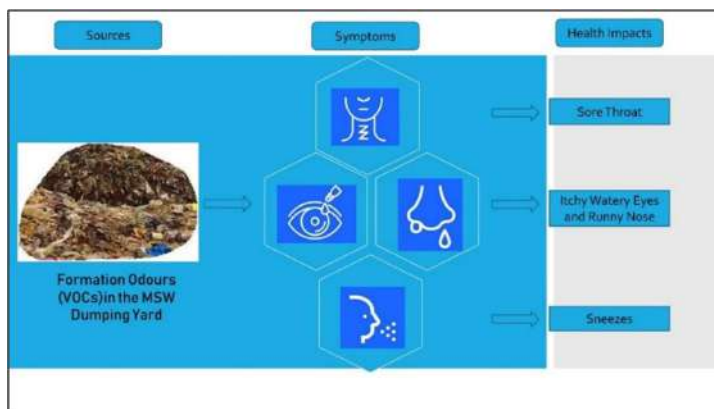
Fig. 7: Allergy Symptoms due to inhalation of Odors at MSW Dumping Yard.

and ethylbenzene can be passed on during communication between the workers in the dumping yard. Due to the presence of chlorobenzene compounds, histopathologic changes in the liver are possible, and ethylbenzene exposure can result in difficulties in the kidney and liver in MSW workers, as Fig. 8 indicates (IRIS 2024).

Methyl chloride compound: In the dumping yard, methanol and hydrogen chloride combine to produce methyl chloride (Holbrook 1992). Methyl chloride can be found in dumping yards indirectly due to burning (Graedel & Keene 1995).

Methyl chloride, also known as chloromethane, is a family of organic compounds. Inhalation is the main route of exposure from the MSW dumping yard. Breathing methyl chloride can irritate the lungs, causing coughing and/or shortness of breath, as shown in Fig. 8 (IRIS 2024).

Methyl ethyl ketone (MEK) compound: In the MSW dumping yard, methyl ethyl ketone (MEK) is frequently found in mixtures with acetone, ethyl acetate, hexane, and toluene. These combinations are composed of chlorofluorocarbons. These VOC compound mixtures are primarily produced in the MSW dumping yard during the biodegradation process (OEHHA 2024a). Inhalation is the main route of exposure from the MSW dumping yard. Low-dose chronic exposure to MEK causes neurological damage, and MEK can be irritating through all modes of exposure. It can be harmful if swallowed, ingested, or come into contact with the skin. In a study involving volunteers, both males and females exposed

to 100 ppm (295 mg.m^{-3}) reported experiencing nose and throat irritation. (US EPA 2003).

Toluene compounds: Toluene is an aromatic chemical compound that is frequently found in mixtures with benzene. In the MSW dumping yard, toluene is frequently contaminated with other polycyclic aromatic hydrocarbons (PAHs). The primary method of exposure from the MSW disposal yard is inhalation. Fig. 9 shows the symptoms of headache, dizziness, a sense of intoxication, and mild eye and nose irritation brought on by inhaling toluene chemicals released in the MSW dumping yard. (Andersen et al.1983).

Trichlorofluoromethane (TCM) compound: The trichlorofluoromethane compound belongs to the chlorofluorocarbons. TCM is broken down in the presence of oxygen and methane, and the decomposition occurs simultaneously with methane's oxidation (Scheutz et al. 2004). Trichlorofluoromethane has no odor at concentrations lower than 20% (by volume in air); at greater concentrations, it has a faint, ethereal odor (Braker & Mossman 1980). Due to the presence of TCM in the MSW dumping yard, it is possible to get irritation on the skin and eyes and also global warming and ozone depletion potential to the environment (Verschueren 1996). Breathing concentrations in the air that are nearly 0% can cause dizziness and tiredness (USCG 1999). The impact of trichlorofluoromethane on MSW dumping yard workers is shown in Fig. 10.
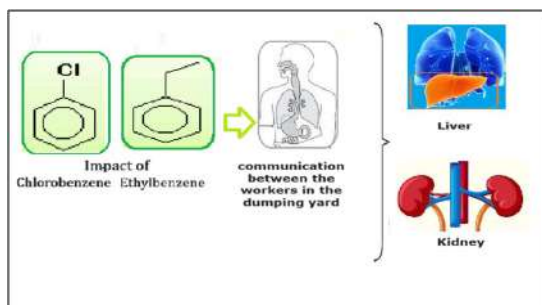
Fig. 8: Exposure of Chlorobenzene and ethylbenzene to MSW Workers.
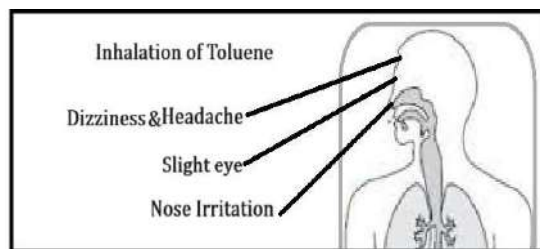
Fig. 9: Symptoms of inhalation of Toluene.
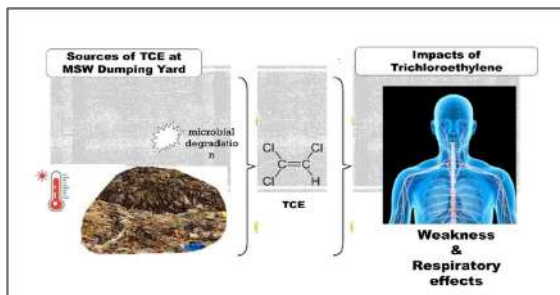
Fig. 10: Formation and impacts of TCE on MSW workers.
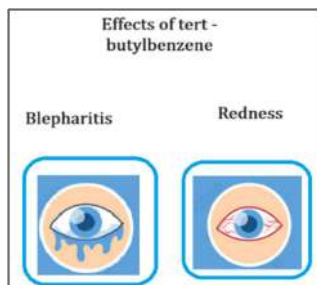
Fig. 11: Impacts of tert-butylbenzene MSW workers.

Trichloroethylene (TCE) compound: The trichloroethylene compound belongs to organic halogen compounds. Vinyl chloride is one of the byproducts of TCE's natural breakdown in the MSW dumping yard. Human health may be adversely affected by TCE across all modes of exposure. Because TCE is present in the MSW dumping yard, dermal and inhalation exposures are the primary routes of exposure. They complement each other regarding strengths and weaknesses. The respiratory effects are attributed to the person working the MSW dumping yard being predisposed to them by inhaling the waste products during the decomposition stage (Blair 1998). Fig. 10 shows the formation and impacts of TCE on MSW workers.

***Tert*-butylbenzene compound:** *Tert*-butylbenzene is an organic chemical compound belonging to the aromatic hydrocarbon family. A carbocation is created when isobutene and a Lewis acid react. Then, benzene and carbohydrate react to form the intermediate product. To allow the tert-butylbenzene to be released into the MSW disposal yard. The MSW Dumping Yard contains tert-butylbenzene, which may cause irritation of the eyes in workers (Blair 1998). Fig. 11 shows the impacts of tert-butylbenzene MSW workers regularly working in dumping yards.

Xylenes (*m,p,o*) compounds: Meta xylenes, para xylenes, and ortho xylenes (m,p,o) are organic chemical compounds that are one of the three isomers of dimethyl benzene. A large number of volatile organic compounds (VOCs), including xylene (m,p,o), present in the MSW dumping yard pose a risk to human health. The substance can get into their eyes, mouths, and skin (Langman 1994). Exposure to low concentrations of xylene (< 200 ppm) can result in temporary adverse effects that do not cause permanent harm. Fig. 12 shows the impacts on xylenes (m,p,o) MSW workers and nearby residents. Continuous exposure can cause nervous problems, headaches, depression, sleeplessness, agitation, and excessive weariness.

CONCLUSIONS

The VOC odor concentration was measured by collecting samples at three different sampling locations selected at the urban municipal solid waste dumping yard. The odor
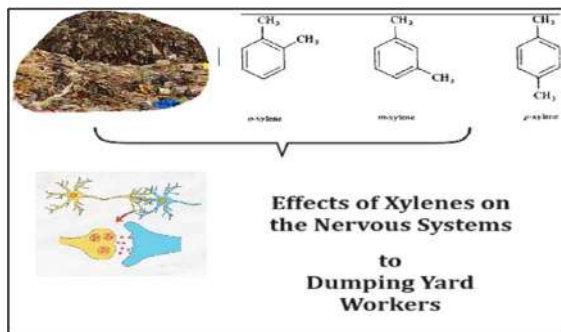
Fig. 12: Effects on MSW workers of xylenes *(m, p, o)*.

emissions were identified in the analysis carried out by the GC-MS 6280N instrument. Three different locations were selected for sampling in the dumping yard. When the dumpsite's total VOC concentrations were monitored in the pre-monsoon, it was discovered that stations 1 and 2 of the dump site, where fresh municipal solid waste is placed, had higher overall VOC concentrations, and more VOCs were detected. The sampling maximum VOC concentration of T-butylbenzene was recorded in the sampling location-1 dumping yard, and the value is 1.41 µg,m^{-3}. The minimum VOC concentration of 0.07 µg.m^{-3} was recorded in sampling station-2 (*sec*-butylbenzene). The MSW fresh waste contains more moisture content, so we only receive a high odor concentration during the disposal of fresh waste. Metrological factors play a major role in the MSW dumping yard. Weather factors like high moisture content or humidity can cause solid waste to hydrate and break down, generating unpleasant odors in the atmosphere. Hence, once the solid waste dumping yard rains during the initial stage of the humidity phase, allergic people may inhale a high concentration of diffused odor emission from the waste material, which can cause an allergic reaction to the surrounding environment, some of which are severe.

Additionally, the odor emissions from the dumpsite pose both carcinogenic and noncarcinogenic risks to the health of the individuals participating in the dumping yard. Thus, it requires adequate management of municipal waste as well as routine health checks for workers at the dumpsite. As a result of these results, it is important to manage odor emissions (VOCs) during composting and take steps to reduce their negative effects on the environment and public health.

REFERENCES

Ahluwalia, I.J. and Patel, U., 2018. *Solid Waste Management in India: An Assessment of Resource Recovery and Environmental Impact*. Indian Council for Research on International Economic Relations (ICRIER), New Delhi, Paper No. 356. Available at: https://hdl.handle.net/10419/203690.

Blair, A., 1998. Mortality and cancer incidence of aircraft maintenance workers exposed to trichloroethylene and other organic solvents and chemicals: Extended follow-up. *Occupational and Environmental Medicine*, 55(3), pp.161–171. doi:10.1136/oem.55.3.161.

Braker, W. and Mossman, A.L., 1980. *Matheson gas data book* (p. 41). Lyndhurst, NJ: Matheson.

Cai, L., Koziel, J. and O'Neal, M., 2007. Determination of characteristic odorants from *Harmonia axyridis* beetles using in vivo solid-phase microextraction and multidimensional gas chromatography-mass spectrometry–olfactometry. *Journal of Chromatography A*, 1147(1), pp.66–78. doi:10.1016/j.chroma.2007.02.044.

Christensen, H., Kjeldsen, P., Albrechtsen, H.J., Heron, G., Nielsen, P.H., Bjerg, P.L. and Holm, P.E., 1994. Attenuation of landfill leachate pollutants in aquifers. *Critical Reviews in Environmental Science and Technology*, 24, pp.119–202.

De la Rosa, D.A., Velasco, A., Rosas, A. and Volke-Sepúlveda, T., 2006. Total gaseous mercury and volatile organic compounds measurements at five municipal solid waste disposal sites surrounding the Mexico City Metropolitan Area. *Atmospheric Environment*, 40(12), pp.2079-2088.

David, E. and Niculescu, V.C., 2021. Volatile organic compounds (VOCs) as environmental pollutants: Occurrence and mitigation using nanomaterials. *International Journal of Environmental Research and Public Health*, 18(24), p.13147. doi:10.3390/ijerph182413147.

Dlamini, B., 2019. *Evaluating the Performance (effectiveness and Efficiency) of Waste Management and Minimization Practices in the District Municipalities (Umkhanyakude and Zululand) in the KwaZulu-Natal Province, South Afric*a. University of Johannesburg

Environmental Protection Agency (EPA), 1997. Integrated Risk Information System (IRIS). Retrieved from https://www.epa.gov/iris. (Accessed 02 March.2024).

Fikri, E., 2024. A projection study of gaseous pollutants formed, potential health effects, and clinical codification in Piyungan landfill. *Nature Environment and Pollution Technology*, 23(1), pp.517–523. doi:10.46488/nept.2024.v23i01.048.

Graedel, T.E. and Keene, W.C., 1995. Tropospheric budget of reactive chlorine. *Global Biochemical Cycles*, 9(1), pp.47–77.

Hohener, P., Werner, D., Balsiger, C. and Pasteris, G., 2003. Worldwide occurrence and fate of chlorofluorocarbons in groundwater. *Critical Reviews in Environmental Science and Technology*, 33, pp.1–29.

Holbrook, M.T., 1992. Chlorocarbons, hydrocarbons (CHCI3). In: Kroschwitz, J.I. and Howe-Grant, M. (eds.) *Kirk-Othmer's Encyclopedia of Chemical Technology*, Fourth edition. John Wiley and Sons, pp.16-34.

IARC, 2012. List of classifications. https://monographs.iarc.fr/list-of-classificationsvolumes, (Accessed 23 March 2024).

Iris assessments | IRIS | US EPA. Available at: https://iris.epa.gov/AtoZ/?list_type=alpha (Accessed: 24 March 2024).

Jayasinghe, P.A., Jalilzadeh, H. and Hettiaratchi, P., 2023. The impact of COVID-19 on waste infrastructure: Lessons learned and opportunities for a sustainable future. *International Journal of Environmental Research and Public Health*, 20(5), p.4310. doi:10.3390/ijerph20054310.

Jin-Feng, W. and Hu, Y., 2012. Environmental health risk detection with Geog Detector. *Environmental Modelling and Software*, 33, pp.114–115. doi:10.1016/j.envsoft.2012.01.015.

Kumarathilaka, P. and Jayawardhana, Y., 2016. Characterizing volatile organic compounds in leachate from Gohagoda municipal solid waste dumpsite, Sri Lanka. *Groundwater for Sustainable Development*, 2–3, pp.1–6. doi:10.1016/j.gsd.2016.04.001.

Langman, J., 1994. M. Xylene: its toxicity, measurement of exposure levels, absorption, metabolism, and clearance. *Pathology*, 26, pp.301–309.

Latugan, P., 2024. Analysis and characterization of municipal solid wastes generated in Ifugao State University Potia Campus: A basis for planning of waste management. *Nature Environment and Pollution Technology*, 23(1), pp.281–294. doi:10.46488/nept.2024.v23i01.024.

Liu, F., Liu, Y., Jiang, D., Zhang, R., Cui, Y. and Li, M., 2014. Health risk assessment of semi-volatile organic pollutants in Lhasa River, China. *Ecotoxicology*, 23(4), pp.567–572.

Liu, J. and Zheng, G., 2020. Emission of volatile organic compounds from a small-scale municipal solid waste transfer station: ozone-formation potential and health risk assessment. *Waste management*, 106, pp.193-202.

Wenjing, L., Zhenhan, D., Dong, L., Jimenez, L.M.C., Yanjun, L., Hanwen, G. and Hongtao, W., 2015. Characterization of odor emission on the working face of landfill and establishing of odorous compounds index. *Waste management*, 42, pp.74-81.

Mahin, T., 2001. Comparison of different approaches used to regulate odors around the world. *Water Science and Technology*, 44(9), pp.87–102. doi:10.2166/wst.2001.0514.

Methyl ethyl ketone (2003). Available at: https://iris.epa.gov/static/pdfs/0071.

Ministry of Environment, Forest and Climate Change, Government of India, 2022. Available at: https://moef.gov.in, (Accessed date: 25.02.2024).

OEHHA 2024a. Oehha.ca.gov. Available at: https://oehha.ca.gov/chemicals/methyl-ethyl-ketone (Accessed: 25 Febrary 2024).

OEHHA 2024b. Oehha.ca.gov. Available at: https://oehha.ca.gov/water/notification-level/proposed-notification-levels-sec-butylbenzene-and-tert-butylbenzene (Accessed: 02 March 2024).

Pan, Q., Liu, Q.-Y., Zheng, J., Li, Y.-H., Xiang, S., Sun, X.-J. and He, X.-S., 2023. Volatile and semi-volatile organic compounds in landfill gas: Composition characteristics and health risks. *Environment International*, 174, p.107886. doi:10.1016/j.envint.2023.107886.

Randazzo, A., Folino, A., Tassi, F., Tatàno, F., de Rosa, S. and Gambioli, A., 2022. Volatile organic compounds from green waste anaerobic degradation at lab-scale: evolution and comparison with landfill gas. *Detritus*, 19, pp.63-74. https://doi.org/ 10.31025/2611-4135/2022.15188.

Saral, A., Demir, S., & Yıldız, Ş. 2009. Assessment of odorous VOCs released from a main MSW landfill site in Istanbul-Turkey via a modelling approach. *Journal of Hazardous Materials*, 168(1), 338-345.

Scaglia, B., Orzi, V., Artola, A., Font, X., Davoli, E., Sanchez, A. and Adani, F., 2011. Odors and volatile organic compounds emitted from municipal solid waste at different stages of decomposition and their relationship with biological stability. *Bioresource Technology,* 102(7), pp.4638–4645. doi:10.1016/j.biortech.2011.01.016.

Scheutz, C., Mosbæk, H. and Kjeldsen, P., 2004. Attenuation of methane and volatile organic compounds in landfill soil covers. *Journal of Environmental Quality,* 33(1), pp.61–71. doi:10.2134/jeq2004.6100.

Su, F.C., Jia, C. and Batterman, S., 2012. Extreme value analyses of VOC exposures and risks: A comparison of RIOPA and NHANES datasets. *Atmospheric environment*, 62, pp.97-106.

U.S. Coast Guard (USCG), 1999. *Chemical Hazard Response Information System (CHRIS) - Hazardous Chemical Data*. Commandant Instruction 16465.12C. Washington, D.C.: U.S. Government Printing Office.

U.S. Environmental Protection Agency (US EPA), 2003. Toxicological Review of Methyl Ethyl Ketone. PA: Washington D.C., US.

Verschueren, K., 1996. *Handbook of Environmental Data on Organic Chemicals*. 3rd ed. New York, NY: Van Nostrand Reinhold Co, p.1016.

Williams, J. and Koppmann, R., 2007. Volatile organic compounds in the atmosphere: An overview. *Environmental Chemistry,* 54, pp.1–32. doi:10.1002/9780470988657.ch1.

World Bank Group, 2023. Solid Waste Management. Retrieved from https://www.worldbank.org/en/topic/urbandevelopment/brief/solid-waste-management, (Accessed 25 February 2024).

Young, P. J.; Heasman, L. A. 1985. Proceedings of GRCDA 8thInternational Landfill Gas Symposium, San Antonio, TX, April1985; pp 93-114

Young, P. and Parker, A., 1984, January. Vapors, odors, and toxic gases from landfills. In *Hazardous and Industrial Waste Management and Testing: Third Symposium, ASTM STP* (Vol. 851, pp. 41-24).

Young, P.J. and Parker, A., 1983. The identification and possible environmental impact of trace gases and vapor in landfill gas. *Waste Management Resources,* 1, pp.213–226.

Original Research Paper | https://doi.org/10.46488/NEPT.2025.v24i01.D1678 | Open Access Journal

Enhancing Social Capital Development Through Environmental Management Model in the Periphery Area of Banjarmasin City

E. Normelani[1†], D. Arisanty[2], Ahmad[3], M. Efendi[1], I. K. Hadi[1], R. Noortyani[4], Rusdiansyah[1] and R. P. Salan[5]

[1]Geography Study Program, Lambung Mangkurat University, Brigjend H. Hasan Basry Road, Banjarmasin 70123, Indonesia
[2]Department of Geography Education, Lambung Mangkurat University, Brigjend H. Hasan Basry Road, Banjarmasin 70123, Indonesia
[3]Department of Management, Lambung Mangkurat University, Brigjend H. Hasan Basry Road, Banjarmasin 70123, Indonesia
[4]Department of Indonesian Language Education, Lambung Mangkurat University, Brigjend H. Hasan Basry Road, Banjarmasin 70123, Indonesia
[5]Agency for Planning, Regional Development, Research and Development of the City of Banjarmasin, Indonesia
†Corresponding author: E. Normelani; ellynormelani@ulm.ac.id

Citation for the Paper:

ABSTRACT

The objective of this research was to determine an environmental management model that integrates social, economic, geographic, and community aspects to promote the growth of social capital among residents in the periphery area of Banjarmasin City. The analysis was conducted with 150 respondents selected through purposive sampling based on specific criteria. A quantitative descriptive method was adopted, and the structural model analysis was conducted using SmartPLS 3.0 software. The structural model analysis consisted of (a) formulation of the structural model theory, (b) analysis of the outer model, (c) analysis of the inner model, and (d) hypothesis testing. The field data analysis and calculations using SmartPLS 3.0 software showed an R^2 value of 0.855. The value showed that the economic, social, geographic, and community indicators could indeed contribute to the development of social capital, including norms, culture, perceptions, and behaviors among residents in the periphery area. Approximately 85.5% of the variation could be explained, while the remaining 14.5% might be influenced by other factors. In terms of the development of social capital, environmental management model was shown by (1) economic, with a T-statistic value of 2.627 and a P-value of 0.009, (2) geographic, with a T-statistic value of 1.982 and a P-value of 0.048, (3) community, with a T-statistic value of 4.211 and a P-value of 0.000, and (4) social with a T-statistic value of 2.057 and a P-value of 0.040. Since the T-statistic values exceeded the T-table threshold of 1.96, and the P-values were less than the significance level of 0.05, it could be concluded that economic, geographic, community, and social, environmental management in the periphery area served as valuable indicators for fostering the sustainable development of social capital among residents of Banjarmasin City.

INTRODUCTION

A city is an area characterized by a higher density of activities, including a wide range of endeavors, from economic transactions to political processes and daily life. The dynamic often results in social disparities, which can be observed from various perspectives, particularly the physical aspects. The periphery of a city functions as a physical manifestation of gentrification, a process in which economically disadvantaged areas experience an influx of middle to upper-middle-class residents who contribute to the development of the region, thereby enhancing its value (Melo & Jenkins 2023). The development often leads to the displacement of existing residents to another area (Liu et al. 2017).

The development of the region often overlooks and does not adequately take into account the unique characteristics of a rurban (rural-urban) environment. The

area is situated on the periphery of the urban area and is influenced by both physical and non-physical attributes while still retaining rural qualities. Area increasingly confronts the complex issues prevalent in an urban environment, and its potential is gradually diminishing. There is an urgent need to manage and develop such potential to enhance community well-being and attain sustainable regional governance (Brontowiyono & Lupiyanto 2011).

A literature review by Haridison (2013) examined the role of social capital and its application in various aspects, including political, human, and economic. In the context of development issues, the concept of social capital has garnered the attention of both academics and practitioners. It is regarded as a valuable theoretical framework within the paradigm of inclusive and sustainable development, which emphasizes a bottom-up method over a top-down one. Social capital forms an important part of social indicators, seeking to integrate three dimensions, including social, economic, and environmental.

The interplay between humans and the environment is profound, with each influencing and benefiting the other. However, the relationship has yet to be fully integrated into a comprehensive system. Environmental damage is an inevitable consequence and has far-reaching impacts on humans (Munandar 2002, Uliyah, 2015). The conventional method to environmental issues primarily addresses physical aspects, such as air quality, water pollution, chemical reactions, soil conditions, climate, ecosystems, temperature, and more. However, some view such issues through a broader lens, incorporating social, economic, and political dimensions. This perspective arises from the realization that the community might not always have wise environmental stewardship. Addressing such issues necessitates a multidisciplinary method, drawing wisdom and expertise from social, political, and economic sciences. Resolving ecological crises transcends scientific and technological advancements. It requires fundamental social, economic, and political transformations. The perspective suggests that the community has the potential to address environmental issues by fostering sustainability (Gyamfi et al. 2023, Ife & Tesoriero, 2008)

Social capital covers several formative elements, including (1) trust, which is the cornerstone used in shaping other components. (2) Value System and Norms, where values and norms form a distinct entity capable of shaping social capital. Values represent traditionally held ideas considered correct and significant by individuals. Additionally, norms play a significant role in guiding the forms of behavior that develop within the community. (3) Acceptance and Diversity: tolerance is integral to social life

and plays a crucial role in shaping social capital. Fostering a tolerant attitude toward community differences, showing respect for those differences, and accepting them with grace and wisdom are essential. (4) Cooperation, which arises from a sense of togetherness and a shared background.

Banjarmasin City faces the challenge of having the highest number of impoverished residents in South Kalimantan province. Over the past three years, the number of the impoverished has witnessed a significant increase, with only a slight decrease in 2022. There were 29.65 thousand impoverished residents in 2019, and the number significantly rose to 31.13 thousand in 2020. By 2021, the count reached 34.84 thousand impoverished residents, and in 2022, it reached 34.01 thousand (Statistics 2023).

The periphery of Banjarmasin City, particularly along the riverbanks, shows high population density and often experiences the development of slums. This density is a consequence of the increasing population and the subsequent demand for land in the area. The social and economic conditions of residents in such areas are relatively low, with 79% having completed only primary to lower-secondary education and 57% being engaged in labor or facing unemployment (Angriani 2021). In line with previous reviews, the geographic distribution of impoverished residents and slum settlements, as outlined in the Decree of the Mayor of Banjarmasin Number 460 Year 2015 regarding the Location of Slum Settlements in Banjarmasin City, includes the slum area spanning 523.19 hectares. The area tends to be distributed across 5 districts and 52 neighborhoods. Generally, the concentration of impoverished residents is observed in the periphery, and their presence in the slum in the city center is a result of unplanned and unregulated development, which has led to a degradation of the living environment, particularly in the periphery area (Ndolu et al. 2017).

The periphery area, defined as an area located on the outskirts of a city, holds a unique regional perspective because it occupies the transitional space between rural and urban domains (Yunus 2008). From a characteristics standpoint, it embodies a harmonious blend of rural and urban elements. Some areas show urban characteristics, while others retain a closer connection to rural attributes. It is frequently referred to as a peri-urban area. In terms of characteristics, the periphery area symbolizes the fusion of rural and urban features, with specific zones showing urban traits while others retain rural traits. Kurts and Eitcher, as cited in Yunus (2008), provided several definitions for the periphery area, including (a) an area where rural and urban land uses converge and border city, (b) the periphery area covers all suburbs, satellite towns, and other territories

located just beyond the city, where non-agricultural labor is predominant, (c) area located outside the official city boundaries but still within commuting distance, (d) open rural area inhabited by individuals working in the city, and (e) zone where the work fields and orientations of both urban and rural life intersect.

The expansion of urban development into the periphery of Banjarmasin City signifies a shift from rural to urban populations. The city center, once synonymous with business activities, industries, government offices, services, and warehouses, has experienced a substantial transformation in land use. Previously, vacant lands in the area have been repurposed to become centers of trade, residential areas, and facilities supporting urban growth. The alteration in land use aims to fulfill physical, economic, and social objectives. The development of the periphery area is anticipated to drive the growth and economy of the city. The transformation of land use due to infrastructure development will bear implications for the neighboring community, particularly in relation to the economic and social dimensions (Latifah, 2014). Based on the theories and research results mentioned above, the examination of the "Environmental Management Model in the Periphery Area Through Development of Social Capital in Banjarmasin City" becomes an intriguing prospect. The objective of this research was to determine an environmental management model that integrates social, economic, geographic, and community aspects to promote the growth of social capital among residents in the periphery area of Banjarmasin City.

Literature Review

Environmental management: Environmental management represents a comprehensive endeavor aimed at preserving the functions of the environment. This included the prudent organization, use, development, maintenance, restoration, monitoring, and control of the environment (Machmud 2012). The environment served as the habitat for living beings, where they found sustenance and possessed distinctive characteristics and functions that interacted with the presence of inhabitants, particularly humans, who played a more complex and substantial role (Setiadi & Kolip 2013). According to Sartain, an American psychologist, the term "environment" included all worldly conditions that, in various ways, influenced behavior, growth, development, or life processes, excluding genetic factors. Genes could be seen as preparing the environment for other genes (to provide environment). Sartain further categorized the environment into three parts, including the natural/external, the internal, and social or community (Ngalim 2014, Zhou & Gu 2024).

Environmental has a broad scope, extending beyond humans, animals, plants, and physical entities to include a wide array of elements, spanning biotic, organic, inorganic, and social. The social environment comprised all those who exerted influence on individuals or others. Direct influences manifested through daily interactions with family, friends, schoolmates, or co-workers. Indirect influences may have occurred through media such as radio, television, reading books, magazines, newspapers, and other means (Dalyono 2019). The origins of social capital date back to 1916, inspired by the work of Lyda Judson Hanifan, "The Rural School Community Centre," where social capital was distinguished from other forms of capital and acknowledged as one of the most important forms in the community (Fathy 2019). It consisted of the outcomes of social relationships particularly trust, institutionalized norms, mutually beneficial relationships, and more (Sunyoto 2018).

Social capital represented a web of interpersonal relationships grounded in networks, norms, and social trust, which facilitated the efficiency and effectiveness of cooperation and coordination toward shared objectives and policies. The dimension expanded within the community, containing values, norms, and patterns of social interaction that regulated the daily lives of its members (Laura et al. 2018).

Periphery area: According to Yunus (2008), the periphery area was situated on the outskirts of the city and had environmental significance, positioned at the crossroads between rural and urban regions. It represented a unique blend of rural and urban elements, where specific areas possessed urban characteristics while others maintained closer ties to rural features. The area was frequently labeled as peri-urban zones. It epitomized the harmonious merger of rural and urban attributes, with specific regions showcasing urban traits and others being closer to rural attributes. Kurts and Eitcher, as referenced in Yunus (2016), offered several definitions of the periphery area, including (1) area where rural and urban land uses converged at the border of the city, (2) a periphery area covered all suburbs, satellite towns, and other territories just beyond the city where non-agricultural labor was prevalent, (3) area located beyond the official city boundaries but still within commuting distance, (4) open rural area inhabited by individuals working in the city, and (5) space where the work fields and orientations of both urban and rural life intersect. Based on the literature review, the conceptual framework is summarized in Fig. 1.

The hypotheses in this research included:

The Influence of the economic environmental on social capital

The impact of the geographic environment on social capital
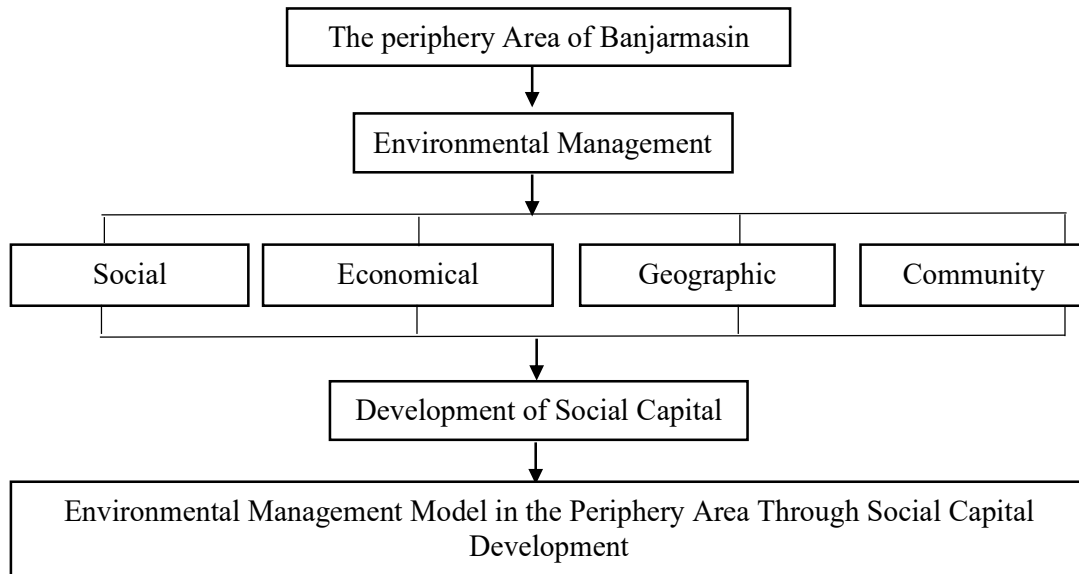
Fig. 1: Research Framework.

The role of the community environment in influencing social capital

The interplay between social environmental and social capital

MATERIALS AND METHODS

The research site was determined using area sampling, specifically focusing on the periphery area of Banjarmasin City. The selection was motivated by significant environmental changes, including a reduction in this area due to extensive infrastructure development, limited environmental management, and a lack of attention from the local government. Table 1 provides the information about the research variables used in the study.

This research adopted a quantitative descriptive method, leveraging numerical data derived from calculations or measurements, including information gathered from questionnaires related to environmental management and the distribution of social capital. Data sources incorporated both primary and secondary. Primary data were directly obtained from respondents in the periphery area, while secondary data were derived from sources supporting this research but were not collected (Sugiyono 2010). Data collection methods included (1) observation, carried out to obtain data on environmental management, social capital, and the profile of residents in the selected area, and (2) questionnaires, used to collect data from respondents, with a focus on environmental management within social, economic, geographic, and community contexts, as well as social capital in the Banjarmasin City.

Sample selection was carried out using purposive sampling, a method used to select the sample based on specific considerations. The sample was not randomly selected but was determined by the analyst. The criteria for the selection were residents residing on the outskirts of Banjarmasin City. Sarwono & Narimawati (2015) recommended a sample size of at least 30-100 for the analysis using Partial Least Squares Structural Equation Modeling (PLS-SEM). In this research, the size was determined using the Slovin Formula, resulting in a total of 150 samples selected from the residents living in the periphery area of Banjarmasin City.

Both Descriptive Statistical Analysis and PLS-SEM were adopted in the analysis. Descriptive statistical analysis was used to obtain a comprehensive and precise overview of the research objectives, with a 5-point Likert scale used. PLS-SEM was adopted to develop or validate an existing theory (Sarwono & Narimawati 2015). The model was also used for structural analysis, facilitated by the SmartPLS 3.0 software. According to Ananda Sabil (2015), the analysis

Table 1: Operational definition of research variables.

Variable	Indicator	Data Source
Environmental Management	• Social environmental • Economic Environmental • Geographic Environmental • Community Environmental	Ngalim (2014)
Social Capital	• Norm • Culture • Perception • Behavior	Fathy (2019) Usman & Ahmad (2018)

of the structural model consisted of (1) formulating the structural model theory, (2) analyzing the outer model, (3) analyzing the inner model, and (4) testing hypotheses.

RESULTS AND DISCUSSION

Physical development in certain areas could give rise to socio-cultural and environmental challenges. Currently, development is often equated with physical growth, while natural elements, the environment, and the community are regarded as supportive components. The interplay between physical development and environmental management as a strategy for attaining sustainability was crucial. However, development in specific areas tended to overlook the periphery, which had characteristics of both urban and rural environments. Without dedicated attention, this area would continue to be influenced by the complex problems associated with urban development.

Banjarmasin became one of the cities experiencing continuous expansion, necessitating land for infrastructure and associated amenities. This invariably resulted in an ongoing reduction in available land for alternative purposes. The shift of development focus from urban hubs to the periphery stemmed from the growing demand for space. Furthermore, the socio-economic fabric of the periphery primarily revolved around agriculture, fisheries, and other industries, making the area crucial

for catering to the needs of Banjarmasin City residents. An important aspect in achieving this was environmental management and the nurturing of social capital within the periphery. Environmental management covers a wide range of aspects, including not only humans, animals, plants, and physical but also biotic, abiotic, and cultural aspects influenced by economic, geographic, community, and social factors.

Norms, culture, beliefs, perceptions, and behavior collectively formed the social capital of the periphery area. The elements required careful observation and development through well-planned environmental management across economic, geographic, community, and social indicators. Consequently, the environmental management model became a requisite for enhancing the community's social capital, enabling the area to contribute to sustainable development and the local economy. It played a crucial role in meeting the needs of Banjarmasin City residents.

The environmental management model, through the development of social capital in Banjarmasin, commenced with the validation of the outer model to assess its validity and reliability. The analysis scrutinized various facets, including Factor Loading, AVE, Discriminant Validity, and Composite Reliability. The results showed that social, economic, geographic, community and social dimensions
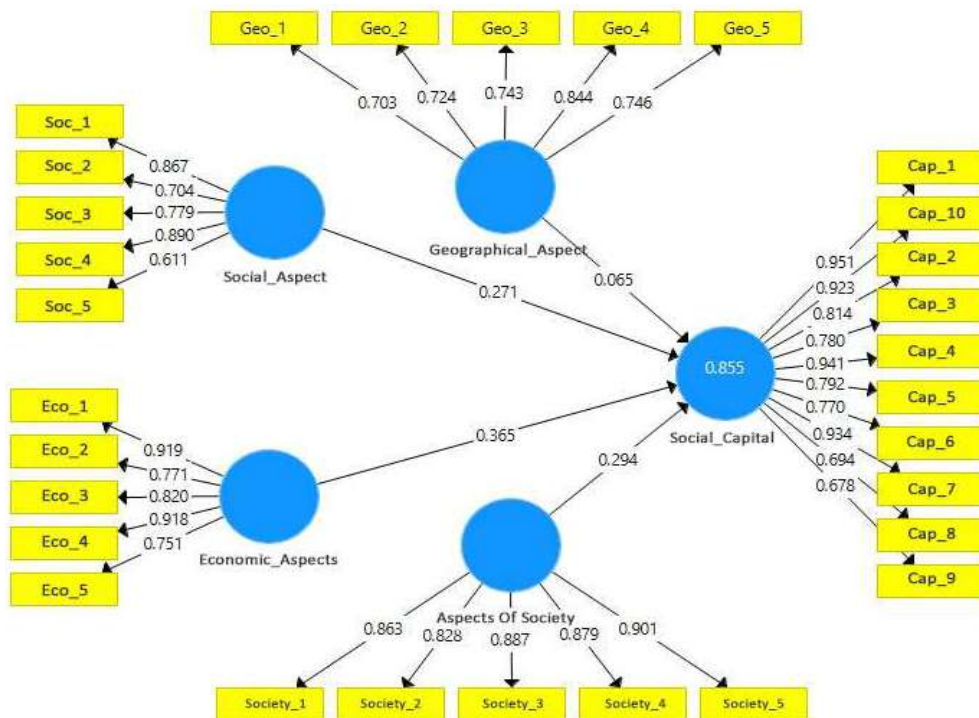
Fig. 2: SmartPls Algorithm for outer model.

met the validity and reliability criteria for the development of social capital, comprising norms, culture, perceptions, and behavior in the periphery of Banjarmasin City. The first phase of model validation testing was Factor Loading, with the requirement that it should exceed 0.6 for an indicator to be considered valid. Any indicators failing to meet such criterion were excluded from the model (Hussain et al. 2015). The results of the outer model analysis are presented in Fig. 2.

Fig. 2 shows that the variables related to environmental management and social capital had factor loading values exceeding the threshold of 0.6 (Hussain et al. 2016). Based on the results, it was evident that environmental management concerning economic, geographic, community, and social aspects was valid in fostering the development of social capital, including norms, culture, perceptions, and behavior among residents in the periphery area of Banjarmasin City.

The correlation values between the supportive variables of the environmental management model in the periphery were assessed through the AVE value. The value played a crucial role in testing convergent validity since it originated from convergent validity outputs. In this research, the expected AVE value exceeded 0.5, and when examining the latent variable, all constructs surpassed the threshold of 0.5. When the square root of the AVE value was greater than the correlation value between one construct and the other in the model, it signified strong discriminant validity (Ghozali & Latan 2015). The AVE value is shown in the Table 2.

The AVE value for environmental management variables with their indicators included (1) economic with an AVE value greater than 0.5, (2) social with an AVE value greater than 0.5, (3) geographic with an AVE value greater than 0.5, and (4) environmental management in terms of community with an AVE value greater than 0.5. Furthermore, the social capital variable has an AVE value exceeding 0.5, showing that the environmental management model in terms of economic, geographic, community, and social aspects was proficient in cultivating social capital such as norms, culture, perceptions, and behavior within the periphery of Banjarmasin City. The results complied with the requirements for convergent validity, with the

AVE value surpassing 0.5 (Ghozali & Latan 2015). The next step was testing discriminant validity.

The assessment of discriminant validity in the environmental management model in the periphery was conducted by examining the cross-loading table. Cross-loading values were indicative of the correlations of constructs with measurement items that exceeded the magnitude of other constructs. This signified that the latent constructs better predicted the variance within their designated category than the variance in other categories (Ghozali & Latan 2012).

Table 3 shows two results, including (1) environmental management in the economic, geographic, community, and social aspects within the periphery has cross-loading values greater than other constructs, and (2) social capital has cross-loading values greater than others in its block. The results affirmed the strong discriminant validity of environmental management in terms of economic, geographic, community, and social aspects with social capital (such as norms, culture, perceptions, and behavior) among residents in the periphery area of Banjarmasin City.

The final step in evaluating the outer model revolved around testing the unidimensionality of the environmental management model within the periphery for the development of social capital in Banjarmasin City. This evaluation adopted composite reliability and Cronbach's alpha values, and it was considered satisfactory when the values exceeded 0.7 (Ghozali & Latan 2015).

Table 4 shows Cronbach's alpha and composite reliability values for social capital, economic, geographic, community, and social aspects, all of which met the reliability criteria by exceeding the threshold of 0.7 (Ghozali & Latan 2015). It substantiated the accuracy, consistency, and precision of the instruments adopted in the environmental management model with all four aspects as part of the initiative to foster social capital development in the outskirts of Banjarmasin City. This compliance with the standard criteria assured the reliability of the research model.

In evaluating the inner model, the focus shifted to the coefficient of determination (R^2 value) to explain the impact of the environmental management model in the outskirts concerning social capital development in Banjarmasin City. The R^2 value served to elucidate the influence of specific exogenous latent variables on endogenous ones. An R^2 value of 0.75, 0.50, and 0.25 was indicative of a strong, moderate, and weak model, respectively (Sarstedt et al. 2019).

The R^2 value of 0.855, which corresponded to 85.5%, placed the model of environmental management through social capital development in the periphery of Banjarmasin

Table 2: Average Variance Extracted (AVE) Values for Environmental Management Through Social Capital Development

Construct	AVE
Economic Environmental	0.704
Social environmental	0.604
Geographic Environmental	0.568
Community Environmental	0.760
Social Capital	0.695

Table 3: Discriminant validity values for environmental management through social capital development.

Construct	Social Capital	Economic Environmental	Geographic Environmental	Community Environmental	Social Environmental
Eco_1	0.914	**0.919**	0.268	0.874	0.911
Eco_2	0.544	**0.771**	0.108	0.533	0.697
Eco_3	0.741	**0.820**	0.232	0.804	0.771
Eco_4	0.914	**0.918**	0.226	0.881	0.914
Eco_5	0.515	**0.751**	0.119	0.514	0.678
Geo_1	0.135	0.153	**0.703**	0.141	0.153
Geo_2	0.145	0.133	**0.724**	0.138	0.150
Geo_3	0.299	0.224	**0.743**	0.234	0.211
Geo_4	0.262	0.244	**0.844**	0.228	0.260
Geo_5	0.117	0.041	**0.746**	0.036	0.058
Society_1	0.862	0.815	0.216	**0.863**	0.822
Society_2	0.622	0.649	0.192	**0.828**	0.620
Society_3	0.832	0.816	0.230	**0.887**	0.823
Society_4	0.632	0.730	0.159	**0.879**	0.716
Society_5	0.706	0.794	0.219	**0.901**	0.745
Soc_1	0.860	0.809	0.185	0.799	**0.867**
Soc_2	0.525	0.627	0.150	0.540	**0.704**
Soc_3	0.672	0.754	0.219	0.744	**0.779**
Soc_4	0.871	0.825	0.241	0.781	**0.890**
Soc_5	0.438	0.607	0.154	0.417	**0.611**
Cap_1	0.951	0.922	0.276	0.879	0.913
Cap_2	**0.814**	0.825	0.284	0.775	0.809
Cap_3	**0.780**	0.525	0.228	0.559	0.535
Cap_4	**0.941**	0.910	0.240	0.862	0.897
Cap_5	**0.792**	0.790	0.259	0.770	0.791
Cap_6	**0.770**	0.515	0.224	0.549	0.524
Cap_7	**0.934**	0.914	0.244	0.876	0.907
Cap_8	**0.694**	0.509	0.183	0.537	0.505
Cap_9	**0.678**	0.462	0.171	0.479	0.443
Cap_10	**0.923**	0.895	0.272	0.850	0.889

City within the strong category (Sarstedt et al. 2019) (Table 5). This showed that the environmental management model (economic, social, geographic, and community) could foster the development of social capital, including norms, culture, perceptions, and community behavior, to an extent of 85.5%. The remaining 14.5% was influenced by other unaccounted factors.

The results were in line with the work of Yuliastuti et al. (2018), emphasizing the role of social capital in environmental quality, particularly in the form of residents' trust, with a substantial influence level of 0.222. A literature

Table 4: Composite reliability values for environmental management through social capital development.

Construct	Cronbach's Alpha	Composite Reliability
Social Capital	0.951	0.957
Economic Environmental	0.898	0.922
Geographic Environmental	0.820	0.867
Community Environmental	0.923	0.941
Social Environmental	0.838	0.882

Table 5: Determination coefficients for environmental management through social capital development.

Construct	R^2	R^2 Adjusted
Social Capital	0.855	0.851

was conducted by Prittaningtyas et al. (2014) at the Faculty of Geography, Gadjah Mada University (2014) on the Analysis of Settlement Environmental Quality in the Outskirts of the city, with the Village of Ngestiharjo, Yogyakarta as case research. The results showed the interplay of socio-economic, biotic, and abiotic factors on the quality of the settlement environment in the village. Furthermore, literature conducted by Balady and Shah (2018), concluded that specific citizens possessed various forms of social capital contributing to their well-being improvement and environmental sustainability when integrated into PLBHK programs.

To validate the credibility of the environmental management model for social capital development among residents in the periphery area of Banjarmasin City, a hypothesis test leveraged the T-statistic coefficient with a 95% confidence level. Abdillah and Hartono (2015) emphasized that the determination of hypothesis acceptance depended on the significance level of its confirmation, determined through the comparison of the T-table value and T-statistic. When the T-statistic value surpassed the T-table

value, it signified support for the hypothesis. In the context of a 95% confidence level (with an alpha of 5%), the T-table value for a two-tailed hypothesis was ≥ 1.96.

In the Bootstrapping Model Smart PLS results and the Research Testing (Fig. 3 and Table 6), it became evident that the environmental management model significantly influenced the development of social capital among residents in the periphery area of Banjarmasin City. The influence was manifested through four key indicators, including (1) community, (2) economic, (3) social, and (4) the geographic aspect. Further explanations of the results related to the environmental management model in the periphery of Banjarmasin City were as follows:

1. Hanifan (1916), as articulated in his book "The Rural School Community Centre," distinguished social capital to be a unique form of capital that held immense significance in the lives of the community. This research supported the assertion of Hanifan by establishing that the environmental management model, with the community indicator, substantially contributed to the
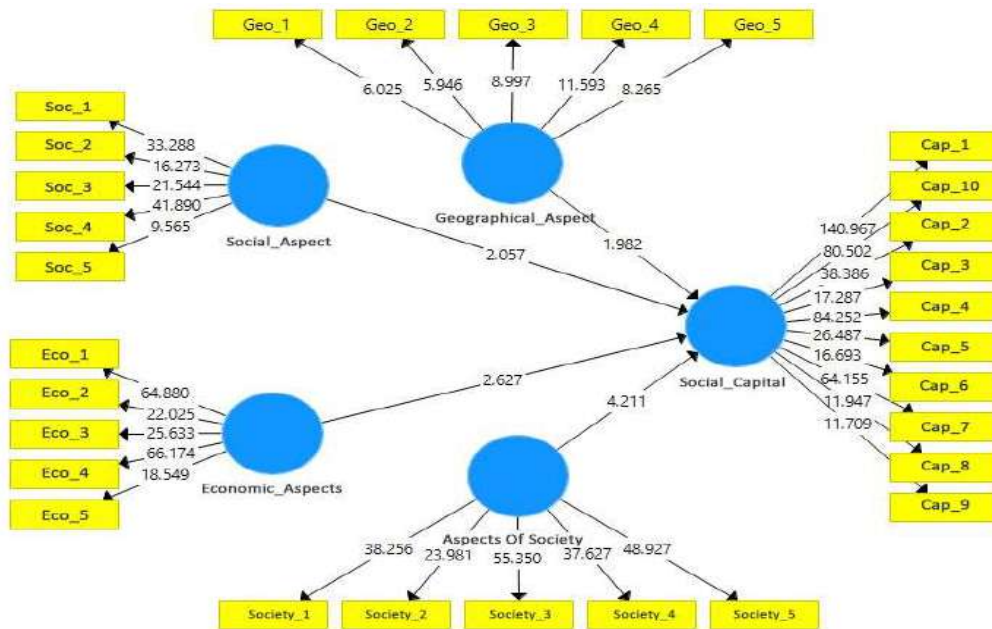
Fig. 3: Bootstrapping of SmartPls Model.

Table 6: Research test on environmental management through social capital development.

Construct	Original Sample (O)	T Statistics (|O/STDEV|)	P Values	Des
Economic Environmental -> Social Capital	0.365	2.627	0.009	Accepted
Geographic Environmental -> Social Capital	0.065	1.982	0.048	Accepted
Community Environmental -> Social Capital	0.294	4.211	0.000	Accepted
Social Environmental -> Social Capital	0.271	2.057	0.040	Accepted

development of social capital. The T-statistic value for the aspect was 4.211 (> 1.96), with a corresponding P-value of 0.000, showing high statistical significance (P < 0.05).

2. Burt (2004) defined social capital as the ability of the community to foster interpersonal connections. This research was in line with the notion of Burt by establishing that the environmental management model, particularly the economic indicator, played a crucial role in developing social capital. It was substantiated by a T-statistic value of 2.627, surpassing the threshold of 1.96, along with a P-value of 0.009, affirming its statistical significance (P < 0.05).

3. Laura et al. (2018) explained that social capital was a system of interpersonal relationships facilitated by networks, norms, and social trust, enhancing cooperative and coordinated endeavors for common objectives and policies. In line with the analysis results, the environmental management model with social indicators significantly contributed to social capital development. The T-statistic value for the aspect was 2.057, exceeding the threshold of 1.96, with a corresponding P-value of 0.040, thereby reinforcing its statistical significance (P < 0.05).

4. The method used to mobilize the physical/geographic environment was closely tied to community social capital. Robust social capital was essential in raising awareness and promoting collective action to meet common needs. Each community has social capital that serves several functions, including fostering social solidarity, encouraging participation, acting as a relationship balancer, promoting self-reliance and self-sufficiency, becoming part of a social issue management mechanism (addressing conflicts and poverty), and nurturing and strengthening social integration in socially vulnerable regions. In line with the research results, the environmental management model with the geographic indicator meaningfully contributed to the development of social capital. The T-statistic value for the aspect was 1.982, surpassing the threshold of 1.96, with a P-value of 0.048, showing its statistical significance (P < 0.05).

Based on the explanations above, it was evident that the environmental management model with indicators, including (1) economic, (2) geographic, (3) community, and (4) social aspects, surpassed the established threshold. The T-statistic values for all the indicators were consistently greater than (>) 1.96, with P-values less than (<) 0.05 (Abdillah & Hartono 2015). The results of these statistics illustrate that environmental management has a significant influence on social capital. Social capital, which includes norms, culture,

perception, and behavior, is determined by the characteristics of the environment in the region. Community knowledge and understanding of the environment turn out to determine perceptions and behaviors in society (Arisanty et al. 2023). Community participation and adaptation to environmental changes are influenced by social capital in society, such as the level of trust in each other towards others, inter-community involvement, and relationships between community groups (Saptutyningsih et al. 2020). Strong social capital can encourage the ability of communities to manage the environment together (Musavengane & Kloppers 2020). Strengthening social capital can also encourage community resilience to various environmental problems, including disaster problems (Aldrich & Meyer 2022).

This compelling evidence reaffirmed that the environmental management model, when scrutinized from economic, geographic, community, and social perspectives, exerted a substantial influence on the norms, culture, perceptions, and behaviors of the periphery area. It underscored the important role of environmental management in contributing to the development of social capital. Therefore, this research used economic, geographic, community, and social environmental management indicators in the pursuit of sustainable social capital development in Banjarmasin City.

CONCLUSIONS

In conclusion, based on field data analysis and comprehensive calculations using Smart PLS 3.0 Software, the results showed:

1. The environmental management model, particularly with an economic aspect in the outskirts, was effective in fostering the development of social capital among residents in the periphery area of Banjarmasin City. The statistical analysis showed a T-statistic value of 2.627, surpassing the T-table threshold of 1.96, and a P-value of 0.009, thereby underscoring its significance at the 0.05 level.

2. The environmental management model, with a geographic focus, served as a valuable tool in cultivating social capital in the periphery area. The Smart PLS analysis showed a T-statistic value of 1.982, which exceeded the T-table standard of 1.96, with a P-value of 0.048, thereby emphasizing its statistical significance at the 0.05 level.

3. The environmental management model with a community aspect played a crucial role in the development of social capital in Banjarmasin City. The Smart PLS analysis results showed a T-statistic value of

4.211, which exceeded the T-table value of 1.96, with a P-value of 0.000, thereby emphasizing its significance at the 0.05 level.

4. The environmental management model with a social aspect contributed significantly to the development of social capital in the periphery area. The Smart PLS analysis results showed a T-statistic value of 2.057, surpassing the T-table value of 1.96, alongside a P-value of 0.040, which solidified its statistical significance at the 0.05 level.

Based on the results above, the following recommendations were proposed.

1. Residents residing in the periphery area, particularly within Banjarmasin City, should prioritize the considerations of environmental management concerning social, economic, geographic, and community aspects, as these exert a substantial influence on the development of social capital.

2. For the local government, it was recommended to dedicate greater attention to environmental management when formulating policies and regulations. The environmental management model, incorporating social, economic, geographic, and community aspects, evidently held the potential to foster social capital within the periphery of Banjarmasin City.

ACKNOWLEDGEMENT

REFERENCES

Abdillah, W. and Hartono, J., 2015. Partial least square (PLS): Alternative structural equation modeling (SEM) in business research. Yogyakarta: Penerbit Andi, 22, pp.103–150.

Aldrich, D.P. and Meyer, M.A., 2022. *Handbook of Environmental Hazards and Society,* Routledge, pp.201–213.

Angriani, D., 2021. The Effect of Organizational Culture and Altruism on Social Competency of Science Teachers. *Journal of Educational Sciences*, 5(4), pp.678-686.

Arisanty, D., Rajiani, I., Mutiani, M., Hastuti, K.P., Abbas, E.W., Rosadi, D. and Muhaimin, M., 2023. Social capital of Banjarese for peatland fire mitigation: Combining of local wisdom and environment. *World,* 4(4), pp.745–757.

Baladi, R.A. and Shah, M.A., 2018. Solar-powered irrigation system for agriculture based on moisture content in the field and saving energy and water with optimum designing. *Asian Journal of Engineering, Sciences & Technology,* 8(1), p.651.

Brontowiyono, W. and Lupiyanto, R., 2011. Development of suburban areas and environmental problems in Nitiprayan art village, Bantul. *Journal of Environmental Science & Technology,* 3(1), pp.31–51.

Burt, R.S., 2004. Structural holes and good ideas. *American Journal of Sociology,* 110(2), pp.349–399.

Fathy, R., 2019. Social capital: Concept, inclusivity, and community empowerment. *Journal of Sociological Thought*, 6(1), pp.1–17.

Ghozali, I. and Latan, H., 2012. *Partial least square: Concept, techniques, and application of SmartPLS 2.0 M3.* Diponegoro University Publishing Agency.

Ghozali, I. and Latan, H., 2015. *Partial Least Squares: Concept, Techniques, and Application Using Smartpls 3.0 for Empirical Research.* Diponegoro University Publishing Agency.

Gyamfi, B.A., Onifade, S.T. and Ofori, E.K., 2023. Synthesizing the impacts of information and communication technology advancement and educational developments on environmental sustainability: A comparative analysis of three economic blocs—BRICS, MINT, and G7 economies. *Sustainable Development,* 31(2), pp.744–759.

Hanifan, L.J., 1916. The rural school community center. *The Annals of the American Academy of Political and Social Science*, 67(1), pp.130–138.

Haridison, A., 2013. Social capital in development. *JISPAR: Journal of Social Sciences, Politics, and Governance*, 4, pp.31–40.

Hussain, M., Khan, M. and Al-Aomar, R., 2016. A framework for supply chain sustainability in the service industry with confirmatory factor analysis. *Renewable and Sustainable Energy Reviews,* 55, pp.1301–1312.

Hussain, M., Khan, M. and Saber, H., 2015. Impact of capacity constraints on the dynamic response of a two-level supply chain. *Logistics, Informatics and Service Science,* 16, pp.201–206.

Ife, J. and Tesoriero, F., 2008. *Community Development: Alternative Approaches to Community Development in the Era of Globalization.* Pustaka Pelajar, p.265.

Latifah, S., 2014. Development of suburban cities (Impact of agricultural land conversion into elite housing). *Paradigm*, 2(3).

Laura, N., Sari, R.D., Setiawan, I. and Herdiyanti, H., 2018. The role of community social capital in managing natural resources as a survival strategy in Dusung Limang, Kelapa District, West Bangka Regency, *Plos One,* p.74.

Liu, Y., Tang, S., Geertman, S., Lin, Y. and van Oort, F., 2017. The chain effects of property-led redevelopment in Shenzhen: Price-shadowing and indirect displacement. *Cities,* 67, pp.31–42.

Machmud, S., 2012. *Environmental Law*. Citra Bhakti.

Melo, V. and Jenkins, P., 2023. The growth of different spaces of middle-classness in Greater Maputo: A methodological approach for assessing processes of this urban transformation. *Cities,* 142, p.104536.

Munandar, S., 2002. *Empowering Social Capital as an Alternative to Anticipate Social Conflict*. National Seminar Paper, ISI, Bogor, West Java.

Musavengane, R. and Kloppers, R., 2020. Social capital: An investment towards community resilience in the collaborative natural resource management of community-based tourism schemes. *Tourism Management Perspectives,* 34, p.100654. https://doi.org/10.1016/j.tmp.2020.100654

Ndolu, C., Effendi, J. and Ramang, R., 2017. Physical environmental conditions of settlements that grow contrary to land use designations and concepts formed from abstracted settlement conditions in the hills of Kelapa Lima Village, Kupang City. *Science,* 17, pp.82–89.

Ngalim, P., 2014. *Educational Psychology*. Bandung: PT Remaja Rosdakarya.

Prittaningtyas, E., Ekartaji, H., Yunus, H.S. and Rahardjo, N., 2014. Study on the quality of residential environments in urban peripheries: A case in Ngestiharjo Village, Yogyakarta. *Indonesian Geography Magazine*, 28(1), pp.96–102.

Saputynigsih, E., Diswandi, D. and Jaung, W., 2020. Does social capital matter in climate change adaptation? A lesson from the agricultural sector in Yogyakarta, Indonesia. *Land Use Policy,* 95, p.104189.

Sarstedt, M., Hair Jr, J.F., Cheah, J.-H., Becker, J.-M. and Ringle, C.M., 2019. How to specify, estimate, and validate higher-order constructs in PLS-SEM. *Australasian Marketing Journal*, 27(3), pp.197–211.

Sarwono, J. and Narimawati, U., 2015. *Writing Theses, Dissertations, and Research Papers Using Partial Least Square SEM (PLS-SEM)*.: Andi.

Setiadi, E.M. and Kolip, U., 2013. *Introduction to Political Sociology.* Kencana.

Statistics, C.B. of 2023. *Banjarmasin in Figures 2023*. Kota Banjarmasin.

Sugiyono, D., 2010. *Understanding Qualitative Research*. Alfabeta.

Sunyoto, U., 2018. *Social Capital*. Pustaka Belajar.

Uliyah, A.M., 2015. *Introduction to Human Basic Needs*. Salemba Medika.

Usman, M. and Ahmad, M.I., 2018. Parallel mediation model of social capital, learning and the adoption of best crop management practices: evidence from Pakistani small farmers. *China Agricultural Economic Review*, *10*(4), pp.589-607.

Yuliastuti, N., Sukmawati, A.M. and Purwoningsih, P., 2018. Utilization of social facilities to reinforce social interaction in formal housing. *International Journal of Architectural Research,* 12(1), pp.134–151.

Yunus, H.S., 2008. *Dynamics of Peri-Urban Areas: Determinants of the City's Future*. Pustaka Pelajar.

Zhou, Y. and Gu, B., 2024. *Earth Critical Zone*, Pustaka Pelajar.

The Impact of Iron Oxide Nanoparticles on Crude Oil Biodegradation with Bacterial Consortium

Suganya Kalaiarasu, K. J. Sharmila, Santhiya Jayakumar, Sreekumar Palanikumar and Priya Chokkalingam†

Department of Biotechnology, Dr. M.G.R. Educational and Research Institute, Chennai, Tamil Nadu, India

†Corresponding author: Priya Chokkalingam; priyamohan.2984@gmail.com

ABSTRACT

This study was performed to determine the effect of synthesized iron oxide nanoparticles on the consortium of isolated bacterial strains from the crude oil-contaminated site. The iron oxide nanoparticle (FeNPs) was synthesized by chemical co-precipitation method and confirmed with its characterization results such as UV-spectroscopy, X-ray Diffraction (XRD), High-Resolution Scanning Electron Microscopy (HR-SEM), Zeta potential and Particle Size Analyser studies. The isolates were cultured in LBBH (Luria-Bertani and Bushnell Haas) medium containing crude oil as a carbon source with incubation for 7 days. This study was performed using FeNPs with four different concentrations (10, 50, 100 and 150mg) incorporated with the isolated microbes clubbed as a consortium. The rate of biodegradation was investigated by gas chromatography-mass spectrometry (GC-MS) analysis. By comparing the control sample (crude oil) there was a better degradation in FeNPs added bacterial culture than consortium degradation. The obtained results conclude that studying different concentrations of FeNPs with the consortium of isolated microbes showed degradation differences, whereas 150mg concentration has a better degradation effect compared to other variations. It should be carried out to avoid agglomeration of nanoparticles by improving their biocompatibility and quality to influence the biodegradation of crude oil.

INTRODUCTION

The pollution of hydrocarbons due to oil and gas exploration and exploitation operations is one of the main environmental issues of the day. The discharge of this vital energy source into the environment is unavoidable and it has disastrous effects on marine/coastal waterways, shorelines, and land as well. Due to the danger that large oil spills pose to the environment, it is crucial to find clean-up methods that are affordable, quick, environmentally friendly, and long-lasting. These methods should also optimize and make it easier for highly petroleum hydrocarbon-inundated terrestrial ecosystems to be bio-restored for agricultural use or ecological balance (Bertha et al. 2021). Following a discharge or spill, a variety of concurrent physicochemical processes control the distribution and destiny of oil. Short-chain volatile chemicals rapidly evaporate after first spreading out on the surface. The amount that the mass of oil is exposed to air and light depends on the physical form of the oil, which affects the rate of oxidation (Yusaf 1985). Accidents involving oil spills have a history of declining in recent decades. The need to continue studying the function of microorganisms in the natural and induced attenuation of pollutants is driven by the greatest industrial catastrophe in history and the continual input of several additional pollutants into the coastal environment. By understanding the role of microorganisms in the restoration of an ecosystem, greater efforts are needed to better understand how these microbial communities function. In situ, investigations at the contaminated sites and simulation experiments in microcosms and mesocosm under controlled

laboratory settings have been the two primary approaches utilized to investigate the microbiological response to oil pollution (Acosta-González et al. 2016). The primary use of environmental biotechnology is bioremediation, which is presently thought of as an emerging technique. This can completely degrade the pollutant into carbon dioxide aerobically or water and methane under anaerobiosis, or it can mineralize the pollutant, partially transforming it into a less dangerous form. Each microbe has a unique tolerance profile, and there are instances where large amounts of organic contaminants might limit microbial activity (San Martín 2011). Although bioremediation has not yet been proven to be efficient for the treatment of open ocean oil after a spill it is far more challenging to assess hydrocarbon biodegradation in situ than it is to do so in lab experiments (Atlas 1995). The restricted accessibility of oil pollutants to microorganisms is the limiting factor in the biodegradation of oil pollution in the environment. Since many complex hydrocarbon molecules are carcinogenic, they also pose a real risk to human health. Here, to solve these issues, nanotechnology has drawn a lot of attention due to its large specific surface areas and has been widely exploited as reductants and/or catalysts to enhance a variety of processes. On the other hand, the impact of nanoparticles on microbes has also attracted a lot of interest. Although nanoparticles can help with microbe activity, there has only been very little research on how they affect the rates of microbiological response. Typically, nanoparticle catalysts increase the speed of microbiological reactions by attaching to cells and promoting microbial activity (El-Sheshtawy et al. 2017). Even if biological methods are effective, the efficiency and efficacy of nanoparticles have been widely employed to remove a range of organic and inorganic toxins from the environment. Nanoparticles make excellent adsorbents and may significantly increase the adsorption capabilities of sorbent materials. Among them, Iron oxide nanoparticles have gained a lot of interest for a variety of applications due to their special characteristics and relatively simple manufacture. Iron oxide nanoparticles with appropriate surface chemistry are prepared by various methods such as wet chemical, dry processes, or microbiological techniques. The most effective and simplest technique to obtain iron oxide nanoparticles is through the Chemical co-precipitation method. The potential of iron oxide nanoparticles for oil clean-up was emphasized by several investigations (Ali et al. 2016 & Alabresm et al. 2018). The method for synthesizing iron oxide nanoparticles is environmentally friendly and requires a short reaction time compared to the physical and chemical methodologies (Oyewole et al. 2019). This research work exhibits the enhancement in crude oil biodegradation of isolated strains as a consortium and with the addition of synthesized iron oxide nanoparticles (FeNPs) was performed and analyzed using GC-MS study.

MATERIALS AND METHODS

Synthesis of Iron Oxide Nanoparticles (FeNPs)

Iron oxide nanoparticles were synthesized using the chemical co-precipitation method (Ganapathe et al. 2022, Kalantari et al. 2014). The iron source was first prepared by dissolving 0.2 M $FeSO_4·2H_2O$ and 0.1 M $FeCl_3·6H_2O$ in 50 mL of distilled water. The base solution was prepared by dissolving 2M NaOH into 200 mL of distilled water. The prepared iron source was added dropwise into the flask containing the base solution under vigorous magnetic stirring of 1000 rpm at 37°C for 30 minutes. At the end of the reaction, the observed black precipitate was centrifuged at 5000 rpm for 10min, and washed thrice with distilled water and ethanol. The precipitate was then dried in a hot air oven at 100°C overnight. The dried black granules were finely ground into powdered form. The sample has been labeled as FeNPs for further reference.

Characterization Studies of Synthesized FeNPs

The UV spectrophotometric analysis of the synthesized iron oxide nanoparticles was carried out at 200 to 800 nm wavelength range (Oyewole et al. 2018). The surface charge and the size distribution were analyzed using a Zeta-potential and Particle Size analyzer. The crystalline nature of synthesized nanoparticles was analyzed using X-ray diffraction (XRD) at an angle range of 2θ (10–80 degrees). The surface morphology of the iron oxide nanoparticles was examined using High-Resolution Scanning Electron Microscopy (HR-SEM) equipped with (EDS) Energy Dispersive Spectroscopy.

Isolation and Identification of Bacteria

The crude oil-polluted soil sample was collected from an oil refinery site, in Chennai, Tamil Nadu (13°10'36" N 80°16'25" E). The sample was serial diluted and inoculated in LBBH medium and kept in a shaking incubator overnight at 37°C at 100 rpm. After initial serial dilution and growth observation, four strains (SH 1- 4) were isolated and maintained as pure cultures (Chikere & Ekwuabu 2014). To assess biodegradation, these isolates were used as a consortium, inoculated in LBBH medium with 2% crude oil, and incubated in a rotary shaker at 37°C in 150 rpm (Li et al. 2019). Flask with LBBH medium and crude oil served as a control for the comparative study.

Degradation of Crude Oil Using Synthesized Iron Oxide Nanoparticles (FeNPs)

For biodegradation activity, LBBH medium was prepared with different concentrations of synthesized nanoparticles
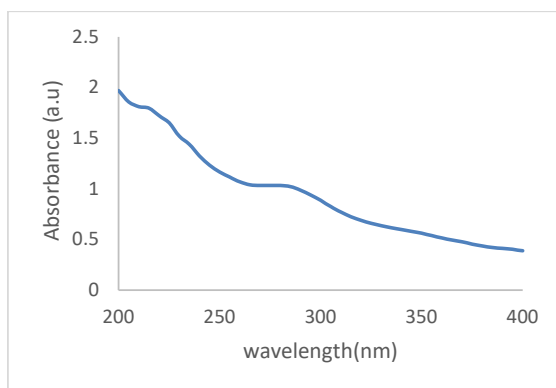
Fig. 1: The UV-visible analysis of FeNPs.
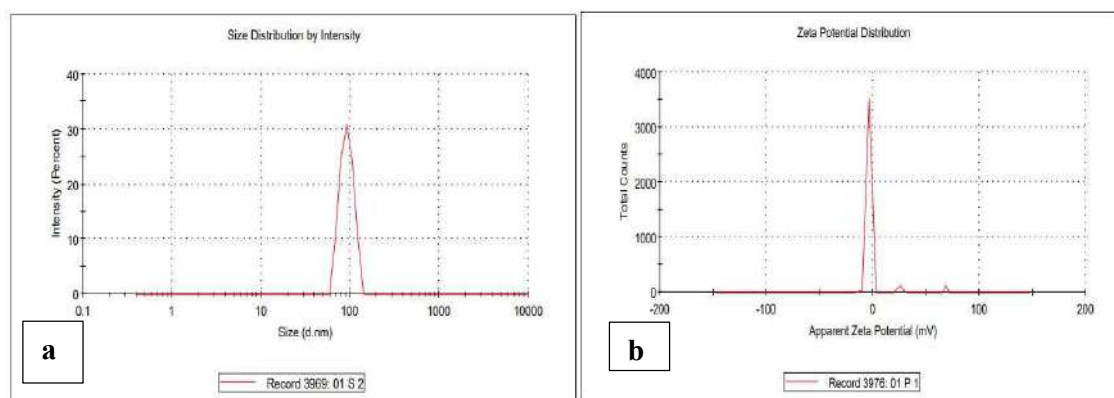
Fig. 2: (a) Particle size and (b) zeta potential distribution of FeNPs.

(10, 50, 100, 150mg), and 2mL of crude oil was added and kept in a shaking incubator at 100rpm for 30 minutes. Then 100μL of overnight incubated consortium culture was added in each medium containing various concentrations of nanoparticles again kept for incubation in a shaker incubator for 7 days at 37°C at 150rpm. A sample containing crude oil without inoculum was taken as a control. The cultures were kept in a shaking incubator at 150 rpm for 7 days (El-Sheshtawy & Ahmed 2017). Degraded crude oil residues were performed by Gas Chromatography-Mass Spectroscopy (GC-MS) analysis equipped with a fused silica capillary column (DB5, 30m long 0.25mm inner diameter). The oven temperature was programmed from 50°C (3 min) to 280°C at 10°C/min. The carrier gas was Helium at a flow rate of 1 mL/min. The injector temperature was 230°C, and the samples were injected for 2mL. The mass spectrum of the components present in the crude oil was confirmed in the National Institute of Standard and Technology (NIST) mass spectra library database to determine the amount of residual crude oil in the analyzed degraded samples (Kazemzadeh et al. 2020, Iwabuchi et al. 2002).

RESULTS

This work evaluates the possibility of using isolated bacterial strains in combination with iron oxide nanoparticles (FeNPs) to improve crude oil biodegradation. FeNPs characterization verifies their applicability, and enhanced degradation is revealed by GC-MS analysis. With ramifications for environmental cleanup initiatives, our findings highlight FeNPs' potential as a potent instrument for enhancing crude oil remediation procedures. The effective production of FeNPs was validated by characterization investigations; UV-Vis examination revealed an absorption peak at 278nm (Fig. 1), which is suggestive of iron oxide nanoparticles.

The Zeta potential and size of particles analysis in Fig. 2 (a) & (b) showed that the FeNPs were stable, with a zeta potential of ±3.53 mV, a particle size of about 148.3 nm, and a PDI of 0.373. Zeta potential was also determined and obtained to be ±3.53 mV signifies the stability of synthesized nanoparticles.

FeNPs' crystalline structure was validated by X-ray diffraction (XRD) research. In X-ray diffraction analysis
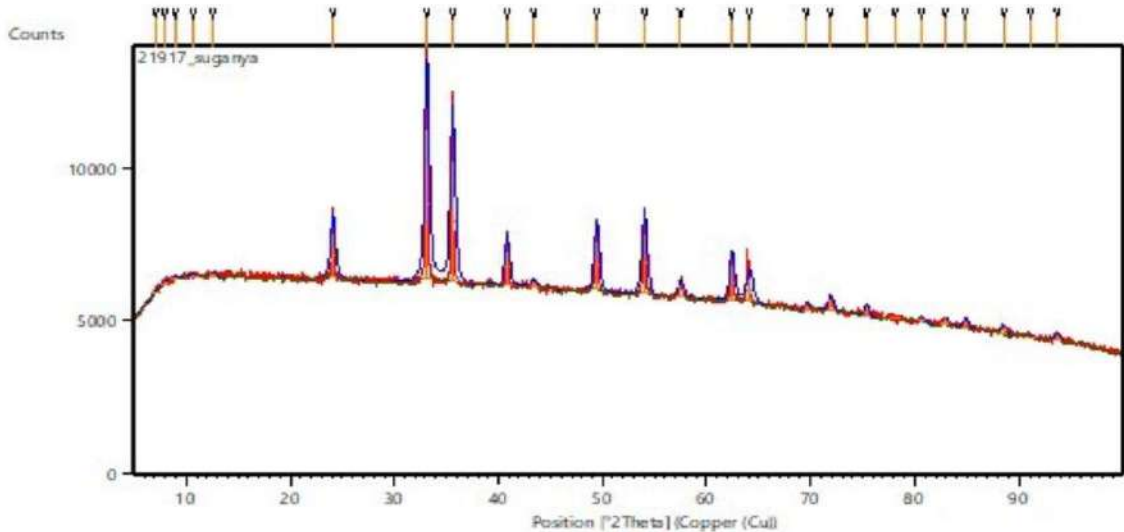
Fig. 3: XRD spectrum of FeNPs.

(Fig. 3) of synthesized FeNPs, a cathode film coating was used to determine the type of crystals of nanoparticles (2 θ = 10–80). The spectrum obtained by the XRD method showed the peak range at $2\theta = 33.50, 38, 41.35, 50.01$, and 63 positions confirming the crystalline structure of nanoparticles.

Morphological Characterization of FeNPs by HR-SEM Analysis

The surface morphology of the iron nanoparticles was examined using HR-SEM and EDX. In Fig. 4 (A & B) and Fig. 5, the results of the synthesized nanoparticles were visible in HR-SEM images as cylindrical and rod-shaped spheres at a magnification of 2 μm, and 500 nm images were confirmed with clear morphology of synthesized FeNPs. Agglomeration in the SEM images of the synthesized nanoparticles might be due to electrostatic interaction between layers of nanoparticles' surface. In terms of EDAX analysis, the main components found in the sample were Fe (81.79 by weight) proved the expected iron oxide nanoparticles.

Molecular Identification of Selected Bacterial Strains

The study involved the isolation and selection of bacterial
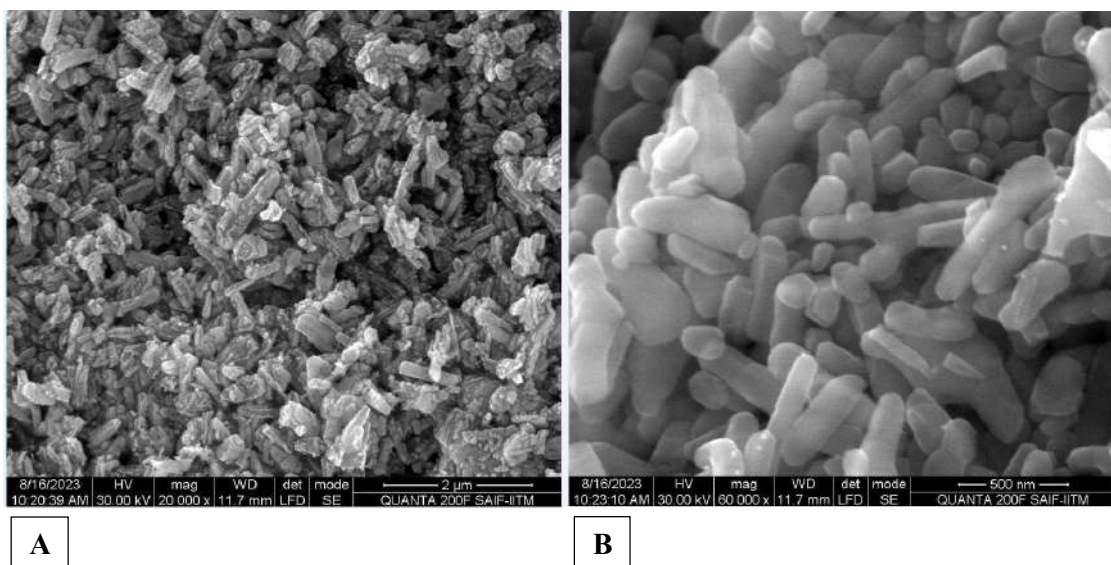
Fig. 4: HR-SEM images (2μm - A and 500nm - B magnification) of FeNPs.
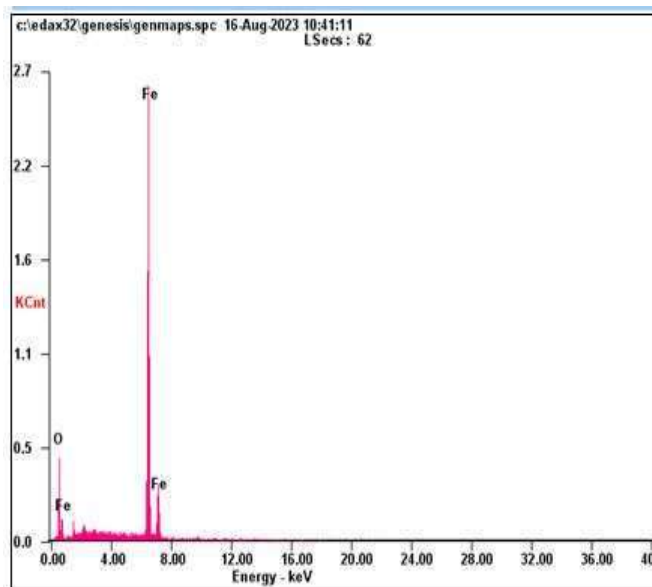
Element	Wt%	At%
OK	18.21	43.73
FeK	81.79	56.27
Matrix	Correction	ZAF

Fig. 5: EDS data of FeNPs.

strains from a soil sample contaminated with crude oil. The collected soil sample was incubated in LBBH medium overnight at 37°C and 100 rpm. After serial dilutions and growth observations, four bacterial strains (SH 1-4) were isolated and maintained as pure cultures. These strains were identified as *Bacillus glycinifermentans* (MN399919.1), *Bacillus subtilis* subsp. *Stercoris* (MN704442.1), *Enterobacter cloacae* (MT367840.1), and *Enterobacter ludwigii* (CP018785.1). To confirm the identities of these strains, molecular-based techniques, specifically PCR amplification, were employed. The obtained 16S rRNA sequences were compared with those available in the database. Subsequently, the selected strains were used in degradation studies, focusing on their ability to utilize crude oil as the sole carbon source (Tian et al. 2018). This research describes improving the biodegradation process by using the consortium of isolated bacteria which confirms the degradation activity and the synthesized nanoparticles tend to break down the crude oil components into simpler forms to provide one of the nutrient sources for microbes. FeNPs are produced by the chemical co-precipitation technique, and their appropriateness and efficacy in promoting biodegradation processes are studied. The separated bacterial strains that are grown from soil samples polluted with crude oil are then mixed with these nanoparticles. Grown in a medium containing FeNPs, the consortium of bacterial strains identified by molecular techniques shows that they can break down crude oil.

GC-MS Analysis of Crude Oil Degradation Studies

Gas chromatography-mass spectrometry (GC-MS) analysis is used to assess the biodegradation process and determine how much crude oil has degraded. The utilization of bacterial consortia and FeNPs in this system presents a promising approach to crude oil pollution remediation, with the potential to yield more environmentally sustainable and effective remediation methods. When using chemically synthesized FeNPs in the consortium of isolated bacterial strains for the biodegradation of crude oil, the results are suitable based on characterization investigations, which demonstrate well-dispersed nanoparticles with the right size and stability. As a consortium, these strains were used to study the biodegradation of crude oil. In GC-MS analysis the group of four distinct bacterial strains were cultivated on LBBH medium with 2% crude oil to evaluate the biodegradation of crude oil. After that, the cultures were kept in an incubator that was shaking and running at 150 rpm for 7 days. To assess their effects and variation in crude oil biodegradation activity, FeNPs were introduced to the consortium in four different concentrations (10, 50, 100, 150 mg). By contrasting the group of organisms and FeNP-treated cultures with a control sample, the biological degradation effectiveness of both was validated using the gas chromatography-mass spectrometry used to assess the amount of biodegradation and detect any alterations in the hydrocarbon component composition of the degraded oil residues during incubation. This all-inclusive method made it possible to evaluate the bacterial consortium's capacity for biodegradation and the impact of FeNPs on crude oil clean-up in detail.

The complicated structure of hydrocarbon chemicals within the crude oil substrate was revealed by the gas chromatography-mass spectrometry (GC-MS) analysis of
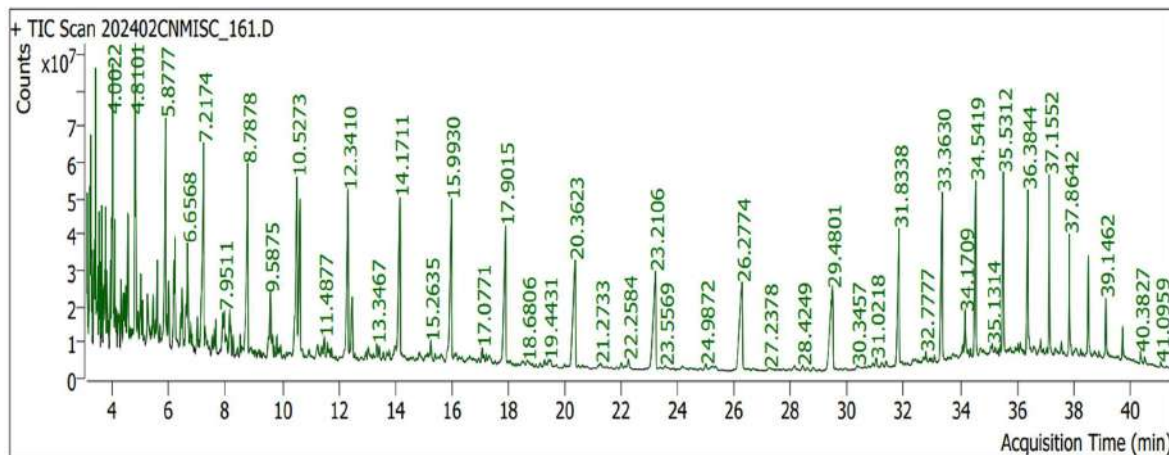
Fig. 6: GC-MS analysis - Control (crude oil).

the control sample (Fig. 6). The complicated character of the crude oil sample was reflected in the wide spectrum of hydrocarbon compounds that were found. This thorough evaluation offered a fundamental comprehension of the hydrocarbon profile found in the raw crude oil and was an essential point of reference for further investigations. The existence of several hydrocarbon compounds emphasized the difficulty of crude oil pollution and the need for efficient clean-up techniques. The control sample's outcomes provided the framework for assessing how well biodegradation processes reduce the pollution caused by crude oil.

When exposed to crude oil, the bacterial consortium showed moderate biodegradation capabilities without the presence of iron oxide nanoparticles (FeNPs). After research, it became clear that the consortium had started a degrading process that resulted in a noticeable drop in the amount of different hydrocarbon compounds (Fig. 7). The consortium's natural capacity to metabolize and degrade complex

hydrocarbons was demonstrated by the mild biodegradation. The consortium's capacity as a natural agent for reducing pollution from crude oil is highlighted by this decrease in hydrocarbon compounds. To maximize the consortium's biodegradation efficiency, more studies may be needed to improve its efficacy in environmental clean-up initiatives. The consortium only includes a restricted amount of bacterial strains (SH 1-4), and this could not be diverse enough to break down every component of crude oil effectively. A microbial community with greater diversity may be able to target a broader variety of hydrocarbon molecules for breakdown.

A significant improvement in crude oil biological degradation was seen at the lowest concentration of 10mg of FeNPs, which outperformed the effectiveness of a control sample (Fig. 8). This result emphasizes how FeNPs, even at comparatively modest dosages, can help bioremediation processes. The effect showed that FeNPs had a beneficial
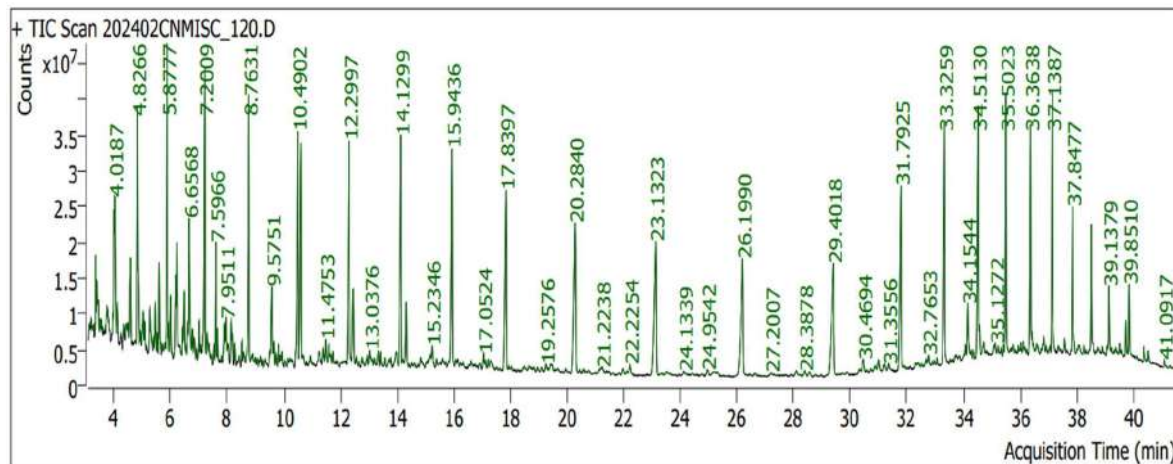
Fig. 7: GC-MS analysis– Consortium (SH 1-4).
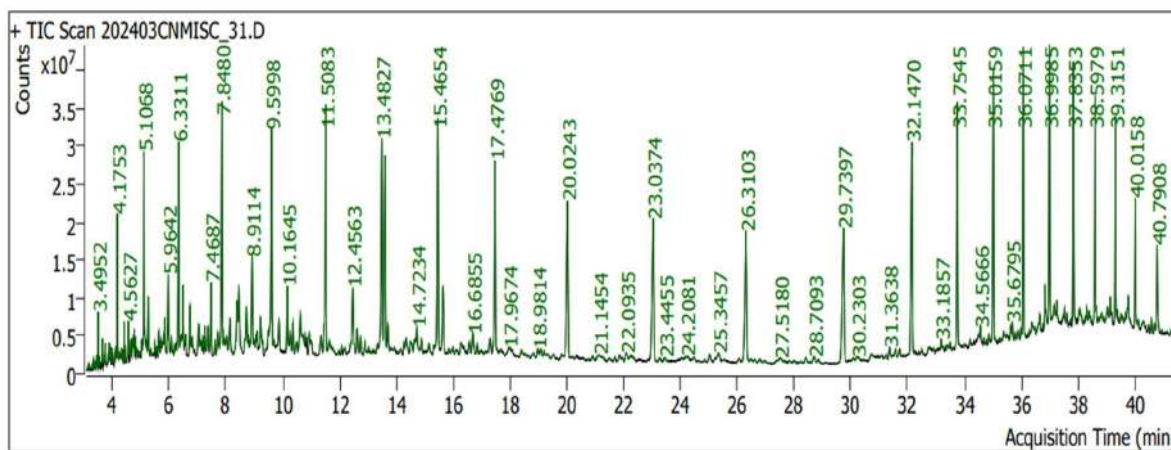
Fig. 8: GC-MS result-10mg concentration.
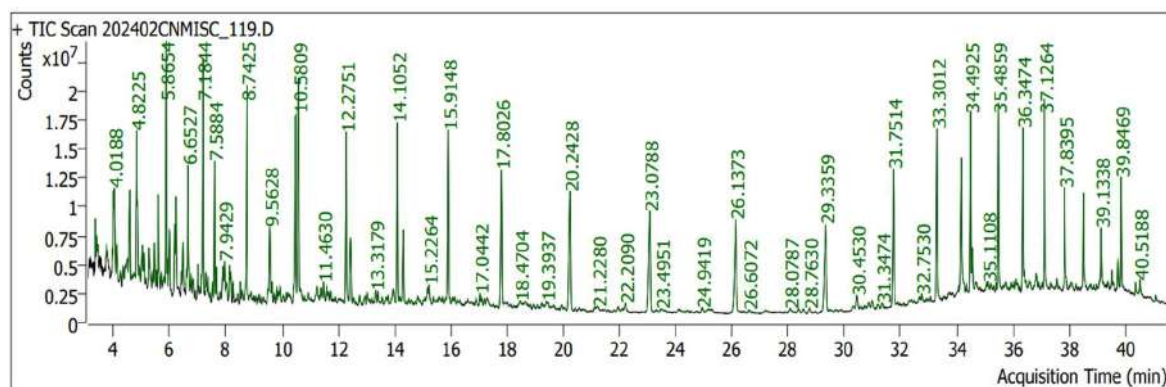
Fig. 9: GC-MS result – 50mg concentration.

effect on hastening the hydrocarbon breakdown of crude oil, even if it was less pronounced than at higher FeNPs concentrations. This study is noteworthy because it implies that FeNPs, even at low concentrations, can aid in environmental clean-up operations. It also emphasizes the versatility and possible application of FeNPs in remediation tactics targeted at treating crude oil contamination.

The biodegradation efficacy significantly improved as the concentration of FeNPs was raised to 50 mg, which is a significant improvement over lesser concentration (Fig. 9). The quantity of hydrocarbon compounds decreased noticeably as the concentration of FeNPs increased, demonstrating the critical role FeNPs play in quickening the degradation process. FeNPs may be able to improve the bacterial consortium's interaction with the crude oil substrate, leading to more effective hydrocarbon compound breakdown, as indicated by the increased efficacy at this concentration.

A much-improved capacity for crude oil clean-up was demonstrated by raising the FeNPs content to 100mg, which

produced an even more noticeable biodegradation effect (Fig. 10). A more thorough clean-up of hydrocarbon compounds from the surroundings and increased rates of degradation were probably caused by higher levels of FeNPs, which also encouraged increased interaction and mutually beneficial outcomes that occurred between FeNPs and the bacterial consortia.

The biodegradation effect peaked at a remarkably high concentration of 150 mg of FeNPs, suggesting that FeNPs have the greatest potential for facilitating crude oil bioremediation (Fig. 11). The hydrocarbon compound abundance was most significantly reduced at this concentration, highlighting the important role that FeNPs play in enhancing the effectiveness and efficiency of the processes involved in the degradation of crude oil. These results imply that a higher number of FeNPs can result in more comprehensive and effective crude oil bioremediation procedures, and they also highlight the significance of optimizing the FeNPs amount for maximum elimination performance. Finally, the study's conclusions highlight the favorable relationship between rising iron
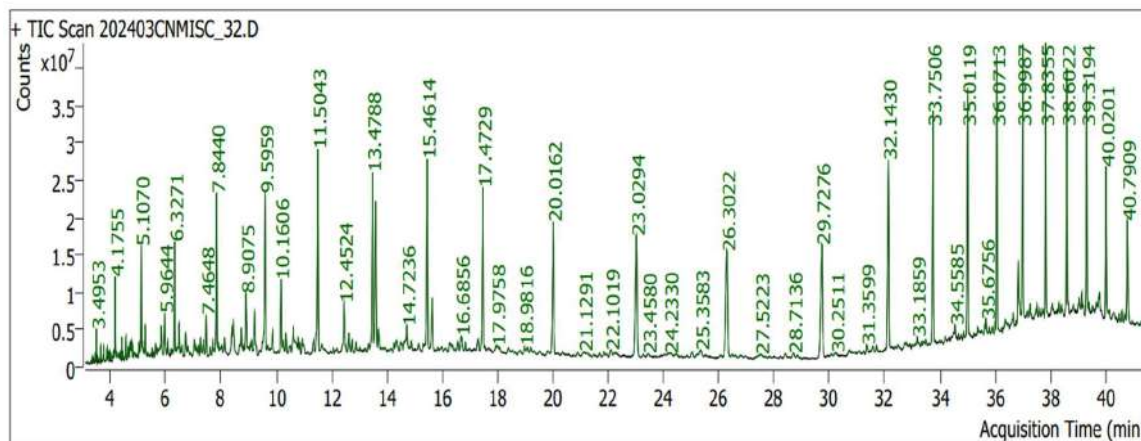
Fig. 10: GC-MS result – 100mg concentration.
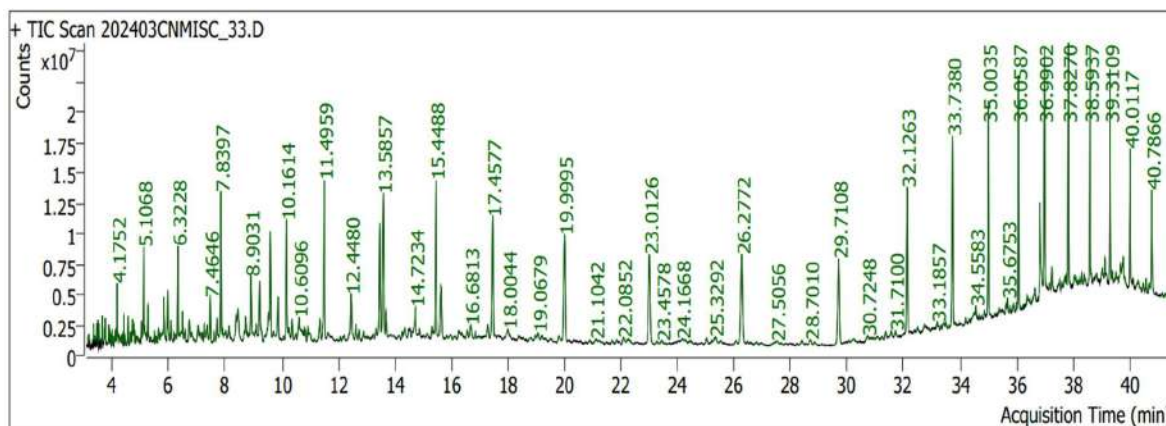
Fig. 11: GC-MS result – 150mg concentration.

oxide nanoparticle (FeNPs) concentrations and improved crude oil biodegradation efficiency. The results indicate that FeNPs play a crucial role in expediting bioremediation processes, as evidenced by the substantial decrease in hydrocarbon compounds observed at the highest dosage of 150 mg. FeNPs ability to support cleanup efforts was further validated by real evidence of crude oil chemical degradation obtained through gas chromatography-mass spectrometry research. These findings suggest that FeNPs may be a viable and long-term instrument for improving the effectiveness of crude oil cleaning operations. These findings have important ramifications for projects aimed at protecting the environment and restoring ecosystems.

DISCUSSION

This work analyses the use of isolated microorganisms in combination with synthetic iron oxide nanoparticles (FeNPs) as a possible remediation approach for the biodegradation of crude oil. The effectiveness of nanoparticles in accelerating the breakdown of crude oil has been found that the various types of nanoparticles have distinct properties that affect how well they work (Bertha et al. 2021). Enhancing reaction speeds also greatly depends on choosing the right microorganisms and nanoparticles. The ideal concentration of nanoparticles must be carefully determined, though, since too much can negatively impact microbial activity and perhaps slow down the breakdown process (Iwabuchi et al. 2002). The purpose of this study's iron oxide nanoparticle creation was to use bacterial isolates to accelerate the breakdown of crude oil. The propensity of iron oxide with bare surfaces to aggregate because of van der Waals forces and extremely energetic surfaces, however, presents a significant obstacle. The ability of the nanoparticles to promote biodegradation may be hampered by this aggregation. Although iron nanoparticles' size distribution, shape, and surface characteristics have been altered in an attempt to improve their biocompatibility, stability is still a major challenge. Iron nanoparticles' strong reactivity with oxidizing substances, especially

when air is present, is a drawback to employing them. This reactivity may cause unintentional oxidation, which could reduce the nanoparticles' usefulness in bioremediation applications. Preparation procedures frequently need to be carried out in anaerobic environments to minimize oxidation and help address this problem. Creating efficient defense mechanisms, including appropriate polymer or biomolecule surface coatings, is also crucial for preserving the stability of nanoparticles and guaranteeing their long-term effectiveness in clean-up operations. Therefore, even though iron oxide nanoparticles have the potential for biodegrading crude oil, resolving issues with stability and reactivity is essential to maximizing their use in environmental remediation. In the work by Rizi et al. (2017), isolated bacterial colonies were cultivated in media containing varied concentrations of TiO_2, Fe_2O_3, and nanoparticles of Fe_3O_4 to examine the effect of nanoparticles on sludge from oil refinery biodegradation. Using GC-MS analysis, the maximum microbial growth was detected at a value of 1mg/ml of Fe_2O_3 and Fe_3O_4 nanoparticles. In contrast, the inclusion of Fe_3O_4 nanoparticles, particularly under light circumstances, resulted in a significant decrease in the amount of cyclosiloxane compound, suggesting improved biodegradation. Furthermore, even in dark settings, bacterial activity in conjunction with Fe_3O_4 nanoparticles led to the elimination of some compounds, whereas the presence of Fe_2O_3 nanoparticles demonstrated a decrease in some chemicals. Overall, the study shows that Fe_2O_3 and Fe_3O_4 nanoparticles have a beneficial effect on the biodegradation of oil sludge. In a further study, El-Sheshtawy & Ahmed (2017) used GC-MS analysis to find variations in total paraffins as samples of leftover crude oil from different microcosms biodegraded. The most efficient breakdown of total paraffins, especially those with long chains (C31–C46), was achieved by adding the biosurfactant containing 0.2g of Fe_2O_3. This finding indicates a new and significant trend in biodegradation, which is enhanced bacterial strain performance and total paraffin consumption when biosurfactant with Fe_2O_3 nanoparticles is present. Cao et al. (2021) produced magnetic nanoparticles adorned with bacteria to mitigate the effects of crude oil. The research focused on the biodegradation of low-molecular-weight chemicals, including aromatics and alkanes. According to GC-MS analysis, when combined with pure bacteria, magnetic nanoparticles improved the breakdown of lower molecular-weight aromatic compounds compared to when pure bacteria were used alone. Moreover, the recovery procedure made it easier to get rid of oil-bacteria clumps, which eliminated high-molecular-weight aromatic compounds. The study's conclusions highlight how magnetic nanoparticles can enhance the biodegradation of crude oil, especially for low-molecular-weight chemicals, potentially leading to improvements in remediation techniques.

CONCLUSIONS

According to the results of this study, the four bacteria species were isolated from the oil-contaminated site to check its crude oil biodegradation activity. Thus, these strains can deteriorate the long complex chains to short chain compounds and there was partial degradation of the complex compounds present in crude oil that was provided as the sole carbon source. The synthesized iron oxide nanoparticles showed heavy components reduction at 150 mg concentration than other used concentrations, which was better than the consortium sample when compared to the control. So, the synthesized iron oxide nanoparticles confirm its efficacy in degrading crude oil. Further, different concentrations of nanoparticles should be performed to analyze the degradation levels and to achieve the complete efficiency of crude oil in a consortium for bioremediation purposes.

ACKNOWLEDGEMENTS

REFERENCES

Acosta-González, A. and Marqués, S., 2016. Bacterial diversity in oil-polluted marine coastal sediments. *Current Opinion in Biotechnology*, 38, pp.24-32.

Alabresm, A., Chen, Y.P., Decho, A.W. and Lead, J., 2018. A novel method for the synergistic remediation of oil-water mixtures using nanoparticles and oil-degrading bacteria. *Science of the Total Environment*, 630, pp.1292-1297.

Atlas, R.M., 1981. Microbial degradation of petroleum hydrocarbons: an environmental perspective. *Microbiology Reviews*, 45(1), pp.180-209.

Cao, Y., Zhang, B., Zhu, Z., Rostami, M., Dong, G., Ling, J. and Chen, B., 2021. Access-dispersion-recovery strategy for enhanced mitigation of heavy crude oil pollution using magnetic nanoparticles decorated bacteria. *Bioresource Technology*, 337, 125404.

Chikere, C.B. and Ekwuabu, C.B., 2014. Molecular characterization of autochthonous hydrocarbon utilizing bacteria in oil-polluted sites at Bodo Community, Ogoni land, Niger Delta, Nigeria. *Nigerian Journal of Biotechnology*, 27, pp.28-33.

Bertha, E.E.C., Chikere, C.B. and Akaranta, O., 2021. Sustained nutrient delivery system: a new perspective in bioremediation. *Journal of Soil Science and Environmental Management*, *12*(4), pp.173-182.

El-Sheshtawy, H.S. and Ahmed, W., 2017. Bioremediation of crude oil by *Bacillus licheniformis* in the presence of different concentration nanoparticles and produced biosurfactant. *International Journal of Environmental Science and Technology*, 14, pp.1603-1614.

El-Sheshtawy, H., Khalil, N., Ahmed, W. and Amin, N., 2017. Enhancement the bioremediation of crude oil by nanoparticle and biosurfactants. *Egyptian Journal of Chemistry*, 60(5), pp.835-848.

Ganapathe, L.S., Kazmi, J., Mohamed, M.A. and Berhanuddin, D.D., 2022. Molarity Effects of Fe and NaOH on Synthesis and Characterisation of

Magnetite (Fe_3O_4) Nanoparticles for Potential Application in Magnetic Hyperthermia Therapy. *Magnetochemistry*, 8(11), p.161.

Iwabuchi, N., Sunairi, M., Urai, M., Itoh, C., Anzai, H., Nakajima, M. and Harayama, S., 2002. Extracellular polysaccharides of *Rhodococcus rhodochrous* S-2 stimulate the degradation of aromatic components in crude oil by indigenous marine bacteria. *Applied and Environmental Microbiology*, 68(5), pp.2337-2343.

Kalantari, K., Ahmad, M.B., Shameli, K., Hussein, M.Z.B., Khandanlou, R. and Khanehzaei, H., 2014. Size-controlled synthesis of Fe_3O_4 magnetic nanoparticles in the layers of montmorillonite. *Journal of Nanomaterials*, 2014, pp.181-185.

Kazemzadeh, S., Naghavi, N.S., Emami-Karvani, Z., Fouladgar, M. and Emtiazi, G., 2020. Gas chromatography-mass spectrometry analyses of crude oil bioremediation by the novel *Klebsiella variicola* SKV2 immobilized in polyurethane polymer scaffold and two-layer microcapsulation. *Bioremediation Journal*, 24(2-3), pp.129-149.

Li, S.W., Liu, M.Y. and Yang, R.Q., 2019. Comparative genome characterization of a petroleum-degrading *Bacillus subtilis* strain DM2. *International Journal of Genomics*.

Oyewole, O.A., Raji, R.O., Musa, I.O., Enemanna, C.E., Abdulsalam, O.N. and Yakubu, J.G., 2019. Enhanced degradation of crude oil with *Alcaligenes faecalis* ADY25 and iron oxide nanoparticle. *International Journal of Applied Biological Research*, 10(2), pp.62-72.

Rizi, M.S.S., Emtiazi, G., Sepahi, A.A., Maal, K.B. and Hosseini, F., 2017. The effect of nanoparticles on oil sludge biodegradation by *Chromohalobacter* sp. isolated from the Bahregan area in the Persian Gulf. *Petroleum Science and Technology*, 35(7), pp.687-695.

San Martín, Y.B., 2011. Bioremediation: a tool for the management of oil pollution in marine ecosystems. *Biotecnología Aplicada*, 28(2), pp.69-76.

Tian, X., Wang, X., Peng, S., Wang, Z., Zhou, R. and Tian, H., 2018. Isolation, screening, and crude oil degradation characteristics of hydrocarbons-degrading bacteria for treatment of oily wastewater. *Water Science and Technology*, 78(12), pp.2626-2638.

Wang, N., Hsu, C., Zhu, L., Tseng, S. and Hsu, J.P., 2013. Influence of metal oxide nanoparticles concentration on their zeta potential. *Journal of Colloid and Interface Science*, 407, pp.22-28.

Yusaf, S., 1985. Bio Effects of Marine Oil Pollution. *Oil & Petrochemical Pollution*, 2, pp.235-264.

Relative Saccharification of Sawdust Materials at Different Incubation pH-values

N. A. Ndukwe[1], J. B. M. Seeletse[2] and J. P. H. van Wyk[2]†

[1]Department of Chemical Sciences, College of Basic and Applied Sciences, Mountain Top University, Magoki, Ogun State, Nigeria

[2]Department of Pharmacology and Therapeutics, Sefako Makgatho Health Sciences University, South Africa

†Corresponding author: J.P.H. van Wyk: bioenergy.res@gmail.com

ABSTRACT

The uncontrolled production of waste is a daily phenomenon that is experienced by most global communities, and the situation worsens due to the lack of effective waste management procedures. Solid waste such as sawdust is primarily produced by the forestry industry and although it is utilized by certain countries as briquettes to make fire or as an absorbent to clean fluid spillage as well as a component of ceilings, most of the sawdust along the Lagos Lagoon in Nigeria is left unattended as waste, contributing to environmental pollution. Cellulose, composed of glucose units is a structural component of sawdust and when saccharified the resulting glucose can be fermented into renewable substances such as bio-ethanol. The cellulose degradation process can be performed with a cellulase enzyme such as available in the fungus *Aspergillus niger* and during the current investigation, this enzyme system was used to bio-convert the cellulose component of sawdust from ten different trees along the Lagoon into glucose. To increase the cellulase action all sawdust materials were delignified before cellulase action with the main aim of determining the optimum pH value for maximum degradation of the various sawdust materials. The pH-related saccharification profile of each type of sawdust was constructed as well as the relative percentage of saccharification and it was concluded that all the materials were optimum degraded at acidic pH-values which varied between pH 5.0 and pH 6.0 that are like optimum pH-values reported for the other types of cellulose materials.

INTRODUCTION

Environmental pollution will become more topical as the amount of waste produced by the global population increases with the negative effect thereof on water resources, in air as well as on land already observed and described (Li et al. 2021). Solid waste is one of the various sectors of rubbish with organic waste a major component of trash composed of materials produced by agriculture, forestry, and households (Janakiram & Sridevi 2010). Organic waste refers to substances of plant origin such as food waste, garden waste (plants, grass, trees), and sawdust which potential to be degraded by cellulase enzymes into glucose, a fermentable sugar at different incubation pH-value was determined during the current investigation. Sawdust is a waste product produced by forestry during the felling of trees tons of this wood material are produced annually along the Lagos Lagoon in Nigeria because of the activities of numerous sawmills (Faremi et al. 2021). Efforts to develop waste through recycling into useful products or commodities are widely applied with the aim not only to protect natural resources but also to limit the use of fossil fuels that could have a positive effect on the environment specifically to control the effects of climate change (Paritosh et al. 2017). Although sawdust has several applications such as an efficient adsorbent for dye removal (Chikri et al. 2020), insulation material (Okino et al. 2021), biosorbent (Giwa et al. 2016),

forms part of ceiling boards (Zeleke & Rotich 2021), its potential to be developed as a resource for the development of bio-chemicals or bio-pharmaceuticals is yet to be realized.

The chemical structure of sawdust makes it a suitable resource for the synthesis carbon carbon-related substances that would replace fossil fuels as feedstock (Babu et al. 2022). Cellulose a glucose bio-polymer is one of the major structural components of sawdust and if degraded into glucose this fermentable sugar could be used as a renewable feedstock for the synthesis of many bio-products such as bio-ethanol (Amaefule et al. 2023). Although cellulose exhibits a relatively high resistance towards different degradation procedures it can be saccharified through the action of cellulase a hydrolytic enzyme (Sartori et al. 2015). To make the cellulose more susceptible to cellulase-catalyzed degradation this biopolymer can be delignified (Kurian et al. 2014), a process that destroys its interaction with lignin, another biopolymer in plant materials. Cellulase enzymes are available from different bacterial (Sethi et al. 2013) and fungal (Ja'afaru 2013) sources with cellulases from *Trichoderma reesei* (De Paula et al. 2018) and *Aspergillus niger* (Lee et al. 2011) known as effective enzyme systems acting on cellulose causing the release of free glucose. The enzymatic or cellulase-catalyzed degradation of cellulose is subjected to several catalytic variables that could affect the effective outcome of the cellulose saccharification process in terms of glucose production. These variables include incubation temperature, incubation time, the pH value at which the incubation takes place, the concentration of the cellulase enzyme used during the degradation process, and the amount of cellulose used during each incubation process. One of the aims of cellulose degradation is to design a saccharification process that results in the maximum amount of sugar produced and this process should include the optimization of catalytic properties of the cellulase enzymes as well as the application of physical and chemical pretreatments rendering the cellulose more susceptible for cellulase catalyzed degradation (Abolore et al. 2024). It is however important to mention that the pretreatment action should be environmentally benign thus making acid and alkaline pretreatment agents less favorable.

The environmental impact of fossil fuel consumption as an energy source or feedstock during the synthesis of chemical-related substances is well-researched and published (Lak et al. 2024). As a result of the negative environmental effects caused by fossil fuel use alternative and renewable energy resources must be identified and developed. Linked to this environmental observation and of concern is the increasing volumes of non-manageable solid waste especially organic waste produced annually. These two phenomena could be resolved simultaneously by developing the cellulose component of organic waste such as sawdust as a resource for bioproduct synthesis thus limiting the amount of solid waste and the dependence on fossil fuels as an energy resource and feedstock for synthetic purposes.

The development of waste cellulose such as sawdust and wastepaper (Mokatse & Van Wyk 2021) as a resource of bio-energy should be initiated by making it more susceptible to degradation and the use of cellulase enzymes should be advisable as the process is environmentally benign (Verma & Kumar 2022). This investigation dealt with the saccharification of sawdust from different trees along the Lagos Lagoon with the cellulase enzyme from *Aspergillus niger* with a focus on the effect of changing incubation pH values when degrading the delignified sawdust materials.

MATERIALS AND METHODS

Sawdust Substrate and Cellulase Enzyme

Delignified sawdust samples from ten different trees along the Lagos Lagoon in Nigeria were transferred in triplicate into test tubes. Names of these sawdust samples are *Erythropleum suaveolens*, *Symphona globulifera*, *Ricindendron heudelotii*, *Pterygota macrocarpa*, *Milicia excels*, *Ipomoeu asarifolia*, *Hallelea ciliate*, *Sacoglottis gabonensis*, *Pycnanthus angolensis*, and *Terminalia superb*. Commercially obtained *Aspergillus niger* cellulase enzyme (0.1g) was dissolved in 0.005 $mol.dm^{-3}$ pH 5.0 tris buffer resulting in an enzyme solution concentration of 2.0 $mg.mL^{-1}$.

Delignification of Sawdust - Kraft Pulping and Hydrogen Peroxide Treatment of the Wood Sawdust

To ensure a maximum cellulose exposure to the cellulase enzyme the various sawdust materials were delignified by subjecting 2kg of each of the different sawdust materials (2.8-5.0 mm particle size) to 350g of NaOH and 140g NaS_2 during the Kraft pulping process. The Kraft pulping chemicals were dissolved in 8 L water and the delignification of the lignocellulosic materials (sawdust) was carried out in a rotary steel digester at 170°C and a pressure of 200 kPa for 1 h 45 min at cooking liquor to the wood ratio of 4:1. After the Kraft pretreatment, the extracted cellulose fibers were washed in turns with deionized water until they were free of the Kraft reagents (Ndukwe et al. 2009).

To remove residual lignin from these Kraft-treated cellulose all these sawdust materials (10 g) were treated with 30% hydrogen peroxide (60 mL) at 40°C for 25-30 min. The relatively small waste volumes of the Kraft and delignification process were kept in containers for further purification treatments.

Cellulase Incubation and Sugar Analyses

The delignified sawdust materials (10 mg) were transferred in triplicate in test tubes and incubated with the *A. niger* cellulase enzyme solution (200 ul) and Tris buffer solutions at pH-values varied between pH 4.0 and pH 7,0 (800 ul) for 2h at an incubation temperature of 50°C. The concentration of sugars released from the sawdust materials during cellulase-catalyzed degradation was determined from a standard glucose calibration curve constructed with glucose standard solutions at concentrations of 0.50 mg.mL^{-1}, 2.00 mg.mL^{-1}, 4.00 mg.mL^{-1}, 6.00 mg.mL^{-1} and 8.00 mg.mL^{-1}. The DNS method as described by Miller was used to calculate the concentration of the sugar produced during *A. niger* action on the waste sawdust (Miller 1959).

Calculation of Resultant Amount of Sugar Produced and Percentage Saccharification

The resultant amount of sugar produced from the delignified and non-delignified sawdust was calculated by subtracting the amount of sugar released from each type of sawdust in the absence of cellulase action from the amount of sugar released when the sawdust was treated with the cellulase enzyme. This amount of sugar known as the resultant amount of sugar was released because of the cellulase action on each type of sawdust material.

The percentage saccharification of each sawdust material was calculated by dividing the resultant mass of sugars produced through cellulase action by the total mass of the sawdust incubated multiplied by a hundred. These values indicate to what extent the sawdust was bio-converted into sugars and can also be used to conclude the relative saccharification of the various sawdust materials.

Statistical Analysis

All the experimental analyses were performed in triplicate, and the mean values with standard deviations were determined with Microsoft Excel.

RESULTS AND DISCUSSION

A major environmental problem facing cities and towns in Nigeria, especially along the Lagos Lagoon is the improper disposal of waste generated daily by activities of sawmills. Waste production relates to living and cannot be avoided, and such is the continuous production of sawdust by sawmills in the Lagos Lagoon area with an estimated number of 2000 sawmills (Sibiya et al. 2020). The abandonment of sawdust at the sawmills causes aesthetic problems as well as air pollution resulting in respiratory problems for many humans similar is the open-air combustion of sawdust which causes the release of carbon dioxide, smoke as well as NOx and the loss of potential useful energy into the environment. The indiscriminate incineration of sawdust is also responsible for producing greenhouse gases (Oluoti et al. 2014). With most sawdust management procedures resulting in negative environmental effects, it is important to consider environmentally benign management procedures

Fig. 1: Effect of changing pH-value on the degradation of delignified sawdust from *Erythropleum suaveolens* by *A. niger* cellulase.

and such an action could be the enzymatically catalyzed bioconversion of the cellulose component of sawdust into glucose a fermentable sugar that could be further developed as a feedstock for the synthesis of bioproducts such as bioethanol. The pH value at which the cellulase enzyme acts on sawdust is one of the catalytic variables which must be optimized during the saccharification with *A. niger* cellulase enzyme and the degradation of the delignified as well sawdust was performed at pH-values ranging between pH 4.0 to pH 7.0.

Fig. 1 represents the effect of changing pH values on the degradation of delignified sawdust from *Erythropleum*

suaveolens. The optimum pH for cellulase action was observed at pH 5.0 which showed the highest sugar production of 3.9 mg.mL^{-1} and a 39% saccharification. The lowest sugar production was obtained at pH 6.0 resulting in a concentration of 1.5 mg.mL^{-1} and a 15% saccharification while the highest amount of sugar produced at pH 5.0 was 2.6 times higher than the lowest amount of sugar produced. The saccharification of delignified cellulose from *Symphona globulifera* is illustrated in Fig. 2 showing optimum sugar production at a pH-value of 6.0 which is less acidic than the optimum pH-value of 5.0 that was observed during the maximum degradation of cellulose from *Erythropleum suaveolens*.

Fig. 2: Effect of changing pH-value on the degradation of delignified sawdust from *Symphonia globulifera* by *A. niger* cellulase.

Fig. 3: Effect of changing pH-value on the degradation of delignified sawdust from *Ricindendron heudelotii* by *A. niger* cellulase.
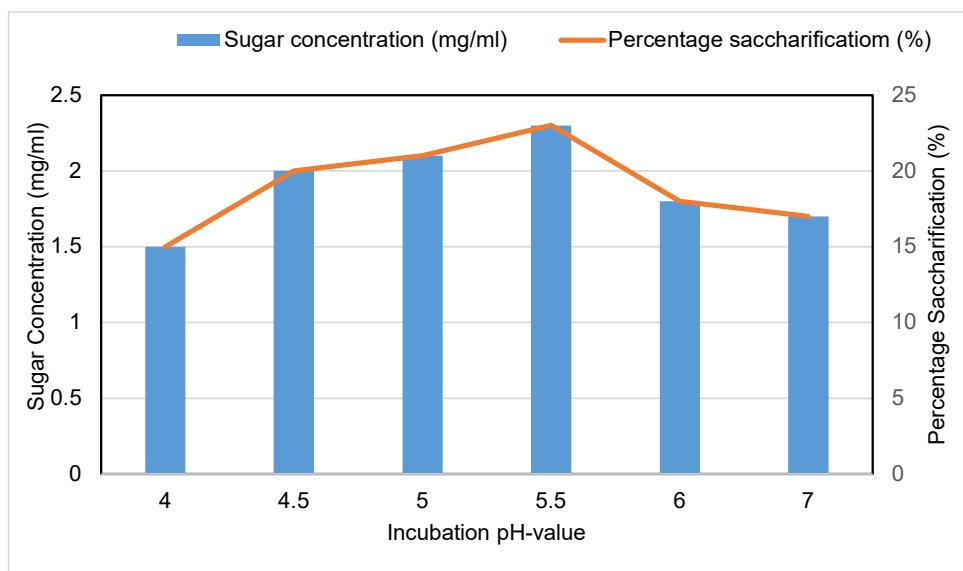
Fig. 4: Effect of changing pH-value on the degradation of delignified sawdust from *Pterygota macrocarpa* by *A. niger* cellulase.

The maximum amount of sugar produced from this *Symphonia globulifera* cellulose was calculated at a concentration of 2.8 mg.mL^{-1} and a 28% saccharification. This sugar concentration was 2.2 times higher than the lowest amount of sugar produced at a concentration of 1.3 mg.mL^{-1} during the saccharification at pH 4.5. The percentage saccharification at this lowest degree of saccharification was 13% while the second highest amount of sugar production was observed at a pH value of 5.0 producing a sugar concentration of 2.3 mg.mL^{-1} and a 23% saccharification. Incubation of this cellulose at a pH value of 7,0 produced also a relatively high sugar amount at a concentration of 2.2 mg.mL^{-1} and a 22% saccharification.

The saccharification of delignified cellulose from *Ricindendron heudelotti* (Fig. 3) showed optimum degradation at pH-values between 5.0 and 6.0 with the maximum amount of sugar produced at a concentration of 3.5 mg.mL^{-1} produced at a pH value of 5.0 which decline to a value of 3.0 mg.mL^{-1} when this bio-polymer was degraded at pH 6.0. During this degradation process the corresponding percentage of degradation declined from 35% to 30% saccharification with the lowest degree of saccharification observed at the pH-values of 4.0, 4.5, and 7.0 producing sugars at concentrations between 2.2 and 2.4 mg.mL^{-1}. The maximum amount of sugar produced at pH 5.0 was 1.6 times higher than the lowest sugar concentration produced when degraded at a pH value of 4.0.

When delignified cellulose from *Pterygota macrocarpa* (Fig. 4) was bio-converted into glucose with cellulase from *A. niger* the maximum amount of sugar was produced at a concentration of 2.3 mg.mL^{-1} resulting in a 3% saccharification. This amount of sugar was 1.5 times higher than the lowest sugar concentration of 1.5 mg.mL^{-1} that was produced when the cellulose was degraded at a pH value of 4.0 causing a 15% saccharification. These results indicate that the delignified cellulose from this tree exhibits a relatively high susceptibility for degradation by the *A. niger* cellulase at all the pH values at which it was incubated. When *Milicia excelsa* cellulose (Fig. 5) was exposed to cellulase degradation the optimum degree of saccharification was obtained when the process was performed at a pH-value of 5.0 resulting in a sugar concentration of 3.0 mg.mL^{-1} (30% saccharification). The produced sugar concentration decreased gradually when the incubation pH value was increased to 7.0 when a sugar concentration of 2.0 mg.mL^{-1} was obtained at a saccharification of 20%. When the incubation pH value was decreased to a value of 4.0 the amount of sugar produced was also calculated at a concentration of 2.0 mg.mL^{-1} which was 1.5 times less than the maximum amount of sugar produced.

The cellulase-catalyzed degradation of delignified sawdust from *Ipomoea asarifolia* (Fig. 6) was optimally degraded at a pH value of 5.0 resulting in a sugar concentration of 3.7 mg.mL^{-1} and a 37% saccharification. The degree of saccharification decreased when saccharified at pH-values higher and lower than pH 5.0 with the minimum amount of sugar produced at a pH-value of 7.0 producing a sugar concentration of 1.5 mg.mL^{-1} and a 15% saccharification. This amount of sugar produced was 2.5 times less than the highest sugar concentration whilst the second lowest
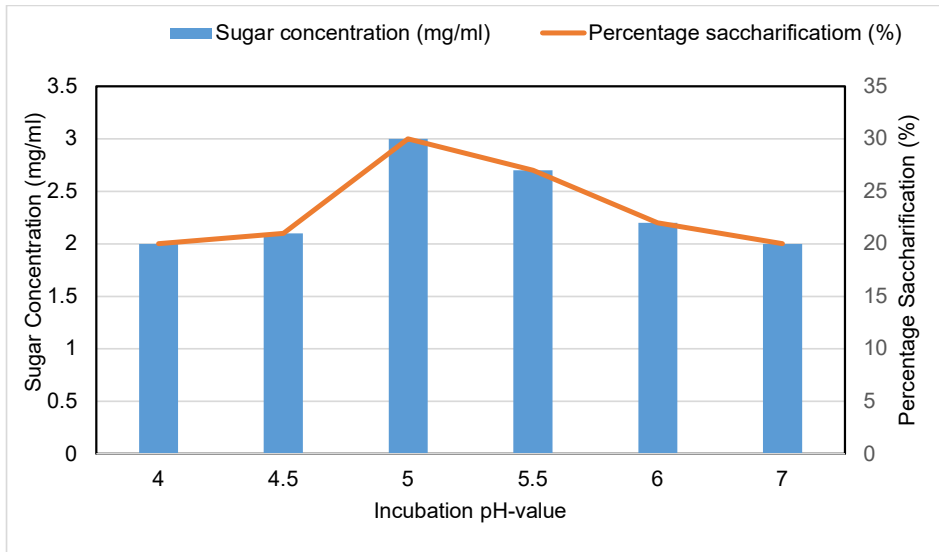
Fig. 5: Effect of changing pH-value on the degradation of delignified sawdust from *Milicia excels* by *A. niger* cellulase.
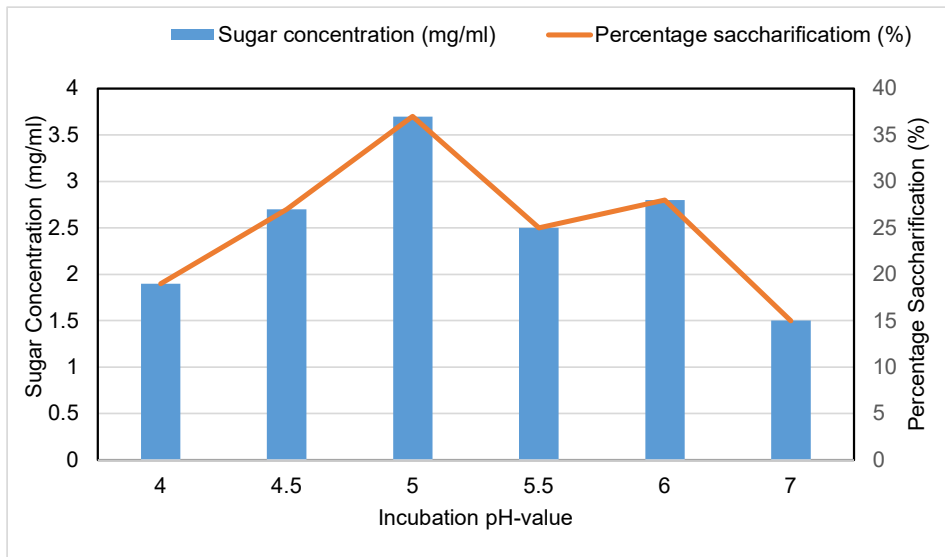
Fig. 6: Effect of changing pH-value on the degradation of delignified sawdust from *Ipomoea asarifolia* by *A. niger* cellulase.

sugar concentration was produced at 1.9 mg.mL^{-1} (19% saccharification) when the cellulase was acting on this sawdust at a pH-value of 4.0. The degradation of cellulose from *Hallea ciliate* with *A. niger* cellulase is illustrated in Fig. 7 showing a saccharification pattern at the different pH values that are different from that obtained during the saccharification of the other sawdust materials. Optimum degradation was obtained over a relatively broad pH range which varied from pH 4.5 to pH 6.0 resulting in a sugar concentration of 2.9 mg.mL^{-1} and a 29% saccharification. The lowest amount of sugar obtained at pH 4.0 and pH 7.0

was calculated at concentrations of 2.0 mg.mL^{-1} and 1.9 mg.mL^{-1}, respectively.

When delignified cellulose from *Sacoglottis gabonensis* was treated with *A. niger* cellulase an optimum sugar concentration of 4.4 mg.mL^{-1} was obtained when this bio-polymer was hydrolyzed at a pH value of 5.0 which resulted in a 44% saccharification (Fig. 8). At the higher pH values of 5.5 and 6.0, the amount of sugar produced decreased to concentrations of 3.3 mg.mL^{-1} and 2.2 mg.mL^{-1}, respectively. During the incubation at a pH value of 7.0, the delignified cellulose showed an increased susceptibility for
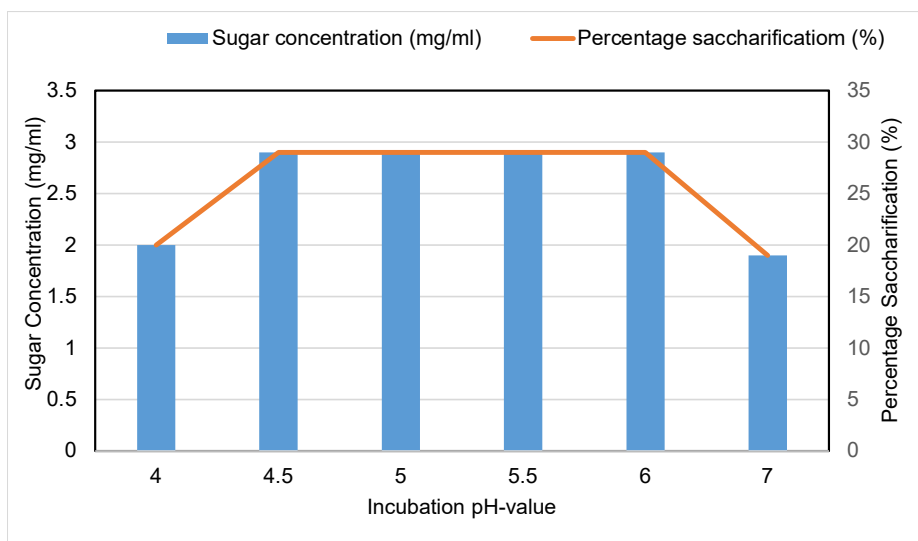
Fig. 7: Effect of changing pH-value on the degradation of delignified sawdust from *Hallea ciliate* by *A. niger* cellulase.
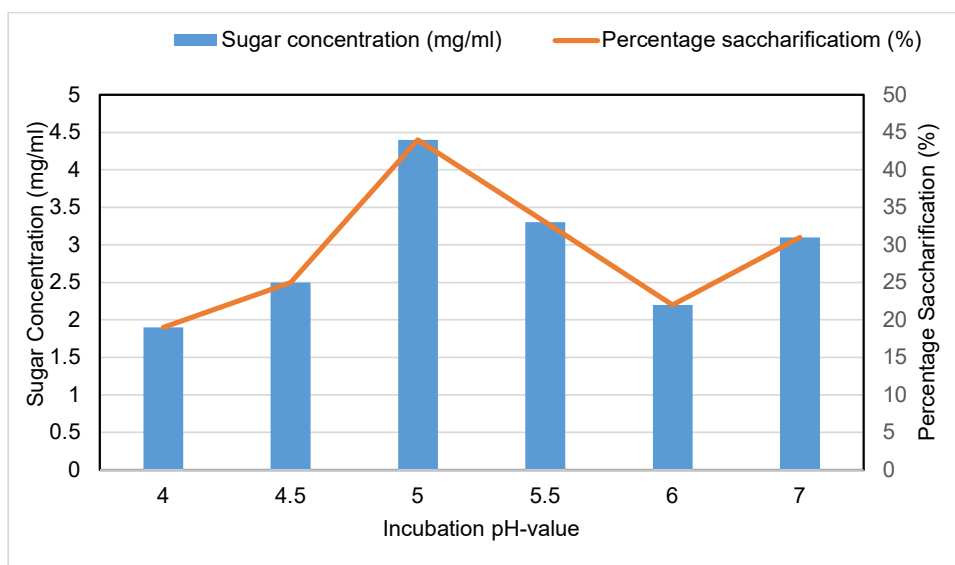
Fig. 8: Effect of changing pH-value on the degradation of delignified sawdust from *Sacoglottis gabonensis* by *A. niger* cellulase.

the cellulase enzyme that resulted in a sugar concentration of 3.1 mg.mL^{-1} (32% saccharification). At pH-values less than 5.0 the degradation of the cellulose component showed a lower degree of saccharification producing the lowest sugar concentration of 1.9 mg.mL^{-1} (19% saccharification) when hydrolyzed with the cellulase enzyme at pH 4.0. The highest amount of sugar produced at pH 5.0 was 2.4 times higher than the lowest degree of saccharification obtained at a pH value of 4.0.

Fig. 9 represents the effect of changing pH values on the degradation of delignified sawdust from *Pycnanthus*

angolensis. Optimum saccharification of this sawdust was obtained at two pH-values of pH 4.0 as well as at a pH value of 5.0 resulting in the formation of sugar at a concentration of 4.6 mg.mL^{-1} (46% saccharification). The lowest degree of saccharification was observed when the incubation was performed at a pH-value of 7,0 which resulted in a sugar concentration of 1.8 mg.mL^{-1} (18% saccharification) that was 2.5 times less than the highest amount of sugar produced. When delignified cellulose from *Terminalia superb* sawdust was degraded with the *A. niger* cellulase (Fig. 10) the amount of sugar produced showed an increased value from
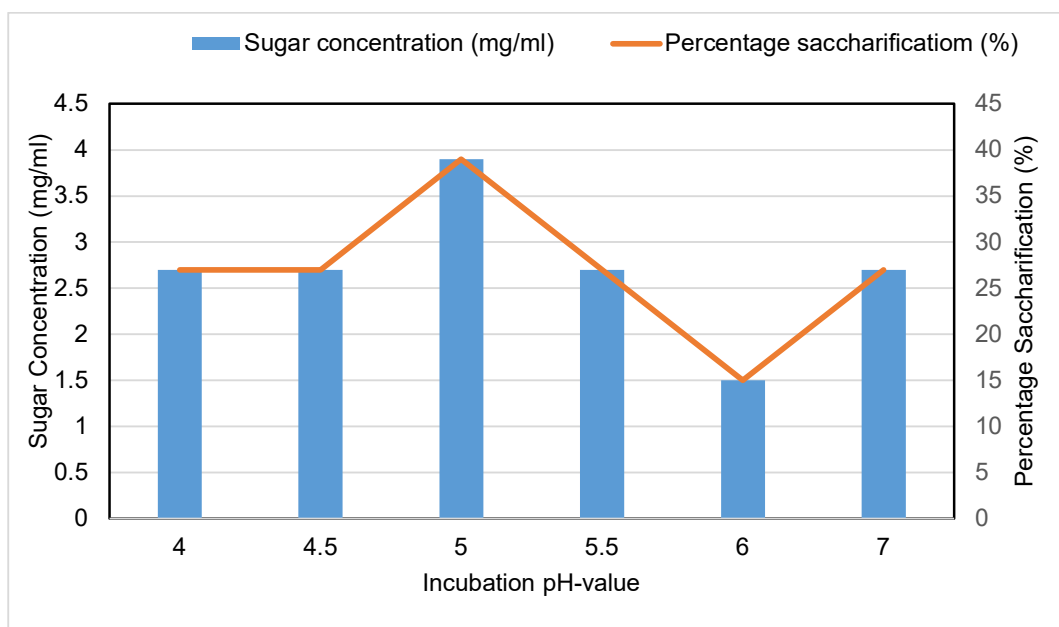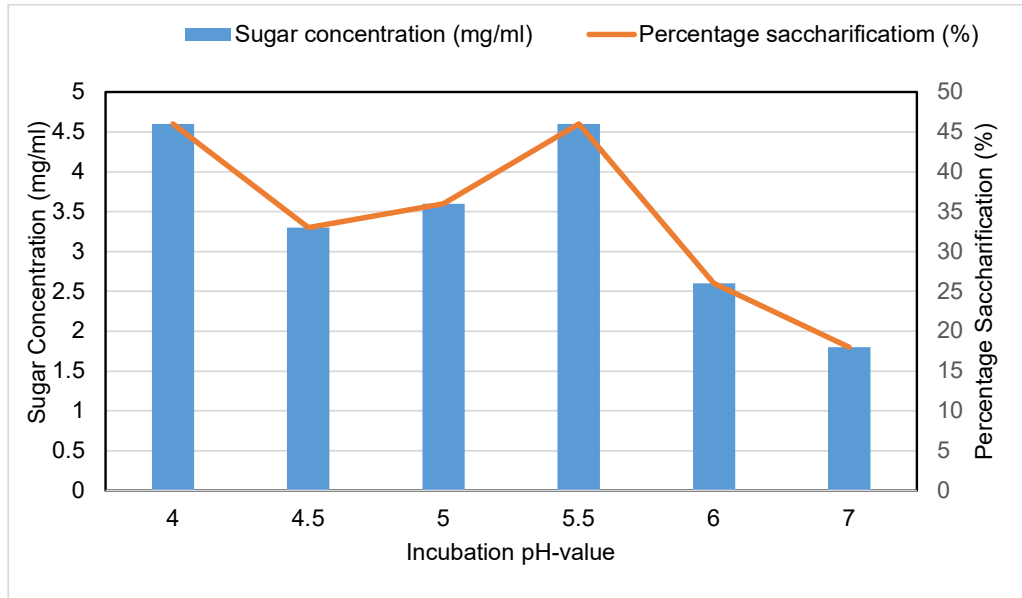
Fig. 9: Effect of changing pH-value on the degradation of delignified sawdust from *Pycnanthus angolensis* by *A. niger* cellulase.

2.4 mg.mL^{-1} when exposed to the enzyme at a pH-value of 4.0 to the maximum amount of sugar produced at a concentration of 3.1 mg.mL^{-1} when degraded at pH 5.5. When exposed to the enzyme at pH-values of 6.0 and 7.0 the amount of sugar produced decreased to values of 1.9 mg.mL^{-1} and 1.0 mg.mL^{-1}, respectively. The lowest amount of sugar produced was 3.1 times less than the highest amount of sugar released at a concentration of 3.1 mg.mL^{-1}.

The pH value at which an enzyme-catalyzed reaction is performed is an important catalytic variable that must be optimized to ensure maximum product formation while converting the reactant (cellulose) into products (sugars). Fig. 11 reflects the pH values at which optimum cellulase activity was obtained while bio-converting the sawdust from different trees along the Lagos Lagoon into sugars, mainly glucose. From these results, it can be concluded that

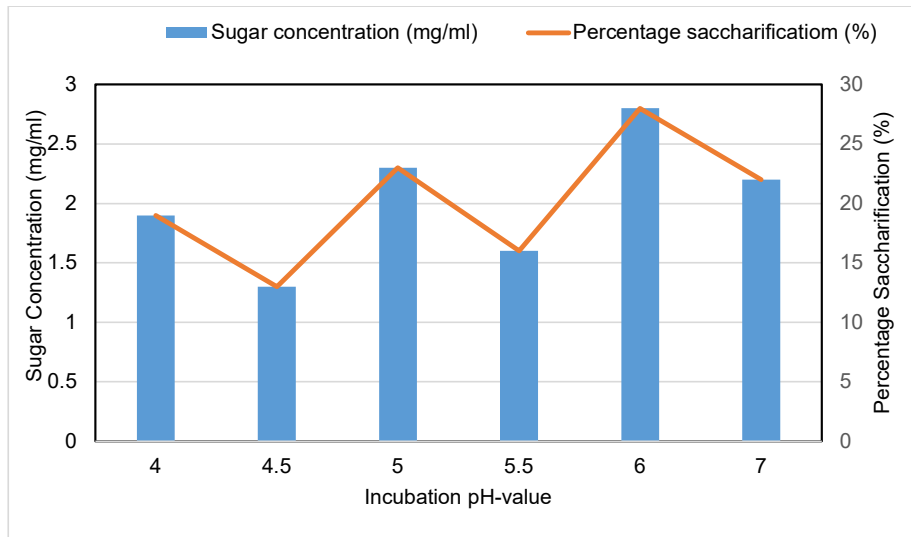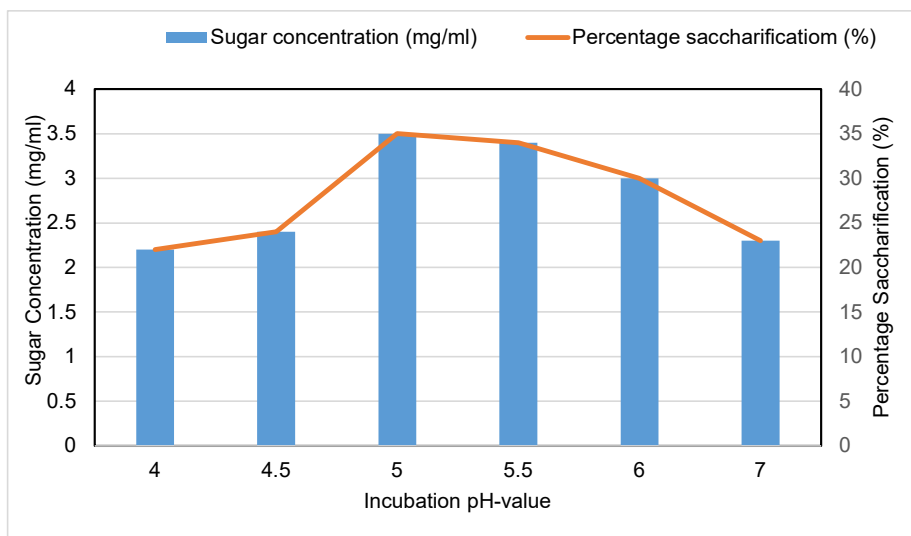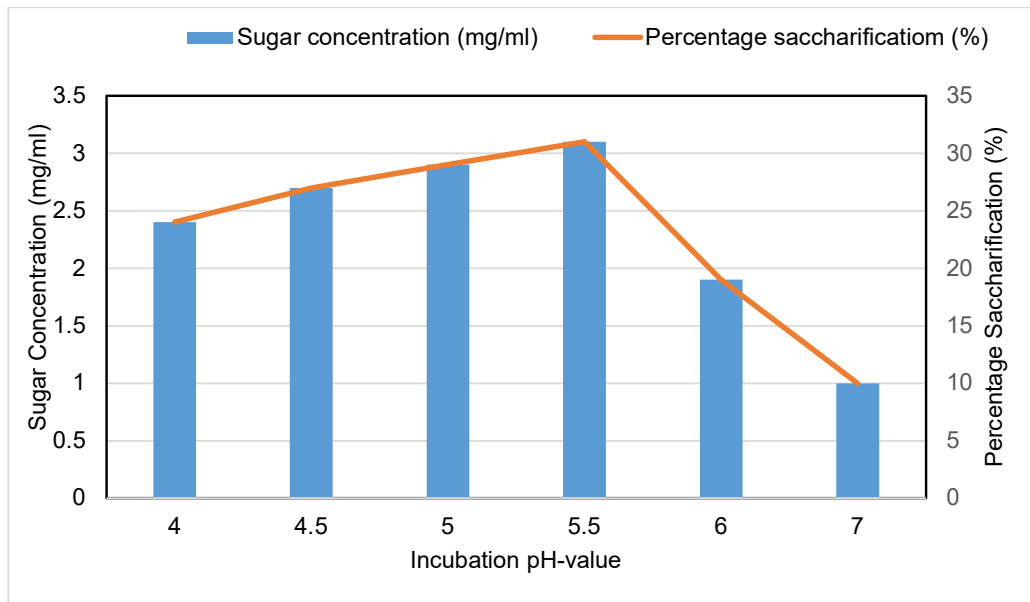Fig. 10: Effect of changing pH-value on the degradation of delignified sawdust from *Terminalia superb* by *A. niger* cellulase.
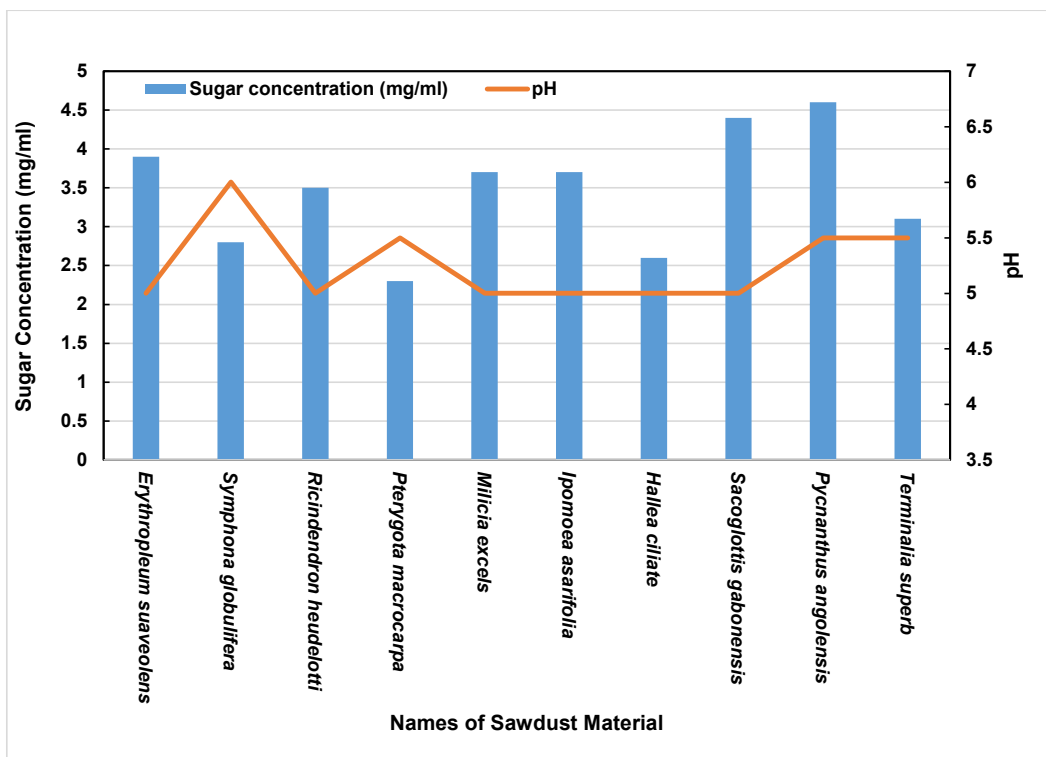
Fig. 11: Optimum pH values for maximum sugar production when sawdust from different trees along the Lagos Lagoon in Nigeria are saccharified with *A. niger* cellulase.

optimum saccharification for all the sawdust materials was obtained at pH values varying between pH 5.0 and pH 6.0 with the sugar concentration varying between 2.3 mg.mL^{-1} and 6 mg.mL^{-1}. These optimum pH values for the *A. niger* cellulase catalyzed degradation of delignified sawdust are like pH values for maximum degradation of agricultural waste at a pH 4.5 by cellulase from *Clostridium thermocellum* (Mutreja et al. 2011), filter paper with cellulase from *Phialophora sp. G5* (Zhao et al. 2012) at a pH value of 6.0,

degradation of carboxymethyl cellulose with cellulase from *Streptomyces argentomyces* at a pH-value of 5.0 (Ventorino et al. 2016) and the optimum activity of cellulase from *Trichoderma reesei* when hydrolyzing the B-D-glycosidic bond in p-nitrophenyl-B-D-cellobioside at a pH-value of 5.5 (He et al. 2019).

The difference in the amount of sugar released from the sawdust materials is an indication of the varying degree of susceptibility of these delignified materials for the *A. niger* cellulase enzyme. Sawdust is a major waste product of the forestry industry, and its cellulose component exhibits a strong potential for degradation into glucose a fermentable sugar that could be used as a feedstock for the synthesis of bioproducts such as bio-ethanol (Vasic et al. 2021). Delignification has been proven to be an effective

pretreatment procedure for wood materials rendering the cellulose component more susceptible to cellulase-catalyzed degradation and the positive effect of this pretreatment of sawdust is well documented (Suryadi et al. 2022). Several structural features of cellulose such as the crystallinity (Park et al. 2010) as well as the amorphous parts (Ruel et al. 2012) influence the degree of cellulose bioconversion as the interaction between cellulose and the cellulase enzyme is dependent on the relative presence of each of these sections in the cellulose molecule. The crystalline section is less susceptible for cellulase degradation although certain components of the cellulase enzyme are aimed to degrade this part of cellulose whilst the amorphous section is more available for cellulase action in general. Delignification aims to destroy the interaction between lignin and cellulose thus rendering cellulose more available for cellulase action by exposing the various sections for attack and action by the cellulase enzyme.

Since delignification results in an increased degree of cellulase-catalyzed degradation of cellulose, the current investigation was performed on delignified sawdust from different trees determining how different incubation pH-values could affect the saccharification of the different sawdust materials when degraded with *A. niger* cellulase.

CONCLUSIONS

Environmental pollution, fossil fuel combustion, and the development of alternative and renewable energy resources are currently topical global issues. The accumulation of solid waste does not only occupy valuable land, but gases released during the fermentation of the organic part of organic solid waste have a negative effect on humans and animals. Simultaneously are gases released during the combustion of fossil fuels described as dangerous to the environment and evidence of this phenomenon is climate change already experienced by many communities. A possible solution to both these two environmental issues could be the development of waste cellulose as a renewable feedstock for the synthesis of bioproducts. In this respect sawdust could be a suitable organic waste material and the development of sawdust would not only assist in limiting the accumulation of solid waste but can also limit the dependence on fossil fuels. When subjected to cellulase-catalyzed saccharification it would be important to optimize the catalytic properties such as the pH value ensuring maximum degradation of organic waste material such as sawdust. For maximum degradation of different waste cellulose materials, it is thus important that the optimum pH value for degradation of each type of organic waste material be determined before performing a large-scale bioconversion into fermentable sugars.

REFERENCES

Abolore, R.S., Jaiswal, S. and Jaiswal, A.K., 2024. Green and sustainable pretreatment methods for cellulose extraction from lignocellulosic biomass and its applications: A review. *Carbohydrate Polymer Technologies and Applications*, 7, p.100396. https://doi.org/10.1016/j.carpta.2023.100396.

Amaefule, D., Nwakaire, J., Ogbuagu, N., Anyadike, C., Ogenyi, C., Ohagwu, C. and Egbuhuzor, O., 2023. Effect of production factors on the bioethanol yield of tropical sawdust. *International Journal of Energy Research*, Article ID 9983840. https://doi.org/10.1155/2023/9983840.

Babu, S., Rathore, S.S., Singh, R., Kumar, S., Singh, V.L., Yadav, S.K., Yadav, V., Raj, R., Yadav, D., Shekhawat, K. and Wani, O.A., 2022. Exploring agricultural waste biomass for energy, food and feed production and pollution mitigation: A review. *Bioresource Technology*, 360, p.127566. https://doi.org/10.1016/j.biortech.2022.127566.

Chikri, R., Elhadiri, N., Benchanaa, M. and Elmaguana, Y., 2020. Efficiency of sawdust as low-cost adsorbent for dyes removal. *Journal of Chemistry*, Article ID 8813420. https://doi.org/10.1155/2020/8813420.

De Paula, R.G., Antoniêto, A.C.C., Ribeiro, L.F.C., Carraro, C.B., Nogueira, K.M.V., Lopes, D.C.V., Silva, A.C., Zerbini, M.T., Pedersoli, W.R., Costa, M.N. and Silva, R.N., 2018. New genomic approaches to enhance biomass degradation by the industrial fungus *Trichoderma reesei*. *International Journal of Genomics*, Article ID 1974151. https://doi.org/10.1155/2018/1974151.

Faremi, O.E., Sogbanmu, T.O. and Adeyemo, O.K., 2021. How sawmill wastes impact surface water, sediment, macrobenthic invertebrates, and fish: a case study of the Lagos lagoon, Okobaba Area, South-western Nigeria. *Environmental Monitoring and Assessment*, 193, p.235. https://doi.org/10.1007/s10661-021-09006-0.

Giwa, A.A., Abdulsalam, K.A., Wewers, F. and Oladipo, M.A., 2016.

Biosorption of Acid Dye in Single and Multidye Systems onto Sawdust of Locust Bean (*Parkia biglobosa*) Tree. *Journal of Chemistry*, Article ID 6436039. https://doi.org/10.1155/2016/6436039.

He, R., Ding, R., Heyman, J.A., Zhang, D. and Tu, R., 2019. Ultra-high-throughput picoliter-droplet microfluidics screening of the industrial cellulase-producing filamentous fungus *Trichoderma reesei*. *Journal of Industrial Microbiology and Biotechnology*, 46, pp.1603-1610. https://doi.org/10.1007/s10295-019-02221-2.

Ja'afaru, M.I., 2013. Screening of fungi isolated from environmental samples for xylanase and cellulase production. *International Scholarly Research Notices*, Article ID 283423. https://doi.org/10.1155/2013/283423.

Janakiram, J. and Sridevi, K., 2010. Conversion of waste into wealth: a study in solid waste management. *Journal of Chemistry*, Article ID 549185. https://doi.org/10.1155/2010/549185.

Kurian, J.K., Gariepy, Y., Lefsrud, M., Orsat, V., Seguin, P., Yaylayan, V. and Raghavan, G.S.V., 2014. Experimental study on calcium hydroxide-assisted delignification of hydrothermally treated sweet sorghum bagasse. *International Journal of Chemical Engineering*, Article ID 684296. https://doi.org/10.1155/2014/684296.

Lak, O.Z., Rezaei, J. and Rahimpour, M.R., 2024. Health and pollution challenges of fossil fuels utilization. In: *Reference Module in Earth Systems and Environmental Sciences*, Elsevier, ISBN 9780124095489. https://doi.org/10.1016/B978-0-323-93940-9.00202-4.

Lee, C.K., Darah, I. and Ibrahim, C.O., 2011. Production and optimization of cellulase enzyme using *Aspergillus niger* USM AI 1 and comparison with *Trichoderma reesei* via solid state fermentation system. *Biotechnology Research International*, Article ID 658493. https://doi.org/10.4061/2011/658493.

Li, X., Tian, Y., Li, Y., Xu, C., Liu, X. and Cheng, B., 2021. Modeling the impact of innovation on economic quality and environmental pollution change under consideration of environmental regulation. *Discrete Dynamics in Nature and Society*, Article ID 3800678. https://doi.org/10.1155/2021/3800678.

Miller, G.L., 1959. Use of dinitrosalicylic acid reagent for determination of reducing sugar. *Analytical Chemistry*, 31, pp.426-428.

Mokatse, K.M. and Van Wyk, J.P.H., 2021. Successive saccharification of waste paper as a resource for bio-product development. *Nature Environment and Pollution Technology*, 20(3), pp.1301-1308. https://doi.org/10.46488/NEPT.2021.v20i03.042.

Mutreja, R., Das, D., Goyal, D. and Goyal, A., 2011. Bioconversion of agricultural waste to ethanol by ssf using recombinant cellulase from *Clostridium thermocellum*. *Enzyme Research*, Article ID 340279. https://doi.org/10.4061/2011/340279.

Ndukwe, N.A., Jenmi, W.O., Okiei, W.O. and Alo, B., 2009. Comparative study of percentage yield of pulp from various Nigerian wood species using the kraft process. *African Journal of Environmental Science and Technology*, 3(1), pp.21-25.

Okino, J., Komakech, A.J., Wanyama, J., Ssegane, H., Olomo, E. and Omara, T., 2021. Performance Characteristics of a Cooking Stove Improved with Sawdust as an Insulation Material. *Journal of Renewable Energy*, Article ID 9969806. https://doi.org/10.1155/2021/9969806.

Oluoti, K., Megwai, G., Pettersson, A. and Richards, T., 2014. Nigerian wood waste: a dependable and renewable fuel option for power production. *World Journal of Engineering and Technology*, 2, pp.234-248.

Paritosh, K., Sandeep, K., Kushwaha, K., Yadav, M., Pareek, N., Chawade, A. and Vivekanand, V., 2017. Food waste to energy: an overview of sustainable approaches for food waste management and nutrient recycling. *BioMed Research International*, Article ID 2370927. https://doi.org/10.1155/2017/2370927.

Park, S., Baker, J.O., Himmel, M.E., Parilla, P.A. and Johnson, D.K., 2010. Cellulose crystallinity index: measurement techniques and their impact on interpreting cellulase performance. *Biotechnology for Biofuels*, 3(10). https://doi.org/10.1186/1754-6834-3-10.

Ruel, K., Nishiyama, Y. and Joseleau, J.-P., 2012. Crystalline and amorphous cellulose in the secondary walls of *Arabidopsis*. *Plant Sciences*, 193–194, pp.48–61.

Sartori, T., Tibolla, H., Prigol, E., Colla, L.M., Costa, J.A.V. and Bertolin, T.E., 2015. Enzymatic saccharification of lignocellulosic residues by cellulases obtained from solid state fermentation using *Trichoderma viride*. *BioMed Research International*, Article ID 342716. https://doi.org/10.1155/2015/342716.

Sethi, S., Datta, A., Gupta, B.A. and Gupta, S., 2013. Optimization of cellulase production from bacteria isolated from soil. *International Scholarly Research Notices*, Article ID 985685. https://doi.org/10.5402/2013/985685.

Sibiya, J.B.M., Ndukwe, N. and Van Wyk, J.P.H., 2020. Saccharification of sawdust masses from the Lagos Lagoon in Nigeria with *Aspergillus niger* cellulase. *Pharmaceutical and Biosciences Journal*, 8(6), pp.24-32. https://doi.org/10.20510/ukjpb/8/i6/1607002257.

Suryadi, H., Judono, J.J., Putri, M.R., Eclessia, A.D., Ulhaq, J.M., Agustina, D.N. and Sumiati, T., 2022. Biodelignification of lignocellulose using ligninolytic enzymes from white-rot fungi. *Heliyon*, 8(2), p.e08865. https://doi.org/10.1016/j.heliyon.2022.e08865.

Vasić, K., Knez, Z. and Leitgeb, M., 2021. Bioethanol production by enzymatic hydrolysis from different lignocellulosic sources. *Molecules*, 26(3), p.753. https://doi.org/10.3390/molecules26030753.

Ventorino, V., Ionata, E., Birolo, L., Montella, S., Marcolongo, L., de Chiaro, A., Espresso, F., Faraco, V. and Pepe, O., 2016. Lignocellulose-adapted endo-cellulase producing streptomyces strains for bioconversion of cellulose-based materials. *Frontiers in Microbiology*, 7, p.2061. https://doi.org/10.3389/fmicb.2016.02061.

Verma, N. and Kumar, V., 2022. Influence of sugars, sugar alcohols and their combinations on environmentally significant cellulase production under liquid state fermentation. *Nature Environment and Pollution Technology*, 21(1), pp.127-139. https://doi.org/10.46488/NEPT.2022.v21i01.014.

Zeleke, Y. and Rotich, G.K., 2021. Design and development of false ceiling board using polyvinyl acetate (pvac) composite reinforced with false banana fibres and filled with sawdust. *International Journal of Polymer Science*, Article ID 5542329. https://doi.org/10.1155/2021/5542329.

Zhao, J., Shi, P., Li, Z., Yang, P., Luo, H., Bai, Y., Wang, Y. and Yao, B., 2012. Two neutral thermostable cellulases from *Phialophora* sp. G5 act synergistically in the hydrolysis of filter paper. *Bioresource Technology*, 122, pp.404-410.

Conversion of Citrus Fruit Peel into a Value-Added Product, Bio-Oil

M. Subathra [ID] **and R. Devika†** [ID]

Department of Biotechnology, Aarupadai Veedu Institute of Technology, Vinayaka Mission's Research Foundation (Deemed to be University), Vinayaka Nagar, Old Mahabalipuram Road, Paiyanoor-603104, Tamil Nadu, India
†Corresponding author: R. Devika; subu110494@gmail.com

ABSTRACT

The present study aimed to investigate the bio-oil from the blended citrus fruit peel by hydrothermal liquefaction process. Huge amounts of fruit peel waste are disposed of in the open environment without any proper management. Such fruit peels are considered a potential bio-resource to be converted into economically valuable products like bio-oil. Since the citrus fruit peel is a rich source of moisture content, a hydrothermal liquefaction process was introduced to produce bio-oil from cellulose, and lignocellulose. The experimental design against temperature, time, and biomass concentration optimization was carried out which was confirmed by the ANOVA f and p test that reveals time and temperature influenced the bio-oil yield drastically. As the time and temperature rise more than 60 min and 280°C, the volatile substance present in the biomass converts itself into solid residue which has a negative impact on bio-oil production, compared with biomass concentration. The maximum yield of bio-oil was recorded as 29.4% at 280°C at 60min reaction time and 80g/200mL concentration as optimized parameters. The GCMS reveals the presence of hydrocarbons and alkanethiol which are flammable and hold the standards of commercial transportation fuel but hold nitrogen and oxygen-containing compounds to pull down the fuel standards. Thus, the produced bio-oil can be blended with the transportation fuel after the upgradation process for efficient results.

INTRODUCTION

Increases in population and waste generation are two interrelated things that are directly proportional to each other (Supangkat & Herdiansyah 2020). Statistical data reveals that the waste generation in the world will rise to 73% by 2050 (The World Bank 2024). As the waste generation increases, to ensure a clean environment the generated waste has to be managed efficiently in a traditional manner to discard waste in a bare land named landfills which may cause various hindrances to mankind and the surrounding ecosystem. Landfills can cause air pollution by releasing a high amount of greenhouse gas into the environment resulting in global warming, and water pollution by discarding the heavy metals into the ground water which results in various health issues. This also pollutes the soil and makes the land unfit causing communicable diseases, eye infections, skin infections, dust allergies, gastrointestinal tract infections, etc. in the nearby population (Parvin & Tareq 2021, Siddiqua et al. 2022). However, waste management awareness among the common man, the 3R concept is booming and reducing the percentage of landfill usage for waste disposal. But a wiser way of utilizing the waste is to convert it into value-added products like bio-oil, biomaterials, and biochemicals, which must be opted for by the population to decrease and efficiently utilize the waste (Bharathiraja et al. 2017, Sadh et al. 2018). Some of the popular methods used in current days to convert waste are thermochemical conversion and biochemical conversion methods (Nanda et al. 2013, Aboagye et al. 2017, Kim et al. 2015). In this study thermal method of treatment has been chosen. Though the thermal method includes various techniques like pyrolysis, gasification, hydrothermal process, etc. hydrothermal

process is been used here since the waste utilized under this method does not need a pretreatment process, thereby saving energy and time consumption.

The waste chosen for treatment here is citrus fruit peel, a lignocellulose waste that has a production rate of 180 billion tons every year globally. Such waste can be efficiently converted into value-added products by the hydrothermal liquefaction process since the process holds several advantages in treating wet biomass, using low temperatures, and reducing energy consumption (Vo et al. 2016). The hydrothermal liquefaction process is well-studied for processing feedstocks from lignocelluloses wet waste which leads to oil products in a mixture of hydrocarbons (gasoline/ jet/ diesel range) (Snowden-Swan et al. 2017). The Hydrothermal Liquefaction process also undergoes a significant thermodynamic change (supercritical phase) at high temperature (200-350°C) and pressure up to 25 MPa for wet biomass which leads to weakening and ionization of H bonds into hydronium (CHO) and hydroxide (OH-) ions (Beims et al. 2020). Hydrothermal Liquefaction influences acid-catalyzed hydrolysis and degradation leading to the breaking down and reforming of biomass to cellulose, hemicellulose, lignin, and ultimately to bio-crude with the higher energy content of 30-35 MJ/kg (Ruiz et al. 2013). Malins et al. (2015) demonstrated the effect of different catalysts in the efficient production of biocrude from sludge and Vardon et al. (2011) carried out Hydrothermal Liquefaction processes with sludge, manure, and algae anaerobically and analyzed various parameters of biocrude. The investigation carried out by Hariram et al. (2023) also utilized avocado fruit seed to extract bio-oil by trans-esterification process. Lignocellulose waste is the major contributor of cellulose, hemicellulose, lignin, and pectin that contribute to producing value-added products by break down mechanism of biomolecules by hydrothermal liquefaction process at temperature ranges from 200°C-450°C and pressure ranges from 5-20 MPa (Baruah et al. 2018, Dimitriadis & Stella 2017). The optimum parameters like temperature, the concentration of biomass, and time were experimentally studied to produce the bio-oil. Gas Chromatography and Mass Spectrometry) GCMS and physicochemical proximate analysis methods were used to analyze the bio-oil. Thus, this research aims to provide a basic understanding of the effect of the Hydrothermal Liquefaction process on the citrus fruit peel in producing the bio-oil.

MATERIALS AND METHODS

Sample Collection

The citrus fruit peel was collected from the canteen of "Aarupadai Veedu Institute of Technology, Chennai". The collected biomass (orange peel lemon peel and sweet lime peel) was made into coarse powder. This fresh sample consists of 78% of moisture content. This also contains 87.4% carbon, 11.2% of nitrogen, 1.1% of hydrogen, and 30.9% of oxygen.

Hydrothermal Liquefaction Process

The hydrothermal liquefaction process was carried out in a thermal autoclave reactor of a capacity of 5 L with an operating temperature of 350°C and a heating rate of 10°C/min. The biomass was loaded in the desired volume to the reactor vessel along with distilled water as solvent. The holding time of the reaction was set as 1 hour with 700 rpm as the speed of rotation. The layer separation method was used for extracting the bio-oil using hexane as solvent. An equal volume of hexane solvent was added to the bio-oil in a separating funnel for the separation of the organic layer from the residue. The bio-oil was further purified by a rotary vacuum evaporator from which the organic layer was separated using a distillation process. The same conditions were repeated in triplets to minimize the error. The bio-oil yield was calculated by weighing the weight of the bio-oil against the weight of the biomass taken for the hydrothermal liquefaction process.

Design of experiment (DOE)

The optimization study was carried out and verified by using the ANOVA p-test. The experiment was carried out with 3 optimizing parameters – temperature (210°C, 220°C, 240°C, 260°C, 280°C, 300°C and 310°C), time (50 min, 60 min, 120 min and 130 min) and biomass concentration (10 g/200mL, 20 g/200mL, 40 g/200mL, 50 g/200mL, 60 g/200mL, 80 g/200mL, 100 g/200mL, 110 g/200mL). The ANOVA p-test analysis was used to confirm the effect of 3 variables on the yield and experimental fitness after 16 runs of the experiment listed in Table 1.

Bio-oil Characterization

The bio-oil produced was characterized by GCMS and property analysis, to find the compounds present in it and ensure the efficiency of the bio-oil. GCMS analyses the compounds present in the bio-oil produced from citrus fruit peel (orange peel, lemon peel, and sweet lime peel). The chromatography utilized here was Agilent 7890 GC outfitted with an Agilent 7683B auto-injector, an HP-5 section, and a flame ionization detector. Helium gas served as a carrier with a flow rate of 1 mL/min and an inlet temperature of 250°C. The start temperature of the detector starts from 50°C per 2 min and rises by 10°C/min. The electron input and scan range were found to be 70eV and 35-335 amu. Property analysis was carried out to find the kinematic viscosity, calorific

value, density, and TAN (Total Acid Number) number to find the efficiency of the bio-oil.

RESULTS AND DISCUSSION

Effect of Parameters on Hydrothermal Liquefaction Process

The effect of the parameters on bio-oil yield was analyzed (Table 1). The bio-oil production was found to increase as the temperature rose from 200°C to 260°C and started to decrease as the temperature rose further to 300°C. From the above analysis, the optimum temperature for thermal liquefaction was found to be 280°C (Fig. 1). The same protocol was implemented to optimize the time. 4 different timings were taken for the process namely – 50 min, 60 min, 120 min, and 130 min. The maximum yield was recorded at 60 min. The above analysis infers, that the optimum time for the best conversion of citrus peel into bio-oil was recorded as 60 min (Fig. 2). To optimize the concentration, the same process was carried out with 20 g/200mL, 40 g/200mL,

Table 1: Design of the experiment.

Experimental run	Variables			Response
	Temperature (°C)	Time (min)	Biomass concentration (g/200mL)	Bio-oil Yield %
1	220	60	20	18.2
2	240	60	40	21.8
3	260	60	60	26.7
4	280	60	80	29.4
5	300	60	100	29.2
6	220	120	20	12.3
7	240	120	40	15
8	260	120	60	16.1
9	280	120	80	19.7
10	300	120	100	21
11	210	50	110	23
12	210	50	10	10.3
13	210	50	50	13.5
14	310	130	110	21.6
15	310	130	10	2
16	310	130	50	4.7
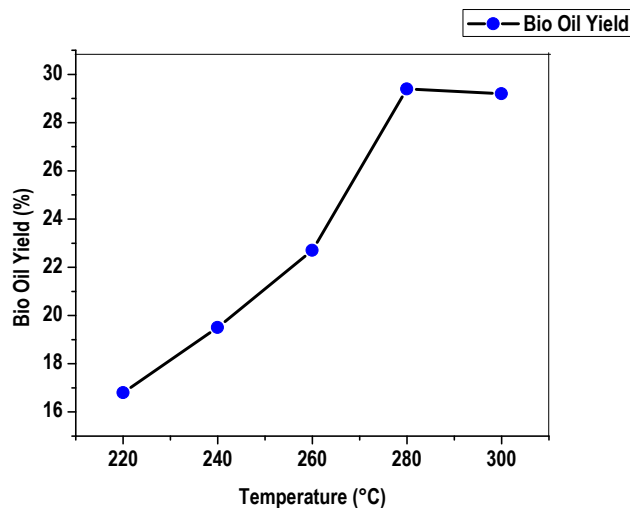
Fig. 1: Mean value of response with temperature.
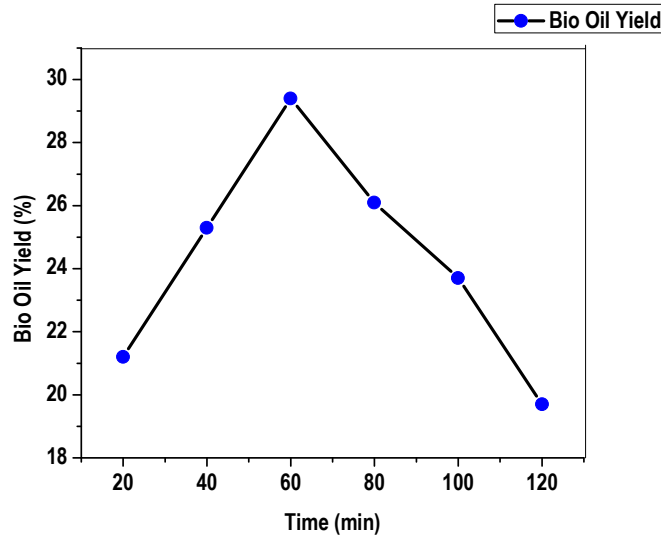
Fig. 2: Mean value of response with time.
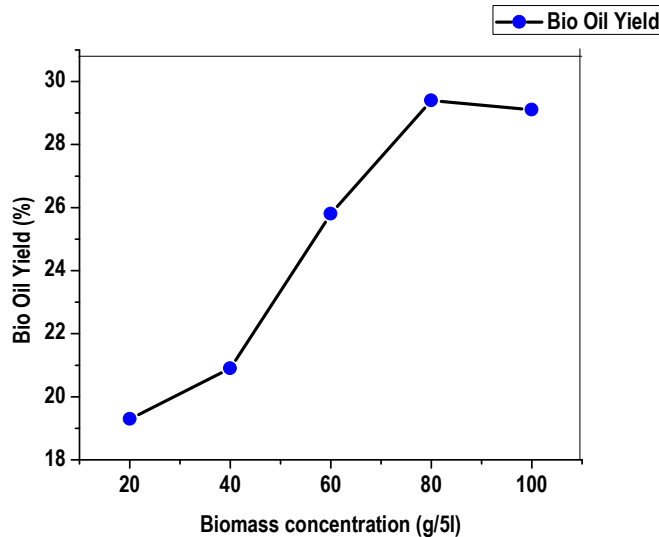
Fig. 3: Mean value of response with biomass concentration.

50 g/200mL, 60 g/200mL, 80 g/200mL, 100 g/200mL, and 110 g/200mL. Among the different concentrations, 80 g/200mL recorded the highest yield of bio-oil and was noted as an optimized concentration (Fig. 3). Thus at 280°C, 60 min, and 80 g/200mL concentration the yield of bio-oil was recorded as 29.4 yield %. Along with bio-oil, biochar was obtained as the by-product which can be used as a bio-fertilizer. Orange peel requires 275°C for effective conversion of biomass into bio-oil due to the presence of elemental carbon (Biller & Ross 2011, Dandamudi et al. 2019, Reddy et al. 2016). The yield recorded by microalgae was found to be higher than the citrus peel biomass due to the presence of lipid content in the microalgae that enhances oil

production at greater temperatures. However, the citrus peel produces the bio-oil at a lesser reaction temperature since the biomass is a rich source of lignocellulose, cellulose, and lignin. On further increasing the temperature, the gasification process is favored and increases the biochar yield. Thus, low temperatures are best suited for lignocellulose-rich biomass for bio-oil production (Mohan et al. 2006). The maximum yield range of biocrude was recorded between 25 to 28% at a temperature of 200 to 275°C and minimum biocrude yield was obtained between 4.4 to 9.5% at a temperature of 275°C, respectively in hydrothermal liquefaction process with orange peel as biomass (Divyabharathi & Subramanian 2021). High volatile matter present in the citrus peel promotes

bio-oil production and less lignin content reduces the biochar yield out of the hydrothermal liquefaction process (Divyabharathi & Subramanian 2021).

ANOVA Evaluation For the Response of Bio-Oil

ANOVA evaluation recorded for the response of bio-oil reveals in Table 2, that the temperature and the reaction time of the hydrothermal liquefaction process significantly affect the bio-oil yield compared with the concentration of the biomass. As the temperature rises, the bio-oil yield also increases significantly till 280°C and slightly falls, on further rise in temperature. The same rise in bio-oil yield was observed when the temperature rose to 60min but, tend to fall further doubling the reaction time. The reason for a fall in the bio-oil yield in the above two parameters is the presence of higher volatile matter that gets converted into solid residue at increased temperature and at prolonged periods of reaction time. Thus, the model is significant and found to fit with both temperature and time. On the other hand, concentration has having lesser impact on bio-oil yield when compared to temperature and time. When the concentration is maintained constant on increasing temperature and time, the conversion rate of the biomass increases until the optimal parameter (280°C and 60 min) and starts to decrease on a further rise. Higher temperature enhances biomass cracking and promotes the hydrolysis process resulting in the production of lower-weight compounds (Changi et al. 2015). Further processes such as decarboxylation, dehydration, and repolymerization in the hydrothermal liquefaction process result in the formation of various intermediate and by-products (Wang et al. 2018). Improved biomass conversion was recorded at increased reaction time during the hydrothermal liquefaction process (Dimitriadis et al. 2017, Xu & Etcheverry 2008). According to the choice of biomass, reaction time tends to differ as recorded in the literature – 10 min for microalgae (Valdez et al. 2012), 15 min for swine manure (Xiu et al. 2010), 30 min for corn stalk (Zhu et al. 2014) and 80 min for bamboo biomass. The water content present during the liquefaction process decides the percentage of the hydrolysis process that enhances the bio-oil yield by promoting maximum conversion. But increasing the biomass concentration the solid residue formation gets elevated and pulls down the bio-oil yield (Qu et al. 2003). Regression coefficients were obtained through the least square technique by Divyabharathi & Subramanian (2021), wherein the effect of linear and quadratic terms was analyzed and proved that there was a significant effect at a 5% level on bio-crude production during the period of study and similar response in terms of aqueous and char yield were 0.822 and 0.937 respectively. The lignin content present in the biomass decides the bio-char production resulting in 0.8 to 6.9% from orange peel by Hydrothermal Liquefaction Process. The lesser the lignin content lesser be bio-char production (Divyabharathi & Subramanian 2021).

Proximate Analysis of Bio-Oil

The proximate analysis of the synthesized bio-oil recorded 31.2 MJ/kg calorific value, holding a density of 937 kg/m^3, the viscous nature of 7.05 mm^2, and TAN as 0.59 KOH/g concentration in Table 3. The bio-oil produced from biomass using the hydrothermal liquefaction process always has a major correlation with the existing biodiesel and diesel standards (Alleman et al. 2016). The properties of biocrude obtained from orange peel were analyzed by Divyabharathi & Subramanian (2021) and registered 32 MJ/kg of heating value, 93°C of flash point, during the period of study, and the properties registered from orange peel had comparable fuel properties with those of biodiesel/diesel and they are potentially used as a marine bunker fuel or furnace oil due to its similar viscosity, flash point and heating value

Table 2: ANOVA response of bio-oil yield.

Source	SOS	DF	MS	F value	P Value	Status
Model	31.517	9	3.501	9.99	0.0010	Significant
A-Concentration	1.333	1	1.333	3.806	0.0820	Not significant
B-Time	2.3105	1	2.310	6.596	0.0302	Significant
C-Temperature	2.482	1	2.482	7.087	0.0259	Significant
AB	3.079	1	3.079	8.792	0.0158	Significant
BC	5.733	1	5.733	16.371	0.0029	Significant
AC	3.308	1	3.308	9.446	0.0132	Significant
A^2	1.776	1	1.776	0.050	0.8268	Not significant
B^2	5.336	1	5.336	15.230	0.0036	Significant
C^2	6.160	1	6.160	17.590	0.0023	Significant

Where, SOS – Sum of Squares, DF –Degree of Freedom, MS – Mean Square

Table 3: Proximate analysis of Bio-oil.

Property	Unit	Bio-oil
Calorific Value	MJ/kg	31.2
Density	kg/m^3	937
Viscosity	mm^2	7.05
TAN Number	KOH/g	0.59

(Hossain et al. 2017). The standard similarity promotes their usage in blending with commercial transportation fuel or replacing its usage. However, proper purification steps like fuel upgradation or downstream techniques, viz. catalytic cracking to perform hydrodeoxygenation, desulphurization, and hydrotreatment must be carried out to remove the excess hydrogen and oxygen from the bio-oil to increase the efficiency (Hossain et al. 2017).

GCMS Analysis of Bio-Oil

GCMS analyzes the organic compounds present in the bio-oil produced. The composition of the bio-oil obtained under optimal operating conditions detected by GCMS was given in Table 4 and Fig. 4. The major compounds eluted out include pentadiene (33.5%) – an organic compound that is volatile and considered a flammable hydrocarbon, tetramethyl 2-hexadecene (24.5%) is an isoprenoid hydrocarbon, a derivative of chlorophyll present in the plant, hexadecane thiol (22.4%) an alkanethiol that forms monolayer by sulfur ions with the atoms present on the surface which is combustible and insoluble in water, trimethoxy methyl dihydroisoquinole (4.3%) used as a flavoring agent and dimethyl octadecanamide (14.7%). All the mentioned compounds were obtained from the decomposition and

Table 4: Major compounds present in bio-oil from citrus peel detected by the GCMS.

Retention time (min)	Area %	Compound name
3.223	0	2-Ethyl-1-pyrrole
4.933	0.1	Tetramethyl-1-dimethyl cyclopentane
5.677	33.5	Pentadien
7.733	0.2	Trimethyl cyclohexanone
8.190	0.1	Pyridine
17.223	0.1	Hydroquinone
21.170	0.1	Benzene 1,2,3-trimethoxy
27.800	24.5	Tetramethyl 2-hexadecene
28.747	22.4	Hexadecanethiol
31.713	4.3	Trimethoxy-methyl-Dihydroisoquinole
33.087	14.7	Dimethyl octadecanamide
Total	100	

depolymerization of the citrus peel. The presence of hydrocarbon was observed since they are derived from plant-based biomass which is regularly used as a flavoring and fragrant-producing agent in industrial sectors (Sharma et al. 2020). The hydrocarbon derivatives increase with an increase in temperature. However, initially during the temperature raised from 200°C to 250°C, nitrogenized compounds were eluting out, as the temperature reached 275°C, hydrocarbon compounds like phenol, alkanes, and isomeric alkenes were produced. This may be the result of decarboxylation and decomposition processes carried out by acids. The amine derivatives oxygenate and cyclic hydrocarbons which are the result of the repolymerization reaction pull down the stability
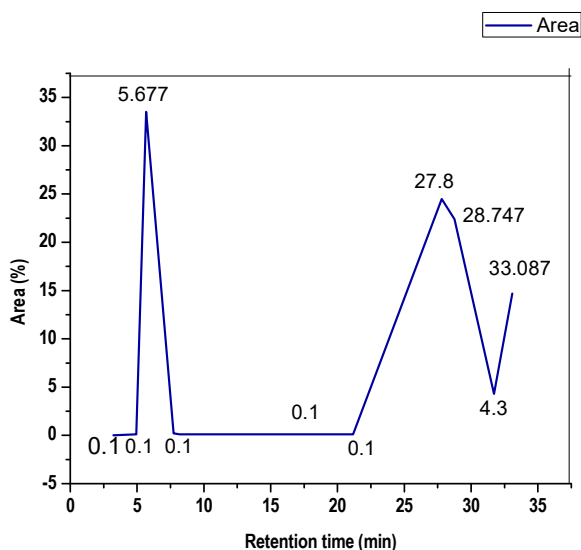
Fig. 4: GCMS of bio-oil from the citrus fruit peel.

of the bio-oil which can be over ruined by undergoing the fuel upgradation process (Palomino et al. 2020, Liu et al. 2013, Chen et al. 2014).

CONCLUSION

Based on the experimental design, the temperature and time influenced the bio-oil yield compared with the concentration of citrus fruit peel as biomass which was confirmed by ANOVA f and p test. The optimized parameters for the bio-oil were recorded at 280°C at 60 min reaction time and 80 g/200mL concentration by undergoing a hydrothermal liquefaction process. The maximum bio-oil yield was recorded as 29.4%. The fuel property of the bio-oil was obtained as 31.2 MJ/kg calorific value, 937 kg/m^3 density, 7.05 mm^2 viscosity, and 0.59 KOH/g TAN number. The GCMS analysis reveals the presence of hydrocarbons and alkanethiol which are flammable and hold the standards of commercial transportation fuel. Thus, the produced bio-oil can be blended along with the transportation fuel after carrying out the fuel upgradation process that removes excess oxygen, sulfur, and nitrogen content or it can be used directly as marine bunker fuel or for furnace purposes.

ACKNOWLEDGEMENTS

REFERENCES

Aboagye, D., Banadda, N., Kiggundu, N. and Kabenge, I., 2017. Assessment of orange peel waste availability in Ghana and potential bio-oil yield using fast pyrolysis. *Renewable and Sustainable Energy Reviews*, 70, pp.814-821. https://doi.org/10.1016/j.rser.2016.11.262.

Alleman, T.L., McCormick, R.L., Christensen, E.D., Fioroni, G., Moriarty, K. and Yanowitz, J., 2016. *Biodiesel handling and use guide* (No. NREL/BK-5400-66521; DOE/GO-102016-4875). National Renewable Energy Lab. (NREL), Golden, CO (United States).

Baruah, J., Nath, B.K., Sharma, R., Kumar, S., Deka, R.C., Baruah, D.C. and Kalita, E., 2018. Recent trends in the pretreatment of lignocellulosic biomass for value-added products. *Frontiers in Energy Research*, 6, p.141. https://doi.org/10.3389/fenrg.2018.00141.

Beims, R.F., Hu, Y., Shui, H. and Xu, C.C., 2020. Hydrothermal liquefaction of biomass to fuels and value-added chemicals: Products applications and challenges to develop large-scale operations. *Biomass and Bioenergy*, 135, p.105510. https://doi.org/10.1016/j.biombioe.2020.105510.

Bharathiraja, B., Jayamuthunagai, J., Sudharsanaa, T., Bharghavi, A., Praveenkumar, R., Chakravarthy, M. and Yuvaraj, D., 2017. Biobutanol–An impending biofuel for future: A review on upstream and downstream processing techniques. *Renewable and Sustainable Energy Reviews*, 68, pp.788-807. https://doi.org/10.1016/j.rser.2016.10.017.

Biller, P. and Ross, A.B., 2011. Potential yields and properties of oil from the hydrothermal liquefaction of microalgae with different biochemical content. *Bioresource Technology*, 102(1), pp.215-225. https://doi.org/10.1016/j.biortech.2010.06.028.

Changi, S.M., Faeth, J.L., Mo, N. and Savage, P.E., 2015. Hydrothermal reactions of biomolecules relevant for microalgae liquefaction. *Industrial & Engineering Chemistry Research*, 54(47), pp.11733-11758. https://doi.org/10.1021/acs.iecr.5b02771.

Chen, W.T., Zhang, Y., Zhang, J., Yu, G., Schideman, L.C., Zhang, P. and Minarick, M., 2014. Hydrothermal liquefaction of mixed-culture algal biomass from wastewater treatment system into bio-crude oil. *Bioresource Technology*, 152, pp.130-139. https://doi.org/10.1016/j.biortech.2013.10.111.

Dandamudi, K.P.R., Muppaneni, T., Markovski, J.S., Lammers, P. and Deng, S., 2019. Hydrothermal liquefaction of green microalga *Kirchneriella* sp. under sub-and super-critical water conditions. *Biomass and Bioenergy*, 120, pp.224-228. https://doi.org/10.1016/j.biombioe.2018.11.021.

Dimitriadis, A. and Bezergianni, S., 2017. Hydrothermal liquefaction of various biomass and waste feedstocks for biocrude production: A state of the art review. *Renewable and Sustainable Energy Reviews*, 68, pp.113-125. https://doi.org/10.1016/j.rser.2016.09.120.

Divyabharathi, R. and Subramanian, P., 2022. Biocrude production from orange (*Citrus reticulata*) peel by hydrothermal liquefaction and process optimization. *Biomass Conversion and Biorefinery*, pp.1-12. https://doi.org/10.1007/s13399-021-01383-3.

Hariram, V., Reddy, P.K., Gajalakshmi, B., Basha, S.S., Saravanan, A., Khamruddin, S.K. and Reddy, B.R., 2023. Synthesis of *Persea Americana* bio-oil and its spectroscopic characterization studies. *Nature Environment and Pollution Technology*, 22(3), pp.1627-1634. https://doi.org/10.46488/NEPT.2023.v22i03.049.

Hossain, F.M., Kosinkova, J., Brown, R.J., Ristovski, Z., Hankamer, B., Stephens, E. and Rainey, T.J., 2017. Experimental investigations of physical and chemical properties for microalgae hydrothermal liquefaction bio-crude using a large batch reactor. *Energies*, 10(4), p.467. https://doi.org/10.3390/en10040467.

Kim, B.S., Kim, Y.M., Jae, J., Watanabe, C., Kim, S., Jung, S.C., Kim, S.C. and Park, Y.K., 2015. Pyrolysis and catalytic upgrading of *Citrus unshiu* peel. *Bioresource Technology*, 194, pp.312-319. https://doi.org/10.1016/j.biortech.2015.07.035.

Liu, H.M., Li, M.F., Yang, S. and Sun, R.C., 2013. Understanding the mechanism of cypress liquefaction in hot-compressed water through characterization of solid residues. *Energies*, 6(3), pp.1590-1603. https://doi.org/10.3390/en6031590.

Malins, K., Kampars, V., Brinks, J., Neibolte, I., Murnieks, R. and Kampare, R., 2015. Bio-oil from thermo-chemical hydro-liquefaction of wet sewage sludge. *Bioresource Technology*, 187, pp.23-29. https://doi.org/10.1016/j.biortech.2015.03.093.

Malins, K., Kampars, V., Brinks, J., Neibolte, I., Murnieks, R., Kampare, R., 2015. Bio-oil from thermo-chemical hydro-liquefaction of wet sewage sludge. *Bioresource Technol.*, 187, pp. 23-29. doi: 10.1016/j.biortech.2015.03.093.

Mohan, D., Pittman Jr, C.U. and Steele, P.H., 2006. Pyrolysis of wood/biomass for bio-oil: a critical review. *Energy & Fuels*, 20(3), pp.848-889. https://doi.org/10.1021/ef0502397.

Nanda, S., Mohammad, J., Reddy, S.N., Kozinski, J.A. and Dalai, A.K., 2014. Pathways of lignocellulosic biomass conversion to renewable fuels. *Biomass Conversion and Biorefinery*, 4, pp.157-191. doi: 10.1007/s13399-013-0097.

Palomino, A., Godoy-Silva, R.D., Raikova, S. and Chuck, C.J., 2020. The storage stability of biocrude obtained by the hydrothermal liquefaction of microalgae. *Renewable Energy*, 145, pp.1720-1729. https://doi.org/10.1016/j.renene.2019.07.084.

Parvin, F. and Tareq, S.M., 2021. Impact of landfill leachate contamination on surface and groundwater of Bangladesh: a systematic review and possible public health risks assessment. *Applied Water Science*, 11(6), p.100. https://doi.org/10.1007/s13201-021-01431-3.

Qu, Y., Wei, X. and Zhong, C., 2003. Experimental study on the direct liquefaction of *Cunninghamia lanceolata* in water. *Energy*, 28(7), pp.597-606. https://doi.org/10.1016/S0360-5442(02)00178-0.

Reddy, H.K., Muppaneni, T., Ponnusamy, S., Sudasinghe, N., Pegallapati, A., Selvaratnam, T., Seger, M., Dungan, B., Nirmalakhandan, N., Schaub, T. and Holguin, F.O., 2016. Temperature effect on hydrothermal liquefaction of *Nannochloropsis gaditana* and *Chlorella* sp. *Applied Energy*, 165, pp.943-951. https://doi.org/10.1016/j.apenergy.2015.11.067.

Ruiz, H.A., Rodríguez-Jasso, R.M., Fernandes, B.D., Vicente, A.A. and Teixeira, J.A., 2013. Hydrothermal processing, as an alternative for upgrading agriculture residues and marine biomass according to the biorefinery concept: a review. *Renewable and Sustainable Energy Reviews*, 21, pp.35-51. https://doi.org/10.1016/j.rser.2012.11.069.

Sadh, P.K., Duhan, S. and Duhan, J.S., 2018. Agro-industrial wastes and their utilization using solid state fermentation: a review. *Bioresources and Bioprocessing*, 5(1), pp.1-15. https://doi.org/10.1186/s40643-017-0187-z.

Sharma, K., Pedersen, T.H., Toor, S.S., Schuurman, Y. and Rosendahl, L.A., 2020. Detailed investigation of compatibility of hydrothermal liquefaction derived biocrude oil with fossil fuel for corefining to drop-in biofuels through structural and compositional analysis. *ACS Sustainable Chemistry & Engineering*, 8(22), pp.8111-8123. https://dx.doi.org/10.1021/acssuschemeng.9b06253.

Siddiqua, A., Hahladakis, J.N. and Al-Attiya, W.A.K., 2022. An overview of the environmental pollution and health effects associated with waste landfilling and open dumping. *Environmental Science and Pollution Research*, 29(39), pp.58514-58536. https://doi.org/10.1007/s11356-022-21578-z.

Snowden-Swan, L.J., Hallen, R.T., Zhu, Y., Hart, T.R., Bearden, M.D., Liu, J., Seiple, T.E., Albrecht, K.O., Jones, S.B., Fox, S.P., Schmidt, A.J., Maupin, G.D., Billing, J.M. and Elliott, D.C., 2017. *Conceptual Biorefinery Design and Research Targeted for 2022: Hydrothermal Liquefaction Processing of Wet Waste to Fuels* [pdf]. Available at: https://www.pnnl.gov/main/publications/external/technical_reports/PNNL-27186.pdf [Accessed 03 January 2025]

Supangkat, S. and Herdiansyah, H., 2020. Analysis correlation of municipal solid waste generation and population: Environmental perspective. In: *IOP Conference Series: Earth and Environmental Science*, 519(1), p. 012056. https://doi.org/10.1088/1755-1315/519/1/012056.

The World Bank (IBRD-IDA), 2024. A global snapshot of solid waste management to 2050 data. Available at: https://datatopics.worldbank.org/what-a-waste/trends_in_solid_waste_management.html. Access date: 3 Jan 2025.

Valdez, P.J., Nelson, M.C., Wang, H.Y., Lin, X.N. and Savage, P.E., 2012. Hydrothermal liquefaction of *Nannochloropsis* sp.: Systematic study of process variables and analysis of the product fractions. *Biomass and Bioenergy*, 46, pp.317-331. https://doi.org/10.1016/j.biombioe.2012.08.009.

Vardon, D.R., Sharma, B.K., Scott, J., Yu, G., Wang, Z., Schideman, L., Zhang, Y. and Strathmann, T.J., 2011. Chemical properties of biocrude oil from the hydrothermal liquefaction of *Spirulina* algae, swine manure, and digested anaerobic sludge. *Bioresource Technology*, 102(17), pp.8295-8303. https://doi.org/10.1016/j.biortech.2011.06.041.

Vo, T.K., Lee, O.K., Lee, E.Y., Kim, C.H., Seo, J.W., Kim, J. and Kim, S.S., 2016. Kinetics study of the hydrothermal liquefaction of the microalga *Aurantiochytrium* sp. KRS101. *Chemical Engineering Journal*, 306, pp.763-771. https://doi.org/10.1016/j.cej.2016.07.104.

Wang, T., Zhai, Y., Zhu, Y., Peng, C., Xu, B., Wang, T., Li, C. and Zeng, G., 2018. Influence of temperature on nitrogen fate during hydrothermal carbonization of food waste. *Bioresource Technology*, 247, pp.182-189. https://doi.org/10.1016/j.biortech.2017.09.076.

Xiu, S., Shahbazi, A., Shirley, V. and Cheng, D., 2010. Hydrothermal pyrolysis of swine manure to bio-oil: Effects of operating parameters on products yield and characterization of bio-oil. *Journal of Analytical and Applied Pyrolysis*, 88(1), pp.73-79. https://doi.org/10.1016/j.jaap.2010.02.011.

Xu, C. and Etcheverry, T., 2008. Hydro-liquefaction of woody biomass in sub-and super-critical ethanol with iron-based catalysts. *Fuel*, 87(3), pp.335-345. https://doi.org/10.1016/j.fuel.2007.05.013.

Zhu, W.W., Zong, Z.M., Yan, H.L., Zhao, Y.P., Lu, Y., Wei, X.Y. and Zhang, D., 2014. Cornstalk liquefaction in methanol/water mixed solvents. *Fuel Processing Technology*, 117, pp.1-7. https://doi.org/10.1016/j.fuproc.2013.04.007.

Original Research Paper

Open Access Journal

Assessing Natural Disaster Vulnerability in Indonesia Using a Weighted Index Method

Faradiba Faradiba[1†] (ORCID), St. Fatimah Azzahra[2], Taat Guswantoro[1], Lodewik Zet[3] (ORCID) and Nathasya Grisella Manullang[1]

[1]Physics Education Study Program, Universitas Kristen, Indonesia
[2]Chemistry Education Study Program, Universitas Kristen, Indonesia
[3]BPS-Statistics Indonesia, Indonesia
†Corresponding author: Faradiba Faradiba; faradiba@uki.ac.id

ABSTRACT

Natural disasters are natural activities that can disrupt various aspects. Natural disasters cannot be avoided, but the impact of natural disasters can be minimized through mitigation. This can be known through event history to determine an area's vulnerability to natural disasters. This research aims to determine regional natural disaster vulnerability by calculating the natural disaster index. The data used in this research refers to data from the 2021 PODES data collection, which contains the intensity of natural disasters and casualties according to the type of natural disaster in Indonesia in 2020. The method used for the calculation is the weighted index method. The results of this research produced 5 clusters based on the level of natural disaster vulnerability according to sub-district/village. The top five provinces in Indonesia that have the highest natural disaster-prone areas are Aceh, North Sumatra, West Java, East Java, and Central Sulawesi. Research shows that sub-districts/villages in Indonesia are known according to their level of vulnerability to natural disasters. These results can be used as a reference for the government to carry out mitigation so that accelerated development in the local area can continue.

INTRODUCTION

Natural disasters are a phenomenon that often haunts Indonesia. As an archipelagic country located on the Pacific Ring of Fire, Indonesia is vulnerable to various types of natural disasters, ranging from earthquakes, volcanic eruptions, floods, and landslides to tsunamis (Hakim & Lee 2020, Malawani et al. 2021, Teh & Khan 2021). The existence of this natural disaster is no stranger to the Indonesian population. Most of them have even experienced it directly. Every year, news about natural disasters graces the mass media, painting a distressing picture of the loss and suffering caused by natural forces.

Not only do they cause material losses, but natural disasters also often cause loss of life. The ever-increasing loss of life is a reflection of how devastating the impact of natural disasters can be. Behind Indonesia's natural fragility, there are factors such as global warming, deforestation, and environmental pollution, which are increasingly making the situation worse. This high level of vulnerability requires alertness and cooperation between the government, society, and humanitarian organizations to reduce the impacts caused by natural disasters.

Apart from geographical factors, human factors also contribute to the frequent occurrence of natural disasters in Indonesia. Rapid population growth causes pressure on natural resources and the environment to increase. Practices such as deforestation, unsustainable agriculture, and irregular development can exacerbate the risk of natural disasters (Azare et al. 2020, Chirwa & Adeyemi 2020, Kumar et al. 2022). Deviations in environmental management and land use can also

increase the impact of natural disasters, such as flooding due to river flows being blocked by rubbish or development on river banks.

Apart from geographical and human factors, climate change is also an increasingly significant cause of increasing the risk of natural disasters in Indonesia (Celik 2020, Ebi & Hess 2020, Faradiba et al. 2024, Merrey et al. 2018, Prarikeslan et al. 2023). Climate change causes unstable weather patterns, increasing the frequency and intensity of extreme rainfall, drought, and tropical storms (Faradiba 2021). This has a direct impact on the occurrence of floods, landslides, and other disasters that damage infrastructure, disrupt livelihoods, and threaten the safety of residents (Faradiba & Zet 2020).

The impact of natural disasters can be very destructive and detrimental to society at large. One of the main impacts is material loss, where infrastructure such as houses, roads, bridges, and other public facilities can be damaged or destroyed due to earthquakes, floods, or volcanic eruptions. These losses not only affect the daily lives of residents but also cause economic activities, such as agricultural production, trade, and industry, to be hampered.

Apart from material losses, natural disasters can also cause human losses, both in terms of fatalities and physical and mental injuries. When a disaster occurs, people are vulnerable to various risks, such as being buried in the ground, drowning in floods, or being injured by building debris. Additionally, the psychological impact of losing a home, possessions, or even family members can cause lasting trauma and stress.

Apart from material and human losses, natural disasters can also cause social losses. Disasters often divide communities, sever social relationships, and result in forced migration. In addition, disasters can also exacerbate social disparities, where those who already live in conditions of economic or social vulnerability become more vulnerable to the impacts of disasters than those who are better off.

A region's vulnerability to natural disasters becomes clear when we look at the intensity and impacts they cause. The high intensity of natural disasters, such as earthquakes, volcanic eruptions, floods, or tsunamis, is a strong indicator of the region's vulnerability. Apart from that, the number of fatalities caused by natural disasters also provides a very important picture in evaluating the vulnerability of an area.

Regions that often experience natural disasters with high intensity and cause a significant number of fatalities show a serious level of vulnerability. For example, areas that are in the path of active earthquakes or close to active volcanoes tend to have a high vulnerability to earthquakes and volcanic eruptions. Likewise, areas are often affected by floods or tsunamis due to their geographical location in lowland or coastal areas.

Apart from geographical factors, social, economic, and infrastructure factors also play a role in determining the level of vulnerability of an area to natural disasters. Areas with high levels of poverty or weak infrastructure tend to be more vulnerable to the impacts of natural disasters due to a lack of access to health facilities, evacuation, and post-disaster assistance.

Natural disasters are a threat that is difficult to avoid because their strength depends on natural factors, which often cannot be predicted with certainty. However, although they cannot be completely avoided, the impacts caused by natural disasters can be minimized through various mitigation efforts. Disaster mitigation is a series of proactive actions aimed at reducing the risk and vulnerability of society to natural disasters.

One important aspect of disaster mitigation is a better understanding of the types of natural disasters that may occur in an area, as well as the factors that influence them. With a deep understanding of potential threats, the government and society can take appropriate preventive steps, such as preparing emergency response plans, developing disaster-resistant infrastructure, and preparedness training.

Apart from that, disaster mitigation also involves efforts to increase public awareness about disaster risks and safe ways to act when a disaster occurs. Education about evacuation, first aid, and the use of technology to monitor and predict disaster threats are also important parts of disaster mitigation. The higher the level of community awareness and preparedness, the more effective the disaster mitigation efforts will be.

In managing natural disaster risks, it is important to have a clear understanding of a region's vulnerability to various types of disasters. To do this, an index that can be used to measure the level of vulnerability to natural disasters in each region is needed. This index serves as a tool to compare levels of vulnerability between regions in Indonesia, thereby enabling stakeholders, including the government, humanitarian organizations, and the general public, to identify the most vulnerable areas and prioritize mitigation efforts.

By using the natural disaster vulnerability index, the government, and other stakeholders can identify areas that require special attention in terms of disaster mitigation (Fig. 1). Steps such as improving disaster-resistant infrastructure, educating the public about disaster risks, and developing effective emergency response plans can help reduce vulnerability and increase regional resilience

Geographical Factors

Indonesia is an archipelagic country located at the confluence of four tectonic plates. In the southern and eastern parts of Indonesia there are volcanic arcs.

Anthropocene

Natural Disasters

Vurnerability

Human activities have a global influence on changes in the Earth's

Climate Change

Increasing global surface temperatures, resulting in more droughts and increased storm intensity. More water vapor evaporates into the atmosphere, more heat in the atmosphere and warmer sea surface temperatures can cause increased wind speeds in tropical storms.

Fig. 1: Research conceptual framework.

to natural disasters. Thus, the use of a natural disaster vulnerability index can be a very valuable tool in efforts to reduce the impact of disasters and protect people's lives and property. Several previous studies related to natural disaster indices have been carried out using several methods, namely the Buffer-From-Cluster Approach (BFCA), index based on mortality, and others (Peduzzi et al. 2009, Pulvirenti et al. 2020, Wannewitz et al. 2016).

There have been many studies analyzing the impact of natural disasters in various regions (Kaniasty 2020, Pramono et al. 2020, Rosselló et al. 2020).

However, there are still only a few that calculate the natural disaster index in the smallest administrative areas. Therefore, this research aims to calculate the natural disaster index in sub-district and rural areas. The results of the research will produce an index for each region, which will be divided according to vulnerability clusters.

MATERIALS AND METHODS

This research uses data from the results of the 2021 Village Potential Data Collection (PODES), which includes information about the intensity of natural disasters and the number of fatalities due to various types of natural disasters in Indonesia during 2020. PODES is a government program that aims to collect data related to the condition of villages. Villages throughout Indonesia, including data related to natural disasters. This data is a rich and comprehensive source of information for analyzing the vulnerability and impact of natural disasters in various regions in Indonesia.

The method used in this research is the weighted index method, which is a statistical approach that is commonly

used to combine several indicators or variables into one single index (Sun et al. 2021, Zhu et al. 2020). In this context, a weighted index is used to calculate the level of vulnerability to natural disasters in various regions in Indonesia. This approach allows researchers to assign appropriate weights to each variable under consideration, such as the intensity of natural disasters and the number of fatalities, thereby providing a more accurate picture of the level of vulnerability.

Weighted index is an average calculation method where each value in a data set has a certain weight that influences its contribution to the overall average value. The general formula for calculating the weighted index is as follows:

$$\text{Weighted Index} = \frac{\sum_{i=1}^{n} W_i \, x \, X_i}{\sum_{i=1}^{n} W_i}$$

Notes:

7 is the weight assigned to each value in the data set.

8 is value of each element in the data set.

$\emptyset$ is the number of elements in the data set.

By using the weighted index method, this research aims to provide a deeper understanding of the level of vulnerability to natural disasters in Indonesia. It is hoped that the results of this analysis can provide valuable input for decision-makers, including governments and humanitarian organizations, in designing effective and targeted disaster mitigation policies and programs. With a better understanding of vulnerability to natural disasters, it is hoped that mitigation efforts can be more targeted and have a significant impact in protecting communities and their assets from the threat of natural disasters.

RESULTS AND DISCUSSION

Based on Table 1, it is found that flood disasters are the type of natural disaster that occurs most frequently in Indonesia. This is not surprising considering Indonesia's geographic and climate characteristics, which are prone to high rainfall and topography, which tends to be swampy and hilly. Various factors, including heavy rain, river overflows, sea tides, and overflowing lakes or dams, can trigger floods. This condition causes flooding to become a constant threat to Indonesian people, especially to those who live in lowland areas or close to large rivers.

The impact of flooding on Indonesian society is very large, both in terms of material losses and casualties. Floods often cause damage to infrastructure, such as houses, roads, bridges, and other public facilities. Apart from that, floods can also disrupt economic activities, such as agriculture, trade, and industry. It is not uncommon for floods to result in loss of life, especially if there is no effective early warning system or adequate emergency response infrastructure.

To overcome the threat of flooding, various mitigation efforts need to be carried out, including building flood-resistant infrastructure, good river and drainage management, and increasing community capacity to face flood risks. Apart from that, it is also important to take adaptation steps to climate change, which could increase the intensity and duration of floods in the future. With coordinated and directed efforts, it is hoped that the level of vulnerability to flood disasters in Indonesia can be reduced so that people can live more safely and prosperously amidst inevitable natural threats.

Based on Table 2, as the intensity of flood disasters increases in Indonesia, the number of fatalities due to flood disasters occupies the top position compared to other types

Table 2: Number of death victims from natural disasters in 2020 by types.

Natural Disaster	Total	Std. Error	[95% Cof. Interval]	
Landslide	526	162,95	206,61	845,38
Flood	13.625	2.360,47	8.998,49	18.251,50
Flash floods	1.019	623,77	-203,59	2241,59
Earthquake	184	31,04	123,15	244,84
Tsunami	0			
Tidal Waves	831	417,81	12,09	1.649,90
Whirlwind/ Tornado/Typhoon	514	141,88	235,90	792,09
Erupting volcano	2	1,41	-0.77	4,77
Forest and Land Fires	667	637,10	-581,72	1.915,73
Drought (Land)	5.228	1.581,06	2.129,12	8.326,87
Abrasion	196	52,74	92,62	299,37

of natural disasters. This phenomenon shows how serious the impact of flooding is on the lives and safety of Indonesian people. Floods can cause huge losses not only in terms of material damage but also threaten human lives.

Flood disasters can cause casualties due to various factors, such as drowning, being swept away by flood currents, being buried by building rubble, or contracting infectious diseases after the flood recedes. Especially in areas that are prone to flooding and have high levels of population density, the risk of loss of life due to flooding is increasingly high. In addition, sometimes, a lack of access to safe evacuation facilities and effective early warning systems also contributes to high death tolls.

The increase in the number of fatalities due to floods highlights the importance of more effective flood mitigation and management efforts. Steps such as improving flood-resistant infrastructure, improving drainage systems, providing adequate evacuation facilities, and increasing

Table 1: Intensity of natural disaster events in 2020 by types.

Natural Disaster	Total	Std. Err.	[95% Cof. Interval]	
Landslide	10.518	174,89	10.175,20	10.860,80
Flood	26.889	278,30	26.343,51	27.434,49
Flash floods	1.054	46,78	962,30	1.145,69
Earthquake	20.881	335,56	20.223,30	21.538,70
Tsunami	19	10,14	-0,89	38,89
Tidal Waves	3.370	112,58	3.149,33	3.590,66
Whirlwind/ Tornado/Typhoon	3.726	75,83	3.577,36	3.874,63
Erupting volcano	321	28,20	265,70	376,29
Forest and Land Fires	1.856	68,44	1.721,84	1.990,15
Drought (Land)	2.750	61,90	2.628,66	2.871,33
Abrasion	1.614	66,35	1.483,94	1.744,05

Table 3: Weight of natural disaster intensity in 2020 by types.

Natural Disaster	Weight
Landslide	0,04754842598427350
Flood	0,12155634400942500
Flash floods	0,00476478807638565
Earthquake	0,09439614783966680
Tsunami	0,00008589276418532
Tidal Waves	0,01523466396339630
Whirlwind/Tornado/Typhoon	0,01684402312392120
Erupting volcano	0,00145113564755199
Forest and Land Fires	0,00839036685936601
Drought (Land)	0,01243184744787530
Abrasion	0,00729636428395299

Table 4: Weight of casualties from natural disasters in 2020 by types.

Natural Disaster	Weight
Landslide	0,0154624429624430
Flood	0,4005243067743070
Flash floods	0,0299548087048087
Earthquake	0,0054089154089154
Tsunami	-
Tidal Waves	0,0244283081783082
Whirlwind/Tornado/Typhoon	0,0151096876096876
Erupting volcano	0,0000587925587926
Forest and Land Fires	0,0196073183573184
Drought (Land)	0,1536837486837490
Abrasion	0,0057616707616708

Table 5: 2020 natural disaster index range by cluster.

Cluster	Range Index
1	0.00
2	0.01-0.0941268
3	0.0941269-0.1286526
4	0.1286527-0.2824877
5	> 0.2824877

public awareness about the dangers of flooding are key to reducing the risk of loss of life due to flood disasters. With coordinated and integrated efforts between the government, society, and various related parties, it is hoped that the number of fatalities due to flooding can be reduced so that Indonesia can become more resilient in facing the inevitable threat of natural disasters.

In Table 3 and Table 4, weight data is used to calculate the natural disaster index. The method used in this calculation is the weighted method, which considers various factors in determining the severity of a natural disaster. In this context, the depth of calculation of the natural disaster index is influenced by two main factors, namely the number of natural disaster events and the number of victims affected.

These factors are then given a certain weight according to the level of impact on society and the environment. This weight is reflected in the Tables mentioned previously, where each natural disaster is given a weight based on

an analysis of the risks and impacts it has. For example, natural disasters with a high number of fatalities will have greater weight than other natural disasters that have a more limited impact.

The results of calculating the natural disaster index are grouped into 5 clusters, as listed in Table 5. The higher the index value, the higher the vulnerability to natural disasters in that area. A value of zero in cluster 1 indicates that the region did not experience natural disasters during the research reference. Based on Fig. 2, if added up for each cluster, most regions in Indonesia do not have natural disasters.

From the data listed in Table 6, it can be seen that the provinces of Aceh, North Sumatra, West Java, East Java, and Central Sulawesi stand out as the regions with the number of villages or sub-districts most vulnerable to natural disasters. This information is presented based on clustering analysis, with a focus on cluster 6, which shows the highest natural disaster vulnerability index. The results of this study are in line with previous research (Ardiansyah et al. 2021, Capah, 2022, Ismana et al. 2022, Kharimah et al. 2022, Samad et al. 2020).

This focus on cluster 6 provides a clear picture of areas where the potential for natural disasters is a very important issue and needs special attention. This highlights the importance of grouping regions based on their level of
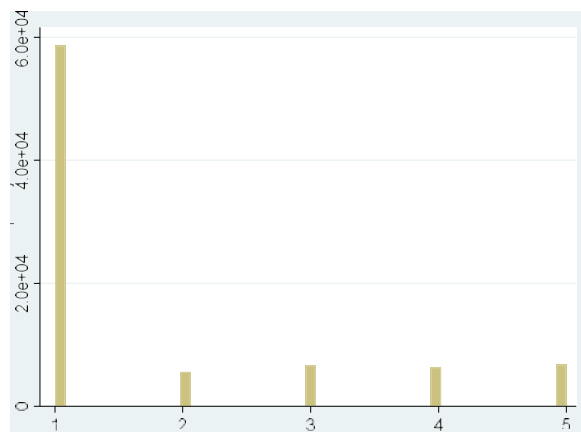
Fig. 2: Number of subdistricts/villages according to natural disaster index clusters in 2020 by cluster.

Table 6: Number of subdistricts/villages according to natural disaster index distribution Clusters and Provinces in 2020.

Province Code	Province	Cluster					Total
		1	2	3	4	5	
11	Aceh	4.550	238	633	466	627	6.514
12	Sumatera Utara	4.136	407	333	317	939	6.132
13	Sumatera Barat	622	98	114	145	308	1.287
14	Riau	1.342	92	186	160	96	1.876
15	Jambi	1.033	40	198	147	144	1.562
16	Sumatera Selatan	2.767	119	200	128	78	3.292
17	Bengkulu	1.227	57	64	79	87	1.514
18	Lampung	2.162	127	142	128	95	2.654
19	Kepulauan Bangka Belitung	285	52	17	21	18	393
21	Kepulauan Riau	300	85	11	16	16	428
31	DKI Jakarta	154	4	58	26	25	267
32	Jawa Barat	3.383	715	610	718	531	5.957
33	Jawa Tengah	6.100	851	711	579	321	8.562
34	DI Yogyakarta	255	79	30	44	30	438
35	Jawa Timur	6.277	473	653	535	558	8.496
36	Banten	956	92	203	147	154	1.552
51	Bali	518	69	45	48	36	716
52	Nusa Tenggara Barat	811	102	59	77	102	1.151
53	Nusa Tenggara Timur	2.368	648	157	189	88	3.450
61	Kalimantan Barat	1.248	68	224	324	284	2.148
62	Kalimantan Tengah	815	36	173	258	294	1.576
63	Kalimantan Selatan	1.379	87	274	165	102	2.007
64	Kalimantan Timur	699	43	100	104	100	1.046
65	Kalimantan Utara	324	15	67	46	30	482
71	Sulawesi Utara	1.183	121	127	136	273	1.840
72	Sulawesi Tengah	1.087	79	209	263	382	2.020
73	Sulawesi Selatan	2.056	243	301	272	179	3.051
74	Sulawesi Tenggara	1.942	118	148	71	30	2.309
75	Gorontalo	372	63	66	102	131	734
76	Sulawesi Barat	266	44	95	108	137	650
81	Maluku	845	154	101	79	69	1.248
82	Maluku Utara	477	58	120	207	341	1.203
91	Papua Barat	1.537	38	135	176	100	1.986
94	Papua	5.182	109	111	83	70	5.555
	Indonesia	58.658	5.624	6.675	6.364	6.775	84.096

vulnerability to natural disasters to help central and regional governments plan more effective mitigation strategies.

The intensity of natural disasters can be reduced significantly by involving active participation from the local level, namely sub-districts and villages, in disaster mitigation efforts. This means giving regions a more important role in preparing for and responding to the threat of natural disasters.

The data listed in Fig. 2 highlights the important role of Central Java Province in terms of early warning systems for natural disasters.

Central Java Province, with the largest number of sub-districts or villages in the natural disaster early warning system, shows high commitment and awareness in terms of disaster mitigation. This reflects investments made in early
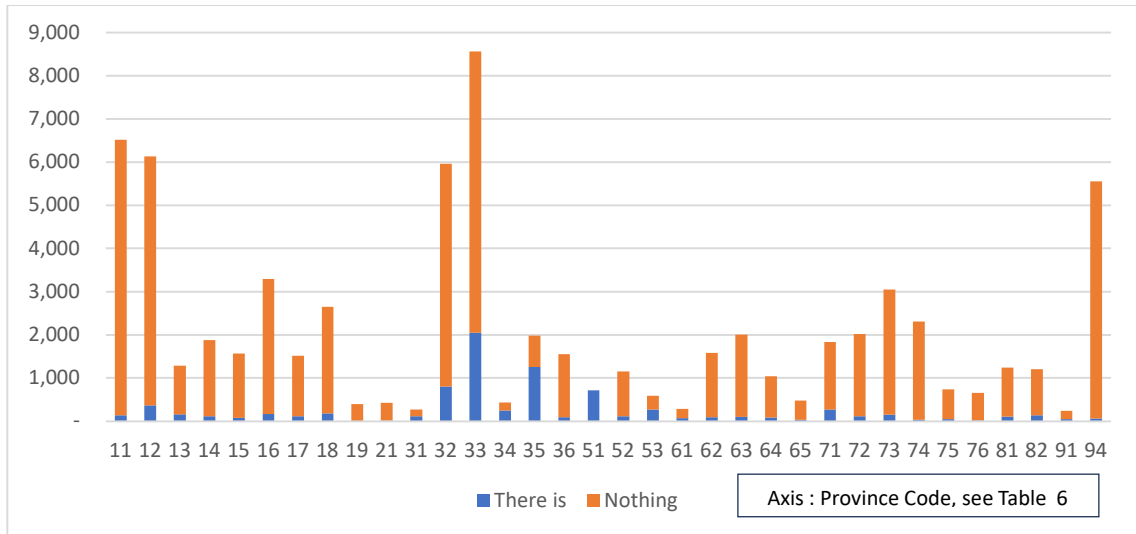
Fig. 2: Number of subdistricts/villages according to the 2020 natural disaster early warning system by Province.
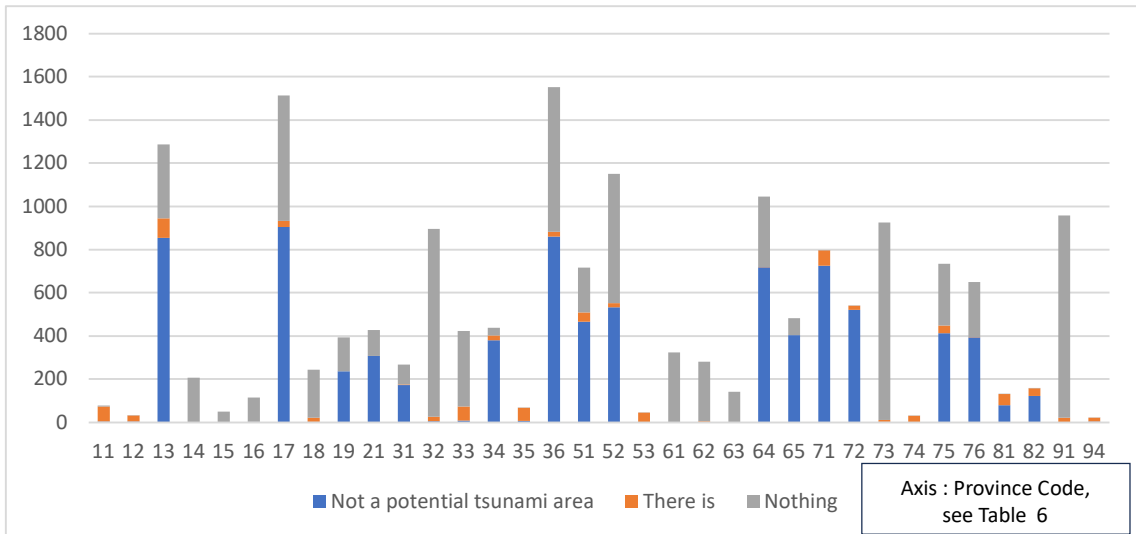
Fig. 3: Number of Subdistricts/Villages According to the 2020 Special Tsunami Early Warning System by Province.

warning infrastructure and the knowledge and skills of local communities in dealing with the threat of natural disasters.

The data depicted in Fig. 3 reveals that Aceh Province stands out as the province that has the largest number of sub-districts or villages integrated into a special tsunami early warning system. The presence of this early warning system reflects high awareness of the risk of tsunami disasters in the region, especially considering the tragic history of the large tsunami in 2004 that hit Aceh and most of the surrounding area.

The bitter experience of the disaster has prompted serious efforts to improve preparedness and mitigation in Aceh, with a particular focus on tsunami early warning. The availability of a widespread early warning system in sub-districts and villages in Aceh shows the commitment of the government and local communities to anticipating and responding to the threat of disaster quickly and effectively.

Aceh Province has a topography that is prone to earthquakes and tsunamis because of its position on the Pacific Ring of Fire. Therefore, investment in early warning infrastructure and community outreach is key in efforts to maintain safety and minimize losses due to the tsunami disaster. The existence of an extensive early warning system in Aceh not only reflects progress in disaster mitigation but also provides an example for other areas potentially exposed to similar threats to improve their preparedness.

The data depicted in Fig. 4 and Fig. 5 confirms that Central Java Province stands out as the province with the largest number of sub-districts or villages equipped with safety equipment and disaster evacuation signs/routes to increase preparedness for natural disasters. The existence of this safety equipment is a concrete step in preparing ourselves to face various potential natural disasters that could occur in the area.

Central Java Province, which is geographically located in the center of Java Island, has a fairly high risk of natural disasters such as earthquakes, floods, landslides, and volcanic eruptions. Therefore, awareness of the importance of disaster preparedness has encouraged serious efforts to provide safety equipment in every sub-district or village.

The data depicted in Fig. 6 shows that South Sumatra Province stands out as the province with the largest number of sub-districts or villages that are actively involved in the construction, maintenance, or normalization of water channels. This indicates a high commitment from the government and local communities to managing water infrastructure to reduce the risk of disasters related to flooding and waterlogging.

Based on Fig. 6, South Sumatra Province, with its geographical characteristics dominated by lowlands and large river flows, is often vulnerable to floods and other water-related problems. Therefore, activities to create, maintain, and normalize water channels are very important to reduce disaster risks and increase community resilience to these threats.
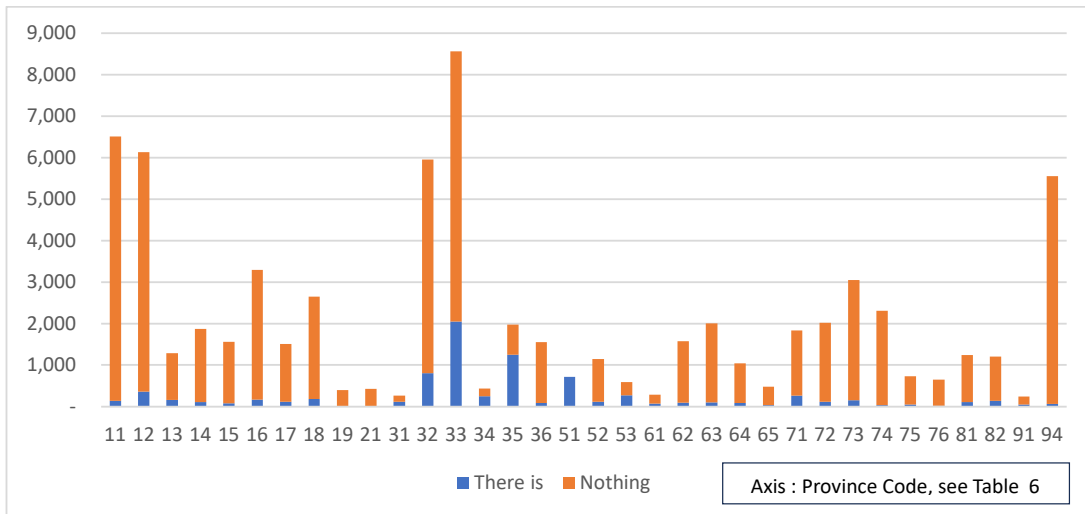
Fig. 4: Number of subdistricts/villages according to safety equipment in 2020 by Province.
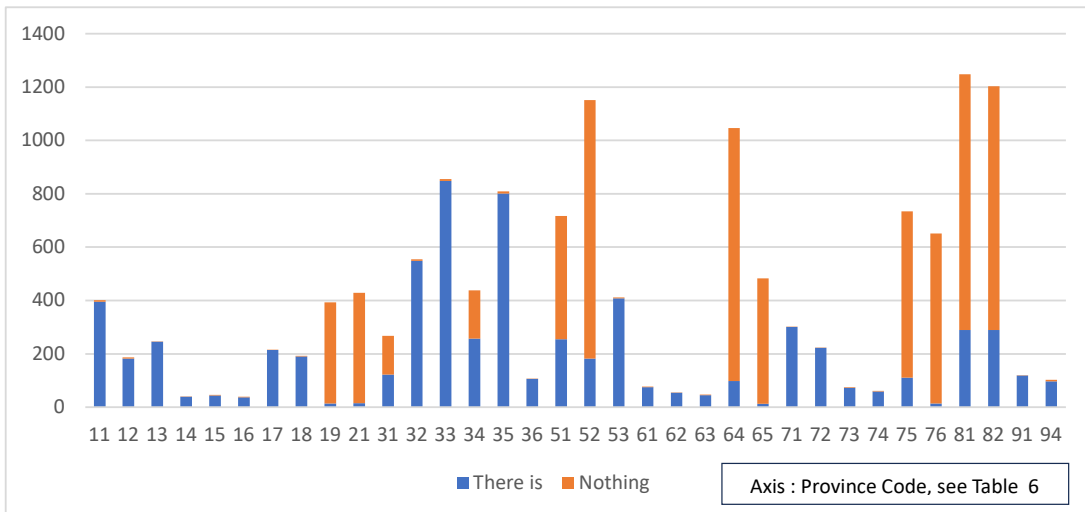
Fig. 5: Number of subdistricts/villages according to signs and disaster evacuation routes in 2020 by Province.
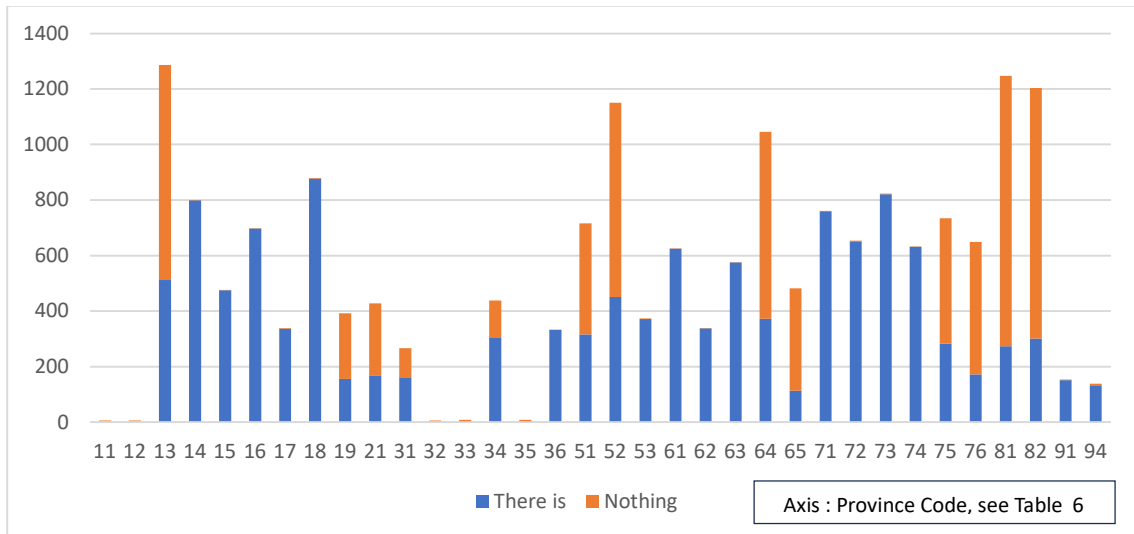
Fig. 6: Number of subdistricts/villages according to construction, maintenance, or normalization of water channels in 2020 by Province.

The active participation of sub-districts and villages in this effort shows the importance of the local role in managing water infrastructure. Local communities have extensive knowledge of local environmental conditions and can make valuable contributions in planning and implementing effective waterway maintenance activities.

Natural disaster mitigation is a crucial effort in anticipating and reducing the negative impacts caused by natural disasters. The main goal of disaster mitigation is to protect human lives, property, and vital infrastructure from damage or loss caused by natural disasters. The importance of disaster mitigation lies in the principle of prevention, which is more effective than handling it after a disaster occurs, thereby minimizing human and material losses.

Natural disaster mitigation is a shared responsibility that various parties must carry out. This includes government, civil society, non-governmental organizations, educational institutions, and the private sector. Each party has a different but interrelated role in achieving optimal disaster mitigation goals.

Through the index that has been calculated in this research, it is hoped that it can help the government in mitigating disaster-prone areas and evacuating areas that have been affected by disasters. The government's role is very important to minimize losses due to natural disasters. Apart from that, the government's role is also needed to repair areas that have been affected by natural disasters so that regional development acceleration can be achieved well.

The government has a central role in coordinating natural disaster mitigation efforts, starting from planning policy implementation to resource allocation. Civil society also has an important role in increasing preparedness and awareness of potential disasters, as well as actively participating in mitigation activities such as evacuation training and risk management. Non-governmental organizations often provide direct assistance to disaster victims and play a role in counseling and advocacy related to disaster mitigation. Meanwhile, the private sector can contribute in the form of technical support, financial resources, and infrastructure that can be used for disaster mitigation.

By actively involving various parties and coordinating natural disasters, mitigation efforts can become more effective and sustainable. Collaboration between government, communities, non-governmental organizations, and the private sector is key in building community resilience to the threat of natural disasters.

CONCLUSIONS

As an archipelagic country located on the Pacific Ring of Fire, Indonesia is vulnerable to various types of natural disasters, ranging from earthquakes, volcanic eruptions, floods, and landslides to tsunamis. Natural disasters are sometimes difficult to avoid, but the negative impacts of natural disasters can be minimized, especially in locations that are indicated to be prone to natural disasters. This research produces regional categorization based on the level of vulnerability to natural disasters. These results can be used as a reference in mitigating natural disasters, especially in areas that have the highest natural disaster index. Synergy is needed from various parties to minimize the negative impact of natural disasters. Through good mitigation, the

development of areas affected by natural disasters can be more alert in facing natural disasters.

ACKNOWLEDGMENT

REFERENCES

Ardiansyah, W., Nuarsa, I.W. and Bhayunagiri, I.B.P., 2021. Analysis of drought disaster risk areas based on geographic information system in Bondowoso Regency, East Java Province. *IOP Conf. Series: Earth and Environmental Science*, 230, pp.6515.

Azare, I.M., Abdullahi, M.S., Adebayo, A.A., Dantata, I.J. and Duala, T., 2020. Deforestation, desert encroachment, climate change and agricultural production in the Sudano-Sahelian Region of Nigeria. *Journal of Applied Sciences and Environmental Management*, 24(1), pp.127–132.

Capah, F.R.A., 2022. The role of the regional disaster management agency in post-disaster handling in Deli Serdang Regency, North Sumatra Province. *Journal Ilmu Pemerintahan Suara Khatulistiwa*, 11, pp.22.

Celik, S., 2020. The effects of climate change on human behaviors. *Environment, Climate, Plant and Vegetation Growth*, pp.577–589.

Chirwa, P.W. and Adeyemi, O., 2020. Deforestation in Africa: implications on food and nutritional security. *Sustainability*, pp.197–211.

Ebi, K.L. and Hess, J.J., 2020. Health risks due to climate change: inequity in causes and consequences: study examines health risks due to climate change. *Health Affairs*, 39(12), pp.2056–2062.

Faradiba, F. and Zet, L., 2020. The impact of climate factors, disaster, and social community in rural development. *The Journal of Asian Finance, Economics and Business*, 7(9), pp.707–717. https://doi.org/https://doi.org/10.13106/jafeb.2020.vol7.no9.707

Faradiba, F., 2021. Analysis of intensity, duration, and frequency of rain daily on Java Island using the Mononobe method. *Journal of Physics: Conference Series*, 1783(1), pp.012107. https://doi.org/10.1088/1742-6596/1783/1/012107

Faradiba, F., Azzahra, S.F., Yuniarti, E., Zet, L., Laia, T.K. and Wulandari, R., 2024. Will development and temperature be reconciled? *Nature Environment and Pollution Technology*, 23(1), pp.151–160. https://doi.org/10.46488/NEPT.2024.v23i01.011

Hakim, W.L. and Lee, C.-W., 2020. A review of remote sensing and GIS applications to monitor natural disasters in Indonesia. *Korean Journal of Remote Sensing*, 36(6_1), pp.1303–1322.

Ismana, D.R., Baehera, S., Fitrianto, A., Sartono, B. and Oktarina, S.D., 2022. Village grouping in West Java based on disaster risk areas. *Indonesian Journal of Statistics and Its Applications*, 6(2), pp.243–252.

Kaniasty, K., 2020. Social support, interpersonal, and community dynamics following disasters caused by natural hazards. *Current Opinion in Psychology*, 32, pp.105–109.

Kharimah, I., Wahyuni, D., Aprilyanto, A. and Widana, I.D.K.K., 2022. Flood disaster mitigation efforts in Pidie Jaya Regency, Aceh Province, to support national security. *PENDIPA Journal of Science Education*, 6(1), pp.57–63.

Kumar, R., Kumar, A. and Saikia, P., 2022. *Deforestation and Forests Degradation: Impacts on the Environment*. Springer, pp.19–46.

Malawani, M.N., Lavigne, F., Gomez, C., Mutaqin, B.W. and Hadmoko, D.S., 2021. Review of local and global impacts of volcanic eruptions and disaster management practices: the Indonesian example. *Geosciences*, 11(3), pp.109.

Merrey, D.J., Hussain, A., Tamang, D.D., Thapa, B. and Prakash, A., 2018. Evolving high altitude livelihoods and climate change: A study from Rasuwa District, Nepal. *Food Security*, 10(4), pp.1055–1071.

Peduzzi, P., Dao, H., Herold, C. and Mouton, F., 2009. Assessing global exposure and vulnerability towards natural hazards: the Disaster Risk Index. *Natural Hazards and Earth System Sciences*, 9(4), pp.1149–1159.

Pramono, J., Kusumastuti, D., Sekarwangi, M. and Choerudin, A., 2020. The community participation in disaster mitigation to manage the impact of natural disasters in Indonesia. *International Journal of Advanced Science and Technology*, 12, pp.2396–2403.

Prarikeslan, W., Sudiar, N.Y., Anugrah, G., Beri, D., Handayani, D., Eka Putri, I.L. and Gautama, M.I., 2023. The impact of climate change on the City of Padang, Indonesia. *Nature Environment and Pollution Technology*, 22(4), pp.2223–2229. https://doi.org/10.46488/NEPT.2023.v22i04.050

Pulvirenti, L., Squicciarino, G. and Fiori, E., 2020. A method to automatically detect changes in multitemporal spectral indices: Application to natural disaster damage assessment. *Remote Sensing*, 12(17), pp.2681.

Rosselló, J., Becken, S. and Santana-Gallego, M., 2020. The effects of natural disasters on international tourism: A global analysis. *Tourism Management*, 79, pp.104080.

Samad, A., Erdiansyah, E. and Wulandari, R., 2020. Evaluation of government policies post-disaster: A case study of the disaster in Central Sulawesi. *Jurnal of Governance and Public Policy*, 9(1), pp.15–24.

Sun, L., Chang, J., Zhang, J., Fu, Z. and Zou, J., 2021. Evaluation of unmanned aerial vehicles' cooperative combat effectiveness based on conditional entropy combination weight method. *Journal of Systems Engineering and Electronics*, 13.

Teh, D. and Khan, T., 2021. Types, *Definition and Classification of Natural Disasters and Threat Level. Handbook of Disaster Risk Reduction for Resilience*. Springer, pp.27–56.

Wannewitz, S., Hagenlocher, M. and Garschagen, M., 2016. Development and validation of a sub-national multi-hazard risk index for the Philippines. *GI_Forum*, 1, pp.133–140.

Zhu, Y., Tian, D. and Yan, F., 2020. Effectiveness of entropy weight method in decision-making. *Mathematical Problems in Engineering*, 20, pp.1–5.

Waste to Wealth: An Approach Towards Sustainable Construction from Pollutants

Kasturima Das† [ID]**, Bikramjit Goswami** [ID] **and Girija T. R.**

Dept. of Civil Engineering, Assam Don Bosco University, Azara, Guwahati, Assam, India

†Corresponding author: Kasturima Das; kasturimadas@gmail.com

ABSTRACT

The global construction industry faces significant challenges related to environmental sustainability and resource scarcity. Researchers are increasingly exploring innovative approaches to repurpose waste materials, aiming to mitigate environmental pollution while producing value-added construction materials. This paper reviews the sustainability of current methodologies for synthesizing construction materials from pollutants, considering industrial by-products, post-consumer waste, and pollutants as potential feedstocks. The evaluation focuses on various recycling, upcycling, and bioconversion techniques, assessing their environmental and technical feasibility. The paper also discusses case studies of successful implementations and emerging trends in the field to highlight practical applications and future research directions. Ultimately, the paper advocates for sustainable practices in the construction sector by promoting a circular economy model, where waste is transformed into valuable resources, fostering wealth development.

INTRODUCTION

Sustainable construction improves the environment by consuming less energy and making less waste in buildings. This makes the industry more resilient, uses fewer natural resources, and requires less maintenance. The materials used in the construction of structures under sustainable construction take social, economic, and environmental factors into consideration (Zavadskas et al. 2018, Figueiredo et al. 2021). They are significant in energy consumption and environmental impacts with their emphasis on fire performance, environmental impact, and structural performance. So, environmentally sustainable and green construction methods help make the construction industry more sustainable.

Ecologically friendly building materials have several benefits. They reduce energy consumption, waste, and harmful impacts on public health and safety in environmental ways. They make the industry resilient and better at using local resources; besides, they are more durable (Danso 2018). Sustainable building materials help to reduce life-cycle costs and have lesser adverse environmental impacts, apart from helping to enhance building health and safety. They also help to reduce harm to humans, lessen the effect of climate change, create less solid waste, improve thermal comfort and flexibility, cause more use of local resources, create homes for all, and use less upkeep. Finally, they reduce the financial stress and economic impact on buildings by increasing energy efficiency (Sahlol et al. 2021).

Sustainable building materials provide an important means of cutting pollution and damage to the environment. Their advantages, therefore, far outweigh their disadvantages, which include greater energy consumption, costs, and resource stress; further problems include carbon emission and design regulation. Among the many advantages are a smaller carbon footprint, involvement with the people, economic

success, and resilience to climate change. Although there are disadvantages, including higher costs and the need for skilled labor, this would make construction project decisions more definite if these are realized in tandem with their advantages. Making sustainability a priority not only reduces ecological destruction but also leads to broader achievement of advancement toward a constructed environment that is more resilient and ecologically responsible (Porfiriev et al. 2017).

Research Gap: Currently, many housing corporations have shown tremendous promise in prioritizing sustainable construction. However, as a result of certain unavoidable requirements, be it skilled labor or complicated treatment processes involved with the usage of sustainable building products such as the acquirement of driftwood and chemical treatment of bamboo, construction projects become somewhat expensive, repelling both contractors as well as buyers from these initiatives. This calls for means of recycling waste in a way that not only saves and uplifts the environment but is also light on the pocket. The present study thus focuses on techniques that utilize plastic waste in a manner that not only reduces the landfill burden but also enhances structural stability as well as the strength of the constructed structure.

Objectives of the Study: Sustainable production of building materials from waste resources, like plastic, fly ash, and industrial by-products, by recycling through creative techniques like carbon capture and utilization constitutes a way of producing environmentally compatible substitutes from pollution. End products may be made by such creative techniques, which can be turned into strong and resource-efficient building components, thus reducing their footprint on the environment. The primary objectives of this investigation are

- To show the viability of turning waste resources into building materials that can be used.
- To illustrate the strength, resilience, and other important characteristics of materials synthesized from pollutants.
- To reduce the environmental pollution.

Impact of Sustainable Construction Materials on Building Resilience

Building resilience needs durability more than functional durability. Materials such as PVC increase vulnerability, enable stressor recovery, enhance environmental and life-cycle performance, and increase durability. This makes them resilient and constructive to all cities and helps in turning metropolitan areas into resilient cities. Since compressed plastic structural components are cheap and eco-friendly, they may significantly increase the earthquake resilience of a building due to their ability to insulate well against heat,

sound, and moisture. In addition to significantly affecting energy use and environmental impacts, sustainable building materials reduce the amount of waste generated, improve industrial resilience, and increase usability (Porfiriev et al. 2017, Marjaba & Chidiac 2016).

Building resilience is made possible through the use of sustainable building materials that include reclaimed wood, bamboo, recycled steel, and straw bales. These materials are durable, energy-efficient, and environmentally friendly, which makes the buildings very resilient against adverse weather conditions and natural disasters. Developers and engineers can make buildings resilient against natural disasters, climate change, and other hazards using these materials. These materials also promote the long-term sustainability of the built environment and are non-degradative, thus reducing the environmental impact of buildings. Such structures could be designed to adjust to environmental changes and remain usable and durable even after many decades. Incorporating resilience elements into sustainability programs helps reduce dependence on single sources of raw materials and the strategic location of the goods to reduce supply chain interruptions. In general, using sustainable building materials increases structural integrity, reduces the environmental impact, and brings about long-term sustainability, all of which increase building resilience (Satterthwaite et al. 2020).

Economic Advantages of Using Sustainable Construction Materials

Eco-friendly building materials are financially beneficial in many ways. Building materials of this nature have high productivity, high added value, and high resource efficiency in developing countries, which in turn promotes GDP development and economic growth. The building owner can enjoy an all-round long-term cost benefit because these reduce the life cycle costs of construction projects. They promote energy efficiency, which translates into reduced operating costs and electricity bills (Liu et al. 2020). Moreover, the use of sustainable materials serves to enhance the environment since it reduces the output of waste and carbon emissions, both of which enhance living and working conditions. Moreover, demand for properties made from sustainable building materials becomes higher since such materials attract eco-conscious renters and buyers (Eco-Tech Building Solutions 2024). This results in a higher market demand for and value of the property. Sustainable building materials make the property more marketable and attract higher levels of occupancy. Building owners and developers can reap monetary rewards through increased rental rates and property prices that come about

because of this enhanced marketability (Marchese et al. 2018).

Such government incentives, for instance, include grants and tax concessions, among others. For instance, corporations like the Indian Green Building Council (IGBC) and Green Rating for Integrated Habitat Assessment (GRIHA) have stepped up to encourage such sustainable construction trends. Certifications received from both these corporations help get significant tax rebates as high as 3% to 7% on building materials, thereby bringing down the construction cost together with improved marketability. Such financial incentives increase the financial advantages of using sustainable building materials as they nudge developers and constructors to adopt more sustainable techniques. In this regard, it is important to consider any possible disadvantages associated with using the materials, such as higher prices of purchase, limited supplies in specific areas, and peculiar installation requirements. These factors can slow building schedules and budgets. In addition, some of the sustainable materials have special handling, storage, or disposal requirements, making the building process complicated (Ivanov 2018). However, the long-term savings, energy efficiency, market demand, and government incentives of using these sustainable building materials make them financially sound to builders and developers. By using sustainable methods and resources, the building industry may help to ensure environmental sustainability and economic growth.

Key Characteristics of Sustainable Construction Materials

Ecologically responsible construction is anchored by important characteristics of sustainable building materials. Key aspects are recyclability, resilience, resource efficiency, and waste and emission reduction, with added social, economic, and environmental factors holistically. Wood is a prime example of a sustainable material due to its outstanding acoustical properties, thermal insulation, and good strength-to-weight ratio. In addition, since wood is renewable and recyclable, it helps the building industry reduce carbon emissions (Asdrubali et al. 2017). Sustainable materials improve environmental stewardship further by reducing energy consumption, maintaining structural integrity, increasing fire safety precautions, and, finally, leading to lower operating expenses.

Economic metrics related to the longevity of the materials, maintenance costs, and running costs are also important aspects in determining the viability of sustainable materials. Human toxicity, climate change, waste, flexibility, thermal comfort, and utilization of local resources are a few examples of essential environmental factors. Social factors, including housing for all, are also quite critical (Bhuiyan & Hammad 2023). Sustainable building materials should also surpass technical performance criteria, have an impact in environmental terms, show resource efficiency, and encompass the perspectives of the stakeholders. A multi-criteria decision-making technique should be adopted while selecting the materials to strike a balance between long-term sustainability and cost-effectiveness.

The use of sustainable construction materials has many benefits, among which some of the most important are waste minimization, environmental preservation, social responsibility, and rigorous technical specifications. Waste generation and related environmental harm can be dramatically minimized by construction techniques, which prioritize the use of materials with the lowest ecological footprint and optimize resource efficiency. Moreover, by contributing to healthier and more equitable societies by using sustainable materials, they respond to issues of social equality. Additionally, building sustainably will open the door to innovation and development in the construction industry since they are designed to meet very strict technical specifications. Building sustainably speaks of the beginning of a potential journey toward an even stronger and more ecologically aware future.

Pollution and Pollutants in the Environment

Pollution from various kinds of sources, including errors in disposing of waste, the emissions of traffic, and industrial pollutants, threatens the environment and public health. The discharge of toxic chemicals into the air, water, and soil brings about an ecological imbalance that will soon prove detrimental to health. The substances of pollution vary; they can be biodegradable substances like organic waste or permanent ones like heavy metals and plastic garbage. To tackle pollution, all-encompassing approaches are needed, including legislative actions, advancements in technology, and public education initiatives. By reducing waste, conserving resources, and embracing clean energy, sustainable behavior is an example that becomes essential in reducing the adverse consequences of pollution and preserving the environment for future generations.

Pollution is the discharge of harmful chemicals into the environment. Contaminants are the term we use for these harmful compounds. Some pollutants are naturally occurring, such as volcanic ash. Human activity can also cause them, like in the case of industry runoff or garbage. Pollutants are harmful to the quality of the air, water, and land (Ukaogo et al. 2020). Pollutants are the main source of environmental contamination; they may be classified into two categories:

biodegradable and non-biodegradable. Waste products that break down naturally without leaving behind any pollutants are known as degradable pollutants. Waste that is incapable of being broken down or destroyed by any biological activity is considered non-degradable pollution (Tian & Bilal 2020). On the basis of their persistence and rate of degradation, pollutant substances that humans have discharged into the environment are normally grouped into two broad categories: biodegradable and non-biodegradable (Wasi et al. 2013). Pollutants that are not biodegradable pose a threat to the environment. It is impossible to eradicate the majority of toxins from the environment, not even after billions of years. Reusing or recycling them to create new and valuable products might help eliminate this kind of non-biodegradable pollution.

Types of Pollutants

Biodegradable pollutants are those that can be metabolized by microorganisms, whether through chemical reactions induced in them or their disintegration. Some examples include certain chemicals such as some detergents and pesticides, as well as organic materials, such as sewage and food wastes. These contaminants will eventually become less harmful through biological processes inducing chemical reactions or degradation. However, they may degrade, and secondary products may be formed and, in doing so, may be just as dangerous in the end. Non-biodegradable pollutants include plastics, heavy metals such as lead and mercury, and some persistent organic pollutants like DDT (Mathew et al. 2017). These pollutants go through little biologically mediated processes and are laid down in the environment and bio-accumulated in species and increase in toxicity.

A multidimensional approach is required for such pollutants to be effectively controlled. This includes tight regulation, eco-friendly waste disposal techniques, advanced technology for pollution control, and public awareness campaigns to reduce the amount of pollution that originates (Al-Jebouri 2023). In addition, switching to more sustainable patterns of production and consumption is a need. This might ultimately reduce pollution and preserve the earth and all its inhabitants. Fig. 1 shows the difference between degradable and non-degradable pollutants. These variations highlight the serious environmental consequences of non-biodegradable pollutants, which have led to the development of new technologies for recycling non-biodegradable materials into useful products. This has the dual goals of reducing the pollution these hazardous pollutants cause to the environment and protecting the natural world for future generations.

Impact of Pollutants on Ecosystems

Pollutants pose a serious threat to ecosystems because they can upset the delicate balance and do much damage to the environment. Pollutants are a hazard, regardless of their biodegradability. Biodegradable environmental contaminants are easier to dispose of than non-biodegradable ones; an example of plastic, in particular, becomes a chronic hazard and is difficult to dispose of (Oberoi & Garg 2021). Because of inefficient manufacturing processes, improper disposal of garbage, and poor recycling processes, plastic, in particular, becomes a major hazard to ecosystems. The increasing availability of plastic refuse poses monstrous problems in waste management, especially in developing countries where populations are growing at a high rate. This is especially so in the case of plastic garbage that settles on land and in water (Godfrey 2019). Besides swamping the present waste management system, this plastic refuse befalls human beings and animals in ruin. Better waste management strategies, environmentally friendly production processes, and greater public knowledge are the ingredients of a global initiative to combat this hazard. The integrity of our ecosystems must be preserved for the betterment of our future generations, and we can only reduce the harmful effects of pollution by cooperating.

Pollution Management Strategies

Pollution control techniques must, therefore, have techniques that include removal, control, and prevention. Waste removal is one of the most crucial aspects of pollution control techniques. Waste management crews are very crucial to any municipality in terms of collection and disposal of residential waste. Separation of the garbage into degradable portions and those that are not is an important procedure at disposal grounds. Recyclable garbage is separated from non-degradable waste, such as bottles, plastics, and various products. Eggshells and other compostable waste are composted during the procedure. This systematic categorization helps ensure that resources are conserved and facilitates easier waste management. Moreover, it allows for material reuse and recycling in addition to waste management (Hoang et al. 2019). For instance, composting turns organic waste into organic compost that can enrich soil fertility and help with farming practices. Communities can significantly reduce the volume of waste they generate, which will help the environment and other generations to come to have a cleaner and healthier habitat.

The strategies required to control pollution in the environment

- Ensure effective garbage collection throughout municipalities. (Musella et al. 2019)
- Identify waste types, such as medical, electrical, or household (Reno 2015).
- Classify waste items as degradable or non-biodegradable (Alaudeen 2019).

- Degradable waste products have several applications, including fertilizer and residential consumption.
- Non-degradable garbage takes hundreds of years to disintegrate. As a result, the disposal of non-biodegradable garbage necessitates creativity and new technology, such as utilizing plastic to produce roads and construction materials (Subramanian 2019).

MATERIALS AND METHODS

The assessment plan of this study has been purely exploratory. The primary objective of this research study is to showcase the feasibility of altering waste materials into fully functional construction products without compromising on the strength and resilience characteristics of the same. In order to achieve this, the study mainly focuses on discarded plastic, which, when mixed with bitumen or sand, not only accommodates tonnes of the same but also enhances the strength parameters.

A thorough study was conducted reviewing the existing literature, conducting industrial visits and interviews with budding entrepreneurs of start-ups dealing with emerging technologies of ways and means to convert different types of non-biodegradable waste products be it glass or plastic, into valuable commodities. It was found in the survey that numerous types of daily wear commodities, be it textiles, shoes, carpets, toys, furniture, etc., get manufactured in bulk from waste plastic waste (Shuttleworth L., 2024). However, these products ended up back at the landfill sites within a very short period. Hence, the main focus of the study was to concentrate on products that were put well into use for a significant duration of time.

RESULTS AND DISCUSSION

Non-Degradable Pollutants

Non-biodegradable pollutants bring another factor to environmental unsustainability as they defeat the natural processes of degradation. Examples include plastics, heavy metals, and other synthetic substances that persist for many years in ecosystems. Hundreds of research studies have evidenced the consequences of their accumulation, which are very dangerous to the well-being of fauna and flora. Not only do these contaminants harm the soil and water bodies, but through the food chain, they also harm humans. Novel and new-age technologies are required to overcome this problem. Non-biodegradable pollutants are often unmanageable by common methods of waste management (Dharmasiri 2019). Novel approaches are required that range from thermal treatment and chemical degradation to bioremediation. To control the production and use of these contaminants,

stringent legislation and policies must be enforced. Solutions for overall development require the cooperation between different governmental, industrial, and research bodies. The protection of ecosystems and human health in future years will require society to find and implement workable solutions that mitigate the dangers non-biodegradable pollutants pose to the environment and human health.

Recycling of Non-Degradable Pollutants

Recycling non-biodegradable pollutants involves the conversion of persistent waste materials into some valuable commodities, hence reducing the environmental impact. The process depends on novel methods such as chemical degradation, thermal transformation, and biological attenuation in the conversion of pollutants into less toxic compounds or their repurposing to useful benefits. Advanced technology and sustainable practices are crucial for the management of these pollutants like plastics, heavy metals, and synthetic derivatives. By the side, supporting principles of circular economy, restricted use of single-use products, and strict regulations can aid in reducing the formation and accumulation of non-biodegradable pollutants (Burelo et al. 2023). Governments, industries, and research organizations need to collaborate in the establishment of viable recycling methods and the promotion of sustainable waste disposal. Supporting the recycling of non-biodegradable pollutants can reduce environmental degradation resource conservation, and protect the health of ecosystems and populations.

Conversion of Non-Degradable Pollutants to Useful Products

Methods that innovatively convert non-degradable pollutants into useful products include the conversion of non-degradable waste materials into reusable products. The techniques of chemical transformation, thermal treatment, and bioremediation break non-degradable pollutants into less harmful components or convert them into valuable products (Guzik et al. 2021). Many materials are known as Polymers, and at present, polymers are making a substantial contribution to our daily activities. Due to their widespread and regular use in numerous industries, polymer production and disposal increased tremendously over time. In that regard, however, polymeric wastes are heavier than organic wastes, and most of them do not degrade (Dwivedi et al. 2019). This is polymeric waste, which can be restored to full-use products as raw materials for the plastic industry, construction works, and recycled plastic products. The main component of sewage sludge ash is silty material with occasional sand-sized particles. It is a byproduct of dewatered sewage sludge burning in an incinerator. Large amounts of organic sludge are produced as a byproduct of

the treatment process as a result of the sewage treatment facilities' fast development. This massive amount of sludge is dried, ground into a powder, and utilized as a raw ingredient to make cement, which is used in concrete buildings (Lynn et al. 2015). Due to their stability, durability, and stress resistance in structures, plastic bottles are also utilized in the construction industry to create bricks and cement mixtures, among other materials (Dadzie et al. 2020).

Converted Products Used in the Construction Field

Products used in construction fields include a wide variety of materials that are necessary for constructing buildings and other infrastructure. These include wood, steel, concrete, and different composite materials made for certain uses. Concrete is a versatile and long-lasting construction material. Steel provides flexibility and strength, which are essential for structural frameworks. Wood is still an abundant resource that is used for flooring, finishing, and framing (Oyedele et al. 2014). Waste from many sources is being used to make a range of building materials. For example, post-consumer waste from households, companies, institutions, and industries is recycled and reused in construction. Examples of these materials 5 include plastic bags for plastic strips, which are commonly used on soil embankments, grounded polyethylene, and as a component of Trex and plastic lumber. Newsprint is used in cellulose insulation, wallpaper, asphalt road surfaces, and color boards. Additional recycled post-consumer goods include rubber tiles manufactured from unused tyres, wool insulation made from recycled textiles, ceiling boards made from recycled plastics, carpet, and carpet pads made from recycled post-consumer fabrics, and so on (Bolden et al. 2013). Waste from building projects may also be used to create new materials or components for other goods. Reducing the net quantity of waste produced by building operations is done effectively (Thomas et al. 2013). Fig 1 shows the classification of the recycled construction materials.

Different Construction Products from Different Pollutants

The construction industry's depletion of natural resources has increased research efforts to promote the use of recyclable waste items, such as scrap tires, as an alternative to non-renewable materials. Waste tires (whole tires, tire shreds, or tire chips) have many unique properties that are useful in engineering applications, particularly geotechnical engineering applications, such as low density, low earth pressure, good insulating properties, good drainage capability, long-term durability, and high compressibility. Tyre waste is used for concrete due to its strength, chloride resistance, and sound barrier (Mashiri et al. 2015).

Rapid changes in equipment production have reduced electronic product costs, leading to consumers discarding old products and embracing new technology. This has resulted in a substantial volume of electronic garbage, which includes computers, mobile phones, televisions, printers, laptops, and home appliances, and is expanding at approximately three times the rate of the global population (WHO 2023). Plastic is one of the most common materials used in electrical gadgets, accounting for around 21% (Kumar et al. 2018). Waste glass material cut from electronic-grade glass strands was utilized as fine aggregate in concrete. Recently, asphalt binders were experimentally changed using electronic waste from recovered computer plastics to increase asphalt binder performance vs standard asphalt binders, and waste printed circuit board powder was employed as an additive in cement mortar (Paul & Gnanendran 2016, Kumar & Bhaskar 2015). Waste plastic bags are used to substitute cement in the manufacturing of building bricks and concrete blocks. Incorporating plastics into concrete blocks not only ensures safe disposal but may also increase concrete qualities such as tensile strength, chemical resistance, drying shrinkage, and creep (Abdel Tawab et al. 2020). Instead of using cement, plastic waste is used to make roof tiles. To make roof tiles, a combination of river sand and polyethylene terephthalate (PET) plastic is utilized. The gained characteristics are marginally superior to those of regular cement (Bamigboye et al. 2019).

Role of Engineering in the Conversion

The creation of waste is an unavoidable byproduct of human activity. Engineering takes care of the transformation of non-biodegradable pollutants into building materials, for example, by designing new technologies for resource recovery and valorization of waste (Bala et al. 2022). Thus, waste materials such as plastics, industrial wastes, and sewage sludge can be changed into high-value products like aggregates, composites, and bricks. Advanced technologies, such as pyrolysis, hydrothermal carbonization, and chemical conversion, are used in this conversion. Engineers design these processes in such a way that they are environmentally friendly, scalable, and effective. These processes are optimized by using innovative catalysts, reactors, and purifying techniques and, at the same time, convert the highest possible amount of waste and have the lowest possible consumption of energy and emissions. Additionally, engineers calculate life cycle analyses to aid in environmentally responsible decision-making and environmental impact assessment of these products (Peng et al. 2023). With technical knowledge, society can increase the demand for building materials in an environmentally sustainable and circular manner.

Used in/as entirely New Product   Used in/as similar Product in New forms

Post Consumer Waste

e.g   e.g

- Grounded Polythene from Plastic Bags
- Wool Insulation from recycled fabrics/clothing
- Cellulose insulation from recycled newsprints

- Rubber tiles from scrap tires
- Wallpaper from newsprint
- Plastic strips and trex lumbers from plastic

Sources of Recycled Construction Products

- Coal fly ash as cement constituents
- Roof shingles cut off, used in hot mixed asphalt
- Granulated Ground Blast Furnace in concrete

- Construction debris as aggregates
- Chip and particle board from used timber
- Used bricks/blocks as aggregate mix

Pre-Consumer Waste   **Construction Generated Waste**

Fig. 1: Recycled construction material classification.

Adopting the 3R concept (Reduce, Reuse, and Recycle), as supported by well-known international organizations, is a strategic step toward environmentally friendly waste management techniques. A lot of emphasis on reduction, reuse, and recycling increases not only waste reduction but also the growth of a circular economy. This approach has enormous promise because it focuses on the use of cleaner manufacturing techniques and the valorization of wastes, which, in other words, means the process of the transformation of thrown-away resources into useful materials and energy sources. The garbage valorization approach is the process of converting waste into useful goods, including materials, fuels, and chemicals. It is a critical step towards minimizing the environmental impact of waste with creativity and resource efficiency (Abdel-Shafy & Mansour 2018). Resource recovery of energy, materials, or products is an integral part of tertiary and quaternary recycling. From this angle, one of the important avenues for resource recovery from plastic waste is the thermolysis of thermoplastics. In a chain reaction that involves the processing of low molecular weight molecules, thermolysis sets off a process that is of paramount importance in this regard. Three principal methods can be considered in the development of this chain reaction: pyrolysis, hydrocracking, and gasification. Pyrolysis involves the decomposition of materials through high temperatures without oxygen. Hydrocracking involves the use of hydrogen to break down large molecules into smaller ones (Okan et al. 2019). Gasification converts materials into synthesis gas, opening a range of flexible

applications. From these perspectives, the effectiveness of the thermolysis technology in mitigating the problems presented by plastic waste is based on these approaches.

The base processes in which the working of this technology is based are three basic processes in thermolysis: gasification, hydrocracking, and pyrolysis. These processes can break down large molecular long-chain polymers into goods suitable for high-temperature building applications (Zhang et al. 2021). Pyrolysis breaks organic material, in the absence of oxygen, into biochar and bio-oil. Hydrocracking uses hydrogenation and converts the heavier hydrocarbons into simpler ones to produce diesel and gasoline. Carbonaceous materials are gasified to produce synthesis gas that is a flexible fuel precursor. All these, when combined, provide creative ways to use resources sustainably and make it easier to produce the materials needed for high-temperature building requirements.

CASE STUDIES

Case Study 1 - Plastic Roads

Waste management efforts in Kerala provide a challenge to the environment and human health, particularly with the usage of plastic rubbish. The state government has introduced new measures, one of which is the creation of roadways through recycled plastic material for garbage management and infrastructure development. The Public Works Department took an important step by re-laying portions

of several roads in the Thiruvananthapuram district with a combination of plastic garbage and asphalt. This brings two advantages together: It recycles spent plastic, and the road becomes stronger and longer-lasting. The PWD has entered into a tie-up with the Clean Kerala Company Ltd, which is a state enterprise responsible for plastic garbage collection, to feed this eco-friendly road construction exercise across the state. This tie-up will buy an additional 15 tons of plastic granules in a month and will show a concerted attempt to use more recycled material in infrastructure activities. Kerala is taking positive steps to undo plastic pollution and enhance infrastructure at the same time through cooperation between government agencies and creative applications. This green approach shows the resolve of the state to protect the environment and the people's welfare.

The CKC is the state's principal agency for processing plastic waste. It carefully collects all plastic waste, including carry bags and other plastic materials, from all sources. These polymers are broken into granules. While the bigger plastics are sold to CKC, those smaller than 50 microns, which are unfit for standard recycling, are processed by combining with bitumen to enhance road construction. Presently, the CKC buys granulated plastics from thousands of places in Kerala at Rs. 15 per kilogram. The agency, therefore, sells these shredded plastic granules to the contractors at a little higher price of Rs. 20 per kilogram. The contractors utilize the granules, in addition to asphalt, to build roads. About 1,700 kg of plastic waste is used to create one kilometer of road, which helps in long-term infrastructure development and helps in effectively resolving plastic pollution issues. The unique partnership of government entities like the Public Works Department and Clean Kerala Company Ltd in the state of Kerala gives an example of an aggressive strategy for reducing plastic pollution and improving the infrastructure. This use of recovered plastic in road building outlines a sustainable solution to environmental and public health issues and sets a good example for others (Gupthan 2017).

Case Study 2 - Bricks from Plastics

There have been numerous steps taken in the last few years toward the conversion of plastic garbage into valuable resources, primarily in highly developed countries. There is, however, a potential path for the creation of new building materials based on plastic waste, as the construction sector dominates most nations and uses enormous amounts of raw material. Recent reports stated that there are advances in combinations of plastic with sand, which are applied for the manufacturing of plastic sand bricks. These, together with further civil engineering applications of these innovative building materials, are very exciting. The composition of plastic sand bricks is fifty-five to sixty-five percent of the weight of plastic sand bricks, plastic comprises twenty-nine to thirty-nine percent, and there are also crushed glass bottles and paper shredded at one percent and five percent, respectively. Interestingly, each brick uses approximately 250 grams of plastic, so the production of bricks involves a significant reduction in plastic pollution. For instance, 2,50,000 kg of plastic garbage will be used to make 10,000 bricks. The approach is not only an urgent answer to the need to decrease plastic pollution but also ensures long-term satisfaction of the needs of the construction industry. The use of plastic sand bricks means a change of thinking in favor of the circular economy, which transmits trash into valuable resources. Besides, they contribute to a reduction in environmental degradation and the preservation of natural resources so that, in the ever-continuing global effort to decrease the levels of plastic pollution and move toward a more resilient, resource-efficient future, they become an innovation and sustainability beacon (Ursua 2019).

The innovative use of recycled plastic bottles in construction as building bricks holds a sustainable solution in multiple ways. The bricks have superior attributes than regular bricks, including reduced thickness and weight, good heat and noise insulation, and an equal strength and durability of traditional materials. In turn, only 20 plastic bottles are needed to make one brick, therefore limiting the amount of plastic waste to be seen in the environmental landscape while consuming less energy than the other recycling methods. Manufacturing them is easy without washing, sorting, or adhesives, hence easing the production process and also creating less stress on the environment. Other than structural applications, plastic bricks can be used for wall fillers, fences, and non-load-bearing walls with proper insulation properties and practicality in building construction. This creative method solves ecological issues without forgetting to depict the possibility of converting trash into useful building material. This creative method solves ecological issues without forgetting how garbage can be turned into useful building material (Lois Zoppi 2019).

LIMITATIONS OF THE STUDY

The main emphasis of the current study is on the product that could be curated/recycled from discarded plastic waste and is not much concerned with its particular types such as LDPE, HDPE, PVC, PET, etc. It does not focus much on the pros and cons of the segregated plastic types and whether they can be clubbed together for recycling.

CONCLUSIONS

In conclusion, it is possible to satisfy the demands for

infrastructure while also improving the environment by using a sustainable method of turning rubbish into construction materials. The use of garbage reduces the destabilizing effects of trash collision on ecosystems and human health by recycling waste to useful sources. It also saves exhausted natural resources and sustainability for a long time. Advanced and state-of-the-art technologies such as carbon capture and utilization make them turn pollutants into high-quality building materials that are safe and efficient. Adopting this pattern shift would make everyone embrace a circular economy model in which trash is considered a source of wealth instead of waste. In addition, the massive use of environmentally friendly building materials pressures many industrial actors to make eco-friendly procedures a priority. This leads to a change in the model of systemic change in the direction of a greener future. An integrated effort between policymakers, academics, and business people is a cardinal virtue that must be done to encourage advances and overcome current hurdles. Ultimately, we would be able to build robust infrastructure in the presence of a beneficial environment for the next generation if we incorporate sustainability into material synthesis processes. This review centers on the need to move toward a circular economy ideology, wherein waste should be considered an asset and not something that should be removed to contribute toward a more successful and green society.

IMPLICATIONS FOR FUTURE RESEARCH

Plastic Bricks that are currently manufactured are typically used for road pavements, footpaths, residential compounds, etc. So far, there has been very minimal research when it comes to manufacturing construction units/blocks that can be used to replace RCC in terms of strength and durability. Thorough research can be done on the same based on such plastic bricks that can be well utilized for building construction. Such an innovation will not only curb the current scenario of plastic pollution but will also lead to earthquake-resilient and affordable housing globally.

REFERENCES

Abdel-Shafy, H.I. and Mansour, M.S., 2018. Solid waste issue: Sources, composition, disposal, recycling, and valorization. *Egyptian Journal of Petroleum*, 27(4), pp.1275-1290.

Abdel Tawab, O.F., Amin, M.R., Ibrahim, M.M., Abdel Wahab, M., Abd El Rahman, E.N., Hassanien, R.H., Hatem, M.H. and Ghaly, A.E., 2020. Recycling waste plastic bags as a replacement for cement in the production of building bricks and concrete blocks. *Journal of Waste Resources and Recycling*, 1(2), p.202.

Al-Jebouri, M.M., 2023. Modelings of infectious diseases and cancers under wars and pollution impacts in Iraq with reference to a novel mathematical model and literature review. Open Journal of Pathology, 13(3), pp.126-139.

Alam Bhuiyan, M.M. and Hammad, A., 2023. A hybrid multi-criteria decision support system for selecting the most sustainable structural material for multistory building construction. *Sustainability*, 15(4), p.3128.

Alaudeen, S.S., 2019. Degradable and Non-Degradable Waste Separation Using Intelligent Approach. *International Journal of Emerging Technology and Innovative Engineering*, 5(5).

Asdrubali, F., Ferracuti, B., Lombardi, L., Guattari, C., Evangelisti, L. and Grazieschi, G., 2017. A review of structural, thermo-physical, acoustical, and environmental properties of wooden materials for building applications. *Building and Environment*, 114, pp.307-332.

Bala, S., Garg, D., Thirumalesh, B.V., Sharma, M., Sridhar, K., Inbaraj, B.S. and Tripathi, M., 2022. Recent strategies for bioremediation of emerging pollutants: a review for a green and sustainable environment. Toxics, 10(8), p.484.

Bamigboye, G.O., Ngene, B.U., Ademola, D. and Jolayemi, J.K., 2019, December. Experimental study on the use of waste polyethylene terephthalate (PET) and river sand in roof tile production. *Journal of Physics: Conference Series*, 1378, p 042105.

Bolden, J., Abu-Lebdeh, T. and Fini, E., 2013. Utilization of recycled and waste materials in various construction applications. *American Journal of Environmental Science*, 9(1), pp.14-24

Burelo, M., Hernández-Varela, J.D., Medina, D.I. and Treviño-Quintanilla, C.D., 2023. Recent developments in bio-based polyethylene: Degradation studies, waste management and recycling. *Heliyon*, 9(11).

Dadzie, D.K., Kaliluthin, A.K. and Kumar, D.R., 2020. Exploration of waste plastic bottles use in construction. *Civil Engineering Journal*, 6(11), pp.2262-2272.

Danso, H., 2018. Identification of key indicators for sustainable construction materials. *Advances in Materials Science and Engineering*, 2018, pp.1-7.

Dharmasiri, L.M., 2019. Waste management in Sri Lanka: challenges and opportunities. *Sri Lanka Journal of Advanced Social Studies*, 9(1), pp.72-85.

Dwivedi, P., Mishra, P.K., Mondal, M.K. and Srivastava, N., 2019. Non-biodegradable polymeric waste pyrolysis for energy recovery. *Heliyon*, 5(8), p.654.

Eco-Tech Building Solutions 2024. Why Contractors Are Choosing Sustainable Materials. Available at https://ecotechnology.ca/blogs/featured-posts-1/building-green-why-contractors-are-choosing-sustainable-materials. Accessed on 16 Jan 2025.

Figueiredo, K., Pierott, R., Hammad, A.W. and Haddad, A., 2021. Sustainable material choice for construction projects: A Life Cycle Sustainability Assessment framework based on BIM and Fuzzy-AHP. *Building and Environment*, 196, p.107805.

Godfrey, L., 2019. Waste plastic, the challenge facing developing countries—ban it, change it, collect it? *Recycling*, 4(1), p.3.

Gupthan, M., 2017. Kerala Hits the Plastic Road! Available at https://www.onmanorama.com/news/kerala/kerala-hits-the-plastic-road.html. Accessed on 16 Jan 2025.

Guzik, M.W., Nitkiewicz, T., Wojnarowska, M., Sołtysik, M., Kenny, S.T., Babu, R.P., Best, M. and O'Connor, K.E., 2021. A robust process for high-yield conversion of non-degradable polyethylene to a biodegradable plastic using a chemo-biotechnological approach. *Waste Management*, 135, pp.60-69.

Hoang, T.C., Black, M.C., Knuteson, S.L. and Roberts, A.P., 2019. Environmental pollution, management, and sustainable development: Strategies for Vietnam and other developing countries. *Environmental Management*, 63, pp.433-436.

Ivanov, D., 2018. Revealing interfaces of supply chain resilience and sustainability: a simulation study. International Journal of Production Research, 56(10), pp.3507-3523.

Liu, Z.J., Pypłacz, P., Ermakova, M. and Konev, P., 2020. Sustainable construction as a competitive advantage. *Sustainability*, 12(15), p.5946.

Lois Zoppi, B.A., 2019. Turning plastic waste into building materials. Available at https://www.azobuild.com/article.aspx?ArticleID=8308. Accessed on 16 Jan 2025

Lynn, C.J., Dhir, R.K., Ghataora, G.S. and West, R.P., 2015. Sewage sludge ash characteristics and potential for use in concrete. *Construction and Building Materials*, 98, pp.767-779.

Marchese, D., Reynolds, E., Bates, M.E., Morgan, H., Clark, S.S. and Linkov, I., 2018. Resilience and sustainability: Similarities and differences in environmental management applications. *Science of the Total Environment*, 613, pp.1275-1283.

Marjaba, G.E. and Chidiac, S.E., 2016. Sustainability and resiliency metrics for buildings: Critical review. *Building and Environment*, 101, pp.116-125.

Mashiri, M.S., Vinod, J.S., Sheikh, M.N. and Tsang, H.H., 2015. Shear strength and dilatancy behavior of sand–tyre chip mixtures. *Soils and Foundations*, 55(3), pp.517-528.

Mathew, B.B., Singh, H., Biju, V.G. and Krishnamurthy, N.B., 2017. Classification, source, and effect of environmental pollutants and their biodegradation. Journal of Environmental Pathology, Toxicology and Oncology, 36(1).

Musella, G., Agovino, M., Casaccia, M. and Crociata, A., 2019. Evaluating waste collection management: the case of macro-areas and municipalities in Italy. *Environment, Development and Sustainability*, 21, pp.2857-2889

Oberoi, G. and Garg, A., 2021. Single-use plastics: A roadmap for sustainability? *Supremo Amicus*, 24, p.585

Okan, M., Aydin, H.M. and Barsbay, M., 2019. Current approaches to waste polymer utilization and minimization: A review. *Journal of Chemical Technology & Biotechnology*, 94(1), pp.8-21.

Oyedele, L.O., Ajayi, S.O. and Kadiri, K.O., 2014. Use of recycled products in UK construction industry: An empirical investigation into critical impediments and strategies for improvement. *Resources, Conservation and Recycling*, 93, pp.23-31

Paul, D.K. and Gnanendran, C.T., 2016. Characterization of lightly stabilized granular base materials using monotonic and cyclic load flexural testing. *Journal of Materials in Civil Engineering*, 28(1), p.04015074.

Peng, X., Jiang, Y., Chen, Z., Osman, A.I., Farghali, M., Rooney, D.W. and Yap, P.S., 2023. Recycling municipal, agricultural and industrial waste into energy, fertilizers, food and construction materials, and economic feasibility: A review. *Environmental Chemistry Letters*, 21(2), pp.765-801.

Porfiriev, B.N., Dmitriev, A., Vladimirova, I. and Tsygankova, A., 2017. Sustainable development planning and green construction for building resilient cities: Russian experiences within the international context. *Environmental Hazards*, 16(2), pp.165-179.

Reno, J., 2015. Waste and waste management. *Annual Review of Anthropology*, 44, pp.557-572.

Sahlol, D.G., Elbeltagi, E., Elzoughiby, M. and Abd Elrahman, M., 2021. Sustainable building materials assessment and selection using system dynamics. *Journal of Building Engineering*, 35, p.101978.

Satterthwaite, D., Archer, D., Colenbrander, S., Dodman, D., Hardoy, J., Mitlin, D. and Patel, S., 2020. Building resilience to climate change in informal settlements. *One Earth*, 2(2), pp.143-156.

Senthil Kumar, K., Premalatha, P.V., Baskar, K., Sankaran Pillai, G. and Shahul Hameed, P., 2018. Assessment of radioactivity in concrete made with e-waste plastic. *Journal of Testing and Evaluation*, 46(2), pp.574-579.

Senthil Kumar, K. and Baskar, K., 2015. Recycling of E-plastic waste as a construction material in developing countries. *Journal of Material Cycles and Waste Management*, 17, pp.718-724.

Shuttleworth, L., 2022. 26 Innovative Recycled Plastic Products to Inspire You. *ClimateSort*. Available at https://climatesort.com/recycled-plastic-products/ Accessed on 16 Jan 2025.

Subramanian, M.N., 2019. *Plastics Waste Management: Processing and Disposal*. John Wiley & Sons.

Thomas, C., Cimentada, A., Polanco, J.A., Setién, J., Méndez, D. and Rico, J., 2013. Influence of recycled aggregates containing sulfur on properties of recycled aggregate mortar and concrete. *Composites Part B: Engineering*, 45(1), pp.474-485.

Tian, K. and Bilal, M., 2020. Research progress of biodegradable materials in reducing environmental pollution. *Abatement of Environmental Pollutants*, 16, pp.313-330.

Ukaogo, P.O., Ewuzie, U. and Onwuka, C.V., 2020. *Environmental Pollution: Causes, Effects, and the Remedies*. Elsevier, pp. 419-429.

Ursua, J.R.S., 2019. Plastic wastes, glass bottles, and paper: Eco-building materials for making sand bricks. *Journal of Natural Allied Sciences*, 3(1), pp.46-52.

Wasi, S., Tabrez, S. and Ahmad, M., 2013. Toxicological effects of major environmental pollutants: an overview. *Environmental Monitoring and Assessment*, 185, pp.2585-2593.

World Health Organization (WHO) n.d. Electronic waste (e-waste) Available at https://www.who.int/news-room/fact-sheets/detail/electronic-waste-(e-waste) Accessed date 16 Jan 2025.

Zavadskas, E.K., Šaparauskas, J. and Antucheviciene, J., 2018. Sustainability in construction engineering. *Sustainability*, 10(7), p.2236.

Zhang, F., Zhao, Y., Wang, D., Yan, M., Zhang, J., Zhang, P., Ding, T., Chen, L. and Chen, C., 2021. Current technologies for plastic waste treatment: A review. *Journal of Cleaner Production*, 282, p.124523.

Isolation of Freshwater Algae from Some Reservoirs of Chiang Mai Rajabhat University, Mae Rim Campus, Chiang Mai

Pongpan Leelahakriengkrai[1,2,†] [iD]**, Phitsanuphakhin Chaimongkhon[1,2]** [iD] **and Tatporn Kunpradid[1,2]** [iD]

[1]Department of Biology, Faculty of Science and Technology, Chiang Mai Rajabhat University, Chiang Mai, Thailand
[2]Centre of Excellence of Biodiversity Research and Implementation for Community, Faculty of Science and Technology, Chiang Mai Rajabhat University, Chiang Mai, Thailand
†Corresponding author: Pongpan Leelahakriengkrai; pongpan_lee@cmru.ac.th

ABSTRACT

A study on the biodiversity and isolation of freshwater algae from some reservoirs of Mae Rim Campus, Chiang Mai Rajabhat University, Chiang Mai Province, collected algal samples and assessed the water quality at four reservoirs, including Wiang Bua Reservoir, Ma Lang Por Reservoir, Education Auditorium reservoir, and Kru Noi Garden Reservoir. One hundred and six species of algae belonging to 8 phyla were found. The most prominent species were *Cylindrospermopsis philippinensis, Trachelomonas volvocina, Peridiniopsis* sp.*,* and *Coelastrum astroideum*, respectively. The overall water quality was categorized as clean according to some physical and chemical parameters by the National Environmental Board of Thailand. However, high BOD values were detected at some sampling points. The algae isolation included 8 isolates, which could be utilized for various purposes in the future, such as biomass, protein, polysaccharide energy, bioactive compounds, antioxidant substances, wastewater treatment, environmental indicators, algal toxins, and phylogenetic studies. All strains were stored at the Centre of Excellence of Biodiversity Research and Implementation for Community, Chiang Mai Rajabhat University, for conservation and future development purposes.

INTRODUCTION

A study on the diversity of algae at Chiang Mai Rajabhat University, Mae Rim Campus, was initiated from 2012 to 2014 (Leelahakriengkrai & Kunpradid 2014, Supahan et al. 2017) revealed a remarkable array of algae in the water resources on the campus. This study identified diverse groups of algae, showcasing a rich biological diversity that can be applied in various applications. The utilization strains as *Scenedesmus* sp. and *Desmodesmus* sp., demonstrated significant bioactivity by extracting bioactive compounds that inhibit virus and bacteria growth (Singab et al. 2018, Ehsani et al. 2023). Moreover, *Botryococcus* spp. emerged as a promising source of hydrocarbon compounds, showcasing potential applications in alternative energy production (Furuhashi et al. 2022).

Several other algal species were various applications, such as bioindicators for water quality and responding to climate change (Giao & Nhien 2020, Barinova & Alster 2021, Tewari 2022, Alombro et al. 2023). Moreover, some groups of freshwater algae can produce toxins such as microcystins and cylindrospermopsin. These toxins are produced by blue-green algae and can be harmful to living organisms, particularly by impacting liver cells (Scoglio 2018, Ziesemer et al. 2022).

At present, the Mae Rim Campus of Chiang Mai Rajabhat University is undergoing extensive construction, including new buildings, roads, and other facilities for academic activities and services. Excavation of various water resources

in the area will intensify for future water consumption. However, these water sources have been impacted by the increased activities, as some of them are designated to receive water from various operations. These activities have resulted in alterations to water quality and the distribution of algae. Therefore, it is essential to consistently monitor the water quality and biodiversity of living organisms, especially among aquatic ecosystem producers. This monitoring is crucial to illustrate data on dispersion and changes from the past to the present, as it may impact the conservation of beneficial algal strains. Consequently, there is an urgent need for the isolation and preservation of algae from water resources, aiming to conserve the algal strains in culture collection for future application. Furthermore, this aligns with the Plant Genetic Conservation Project under the royal initiative of Her Royal Highness Princess Maha Chakri Sirindhorn on the resource-based and sustainable utilization of algae.

MATERIALS AND METHODS

The Study Sites

The study sites were chosen from four important Chiang Mai Rajabhat University, Mae Rim Campus reservoirs. The four sites include Wiang Bua Reservoir (WB), Ma Lang Por Reservoir (MP), Education Auditorium Reservoir (ED) and Kru Noi Garden Reservoir (KN) which is located in the Mae Rim Campus of Chiang Mai Rajabhat University, Chiang Mai Province, Thailand (Fig. 1) during July 2022

(rainy season), December 2022 (cool, dry season) and May 2023 (summer).

The Physical and Chemical Properties of Water

The water samples were collected from the surface of the reservoirs, focusing on their physical and chemical properties according to the standard methods outlined in the Standard Methods for the Examination of Water and Wastewater (2017). The parameters measured included water temperature and air temperature, transparency, pH, conductivity, total dissolved solids, dissolved oxygen (DO), Biochemical oxygen demand (BOD), nitrate nitrogen, ammonium nitrogen, and orthophosphate. Differences in the physical and chemical properties of water among sampling sites were assessed using analysis of variance (ANOVA) and the Least Significant Difference (LSD) test. Water quality was evaluated by comparing it to surface water quality standards established by the National Environmental Board Thailand (Simachaya 2000).

Algal Diversity Study

Phytoplankton samples were collected from the surface water in the area with the greatest depth of the reservoir. Water samples of approximately 10 L in volume were obtained and filtered through a plankton net with a mesh size of 10 μm. The filtered phytoplankton samples were then placed into sample bottles. Samples of attached algae were gathered by inspecting different substrate materials, including stones, hard surfaces like aquatic plants, and artificial substrates,

Fig.1: Aerial photograph of Mae Rim Campus of Chiang Mai Rajabhat University and 4 sampling sites including Wiang Bua Reservoir (WB), Ma Lang Por Reservoir (MP), Education Auditorium Reservoir (ED) and Kru Noi Garden Reservoir (KN).

Table 1: Results of the physical and chemical factors of 4 sampling sites at Mae Rim Campus of Chiang Mai Rajabhat University (n=3).

Sampling sites	Air Temperature [°C]	Water Temperature [°C]	Transparency [cm]	Turbidity [NTU]	pH	Conductivity [μs/cm⁻¹]	TDS [mg.L⁻¹]	DO [mg.L⁻¹]	BOD [mg.L⁻¹]	NO_3^--N [mg.L⁻¹]	NH_4^+-N [mg.L⁻¹]	SRP [mg.L⁻¹]
WB-Jul	33.0±0.0	31.0±0.0	44.0±1.0[d]	30.0±1.0[d]	8.54±0.06[f]	136.00±2.00[c]	80.33±1.53[c]	6.07±0.12[b]	2.20±0.00[de]	nd	0.68±0.08[de]	0.010.00+[ab]
WB-Dec	30.0±0.0	31.0±0.0	59.0±0.0[e]	35.0±1.0[e]	8.01±0.09[cd]	127.67±1.53[b]	73.00±1.00[b]	6.67±0.12[d]	2.00±0.00[cd]	nd	0.18±0.02[a]	nd
WB-May	34.0±0.0	33.0±0.0	21.0±0.0[b]	137.0±3.0[i]	8.63±0.02[f]	103.88±2.69[a]	67.26±2.15[a]	6.27±0.12[c]	2.40±0.20[e]	nd	0.68±0.08[de]	0.08±0.02[d]
MP-Jul	33.0±0.0	31.0±0.0	81.0±1.0[i]	17.0±1.0[a]	7.98±0.03[cd]	234.33±1.53[i]	143.66±1.00[i]	5.00±0.00[a]	4.10±0.10[h]	nd	0.64±0.01[cd]	0.02±0.00[bc]
MP-Dec	31.0±0.0	30.0±0.0	30.0±1.0[c]	41.0±1.0[f]	7.89±0.09[c]	176.00±1.00[f]	96.33±0.58[e]	7.33±0.12[e]	2.80±0.00[f]	nd	0.21±0.04[a]	0.19±0.02[e]
MP-May	35.0±0.0	33.0±0.0	68.0±1.0[g]	27.0±1.0[c]	8.06±0.12[d]	149.04±3.92[e]	86.66±1.53[d]	6.13±0.12[bc]	1.90±0.10[c]	0.8±0.3[b]	0.67±0.06[de]	0.09±0.00[d]
ED-Jul	32.0±0.0	31.0±0.0	15.0±0.0[a]	110.0±2.0[h]	7.98±0.03[cd]	144.00±1.00[d]	82.00±1.00[c]	8.00±0.00[f]	3.50±0.10[g]	0.9±0.1[bc]	0.54±0.08[c]	0.02±0.00[bc]
ED-Dec	32.0±0.0	30.0±0.0	107.0±2.0[j]	15.0±1.0[a]	7.56±0.10[b]	234.66±0.58[i]	134.66±0.58[h]	5.00±0.00[a]	0.40±0.00[a]	1.4±0.2[d]	0.19±0.04[a]	0.01±0.00[ab]
ED-May	33.0±0.0	34.0±0.0	60.0±1.0[e]	37.0±2.0[e]	7.42±0.14[a]	245.21±4.89[j]	144.33±2.08[i]	5.13±0.12[a]	1.30±0.20[b]	0.3±0.2[a]	0.66±0.08[de]	0.09±0.01[d]
KN-Jul	32.0±0.0	31.0±0.0	70.0±1.0[h]	15.0±0.0[a]	8.38±0.08[e]	183.66±1.53[g]	104.00±2.65[f]	9.07±0.12[g]	5.50±0.10[i]	1.10.2+[c]	0.37±0.04[b]	0.01±0.00[ab]
KN-Dec	32.0±0.0	30.0±0.0	64.0±1.0[f]	20.0±0.0[b]	7.89±0.07[c]	174.00±1.00[f]	102.00±1.00[f]	6.60±0.00[d]	1.80±0.00[c]	nd	0.14±0.02[a]	0.03±0.02[c]
KN-May	35.0±0.0	34.0±0.0	29.0±1.0[c]	53.0±4.0[g]	7.98±0.06[cd]	188.77±4.72[h]	121.00±4.00[g]	6.07±0.12[b]	2.00±0.20[cd]	nd	0.76±0.04[f]	0.09±0.01[d]

Notes: Values expressing the Mean±SD followed by similar letters in a column do not differ significantly at p<0.05

*nd = not detected

Table 2: Taxonomic categories and distribution of freshwater algae of 4 sampling sites of Chiang Mai Rajabhat University, Mae Rim Campus in July 2022 (rainy season), December 2022 (cool dry season) and May 2023 (summer).

Species lists	WB	MP	ED	KN
Phylum Chlorophyta				
Ankistrodesmus arcuatus	-/-/-	+/-/-	-/-/+	-/-/-
Ankistrodesmus densus	+/-/-	-/-/-	-/-/-	+/-/+
Ankistrodesmus fusiformis	-/-/-	-/-/-	-/-/-	+/-/-
Actinastrum hantzschii	-/-/-	+/-/-	-/-/-	-/-/-
Coelastrum astroideum	+/+/+	+/-/+	+/-/-	*/*/+
Coelastrum microsporum	-/-/-	-/-/-	+/-/+	-/-/-
Coelastrum reticulatum	-/-/-	-/-/-	+/-/-	-/-/-
Coelastrum sp.1	-/-/-	-/+/-	-/-/-	-/-/-
Coelastrum sp.2	-/-/-	-/-/-	-/+/-	-/-/-
Chlorella sp.	-/-/-	+/-/-	+/-/-	+/-/-
Chlorococcum sp.	+/-/-	-/-/-	-/-/-	+/-/-
Dictyosphaerium ehrenbergianum	-/-/-	-/+/-	-/-/-	-/-/-
Dictyosphaerium sp.	-/-/-	-/-/-	-/-/-	+/-/-
Didymocystis sp.	-/-/-	-/-/+	-/-/-	-/-/+
Desmodesmus armatus	+/+/-	-/-/-	-/-/-	-/+/-
Desmodesmus dispar	+/-/-	-/-/-	-/-/-	-/-/-
Desmodesmus hystrix	-/-/-	-/-/-	-/-/-	-/+/-
Desmodesmus perforates	-/-/-	-/+/-	-/+/-	-/-/-
Desmodesmus communis	+/-/-	-/+/-	-/+/+	-/-/-
Desmodesmus opoliensis var. *alatus*	+/-/-	-/-/-	-/+/-	-/-/-
Eudorina elegans	-/-/-	-/-/-	-/-/-	+/-/-
Kirchneriella aperta	-/-/-	+/-/-	-/-/-	-/-/-
Golenkinia sp.	+/-/-	-/-/-	-/-/-	-/-/-
Nephrocytium sp.	-/-/-	-/-/-	+/-/-	-/-/-
Micractinium pusillum	-/-/-	-/-/-	-/+/-	-/-/-
Monoraphidium controtum	*/+/-	-/-/-	-/-/-	*/-/-
Monoraphidium griffithii	-/+/-	-/-/-	-/-/-	-/-/-
Monoraphidium tortile	+/-/-	-/-/-	-/-/-	-/-/-
Mougeotia sp.	-/-/-	-/-/+	-/-/-	-/-/+
Oocystis marssonii	-/-/-	-/-/+	+/-/-	-/+/+
Pediastrum duplex var. *genuinum*	-/-/-	-/-/-	-/+/-	-/-/-
Pediastrum simplex var. *clathratum*	-/-/-	-/-/+	-/+/-	-/-/+
Pediastrum simplex var. *simplex*	-/-/-	+/+/-	*/+/-	-/-/-
Pediastrum simplex var. *sturmii*	-/-/-	-/-/-	+/-/-	-/-/-
Pediastrum simplex var. *echinulatum*	+/+/+	-/+/-	-/-/-	-/-/-
Pediastrum biwae	-/+/+	-/-/+	-/-/+	-/+/+
Pediastrum tetras var. *excisum*	-/-/-	-/-/-	-/+/-	-/-/-
Scenedesmus acuminatus	+/-/-	-/-/-	-/-/-	-/-/-
Scenedesmus sp.1	-/-/-	-/-/-	-/+/-	-/-/-
Scenedesmus sp.2	-/+/-	-/-/-	-/-/-	-/-/-
Sphaerellopsis sp.	-/-/-	-/-/-	+/-/-	+/-/-
Stichococcus bacillaris	-/-/-	+/-/-	-/-/-	-/-/-

Species lists	WB	MP	ED	KN
Tetraedron sp.	+/-/-	-/-/-	-/-/-	+/-/-
Phylum Charophyta				
Closterium sp.	-/-/-	-/-/-	-/+/-	-/+/-
Cosmarium quadrum	-/-/-	-/*/-	-/+/+	-/+/-
Cosmarium sp.1	+/-/-	-/-/-	-/-/-	-/-/-
Cosmarium sp.2	-/+/-	-/-/-	-/+/-	-/+/-
Cosmarium sp.3	-/-/-	-/+/-	-/-/-	-/-/-
Elakatothrix sp.	-/-/-	-/-/-	-/-/+	-/+/+
Staurastrum tetracerum	+/+/+	-/+/-	*/+/-	-/+/-
Staurastrum gracile	-/+/-	-/-/-	-/+/-	-/-/-
Phylum Bacillariophyta				
Achnanthidium sp.	-/+/+	-/*/-	-/*/-	-/+/-
Anomoeoneis sp.	-/-/-	-/-/-	-/-/-	+/-/-
Brachysira neoexilis	+/-/-	-/-/-	-/-/-	-/-/-
Cyclotella sp.	+/*/-	+/-/-	-/-/-	-/-/-
Cymbella sp.	-/-/-	-/+/-	-/+/-	-/-/-
Entomoneis sp.	-/-/-	-/+/-	-/-/-	-/-/-
Eunotia sp.	-/-/-	-/-/-	-/+/-	-/-/-
Frustulia rhomboides	-/+/-	-/-/-	-/-/-	-/-/-
Gomphonema lagenula	-/+/-	-/-/+	-/+/+	-/-/-
Gomphonema parvulum	-/-/-	-/+/-	-/+/-	-/-/-
Nitzschia sp.	+/+/-	-/-/-	-/+/-	+/-/-
Navicula sp.1	-/+/-	-/-/-	-/-/-	-/-/-
Navicula sp.2	-/-/-	-/-/-	-/-/-	+/+/-
Neidium sp.	-/-/-	-/-/-	-/+/-	-/-/-
Surirella robusta	-/-/-	-/-/-	-/+/-	-/-/-
Phylum Cyanobacteria				
Anabaena cylindrica	+/-/+	-/-/+	-/-/+	-/-/+
Coelomoron sp.	-/-/-	-/-/-	-/+/-	-/-/-
Cylindrospermopsis philippinensis	*/*/*	-/-/+	-/-/-	-/-/-
Merismopedia elegans	+/-/-	-/-/-	-/-/-	-/+/-
Merismopedia pinctata	+/-/-	-/-/+	-/-/-	-/-/-
Microcystis aeruginosa	+/-/-	-/-/-	-/-/-	-/*/-
Oscillatoria sp.	-/-/+	-/-/-	-/-/+	-/-/-
Planktothrix sp.	-/-/-	-/-/-	+/-/-	-/-/-
Pseudanabena limnetica	+/-/-	-/-/-	+/-/-	-/-/-
Phylum Miozoa				
Tripos furca	-/-/-	-/-/-	-/+/-	-/+/-
Peridiniopsis sp.1	+/+/-	-/-/*	*/*/+	-/-/-
Peridiniopsis sp.2	-/+/-	-/-/-	-/-/-	-/*/*
Peridinium sp.	-/-/-	-/-/-	-/-/-	-/+/-
Phylum Ochrophyta				
Centritractus sp.	-/-/-	-/+/-	-/-/-	-/-/-
Dinobryon divergens	+/-/-	-/-/-	-/-/-	-/+/-
Isthmochloron sp.	-/-/-	-/-/-	-/-/-	-/+/-
Mallomonas sp.	-/-/-	-/-/-	-/+/-	-/-/-
Phylum Cryptista				
Cryptomonas sp.	-/-/-	+/-/-	-/-/-	-/-/-
Phylum Euglenozoa				
Euglena caudata	+/-/+	-/-/-	-/-/-	-/-/-

Species lists	WB	MP	ED	KN
Euglena viridis	-/-/-	-/-/-	-/-/-	+/-/+
Euglena sp.1	-/-/-	+/-/+	-/-/-	-/-/-
Euglena sp.2	-/-/-	+/-/-	-/-/-	-/-/-
Euglena sp.3	-/+/-	-/-/-	-/-/-	-/-/-
Euglena sp.4	-/-/-	-/-/-	-/+/-	-/-/-
Lepocinclis acus	-/-/-	-/-/-	-/+/*	-/-/-
Lepocinclis oxyuris	-/-/-	-/-/-	-/-/-	-/+/-
Lepocinclis sp.	-/+/-	-/-/-	-/-/-	-/-/-
Phacus elegans	-/+/-	+/+/-	-/*/-	-/-/-
Strombomonas acuminata	-/+/+	-/-/*	-/-/*	-/-/*
Strombomonas schauinslandii	-/-/+	-/-/-	-/-/-	-/+/*
Strombomonas sp.	+/-/-	-/-/-	-/-/-	+/-/-
Trachelomonas armata	-/-/-	+/-/-	-/-/-	-/-/-
Trachelomonas aspera	-/-/-	-/-/-	-/+/-	-/-/-
Trachelomonas hirta var. duplex	-/-/-	-/+/-	-/+/-	-/-/-
Trachelomonas planctonica	-/-/-	-/+/-	-/-/-	-/-/-
Trachelomonas venusta	-/+/-	-/-/-	-/-/-	-/-/-
Trachelomonas volvocina	+/+/*	*/*/*	-/+/*	-/-/-
Trachelomonas sp.1	+/-/-	+/-/-	-/-/-	+/-/-
Trachelomonas sp.2	-/-/-	-/-/-	-/-/-	+/-/-
Trachelomonas sp.3	-/-/-	-/-/-	-/-/-	+/-/-

+ = present; - = absent; * = dominant in July 2022/December 2022 /May 2023, respectively

WB = Wiang Bua reservoir, MP = Ma Lang Por reservoir, ED = Education Auditorium reservoir, KN = Kru Noi Garden Reservoir.

using a toothbrush, scraper, and knife. The collected attached algae samples were transferred into plastic containers. The two groups of algae samples were divided into two parts. The first part was preserved with Lugol's solution for species identification and counting (Bellinger & Sigee 2015). The second part was stored at approximately 0-4 °C for isolation to obtain a pure culture in the laboratory.

Algal Isolation and Collection

The isolation of algae was conducted using various methods, including micropipetting (Tsuchikane et al. 2018), streak plates, and spray plates. The BG11 medium was used for blue-green algae, Jaworski's medium for green algae and diatoms, and modified Hutner's medium for euglenoids. The pure culture algae will be stored in an incubator for preservation and further study of potential applications at the Centre of Excellence of Biodiversity Research and Implementation for Community, Chiang Mai Rajabhat University.

RESULTS AND DISCUSSION

The physical and chemical water quality parameters in the Wiang Bua Reservoir (WB), Ma Lang Por Reservoir (MP), Education Auditorium Reservoir (ED), and Kru Noi Garden Reservoir (KN) during July 2022, December 2022, and May 2023 are presented in Table 1. Statistically significant differences were observed in the physical and chemical water quality at each reservoir, influenced and characterized by human use and the surrounding environment. Upon conducting a comparative analysis of the physical and chemical water quality parameters at all four sampling points against the surface water quality standards set by the National Environmental Board across various factors, it was found that all four water sources receive discharges from specific types of activities. Nevertheless, they have the potential to be beneficial for consumption and utilization, provided they undergo regular pathogen disinfection and general water quality improvement processes. When categorizing the water properties based on specific water quality parameters (Simachaya 2000) to indicate their potential uses, it was found that the majority of the sampled sources fall into Category 2 (Very clean). This indicates that the water resources could be used for aquatic conservation, fishery, and water sports. However, the results for biochemical oxygen demand revealed elevated values in rainy during July at all sampling points, categorizing them into Category 3-4 (Medium clean to Fairly clean). These sources can be used for agriculture and industrial purposes. The findings suggest that certain water sources accumulate high levels of organic matter during specific seasons, posing potential implications for the occurrence of eutrophication in the future (Reinl et al. 2022).

A total of 106 species in 8 Phyla of freshwater algae were discovered (Table 2 and Fig. 2). The Wiang Bua reservoir contained 8 Phyla and 46 species, while Ma Lang Por reservoir revealed 8 Phyla and 42 species. Education Auditorium reservoir yielded 7 Phyla and 50 species, and Kru Noi Garden reservoir contained 7 Phyla and 43 species. These freshwater algae, commonly encountered in subtropical reservoirs, are predominantly Chlorophyta (Sharma & Sharma 2021, Rahayu et al. 2020, Ngearnpat et al. 2018, Martinet et al. 2016). The *Staurastrum tetracerum* and *Coelastrum astroideum* were common species of all sampling sites. Their abundance was observed to increase with higher nitrogen and phosphorus levels in the water sources (Krzebietke 2011, Felisberto et al. 2011). Additionally, a total of 22 species of Phylum Euglenozoa were identified, particularly within the genera *Euglena* spp., *Strombomonas* spp., and *Trachelomonas* spp. Freshwater algae in this group are typically abundant in small reservoirs with high nutrient levels (Wehr et al. 2015), similar to green algae such as *Pediastrum* spp., *Scenedesmus* spp., and *Desmodesmus* spp., which collectively comprised 18 species. These algae are commonly found in waters with elevated nitrogen and phosphorus levels, ranging from moderate to high (Meso-eutrophic) (Prasertsin et al. 2014, Rishi et al. 2017).
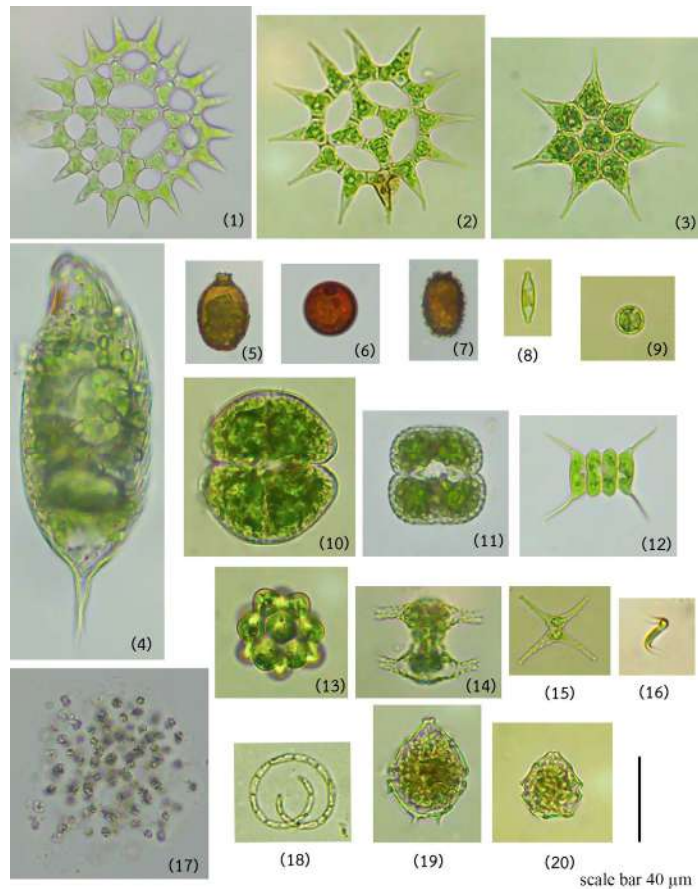
Fig. 2: The dominance species of freshwater algae in 4 sampling sites of Chiang Mai Rajabhat University, Mae Rim Campus.
(1-2) *Pediastrum biwae* (3) *Pediastrum simplex* var.*echinulatu* (4) *Lepocinclis oxyuris* (5) *Trachelomonas planctonica* (6) *Trachelomonas volvocina* (7) *Trachelomonas hirta* var. *duplex* (8) *Achnanthidium* sp. (9) *Cyclotella* sp. (10) *Cosmarium* sp.1 (11) *Cosmarium* sp.2 (12) *Desmodesmus communis* (13) *Coelastrum astroideum* (14) *Staurastrum gracile* (15) *Staurastrum tetracerum* (16) *Monoraphidium controtum* (17) *Microcystis aeruginosa* (18) *Cylindrospermopsis philippinensis* (19) *Peridiniopsis* sp.1 (20) *Peridiniopsis* sp.2.

Table 3: Guidelines for the possible utilization of some freshwater algae isolations from the water resource of Chiang Mai Rajabhat University, Mae Rim Campus.

Algae isolation	Applications	Reference
Chlorococcum sp.	biofuel	(Kookal et al. 2016)
Desmodesmus spp.	biomass and wastewater treatment	(Cheban et al. 2015)
Monoraphidium sp.	biocompounds	(Lin et al. 2019)
Microcystis aeruginosa	algae hepatotoxin microcystins (MCs)	(Scoglio, 2018)
Anabaena cylindrica	biological fertilizer	(Kholssi et al. 2022)
Trachelomonas sp.	environmental indicators	(Wehr et al., 2015)
Actinastrum hantzschii	biomass and biofuel	(Lyon et al., 2015)
Chlorella sp.	biofuel and protein	(Guccione et al., 2014)
Kirchneriella sp.	biomass	(Shukla et al., 2016)
Pediastrum spp.	environmental indicators	(Jovanović et al. 2017)
Stichococcus bacillaris	biofuel	(Sivakumar et al. 2014)
Coelastrum spp.	antioxidant substances	(Kaha et al. 2021)
Nephrocytium sp.	morphology and phylogenetic studies	(Lui et al. 2017)
Oocystis sp.	biomass	(Na et al. 2021)
Sphaerellopsis sp. (*Vitreochlamys* sp.)	morphology and phylogenetic studies	(Nakada et al. 2016)

Furthermore, in the Wiang Bua reservoir, *Cylindrospermopsis philippinensis* was consistently found as a prominent species in every sampling event. This blue-green algae can produce the toxin cylindrospermopsin (CYN), which inhibits protein synthesis and is carcinogenic, particularly affecting the liver (Falconer & Humpage 2006). Additionally, reports are indicating its detrimental effects on other organs, such as the kidneys, lungs, and heart (Pichardo et al. 2017). Compared to other toxins from blue-green algae, CYN is primarily produced and released extracellularly (Bormans et al. 2014), leading to its accumulation in aquatic organisms and subsequent transfer through the food chain. Although *Cylindrospermopsis philippinensis* was identified as a prominent species in this study, no bloom events were observed. Therefore, continuous monitoring and vigilance are necessary to prevent potential bloom occurrences. The presence of freshwater algae indicative of high nutrient levels aligns with the assessment of water quality based on physical and chemical parameters. Hence, continuous monitoring and assessment of water quality at all sampling points are essential to mitigate the risk of eutrophication in the future.

Twenty eight isolations were screened from 4 sampling sites within Mae Rim Campus, Rajabhat Chiang Mai University. The Twenty isolates belonged to Chlorophyta, including *Actinastrum hantzschii* Lagerheim, *Ankistrodesmus densus* Korshikov, *Ankistrodesmus fusiformis* Corda, *Chlorella* sp., *Chlorococcum* sp., *Coelastrum astroideum* De Notaris, *Coelastrum microsporum* Nägeli, *Coelastrum reticulatum* (Dangeard) Senn, *Desmodesmus armatus* (Chodat) Hegewald, *Desmodesmus hystrix* (Lagerheim) E.Hegewald, *Desmodesmus* sp., *Dictyosphaerium* sp., *Kirchneriella aperta* Teiling, *Monoraphidium tortile* (West & G.S.West) Komárková-Legnerová, *Nephrocytium* sp., *Oocystis marssonii* Lemmermann, *Pediastrum simplex* Meyen, *Sphaerellopsis* sp., *Staurastrum tetracerum* Ralfs ex Ralfs and *Stichococcus bacillaris* Butcher. The three isolates of Cyanophyta were *Anabaena cylindrica* Lemmermann, *Microcystis aeruginosa* (Kützing) Kützing, and *Planktothrix* sp. The three isolates were *Anomoeoneis* sp., *Navicula* sp., and *Nitzschia* sp. in Bacillariophyta, and two isolates of Euglenozoa were *Euglena viridis* (O.F.Müller) Ehrenberg and *Trachelomonas* sp. Upon comparison with relevant literature, it is evident that the algae isolated in this study have potential for various future applications. These applications include biomass, protein, biofuel, bioactive compounds, antioxidant substances, biological fertilizer, wastewater treatment, environmental indicators, algal toxin, morphology, and phylogenetic studies, as detailed in Table 3.

CONCLUSIONS

The physical and chemical qualities of water according to the announcement of the National Environmental Committee, it was found that the water quality is generally clean. However, in some areas, the BOD (Biochemical Oxygen Demand) levels are high, which could affect the water quality and biodiversity of organisms living in water sources in the future. A study of the biodiversity of phytoplankton found a total of 8 phyla and 106 species, indicating a high biodiversity area. However, the dominance of green algae and euglenoids served as indicators of water sources with moderate to high nutrient levels, consistent with the findings of physical and chemical water quality. Additionally, blue-green algae capable of producing toxins were notably present at some sampling points. Therefore, regular monitoring and quality assessment of water are necessary.

In the isolation of freshwater algae, a total of 28 isolates were obtained, which could be utilized for various purposes in the future. All strains were preserved at the Centre of Excellence of Biodiversity Research and Implementation for Community, Chiang Mai Rajabhat University, in response to the Plant Genetic Conservation Project under the royal initiative of Her Royal Highness Princess Maha Chakri Sirindhorn. This development aims to harness these resources for future benefits.

ACKNOWLEDGMENTS

REFERENCES

Alombro, N.C., Guiamadil, R.C., Datumama, W.U., Catipay, J.P.A. and de Vera, P.J.D., 2023. Evaluation of Organic Pollution Using Algal Diversity in Rivers of Cotabato City, Bangsamoro Autonomous Region in Muslim Mindanao (BARMM), Mindanao Island, Philippines. *Nature Environment and Pollution Technology*, 22(4), pp. 2231-2237. https://doi.org/10.46488/NEPT.2023.v22i04.051.

American Public Health Association, 2017. *Standard Methods for the Examination of Water and Wastewater*. American Water Works Association.

Barinova, S. and Alster, A., 2021. Algae and cyanobacteria diversity and bioindication of long-term changes in the Hula Nature Reserve, Israel. *Diversity*, 13, pp.583. https://doi.org/10.3390/d13110583.

Bellinger, E.G. and Sigee, D.C., 2015. *Freshwater Algae: Identification, Enumeration and Use as Bioindicators*. John Wiley and Sons, Ltd.

Bormans, M., Lengronne, M., Brient, L. and Duval, C., 2014. Cylindrospermopsin accumulation and release by the benthic cyanobacterium Oscillatoria sp. PCC 6506 under different light conditions and growth phases. *Bulletin of Environmental Contamination and Toxicology*, 92(2), pp.243–247. https://doi.org/10.1007/s00128-013-1144-y.

Cheban, L., Malischuk, I. and Marchenko, M., 2015. Cultivating Desmodesmus armatus (Chod.) Hegew. in recirculating aquaculture systems (RAS) waste water. *Archives of Polish Fisheries*, 23, pp.155-162.

Ehsani, M., Alizadeh, B., Mahboubi, A., Hosseinabadi, T. and Tabarzad, M., 2023. Antioxidant and antimicrobial activities of peptide fractions derived from enzymatic digestion of Desmodesmus sp. protein extract: Bioactivity of peptides derived from Desmodesmus sp. *Trends in Peptide and Protein Science*, 8(1), pp.1–8 (e8). https://doi.org/10.22037/tpps.v8i1.43836.

Falconer, I.R. and Humpage, A.R., 2006. Cyanobacterial (Blue-Green Algal) toxins in water supplies: Cylindrospermopsins. *Environmental Toxicology*, 21(4), pp.299–304. https://doi.org/10.1002/tox.20194.

Felisberto, S.A., Leandrini, J.A. and Rodrigues, L., 2011. Effects of nutrients enrichment on algal communities: an experimental in mesocosms approach. *Acta Limnologica Brasiliensia*, 23(2), pp.128–137.

Furuhashi, K., Magota, A., Liu, Y., Hasegawa, F., Okada, S., Kaizu, Y. and Imou, K., 2022. Thinning of Botryococcus braunii colony sheath by pretreatment enhances solvent-based hydrocarbon recovery. *Phycol.*, 2, pp.363–373. https://doi.org/10.3390/phycology2040020.

Giao, N.T. and Nhien, H.T.H., 2020. Phytoplankton-water quality relationship in water bodies in the Mekong Delta, Vietnam. *Applied Environmental Research*, 42(2), pp.1–12. https://doi.org/10.35762/AER.2020.42.2.1.

Guccione, A., Biondi, N., Sampietro, G., Rodolfi, L., Bassi, N. and Tredici, M.R., 2014. Chlorella for protein and biofuels: from strain selection to outdoor cultivation in a Green Wall Panel photobioreactor. *Biotechnology for Biofuels and Bioproducts*, 7(84), pp.1–12. https://doi.org/10.1186/1754-6834-7-84.

Jovanović, J., Trbojević, I., Simić, G.S., Popović, S., Predojević, D., Blagojević, A. and Karadžić, V., 2017. The effect of meteorological and chemical parameters on summer phytoplankton assemblages in an urban recreational lake. *Knowledge and Management of Aquatic Ecosystems*, 418, pp.48. https://doi.org/10.1051/kmae/2017038.

Kaha, M., Iwamoto, K., Yahya, N.A., Suhaimi, N., Sugiura, N., Hara, H., Othman, N., Zakaria, Z. and Suzuki, K., 2021. Enhancement of astaxanthin accumulation using black light in Coelastrum and Monoraphidium isolated from Malaysia. *Scientific Reports*, 11(1), pp.11708. https://doi:10.1038/s41598-021-91128-z.

Kholssi, R., Marks, E.A.N., Miñón, J., Montero, O., Lorentz, J., Debdoubi, A. and Rad, C., 2022. Biofertilizing effects of Anabaena cylindrical biomass on the growth and nitrogen uptake of wheat. *Communications in Soil Science and Plant Analysis*, 53(6), pp.1–10. https://doi.org/10.1080/00103624.2022.2043350.

Kookal, S., Santhakumaran, P. and Ray, J.G., 2016. Chlorococcum humicola (Nageli) Rabenhorst as a renewable source of bioproducts and biofuel. *Journal of Plant Studies*, 5(1), pp.48–57.

Krzebietke, A.N., 2011. Dynamics and structure of phytoplankton in fishponds fed with treated wastewater. *Polish Journal of Environmental Studies*, 20(1), pp.157–166

Leelahakriengkrai, P. and Kunpradid, T., 2014. Water quality and biodiversity of phytoplankton and benthos in the reservoirs at Saluang Campus Chiang Mai Rajabhat University. *Rajabhat Journal of Science, Humanities and Social Sciences*, 15(1), pp.87–97.

Lin, Y., Ge, J., Zhang, Y., Ling, H., Yan, X. and Ping, W., 2019. Monoraphidium sp. HDMA-20 is a new potential source of α-linolenic acid and eicosatetraenoic acid. *Lipids in Health and Disease*, 18(56), pp.1–10. https://doi.org/10.1186/s12944-019-0996-5.

Lui, X., Zhu, H., Liu, B., Liu, G. and Hu, Z., 2017. Phylogeny and morphology of genus *Nephrocytium* (Sphaeropleales, Chlorophyceae, Chlorophyta) from China. *Phytotaxa*, 319(1), pp.84–92.

Lyon, S.R., Ahmadzadeh, H. and Murry, M.A., 2015. *Algae-Based wastewater treatment for biofuel production: Processes, species, and extraction methods*. Springer.

Martinet, J., Guédant, P. and Descloux, S., 2016. Phytoplankton community and trophic status assessment of a newly impounded sub-tropical reservoir: Case study of the Nam Theun 2 reservoir (Lao PDR, Southeast Asia). *Hydroécologie Appliquée*, 19, pp.173–195.

Na, H., Jo, S.W., Do, J.M., Kim, I.S. and Yoon, H.S., 2021. Production of algal biomass and high-value compounds mediated by interaction of microalgal *Oocystis* sp. KNUA044 and bacterium *Sphingomonas* KNU100. *Journal of Microbiology and Biotechnology*, 31(3), pp.387–397.

Nakada, T., Ito, T. and Tomita, M., 2016. 18S ribosomal RNA gene phylogeny of a colonial Volvocalean lineage (Tetrabaenaceae-Goniaceae-Volvocaceae, Volvocales, Chlorophyceae) and its close relatives. *Journal of Japanese Botany*, 91, pp.345–354.

Ngearnpat, N., Klayluk, B., Kumla, A., Ngamtad, S. and Issakul, K., 2018. Phytoplankton composition and water quality of Kwan Phayao reservoir, Thailand, during rainy and cold dry seasons. *Journal of Food, Health and Bioenvironmental Science*, 11(2), pp.46–55.

Pichardo, S., Cameán, A.M. and Jos, Á., 2017. In vitro toxicological assessment of cylindrospermopsin: A review. *Toxins*, 9(12), pp.402. https://doi.org/10.3390/toxins9120402.

Prasertsin, T., Pekkoh, J., Pathom-aree, W. and Peerapornpisal, Y., 2014. Diversity, new and rare taxa of *Pediastrum* spp.. in some freshwater resources in Thailand. *Chiang Mai Journal of Science*, 41(5.1), pp.1065–1076.

Rahayu, R.U.S.D., Anggoro, S. and Soeprobowati, T.R., 2020. Plankton community structure and trophic status of Wadaslintang Reservoir, Indonesia. *AACL Bioflux*, 13(2), pp.1138–1151.

Reinl, K., Harris, T., Elfferich, I., Coker, A., Zhan, Q., Domis, L., Morales-Williams, A.M., Bhattacharya, R., Grossart, H., North, R.L. and Sweetman, J.N., 2022. The role of organic nutrients in structuring freshwater phytoplankton communities in a rapidly changing world. *Water Research*, 219, p.118573. https://doi.org/10.1016/j.watres.2022.118573.

Rishi, V., Tripathi, S. and Awasthi, A.K., 2016. Diversity and significance of genus *Scenedesmus* (Meyen) in River Ganga at Kanpur, India. *International Journal of Current Microbiology and Applied Sciences*, 5(8), pp.584–592.

Scoglio, S., 2018. Microcystins in water and in microalgae: Do microcystins as microalgae contaminants warrant the current public alarm? *Toxicology Reports*, 5, pp.785–792. https://doi.org/10.1016/j.toxrep.2018.07.002.

Sharma, B.K. and Sharma, S., 2021. Phytoplankton diversity of a subtropical reservoir of Meghalaya State of Northeast India. *Aquatic Science and Engineering*, 36(2), pp.51–65. https://doi.org/10.26650/ASE2020740218.

Shukla, M., Tabassum, R., Singh, R. and Dhar, D.W., 2016. Influence of light intensity, temperature and CO_2 concentration on growth and lipids in green algae and cyanobacteria. *Indian Journal of Experimental Biology*, 54(7), pp.482–487.

Simachaya, W., 2000. *Water Quality Management in Thailand*. Workshop on Environmentally Sound Technology on Water Quality Management, UNEP, Mekong River Commission.

Singab, A.N.B., Ibrahim, N.A., El-Sayed, A.E.B., El-Senousy, W.M., Aly, H., Elsamiae, A.S.A. and Matloub, A.A., 2018. Antiviral, cytotoxic, antioxidant and anticholinesterase activities of polysaccharides isolated from microalgae Spirulina platensis, Scenedesmus obliquus, and Dunaliella salina. *Archives of Pharmaceutical Sciences, Ain Shams University*, 2(2), pp.121–137. https://doi.org/10.21608/aps.2018.18740.

Sivakumar, G., Jeong, K. and Lay, J.O., 2014. Bioprocessing of *Stichococcus bacillaris* strain Siva 2011. *Biotechnology for Biofuels and Bioproducts*, 7(62), pp.1–9. https://doi.org/10.1186/1754-6834-7-62.

Supahan, N., Kunpradid, T., Joradol, A. and Leelahakriengkrai, P., 2017. Diversity of some organisms in Chiang Mai Rajabhat University, Mae Rim Campus, Chiang Mai Province. *Science and Technology RMUTT Journal*, 7(2), pp.1–14.

Tewari, K., 2022. A review of climate change impact studies on harmful algal blooms. *Phycol.*, 2, pp.244–253. https://doi.org/10.3390/phycology2020013.

Tsuchikane, Y., Hamaji, T., Ota, K. and Kato, S., 2018. Establishment of a clonal culture of unicellular conjugating algae. *Journal of Visualized Experiments*, 4(137), p.57761. https://doi.org/10.3791/57761.

Wehr, J.D., Sheath, R. and Kociolek, P., 2015. *Freshwater Algae of North America: Ecology and Classification*. Academic Press.

Ziesemer, S., Meyer, S., Edelmann, J., Vennmann, J., Gudra, C., Arndt, D., Effenberg, M., Hayas, O., Hayas, A., Thomassen, J.S., Kubickova, B., Pöther, D. and Hildebrandt, J., 2022. Target mechanisms of the cyanotoxin cylindrospermopsin in immortalized human airway epithelial cells. *Toxins*, 14, p.785. https://doi.org/10.3390/toxins14110785.

Adoption Intention of Technology-Based Water Generation and Management Through W-TAM

Rajashree Jain[1]† , Sarika Sharma[1] , Deepthi Setlur[2], Aditya Bajaj[1] and Dhwani Parekh[1]

[1]Symbiosis Institute of Computer Studies and Research, Symbiosis International University, Pune, India
[2]Fruition Technology Labs and AquaVapor, Cypress, Texas, United States
†Corresponding author: Rajashree Jain; rajashreejain@gmail.com

ABSTRACT

Increasing concerns related to climate change and extensive use of water resources have depleted the available water for use. For water as an essential requirement for humans to carry onto their day-to-day chores, access and availability of water becomes the highest priority. Technology-based solutions support water generation, filtration, quality testing, water distribution, and many other areas. The present paper dwells on the user acceptance of these technologies. A conceptual model was developed through a literature review and named as Water-Technology Acceptance Model (W-TAM). The data was collected through a self-designed survey instrument to empirically test the proposed model. Analysis of this data was done with confirmatory factor analysis and structural equation modeling. It was observed that the actual use of these technologies depends on the ease of use and usefulness. Attitude to use them also matters. Although perceived risks and affordability did affect the use of W-TAM, trust, and regulatory aspects did not confirm their role in the adaptation of W-TAM. These findings will provide meaningful insights to the stakeholders and will help them in the practical implementation of these water-based technologies. This may also help service providers in the formulation of policies for technology-based water generation.

INTRODUCTION

The widespread adoption and use of technology have become an integral part of modern life, with individuals using technology for various tasks and activities daily. The evolution of smartphones and mobile applications seamlessly integrates into our daily lives (Lee et al. 2014). Acceptance of the internet and the rise of bottled water consumption are some examples of such transformations. These changes have had far-reaching social, economic, and environmental implications. As per the World Resources Institute, more and more countries are now entering in water stress ranking, which is a matter of concern (Kuzma et al. 2023). Technological solutions for alternate sources of water generation are the need of the hour to tackle this crucial situation. Atmospheric water generation (AWG) seems to be a sustainable solution, which is researched, and advancements that happened in the last decade are quite promising (Raveesh et al. 2021, Gido et al. 2016).

Water Resource and Technologies: A Background

Water, a vital natural resource, holds cultural and ecological significance, paralleling the impact of technology on communication. Being a scarce resource, it also plays a critical role in sustaining life and supporting various ecosystems. Concerns about water pollution, scarcity, and excessive consumption highlight the need for responsible water usage. The surge in bottled water consumption raises concerns about convenience and environmental impact, with manufacturing and disposal contributing to resource depletion, greenhouse gas emissions, and

pollution. Awareness drives the search for alternatives like reusable bottles and improved water infrastructure to address convenience and environmental concerns (Gleick & Cooley 2009).

Water scarcity is not only a local issue; it is one of the Sustainable Development Goals (SDGs) recognized by the United Nations. It highlights the importance of equitable access to clean water and sanitation services, protection of water resources, and the adoption of sustainable practices (Bhaduri, 2016). To ensure a sustainable future, it is crucial to develop and implement innovative and sustainable technologies for water generation, management, and conservation. Investing in technologies such as atmospheric water generators can help alleviate the pressures of water scarcity and ensure a more secure water future for all (Almusaied & Asiabanpour 2017).

In addition to the importance of sustainable technology for water sustainability, it is crucial to consider the acceptance and adoption of these technologies. Recognizing that the implementation of technology related to such a vital resource as water can be challenging for people, the Technological Acceptance Model (TAM) comes into play. The present paper dwells on exploring the TAM and especially on the acceptance of technology-based water sources other than natural resources. We present an incremental model based on the traditional TAM proposed by Davis (1989) and referred to here as W-TAM, a Water Technology Acceptance Model.

Need of the Study and Research Questions

A recent report from the UN Water conference held in March 2023, states the surge in water supply demand by 40% by 2030. The report also raises concerns and urges an overhaul of wasteful water practices around the world. On the other hand, ongoing efforts are also seen in mitigating continued water stress. Literature shares several examples of deep penetration of water-based technologies. Digitalization of water supply systems aligning with Water 4.0 models (Adedeji et al. 2022), Water generation (Raveesh et al. 2021), to user acceptance of water treatment technologies (Contzen et al. 2023) are available in the literature. However, most of these user acceptance models were studied from clusters like employees of municipalities for technology adoption or use of smart devices for water management and a few are available on water treatment. Researchers have considered the use of ICT and IOT-based technology for water management and water services department employees (Morienyane et al. 2019). TAM was extended for smart meter usage along with a few moderating variables like personal environment concerns and innovation (Madias et al. 2023). It is also important to note the end-user acceptance

of these technologies. However, the impact of trust in water technologies and regulatory policies from the public was not found in the study. A study in particular to show user acceptance of technologies used for water or W-TAM was not available. Hence, an extended TAM for water technologies was felt. The present paper proposes W-TAM with extended parameters. With this backdrop, the study attempts to seek answers to these research questions:

Research Question 1: Whether technology for water generation, water treatment, and water management are acceptable to users?

Research Question 2: What factors can influence the acceptance of water technologies in W-TAM?

LITERATURE REVIEW

As part of this study, a critical literature review was conducted about water, technologies used for water quality and generation and their acceptance-related contexts. Therefore, the technology acceptance model was included in the context of water technologies.

Water Generation Technologies

AWGs are devices that extract water vapor from the air, condense it into liquid water, and have been designed as an innovative solution for regions with medium to high humidity (Peters et al. 2013). Shafeian et al. (2022), in their study, examined the environmental claims of Air Water Generators (AWGs), and their acceptance by the selected individuals or communities. Jarimi et al. (2020) presented a technology review and the merits of fog and dew-based AWGs.

Pontious et al. (2016) provided two sustainable engineering designs adhering to minimum energy consumption and cost compared to existing AWGs in the market. Tripathi et al. (2016) designed and presented an AWG that can be powered either through a bicycle-gear arrangement or by utilizing renewable energy sources like solar or wind power. By implementing this solution, the project aimed to provide safe and clean drinking water to the affected regions. Another part of the study was the acceptance of such water generators by the users and the study on the market penetration.

In another study, Das (2018) assessed AWGs for rural and remote India. The study builds the capacity towards the "Har Ghar Lal" initiative of the Government of India. The concern for the use of AWGs remains about the cost. Hybrid technologies and frugal engineering with renewable energy sources may be considered in the future for the mass reach of AWGs. In another context from Jordan, the study focused on the benefits of recovering water generated from air conditioners. The authors examined the quality of such

condensed water and the social implications and acceptance of reusing condensed water (Shourideh et al. 2018, Matarneh et al. 2023).

Water Technology Acceptance Model (W-TAM)

The Technology Acceptance Model (also known as TAM) proposed by Davis (1989) is a widely used theoretical model that explains how individuals come to accept and use technology and identifies perceived usefulness and ease of use as key factors that influence the decision to use technology. An extended model was also proposed later by Venkatesh & Davis (2000). It suggests that users' intention to use technology is influenced by perceived usefulness (how it enhances performance) and perceived ease of use (how user-friendly it is). These factors influence users' attitudes toward technology usage, ultimately affecting their behavioral intention. According to Adams et al. (1992), the decision to use technology is influenced by two main factors, which are 'Perceived usefulness (PU)' and 'Perceived Ease of Use (PEU)'.

Perceived Usefulness (PU)

It represents users' perspective towards a technology from a benefit point of view. In case we believe that the technology is useful for completing our routine tasks and helping us improve our efficiency it is likely that we perceive it as useful. It may be subjective for individuals and vary from person to person.

Perceived Ease of Use (PEU)

Apart from perceived usefulness, perceived ease of use will also play an important role in the acceptance of technology. If a person finds it easy to use with minimum effort to understand for operating a technology, it is more likely that the technology can be used actually.

On the other hand, if a technology appears complex, cumbersome, or requires extensive training, it may be perceived as difficult to use, which can hinder its adoption.

Further to this model, there were several studies conducted, which used the original TAM or the TAM versions. Lee et al. (2003) in their study examined the TAM, especially the uses of accepting technology for Information Systems (IS). Some researchers tested the basic TAM model and some additional significant for usage in the information technology domain (Legris et al. 2003, Davis 1993, Bajaj et al. 1998). Apart from the PU and PEU variables, more behavioral variables were added to the model, like attitude towards using and actual usage behavior and more. Turner et al. (2010) examine the evidence regarding the Technology Acceptance Model (TAM) and its ability to predict actual usage using subjective and objective measures.

Sharp (2007), in his review article, presented several factors influencing individuals' acceptance or rejection of specific technologies, considering the wide range of technologies being implemented. The paper highlighted that the strength of TAM lies in its flexibility and applicability, enabling in-depth analysis and understanding of diverse applied technologies. A meta-analysis of the Technology Acceptance Model (TAM) was presented and concluded that the results obtained from TAM are highly reliable across various contexts. According to King (2006), the analysis highlighted the existence of robust models for applicability.

In the present study, we have used a two-way strategy to understand the Technology Acceptance Model (TAM) and secondly its extension to water-based technologies. It considers the factors from the existing model and is customized for water-related technological innovations.

Perceived Usefulness of Water-Based Technology (PUWT)

It measured the perceptions of users on the extent to which they find water-based technology beneficial to their daily chores. It also examines whether the existing water-based challenges were addressed. A higher PUWT increases the likelihood of technology adoption. This factor also evaluates the level of awareness and knowledge individuals have about the existence and functionalities of water-based technologies. Effective communication and promotion of the technology's benefits can significantly influence individuals' awareness and increase their interest in adopting the technology (Contzen et al. 2023). The following hypothesis is posited:

H1: Perceived Usefulness of Water-Based Technology significantly affects the attitude to the use of water-based technology.

Perceived Ease of Use of Water-Based Technology (PEUWT)

PEUWT measures the degree to which individuals believe that using water-based technology is simple, effortless, and requires minimal effort to operate. The technology was accepted in the past based on the perceived ease of use of several technology penetrations like online ticketing, e-learning services, and IOT-based water meters by several researchers (Renny et al. 2013, Lee et al. 2013, Willis et al. 2010). PEUWT affects the intentions and may influence the users towards a specific technology. An intuitive and user-friendly interface, along with straightforward instructions, can enhance the perceived ease of use, making the technology more appealing to potential users. Therefore, we considered the Hypothesis as follows:

H2: Perceived Ease of Use of Water-Based Technology significantly affects the attitude toward to use of water-based technology.

Trust in Water-based Technology (TWBT)

Trust plays a crucial role in technology adoption. It has been seen as an important factor in influencing online behaviors, especially towards e-commerce (Lee et al. 2013, Pavlou 2003). TWBT assesses the level of confidence individuals have in the water-based technology's reliability, security, and performance. Strong trust in the technology fosters a positive attitude toward its adoption (Wu et al. 2000).

H3: Trust in Water-Based Technology significantly affects the attitude to use water-based technology.

Regulatory and Policy Support (RPS)

Wolsink (2010) discussed a comparative analysis of acceptance of technology based on the policies and regulatory framework. The author presented the case based on several dimensions of technology acceptance, including a policy point of view. These are socio-political, community, and market acceptance of public and private infrastructure in the three case study areas considered. The three areas considered for this acceptance framework were renewable energy, space-water management, and waste management. RPS assesses the impact of government policies, regulations, and incentives that either facilitate or hinder the adoption of water-based technology. Supportive policies can encourage wider adoption. The present study dwells on testing them as:

H4: Regulatory and Policy Support (RPS) significantly affects the attitude to use water-based technology.

Attitude to Use Water-based Technologies

From the original TAM model, this can be adopted that the attitude to use water-based technology impacts the actual use of water-based technology and thus hypothesized as:

H5: Attitude to use water-based technology significantly affects the actual use of water-based technology.

Other Moderators

There are two more factors identified that can moderate between the attitude to use and the actual use of the water-based technology. These are:

a) **Perceived Cost and Affordability (PCA):** PCA evaluates the financial implications associated with adopting the water-based technology. This includes the initial investment, maintenance costs, and the perceived value of the technology to its cost.

   H6: The Perceived Cost and Affordability play a moderating role between attitude to use water-based technology and attitude to use water-based technology

b) **Perceived Risks (PR):** PR explores individuals' perceptions of potential risks associated with using
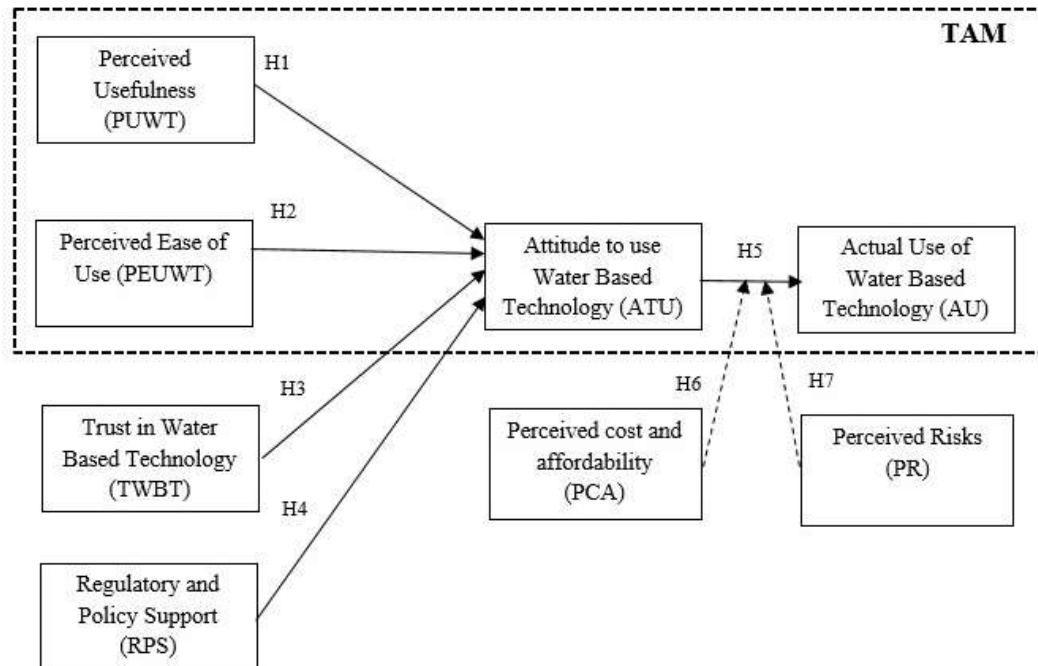
Fig. 1: Conceptual hypothesized model.

water-based technology, such as technical failures, data security issues, or adverse environmental effects. Lower perceived risks positively affect technology adoption.

H7: The Perceived Risks play a moderating role between attitude to use water-based technology and attitude to use water-based technology

Based on the above discussion, the hypothesized theoretical framework is exhibited in Fig. 1. The present paper delves into the user acceptance perspective on AWGs. The present work presents a twofold strategy adopted in conducting the present research, the first one being TAM and the second one is on a very futuristic water-based Technology for which we are referring as the Water-Based Technology Acceptance Model (W-TAM). The proposed W-TAM model provides a comprehensive framework to analyze the various factors influencing the acceptance and adoption of water-based technologies. The details of the methodology used are detailed in the next section.

MATERIALS AND METHODS

To empirically test the model proposed (Fig. 1), a survey was conducted and data was collected. The study is based on the perception and adoption of the use of technology-based water generation, therefore, the respondents were people who are using or intending to use it from various cities of India. The study focused on six major cities in India, namely Pune, Delhi, Ahmedabad, Chennai, and Bengaluru. These cities were selected due to their varied demographics, geographical locations, and differing levels of exposure to water-related challenges, making them suitable representatives of the larger Indian urban population (the data collection period is November 2023 to February 2024). A convenience sampling method was adopted for data collection. An electronic form was designed and sent to the respondents through electronic and social media channels. The 223 responses were collected and considered for data analysis (see demographics Table 1).

Survey Instrument

A questionnaire was designed to collect data through the survey method. The Likert's five-point agreement scale (5: Strongly Agree to 1: Strongly disagree) was included. It was administered using a Google Form to gather quantitative data from a wider audience of stakeholders. The research employed a mixed-methods approach to investigate the technological acceptance of Atmospheric Water Generators (AWGs). The study utilized personal interviews conducted as telephonic conversations and online surveys distributed via a Google Form. The questionnaires for each criterion group were carefully designed to elicit information about the factors influencing technological acceptance. Questions focused on

Table 1: Demographics (N =223).

Factor	Category	Count
Age (in years)	10-30	74
	31-50	99
	51-70	44
	>70	6
Gender	Female	129
	Male	92
	Prefer not to say	2
Place of Residence	District	137
	Town	78
	Village	8
Number of members in the Family	Four	135
	Five	47
	Six	23
	More than six	18
Type of House	Gated township	22
	Independent home	107
	Multistory apartment	94
Occupation	Employed	127
	Housemaker	26
	Student	39
	Other	31
Annual Income (INR)	< 5 lacs	88
	< 7 lacs	25
	< 10 lacs	39
	> 10 lacs	71
Water Purifier Installed at home	Yes	202
	No	21
Type of water Purifier used	Use of RO (reverse osmosis) based filter	116
	Use of Sedimentary Filtration	47
	Use of UV Filtering	34
	Don't Know	5
	Not Applicable	21
Total		223

participants' knowledge of AWGs, perceived benefits and drawbacks, concerns regarding reliability and efficiency, and willingness to adopt the technology. The questionnaires also explored participants' attitudes towards sustainable practices and environmental consciousness. The surveys were tailored to each criterion group, addressing specific concerns and interests related to AWGs. The reliability of the scales used was tested with Cronbach's Alpha (obtained value is 0.923), which is more than 0.8 (Fornell & Larcker 1981), and hence reliability is good for the survey instrument.

RESULTS AND DISCUSSION

To address the content validity, a rigorous literature review was conducted for the model development. In addition, telephonic interviews were conducted with key stakeholders, including industry experts, retailers, suppliers, and decision-makers, to gain in-depth insights into their perceptions, experiences, and attitudes toward AWGs. Structural equation modeling (SEM) is a widely adopted statistical method that leads to the development of path models using regression analyses involving independent and dependent variables (Saris & Stronkhorst 1984). Software SPSS 16.0 and AMOS 22.0 were used for data analysis. In the first phase, a confirmatory factor analysis (CFA) was performed for model fitness and validity and in the second phase, SEM was performed. The model fitness indices suggested by Hair et

al. (2010) are adopted in this study. We obtained values for Chi-square/degree of freedom (CMIN/DF) as 1.249, which is less than 3, Comparative fit index (CFI) as 0.965, which is > 0.9, and Tucker Lewis index (TLI) as 0.958 which is > 0.9, for the goodness of fit. The root mean square error of approximation (RMSEA) value was obtained as 0.05, which is less than 0.1 for the badness of fit. As all the values are in the suggested range, therefore, it can be analyzed that the model is fit for the application of SEM.

Factor loadings obtained from Confirmatory factor analysis were used to address validity concerns, which are presented in (Fig. 2, Table 2, and Table 3). Convergent Validity is measured with a) Composite Reliability (CR), whose values should be more than 0.7 (Jöreskog 1971), b) Average variance explained (AVE): whose values should
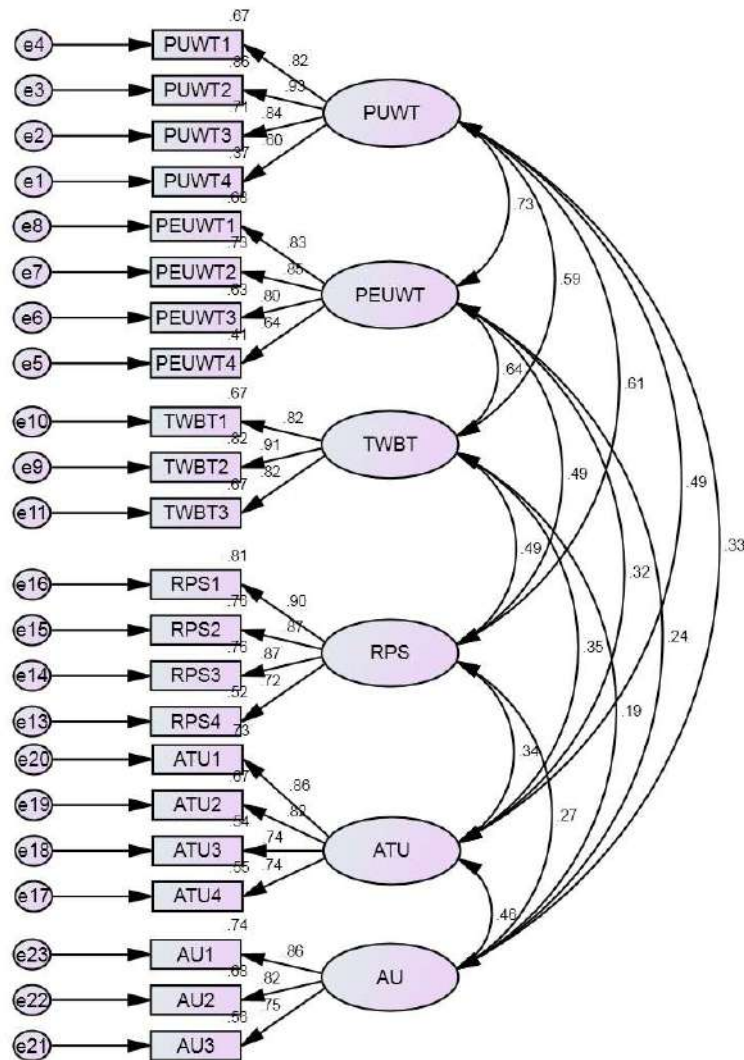
Fig. 2: Confirmatory Factor Analysis (CFA).

Table 2: Item loadings, composite reliability, and average variance explained.

Construct	Items	IL	CR	AVE
Perceived Usefulness of Water Technologies (PUWT)	PUWT1	0.82	0.879	0.651
	PUWT 2	0.93		
	PUWT 3	0.84		
	PUWT 4	0.60		
Perceived Ease of Use of Water Technologies (PEUWT)	PEUWT1	0.83	0.863	0.615
	PEUWT2	0.85		
	PEUWT 3	0.80		
	PEUWT4	0.64		
Trust in Water Based Technology (TWBT)	TWBT1	0.82	0.887	0.724
	TWBT2	0.91		
	TWBT3	0.82		
Regulatory and Policy Support (RPS)	RPS1	0.90	0.907	0.711
	RPS2	0.87		
	RPS3	0.87		
	RPS4	0.72		
Attitude to use Water Based Technology (ATU)	ATU1	0.86	0.870	0.627
	ATU2	0.82		
	ATU3	0.74		
	ATU4	0.74		
Actual Use of Water-Based Technology (AU)	AU1	0.86	0.852	0.658
	AU2	0.82		
	AU3	0.75		

be above 0.5 (Hair et al. 2010), and c) CR should be more than AVE. These three conditions/validity are achieved for all the constructs. For the discriminant Validity, AVE should be greater than MSV (Maximum shared variance), which is also achieved. After all the validity addressed in the proposed model, analysis using SEM was conducted and presented in the next sub-section.

Path Analysis of the Proposed Model

Structural Equation Modeling (SEM) was carried out for the proposed model, which, according to Hair et al. (2010)

(Fig. 3). There were five hypotheses (H1 to H5) proposed in the study. The hypotheses testing is presented in Table 4.

The hypotheses were tested through the above SEM, and results can be interpreted for each hypothesis. The first hypothesis was about the impact of user satisfaction on attitude. From the above table (Table 4), it can be interpreted that the perceived usability of water technologies and perceived ease of use of water technologies positively and significantly affect a person's attitude to using water technologies. Further, it can be stated from the table that attitude affects the actual use of water technologies. Thus, hypotheses H1, H2, and H5 are accepted. hypotheses H3 and H4 are rejected in this study, which means there was no significant impact of trust in water-based technology and regulatory and policy support on attitude to use water-based technology.

The Mediation Impact

The model has two mediating variables whose effect is to be analyzed between the variable's attitude to use water-based technologies and actual use. These are perceived cost and affordability and perceived risks. Respondents were asked whether they find water-based technologies affordable and cost-effective. Also in another question, respondents were asked whether they feel any risks are associated with water-based technologies. For both questions, the responses are recorded as 'yes' or 'no', considering them categorical variables. The data set was split based on the variables 'perceived cost and affordability' and then for 'perceived risks'. The mediation impact was tested through the Z test, which was carried out through software 16.0. If the obtained Z value is <1.96, The null hypothesis is to be accepted, which means that there is no significant difference exists, and there is no mediating role of variables 'perceived cost and affordability' and 'perceived risks'. For hypothesis, H6 and H7 results are presented in Table 5.

The mediating role of perceived cost and affordability (yes or no) can be expressed as:

$$\text{Actual Use} = a + b_{(Yes)} (ATU)$$

Table 3: Correlation matrix.

	CR	AVE	MSV	MaxR(H)	TWBT	PUWT	PEUWT	RPS	ATU	AU
TWBT	0.884	0.718	0.410	0.895	0.847					
PUWT	0.880	0.652	0.534	0.920	0.587	0.807				
PEUWT	0.862	0.613	0.534	0.878	0.640	0.731	0.783			
RPS	0.907	0.712	0.370	0.921	0.489	0.608	0.491	0.844		
ATU	0.870	0.626	0.243	0.878	0.347	0.493	0.320	0.344	0.791	
AU	0.853	0.659	0.209	0.861	0.192	0.327	0.238	0.267	0.457	0.812
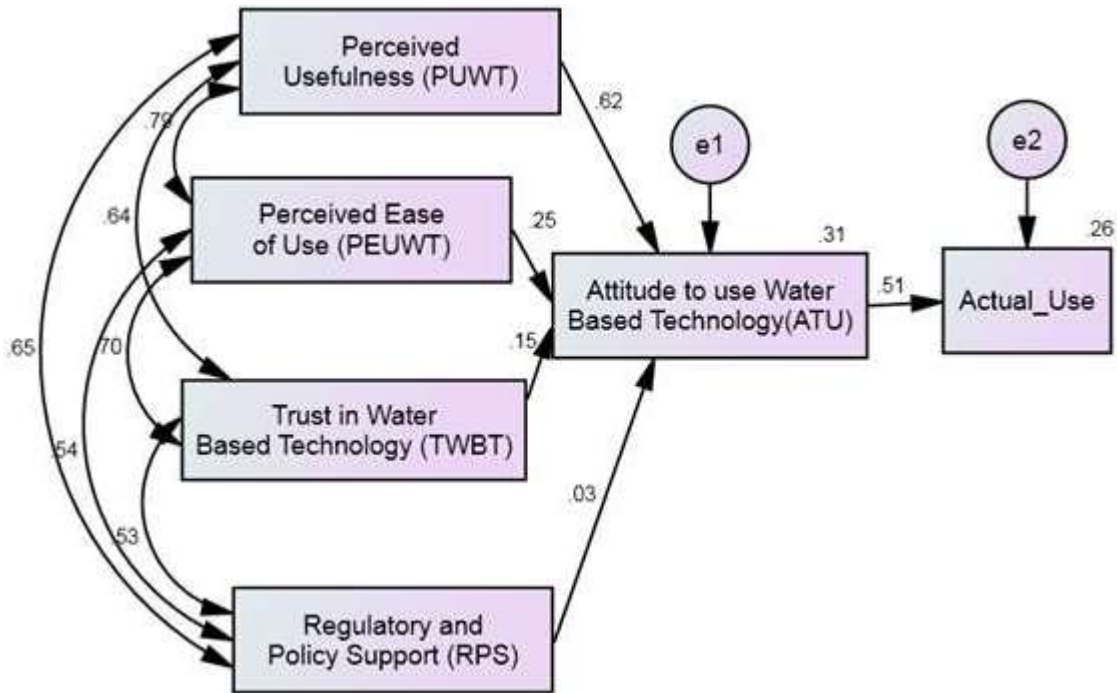
Fig. 3: Path analysis using SEM.

Table 4: Key findings of SEM and Hypotheses testing.

Hypothesis	Path Coefficient (β)	p Values	Significance (p<0.05)	Finding and Hypothesis (Accepted/rejected)
H1: PUWT -> ATU	0.62	0.000	Yes	Accepted
H2: PEUWT -> ATU	0.25	0.040	Yes	Accepted
H3: TWBT -> ATU	0.15	0.216	No	Rejected
H4: RPS -> ATU	0.03	0.775	No	Rejected
H5: ATU -> AU	0.51	0.000	Yes	Accepted

Table 5: Mediating role of variables.

Perceived cost and affordability (PCA) Yes: 49 No: 174	B (PCA-Yes)	B (PCA-No)	Standard error (PCA-Yes)	Standard error (PCA-No)	Z value
Between attitude to use water-based technologies and actual use	0.018	0.641	0.292	0.102	2.014
Perceived risks (PR) Yes: 128 No: 95	B (PR-Yes)	B (PR -No)	Standard error (PR -Yes)	The standard error (PR -No)	Z value
Between attitude to use water-based technologies and actual use	.489	.268	.125	.279	0.722

Actual Use = a + b $_{(No)}$ (ATU)

Where *a* is the intercept and *b* is the regression coefficient of the independent variable, which is 'attitude to use water-based technologies'.

From Table 5, it can be interpreted that a) the Z value for the mediating variable 'Perceived cost and affordability'

is 2.014, which is greater than 1.96. Therefore, there exists a difference between the values and it can be said that 'Perceived cost and affordability' mediates and impacts between attitude to use water-based technologies and actual use. However, for the mediating variable 'Perceived Risks', there is no mediating impact as the Z value is 0.722, which is less than 1.96.

CONCLUSIONS

This study proposed a concept through an extensive literature review. Additional factors were identified and were used to extend the existing TAM (Davis 1993) in the context of water technologies. The analysis of the present study adopted for W-TAM shows that both perceived Usefulness of Water Technologies (PUWT) and Perceived ease of Use (PEUWT) affect user's Attitudes to Use Water Based Technology. (ATU). This is accepted by several past research findings (Davis 1993, 1989, Lule 2012). These have positively impacted the Actual Use of Water Technologies. Whereas it was observed that the perceived cost and affordability matter when it comes to the actual use of W-TAM on the other hand, responses stated that the perceived risk has no moderating effect on the actual use. Trust is a belief and has always been uncertain from users' point of view. In e-commerce, retail, banking, and finance sectors, this has been a major influencer in accepting the changes and technological developments. However, for water is an essential requirement for humans to carry onto their day-to-day chores, access and availability of water becomes the highest priority than the policy and regulatory framework and trust. Accordingly, the study rejected the hypothesis of Regulatory and Policy Support (RPS). Wolsingk (2010) argued that in the context of renewable water and waste energies, infrastructure regulations and uniform and standardized solutions seldom lead to success. Diversity and local management is the key. Regulations are usually implemented from the point of view of vendors and service providers. In this study the perspective of the user is considered, hence the regulatory policy support may not be an important factor for users to adopt water-based technology. Similarly, Trust in Water Based Technology (TWBT) may not be a sufficient factor to adopt water-based technologies there may be other significant factors to adopt the same. Affordability is another imperative dimension of the adoption of any technology and here, it is also identified as one of the mediating factors. Users find no risk in the adoption of water technologies as per the data analysis in the previous section.

Theoretical Implications: The study adds to the literature body of important and emerging fields of environment and water-based technologies. Through the relevant studies, a theoretical conceptual model was proposed and was tested empirically. The quantitative approach used in this study may be the basis of further investigation in this field.

Practical Implications: This relatively new field of water technologies was studied from the user's perspective and the factors that may affect their decision to use water-based technologies. The quantitative nature of this study provides meaningful insights into user acceptance. The findings may help stakeholders formulate their policies, and cost-related aspects can be taken care of.

Limitations and Future Scope

The present study was conducted based on convenience sampling and has a scope of testing based on stratified, much wider, and larger samples. There is also scope to extend the study for testing it among communities or clusters like among the residential community, the business community and the policymakers at large. The present model, shown in Fig. 1, is individual, and the findings are for individual users.

As an extension of the study, it may be considered for testing the model in a single article but for distinct technologies used: water generation, water processing, water Filtering, water management, and, in general, "Smart Water Technologies".

ACKNOWLEDGMENTS

REFERENCES

Adams, D.A., Nelson, R.R. and Todd, P.A. 1992. Perceived usefulness, ease of use, and usage of information technology: A replication. *MIS Quarterly*, 16(2), pp.227-247.

Adedeji, K.B., Akinlolu A.P., Adnan M.A. and Anish M.K., 2022. Towards digitalization of water supply systems for sustainable smart city development-water 4.0. *Applied Sciences*, 12(18), pp.1:25, https://doi.org/10.3390/app12189174.

Almusaied, Z. and Asiabanpour, B., 2017. Atmospheric Water Generation: Technologies and influential factors, IIE Annual Conference Proceedings, pp.1448–1453.

Bajaj, A. and Sarma, R.N., 1998. A feedback model to understand information system usage. *Information & Management*, 33(4), pp. 213-224. https://doi.org/10.1016/S0378-7206(98)00026-3.

Bhaduri, A., Bogardi, J., Siddiqi, A., Voigt, H., Vörösmarty, C., Pahl-Wostl, C., Bunn, S.E., Shrivastava, P., Lawford, R., Foster, S., Kremer, H., Renaud, F.G., Bruns, A. and Osuna, V.R., 2016. Achieving sustainable development goals from a water perspective. *Frontiers in Environmental Science*, 4(64), pp.1-13.

Contzen, N., Kollmann, J. and Mosler, H.J., 2023. The importance of user acceptance, support, and behavior change for the implementation of decentralized water technologies. *Nature Water*, 1(2), pp.138-150.

Das, S.D., 2018. Assessment of atmospheric water generator for rural and remote India. *IOSR Journal of Electrical and Electronics Engineering*, 13(2), pp.67-74.

Davis F.D., 1993. User acceptance of information technology: system characteristics, user perceptions, and behavioral impacts. *International Journal of Man-Machine Studies*, 38(3), pp.475-487. https://doi.org/10.1006/imms.1993.1022.

Davis, F.D., 1989. Perceived usefulness, perceived ease of use, and user acceptance of information technology. *MIS Quarterly*, 13(3), pp.319–340. https://doi.org/10.2307/249008.

Fornell, C. and Larcker, D.F., 1981. Structural equation models with unobservable variables and measurement error: Algebra and statistics. *Journal of Marketing Research*, 18(3), pp.382-388.

Gido, B., Friedler, E. and Broday, D.M., 2016. Assessment of atmospheric moisture harvesting by direct cooling, *Atmospheric Research*, 182 (1), pp.156-162. https://doi.org/10.1016/j.atmosres.2016.07.029.

Gleick, P. and Cooley, H., 2009. Energy Implications of Bottled Water. *Environmental Research Letters*, 4(1), pp.1-6. doi: 10.1088/1748-9326/4/1/014009.

Hair, J.F., Black, W.C., Babin, B.J. and Anderson, R.E., 2010. *Multivariate Data Analysis (7th ed.)*. Upper Saddle River, NJ: Prentice Hall.

Jarimi, H., Powell, R. and Riffat, S., 2020. Review of sustainable methods for atmospheric water harvesting. *International Journal of Low-Carbon Technologies*, 15(2), pp.253-276.

Jöreskog, K.G., 1971. Simultaneous factor analysis in several populations. *Psychometrika*, 36(4), pp.409-426.

King, W.R. and He, J., 2006. A meta-analysis of the technology acceptance model. *Information Management*, 43(1), pp.740–755.

Kuzma, S., Saccoccia, L. and Chertock, M., 2023. 25 *Countries, Housing One-quarter of the Population, Face Extremely High Water Stress*. World Resources Institute. Retrieved July 2, 2024, from https://www.wri.org/insights/highest-water-stressed-countries.

Lee, Y.K., Chang, C.T., Lin, Y. and Cheng, Z.H., 2014. The dark side of smartphone usage: Psychological traits, compulsive behavior, and technostress. *Computers in Human Behavior*, 31(1), pp.373-383.

Lee, Y.H., Hsieh, Y.C. and Chen, Y.H., 2013. An investigation of employees' use of e-learning systems: applying the technology acceptance model, *Behaviour and Information Technology*, 32(2), pp.173–189. https://doi.org/10.1080/0144929X.2011.577190

Lee, Y., Kozar, K.A. and Larsen, K.R.T., 2003. The technology acceptance model: past, present, and future. *Communication Association Information Systems*, 12(50), pp.752–780.

Legris, P., Ingham, J. and Collerette, P., 2003. Why do people use information technology? A critical review of the technology acceptance model. *Information and Management*, 40(3), pp.191-204.

Lule, I., Omwansa, T.K. and Waema, T.M., 2012. Application of technology acceptance model (TAM) in m-banking adoption in Kenya. *International journal of computing & ICT research*, 6(1), pp.31-42.

Madias, K., Szymkowiak, A. and Borusiak, B., 2023. What builds consumer intention to use smart water meters–Extended TAM-based explanation. *Water Resources and Economics*, 44, pp.1-33.

Matarneh, S., AlQaraleh, L., Alkhrissat, T. and Abdel-Jaber, M., 2023. Assessing water production from air conditioning systems as an unconventional supply source: A focus on water quality and social acceptance perspectives. *Case Studies in Chemical and Environmental Engineering*, 9, pp.1-13.

Morienyane, L.D. and Marnewick, A., 2019. Technology Acceptance Model of Internet of Things for Water Management at a Local Municipality. *Technology & Engineering Management*, 61, pp.1-6.

Peters, G.M, Blackburn, N.J. and Armedion, M., 2013. Environmental assessment of air to water machines-triangulation to manage scope uncertainty. *Springer-Vsuccumbed Berlin Heidelberg*, 18, pp.1149-1157.

Pontious, K., Weidner, B., Guerin, N., Dates, A., Pierrakos, O. and Altaii, K., 2016. Design of an atmospheric water generator: Harvesting water out of thin air. *Information and Electronic Systems*, 41, pp.6-11. doi: 10.1109/SIEDS.2016.7489327.

Pavlou, P.A., 2003. Consumer acceptance of electronic commerce: Integrating trust and risk with the technology acceptance model. *International Journal of Electronic Commerce*, 7(3), pp.101-134.

Raveesh G., Goyal, R. and Tyagi, S.K., 2021. Advances in atmospheric water generation technologies. *Energy Conversion and Management*, 239, https://doi.org/10.1016/j.enconman.2021.114226.

Renny, M., Guritno, S. and Siringoringo, H., 2013. Perceived usefulness, ease of use, and attitude towards online shopping usefulness towards online airline ticket purchase. *Procedia - Social and Behavioral Sciences*, 81, pp.212–216. https://doi.org/10.1016/j.sbspro.2013.06.415

Saris, W.E. and Stronkhorst, L.H., 1984. *Causal Modelling in Nonexperimental Research: An Introduction to the LISREL Approach*. Sociometric Research Foundation.

Sharp, J.H., 2007. Development, extension, and application: a review of the technology acceptance model. *Information Systems Education Journal*, 5(9), pp.1–11.

Shafeian, N., Ranjbar, A.A. and Gorji, T.B., 2002. Progress in atmospheric water generation systems: A review. *Renewable and Sustainable Energy Reviews*, 161, https://doi.org/10.1016/j.rser.2022.112325

Shourideh, A., Ajram, W.B., Lami, J.A., Haggag, S. and Mansouri, A., 2018. A comprehensive study of an atmospheric water generator using the Peltier effect. *Thermal Science and Engineering Progress*, 6, pp.14-26.

Tripathi, A., Tushar, S., Pal, S., Lodh, S., Tiwari, S. and Desai, R.S., 2016. Atmospheric Water Generator. International Journal of Enhanced Research in Science. *Technology & Engineering*, 5(4), pp.231-242.

Turner, M., Kitchenham, B., Brereton, P., Charters, S. and Budgen, D., 2010. Does the technology acceptance model predict actual use? A systematic literature review. *Information Software Technology*, 52, pp.463-479.

Venkatesh, V. and Davis, F.D., 2000. A theoretical extension of the technology acceptance model: four longitudinal field studies, *Management Science*, 46 (2), pp.186–204. https://doi.org/10.1287/mnsc.46.2.186.11926.

Willis, R.M., Stewart, R.A., Panuwatwanich, K., Jones, S. and Kyriakides. A., 2010. Alarming visual display monitors affecting shower end-use water and energy conservation in Australian residential households. *Resources Conservation and Recycling*, 54(12), pp.1117–1127. https://doi.org/10.1016/j.resconrec.2010.03.004

Wolsink, M., 2010. Contested environmental policy infrastructure: Socio-political acceptance of renewable energy, water, and waste facilities. *Environmental Impact Assessment Review*, 30(5), pp.302-311.

Wu, K., Zhao, Y., Zhu, Q., Tan, X. and Zheng, H., 2011. A meta-analysis of the impact of trust on technology acceptance model: Investigation of the moderating influence of subject and context type. *International Journal of Information Management*, 31(6), pp.572-581.

Original Research Paper | https://doi.org/10.46488/NEPT.2025.v24i01.D1698 | Open Access Journal

Evaluation of Physicochemical Parameters in Sandy Soils After Applying Biochar as an Organic Amendment

Alex Huamán De La Cruz[1,3]† , Gina Luna-Canchari[2], Nicole Mendoza-Soto[2], Daniel Alvarez Tolentino[3], Ronald Jacobi Lorenzo[4], Armando Calcina Colqui[4], Geovany Vilchez Casas[4], Julio Mariños Alfaro[3] and Roger Aguilar Rojas[3]

[1]Facultad de Derecho, Universidad Tecnológica del Perú, San Agustín de Cajas 12007, Huancayo 12001, Peru

[2]Escuela Profesional de Ingeniería Ambiental, Universidad Peruana Unión, Lima, Peru

[3]Escuela Profesional de Ingeniería Ambiental, Universidad Nacional Intercultural de la Selva Central Juan Santos Atahualpa, Jr. Los Cedros N°141, Chanchamayo, Perú

[4]Escuela Profesional de Ingeniería Civil, Universidad Nacional Intercultural de la Selva Central Juan Santos Atahualpa, Jr. Los Cedros N°141, Chanchamayo, Perú

†Corresponding author: Alex Huamán De La Cruz; alebut2@hotmail.com

ABSTRACT

Sandy soils are not suitable for agriculture because they do not retain nutrients, and water drains quickly. The biochar applied to these soils provides nutrients, improves their fertility, and favors crop yields. Thus, this work aimed to evaluate the effect of the application of pine biochar and the pruning of green areas obtained by slow pyrolysis on the physicochemical attributes of sandy soil. For this purpose, a greenhouse experiment was conducted in fifteen pots randomly divided into three groups (five replicas) of treatment depending on the dose of biochar: 0% (0 g/pot, T1 control treatment), 10% (100 g/pot, T2), and 25% (250 g/pot, T3) calculated according to the volume of the soil. Likewise, 05 seeds of turnip (*Brassica rapa* subsp. *rapa*) were placed in each pot, where their germination and growth were monitored. Application of biochar reported an increase in organic matter, porosity, pH, electrical conductivity, cation exchange capacity, NO_3^-, K, and Mg (without significant differences) and a reduction in bulk density, P, and Ca (without significant differences). These behaviors were higher in T3, followed by T2, compared to T1. Similarly, T3 (68%, 7.5 ± 0.9 cm) showed a higher number of turnip germinations and growth compared to T2 (48%, 7 ± 0.6 cm) and T1 (28% 6 ± 0.4 cm). The biochar applied improved the attributes of the sandy soil, strengthening it against possible erosion and promoting the preservation of terrestrial ecosystems.

INTRODUCTION

Land degradation is a problem that is growing at alarming rates, threatening land productivity and fertility, as well as food security, sustainable development, and healthy ecosystems in many countries around the world (Jie et al. 2002). The Intergovernmental Science-policy Platform on Biodiversity and Ecosystem Services (IPBES) indicates that only a quarter of the world's land is free from anthropogenic impact and that by 2050 this will be reduced to one-tenth (IPBES 2018). Likewise, the United Nations (UN) maintains that every year 24000 million tons of fertile soil are lost as a result of desertification, which puts at risk the well-being of 3200 million people (ONU 2019). In Latin America, Brazil and Honduras show the highest deforestation, while Mexico, Argentina, Bolivia, Chile, and Peru have the highest desertification (Ontiveros 2014).

In Peru, desertification is classified according to its geographical regions. In the Sierra, due to overgrazing, water and wind erosion and pollution, on the coast by salinization, and the jungle mainly by water erosion (Eguren & Marapi 2015). Peru

faces significant soil degradation challenges due to erosion in the Andes, deforestation in the Amazon, overgrazing in highland pastures, and unsustainable agricultural practices like monoculture and excessive chemical use (Tito et al. 2022). Mining activities contribute to soil contamination and erosion, while climate change exacerbates these issues with extreme weather events (Bech et al. 2017). Additionally, irrigation-induced salinization and rapid urbanization further degrade soil quality, complicating efforts to maintain soil health. For instance, the National Forest and Wildlife Service (SERFOR) identified 8.2 million degraded hectares in Peru, with 2.2 million referring to the Sierra, 519,000 in the Jungle, and 149,000 in the Coast (Andina 2021). Among the main problems of soil degradation in Peru are the loss of vegetation cover and biodiversity, burning of pastures and forest fires, reduction of ecosystem services, overgrazing, poor agricultural practices, inadequate water use, change of land use (overuse), erosion, etc. (Andina 2021). Soil degradation occurs when it loses or is altered its chemical, physical, ecological, and biological properties as a result of natural or anthropogenic disturbances (population growth, industrialization, and climate change) (FAO 2015).

Soil degradation processes include erosion, nutrient, and organic matter depletion, loss of organic carbon, desertification, acidification, and pollution (Samec et al. 2023).

Sandy soils are prone to erosion, especially in areas with minimal vegetation cover or where the wind is strong, which degrades soil quality over time (Flumignan et al. 2023). Much of Peru's sandy soils are found along the coastal regions, particularly in the desert areas, which is a major agricultural hub, producing a variety of high-value crops such as asparagus, avocados, grapes, and various fruits and vegetables for domestic consumption and export (Olarte et al. 2023). Thus, this degradation could be reversed if sustainable management practices and the use of appropriate technologies are put into practice.

Biochar is a carbon-rich material, a highly porous product that can be obtained from the carbonization (thermal decomposition) of organic materials through the process of pyrolysis (combustion in the absence of oxygen) with temperatures below 700°C. Its application is considered as a promising soil amendment in for several reasons, such as i) soil health improvement because it enhances soil structure, increases nutrient retention, and boosts microbial activity (Yadav et al. 2023), ii) carbon sequestration due to that reduces greenhouse gas emissions and long-term carbon storage (Zhang et al. 2023), iii) environmental benefits because reduces pollution and water quality improvements (Oni et al. 2019), iv) sustainable agriculture due to that enhanced crop yields and reuse agricultural and forestry residues (Liu et al. 2023), and v) climate resilience because improve drought resistance and extreme weather conditions (Lehmann et al. 2021). Furthermore, due to its high specific surface, high porosity, and strong adsorption capacity, biochar as an organic amendment can remedy soils contaminated by different pesticides (Brassard et al. 2019, Pan et al. 2022) and metals (Haider et al. 2022, Xiong et al. 2024). In plants, biochar improves the biological nitrogen fixation processes by stimulating bacterial nitrification rates. Likewise increases the availability of C, Ca, Mg, K, and P to plants. Biochar-added modified soil microbial habitats and directly affect microbial metabolisms, which together induce changes in microbial community and activity (Zhu et al. 2017).

In addition, recent studies reported that the application of biochar in soils helped to minimize the absorption of metals, thus reducing the toxicity of the metal in different plants such for example wheat (*Triticum aestivum* L.) (Rehman et al. 2020), alfalfa (*Medicago sativa* L.) (Zhang et al. 2019), and lettuce (*Lactuca sativa* L.) (Vannini et al. 2021, Rivera et al. 2022).

Avoiding, reducing, and reversing the problem of contaminated and degraded soils will protect biological diversity and ecosystem services important for life on Earth and ensure human well-being. Therefore, the objective of this work was to determine the effect of the application of biochar on the physicochemical properties of sandy soils and to evaluate their germination and growth of turnips.

MATERIALS AND METHODS

Soil Sampling and Characterization

The potting experiments were conducted under greenhouse

Table 1: Characterization of physicochemical properties of soil used in biochar experiments.

Parameter	Value
Bulk density (B. D.)	2.20 g.cm^{-3}
Real density (R.D)	2.74 g.cm^{-3}
Porosity (PO)	19.87%
pH	7.77
Electrical conductivity (EC)	726 uS.cm^{-1}
Cation Exchange Capacity (CIC)	0.9 meq.100g^{-1}
Organic matter (OM)	(3.23%)
Texture	Sandy loam
Nitrate (NO$_3$)	1.40 mg.L^{-1}
Potassium (K)	4.5 mg.L^{-1}
Phosphorus (P)	1.10 mg.L^{-1}
Calcium (Ca)	165 mg.L^{-1}
Magnesium ((Mg)	20 mg.Lv1
Color	Wet: Dark Brown
	Dry: Yellowish Brown

conditions using soils sampled within the plant's facilities of the Universidad Peruana Unión (11°59'24" S, 76°50'29" O), Lurigancho-Chosica, Lima (Perú). The soils were obtained by sampling an area of 25 m² at 30 cm depth, applying the methodology of patterns with uniform distribution described in the "Guide for Soil Sampling" of the Ministry of the Environment (MINAM) (MINAM 2014). In total, 25 subsamples were collected (1 kg per m²), which were gathered, homogenized, sieved (Size 1.18 mm with ASTM-E-11 specifications), and quartered to obtain 25 representative samples of 1 kg. One of the samples was randomly characterized as physicochemical (Table 1), presenting a sandy loam texture.

Production and Characterization of Biochar

A pyrolytic furnace of 20 kg capacity was designed and manufactured with two metal cylinders (Fig. 1). An external one (70 cm in height and 58 cm in diameter) produces the biochar with perforations to release volatile gases and energy. An internal one (40 cm in height and 38 cm in diameter) that allowed to feed the residual biomass and increase the temperature of pyrolysis and perforations to regulate the aeration and collect the ashes through the sieving. It is important to mention that the system had a hermetic lid with a chimney (10 cm height and 5 cm height) that allowed the moderate entry and exit of oxygen.

Plant biomass (branches, trunks, and leaves mainly of the pine tree, plant remains, and grasses) corresponding to the pruning of green areas and gardens of the District of Chaclacayo, Lima (Peru) was used as raw material (RM).

This RM was subjected to the process of slow pyrolysis in the pyrolytic furnace, starting with a temperature of 0°C to 200°C (first stage for evaporation of moisture and light volatiles) with a heating rate of 5 °C.s⁻¹ to reach 450 °C (the second stage where hemicellulose and cellulose were devolatilized and decomposed) and with a residence time of 45 min.

Plant biomass (branches, trunks, and leaves mainly of the pine tree, plant remains, and grasses) corresponding to the pruning of green areas and gardens of the District of Chaclacayo, Lima (Peru) was used as raw material (RM). This RM was subjected to the process of slow pyrolysis in the pyrolytic furnace, starting with a temperature of 200°C with a heating rate of 5°C.s⁻¹ to reach 450°C and with a residence time of 45 min.

The biochar obtained was transferred to the laboratory, after which it was crushed using a mortar and sieved to obtain particles smaller than 2 mm (ASTM-E-11 specifications) (Fig. 2) before its use as an organic amendment. From a total of 12.5 kg of biomass, 4.85 kg (38.8% yield) of biochar was obtained.

Application of Biochar Pots with Turnip Seeds (*Brassica rapa* subsp. *rapa*)

To experiment was carried out in fifteen pots, where was added 1 kg of soil, which were divided into five pots (five repetitions) in three treatments: control treatment (T1) had a concentration of 0% (0 g of biochar), treatment two (T2) had a concentration of 10% (0.1 kg of biochar) and treatment three (T3) was 25% (0.25 kg of biochar). Likewise, 05 seeds of turnip (*Brassica rapa* subsp. *rapa*) were placed
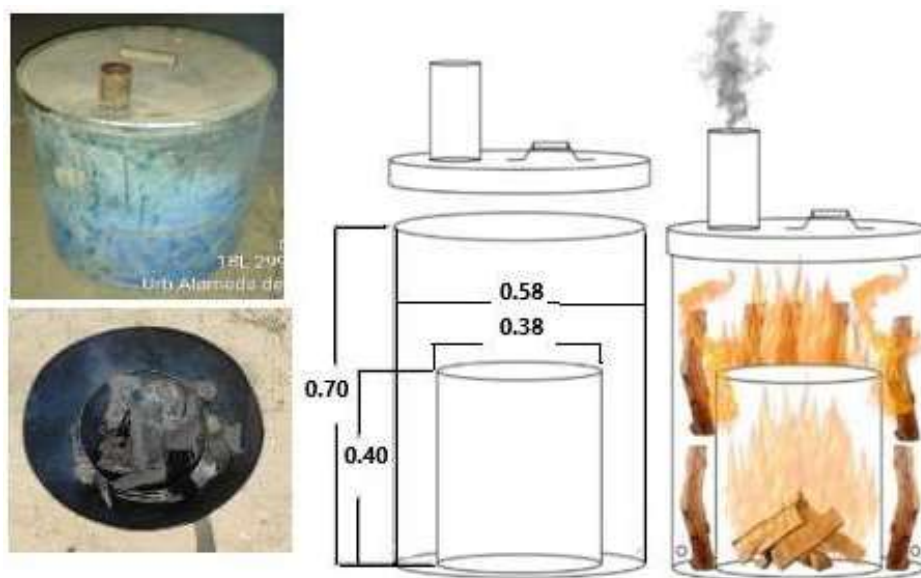
Fig. 1: Desing and use of pyrolytic furnace to produce biochar.

Fig. 2: Crushing and sieving of biochar produced.

Table 2: Physicochemical parameters to be evaluated.

Parameter	Unity	Methodology	Ideal ranges	References
Bulk density (BD)	$g.cm^{-3}$	Cylinder	Low: ≤ 0.7 Ideal: 0.7-0.8 High: 09-1.2 ≥ 1.2	(Reyes 2001)
Real density (DR)	$g.cm^{-3}$	Pycnometer	Around 2.65 g,cm^{-3} *Always minor to BD	(Volverás-Mambuscay et al. 2020)
Porosity (P)	%	Relation between RD and BD	Very low: 30-35 Low: 35-40 Medium: 40-45 High: 45-55 Very high: 55-60	(Reyes 2001)
pH		Potentiometer	Low: < 5 Medium: 5-6 Optimal: 6-7 High: >7	(Meléndez & Molina 2001)
Electrical conductivity (EC)	$\mu s.cm^{-1}$	Potentiometer	Non-saline: 0-2 $dS.m^{-1}$ Slightly saline: 2-4 $dS.m^{-1}$ Moderately saline: 4-8 $dS.m^{-1}$ Strongly saline: 8-16 $dS.m^{-1}$ Very strong saline: >16 $dS.m^{-1}$ *$1000\mu S.cm^{-1} = 1\ dS.m^{-1}$	(Gallart 2017)
Cation exchange capacity (CIC)	$meq.100g^{-1}$	Vacuum pump	Very low: <5 $cmol.Kg^{-1}$ Low: 5-10 Moderately: 10-15 High: 15-20 Very high: >20	(Ortega 1995)
Texture		Bouyoucos	Ideal: loam Good: Sandy loam Acceptable: Approaching or within loamy loam, clay loam, or sandy loam Regular: Approaching or inside silty, clayey, or sandy	(Salinas & García 1979)
Organic matter	%	Titrimetric	Low: <2 Medium: 2-5 Óptimal: 5-10 High:>10	(Meléndez & Molina 2001)
Nitrate (NO_3)	$mg.L^{-1}$	Photometry	Optimal: 2 $mg.kg^{-1}$ - 8 $mq.kg^{-1}$	HORIBA (AOAC 2023)

Table Cont....

Parameter	Unity	Methodology	Ideal ranges	References
Potassium (K)	$mg.L^{-1}$	Photometry	Very low: <0.10 Low: 0.10 – 0.20 Moderate: 0.21-0.30 High: 0.31-0.40 Very high: >0.40	(Ortega 1995)
Phosphorus (P)	$mg.L^{-1}$	Photometry	Low: <12 $mg.L^{-1}$ Medium:12-20 $mg.L^{-}$ Óptimal: 20-50 $mg.L^{-1}$ High: >50 $mg.L^{-}$	(Meléndez & Molina 2001)
Magnesium (Mg)	$mg.L^{-1}$	Photometry	Low: <1 Medium: 1-3 Óptimal:6-3 High: > 6 *cmol/L =10 $mmol.L^{-}$ 1mmool/L = 1ppm ÷ (24.3) 1ppm = $1mg.L^{-1}$	(Meléndez & Molina 2001)
Calcium (Ca)	$mg.L^{-1}$	Photometry	Low: <4 $cmol.L^{-1}$ Medium: 4-6 $cmol.L^{-1}$ Óptimal:15-6 $cmol.L^{-1}$ High: >15 $cmol.L^{-1}$ *cmol/L =10 $mmol.L^{-1}$ $1mmol.L^{-}$ = 1ppm ÷ (40) 1ppm = $1mg.L^{-1}$	(Meléndez & Molina 2001)

in each pot and irrigated with 250 mL of water every two days.

Germination and stem height were monitored every 10 days in the three treatments for 40 days.

Physicochemical Parameters Evaluated

The physicochemical parameters measured at the beginning and end of the experiments, their units, the methodology used, and ideal ranges for the physicochemical properties of soil are presented in Table 2.

Statistical Analysis

The data obtained was subjected to the normality test. Subsequently, the data were submitted to the ANOVA analysis of variance and the Tukey multiple comparison tests (p-value < 0.05) to see differences between the treatments. All statistical treatments were carried out in the free software RStudio (R Team Core 2019) version 4.2.6.

RESULTS AND DISCUSSION

Physicochemical Characterization

Fig. 3 shows the characterization of physical parameters (Bulk Density, organic matter, Porosity, pH, Electrical Conductivity, and Cation Exchange Capacity) measured in the treatments: T1 (0% biochar, control treatment), T2 (10% biochar), and T3 (25% biochar).

Bulk Density (BD) shows that there is a significant difference (p<0.05) between treatments (Fig. 3a). The T3

treatment presented the lowest bulk density with 1.82 ± 0.01 $g.cm^{-3}$, while the control treatment obtained the highest bulk density with (2.22 ± 0.06 $g.cm^{-3}$), showing to be higher by 18.0%. Likewise, it is observed that the addition of biochar to the soil decreases the bulk density by increasing the dose of biochar. Delaye et al. (2020) reported reduced bulk density by adding biochar in soils collected at different soil depths (0-5 cm, 5-10 cm, 10-20 cm, and 20-30 cm). Li et al. (2023) reported a soil bulk density decreasing from 1.30 to 1.10 $\mu g.cm^{-3}$ when was added more corn straw biochar on light sierom soil (0-20 cm). Likewise, the authors reported a reduction of soil thermal conductivity and soil thermal diffusivity but no effects on the soil thermal capacity with the increase of biochar amendment rate. Singh et al. (2022) found a significant reduction in the bulk density of soils with biochar compared to control soils, with greater emphasis on greenhouse studies (62%) than laboratory studies (30%) and field studies (23%). Although the ideal range (0.7- 0.8 $g.cm^{-3}$) of BD was not reached, a reduction in BD could be observed with the increase in the amount of biochar, which could perhaps be achieved if working with for example, 50% dose (500 g biochar) (Reyes 2001). Agbede & Adekiya (2020), after applying biochar of maize on sandy soil, found a significantly improved grain yield and soil chemical properties (reduction bulk density, penetration resistance, and increased porosity).

The organic matter (O.M.) shows significant differences (p<0.05) between the treatments evaluated (Fig. 3b). The highest concentration of O.M. was found in T3 (24%) with an increase of 1044% followed by T2 (13.3%), with an increase

of 578%, both compared to the T1 control treatment (2.3%). It is observed that with an increase in biochar, the amount of MO increases. Biochar has the potential to sequester carbon in the soil, mainly in soils that lose organic matter (Rebolledo et al. 2016). Oses (2013) argues that this happens because Biochar is an amendment with a high content of Organic Matter, and when incorporated into the soil can have positive effects on physicochemical parameters, specifically MO. Likewise, Fiallos-Ortega et al. (2015) reported higher MO content after the addition of Biochar to the soil. Based on the classification of Meléndez and Molina (2001), the organic matter in the control treatment (T1, 2.13%) was at the intermediate level (2-5%), and after adding the biochar, the T2 (13.3%) and T3 (24%) began to present a high level of MO (>10%).

Porosity (Fig. 3c) showed differences (p>0.05) between the three treatments (T1, T2, and T3). An increase in porosity is observed when biochar is added to treatments. T3 presented the highest porosity of 23.2%, followed by T2 with 21.4%, and finally T1 with 19.8%. Baiamonte et al. (2019) found that biochar applied to desert sandy soil from the United Arab Emirates significantly increased soil porosity and the amount of storage pores. Likewise, this behavior of increased porosity and reduction in the BD is in agreement with works previously published in the scientific literature (Toková et al. 2020, Chang et al. 2021, Singh et al. 2022). According to the classification of Reyes (2001), the porosity of T2 and T3 found are within the very low level (30%-35%). However, increases of 20% (T3) and 8% (T2) were achieved compared to the T1 control treatment. Singh et al. (2022) found higher porosity (31% to 66%) when biochar is prepared at higher temperatures (>500°C), while at lower pyrolytic temperatures (<500°C), it has a greater effect on biological diversity, some that were not measured in this work. Based on this, our very low porosity could be related to the low pyrolytic temperature used (450°C).

The pH measured showed differences (p>0.05) between the three treatments (Fig. 3d). pH is an indicator of soil quality because it affects soil function and nutrient availability for plants, pesticide yield, and decomposition of organic matter (Penn & Camberato 2019). There is an increase in pH in T3 (8.05) of 3.6% and 2.3% in T2 (7.95) compared to T1 (7.77) when biochar is added. Lima et al. (2018) applied biochar of coffee residues on sandy soil and found an increase in pH in the function of the doses. Similar findings of pH increase were reported when the percentage of biochar types was increased on different types of soils (Toková et al. 2020, Chang et al. 2021, Singh et al. 2022, Xiong et al. 2024). An optimal pH range varies from 6 to 7 (Meléndez & Molina 2001). Here, the pH varies from 7.77 to 7.95, which is characterized as high (>7). However, this

slightly alkaline scale is also considered suitable for growing any plant and can immobilize metals in the soil.

Regarding Electrical Conductivity (EC), statistical differences (p>0.05) were found between treatments (Fig. 3e). Fig. 3(e) shows an increase in EC with increasing biochar dose, i.e., T2 increased by 74% and T3 by 154% concerning T1, respectively. Kane et al. (2021) indicated that the increase in EC differs depending on the pyrolysis temperature, catalyst used, raw material, and heating rate. For instance, Singh et al. (2022), after doing review work, found an increase in EC of 78% when used as raw material herbaceous, 55% in fine-textured soils, and 51% in biochar prepared at low temperatures (<500°C), all compared to the control group. Thus, the increase in EC in the soil could be related to the fact that pine and garden pruning debris were used as raw materials, which were subjected to a slow pyrolysis of low temperature (450°C) to obtain the biochar. Likewise, all the results are in the category "Non-saline" (Table 2) considered of good quality for agricultural productivity, these results are positive since the low concentration of EC allows the soil not to store salts that could interfere with productivity. This event may be because biochar does not contain high concentrations of salts, unlike synthetic fertilizers.

Fig. 3(f) shows that the values of the Cation Exchange Capacity (CEC) present differences (p>0.05) between the treatments. Likewise, an increase in CEC was observed in T2 treatment (1.3 ± 0.6 meq.100g^{-1}) and T3 (1.9 ± 1.3 meq.100g^{-1}) compared to T1 (0.9 ± 0.5 meq.100g^{-1}). This shows that the application of biochar contributes to increasing the ability of sandy soil to retain cations (Ca, Mg, Na, etc.). Despite showing a growing trend, the concentration of all treatments was less than 5 meq.100g^{-1} is considered a "very low" CEC for agricultural soil (Ortega 1995). However, it is important to note that the chemical properties require more time under study to obtain significant results. Rebolledo et al. (2016) argued that the increase in CEC is probably due to the high negative surface charge, high charge density, and high specific surface area of the Biochar. Chinchajoy (2021) also presented an increase in CEC in treatments with the application of biochar in the soil, which he mentions is related to the oxidation of aromatic carbon and the formation of negatively charged carboxyl.

Fig. 4 shows the chemical parameters of Nitrate (NO$_3$$^-$), potassium (K), phosphorus (P), magnesium (Mg), and Calcium measured in the three treatments: control T1 (0% biochar), T2 (10% biochar), T3 (25% biochar) applied in sandy soils.

Fig. 4(a) shows significant differences (p<0.05) between treatments for nitrate (NO$_3$), with a higher value in T3 (7.6 ± 2.7 mg.kg^{-1}), followed by T2 (4.3 ± 2.1 mg.kg^{-1}), and
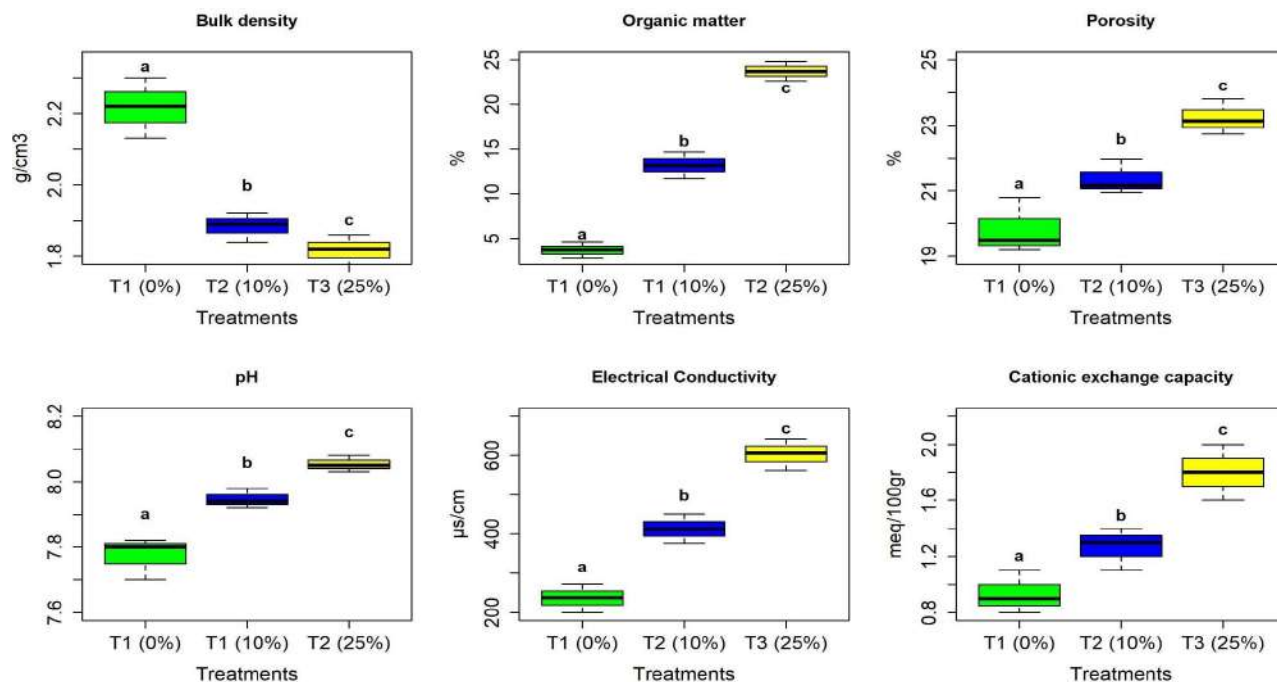
Fig. 3: Physical parameters: (a) Bulk density; (b) Organic matter; (c) Porosity; (d) pH; (e) Electrical conductivity; and (f) Cationic exchange capacity.
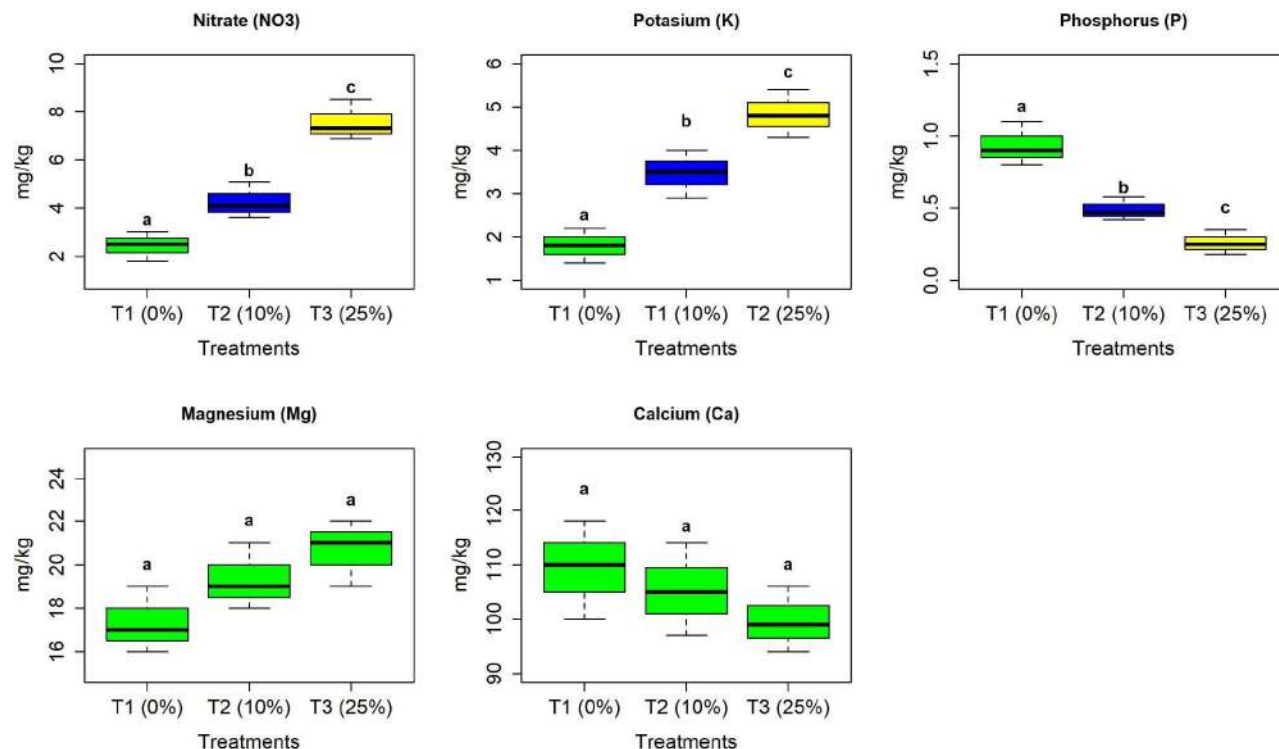
Fig. 4: Result of chemical parameters: (a) nitrate; (b) Potassium (K); (c) Phosphorus (P); (d) Magnesium (Mg); and (e) Calcium (Ca).

T1 (2.4 ± 1.3 mg.kg^{-1}). From Fig. 4(a), it is observed that the addition of biochar increased the amount of nitrate in T2 (79%) and T3 (216%) compared to T1. Hu et al. (Hu et al. 2023) reported an increase of 4.7% to 32.3% when adding

biochar concentrations between 1% to 4% on cropland. Our results were higher probably because higher concentrations of biochar were added to the soil. Nitrate measures the amount of nitrogen (N) available in the soil that can be immediately absorbed by plants (Horiba 2015). Nitrogen in the soil is a complex parameter. It is involved in a whole cycle and is essential for plant growth and ecosystem health (Dong et al. 2022). A higher percentage of nitrogen is found in the atmosphere, which plants cannot capture without microbial help; for that reason, the percentage of MO in the soil is vital to determining the availability of nitrogen (Anas et al. 2020). Pacheco-Avila et al. (2002) mention that the degradation of MO releases Ammonium (NH_4), part of this compound is used by plants, and the rest is transformed into nitrites (NO_2), the same that are oxidized to nitrates (NO_3), a compound that serves as fertilizer for plants. The addition of biochar can improve N recycling in agricultural soil-plant systems, reduce N_2O emissions, control N leaching, and increase microbial activity and crop productivity (Gul & Whalen 2016, Liao et al. 2020). According to Wilson (2017), our values (4.3 to 7.6 mg.L^{-1}) are within the optimal range (2 mg.L^{-1} to 8 mg.L^{-1}) for cropland.

The potassium result (K) is presented in Fig. 4b, where the treatments showed a significant difference ($p > 0.05$). An increase in K in T2 (3.47 ± 1.73 mg.L^{-1}) and T3 (4.83 ± 2.39 mg.L^{-1}) was noted concerning the T1 control treatment (1.80 ± 0.90 mg.L^{-1}). Doulgeris et al. (2023) and Farrar et al. (2022) reported that an increase in the proportion of biochar above the soil increased available K. Likewise, Farrar et al. (2022) argue that the addition of biochar causes less K to be leached, causing more K to be retained, which could explain the increase in K when higher concentrations of biochar is applied.

Fig. 4(c) shows significant differences ($p > 0.05$) between the three treatments, with a reduction in phosphorus (P) by 47% for T2 (0.49 ± 0.25 mg.L^{-1}) and 72% for T3 (0.26 ± 0.14 mg.L^{-1}) compared to control treatment T1 (0.93 ± 0.47 mg.L^{-1}). P is a vital element for plant growth; its reduction in soils indicates soil degradation and environmental pollution (Xu et al. 2019). The availability of P is a function of the pH level of the soil (optimal range between 6.5 to 7.5), showing a high affinity for Al, Fe, and Ca, with which it can form insoluble precipitates dependent on the acidity of the soil. For instance, Penn and Camberato (2019) indicate that phosphate solubility is affected at a pH greater than 6.5. Likewise, Chang et al. (2021) argued that P becomes insoluble at pH less than 6.5, while at higher values, it becomes soluble. Thus, the reduction of available P observed in the soil added with biochar could be related to the increase in pH (7.95 to 8.05) (Fig. 3c) and the formation of precipitates with calcium.

For Magnesium (Mg), the behavior of the results between the treatments did not show significant differences ($p > 0.05$), but there was a slight increase of 11.5% in T2 (19.3 ± 9.5 mg.L^{-1}) and 19.3% for T3 (20.7 ± 8.4 mg.L^{-1}) compared to T1 (17.3 ± 8.6 mg.L^{-1}) (Fig. 4d). These meetings show that the application of Biochar had a positive change on the Mg parameter. Arévalo (2020) reported an increase of 24% (from 1.04 to 1.29 meq.100mL^{-1}) when adding 2.5 kg pine biochar above ground. A greater increase in Mg is probably related to the greater amount of biochar added. Likewise, Wu et al. (2020) reported an increase in Mg (control = 12.9 mg.kg^{-1}) of 24.5% (16.2 mg.kg^{-1}), 65.7% (21.5 mg.kg^{-1}), and 24.2% (16.12 mg.kg^{-1}) when straw, rice, and corn biochar were added, respectively.

Fig. 4(e) shows a reduction in calcium (Ca) concentration of 3.7% in T2 (105 mg.kg^{-1}) and 8.7% for T3 (100 mg.kg^{-1}) compared to T1 (109 mg.kg^{-1}). However, there was no significant difference ($p < 0.05$) between treatments. Ca is an essential component of soil and plants and is key in regulating the acidity, structure, and function of ecosystems (Luo et al. 2023). Arévalo (2020) reported a Ca reduction of 15% and 21% in two 2x2 m soil plots when 2.5 kg of biochar was added as an organic amendment. Wu et al. (2020) found a reduction of Ca by 0.6% when corn biochar was added, .26% with straw biochar, and 48% when wheat biochar was applied. These findings corroborate the report by Singh et al. (2022), who indicate that the effect of biochar on chemical properties is dependent on the raw material used.

*

Effect of Biochar on Turnip Germination

Germination and height were measured every 10 days in the three treatments for 40 days (Table 3). Table 3 shows that the addition of biochar significantly increased ($p > 0.05$) the germination of seeds of T3 (68% germinated) and T2 (48% germinated) concerning T1 (28% germinated). It was also noted that 02 seeds took more than 20 days to germinate in T1, which could be related to the physicochemical characteristics of the control soil. About the height of the stems was observed a greater growth in treatments T1 and T2 without significant difference between these, but if compared to T1. Therefore, it could be attributed that higher germination of seeds is related to a higher dose (% biochar) added. Tammeorg et al. (2014) reported a similar encounter, where a greater number of turnip seeds germinated when biochar was added compared to the control treatment. Murtaza et al. (2023) reported that the addition of biochar on sandy soil caused the growth of corn to increase as a response to the increase in the rate of photosynthesis, reduction of bulk density, moisture retention, and the relationship between plant water and soil. Thus, the addition of biochar

Table 3: Germination and growing of turnip.

Treatment	Day	Germinated plants	Stem height [cm]
T1 (n = 25)	10	01	1
	20	04	3.5
	30	02	4
	40	0	6 ± 0.4
Total		07 a	
T2 (n = 25)	10	5	2
	20	7	4
	30	0	6
	40	0	7
Total		12 b	7 ± 0.6 a
T3 (n = 25)	10	9	2.2
	20	8	4.5
	30	0	6.3
	40	0	7.5
Total		17 c	7.5 ± 0.9 a

could control poor germination and plant growth resulting from poor soil attributes (Furtado et al. 2016). Likewise, an increase in crop productivity after applying biochar was reported in leguminous crops (21.2%), corn (14.3%), and wheat (8.0%) (Zhang et al. 2022). It is important to note that this type of work is influenced by different factors and interactions between, for example, the type of soil, raw material to produce biochar, pyrolysis method, and dose to be added, which must still be studied more extensively.

The application of biochar based on pine and remains of tree pruning on sandy loam soil improved the physicochemical parameters of the soil through the increase of porosity, organic matter, CEC, and K, stabilized the pH, electrical conductivity, there was a slight increase in Mg and maintained the Ca. The physicochemical parameters showed a greater increase (T3 followed by T2) when higher doses (25% and 10%) were added of biochar, compared to T1 (0% control). The sandy soil became ideal for plant development. The seeds germinated in greater quantity and volume in T2. Therefore, it is inferred that the higher the dose of biochar the results are more favorable, without detracting from the results obtained in T2 since a large part of its parameters fall into the quality range.

Biochar offers practical benefits for farmers by enhancing soil fertility, improving water retention, and boosting crop yields, particularly in degraded soils. It helps sequester carbon, supporting climate change mitigation efforts. For policymakers, promoting biochar use aligns with sustainable agriculture goals, reducing the need for chemical fertilizers and addressing soil degradation. Integrating biochar into

agricultural policies can lead to long-term environmental and economic benefits, making farming more resilient and sustainable.

As a recommendation, for sandy soils, apply biochar at 5-10 tons per hectare, mixing it into the top 15-20 cm along with compost or manure. Incorporate it during land preparation or post-harvest, and use cover crops and drip irrigation to enhance its benefits. Regularly test soil and monitor crop performance to adjust application practices for optimal results.

CONCLUSIONS

The application of biochar based on pine and remains of tree pruning on sandy loam soil improved the physicochemical parameters of the soil through the increase of porosity, organic matter, CEC, and K, stabilized the pH, electrical conductivity, there was a slight increase in Mg and maintained the Ca. The physicochemical parameters showed a greater increase (T3 followed by T2) when higher doses (25% and 10%) were added of biochar, compared to T1 (0% control). The sandy soil became ideal for plant development. The seeds germinated in greater quantity and volume in T2. Therefore, it is inferred that the higher the dose of biochar the results are more favorable, without detracting from the results obtained in T2 since a large part of its parameters fall into the quality range. Finally, it is concluded that the biochar used as an organic amendment contributes significantly to the improvement of the physicochemical parameters of the soil, positively impacting the environment.

Future research on biochar should focus on long-term impact studies and examine the effects of biochar on soil health, crop productivity, and carbon sequestration over extended periods. Likewise, to explore how different biochar types and feedstocks affect the soil properties and plant growth.

ACKNOWLEDGMENTS

REFERENCES

Agbede, T.M. and Adekiya, A.O., 2020. Influence of biochar on soil physicochemical properties, erosion potential, and maize (Zea mays L.) grain yield under sandy soil condition. *Communications in Soil Science and Plant Analysis*, 51, pp.2559–2568.

Anas, M., Liao, F., Verma, K.K., Sarwar, M.A., Mahmood, A., Chen, Z.L., et al., 2020. Fate of nitrogen in agriculture and environment: Agronomic, eco-physiological and molecular approaches to improve nitrogen use efficiency. *Biological Research*, 53, pp.1–20.

Andina, 2021. Serfor identifica 8.2 millones de hectáreas degradadas para restaurar en el Perú. *Agencia Peruana de Noticias*. Retrieved 25

August 2023, from https://andina.pe/agencia/noticia-serfor-identifica-82-millones-hectareas-degradadas-para-restaurar-el-peru-833166.aspx.

AOAC, 2023. Nitrogen. *Official Methods of Analysis of AOAC INTERNATIONAL*, Oxford University Press, pp.12–21.

Arévalo, N.M., 2020. *Assessment of Soil Quality Through the Application of Pine Needle Biochar (Pinus Patula) in the Machángara - Saucay Basin*. Salesian Polytechnic University, Cuenca Campus. Pp.1–112.

Baiamonte, G., Crescimanno, G., Parrino, F. and De Pasquale, C., 2019. Effect of biochar on the physical and structural properties of a sandy soil. *CATENA*, 175, pp.294–303.

Bech, J., Roca, N. and Tume, P., 2017. *Hazardous Element Accumulation in Soils and Native Plants in Areas Affected by Mining Activities in South America*. In: *Assessment, Restoration, and Reclamation of Mining Influenced Soils*. Elsevier Inc., pp.419–461.

Brassard, P., Godbout, S., Lévesque, V., Palacios, J.H., RaghavanV. and Ahmed, A., 2019. Biochar for soil amendment. In: Char and Carbon Materials Derived from Biomass, Elsevier, pp. 109–146.

Chang, Y., Rossi, L., Zotarelli, L., Gao, B., Shahid, M.A. and Sarkhosh, A., 2021. Biochar improves soil physical characteristics and strengthens root architecture in Muscadine grape (Vitis rotundifolia L.). *Chemical and Biological Technologies in Agriculture*, 8, pp.1–11.

Chinchajoy, J.A.B., 2021. *Effect of Biochar Addition as a Soil Amendment on Microorganisms Related to the Carbon Cycle* Universidad de la Salle, pp.1–49.

Delaye, L.A.M., Ullé, J.Á. and Andriulo, A.E., 2020. Biochar application in degraded soil under sweet potato production effect on edaphic properties. *Ciencia del Suelo*, 38, pp. 162–173.

Dong, J., Cui, X., Niu, H., Zhang, J., Zhu, C., Li, L. and Zhang, X., 2022. Effects of nitrogen addition on plant properties and microbiomes under high phosphorus addition level in the Alpine Steppe. *Frontiers in Plant Science*, 13, pp.1–11.

Doulgeris, C., Kypritidou, Z., Kinigopoulou, V. and Hatzigiannakis, E., 2023. Simulation of potassium availability in the application of biochar in agricultural soil. *Agronomy*, 13, p.784.

Eguren, F. and Marapi, R., 2015. The soils in Peru: A fundamental resource for creating and sustaining life. *La Revista Agraria*, 170, p.1–16.

FAO, 2015. Soils Are Endangered, But the Degradation Can Be Rolled Back. Food and Agriculture Organization of the United Nations. Retrieved 23 August 2023, fromhttps://www.fao.org/news/story/en/item/357059/icode/.

Farrar, M.B., Wallace, H.M., Xu, C.-Y., Joseph, S., Nguyen, T.T.N., Dunn, P.K. and Smith, R., 2022. Biochar compound fertilisers increase plant potassium uptake 2 years after application without additional organic fertiliser. *Environmental Science and Pollution Research*, 29, p.7170–7184.

Fiallos-Ortega, L.R., Flores-Mancheno, G., Duchi-Duchi, N., Flores-Mancheno, I., Baño-Ayala, D. and Estrada-Orozco, L., 2015. Soil ecological restoration applying biochar (charcoal) and its effects on the Medicago sativa production. *Rev Cien Agri*, 12, p.13–20.

Flumignan, D.L., Gomes, L.D., Motomiya, A.V.A., Oliveira, G.Q. De and Vieira Filho, P.S., 2023. Soil cover is strategic to remedy erosion in sandy soils. *Engenharia Agrícola*, 43, p.1–2.

Furtado, G. de F., Chaves, L.H.G., de Sousa, J.R.M., Arriel, N.H.C., Xavier, D.A. and de Lima, G.S., 2016. Soil chemical properties, growth and production of sunflower under fertilization with biochar and NPK. *Australian Journal of Crop Science*, 10, p.418–424.

Gallart, F., 2017. *The Electrical Conductivity of Soil as an Indicator of Soil Use Capacity in the Northern Area of the Albufera Natural Park in Valencia*. Universitat Politecnica de Valencia, p.1–34.

Gul, S. and Whalen, J.K., 2016. Biochemical cycling of nitrogen and phosphorus in biochar-amended soils. *Soil Biology and Biochemistry*, 103, p.1–15.

Haider, F.U., Wang, X., Farooq, M., Hussain, S., Cheema, S.A., Ain, N. ul, and Zhang, L., 2022. Biochar application for the remediation of trace metals in contaminated soils: Implications for stress tolerance and crop production. *Ecotoxicology and Environmental Safety*, 230, p.113165.

Horiba, M. 2015. Soil nitrate measurement for determination of plant-available nitrogen. *ASPLM*, 6, pp.2–3.

Hu, T., Wei, J., Du, L., Chen, J. and Zhang, J., 2023. The effect of biochar on nitrogen availability and bacterial community in farmland. *Annals of Microbiology*, 73, p.1–11.

IPBES, 2018. Press Release: Global Soil Degradation Worsens and Is Now "Critical," Threatening the Well-being of 3.2 Billion People. Science and Policy for People and Nature.. Retrieved 24 August 2023, from https://www.ipbes.net/news/comunicado-de-prensa-la-degradación-del-suelo-nivel-mundial-empeora-y-ahora-es-crítica-poniendo.

Jie, C., Jing-zhang, C., Man-zhi, T. and Zi-tong, G., 2002. Soil degradation: A global problem endangering sustainable development. *Journal of Geographical Sciences*, 12, p.243–252.

Kane, S., Ulrich, R., Harrington, A., Stadie, N.P. and Ryan, C., 2021. Physical and chemical mechanisms that influence the electrical conductivity of lignin-derived biochar. *Carbon Trends*, 5, p.100088.

Lehmann, J., Cowie, A., Masiello, C.A., Kammann, C., Woolf, D., Amonette, J.E. and Smith, R., 2021. Biochar in climate change mitigation. *Nature Geoscience*, 14, p.883–892.

Li, Y.Q., Li, L.J., Zhao, B.W., Zhao, Y., Zhang, X., Dong, X. and Wang, Y., 2023. Effects of corn straw biochar, soil bulk density and soil water content on thermal properties of a light sierozem soil. *Nature Environment and Pollution Technology*, 22, p.895–903.

Liao, J., Liu, X., Hu, A., Song, H., Chen, X. and Zhang, Z., 2020. Effects of biochar-based controlled release nitrogen fertilizer on nitrogen-use efficiency of oilseed rape (Brassica napus L.). *Scientific Reports*, 10, p.1–14.

Lima, J.R. de Moraes Silva, W., de Medeiros, E.V., Duda, G.P., Corrêa, M.M., Martins Filho, A.P. and Pereira, F., 2018. Effect of biochar on physicochemical properties of a sandy soil and maize growth in a greenhouse experiment. *Geoderma*, 319, p.14–23.

Liu, Z., Ju, X., Zheng, L. and Yu, F., 2023. The Bright Future of Biochar in Sustainable Agriculture: A Bibliometric Analysis. *Journal of Soil Science and Plant Nutrition*, 23, p.5036–5047.

Luo, Y., Shi, C., Yang, S., Liu, Y., Zhao, S. and Zhang, C., 2023. Characteristics of soil calcium content distribution in Karst dry-hot valley and its influencing factors. *Water*, 15, p.1119.

Meléndez, G. and Molina, E., 2001. Soil fertility and crop nutrition management in Costa Rica. *Plos One,* 715, pp.102134–102148

MINAM, 2014. *Guide for Soil Sampling*. MINAM p.72.

Murtaza, G., Ahmed, Z., Eldin, S.M., Ali, B., Bawazeer, S., Usman, M. and Zhang, L., 2023. Biochar-Soil-Plant interactions: A cross talk for sustainable agriculture under changing climate. *Frontiers in Environmental Science*, 11, p.1–16.

Olarte, D.L., Aguilar-Bardales, Z. and Calderón-Cahuana, D.L., 2023. Estimation of the soil-water characteristic curve in sandy soils using the filter paper method. *TECNIA*, 33, p.42–51.

Oni, B.A., Oziegbe, O. and Olawole, O.O., 2019. Significance of biochar application to the environment and economy. *Annals of Agricultural Sciences*, 64, p.222–236.

Ontiveros, R., 2014. *Methodological Guide, Climate Change and Soil Degradation in Latin America*. EuroClima, pp.1–192.

ONU, 2019. Around 24 Billion Tons of Fertile Soil Are Lost Each Year Due to Desertification. United Nations. Retrieved 24 August 2024, from https://news.un.org/es/story/2019/06/1457861.

Ortega, D., 1995. *Soils of Colombia: Origin, Evolution, Classification, Distribution, and Use*. In: *Agrológica*. Colombia, p.632.

Oses, A.O., 2013. *Effects of Biochar Application in the Hierarchical Aggregation Model of a Forest Soil Under Oceanic Conditions*. Springer, 96p.

Pacheco-Avila, J., Pat-Canul, R. and Cabrera-Sansores, A., 2002. Analysis

of the nitrogen cycle in the environment in relation to groundwater and its effect on living beings. *Ingeniería*, 6, pp.73–81.

Pan, L., Mao, L., Zhang, H., Wang, P., Wu, C., Xie, J. and et al., 2022. Modified biochar as a more promising amendment agent for remediation of pesticide-contaminated soils: Modification methods, mechanisms, applications, and future perspectives. *Applied Sciences (Switzerland)*, 12, p.651.

Penn, C. and Camberato, J., 2019. A critical review of soil chemical processes that control how soil pH affects phosphorus availability to plants. *Agriculture*, 9, p.120.

R Team Core, 2019. *A Language and Environment for Statistical Computing*. R Foundation for Statistical Computing.

Rebolledo, A.E., López, G.P. and Moreno, C.H., 2016. Biocarbón (biochar) I: Naturaleza, historia, fabricación y uso en el suelo. *Terra Latinoamericana*, 34, pp.367–382.

Rehman, M.Z. ur, Zafar, M., Waris, A.A., Rizwan, M., Ali, S. and Sabir, M., 2020. Residual effects of frequently available organic amendments on cadmium bioavailability and accumulation in wheat. *Chemosphere*, 244, p.125548.

Reyes, M.L., 2001. Soil degradation in Sonora: The problem of erosion in soils used for livestock. *Región y sociedad*, 13, pp.1–25.

Rivera, J., Reyes, J., Cuervo, J., Martínez-Cordón, M. and Zamudio, A., 2022. Effect of biochar amendments on the growth and development of "Vera" crisp lettuce in four soils contaminated with cadmium. *Chilean Journal of Agricultural Research*, 82, pp.244–255.

Salinas, J.G. and García, R., 1979. *Analytical Methods for Acid Soils and Plants*. Colombia Publication, p.62

Samec, P., Kučera, A. and Tomášová, G., 2023. *Forest Degradation Under Global Change, Sustainable Development*, Oxford Publications, pp.1–62.

Singh, H., Northup, B.K., Rice, C.W. and Prasad, P.V.V., 2022. Biochar applications influence soil physical and chemical properties, microbial diversity, and crop productivity: A meta-analysis. *Biochar*, 4, pp.1–17.

Tammeorg, P., Simojoki, A., Mäkelä, P., Stoddard, F.L., Alakukku, L. and Helenius, J., 2014. Biochar application to a fertile sandy clay loam in boreal conditions: effects on soil properties and yield formation of wheat, turnip rape, and faba bean. *Plant and Soil*, 374, pp.89–107.

Tito, R., Salinas, N., Cosio, E.G., Boza Espinoza, T.E., Muñiz, J.G. and Aragón, S., 2022. Secondary forests in Peru: differential provision of ecosystem services compared to other post-deforestation forest transitions. *Ecology and Society*, 27, art.12.

Toková, L., Igaz, D., Horák, J. and Aydin, E., 2020. Effect of biochar application and re-application on soil bulk density, porosity, saturated hydraulic conductivity, water content and soil water availability in a silty loam haplic luvisol. *Agronomy*, 10, p.1005.

Vannini, A., Bianchi, E., Avi, D., Damaggio, N., Di Lella, L. and Nannoni, F., 2021. Biochar amendment reduces the availability of Pb in the soil and its uptake in lettuce. *Toxics*, 9, p.268.

Volverás-Mambuscay, B., Campo-Quesada, J.M., Merchancano-Rosero, J.D. and López-Rendón, J.F., 2020. Physical properties of soil in the Wachado planting system in Nariño, Colombia. *Agronomía Mesoamericana*, 31, pp.743–760.

Wu, C., Hou, Y., Bie, Y., Chen, X., Dong, Y. and Lin, L., 2020. Effects of biochar on soil water-soluble sodium, calcium, magnesium and soil enzyme activity of peach seedlings. *IOP Conference Series: Earth and Environmental Science*, 446, p.032007.

Xiong, M., Dai, G.Q., Sun, R.G. and Zhao, Z., 2024. Passivation effect of corn vinasse biochar on heavy metal lead in paddy soil of Pb-Zn mining area. *Nature Environment and Pollution Technology*, 23, pp.419–426.

Xu, M., Wu, J., Yang, G., Zhang, X., Peng, H., Yu, X. and et al., 2019. Biochar addition to soil highly increases P retention and decreases the risk of phosphate contamination of waters. *Environmental Chemistry Letters*, 17, pp.533–541.

Yadav, S.P.S., Bhandari, S., Bhatta, D., Poudel, A., Bhattarai, S. and Yadav, P. 2023. Biochar application: A sustainable approach to improve soil health. *Journal of Agriculture and Food Research*, 11, p.100498.

Zhang, F., Liu, M., Li, Y., Che, Y. and Xiao, Y., 2019. Effects of arbuscular mycorrhizal fungi, biochar and cadmium on the yield and element uptake of Medicago sativa. *Science of the Total Environment*, 655, pp.1150–1158.

Zhang, L., Wu, Z., Zhou, J., Zhou, L., Lu, Y. and Xiang, Y., 2022. Meta-analysis of the response of the productivity of different crops to parameters and processes in soil nitrogen cycle under biochar addition. *Agronomy*, 12, p.1857.

Zhang, T., Tang, Y., Li, H., Hu, W., Cheng, J. and Lee, X., 2023. A bibliometric review of biochar for soil carbon sequestration and mitigation from 2001 to 2020. *Ecotoxicology and Environmental Safety*, 264, p.115438.

Zhu, X., Chen, B., Zhu, L. and Xing, B., 2017. Effects and mechanisms of biochar-microbe interactions in soil improvement and pollution remediation: A review. *Environmental Pollution*, 227, pp.98–115.

Original Research Paper | https://doi.org/10.46488/NEPT.2025.v24i01.B4226 | **Open Access Journal**

GIS-Based Assessment of Soil Erosion Using the Revised Universal Soil Loss Equation (RUSLE) Model in Morigaon District, Assam, India

Ananya Saikia [ID] **, Monjit Borthakur†** [ID] **and Bikash Jyoti Gautam**
Department of Geography, Cotton University, Guwahati, Assam, India
†Corresponding author: Monjit Borthakur; monjit.borthakur@cottonuniversity.ac.in

ABSTRACT

Soil erosion in the agricultural landscape of Assam has been impacting the livelihoods of millions. In administrative regions like districts, which are vulnerable to natural disasters like floods and bank erosion, GIS-based soil erosion estimating studies can help planners and policymakers identify areas of soil erosion to implement scientific conservation measures. The main purpose of this study is to estimate soil loss and to determine soil loss zones in the Morigaon district of Assam. The Revised Universal Soil Loss Equation (RUSLE) combined with GIS has been incorporated into the present study. The five parameters of RUSLE, namely, rainfall-runoff erosivity, soil erodibility, topographic factor, cover management, and conservation practices, are individually estimated from relevant and authentic data sources, and all these parameters are quantified in GIS. The research findings show that 46.89% of areas in the district are in moderate soil loss zone, eroding 0.78 ton/ha/year, 34.27% of areas are in low soil loss zone, 15.36% of areas are in high soil loss zone, eroding about 12.22 ton/ha/year and 3.47% of areas are in a very high soil loss zone, eroding 192.8 ton/ha/year. The high soil loss zones mainly cover the riverine areas and bare lands in the district. As per our estimation, there is an average of 205.85 tonnes of soil loss in the district per hectare per year.

INTRODUCTION

Soil erosion, in general, involves the removal and transport of the top layer of soil. It is a global problem affecting natural resources, ecosystems, and agricultural production over the decades (Bakker et al. 2005, Ighodaro et al. 2013, Koirala et al. 2019, Littleboy et al. 1992, Parveen & Kumar, 2012, Pimentel 2006, Thapa 2020). Soil loss due to soil erosion is more common, especially in mountainous areas. Generally, soil erosion is induced by two factors: wind (aeolian process) and water (fluvial process), of which water is considered as the primary one. In India, the soil is eroded at an average annual rate of 5.3 billion tons per year (Narayana & Babu 1983), and the average annual soil loss at the national level is 4.9 billion tons (Singh et al. 1992). However, soil loss due to erosion is more common in the Himalayan region and Western Ghats as compared to other parts of the country (Pandey et al. 2007). The surface water flow and resulting soil erosion are mainly induced by five factors, namely rainfall, soil erodibility, topography, cover management, and support practices (Renard 1997).

To estimate annual soil loss due to water erosion, the Science and Education Administration of the National Runoff and Soil Loss Data Centre developed the Universal Soil Loss Equation (USLE) model in 1954 (Wischmeier & Smith 1978), which is the most empirical method for estimating soil loss. USLE is the most widely accepted method for estimating average annual soil loss and its effectiveness in determining conservation measures. However, in 1993, the USDA Soil and Water Conservation Service introduced the Revised Universal

Soil Loss Equation (RUSLE), which is an improved and diverse version of USLE. Both the models are the same, but RUSLE includes more accurate slope length and slope gradient calculations and more detailed calculations for soil cover and conservation practices along with development in iso-erodent maps (Renard 1997). Over the last few decades, numerous studies have been carried out on soil loss estimation studies by many researchers using GIS and remote sensing techniques due to their accuracy and reliability. The majority of the literature found on the study of soil erosion is mainly on river basins or watersheds in India (Abdul Rahaman et al. 2015, Balasubramani et al. 2015, Das & Sarma 2017, Devatha et al. 2015, Ganasri & Ramesh 2016, Gelagay & Minale 2016, Kalita et al. 2018, Kalita & Bhattacharjee 2024, Krishna Bahadur 2009, Pandey et al. 2007, Thakuriah, 2023). However, there are only a few studies on soil loss estimation in the context of state, e.g., soil loss estimation studies in a broader perspective have been made on a state like Goa in India, which is a diversified state surrounded by coasts and Western Ghats (Gaonkar et al. 2024) and in districts or such administrative regions (Budhathoki et al. 2023, Das et al. 2020, Handique et al. 2023, Koirala et al. 2019, Lewis 1985, Nagaraju et al. 2011, Niyonsenga et al. 2021, Thapa 2020).

Measuring soil loss in an area or a region is necessary because it helps design soil conservation measures in an area or a river basin, designing dams and reservoirs, etc. Understanding the rate and patterns of soil loss helps in implementing effective soil conservation techniques such as contour farming, terracing, and afforestation. In the agricultural sector, such studies can help to maintain soil health and ensure long-term productivity. Against the above backdrops, the present study attempts to assess soil loss in the Morigaon district of Assam, which is predominantly an agrarian district of the state. This is the first-ever study on soil loss estimation in the district.

STUDY AREA

Morigaon district of Assam is in the middle part of Assam with a geographical extension of latitude 26°15′ N and 26°50′ N and 92° E and 92°50′ E longitude. The district is bounded by the mighty river Brahmaputra and Darrang district on the north, Karbi Anglong district on the south, Nagaon district on the east, and Kamrup district on the west (Fig. 1.). The total geographical area of the district is 1551 sq. km. The district is characterized by alluvial plains with several rivers and numerous wetlands and is mainly drained by the Brahmaputra, Kopili, Kolong, Sonai, Killing, and Pokoriya rivers. The soil of the district is alluvial and mostly loamy, comprising sand and clay. The district falls under Central Brahmaputra Valley agro-climatic zones under the Eastern
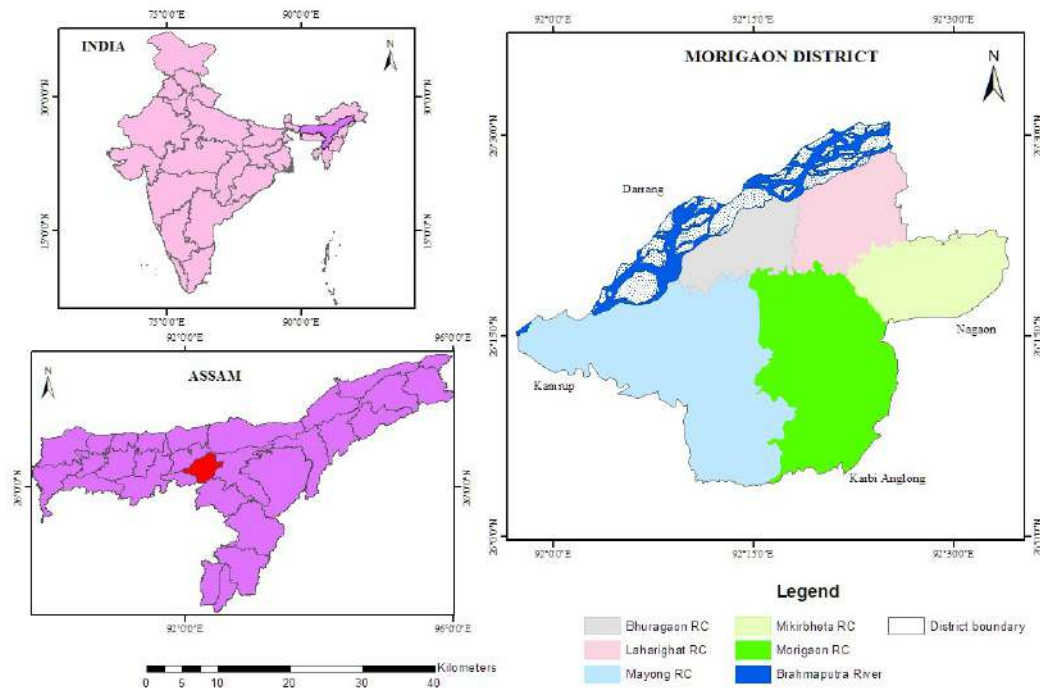
Fig. 1: Location of Morigaon district.

Table 1: Details of the database used in the present study.

Data	Year	Source	Description
Topographical maps	1963	Survey of India (SOI)	78 N15, N16,83 B (03, 04, 06, 07, 08 and 12), 1: 50000
Rainfall data	2012-2021	https://crudata.uea.ac.uk/cru/data/hrg/	High-resolution gridded datasets (CRU TS, CRU CY, CRU CL: 1901-2022 global land data for multiple variables on a 0.5° x 0.5° or finer grid)
Thematic Maps		National Bureau of Soil Survey and Land Use Planning (NBSS & LUP), Nagpur	Soil texture
Satellite image	2021	Copernicus	Sentinel 2A, 10m
	2009	JAXA and Alaska Satellite Facility (ASF)	ALOS PALSAR DEM, 12.5 m

Himalayan Region, for which it is suitable for agricultural production and agriculture is the primary economic activity of the rural households in the district.

MATERIALS AND METHODS

The advent of remote sensing has made it easier to derive spatial information since they are handy and cost-effective. The integrated use of remote sensing and GIS technologies helps to assess soil loss at various scales. Table 1 indicates the data sets used to prepare thematic maps in a GIS environment. The district boundary of Morigaon is derived from the topographical maps of the Survey of India.

RUSLE Model

The RUSLE model estimates the amount of soil loss due to erosion. It is a result of the cooperative effort of scientists and users to update the age-old USLE model. Moreover, the combined use of GIS and RUSLE has been proven to be an effective approach to estimating potential soil loss in a given area (Fernandez et al. 2003, Yitayew et al. 1999). The estimated soil loss equation is very effective in soil conservation studies. The soil loss equation is:

$$A = R \times K \times L \times S \times C \times P \qquad \ldots(1)$$

where, A= Amount of estimated soil eroded, R = rainfall runoff, K = erodibility of soil, L= slope length factor, S =
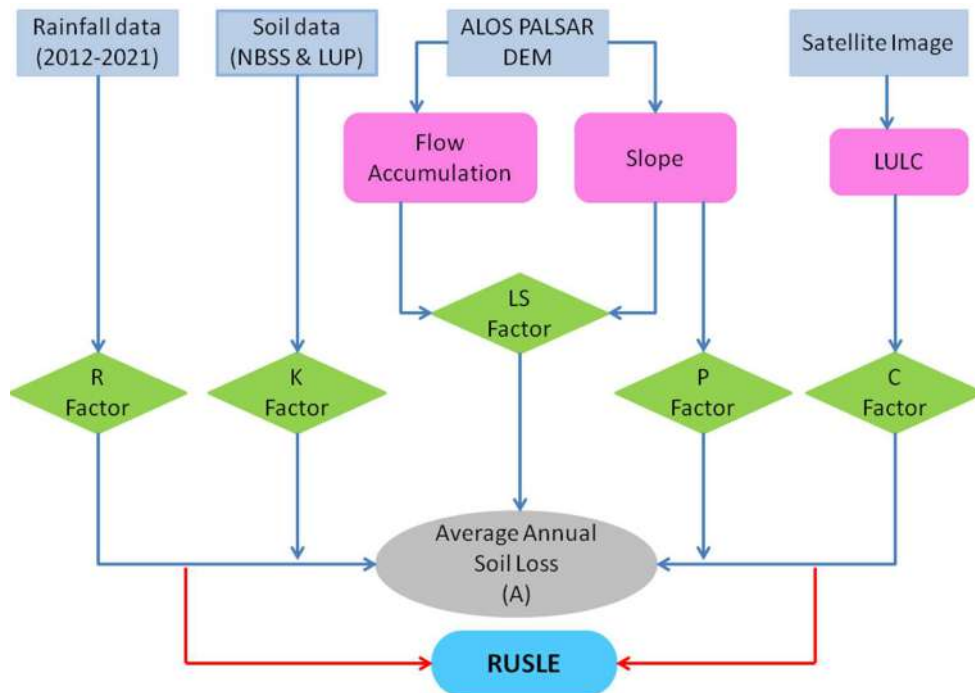
Fig. 2: Flow chart of RUSLE.

slope steepness, C = cover management and P = support practice factor.

Derivations of Parameters of RUSLE

The parameters of RUSLE can be easily integrated with GIS, for which the model acts as an advantage in the present soil loss study. The flow chart of the methodology of the RUSLE model used in this study is presented in Fig. 2.

Rainfall-Runoff Erosivity Factor (R)

Erosivity is the power of wind or water to cause erosion. The higher erosivity results in higher erosion. The rainfall erosion index is a numerical evaluation of rainfall patterns or storms that can erode the topsoil (Wischmeier 1959). It can also be regarded as *'the raindrop impact'* because raindrop impact leads to sheet erosion, which removes the top soil layers. For the R- R-factor, rainfall data has been taken for a period of 10 years i.e., from 2012 to 2021. The ten years of monthly rainfall data have been converted to average yearly data using a raster calculator in GIS. The data is in grid cells, which are further converted to point data, and an isoerodent map has been prepared by adopting the Inverse Distance Weighted (IDW) interpolation technique (Fig. 3). The R factor is calculated using the following equation: (Koirala et al. 2019, Stocking, 1984, Thapa 2020).

$$R = 38.5 + 0.35P \qquad \qquad \dots(2)$$

Table 2: K factor values of different soil textures in the Morigaon district.

Soil texture	K- Factor
Fine loam	0.07
Fine silt	0.40
Coarse loam	0.07
Clay	0.22
Fine	0.05

Soil Erodibility Factor (K)

Soil erodibility is the susceptibility of soil to erode and is related to organic components, soil structure, texture, steepness, etc., which influence the detachment and transportation process (Panagos et al. 2014). It is related to soil infiltration as more infiltration capacity lessens the runoff volume. If runoff is less, soil erosion is also less. Soils containing a high percentage of sand and silt are more susceptible to detachment. However, an increase in the organic and clay content of the soil decreases erodibility as it aggregates the soil, and a higher raindrop impact will be required to break down the soil. Clay has a resisting capacity; however, it is easily transportable once detached. The soil texture of the district and related K factor values has been presented in Table 2. The K factor in the study area ranges from 0.04 to 0.4 (Fig. 4).

Topographic Factor (LS)

The topographic factor comprises the slope length and
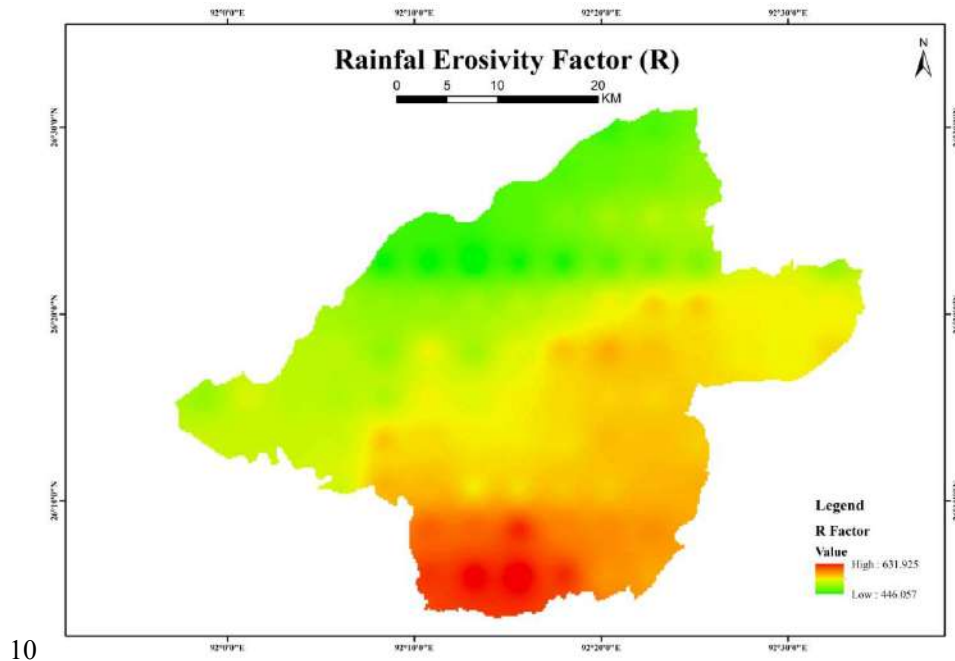
Fig. 3: R factor map of Morigaon district.
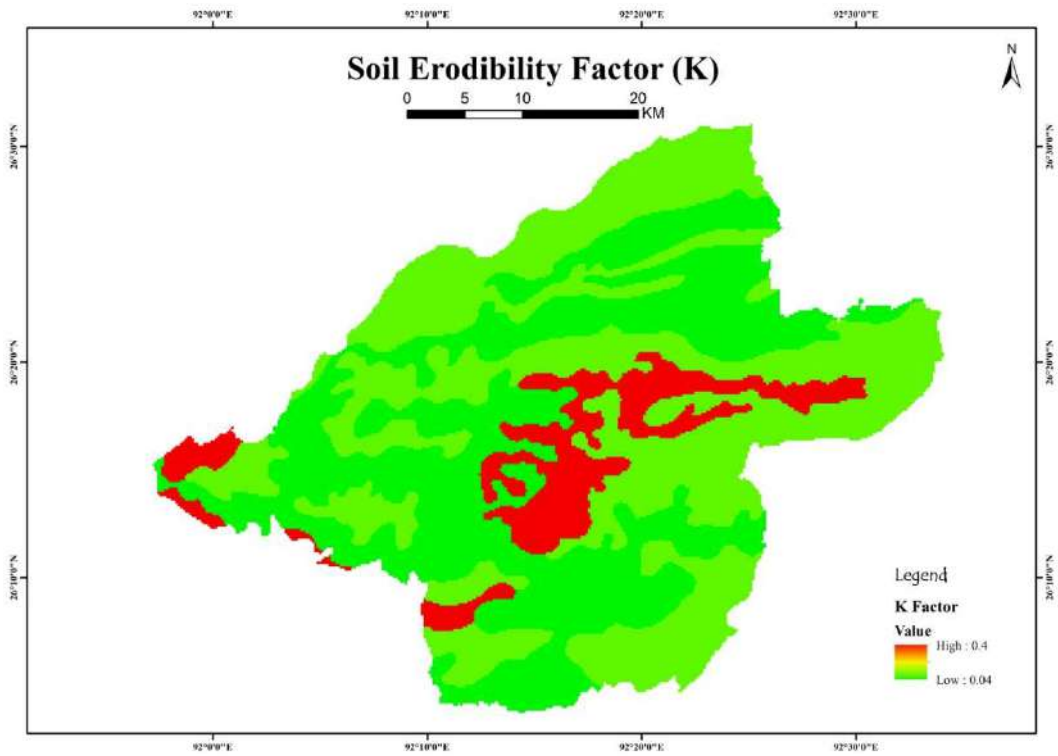
Fig. 4: K factor map of Morigaon district.

slope steepness, which directly influence the surface runoff (Koirala et al. 2019). The degree of slope is the dominant factor of soil erosion. The steeper and longer the slope, the higher the risk for erosion. In a steeper and longer slope, increased surface runoff reduces soil stability. The combined LS factor is computed by following the equation proposed by (Moore & Burch 1986). The LS factor in the study area ranges from 0 to 2.335 (Fig. 5).
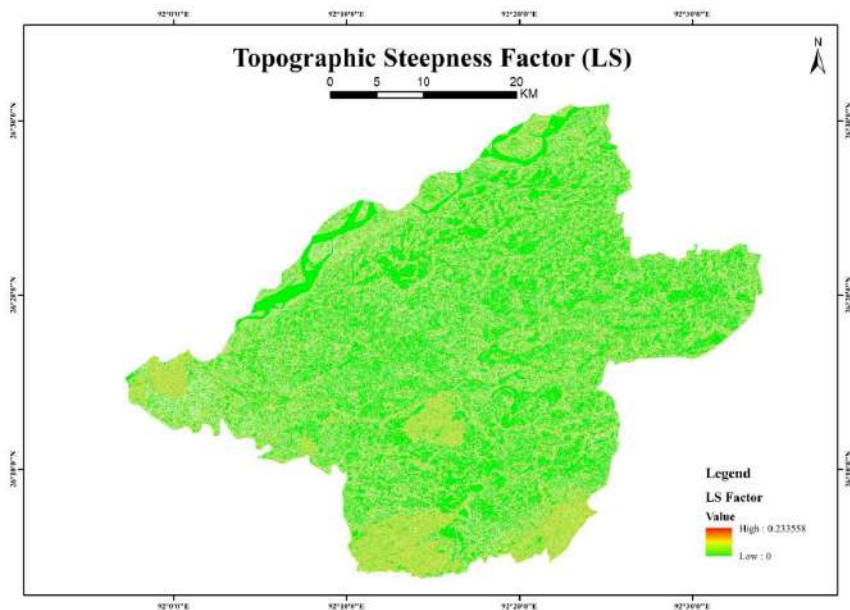
Fig. 5: LS factor map of Morigaon district.
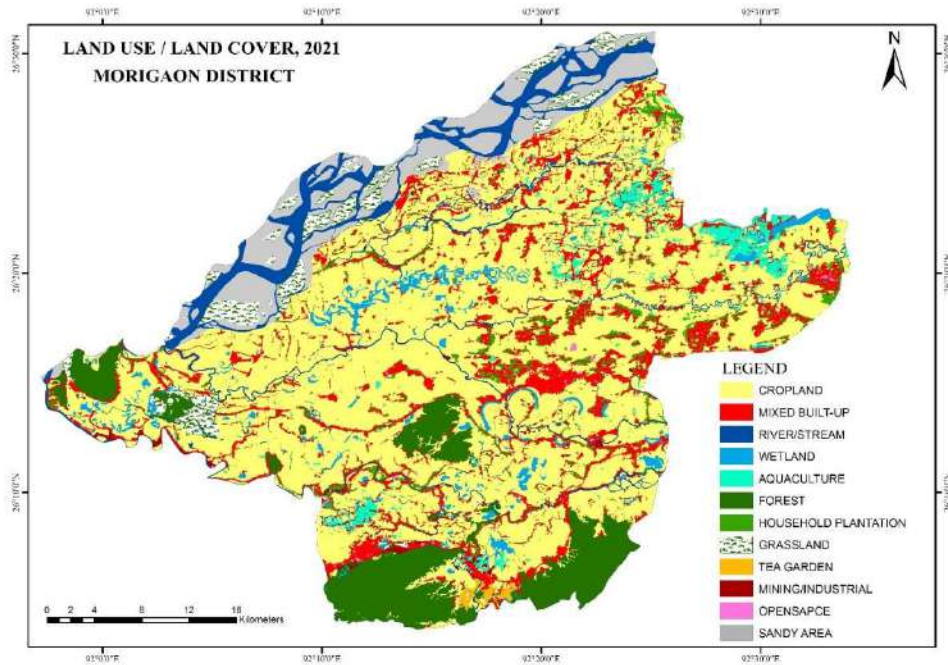
Fig. 6: Land use/land cover map of Morigaon district.

$$LS = \left\{ FA \times \left(cell\, \frac{size}{23.13} \right) \right\}^{0.4} \times$$

$$\{\sin(slope\ of\ DEM \times 0.01745/0.09)\}^{1.3} \times 1.6 \quad \ldots(3)$$

Where LS = Slope length and Steepness factor and FA = Flow accumulation

Cover Management Factor (C)

Cover management implies the ratio of soil loss from an identical area covered under specified land use. Cover management implies the vegetative cover of the area, and

Table 3: Land use classes and associated C values in Morigaon district.

Land cover type	C value	Source
Cropland	0.55	(Yang et al. 2003)
Forest	0.17	(Yang et al. 2003)
Mixed built-up	0	(Koirala et al. 2019)
Mining/Industrial	0.08	(Wang et al. 2016)
Household Plantation	0.03	(Yang et al. 2003)
Agri lands	0.4	(Yang et al. 2003)
Tea garden	0.01	(Wang et al. 2016)
Grassland	0.06	(Yang, 2014)
Open Space	0.35	(Yang et al. 2003)
River/Stream	0	(Koirala et al. 2019)
Wetlands	0.05	(Yang et al. 2003)
Sandy area	1	(Bouguerra et al. 2017)

understanding the specific land use patterns, the risk of soil erosion can be assessed. Major land use classes of a region are an important parameter in assessing soil erosion (Erencin 2000, Folly et al. 1996). Since land use and land cover changes are the most sensitive indicators of the interactions between humans and the environment, they continue to be important areas of research (Alkharabsheh et al. 2013). Fig. 6 shows the land use and land cover map of the Morigaon district, and land cover is classified through visual interpretation techniques using Sentinel data. The C factor has been mapped from land cover classification (Fig. 7), and the C factor values used in different land use classes in the study are represented in Table 3. The C factor in the study area ranges from 0 to 1.

Support Practice Factor (P)

The support practice factor implies the soil loss ratio with support practices like contouring, strip cropping, or terracing in slope (Wischmeier & Smith 1978). For the study area, the P values are obtained following Table 4. P factor map (Fig. 8) has been prepared from the slope map of the district by following the equation:

$$P = 0.2 + 0.3\ S \qquad \ldots(4)$$

Where S is the slope.

RESULTS AND DISCUSSION

In this study, geospatial techniques are incorporated to
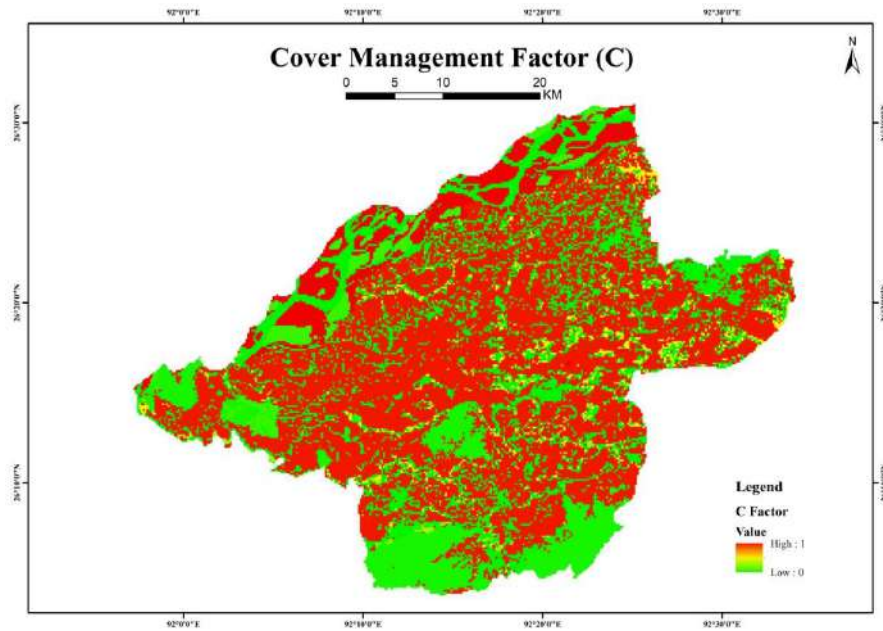
Fig. 7: C factor map of Morigaon district.

Table 4: Support practice factor according to slope (Balabathina et al. 2020, Budhathoki et al. 2023, Koirala et al. 2019).

Slope [%]	Contouring	Strip cropping	Terracing
0.0-7.0	0.55	0.27	0.10
7.0-11.3	0.60	0.30	0.12
11.3-17.6	0.80	0.40	0.16
17.6-26.8	0.90	0.45	0.18
26.8>	1	0.50	0.20

estimate soil erosion using the RUSLE model. The soil erosion or estimated soil loss map was generated (Fig. 9), and the erosion map of the study area is categorized into four soil loss categories, namely, low, moderate, high, and very high. The estimated results show that 3.47% area in the district is in a very high category of soil loss, where about 192.8 tons. ha^{-1} of soil is being eroded annually. The maximum soil loss category in the district lies in the moderate soil loss category (46.89%), followed by the low soil loss category (34.27%
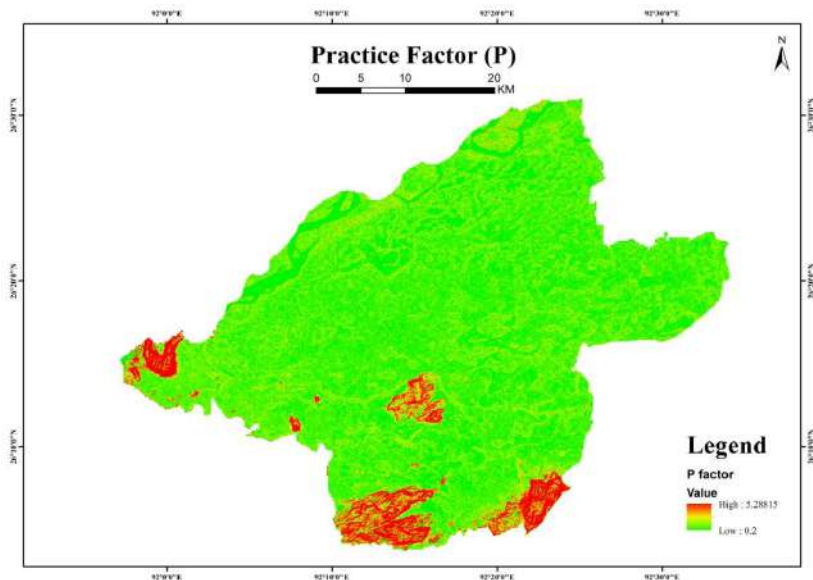
Fig. 8: P factor map of Morigaon district.
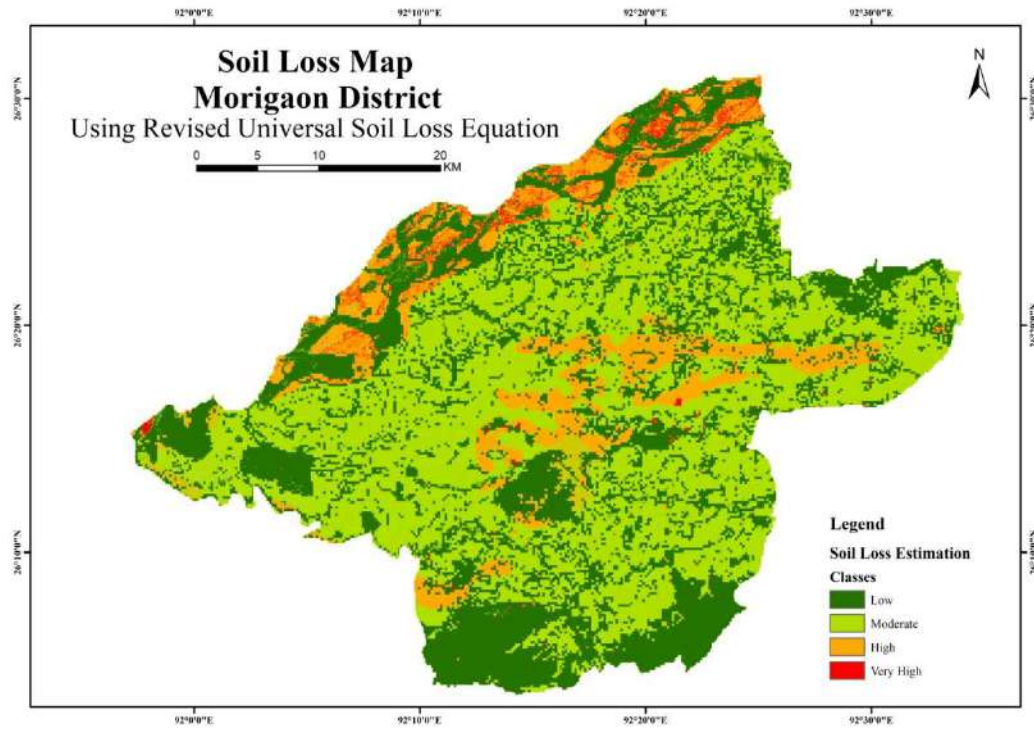
Fig. 9: Annual soil loss estimation map based on RUSLE in Morigaon district.

Table 5: Estimated value of soil loss in Morigaon district.

Soil loss category/zone	% of area within each category	Average soil loss (ton/ha/year)
Low	34.27	0.05
Moderate	46.89	0.78
High	15.36	12.22
Very high	3.47	192.8

area). In the moderate soil loss, about 0.78 ton/ha of soil is being eroded annually (Table 5).

The high and very high soil loss zone has been seen in the Brahmaputra riverbed in the northern part of the district comprising Laharighat Revenue Circle, Bhuragaon Revenue Circle, and Mayong Revenue Circle. These three revenue circles are more vulnerable to flood hazards and bank erosion. Due to detachment and transportation of top soils and the deposition of silts, it reduces the carrying capacity of the rivers which leads to flooding. In addition, the soil type of these revenue circles is of fine loamy of typic udifluvents origin. The soil of these revenue circles is moderately well-drained fine soils that occur on the level and active flood plains having loamy surfaces with erosion and severe flooding. Erosion hazards are more common in these three revenue circles, affecting the populations by permanently displacing them from their place of origin.

However, a high erosion zone is also seen in the central part of the district, where there are several wetlands along the Sonai and Pokoriya river courses. The soil type of that area is fine silty, which mainly occurs in gently sloping floodplains with moderate flooding.

The low erosion zones are seen in the hilly areas of the district. Morigaon district is mainly an alluvial plain with some isolated residual hillocks. The minimum slope of the district is 2.36°, and the maximum slope is 60.19°. It can be said that the district has a gentle slope ranging from 2.36° to 7.8°. The hilly terrain of Burha Mayong Reserved Forest in the extreme west of the district indicates a low erosion zone area. Likewise, Sonai Kuchi Reserve Forest in the southwest, Kholahat Reserved Forest in the southeast, and Tetelia Baghara Reserved Forest in the south-central part of the district show a low soil loss zone area. These zones are mainly covered with a canopy of vegetation, which influences the interception of rain. The thick canopy absorbs raindrop impacts on the ground. Although steepness is high in these areas, the expected higher erosivity is reduced by the forest land use type. The thick canopy of these areas has also increased the soil stability. In addition, these residual hills have clayey soil, which is very deep and fine with slight stoniness and, therefore, is moderately susceptible to erosion.

The soil loss vulnerability map shows that soil loss is higher in the riverine areas and degraded forest areas of the district. Similar findings have also been found by other researchers in their respective studies (Das et al. 2020, Kalita & Bhattacharjee 2024). Studying soil loss over a long period, i.e., spatio-temporal variations like the soil loss study made in Chengde city of China for fifteen years (Yan et al. 2022), the spatio-temporal study will give a better vision of the pattern of soil loss, changing process of soil loss from emergence to extinction and the identification of the most influential factor of soil loss.

CONCLUSIONS

The present study attempts to apply the RUSLE model in an administrative unit like a district, and this is the first-ever study on soil loss estimation in the Morigaon district of Assam, India. It is believed that soil loss studies of this kind on administrative units will be helpful for land use planners and policymakers to formulate effective soil conservation measures. Soil erosion vulnerability map helps to identify erosion-prone areas to implement scientific soil conservation measures. The soil loss estimation maps of the study area reveal that about 46.89% of the district is in the moderate zone of soil loss, and 15.36% area is in the high soil loss zone. The moderate soil loss zone has the sensitivity to falling in the zone of high soil loss. So, proper conservation strategies are needed. In addition, the high soil loss zone, if not conserved immediately, will lead to extreme land degradation in the district.

REFERENCES

Abdul Rahaman, S., Aruchamy, S., Jegankumar, R. and Abdul Ajeez, S., 2015. Estimation of annual average soil loss, based on RUSLE model in Kallar watershed, Bhavani Basin, Tamil Nadu, India. *ISPRS Annals of the Photogrammetry, Remote Sensing and Spatial Information Sciences*, II-2/W2, pp.207-214. https://doi.org/10.5194/isprsannals-II-2-W2-207-2015

Alkharabsheh, M.M., Alexandridis, T.K., Bilas, G., Misopolinos, N. and Silleos, N., 2013. Impact of land cover change on soil erosion hazard in Northern Jordan Using Remote Sensing and GIS. *Procedia Environmental Sciences*, 19, pp.912-921. https://doi.org/10.1016/j.proenv.2013.06.101

Bakker, M.M., Govers, G., Kosmas, C., Vanacker, V., Oost, K. van and Rounsevell, M., 2005. Soil erosion as a driver of land-use change. *Agriculture, Ecosystems & Environment*, 105(3), pp.467-481.

Balabathina, V.N., Raju, R.P., Mulualem, W. and Tadele, G., 2020. Estimation of soil loss using remote sensing and GIS-based universal soil loss equation in the northern catchment of Lake Tana Sub-basin, Upper Blue Nile Basin, Northwest Ethiopia. *Environmental Systems Research*, 9(1), p.35. https://doi.org/10.1186/s40068-020-00203-3

Balasubramani, K., Veena, M., Kumaraswamy, K. and Saravanabavan, V., 2015. Estimation of soil erosion in a semi-arid watershed of Tamil Nadu (India) using revised universal soil loss equation (RUSLE) model through GIS. *Modeling Earth Systems and Environment*, 1(3), p.10. https://doi.org/10.1007/s40808-015-0015-4

Bouguerra, H., Bouanani, A., Khanchoul, K., Derdous, O. and Tachi, S.E., 2017. Mapping erosion-prone areas in the Bouhamdane watershed (Algeria) using the Revised Universal Soil Loss Equation through GIS. *Journal of Water and Land Development*, 32(1), pp.13-23. https://doi.org/10.1515/jwld-2017-0002

Budhathoki, S., Poudel, A. and Shrestha, H.L., 2023. Soil Erosion Analysis Using GIS and RS in Makawanpur District, Nepal. *Journal of Forest and Natural Resource Management*, 3(1), pp.68-81. https://doi.org/10.3126/jfnrm.v3i1.60110

Das, R., Gogoi, B. and Jaiswal, M.K., 2020. Soil loss assessment in Sadiya Region, Assam, India, using remote sensing and GIS. *Indian Journal of Science and Technology*, 13(23), pp.2319-2327. https://doi.org/10.17485/IJST/v13i23.588

Das, T. and Sarma, A.K., 2017. Estimation of annual average soil loss and preparation of spatially distributed soil loss map: A case study of Dhansiri River Basin. *Indian Institute of Technology Guwahati*, Guwahati, India, p.38.

Devatha, C.P., Deshpande, V. and Renukaprasad, M.S., 2015. Estimation of soil loss using USLE Model for Kulhan Watershed, Chattisgarh- A Case Study. *Aquatic Procedia*, 4, pp.1429-1436. https://doi.org/10.1016/j.aqpro.2015.02.185

Erencin, Z., 2000. *C-Factor Mapping Using Remote Sensing and GIS: A Case Study of Lom Sak/Lom Kao, Thailand*. Soil Science Division International Institute For Aerospace Survey And Earth Sciences Enschede, The Netherlands

Fernandez, C., Wu, J.Q., McCool, D.K. and Stöckle, C.O., 2003. Estimating water erosion and sediment yield with GIS, RUSLE, and SEDD. *Journal of Soil and Water Conservation*, 58(3), pp.128-136.

Folly, A., Bronsveld, M.C. and Clavaux, M., 1996. A knowledge-based approach for C-factor mapping in Spain using Landsat TM and GIS. *International Journal of Remote Sensing*, 17(12), pp.2401–2415. https://doi.org/10.1080/01431169608948780

Ganasri, B.P. and Ramesh, H., 2016. Assessment of soil erosion by RUSLE model using remote sensing and GIS - A case study of Nethravathi Basin. *Geoscience Frontiers*, 7(6), pp.953–961. https://doi.org/10.1016/j.gsf.2015.10.007

Gaonkar, V.G.P., Nadaf, F.M. and Kapale, V., 2024. Mapping and quantifying integrated land degradation status of Goa using geostatistical approach and remote sensing data. *Nature Environment and Pollution Technology*, 23(1), pp.295-309. https://doi.org/10.46488/NEPT.2024.v23i01.025

Gelagay, H.S. and Minale, A.S., 2016. Soil loss estimation using GIS and remote sensing techniques: A case of Koga watershed, Northwestern Ethiopia. *International Soil and Water Conservation Research*, 4(2), pp.126–136. https://doi.org/10.1016/j.iswcr.2016.01.002

Handique, A., Dey, P. and Patnaik, S.K., 2023. Application of Revised Universal Soil Loss Equation (RUSLE) model for the estimation of soil erosion and prioritization of erosion-prone areas in Majuli Island, Assam, India. *Journal of Applied and Natural Science*, 15(4), pp.1667–1678. https://doi.org/10.31018/jans.v15i4.5176

Ighodaro, I.D., Lategan, F.S. and Yusuf, S.F.G., 2013. The impact of soil erosion on agricultural potential and performance of Sheshegu community farmers in the Eastern Cape of South Africa. *Journal of Agricultural Science*, 5(5). https://doi.org/10.5539/jas.v5n5p140

Kalita, N. and Bhattacharjee, N., 2024. Estimation of soil loss in the Nanoi River Basin using geospatial techniques. *Indian Journal of Science and Technology*, 17(18), pp.1845–1853. https://doi.org/10.17485/IJST/v17i18.1382

Kalita, N., Borgohain, A., Sahariah, D. and Sarma, S., 2018. Estimation of soil loss sensitivity in the Jinari River basin using the Universal Soil Loss Equation. *Natl Geogr J India*, 64(1–2), pp.118–127.

Koirala, P., Thakuri, S., Joshi, S. and Chauhan, R., 2019. Estimation of soil erosion in Nepal using a RUSLE modeling and geospatial tool. *Geosciences*, 9(4), p.147. https://doi.org/10.3390/geosciences9040147

Krishna Bahadur, K.C., 2009. Mapping soil erosion susceptibility using remote sensing and GIS: A case of the Upper Nam Wa Watershed, Nan Province, Thailand. *Environmental Geology*, 57(3), pp.695–705. https://doi.org/10.1007/s00254-008-1348-3

Lewis, L.A., 1985. Assessing soil loss in Kiambu and Murang'a Districts, Kenya. *Geografiska Annaler: Series A, Physical Geography*, 67(3–4), pp.273–284. https://doi.org/10.1080/04353676.1985.11880152

Littleboy, M., Silburn, D., Freebairn, D., Woodruff, D., Hammer, G. and Leslie, J., 1992. Impact of soil erosion on production in cropping systems. I. Development and validation of a simulation model. *Soil Research*, 30(5), p.757. https://doi.org/10.1071/SR9920757

Moore, I.D. and Burch, G.J., 1986. The physical basis of the length-slope factor in the Universal Soil Loss Equation. *Soil Science Society of America Journal*, 50(5), pp.1294–1298. https://doi.org/10.2136/sssaj1986.03615995005000050042x

Nagaraju, M.S.S., Obi Reddy, G.P., Maji, A.K., Srivastava, R., Raja, P. and Barthwal, A.K., 2011. Soil loss mapping for sustainable development and management of land resources in Warora Tehsil of Chandrapur District of Maharashtra: An integrated approach using remote sensing and GIS. *Journal of the Indian Society of Remote Sensing*, 39(1), pp.51–61. https://doi.org/10.1007/s12524-010-0055-1

Narayana, D.V.V. and Babu, R., 1983. Estimation of soil erosion in India. *Journal of Irrigation and Drainage Engineering*, 109(4), pp.419–434. https://doi.org/10.1061/(ASCE)0733-9437(1983)109:4(419)

Niyonsenga, J.D., Mugabowindekwe, M. and Mupenzi, C., 2021. Spatial analysis of soil erosion sensitivity using the Revised Universal Soil Loss Equation model in Nyamasheke District, Western Province of Rwanda. *Transactions in GIS*, 25(2), pp.735–750. https://doi.org/10.1111/tgis.12701

Panagos, P., Meusburger, K., Ballabio, C., Borrelli, P. and Alewell, C., 2014. Soil erodibility in Europe: A high-resolution dataset based on LUCAS. *Science of The Total Environment*, 479–480, pp.189–200. https://doi.org/10.1016/j.scitotenv.2014.02.010

Pandey, A., Chowdary, V.M. and Mal, B.C., 2007. Identification of critical erosion-prone areas in the small agricultural watershed using USLE, GIS, and remote sensing. *Water Resources Management*, 21(4), pp.729–746. https://doi.org/10.1007/s11269-006-9061-z

Parveen, R. and Kumar, U., 2012. Integrated approach of Universal Soil Loss Equation (USLE) and Geographical Information System (GIS) for soil loss risk assessment in Upper South Koel Basin, Jharkhand. *Journal of Geographic Information System*, 04(06), pp.588–596. https://doi.org/10.4236/jgis.2012.46061

Pimentel, D., 2006. Soil erosion: A food and environmental threat. *Environment, Development and Sustainability*, 8(1), pp.119–137. https://doi.org/10.1007/s10668-005-1262-8

Renard, K.G., 1997. *Predicting Soil Erosion by Water: A Guide to Conservation Planning with the Revised Universal Soil Loss Equation (RUSLE)*. US Department of Agriculture, Agricultural Research Service.

Singh, G., Babu, R., Narain, P., Bhushan, L.S. and Abrol, I.P., 1992. Soil erosion rates in India. *Journal of Soil and Water Conservation*, 47(1), pp.97–99.

Stocking, M., 1984. Rates of erosion and sediment yield in the African environment. In D.E. Walling, S.S.D. Foster and P. Wurzel, (eds.) *Challenges in African Hydrology and Water Resources*. IAHS Publication, pp.285–293

Thakuriah, G., 2023. GIS-based revised universal soil loss equation for estimating annual soil erosion: A case of lower Kulsi basin, India. *SN Applied Sciences*, 5(3), p.81. https://doi.org/10.1007/s42452-023-05303-0

Thapa, P., 2020. Spatial estimation of soil erosion using RUSLE modeling: A case study of Dolakha district, Nepal. *Environmental Systems Research*, 9(1), p.15. https://doi.org/10.1186/s40068-020-00177-2

Wang, R., Zhang, S., Yang, J., Pu, L., Yang, C., Yu, L., Chang, L. and Bu, K., 2016. Integrated use of GCM, RS, and GIS for the assessment of hillslope and gully erosion in the Mushi River Sub-Catchment, Northeast China. *Sustainability*, 8(4), p.317. https://doi.org/10.3390/su8040317

Wischmeier, W.H., 1959. A rainfall erosion index for a universal soil‐loss equation. *Soil Science Society of America Journal*, 23(3), pp.246–249. https://doi.org/10.2136/sssaj1959.03615995002300030027x

Wischmeier, W.H. and Smith, D.D., 1978. *Predicting Rainfall Erosion Losses: A Guide to Conservation Planning*. Department of Agriculture, Science, and Education Administration.

Yan, X., Wu, L., Xie, J., Wang, Y., Wang, C. and Ling, B., 2022. Dynamic changes and precision governance of soil erosion in Chengde City using the GIS techniques and RUSLE model. *Nature Environment and Pollution Technology*, 21(3), pp.1027–1037. https://doi.org/10.46488/NEPT.2022.v21i03.009

Yang, D., Kanae, S., Oki, T., Koike, T. and Musiake, K., 2003. Global potential soil erosion with reference to land use and climate changes. *Hydrological Processes*, 17(14), pp.2913–2928. https://doi.org/10.1002/hyp.1441

Yang, X., 2014. Deriving RUSLE cover factor from time-series fractional vegetation cover for hillslope erosion modelling in New South Wales. *Soil Research*, 52(3), p.253. https://doi.org/10.1071/SR13297

Yitayew, M., Pokrzywka, S.J. and Renard, K.G., 1999. Using GIS for facilitating erosion estimation. *Applied Engineering in Agriculture*, 15(4), pp.295–301. https://doi.org/10.13031/2013.5780

The Synthesis of AgNPs/SAC Using Banana Frond Extract as a Bioreducing Agent and its Application as Photocatalyst in Methylene Blue Degradation

Anti Kolonial Prodjosantoso†[ID]**, Tengku Khadijah Nurul Hanifah**[ID]**, Maximus Pranjoto Utomo**[ID]**, Cornelia Budimarwanti**[ID] **and Lis Permana Sari**[ID]

Department of Chemistry, Yogyakarta State University, Yogyakarta, Indonesia
†Corresponding author: Anti Kolonial Prodjosantoso; prodjosantoso@uny.ac.id

ABSTRACT

Silver nanoparticles (AgNPs) were synthesized utilizing various methods, including bioreducing agents. The synthesis involved the use of silver nitrate ($AgNO_3$) as the precursor and banana frond extract as the bioreducing agent, with different volume ratios being tested. Subsequently, the most optimal variant of AgNPs was immobilized onto activated carbon (AC) derived from soybean seeds. The AgNPs/SAC composite was subjected to thorough characterization using UV-Vis diffuse reflectance spectroscopy and X-ray diffraction (XRD). A series of degradation experiments were then conducted using methylene blue, with the reaction duration following a specific protocol. A comparison of methylene blue concentrations before and after the photodegradation process was made to assess the reaction's efficacy. The findings revealed that the ideal ratio between the bioreducing agent and precursor was 9:30 (v/v). The AgNPs/SAC composite exhibited a peak absorption at a wavelength of 420-440 nm. The UV-DRS characterization of AgNPs/SAC unveiled a band gap energy of 1.52 eV. The AgNPs supported on AC displayed a peak absorption wavelength of 5,438.5 nm, showcasing a face-centered cubic (FCC) structure. The AgNPs/SAC effectively decreased the concentration of methylene blue through a combination of adsorption and photodegradation mechanisms, achieving efficiencies of 35.3813% and 81.1636%, respectively. The AgNPs/SAC composite demonstrates significant potential for efficient and sustainable water treatment.

INTRODUCTION

The textile industry generates 10-15% of the total dyestuff waste during dyeing (Jyoti & Singh 2016). Dyes are organic compounds with aromatic structures, known for their high stability and difficulty to degrade (Daneshvar et al. 2007). One of the most commonly used dyes is methylene blue. The issue of dye waste can be mitigated through various methods, including biosensing, adsorption, filtration, electrolysis, coagulation, and sedimentation (Ong 2011, Thenarasu et al. 2024). These methods, when implemented, often do not yield optimal results, are difficult to execute, and can sometimes even create new problems. The method of waste treatment using photocatalysts was developed due to its advantages.

Nanoparticles have a high surface-to-volume ratio, enhancing their reactivity and allowing for the development of more efficient and effective water treatment technologies (Cao et al. 2024). Among the nanoparticles that can be employed as photocatalysts are silver nanoparticles (AgNPs). Silver metal (Ag) exhibits excellent photocatalytic properties (Wahyuni et al. 2017). A variety of techniques have been developed for synthesizing AgNPs, including chemical reduction methods (Kumar et al. 2015), electrochemical reduction, bioreduction (Mubarak et al. 2011, Silambarasan & Jayanthi 2013), sol-gel (Lenzi et al. 2011), and photoreduction (Chan & Barteau

2005). The bioreduction method is known as environmentally friendly (Jyoti & Singh 2016, Ma et al. 2024).

Plant extracts contain a variety of secondary metabolites, including alkaloids, tannins, flavonoids, steroids, and phenols. These compounds can act as reducing and stabilizing agents of silver nanoparticles. One example of a plant that contains secondary metabolites is the banana frond. The ethanolic extract of banana frond contains flavonoids, tannins, and saponins (Fatma 2018).

Nanoparticles supported within larger materials are employed to enable the repeated use of nanoparticles, which are firmly anchored to the supporting material. Activated carbon stands out as a suitable support material due to its beneficial characteristics, such as large surface area, resilience to acidic and alkaline conditions, and the ability to modify its functional groups. The functional groups on the surface of carbon can function as a support for the developed metal catalyst or become active sites for specific catalytic reactions (Gläsel 2015). Soybeans are one of the natural sources from which activated carbon can be derived.

Based on the preceding description, this study focuses on the synthesis of AgNPs/SAC using the banana frond extract (*Musa balbisiana*) as a bioreducing agent and its application as a photocatalyst for methylene blue degradation. The resulting AgNPs/SAC were characterized using UV-Vis DRS and XRD, and then their photocatalytic effectiveness against methylene blue was evaluated.

MATERIALS AND METHODS

The main materials used in the experiment include $AgNO_3$ (Sigma Aldrich 99.9999%), methylene blue (Sigma Aldrich >995%), and banana frond extract (*Musa balbisiana*); and the instruments were UV-Vis Spectrophotometer (Shimadzu 2400 PC Series), UV-Vis DRS (Shimadzu UV-2450 spectrophotometer), XRD (Rigaku miniflex 600, and photochemical reactor (Techinstro).

The banana frond extract was obtained by using an extraction procedure implemented following the methodology proposed by Prodjosantoso et al. (2019). The frond of the banana was cut into small pieces, washed, and dried at room temperature. A total of 25 grams of dried banana frond were combined with 150 milliliters of distilled water and blended for five minutes using a blender. Subsequently, filtration was conducted using filter paper (Whatman Grade 42).

The activated carbon (AC) preparation method was carried out by modifying the Hatina method (Rampe & Tiwow 2018). Soybean seeds were first washed with distilled water and then sun-dried for four hours. They were subsequently oven-dried at a temperature of 105°C for 24 hours. A total of dry 250 grams of soybean seeds were then subjected to a heating process at a temperature of 500°C for four hours. Following this, the seeds were washed and activated using a solution of hydrochloric acid (HCl 0.1 M) in a ratio of 1:2 (w/v) for ten hours. The seeds were then rinsed with distilled water and activated using sodium hydroxide (NaOH 0.1 M) in a ratio of 1:2 (w/v) for ten hours. Finally, the seeds were rinsed again with distilled water and dried in an oven at a temperature of 105 °C for two hours.

A total of 30 mL of $AgNO_3$ 0.01 M solution was prepared in six separate Erlenmeyer flasks. Subsequently, add 3, 4.5, 6, 7.5, 9, and 10.5 mL of banana frond extract to respective flasks. The mixture is then stirred with a magnetic stirrer for two hours. After stirring, the solutions were analyzed using a UV-Vis spectrophotometer to determine the optimal variation.

The synthesis of AgNPs in this study followed the method developed by Taba et al. (2022). First, 100 mL of 0.01 M $AgNO_3$ was introduced into the beaker, and a specific quantity of banana frond extract was added according to the optimal composition. The mixture was then stirred for two hours using a magnetic stirrer. The impregnation of AgNPs onto SAC was adapted from the Nguyen et al. (2020) method. Subsequently, 25 g of activated carbon was added to the mixture, which was then tightly covered using aluminum foil. The mixture was then shaken for 24 hours. The AgNPs/SAC were then filtered, washed with ethanol, and dried in an oven at 110°C oven for 2 hours. The resulting AgNPs/SAC were characterized using UV-Vis DRS and XRD methods.

A 100 ppm stock solution was prepared by dissolving 100 mg of methylene blue in 1 L of distilled water. This stock solution was then diluted to prepare standard solutions with concentrations of 1, 2, 4, 6, and 8 ppm. The absorbance of these standard solutions was measured using a UV-Vis spectrophotometer.

Photodegradation was studied by using the method published by Prodjosantoso (2019), which was by adding 1 g of AgNPs/SAC into 100 mL of a 50 ppm methylene blue solution. The mixture was placed in an Erlenmeyer flask and agitated at various time intervals (0, 5, 10, 15, 30, 60, 120, and 180 minutes) in the dark. After 24 hours, the mixture was exposed to the sunlight for photodegradation within time intervals of 0, 5, 10, 15, 30, 60, 120, and 180 minutes. The final concentration of methylene blue was then measured using a UV-Vis spectrophotometer to calculate the photodegradation effectiveness.

RESULTS AND DISCUSSION

The optimal bioreducing agent and the precursor volume ratio were of interest in the formation of AgNPs. The optimal

composition is determined by the highest absorbance of the typical wavelengths of the analyzed particles. Qualitatively, a higher absorbance indicates a greater number of AgNPs formed, implying a higher concentration of AgNPs in the solution. The shifting of the wavelength position to the larger wavelength indicates the lower stability of the AgNPs (De Leersnyder et al. 2019).

A combination treatment of agitating and stirring of the mixtures of $AgNO_3$ 0.01 M solution and bioreducing agents resulted in the formation of silver nanoparticles characterized by the solution color change from yellow to brownish. This color change is assumed due to the reduction of Ag^+ ions to Ag^0 by secondary metabolites in the banana frond extract. This phenomenon, known as surface plasmon resonance (SPR), can be observed using a UV-Vis spectrophotometer in the range of 400-500 nm (Melkamu & Bitew 2021). The coloration observed in the solution of AgNPs is illustrated in Fig. 1.a.

Fig. 1.b. Indicates that the most stable AgNPs are achieved with a 9 mL variation of bioreducing agent. Additionally, the differences in wavelength can indicate

variations in the particle size of AgNPs, with smaller particles being characterized by shorter wavelengths (Asif et al. 2022). From the absorbance perspective, the 9 mL variation exhibits the highest absorbance value of 0.242. The high absorbance is directly proportional to the number of AgNPs formed. Consequently, the 9:30 (v/v) variation was selected as the optimal composition, as it exhibited the most intense brown color, the highest absorbance, and the shortest wavelength.

The bandgap energy disparity also influences the energy of photons or the quantity of light required. The reduction in bandgap energy necessitates a proportional decrease in light energy, and vice-versa (Dhankhar et al. 2014). Consequently, the bandgap energy is determined to ascertain the photocatalytic activity of a photocatalyst. In this study, the bandgap energy was determined using a DRS spectrophotometer instrument in the ultraviolet-visible light area. To obtain the bandgap energy, the data is processed using the Kubelka-Munk equation, as follows:

Where F (R) is the Kubelka-Munk factor, R is the reflectance, A is the proportional constant, and Eg is the gap energy (eV) (Landi et al. 2022). The results of these
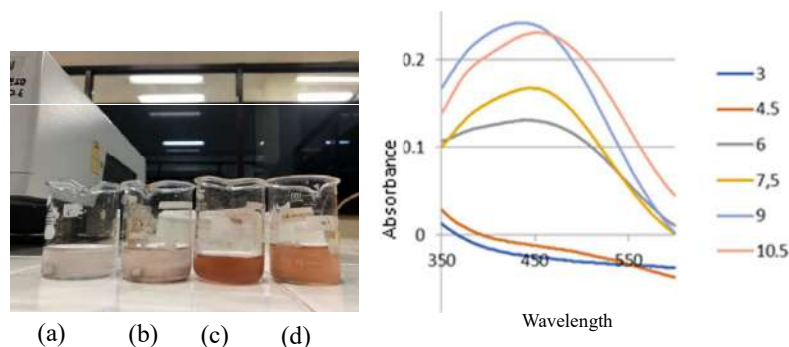
Fig. 1: (a) AgNPs color solutions obtained by adding a) 6 mL, b) 7.5 mL, c) 9 mL, and d) 10.5 mL bioreducing agent; and (b) Bioreducing agent composition optimization curve.
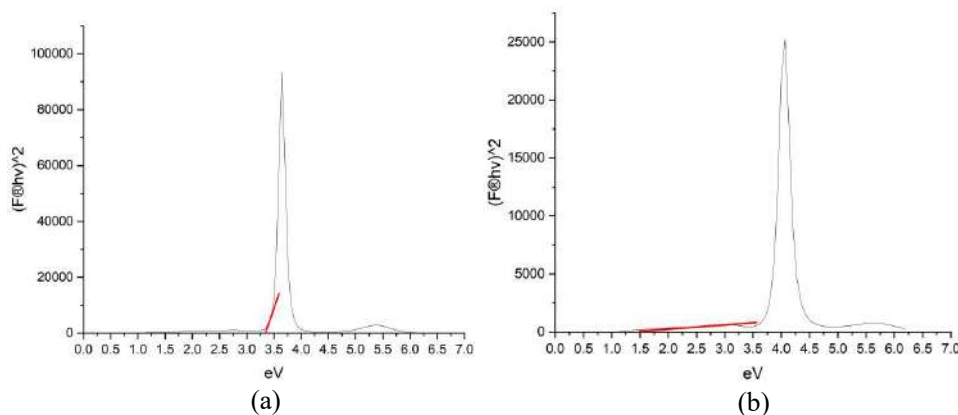
Fig. 2: Bandgap Energy Curves of a) AC and b) AgNPs/SAC.

calculations are then processed into curves. The linear portion of the curve is extrapolated in a direction perpendicular to the X-axis to obtain the bandgap energy value. The bandgap energy curve is presented in Fig. 2.

Fig. 2 indicates that the bandgap energies of AC and AgNPs/SAC are 3.33 eV and 1.52 eV, respectively. These findings demonstrate that the incorporation of AgNPs into SAC results in a significant reduction in the bandgap energy. This reduction can be attributed to the formation of new electronic levels. A lower bandgap energy indicates that electrons are more readily excited from the valence band to the conduction band when exposed to photon energy. According to Rizki et al., the bandgap energy reduction of composites can facilitate the formation of electron-hole $(e^- - h^+)$ pairs during light irradiation, thereby enhancing photocatalytic activity (Rizki et al. 2023).

The X-ray diffraction (XRD) method is a widely utilized analytical technique for analyzing crystal structures and particle sizes (Kumar & Hymavathi 2017). Each crystal exhibits a unique diffraction pattern. In this study, XRD characterization was conducted using Cu-Kα radiation sources at 2θ angles between 10-90º to determine the crystal size of AgNPs supported by AC. The diffractograms of AC and AgNPs/SAC were compared to identify the specific peaks of AgNPs. These peaks were then compared to data from COD (Crystallography Open Database). The XRD analysis results indicate that AC is an amorphous material. The diffractogram pattern of AC is presented in Fig. 3.

Fig. 3.a illustrates the presence of multiple peaks, two observed at 2θ angles of approximately 26° and 46°. This is consistent with the findings of Jain et al. (2021), which indicate that the amorphous peak of AC occurs at 2θ around 26° and 43°. The peak at 2θ about 25° corresponds to the

diffraction (002) derived from graphite (Ahmad et al. 2003). The diffraction pattern of AgNPs/SAC differs slightly from that of AC. The appearance of sharp peaks in the AgNP/AC diffractogram indicates that AgNPs have been successfully loaded onto the AC (Tuan et al. 2011). Wide peaks indicate small particle sizes (Sudhakar & Soni 2018).

Some peaks have emerged at 2θ values of 38.40°; 44.45°; 64.65°; 77.43°; and 81.83°, which respectively represent the hkl planes (111), (002), (022), (113), and (222) (Fig. 3.b). The (111) plane was the most intense, indicating that the AgNPs orientation was along this plane. This finding is consistent with the results of the research conducted by Isa and Lockman (2019). The analysis results indicated the formation of AgNPs with a face-centered cubic (FCC) structure, which aligns with previous research by Isa & Lockman (2019).

X-ray diffraction (XRD) data are also employed to determine the crystal size of AgNPs. The determination of the crystal size is calculated using the Debye-Scherrer equation:

$$D = \frac{k\lambda}{\beta\cos\theta}$$

Where D represents the crystal size in nanometers, k is a dimensionless shape factor (typically 0.89), λ is the wavelength (nm), β is the FWHM (full width at half maximum) value, and θ is the Bragg angle (deg) (Radha & Thamilselvi 2013). The calculations indicate that AgNPs supported by AC have an average size of 5.4385 nm. These results are similar to those found in Nisa's (2024) research where she synthesized AgNPs/SAC using banana pith extract, obtaining a particle size of 13.69±5.11 nm.

The methylene blue adsorption on the AgNPs/SAC was studied in the dark to prevent photocatalysis. This dark state is achieved by covering the surface of the Erlenmeyer flask
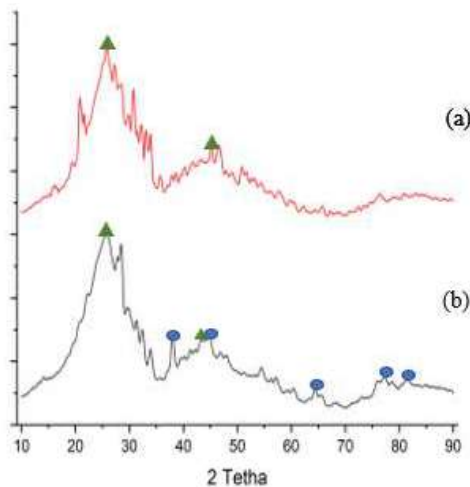
Fig. 3: XRD pattern of a) AC and b) AgNPs/SAC.

Table 1: Methylene blue in the solutions.

Time (minutes)	0	5	10	15	30	60	120	180
Concentration (ppm)	50.81752	48.79924	47.27605	45.84606	42.30494	39.68738	38.05468	32.83763

Table 2: Methylene blue in the solution after the photodegradation processes.

Time (minutes)	0	5	10	15	30	60	120	180
Concentration (ppm)	31.73829	29.88906	28.28117	26.50954	21.82125	15.597	8.73449	5.97836

with aluminum foil. The shaking process is carried out at specific time intervals. The data on the concentrations of methylene blue at various time intervals can be found in Table 1.

The data (Table 1.) indicate that the concentration of methylene blue decreases along with increasing light exposure time. The relationship between reaction rate and concentration can be determined using the reaction order equation, as follows:

1) Zero Reaction Order
$$C_t = -kt + C_0$$

2) First Reaction Order
$$ln C_t = -kt + ln\,C_0$$

3) Second Reaction Order
$$1/C_t = -kt + 1/\,C_0$$

The concentration of methylene blue at time t (ppm), k is the rate constant; t is the time (minutes); and C_0 is the initial concentration of methylene blue (ppm) (Sun 2014). The reaction order is determined by comparing the R^2 values for each reaction order curve. The reaction order with the greatest R^2 value indicates the order of the reaction. The R^2 values for the zero-order, first-order, and second-order reactions were 0.8873, 0.9175, and 0.9829, respectively. These results indicate that the adsorption reaction follows the second-order kinetics.

The adsorption effectiveness of methylene blue is calculated using the following equation:

$$\%\text{Efficacy} = \frac{C_0 - C_e}{C_o} \times 100\%$$

The calculations indicate that the effectiveness of AC adsorption is 35.3813%.

Following 24 hours of adsorption in the absence of light, photodegradation of methylene blue is initiated. This study assumes that after a 24-hour adsorption period, no further adsorption occurs and that the subsequent reaction is solely a photodegradation reaction of AgNPs. It should be noted, however, that this study does not guarantee that the photodegradation process occurs without a simultaneous adsorption process.

The photodegradation process is conducted under sunlight, with time intervals of 0, 5, 10, 15, 30, 60, 120, and 180 minutes. The utilization of sunlight as a light source is predicated on the energy value of the band gap of AgNPs, wherein AgNPs exhibit photocatalytic activity in the visible light spectrum. Sunlight is comprised of 38.9% visible light, 6.8% ultraviolet light, and 54.3% infrared light. Furthermore, the use of solar energy, particularly sunlight, is energy-saving, given that the sun is a renewable energy source. The photodegradation process was conducted between 10:00 a.m. and 1:00 p.m., with the measured light intensity on the lux meter ranging from 4,000 to 8,000 lux. When the catalyst in solution is irradiated by light, electron-hole pairs are formed on the catalyst surface. The excitation of electrons from the valence band to the conduction band is accompanied by the formation of a positive hole, resulting in the production of an electron-hole pair. Both charge carriers will undergo redox reactions to produce hydroxyl radicals (OH*) and superoxide radicals (O*). Hydroxyl radicals possess strong oxidizing properties and exhibit a considerable redox potential, enabling them to oxidize most organic substances into water, hydroxyl acids, and carbon dioxide (Wat et al. 2011). Consequently, the concentration of organic substances, such as methylene blue, is reduced. The results of the photodegradation process, as evidenced by a decrease in the concentration of methylene blue, are presented in Table 2.

The rate of photodegradation can be determined based on the equation of the line on the second-order curve, using the following equation:

$$r = k\,C^n$$

Where r is the reaction rate (ppm/min), C is the concentration (ppm), k is the reaction rate constant, and n is the reaction order (Chiu 2019). The photodegradation reaction rate of methylene blue using AgNPs was calculated to be 0.8058 ppm/minute. The efficacy of the photodegradation process was evaluated by comparing the decline in the concentration of methylene blue to its initial concentration. The results demonstrated a reduction in the concentration of methylene blue from 31.73829 ppm to 5.97836 ppm,

indicating an 81.1636% effectiveness of methylene blue photodegradation by AgNPs/SAC. Consequently, the effectiveness of photodegradation is greater than that of adsorption.

CONCLUSIONS

The research findings reveal that the optimal proportion of banana frond extract combined with precursors is 9:30 (v/v), demonstrating the highest absorbance value at the 437 nm wavelength. The bandgap energy of AgNPs/SAC is 1.52 eV, with AgNPs particles supported on AC exhibiting an FCC structure and an average particle size of 5.4385 nm. The adsorption efficiency of AgNPs/SAC stands at 35.3813%, while the photodegradation effectiveness reaches 81.1636%. The application of AgNPs/SAC proves to be highly effective in water treatment.

ACKNOWLEDGMENTS

REFERENCES

Ahmad, A., Senapati, S., Khan, M.I., Kumar, R. and Sastry, M., 2003. Extracellular biosynthesis of monodisperse gold nanoparticles by a novel extremophilic actinomycete, *Thermomonospora* sp. *Langmuir*, 19(8), pp.3550-3553.

Amri, F.S. and Hossain, M.A., 2018. Comparison of total phenols, flavonoids and antioxidant potential of local and imported ripe bananas. *Egyptian Journal of Basic and Applied Sciences*, 5(4), pp.245-251.

Asif, M., Yasmin, R., Asif, R., Ambreen, A., Mustafa, M. and Umbreen, S., 2022. Green synthesis of silver nanoparticles (AgNPs), structural characterization, and their antibacterial potential. *Dose-Response: A Publication of International Hormesis Society*, 20(1), p.15593258221088709.

Cao, V., Cao, P.A., Han, D.L., Ngo, M.T., Vuong, T.X. and Manh, H.N., 2024. The suitability of Fe3O4/graphene oxide nanocomposite for adsorptive removal of methylene blue and congo red. *Nature Environment & Pollution Technology*, 23(1).

Chan, S.C. and Barteau, M.A., 2005. Preparation of highly uniform Ag/TiO2 and Au/TiO2 supported nanoparticle catalysts by photodeposition. *Langmuir*, 21(12), pp.5588-5595.

Chiu, Y.-H., Chang, T.-F.M., Chen, C.-Y., Sone, M. and Hsu, Y.-J., 2019. Mechanistic insights into photodegradation of organic dyes using heterostructure photocatalysts. *Catalysts*, 9(5), p.430.

Daneshvar, N., Ayazloo, M., Khataee, A.R. and Pourhassan, M., 2007. Biological decolorization of dye solution containing malachite green by microalgae *Cosmarium* sp. *Bioresource Technology*, 98(6), pp.1176-1182.

De Leersnyder, I., De Gelder, L., Van Driessche, I. and Vermeir, P., 2019. Revealing the importance of aging, environment, size and stabilization mechanisms on the stability of metal nanoparticles: a case study for silver nanoparticles in a minimally defined and complex undefined bacterial growth medium. *Nanomaterials (Basel)*, 9(12), p.1684.

Dhankhar, M., Singh, O. and Singh, V.N., 2014. Physical principles of losses in thin film solar cells and efficiency enhancement methods. *Renewable and Sustainable Energy Reviews*, 40, pp.214-223.

Gläsel, J., Diao, J., Feng, Z., Hilgart, H., Wolker, T., Su, D.S. and Etzold, B.J.M., 2015. Mesoporous and graphitic carbide-derived carbons as selective and stable catalysts for the dehydrogenation reaction. *Chemistry of Materials*, 27(16), pp.5719-5725.

Isa, N. and Lockman, Z., 2019. Methylene blue dye removal on silver nanoparticles reduced by *Kyllinga brevifolia*. *Environmental Science and Pollution Research*, 26(11).

Jyoti, K. and Singh, A., 2016. Green synthesis of nanostructured silver particles and their catalytic application in dye degradation. *Journal of Genetic Engineering and Biotechnology*, 14(2), pp.311-317.

Kumar, B.R. and Hymavathi, B., 2017. X-ray peak profile analysis of solid-state sintered alumina doped zinc oxide ceramics by Williamson–Hall and size-strain plot methods. *Journal of Asian Ceramic Societies*, 5(2).

Kumar, R., Rashid, J. and Barakat, M.A., 2015. Zero valent Ag deposited TiO2 for the efficient photocatalysis of methylene blue under UV-C light irradiation. *Colloids and Interface Science Communications*, 5, pp.1-4.

Landi, S., Segundo, I.R., Freitas, E., Vasilevskiy, M., Carneiro, J. and Tavares, C.J., 2022. Use and misuse of the Kubelka-Munk function to obtain the band gap energy from diffuse reflectance measurements. *Solid State Communications*, 341. https://doi.org/10.1016/j.ssc.2021.114573.

Lenzi, G.G., Fávero, C.V.B., Colpini, L.M.S., Bernabe, H., Baesso, M.L., Specchia, S. and Santos, O.A.A., 2011. Photocatalytic reduction of Hg(II) on TiO2 and Ag/TiO2 prepared by the sol-gel and impregnation methods. *Desalination*, 270(1-3), pp.241-247.

Ma, L., Chen, N., Feng, C. and Yang, Q., 2024. Recent advances in enhanced technology of Cr(VI) bioreduction in aqueous condition: A review. *Chemosphere*, 351(3), p.141176.

Melkamu, W.W. and Bitew, L.T., 2021. Green synthesis of silver nanoparticles using *Hagenia abyssinica* (Bruce) J.F. Gmel plant leaf extract and their antibacterial and anti-oxidant activities. *Heliyon*, 7(11).

Mubarak, D.A., Sasikala, M., Gunasekaran, M. and Thajuddin, N., 2011. Biosynthesis and characterization of silver nanoparticles using marine cyanobacterium, *Oscillatoria willei* NTDM01. *Digest Journal of Nanomaterials and Biostructures*, 6(2), pp.385–390.

Nisa, S.K., 2024. Sintesis AgNPs/SAC menggunakan ekstrak empulur pisang (Musa balbisiana) dan aplikasinya sebagai fotokatalis degradasi metilen biru. Skripsi. Universitas Negeri Yogyakarta.

Ong, S.T., Keng, P.S., Nam, L., Tiong, H. and Hung, Y.T., 2011. Dye Waste Treatment. *Water*, 3, pp.157-176.

Prodjosantoso, A.K., Kamilia, S., Utomo, M.P. and Budiasih, K.S., 2019. Silica supported copper-nickel oxide catalyst for photodegradation of methylene blue. *Asian Journal of Chemistry*, 31(12), pp.2891–2896.

Prodjosantoso, A.K., Prawoko, O.S., Utomo, M.P. and Sari, L.P., 2019. Green synthesis of silver nanoparticles using *Salacca zalacca* extract as reducing agent and it's antibacterial activity. *Asian Journal of Chemistry*, 31(12).

Radha, K.V. and Thamilselvi, V., 2013. Synthesis of silver nanoparticles from *Pseudomonas putida* NCIM 2650 in silver nitrate supplemented growth medium and optimization using response surface methodology. *Digest Journal of Nanomaterials and Biostructures*, 8(3), pp.1101–1111.

Rampe, M.J. and Tiwow, V.A., 2018. Fabrication and characterization of activated carbon from charcoal coconut shell Minahasa, Indonesia. *In Journal of Physics: Conference Series* (Vol. 1028, No. 1, p. 012033). IOP Publishing.

Rizki, I.N., Inoue, T., Chuaicham, C., Shenoy, S., Srikhaow, A., Sekar, K. and Sasaki, K., 2023. Fabrication of reduced Ag nanoparticle using crude extract of cinnamon decorated on ZnO as a photocatalyst for hexavalent chromium reduction. *Catalysts*, 13(2).

Silambarasan, S. and Jayanthi, A., 2013. Biosynthesis of silver nanoparticles using *Pseudomonas fluorescens. Research Journal of Biotechnology*, 8(3), pp.71-74.

Sudhakar, P. and Soni, H., 2018. Catalytic reduction of nitrophenols using silver nanoparticles-supported activated carbon derived from agro-waste. *Journal of Environmental Chemical Engineering*, 6(1).

Sun, J., 2014. Development of inorganic-organic hybrid materials for waste water treatment. Thesis. National University of Singapore.

Thenarasu, A., Chai, M.K., Tan, Y.H., Wong, L.S., Rajamani, R. and Djearamane, S., 2024. Study of *Chlorella vulgaris* from different growth phases as biosensor for detection of titanium and silver nanoparticles in water. *Nature Environment & Pollution Technology*, 23(2).

Trinh, V.T., Nguyen, T.M.P., Van, H.T., Hoang, L.P., Nguyen, T.V., Ha, L.T., Vu, X.H., Pham, T.T., Nguyen, T.N., Quang, N.V. and Nguyen, X.C., 2020. Phosphate adsorption by silver nanoparticles-loaded activated carbon derived from tea residue. *Scientific Reports*, 10(1), pp.1-13.

Tuan, T.Q., Son, N., Dung, H.T.K., Luong, N.H., Thuy, B.T., Anh, N.T., Hoa, N.D. and Hai, N.H., 2011. Preparation and properties of silver nanoparticles loaded in activated carbon for biological and environmental applications. *Journal of Hazardous Materials*, 192(3).

Wahyuni, E.T., Roto, R. and Prameswari, M., 2017. TiO2/Ag-nanoparticle as a photocatalyst for dyes degradation. In: *International Conference on Environmental Science and Technology*. CEST.

Wat, M.J., Veenma, D., Hogue, J., Holder, A.M., Yu, Z., Wat, J.J., Hanchard, N., Shchelochkov, O.A., Fernandes, C.J., Johnson, A., Lally, K.P., Slavotinek, A., Danhaive, O., Schaible, T., Cheung, S.W., Rauen, K.A., Tonk, V.S., Tibboel, D., de Klein, A. and Scott, D.A., 2011. Genomic alterations that contribute to the development of isolated and non-isolated congenital diaphragmatic hernia. *Journal of Medical Genetics*, 48(5), pp.299-307.

High-Performance, Eco-Friendly Blocks from Iron Ore Tailings: A Solution for Sustainable Construction

S. A. Kakodkar† [ID] **and Ulhas G. Sawaiker**

Department of Civil Engineering, Goa College of Engineering, Farmagudi, Goa 403401, India
†Corresponding author: S. A. Kakodkar; satyeshk@gmail.com

ABSTRACT

Goa's iron ore mining industry has generated over 7.7 million tonnes of iron ore tailings (IOTs) in the past two decades. These IOTs pose a significant environmental threat due to heavy metal contamination, dust generation, and acid mine drainage. While some IOTs are used for backfilling, the majority are stored in tailings storage facilities (TSFs), posing long-term risks to surrounding water resources, ecosystems, and land use. Large-scale utilization technologies are crucial for sustainable IOT management. This study investigates the feasibility of incorporating IOTs in construction block production, aiming for high-volume waste consumption and improved resource efficiency. This approach offers a potential pathway to remediate the environmental impact of IOTs. The proposed method replaces 85% of the cement content with a cementitious material comprising 65% Ground Granulated Blast Furnace Slag (GGBS), 10% Fly Ash, and 10% Lime. It also utilizes IOTs entirely as a substitute for sand, with ceramic waste partially replacing coarse aggregates. While partial substitution of coarse aggregates with ceramic waste was attempted, it decreased workability. The optimal mix design, achieving the highest compressive strength, utilizes 15% cement, 65% GGBS, 10% Fly Ash and Lime, and 100% IOTs as fine aggregate with 100% basaltic aggregates. This formulation successfully demonstrates the potential use of IOTs in manufacturing construction blocks that reach compressive strengths of 10.91 N.mm⁻² and 15.92 N.mm⁻² at 7 and 28 days, respectively, satisfying the IS 2185-Part 1 (2005) code requirement. The block density was 2.20 g.cm⁻³. This research demonstrates the potential to convert a significant environmental challenge into a sustainable solution. By utilizing IOTs in construction block production, we can effectively achieve waste remediation; and create resource-efficient and eco-friendly building materials, offering substantial dual benefits for Goa's environment and construction sector.

INTRODUCTION

Mineral extraction, which involves the extraction of raw materials from the Earth's crust, encompasses the entire mining value chain comprehensively. This chain traverses the initial exploration and discovery stage through exploitation and processing, culminating in post-closure land use planning. Across all sub-processes, advances in geoscientific prospecting, extraction methodologies, beneficiation techniques, material characterization, safety protocols, and environmental mitigation strategies contribute significantly to improving efficiency and sustainability within the mining sector (Das et al. 2023). The mining sector plays a crucial role in driving socioeconomic advancement for nations endowed with economically viable mineral deposits (Mouih et al. 2023). Iron, being the second most plentiful metal in the Earth's crust, significantly impacts this dynamic. However, the very extraction of these vital resources, while driving economies, generates a significant waste stream, predominantly tailings and overburden (Tayebi et al. 2019, Gou et al. 2019). Iron ore beneficiation, crucial for the refining of iron ore, inadvertently generates IOTs as a by-product. However, the rising global demand for iron and steel products has led to the exploitation of lower-grade ores, resulting in a dramatic increase

in IOT production, which poses significant environmental challenges (Zhang et al. 2021).

Surging population growth and accelerated industrialization in recent years have driven a substantial increase in resource consumption, particularly of finite natural materials. These conventional construction materials, employed in the dominant paradigm, often bear a significant environmental footprint. Consequently, within the imperative of sustainable development, there is a critical need to shift toward alternative elements for building material production (Mouih et al. 2023). India faces the challenge of unutilized iron ore reserves, which constitute 10 to 15% of its mined ore, a consequence of the economic infeasibility of extracting valuable iron from low-grade deposits (Lamani et al. 2015). The large-scale accumulation of IOTs within confined impoundment structures (tailing dams) presents significant challenges. Beyond direct land footprint encroachment, substantial capital expenditures associated with both construction and ongoing maintenance of these extensive containment facilities are incurred (Zhang et al. 2021).

In the coastal Indian state of Goa, iron and manganese extraction employs the open pit mining technique, necessitating the pre-stripping of overburden to access the underlying ore bodies. This approach currently covers approximately 30,325 hectares, representing approximately 8% of the total landmass of the state, and the target mineral deposits occupy geological formations beneath the surface material removed (Sebastian et al. 2017). The process of extracting iron ore may present significant challenges during the removal of the overlying material, impacting storage, handling, and subsequent land reclamation efforts. The abundance of iron ore deposits within the banded iron formations of Goa, coupled with their flexibility for beneficiation, has resulted in the setting up of multiple iron ore processing plants. Surface mining operations in Goa exhibit a high stripping ratio (waste-to-ore ratio) compared to the national average. During the 2017-2018 fiscal year, a total of 86 operational mines in Goa produced 10,279 tonnes of iron ore (MoM-GoI 2022). Considering the prevailing waste-to-ore ratio (stripping ratio) for open-pit mining practices in Goa, which typically ranges from 3:1 to 5:1 due to site-specific geological considerations (TERI 2001, Yellishetty et al. 2009, Sebastian et al. 2017, Jakati 2021), we can anticipate related waste generation due to ore processing. In India, tailings generation is about 10% to 25% by weight of total iron ore mine production (Zhang et al. 2021), and in the last two decades, Goa's IOTs generation has been 7.7 million tons. Extensive IOT generation, if not managed, presents a significant environmental and public health risk within the region. A primary concern among these tailing-related risks is the potential for acid mine drainage (AMD). Groundwater

contamination, dust pollution, and land desertification are serious environmental threats in the vicinity of IOTs dams.

Apart from environmental devastation, the tailing dams pose a direct and alarming hazard to the well-being and safety of nearby inhabitants. Tailing dams represent a higher risk of collapse than reservoir dams due to their specific mechanical properties and operating style (Zhang et al. 2021). Fuelled by a growing global demand for recycled and environmentally friendly materials, the construction sector presents a perfect opportunity to address the challenge of managing Iron Ore Tailings. The granulometry and chemical composition of IOTs make them suitable for various construction applications (Franco et al. 2022). Through strategic repurposing of mine tailings into geopolymers, aggregates, and composite blocks, we can simultaneously realize a triple bottom line: environmental mitigation through reduced waste generation and cleaner production (Kuranchie et al. 2015), resource creation with novel sustainable construction materials and economic advantages through cost savings and market diversification (Haibin & Zhenling 2010, Thejas et al. 2022). This approach presents a potentially viable long-term solution to tailings management while simultaneously conserving precious resources. Implementing comprehensive tailings reuse strategies can empower Goa's iron ore mining industry not only to remediate the environmental burdens inherent in its operations but also to propel it towards a sustainable and economically tough future.

Integration of waste materials into construction materials has ignited a growing research interest, particularly in the pursuit of Fly Ash, slag, and silica fume as robust alternatives to traditional materials. These efforts have produced encouraging results, propelling the advancement of novel and innovative construction materials. Driven by the pursuit of economic and environmental sustainability, researchers have revealed an overabundance of novel construction materials that incorporate waste materials such as IOTs, as demonstrated by Thejas et al. (2022) and Elahi et al. (2021). These advances offer the construction industry not only cost-effective alternatives but also a strategic avenue to reduce its environmental footprint and enter a lucrative circular economy, promoting resource efficiency and economic diversification.

This paper examines the utilization of iron ore tailings (IOT) in manufacturing construction blocks. It explores the potential of replacing sand and cement with cementitious binders to evaluate their suitability as an eco-friendly and sustainable solution for the construction industry.

MATERIALS AND METHODS

Material Collection and Characterization

To manufacture the construction block, the sample of Iron

a) Cement b) GGBS c) Fly Ash d) Lime e) Iron Ore Tailings f) Aggregate

Fig. 1: Materials used to cast construction blocks

Ore Tailings (IOTs) was collected from a specified mine within Dharbandora Taluka, South Goa district, India (15.3366411°N, 74.24727°E). Ground Granulated Blast Slag (GGBS) and Fly Ash for this study were sourced from JSW Cement Ltd. Cement, Lime, and basaltic aggregate were purchased from local vendors. To comprehensively assess their physicochemical properties, the IOTs, GGBS, Fly Ash, and ceramic waste were subjected to rigorous analyses using standardized protocols. X-ray fluorescence (XRF) spectroscopy provided a comprehensive elemental analysis of all materials, revealing their key oxide compositions. These data are crucial for determining the reactivity, potential pozzolanic activity, and suitability. Fig. 1 shows the different materials used to cast construction blocks.

The sieve analysis for particle size distribution, specific gravity for density determination, and loss-on-ignition (LOI) for residual organic content were carried out on IOTs. GGBS and Fly Ash were analyzed for specific gravity, LOI, Moisture Content, Fineness, and residue on the sieve. Ceramic waste and basalt aggregate were analyzed for specific gravity and sieve analysis.

Mix Proportions

Based on the substantial demand and requirements for building materials within the construction sector, a novel approach that uses IOTs in construction units was explored. This involved the development of four distinct mix design trials: a baseline mix with 10mm aggregate and three experimental mixes that combined 10 mm and 4.75 mm ceramic waste in varying ratios. Table 1 presents the detailed aggregate proportions for each mix design. The process of determining the optimal concrete mix design involves a

Table 1: Percentage breakdown of aggregates in the mix.

Trial	10 mm aggregate in %	Ceramic waste in %
1	100	-
2	90	10
3	80	20
4	70	30

series of interrelated steps. It begins with the calculation of the target strength, which is derived by adding 1.65 times the standard deviation (as specified in Table 1 of IS 10262 (2019) to the characteristic compressive strength (f_{ck}). Subsequently, the water-cement ratio is carefully selected, guided by the values outlined in Table 5 of IS 456 (2000) *(Reaffirmed Year: 2021)*.

The maximum water content is then determined from Table 2 of IS 10262 (2019), taking into account the nominal maximum size of the aggregate. With these parameters established, the Cement content is determined. Proceeding further, the proportion of coarse aggregate is estimated based on the recommendations in Table 3 of IS 10262 (2019). This paves the way for the crucial step of accurately estimating the quantities of each mixed ingredient. In particular, adjustments may be necessary to account for the moisture content of the aggregates. The culmination of this meticulous process involves the preparation of concrete trial mixes that serve to validate and refine the proportions of the designed mix.

Cube Casting

The fractions of material were mixed according to the percentage stated in Table 2 to cast the cubes to decide the optimal mix.

Table 2: Percentage of material used in test cubes.

Trial	Percentage of Cementitious Material				Percentage of IOTs in replacement of sand	Percentage of Coarse Aggregate	Percentage of Ceramic Waste
	Cement	GGBS	Fly Ash	Lime			
1	15.00	65.00	10.00	10.00	100.00	100.00	--
2	15.00	65.00	10.00	10.00	100.00	90.00	10.00
3	15.00	65.00	10.00	10.00	100.00	80.00	20.00
4	15.00	65.00	10.00	10.00	100.00	70.00	30.00

A controlled water addition rule yielded a homogeneous cohesive paste without air voids. Standardized mixing parameters optimize workability and uniformity. Pre-treatment with a mold release agent facilitated smooth specimen extraction. Optimal filling and compaction were achieved through standardized procedures. Controlled vibration further enhanced the internal packing density, promoting optimal strength development. Standardized surface finishing techniques ensured both aesthetic appeal and test precision. A controlled humidity environment followed by immersion in water facilitated optimal curing conditions. The precise positioning of the specimen and the controlled loading rate within the testing apparatus ensured accurate and reliable compressive strength data. These meticulously controlled procedures guaranteed the creation of robust and reliable concrete samples suitable for their designated structural applications.

Test Methods

To identify the optimal concrete mixture, in each trial, 6 cubes were cast and cured at ambient temperature. The cubes were tested for compressive strength at 7 and 28 days. The tests were conducted in accordance with IS Code IS 516 (1959) *(Reaffirmed Year: 2018)*. During compression testing, the cubes were placed sideways, nestled between the sturdy steel plates of a 200-ton machine of Venus make.

The load was applied gradually, without shock, and continuously increased at a rate of approximately 140 kg.cm² .min^{-1} until the sample's resistance broke down and it could no longer sustain a higher load. This relentless pressure continued until the resistance of the cube was crushed, and its capacity to bear the burden was finally exhausted. In simpler terms, the steadily increasing pressure eventually overpowered the cube, revealing its breaking point. When these concrete cubes were subjected to this controlled trial, the researchers could analyze their individual strengths and weaknesses, ultimately paving the way for the selection of the most robust and reliable concrete mix for the intended application.

Casting of Block

After identifying the optimal concrete mix based on the compressive strength of the test cube, block production commenced at an industrial facility situated within the Kakoda Industrial Estate in Goa, India. At this location, the necessary ingredients were mixed and subsequently transformed into robust building blocks.

The process started with the IOTs poured into a pan mixer. This was followed by the addition of GGBS, Fly Ash, Cement, and Lime in precise proportions determined by laboratory tests. For nearly two minutes, the mixer agitated, ensuring a uniform blend of the finer ingredients. This homogeneous mix is crucial to creating strong and consistent blocks. Once the finer materials were well combined, a 10mm basaltic aggregate was added to the mix. These small stones provide additional strength and structure to the blocks. Water was carefully added until the mixture reached a perfect consistency for block manufacturing. Imagine a doughy texture, not too wet and not too dry. The prepared mixture was then transferred to the block-making machine. Here, a powerful hydraulic press applied 80 tons of pressure, compacting the mixture into sturdy blocks. The newly formed blocks were then carefully cured. This process helps the concrete harden properly and reach its full strength. To ensure the quality of the blocks, various tests were performed. These included dimension test, compressive strength and bulk density, water absorption, and efflorescence. Each test provides valuable information on the suitability of the block for construction.

The following paragraphs describe the various procedures adopted for testing.

Dimension Test

Block dimension verification must adhere to the established guidelines outlined in IS 2185-Part 1 (2005). This procedure involves the random selection of twenty or more blocks, followed by their orderly arrangement in rows. Subsequently, a precise measurement of their respective dimensions is conducted to the nearest millimeters. The total lengths of the aligned blocks are meticulously determined using calibrated steel tape. This ensures a consistent and accurate assessment of the longitudinal dimension throughout the row. Similar to length measurement, the width and depth of the arranged blocks are meticulously assessed. This involves using a standardized technique that uses a straight-line reference along each dimension.

Compressive Strength and Dry Bulk Density

A digital compression testing machine was used to conduct compression testing following the procedure outlined in IS 2185-Part 1 (2005). This test apparatus applies an axial load with a consistent rate of 14 N.mm² per minute, incrementally increasing the pressure until the specimen exhibits definitive failure. Subsequently, the compressive strength quantified in N.mm² was determined using Equation (1).

Compressive strength (N.mm^{-2}) =

$$\frac{Maximum\ Load\ (N)}{Leng\ \ (mm) X\ Bread\ \ (mm)} \qquad \ldots(1)$$

The bulk density of each sample was evaluated according to the established protocol described in IS 2185-Part 1

(2005). Before measurement, the three blocks were dried in a controlled oven environment. They were kept at a constant temperature of 100°C for 24 hours to ensure complete moisture removal. After the drying period, the samples were cooled to ambient temperature and subsequently weighed using a calibrated balance. To determine the volume of the sample, precise measurements of length, width, and thickness were made at three different locations for each dimension. The average values were calculated for each dimension to account for possible minor variations within the block. Using Equation (2), the bulk density of each sample was subsequently calculated.

$$\text{Density by volume } (kg.m^{-3}) = \frac{Weigh\ of\ block\ (kg)}{(length\ (m) \times width\ (m) \times thickness\ (m))} \qquad \dots(2)$$

Water Absorption

The experiment involved submerging the test samples entirely in water at ambient temperature for a duration of 24 hours. This ensured a thorough saturation of the material. After the immersion period, the samples were weighed while suspended in water using a fine metal wire, eliminating any buoyancy effects. To standardize surface water removal, samples were gently drained for one minute on a 10mm or larger wire mesh. Before conducting the initial submerged weight measurement (M2), any remaining visible superficial water was carefully removed using a moist cloth. To obtain the saturated mass, all samples were subsequently subjected to oven drying at a temperature of 100°C to 115°C under controlled conditions for a minimum of 24 h and weighed (M1). This rigorous procedure, which employs standardized immersion, drainage, and drying protocols, ensures an accurate and reproducible measurement of water absorption capacity, a crucial parameter for evaluating the durability and performance of construction materials. Subsequently, water absorption, expressed as a percentage of mass, was calculated by applying the formula provided in Equation (3), which provides a quantitative measure of the ability of the blocks to absorb and retain water.

$$\text{Water absorption } (\%) = \frac{M2 - M1}{M1} \qquad \dots(3)$$

Efflorescence

The efflorescence assessment of the block samples adhered to the procedures outlined in IS 3495- Part 3: 1992 (Reaffirmed Year: 2016). Each sample was placed in a shallow plate, with one end submerged in water to a predetermined depth of 25 mm. This immersion continued until the water was completely absorbed by the sample and the subsequent evaporation of excess water from the dish. Following this initial drying cycle, a repeat step of adding water was performed. Finally, an examination of the blocks after the second evaporation identified any potential efflorescence manifested as discernible deposits on the surface.

RESULTS AND DISCUSSION

Before optimizing the material combination for maximum compressive strength, a comprehensive characterization of GGBS, Fly Ash, and IOTs was conducted. Table 3 presents the physical and chemical properties of the material. Chemical analyses for IOTs, GGBS, and Fly Ash included SiO_2, Al_2O_3, Fe_2O_3, CaO, MgO, and ignition loss. Specific gravity was determined for GGBS, Fly Ash, and IOTs, while fineness and residue on the sieve were determined for GGBS and Fly Ash (Kakodkar & Sawaiker 2023).

To obtain an optimal concrete mix design that balances high performance and economic feasibility, following the established guidelines outlined in IS 10262 (2019), the cubes were cast. Table 4 shows the amount of material and the proportions of constituents implemented in the mix design while Table 5 presents the compressive strength obtained on cubes. The compressive strength of the molded cubes, evaluated after 7 and 28 days, is shown graphically in Fig. 2.

Trial 1 achieved a compressive strength of 7.76 N.mm^{-2} at 7 days and 8.53 N.mm^{-2} at 28 days. Given the importance of compressive strength as a measure of resistance to forces (Castillo et al. 2021), masonry blocks were considered a suitable alternative due to their adhesion to IS codes and the significant demand in construction.

Tests on Blocks

Dimension test: The blocks were arranged lengthwise, and their dimensions were measured. This step was repeated

Table 3: Physical and Chemical Properties of a Material used to cast Construction Blocks.

Property	Raw Material			
	IOTs	GGBS	Fly Ash	Ceramic Waste
Specific Gravity	3.255	2.91	2.30	2.25
Fineness M^2.kg^{-1}	--	379	325	--
Residue on Sieve [%]	--	4.80	23.1	--
SiO_2 [%]	17.90	34.81	56.61	60.30
Al_2O_3 [%]	5.80	17.92	27.54	17.60
Fe_2O_3 [%]	63.09	1.36	4.80	4.00
CaO [%]	0.018	37.63	5.00	2.40
MgO [%]	0.135	7.83	0.60	4.20
LOI [%]	11.66	0.18	3.10	1.80

Table 4: Material used for mix design along with proportion.

Trial	Cementitious Material in kg				IOTs in kg	Coarse Aggregate in kg	Ceramic Waste in kg	Remarks
	GGBS	Fly Ash	Cement	Lime				
1	300.95	46.3	69.45	46.3	678.96	934.95	--	100%
2	300.95	46.3	69.45	46.3	678.96	826.20	84.51	90%+10%
3	300.95	46.3	69.45	46.3	678.96	712.72	164.04	80%+20%
4	300.95	46.3	69.45	46.3	678.96	618.96	244.18	70%+30%

Table 5: Compressive strength obtained on cubes.

Trial	T1 (N/mm^2)		T2 (N/mm^2)		T3 (N/mm^2)		T4 (N/mm^2)	
	7days	28 days	7days	28 days	7days	28 days	7days	28 days
1	7.73	8.50	7.25	7.97	7.32	8.05	7.40	8.14
2	7.82	8.59	7.20	7.92	7.29	8.02	7.42	8.15
3	7.75	8.52	7.17	7.88	7.35	8.08	7.46	8.20
Average	7.76	8.53	7.20	7.92	7.32	8.05	7.43	8.16
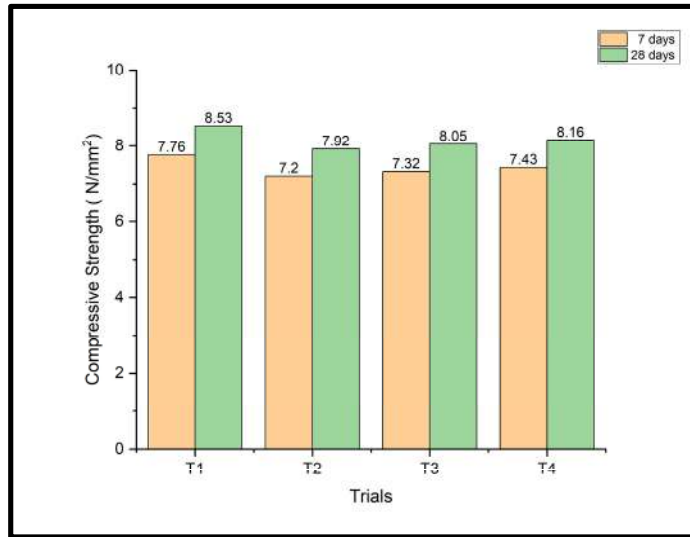
Fig. 2: 7 and 28 days Compressive strength obtained by Trials.

thrice by rearranging the blocks, and the average length was recorded. A similar process was carried out for width and thickness. Table 6 presents the Dimension Test on blocks.

Compressive Strength and Density of the Cast Block

Masonry material exhibits strong behavior under compression but is vulnerable under tension. Consequently, when choosing blocks for load-bearing structures, understanding their capacity for compressive stress is vital. In this research,

the average compressive strength was 10.91 N.mm^{-2} for 7 days and 15.92 N.mm^{-2} for 28 days when 65% of GGBS and 15% of Fly Ash were used in addition to 100% IOTs as fine aggregate and 10mm basaltic aggregate. Thejas and Hossiney (2022) performed five different block trials and found the maximum average compressive strength of 7.7 N.mm^{-2} in one of the trials wherein 42% IOTs and 44% GGBS were used. Such enhancements can be credited to the intricate reaction mechanisms of GGBS and Lime with IOTs. The complex

Table 6: Dimension Test on Construction Blocks.

Dimensions	No. of units	Dimensions [mm]	Average Dimensions [mm]	Code recommendations [mm]	
L	20	290	295	5680	5920
B		190	192	3720	3880
H		140	142	2740	2860

reaction mechanisms between GGBS, Lime, and IOTs play an important role. The GGBS and Lime interact with the IOTs through two primary mechanisms: an exothermic reaction and quick ion exchange, as well as a gradual, slower chemical reaction between calcium hydroxide and pozzolanic materials. Furthermore, the extended chemical reaction between calcium and the silica-alumina compounds in IOTs results in highly stable silicates and aluminates, providing a stronger bond and an ability to resist deterioration over time. These findings align with those of Oti et al. (2009), who observed similar reactions of GGBS and Lime to improve soil properties for construction applications. Elahi et al. (2021) reported an average compressive stress capacity of 4.4 $N.mm^{-2}$ when 21% Fly Ash was used along with soil and Cement. Nagaraj and Shreyasvi (2017) used Cement, quarry dust, and Lime along with mining waste materials and observed that at 40% replacement with mining waste material, the compressive stress capacity was 3.5 $N.mm^{-2}$. Sekhar and Nayak(2018) manufactured blocks using 75% fine-grained sedimentary rock along with 25% GGBS and 12% Cement and witnessed a compressive stress capacity of 5.5 $N.mm^{-2}$ at 28 days. Table 7 presents the compressive strength obtained by block at 7 and 28 days.

The influence of IOTs on block density, a crucial parameter in the design of masonry, was investigated.

The incorporation of IOTs resulted in a marginally higher density ranging between 2.09 to 2.28 $g.cm^{-3}$ across different block samples, with an average of 2.20 $g.cm^{-3}$. This is consistent with the observations of Abdulrahman (2015), who reported an increase in density in the Sand Crete Blocks (SCB) due to the IOTs replacing sand (ranging from 10% to 30%) in a Cement-to-sand mix of 1 6. The denser nature of the IOTs compared to that of sand was cited as a contributing factor. Similarly, James et al. (2016) observed a bulk density of 1.85 $g.cm^{-3}$ when using IOTs. The observed density enhancements in this study may be linked to the tighter arrangement of fine IOT particles and their marginally greater specific gravity in contrast to conventional earthen blocks, which usually demonstrate densities ranging between

Table 7: Compressive Strength of Construction Blocks.

Block	Compressive strength [$N.mm^{-2}$]	
	7 Days	28 Days
1	10.59	15.55
2	10.78	15.86
3	11.45	16.32
4	10.67	15.76
5	11.08	16.13
Average	10.91	15.92

Table 8: Density of Construction Blocks.

Block	Block density [$g.cm^{-3}$]
1	2.09
2	2.28
3	2.21
4	2.18
5	2.25

1.8 and 1.9 $g.cm^{-3}$. Table 8 summarizes the block densities of the investigated samples.

Water Absorption

The water absorption of masonry units plays a crucial role in their durability, particularly in their resistance to freeze-thaw damage. Lower water absorption indicates a smaller pore volume within the unit, leading to enhanced frost resistance. Typically, standards recommend that the water absorption rate for clay bricks and blocks be below 20%. The present study uses 100% IOTs as fine aggregate, which constitutes 35% of the total volume of the mixture, resulting in a favorable water absorption rate of 4.64%. Furthermore, the incorporation of GGBS and Fly Ash improves pore filling via their fine particle size and reactive products formed during pozzolanic reactions, further reducing water absorption. Thejas & Hossiney (2022) reported optimal performance for 42I-44G blocks (42% IOTs, 44% GGBS) with water absorption of 13%, observing a correlation between an increase in IOTs content and an increase in water absorption. Table 9 presents the measured water absorption values. Nagaraj et al. (2014) studied compressed stabilized earth blocks (CSEB) that incorporate Lime and Cement, achieving minimum water absorption of 7% for a mixture of 92% soil, 4% Cement, and 4% Lime. Table 9 summarizes the water absorption data for these cast blocks. Kumar and Surendra (2020) reported water absorption below 18% in all of their tests with varying Cement percentages.

Efflorescence

Block efflorescence arises from the deposition of soluble

Table 9: Water Absorption of Construction Blocks.

Brick	Dry weight [kg]	Wet weight [kg]	Water Absorption [%]
1	19.05	20.04	5.19
2	19.18	19.94	3.96
3	19.48	20.41	4.77
4	18.98	19.81	4.37
5	20.15	21.14	4.91
Average			4.64

salts on the surface. This phenomenon occurs readily in the presence of three key elements: water-soluble salts, moisture, and a porous block medium. In particular, severe efflorescence can compromise wall plaster and paint adhesion and negatively impact aesthetics, even on unplastered surfaces. Consequently, efflorescence-free blocks are preferred. IS 3495 - Part 3: 1992 (Reaffirmed Year: 2016) establishes an efflorescence classification system based on the quantity of salt deposits on the surface of the block.

Thejas & Hossiney (2022) observed a correlation between increased IOT content and higher efflorescence, with their 82% IOT block showing significant salt deposition compared to their other trials without visible deposits. This suggests that a higher IOT content potentially facilitates salt migration. In contrast, incorporating GGBS and Fly Ash into blocks can elevate the alumina content, fostering stronger cross-linking within the binder phase and restricting the movement of alkali, thereby mitigating efflorescence. In our study, the use of IOT content did not result in efflorescence, possibly due to the aforementioned mechanisms.

CONCLUSIONS

The project addressed the significant environmental impact of iron ore tailings (IOTs) by exploring remediation strategies. It aimed to develop a sustainable composite construction block utilizing readily available IOTs from Goa's mines. This objective was achieved by testing various combinations of IOTs, Ground Granulated Blast Furnace Slag (GGBS), and Fly Ash. The optimal mix design, achieving the highest compressive strength, consisted of 15% cement, 65% GGBS, 10% fly ash, and lime and utilized 100% IOTs as fine aggregate along with 100% basaltic aggregates. The manufactured blocks met the dimensional criteria stipulated in IS 2185-Part 1 (2005). Their compressive strength even surpassed the code requirements, reaching 10.91 N.mm² at 7 days and 15.92 N.mm² at 28 days. While the block density of 2.20 g/cm³ was slightly higher than standard blocks, the average water absorption of %4.64 remained within the limits of IS 2185-Part 1 (2005). Importantly, no efflorescence was observed on the blocks. This study successfully developed an eco-friendly composite block from mine waste, offering a potential pathway for remediating the environmental impact of iron ore tailings (IOTs). The blocks comply with relevant building code requirements, paving the way for sustainable waste management and resource utilization, particularly by utilizing IOTs as a viable construction material.

ACKNOWLEDGEMENT

REFERENCES

Abdulrahman, H.S., 2015. Potential use of iron ore tailings in sandcrete block making. *International Journal of Research in Engineering and Technology*, 4(4), pp.409–414.

Castillo, H., Collado, H., Droguett, T., Sánchez, S., Vesely, M., Garrido, P. and Palma, S., 2021. Factors affecting the compressive strength of geopolymers: A review. *Minerals*, 11(12), p.271. https://doi.org/10.3390/min11121317

Das, M.R., Satapathy, S. and Pothal, L.K., 2023. A study on waste management in iron mining. *Materials Today: Proceedings*, 42, p.368. https://doi.org/10.1016/j.matpr.2023.06.368

Elahi, T.E., Shahriar, A.R. and Islam, M.S., 2021. Engineering characteristics of compressed earth blocks stabilized with cement and fly ash. *Construction and Building Materials*, 277, p.1061. https://doi.org/10.1016/j.conbuildmat.2021.122367

Franco, J.deA.B., Domingues, A.M., Africano, N.deA., Deus, R.M. and Battistelle, R.A.G., 2022. Sustainability in the civil construction sector supported by Industry 4.0 technologies: Challenges and opportunities. *Infrastructures*, 7(3). https://doi.org/10.3390/infrastructures7030043

Gou, M., Zhou, L. and Then, N.W.Y., 2019. Utilization of tailings in cement and concrete: A review. *Science and Engineering of Composite Materials*, 26(1), pp.449–464. https://doi.org/10.1515/secm-2019-0029

Haibin, L. and Zhenling, L., 2010. Recycling utilization patterns of coal mining waste in China. *Resources, Conservation and Recycling*, 54(12), pp.1331–1340. https://doi.org/10.1016/j.resconrec.2010.05.005

IS 456, 2000. *Plain and Reinforced Concrete - Code of Practice*. Bureau of Indian Standard.

IS 516, 1959. *Method of Tests for Strength of Concrete*. Bureau of Indian Standard.

IS 2185-Part 1, 2005. *Concrete Masonry Units — Specification, Part 1 Hollow and Solid Concrete Blocks*. Bureau of Indian Standard.

IS 3495-Part 3: 1992 (Reaffirmed Year: 2016). *Methods of tests of burnt clay building bricks: Part 3: Determination of efflorescence*. Bureau of Indian Standard.

IS 10262, 2019. *Concrete Mix Proportioning — Guidelines*. Bureau of Indian Standard.

Jakati, D.M., 2021. Development of mining in Goa and its environmental impacts – A geographical perspective. *International Journal of Research*, 18(7), pp.2979–2988.

James, J., Pandian, P.K., Deepika, K., Manikanda Venkatesh, J., Manikandan, V. and Manikumaran, P., 2016. Cement-stabilized soil blocks are mixed with sugarcane bagasse ash. *Journal of Engineering*, 16, pp.21-33. https://doi.org/10.1155/2016/7940239

Kakodkar, S. and Sawaiker, U., 2023. Composite material design for brick manufacturing. *Materials Today: Proceedings*, 12, p.54. https://doi.org/10.1016/j.matpr.2023.05.663

Kumar, V. and Surendra, B.V., 2020. Strength and water absorption characteristics of cement stabilized masonry blocks using brick masonry waste. *Lecture Notes in Civil Engineering*, 75, pp.131–143. https://doi.org/10.1007/978-981-15-3361-7_10

Kuranchie, F.A., Shukla, S.K., Habibi, D. and Mohyeddin, A., 2015. Utilisation of iron ore tailings as aggregates in concrete. *Cogent Engineering*, 2(1), pp.1083137. https://doi.org/10.1080/23311916.2015.1083137

Lamani, S.R., Aruna, M., Vardhan, H. and Shanth, A.T., 2015. Development of value-added product using iron ore waste for its effective utilization. *International Journal of Advanced and Applied Sciences*, 2(12), pp.30–35.

Ministry of Mines, Government of India, Annual Report 2021-2022. https://mines.gov.in

Mouih, K., Hakkou, R., Taha, Y. and Benzaazoua, M., 2023. Performances of compressed stabilized bricks using phosphate waste rock for sustainable construction. *Construction and Building Materials*, 388, p.131577. https://doi.org/10.1016/j.conbuildmat.2023.131577

Nagaraj, H.B. and Shreyasvi, C., 2017. Compressed Stabilized Earth Blocks Using Iron Mine Spoil Waste - An Explorative Study. *Procedia Engineering*, 180, pp.1203–1212. https://doi.org/10.1016/j.proeng.2017.04.281

Nagaraj, H.B., Sravan, M.V., Arun, T.G. and Jagadish, K.S., 2014. Role of lime with cement in long-term strength of Compressed Stabilized Earth Blocks. *International Journal of Sustainable Built Environment*, 3(1), pp.54–61. https://doi.org/10.1016/j.ijsbe.2014.03.001

Oti, J.E., Kinuthia, J.M. and Bai, J., 2009. Engineering properties of unfired clay masonry bricks. *Engineering Geology*, 107(3-4), pp.130–139. https://doi.org/10.1016/j.enggeo.2009.05.002

Sebastian, T., Nath, B.N., Naik, S., Borole, D.V., Pierre, S. and Yazing, A.K., 2017. Offshore sediments record the history of onshore iron ore mining in Goa State, India. *Marine Pollution Bulletin*, 114(2), pp.805–815. https://doi.org/10.1016/j.marpolbul.2016.10.075

Sekhar, D.C. and Nayak, S., 2018. Utilization of granulated blast furnace slag and cement in the manufacture of compressed stabilized earth blocks. *Construction and Building Materials*, 166, pp.531–536. https://doi.org/10.1016/j.conbuildmat.2018.01.125

Tayebi-Khorami, M., Edraki, M., Corder, G. and Golev, A., 2019. Re-Thinking Mining Waste through an integrative approach led by circular economy aspirations. *Minerals*, 9(5), p.286. https://doi.org/10.3390/min9050286

The Energy and Resources Institute, 2001. Overview of Mining and Mineral Industry in India, Tata Energy Research Institute. New Delhi.

Thejas, H.K., Hossiney, N. and Shukla, S.K., 2022. Compressed unfired blocks made with iron ore tailings and slag. *Cogent Engineering*, 9(1), p.75. https://doi.org/10.1080/23311916.2022.2032975

Yellishetty, M., Ranjith, P.G. and Kumar, D.L., 2009. Metal concentrations and metal mobility in unsaturated mine wastes in mining areas of Goa, India. *Resources, Conservation and Recycling*, 53(7), pp.379–385. https://doi.org/10.1016/j.resconrec.2009.02.005

Zhang, N., Tang, B. and Liu, X., 2021. The cementitious activity of iron ore tailing and its utilization in cementitious materials, bricks, and concrete. *Construction and Building Materials*, 288, p.123022. https://doi.org/10.1016/j.conbuildmat.2021.123022

Phenopalynological Study of Some Ornamental Species in the Giza Region, Egypt

W. K. Taia[1†] 🔵 **, W. M. Amer[2]** 🔵 **, A. B. Hamed[2]** 🔵 **and A. M. Abd El-Maged[3]** 🔵

[1]Department of Botany and Microbiology, Faculty of Science, Alexandria University, Alexandria, Egypt
[2]Department of Botany and Microbiology, Faculty of Science, Cairo University, Giza 12613, Egypt
[3]Department of Biology and Geology, Alexandria University, Faculty of Education, Alexandria, Egypt
†Corresponding author; Wafaa K. Taia; taia55taxonomy@hotmail.com

ABSTRACT

Mature flower buds were collected from twenty species planted on the different roads in the Giza district from May to September 2022 and 2023. The pollen grains were examined carefully and photographed using a 40x10x magnification lens in an OPTICA (B-150D) light microscope fitted with a USB digital video Camera and Computer Software. At least 30 pollen grains/each species were measured and described. Non-catalyzed pollens were sputtered onto Aluminum stubs, coated with 30 nm gold, and examined and photographed using JEOL JSL IT 200 SEM. The morphological characters of the pollen grains were examined. According to the pollen size _Acalypha wilkesiana_ and _Tecoma stans_ were the smallest pollen grains, from 20.0µm to 26.0µm, which facilitate their introduction to the nose causing asthma and rhinitis. _Clerodendrum inerme_ pollen grains have echinate exine surface, which causes allergic symptoms more than the psilate ones. _Plumbago capensis_ has intectate exine with echinate columella causing human disorders. This study demonstrates the critical position of air pollution in this area with the change in the phenological aspects of the plants resulting in producing immature pollen grains in huge amounts, which cause human disorders and pollinosis. Our results showed that the studied species can induce allergy in one way or another if we consider the situation of the studied area, weather pattern, and pollen characteristics.

INTRODUCTION

Climate change has led to an increase in people suffering from different types of allergies and respiratory problems. Pollen allergy is one of the severe respiratory disorders resulting from inhaling the pollen grains carried by wind. The exact knowledge of the plants causing allergies is still a matter of investigation. Many studies have been carried out to investigate the exact plants causing pollinosis, i.e. pollen allergy, in different countries and cities. Mansouritorghabeh et al. (2019), besides many other authors, mentioned that trees belonging to certain orders, such as Fabales, Fagales, Lamiales, Proteales, and Pinales, are from the most allergen pollens. Taia (2020) mentioned that allergy is not restricted to certain trees, shrubs, or herbs, but it depends on the quantity of pollen grains carried by air, pollen grain size, beside other environmental factors. Thakur & Sharma (2018) found that symptoms of pollinosis have increased nowadays due to climate change, heat waves, beside various environmental factors. The increase in the planting of the city's ornamental trees, besides air pollution as a result of urbanization, constitutes harmful conducive to allergies (Aerts et al. 2021).

The study of pollen grains as the cause of allergy has been investigated by many authors (Shea et al. 2008, Aboulaich et al. 2013, Pawankar et al. 2013, Bohwmik et al. 2021, Taia 2020, Taia & Bassioni 2022). Mansouritorghabeh et

al. (2019) mentioned that there are two categories of risk factors for allergy, first is patient characteristics, and the second is environmental factors. They reported that 40% of allergic people have been affected by pollen grains besides the global climate change, especially in the Middle East area. Oh (2022) found that increases in CO_2 concentration and atmospheric temperature raise pollen concentration. Many studies clarified the significant impact of climate fluctuation on the phenology of the plants in many areas around the world, besides the other aeroallergens and their impact on public health (Beggs 2004, Assarehzadegan et al. 2013). This change in the phenology of the plants resulted in producing pollen grains at unsuitable times for fertilization and kept huge amounts of pollen carried by air. This fact promotes the need for continuous studies of allergenic tree pollens in each region and city.

Although many researchers have investigated the relationship between urban vegetation and air pollution, few studies have focused on the role of pollen grains as air pollutants. El-Shamy et al. (2023) found that six different plants belonging to the Fabaceae family (*Bauhinia variegate*, *Cassia javanica*, *Delonix regia*, *Peltophorum africanum*, *Senna didymobotrya* and *Senna surattensis*) and four different plants belonging to Poaceae family (*Avena sativa*, *Setaria viridis*, *Sorghum bicolour* and *Zea mays*) have hydrophilic proteins antigen in their pollens. They concluded that pollen grains related to the Fabaceae and Poaceae families are responsible for allergic patients in Egypt. García-Mozo (2017) concluded that the family Poaceae is the main family responsible for pollen allergy. Pollen allergens must be water-soluble proteins, glycoproteins, starch, or fats, which make them capable of evoking an IgE antibody-mediated allergic reaction immediately in sensitive people. Stewart et al. (2009) identified 15 distinct groups of proteins with different biochemical properties as allergens in taxa of the subfamily Pooideae, family Poaceae. Pollinosis is an illness induced by glycoprotein derivatives which are in the external part of the pollen cell wall (Exine). These glycoprotein derivatives bond to certain receptors situated in the mucous membranes, stimulating the secretion of histamine and causing inflammation symptoms (Taia & Zayed 2021).

This work aimed to investigate the pollen characteristic of the twenty species of the most common ornamental species planted in the roads of the Giza district within the great Cairo. Giza has its characteristic weather all through the year. It is dry-hot during the summer and exposed to windstorms during the winter. It is affected by the surrounding factories, which make the air polluted by a great number of gases, dust, pollen grains, and fungal spores.

MATERIALS AND METHODS

Study Area

Cairo, the capital of Egypt, is considered one of the most highly polluted cities in the world. The city is highly crowded with people, vehicles, and cars. The dense gas evolved by cars, transportation, and industrialization processes made the air highly polluted. The Giza district lies west of Cairo and is considered an important part of Cairo city. It is visited by tourists for the most important Egyptian monuments and historical places. A narrow strip of Giza Governorate lies on the west bank of the river Nile and has two industrial centers. Giza is surrounded by El-Mokatam plateau and Shobra El-Khema, which is a big industrial area. Giza city has brick industries along the western bank of the river Nile, north and south of Giza. Accordingly, the air quality in Giza is full of industrial emissions besides the dust storms from the El-Mokatam Plateau and CO_2 gas from agricultural waste burning in the delta Nile valley (Hassan & Khoder 2017).

Pollen Grains Collection

Mature flower buds were collected from twenty species planted on the different roads in the Giza district from May to September 2022 and 2023. The name of the trees is present in Table 1. Each species is represented by ten flower buds from five different trees. The buds were carefully opened to release the stamens. The pollen grains were sputtered onto a clean glass slide with a few drops of glycerol, covered by cover slides, and sealed with wax for light microscope examination. The pollen grains were examined and photographed using a 40x10x magnification lens in an OPTICA (B-150D) light microscope fitted with USB digital video Camera and Computer Software. At least 30 pollen grains/each species were measured and described. Non-acetolyzed pollens were sputtered onto Aluminum stubs, coated with 30 nm gold, and examined and photographed using JEOL JSL IT 200 SEM allocated at the Faculty of Science, Alexandria University at 15 Kev. For pollen description, the terminology used here is that of Walker & Doyle (1976).

RESULTS

Pollen Morphology of the Studied Taxa

Pollen grains of the studied trees are mostly of medium size. Only two species have small pollen grains from 20.0 to 25.0 µm; *Acalypha wilkesiana* and *Tecoma stans*; and another three species have large pollen grains over 50.0 µm, *Plumbago capensis*, *Senna surattensis* and *Jacaranda mimosifolia*. The pollen size categories are not related to the state of the tree, deciduous or evergreen. Pollen

Table 1: Studied trees and their taxonomic position, citation and place of origin.

No.	Species	Family	Date of collection	Citation	Origin
1.	*Plumbago capensis* Thunb.	Plumbaginaceae	22/5/2022	Lam., Encycl. 2: 270 (1786)	S. Africa
2.	*Calliandra haematocephala* Hassk.	Fabaceae	20/6/2023	Retzia 1:216 (1855)	South America.
3.	*Cassia fistula* L.		20/6/2023	Sp. Pl. 377. 1753	India, Malaysia and Southeast Asia
4.	*Cassia javanica* L.		19/5/2022	Sp. Pl.: 379 (1753	South East Asia
5.	*Delonix regia* (Bojer ex Hook.) Raf.		19/7/2022	Sp. Pl.: 379 (1753	Madagascar
6.	*Senna surattensis* (Burm. f.) Irwin & Barenby		20/7/2022	Mem. New York Bot. Gard.35(1): 81 (1982)	Tropical Asia to Australia.
7.	*Lagerstroemia indica* L.	Lythraceae	19/7/2022	Syst. Nat. ed. 10, 2: 1076 (1759)	Himalaya to South Asia
8.	*Punica granatum* L.		24/8/2023	Sp. Pl. : 472 (1753)	Afghanistan and Iran.
9.	*Euphorbia milii* Des Moul.	Euphorbiaceae	20/6/2023	Bull. Hist. Nat. Soc. Linn. Bordeaux 1: 27 (1826)	Madagascar
10.	*Acalypha wilkesiana* Mull. Arg.		24/8/2023	Prodr. 15(2): 817 (1866)	Micronesia
11.	*Cascabela thevetia* (L.) Lippold	Apocynaceae	19/7/2022	Feddes Repert. 91: 52. 1980	Argentina and Bolivia.
12.	*Catharanthus roseus* (L.) G. Don		20/6/2023	Gen. Hist. 4: 95 (1837)	Madagascar
13.	*Nerium oleander* L.		24/8/2023	Sp. Pl.: 209 (1753)	Mediterranean to Japan
14.	*Plumeria rubra* L.		19/7/2022	Sp. Pl. : 209 (1753)	Mexico and Panama
15.	*Withania somnifera* (L.) Dunal	Solanaceae	11/6/2022	Prodr. [A.P. de Candolle] 13(1): 453. 1852	India
16.	*Jacaranda mimosifolia* D. Don	Bignoniaceae	19/7/2022	Bot. Reg. 8: t.631 (1822)	Argentina and Bolivia.
17.	*Tecoma stans* (L.) Juss. ex Kun*th*		11/6/2022	Nov. Gen. Sp. Pl. 3:144	S. America
18.	*Clerodendrum inerme* Gaertin.	Lamiaceae	24/8/2023	Sp. Pl. : 637 (1753)	China, India and Australia
19.	*Vitex agnus-castus* L.		19/7/2022	Sp. Pl.: 638 (1753)	Mediterranean region
20.	*Lantana camara* L.	Verbenaceae	24/8/2023	Sp. Pl. : 627 (1753)	Central and South America

phenocharacters of the studied trees are summarized in Table 2.

1. *Plumbago capensis* Thunb. Plum, Baginaceae, evergreen tree (Figs. 1-4)

Pollen grains are dispersed as monads, radiosymmetric, and isopolar with large pollen grains. The mean polar axis length is 55.8 μm while the mean equatorial axis diameter is 38.9 μm with P/E equal to 1.4. Their shapes are prolate with three zonocolpate apertures (Figs. 1, 2). The colpi are nearly the same length as the polar axis but still free (Figs. 2, 3). The apocolpi are narrow, and the colpi membranes are smooth. Exine thickness is 2.8 μm, intectate with long bacullae and pointed echinated capitae (Fig. 4).

2. *Calliandra haematocephala* Hassk. Fabaceae, Mimosoideae, evergreen tree (Figs. 5, 6)

Pollen grains dispersed in polyads consist of seven to nine pollen grains (Fig. 6). The polyads are non-appendiculate (Fig. 5). The apical pollen grain is acute.

3. *Cassia fistula* L. Fabaceae, Caesalpinoideae, Deciduous tree (Figs. 7-10)

Pollen grains are dispersed in monads, radiosymmetric, and isopolar with medium pollen grains. The mean polar axis length is 40.7 μm while the mean equatorial axis diameter is 32.6 μm with P/E equal to 1.2. Their shapes are subprolate with three zonocolporate apertures (Figs. 7, 9). The colpi are nearly the same length as the polar axis but still free

(Fig. 8). The apocolpi are narrow, and the colpi membranes are smooth. The pores are lolongate, small, and covered by an exinous bridge. Exine thickness is 2.2 μm, and tectate perforate with rugate ectexine (Fig. 10).

4.   *Cassia javanica* L. Fabaceae, Caesalpinoideae, Deciduous tree (Figs. 11-14)

Pollen grains are dispersed in monads, radiosymmetric, and isopolar with medium pollen grains. The mean polar axis length is 38.2 μm while the mean equatorial axis diameter is 28.5 μm with P/E equal to 1.3. Their shapes are prolate with three zonocolporate apertures (Figs. 11, 12). The colpi are nearly the same length as the polar axis but still free (Figs. 12, 13, 14). The apocolpi are narrow, and the colpi membranes are smooth. The pores are lolongate, oval and exposed. Exine thickness is 2.5 μm, and tectate perforate with foveolate ectexine (Fig. 14).

5.   *Delonix regia* (Bojer ex Hook.) Raf. Fabaceae, Caesalpinoideae, Deciduous tree (Figs. 15, 16)

Pollen grains are dispersed in monads, radiosymmetric, and isopolar with medium pollen grains. The mean polar axis length is 36.3 μm while the mean equatorial axis diameter is 36.3 μm with P/E equal to 1.0. Their shapes are spheroidal with three zonocolporate apertures (Fig. 15). The colpi are short with rounded ends (Fig. 16). The apocolpi are wide, and the colpi membranes are granulated. The pores are lolongate, small and exposed. Exine thickness is 1.8 μm, tectate perforate with reticulate ectexine (Fig. 16). The luminae are enriched with rounded granules.

6.   *Senna surattensis* (Burm. f.) Irwin & Barenby Fabaceae, Caesalpinoideae, evergreen tree (Figs. 17, 18)

Pollen grains are dispersed in monads, radiosymmetric, and isopolar with large pollen grains. The mean polar axis length is 52.8 μm while the mean equatorial axis diameter is 47.2 μm with P/E equal to 1.1. Their shapes are subprolate with three zonocolporate apertures (Figs. 17, 18). The colpi are shorter than the polar axis (Fig. 17). The apocolpi are wide, and the colpi membranes are smooth. The pores are small and plugged. Exine thickness is 2.5 μm, tectate inperforate with punctate ectexine (Fig. 18).

7.   *Lagerstroemia indica* L. Lythraceae, deciduous tree (Figs. 19-22)

Pollen grains are dispersed in monads, radiosymmetric, and isopolar with medium pollen grains. The mean polar axis length is 48.5 μm while the mean equatorial axis diameter is 40.5 μm with P/E equal to 1.2. Their shapes are subprolate with three zonocolporate apertures (Figs. 19, 20). The colpi are shorter than the polar axis (Fig. 20). The apocolpi are wide, and the colpi membranes are granulated. The pores are very small and plugged. Exine thickness is 2.5 μm, and

tectate perforate with rugate ectexine (Fig. 21, 22).

8.   *Punica granatum* L. Lythraceae, deciduous tree (Figs. 23-26)

Pollen grains are dispersed in monads, radiosymmetric, and isopolar with medium pollen grains. The mean polar axis length is 42.8 μm while the mean equatorial axis diameter is 31.5 μm with P/E equal to 1.4. Their shapes are perprolate with three zonocolporate apertures (Figs. 23, 24). The colpi are shorter than the polar axis (Fig. 25). The apocolpi are wide, and the colpi membranes are granulated. The pores are lolongate, small, oval and plugged. Exine thickness is 2.2 μm, and tectate imperforate with scabrate ectexine (Fig. 26).

9.   *Euphorbia milii* Des Moul. Euphorbiaceae, evergreen tree (Figs. 27-30)

Pollen grains are dispersed in monads, radiosymmetric, and isopolar, with medium pollen grains. The mean polar axis length is 40.2 μm, and the mean equatorial diameter is 24.8 μm with P/E equal to 1.6. Their shapes are perprolate with three zonocolporate apertures (Figs. 26, 27). Colpus is shorter than the polar axis (Figs. 27, 28, 29). The apocolpi are wide, and the colpi membranes are smooth. The pores are lolongate, small and plugged. Exine thickness is 2.8 μm, and tectate perforate with reticulate ectexine (Fig. 30).

10. *Acalypha wilkesiana* Mull.Arg. Euphorbiaceae, evergreen tree (Figs. 31-34)

Pollen grains are dispersed in monads, radiosymmetric, isopolar, and small pollen grains. The mean polar axis length is 20.2 μm, and the mean equatorial diameter is 20.2 μm with P/E equal to 1.0. Their shapes are spherical with three zonocolporate apertures (Figs. 31, 32). The colpi are shorter than the polar axis (Fig. 33). The apocolpi are wide, and the colpi membranes are granulated. The pores are lolongate, small and plugged. Exine thickness is 1.2 μm, and tectate perforate with rugate ectexine (Fig. 34).

11. *Cascabela thevetia* (L.) Lippold Apocynaceae, evergreen tree (Figs. 35-38)

Pollen grains are dispersed in monads, radiosymmetric, and isopolar, with medium pollen grains. The mean polar axis length is 35.2 μm, and the mean equatorial diameter is 28.2 μm with P/E equal to 1.3. Their shapes are prolate with three zonocolporate apertures (Figs. 35, 36, 37). The colpi are shorter than the polar axis (Fig. 35). The apocolpi are wide, and the colpi membranes are smooth. The pores are lolongate, wide and covered by an exinous bridge (Fig. 37). Exine thickness is 1.8 μm, and tectate perforate with rugate ectexine (Fig. 38).

12. *Catharanthus roseus* (L.) G. Don Apocynaceae, evergreen tree (Figs. 39- 42)

Pollen grains are dispersed in monads, radiosymmetric, and isopolar, with medium pollen grains. The mean polar axis length is 38.2 µm, and the mean equatorial diameter is 30.4 µm with P/E equal to 1.3. Their shapes are prolate with three zonocolporate apertures (Figs. 39, 40). The colpi are shorter than the polar axis (Fig. 41). The apocolpi are wide, and the colpi membranes are smooth. The pores are lolongate, wide and exposed (Fig. 40). Exine thickness is 1.8 µm, and tectate inperforate with punctate ectexine (Fig. 42).

13. *Nerium oleade* L. Apocynaceae, evergreen tree (Figs. 43-45)

Pollen grains are dispersed in monads, radiosymmetric, and isopolar, with medium pollen grains. The mean polar axis length measures 34.8 µm, and the mean equatorial diameter is 30.2 µm with P/E equal to 1.2. Their shapes are subprolate with three zonocolporate apertures (Figs. 43, 44). The colpi are shorter than the polar axis (Fig. 43). The apocolpi are wide, and the colpi membranes are smooth. The pores are lolongate, small and covered by an exinous bridge (Fig. 44). Exine thickness is 2.8 µm, dictating perforate with foveolate ectexine (Fig. 45).

14. *Plumeria rubra* L. Apocynaceae, deciduous tree (Figs. 46-48)

Pollen grains are dispersed in monads, radiosymmetric, and isopolar, with medium pollen grains. The mean polar axis length is 32.8 µm, and the mean equatorial diameter is 24.6 µm with P/E equal to 1.3. Their shapes are subprolate with three zonocolporate apertures (Fig. 46). The colpi are shorter than the polar axis (Fig. 47). The apocolpi are wide, and the colpi membranes are smooth. The pores are lolongate, oval and plugged (Fig. 47). Exine thickness is 2.4 µm and tectate perforate with scabrate ectexine (Fig. 48).

15. *Withania somnifera* (L.) Dunal *Withania somnifera* (L.) Dunal Solanaceae, evergreen tree (Figs. 49-51)

Pollen grains are dispersed in monads, radiosymmetric, and isopolar, with medium pollen grains. The mean polar axis length is 44.6 µm, and the mean equatorial diameter is 28.8 µm with P/E equal to 1.5. Their shapes are perprolate with three zonocolpate apertures (Fig. 49). The colpi are free and long and extend near the poles (Fig. 50). The apocolpi are narrow, and the colpi membranes are granulated. Exine thickness is 2.0 µm, and tectate perforate with reticulate ectexine (Fig. 51).

16. *Jacaranda mimosifolia* D. Don Bignoniaceae, deciduous tree (Figs. 52-55)

Pollen grains are dispersed in monads, radiosymmetric, and isopolar, with large pollen grains. The mean polar axis length is 52.6 µm, and the mean equatorial diameter is 32.4 µm, with P/E equal to 1.6. Their shapes are perprolate with three zonocolpate apertures (Figs. 52, 53). The colpi are free, long and extend near the poles (Fig. 54). The apocolpi are narrow, and the colpi membranes are granulated. Exine thickness is 2.2 µm, and tectate perforate with foveolate ectexine (Fig. 55).

17. *Tecoma stans* (L.) Juss. ex Kunth Bignoniaceae, evergreen tree (Figs. 56-58)

Pollen grains are dispersed in monads, radiosymmetric, and isopolar, with small pollen grains. The mean polar axis length is 25.0 µm, and the mean equatorial diameter is 16.5 µm with P/E equal to 1.5. Their shapes are perprolate with three zonocolpate apertures (Fig. 56). The colpi are syncolpate, long and unitted at the poles (Figs. 57, 58). The colpi membranes are granulated. Exine thickness is 2.4 µm, and tectate perforate with reticulate ectexine (Fig. 58).

18. *Clerodendrum inerme* Gaertin. Lamiaceae, evergreen tree (Figs. 59-63)

Pollen grains are dispersed in monads, radiosymmetric, and isopolar, with medium pollen grains. The mean polar axis length is 40.2 µm, and the mean equatorial diameter is 29.8 µm with P/E equal to 1.3. Their shapes are subprolate with three zonocolpate apertures (Figs. 59, 60, 61). The colpi are shorter than the polar axis (Fig. 61). The apocolpi are wide, and the colpi membranes are smooth (Figs. 59, 60). Exine thickness is 2.2 µm, and tectate inperforate with echinate ectexine (Fig. 63).

19. *Vitex agnus-castus* L., Lamiaceae, deciduous tree (Figs. 64-68)

Pollen grains are dispersed in monads, radiosymmetric, and isopolar, with medium pollen grains. The mean polar axis length is 42.8 µm, and the mean equatorial diameter is 32.6 µm with P/E equal to 1.3. Their shapes are subprolate with three zonocolpate apertures (Figs. 64, 65). The colpi are as long as the polar axis (Figs. 66, 67). The apocolpi are narrow, and the colpi membranes are smooth. Exine thickness is 1.8 µm, and tectate perforate with reticulate ectexine (Fig. 68).

20. *Lantana camara* L. Verbenaceae, evergreen tree (Figs. 69-72)

Pollen grains are dispersed in monads, radiosymmetric, and isopolar, with medium pollen grains. The mean polar axis length is 38.0 µm, and the mean equatorial diameter is 37.8 µm, with P/E equal to 1.0. Their shapes are spheroidal with three zonocolporate apertures (Figs. 69, 70). The colpi are as long as the polar axis (Fig. 71). The apocolpi are narrow, and the colpi membranes are smooth. The pores are small lolongate (Fig. 71). Exine thickness is 2.4 µm, and tectate perforates with rugate ectexine (Fig. 72).

Table 2: Pollen phenocharacters of the studied trees.

| No. | Species | Status | Pollen characters | | | | | | Aperture | | Exine | |
			Dis	P.A.L μm M±SD	E.A.D μm M±SD	P/E	Shape	Size	No	Type	Th	Or
1.	Plumbago capensis	Eg	M	55.8±1.26	38.9±2.65	1.4	P	L	3	Col	2.8	IT
2.	*Calliandra haematocephala*	Eg	Po	--	--	--		--	--	--	--	--
3.	*Cassia fistula*	D	M	40.7±2.35	32.6±1.89	1.2	SP	Me	3	Colp	2.2	Ru
4.	*Cassia javanica*	D	M	38.2±1.95	28.5±2.25	1.3	P	Me	3	Colp	2.5	Fv
5.	*Delonix regia*	D	M	36.3±2.95	36.3±2.95	1.0	Sph	Me	3	Colp	1.8	R
6.	*Senna surattensis*	Eg	M	52.8±2.98	47.2±2.42	1.1	SP	L	3	Colp	2.5	Pu
7.	*Lagerstroemia indica*	D	M	48.5±2.82	40.5±1.82	1.2	SP	Me	3	Colp	2.5	Ru
8.	*Punica granatum*	D	M	42.8±2.1	31.5±2.85	1.4	PP	Me	3	Colp	2.2	Sc
9.	*Euphorbia milii*	Eg	M	40.2±2.8	24.8±2.6	1.6	PP	Me	3	Colp	2.8	R
10.	*Acalypha wilkesiana*	Eg	M	20.2±1.2	20.2±1.2	1.0	Sph	S	4	Colp	1.2	Ru
11.	*Cascabela thevetia*	Eg	M	35.2±2.6	28.2±2.8	1.3	P	Me	3	Colp	1.8	Ru
12.	*Catharanthus roseus*	Eg	M	38.2±2.4	30.4±1.8	1.3	p	Me	3	Colp	1.8	Pu
13.	*Nerium oleander*	Eg	M	34.8±2.2	30.2±2.4	1.2	SP	Me	3	Colp	2.8	Fv
14.	*Plumeria rubra*	D	M	32.8±2.4	24.6±1.8	1.3	Sp	Me	3	Colp	2.4	Sc
15.	*Withania somnifera*	Eg	M	44.6±2.2	28.8±2.6	1.5	PP	Me	3	Col	2.0	R
16.	*Jacaranda mimosifolia*	D	M	52.6±1.2	32.4±2.2	1.6	PP	L	3	Col	2.2	Fv
17.	*Tecoma stans*	Eg	M	25.0±3.2	16.5±1.8	1.5	PP	S	3	Col	2.4	R
18.	Clerodendrum inerme	Eg	M	40.2±1.8	29.8±2.2	1.3	P	Me	3	Col	2.2	Ec
19.	Vitex agnus-castus	D	M	42.2±0.8	32.6±1.2	1.3	P	Me	3	Col	1.8	R
20.	Lantana camara	Eg	M	38.0±1.2	37.8±1.8	1.0	Sph	Me	3	Colp	2.4	Ru

Abbreviations: Col=Colpate; Colp=Colporate; D=Deciduous; Dis=Dispersal; E.A.D=Equatorial axis diameter; Ec=Echinate; Eg=Evergreen; Fv=Foveolate; IT=Intectate; L=Large; M=Monad; Me=Medium; No=Number; P=Prolate; Po=Polinium; PP=Perprolate; Pu=Punctate; R=Reticulate; Ru=Rugate; S=Small; Sc=Scabrate; SP=Subprolate; Sph=Spheroidal

DISCUSSION

Street planting with roadside trees is essential to make the city livable, improve the environment, enhance public health and support, and advance the infrastructure. Meanwhile, some plants cause health troubles for people, such as allergies. Plants causing allergies are still unidentified. In urban areas with crowded populations, many buildings and factories besides the gases emitted from the traffic and automobiles, can accelerate allergic symptoms. The wind-pollinated trees are considered an important cause of pollen allergy, for being widespread and dense in the human environment, besides their huge production by flowers (Oh 2022). Pollen released by street trees, in combination with air pollutants, has a considerable adverse impact on human health. Pollen allergy; is known as pollinosis hay fever or seasonal allergic rhinitis, increases during spring, summer, and autumn. The pollen grains have specific proteins which are released during their dehydration causing allergic reactions in sensitive people (Elshemy & Abobakr 2013). The most effective

pollens are those with small sizes ranging from 10 μm to less than 50 μm, which can penetrate the bronchitis, causing symptoms of allergy (Thakur & Sharma 2018). The small pollen grains are easily carried by air and transferred by wind for long distances. The onset of pollen grains differs annually according to both the species and weather variability (Zhang et al. 2014, Oh 2018). CO_2 concentration in the air is an important factor affecting the quantity of pollen onset by plants (Oh 2018). In an area like Giza is a crowded region with more air pollutants, pollen grains become more harmful, and in combination with the pollutants, symptoms of allergy become severe.

From the results obtained, both *Acalypha wilkesiana* and *Tecoma stans* have the smallest pollen grains, from 20.0μm to 26.0μm, which facilitate their introduction to the nose causing asthma and rhinitis. Mampage et al. (2022) pointed to the severe impacts of bioaerosols on human health depending on their size and considered the pollen grains range from 10 to 100 μm causatives to allergy. According to Mampage et
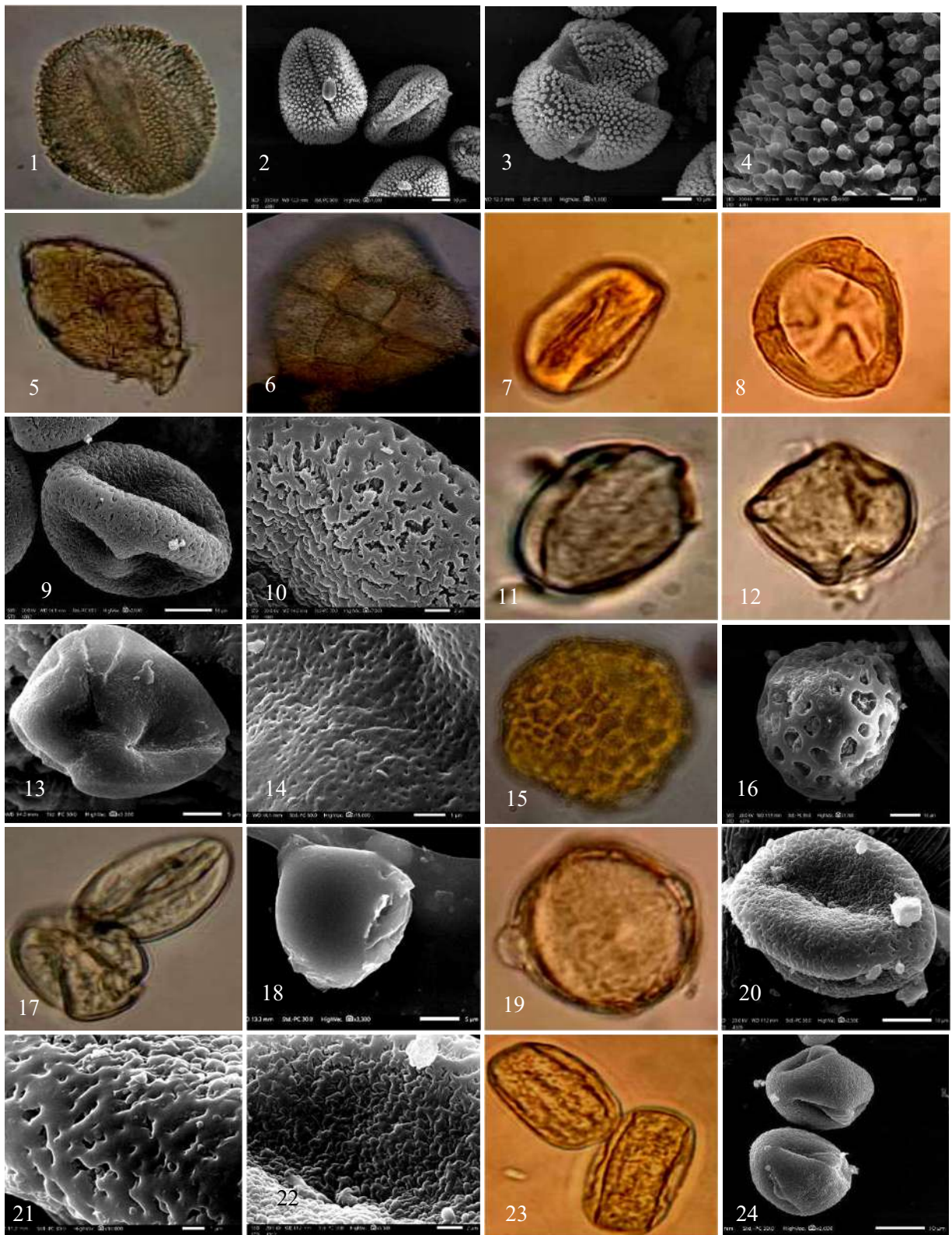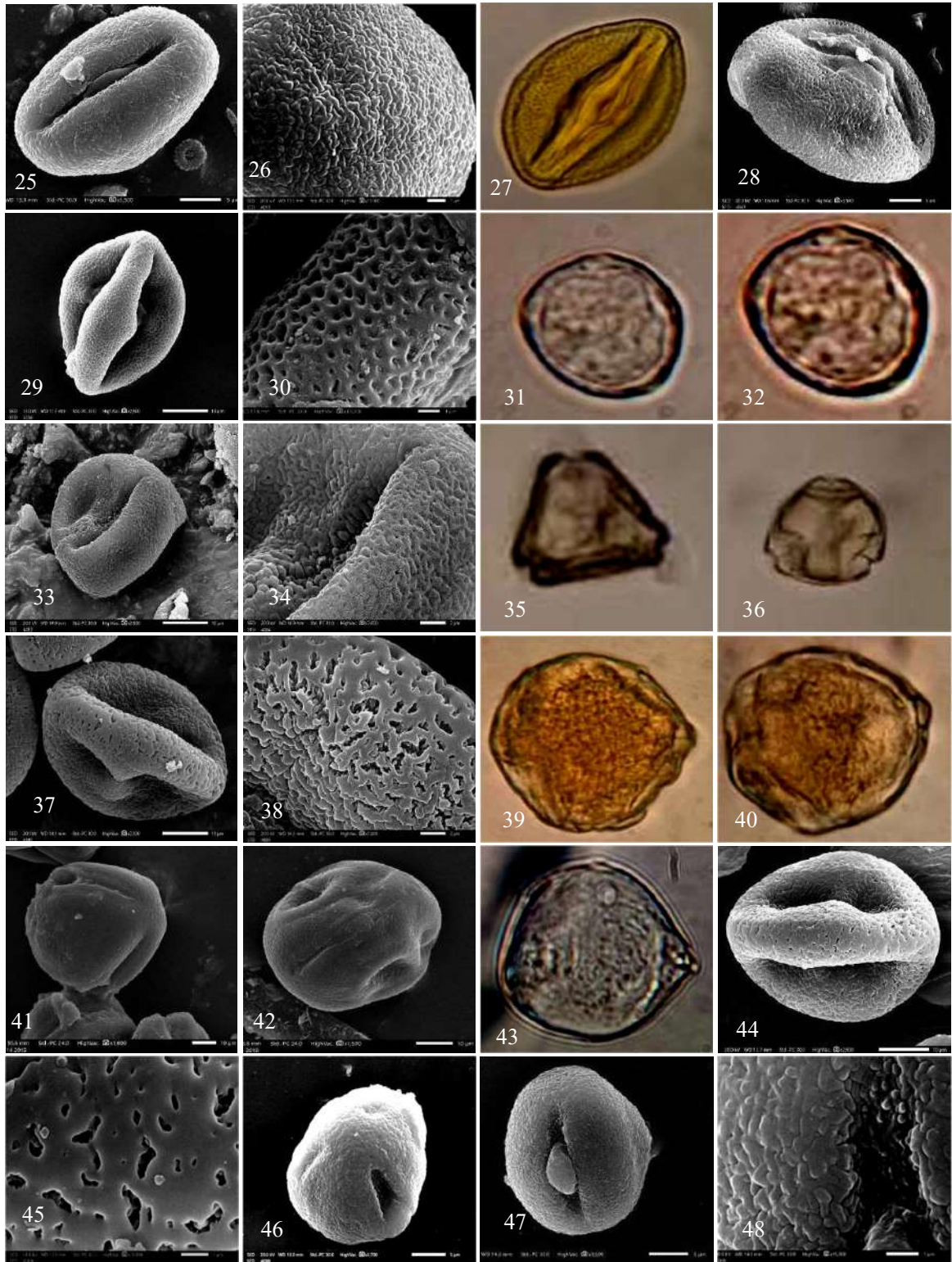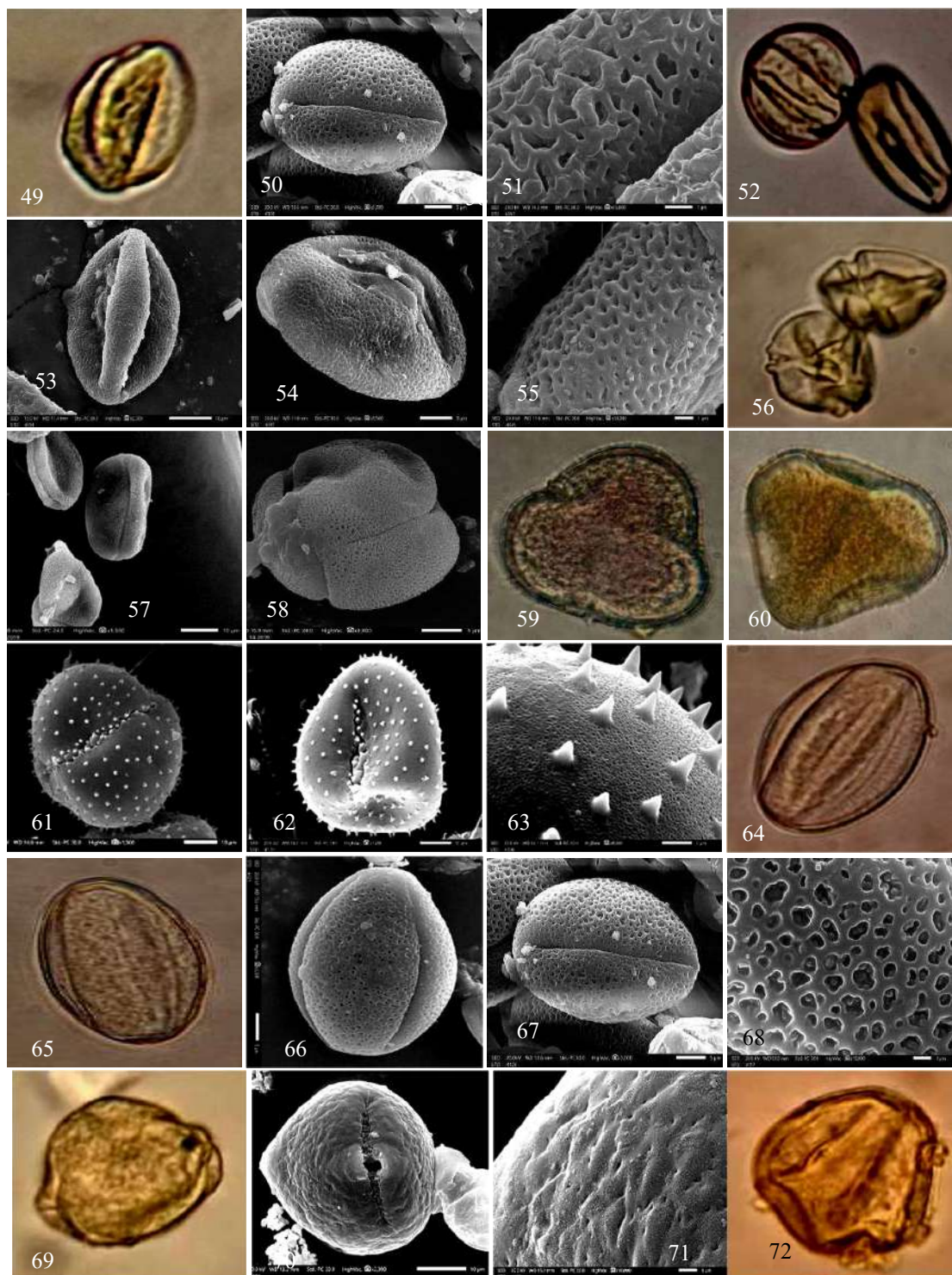
Figs. 1-72: LM and SEM photographs of the pollen grains of the studied species. 1-4 Plumbago capensis, 5-6 polyads of *Calliandra haematocephala*, 7- 10 *Cassia fistula* 11-14 *Casia javanica*, 15-16 *Delonix regia*, 17-18 *Senna surathensis*, 19-22 *Lagerstroemia indica*, 23-26 *Punica granatum*, 27- 30 *Euphorbia milii*, 31-34 *Acalypha wilkesiana*, 34- 38 *Cascabela thevetia*, 39-42 *Catharanthus roseus*, 43-45 *Nerium oleander*, 46-48 *Plumeria rubra*, 49-51 *Withania somnifera*, 52- 55 *Jacaranda mimosifolia*, 56-58 *Tecoma stans*, 59-63 *Clerodendrum inerme*, 64-68- *Vitex agnus-castus*, 69-72 *Lantana camara*.

al. (2022), all the studied pollen trees are allergic and can induce trouble for human health. Oh (2022) pointed to the huge effect of pollen grains as causative and triggering agents of respiratory allergy, and people suffering from pollinosis increased as a result of environmental changes. He pointed to the most allergens pollen grains sizes range from 20 to 60 µm. According to both opinions, all the pollen grains of the studied species are causatives of allergy. The sizes of the studied trees' pollen grains range from 20 to 55 µm, which means that all of them can trigger allergic symptoms. If we add the exine ornamentation, as it can cause itching in their intact eyes and skin, we can say that the echinate surfaces recorded in *Clerodendrum inerme* cause allergic symptoms more than the psilate ones. Dbouk et al. (2022) mentioned that the WHO announced that by 2050, one out of two people will suffer from allergy disorders due to the combination of air pollution beside pollen grains. This warning stimulated scientists to find protection from this harmful combination. Sedghy et al. (2018) considered pollen grains not only as allergen carriers but they can elicit allergic responses in sensitized people. They mentioned that interaction between air pollutants and pollen grains damages the pollen cell wall and increases the number of allergens released into the environment. They considered the big-sized pollen grains that cannot penetrate the bronchitis to have pollen-derived particles, smaller than the pollens themselves, which can induce asthma-related symptoms. Our results showed that the studied trees can induce allergy in one way or another if we consider the situation of the studied area and the weather pattern.

Aperture type and number don't have a considerable role in allergy. They can affect the hydration state of the pollen grains and the secretion of lipids and glycoproteins, stimulating allergy. All the studied trees have tricolpate or tricolporate apertures. This means that all the pollens have the same chance to release the chemical stimulants. Božič & Šiber (2022) made a model illustrating the bursting of the porate pollen grains to release their contents. They mentioned that the air humidity and the environment can desiccate the pollen and make in fold on the surface or swell the pollen and burst it. In the latter case, the release of lipids, proteins, and pollen derivative particles becomes easier and causes many disorders in humans. Thus, if we consider the studied area beside the weather patterns and air pollutants and specks of dust, all together can combine, resulting in delaying the anther opening and releasing the pollens. In this case, the pollen grains become more mature with more allergens (Oh 2022).

CONCLUSIONS

This study clarified the different morphological characteristics of the ornamental species in the Giza district, Egypt. It demonstrates the critical position of air pollution in this area with the change in the phenological aspects of the plants, resulting in the production of immature pollen grains in huge amounts, which cause human disorders and pollinosis. Our results showed that the studied species can induce allergy in one way or another if we consider the situation of the studied area, weather pattern, and pollen characteristics.

REFERENCES

Aboulaich, N., Achmakh, L., Bouziane, H., Mar Trigo, M., Recio, M., Kadiri, M., Cabezudo, B., Riadi, H. and Kazzaz, M., 2013. Effect of meteorological parameters on Poaceae pollen in the atmosphere of Tetouan (NW Morocco). *International Journal of Biometeorology*, 57, pp.197-205. DOI: 10.1007/s00484-012-0566-2.

Aerts, R., Bruffaerts, N., Somers, B., Demoury, C., Plusquin, M., Nawrot, T.S. and Hendrickx, M., 2021. Tree pollen allergy risks and changes across scenarios in urban green spaces in Brussels, Belgium. *Landscape and Urban Planning*, 207, p.104001. DOI: 10.1016/j.landurbplan.2020.104001.

Assarehzadegan, M.A., Shakurnia, A. and Amini, A., 2013. The most common aeroallergens in a tropical region in Southwestern Iran. *World Allergy Organization Journal*, 6, pp.1-7. DOI: 10.1186/1939-4551-6-7.

Beggs, P.J., 2004. Impacts of climate change on aeroallergens: past and future. *Clinical and Experimental Allergy*, 34(10), pp.1507-1513. DOI: 10.1111/j.1365-2222.2004.02061.x.

Bohwmik, M., Ghosh, N. and Bhattacharya, S.G., 2021. Allergenicity assessment of Delonix regia pollen grain and identification of allergens by immunoproteomic approach. *Heliyon*, 7(2), p.e06014. DOI: 10.1016/j.heliyon.2021.e06014.

Božič, A. and Šiber, A., 2022. Mechanics of inactive swelling and bursting of porate pollen grains. *Biophysical Journal*, 121(5), pp.782-792. DOI: 10.1016/j.bpj.2022.01.019.

Dbouk, T., Visez, N., Ali, S., Shahrour, I. and Drikakis, D., 2022. Risk assessment of pollen allergy in urban environments. *Scientific Reports*, 12(1), p.21076. DOI: 10.1038/s41598-022-24819-w.

EL-shamy, H.M., Abdel-Rahman, B., Abdel Ghaffar, A.B. and Elwan, Z.A., 2023. Identification of some allergenic pollen proteins of some Fabaceae and Poaceae species using the SDS-PAGE technique. *Egyptian Journal of Pure and Applied Science*, 61(2), pp.28-41. DOI: 10.21608/ejaps.2023.196823.1056.

Elshemy, A. and Abobakr, M., 2013. Allergic Reaction: Symptoms, Diagnosis, Treatment and Management. *World Journal of Innovative Research*, 2(1), pp. 123-144.

García-Mozo, H., 2017. Poaceae pollen as the leading aeroallergen worldwide: A review. *Allergy*, 72(12), pp. 1849-1858. DOI: 10.1111/all.13210.

Hassan, S.K. and Khoder, M.I., 2017. Chemical characteristics of atmospheric PM2.5 loads during air pollution episodes in Giza, Egypt. *Atmospheric Environment*, 150, pp. 346-355. DOI: 10.1016/j.atmosenv.2016.11.026.

Mampage, C.B.A., Hughes, D.D., Jones, L.M., Metwali, N., Thorne, P.S. and Stone, E.A., 2022. Characterization of sub-pollen particles in size-resolved atmospheric aerosol using chemical tracers. *Atmospheric Environment X*, 15(2), 100177. DOI: 10.1016/j.aeaoa.2022.100177.

Mansouritorghabeh, H., Jabbari-Azad, F., Sankian, M., Varasteh, A. and Farid-Hasseini, R., 2019. The most common allergenic tree pollen grains in the Middle East: A narrative review. *Iranian Journal of Medical Sciences*, 44(2), pp.87-98. DOI: 10.30476/ijms.2019.44521.

Oh, J.W., 2018. The formation of pollen. In: Oh, J.W. (ed.) *Pollen Allergy in A Changing World: A Guide to Scientific Understanding and Clinical Practice*. Springer Nature, pp.9-19.

Oh, J.W., 2022. Pollen allergy in a changing planetary environment. *Allergy, Asthma & Immunology Research*, 14(2), pp.168-181. DOI: 10.4168/aair.2022.14.2.168.

Sedghy, F., Varasteh, A.R., Sankian, M. and Moghadam, M., 2018. Interaction between air pollutants and pollen grains: The role on the rising trend in allergy. *Reports of Biochemistry and Molecular Biology*, 6(2), pp.219-224.

Shea, K.M., Truckner, R.T., Weber, R.W. and Peden, D.B., 2008. Climate change and allergic disease. *Journal of Allergy and Clinical Immunology*, 122(3), pp.443-453. DOI: 10.1016/j.jaci.2008.06.032.

Stewart, G.A., Richardson, J.P., Zhang, J. and Robinson, C., 2009. The structure and function of allergens. In: Middleton's *Allergy: Principles and Practice*, pp.569-608. DOI: 10.1016/B978-323-08593-9.00027-9.

Pawankar, R., Canonica, G.W., Holgate, S.T., Lockey, R.F. and Blaiss, M., 2013. White Book on Allergy. *World Allergy Organization*, pp.95-100.

Taia, W.K., 2020. Pollen Allergens of some Road Trees, Shrubs and Herbs in Alexandria, Egypt. *Journal of Biomedicine and Science*, 1(5), pp.187-190. DOI: 10.38125/OAJBS.000143.

Taia, W.K. and Bassiouni, E.M., 2022. Airborne Allergenic Pollen Grains in Alexandria City, Egypt. *Acta Scientific Microbiology*, 5(6), pp.102-109. DOI: 10.31080/ASMI.2022.05.1088.

Taia, W.K. and Zayed, A.H., 2021. Road tree pollen grain contents and effect on the immune system. *Quantum Journal of Medical and Health Sciences*, 1(4), pp.34-50.

Thakur, N. and Sharma, S., 2018. Allergies, Pollen grain, Human health and Factors responsible: A Review. *International Journal of Research*, 7(4), pp.1118-1124.

Walker, J.W. and Doyle, J.A., 1976. The basis of Angiosperm phylogeny: Palynology. *Annals of the Missouri Botanical Garden*, 62, pp.666-723.

Zhang, Y., Bielory, L. and Georgopoulos, P.G., 2014. Climate change effect on Betula (birch) and Quercus (oak) pollen seasons in the United States. *International Journal of Biometeorology*, 58(5), pp.909-919. DOI: 10.1007/s00484-013-0674-7.

Isolation, Identification, and Characterization of Putative Dye-Degrading Bacteria from Polluted Soil: Bioremediation Investigations

M. M. Sahila[1], M. Shonima Govindan[2], N. K. Shainy[3]† , P. Nubla[3] and M. Kulandhaivel[4]†

[1]Department of Bioinformatics, SAFI Institute of Advanced Study, Vazhayur East, Malappuram District, Kerala, India
[2]Department of Biochemistry, SAFI Institute of Advanced Study, Vazhayur East, Malappuram District, Kerala, India
[3]Department of Microbiology, SAFI Institute of Advanced Study, Vazhayur East, Malappuram District, Kerala, India
[4]Department of Microbiology, Karpagam Academy of Higher Education, Coimbatore, Tamil Nadu, India
†Corresponding author: N. K. Shainy; shain.sias@siasindia.org

Citation for the Paper:

Sahila, M. M., Govindan, M. S., Shainy, N. K., Nubla, P. and Kulandhaivel, M., 2025. Isolation, identification, and characterization of putative dye-degrading bacteria from polluted soil: Bioremediation investigations. *Nature Environment and Pollution Technology*, 24(1), B4229. https://doi.org/10.46488/NEPT.2025.v24i01.B4229.

Note: From year 2025, the journal uses Article ID instead of page numbers in citation of the published articles.

ABSTRACT

The residual dye within the soil from the synthetic dye manufacturing and fabric industries is a global state of affairs. The discharge consists of an excessive content of pigments and other components, creating complicated structures. It leads to damage to the soil structure and its fertility. Amid existing amputation methods, microbial remediation takes significant consideration owing to its subordinate charge, sophisticated proficiency, and fewer influences on the milieu. The current study was premeditated for the seclusion and portrayal of azo dye- dye-decolorizing bacteria, which is a criterion for emerging a microorganism-facilitated treatment of adulterating dyes. In this present investigation, twenty sorts of bacteria that were talented to decolorize seven kinds of azo dyes (Crystal Violet, Methylene Blue, Safranine, Congo Red, Methyl Orange, Malachite Green, and Carbol Fuchsin) were isolated from dye-polluted soil from the dying industry near the railway station; in Calicut. Based on 16S rDNA scrutiny, the most resourceful decolourizing bacteria for these azo dyes was identified as *Priestia megaterium* strain *NRBC 15308*. After characterization, *Priestia megaterium* was found to be optimally nurtured at 35°C, on a pH of 7, with a 1.5% glucose concentration in a minimal salt medium. 100% decolorization of a 6% dye solution was found at optimal conditions by *Priestia megaterium*. *Priestia megaterium* can decolorize cotton and gauze suspended in the dye solution in 24 hours. Bioremediation studies with the isolate proved that the inhibition effect of the dye solution on seed germination could be removed by the application of *Prestia megaterium*. The isolation of *Priestia megaterium* strain NRBC 15308 as a dye-degrading bacterium holds immense promise for remediating dye-contaminated soil.

INTRODUCTION

Soil performs a vital role in the environment. complex composition of inorganic factors (minerals) derived from disintegrated rocks, humus, water, and so on. Conjointly have an impact on the homes of the soil. The same old American Society for Checking Out and Substances (ASTM) model of the Unified Soil category device has categorized soil on the premise of grain size and texture in clay, gravel, organic clay, natural slit, peat, sand, and silt (ASTM 2017). The clay fraction has an excessive floor area and holds many chemical and biological properties of arable soil. While sand and silt fractions ordinarily manage the bodily person, In contrast to minerals, the soil consists especially of number one (chemically unaltered) and secondary (chemically altered) rocks, silicates and non-silicates, and crystalline and non-crystalline minerals (Schulze 2002). Likewise, Kumar et al. (2024) argue biotechnological advancements are essentially dangerous to the environment because they have the potential to reduce metal pollution. Pollutants in the environment can be efficiently removed using bioremediation. Both native and introduced species can thrive in a microorganism-friendly environment.

Alongside this, soils provide anchorage to roots, clench water, and provide nutrients. As cliché goes, "We build on the soil as well as with it and in it." The attention to heterogeneous materials varies due to many factors, which include metals, chemical compounds (monomers, solvents, reactive initiators, dyes, and pigments) leaching from municipal and chemical industries, unintentional spillage, and underground leakage that cause soil pollutants (Calacea et al. 2005). Those troubles are of primary concern as the contaminated websites are considerably expanding and growing to be appealing. Inside America, more than 40,000 websites have been determined to be contaminated with the above contaminants, in accordance with a document by the Environmental Safety Corporation (EPA) (Sharma & Pandey 2014, Zhao et al. 2016).

The removal of contaminants from soil depends on the complicated interaction of physical, chemical, and organic factors within the surroundings. The bioremediation era is a powerful approach that utilizes organisms to neutralize pollution (Baocheng et al. 2008). The bioremediation procedure of dye remedy from infected soil could be very powerful and can be called a sustainable method. It's a low-budget and effective treatment manner. The consumption of the strength all through the remedy of dye-containing soil is very low. Remedy of carcinogenic dye may also be very beneficial by way of the usage of microbes, as microbes digested the level of carcinogenicity of the dye. Yadav et al. (2021) confirmed that laccase is responsible for lessening the level of dye carcinogenicity. The authors used *Allium cepa* to check the toxicity and observed that laccase reduced the toxicity of the dye.

Microbial degradation of hydrophobic compounds takes place because of their shape, the availability of microorganisms, and the physico-chemical situations that affect the metabolic competence of the microorganisms (Heng et al. 2008). It consists of various good-sized parameters, which include pH, water, aeration repute (redox ability), presence of oxygen, vitamins, and temperature. Biodegradation of organic contaminants can be performed as it should be, but in keeping with some authors, microorganisms and their ecology need to be fully understood. Holden et al. (1997) cautioned against deciding the elements regulating the preferred metabolic pathway and the distribution of degrading microbial groups relative to pollutants.

A lot of bodily and chemical treatment techniques, together with oxidation, reduction, adsorption, chemical precipitation and flocculation, electrochemical remedy, and ion-pair extraction, are used to do away with dyes from wastewater effluents (Fan et al. 2009). Those strategies are attractive due to their performance; however, they are complex and steeply priced (Robinson et al. 2001). On the other hand, biological techniques have obtained revolutionary attention because of their fee, effectiveness, capability to produce much less sludge, and environmental harmlessness. Those procedures can convert this complex natural pollution into water, carbon dioxide, and inorganic salts (Daneshvar et al. 2007). A huge variety of microorganisms can decolorize or maybe completely mineralize an extensive variety of dyes, along with microorganisms (Dave & Dave 2008), fungi, and algae (Ghanem et al. 2011, Ramya et al. 2010). The most promising microorganisms for wastewater remedy are the ones remoted from websites infected with dyes (Indigenous) due to the fact they've adapted to survive in negative situations (Dave & Dave 2008).

A study carried out with the sample dye-infected water showed ninety-five% degradation of all dyes by *Bacillus megaterium*, and then they concluded that *Bacillus megaterium* can be used for the treatment of the dye-infected soil and water (Lekha & Nair 2017).

Based totally on laboratory effects, efforts have to then be made to scale up and apply bacterial decolorization strategies in real industrial effluents. In addition, with the trendy advances in genomics and proteomics, there's a possibility to improve the overall performance of bacterial or enzymatic remedies for textile wastewater. With all the advantageous study findings and ongoing tendencies, microbiological treatment is hoped to be essential in the elimination of dyes and poisonous chemical compounds in fabric wastewater. In addition, the sample from textile wastewater effluent was determined to contain *Bacillus megaterium* KY848339.1, a bacterial stress that should remove ninety-one percent of AR377 azo dye at the concentration of 500 mg.L^{-1} within 24 h (Tahir et al. 2021). From estuarine sediments (Velar Estuary, Porto novo, Tamil Nadu, India), isolate *Bacillus megaterium* PNS15 confirmed an appreciable synthesis of dye-degrading enzymes (azo reductase and laccase). Sivasubramani et al. (2021) selected the isolate that changed into *Bacillus megaterium* and confirmed maximum decolorization of turquoise blue dye within forty-eight hours at pH 7.00. The isolated subculture can decolorize turquoise blue dye awareness by as much as 5 mg in herbal conditions. The remote pressure is even able to degrade a huge variety of dyes. Similarly, *Bacillus megaterium* species may be carried out and examined at large-scale degradation of this dye (Joshi et al 2013). The present investigation aims to isolate and identify an indigenous bacterial strain from dye enterprise effluent that can degrade diverse azo dyes. Compare and optimize the biodegradation functionality of such traces and their application in bioremediation.

MATERIALS AND METHODS

Collection of Soil Samples

The sample was collected from soil contaminated with dyes from a dying industry near a railway station in Calicut, Kerala (Fig. 1). The soil sample is highly polluted with dye and other chemicals used in the dying industry. The soil sample had an alkali pH of about 9.5. The soil was dark in color. The soil was air-dried to remove excess moisture, and the samples were minced into a fine powder via a grout and pounder and used for study.

Preparation of an Azo dye Solution

1% standard solutions are prepared by dissolving 1 g of a piece of powder dye into 100 mL of autoclaved purified water, followed by percolation. Table 1 shows the composition of azo dye.

Selective Media Used for the Study

Minimal salt agar: Prepare MS medium supplemented with a 1% azo dye solution for primary screening studies.

Preliminary screening: The screening methods were based on the modified methodology of Sriram et al. (2013). The minimal salt agar prepared was inoculated with a serially diluted soil sample with a 1% dye solution for preliminary screening. The colonies developed on the plates were subcultures and used for further screening.

Fig. 1: Soil sample used for the study.

Table. 1: Composition of Azo Dye.

Crystal Violet	1 mL
Methylene Blue	1 mL
Safranine	1 mL
Congo Red	1 mL
Methyl Orange	1 mL
Malachite Green	1 mL
Carbol fuchsin	1 mL

Secondary screening: For each subsequent acclimatization step, MSA plates were prepared with incremental increases in dye concentration (e.g., 2%, 3%, 4%, 5%, and 6%), and the colonies isolated in the initial screening were inoculated into these plates and incubated at 37°C. The organism accomplished the highest concentration of dye solution, which was used for further studies (Sriram et al. 2013)

Identification of Selected Bacterial Strains (Afrin et al. 2021) (Bergey's Manual)

The isolated bacterial culture was enhanced in the nutrient broth medium. Later, the 24-hour streaking plate method was done through nutrient agar media; therefore, sole and untainted colonies were electrified, which meant forced entails. These microbial strains were identified through morphologic and gram-staining physical appearance, biochemical, and molecular credentials classification.

Morphological and Biochemical Classification

The quarantines were identified based on morphological studies and biochemical characterization. Bergey's manual was rummage-sale as a reference to identify the isolates. Microscopic features were recorded for all colonies: color, size, and shape, and then further staining was done. Isolates were analyzed for motility test by hanging drop technique, oxidase, catalase, indole, MR-VP, citrate utilization, and Urease test (Garrity et al. 2006)

Molecular Characterization

The complete identification of the isolate was done according to the method suggested by Saitou and Nei (1987). The genome of the isolate was isolated, amplified, and analyzed.

Isolation of Genomic DNA from an Isolated Culture and PCR Amplification

Isolation of DNA was done by using the Hi Pur ATM Bacterial Genomic DNA Purification Kit (MB505, Himedia). The polymerase chain reaction cast off to the 16S rDNA sequencing with forward primer: 5'GAGTTTGATCCTGGCTCA 3' and reverse primer: 5'ACGGCTAACTTGTTACGACT 3'were purchased from Eurofins, Bangalore. The PCR was performed with the following modification: the reactions were run with 10 µL of Master Mix (Emerald Amp GT PCR, 2X premix), 0.2µ M forward and reverse primers, DNA <500ng, and molecular biology grade water. We performed the amplification via the ensuing cycling conditions: 98°C for 30 s, followed by 30 cycles of 98°C for 10 s and 55-60°C for 30 seconds, then 72°C for 1 min, and a final extension at 72°C for 10 min The amplified PCR products were visually proven under ultraviolet light via a 1% agarose gel stained

with ethidium bromide (EtBr). The amplified products were succumbed for sequencing through both forward and reverse primers at Macrogen, Inc.

Phylogenetic Tree Construction

The PCR product is then subjected to a cleanup procedure, followed by sequencing using 27F and 1492R worldwide primers. Sequencing reactions were executed with an ABI PRISM® BigDyeTM Terminator Cycle Sequencing Kit with AmpliTaq® DNA polymerase (FS enzyme) (Applied Biosystems). The sequencing file remained open in Snap Gene Viewer, and the raw data was checked for the length of the quality and read. The sequence is then blasted using the BLASTn tool to identify the sequence of the organism to which the data is aligned with maximum score and coverage. A phylogenetic tree was constructed using MEGA 11.0.13 version software with the neighbor-joining hood method.

Dye Decolorization Assay

Minimal salt broth medium amended with 2% dye solution was inoculated with microbial quarantine (1% v/v) and incubated at 37°C under a shuddering condition. Samples were withdrawn after 24 h and analyzed for growth and decolorization. Decolorization was determined by measuring the absorption spectra at the lambda max (λ max) of the dye (410 nm) for the clear supernatant and growth using the absorbance of the culture supernatant (640 nm) using a spectrophotometer. A medium containing dye without the inoculum was considered a control. The color elimination efficacy was specified as the percentage ratio built on the ensuing equation. Respectively, testing was executed in triplicate, and the mean values were documented.

Percent decolorization = (initial absorbance – Final absorbance value) ×100/Initial absorbance

Optimization Studies

All the activities of the organisms will be at their maximum in their optimal conditions. So, the optimization of environmental and nutrient conditions like media composition, pH, temperature, and concentration of glucose as a co-substrate was conducted to ensure the maximum enhancement of the decolorization property of the organism.

Optimization of Media

Minimal Salt Broth, Minimal Mineral Broth, and Bushnell Haas Broth were selected for the study, and 50 mL of each medium was inoculated in one ml culture of the quarantine and incubated for 24 hours at 37°C. Media that showed maximum color removal efficiency was used for further

degradation studies. Individual trials were executed in triplicate, and the mean values were verified.

Optimization of pH, Temperature Glucose, and Salinity Levels

Optimization of various parameters like pH (3.5, 4.5, 7, 8.5, 9.5.), temperature (15°C, 25°C, 35°C, 45°C, 55°C), glucose (0, 1%,1.5%, 2%, 2.5%), and salinity levels (1, 3, 5, and 7 % NaCl) for decolorization of azo dye solution was complete with some amendments by Shah (2013) and Prasad and Rao (2013). The enhanced media with 5% (v/v) dye solution was inoculated with a 1% (v/v) microbial isolate and incubated for 24 hours. Uninoculated medium with azo dye solutions was kept back as a control. Respectively, research was accomplished in triplicate, and the mean standards were documented.

Application Studies

The isolated bacterium, after optimization and decolorization assay, was used to analyze the efficiency of color removal from cotton and gauze and also to understand the bioremediation capacity of the organism.

Cotton and Gauze Roll Decolorization Study

Minimal salt broth amended with 5% (v/v) of azo dye solution was inoculated with 1 ml of the isolated bacterium. Cotton roll and Gauze roll, each weighing 2.340 g, were added to the medium in separate flasks and incubated under optimized conditions for 24 h. A control was maintained without adding any organisms to the medium. The color removal efficiency of the organism from the test materials was calculated using the formula along with the growth of the organism in the medium as described above.

Bioremediation Studies (Ajisha et al. 2021)

Seeds used: Okra seeds were collected from the "green leaves" nursery in Vellangallur, Thrissur. For this experiment, we used okra seed due to its fast germination. The procedure was done in aseptic conditions.

Soil used: A red loamy type of soil, which was collected from the SIAS campus in Vazhayur East, was sterilized for three consecutive days to avoid any spore and fungal contamination. The soil pH of 6.1 also ought to have a virtuous aquatic holding capacity.

Germination test in soil: The bushy cell deferment of *Priestia megaterium* cells prepared stood castoff for inoculating the loam. 3 ml of the cell suspension was further added to 60 gm of dirt containing 20% moisture and 6% and 8% dye, engaged in flexible cups, and assorted meticulously to guarantee even dispersal. Seeds were sown immediately,
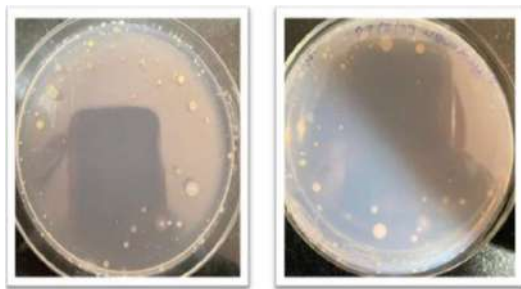
Fig. 2: Primary screening.

separately in five sets with triplicates: set 1 (soil+ seed), set 2 (soil+ seed+ organism), set 3 (soil+ seed+ dye), set 4 (soil+ seed+ dye (6%) + organism), and set 5 (soil+ seed+ dye (6%) + organism).

RESULTS AND DISCUSSION

Screening and Isolation of Azo Dye-Debasing Microorganisms

The serially diluted sample plated on the minimal salt agar with 1% of the dye solution produced different types of colonies after incubation for 24 h. The bacterial colonies were marked as D01 to D20, and the fungal colonies found on the plates were named F01 and F02. The detailed colony morphology of the isolates is given in Table 2. The organisms that could utilize the dyes provided in the medium as a carbon source showed growth in the medium (Fig. 2).

Secondary Screening

When the MS agar plates had an incremental increase in dye concentrations of 2%, 3%, 4%, 5%, and 6%, only one bacterium named D20 could survive. Mahmood et al. (2012) and Karthikeyan & Anbusaravanan (2013) have stated the seclusion and screening of microbes were accomplished by decolorizing several azo dyes since sludge samples collected from sewer water handling places polluted with dyes in the comparable method. Jamee & Siddique (2019) observed that synthetic dye degradation by microbes is facilitated by their oxidase. Prevalently, the azo reductase places the utmost dynamic part in decolorization by breaking down azo bonds. Microbial oxidoreductase enzymes are significant in the squalor of artificial dyes. This energetic metabolism of microorganisms empowers them to exploit multifaceted xenobiotic amalgams of the dyestuff as a substratum. Among the development, they are cracked down to a reduced number

Table 2: The colony morphology of various organisms grown in the MS agar on preliminary screening.

Organism	Shape	Color	Margin	Opacity	Dry/wet	Size
D1	Circular	Yellow	Regular	Opaque, flat	Wet	Medium
D2	Circular	Pinkish white	Irregular	Opaque, flat	Dry	Small
D3	Circular	Light yellow	Regular	Opaque, mucoid	Dry	Small
D4	Circular	Off white	Irregular	Opaque	Wet	Small
D5	Circular	Cream	Regular	Opaque	Wet	Medium
D6	Circular	Light white	Regular	Opaque	Wet	Medium
D7	No shape	Pinkish white	Irregular	Opaque	Dry	Small
D8	Circular	Yellow	Regular	Opaque	Wet	Large
D9	Circular	Yellow	Regular	Opaque	Dry	Medium
D10	Circular	Yellow	Regular	Opaque	Wet	Small
D11	Circular	Pinkish white	Regular	Opaque	Wet	Small
D12	Circular	White	Regular	Opaque	Wet	Large
D13	Circular	Pinkish white	Regular	Opaque	Wet	Small
D14	Circular	White	Regular	Opaque	Dry	Medium
D15	Circular	Transparent	Regular	Transparent	Wet	Medium
D16	Circular	White	Irregular	Opaque	Dry	Small
D17	Circular	White	Regular	Opaque	Wet	Small
D18	Circular	White	Regular	Opaque	Dry	Medium
D19	Circular	Pink	Irregular	Opaque	Wet	Medium
D20	No shape	Milky white,	Irregular	Opaque	Wet	Large
F01	A	White	Fungal	Colony	-	-
F02	A	Black	Fungal	Colony	-	-

Fig. 3: Secondary screening.

of intricate metabolites. A benefit of procuring microbes from authentic places of effluent removal is that they are more likely to partake in the enzymes stimulated, which enable the putrefaction of dyes. Fig. 3.

Identification of the Selected Bacterial Strain

The morphological and biochemical characterization of isolated bacteria was studied. Findings are tabulated in Table 3 and Fig. 4.

Molecular Identification

D20 genomic DNA was isolated and verified (Fig. 5); the template (DNA) was used to amplify the 16SrRNA. DNA sequence by PCR (Fig. 6) The PCR product was then

Table. 3: Biochemical characteristics (Positive+, Negative-).

S. No.	Characters	Result
1.	Gram staining	Gram positive diplobacillus
2.	Morphology	Milky white, irregular, mucoid, raised
3.	Motility	motile
4.	Spore	Spore forming
5.	Indole	Negative
6.	Methyl Red	Negative
7.	Voges-Proskauer	Positive
8.	Citrate test	Positive
9.	Catalase test	Positive
10.	Oxidase test	Negative
11.	Urease	Positive

Fig. 4: Gram-positive diplobacillus.

subjected to PCR clean-up followed by sequencing. The nucleotide sequence obtained after sequencing was blasted using the BLASTn program. The bacteria were identified as *Priestia megaterium NRBC* 15308=*ATCC* 14581. Sanger sequencing, also known as the Hawser termination technique, is used to determine the nucleotide sequence of DNA. Coli DNA polymerase l (pol l) or its proteolytic (Klenow) fragment was chosen by Dr. Sanger for his dideoxy sequencing chemistry (Sanger et al. 1977). The rudimentary local alignment search tool (BLAST) finds regions of local resemblance among sequences. The program likens nucleotide or protein sequences to sequence databases and computes the statistical implications.

Phylogenetic Tree

Phylogenetic investigation delivers an in-depth understanding of how species progress through genetic vicissitudes (Fig. 7). Through phylogenetics, experts can appraise the pathway that links a current organism with inherited derivation, as well as forecast the heritable discrepancy that might arise in the future. Subsequently, in molecular identification, the isolate was identified as *Priestia megaterium* (NRBC 15308=ATCC 14581, Fig.7). Have 1.5 kb of molecular weight, wi*th* 99% identities. Maximum score: 1376, E-value: 0.0, accession number: NR1126361. The research was done by Afrin et al. (2021) and found that
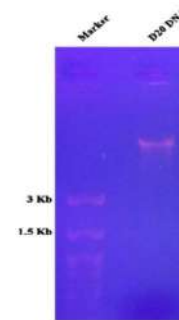
Fig. 5: DNA isolated from D20 run in 0.8% agarose gel.
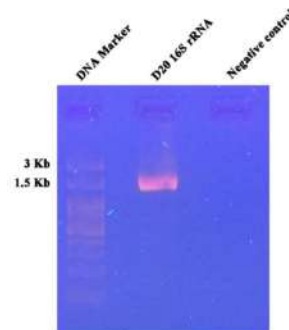
Fig. 6: PCR amplification of 16S rRNA of D20.
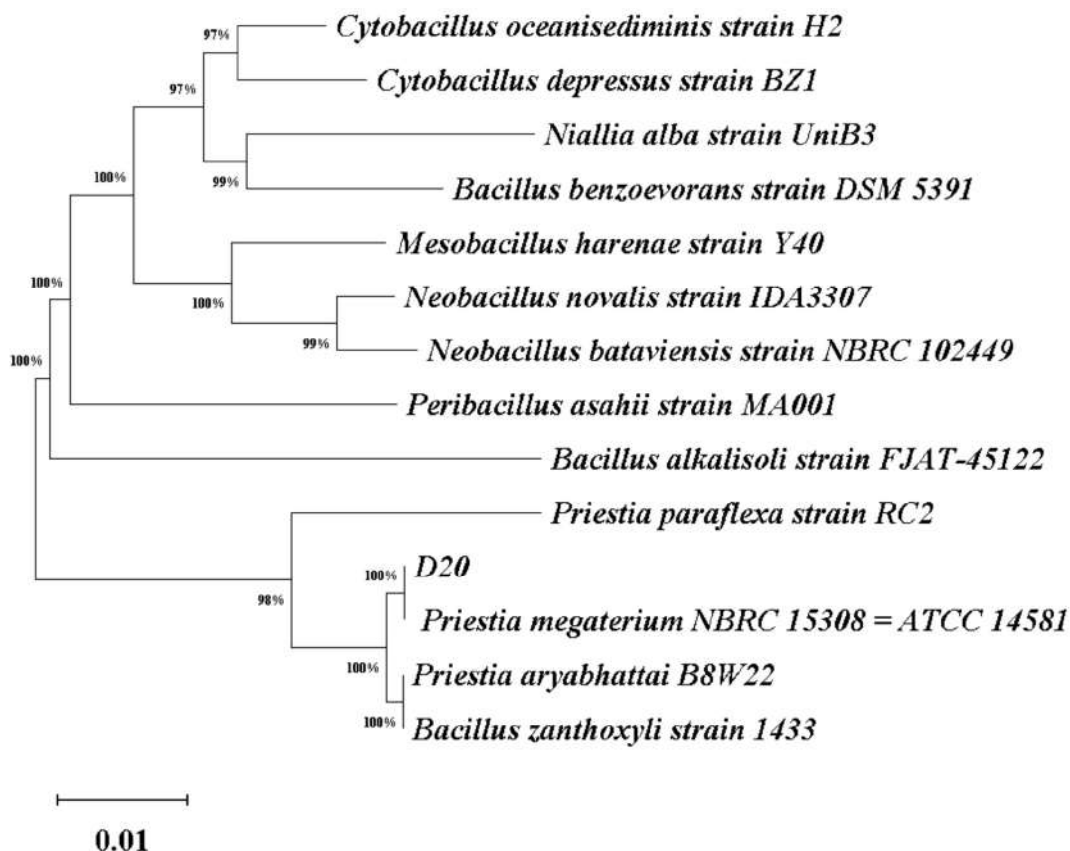
Fig. 7: Phylogenetic placement of 16S rRNA sequences.

similar organisms can degrade maximum dye: *Enterococcus faecium* and two strains of *Pseudomonas aeruginosa* after molecular identification. The maximum decolorization occurred in the range of 37ºC under aerobic conditions. Similarly, the research done by Sulthana (2017) identified three important bacterial species, *Enterococcus faecium*, *Bacillus pumilis*, and *Bacillus thuringiensis*, through a biological identification system. A soil sample was collected from local textile effluent. Another research (Fareed et al. 2022) found that the maximum decolorization by the bacteria was identified as *Bacillus cereus* strain *ROC*. The soil sample was collected from contaminated industrial areas. The research was done by Fareed et al. (2022), who identified *Bacillus cereus ROC* as being highly proficient in degrading dyes with a decolorization rate of 83%.

Dye Decolorization Assay

The test done in triplicate showed an average of 82.4 % degradation when provided with 2% dye Table 4.

Optimization of Media

Media optimization studies with different media like Minimal Salt Broth, Minimal Mineral Broth, and Bushnell Haas Broth proved that Minimal salt agar is the most efficient media for maximum decolorization of dye. One flask from each is considered a control. Inoculated 100 µl of inoculum into 3 broths. I observed the color change after overnight incubation. The decolorization of dye by *Priestia megaterium* in the tested media is provided in Fig. 8. Observed the maximum decolorization efficiency (100%) in minimal salt broth compared to minimal mineral broth and Bushnell Haas broth Table 5. The organism could complete decolorization of 5% of the azo dye solution; normally, *Priestia megaterium* is grown in minimal media. Radia Jamee & Romana Siddique

Table 4: Decolourisation rate of Decolourisation rate of 2% of azo dye in the minimal salt medium at OD 410nm.

Conditions	Control	MS Broth (1)	MS Broth (2)	MS Broth(3)
Before inoculation	0.00	0.00	0.00	
Initial absorbance	0.00	0.17	0.16	0.17
Final absorbance	0.00	0.03	0.02	0.03
Percentage of decolorisation	0	82.4	87.5	82.4

Table 5: Optimisation of media OD at 410 nm.

Conditions	Control	Minimal Salt Broth	Minimal Mineral Broth	Bushnell Haas Broth
Before inoculation	0.00	0.00	0.00	0.00
Initial absorbance	0.00	1.27	1.22	1.25
Final absorbance	0.00	0.00	0.17	0.12
% of decolorisation	0	100	86	90.4
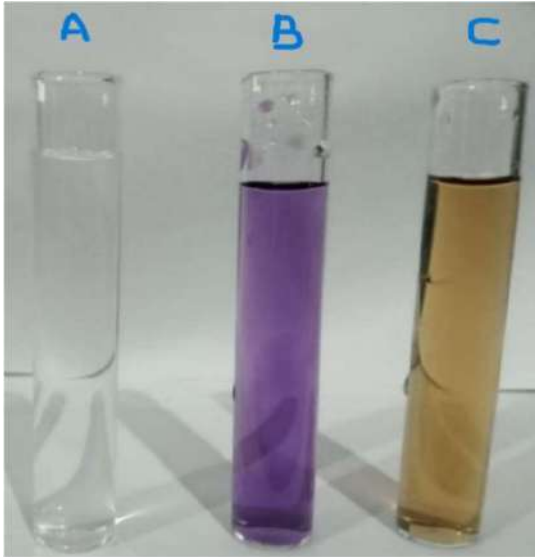
Fig. 8: Supernatant of the decolorized medium after 24 hours
A- Minimal Salt Broth, B- Bushnell Haas Broth, C- Minimal
Mineral Broth.

(2019) observed that the filth of artificial dyes by microbes is eased by their oxidases. In the instance of azo dyes, azo reductase plays the most vigorous part in decolorization by flouting down azo bonds. Approximately microbes have been deliberately to worsen dyes below the aerophilic state. The current study shows its maximum decolorization was 100% (Table 5).

Optimization of pH, Temperature and Glucose

The selected D20 organism has optimal growth conditions like pH, temperature, and glucose. Here, the decolorization amount is higher at the ideal pH and decreases with further acidic or alkaline pH; the optimal pH is between 7 and 8.5. Besides, it remains experiential that a cumulative temperature of 35°C - 45°C raises the decolorization percentage; further cumulative temperature might decrease the decolorization rate.

Optimization of pH

The research revealed that the ratio of azo dye degradation had improved with the modification of pH in the broth. The higher dilapidation remained pragmatic at pH 7. The optimal decolorization was at pH 7 (100%), even though the organism could decolorize the dye at an alkaline pH of 9.5 (92%). But at an acidic pH, the organism gets less reactive. The azo dye had an alkaline pH so that *Priestia megaterium* could degrade the azo dyes at this pH level. Several researchers have evidenced that biosorption developments via microorganisms remained highly pH-dependent (Aksu & Tezer 2005, Kumar et al. 2006). According to popular alternative research done by Wang et al. (2009), the *Citrobacter* sp. CK3 must have accomplished the finest decolorization of the sensitive red 180 (96%) at pH 6.0-7.0. According to Bishnoi et al. (2024), phenanthrene degradation increased with an increase in pH from 5.0 to 7.0 and again decreased with a further increase in pH from 7.0 to 9.0. Maximum degradation of PAH was observed at pH. In the instance of red azo dye decolorization by *Aspergillus niger*, it might be detected that the exclusion percent upsurge with the rise of pH and the extreme decolorization competence stood touched (99.69) at pH 9.0 (Mahmoud et al. 2017). In my study, the azo dye solution was completely decolorized (100%) by *Priestia megaterium* at pH 7 (Table 6).

Optimization of temperature

The maximum (100%) of azo dye decolorization was observed at 35ºC as represented in Table. 7: Microbes need an optimal temperature for development. Meanwhile, dye decolorization is a metabolic progression; the alteration in temperature causes a modification from the ideal result into a deterioration of dye decolorization. The dying industries had different temperature zones, and sometimes increased temperatures, and the organism *Priestia megaterium* could decolorize 84.4% of azo dyes at a temperature of 45ºC. If an increase in temperature occurs, the treatment should be conducted at the optimum temperature. A comparable outcome of temperature was achieved by *Bacillus subtilis* in crystal violet dye filth (Kochher & Kumar 2011). Lalnunhlimi & Krishnaswamy (2016) described that bacterial cultures exhibit optimum dilapidation effectiveness through temperature ranges of 30-35ºC. Another researcher observed that the optimum temperature for the decolorization of

Table 6: The effect of pH on azo dye degradation by *Priestia megaterium*.

MS Broth	pH	Initial absorbance	Final absorbance	Percentage of decolorisation
	3.5	1.24	0.92	25.8
	4.5	1.22	0.53	56.5
	7	1.26	0.00	100
	8.5	1.23	0.04	96.7
	9.5	1.22	0.10	92

Table 7: The effect of temperature on azo dye degradation is *Priestia megaterium*.

MS Broth	Temperature °C	Initial absorbance	Final absorbance	Percentage of decolorisation
	15	1.24	0.61	50.8
	25	1.23	0.22	82.1
	35	1.24	0.00	100
	45	1.22	0.19	84.4
	55	1.24	1.20	3.2

Table 8: The effect of glucose concentration on azo dye degradation by *Priestia megaterium*.

MS Broth	Glucose Concentration	Initial absorbance	Final absorbance	Percentage of decolorisation
	1	1.24	0.56	54.8
	1.5	1.22	0.29	76.2
	2	1.23	0.03	97.6
	2.5	1.24	0.80	30.6
	3	1.24	0.89	28.2

malachite green was achieved via an innovative enzyme from *Bacillus cereus* Wanyonyi et al. (2017). Similarly, in Bishnoi et al. (2024), the optimal temperature for the degradation of phenanthrene was observed at 30°C, whereas biodegradation efficiency decreased as temperature increased or decreased.

Optimization of Glucose Concentration

There is an optimal pH for the organism. D20 is between 7 and 8.5; the optimum temperature for D20 is between 35 and 45, and the optimum glucose concentration is between 0.5 and 1. The maximum degradation of azo dye was observed at 0.15 a concentration Table 8. At this glucose concentration, the maximum decolorization was about 97.6%.

Application of Studies

Cotton roll and gauze roll decolorization: Cotton and gauze rolls in minimal salt broth amended with 5% dye absorbed the color in one hour, changing their color to deep purple. The medium inoculated with *Priestia megaterium* for 24 hs showed decolorization of cotton and gauze rolls. Another flask with cotton and gauze rolls without adding *Priestia megaterium* was kept as a control for the study (Fig. 9).

From the experiment, it was observed that the cotton roll was more decolorized than the gauze roll. Gauze roll is the same as cotton stuff. This experiment showed that the *Priestia megaterium* can decolorize the dye in cloths. Similar works done by Thirupathi et al. (2021) also found similar results, where nine ligninolytic microbial strains were isolated from loam samples. Entirely the strains were talented enough to decolorize a blend of azo dyes (DR 23, DB 15, and DY 12). Tiercelatent strains with extreme dye decolorizing proficiency were designated and identified by 16S rRNA gene sequencing studies. The ligninolytic microbial consortium WGC-D was found to be extra-operative,
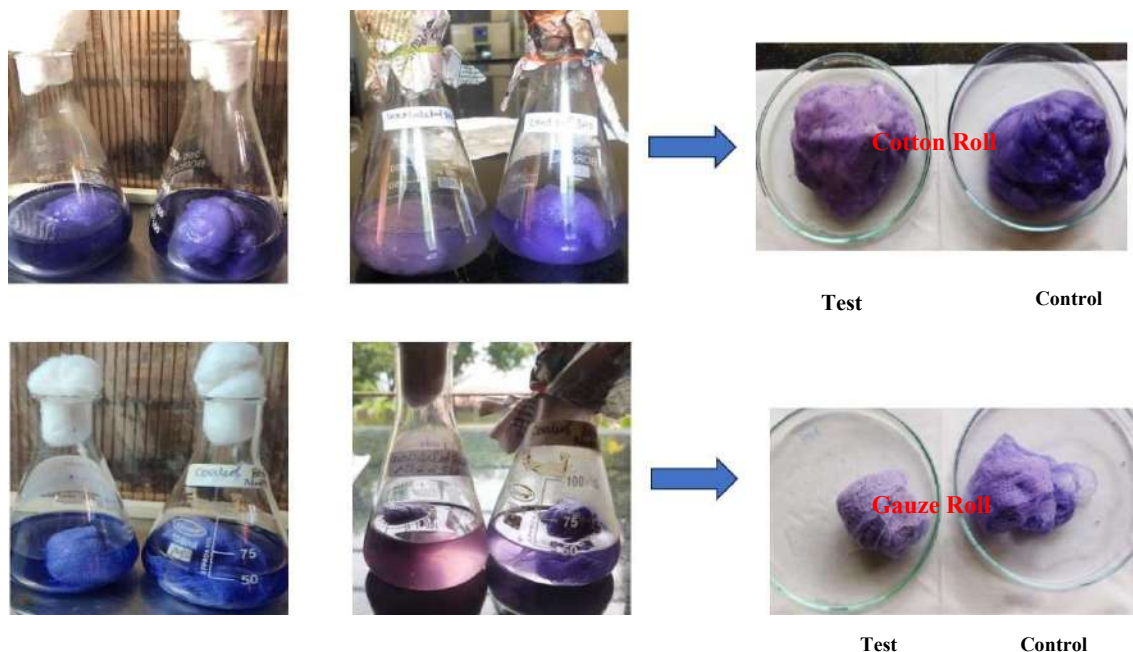
Fig. 9: Cotton roll and gauze roll decolourization.

Table 9: Cotton Roll and Gauze Roll Decolourization.

Minimal salt broth with 5% of dye	Cotton Roll Decolourization OD 410 nm	Gauze Roll Decolourization OD 410 nm
Initial Absorbance	1.25	1.25
Final Absorbance	0.09	0.10
% of decolorization	92.8	92

which decolorized up to 75% of the dye represented in Table. 9.

Bioremediation Studies

The 15 pots planted with 10 okra seeds each were keenly observed for germination for a period of one week. Each day's result was recorded, and the number of seeds that sprouted was checked. The result emphasized the possibility of *Priestia megaterium* as a growth-promoting bacteria.

The results from the study indicate that *Priestia megaterium* has growth-promoting activity, which is helping in the seed germination process. The excellent growth in the presence of *Priestia megaterium* in the soil with dye indicates the presence of nutrients, which can be intermediate

metabolites produced by the bacteria, as represented in Fig. 10.

Similar works were conducted by Ebency et al. (2013), who germinated different plants, such as green gram, kidney beans, and fenugreek, with *Bacillus* sp. Nope, phytotoxicity was pragmatic for the attentiveness of the dye castoff in the study. Upright sprouting and shoot, root length of the floras was experiential for both dye and tainted dye unprotected kernels, subsequently likening with control. The isolate from the seepage liberation site exposed latent debasing dyes in quicker proportion with a bid of virtuous seed sprouting proficiency.

Set-1: Soil + Seed = Seeds showed normal growth.

Set-2: Soil + Seed + Organism = A healthier growth than normal growth in the presence of *Priestia megaterium* was observed.

Set-3: Soil + Seed+ Dye (6%) = no seed germination even after 6 days.

Set-4: Soil + Seed + Dye (6%) + Organism = All the seeds were germinated and showed maximum growth in terms of shoot length

Set-5: Soil + Seed + Dye (8%) + Organism = seed

Fig. 10: Germination studies for bioremediation.

germination was observed for 7-8 seeds, and the seedlings produced were in good health

CONCLUSIONS

Azo dyes are now crucial in a variety of businesses, particularly as consumers' preferences are heavily influenced by color. However, as azo dye use has increased, several health and environmental issues have surfaced, some of which are brought on by azo dyes and their metabolites. Bioremediation should be utilized since contemporary civilizations strive for environmentally friendly solutions. Microorganisms have demonstrated adaptable performance not only in the biomedical field but also in the application areas of the environment. There is a lot of untapped potential in microorganisms, and numerous enzymes from various microbes need to be further examined. Also important to consider is how well these microbes can tolerate a variety of xenobiotics. Over the years, modern technology has made enormous strides.

In conclusion, the isolation, identification, and partial characterization of *Priestia megaterium* strain NRBC 15308 as a potential dye-degrading bacterium provides valuable insights into sustainable environmental practices. The utilization of this bacterium in bioremediation efforts holds promise for effectively addressing dye contamination in soil while promoting eco-friendly solutions for a cleaner and healthier environment.

Priestia megaterium strain NRBC 15308 might be castoff as an auspicious for real-world bids in decolorizing and concurrently lessening the harmfulness of textile dyes. The metabolites molded after the decolorization of dye are prerequisites to be analyzed; therefore, they can be used as castoffs as admirable bio-agents for the biodegradation of textile dyes. As we move towards a more sustainable future, such studies play a crucial role in fostering responsible environmental stewardship.

ACKNOWLEDGMENT

REFERENCES

Afrin, S., Rahman Shuvo, H., Sultana, B., Islam, F., Abu Rus'd, A., Begum, S. and Hossain, M.N., 2021. The degradation of textile industry dyes using the effective bacterial consortium. *Journal of Heliyon*, 7, e08102.

Ajisha, M., Shaima, T.C., Soumya, V., Menon, A. and Mohammad Kunhi, A., 2021. Bioaugmentation of soil with *Pseudomonas monteilii* strain eliminates inhibition of okra (*Abelmoschus esculentus*) seed germination by m-cresol. *Journal of Current Microbiology*, 78, pp.1892–1902.

Aksu, Z. and Tezer, S., 2005. Biosorption of reactive dyes on the green alga *Chlorella vulgaris*. *Process Biochemistry*, 40, pp.1347-1361.

ASTM, 2017. Standard practice for classification of soils for engineering purposes (unified soil classification system). *Annual Book of ASTM Standards*, 4(8), pp.249–260. D18.07.

Bishnoi, K., Rani, P., Karwal, M. and Bishnoi, N.R., 2024. PAHs biodegradation by locally isolated *Phanerochaete chrysosporium* and *Penicillium citrinum* from liquid and spiked soil. *Nature Environment & Pollution Technology*, 23(2), pp.785-795.

Calacea, N., Campisib, T., Iacondinib, A., Leonia, M., Petronioa, B.M. and Pietroletti, M., 2005. Metal-contaminated soil remediation by means of paper mill sludges addition: chemical and ecotoxicological evaluation. *Environmental Pollution*, 136(3), pp.485–492.

Daneshvar, N., Khataee, A.R., Rasoulifard, M.H. and Pourhassan, M., 2007. Biodegradation of dye solution containing Malachite Green: Optimization of effective parameters using Taguchi method. *Journal of Hazardous Materials*, 143, pp.214–219.

Dave, S.R. and Dave, H.R., 2008. Isolation and characterization of *Bacillus thuringiensis* for acid red 119 dye decolourisation. *Journal of Bioresource Technology*, 100, pp.249–253.

Ebency, C.I.L., Rajan, S., Murugesan, A.G., Rajesh, R. and Elayarajah, B., 2013. Journal article. *International Journal of Current Microbiology and Applied Sciences*, 2(10), pp.496–505.

Fan, H.J., Huang, S.T., Chung, W.H., Jan, J.L., Lin, W.Y. and Chen, C.C., 2009. Degradation pathways of crystal violet by Fenton and Fenton-like systems: Condition optimization and intermediate separation and identification. *Journal of Hazardous Materials*, 171, pp.1032–1044.

Fareed, A., Zaffar, H., Bilal, M., Hussain, J., Jackson, C. and Naqvi, T.A., 2022. Decolorization of azo dyes by a novel aerobic bacterial strain *Bacillus cereus* strain ROC. *PLoS ONE*, 17(6), e0269559.

Garrity, G., Staley, J.T., Boone, D.R., De Vos, P., Goodfellow, M. and Rainey, F.A., 2006. *Bergey's Manual of Systematic Bacteriology: The Photobacteria*, 2nd ed. Berlin: Springer Science & Business Media.

Ghanem, K.M., Al-Garni, S.M. and Biag, A.K., 2011. Statistical optimization of cultural conditions for decolorization of methylene blue by mono and mixed bacterial culture techniques. *African Journal of Microbiology Research*, 5(15), pp.2187–2197.

Heng, Q.U., Zhou, J., Xuemin, X., Chunli, Z., Zhao, H. and Zhou, X., 2008. Adsorption behavior of Azo Dye CI Acid Red 14 in aqueous solution on surface soils. *Journal of Environmental Science*, 20(6), pp.704–719.

Holden, P.A., Halverson, L.J. and Firestone, M.K., 1997. Water stress effects on toluene biodegradation by *Pseudomonas putida*. *Biodegradation*, 8(3), pp.143–151.

Jamee, R. and Siddique, R., 2019. Biodegradation of synthetic dyes of textile effluent by microorganisms: An environmentally and economically sustainable approach. *European Journal of Immunology*, 9(4), pp.114-118.

Joshi, B., Kabariya, K., Nakrani, S., Khan, A., Parabia, F.M., Doshi, H.V. and Thakur, M.C., 2013. Biodegradation of turquoise blue dye by *Bacillus megaterium* isolated from industrial effluent. *American Journal of Environmental Protection*, 1(2), pp.42-47.

Karthikeyan, S. and Anbusaravanan, N., 2013. Isolation, identification, and characterization of dye-adapted bacteria from textile effluents mixed with sewage released into the River Amaravathy, Karur, Tamil Nadu, India. *IOSR Journal of Environmental Science, Toxicology and Food Technology*, 7(2), pp.51-57

Kochher, S. and Kumar, J., 2011. Microbial decolorization of crystal violet by *Bacillus subtilis*. *Biological Forum - An International Journal*, 3(1), pp.82–86.

Kumar, A., Mukherjee, G. and Gupta, S., 2024. Role of biotechnology and genetic engineering in bioremediation of cadmium pollution. *Nature Environment & Pollution Technology*, 23(2), pp.633-648.

Kumar, R., Ramamurthi, S., Sivanesan, S., Kumar, K.V., Ramamurthi, V.

and Sivanesan, S., 2006. Biosorption of malachite green, a cationic dye, onto *Pithophora* sp., a freshwater alga. *Dyes and Pigments*, 69, pp.102–107.

Lalnunhlimi, S. and Krishnaswamy, V., 2016. Decolorization of azo dyes (Direct Blue 151 and Direct Red 31) by moderately alkaliphilic bacterial consortium. *Brazilian Journal of Microbiology*, 47(1), pp.39-46.

Lekha, K. and Nair, R., 2017. Biodegradation of Azo Dyes Using *Bacillus megaterium* and Its Phytotoxicity Study. *IOSR Journal of Environmental Science, Toxicology and Food Technology*, 11(7), pp.12-20.

Mahmood, R., Sharif, F., Ali, S., Hayyat, M.U. and Akbar Cheema, T., 2012. Isolation of bacterial consortia with probiotic potential from the rumen of tropical calves. *Biologia*, 58(1&2), pp.53–60.

Mahmoud, M.S., Mostafa, M.K., Mohamed, S.A., Sobhy, N.A. and Nasr, M., 2017. Bioremediation of red azo dye from aqueous solutions by *Aspergillus niger* strain isolated from textile wastewater. *Journal of Environmental Chemical Engineering*, 5, pp.547–554.

Prasad, A.A. and Rao, K.B., 2013. Aerobic biodegradation of azo dye by *Bacillus cohnii* MTCC 3616; an obligately alkaliphilic bacterium and toxicity evaluation of metabolites by different bioassay systems. *Applied Microbiology and Biotechnology*, 97, pp.7469–7481.

Ramya, M., Iyappan, S., Manju, A. and Jiffe, J.S., 2010. Biodegradation and decolorization of acid red by Acinetobacter radio resistance. *Journal of Bioremediation and Biodegradation*, 1, pp.105–111.

Robinson, T., McMullan, G., Marchant, R. and Nigam, P., 2001. Remediation of dyes in textile effluent: A critical review on current treatment technologies with a proposed alternative. *Bioresource Technology*, 77, pp.247.

Saitou, N. and Nei, M., 1987. The neighbor-joining method: a new method for reconstructing phylogenetic trees. *Molecular Biology and Evolution*, 4(4), pp.406–425.

Sanger, F., Nicklen, S. and Coulson, A.R., 1977. DNA sequencing with chain-terminating inhibitors. *PMCID*, PMC431765, PMID: 271968.

Schulze, D.G., 2002. An introduction to soil mineralogy. *Soil Mineralogy with Environmental Applications*, 19, pp.1–35.

Shah, M.P., 2013. Microbial degradation of textile dye (Remazol Black B) by *Bacillus spp*. ETL-2012. *Journal of Applied & Environmental Microbiology*, 1, pp.6–11.

Sharma, P. and Pandey, S., 2014. Status of phytoremediation in the world scenario. *International Journal of Environmental Bioremediation and Biodegradation*, 2(4), pp.178–191.

Sivasubramani, K., Ganesh, P., Sivagurunathan, P., Kolanjinathan, K. and Raman, H., 2021. Biodegradation potential of an estuarine bacterium *Bacillus megaterium* PNS 15 against an azo dye, Reactive blue 194. *Journal of Applied Biology and Biotechnology*, 9(4), pp.126-132.

Sriram, N., Reetha, D. and Saranraj, P., 2013. Biological degradation of reactive dye by using bacteria isolated from dye-effluent contaminated soil. *Middle-East Journal of Scientific Research*, 17(12), pp.1695-1700.

Sulthana, B., 2017. Degradation of dyes used in textile industries by bacteria isolated from local textile effluents. Submitted by BRAC University. ID No: 15176007.

Tahir, U., Nawaz, S., Hassan Khan, U. and Yasmin, A., 2021. Assessment of bio decolorization potentials of biofilm-forming bacteria from two different genera for Mordant Black 11 dye. *Bioremediation Journal*, 25(3), pp.252–270.

Thirupathi, K., Rangasamy, K., Ramasamy, M. and Muthu, D., 2021. Evaluation of textile dye degrading potential of ligninolytic bacterial consortia. *Environmental Challenges*, 4, 100078.

Wang, H., Su, J.Q., Zheng, X.W., Tian, Y., Xiong, X.J. and Zheng, T.L., 2009. Bacterial decolorization and degradation of the reactive dye Reactive Red 180 by *Citrobacter* sp. CK3. *International Biodeterioration & Biodegradation*, 63, pp.395–399.

Wanyonyi, W.C., Onyari, J.M., Shiundu, P.M. and Mulaa, F.J., 2017. Biodegradation and detoxification of malachite green dye using novel enzymes from *Bacillus cereus* strain KM201428: Kinetic and metabolite analysis. *Energy Procedia*, 119, pp.38–51.

Yadav, A., Yadav, P., Singh, A.K., Kumar, V., Sonawane, V.C., Markandeya, Bhargava, R.M. and Raj, A., 2021. Decolourisation of textile dye by laccase: process evaluation and assessment of its degradation bioproducts. *Bioresource Technology*, 340, pp.125591.

Zhao, F., Ma, Y., Zhu, Y., Tang, Z. and McGrath, S.P., 2016. Soil contamination in China: current status and mitigation strategies. *Environmental Bioremediation Technologies*, 49(2), pp.750–759.

The Potential of Blue Light as a Disinfection Strategy in Indoor Environments

F. Llinares Pinel[1], M. J. Pozuelo de Felipe[1], D. Uruburu Ferrón[1], D. Baeza Moyano[2], S. Bueno Fernández[2], T. Awad Parada[3,4] and R.A. González Lezcano[5†]

[1]Department Pharmaceutical and Health Sciences, Pharmaceutics and Pharmaceutical Technology, University San Pablo CEU, Campus Montepríncipe, Alcorcón, 28668, Madrid, Spain

[2]Department of Chemistry and Biochemistry University San Pablo CEU, Campus Montepríncipe, Al-corcón, 28668, Madrid, Spain

[3]Department of Mechanical Engineering Technical School of Engineering at ICAI Comillas Pontifical University, Alberto Aguilera 25, 28015, Madrid, Spain

[4]UDIT Universidad de Diseño y Tecnología, Av. Alfonso XIII,97, 28016 Madrid, Spain

[5]Architecture and Design Department. Escuela Politécnica Superior. University San Pablo CEU, Campus Montepríncipe, Alcorcón, 28668, Madrid, Spain

†Corresponding author: R. A. González Lezcano; rgonzalezcano@ceu.es

ABSTRACT

Microbially contaminated objects used in everyday life have been shown to impact human health by harboring infections through direct or indirect contact. For this reason, the development of alternative methods for bacterial elimination that do not lead to resistant microorganisms, large quantities of residues, or human cytotoxicity is warranted. Due to their proven bactericidal power, the use of electromagnetic waves lower than ultraviolet-C radiation would constitute a possible alternative. The main aim of this research was to determine the effect of 462 nm radiation emitted by light-emitting diodes (LEDs) on the most frequent bacteria contaminating everyday objects and surfaces in residential and hospital environments. The rationale behind the selection of this specific frequency within the blue light spectrum, in contrast to previous research exploring the application of higher frequencies, was its safety for individuals' eyes and skin. The findings suggest that the use of low-frequency blue light can be effective in destroying environmental microorganisms stemming from the skin microbiome and mucous membranes, and even fecal bacteria, present in the surfaces of everyday objects such as *inter alia,* mobile phones, remote controls, credit cards, and of which some present high antibiotic resistance.

INTRODUCTION

LED Phototherapy Features

Currently, 80%-90% of the time is spent indoors, especially in homes (Klepeis et al. 2001), in developed countries, as the presence at home ranges from 60% to 90% of the day and 30% of the time is spent sleeping (Borsboom et al. 2016, Hormigos et al. 2018).

Homes, which are the indoor places with the highest exposure, contain the air that is breathed in the majority of the time. According to Wargocki (2016), the indoor atmosphere in a home should promote rest and recovery. However, since poor indoor air quality (IAQ) has detrimental impacts on health, this goal is prevented.

Buildings have become more airtight since the energy crisis of the 1970s, which has caused the emergence of illnesses connected to indoor air quality, such as sick building syndrome (SBS) (Cao et al. 2014). Moreover, studies have shown a connection between ventilation-related air movement in buildings and the spread of infectious diseases (Sanglier et al. 020). Low IAQ also reduces productivity,

which has a considerable negative impact on the economy (Sherman 2008). As a result, since the turn of the century, efforts have been concentrated on striking a balance between energy efficiency and air distribution characteristics, IAQ, and thermal comfort (Chung & Hsu 2001). The advantages of indoor air exchange have been demonstrated in this context. However, it is unclear how much ventilation affects the transmission of infectious diseases (Cao et al. 2014). As airflow rates have no quantifiable impact on health, ventilation rates stipulated in regulations are often established following comfort standards (perceived circumstances) (Wargocki 2015).

Nonetheless, following some techniques can result in a healthy indoor environment by implementing the necessary IAQ improvement strategies, which also include increasing the supply of fresh air, reducing pollution from emission sources, air cleaning, and improving ventilation efficiency (Van Tran et al. 2020), the latter is covered by this study. The distribution of fresh air throughout a space is shown by the ventilation efficiency, providing a qualitative assessment of the effectiveness of the ventilation system. Moreover, it can be utilized as an IAQ indicator if the air supply is of good quality (Chen et al. 2020). The goal of the ventilation system, such as heat removal, contamination removal, cross-infection prevention, or supply of fresh air to the breathing zone, should be taken into consideration when evaluating ventilation efficiency (Zhou et al. 2021).

The breathing zone is defined as the volume of air contained within a hemisphere with a radius of 0.3 m that extends in front of a person's face per ISO 15202-1 (Cao et al. 2014). The midpoint of the imaginary line connecting the ears serves as the hemisphere's center, and the larynx, the top of the head, and that line's intersection create the hemisphere's base. Better or worse, IAQ will be perceived in the breathing zone depending on the flow pattern, and, as a result, depending on the distribution of the age of the air inside a space. As a result of the amount of time spent inside the breathing zone, which results in high exposure, it is vital to evaluate the air quality in the building, particularly in bedrooms (Hormigos et al. 2019).

The use of lamps for therapeutic purposes, i.e., phototherapy and specifically for pathogen elimination, has been known for more than 80 years. The earliest research pointing to the beneficial properties of Ultraviolet (UV) light lamps dates back to 1937 when UV light lamps were used to irradiate classrooms and other school areas to disinfect and sanitize the air to eradicate and prevent the spread of pathogens such as measles, mumps, and chickenpox. Said study provided conclusive findings on the virucidal power of UV light as an effective light therapy (Wells et al.1941),

although, at the time, no information was available on its carcinogenic effect in humans.

Since its inception, phototherapy has evolved considerably. The increasing number of multidrug-resistant bacterial strains, together with the difficulty of obtaining new antibiotics, have rendered novel microbial control techniques essential. One of the strategies that has since demonstrated potential for pathogen destruction is the use of light-emitting diode (LED) lamps or light systems, which, in addition to being low cost, have a low environmental impact [16] and do not pose a health hazard for humans and animals (Angarano et al. 2020, Gillespie et al. 2017).

LEDs emit light because of the flow of electric current through two semiconductors, whose material determines the light emission wavelength (Prasad et al. 2019). The bactericidal effect of LEDs is due to the presence of endogenous photosensitizers (EPs), such as porphyrin-containing cytochromes, ubiquinones, or flavin-containing enzymes (Kim et al. 2021), which are commonly found on the inner membrane of the bacterial cell. The excitation of EPs, i.e., the release and transfer of an electron into an oxygen molecule for EPs stabilization, takes place when these are irradiated by a certain wavelength of light. This change of charge at the molecular level is responsible for the appearance of Reactive Oxygen Species (ROS) such as superoxide anion, hydroxyl radicals, and hydrogen peroxide, which damage bacterial structural components such as DNA, RNA, lipids, and proteins (Kim & Kang 2021, Angarano et al. 2020).

Exposing different foods to 405 nm LED light has been previously shown to reduce their pathogenic bacterial load. Moreover, Li et al. (2018) found a considerable decrease of *Salmonella* spp. and *Listeria monocytogenes* present in fresh ready-to-eat salmon, and Kim et al. (2017) obtained analogous results with *Salmonella* spp. in fresh fruit. In like manner, the load of *Escherichia coli 0157:H7* on the surface of dried fruits was found to lessen after LED light exposure (Lacombe et al. 2016). Despite the lower antibacterial efficacy of LED light compared to other methods, e.g., high-temperature heating or UV or ionizing radiation, low-energy photons avoid material degradation or tissue damage while also not compromising food quality.

The need to control microbial contamination in hospital environments gave rise to research assessing the effect of LED light on bacteria frequently found in those settings, such as methicillin-resistant *Staphylococcus aureus*, and obtaining antibacterial levels similar to that of laser light (Masson-Meyers et al. 2015). Additionally, the technology has been considered for potential medical use, entailing wound decontamination (McDonald et al. 2011) and sterilization of tissue matrices such as collagen (Smith et al. 2009).

Most existing studies have based their research on lamps with peak emission at 405 nm, whose oxidizing power can induce skin and retina damage. Thus, the present research adopted a wavelength of 462 nm, which does not present the oxidizing power of wavelengths closer to Ultraviolet-A (UVA) and hence does not incur any damage at high intensity (Wang et al. 2007, ICNIRP 2013, Roehlecke et al. 2013, Lawrence et al. 2018).

One of the primary environments affecting quality of life has been identified as the residential indoor environment (QoL). The relationship between home indoor environment and quality of life is complex. Nevertheless, studies often focus on a small number of residential environmental elements and their impact on QoL (Rajagopalan & Goodman 2021). Consequently, based on the results of the home environment and health survey, the purpose of this study is to determine the correlations between the overall residential interior environment and quality of life, as well as how such associations can be altered by various confounding factors. The findings indicated that participants' top cited home environmental concerns were thermal issues. Even after adjusting for age, sex, education, smoking, drinking, number of residents per household, and other factors, there was a statistically significant correlation between the increase in physical/mental health conditions and the decrease in reported frequency of residential environmental problems, including thermal, indoor air quality, lighting, acoustics, hygiene, safe and security environment (Vardoulakis et al. 2020). After controlling for confounding variables, it was discovered that coupled home environmental issues such as temperature and humidity, thermal environment and air quality/noise/mold, air quality and noise, and fall and wet had substantial combined effects on physical/mental health. This study tried to unravel the intricate connections between indoor living conditions and quality of life, which would serve as a foundation for developing QoL-improving measures (Marć et al. 2019).

The research of Haraldstad et al. (2019) in the fields of biomedicine, social science, clinical medicine, and health services must now take quality of life (QoL) into account as a significant health outcome metric. The World Health Organization (WHO) recognized environmental factors as the primary drivers of quality of life (QoL) (Skevington et al. 2004). Without a doubt, the residential indoor environment is acknowledged as one of the most significant environmental factors. People spend roughly 66% of their time in residential structures on average (Zhang et al. 2021). Because of restrictions on outside activities, this percentage is especially greater during the COVID-19 epidemic. This statistic alone demonstrates the necessity of researching how residential indoor environments affect quality of life.

Over the past ten years, there has been a rapid advance in the recognition and comprehension of the impact the home indoor environment has on health. Numerous studies have examined the relationship between indoor environmental factors (primarily indoor air pollutants, noise, lighting, and comfort factors) and adverse health outcomes, including mortality (Ma et al. 2020), respiratory issues (Raju et al. 2020), allergy (Svendsen et al. 2018), sleep disturbance (Ricketts et al. 2022), lung cancer (Caracci et al. 2021), mental health (Zhang et al. 2023) and cardiovascular disease (Xia et al. 2021), has been developed. QoL might thus be thought of as "the missing measurement in health." The WHO defines QoL (1998) as "individuals' impressions of their situation in life in relation to their objectives, aspirations, standards, and worries and in the context of the culture and value systems in which they live."

Also, the increase in life expectancy over the previous century has caused a change away from considering health in terms of survival (mortality), leading to an emphasis on being disease-free and, more recently, an emphasis on quality of life (QoL) (McDowell 2006). That underlines even more how crucial it is to incorporate QoL into environmental health research.

Although the home indoor environment has been frequently discussed for its major impact on QoL, quantifying the relationship between them remains a significant problem. Some examples could clarify this: Environmental exposure that occurs on multiple occasions and simultaneously is common in residential indoor environments. For instance, data from numerous international surveys revealed that multiple risk factors, including noise, indoor air pollution, thermal issues, moisture and mildew, water quality, and the lack of daylight, commonly affected the home indoor environment (Ormandy 2009). The body of research on the relationships between indoor air quality, the temperature environment, sound, and light is also expanding. Interactions might change the home's occupants' ability to live in a comfortable and healthy atmosphere (ASHRAE 2011).

Also, to advance the research, it is proposed to take into account the convective effects caused by people's presence and the way they breathe when evaluating the airflow patterns inside an enclosure (Moreno-Rangel et al. 2018).

Bacterial Pathogenicity

Hospital-acquired infections brought about by direct or indirect contact with everyday surfaces and objects have been extensively studied (Suleyman et al. 2018). The survival of common bacteria indoors on the individual's skin and mucous membranes, as well as microorganisms in bioaerosols from plants, the air, and the soil, facilitates the

acquisition of infections, especially in immunocompromised and hospitalized individuals (Kumar & Ison, 2019, Kurizky et al. 2020). Patients undergoing oncological or immunosuppressive treatments are also more susceptible to community-acquired pathogens, making microbial elimination or reduction in their usual environment advisable.

The genus *Pseudomonas aeruginosa* and *Acinetobacter* spp. stand out among the environmental microorganisms most frequently linked to colonization and indirect disease transmission through contact with contaminated objects, e.g., mobile phones, computer keyboards, and doorknobs (Isaacs et al. 1998, Borer et al. 2005, Malta et al. 2020). With a high survival rate on inanimate surfaces, these can form biofilms with high tolerance to disinfecting agents and, therefore, promote pathogen transmission by hands and medical equipment, in turn reaching at-risk individuals (Yang et al. 2020, Angarano et al. 2020). The clinical relevance of biofilm formation lies in its multiple drug resistance in hospital settings, as well as its potent pathogenicity in nosocomial infections (Olu-Taiwo et al. 2020, Malta et al. 2020). LED illumination was shown to increase the sensitivity of *Pseudomonas aeruginosa* biofilms to antibacterial agents, such as chlorhexidine and benzalkonium chloride, thus facilitating their inactivation and elimination (Yang et al. 2020).

By the same token, common human gut colonizing bacteria such as *Escherichia coli* and *Enterococcus*, or those present on mucous membranes, e.g., *Staphylococcus aureus* and *Streptococcus pyogenes,* persist in their environment for long periods, allowing it to spread through direct or indirect contact and potentially originate infectious outbreaks (Dancer 2008, Yoon et al. 2009, Kramer & Assadian 2014, Kanamori et al. 2016). Their high antibiotic resistance rates pose treatment challenges by narrowing the therapeutic options available (Lakhundi & Zhang 2018).

The overarching aim of this research was to determine whether radiation far removed from UVA, specifically blue light at a wavelength of 462 nm, displays bactericidal power for personal and everyday objects. On the assumption that the bactericidal power is confirmed, the authors would proceed to test the reduction or elimination of the microbial load on small surfaces, objects, or devices for everyday and clinical use.

MATERIALS AND METHODS

462 nm blue LED lamps were used and placed at a distance of 1.5 cm from the sample. When switched on, their temperature was 28°C, while the ambient temperature of the laboratory neared 26°C. The bacterial suspensions were placed on Parafilm under the lamps.

The microorganisms employed in the research were retrieved from the culture collection of the Microbiology Section of the Faculty of Pharmacy at CEU San Pablo University. The Gram-positive bacteria were the genus *Staphylococcus aureus*, *Enterococcus faecalis*, and *Streptococcus pyogenes,* while the Gram-negative bacteria were *Escherichia coli*, *Pseudomonas aeruginosa* and *Acinetobacter baumannii.*

All microorganisms were stored at 20°C in a freezer in the microbiology laboratory. The *Streptococcus pyogenes* samples were cultured in blood-agar medium, the *Enterococcus faecalis* samples in Slanetz-Bartley agar, the *Staphylococcus aureus* samples in Baird-Parker agar, and the *Escherichia coli, Pseudomonas aeruginosa*, and *Acinetobacter baumannii* samples in nutrient-agar media. All media were provided by OXOID. The experimental light exposure was carried out in a laminar flow cabinet. Drops of 200 µl volume containing bacterial suspensions in saline solution were placed on Parafilm inside the cabinet, under the LED light beam at 1.5 cm from the emitting source. The LEDs, whose characteristics were described in section 3, functioned continuously for one to four hours. Non-irradiated control samples were additionally prepared under the same conditions. The bacterial suspensions were adjusted according to the 0.5 McFarland turbidity Standard. To prevent sample desiccation, 105 µL and 90 µL of saline solution were added to the irradiated and control samples, respectively, every hour. All experiments were performed in triplicate.

The irradiated bacterial samples and their respective controls were collected every hour and diluted 10,000-fold by means of two successive 1/100 dilutions in saline solution. Subsequently, 100 µl were taken and spread following the Drigalski-spatula technique on the agar plates mentioned in section 3.2. After a 24-hour incubation period in an oven at 37°C, the colony-forming units (CFUs) were counted. The Student's t-test was performed to determine the differences between the irradiated and the non-irradiated samples.

RESULTS

A significant reduction in CFUs was obtained within the first hour of exposure for the *Staphylococcus aureus* and *Streptococcus pyogenes* ($p > 0.01$) samples and from the second hour of exposure ($p > 0.05$) for the *Enterococcus faecalis* sample (Table 1). Two hours of exposure were necessary for reaching the sterilization of the *Streptococcus pyogenes* sample, while three hours were required for the inactivation of the *Staphylococcus aureus* and *Enterococcus faecalis*, slightly longer than the 80 minutes reported in previous research (Maclean et al. 2009). A possible

explanation for this discrepancy may lie in the disparate characteristics of the lamps used in the studies. The present research employed a blue light lamp with a peak emission wavelength of 462 nm and an irradiance of 3.01 mW.cm^{-2}, whilst Maclean et al. (2009) used a lamp peaking at 405 nm with an irradiance of 10 mW/cm^{-2}. Although the distance between the LEDs and the sample was somewhat smaller in our testing procedure (1.5 cm versus 2 cm implemented in the latter), the different emission powers could be an explaining factor for the gap between the two studies' findings.

As for the experiments with the Gram-negative bacteria, a noteworthy reduction in CFUs was yielded within the first hour of exposure for the *Escherichia coli* sample, within two hours for *Acinetobacter baumannii,* and three hours for *Pseudomonas aeruginosa* (Table 2). None of the samples attained full bacterial eradication, including after four hours of irradiation. These outcomes are in line with those of Maclean et al. (2009), who found a 4-log reduction of CFU as a result of two to four hours of blue light exposure. The present study observed a lesser reduction in Gram-negative bacteria, which could also be attributed to the different emission powers of the lamps. Table 1 shows the effect of blue light therapy on Gram-positive bacteria. A significant impact is shown * p>0.05* and ** p>0.01** in the Student's t-test of the irradiated samples versus controls at each hour of exposure. Table 2 shows the effect of blue light therapy on Gram-negative bacteria. A significant impact is shown * p>0.05* and ** p>0.01** in the Student's t-test of the irradiated samples versus controls at each hour of exposure.

DISCUSSION AND CONCLUSIONS

The development of alternative disinfection methods has led to consider the potential of a raft of biological techniques as the use of bacteriophage therapy (Lin et al. 2017), i.e. bacteria-killing viruses, bacteriocins, i.e. antimicrobial peptides produced by bacteria that are active against other strains of the same or related species, and physical methods such as the use of low-frequency electromagnetic radiation as an alternative to Ultraviolet-C light or ionizing radiation, which poses a danger to human health (ICNRP 2013).

The thermal environment, indoor air quality, acoustic environment, lighting environment, hygiene environment, safety environment, and security environment conform to the healthy home environment as described by the WHO (2018) and Harvard T.H. Chan School of Public Health. (J.G. Allen et al. 2017).

The results obtained suggest that blue light therapy does not bear an equal effect on all bacteria types, similar to what happens with chemical disinfectants. Specifically, blue light exhibited a diminished bactericidal effect on the Gram-negative bacteria tested when compared to Gram-positive ones, which is aligned with previous research (Maclean et al. 2009, Moyano et al. 2020). This mismatch in efficacy could be due to Gram-positive and Gram-negative bacteria having different endogenous porphyrin compositions, with a concurrent impact on bacterial photoinactivation and elimination levels (Guffey & Wilborn 2006, Kim et al. 2017, Hessling et al. 2017). Numerous studies have

Table 1: Effect of blue light therapy on Gram-positive bacteria. Med.: Mean value of log CFU, SD: Standard deviation.

	Staphylococcus aureus				*Streptococcus pyogenes*				*Enterococcus faecalis*			
	Control		Irradiated		Control		Irradiated		Control		Irradiated	
Hours	Med.	SD	Med.	SD.	Med.	SD	Med.	SD	Med.	SD	Med.	SD
0	6,9	0,01	6,9	0,01	6,8	0,6	6,8	0,6	5,9	0,8	5,9	0,8
1	6,79	0,02	6,62*	0,04	5,2	1	2,45**	0,7	5,55	1	4,06**	1,2
2	5,51	0,02	3,12**	0,03	4,1	0,9	0**	0	4,4	1	2,61**	0,3
3	5,1	0,02	0**	0	3,03	1,1	0**	0	3,9	0,4	0**	0
4	4,7	0,02	0**	0	2,21	1	0**	0	3,2	0,5	0**	0

Table 2: Effect of blue light therapy on Gram-negative bacteria. Med.: Mean value of log CFU, SD: Standard deviation.

	Escherichia coli				*Acinetobacter baumannii*				*Pseudomonas aeruginosa*			
	Control		Irradiated		Control		Irradiated		Control		Irradiated	
Hours	Med.	SD	Med.	SD	Med.	SD	Med.	SD	Med.	SD	Med.	SD
0	6,9	0,6	6,9	0,6	6,5	0,8	6,5	0,8	5,5	0,8	5,5	0,8
1	6,6	0,5	3,8**	0,4	5,9	1	5,2	0,9	5,1	0,5	4,4	0,6
2	5,4	0,4	2,8**	0,5	5,7	0,4	4,6*	0,6	4,6	0,4	4,1	0,6
3	5,1	0,2	2,1**	0,5	5,3	0,7	3,93**	0,4	4,11	0,6	2,9*	0,7
4	4,9	0,3	1,4**	0,5	4,9	0,5	3,51**	0,7	3,66	0,7	1,12**	1,1

established the correlation between the efficacy of bacterial photoinactivation at different wavelengths to the endogenous porphyrins that bacteria can synthesize or to the different precursors of porphyrin synthesis that can be used as photosensitizers (Hessling et al. 2017).

Residents often consider thermal issues to be more significant than other environmental factors, including sound, light, and indoor air quality (Dimitroulopoulou 2012). This study also shows a substantial correlation between the rise in physical and mental health issues and the decline in reported thermal problem frequency. These results were consistent with other research that revealed relationships between thermal variables such as dry bulb temperature, radiant temperature, humidity, air speed, and mental/physical well-being. (Jingyi et al. 2021)

According to a number of studies, particularly those conducted in the winter, more than one-third of people reported experiencing indoor air quality issues that may be related to CO_2 (37%), HCHO (53%), and TVOC (40%) (Huang et al. 2018).

According to Spengler et al. (2001), temperature and humidity can directly affect both physical and mental health. Blue light excited endogenous porphyrins result in ROS and free radicals, which are responsible for non-specific damage to different structural components of the bacteria, e.g., proteins, the plasma membrane, and genetic material. Protoporphyrin IX, a very abundant endogenous photosensitizer in *Staphylococcus aureus* located in the cytoplasm, is catalyzed by ferrochelatase, which is the terminal cytoplasmic enzyme of the heme biosynthetic pathway involved in iron incorporation (Kim et al. 2017). According to the previous research, in addition to causing DNA damage, ROS inhibits the enzyme ATPase, as well as the activity of other pumps such as the phosphoenolpyruvate (PEP): carbohydrate phospho-transferase system (PTS) (glucose uptake pump). More recently, Kim & Kang (2021) suggested that damage also occurs at the plasma membrane level with the loss of respiratory activity when exposed to blue light wavelengths.

Other molecules susceptible to induce bacterial photoinactivation by means of ROS production are flavins. A previous study conducted by Plavskii et al. (2018) on *Staphylococcus aureus* and *Escherichia coli* evidenced that the photosensitization of endogenous porphyrins and flavins occur most effectively under 405 nm light and 445 nm, respectively. Reducing the microbial load on objects and surfaces minimizes the risk of cross-infection. Most chemical disinfectants do not sterilize nor completely eradicate microorganisms, so on that level, blue LED therapy would not fall behind conventional ones. Its

main drawback, however, lies in the time necessary for significant bacterial decrease, which averages two hours. It would be interesting for future work to examine whether repeated irradiation at 15-min or 30-min intervals could increase the bactericidal power of blue light, as obtained by Masson-Meyers et al. (2015) in their experiments with *Staphylococcus aureus*.

On the other hand, Gillespie et al. (2017) and Mori et al. (2017) state that pulsed light can be as effective as continuous light since only one photon is needed for porphyrin excitation. Bacteria do not absorb photons while the molecule is in an excited state, so the use of continuous light would convey a rapid saturation and loss of the latter. Conversely, pulsed light would allow for energy savings whilst obtaining analogous effects. According to certain investigations by Wu et al. (2020), high noise levels were strongly linked to less thermal comfort than usual thermal conditions. Noises tend to increase the intensity of interior odours and lower perceived air quality (Sarigiannis 2014). Additionally, it aims to evaluate how the air is distributed while taking into account factors like the quality of the indoor air and occupant behaviour, as well as energy efficiency standards (Domínguez-Amarillo et al. 2020).

The use of LED light as a disinfectant in the food industry and hospital environments for material disinfection and wound treatment (McDonald et al. 2011) led the authors to assess its antibacterial activity on the most frequent bacteria contaminating everyday objects and surfaces in residential and hospital settings. On the proviso that its efficacy was confirmed, we would proceed to develop a series of lamps capable of sterilizing the surfaces most susceptible to microbial contamination, such as *inter alia,* lift buttons, switches, doorknobs, push-buttons, washbasins, and toilets. Due to the nature of these surfaces, the safety of prolonged use of the disinfecting light was a necessary condition, namely for eyes and skin. Furthermore, to avoid toxic effects brought about by the external photosensitization of microorganisms, no chemical compound susceptive to radiation-induced alteration should be used.

The use of said type of lamps in households and public places could positively impact the consumption of chemicals currently used for the same purpose, which would lower the production of these compounds and packaging and, in turn, decrease energy consumption and single-use plastic waste.

LED luminaires emitting longer wavelengths in the blue light spectrum, such as those used for the present experimental research, may take longer to inhibit pathogens in contact surfaces than those with shorter wavelengths but provide the advantage of being innocuous to the skin and eyes of people even near the emitting source.

Direct 642 nm blue LED irradiation significantly reduced the populations of Gram-negative bacteria and completely eradicated Gram-positive ones tested after three hours of exposure.

Further analysis should be carried out using higher-power blue lamps in pulsed or continuous mode to analyze their impact on exposure time reduction and the elimination of Gram-negative bacteria.

REFERENCES

Allen, J.G., Bernstein, A. and Cao, X., 2017. The 9 foundations of a healthy building. Harvard T.H. Chan School of Public Health.

Angarano, V., Smet, C., Akkermans, S., Watt, C., Chieffi, A., Van Impe, J.F.M., 2020. Visible light as an antimicrobial strategy for inactivation of *Pseudomonas fluorescens* and *Staphylococcus epidermidis* biofilms. *Antibiotics*, 9(4), pp.171-194.

ASHRAE, 2011. *Guideline 10: Interactions Affecting the Achievement of Acceptable Indoor Environments*. The American Society of Heating, Refrigerating and Air-Conditioning Engineers.

Borer, A., Gilad, J., Smolyakov, R., Eskira, S., Peled, N., Porat, N., Hyam, E., Trefler, R., Riesenberg, K. and Schlaeffer, F., 2005. Cell phones and Acinetobacter transmission. *Emerging infectious diseases*, 11(7), p.1160.

Borsboom, W., De Gids, W., Logue, J., Sherman, M. and Wargocki, P., 2016. *Technical Note 68*. *Residential Ventilation and Health*. Air Infiltration and Ventilation Centre (AIVC).

Caracci, E., Stabile, L., Buonanno, G., 2021. A simplified approach to evaluate the lung cancer risk related to airborne particles emitted by indoor sources. *Building and Environment*, 204, p.108143.

Cao, X., Dai, X. and Liu, J., 2016. Building energy-consumption status worldwide and the state-of-the-art technologies for zero-energy buildings during the past decade. *Energy and Buildings*, 128, pp.198–213.

Chen, T., Feng, Z. and Cao, S.J., 2020. The effect of vent inlet aspect ratio and its location on ventilation efficiency. *Indoor and Built Environment*, 29(2), pp.180-195. https://doi.org/10.1177/1420326X19865930.

Chung, K. and Hsu, S., 2001. Effect of ventilation pattern on room air and contaminant distribution. *Building and Environment*, 36, pp.989–998.

Dancer, S.J., 2008. Importance of the environment in meticillin-resistant *Staphylococcus aureus* acquisition: the case for hospital cleaning. *The Lancet Infectious Diseases*, 8(2), pp.101-113. https://doi.org/10.1016/S1473-3099(07)70241-4.

Domínguez-amarillo, S., Fernández-agüera, J., Cesteros-garcía, S. and González-lezcano, R.A., 2020. Bad air can also kill Residential indoor air quality and pollutant exposure risk during the COVID-19 crisis. *International Journal of Environmental Research and Public Health*, 17(19), pp.1–34. https://doi.org/10.3390/ijerph17197183.

Dimitroulopoulou, C., 2012. Ventilation in European dwellings: A review. *Building and Environment*, 47, pp.109–125. https://doi.org/10.1016/j.buildenv.2011.07.016.

Frontczak, M. and Wargocki, P., 2011. Literature survey on how different factors influence human comfort in indoor environments. *Building and Environment*, 46, pp.922–937.

Gillespie, J.B., Maclean, M., Given, M.J., Wilson, M.P., Judd, M.D., Timoshkin, I.V. and MacGregor, S.J., 2017. Efficacy of pulsed 405-nm light-emitting diodes for antimicrobial photodynamic inactivation: effects of intensity, frequency, and duty cycle. *Photomedicine and laser surgery*, 35(3), pp.150-156.

Guffey, J.S. and Wilborn, J., 2006. In vitro bactericidal effects of 405-nm and 470 nm blue light. *Photomedicine and Laser Surgery*, 24(6), pp.684-688.

Haraldstad, K., Wahl, A., Andenæs, R., Andersen, J.R., Andersen, M.H., Beisland, E., Borge, C.R., Engebretsen, E., Eisemann, M., Halvorsrud, L. and Hanssen, T.A., 2019. A systematic review of quality of life research in medicine and health sciences. *Quality of life Research*, 28, pp.2641-2650.

Hessling, M., Spellerberg, B. and Hoenes, K., 2017. Photoinactivation of bacteria by endogenous photosensitizers and exposure to visible light of different wavelengths – A review of existing data. *FEMS Microbiology Letters*, 364(2), p.fnw270. https://doi.org/10.1093/femsle/fnw270.

Hormigos-Jimenez, S., Padilla-Marcos, M.Á., Meiss, A., Gonzalez-Lezcano, R.A. and Feijó-Muñoz, J., 2018. Computational fluid dynamics evaluation of the furniture arrangement for ventilation efficiency. *Building Services Engineering Research and Technology*, 39(5), pp.557–571. https://doi.org/10.1177/0143624418759783.

Hormigos-Jimenez, S., Padilla-Marcos, M.Á., Meiss, A., Gonzalez-Lezcano, R.A. and Feijó-Muñoz, J., 2019. Assessment of the ventilation efficiency in the breathing zone during sleep through computational fluid dynamics techniques. *Journal of Building Physics*, 42(4), pp.458–483. https://doi.org/10.1177/1744259118771314.

Huang, K., Song, J., Feng, G., Chang, Q., Jiang, B., Wang, J., Sun, W., Li, H., Wang, J. and Fang, X., 2018. Indoor air quality analysis of residential buildings in northeast China based on field measurements and longtime monitoring. *Building and Environment*, 144, pp.171-183.

International Commission on Non-ionizing Radiation Protection (ICNRP), 2013. Guidelines on limits of exposure to incoherent visible and infrared radiation. *Health Physics*, 105, pp.74-96.

Isaacs, D., Daley, A., Dalton, D., Hardiman, R. and Nallusamy, R., 1998. Swabbing computers in search of nosocomial bacteria. *The Pediatric Infectious Disease Journal*, 17(6), p.533. https://doi.org/10.1097/00006454-199806000-00025.

Jingyi, M., Shanshan, Z. and Wu, Y., 2022. The influence of physical environmental factors on older adults in residential care facilities in Northeast China. *Health Environments Research and Design Journal*, 15(1), pp.131–149. https://doi.org/10.1177/19375867211036705.

Kanamori, H., Weber, D.J. and Rutala, W.A., 2016. Healthcare outbreaks associated with a water reservoir and infection prevention strategies. *Clinical Infectious Diseases*, 62(11), pp.1423-1435. https://doi.org/10.1093/cid/ciw122.

Klepeis, N.E., Nelson, W.C., Ott, W.R., Robinson, J.P., Tsang, A.M., Switzer, P. and Engelmann, W.H., 2001. The National Human Activity Pattern Survey (NHAPS): A resource for assessing exposure to environmental pollutants. *Journal of Exposure Science and Environmental Epidemiology*, 11(3), pp.231.

Kim, D. and Kang, D., 2021. Efficacy of light-emitting diodes emitting 395, 405, 415, and 425 nm blue light for bacterial inactivation and the microbicidal mechanism. *Food Research International*, 141, p.110105. https://doi.org/10.1016/j.foodres.2021.110105.

Kim, M.J., Bang, W.S. and Yuk, H.G., 2017. 405±5 nm light emitting diode illumination causes photodynamic inactivation of *Salmonella* spp. on fresh-cut papaya without deterioration. *Food Microbiology*, 62, pp.124-132.

Kramer, A. and Assadian, O., 2014. Survival of microorganisms on inanimate surfaces. In: Borkow, G. (ed.) Use of Biocidal Surfaces for Reduction of Healthcare Acquired Infections. Springer Cham. https://doi.org/10.1007/978-3-319-08057-4_2.

Kumar, R. and Ison, M.G., 2019. Opportunistic infections in transplant patients. *Infectious Disease Clinics of North America*, 33(4), pp.1143-1157. https://doi.org/10.1016/j.idc.2019.05.008.

Kurizky, P.S., dos Santos Neto, L.L., Aires, R.B., da Mota, L.M.H. and Gomes, C.M., 2020. Opportunistic tropical infections in immunosuppressed patients. *Best Practice & Research Clinical Rheumatology*, 34(4), p.101509. https://doi.org/10.1016/j.berh.2020.101509.

Lacombe, A., Niemira, B.A., Sites, J., Boyd, G., Gurtler, J.B., Tyrell, B. and Fleck, M., 2016. Reduction of bacterial pathogens and

potential surrogates on the surface of almonds using high-intensity 405-nanometer light. *Journal of food protection*, 79(11), pp.1840-1845.

Lakhundi, S. and Zhang, K., 2018. Methicillin-resistant *Staphylococcus aureus*: Molecular characterization, evolution, and epidemiology. *Clinical Microbiology Reviews*, 31(4), p.e00020-18. https://doi.org/10.1128/CMR.00020-18.

Lan, L., Wargocki, P., Wyon, D.P. and Lian, Z., 2011. Effects of thermal discomfort in an office on perceived air quality, SBS symptoms, physiological responses, and human performance. *Indoor Air*, 21, pp.376–390.

Lawrence, K.P., Douki, T., Sarkany, R.P.E., Acker, S., Herzog, B. and Young, A.R., 2018. The UV/Visible radiation boundary region (385-405 nm) damages skin cells and induces "dark" cyclobutane pyrimidine dimers in human skin in vivo. *Scientific Reports*, 8(1), p.12722. https://doi.org/10.1038/s41598-018-30738-6.

Li, X., Kim, M.J. and Yuk, H.G., 2018. Influence of 405 nm light-emitting diode illumination on the inactivation of *Listeria monocytogenes* and *Salmonella* spp. on ready-to-eat fresh salmon surface at chilling storage for 8 h and their susceptibility to simulated gastric fluid. *Food Control*, 88, pp.61-68.

Lin, D.M., Koskella, B. and Lin, H.C., 2017. Phage therapy: An alternative to antibiotics in the age of multi-drug resistance. *World Journal of Gastrointestinal Pharmacology and Therapeutics*, 8(3), pp.162-173.

Ma, Y., Zhang, Y., Cheng, B., Feng, F., Jiao, H., Zhao, X., Ma, B. and Yu, Z., 2020. A review of the impact of outdoor and indoor environmental factors on human health in China. *Environmental Science and Pollution Research*, 27, pp.42335-42345.

Maclean, M., MacGregor, S.J., Anderson, J.G. and Woolsey, G., 2009. Inactivation of bacterial pathogens following exposure to light from a 405-nanometer light-emitting diode array. *Applied and Environmental Microbiology*, 75(7), pp.1932-1937.

Malta, R.C.R., Ramos, P., Paiva Anciens, G.L. and Nascimento, J.D.S., 2020. From food to hospital: We need to talk about *Acinetobacter* spp. *Germs*, 10(4), pp.210-217.

Marć, M., Śmiełowska, M., Namieśnik, J. and Zabiegała, B., 2018. The indoor air quality of everyday use spaces dedicated to specific purposes—a review. *Environmental Science and Pollution Research*. Springer Verlag. https://doi.org/10.1007/s11356-017-0839-8.

Masson-Meyers, D.S., Bumah, V.V., Biener, G., Raicu, V. and Enwemeka, C.S., 2015. The relative antimicrobial effect of blue 405 nm LED and blue 405 nm laser on methicillin-resistant *Staphylococcus aureus*. *Lasers in Medical Science*, 30(9), pp.2265-2271. https://doi.org/10.1007/s10103-015-1799-1.

McDonald, R., MacGregor, S.J., Anderson, J.G., Maclean, M. and Grant, M.H., 2011. Effect of 405-nm high-intensity narrow-spectrum light on fibroblast-populated collagen lattices: an in vitro model of wound healing. *Journal of biomedical optics*, 16(4), pp.048003-048003. https://doi.org/10.1117/1.3561903.

McDowell, I., 2006. *Measuring Health: A Guide to Rating Scales and Questionnaires* Oxford University Press.

Moreno-Rangel, A., Sharpe, T., Musau, F. and McGill, G., 2018. Field evaluation of a low-cost indoor air quality monitor to quantify exposure to pollutants in residential environments. *Journal of Sensors and Sensor Systems*, 7(1), pp.373–388. https://doi.org/10.5194/jsss-7-373-2018.

Mori, M., Hamamoto, A., Takahashi, A., Nakano, M., Wakikawa, N., Tachibana, S., Ikehara, T., Nakaya, Y., Akutagawa, M. and Kinouchi, Y., 2007. Development of a new water sterilization device with a 365 nm UV-LED. *Medical & biological engineering & computing*, 45, pp.1237-1241.

Moyano, D.B., Sola, Y. and González-Lezcano, R.A., 2020. Blue-light levels are emitted from portable electronic devices compared to sunlight. *Energies*, 13(6), p.642. https://doi.org/10.3390/en13164276.

Olu-Taiwo, M., Opintan, J.A., Codjoe, F.S. and Obeng Forson, A., 2020. Metallo-beta-lactamase-producing *Acinetobacter* spp. from

clinical isolates at a tertiary care hospital in Ghana. *BioMed Research International*, 20, p.3852419. https://doi.org/10.1155/2020/3852419.

Ormandy, D., 2009. *Housing and Health in Europe*. Routledge.

Plavskii, V.Y., Mikulich, A.V., Tretyakova, A.I., Leusenka, I.A., Plavskaya, L.G., Kazyuchits, O.A., Dobysh, I.I. and Krasnenkova, T.P., 2018. Porphyrins and flavins as endogenous acceptors of optical radiation of blue spectral region determining photoinactivation of microbial cells. *Journal of Photochemistry and Photobiology B: Biology*, 183, pp.172-183.

Prasad, A., Gänzle, M. and Roopesh, M.S., 2019. Inactivation of *Escherichia coli* and *Salmonella* using 365 and 395 nm high-intensity pulsed light-emitting diodes. *Foods*, 8(12), pp.679-694.

Rajagopalan, P. and Goodman, N., 2021. Improving the indoor air quality of residential buildings during bushfire smoke events. *Climate*, 9(2), pp.1–14. https://doi.org/10.3390/cli9020032.

Raju, S., Siddharthan, T. and McCormack, M.C., 2020. Indoor air pollution and respiratory health. *Clinics in Chest Medicine*, 41, pp.825-843.

Ricketts, E.J., Joyce, D.S. and Rissman, A.J., 2022. Electric lighting, adolescent sleep and circadian outcomes, and recommendations for improving light health. *Sleep Medicine Reviews*, 64, p.101667.

Roehlecke, C., Schumann, U., Ader, M., Brunssen, C., Bramke, S., Morawietz, H. and Funk, R.H., 2013. Stress reaction in outer segments of photoreceptors after blue light irradiation. *PLoS One*, 8(9), p.e71570. https://doi.org/10.1371/journal.pone.0071570.

Sanglier-Contreras, G., López-Fernández, E.J. and González-Lezcano, R.A., 2021. Poor ventilation habits in nursing homes have favoured a high number of COVID-19 infections. *Sustainability (Switzerland)*, 13(21). https://doi.org/10.3390/su132111898.

Sarigiannis, D.A., 2014. Combined or multiple exposure to health stressors in indoor built environments. WHO Regional Office for Europe.

Sherman, M.H., 2008. Multizone age-of-air analysis. *International Journal of Ventilation*, 7, pp.159–167.

Skevington, S.M., Lotfy, M. and O'Connell, K.A., 2004. The World Health Organization's WHOQOL-BREF quality of life assessment: Psychometric properties and results of the international field trial. A report from the WHOQOL Group. *Quality of Life Research*, 13, pp.299–310.

Smith, S., Maclean, M., MacGregor, S.J., Anderson, J.G. and Grant, M.H., 2009. Exposure of 3T3 mouse fibroblasts and collagen to high intensity blue light. In *13th International Conference on Biomedical Engineering: ICBME 2008 3–6 December 2008 Singapore* (pp. 1352-1355). Springer Berlin Heidelberg.

Spengler, J.D., Samet, J.M. and McCarthy, J.F., 2001. *Indoor Air Quality Handbook*. McGraw-Hill.

Suleyman, G., Alangaden, G. and Bardossy, A., 2018. The role of environmental contamination in the transmission of nosocomial pathogens and healthcare-associated infections. *Current Infectious Disease Reports*, 20(6), p.12. https://doi.org/10.1007/s11908-018-0620-2.

Svendsen, E.R., Gonzales, M. and Commodore, A., 2018. The role of the indoor environment: Residential determinants of allergy, asthma and pulmonary function in children from a US-Mexico border community. *Science of The Total Environment*, 616, pp.1513-1523.

The WHO defines QoL, 1998. Development of the WHOQOL-BREF quality of life assessment. *Psychological Medicine*, 28, pp.551-558.

Van Tran, V., Park, D. and Lee, Y.C., 2020. Indoor air pollution, related human diseases, and recent trends in the control and improvement of indoor air quality. *International Journal of Environmental Research and Public Health*, 70, p.896. https://doi.org/10.3390/ijerph17082927.

Vardoulakis, S., Giagloglou, E., Steinle, S., Davis, A., Sleeuwenhoek, A., Galea, K.S., Dixon, K. and Crawford, J.O., 2020. Indoor exposure to selected air pollutants in the home environment: a systematic review. *International journal of environmental research and public health*, 17(23), p.8972. https://doi.org/10.3390/ijerph17238972.

Wang, L.M., Keller, J., Dillon, E.R. and Gaillard, 2007. Oxidation of A2E results in the formation of highly reactive aldehydes and ketones. *Photochemistry and Photobiology*, 82, pp.1251–1257.

Wargocki, P., 2015. What are indoor air quality priorities for energy-efficient buildings? *Indoor and Built Environment*, 24(5), pp.579–582. doi:10.1177/1420326x15587824.

Wargocki, P., 2016. *Ergonomic Workplace Design for Health, Wellness, and Productivity*. CRC Press.

Wells, W.F., Wells, M.W. and Wilder, T.S., 1941. The environmental control of epidemic contagion. *American Journal of Epidemiology*. https://academic.oup.com/aje/article/35/1/97/85502.

WHO, 2018. *Housing and Health Guidelines*. World Health Organization.

Wu, H., Wu, Y., Sun, X. and Liu, J., 2020. Combined effects of acoustic, thermal, and illumination on human perception and performance: A review. *Building and Environment*, 169, p.106593.

Xia, X., Chan, K.H. and Lam, K.B.H., 2021. Effectiveness of indoor air purification intervention in improving cardiovascular health: A systematic review and meta-analysis of randomized controlled trials. *Science of The Total Environment*, 789, p.147882.

Yang, Y., Ma, S., Xie, Y., Wang, M., Cai, T., Li, J., Guo, D., Zhao, L., Xu, Y., Liang, S. and Xia, X., 2020. Inactivation of Pseudomonas aeruginosa biofilms by 405-nanometer-light-emitting diode illumination. *Applied and Environmental Microbiology*, *86*(10), pp.e00092-20. https://doi.org/10.1128/AEM.00092-20.

Yoon, Y.K., Sim, H.S. and Kim, J.Y., 2009. Epidemiology and control of an outbreak of vancomycin-resistant enterococci in the intensive care units. *Yonsei Medical Journal*, 50(5), pp.637–643. https://doi.org/10.3349/ymj.2009.50.5.637.

Zhang, J., Browning, M.H.E.M. and Liu, J., 2023. Is indoor and outdoor greenery associated with fewer depressive symptoms during COVID-19 lockdowns? A mechanistic study in Shanghai, China. *Building and Environment*, 227, p.109799.

Zhang, Y., Hopke, P.K. and Mandin, C., 2021. *Handbook of Indoor Air Quality*. Springer Nature Singapore Pte Ltd.

Zhou, J., Hua, Y., Xiao, Y., Ye, C. and Yang, W., 2021. Analysis of ventilation efficiency and effective ventilation flow rate for wind-driven single-sided ventilation buildings. *Aerosol and Air Quality Research*, 21(5), p.383. https://doi.org/10.4209/aaqr.200383.

Evaluation of Toxicity of Few Novel Insecticides Against Different Aphid Species (*Rhopalosiphum maidis*, *Myzus persicae*, *Liphaphis erysimi*)

Ajinkya Markad, Pritha Ghosh†🔵 **and Matangi Mishra**

Department of Entomology, School of Agriculture, Lovely Professional University, 144411, Phagwara, Punjab, India
†Corresponding author: Pritha Ghosh; pritha.26967@lpu.co.in

ABSTRACT

Aphids are important insect pests and are considered a major threat to various crops. In the laboratory experiment, our objective is to assess the toxicity level of some newer synthetic insecticides, *viz.* Imidacloprid, Flonicamid, and Spirotetramat against different species of aphids *viz.* maize leaf aphids (*Rhopalosiphum maidis*), green peach aphids (*Myzus persicae*), and mustard aphids (*Liphaphis erysimi*). The leaf dip bioassay was conducted to evaluate the LC_{50} and LT_{50} values. Among these novel molecules, Spirotetramat was the most toxic insecticide against *R. maidis* and *M. persicae,* with median lethal concentrations (LC_{50}) of 0.68 and 3.99 ppm, and Flonicamid was the most toxic against *L. erysimi* with an LC_{50} value of 5.79 ppm. The median lethal concentrations for the Imidacloprid, Flonicamid, and Spirotetramat are different for each species of aphids. The LT_{50} values of the given insecticides revealed that the Imidacloprid has the potential for giving effective control of *R. maidis, M. persicae,* and *L. erysimi* species, as evidenced by the shorter time required for 50% mortality with LT_{50} values of 44.53, 49.19 and 44.90 hrs respectively with median lethal concentrations of 4.20, 5.14 and 10.86 ppm. The results indicated variations in toxicity among these different chemicals against different insect species.

INTRODUCTION

Aphids are one of the most known herbivorous pests worldwide and have effectively taken advantage of the agricultural environment (Srigiriraju et al. 2010). Aphids are the common insect pests of crops that cause major economic loss (Dewhirset et al. 2010).

Maize aphid is also known as corn leaf aphid (*Rhopalosiphum maidis*, Hemiptera: Aphididae). *R. maidis* has a wide range of hosts of the Graminae, which includes 30 genera of cereal crops, specifically corn, barley, sorghum, and *Miscanthus sinensis* grass (Kieckhefer & Kantack 1980, Pointeau et al. 2014). *R. maidis* is a polyphagous, sap-sucking insect pest that may cause a 40% yield loss (Table 1) (Alam et al. 2019). It is distributed all over India, and the maize dwarf mosaic virus and maize leaf fleck virus are transmitted by *R. maidis* (So et al. 2010). The infestation of *R. maidis* is found in the whorl stage of plants. The infestation increases during the tassel emergence stage. Infestation of aphids in maize tassel reduces pollination and transmits bacteria, viruses, and fungi in cob, leaf, and other parts of the plant (Alam et al. 2020). Adults of the *R. maidis* are bluish-green. The wingless females are parthenogenetic (reproducing without mating) and of green or whitish green. Most of the time, *R. maidis* reproduces parthenogenetically (Blackman & Eastop 2000, Kumar et al. 2018).

The green peach aphid, *Myzus persicae* (Sulzer) (Aphididae: Hemiptera), is an extremely polyphagous aphid species that has been reported to feed on over 500 species of host plants from at least forty different families, involving several important crops (Van Emden 2017). *M. persicae* is the major pest in potato

crops, causing major losses (Table 1) in yield indirectly by transmitting many plant viruses (Table 2) that lead to the degeneration of the seed tubers (Kreuze et al. 2020). The wingless adult aphids are greenish or yellowish and have lateral stripes on the body.

Lipaphis erysimi (Kalt.) is the primary pest in all mustard-growing regions of the country. It mainly affects the different cruciferous crops such as cabbage, radish, and rape. But mainly harms the crops of the Brassicaceae family *e.g.*, mustard and rapeseed (Koramutla et al. 2016). The mustard aphid's nymphs and adults suck the cell sap from the leaves, inflorescences, and immature pods, resulting in poor yield. They have also been discovered to prefer flowers over leaves for feeding (Dewhirst et al. 2010). This species transmits over 13 different viruses in the Brassicaceae family (Adhab & Schoelz 2015). The heavy infestation of *L. erysimi* shows many symptoms in mustard plants, which results in stunted growth, crinkling of leaves, yellowing, and dried-up plants. The wingless or apterous aphids of *L. erysimi* are yellowish-green or grey-green, small in size, faded, waxy white coating on the body (Gautam et al. 2019).

Due to the high capacity of virus transmission of those above-mentioned aphid species, heavy economic loss has been recorded in the crop yield by various scientists (Harris & Maramorosch 2014). Adverse effects of insecticides, especially due to organophosphate and carbamates, insecticides,

Table 1: Yield losses(%) caused by aphid vectors in different crops.

S.No.	Aphid species	Crop	Yield loss	Reference
1.	*Rhopalosiphum maidis*	Barley	30%	(Maanju et al. 2023)
		Barley	17.1–30%	(Murti et al. 1968, Bhatia et al. 1973)
		Corn	28.14%	(Al-Eryan & Al-Tabbakh 2004)
		Maize	40%	(Alam et al. 2019)
		Maize	10–20%	(Subedi 2015)
2.	*Myzus persicae*	Sweet pepper	31.49-100%	(Sharma et al. 2021)
		Potato	90%	(Sidauruk & Sipayung 2018)
3.	*Lipaphis erysimi*	Mustard	35.4 to 91.3%	(Brar et al. 1987)
		Mustard	100%	(Singh & Sachan 1999)
		Mustard	91%	(Bunker et al. 2006, Kular & Kumar 2011)
		Brassica spp.	65 to 96%	(Dhillon et al. 2022)

Table 2: List of aphid vectors and their disease transmission.

S.No.	Aphid species	Virus	Reference
1.	*Myzus persicae*	Turnip Yellow Virus (TuYV)	(Nancarrow et al. 2022)
		Cucumber mosaic virus	(Ali et al. 2021, Blackman & Eastop 2000, Naga et al. 2020, Capinera 2001, Eigenbrode et al. 2002, Qi et al. 2021)
		Potato leafroll virus (PLV)	
		Lettuce mosaic virus	
		Watermelon mosaic viruses	
		Potato virus Y (PVY)	
		Beet Yellow Virus (BYV)	(Hossain et al. 2021)
		Pea Enation Mosaic Virus(PEMV)	(Doumayrou et al. 2016)
		Potato Leafroll Virus (PLRV)	(Kumar et al. 2020)
		Tobacco necrotic dwarf virus (TNDV)	(Tolin 2008)
2.	*Rhopalosiphum maidis*	Sunflower Mosaic Virus(SMV)	(Gulya et al. 2002)
		Johnsongrass mosaic virus (JGMV), Maize dwarf mosaic virus (MDMV), Sugarcane mosaic virus (SCMV), and Sorghum mosaic virus (SRMV)	(Klein & Smith 2020)
3.	*Lipaphis erysimi*	Turnip mosaic virus	(Devi et al. 2004)
		Cauliflower mosaic virus Caulimovirus	(Adhab & Schoelz 2015)

neurotoxic impact, and fatality, have been observed in beneficial insects, birds, amphibians, and mammals. Inappropriate use of those toxicants and their persistence have become a significant threat to the environment (Singh et al. 2023). Because of these reasons, our focus was to find the efficacy of some novel insecticides on the aphid population, which has less hazardous consequences on the environment and other beneficial organisms of the crop ecosystem. We had planned laboratory assays for evaluating the lethal concentration. Three insecticides which are mainly novel and used by the farmers for sucking pests, especially against these aphid species, have been considered for our trials, like Flonicamid, Spirotetramat, and Imidacloprid. These chemical insecticides have a specific mode of action. Flonicamid disrupts insect chordotonal organs, and Spirotetramat acts as a lipid biosynthesis inhibitor which decreases the reproductivity and fertility of sucking insect pests (Salazar et al. 2016). Imidacloprid blocks the nicotinic acetylcholine receptor in the central nervous system. Because of this mode of action, we selected these insecticides in the present study to assess their bio-efficacy.

MATERIALS AND METHODS

Experiments of the relative toxicity of insecticides were carried out in the laboratory of the Department of Entomology, Lovely Professional University, Phagwara (Punjab) (31.2560°N, 75.7051°E). *R. maidis, L. erysimi, and M. persicae* populations were collected from their host plant, *viz*., maize, mustard, and potato, respectively. The Species of the aphids, *R. maidis, L. erysimi*, and *M. persicae*, were collected in different seasons. *R. maidis* was collected in the *Kharif* season (June-October), and *M. persicae* and *L. erysimi* were collected in the *Rabi* season (November-April). These species of aphids were collected from the field of the university and its nearby places. *R. maidis* species were collected from the maize, and *M. persicae* was collected from the field of the Potato. *L.erysimi* species were collected from the mustard crop of LPU fields. These aphid species were identified morphologically by using taxonomic keys. We reared *R. maidis* on the leaves of maize or corn, and *M. persicae* on the flower and leaves of the potato, *L. erysimi* on the floral part of the mustard plant in laboratory conditions, where the incubator temperature was atat ± 25°. Required insecticides for the evaluation of toxicity are enlisted in Table 3.

Table 3: Different insecticides were used for the evaluation.

Trade Name	Active ingredient	Company
Shandor	Imidacloprid 17.8% SL	Shanro Agritech
Ulala	Flonicamid 50 WG	UPL
Movento	Spirotetramat 15.31% OD	Bayer

Insecticidal Bioassay

The bioassay process was conducted according to the leaf dip method as given by the IRAC test method with some modifications (https://irac-online.org/methods/aphids-adultnymphs/). The healthy leaves of the different hosts of aphids were collected from the field and washed thoroughly. Later, different concentration levels of each formulation were made by diluting it in distilled water. After that, we make the leaf disc or stripes as per the suitability of the host's leaf. One end of these stripes was covered with a wet cotton plug to avoid dryness. Later on, each bunch of stripes or discs was dipped or treated with insecticide concentrations for 15-20 seconds. The treated leaves were dried up for 15 to 20 minutes. After the drying of treated leaf stripes or discs, those were placed onto the paper cups. On each bunch, 20 apterous aphids of the 3rd nymphal instar were transferred on the treated leaves with the help of a fine pointed brush. The paper cups were covered with a muslin cloth. The cups were further kept in the incubator at ± 25°C and 65 ± 10% relative humidity (RH), with a 16:8 h (L:D) photoperiod. The observation was recorded periodically after 24 hours. The response of aphids was categorized as the live, morbid, and dead insects. Aphids were considered alive if they showed movements or held themselves normally. If their movements or posture are abnormal then those were considered morbid.

Statistical Analysis

The result was interpreted by using percentage mortality and control treatment mortality by using corrected mortality by using Abott's formula (Abbott 1925).

$$\text{Corrected mortality \%} = \frac{\text{Test mortality (\%) - Control mortality (\%)}}{100 - \text{Control mortality (\%)}}$$

The mortality data was calculated by Probit analysis by using Finney's table for the transformation of the percentage of mortality. The statistical analysis was done by using the Poloplus software (2.0 version).

RESULTS

There are differences between the responses of the *R.maidis, M. persicae,* and *L. erysimi* populations against tested chemicals, showing a change in the sensitivity to insecticides within the different species.

Relative Toxicity of Insecticides Against *R. maidis*

Laboratory bioassay revealed that Spirotetramat is the most toxic insecticide against *R. maidis,* with an LC_{50} value of

Table 4: Relative toxicity of the tested insecticides against R. maidis, M. persicae, and L. erysimi with values of LC_{50} and LC_{90}.

Sr. No.	Insecticide	LC_{50} ppm	Fiducial limit 95% Ppm	LC_{90} ppm	Chi-square value	df	Heterogeneity
R. maidis							
1	Flonicamid	4.20	2.93-5.31	12.00	3.21	3	1.07
2	Spirotetramat	0.68	0.55-0.832	1.38	3.08	3	1.03
3	Imidacloprid	6.33	5.55-7.11	14.38	2.94	3	0.98
M. persicae							
1	Flonicamid	5.12	2.60-7.61	18.43	4.82	3	1.61
2	Spirotetramat	3.99	2.70-5.30	11.49	3.98	3	1.33
3	Imidacloprid	5.14	4.40- 5.90	14.69	1.54	3	0.51
L. erysimi							
1	Flonicamid	5.79	3.01- 7.89	11.53	5.26	3	1.76
2	Spirotetramat	15.19	14.40- 15.90	21.49	1.76	3	0.59
3	Imidacloprid	10.86	5.27-14.39	30.26	5.92	3	1.97

0.68 ppm and an LC_{90} value of 1.38 ppm when compared with imidacloprid and Flonicamid (Table 4). Whereas the toxicity level of Imidacloprid and Flonicamid was comparatively less, with an LC_{50} value of 6.33 and 4.20 ppm, respectively. LC_{90} values were found at 13.61 and 13.46 ppm, respectively. However, there is a minute difference in the toxicity level of Imidacloprid and Flonicamid. Dose dose-specific response of the aphids against each level of concentration of insecticides was graphically presented in (Fig.1).

Relative Toxicity of Insecticides against *M. persicae*

Relative toxicity of the insecticides against *M. persicae* was analyzed, and the outcomes showed that Spirotetramat was the most toxic insecticide with a value of LC_{50} at 3.99 ppm (fiducial limit 1.55-7.44), and the insecticidal response was

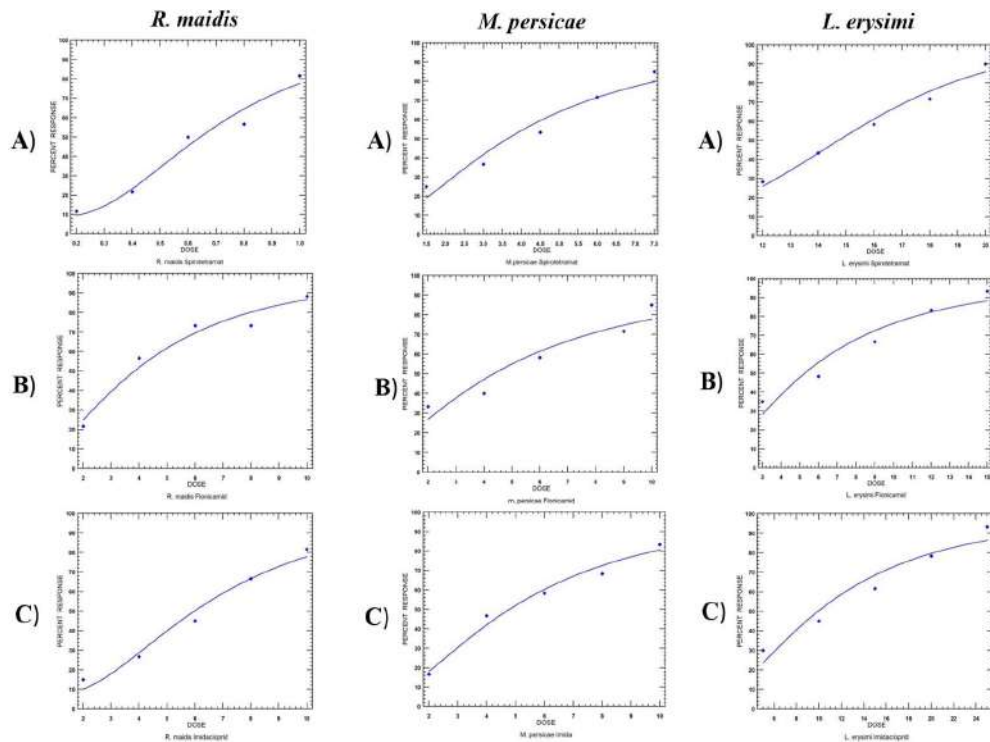

Fig. 1: Graphical representation of the insecticidal responses of the R. maidis, M. persicae, and L. erysimi against insecticides A) Spirotetramat B) Flonicamid C) Imidacloprid. Where response showed the mortality percentage of aphids against each insecticide with their particular level of concentration.

also analyzed in (Fig.1). Bioassay findings of Imidacloprid was evaluated, and the resulted toxicity level was found with an LC_{50} value of 5.14 ppm (Table 4). Flonicamid was found to the toxic as compared to Spirotetramat, with an LC_{50} value of 5.12 ppm. The LC_{90} values of Spirotetramat, Flonicamid, and Imidacloprid were found as 11.49, 18.43, and 14.69 ppm, respectively.

Relative Toxicity of Insecticides against *L. erysimi*

The results of the laboratory bioassay indicate that Flonicamid was found to be the most effective insecticide against *L. erysimi* with an LC_{50} value of 5.79 ppm and LC_{90} value of 11.53 ppm (fiducial limit of 3.01-7.89 ppm) (Table 4). The toxicity level of Imidacloprid showed an LC_{50} value of 10.86 ppm and an LC_{90} value of 30.26 ppm. The effect of the Spirotetramat was seen as less toxic, with LC_{50} value at 15.19 ppm and LC_{90} at 21.49 ppm. At the same time, the toxicity level of Flonicamid was more than the toxicity level of Imidacloprid and Spirotetramat. The insecticidal response of *L. erysimi* against tested formulations is represented in (Fig. 1).

Among all the tested insecticides against different aphid species, our results indicated that Spirotetramat was the most toxic insecticide against *R. maidis* and *M. persicae* with an LC_{50} value of 0.68 and 3.99 ppm except in the case of *L. erysimi*. However, Flonicamide was found to be the most toxic against *L. erysimi*. As per the estimated LC_{50} values, Flonicamid was found to be the second most toxic insecticide against *R. maidis* and *M. persicae*, with an LC_{50} Value of 4.20 and 5.12 ppm, respectively, where Imidacloprid was found to be as least toxic as compared to the other tested insecticides.

Median Lethal Time (LT_{50} and LT_{90}) for Aphid Species Treated with Different Insecticides

In this study, we evaluate the median lethal time LT_{50} and LT_{90} for aphid species *R. maidis*, *M. persicae*, and *L. erysimi* were treated with the insecticides *viz.* Spirotetramat, Flonicamid, and Imidacloprid. We checked the LT_{50} values of the mentioned insecticide based on the LC_{50} value of each insecticide.

In the case of *R.maidis,* for the bioassay, we prepared levels of concentrations of insecticides as Imidacloprid (6.33 ppm), Floniamid (4.20 ppm), and Spirotetramat (0.68 ppm). Here, laboratory bioassay results indicated that Imidacloprid is the most effective insecticide with an LT_{50} value of 44.53 h. (fiducial limit 33.89-57.88 h) and LT_{90} value at 112.16 h. followed by Flonicamide and Spirotetramat with an LT_{50} value of 58.30 and 64.30 h, respectively, and the LT_{90} values of the insecticides are 144.58 and 162.48 h, respectively (Table 5).

In the case of *M. persicae*, the concentration levels of Imidacloprid (5.14 ppm), Flonicamid (5.12 ppm), and Spirotetramat (3.99 ppm) were used for the assessment of LT_{50} values. After the treatment of insecticides, we observed the duration-wise mortality. The findings of the bioassay showed that the lethal time (LT_{50}) for Imidacloprid was determined to be 49.19 h with a fiducial limit ranging from 39.50 to 61.31 h and LT_{90} value at 173.06 h (Table 5). The LT_{50} values of the Flonicamid and Spirotetramat are 57.45 and 61.99 h, respectively, whereas LT_{90} values are 162.19 and 172.15 h, respectively. However, there is a slight difference between the LT_{50} values of Flonicamid and Imidacloprid.

In the case of *L. erysimi*, the prepared concentrations of Imidacloprid (10.86 ppm), Flonicamid (5.79 ppm), and Spiroteramat (15.19 ppm) were used for the laboratory bioassay. The result indicated that imidacloprid has an LT_{50} at 44.90 h, where the fiducial limit ranges from

Table 5: Relative toxicity of insecticides against different aphid species with the value of an LT_{50} (Median lethal time).

Sr. No.	Insecticide	LT_{50} h	Fiducial limit 95% h	LT_{90} h	Chi-square value	*df*	Heterogeneity
R. maidis							
1	Flonicamid	58.30	36.49-83.24	144.58	3.00	3	1.00
2	Spirotetramat	64.30	51.93-85.18	162.48	6.64	6	1.10
3	Imidacloprid	44.53	33.85-57.88	112.16	5.74	5	1.14
M. persicae							
1	Flonicamid	57.45	44.23-71.85	162.19	2.83	3	0.94
2	Spirotetramat	61.99	52.10-76.48	172.15	3.91	6	0.98
3	Imidacloprid	49.19	39.50-61.31	173.06	1.953	6	0.32
L. erysimi							
1	Flonicamid	47.82	33.32-61.23	156.97	2.47	3	0.82
2	Spirotetramat	49.54	32.84-63.25	189.61	2.96	3	0.98
3	Imidacloprid	44.90	25.29-61.24	208.14	2.73	3	0.91

25.29 to 61.24 h, and has an LT_{90} at 208.14 h. The LT_{50} values of the Flonicamid and Spirotetramat were found at 47.82 and 49.54 h, and the LT_{90} values were 156.97 and 189.61 h, respectively.

According to the results of the median lethal time (LT_{50}), Imidacloprid was found to be the most effective insecticide against *R. maidis*, *M. persicae*, and *L. erysimi,* with an LT_{50} value of 44.53, 49.19, 44.90 h., respectively. Next in the line, Flonicamid, found as the second most effective insecticide against the aphid species with LT_{50} values, was 58.30 h. (*R. maidis*), 57.45 h (*M. persicae*), and 47.82 h. (*L. erysimi*). Interestingly, we observed that in the results of relative toxicity, Spirotetramat was found as the most toxic insecticide, but as per the median lethal time, it was observed as the less effective as compared to the other insecticides with LT_{50} values of 64.30, 61.99, and 49.54 against the *R. maidis*, *M. persicae*, and *L. erysimi* respectively.

DISCUSSION

Selected novel insecticides have different modes of action, and they belong to different classes of insecticides. Spirotetramat belongs to a class known as tetronic acid derivative, which acts as a lipid biosynthesis inhibitor (Brück et al. 2009), whereas Flonicamid belongs to pyridine carboxamides, which mainly acts as an antifeedant and has a unique mode of action targeted to the nervous system of insects (Morita et al. 2007) and Imidacloprid belongs to the neonicotinoid class which mainly targets the nervous system of insects by acting as nicotinic acetylcholine receptor (nAChR) agonists (Bass et al. 2015). Due to these unique modes of action, these insecticides exhibit high insecticidal effectiveness as compared to other synthetic insecticides since we are focusing on these insecticides for our experiment.

The studies carried out by Nauen et al. (2008) showed that Spirotetramat is considered a wide-spectrum insecticide with a new mode of action and is effective against different hemipteran insects, *viz.,* aphids, whiteflies, and psyllids. Also, in a similar research performed by Laurent et al. (2023), it was shown that Spirotetramat and Flonicamid insecticides are effective in controlling aphid species up to 85.6% and 79.9%, respectively, in cabbage crops. The result showed the efficacy of Spirotetramat against *R. maidis*, *M. persicae*, and *L. erysimi* with an LC_{50} value of (0.68, 3.99, and 15.19 ppm, respectively). The present findings are supported by the study conducted by Iftikhar et al. (2022), who showed the efficacy of Spirotetramat 240 SC against cabbage aphids (*B. brassicae*) with an LC_{50} value of 1.304 mgL^{-1}. Udtewar et al. (2021) reported that Flonicamid has a high toxicity level against *R. maidis* with an LC_{50} value of 6.682 ppm, and also

recorded that Imidacloprid was less toxic as compared to Flonicamid with an LC_{50} value of 9.028 ppm. As per these results, our study showed a similar trend, with an LC_{50} value of Flonicamid (4.20 ppm) and Imidacloprid (6.33 ppm) against *R. maidis*. In the findings of Neupane and Subedi (2022), the evaluation of insecticidal efficacy against *R. maidis* revealed that the field efficacy of Flonicamid was the most effective insecticide against *R. maidis* and also showed low colony percentage (2.85%), aphid score (2.63%), aphid infestation per plant (7.33%) and high yield production 7904 kg.ha^{-1} with a dose of 0.5 g.ha^{-1}.

As per the studies of Umina et al. (2022), the toxicity of Spirotetramat 240 SC against collected populations of *Myzus persicae* from different locations was assessed. The LC_{50} values were found to be 0.095, 0.571, 13.121, 1.515, and 2.447 mg.L^{-1}. According to the study conducted by Naga et al. (2021), their laboratory experiment revealed that Flonicamid was a toxic insecticide against a laboratory population and Jalandhar population of *M. persicae* with an LC_{50} value of 1.195 and 28.420 ppm, respectively, which in line with present finding. Imidacloprid showed toxicity with an LC_{50} value of 4.214 ppm against a laboratory population, while the LC_{50} against the Jalandhar population was 53.345 ppm, which is also in accordance with the Laboratory population of our study, where the LC_{50} value of the Flonicamid and Imidacloprid was 5.12 and 5.14 ppm respectively against *M. persicae*. Similarly, Halder and Rai (2018) observed an LC_{50} value of 19.17 ppm for Flonicamid against *M. persicae*, and Imidacloprid showed toxicity with an LC_{50} at 5.019 ppm. However, in this study, Imidacloprid was found to be the most toxic insecticide against *M. persicae*.

The studies of Udtewar et al.(2021) reported that Flonicamid was a toxic insecticide against *L. erysimi* with an LC_{50} value of 10.829 ppm and an LC_{50} value of Imidacloprid at 17.968 ppm. Similarly, an experiment conducted by Halder & Rai (2018) indicated that Imidacloprid was more toxic as compared to Flonicamid, with an LC_{50} value of 5.197 ppm and Flonicamide, with LC_{50} at 33.09 ppm. As per our results of toxicity, Floniamid was found as the most toxic insecticide against *L. erysimi,* with an LC_{50} value of 5.79 ppm, and Imidacloprid, with an LC_{50} of 10.86 ppm, respectively.

CONCLUSION

In general, the research highlights the toxicity level of the different insecticides against different species of aphids. The results indicated fluctuation in the effectiveness of the Spirotetramat, Imidacloprid, and Flonicamid when observed in the insect population and species.

We found that Spiroteramat is a highly toxic insecticide against the *R. maidis* and *M. persicae* because of the distinct mode of action. Whereas, the toxicity level of the Flonicamid is higher in the case of *L. erysimi*. These insecticide has different modes of action and can be used as alternatives in the insect pest management of different crops. The use of regular insecticides over the years causes, increases the resistance capacity of many insect pests. Therefore use of novel and efficient insecticides with proper doses is of utmost importance to combat resistance problems. We found that Imidacloprid showed 50% mortality within a short duration of time. Although Flonicamid 50 WG, Spirotetramat 15.31% OD, and Imidacloprid 17.8% SL, these novel insecticides are suitable and efficient insecticides for managing aphid infestations depending on aphid species, their efficiency level may differ. Hence, advocating proper insecticides for chemical management and employing rotation of the insecticides and the use of newer molecules with unique modes of action could be the safer strategy to counteract with development of resistance in the aphid populations.

ACKNOWLEDGMENT

REFERENCES

Abbott, W.S., 1925. A method of computing the effectiveness of an insecticide. *Journal of Economic Entomology*, 18(2), pp.265-267.

Adhab, M.A. and Schoelz, J.E., 2015. Report of the turnip aphid, *Lipaphis erysimi* (Kaltenbach, 1843) from Missouri, USA. *Journal of Plant Protection Research,* 11, p.121.

Alam, M.J., Ahmed, K.S., Hoque, M., Mansura, A., Rony, M.N.H. and Haque, M.S., 2019. Bio-efficacy of some bio-pesticides against maize aphid, *Rhopalosiphum maidis*, a threatening pest of maize. *Journal of Science, Technology and Environment Informatics*, 8(01), pp.563-573.

Alam, M.J., Ahmed, K.S., Hoque, M., Mansura, A., Rony, M.N.H. and Haque, M.S., 2019. Bio-efficacy of some bio-pesticides against maize aphid, *Rhopalosiphum maidis*, a threatening pest of maize. *Journal of Science, Technology and Environment Informatics*, 8(01), pp.563-573.

Alam, M.J., Mukta, L.N., Nahar, N., Haque, M.S. and Razib, S.M.H., 2020. Management practices of aphid (*Rhopalosiphum maidis*) in an infested maize field. *Bangladesh Journal of Environmental Science*, 38, pp.23-28.

Al-Eryan, M.A.S. and El-Tabbakh, S.S., 2004. Forecasting yield of corn, *Zea mays* infested with corn leaf aphid, *Rhopalosiphum maidis*. *Journal of Applied Entomology*, 128(4), pp.312-315.

Ali, J., Covaci, A.D., Roberts, J.M., Sobhy, I.S., Kirk, W.D. and Bruce, T.J., 2021. Effects of cis-jasmone treatment of brassicas on interactions with *Myzus persicae* aphids and their parasitoid *Diaeretiella rapae*. *Frontiers in Plant Science*, 12, p.711896.

Bass, C., Denholm, I., Williamson, M.S. and Nauen, R., 2015. The global status of insect resistance to neonicotinoid insecticides. *Pesticide Biochemistry and Physiology*, 121, pp.78-87.

Bass, C., Puinean, A.M., Zimmer, C.T., Denholm, I., Field, L.M., Foster, S.P., Gutbrod, O., Nauen, R., Slater, R. and Williamson, M.S., 2014. The evolution of insecticide resistance in the peach potato aphid, *Myzus persicae*. *Insect Biochemistry and Molecular Biology*, 51, pp.41-51.

Bhatia, S.K., Young, W.R., Phadke, K.G. and Srivastava, A.N., 1973. Control of corn leaf aphid on barley in India. *Journal of Economic Entomology*, 66(2), pp.463-467.

Blackman, R.L. and Eastop, V.F., 2000. *Aphids on the World's Crops: An Identification and Information Guide*. Springer

Brar, K.S., Bakhetia, D.R.C. and Sekhon, B.S., 1987. Estimation of losses in yield of rapeseed and mustard due to mustard aphid. *Journal of Oilseeds Research (India)*, 4(2), pp.65-73.

Brück, E., Elbert, A., Fischer, R., Krueger, S., Kühnhold, J., Klueken, A.M. and van Waetermeulen, X., 2009. Movento®, an innovative ambimobile insecticide for sucking insect pest control in agriculture: biological profile and field performance. *Crop Protection*, 28(10), pp.838-844.

Bunker, G.K., Rana, B.S. and Ameto, O.P., 2006. Efficacy of some plant products against mustard aphid, *Lipaphis erysimi* (Kalt.) under different intercropping systems. *Pestology*, 6, pp.28-32.

Capinera, J.L., 2001. Green peach aphid, *Myzus persicae* (Sulzer)(Insecta: Hemiptera: Aphididae). Panama City, FL, USA: University of Florida Cooperative Extension Service, Institute of Food and Agricultural Sciences, EDIS.

Devi, P.S., Bhat, A.I., Devi, L.R. and Das, M.L., 2004. Occurrence, transmission, and genotype response of a filamentous virus associated with leaf mustard (*Brassica juncea* var. rugosa) in Manipur. *Indian Phytopathology*, 57(4), pp.488-493.

Dewhirst, S.Y., Pickett, J.A. and Hardie, J., 2010. Aphid pheromones. *Vitamins & Hormones*, 83, pp.551-574.

Dhillon, M.K., Singh, N. and Yadava, D.K., 2022. Preventable yield losses and management of mustard aphid *Lipaphis erysimi* (Kaltenbach) in different cultivars of *Brassica juncea* (L.) Czern & Coss. *Crop Protection*, 161, p.106070.

Doumayrou, J., Sheber, M., Bonning, B.C. and Miller, W.A., 2016. Role of pea enation mosaic virus coat protein in the host plant and aphid vector. *Viruses*, 8(11), p.312.

Eigenbrode, S.D., Ding, H., Shiel, P. and Berger, P.H., 2002. Volatiles from potato plants infected with the potato leafroll virus attract and arrest the virus vector *Myzus persicae* (Homoptera: Aphididae). *Proceedings of the Royal Society of London. Series B: Biological Sciences*, 269(1490), pp.455-460.

Gautam, M.P., Singh, S.N., Kumar, P., Yadav, S.K., Singh, D.P. and Pandey, M.K., 2019. Mustard aphid, *Lipaphis erysimi* (Kalt)(Hemiptera: Aphididae): A review. *The Pharma Innovation Journal*, 8(9), pp.90-95.

Gavkare, O., Kumar, S., Sharma, N. and Sharma, P.L., 2013. Evaluation of some novel insecticides against *Myzus persicae* (Sulzer). *The Bioscan*, 8(3), pp.1119-1121.

Gulya, T.J., Shiel, P.J., Freeman, T., Jordan, R.L., Isakeit, T. and Berger, P.H., 2002. Host range and characterization of Sunflower mosaic virus. *Phytopathology*, 92(7), pp.694-702.

Halder, J. and Rai, A.B., 2018. Aphidicidal activity of some systemic insecticides and change in susceptibility level of *Myzus persicae* Sulzer in the vegetable ecosystem in Varanasi, India. *Pesticide Research Journal*, 30(2), pp.219-223.

Harris, K.F. and Maramorosch, K., eds., 2014. *Aphids as Virus Vectors*. Elsevier.

Hossain, R., Menzel, W., Lachmann, C. and Varrelmann, M., 2021. New insights into virus yellows distribution in Europe and effects of beet yellows virus, beet mild yellowing virus, and beet chlorosis virus on sugar beet yield following field inoculation. *Plant Pathology*, 70(3), pp.584-593.

Iftikhar, A., Hafeez, F., Aziz, M.A., Hashim, M., Naeem, A., Yousaf, H.K.,

Saleem, M.J., Hussain, S., Hafeez, M., Ali, Q. and Rehman, M., 2022. Assessment of sublethal and transgenerational effects of spirotetramat on population growth of cabbage aphid, *Brevicoryne brassicae* L. (Hemiptera: Aphididae). *Frontiers in Physiology*, 13, p.1014190.

Kieckhefer, R.W. and Kantack, B.H., 1980. Losses in yield in spring wheat in South Dakota caused by cereal aphids. *Journal of Economic Entomology*, 73(4), pp.582-585.

Klein, P. and Smith, C.M., 2020. Host plant selection and virus transmission by *Rhopalosiphum maidis* are conditioned by potyvirus infection in *Sorghum bicolor*. *Arthropod-Plant Interactions*, 14(6), pp.811-823.

Koramutla, M.K., Aminedi, R. and Bhattacharya, R., 2016. A comprehensive evaluation of candidate reference genes for qRT-PCR studies of gene expression in mustard aphid, *Lipaphis erysimi* (Kalt). *Scientific Reports*, 6(1), p.25883.

Kreuze, J.F., Souza-Dias, J.A.C., Jeevalatha, A., Figueira, A.R., Valkonen, J.P.T. and Jones, R.A.C., 2020. *The Potato Crop: Its Agricultural, Nutritional and Social Contribution to Humankind*. Springer, pp.389-430.

Kular, J. and Kumar, S., 2011. Quantification of avoidable yield losses in oilseed Brassica caused by insect pests. *Journal of Plant Protection Research*, 51, pp.11-17. 10.2478/v10045-011-0007-y.

Kumar, P., Kaur, J., Suby, S.B., Sekhar, J.C. and Lakshmi, S.P., 2018. *Pests and Their Management*, Oxford Publications, pp.51-79.

Kumar, R.R., Ansar, M., Rajani, K., Kumar, J. and Ranjan, T., 2020. First report on the molecular basis of potato leaf roll virus (PLRV) aggravation by the combined effect of tuber and prevailing aphid. *BMC Research Notes*, 13, pp.1-4.

Laurent, A., Favrot, A., Maupas, F., Royer, C. and Makowski, D., 2023. Assessment of non-neonicotinoid treatments against aphids on sugar beets. *Crop Protection*, 164, p.106140.

Maanju, S., Jasrotia, P., Yadav, S.S., Kashyap, P.L., Kumar, S., Jat, M.K., Lal, C., Sharma, P., Singh, G. and Singh, G.P., 2023. Deciphering the genetic diversity and population structure of wild barley germplasm against corn leaf aphid, *Rhopalosiphum maidis* (Fitch). *Scientific Reports*, 13(1), p.17313.

Morita, M., Ueda, T., Yoneda, T., Koyanagi, T. and Haga, T., 2007. Flonicamid is a novel insecticide with a rapid inhibitory effect on aphid feeding. *Pesticide Science*, 63(10), pp.969-973.

Murty, B.N., Jain, K.B.L., Mathur, V.S., Gulati, S.C. and Satyawali, D., 1968. Aphid resistance in barley, *Crop Protection*, 18, pp.21-36.

Naga, K.C., Buckseth, T., Subhash, S., Bairwa, A., Verma, G., Kumar, R., Malik, K., Sharma, S. and Chakrabarti, S.K., 2020. Transmission efficiency of Potato leaf roll virus (PLRV) by potato aphid *Aulacorthum solani* and green peach aphid *Myzus persicae*. *Indian Journal of Entomology*, 82(1), pp.68-71.

Naga, K.C., Kumar, A., Tiwari, R.K., Kumar, R., Subhash, S., Verma, G. and Sharma, S., 2021. Evaluation of newer insecticides for the management of *Myzus persicae* (Sulzer). *Executive Council*, p.161.

Nancarrow, N., Aftab, M., Hollaway, G., Rodoni, B. and Trębicki, P., 2022. Symptomless turnip yellows virus infection causes grain yield loss in lentil and field pea: A three-year field study in south-eastern Australia. *Frontiers in Plant Science*, 13, p.1049905.

Nauen, R., Reckmann, U., Thomzik, J. and Thielert, W., 2008. Biological profile of spirotetramat (Movento®)–a new two-way systemic (ambimobile) insecticide against sucking pest species. *Bayer CropScience Journal*, 61(2), pp.245-278.

Neupane, S. and Subedi, S., 2022. Evaluation of insecticidal efficacy against maize leaf aphid [*Rhopalosiphum maidis* (Fitch)] under inner terai condition of Nepal. *Archives of Agriculture and Environmental Science*, 7(4), pp.601-605.

Pointeau, S., Jaguenet, E., Couty, A., Dubois, F., Rambaud, C. and Ameline, A., 2014. Differential performance and behavior of the corn leaf aphid, *Rhopalosiphum maidis*, on three species of the biomass crop miscanthus. *Industrial Crops and Products*, 54, pp.135-141.

Qi, Y.H., He, Y.J., Wang, X., Zhang, C.X., Chen, J.P., Lu, G. and Li, J.M., 2021. Physical contact transmission of Cucumber green mottle mosaic virus by *Myzus persicae*. *PLOS One*, 16(6), p.e0252856.

Salazar-López, N.J., Aldana-Madrid, M.L., Silveira-Gramont, M.I. and Aguiar, J.L., 2016. *Spirotetramat*. London, IntechOpen, pp.41-55.

Sharma, S., Sood, A.K. and Ghongade, D.S., 2022. Assessment of losses inflicted by the aphid *Myzus persicae* (Sulzer) to sweet pepper under a protected environment in the northwestern Indian Himalayan region. *Phytoparasitica*, 50(1), pp.51-62.

Sidauruk, L. and Sipayung, P., 2018, November. The population of *Myzus persicae* (Sulzer) and insect diversity on intercropping potatoes with other plants that were planted at different times. *IOP Conference Series: Earth and Environmental Science*, 205, p. 012018

Singh, A., Singh, A., Singh, A., Singh, P., Singh, V., Singh, Y. and Chauhan, A., 2023. Chemistry, Metabolism, and neurotoxicity of organophosphorus insecticides: A review. *Nature Environment & Pollution Technology*, 22(4).

Singh, C.P. and Sachan, G.C., 1999, September. Ecofriendly management of *Lipaphis erysimi* (Kalt.) in *Brassica carinata*. In: *Proceedings of the 10th International Rapeseed Congress*, Canberra, Australia, The Regional Institute Ltd., pp. 26-29.

So, Y.S., Ji, H.C. and Brewbaker, J.L., 2010. Resistance to corn leaf aphid (*Rhopalosiphum maidis* Fitch) in tropical corn (*Zea mays* L.). *Euphytica*, 172, pp.373-381.

Srigiriraju, L., Semtner, P.J. anderson, T.D. and Bloomquist, J.R., 2010. Monitoring for MACE resistance in the tobacco-adapted form of the green peach aphid, *Myzus persicae* (Sulzer)(Hemiptera: Aphididae) in the eastern United States. *Crop Protection*, 29(2), pp.197-202.

Subedi, S., 2015. A review of important maize diseases and their management in Nepal. *Pest Management*, 6(4), pp.181-196

Udtewar, P.G., Bhede, B.V. and Khandare, A.S., 2021. Relative toxicity of insecticides against various species of aphids. *The Pharma Innovation Journal*, SP-10(10), pp.417-420.

Umina, P.A., Bass, C., van Rooyen, A., Chirgwin, E., Arthur, A.L., Pym, A., Mackisack, J., Mathews, A. and Kirkland, L., 2022. Spirotetramat resistance in *Myzus persicae* (Sulzer) (Hemiptera: Aphididae) and its association with the presence of the A2666V mutation. *Pest Management Science*, 78(11), pp.4822-4831.

Van Emden, H.F., 2017. Integrated pest management of aphids and introduction to IPM case studies. *Plos One*, 75, pp.6512-6523.

Using Immobilized Algae (*Scenendesmus quadricauda*) to Reduce Copper Element Toxicity in Common Carp Fish (*Cyprinus carpio*)

Athraa Ismaal, Jasim M. Salman† [ID] **and Moayed J. Yass**

Department of Biology, College of Science, University of Babylon, Iraq

†Corresponding author: Jasim M. Salman; jasimsalman@uobabylon.edu.iq

ABSTRACT

The study assessed the efficiency of immobilized algae (*Scenedesmus quadricauda* (Turpin) Brébisson) in treating copper toxicity in common carp fish. Acute toxicity of copper towards carp fish was determined. Fish were exposed in aqueous tanks to different heavy metal concentrations (10, 15, 25, and 35 ppm) for 96 h to examine their response. The lethal concentration (LC50) of copper for common carp over 96 h was found to be 1.4 ppm, with fish mortality increasing gradually with higher metal concentrations. Subsequently, half of the LC50 concentration (0.7 ppm) was used as a chronic toxicity concentration, and fish were treated for 21 days to assess copper accumulation in their gills and muscles. Copper concentration in gills on day 5 of the experiment was 16.89 ± 2.2 mg.kg^{-1} (Mean ± S.D), a significant increase from in muscles, which recorded 10.72 ± 1.1 mg.kg^{-1} (Mean ± S.D). On day 21, the copper concentration decreased significantly in both gills (4.73 ± 0.5 mg.kg^{-1}) and muscles (8.4 ± 4.5 mg.kg^{-1}) compared to the control group (significant LSD 0.05). But the copper and algae group recorded on day 21 of the experiment (a significant decrease LSD 0.05) in both the gills (mg.kg^{-1}) Mean± S.D (4.73 ± 0.5) and the muscles (mg.kg^{-1}) Mean± S.D (8.4 ± 4.5) compared to the copper group. The removal rate in the gills was 75.57%, and in the muscles was 21.17%. Therefore, treatment with immobilized algae is an efficient and promising method for treating copper toxicity in aquatic environments.

Copyright: © 2025 by the authors
Licensee: Technoscience Publications
This article is an open access article distributed under the terms and conditions of the Creative Commons Attribution (CC BY) license (https://creativecommons.org/licenses/by/4.0/).

INTRODUCTION

Heavy metal pollution in water bodies is a major concern and has a serious impact on associated organisms, especially fish (Shahjahan et al. 2022). Heavy metals enter aquatic systems, dissolve in the water, and easily accumulate in various parts of aquatic organisms, including algae, bivalves, and fish, and then enter the contaminated fish's consumers (Cordoba-Tovar et al. 2022). Some HMs, including cobalt, copper, chromium, iron, manganese, molybdenum, nickel, selenium, and zinc, are toxic to organisms (Ogbuene et al. 2024).

Heavy metals can damage the fish's nervous system, which negatively disrupts the fish's interaction with the surrounding environment (Jamil et al. 2023).

Copper is a bioactive trace metal in aquatic environments and an important micronutrient for many aquatic species. It is an essential micronutrient that plays an important role as a cofactor in critical enzyme reactions related to body processes essential for survival in both humans and animals (Stern et al. 2010). The presence of excessive amounts of copper in the fish diet reduced fish appetite, which negatively affected feed utilization and fish growth (Takasusuki et al. 2004). Moreover, copper toxicity not only led to malformation of the reproductive organs but also led to a significant decrease in the fertility, fertilization, and hatching rates of many fish species (Forouhar et al. 2020).

Copper accumulates in fish when they are exposed to copper in high concentrations. Fish typically consume copper for metabolic functions; However,

it becomes toxic if fish are exposed to a higher concentration for a longer period. The gills are the first organ to accumulate heavy metals at a level above the concentration that is considered toxic through absorption along the surface of the gills, gut wall, and muscles (Annabi et al. 2013). The Copper accumulation is then distributed and bioaccumulated in major organs of fish, including the liver, spleen, and kidneys, and is transmitted through the blood (Tao et al. 2002).

Although many physical and chemical methods are available to remove these toxic heavy metals, most of these techniques appear ineffective when metal concentrations are less than 100 mg.L^{-1} (Salman et al. 2022). Since many heavy metals are water-soluble and dissolve in contaminated water, it is difficult to separate them by applying physical methods (Ahluwalia & Goyal 2007). In this case, biological methods such as bioremediation can be an attractive solution to correct the natural state of the environment from heavy metal pollution. The bioremediation process is very effective in reducing the toxicity of heavy metals by converting them into less harmful forms with the help of certain organisms or their enzymes to reduce pollution. This is an environmentally friendly and cost-effective way to revitalize the polluted environment (Ma et al. 2016).

Many biological agents are used to remove heavy metals from the aquatic environment (Tarekegn et al. 2020). Although heavy metals are usually toxic, organisms have developed specific resistance mechanisms and complex intracellular pathways. To utilize and detoxify heavy metals (de Alencar et al. 2017).

Algae are used in biotechnology to remove heavy metals from polluted aquatic environments because it has exhibit high biosorption capacity, allowing them to remove toxic heavy metals such as cadmium, copper, and lead (Abbas et al. 2014, Cirillo et al. 2012). This degradation is attributed to their ability to photosynthesize and secrete oxygen (Salman et al. 2023a), which leads to the breakdown of toxic organic elements, including heavy metals (Kumar et al. 2021). The removal mechanisms are the use of the algal cell wall containing substances such as fucoidan and alginate that act as heavy metal binding sites (Park et al. 2016, Mantzorou et al. 2018). In addition, algae produce compounds such as metallothioneins and phytochelatins that help in safely converting and storing heavy metals (Perales-Vela et al. 2006). Algae also exhibit cellular defense mechanisms that include anti-free radical systems, which help them adapt to the toxicity of heavy metals such as copper, such as superoxide dismutase (SOD) and catalase (CAT) activity (Morelli & Scarano 2004).

To overcome this problem, the culture of immobilized algae has been proposed in which the algae are trapped within a polymeric matrix that allows nutrient access, improves nutrient removal efficiency, resists toxins, and protects them from predators (de-Bashan & Bashan 2010). Natural polymers such as alginate are commonly used in these matrices due to their availability, non-toxicity, and allowing the light transmittance necessary for photosynthesis processes (Moreno-Garrido 2008).

Immobilized algae systems have been tested by numerous studies for their efficiency in removing heavy metals. Significant uptake of Co, Zn, and Mn has been reported for Chlorella salina cells bound in alginate beads (Garnham et al. 1992). In another study, alginate beads of restricted algae *S. quadricauda* were used to monitor water quality in fish (tilapia) farming(Chen (2001); also, many studies deal with study the role of immobilized algae in removing pharmaceutical waste and evaluate to reduce toxicity by these algae (Obaid et al. 2024b, Obaid et al. 2023, Salman et al. 2022).

This study aims to evaluate the toxicological properties of common carp fish after exposure to copper, evaluate the extent of copper bioaccumulation in the gills and muscles of fish, and the ability of immobilized algae (*S. quadricauda*) to reduce copper toxicity in fish.

MATERIALS AND METHODS

Collecting and Acclimating Fish Samples

The fish used in this study, common carp (*Cyprinuscarpio* Linnaeus), was obtained from a fish farm. The primary types of nets used for fishing are drift nets, surrounding nets, and trap nets on Al-Mahawil regain from Babil Governorate, middle of Iraq. The samples were transferred using plastic containers to the Advanced Environmental Laboratory in the Department of Biology, College of Science.   The experiment was conducted in December 2023 and February 2024. Healthy fish were selected, and abnormal fish were excluded. The fish were acclimated to laboratory conditions for 21 days in aerated dechlorinated freshwater, changed every 48 h, and were fed twice daily with commercial fish food (Mostakim et al. 2015).

The fish samples were placed in an oval-shaped plastic aquarium with a capacity of 100 liters. Oxygen was maintained continuously for an average of 24 hours per day by aerating the containers. Chlorine-free water was used by storing tap water in tanks for 72 hours. The water temperature is adjusted using the air conditioner in the laboratory. Throughout the experiment, the water was changed every 48 hours.

Preparation of Heavy Metal Solutions

To prepare 1000 mL of a 0.1 mol.L^{-1} solution of Copper(II)

nitrate, we have to dissolve 29.5646 g of $Cu(NO_3)_2 \times 6H_2O$ (100 % purity) in deionized or distilled water. After the solid is completely dissolved, dilute the solution to a final volume with deionized (distilled) water to prepare (10,15,20,25,35) mg.L^{-1} from $Cu(NO_3)_2$.

Preparation of Green Algal Media

Chu-10 modified growth media for green algae was used, and 2.5 mL of each stock solution was taken and supplemented to 1 L of distilled water, then sterilized using an autoclave, except for the stock solution (K_2HPO_4), which was added at the end after sterilization to obtain 1 liter of Chu-10. The pH of Chu-10 was adjusted to 6.4 using 0.01(N) NaOH or HCl, and the medium was left until the next day for use in algal growth (Kasim et al. 1999).

Preparation of Immobilized Algae

A 10 mL of algal cultured was placed in a beaker containing 100 mL of Chu-10 medium and cultured for 15 days under controlled conditions of 286 µE.m^{2}.s^{-1}, a light-dark period of 16:8 h, and a temperature of 25± 2°C in a growth chamber (Chia et al. 2013). Then, 100 mL of cultured algae were placed in a beaker with 1000 mL of Chu-10 medium and incubated for 14 days (Tredici 2004). Each 50 mL algal sample taken in stationary phase at 12 and 14 days was centrifuged for 15 min at 3000 rpm to prepare immobilized algae with the following steps:

1. The concentrated algae were taken, an equal amount of sodium alginate solution (2%) was added, and it was shaken well to homogenize the ingredients.

2. Then this mixture (algae and alginates) is placed in a medical syringe or separating funnel. The mixture is dripped drop by drop into a beaker containing a 3% solution of calcium chloride with constant stirring. It is noted that the drops that come down from the syringe solidify in the calcium chloride solution, and then we use a tea strainer to remove the beads (frozen organisms) from the calcium chloride solution. It is then preserved in distilled water in a cold place (Adlercreutz & Mattiasson 1982, Al Mosawi et al. 2022).

Water Quality

Water temperature, electrical conductivity, salinity, and pH were measured directly by a portable digital multimeter, Model 340i h SET, WTW, made in Germany after titration with standard solutions at (4.1, 7, 10.1) and a special buffer solution.

Estimation of LC$_{50}$

Healthy and active fish were common carp (*Cyprinus carpio*) (n = 72), with total length and weight of fish of 18.5 ± 1.45 cm and 89.8 ± 5.6 g, respectively, and were kept in continuously aerated aquariums for laboratory acclimation. Conditions for 2 weeks under controlled natural lighting (12:12 h, light-dark).

The water in the containers was continuously oxygenated (air bubble drivers), and the water was replaced every 48 hours. The temperature was maintained at 19 ± 2 °C. For acclimation and experimental periods, commercial fish food was given to fish twice a day, but fish were deprived of food for 24 hours before the experiment and throughout the acute toxicity test (Mostakim et al. 2015).

The fish were exposed to different concentrations (10, 15, 20, 25, and 35 mg.L^{-1}) of copper in the form of copper nitrate Cu $(NO_3)_2$.

To determine LC$_{50}$ values for 96 h. Three aquaria were used for each concentration, each containing six fish in 70 L of dechlorinated tap water (Svoboda et al. 2001). One control group contained the same number of fish and the same volume of water but without Copper. Before planting the fish in the container, copper is added, and the water is aerated for an hour to distribute the element homogeneously in the water. In addition, the water in the container is replaced every 48 hours.

Mortality was recorded 24, 48, 72, and 96 h after exposure. Dead fish were removed to avoid possible deterioration in water quality (Gooley 2001). The lethal concentration (LC50) for 96 h was calculated using the probit method (Finney 1971). The water is changed every 48 hours, according to (Reish & Oshida 1987), who emphasized that the concentration in aquariums must be re-concentrated.

Sub-Chronic Toxicity

Fish were exposed to 0.7 ppm Cu consecutively for 21 days as a sub-lethal concentration to estimate the chronic toxic effect using 35 experimental organisms.

Removal Efficiency (R.E.)

$$R.E.\% = \frac{C1 - C2}{C1} \times 100$$

Where: R.E%: Removal efficiency, Cl: Heavy metal concentration before treatment, C2: Heavy metal concentration after treatment (Al Mosawi et al. 2022).

Estimation of Copper Residues in Fish

Heavy metals were determined in fish samples (collected, dried, and ground), where the fishmeal was digested by the acid digestion method (APHA 2017).

Where 3 g of the fish sample powder to be digested was placed inside a volumetric flask (25 mL), then (3 mL) of concentrated Perchloric acid solution ($HClO_4$) was added to it. The beaker was covered using an hourglass bottle, and it was heated quietly on a hot plate, and we raised the temperature. Heat gradually until the digestion process is complete. When the mixture reaches the dryness stage, we leave the cup to cool and add again (3 mL) of concentrated nitric acid solution (HNO_3). Cover the cup and continue heating until the digestion process ends, as obtain a mixture consisting of delicate colors, and a light one is called (a light-colored digester). Also, evaporate it until the dryness stage, and add 5 mL of hydrochloric acid (HCl) solution diluted with water in a ratio (1:1), then heat it so that the sample remaining after digestion dissolves, then add distilled water. The filtration process was carried out to eliminate remaining and insoluble substances, and the volume of the solution was adjusted according to the expected concentration in the samples to a volume of 100 mL, 50 mL, or less so that the sample is ready for analysis using an atomic absorption spectrophotometer (Shimadzu AA 7000).

Statistical Analysis

This study used the analysis of variance (ANOVA), LSD, median, standard deviation, minimum, and maximum to find the significance among the study variances by using SPSS statistical program software (version 17).

RESULTS

Water Quality in the Aquarium

The water quality result had the following characteristics:

Table 1: The log of concentration and probit mortality for *C. carpio*.

Concentration mg.L^{-1}	Log of Concentration	Mortality rates %	Probit Mortality
0	0	0%	0
10	1	0	0
15	1.176091	20	4.16
25	1.39794	40	4.75
35	1.544068	60	5.25

pH 8.5±0.3, temperature 19±2°C, dissolved oxygen 6.4± 0.45 mg.L^{-1}, salinity 1.2±0.1 %0 ,E.C. 2360 ± 48 μS.cm^{-1}.

Lethal Concentration 50 (LC$_{50}$)

The half-lethal concentration (LC$_{50}$) of C. carpio was calculated within 96 h, and different concentrations of copper were used (10, 15, 25, and 35 ppm). It was observed that the rate of fish mortality increased with an increase in the copper concentration and duration of exposure. The concentration and probit mortality rate were recorded in Table 1.

The LC$_{50}$ was determined by plotting a log graph of the concentration against the probate mortality of *C. carpio* exposed to copper (Fig. 1), and then the LC50 was calculated from the straight line equation and found to be 1.4 ppm. The fish were exposed for 21 days (chronic exposure) to a single concentration of 50% of the lethal dose (0.7 ppm).

Estimation of Copper Residues in Fish

The concentration of copper in the gills and muscles of the control group, the copper group, the copper group, and the restricted algae is shown in Table 2 and Figs. 2 and 3. The concentration of copper in the gills was significantly higher

y = 8.8004x - 7.7203
R² = 0.7736

Series1, 1.397940009, 4.75
Series1, 1.176091259, 4.16
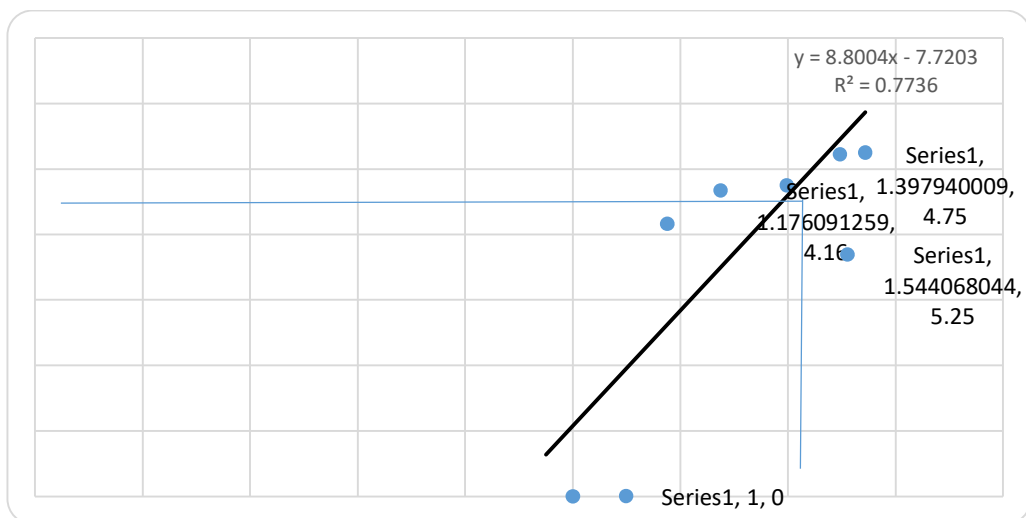Series1, 1.544068044, 5.25
Series1, 1, 0

Fig. 1: Linear regression of toxicity in *C. carpio* exposed to copper (y = probability, X = concentration).

than in the muscles at different times after treatment in all groups in the experimental groups, and it was statistically significant (LSD 0.05).

The amount of copper remaining in the gills of the fish in the copper-treated group recorded a Mean ±S.D. of 16.89±2.2 on the fifth day of the experiment, a significant increase (LSD 0.05) compared to the control group of 1.45±0.2 Mean ±S.D. As for the twenty-first day of the experiment, the copper group recorded a Mean ±S.D. 8.11±1.9 Significant increase (LSD 0.05) compared to the control group 1.33±0.19 Mean±S.D. The amount of residual copper in the gills of the fish of the copper and restricted algae group, Mean±S.D., was 19.02±2.6. On the fifth day of the experiment, a significant increase was recorded (LSD 0.05) compared to the copper group, Mean±S.D., 16.89±2.2. On the twenty-first day of the experiment, the copper and algae group recorded a Restricted Mean±S.D 4.73±0.5 Significant decrease LSD 0.05) compared to the copper group Mean±S.D 8.11±1.9.

The amount of copper remaining in the muscles of the fish in the copper-treated group recorded a Mean ±S.D of 10.72±1.1 on the fifth day of the experiment, a significant increase (LSD) (0.05) compared to the control group (0.81±0.02 Mean ±S.D), while on the twenty-first day of the experiment the copper group recorded a Mean ±S.D. 6.33±1.8 Significant increase (LSD 0.05) compared to the control group 0.57±0.01 Mean±S.D. The amount of copper remaining in the muscles of the fish of the copper and restricted algae group, Mean±S.D., was 6.17±1.3. On the fifth day of the experiment, a significant decrease (LSD 0.05) was recorded compared to the copper group, Mean±S.D.,

Table 2: Copper residues (mg.L^{-1}) in the gills and muscles of carp fish in the copper group, copper with immobilized algae group, and the control group.

Parameters	Treatment (A)	Cu [mg.kg^{-1}]	
	Day (B)	Gills	Muscles
		Mean±S.D	
Control	5	1.45±0.2	0.81±0.02
	21	1.33±0.1	0.57±0.01
Fish +Cu	5	16.89±2.2	10.72±1.1
	21	8.11±1.9	6.33±1.8
Fish +Cu+ Immobilized algae	5	19.02±2.6	6.17±1.3
	21	4.73±0.5	8.45±1.7
LSD(0.05) (A*B)		3.011	4.165

Table 3: Concentration of copper (mg.L^{-1}) before & after treatment and removal efficiency of immobilized algae.

Treatment	Gills	Muscles
Cu group (day-5)	16.89±2.2Mean± S.D	10.72±1.1Mean± S.D
Cu + algae group (day-21)	4.73±0.5Mean± S.D	8.45±1.7Mean± S.D
Removal Efficiency%	75.57	21.17

10.72±1.1. On the twenty-first day of the experiment, the copper and algae group recorded Restricted Mean±S.D 8.45±1.7 Non-significant increase compared with the copper group Mean±S.D 6.33±1.8.

DISCUSSION

Despite the importance of copper as a micronutrient in the metabolism of aquatic organisms, several studies have shown
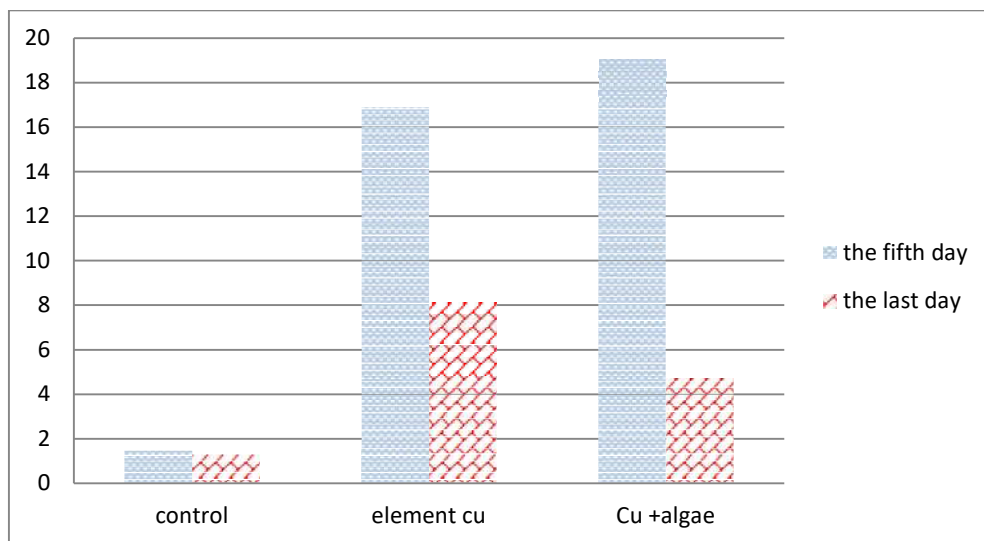

Fig. 2: Accumulation of copper (Cu) in the gills of common carp fish after exposure to copper.
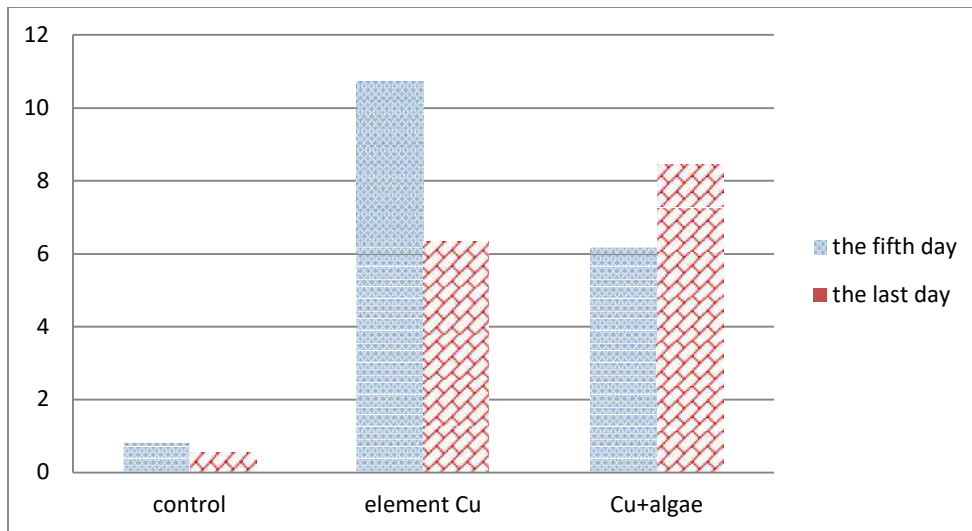
Fig. 3: Accumulation of copper (Cu) in the muscles of common carp fish after exposure to copper.

that even in very low concentrations, this mineral may affect fish survival (Farhangi & Jafaryan 2019). Human activities can release copper into the environment, especially into the land. Mining operations, along with incineration, are the main sources of copper release. Release into water occurs from the weathering of soil, industrial discharge, sewage treatment plants, and antifouling paints (Comber et al. 2022).

In the present study, the 96-hour LC_{50} value of copper was found to be 1.4 ppm by the probit-phenylic analysis method to evaluate the data of the acute toxicity bioassay. Based on these results, it was found that there is a positive relationship between concentration levels and mortality rate. When the concentration level increased, the mortality rate also increased. The mortality rate was also related to the retention time of the copper in the water, as the longer the retention time of the copper in the water, the greater the mortality rate of the fish (Yustiati et al. 2024).

In a study by Goswami et al. (2021), carp fish were exposed to seven different concentrations of copper sulfate. It was found that the average lethal concentration (LC_{50}) of copper in Amur carp fish for 96 h was 1.811. It was also noted that as the metal concentration increased, fish mortality also gradually increased. Other studies showed that (carp fish were exposed to seven different concentrations of copper. It was found that the average lethal concentration (LC50) of copper in *Cyprinuscarpio* L. for 96 h was 2.65 mg.L^{-1} (Al-Tamimi & Al-Azzawi 2015).

Mariyappan & Karuppasamy (2014) found that the mean LC50 of copper for *Cyprinus carpio* L. was 38.36 mg.L^{-1}. This variation in toxicity is due to several factors, such as the sensitivity of the test organisms, which is reflected in their tolerance to toxic substances; The size of the organisms used in each bioassay; and the subjective factors of each individual (Farhangi & Jafaryan 2019).

Fish are naturally exposed to a variety of metals, including essential and non-essential elements. Copper is one of the essential minerals that, after being absorbed from the gills and intestines, is transported by metallothionein into the blood circulation, and some of it accumulates in various internal organs such as the liver, kidneys, and muscles (Peyghan et al. 2003). According to the results, the copper concentration in the gills in the 21st tom of the experiment was Mean ±S.D 6.33±1.8 in all groups. Since the gills are directly exposed to water and thus to toxic compounds, the percentage of pollutants in them is greater than that in the muscles (De Sousa et al. 1981). The present study results on the twenty-first day of the experiment are consistent with Kareem et al. (2022). Note that the concentration of some heavy metals in the muscles is 6.22 (1.45) (mg.kg^{-1}) Mean (SD) and gills Mean (SD). 7.03 (0.95) (mg.kg^{-1}) for common carp (*Cyprinus carpio*) from Dokan Lake, Sulaymaniyah, Iraq. As well as an approach to the results of Sobhanardakani & Jafari (2014), it was found that the copper concentration in the muscles of *Cyprinus carpio* fish h g was 4.0±1.0 in Tahm Dam Lake, Iran.

The reason for the difference in results may be due to the size of the fish and the conditions of the study environment. A decrease in copper accumulation was observed on the twenty-first day of the experiment compared to the fifth day of the experiment in the gills and muscles, indicating that fish can reduce copper accumulation through several strategies, as fish increase the production of copper-binding proteins,

such as metallothionein, to reduce its toxic effect, as well as increase the production of copper-binding proteins. Copper excretion rates through the gills and kidneys for elimination (Kamunde et al. 2002). It increases the production of antioxidants such as glutathione to protect against oxidative copper damage (Monteiro et al. 2005).

According to US EPA standards, the maximum permissible concentration of lead is 0.015 mg.L^{-1} as it tends to have a high biological half-life thanks to its non-biodegradable nature, causing bioaccumulation and biomagnification in the food chain, which leads to serious environmental and health consequences (Obaid et al. 2024a). Many techniques are implemented to remove heavy metal ions, which are broadly classified as physical, chemical, and biological methods. Traditional physical and chemical methods are very expensive, inoperable at low concentrations of heavy metals below 100 mg.L^{-1}, and release hazardous derivatives solvents. In high quantities that are harmful to the environment, bioremediation is one of the most environmentally friendly and sustainable ways to reduce aquatic pollution, which plays an important role in improving the production of associated aquaculture systems (Jeyakumar et al. 2023).

Bioremediation of water contaminated with heavy metals using immobilized algae inside a polymeric matrix of alginate that allows the access of nutrients improves the efficiency of nutrient removal, resists toxins, and protects it from predators. These algae can be easily removed from the environment after treatment (Salman et al. 2023b), and therefore, it is an effective way to reduce the toxicity of heavy metals (de-Bashan & Bashan 2010).

In the current study, the group of copper and restricted algae, we observed an insignificant increase (LSD 0.05) in the concentration of copper in the gills on the fifth day of the experiment, 19.02±2.6 Mean±S.D (mg.kg^{-1}) compared to the copper group, 16.89±2.2 Mean±S.D (mg.kg^{-1}).

The reason for this increase despite treatment with algae is the short treatment time (5 days). On the twenty-first day of the experiment, the concentration of residual copper in the gills of the fish of the copper group and the restricted algae was 4.73±0.5 Mean±S.D. mg.kg^{-1}. The treatment with algae led to There was a significant decrease in LSD (0.05) compared to the copper group 8.11±1.9 Mean±S.D (mg.kg^{-1}).

As for the muscles in the copper and algae-restricted group, we noticed a decrease in the copper concentration (LSD 0.05) on the fifth day of the experiment, 6.17±1.3 Mean±S.D (mg.kg^{-1}), compared to the copper group, 10.72±1.1 Mean±S.D (mg.kg^{-1}). This indicates the ability of algae to reduce the amount of copper in the water, which

leads to a reduction in the amount of copper in the muscles. On day 21 of the experiment, an insignificant increase in copper concentration was recorded in the copper and algae group, 8.45±1.7 Mean±S.D (mg.kg^{-1}) compared to the copper group. This indicates that copper accumulation in the muscles is processed more slowly compared to the gills. The accumulation of heavy metals causes histological changes in fish muscles, providing an opportunity to assess fish health and information about potential health risks from their environment (Jaber et al. 2021). The use of natural products such as immobile algae in bioremediation is an effective way to reduce copper toxicity in aquatic environments.

A study has shown that fish can contract serious diseases such as blood poisoning when the fish are under stressful or unsuitable environmental conditions. This is considered the main cause of economic losses and public health impacts due to eating, handling, and transportation (Abaychi & Al-Saad 1988).

CONCLUSION

The presence of copper in the water of fish farms at the half-lethal concentration LC50, although it did not cause deaths in the fish, may be lead to bioaccumulation of copper in the gills and muscles of the fish, thus causing potential risk to the fish and causing economic losses and impacts on the public health of those eating these fish in the event of contamination, but it was for biological treatment. Using immobilized algae has a significant effect on reducing the amount of copper through its high ability to absorb it from polluted water. Therefore, this technique is very suitable for controlling water quality and aquaculture.

ACKNOWLEDGMENTS

REFERENCES

Abaychi, J. and Al-Saad, H.T., 1988. Trace elements in fish from the Arabian Gulf and the Shatt al-Arab River, Iraq. *Bulletin of Environmental Contamination and Toxicology,* 40, pp. 226–232.

Abbas, S.H., Ismail, I.M., Mostafa, T.M. and Sulaymon, A.H., 2014. Biosorption of heavy metals: A review. *Journal of Chemical Science and Technology,* 3, pp.74–102.

Adlercreutz, P.K. and Mattiasson, B., 1982. Oxygen supply immobilized cells: 3. Oxygen supply by hemoglobin or emulsions of perfluorochemicals. *European Journal of Applied Microbiology and Biotechnology,* 16(4), pp.165–170.

Ahluwalia, S.S. and Goyal, D., 2007. Microbial and plant-derived biomass for removal of heavy metals from wastewater. *Bioresource Technology,* 98, pp.2243–2257.

Al Mosawi, Z.H., Ajanabi, A.O. and Al Mamoori, A.M., 2022. Immobilize algae to remove copper and lead from aquatic ecosystems. *NVEO-Natural Volatiles & Essential Oils Journal*, 5, pp.850–860.

Al-Tamimi, A.H. and Al-Azzawi, A.J., 2015. The acute and chronic toxicity of copper on the behavioral responses and hematological parameters of freshwater fish, common carp (*Cyprinus carpio* L.). *Iraqi Journal of Science*, 56(4A), pp.2835–2845.

Annabi, A., Said, K. and Messaoudi, I., 2013. Cadmium: Bioaccumulation, histopathology and detoxifying mechanisms in fish. *American Journal of Research Communication*, 4(1), pp.60–79.

APHA (American Public Health Association), 2017. *Standard Methods for the Examination of Water and Wastewater*. APHA.

Chen, Y.C., 2001. Immobilized microalga *Scenedesmus quadricauda* (Chlorophyta, Chlorococcales) for long-term storage and application in water quality control in fish culture. *Aquaculture*, 195(1-2), pp.71–80.

Chia, M.A., Odoh, O.A. and Ladan, Z., 2014. The indigo blue dye decolorization potential of immobilized *Scenedesmus quadricauda*. *Water, Air, & Soil Pollution*, 225, p.19.

Cirillo, T., Amodio Cocchieri, R., Fasano, E., Lucisano, A., Tafuri, S., Ferrante, M.C., Carpenè, E., Andreani, G. and Isani, G., 2012. Cadmium accumulation and antioxidant responses in *Sparus aurata* exposed to waterborne cadmium. *Archives of Environmental Contamination and Toxicology*, 62, pp.118–126.

Comber, S., Deviller, G., Wilson, I., Peters, A., Merrington, G., Borrelli, P. and Baken, S., 2022. Sources of copper into the European aquatic environment. *Integrated Environmental Assessment and Management*, 203, pp.1031–1047.

Cordoba-Tovar, L., Marrugo-Negrete, J., Baron, P.R. and Diez, S., 2022. Drivers of biomagnification of Hg, As and Se in aquatic food webs: A review. *Environmental Research*, 204, p.112226.

de-Bashan, L.E. and Bashan, Y., 2010. Immobilized microalgae for removal of pollutants: Review of practical aspects. *Bioresource Technology*, 101, pp.1611–1627.

Farhangi, M. and Jafaryan, H., 2019. The comparison of acute toxicity (96h) of copper (CuSO₄) in *Cyprinus carpio* and *Rutilus rutilus*. *Environment and Pollution*, 8(2), pp.21–30.

Forouhar Vajargah, M., Mohamadi Yalsuyi, A., Sattari, M., Prokić, M.D. and Faggio, C., 2020. Effects of copper oxide nanoparticles (CuO-NPs) on parturition time, survival rate, and reproductive success of guppy fish (*Poecilia reticulata*). *Journal of Cluster Science*, 31, pp.499–506.

Goswami, K., Nada, V. and Ram, R.N., 2021. Estimation of median lethal concentration (LC50) and behavioral alterations of amur carp (*Cyprinus carpio haematopterus*) in response to copper sulfate. *Journal of Entomology and Zoology Studies*, 9(1), pp.469–472.

Jaber, M.M., Al-Jumaa, Z.M., Al-Taee, S.K., Nahi, H.H., Al-Hamdany, M.O., Al-Salh, M.A. and Al-Mayahi, B., 2021. Bioaccumulation of heavy metals and histopathological changes in muscles of common carp (*Cyprinus carpio* L.) in the Iraqi rivers. *Iraqi Journal of Veterinary Sciences*, 35(2), pp.245–249.

Jeyakumar, P., Demnath, C., Vijayaraghavan, R. and Muthuraj, M., 2023. Trends in bioremediation of heavy metal contaminations. *Environmental Engineering Research*, 28(4), pp.47-53.

Kamunde, C., Grosell, M., Higgs, D. and Wood, C.M., 2002. Copper metabolism in actively growing rainbow trout (*Oncorhynchus mykiss*): interactions between dietary and waterborne copper uptake. *Journal of Experimental Biology*, 205(2), pp.279-290.

Kareem, S.I., Hussein, R.H. and Rasheed, R.O., 2022. Bioaccumulation of heavy metals in common carp fish (*Cyprinus carpio*) and its relationship with the protein content. *Iraqi Journal of Veterinary Sciences*, 36(1), pp.173-178.

Kasim, T.I.H., Al-Saadi, H.A. and Salman, N.A., 1999. Production of some phytoplankton and zooplankton and their use as live food for fish larvae. *Iraqi Journal of Agriculture: Proceedings of the 2nd Scientific Conference*, 4(5), pp.188-201.

Ma, Y., Rajkumar, M., Zhang, C. and Freitas, H., 2016. The beneficial role of bacterial endophytes in heavy metal phytoremediation. *Journal of Environmental Management*, 174, pp.14-25.

Mantzorou, A., Navakoudis, E., Paschalidis, K. and Ververidis, F., 2018. Microalgae: A potential tool for remediating aquatic environments from toxic metals. *International Journal of Environmental Science and Technology*, 15, pp.1815-1830.

Mariyappan, M. and Karuppasamy, R., 2014. The acute toxicity effect of copper and cadmium in single and binary exposure on mortality rate and behavioral responses of freshwater fish (*Cyprinus carpio*). *International Journal of Current Research*, 6(3), pp. 5906-5913.

Monteiro, S.M., Mancera, J.M. and Fontaínhas-Fernandes, A., 2005. Copper-induced alterations of biochemical parameters in the gill and plasma of *Oreochromis niloticus*. *Comparative Biochemistry and Physiology Part C: Toxicology & Pharmacology*, 141(4), pp.375-383.

Moreno-Garrido, I., 2008. Microalgae immobilization: current techniques and uses. *Bioresource Technology*, 99, pp.3949-3964.

Mostakim, G.M., Zahangir, M.M., Mishu, M.M., Rahman, M.K. and Islam, M.S., 2015. Alteration of blood parameters and histoarchitecture of liver and kidney of silver barb after chronic exposure to quinalphos. *Journal of Toxicology*. https://doi.org/10.1155/2015/415984.

Obaid, Z.H., Juda, S.A., Kaizal, A.F. and Salman, J.M., 2024a. Biosynthesis of silver nanoparticles (AgNPs) from blue-green algae (*Arthrospira platensis*) and their anti-pathogenic applications. *Journal of King Saud University - Science*, 36(7), p.103264.

Obaid, Z.H., Kadhim, N.F. and Salman, J.M., 2024b. The role of *Chlorella vulgaris* in reducing some pharmaceutical wastes toxicity in clam *Pseudodontopsis euphraticus*. *Baghdad Science Journal*, 21(2), pp.0289-0304.

Obaid, Z.H., Salman, J.M. and Kadhim, N.F., 2023. Review on toxicity and removal of pharmaceutical pollutants using immobilized microalgae. *Ecological Engineering & Environmental Technology*, 6, pp.44-60.

Ogbuene, E.B., Oroke, A.M., Eze, C.T., Etuk, E., Aloh, O.G., Achoru, F.E., Ogbuka, J.C., Okolo, O.J., Ozorme, A.V., Ibekwe, C.J. and Eze, C.A., 2024. Heavy metal concentration in fish species *Clarias gariepinus* (catfish) and *Oreochromis niloticus* (Nile tilapia) from Anambra River, Nigeria. *Nature Environment & Pollution Technology*, 23(2). https://doi.org/10.46488.NEPT.2024.v23i02.052

Park, D., Reed, D.W., Yung, M., Eslamimanesh, A., Lencka, M.M., Fujita, Y., Riman, R.E., Navrotsky, A. and Jiao, Y., 2016. Bioadsorption of rare earth elements through cell surface display of lanthanide binding tags. *Environmental Science & Technology*, 50, pp.2735–2742.

Perales-Vela, H.V., Peña-Castro, J.M. and Cañizares-Villanueva, R.O., 2006. Heavy metal detoxification in eukaryotic microalgae. *Chemosphere*, 64, pp.1–10.

Peyghan, R., Razijalaly, M., Baiat, M. and Rasekh, A., 2003. Study of bioaccumulation of copper in liver and muscle of common carp *Cyprinus carpio* after copper sulfate bath. *Aquaculture International*, 11, pp. 597-604.

Salman, J.M., Kadhim, N.F. and Juda, S.A., 2022. Algal immobilization as a green technology for domestic wastewater treatment. *IOP Conference Series: Earth and Environmental Science*, 1088, p.012000.

Salman, J.M., Majrashi, N., Hassan, F.M., Al-Sabri, A., Esraa Abdul-Adel Jabar, E.A. and Ameen, F., 2023a. Cultivation of blue-green algae (*Arthrospira platensis* Gomont, 1892) in wastewater for biodiesel production. *Chemosphere*, 335, p.139107.

Salman, J.M., Obaid, Z.H. and Kadhim, N.F., 2023b. A histological study on the use of immobilized algae as bioremediators to amoxicillin in *Pseudodontopsis euphraticus*. *Mesopotamian Environment Journal*, 7(2), pp.36-45.

Shahjahan, M., Taslima, K., Rahman, M.S., Al-Emran, M., Alam, S.I. and Faggio, C., 2022. Effects of heavy metals on fish physiology—A review. *Chemosphere*, 300, p.134519.

Sobhanardakani, S. and Jafari, S.M., 2014. Investigation of As, Hg, Zn, Pb,

Cd, and Cu concentrations in muscle tissue of *Cyprinus carpio*. *Journal of Mazandaran University of Medical Sciences*, 24(116), pp.184-195.

Stern, B.R., 2010. Essentiality and toxicity in copper health risk assessment: overview, update, and regulatory considerations. *Journal of Toxicology and Environmental Health, Part A*, 73, pp.114–127.

Takasusuki, J., Araujo, M.R.R. and Fernandes, M.N., 2004. Effect of water pH on copper toxicity in the neotropical fish, *Prochilodus scrofa* (Prochilodondidae). *Bulletin of Environmental Contamination and Toxicology*, 72, pp.1075–1082.

Tao, S., Long, A., Dawson, R.W., Xu, F., Li, B., Cao, J. and Fang, J., 2002. Copper speciation and accumulation in the gill microenvironment of carp (*Cyprinus carpio*) in the presence of kaolin particles. *Archives of Environmental Contamination and Toxicology*, 42(3), pp.325–331.

Tredici, M.R., 2004. Mass production of microalgae: photobioreactors. *Handbook of Microalgal Culture: Biotechnology and Applied Phycology*, 1, pp.178–214.

Yustiati, A., Palsa, A.A., Herawati, T., Grandiosa, R., Suryadi, I.B.B. and Bari, I.N., 2024. The growth and immunity performance of Nile tilapia (*Oreochromis niloticus*) is challenged by the toxicity of bio-insecticide with active ingredients eugenol and azadirachtin. *Nature Environment & Pollution Technology*, 23(1). https://doi.org/10.46488/NEPT.2024.v23i01.007

Original Research Paper | https://doi.org/10.46488/NEPT.2025.v24i01.B4216 | Open Access Journal

Estimation of Flood Hazard Zones of Noa River Basin Using Maximum Entropy Model in GIS

Nilotpal Kalita[1†] [ORCID], **Niranjan Bhattacharjee[2]** [ORCID], **Nirmali Sarmah[2]** [ORCID] and **Manash Jyoti Nath[3]** [ORCID]

[1]Department of Geography, Nowgong Girls' College, Assam, India
[2]Department of Geography, Pandu College, Guwahati, Assam, India
[3]Department of Geography, Gauhati University, Guwahati, Assam, India
†Corresponding author: Nilotpal Kalita; nilotpalkalita4@gmail.com

Citation for the Paper:

Kalita, N., Bhattacharjee, N., Sarmah, N. and Nath, M. J., 2025. Estimation of flood hazard zones of Noa river basin using maximum entropy model in GIS. *Nature Environment and Pollution Technology*, 24(1), B4216. https://doi.org/10.46488/NEPT.2025.v24i01.B4216.

Note: From year 2025, the journal uses Article ID instead of page numbers in citation of the published articles.

ABSTRACT

This study aims to develop a comprehensive flood hazard map for effective hazard management in the Noa river basin, located in Assam, India, through the integration of Geographic Information System (GIS) tools and a Maximum Entropy (MaxEnt) model. The MaxEnt machine learning algorithm was employed, utilizing eight selected geographic and environmental parameters as predictors to generate the flood hazard map. The accuracy of the generated map was evaluated using the Area Under the Curve (AUC) metric. Key findings of the study identified elevation and slope as critical parameters in the assessment of flood risk. Results revealed that the flood hazard map produced by the MaxEnt model achieved an AUC value of 0.85, indicating high predictive accuracy. The research underscores the significance of flood hazard maps as essential tools for policymakers, enabling the identification of areas vulnerable to severe environmental and economic damage. By providing a reliable and precise assessment of flood-prone zones, this study contributes valuable insights for the formulation of effective flood management strategies and mitigation measures. The implementation of such hazard maps is crucial in enhancing preparedness and resilience against flooding events, ultimately safeguarding lives, property, and infrastructure in the Noa River basin.

INTRODUCTION

Rivers are dynamic entities having hydrologic, geomorphic, ecologic, environmental and economic significance. It causes hazards and sometimes disasters, particularly in riverine areas with high to medium rainfall and dense human habitation. However, one of the most significant developments of rivers is the flooding. Floods in some riverine areas, primarily in moist climatic regions, have been rapidly increasing, impacting various geomorphological forms and patterns. The Mangaldai Sub-division, a part of a riverine built-up plain composed of fine alluvial sediments and washed by streams like Bega-*nadi*, Nanoi, Bar-*nadi*, Mangaldai-*nadi*, and Noa-*nadi*, etc., has of late, witnessed increasing floods. The *nadi* is the local term for a river. The river Noa is causing sheet flooding, river bank erosion, and channel shifting. The alarming situation with rivers and floods as geomorphological agents in the sub-division has caused serious damage to geomorphic features, land, the habitat of floodplain dwellers, standing crops, and the environment.

Floods are a natural hazard as well as disaster that has affected human civilizations since time immemorial. They are often caused by heavy rainfall, melting of snow, storm surges, and the collapse of dams and embankments. Understanding floods is crucial for creating strategies to reduce their danger and harm (Garg & Babu 2023). Flood hazard is often referred to as the potential risk and adverse effects associated with the loss of life and property. The effects of flood

hazards can not be controlled fully, but they can be reduced or mitigated by proper planning strategies (Harshasimha & Bhatt 2023).

Anthropogenic activities such as deforestation, unsustainable agricultural practices, and construction projects can lead to the drastic modification of ecosystems (Cerdà 2007, Kavian 2017, Javidan 2021). Physical phenomena like gully erosion, landslides, and floods occur over geological timescales and exhibit variability in both time and space (Achour & Pourghasemi 2020). These are categorized as hazard events with the potential to be influenced by human activities or occur naturally (Kelarestaghi & Ahmadi 2009).

MATERIALS AND METHODS

The study employs eight spatial variables to estimate flood hazard zones in the Noa-*Nadi* river basin. Table 1 provides a list of the data sets used and their sources. All the factors were processed into a raster grid of 30-arc-second grid cells. These raster layers were then converted into the Universal Transverse Mercator spheroid with datum WGS1984.

Additional related maps were generated from SRTM DEM using appropriate spatial analysis tools in ArcGIS (Fig. 1). The spatial variables used are primarily continuous, and some of them were classified into different categories based on expert knowledge and a literature review.

Study Area

The Noa-*nadi* (Fig. 2), extending from 91°55'30" E to 92°2'30" E and 26°55'10" N to 26°21' 55" N, is a north bank tributary of the mighty Brahmaputra River in Assam, India. The basin covers an area of 241.85 sq.km, with the river stretching for about 104.275 kilometers in length. The Noa River is located in the Udalguri district (to the north) and Darrang district (to the south) in the Brahmaputra valley, Assam. It starts at 520 meters above sea level near Bhutiachang on the southern slope of the Bhutan Himalayas and has three tributaries: Bhola, Lakshmi, and Batiamari. The middle part of the river is called Kuyapani, and in the Rik Veda, it is referred to as the Anjashi River (Noa). The river separates from Khampajuli in Bhutan and bends eastward after passing Bhutiachang in Silputa Mouza. It
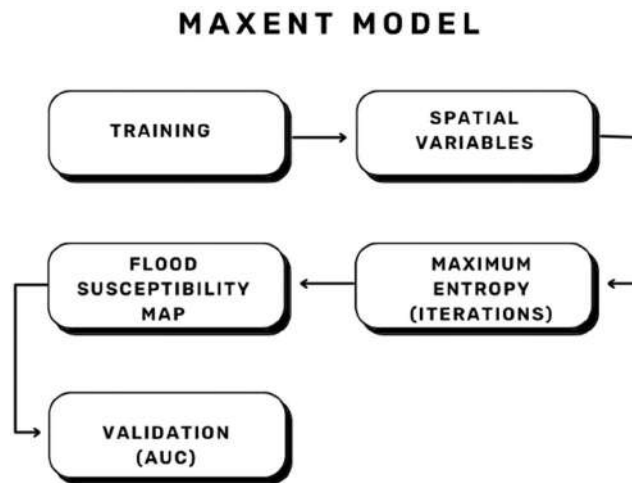
MAXENT MODEL

Fig. 1: Flowchart showing MAXENT modeling.

Table 1: List of the data sets used and their sources.

Spatial variables	Source
Elevation	worldclim.org
Slope	SRTM (Shuttle Radar Topography Mission)
Topographic Werness Index (TWI)	Derived from SRTM DEM
Soil Texture	FAO soil portal
Distance from River Channel	https://www.diva-gis.org/gdata
Distance from road	https://www.diva-gis.org/gdata
Precipitation	https://power.larc.nasa.gov/data-access-viewer/
Population density	NASA SEDAC (Socioeconomic Data and Applications Center) databases
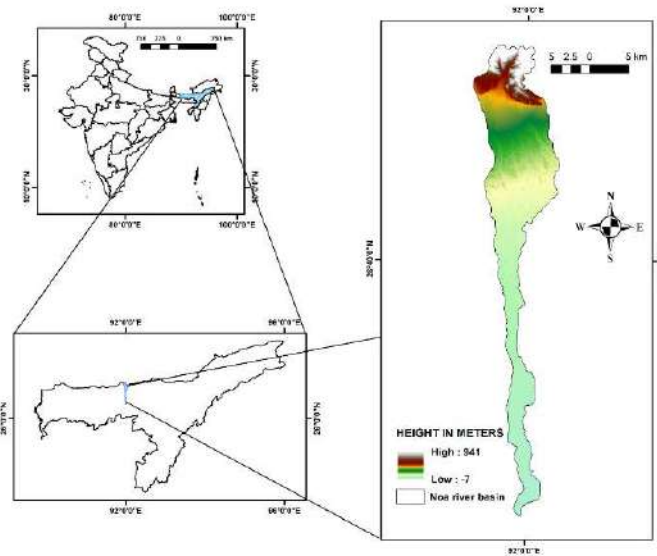
Fig. 2: Study area.

flows southward, crossing National Highway 52, and joins the Mangaldai River in Darrang district. The Noa River, like other rivers, cannot form meanders if the banks are too hard or too unstable. The elevation drops 350 meters from the Assam-Bhutan border to its mouth, giving an average gradient of 5.69 meters per kilometer. The gradient varies across different parts of the river: 10.86 meters/km in the upper part, 4.41 meters/km in the middle, and 0.76 meters/km in the lower part. The river has a mean annual maximum discharge of 73.13 cubic meters per second, a mean maximum water level of 58.33 meters, and carries 166 tons of sediment per square kilometer each year (Bhattacharjee 2008).

Spatial Variables

In this study, eight spatial variables (Fig. 4) are utilized: Elevation, Slope, Soil Texture, Topographical Wetness Index, Distance from river, Distance from road, Precipitation, and Population density.

Elevation

Elevation plays a crucial role in identifying flood hazards and mapping flood zones, especially during the monsoon season when downstream areas are at high risk due to sedimentation and increased river flow. Accurate flood mapping requires analyzing factors influencing natural and human-made hazards. Understanding elevation variation is essential for predicting flood propagation in river basins. The Elevation data is downloaded from worldclim.org, and other datasets are clipped and resampled to 1 km spatial resolution using the nearest neighbor resampling technique. Furthermore, to enable model performance, all data layers have been converted to ASCII grid format.

Slope

The topography of a region, particularly its steepness and length, significantly influences discharge and flooding. Steep or high slopes lead to rapid precipitation runoff, while low or flat slopes are susceptible to waterlogging and high infiltration. A slope map was generated using SRTM data to depict these variations in terrain.

Fig. 3: Flood point of the study area.

Topographic Wetness Index

The slope map, generated from DEM data, illustrates the topographic characteristics of the area. TWI (Topographic Wetness Index) indicates the movement of water down the slope based on gravitational forces and wetness distribution. This index, derived from DEM, plays a cr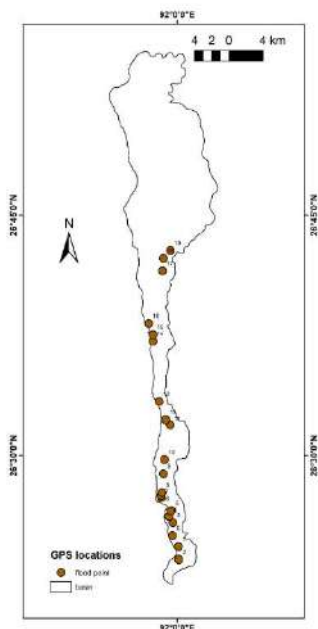ucial role in regulating surface runoff, with wetter areas experiencing higher runoff rates. Additionally, Land Use Land Cover (LULC) data is essential for understanding surface runoff regulation. The general formula of TWI is $TWI = \ln(a/\tan\beta)$. Here, a is the upslope contributing area per unit contour length, and $\tan\beta$ represents the local slope gradient.

Step for TWI in ArcGIS

DEM>Fill>FDR>Flow Accumulation>Slope in degree>Radians of slope=(slope in degree*1.570796)/90>Tan slope= con (slope>0, tan(slope),0.001)> flow accumulation scaled=(flow accumulation+1)*cell size> TWI=ln (flow accumulation scaled/tan slope).

Soil Texture

Soil texture is recognized as a significant factor influencing both infiltration and runoff generation, as well as hazard occurrence. The data for this layer was obtained from the FAO soil portal, revealing that the soil texture in the study area consists mainly of loam and clay.

- Ao- Orthic Acrisols: The Orthic Acrisols soil type is characterized by a very deep, well-drained, dark brown loamy soil.
- Rd- Dystric Regosols: These are soils made up of loose mineral material that is not too coarse and doesn't have fluvic properties.

Distance from River Channel

The distance from the river basin region to the natural drainage, including all streams and rivers in the study area, was calculated using the Euclidean Distance tool in ArcGIS. This tool provides an estimate of the distance from the river basin to the natural drainage features within the study region.

Distance from Road

In ArcGIS mapping, considering the distance from roads can be crucial for various spatial analyses and decision-making processes. The distance from roads can provide valuable insights into accessibility, infrastructure planning, environmental impact assessment, and emergency response planning. In this study, the Euclidean Distance tool is utilized as it calculates the straight-line distance from each cell in a raster to the nearest road. While it is useful for basic distance analysis, but does not consider terrain or obstacles.

Precipitation

Rainfall is a crucial factor in this study as floods primarily occur during the monsoon season, often termed "rain-induced floods." The rainfall map for the study area was created using the Inverse Distance Weighted (IDW) approach, utilizing NASA's POWER data access viewer. https://power.larc.nasa.gov/data-access-viewer/

The map reflects the annual total rainfall of the year 2020, which was selected as it was considered a particularly flood-prone year.

Population Density

Population density is a critical factor in flood vulnerability research, as it helps analyze the social loss and damage suffered by communities in flood-prone areas. The data for this study was downloaded from SEDAC databases, which are estimates for the year 2020.

MaxEnt Modeling

A field survey was conducted frequently to cover different seasons (peak monsoon months and non-monsoon months), and samples were collected at various stages from the Noa River basin (Fig. 3). Field observations were recorded in a field notebook, and photographs were taken with an SLR camera (Canon SX 530 HS). For GPS locations, a"Garmin eTrex" model was used. In the present study, 70% of each hazard dataset was considered for model construction (training), while the remaining 30% of each hazard was used for validation in Maxent. The formula of maximum entropy used in maxent is

$$P^*(z(x_i)) = \exp(z(x_i)l)/ \sum\nolimits_i \exp(z(x_i)l)$$

Here, z is a vector of environmental variables at location x_i, and l is a vector of regression coefficients.

The Maxent model (Phillips & Dudik 2008), initially conceived at the American Museum of Natural History in partnership with AT&T-Research, continues to be developed and maintained by Steven J. Phillips and his team. Introduced in 2004 by Steven J. Phillips, Miroslav Dudík, and Robert E. Schapire, Maxent employs maximum entropy-based machine learning to estimate species distribution probabilities based on environmental parameters, gaining popularity among scientists for species distribution modeling.

Model Calibration and Validation

The model was run with 500 iterations with 10 training samples and 4 test samples. The test AUC and training AUC
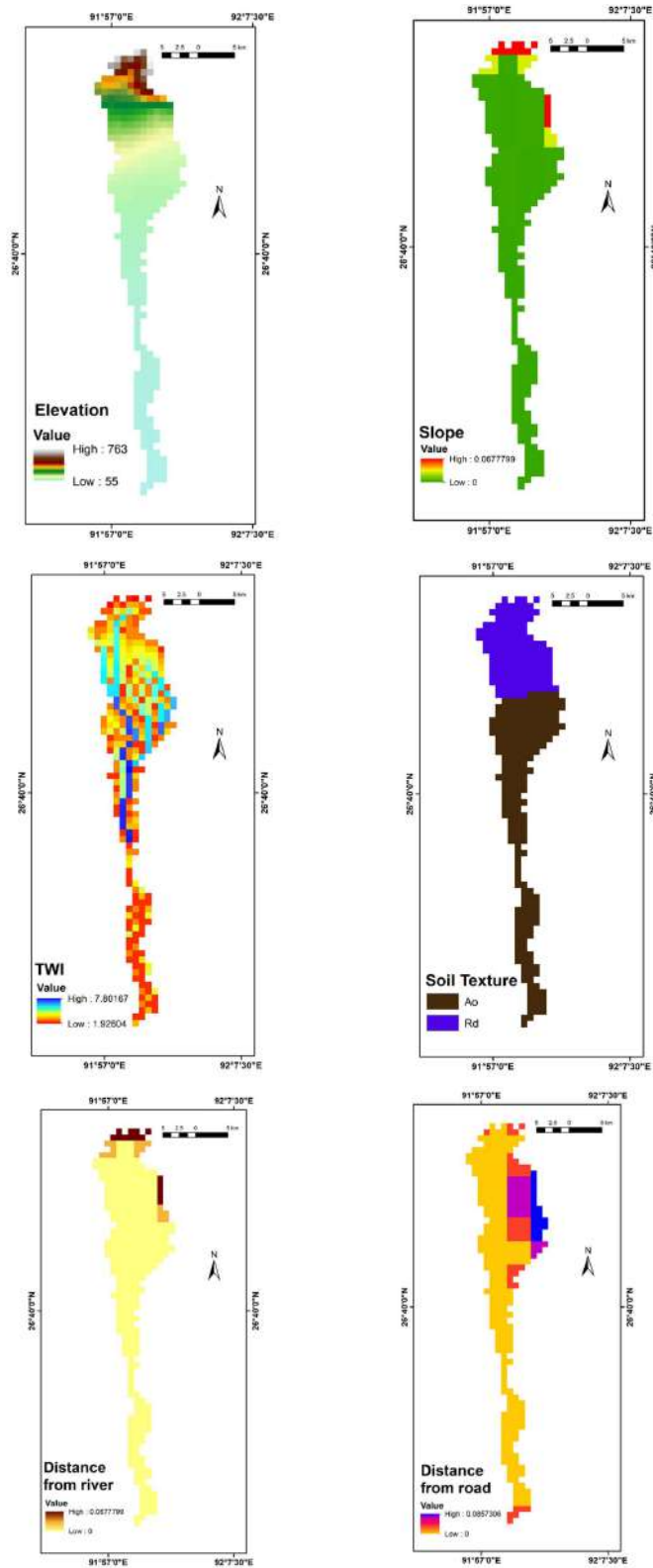
Figure Cont....
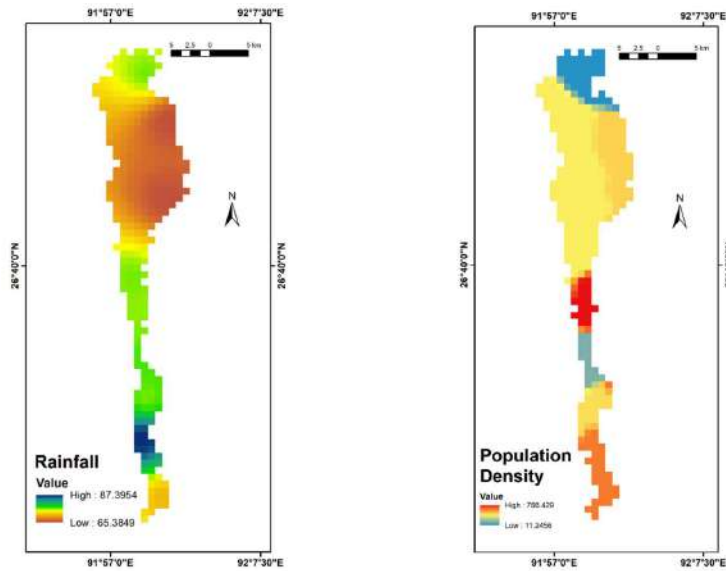
Fig. 4: Spatial variables used in MaxEnt modeling.
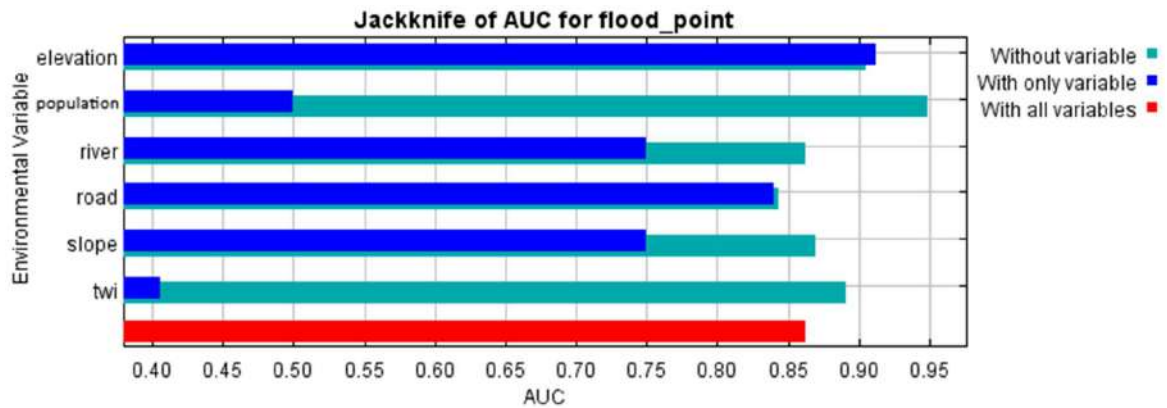
Fig. 5: Jackcknife test for evaluating the relative importance of environmental variables.

of the maxent model are both 0.85. The model utilized 10000 background points, and a total of 100 runs were conducted for the model. The area under the receiving operator curve (AUC) was used as the criterion for the goodness of fit, with the model showing the best AUC being selected for further analysis. The jackknife test (Fig. 5) was conducted to assess the importance of the variables. The final map of flood suitability was prepared with four different classes: high potential, moderate potential, low potential, and very low potential.

RESULTS AND DISCUSSION

The high flood hazard zones (Fig. 6) are estimated from the model to be within the low-lying area of the basin. The model also suggests that the soil (60% contribution) and rainfall

(32% contribution) play significant roles in the estimation of spatial distribution of the flood hazard zones. Out of the total area of 241.85 sq. Km; 48 Sq. The km (20%) area is demarcated as having good and high flood potential. The total population in the river basin was 1,28,142 persons in 2001, out of which 57,159 persons were affected by flood. By the year 2011, the population increased to 1,41,146, with 63,044 persons directly and indirectly affected by floods. The population data are extracted from the district census handbook of Assam, India.

Relevant findings were also observed from different river systems within India, including Yamuna River (Sneha et al. 2018), Subarnarekha Basin (Das & Gupta 2021), Jia Bharali (Debnath et al. 2023), Rapti River (Khan et al. 2023), Ganga River (Yaseen 2024), and many others. Most of these studies
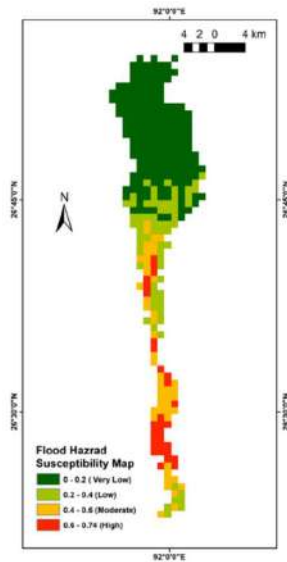
Fig. 6: Flood hazard susceptibility map.

depict flood hazards in river basins with varied topography and consistent rainfall, utilizing Analytical Hierarch Process (AHP) techniques for flood hazard mapping. However, the present study focuses on Maximum Entropy (MaxEnt) based modeling to identify probable flood hazard zones and yields similar results for the Noa basin, which is also characterized by mostly flat topography and ample rainfall (average of 210 cm).

CONCLUSION

This study is the first attempt to estimate probable flood hazard zones of the Noa river basin using Maximum Entropy modeling in GIS, integrating eight spatial variables: Elevation, Slope, Soil Texture, Topographical Wetness Index, Distance from river, Distance from road, Precipitation, and Population density. The flood hazard susceptibility map depicts flood-prone areas in mostly low-lying areas of the basin. Twenty percent of the area (48 sq. km) is affected by moderate and high floods during the monsoon months. Although this area is relatively small in percentage, the basin is highly populated (141,146 people in 2011), and 63,044 persons are affected by floods. The results generated by the MaxEnt model provide a quick estimation of the probable flood hazard zones. This is of great concern for policymakers, as it not only saves time but also provides valuable information for further investigation.

REFERENCES

Achour, Y. and Pourghasemi, H.R., 2020. How do machine learning techniques help in increasing the accuracy of landslide susceptibility maps? *Geoscience Frontiers*, 11(3), pp.871-883.

Bhattacharjee, N., 2008. Flood and Bank Erosion Problems in Darrang District, Assam: A Fluvio-Geomorphological study. Ph.D. thesis, Gauhati University, India.

Cerdà, A., 2007. Soil water erosion on road embankments in eastern Spain. *Science of the Total Environment*, 378(1-2), pp.151-155.

Das, S. and Gupta, A., 2021. Multi-criteria decision-based geospatial mapping of flood susceptibility and temporal hydro-geomorphic changes in the Subarnarekha basin, India. *Geoscience Frontiers*, 12(5), 101206.

Debnath, J., Sahariah, D., Nath, N., Saikia, A., Lahon, D., Islam, M.N. and Chand, K., 2023. Modelling on assessment of flood risk susceptibility at the Jia Bharali River basin in Eastern Himalayas by integrating multicollinearity tests and geospatial techniques. *Modeling Earth Systems and Environment*, 106, pp.1-27.

Garg, C. and Babu, A., 2023. Extreme flood calibration and simulation using a 2d hydrodynamic model under a multipurpose reservoir. *Nature Environment and Pollution Technology*, 22(2), pp.977-983.

Harshasimha, A.C. and Bhatt, C.M., 2023. Flood vulnerability mapping using maxent machine learning and analytical hierarchy process (AHP) of Kamrup Metropolitan District, Assam. *Environmental Science Proceedings*, 25(1), p.73.

Javidan, N., Kavian, A., Pourghasemi, H.R., Conoscenti, C., Jafarian, Z. and Rodrigo-Comino, J., 2021. Evaluation of multi-hazard map produced using MaxEnt machine learning technique. *Scientific Reports*, 11(1), p.6496.

Kavian, A., Hoseinpoor Sabet, S., Solaimani, K. and Jafari, B., 2017. Simulating the effects of land use changes on soil erosion using RUSLE model. *Geocarto International*, 32(1), pp.97-111.

Kelarestaghi, A. and Ahmadi, H., 2009. Landslide susceptibility analysis with a bivariate approach and GIS in Northern Iran. *Arabian Journal of Geosciences*, 2(1), pp.95-101.

Khan, R., Anwar, J., Said, S., Ansari, S., Pathan, A.I. and Sidek, L.M., 2023. GIS Based Flood Hazard and Risk Assessment Using Multi Criteria Decision Making Approach in Rapti River Watershed, India. In *International Conference on Intelligent Computing & Optimization*, pp.95-103. Cham: Springer Nature Switzerland.

Phillips, S.J. and Dudík, M., 2008. Modeling of species distributions with Maxent: new extensions and a comprehensive evaluation. *Ecography*, 31(2), pp.161-175.

Sneha, S.M., Nagar, V., Moral, S. and Teli, B., 2018. Preparation of flood model and hazard estimation on Yamuna River (using GIS and remote sensing). *International Research Journal of Engineering and Technology*, 5(3), pp.3591-3597.

Yaseen, Z.M., 2024. Flood hazards and susceptibility detection for Ganga River, Bihar state, India: Employment of remote sensing and statistical approaches. *Results in Engineering*, 21, p.101665.

Wind Analysis for Power Generation in the South of Iraq

Taghreed Ali Abbas[1][†] , Monim H. Al-Jiboori[1] and Amani I. Altmimi[2]

[1]Atmospheric Sciences Department, College of Science, Mustansiriyah University, 10011, Baghdad, Iraq

[2]Remote Sensing and Geophysics College-Al-Kharkh University, 10081, Baghdad, Iraq

†Corresponding author: Taghreed Ali Abbas; taghreed.ali891@gmail.com

ABSTRACT

The spectrum of the wind speed is expressed as the total wind speed that results from events split up into space, time, or both. It is the relationship shown between the energy or magnitude of any given parameter versus the frequency. In this study, the spectra of the wind speed at the Al-Reem site in Iraq were presented. Since the goal of the current research is to analyze wind speed and direction using the Fast-Fourier-Transform, experimental measurements for the wind speed and wind direction were taken every ten minutes for a year, from December 2014 to December 2015 at heights (10, 30, 50 m). Based on the performance of the Fast-Fourier-Transform, the peak with the highest spectral density, measured at 226,236.282 m/s at the frequency of 2 Hz, was found to be at a height of 50 m throughout the night, while the peak with the lowest height level. The spectral density was 115,863.7 m/s at a frequency of 2 Hz, at a height of (10 m) all into the night. Winds coming from the west and northwest were the most common direction in the region. In the morning, the wind was blowing faster than at night.

INTRODUCTION

The utilization of wind energy has received significant attention worldwide as a clean and renewable source of power generation. In the context of Iraq, especially the southern region, understanding wind speed characteristics is crucial for the effective deployment of wind energy conversion systems. The wind speed parameter (WS) fluctuates greatly. Using the power spectrum to explain the variable nature of wind speed is one of the most preferred approaches. Researchers, particularly those conducting wind energy evaluation studies, can greatly benefit from knowing the wind speed range (Ahmed et al. 2021). Al-Jiboori (2010) conducted a study to analyze the slow response observations for the Baghdad area and concluded that the values of the wind speed within the urban canopy are small at low levels and increase upwards.

Accurate analysis of WS in power generation systems in southern Iraq faces challenges such as the need for statistical analysis to determine wind energy potential (Jabbar 2021), the importance of selecting ideal locations and appropriate wind turbines based on estimated power and cost (Al-Rufaee et al. 2020), and the requirements for theoretical extrapolation between wind speed and height using logarithmic law and power law to calculate wind shear coefficients (Bashaer et al. 2019). Solutions include utilizing the Weibull distribution functions for statistical analysis of wind speed measurements (Mohammed et al. 2020). In 2018, Al-Jiboori et al. (2018) presented research regarding the selection of related low heights for the operation of a wind turbine in Baghdad, and the results showed that 75% of the wind at the site is not promising for wind harvesting due to the tall building and trees in the site (Al-Jiboori et al. 2018). In 2019 it is following a research paper showed that the height of 78 m at Mustansiriyah University in Baghdad is

the best height level for wind turbine generation (Hadad et al. 2019). Developing software tools (such as MATLAB) based wind energy analysis tools for in-depth wind energy analysis, turbine selection, and implementing wind energy systems in ideal locations (such as Alhay in southern Iraq) to provide sufficient electricity for cities. In 2022, Mahmoud et al. (2022) and Mishaal et al. (2020) conducted a study and concluded that the wind profile gives better results at night time.

When it comes to studying wind evaluation, the spectroscopy method is very important and effective.

The spectrum of any variable consists primarily of the total wind speed resulting from events divided in time or space or as a combination of both (Abbas et al. 2019, Hadi et al. 2020). The research was conducted to identify wind energy in the Al-Reem and Al-Shehabi regions in southern Iraq through the Iraqi Zero Map Project, which identified the Al-Reem region as a suitable area for wind energy generation (Resen 2015). In addition, Abbas et al. 2019 conducted a thorough analysis of the WS parameter in the Ali Al-Gharbi area to demonstrate the WS spectrum and concluded that WS at the Ali Al-Gharbi location has specified that it is a favorable site for utilizing wind power generation (Abbas et al. 2019). Resen (2015) studied the region and used the

WAsP model to map and analyze wind and climate. To better understand the characteristics of the wind speed in this region, this study aims to conduct a comprehensive analysis of wind speed data in the southern region of Iraq, to evaluate the characteristics of the wind spectrum for the Al-Reem region in the Maysan district of southern Iraq for the period from December 2014 to December 2015. It would make a significant contribution to our knowledge of the characteristics of the wind speed in this region.

STUDY AREA

The topography of the research area is the primary determinant of the wind assessment study. The site is situated in the Maysan Governorate. Al-Reem region is located approximately 238 kilometers away from the Iraqi capital, Baghdad, with coordinates approximately 32.27° North 46.41° East, and at an altitude of 14 m. Fig. 1 depicts the location of the chosen Al-Reem site in the southern region of Iraq. This region experiences hot desert climates (Köppen climate classification BWh-hot desert climate), characterized by hot, dry, and cool summers, just above 40°C. Winters are wet, and rainfall is greater during the winter months, averaging 177 mm annually. The area was formerly covered by marshes, which supported a variety

Table 1: Features for the researched region (Abbas et al. 2019).

Height [meter]	Daily WS [m.s^{-1}]	Standard deviation	Median	Minimum [m.sec^{-1}]	Maximum [m.sec^{-1}]
10-m	3.771	03.141	3.271	0.351	17.03
30-m	5.41	03.49	4.93	0.382	19.69
50-m	06.14	03.79	5.51	0.331	20.61

Fig. 1: Location of the chosen site (www.google earth.com).

of livelihoods. At present, the terrain consists of about 25% land and more than 50% desert. The Tigris River passes through Maysan, providing moisture to the marshes. Table 1 provides a summary of wind characteristics in this region (Resen 2015, Maysan Governorate 2024).

MATERIALS AND METHODS

A meteorological tower in Al Reem provided wind speed data, which was examined at three different altitudes (10, 30, and 50 meters) over a year. The data was reorganized and analyzed using the Origin 9.0 software to find the peak of the power spectrum. The programs Original 9.0 and Sigma Plot were used to examine the data. The meteorological mast, set up and operated by the Ministry of Science and Technology in Iraq, provided the data.

The Weibull Distribution

It is a statistical technique that can be used to determine a location's wind energy potential and evaluate the wind energy available there. Many probability functions can be employed to determine the statistical distribution of wind speed (WS) and are suitable for wind computations. With an appropriate level of accuracy, the Weibull distribution is considered the most accurate among other procedures. One benefit of this approach is that it can be used to quickly ascertain the average wind energy density for a given site (Mohammed et al. 2020). Equation (1) can be used to calculate the probability density function for wind speed (Mishaal et al. 2020, Resen 2015):

$$f(v) = \frac{k}{c} \left(\frac{v}{c}\right)^{k-1} exp\left[-\left(\frac{v}{c}\right)^k\right]$$

with $\quad k > 0, \ v > 0, \ c > 1$ …(1)

The Weibull scale parameter is represented by (c), the dimensionless Weibull shape parameter is known as (k), the recorded wind speed probability is denoted by f (v), and the wind speed is (v). The wind potential in the research area is described by the Weibull shape parameter (k) and the Weibull scale parameter (c). In simple terms, the scale parameter (c) is employed for the site consideration to show how much wind is blowing there, while the shape parameter (k) represents the peak of the wind speed (WS) distribution. (Abbas et al. 2019)

The Wind Rose

In wind assessment studies, determining the prevailing wind speed direction is crucial because it clarifies how local topography affects the wind. Using a plot known as a wind rose, which is a 360-degree cycle divided into a, 8,16, or 32 sectors, we can plot wind frequencies over a period of time

by the direction of the wind, with color sets showing ranges of the WS. This graphical tool is very useful and used in many wind studies because it may depict the wind's direction and speed at any altitude and any specific location. Table 1 illustrates how the wind speed is adjusted at heights of 10, 30, and 50 meters (Bashaer et al. 2019).

The Constructed Spectrum of Wind

Although the wind spectrum is thought to be complex, there is a form similarity when utilizing different wind speed data sets. The spectral analysis process discounts the wind energy distribution for every frequency by converting the time series of wind speed data into the wind spectrum. This is a transformation from the time domain to the frequency domain and is more accurately implemented using a mathematical tool known as the Fast-Fourier-Transform (FFT). The spectral analysis procedure is based on the theory that the wind parameter could be formulated as a constant, Gaussian random process (Abbas et al. 2019). Normally, the wind spectrum appears as a continuous curve that connects the discrete points produced by Fourier analysis (Mahmood et al. 2022).

RESULTS AND DISCUSSION

Data from the meteorological mast at the specific site, with instruments in place for at least a year for non-stop wind measurements on-site, is essential for any wind assessment to calculate and interpret wind speed. In 2015, data were collected at a height of 10 meters using a cup anemometer. The data must be sorted before any analysis can begin. To do this, a daily ten-minute dataset was normalized to average morning and night hours as well as three different height levels (10, 30, 50 m). Next, we started performing the spectrum analysis using FFT.

Wind Speed's Statistical Analysis

Data were averaged daily so that they could be processed. Then, each day was split into two sets, that is, the morning and night hours. Following that, we began the statistical analysis of the data sets, and the results are shown in Table 2 with the statistical parameters that were reached.

Table 2 shows that the highest WS was at 50 m because, at these heights, the effect of surface roughness is eliminated. The lowest daily WS was at 10 m height level for both morning and night hours. The estimated value of the average daily WS for the morning hours was 5.6 m.sec^{-1} at 50 m, while the average daily wind speed for the night hours was 6.1 m.s^{-1} at 50 m. The values of the night hours are higher than those in the morning.

Results of Weibull Distribution

The Weibull probability function has been used to estimate the frequency distributions of WS, and it is clear from the table summary and graphical result that the Weibull distribution closely matches the actual distribution data. For each height, the values of the shape parameter (k) of the Weibull function and the scale parameter (c) were determined and are shown in Table 3. According to Fig. 2, 3, and 4, the average wind speed in the Reem had the highest probability of repeating at (4.8) m.s^{-1} at 30 m. At night, the lowest is 2.1 m.s^{-1} at 10 pm.

Table 2: Wind speed's statistical measures.

| Day-hours									
Height [m]	WS [m.s^{-1}]	Maximum [m.s^{-1}]	Minimum [m.s^{-1}]	The range	The median	Standard deviation	The Skewness	Kurtosis	Confidence level (95%)
10	4.26847	13.85986	0.0075	13.852	3.86	2.771	0.9985	0.583	0.284
30	5.17	16.0018	0.01	15.9	4.75	3.07	0.99	0.60	0.31
50	5.600	17.01194	0.014	16.99	5.148	3.235	0.984	0.582	0.332
Night-hours									
10	3.215	10.09528	0.42	9.668	2.761	1.968	1.17	1.071	0.202
30	5.181	12.425	0.444	11.98	4.895	2.318	0.632	0.247	0.238
50	6.1348	13.945	0.351	13.593	5.840	2.7	0.451	0.108	0.277
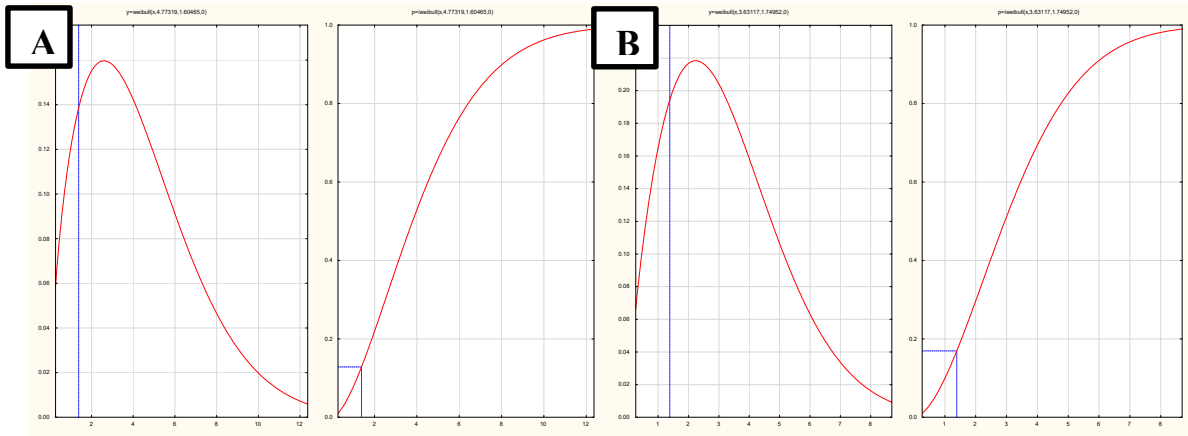
Fig. 2: The Weibull distribution for WS at 10 m throughout (A -morning time, B -night time).
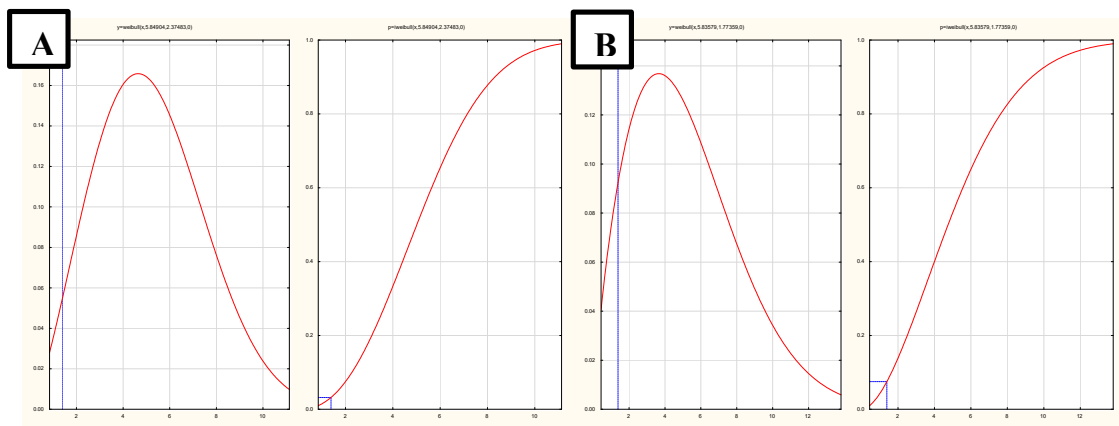
Fig. 3: The Weibull distribution for WS at 30 m throughout (A -morning time , B -night time).
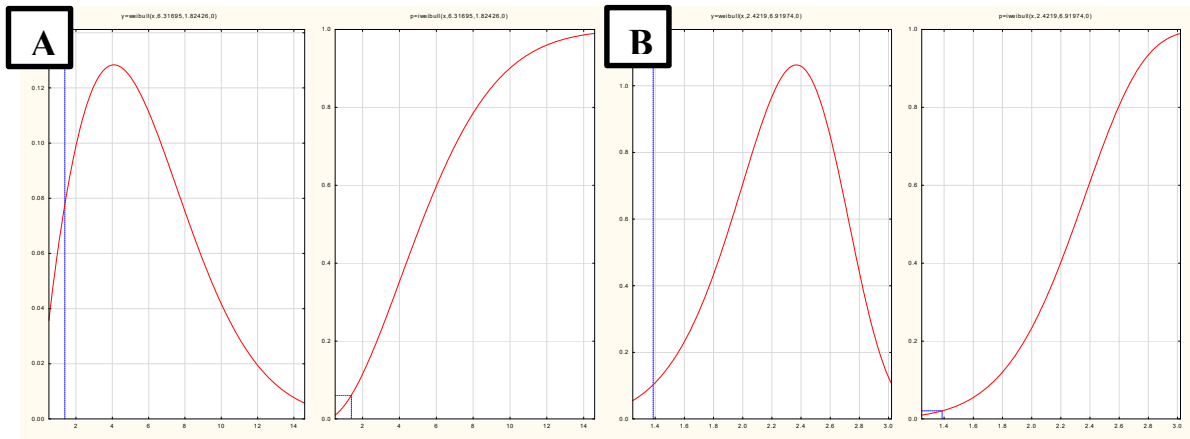
Fig. 4: The Weibull distribution for WS at 50 m throughout (A -morning time, B -night time).

Table 3: The Weibull both scale parameter and shape parameters.

The morning hours		
level (m)	The scale parameter	The shape parameter
10	4.81	1.60
30	5.93	1.82
50	6.41	1.82
The night hours		
10	3.62	1.74
30	5.92	2.37
50	7.0	2.42

The Wind Rose Analysis

Data for wind rose diagrams, which show the wind speed trend at the three chosen elevation levels as well as in the morning and at night, were collected at 10-minute intervals. Table 4 shows this as follows: For a height of 10 m, the maximum mean WS was in the 280°-300° sector with a value of 17.3 m.s^{-1}, and the lowest mean speed was in the 200°-220° sector with a value of 1.8 m.s^{-1}. Likewise, for the 30 m range, the lowest mean wind speed in the 200°–220° sector was 1.7 m.s^{-1}, and the maximum mean WS, measured was 17.3 m.s^{-1}, between 280° and 300°. The maximum mean WS recorded at 50 m was 25.3 m/s in the 300°-320° direction, and the minimum was 1.7 m.s^{-1} in the 200°-220° direction. Winds at the site were mostly blowing from the northwest, specifically from the west, northwest, and northwest (NW-NW), but winds were also blowing from the southwest, west, and southwest (SW-SW).

Time Series Construction of Wind Speed Data

To show the general trend in wind speed, a daily time series was generated. Based on the results, it is found to be about (6.1 m/sec) represents the average WS at 50 m throughout the night, while the value (3.2 m.sec^{-1}) represents the average WS at 10 m throughout the night.

Wind Power Density Spectrum

The Fast Fourier Transform (FFT) was used to quickly and efficiently construct the wind spectrum of the time series of the measured data. Through a series of calculations, the wind speed spectrum for the Al Reem site was obtained at

Table 4: Wind speed and its direction for the selected area at three levels.

Direction sector [°]	Mean value of WS at 10 m	Mean value of WS at 30 m	Mean value of WS at 50 m
0 – 20.	3.44854	3.39466	3.06943
20 – 40.	2.67685	3.49858	2.47671
40 – 60.	2.97321	4.56277	2.57871
60 – 80.	3.6506	4.11631	3.20414
80 – 100.	3.74682	4.91302	4.89762
100 – 120.	6.04072	7.34932	7.99207
120 – 140.	6.99523	5.17859	5.86752
140 – 160.	4.71673	3.37926	3.70064
160 – 180.	3.22531	2.32276	2.44592
180 – 200.	2.32469	1.94173	1.93018
200 – 220.	1.89362	1.75314	1.71465
220 – 240.	1.8609	2.23424	1.81857
240 – 260.	2.15534	2.79617	2.20345
260 – 280.	3.22916	5.63082	3.70834
280 – 300.	8.42699	17.37357	12.44131
300 – 320.	24.68825	19.36725	25.3387
320 – 340.	13.02248	6.41598	10.38026
340 – 360.	4.81872	3.71219	4.15095
Calm WS value	0.1058	0.05966	0.08083
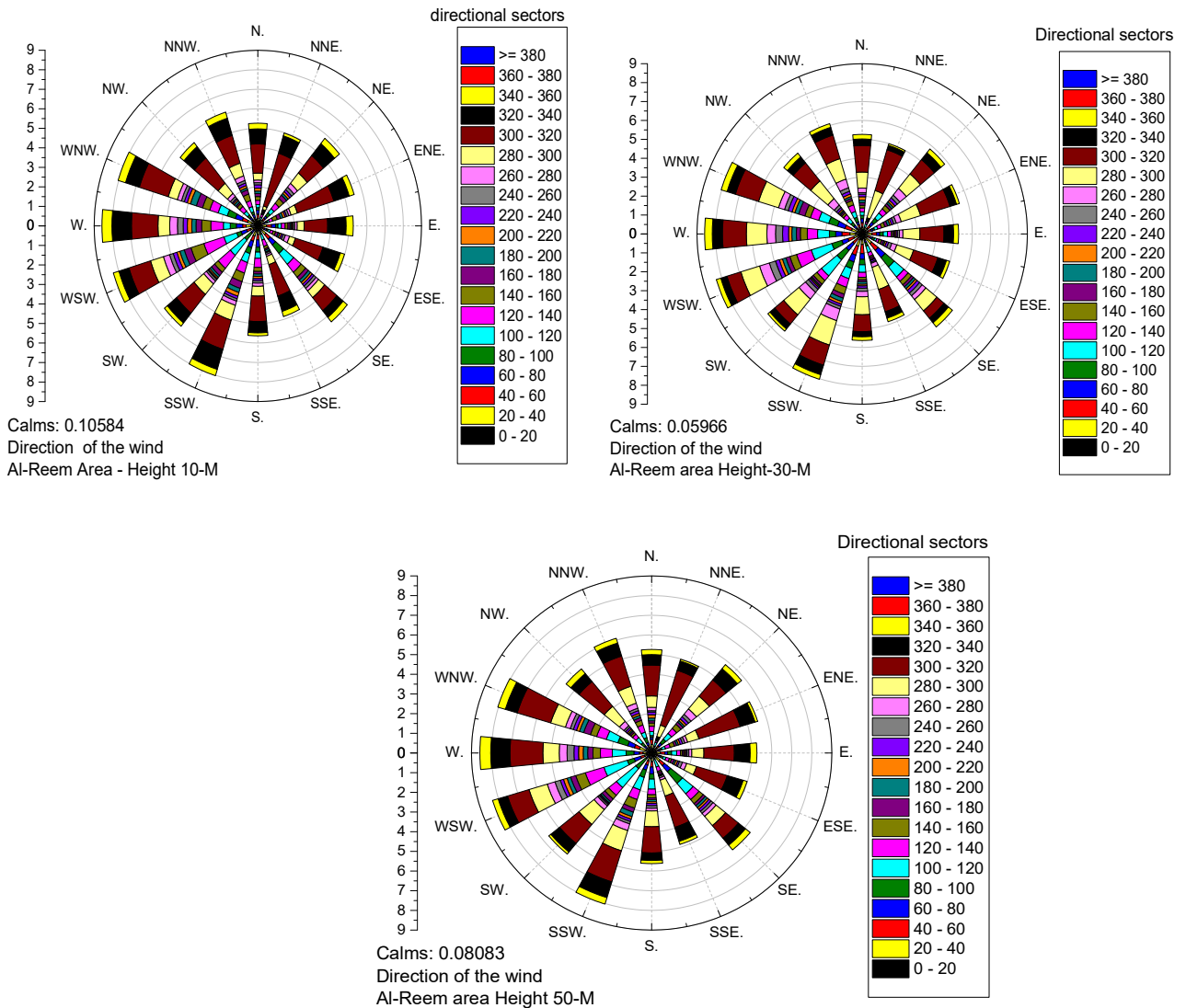
Fig. 5: The wind rose plots for the heights of (10, 30, and 50 m).

three different height levels (10, 30, and 50 m) during the day and night. The spectrum calculation process consists of several basic steps: finalizing the time series, obtaining daily mean WS data from the 10-minute data, and running the fast Fourier transform. Then, the data is filtered and smoothed. The highest spectral density was recorded in the Al-Reem region at 226,236.282 m.s^{-1} at a frequency of 2 Hz at 50 m during the night, while the lowest spectral density was recorded at 115,863.7 m.s^{-1} at a frequency of 2 Hz at 10 m. m rise during the same period. These results are clear from the peaks in Fig. 7.

CONCLUSIONS

To determine the shape of the WS spectrum at the Al-Reem

region, wind measurements were analyzed at heights of 10, 30, and 50 m above the ground. The results can be summarized as follows:

1. Compared to night, morning hours yield higher wind speed data. During the morning hours of the research year, the average standard deviation and maximum wind speed at a height of 50 meters were calculated as 3.235 m.s^{-1} and 5.60011 m.s^{-1}, respectively.

2. There is a strong correlation between the data obtained from actual observations and the Weibull distribution function at heights of (10, 30, 50 m).

3. The plots for the wind rose disclosed that the WNW and the NNW are the predominant wind directions.
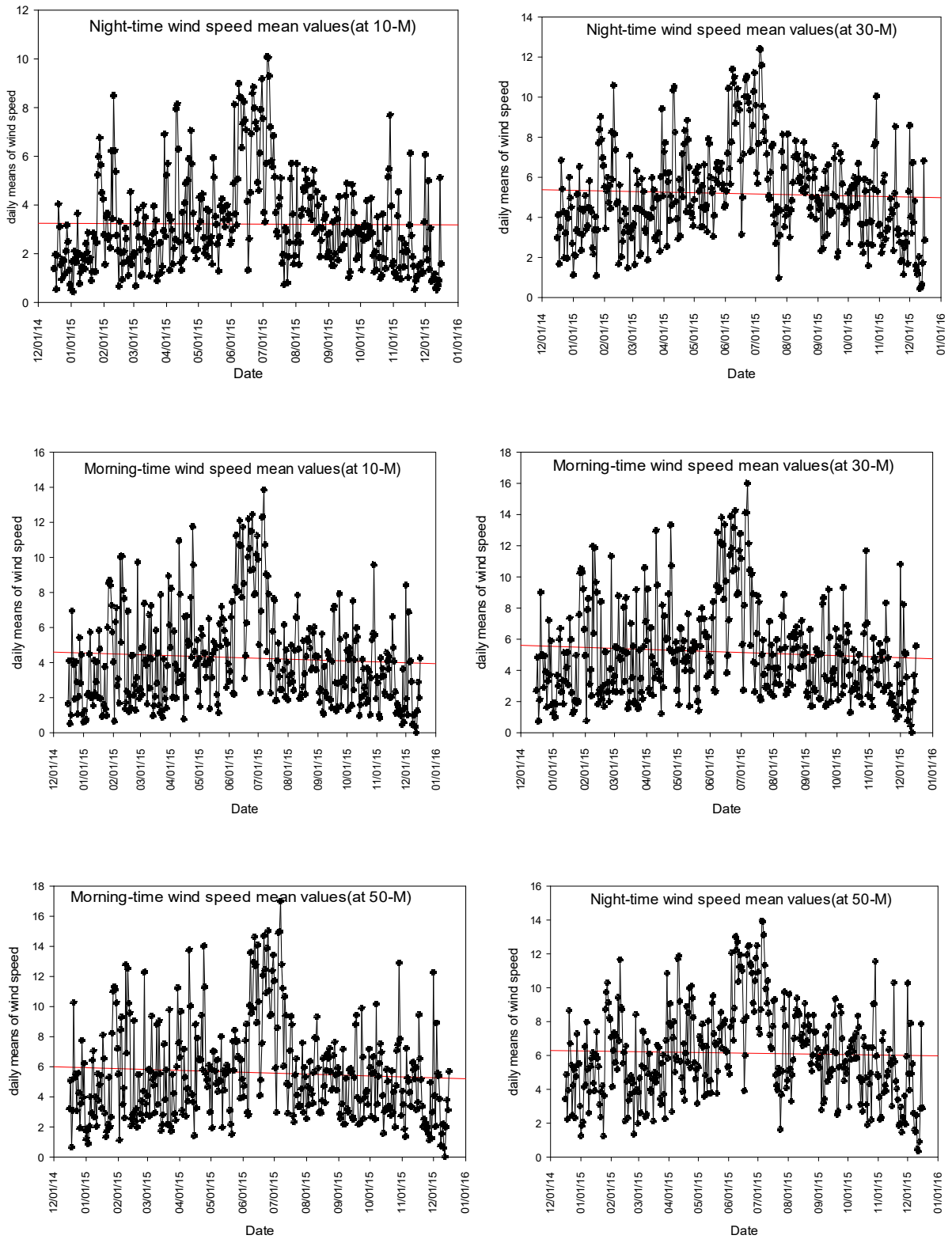
Fig. 6: The time series for both day and night at 10, 30 and 50 m.
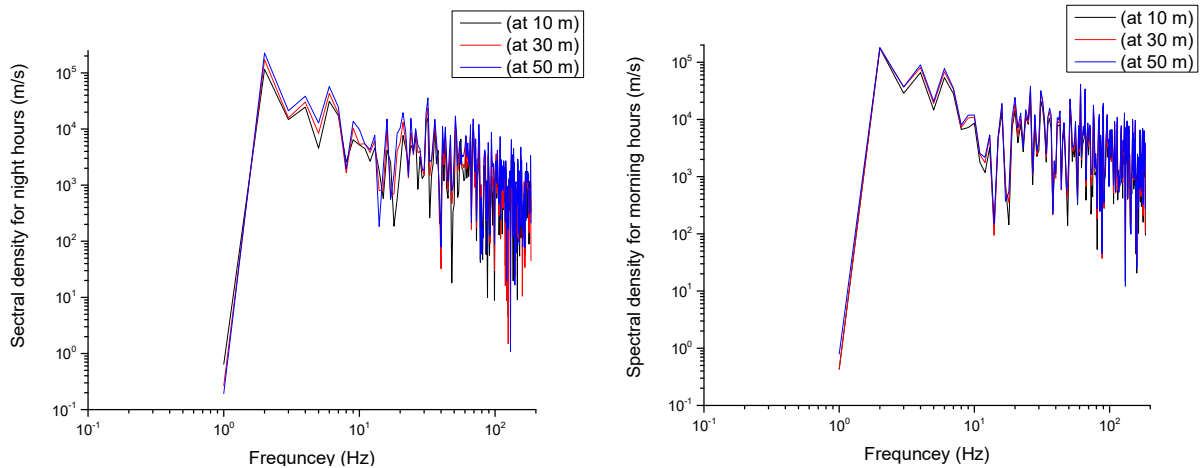
Fig. 7: The spectrum of wind speed at (10, 30, 50 m) during morning hours and night hours.

4. For the heights of 10, 30, and 50 m, the spectral peaks for Al-Reem during the day exhibit a better agreement than those during the night.

5. According to this analysis of the wind speed data at the Al-Reem region, there is a good chance that wind power presents a great way of generating clean power.

REFERENCES

Abbas, T.A., Al-Jiboori, M.H. and Altmimi, A.I., 2019. Spectral and statistical analysis of wind spectrum for Ali Al-Gharbi area in Iraq. *Iraqi Journal of Science*, 64, pp.1649-1657.

Ahmed, B., Khamees, S., Yaseen, F., Khalid, S., Heni, M., Mudar, A. and Abdulsattar, A., 2021. Evaluation of wind data reliability by using logarithmic and power laws: A case study in Southern Iraq. *Journal of Modern Science*, 17, p.31. https://doi.org/10.33640/2405-609X.3123

Al-Jiboori, M.H. and Qassim, M.S., 2018. Choosing the relevant low height for operation of wind turbines over urban Baghdad city. *Journal of Physics: Conference Series*, 1032(1). IOP Publishing. https://doi.org/10.1088/1742-6596/1032/1/012207

Al-Jiboori, M.H., 2010. Determining of neutral and unstable wind profiles over Baghdad city. *Iraqi Journal of Science*, 51(2), pp.343-350.

Al-Rufaee, F.M., Abd, L.M., Kuvshinov, V.V. and Yakimovich, B.A., 2020. Assessment of the potential of wind energy resources in Southern Iraq. *Energy Reports*, 3, pp.105-113. https://doi.org/10.22213/2413-1172-2020-3-105-113

Bashaer, M.L., Al-Tamimi, A.I. and Abdullah, O.I., 2019. Design and implementation of wind energy analysis tool (WEATb) in Iraq.

AIP Conference Proceedings, 2129(1), p.0123075. https://doi.org/10.1063/1.5123075

Hadad, M.S. and Al-Jiboori, M.H., 2019. Choosing minimum height for continuing operation wind energy generation over urban cities. *J. Educ. Pure Sci. Univ. Thi-Qar*, 9, pp.193-203.

Hadi, F. A., Abdulsada Al-Knani, B., & Abdulwahab, R. A. (2020). An assessment the wind potential energy as a generator of electrical energy in the coastal area of southern Iraq. *Scientific Review Engineering and Environmental Sciences*, **29**(1), pp.37-53.

Jabbar, R.I., 2021. Statistical analysis of wind speed data and assessment of wind power density using Weibull distribution function (case study: Four regions in Iraq). *IOP Conference Series: Materials Science and Engineering*, 1804(1), p.012010. https://doi.org/10.1088/1742-6596/1804/1/012010

Mahmood, D.A., Naif, S.S., Al-Jiboori, M.H. and Al-Rbayee, T., 2022. Improving Hufnagel-Andrews-Phillips model for prediction Cn2 using empirical wind speed profiles. *Journal of Atmospheric and Solar-Terrestrial Physics*, 240, p.105952. https://doi.org/10.1016/j.jastp.2022.105952

Maysan Governorate, 2024. Wikipedia. Available at https://en.wikipedia.org/wiki/Maysan_Governorate. Accessed on 5th Feb 2025.

Mishaal, A.K., Abd Ali, A.M. and Khamees, A.B., 2020. Wind distribution map of Iraq: A comparative study. *IOP Conference Series: Materials Science and Engineering*, 928(2), p.022044. IOP Publishing. https://doi.org/10.1088/1757-899X/928/2/022044

Mohammed, B., Abdullah, O.I. and Al-Tamimi, A.I., 2020. Investigation and analysis of wind turbines' optimal locations and performance in Iraq. *FME Transactions*. https://doi.org/10.5937/FMET2001155B

Resen, A., 2015. Wind resource estimation and mapping at the Ali Al-Gharbi site (East-South of Iraq) using the WAsP model. *Iraqi Journal of Science*, 56(2A), pp.1216-1223.

Food and Water Safety Surveillance at Galala Port in Ambon, Indonesia: An Investigation Study

E. Fikri[1,2], Y. W. Firmansyah[3,4], S. Suhardono[5]†, W. Mikana[6] and L. Y. J. Noya[7]

[1]Department of Environmental Sanitation, Bandung Health Polytechnic, Bandung City, 40171, Indonesia

[2]Center of Excellence on Utilization of Local Materials for Health Improvement, Bandung Health Polytechnic, Bandung, 40171, Indonesia

[3]Department of Occupational Health and Safety, Polytechnic of Kesdam VI Banjarmasin, Banjarmasin 70118, Indonesia

[4]Department of Environmental Science Doctoral, Graduate School of Universitas Sebelas Maret, Surakarta City, 57126, Indonesia

[5]Environmental Sciences Study Program, Faculty of Mathematics and Natural Sciences, Universitas Sebelas Maret, Surakarta, 57126, Indonesia

[6]Department of Nursing, Health Science Faculty of Santo Borromeus University, West Bandung Regency, 40553, Indonesia

[7]Technical Center for Environmental Health and Disease Control (BTKLPP), 97100 Ambon City, Indonesia

†Corresponding author: S. Suhardono; sapta.suhardono@staff.uns.ac.id

ABSTRACT

The port is a place for ships as sea transportation to dock. The port, as a place of entry and exit for goods or passengers from various regions, places, and environments, encourages the potential for disease transmission to a new environment. Pathogens present in the environment can directly contact the human body through air, touch, and transmission through food around areas with high mobilization. Therefore, this study aims to look at the results of hygiene observations and laboratory testing related to food, drinking water, and air samples at Galala Port, Ambon City. This study used descriptive research with a cross-sectional research design. From all parameter examination results, several examination results do not meet the standards such as food microbiology examination results (E. coli bacteria > 3.6MPN/gr), sanitation (walls and floors are not watertight), the presence of mosquito larvae (seven *Aedes albopictus* mosquito larvae), drinking water microbiology (total Coliforms 64 CFU.100 mL^{-1}), and clean water microbiology (*E. coli* > 250 CFU. 100 mL^{-1} and total Coliforms 8 CFU.100 mL^{-1}). Therefore, it can be concluded that the inspection of restaurants carried out at Galala port, Ambon City, is not appropriate and does not meet the standards according to the Minister of Health Decree number 942 of 2003.

INTRODUCTION

Food is a basic human need that contains nutrients and essential substances that are good for the growth, repair, and maintenance of body tissues and play a role in regulating vital body processes (Munteanu & Schwartz 2022). Although the body needs food to fulfill the body's nutrients, excessive food consumption or a poor diet is a problem (Gao et al. 2021). Poor food hygiene is a current public health concern (Food and Agriculture Organization of the United Nations 2019).

Globally, there are 420,000 deaths and 600 million cases of foodborne illness each year. Children under the age of five account for 30% of foodborne deaths (World Health Organization, 2024). Meanwhile, excess foodborne disease is contributed by the world's number one disease, cardiovascular disease, with 17.9 million deaths annually, with 85% caused by heart attacks and strokes (World Health Organization 2021). In the Asia-Pacific region, more than 275 million cases of food poisoning are reported per year (Nations 2019). Cardiovascular cases in Asia cause 10.8 million deaths, or about 35% of total deaths in Asia (Zhao 2021).

In 2020, The Indonesian Food and Drug Authority reported there were 45 outbreaks with 3,276 people exposed, so 1,528 of them were sick, and 6 people were declared dead. In Indonesia, cardiovascular disease is dominated by 34.1% hypertension, 10.9 per mile incidence of stroke, 1.5% coronary heart disease, and 0.38% chronic kidney failure (Ministry of Health 2021).

Public transportation is an environment that people visit daily, which affects the level of density and contact between passengers, which can affect the increase and transmission of disease or health problems (Goscé & Johansson 2018). Over the years, there has been an increase in the number of international travelers, more international refugees and migrants, shipping capacity by sea, and a greater volume of international air travel passengers (Findlater & Bogoch 2018). Mobility and length of stay at the destination, as well as spatially controlled mobility of individuals, affect the dynamics of an epidemic (Espinoza et al. 2020).

Load distribution and increased tissue density contribute to the spread of epidemics. Increased global mobility of people, non-human animals, plants, and products drives the introduction of infectious diseases to new locations. Many factors contribute to the global spread of infectious diseases, including the increased speed and range of human mobility, increased volumes of trade and tourism, and changes in the geographic distribution of disease vectors (Yang et al. 2017). Therefore, this study aims to look at the results of hygiene observations and laboratory testing related to food, drinking water, and air samples at Galala Port, Ambon City, Indonesia.

MATERIALS AND METHODS

This study uses descriptive research which aims to the results of laboratory examination of food samples, drinking water samples, and clean water samples at Galala Port. The research design uses a longitudinal design using primary and secondary data sources. Data collection using the *grab sampling* technique was conducted in 2024 at the entrance of Galala Ambon Port, Maluku Province, Indonesia. This study took 50 human samples and food samples taken at eating places around the port entrance. Food and water samples were tested with the identification of physical, chemical, and biological parameters conducted by the Technical Center for Environmental Health and Disease Control (BTKLPP) of Ambon City. Data analysis was done descriptively to describe the test results.

RESULTS AND DISCUSSION

Table 1 shows the chemical test results of food samples at X restaurant were not found to contain harmful additives with negative results, so it was declared safe according to the National Food and Drug Testing Development Center of the Republic of Indonesia, number 07/MM/2000. The use, restriction, and prohibition of Food Additives (BTP) have been regulated in Minister of Health Regulation No. 033 of 2012 and No. 239/Menkes/Per/V/1985 regarding food additives and prohibition of hazardous BTP (Pandey & Upadhyay 2012).

The ban on the use of Borax, Formalin, Rhodamin B, and Methail Yellow in food is due to the effects of the substances themselves on the body. Borax, Formalin, Rhodamin B, and Methail Yellow have toxic properties that cause body disorders such as throat burning, irritation, headaches and nausea, decreased immunity, hormonal imbalances, premature birth, concentration or cognitive impairment, psychological disorders, while long-term effects (chronic/

Table 1: Results of chemical examination of food samples of the restaurant X at Galala Harbor in Ambon City, Year 2024.

Food Name	Test Sample No.	Unit	Inspection Result				
			Borax	Formalin	Rhodamine B	Methai l Yellow	Description
Restaurant X							
1). Yellow Noodles	K.237	/25mg	Negative	Negative	Negative	Negative	Eligible
2). White Rice	K.238	/25mg	Negative	Negative	Negative	Negative	Eligible
3). Meatball frontman	K.239	/25mg	Negative	Negative	Negative	Negative	Eligible

Table 2: Results of microbiological examination of food samples restaurant X at Galala Port Ambon City, Year 2024.

No.	Food Name	Test Sample No.	Unit	Restaurant "X"		Description
				Total Coliform	*E. coli* / Limit Condition $<3.6MPN.g^{-1}$	
1	Yellow Noodles	B.211	$MPN.g^{-1}$	Negative	14	*E.coli* not eligible
2	White Rice	B.212	$MPN.g^{-1}$	Negative	350	*E.coli* not eligible
3	Meatball frontman	B.213	$MPN.g^{-1}$	Negative	<1.3	not eligible

accumulative) are caused such as respiratory system disorders, kidney and liver disorders, reproductive system disorders, nervous system disorders, other chronic diseases, cancer, and death (Sujarwo et al. 2020, Hadrup et al. 2021, Agency for Toxic Substances and Disease Registry 2014, Ghosh et al. 2017, Ridha et al. 2023).

From the results of the samples that were subjected to microbiological examination, only the meatball sample met the criteria for food that is safe for consumption according to Minister of Health Regulation RI No. 2 of 2023 concerning Regulations for the Implementation of Government Regulation No. 66 of 2014 concerning Environmental Health (Hukum Online 2023). Meanwhile, the samples of yellow noodles and white rice did not meet the requirements because they were found to contain *E. coli*.

The discovery of *E.coli* in food at Restaurant "X" that exceeds the threshold limit can increase the *E.coli* pathogenic strains in the body. These pathogens are associated with intestinal problems that cause generalized diarrhea to bloody diarrhea (*Hemorrhagic Colitis*), urinary tract infections due to contamination of other organs, and death. Despite treatment with antibiotics, *E. coli* leaves behind a higher toxin load when the bacteria die. (National 2017, Daneman et al. 2023, Mueller & Tainter 2024). The two samples containing *E.coli* in Table 2 are considered unfit for consumption, so there needs to be attention from Restaurant owners and vigilance from the community towards food hygiene. This is important to do to avoid the onset of disease for port visitors, especially people who want to use ship transportation.

The results of the sanitation inspection at "X" restaurant (Table 3) found that the restaurant service did not wear work clothes, and the walls of the dining room and the floor were not watertight, so it was stated that "X" restaurant did not meet the requirements of Hygiene Sanitation of Eateries and Restaurants as stated in KepMenKes No.942 of 2003

Table 3: Sanitation inspection results of Restaurant X in Galala Port Ambon Year 2024.

Variable	Inspection Result Sanitation	Description
1	2	3
Food Service		
Personal Hygiene	Eligible	
Health Of The Handler In The Last 1 Month	Healthy	
Wear Work Clothes While Working	No	Not Workwear
Finished Food Storage		
Clean	Yes	
Food Containers Used	Eligible	
Enclosed/Protected From Dust/Insects/Other Disturbances	Yes	The Storage Area Does Not Allow Food To Be Polluted/Contaminated
Cutlery/Drinking Utensil Requirements		
Glass/Spoon/Fork Cleanliness	Eligible	
Storage Method	Eligible	
Dining Table Is Always Clean	Yes	
Dining Room Sanitation		
Waterproof Floor	No	
Waterproof Wall	No	Still Using The Board
Cleanliness Of The Skies	Not Eligible	
Adequate Room Ventilation	Not Eligible	
Porcelain Handwashing Station	Not Eligible	
Lighting Is Sufficient	Eligible	
Always Maintain General Hygiene	Eligible	
Storage Requirements Food Ingredients		
Between One Type Of Foodstuff Stored Separately	Yes	
Made Of Strong And Clean Materials	Yes	
Clean Water Needs Are Sufficient	Yes	

Table 4: Results of *Aedes albopictus* mosquito inspection in broken speedboats at Galala Harbor in Ambon City 2024.

No.	Container Type	Flick Check		Total
		Positive	Negative	
1	In Broken Spead	7	0	7

(Kementerian Kesehatan Republik Indonesia 2021).

The use of clean work clothes only on duty is one of the protocols for food handlers as well as controlling food-borne diseases so that there is no contamination from the outside environment when guests travel from their place of residence to the work environment (Hasriani & Zulfan 2022). Watertight wall criteria are needed to withstand wind and rainwater and protect the area inside the restaurant and the processed food inside from being damaged by direct sun exposure and dust from the outside environment. Impermeable floors are associated with moisture, when floors become damp, there is potential for bacterial growth in a building (Keman 2007).

Table 4 shows positive results with the presence of 7 *Aedes albopictus* mosquito larvae in the Broken *Speedboat*. Just like *A. aegypti*, *A. albopictus* can transmit all four serotypes of dengue virus, yellow fever virus, chikungunya virus, and Zika virus and is suspected to have the potential for *Venezuelan Equine Encephalitis virus* (Lwande et al. 2020)

Females *Aedes* lay eggs in domestic or natural water reservoirs and disperse their eggs in two or more places. The breeding and distribution of *Aedes* larvae is influenced by the size of the container, the use of the container or the water in the container, the water temperature, the water source (especially the pH of the water), and the location of the container (Waewwab et al. 2019, Firmansyah et al. 2024). The use of an environment also influences the distribution of *Aedes* mosquitoes across different landscapes, including urban, suburban, rural, forest, and agricultural areas (Rahman et al. 2021, Vannavong et al. 2017). The port is one of the

places where the import of goods or the entry and exit of people between districts, provinces, and even countries. The spread of *A. albopictus* is a more frequent spread on local transportation departures compared to *A. aegypti* (Irayanti et al. 2022). This local outbreak usually occurs within 5-15 years after the infestation of *A. albopictus* (Kraemer et al. 2019).

To prevent introductions, countries should strengthen entomological surveillance, particularly around high-risk introduction routes such as ports and highways, and develop rapid response protocols for vector control to prevent introduced mosquitoes from establishing permanent populations (European Centre for Disease Prevention and Control 2017, Ridha et al. 2023, McGregor & Connelly 2021, Cahyanti et al. 2024).

Examination of physical and chemical parameters of drinking water taken in kettles Restaurant "X" (Table 5) obtained that the restaurant has met the requirements of drinking water quality standards attached in Minister of Health Regulation number 492/MENKES/PER/IV/2010 regarding standardization of drinking water quality (Permenkes 2010) with the highest lab result on *Total Dissolved Solid* (TDS) 45.4 mg.L^{-1}. TDS can come from the place where drinking water sources are taken, exposure from the environment, and places used to store water (Wang 2021). Drinking water should be tasteless and should not contain ions such as calcium, magnesium, potassium, sodium, and other ions. The nitrite parameter showed a result of 0.8018 with a maximum level of 20 mg.L^{-1}. High nitrite in drinking water can cause health problems due to heavy metal consumption and poisoning (Moreno et al. 2020, Nowicki et al. 2020).

Drinking water that goes through the heating process in kettles and pipes triggers the formation of calcium, magnesium, and nitrate ions. These substances have the potential to form N-nitroso compounds (NOCs) that pose a non-carcinogenic threat. Indirect contamination of drinking water can continue to occur if the host is unable to provide the necessary components

Table 5: Results of examination of physical and chemical parameters of drinking water from kettles at restaurant X Port Galala Ambon City, Year 2024.

No.	Parameters	Unit	Max Allowable Level	Laboratory Test Results K.241	Description
A.	PHYSICAL				
1	Color	NTU	10	Not Detected	Eligible
1	Turbidity	NTU	5	0,48	Eligible
2	Smell	-	Odorless	Odorless	Eligible
4	Temperature	^{o}C	-	30,4	Eligible
5	TDS	mg.L^{-1}	500	45,4	Eligible
B.	CHEMICAL				
1	Nitrite (as NO$_2$)	mg.L^{-1}	20	0,8018	Eligible

Table 6: Results of biological parameter examination of drinking water taken in kettles at RM. "X" Port Galala, Year 2024.

No.	Microbiological Parameters	Unit	Limit Terms	Laboratory Test Results B.0214	Description
1	*E.coli*	CFU.100 mL^{-1}	0	0	Eligible
2	Total *Coliforms*	CFU.100 mL^{-1}	0	64	Not Eligible

for water treatment and measures to prevent it (Muryanto et al. 2014, Shoukat et al. 2020, Ward et al. 2018, Dippong et al. 2019).

Examination of the biological parameters of drinking water taken from kettles (Table 6) obtained unqualified results with Total Coliform 64 CFU.100 mL^{-1}. The excess microbiological standards of drinking water are in accordance with those stipulated in Minister of Health Regulation number 32 of 2017 concerning Environmental Health Quality Standards and Water Health Requirements for Sanitary Hygiene Purposes, Swimming Pools, Solus perAgua and Public Baths (Permenkes 2017).

Coliform bacteria are bacteria found in the human environment and feces of warm-blooded animals that should not be found in food (Hammad et al. 2022). The presence of coliforms in drinking water indicates the presence of disease-causing organisms (pathogens) in the water system. Coliforms in the water supply may indicate the ineffectiveness of the water treatment system as well as contamination included in the water supply distribution system and corresponding quality reports (Martin et al. 2016). The presence of coliforms, expressed in concentration, is an indicator to determine the contamination of drinking water (Bahagian 2019). Typically, health symptoms associated with contaminated drinking water range from no ill effects to diarrhea (indigestion) (Martin et al. 2016).

Clean water in "X" restaurants (Table 7) is declared not to meet the criteria for clean water quality standards by the Sanitation Minister of Health Regulation number 32 of 2017 (Permenkes 2017), as evidenced by the results of TDS 511.6 mg. L^{-1}.

TDS, which is total solids, refers to the residual material left in storage. Increasing TDS concentrations in clean water cause scaling and corrosion of cooling water and boilers, thereby limiting water functions for drinking, power generation, industrial cooling, supporting biodiversity, ecosystem services, recreation, transportation routes, waste disposal, agricultural production, irrigation, energy production, regional planning, and fish farming, resulting in significant economic losses (Dey & Vijay 2021, Dörnhöfer &

Table 7: Results of examination of physical and chemical parameters of clean water taken in containment (bucket) at RM. "X" Port Galala, Year 2024.

No.	Parameters	Unit	Max. Allowable Level	Laboratory Test Results K.240	Description
A.	PHYSICAL				
1	Color	TCU	10	Not Detected	Eligible
2	Turbidity	NTU	5	0.43	Eligible
3	Smell	-	Odorless	Odorless	Eligible
4	Temperature	°C	-	30.4	Eligible
5	TDS	mg.L^{-1}	300	511>6	Eligible
B.	CHEMICAL				
1	Nitrite (as NO$_2$)	mg.L^{-1}	20	17.0902	Eligible

Table 8: Results of examination of physical and chemical parameters of drinking water taken in containment (bucket) at RM. "X" Port Galala, Year 2024.

No.	Parameters	Unit	Max Allowable Level	Laboratory Test Results K.240	Description
B.	CHEMICAL				
1	Dissolved Iron (Fe)	mg.L^{-1}	0.2	< 0,0322	Eligible
2	Nitrite (as NO$_2$)	mg.L^{-1}	0,2	0,0017	Eligible
3	pH	-	6,5-8,5	7,12	Eligible
4	Dissolved Manganese (Mn)	mg.L^{-1}	0,1	< 0,0325	Eligible

Table 9: Results of microbiological parameter examination of clean water taken in containment (bucket) at restaurant X, Port Galala, Year 2024.

No.	Microbiological Parameters	Unit	Limit Terms	Laboratory Test Results B.0215	Description
1	*E. coli*	CFU.100 mL^{-1}	0	>250	Not Eligible
2	Total Coliform	CFU.100 mL^{-1}	0	8	Not Eligible

Oppelt 2016, Cheng et al. 2022, Dube et al. 2015, Giao et al. 2021, Ismail et al. 2019). Swimming and boating in impaired waters can also lead to respiratory and gastrointestinal illnesses (Adjovu et al. 2023).

The results of the examination of physical and chemical parameters of drinking water in "X" Restaurant taken from buckets (Table 8) have met the drinking water safety requirements in accordance with Minister of Health Regulation number 492/MENKES/PER/IV/ of 2010 concerning Drinking Water Quality requirements (Permenkes 2010).

All parameters of the microbiological examination of clean water taken from the Restaurant "X" (Table 9) bucket did not meet the requirements of the clean water criteria listed in Minister of Health Regulation number 32 of 2017 concerning Environmental Health Quality Standards and Water Health Requirements for Sanitary Hygiene Purposes, Swimming Pools, Solus per Aqua and Public Baths. (Permenkes 2017) with *E. coli* >250 CFU.100 mL^{-1} and Total Coliform 8 CFU.100 mL^{-1}.

Clean water has a variety of uses in food production, for cleaning, sanitation, and manufacturing purposes. Clean water is used for various activities in the food industry, such as for growing, unloading, fluming, washing, salting, ice making, and in sanitation and hygiene programs (Mahaza et al. 2025). Poor water quality has a detrimental impact on processed food through the pathogenic growth of bacteria, viruses, and microorganisms that produce toxic substances and contaminate water that can cause harm to consumers (Bhagwat 2019, Senami 2021, World Health Organization 2019).

Clean water contaminates food through water-borne microorganisms (Golic et al. 2023). Microorganisms then colonize and multiply on food or equipment used in the processing process, especially during washing. Microorganisms can survive for years to adapt to environmental conditions and leave toxic substances after cleaning (Badan Standarisasi Nasional 2017).

CONCLUSIONS

Hygiene observations and laboratory testing of food, drinking water, and air samples at Galala Harbour, Ambon City. Observations showed that chemical examination of food samples of the Restaurant. Microbiological Examination of Food Samples found that only the meatball pentolan sample met the criteria for safe food consumption according to Minister of Health Regulation Republic of Indonesia number 2 of 2023, while the other 2 samples found *E.coli* that exceeded the threshold, which could increase the pathogenic strain of *E.coli* in the body. Examination of the biological parameters of drinking water taken from the kettle gave unqualified results with Total *Coliform* 64 CFU.100 mL^{-1}. The results of the examination of the physical and chemical parameters of clean water taken in the shelter (bucket) are stated to have not met the criteria for clean water quality standards as sanitation Minister of Health Regulation number 32 of 2017 as evidenced by the TDS result of 511.6 mg.L^{-1}. TDS, which is total solids, refers to the remaining material left in the storage area. Drinking water samples were taken from the reservoir in the restaurant kettle. Drinking water passing through the heating process in the kettle and pipes can trigger the formation of calcium, magnesium, and nitrate ions.

Hygiene observations were also made at the site, and 7 *Aedes albopictus* mosquito larvae were found in the Broken Speedboat. Females *Aedes* lay eggs in domestic or natural water reservoirs and spread their eggs in two or even more places. Albopictus was found more in local transport departures than Ae. This study also highlighted the disease found from Galala Port activities in Ambon City, with many risk factors that can occur.

REFERENCES

Adjovu, G.E., Stephen, H., James, D. and Ahmad, S., 2023. Measurement of Total Dissolved Solids and Total Suspended Solids in Water Systems: A Review of the Issues, Conventional, and Remote Sensing Techniques. *Remote Sensing*, 15(14), pp.3534. https://doi.org/10.3390/rs15143534

Agency for Toxic Substances and Disease Registry, 2014. Medical Management Guidelines for Formaldehyde. Retrieved May 23, 2024, from https://wwwn.cdc.gov/TSP/MMG/MMGDetails.aspx?mmgid=216&toxid=39

Badan Standarisasi Nasional, 2017. The Maximum Limit of Microbial Contamination in Food. BSN

Bahagian, A.S., 2019. Environmental Quality Report – Department of Environment. Retrieved May 23, 2024, from https://www.doe.gov.my/en/environmental-quality-report/

Bhagwat, V.R., 2019. Safety of water used in food production. *Food Safety and Human Health*, 65, pp.219–247. https://doi.org/10.1016/B978-0-12-816333-7.00009-6

Cahyanti, N.D., Firmansyah, Y.W., and Angelia, I., 2024. Demonstration of peppermint emulgel making as anti-mosquito in dengue hemorrhagic fever prevention at SMK Kartini Bhakti Mandiri. Selaparang: *Journal of Advancing Community Service*, 8(4), pp. 3870-3875. https://doi.org/10.31764/jpmb.v8i4.27564

Cheng, C., Zhang, F., Shi, J. and Kung, H.-T., 2022. What is the relationship between land use and surface water quality? A review and prospects from a remote sensing perspective. *Environmental Science and Pollution Research*, 29(38), pp.56887–56907. https://doi.org/10.1007/s11356-022-21348-x

Daneman, N., Fridman, D., Johnstone, J., Langford, B.J., Lee, S.M., MacFadden, D.M. and Brown, K.A., 2023. Antimicrobial resistance and mortality following E. coli bacteremia. *ClinicalMedicine*, 56, pp.101781. https://doi.org/10.1016/j.eclinm.2022.101781

Dey, J. and Vijay, R., 2021. A critical and intensive review on assessment of water quality parameters through geospatial techniques. *Environmental Science and Pollution Research International*, 28(31), pp.41612–41626. https://doi.org/10.1007/s11356-021-14726-4

Dippong, T., Mihali, C., Hoaghia, M.-A., Cical, E. and Cosma, A., 2019. Chemical modeling of groundwater quality in the aquifer of Seini town – Someş Plain, Northwestern Romania. *Ecotoxicology and Environmental Safety*, 168, pp.88–101. https://doi.org/10.1016/j.ecoenv.2018.10.030

Dörnhöfer, K. and Oppelt, N., 2016. Remote sensing for lake research and monitoring – Recent advances. *Ecological Indicators*, 64, pp.105–122. https://doi.org/10.1016/j.ecolind.2015.12.009

Dube, T., Mutanga, O., Seutloali, K., Adelabu, S. and Shoko, C., 2015. Water quality monitoring in sub-Saharan African lakes: A review of remote sensing applications. *African Journal of Aquatic Science*, 40(1), pp.1–7. https://doi.org/10.2989/16085914.2015.1014994

Espinoza, B., Castillo-Chavez, C. and Perrings, C., 2020. Mobility restrictions for the control of epidemics: When do they work? *PLOS ONE*, 15(7), p.e0235731. https://doi.org/10.1371/journal.pone.0235731

European Centre for Disease Prevention and Control, 2017. Vector Control With a Focus on Aedes Aegypti and Aedes Albopictus Mosquitoes Literature Review and Analysis. Retrieved May 23, 2024, from https://www.ecdc.europa.eu/en/publications-data/vector-control-focus-aedes-aegypti-and-aedes-albopictus-mosquitoes-literature

Findlater, A. and Bogoch, I.I., 2018. Human Mobility and the Global Spread of Infectious Diseases: A Focus on Air Travel. *Trends in Parasitology*, 34(9), pp.772–783. https://doi.org/10.1016/j.pt.2018.07.004

Firmansyah, Y. W., Parulian, A. A., Kristiawan, H., & Prasaja, B. J. (2024). Occurrences of dengue fever, dengue hemorrhagic fever, dengue shock syndrome, severe dengue, dengue warning signs in Bandung city: an spatial study based on moran index. *Lontara Journal of Health Science and Technology*, 5(2), pp. 154–170. https://doi.org/10.53861/lontarariset.v5i2.495

Food and Agriculture Organization of the United Nations, 2019. Foodborne Illnesses in Asia-Pacific 'needlessly' sicken 275 million annually and threaten trade. Retrieved May 23, 2024, from https://www.fao.org/asiapacific/news/detail-events/en/c/1197008/

Gao, M., Jebb, S.A., Aveyard, P., Ambrosini, G.L., Perez-Cornago, A., Carter, J. and Piernas, C., 2021. Associations between dietary patterns and the incidence of total and fatal cardiovascular disease and all-cause mortality in 116,806 individuals from the UK Biobank: A prospective cohort study. *BMC Medicine*, 19(1), p.83. https://doi.org/10.1186/s12916-021-01958-x

Ghosh, D.S., Ghosh, D., Firdaus, S.B. and Singha, P.S., 2017. Metanil yellow: The toxic food colorant. *Asian Pacific Journal of Health Sciences*, 4(4), pp.65–66. https://doi.org/10.21276/apjhs.2017.4.4.16

Giao, N.T., Cong, N.V. and Nhien, H.T.H., 2021. Using remote sensing and multivariate statistics in analyzing the relationship between land use pattern and water quality in Tien Giang Province, Vietnam. *Water*, 13(8), p.1093. https://doi.org/10.3390/w13081093

Golic, B., Касагић, Д., Pecanac, B. and Knežević, D., 2023. *Microbiological Status of Water in the Food Industry*. Springer

Goscé, L. and Johansson, A., 2018. Analyzing the link between public transport use and airborne transmission: Mobility and contagion in the London underground. *Environmental Health*, 17(1), p.84. https://doi.org/10.1186/s12940-018-0427-5

Hadrup, N., Frederiksen, M. and Sharma, A.K., 2021. Toxicity of boric acid, borax, and other boron-containing compounds: A review. *Regulatory Toxicology and Pharmacology:* 121, p.104873. https://doi.org/10.1016/j.yrtph.2021.104873

Hammad, A.M., Eltahan, A., Hassan, H.A., Abbas, N.H., Hussien, H. and Shimamoto, T., 2022. Loads of coliforms and fecal coliforms and characterization of thermotolerant *Escherichia coli* in fresh raw milk cheese. *Foods*, 11(3), p.332. https://doi.org/10.3390/foods11030332

Hasriani, E. and Zulfan, M., 2022. Application of healthy behavior of food handlers during a pandemic at the Aji Bata tourism object, Toba Regency. *TEHBMJ (Tourism Economics Hospitality and Business Management Journal), 2*(2), pp.205-218. https://doi.org/10.36983/tehbmj.v2i2.390

Hukum Online, 2023. Environmental Health Quality Standards Are to Be Implemented in Line With Four Types Of Environments. Retrieved May 23, 2024, from Hukumonline.com website: https://pro.hukumonline.com/a/lt63fc61d8dd9dc/environmental-health-quality-standards-to-be-implemented-in-line-with-four-types-of-environments/

Irayanti, I., Martini, M., Wurjanto, A., Susanto, H. S., Firmansyah, Y. W. and Ramadhansyah, M. F. 2022. Status Kerentanan Larva Aedes aegypti Terhadap Temephos Di Wilayah Kerja Pelabuhan KKP Kelas II Tarakan. *Jurnal Rekam Medis & Manajemen Infomasi Kesehatan*, 2(1), pp. 19–27. doi: 10.53416/jurmik.v2i1.80.

Ismail, K., Boudhar, A., Abdelkrim, A., Mohammed, H., Mouatassime, S.E., Kamal, A.O. and Nouaim, W., 2019. Evaluating the potential of Sentinel-2 satellite images for water quality characterization of artificial reservoirs: The Bin El Ouidane Reservoir case study (Morocco). *Meteorology Hydrology and Water Management*, 7(1), pp.31-39. https://doi.org/10.26491/mhwm/95087

Keman, S., 2007. Six fundamental needs of healthy housing. *Jurnal Kesehatan Lingkungan Unair,* 3(2), pp.3933.

Kementerian Kesehatan Republik Indonesia, 2021. Coronary Heart Disease Dominates Urban Communities. Retrieved May 23, 2024, from https://sehatnegeriku.kemkes.go.id/baca/umum/20210927/5638626/penyakit-jantung-koroner-didominasi-masyarakat-kota/

Kraemer, M.U.G., Reiner, R.C., Brady, O.J., Messina, J.P., Gilbert, M., Pigott, D.M. and Golding, N., 2019. Past and future spread of the arbovirus vectors Aedes aegypti and Aedes albopictus. *Nature Microbiology*, 4(5), pp.854-863. https://doi.org/10.1038/s41564-019-0376-y

Lwande, O.W., Obanda, V., Lindström, A., Ahlm, C., Evander, M., Näslund, J. and Bucht, G., 2020. Globe-trotting Aedes aegypti and Aedes albopictus: Risk factors for arbovirus pandemics. *Vector Borne and Zoonotic Diseases Journal*, 20(2), pp.71-81. https://doi.org/10.1089/vbz.2019.2486

Mahaza, S., Suhardono, S., Firmansyah, Y.W., Hardjanti, M., and Noya, L.Y.J., 2024. Food and water safety monitoring at Pattimura airport, Ambon City. *International Journal of Environmental Impacts*, 7(4), pp.723–729. https://doi.org/10.18280/ijei.070413

Martin, N.H., Trmčić, A., Hsieh, T.-H., Boor, K.J. and Wiedmann, M., 2016. The evolving role of coliforms as indicators of unhygienic processing

conditions in dairy foods. *Frontiers in Microbiology,* 7, p.154. https://doi.org/10.3389/fmicb.2016.01549

McGregor, B.L. and Connelly, C.R., 2021. A review of the control of Aedes aegypti (Diptera: Culicidae) in the continental United States. *Journal of Medical Entomology,* 58(1), pp.10-25. https://doi.org/10.1093/jme/tjaa157

Moreno, L., Pozo, M., Vancraeynest, K., Bain, R., Palacios, J. and Jácome, F., 2020. Integrating water-quality analysis in national household surveys: Water and sanitation sector learnings of Ecuador. *NPJ Clean Water,* 3, p.23. https://doi.org/10.1038/s41545-020-0070-x

Mueller, M. and Tainter, C.R., 2024. *Escherichia coli* Infection. StatPearls Publishing.

Munteanu, C. and Schwartz, B., 2022. The relationship between nutrition and the immune system. *Frontiers in Nutrition,* 9, p.50. https://doi.org/10.3389/fnut.2022.1082500

Muryanto, S., Bayuseno, A., Ma'mun, H., Usamah, M. and Jotho, 2014. Calcium carbonate scale formation in pipes: Effect of flow rates, temperature, and malic acid as additives on the mass and morphology of the scale. *Procedia Chemistry,* 9, pp.69-76. https://doi.org/10.1016/j.proche.2014.05.009

Nowicki, S., Koehler, J. and Charles, K., 2020. Including water quality monitoring in rural water services: Why safe water requires challenging the quantity versus quality dichotomy. *NPJ Clean Water,* 3, p.62. https://doi.org/10.1038/s41545-020-0062-x

Pandey, R. and Upadhyay, S., 2012. Food Additive. https://doi.org/10.5772/34455

Permenkes, 2010. Peraturan Menteri Kesehatan No 492 Tahun 2010 Persyaratan Kualitas Air Minum.

Permenkes, 2017. Peraturan Menteri Kesehatan No 32 Tahun 2017 tentang Standar Baku Mutu Kesehatan Lingkungan dan Persyaratan Kesehatan Air Untuk Keperluan Higiene Sanitasi, Kolam Renang, Solus Per Aqua, dan Pemandian Umum.

Rahman, M.S., Ekalaksananan, T., Zafar, S., Poolphol, P., Shipin, O., Haque, U. and Overgaard, H.J., 2021. Ecological, Social, and Other Environmental Determinants of Dengue Vector Abundance in Urban and Rural Areas of Northeastern Thailand. *International Journal of Environmental Research and Public Health, 18*(11), p.5971. https://doi.org/10.3390/ijerph18115971

Ridha, M.R., Marlinae, L., Zubaidah, T., Fadillah, N.A., Widjaja, J., Rosadi, D. and Sofyandi, A., 2023. Control Methods for Invasive Mosquitoes of *Aedes Aegypti* and *Aedes Albopictus* (Diptera: Culicidae) in Indonesia. https://doi.org/10.14202/vetworld.2023.1952-1963

Senami, C., 2021. The Importance of food quality in dining at restaurants. *Journal of Food Technology and Preservation, 5*(9), p.1.

Shoukat, A., Hussain, M. and Shoukat, A., 2020, February 26. Effects of Temperature on Total dissolved Solid in water.

Sujarwo, S., Latif, R.V.N. and Priharwanti, A., 2020. Kajian Kandungan Bahan Tambahan Pangan Berbahaya 2018– 2019 Se-Kota Pekalongan dan Implementasi Perda Kota Pekalongan Nomor 07 Tahun 2013. *JURNAL LITBANG KOTA PEKALONGAN, 18*(2). https://doi.org/10.54911/litbang.v19i0.123

Vannavong, N., Seidu, R., Stenström, T.-A., Dada, N. and Overgaard, H.J., 2017. Effects of socio-demographic characteristics and household water management on *Aedes aegypti* production in suburban and rural villages in Laos and Thailand. *Parasites & Vectors,* 10(1), p.170. https://doi.org/10.1186/s13071-017-2107-7

Waewwab, P., Sungvornyothin, S., Okanurak, K., Soonthornworasiri, N., Potiwat, R. and Raksakoon, C., 2019. Characteristics of water containers influencing the presence of *Aedes immatures* in an ecotourism area of Bang Kachao Riverbend, Thailand. *Journal of Health Research,* 16, p.96 https://doi.org/10.1108/JHR-09-2018-0096

Wang, B., 2021. Research on drinking water purification technologies for household use by reducing total dissolved solids (TDS). *PLOS ONE,* 16, p.e0257865. https://doi.org/10.1371/journal.pone.0257865

Ward, M.H., Jones, R.R., Brender, J.D., de Kok, T.M., Weyer, P.J., Nolan, B.T. and van Breda, S.G., 2018. Drinking Water Nitrate and Human Health: An Updated Review. *International Journal of Environmental Research and Public Health,* 15(7), p.1557. https://doi.org/10.3390/ijerph15071557

World Health Organization, 2019. Safety and Quality of Water Used in Food Production and Processing: Meeting Report. Retrieved May 23, 2024, from https://www.who.int/publications-detail-redirect/9789241516402

World Health Organization, 2021. Cardiovascular Diseases. Retrieved May 23, 2024, from https://www.who.int/health-topics/cardiovascular-diseases

World Health Organization, 2024. Estimating the Burden of Foodborne Diseases. Retrieved May 23, 2024, from https://www.who.int/activities/estimating-the-burden-of-foodborne-diseases

Yang, Y.M., Hsu, C.Y., Lai, C.C., Yen, M.F., Wikramaratna, P.S., Chen, H.H. and Wang, T.H., 2017. Impact of comorbidity on fatality rate of patients with Middle East respiratory syndrome. *Scientific Reports,* 7(1), p.11307. https://doi.org/10.1038/s41598-017-10402-1

Zhao, D., 2021. Epidemiological features of cardiovascular disease in Asia. *JACC: Asia,* 1(1), pp.1-13. https://doi.org/10.1016/j.jacasi.2021.04.007

The Saprobic Index for Water Quality Based on Fish Aquaculture: A Case Study of White Snapper (*Lates calcarifer*) in Floating Net Cages at Sendang Biru Water, Indonesia

Dewi Hidayati[1][†] iD **, Rifqi Aldrian Abrar Syauqa[1], Dian Saptarini[1], Carolyn Melissa Payus[2], Nur Syahroni[3] and Yeyes Mulyadi[3]**

[1]Department of Biology, Faculty of Science and Data Analytics, Institut Teknologi Sepuluh Nopember (ITS), East Java, Indonesia
[2]Faculty of Science & Natural Resources, University Malaysia Sabah (UMS), Sabah, Malaysia
[3]Department of Ocean Engineering, Faculty of Marine Technology, Institut Teknologi Sepuluh Nopember (ITS), East Java, Indonesia
†Corresponding author: Dewi Hidayati; dewi_hidayati@ymail.com

ABSTRACT

The impact of water organic pollution from leftover fish feed and metabolic waste in floating net cages (FNC) aquaculture can lead to detrimental effects on coastal marine biota. This underscores the necessity for continuous monitoring of water quality in areas surrounding FNCs to mitigate the environmental impacts of aquaculture. One method of evaluating water quality is through the Saprobic Index, which quantitatively analyzes pollution status based on the presence and composition of various organisms, including plankton. This study aims to evaluate the organic pollution potential derived from fish feed in the vicinity of the FNCs at Sendang Biru waters by employing the Saprobic Index. The research identified five classes of phytoplankton in the FNC area: Bacillariophyceae, Dinophyceae, Chrysophyceae, Cyanophyceae, and Globothalamea. Analysis of the phytoplankton composition indicated that the waters surrounding Sendang Biru FNC can be classified as ranging from Oligosaprobic to β-Meso/Oligosaprobic. These findings suggest that the aquaculture practices utilizing the FNC system contribute to a light level of organic pollution in the water. This emphasizes the importance of effective management and monitoring strategies to minimize the environmental impact and ensure the sustainability of aquaculture in coastal marine ecosystems.

INTRODUCTION

Sendang Biru water, located in Malang Regency and part of the Indian Ocean, boasts a high diversity of pelagic fish including Tuna Fish (Jaya et al. 2017). Alongside the wild catch from fishing activities, aquaculture in Sendang Biru, using floating net cages (FNC), has also developed to support ecotourism. FNC is a popular aquaculture cultivation technique among fish cultivation circles. It is space-efficient and does not require any water management, as it utilizes rafts connected to cages around coastal waters (Sadhu et al. 2015). Moreover, the manufacturing cost is low and the harvesting process is simple. However, there are a few problems while applying this method, including air quality, disease transmission, changes in food webs, and requirements for comprehensive feed (Dias 2012).

There are three types of food for fish aquaculture, natural feeds, supplementary feeds, and complete feeds. Natural food, including plankton, worms, shrimp, and small fish, can be easily found in culture areas. Meanwhile, supplementary feeds are made from agriculture byproducts and fish waste bodies and are regularly given to the culture fish. Whereas the complete feeds are made from various ingredients containing complete nutrients for fish growth and the shape should facilitate easy

consumption (FAO 2023). Since fish culture in Sendang Biru FNC is semi-intensive, natural food is available. However, the fish are still fed with supplemental feeds.

Hlavac et al. (2014), Madireddy & Brayboy (2022) and Pfeffer (1990) reported that fish-feeding activity is the major contributor to water pollution, particularly nitrates and phosphates from the leftover, feces, which are excreted via gills and kidneys. Since this organic waste creates a considerable threat to the environment. Some organisms, like plankton, are sensitive to this pollutant. Thus, plankton especially phytoplankton, is commonly used as a bioindicator (Pourafrasyabi & Ramenzapour 2014, Awaludin et al. 2015). Bioindicators will quickly provide information regarding water quality (Yeanny 2018).

To evaluate water quality, a saprobic system is employed, involving taxonomic and quantitative analysis of all relevant biocoenosis components, including lower algae and protozoans. The saprobic index is defined as the ratio between the sum of abundance products (the value of saprobic) and the indication weight of individual species (Zahradkova & Soldan 2013). The saprobic index is used to determine the level and status of organic pollution in waters (Canning & Death 2019) by measuring the content of nutrients and pollutants. The approach involves understanding the relationship between the level of organic pollution and the abundance of organisms as a parameter (Indrayani et al. 2014, Szczerbinka & Malgorzata 2015). The saprobic index is commonly employed to assess water quality, thereby enhancing the success rate of fishing businesses in public waters (Sagala 2011). Therefore, it is necessary to conduct research on water quality analysis based on the saprobic plankton index. This research aims to determine the level of pollution, especially organic pollution, in the waters around floating net cages.

MATERIALS AND METHODS

Study Area

Water samples were collected from three sampling sites in Sendang Biru FNC-aquaculture area with coordinates of 8°26'14" S; 112°40'49" E (Fig. 1), including one site at FNC (S1) and two sites at FNC's surrounding area (S2 and S3).

Procedures

Measurement of Physico-Chemical Parameters of Water

Physico-chemical parameter measurements were carried out to measure the water quality in FNC-aquaculture and its surrounding area. The in-situ parameters, including dissolved oxygen (DO), temperature, pH, and salinity were measured using portable DO meter AMT08, digital thermometer, portable pH Meter pH, and Atago handheld refractometer, respectively. The water flow speed was measured on-site with the floating method according to FAO (2023). The concentration of nitrate (NO_3) and phosphate (PO_4) were analyzed in the laboratory using the spectrophotometric method following The Indonesian National Standard Procedure (SNI 2011, SNI 2005).

Analysis of Proximate Content of Fish Feeds

The fish in the Sendang Biru FNC-aquaculture system were

Fig. 1: Three sampling sites around Sendang Biru FNC-aquaculture area. FNC= Floating Net Cage.; S1=Sampling sire 1; S2= Sampling site 2; S3=Sampling site 3. (Google Earth (Jul 2 2020). Sendang Biru Malang. Retrieved from https://www.google.com/earth)Sendang Biru Malang. Retrieved from https://www.google.com/earth

fed with supplementary feed, like fish waste body pieces and pellets. The proximate values of fish waste body pieces, including protein, fat, ash, and crude fiber content, were analyzed according to The Indonesian National Standard Procedure (SNI 1996). For the proximate test of @Megami GR-5 pellets as artificial feed, utilize the proximate data provided on the packaging.

Plankton Sampling

Plankton sampling was carried out in the morning (08.00-11.00 a.m.) using the horizontal tows method from a boat. The plankton net was towed horizontally at a speed of approximately 1 knot for 1 minute according to the National Standard for plankton sampling (SNI 1998) using a Kitahara-type plankton net with a diameter of 0.3 m and a mesh size of 80 μm. The filtered sample was collected in the 60 mL sample container and then preserved in a 10% formalin solution. (USEPA 2021).

Data Analysis

Plankton Sample Analysis

1 ml of filtered sample was taken using a pipette, then dropped onto a Sedgwick Rafter glass and covered with a glass object. The samples were observed using a compound microscope and identified using identification books (Nontji 2008, Yamaji 1979). The plankton samples found were calculated to determine the individual abundance of each species using the Sedgwick Rafter Counting method according to Fachrul et al. (2007). The results of the plankton abundance calculation are then converted into ind./L with the formula below:

$$N = n \times \frac{Vr}{Vo} \times \frac{1}{Vs} \qquad …(1)$$

Where,

N: Number of individual plankton per liter (ind./L)

n : Number of plankton counted in the subsample

Vt: Filtered sample volume (mL)

Vo: Sub sample volume that counted in Sedgwick rafter

Vs: Amount of filtered water (liter)

The calculation of ecological indexes includes the Shannon diversity index (Spellerberg & Fedor 2003). The index of evenness and dominance refers to (Odum 1971) with the formulas as follows.

$$H' = -\sum pi\,[\ln(pi)] \qquad …(2)$$

Where,

H' = Shannon Diversity Index

pi = Relative abundance of species "i"

pi = ni/N, where ni = number of individuals of species "i" and N = total number of individuals of all species

$$E = \frac{H'}{H'maks} \qquad …(3)$$

Where,

E: Evenness index

H': Diversity index value

H' max: ln S

S: Number of Types

$$D = \left(\frac{ni}{N}\right) \wedge 2 \qquad …(4)$$

Where,

D: Dominance index

ni: Number of individuals per genus

N: Total individuals of the entire species

Moreover, the saprobic index was calculated using the formula referred to (Dresscher & Mark 1976, Samudra et al. 2022).

$$X = \left(\frac{C + 3D - B - 3A}{A + B + C + D}\right) \qquad …(5)$$

Where,

X: Saprobic index

A: Cyanophyceae group

B: Dinophyceae group

C: Chlorophyceae group

D: Bacillariophyceae group

RESULTS AND DISCUSSION

Analysis of Proximate of Fish Foods

The proximate analysis of fish food (trash of small tuna fish *(Euthynnus affinis)* and @Megami GR-5 pellets) that was distributed to fish culture in Sendang Biru FNC is given in Table 1.

As shown in Table 1, both types of fish foods contain a high nutrient, particularly protein which is essential

Table 1: Proximate test results of fish feed.

Fish feed	Proximate Test Results			
	Ash (%)	Protein (%)	Fat (%)	Crude Fiber (%)
Trash of small tuna fish	1.64	21.57	3.15	1.09
Pelet @Megami GR-5	10	48	10	2

for fish growth. Protein plays an important role in fish growth, as it contains essential and non-essential amino acids. The protein content in the trash of small Tuna Fish and @Megami GR-5 was 21.57% and 48%, respectively. This protein level falls within the range of 25-50%, which is sufficient for supporting fish growth Iskandar & Fitriadi (2017). However, high protein concentration in fish food results in nitrate and phosphate pollution in the water (Hlavac et al. 2014, Madireddy & Brayboy 2022, Pfeffer 1990). Thus, the evaluation of water quality in the FNC aquaculture system in the Sendang Biru area is important.

Measurement of Physico-Chemical Parameters of Water

In this research, the physico-chemical parameters of FNC water and the surrounding area, including temperature, pH, DO, flow speed, salinity, nitrate, and phosphate levels, were measured. The results are given in Table 2.

The result of the water quality analysis (Table 2) displayed that the temperature in FNC water and its surrounding area was in the range of 21.7-22.5ºC, which indicated that there was no abrupt change (Joseph et al. 2010). Temperature is involved in regulating aquatic ecosystem life, such as metabolic activity and the distribution of aerial organisms (Nontji 2005). Moreover, the temperature, ranging from 20-30 ºC, is suitable for plankton growth as well (Kusumaningtyas et al. 2014). pH values in FNC water and its surrounding area are in the range of 7.35-7.61, which is suitable for marine biota (Joseph et al. 2010), including plankton (Berge 2010). Besides, pH is involved in maintaining water stability. As for the salinity in FNC water and its surrounding area, it ranged from 34 to 37 ppt, which closely aligns with the salinity of the open ocean (33-37 ppt), an optimum range for marine life (Patty 2013). DO levels in FNC water and its surrounding area were in the range of 7.3-8.1 mg/L, which aligns with the optimum level for organisms (3-7 mg/L).

The flow speed in FNC water and its surroundings was in the range of 0.01-0.58 m/s with the current moving from east to west. The water current pattern in South Malang waters follows the South Java current pattern which has the same pattern throughout the year (Sartimbul et al. 2017). The water flow measured in FNC was at the level of 0.01 m/s, which is suitable for feeding activities in the FNC site. Pilditch & Grant (1999) revealed that waters with flow speeds of 0.15-0.1 m/s may inhibit feeding. While the water flow in the FNC water surrounding area was 0.43-0.48 m/s, which is useful to maintain the water flow and DO in FNC.

Nitrate levels in FNC water and its surrounding area were 0.001 mg/L in September, while after one month of fish culture activities (October), it increased around 0.08-0.32 mg/L. This nitrate level in October was higher than standard (Table 2). This incline is possibly related to the feeding activity. Fish culture activity from September to October resulted in the accumulation of leftover, feces and urine, due to an increase in nitrate concentration (Madireddy & Brayboy 2022). Phosphate concentration in all sampling sites is also higher than standard. However, the value fluctuated and there was no indication of increasing concentration from September to October. It is assumed that the source of phosphate concentration in FNC waters may come from inshore anthropogenic activities or natural resources such as weathering and dead organism artifacts (Ruttenberg 2004, Paytan & McLaughlin 2007). The fluctuating value of phosphate is possibly caused by the natural process of phosphate in the soil layer, which is not stable due to its reaction with the aforementioned water flow (Golterman 2004).

Overall, the quality of temperature, DO, pH, and salinity fall within the standards suitable for marine life. Meanwhile, the nitrate and phosphate did not fit the standard according to the previous report by Joseph et al. (2010), Nordin et al. (2009) and KLH (2004). Phosphate is essential for the

Table 2: Results of measurement of water physico-chemical parameters.

| Parameter | Water Criteria for Marine Life and Aquaculture *) | Sampling Period/Location Parameters | | | | | |
| | | September | | | October | | |
		S1	S2	S3	S1	S2	S3
Temperature (ºC)	No abrupt change	22	22.5	22.1	22	21.9	21.7
pH	7.8-8.4	7.35	7.51	7.45	7.32	7.61	7.60
Salinity (ppt)	25- 40	36	36	37	35	34	34
DO (mg/L)	>4 mg/L	7.4	7.7	7.5	7.3	8.1	7.9
Flow speed (m/s)	-	0.01	0.50	0.43	0.01	0.58	0.45
NO_3 (mg/L)	0.008 mg/ L	0.001	0.001	0.001	0.08	0.12	0.32
PO_4 (mg/L)	0.015 mg/ L	0.15	0.11	0.56	0.12	0.50	0.23

* References of water criteria: Joseph et al. 2010, Nordin et al. 2009, KLH 2004.
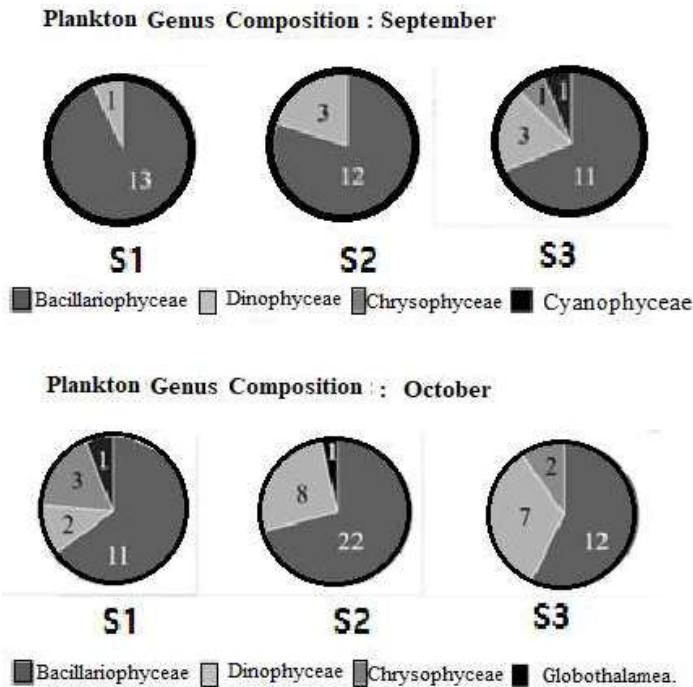
Fig. 2: Plankton genus composition.

growth and metabolism processes of phytoplankton and other organisms. Phosphate levels in FNC water and its surrounding area range from 0.11 to 0.56 mg/L, which fall within the scope of phosphate levels in marine water (0.00031-0.124 mg/L). Phosphate levels on the water surface are generally lower than those on the seafloor primarily because of phosphate consumption by phytoplankton (Patty 2013).

Phytoplankton Composition and Abundance

The phytoplankton found in FNC water and its surrounding areas mainly belongs to the classes of Bacillariophyceae,

Dinophyceae, Cyanophyceae, Chrysophyceae and Globothalamea, and they are divided into 44 genera.

As shown in Fig. 2, in September, the phytoplankton in all sampling sites was dominated by Bacillariophyceae ranging from 11 to 13 genera. Other phytoplankton that were found with less number were Dinophyceae, Cyanophyceae and Chrysophyceae (1-3 genera). In October, a similar phenomenon occurred in Bacillariophyceae for its highest class found in all sampling sites. Phytoplankton, in the Bacillariophyceae class, is commonly found in marine waters and is characterized by a high level of adaptation,
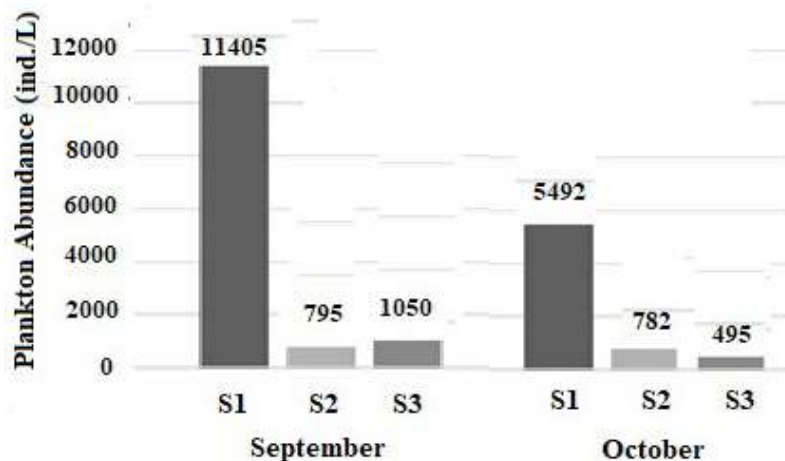
Fig. 3: Abundance of phytoplankton in site (S1) and surrounding FNC waters (S2 and S3).

Table 3: Phytoplankton ecological indexes.

Sampling Period	Sampling Site	H'	E	D
September	S1	1.60	0.83	0.25
	S2	1.47	0.76	0.30
	S3	1.97	0.86	0.16
October	S1	1.85	0.83	0.19
	S2	2.43	0.90	0.10
	S3	2.36	0.95	0.10

Notes: Shanon Diversity Index (H'), Evenness Index (E) and Dominance Index (D)

cosmopolitan nature, and wide distribution (Mann et al. 2017).

The abundance of phytoplankton in FNC water and its surrounding area ranged from 495 to 11,405 ind/L (Fig. 3). S1 in two different sampling periods, September and October, was classified as mesotrophic water with a moderate level of fertility, which is indicated by the phytoplankton abundance ranging from 2,000-15,000 ind/L (Iswanto et al. 2015). Meanwhile S2 and S3, in two sampling periods, were classified as oligotrophic water with a low fertility level indicated by the phytoplankton abundance ranging from 0 to 2,000 ind./L. The high abundance of phytoplankton in S1 was caused by the cultivating place for White Snapper (*Lates calcarifer*) with intensive feeding. Therefore, it resulted in high availability of organic material which could be consumed by phytoplankton. While at S2 and S3 in the two sampling periods, the abundance of phytoplankton was lower due to the ocean currents that distribute phytoplankton to the surrounding water (Font-Muñoz et al. 2017).

Phytoplankton Ecological Indexes

Diversity Index, Evenness Index and Dominance Index: Calculation of the phytoplankton ecological index includes the Shanon Diversity Index (H'), Evenness Index (E) and Dominance Index (D). As shown in Table 3, the phytoplankton diversity index (H') value in FNC water and its surroundings, in September, ranged from 1.47 to 1.97. In October, the phytoplankton diversity index value ranged from 1.85 to 2.43. In general, the phytoplankton diversity

index value increased from September to October, which is classified as stable to very stable with moderate to very good aquatic environmental conditions (Wibisono 2005).

As shown in Table 3, the phytoplankton evenness index value ranged from 0.76 to 0.86 and from 0.83 to 0.95 in September and October, respectively. Overall, the phytoplankton evenness index value of FNC water and its surroundings was relatively high. If the E value is close to 1, it indicates that the level of uniformity in a community is high, and the number of individuals per species is evenly distributed (Kvalseth 2015). The phytoplankton dominance index value ranged from 0.16 to 0.30 and from 0.10 to 0.19 in September and October, respectively. It is classified as low, which indicates that there are no dominating phytoplankton species in FNC water and its surroundings (Wibisono 2005).

Saprobity Index: The saprobity value of water describes the pollution level in the water, measured by the content of nutrients and pollutants. Increasing nutrient content can cause phytoplankton blooms which result in water turbidity and decreased brightness. However, sufficient nutrient content will increase phytoplankton productivity, thereby enhancing the productivity of other organisms with a higher trophic level. Saprobity is measured using phytoplankton as an indicator because each type of phytoplankton is part of a certain saprobic group which will influence the saprobity value (Zahradkova & Soldan 2013, Canning & Death 2019).As shown in Table 4, the saprobity value of FNC water and its surroundings, in September, ranged from +2.8 to +2.36, which belongs to the Oligosaprobic category (Sagala et al. 2011). The Oligosaprobic phase is characterized by blue and clear water with high DO levels, a small number of bacteria in the water, pH- and DO-sensitive organisms, such as planarians, insect larvae, and aquatic moss (Barinova 2017). In addition, there is a breakdown process of organic materials by microorganisms in the water. Consistent with this finding, the data on DO levels in FNC water and its surroundings are classified as high (7.4-7.7 mg/L). In general, the pollution in FNC water and its surroundings in September was vague. This was due to ocean currents which evenly distribute the organic materials in the water (Indrayana et al. 2014).

Table 4: Results of Saprobic Index.

Sampling Period	Sampling Point	Saprobic Index	Saprobic Zone	Degree of Pollution
September	S1	+ 2.80	Oligosaprobic	Very light
	S2	+ 2.55	Oligosaprobic	Very light
	S3	+ 2.36	Oligosaprobic	Very light
October	S1	+ 1.40	β-Meso/ Oligosaprobic	Light
	S2	+ 1.94	β-Oligo/ Oligosaprobic	Very light
	S3	+ 1.27	β-Oligo/ Oligosaprobic	Light

In October, S1 showed water a saprobity value of +1.40, which was classified into β-Meso/Oligosaprobic with mild pollution. Furthermore, the sampling site of S2 was measured with the saprobity value of +1.94 which is categorized into -Oligo/Mesosaprobic with an extremely light degree of pollution. Meanwhile, S3 was measured with the value of +1.27, which was categorized into β-Meso/Oligosaprobic with a light degree of pollution. In October, the quality of FNC water and its surroundings declined because of the accumulation of food residues when cultivating white sea bass. This decrease was inversely proportional to the DO level, with a value of 7.3-8.1 mg/L. This denotes that the organic materials causing the decline in water quality are relatively low because of the bacterial activity in oxidizing organic materials that are consumed (Hamzah & Trenggono 2014). Water belonging to the Mesosaprobic phase is characterized by transparent, slightly turbid, odorless, and colorless water (Barinova 2017).

Overall, FNC water and its surroundings are categorized as a suitable environment for aquatic organism life. Phytoplankton from the Bacillariophyceae class is found in all sampling points as part of the saprobity group. The presence of diatoms (Bacillariophyceae) at all stations indicates mild to moderate water pollution. The Bacillariophyceae class has a wide tolerance range for organic material pollution and serves as a bioindicator in moderate to heavy polluted water.

CONCLUSIONS

It can be concluded that the water quality at sea bass culture in Sendang Biru FNC is classified as Oligosaprobic to β-Meso/Oligosaprobic, which indicates light water pollution. Commonly found phytoplankton belong to the Bacillariophyceae class, with only a small number belonging to Dinophyceae, Cyanophyceae, Chrysophyceae, and Globothalamea classes. This result revealed that aquaculture using the FNC system may contribute the water pollution and regular biomonitoring is required.

ACKNOWLEDGEMENTS

REFERENCES

Awaludin, A.S., Dewi, N.K. and Ngabekti, S., 2015. Saprobic coefficient of plankton in Universitas Negeri Semarang Reservoir (Indonesian: Koefisien saprobik plankton di Perairan Embung Universitas Negeri Semarang). *Indonesian Journal of Mathematics and Natural Sciences*, 38(2), pp.115-120. https://doi.org/10.15294/ijmns.v38i2.5780.

Barinova, S., 2017. Essential and practical bioindication methods and system for the water quality assessment. *International Journal of Environmental Science & Natural Resources*, 2(3), pp.1-11. https://doi.org/10.19080/IJESNR.2017.02.555588.

Berge, T.N., Daugbjerg, D., Andersen, D. and Hansen, P.J., 2010. Effect of lowered pH on marine phytoplankton growth rates. *Marine Ecology Progress Series*, pp.79-91.

Canning, A.D. and Death, R.G., 2019. Ecosystem health indicators—freshwater environments, in *Encyclopedia of Ecology* (Second Edition).

Dias, J.D., Simoes, N.R. and Bonecker, C.C., 2012. Net Cages in fish farming: a scientometric analysis. *Acta Limnologica Brasiliensia*, 24(1), pp.12-17.

Dresscher, T. and Mark, H., 1976. A simplified method for the biological assessment of the quality of fresh and slightly brackish water. *Hydrobiologia*, 48(3), pp.199-201. https://doi.org/10.1007/BF00028691.

Fachrul, M.F., 2007. *Bioecological Sampling Methods* (Indonesian: Metode Sampling Bioekologi). Published by PT. Bumi Aksara and Longman, Jakarta, Indonesia.

FAO, 2023. Water. Chapter 3: Estimates of water flow. Available at: https://www.fao.org/fishery/static/FAO_Training/FAO_Training/General/x6705e/F1.htm

Font-Muñoz, J.S., Jordi, A., Tuval, I., Arrieta, J.J., Anglès, S. and Basterretxea, G., 2017. Advection by ocean currents modifies phytoplankton size structure. *Journal of the Royal Society Interface*, 14, p.20170046. https://doi.org/10.1098/rsif.2017.0046.

Golterman, H.L., 2004. *The Chemistry of Phosphate and Nitrogen Compounds in Sediments*. Kluwer Academic Publishers, New York.

Hamzah, F. and Trenggono, M., 2014. Dissolved oxygen in Lombok Strait (Indonesian: Oksigen terlarut di Selat Lombok). *Jurnal Kelautan Nasional*, 9(1), p.21. https://doi.org/10.15578/jkn.v9i1.6199.

Hlavac, D., Adamek, Z., Hartman, P. and Masílko, J., 2014. Effects of supplementary feeding in carp ponds on discharge water quality: A review. *Aquaculture International*, 22(1), pp.299-320. https://doi.org/10.1007/s10499-013-9718-6.

Indrayana, R., Yusuf, M. and Rifai, A., 2014. The influence of surface currents on the distribution of water quality in Genuk Waters, Semarang (Indonesian: Pengaruh arus permukaan terhadap sebaran kualitas air di Perairan Genuk Semarang). *Journal of Oceanography*, 3(4), pp.651-659.

Indrayani, N., Sutrisno, A. and Agung, S., 2014. Saprobic-trophic index as an indicator of water quality in Kembang Kempis Wedung Dam, Demak Regency (Indonesian: Indeks trofik-saprobik sebagai indikator kualitas air di Bendung Kembang Kempis Wedung, Kabupaten Demak). *Diponegoro Management of Aquatic Resources Journal* (MAQUARES), 3(4), pp.161-168. https://doi.org/10.14710/marj.v3i4.7051.

Iskandar, R. and Fitriadi, S., 2017. Analisa Proksimat Pakan Hasil Olahan Pembudidayaan Ikan di Kabupaten Banjar Kalimantan Selatan. *ZIRA'AH*, 42, pp.65-68.

Iswanto, C.Y., Hutabarat, S. and Purnomo, P.W., 2015. Water fertility analysis based on plankton biodiversity, nitrate and phosphate in Jali River and Lereng River Keburuhan Village, Purworejo (Indonesian: Analisis kesuburan perairan berdasarkan keanekaragaman plankton, nitrat dan fosfat di Sungai Jali dan sungai lereng Desa Keburuhan, Purworejo). *Journal of Management of Aquatic Resources*, 4(3), pp.84-90.

Jaya, M.M., Budy, W. and Domu, S., 2017. Sustainability of tuna fisheries in Sendangbiru Malang District. (Indonesian: Keberlanjutan perikanan tuna di Perairan Sendang Biru Kabupaten Malang). *ALBACORE*, 1(1), pp.111-125. https://doi.org/10.29244/core.1.1.111-125.

Joseph, I., Joseph, S., Ignatius, B., Syda, R.G., Sobhana, K.S., Prema, D. and Varghese, M., 2010. A pilot study on culture of Asian seabass *Lates calcarifer* (Bloch) in open sea cage at Munambam, Cochin Coast, India. *Indian Journal of Fisheries*, 57(3), pp.29-33.

KLH, 2004. Seawater quality standard for marine life. The state of the Environment Minister's Decision No. 51 of 2004.

Kusumaningtyas, M.A., Bramawanto, R., Daulat, A. and Daulat, W.S., 2014. The water quality of Natuna coastal water during transitional season (Indonesian: Kualitas perairan natuna pada musim transisi). *Depik*, 3(1), pp.10-20. https://doi.org/10.13170/depik.3.1.1277.

Kvalseth, T.O., 2015. Evenness indices once again: critical analysis of properties. *Springerplus*, 4, p.232. https://doi.org/10.1186/s40064-015-0944-4.

Madireddy, S. and Brayboy, L., 2022. Effects of protein concentration in fish feed on physical and chemical water pollution. *Journal of Student Research*, 11(1). https://doi.org/10.47611/jsrhs.v11i1.2393.

Mann, D.G., Crawford, R.M. and Round, F.E., 2017. Bacillariophyta. In: Archibald, J.M., Simpson, A.G.B. and Slamovits, C.H. (Eds.) *Handbook of the Protists*, pp.205-266.

Nontji, A., 2005. *Nusantara's Marine* (Indonesian: Laut Nusantara). Published by Djambatan, Jakarta.

Nontji, A., 2008. *Marine Plankton* (Indonesian: Plankton Laut). Published by LIPI Press, Jakarta.

Nordin, R.N. and Pommen, L.W., Meays, C.L., 2009. Water Quality Guidelines for Nitrogen.

Odum, E.P., 1971. *Fundamentals of Ecology*. W.B. Saunders Company, Toronto.

Patty, S.I., 2013. Distribution temperature, salinity and dissolved oxygen in waters Kema, North Sulawesi. *Jurnal Ilmiah Platax*, 1(3), pp.148-157. DOI: https://doi.org/10.35800/jip.1.3.2013.2580.

Paytan, A. and McLaughlin, K., 2007. The Oceanic Phosphorus Cycle. *Chemical Reviews*, 107(2), pp. 563-576.

Pfeffer, E., 1990. The pollution of water by fish feeding [Article in German]. *Deutsche Tierärztliche Wochenschrift*, 97(7), pp.273-275.

Pilditch, C.A. and Grant, J., 1999. Effect of variations in flow velocity and phytoplankton concentration on sea scallop (*Placopecten magellanicus*) grazing rates. *Journal of Experimental Marine Biology and Ecology*, 240(1), pp. 111-136. https://doi.org/10.1016/S0022-0981(99)00052-0

Pourafrasyabi, M. and Ramenzapour, Z., 2014. Phytoplankton as bio-indicator of water quality in Sefid Rud-River-Iran (South Caspian Sea). *Caspian Journal of Environmental Sciences*, 12(1), pp.31-40.

Ruttenberg, K.C., 2004. The Global Phosphorus Cycle. *Treatise on Geochemistry*, 8, pp.585-643. https://doi.org/10.1016/B0-08-043751-6/08153-6.

Sadhu, N., Sharma, K.S.R., Praveen, N.D., Shoji, J. and Philipose, K.K., 2015. First result of culture of Asian seabass (*Lates calcarifer*, Bloch) in open sea floating net cages in India: Effect of stocking density on survival and growth. *Indian Journal of Geo-Marine Sciences*, 44(10), pp.1540-1544.

Sagala, E.P., 2011. Community Saprobic Index in determining the level of pollution in marine waters between the Benu River and Betet Island, Banyuasin Regency, South Sumatra Province (Indonesian: Indeks saprobik komunitas dalam menentukan tingkat pencemaran di perairan laut antara Sungai Benu dan Pulau Betet, Kabupaten Banyuasin, Provinsi Sumatera Selatan). *Maspari Journal*, 2(1), pp.11-18. https://doi.org/10.56064/maspari.v2i1.1125.

Samudra, S.R., Fitriadi, R., Baedowi, M. and Sari, L.K., 2022. Pollution level of Banjaran River, Banyumas District, Indonesia: A study based on the Saprobic Index of periphytic microalgae. *Biodiversitas*, 23(3), pp.1527-1534. https://doi.org/10.13057/biodiv/d230342.

Sartimbul, A., Larasati, A.A., Sari, S.H.J., Rohadi, E. and Yona, D., 2017. Variations in plankton communities and oceanographic parameters in pelagic fishing areas in South Malang Waters (Indonesian: Variasi komunitas plankton dan parameter oseanografi di daerah penangkapan ikan pelagis di Perairan Malang Selatan). *Journal of Fisheries and Marine Science*, 1(2), pp.55-64. https://doi.org/10.21776/ub.jfmr.2017.001.02.2.

Simanjuntak, M., 2012. Sea water quality observed from nutrient aspect, dissolved oxygen and pH in The Banggai Waters, Central Sulawesi (Indonesian: Kualitas Air Laut Ditinjau dari Aspek Zat Hara, Oksigen Terlarut dan pH di Perairan Banggai, Sulawesi Tengah). *Jurnal Ilmu dan Teknologi Kelautan Tropis FPIK-IPB*, 4(2), pp.290-303.

SNI, 1996. Indonesian National Standard No. 2715. Fish Meal as Raw Material for Feed (Indonesian: Tentang Tepung Ikan Bahan Baku Pakan).

SNI, 1998. Indonesian National Standard Procedure No. 03-4717. National Standard Procedure for taking plankton samples (Indonesian: Tata-pengambilan-percontoh-plankton).

SNI, 2005. Indonesian National Standard No. 6989. How to Test Phosphate Levels with a Spectrophotometer using Ascorbic Acid (Indonesian: Tentang Cara Uji Kadar Fosfat dengan Spektrofotometer secara Asam Askorbat).

SNI, 2011. Indonesian National Standard No. 6989. Methods for Testing Nitrate (NO3-N) with a UV-Visible Spectrophotometer with Cadmium Reduction (Indonesian: Tentang Cara Uji Nitrat (NO3-N) dengan Spektrofotometer UV-Visible secara Reduksi Kadmium).

Spellerberg, I.F. and Fedor, P., 2003. A tribute to Claude Shannon (1916–2001) and a plea for more rigorous use of species richness, species diversity and the 'Shannon–Wiener' Index. *Global Ecology & Biogeography*, 12(3), pp.177-179.

Szczerbinka, N. and Malgorzata, G., 2015. Biological method used to assess surface water quality. *Archives of Polish Fisheries*, 23(4), pp.185-196.

USEPA, 2021. Standard Operating Procedure for Phytoplankton Analysis. Available at: <https://www.epa.gov/system/files/documents/2021-12/lg401.v07-phytoplankton-analysis_rfa.pdf>.

Wibisono, M.S., 2005. *Introduction of Marine Science* (Indonesian: Pengantar Ilmu Kelautan). Published by PT. Gramedia Widiasarana Indonesia, Jakarta.

Yamaji, I., 1979. *Illustrations of Marine Phytoplankton of Japan*. Hoikusha Publishing, Osaka.

Yeanny, M.S., 2018. Phytoplankton Community as bio-indicator of fertility in Belawan river. *IOP Conference Series: Earth and Environmental Science*, 130, p.012030. https://doi.org/10.1088/1755-1315/130/1/012030.

Zahradkova, S. and Soldan, T., 2013. Saprobic System. In: *Reference Module in Earth Systems and Environmental Sciences*.

Original Research Paper

doi https://doi.org/10.46488/NEPT.2025.v24i01.D1686

Open Access Journal

Studies of Outdoor Thermal Comfort in Bogor Botanical Gardens

Nofi Yendri Sudiar[1†] [ID]**, Yonny Koesmaryono[2], Perdinan[2], Hadi Susilo Arifin[3] and Randy Putra[1]**

[1]Departemen Fisika FMIPA UNP, Kampus Air Tawar Padang, Sumatera Barat, 25131, Indonesia

[2]Departemen Geofisika dan Meteorologi FMIPA IPB, Kampus Dramaga Bogor, Jawa Barat, 16680, Indonesia

[3]Departemen Arsitektur Lansekap Fak, Pertanian IPB, Kampus Dramaga Bogor, Jawa Barat, 16680, Indonesia

†Corresponding author: Nofi Yendri Sudiar; nysudiar@fmipa.unp.ac.id

ABSTRACT

This study investigates the use of thermal indexes, specifically Physiologically Equivalent Temperature (PET) and Universal Thermal Climate Index (UTCI), to determine outdoor comfort in the Bogor Botanical Gardens (KRB). This park is centrally located in Bogor city, with elevations ranging from 215-260 m above sea level. The thermal sensation was determined using seven references: PET in Europe, Taiwan, Tianjin, Tel Aviv, and UTCI in the Mediterranean, Tianjin, and general contexts. The study involved 284 visitors surveyed for their thermal comfort perceptions. Findings indicate that, based on thermal sensation criteria from the seven references, KRB is generally not within the comfort zone throughout the year, except for the PET in Taiwan, which is comfortable year-round. In-situ measurements show an average daily PET of 33.8°C and UTCI of 34.4°C. According to the Taiwan PET range, the thermal sensation is categorized as somewhat warm to warm (uncomfortable). However, 69.4% of visitors reported feeling comfortable, likely due to the environmental conditions, with 70.3% tree coverage in the 54.7 ha park area.

INTRODUCTION

In the last few years or even a decade, research on thermal comfort has increased due to climate change and increasing urban temperatures. However, there is relatively less research on outdoors compared to indoors.

Thermal comfort for rooms began in 1960 when 4 climatic parameters were used separately, namely: ambient temperature or room temperature, radiation temperature such as radiation from walls, air humidity, and airflow velocity (Mayer & Höppe 1987). All these parameters are always used to create an index of thermal comfort or discomfort in a room. The concept of effective temperature (ET) or standard effective temperature (SET) by adding two other parameters, viz: the difference in the degree of insulation measured from clothing or the term "clo" and the degree of physical activity measured from metabolism or the term "met" (Gagge et al. 1972). The Predicted Mean Values (PMV) comfort or discomfort diagram was developed from the comfortable situation created in an air-conditioned room that depends on clothing and physical activity (Fanger 1970).

The index was designed with indoor use in mind. This need can also be met outside, but SET cannot be used outside without being modified (Spagnolo & de Dear 2003). The primary challenge in evaluating outside thermal conditions is the possibility of far greater climate variability than in indoor environments. Physiological Equivalent Temperature (PET), which seeks to obtain a better approximation for outdoor circumstances, was developed to explain this difficulty (Mayer & Höppe 1987). Furthermore, thermophysiological considerations and climate parameters provide the assumption that outdoor conditions are equivalent to indoors. For example, the human body heat balance indoors with light activity

is 80 W, and clothing is 0.9 CLO. This value is also used for outdoor conditions.

Air conditioners (AC) are a simple way to modify the indoor climate, but there are very few ways to create a comfortable outside environment. The interior comfort index is often used to determine outdoor comfort. It is usually questionable when studies are conducted on thermal comfort for outdoor circumstances, and ideas created for interior conditions are applied to outside conditions without modification (Spagnolo & de Dear 2003). In addition to using human elements (clothing and metabolism) and meteorological variables (air temperature, humidity, radiation, and wind speed), an outdoor comfort index based on the energy balance of the human body should also take these into account. When evaluating outdoor comfort indices, however, the greater range of meteorological elements and human characteristics provide more challenges than when evaluating indices for interior situations. The study of outdoor thermal comfort makes use of predicted mean vote (PMV), physiologically equivalent temperature (PET), and standard effective temperature (SET) (Farajzadeh & Matzarakis 2012, Matzarakis et al. 2014, Matzarakis & Matzarakis 2016) and Universal Thermal Climate Index (UTCI) (Blazejczyk et al. 2012, Park et al. 2014) is the index that is most frequently used. Having the same meteorological inputs—wind speed, air temperature, air humidity, and the flux of short- and long-wave radiation—allows these thermal indices to have an advantage over one another.

Because PET integrates air temperature, humidity, wind speed, and cloud cover, it delivers more accurate information regarding environmental thermal conditions (Farajzadeh & Matzarakis 2012). Similarly, using UTCI can yield accurate forecasts for outdoor thermal comfort (Lai et al. 2014). The majority of studies on thermal comfort for Indonesian tourist destinations still utilize the Thermal Humidity Index, with very few using PET and UTCI (Hadi 2012). Because Indonesia's climate has equatorial, monsoon, and local patterns, it is crucial to conduct a thorough analysis of the application of these indices for tourist destinations.

Northern Taiwan is the only region in Taiwan with a tropical climate; most prior research and assessments of the usage of PET and UTCI were conducted in sub-tropical and temperate regions. Compared to Taiwan and Europe, North China's PET thermal feeling range is distinct (Lai et al. 2014). Since there are differences in the classifications, it is crucial to classify thermal perception for each region (Lin & Matzarakis 2011). The PET and UTCI calculations in a number of areas have been adjusted, including UTCI in the Mediterranean, UTCI in Tianjin, UTCI in Europe, UTCI in Taiwan, and UTCI in Tel Aviv.

This study aims to address this research gap by assessing outdoor thermal comfort in the tropical climate of Indonesia, specifically in the Bogor Botanical Gardens. There is no classification for thermal sensation in Indonesia, a country with a tropical climate, unlike the sub-tropical areas for which it was formerly employed (Sudiar & Gautama 2023). By comparing thermal sensation categories from seven PET and UTCI references with visitor survey results, this study provides a comprehensive analysis of thermal comfort for outdoor activities in natural tourist destinations in tropical climates.

MATERIAL AND METHODS

Location of Research

This study was carried out at the Bogor Botanical Garden (KRB), which is situated in the center of Bogor city at an elevation of between 215-260 meters above sea level and enjoys a tropical environment. KRB area which has an area of about 77.8 ha with topography including flat with slopes varying from 3-15%. Slightly steep on the banks of the Ciliwung River, which divides the KRB. Schmidt-Ferguson's classification of climate states that KRB has a type A value of Q = 7.8%. Koeppen's classification of climate states that KRB has a tropical forest climate, or climate A, with high temperatures. KRB is more precisely classified as having a tropical rainforest climate, with at least 60 mm of rainfall in the driest month (Af). With January having the lowest temperature of 25.9°C and September having the highest temperature of 27.5°C, the average yearly temperature is 26.9°C. The total amount of rainfall every year is 4,308 mm, with November receiving the most at 610 mm and July receiving the least at 206 mm. The average annual temperature is 78%, the average daily sunshine amount is 6.4 h, and the average annual wind speed is 1.7 km.h^{-1} (Sudiar et al. 2019).

Data

The data used in this study are climate data of Bogor Botanical Garden (KRB) station for 6 years (2012-2017) and Baranangsiang Climatology station for 4 years (2012-2015). In April and May 2018, air temperature, air humidity, and wind speed were monitored in situ at KRB (Table 1). The weather measuring device in use is an ABH-4224 type Lutron brand anemometer that satisfies ISO 9001 standards. Measurements and surveys were carried out during the day from 09:00 to 18:00 WIB. The time range was chosen to adjust to the arrival time of visitors. Measurements were grouped into hours. For each hour, a minimum of five measurements and interviews were conducted. 284 visitors

Table 1: Weather parameter measuring instrument specifications.

Parameters	Range	Resolution	Accuracy
Anemometer	0,9 – 35,0 m/s	0,1 m/s	± (2% + 0.2 m/s)
Temperature	0°C - 50°C	0,1°C	± 0,8°C
Humidity	10% - 95% RH	0,1% RH	≥ 70% RH ± (3% *reading* + 1% RH) < 70% RH – 3% RH ± 3% RH

in total participated in this survey as respondents. Simple random sampling, or the taking of samples at random, was used to choose the responders. The parking lot, the regions around trees, shrubs, ponds, and water fields, as well as pedestrian pathways, major thoroughfares, rest facilities (saung, gazebos, and park benches), and other locations were sampled both inside and outside the tourist area.

Thermal Comfort Index

The Universal Thermal Climate Index (UTCI) and Physiologically Equivalent Temperature (PET) are the two thermal comfort indices utilized. Equation (1) is used for the PET calculation, and equation (2) is utilized for the UTCI calculation. Rayman Pro software version 2.3 Beta is used to make the computation easier.

The Munich energy balancing model for humans (MEMI Model), a thermo-physiological heat balance model, serves as the foundation for the PET index (Lai et al. 2014). PET refers to the concept of a perfectly equal indoor and outdoor temperature or balanced temperature. This specific chamber features calm air (<0.1 m.s^{-1}), 1200 Pa air pressure (50% relative humidity at 20°C), and no radiation (Tmrt = Ta). As a result, PET enables the average person to contrast the effects of outdoor temperature conditions with their personal inside experience.
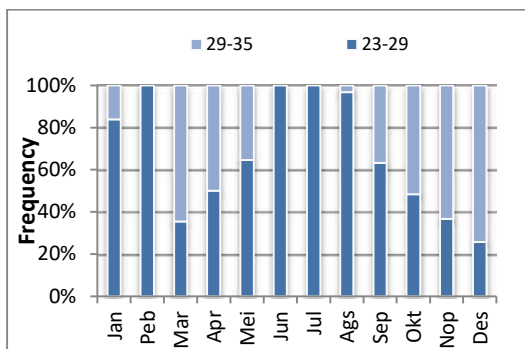
$$M + W + R + C + ED + ER.e + ESW + S = 0 \qquad …(1)$$

Where M represents the rate at which energy is produced internally, W stands for work output, R for net radiation from the body, C for convective heat flow, ED for latent heat flow used to evaporate water that is diffusing through the skin rather than sweat, ER.e for the amount of heat flow used to heat and humidify the air, ESW for heat flow from sweat evaporation, and S for stored heat flow used to heat or cool the body mass.

The air temperature (Ta) of the reference condition that results in the same model response as the real condition is known as the Universal Thermal Climate Index (UTCI). The mean radiant temperature (Tmrt), wind speed (va), humidity represented as relative humidity (RH) or water vapor pressure (vp), and actual air temperature all affect the offset or the difference between the UTCI and air temperature. It is expressed mathematically;

$$U \quad TCI = f (Ta; Tmrt; va; vp) = Ta + Offset (Ta; Tmrt; va; vp) \qquad ...(2)$$

For the reference environment, assumptions are used:

- Wind speed (va) $\cong$ 0.5 m.s^{-1} at 10 m height (approximately $\cong$ 0.3 m.s^{-1} at 1.1 m height)

- Average radiation temperature (Tmrt) = air temperature (Ta)

- At high air temperatures (>29°C), the reference humidity is assumed to be constant at a pressure of 20 hPa. Vapor pressure (vp), reflecting 50% relative humidity.

RESULTS

Historical Thermal Comfort

Thermal comfort was calculated with historical data spanning six years (2012-2017) and using PET and UTCI. Daily values are UTCI and PET. In June, the lowest daily average PET score is 27.4°C, while in December, the maximum value

Fig. 1: Daily European PET.

Fig. 2: Daily Taiwan PET.

is 29.3°C. The variation in the PET score during the year was 1.9°C. Between the rainy and dry seasons, there is no discernible difference in PET scores. In every season, there aren't any extraordinary scores.

Multiple references were consulted to ascertain the KRB area's temperature perception, including PET Europe, PET Taiwan, PET Tianjin, and PET Tel Aviv (Table 2). The thermal sensation of the KRB area on PET Europe is slightly warm and warm. In June and July, the thermal sensation is fully slightly warm. Throughout the year, the frequency of slightly warm (dark shading) was 244 days and warm (light shading) 121 days (Fig. 1).

The thermal sensation of the KRB area in PET Taiwan is slightly cool, comfortable, and slightly warm. Dominant throughout the year the KRB area is comfortable (dark shading) for 357 days. Somewhat cool (light shading) only

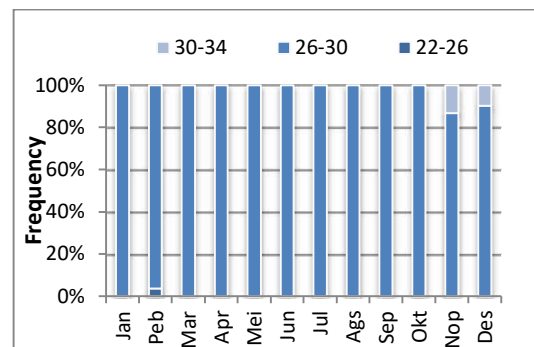one day and slightly warm (light shading) 7 days (Fig. 2).

The thermal sensation of the KRB area in Tianjin PET is slightly warm (dark shading) throughout the year (Fig. 3).

The thermal sensation of the KRB area in PET Tel Aviv is comfortable, slightly warm, and warm. Comfortable sensation (light shading) is only 1 day in February. The frequency of warm sensation (dark shading) is 262 days more than slightly warm (light shading), which is 102 days. March and September were the fully warm months (Fig. 4).

The average temperature measured by the UTCI was 29.0°C in February, the lowest, and 30.6°C in May. The 1.6°C variation in UTCI score throughout the year is not very significant. UTCI Mediterranean, UTCI Tianjin, and UTCI are the references we use to determine the thermal sensation of the KRB area (Table 3).

The thermal sensation of the KRB area in the Mediterranean UTCI is moderately hot and very hot. The very hot sensation (dark shading) is more dominant at 321 days, while the moderately hot sensation (light shading) is 44 days (Fig. 5).

The thermal sensation of the KRB area in UTCI Tianjin is moderately hot (dark shading) throughout the year (Fig. 6).

Table 2: Thermal sensation of PET.

Thermal sensation	PET Eropa (°C)[1]	PET Taiwan (°C)[1]	PET Tianjin (°C)[1]	PET Tel Aviv (°C)[2]
very cold	< 4	< 14	< -16*	< 8
cold	4 – 8	14 - 18	-16 - (-11)*	8 - 12
cool	8 – 13	18 - 22	-11 - (-6)*	12 - 15
slightly cool	13 – 18	22 - 26	-6 - 11	15 - 19
comfortable	18 – 23	26 - 30	11 - 24	19 - 26
slightly warm	23 – 29	30 - 34	24 - 31	26 - 28
warm	29 - 35	34 - 38	31 – 36	28 – 34
hot	35 - 41	38 - 42	36 - 46*	34 – 40
very hot	> 41	> 42	> 46*	> 40

Table 3: UTCI thermal sensation.

Thermal sensation	UTCI Mediterania (°C)[1]	UTCI di Tianjin (°C)[1]	UTCI (°C)[1]
extreme cold	< 4,1	< -21*	< -40
very strong cold	4,1 - 5,9	-21 - (-16)*	-40 - (-27)
very cold	5,9 - 9,1	-16 - (-11)*	-27 - (-13)
moderately cold	9,1 - 14,0	-11 - (-6)*	-13 – 0
somewhat cold	14,0 - 17,4	-6 - 12	0 – 9
Comfortable	17,4 - 24,5	12 - 25	9 – 26
moderately hot	24,5 - 29,1	25 - 33	26 – 32
very hot	29,1 - 34,1	33 - 39	32 – 38
very strong heat	34,1 - 37,7	39 - 47*	38 – 46
extreme heat	> 37,7	> 47*	> 46

Notes:
* = sensation value obtained from linear regression
1 = (Lai et al. 2014)
2 = (Cohen et al. 2013)

Fig. 3: Tianjin daily PET.

Fig. 4: Daily Tel Aviv PET.
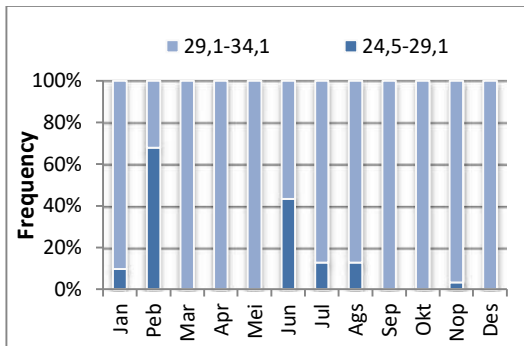
Fig. 5: Daily Mediterranean UTCI.
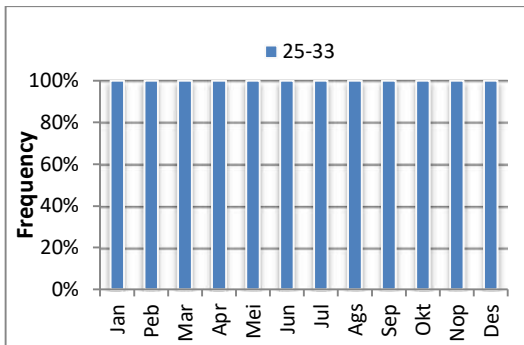
Fig. 6. Daily Tianjin UTCI.
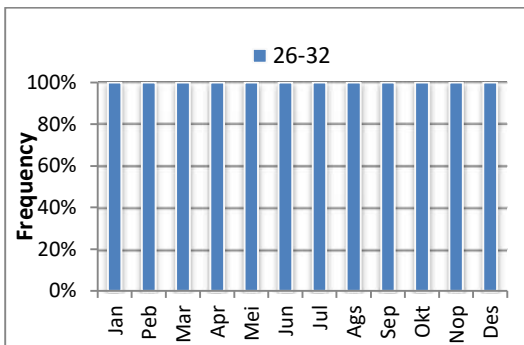
Fig. 7. Daily UTCI.

The thermal sensation of the KRB area at UTCI is moderately hot (dark shading) throughout the year (Fig. 7).

Thermal Comfort During Survey

Based on the responses to the questionnaire, the assessment of the thermal experience that guests to the KRB tourist region experienced. The temperature impression experienced by the visitors was elicited using closed-ended questions. The answer selections are grouped into seven categories: very cold, very cold, moderately cold, hot, hot, and slightly hot. Measurements of the atmospheric temperature, humidity,

Table 4. Weather parameter measurements in KRB.

	Temperature (°C)	Humidity (%)	Wind speed (m/s)
Minimum	28,3	48,2	0.1
Average	32,0	62,0	0.5
Maximum	36,0	78,7	2.0

and wind speed were taken simultaneously before visitors responded (Table 4).

Of the 284 respondents asked, 197 people (69.4%) answered that the thermal sensation of the KRB area was moderate, 30 people (10.6%) answered rather hot, 24 people (8.5%) answered hot, and 22 people (7.7%) answered rather cold (Fig. 8). Most guests agree that the temperature is ideal for tourist visits. The following results are obtained from the calculation of thermal comfort using in situ data: daily average PET = 33.8°C and daily average UTCI = 34.4°C. These results show that most visitors reported a moderate temperature sensation, with PET and UTCI values of about 33.8°C and 34.4°C, respectively. When it comes to the thermal sensation category, 33.8°C and 34.4°C fall into the categories of extremely hot and intense heat (thermal
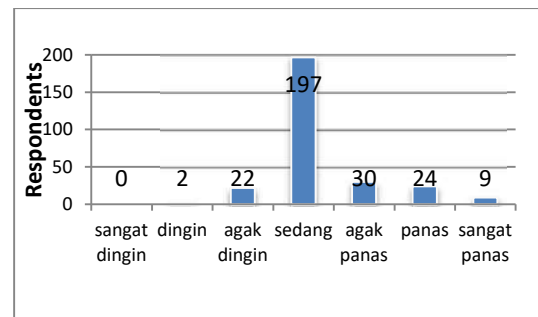
Fig. 8. Thermal sensations felt by visitors in the KRB area.

Table 5. Data collection locations.

Landscape	Number (People)	Percentage (%)
Parking lot	0	0
Trees	66	23,2
Shrubs	31	10,9
Shrubs	1	0,35
Grass	73	25,7
Water tourism	4	1,4
Pedestrian path	30	10,6
Main path	48	16,9
Rest area (gazebo/park bench)	30	10,6
Others	1	0,35
Total	284	100

sensation UTCI) and quite warm and warm (thermal sensation PET).

A total of 264 people (93%) visitors were interviewed inside the KRB tourist sites and 20 people (7%) outside the KRB area. The locations where visitors were interviewed and weather parameters were measured included parking lots, around trees, around shrubs, around bushes, grassy areas, water tourism, pedestrian paths, rest areas (gazebos/park benches), and main roads (Table 5). Most visitors were interviewed around grass (25.7%) and around trees (23.2%).

DISCUSSION

The KRB area is not in the thermal comfort zone throughout the year, except for PET Taiwan, according to reference thermal comfort categories (PET Europe, PET Taiwan, PET Tianjin, PET Tel Aviv, UTCI Mediterranean, UTCI Tianjin, and UTCI). The daily average PET in the KRB area throughout the year is in the range of 26-30°C, which means it is in the comfort zone based on Taiwan PET (Fig. 9). Conversely, the majority of tourists who participated in interviews reported moderate temperatures, with an average PET score of 33.8°C and an average UTCI of 34.4°C. Given that portions of Taiwan are in the tropics, PET Taiwan's UTCI and PET computation scores indicate values that are near the thermal comfort zone when combined with the findings of visitor interviews. These findings put our ability to categorize thermal comfort-particularly in the tropics-to the test.

According to the findings of the respondent interviews, the reason why local tourists feel at ease in the uncomfortable zone relative to existing references is the relatively low annual temperature change (<2°C). Locals have probably adjusted to make themselves comfortable in this circumstance. Additionally, there is not much of a temperature variation between the rainy and dry seasons. Additionally, the comfort of visitors is also influenced by environmental factors.
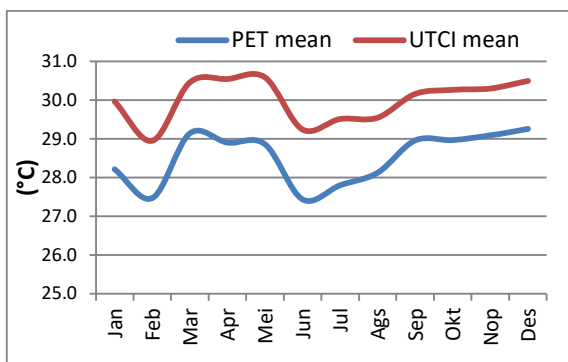
Fig. 9: Average PET and average UTCI in the KRB area for the period 2012-2017.

Interviews with most tourists took place in the shade. Visitors feel comfortable despite the "high" estimated air temperature, thanks to the presence of trees, footpaths, and rest spaces. The tree canopy contributes as a microclimate by reducing daytime air temperatures during hot days and thus increasing human thermal comfort during hot daytime conditions (Coutts et al. 2015).

We can infer from the study's findings that it's critical to classify thermal perception in Indonesia. Further research is required to fully understand the range of thermal comfort and to provide a description that is suitable for each region. Because Indonesia is on the equator, there are very few seasonal fluctuations in temperature. The dry and rainy seasons do not considerably differ in PET and UTCI ratings. PET and UTCI scores tend to be lower in the dry season due to low air humidity during this period. In the transitional season, PET and UTCI scores rise again because the sun reaches its culmination point at the equator, and the energy received in the equatorial region is maximum (Bayong Tjasyono, 2003), which results in temperatures tending to rise. Furthermore, the equator experiences low pressure, which is sufficient to boost convectiveness and have an impact on how solar energy is absorbed by the Earth's surface layer (Fadholi 2013).

CONCLUSIONS

The KRB area is not in the comfort zone throughout the year, except for PET in Taiwan, based on thermal sensation criteria from seven references (PET in Europe, PET in Taiwan, PET in Tianjin, PET in Tel Aviv, UTCI in the Mediterranean, UTCI in Tianjin, and UTCI). The PET and UTCI score fluctuations are negligible (<2°C), indicating no discernible change between the wet and dry seasons.

The daily average UTCI is 34.4°C, while the daily average PET score is 33.8°C based on in situ observations. Based on PET Taiwan's thermal sensation range, the area falls into the warm (uncomfortable) category. However, visitor responses indicate that they feel comfortable, likely due to their adaptation to the climate and the relatively little temperature variation throughout the year. Most visitors were interviewed in shaded areas like among trees, walking trails, and rest spots, suggesting that environmental factors also significantly influence their comfort levels.

To enhance thermal comfort in KRB, it is recommended to expand shaded areas through additional tree planting and shaded rest spots, introduce cooling features like fountains and misting systems to lower ambient temperatures, use reflective and light-colored materials for pathways and seating areas to reduce heat absorption, and design open spaces to promote natural ventilation and improve air circulation.

Future research should include long-term monitoring to evaluate the effectiveness of implemented strategies across seasons, expand studies to diverse tropical climates to understand thermal indices comprehensively, investigate the impact of visitor behavior and clothing on thermal comfort, utilize modern technology like wearable sensors and mobile apps for real-time data collection, and study adaptive strategies used by locals and tourists to inform the design of more comfortable outdoor spaces.

REFERENCES

Bayong Tjasyono, 2003. *Geosains*. ITB.

Blazejczyk, K., Epstein, Y., Jendritzky, G., Staiger, H. and Tinz, B., 2012. Comparison of UTCI to selected thermal indices. *International Journal of Biometeorology*, 56(3), pp.515–535. https://doi.org/10.1007/s00484-011-0453-2

Cohen, P., Potchter, O. and Matzarakis, A., 2013. Human thermal perception of Coastal Mediterranean outdoor urban environments. *Applied Geography*, 37(1), pp.1–10. https://doi.org/10.1016/j.apgeog.2012.11.001

Fadholi, A., 2013. Uji Perubahan Rata-Rata Suhu Udara Dan Curah Hujan Di Kota Pangkalpinang. *Jurnal Matematika Sains Dan Teknologi*, 14(1), pp.11–25. https://doi.org/10.33830/jmst.v14i1.309.2013

Fanger, P.O., 1970. *Thermal Comfort: Analysis and Applications in Environmental Engineering*. Danish Technical Press.

Farajzadeh, H. and Matzarakis, A., 2012. Evaluation of thermal comfort conditions in Ourmieh Lake, Iran. *Theoretical and Applied Climatology*, 107(3–4), pp.451–459. https://doi.org/10.1007/s00704-011-0492-y

Gagge, A.P., Stolwijk, J.A. and Nishi, Y., 1972. An effective temperature scale based on a simple model of human physiological regulatory response. *Memoirs of the Faculty of Engineering, Hokkaido University*, 13(Suppl), pp.21-36.

Hadi, R., 2012. Evaluation of the Comfort Index of Urban Parks (Puputan Badung Field, I Gusti Ngurah Made Agung) in Denpasar, Bali. *E-Jurnal Agroekoteknologi Tropika*, 1(1), pp.34–45. https://doi.org/E-Jurnal Agroekoteknologi Tropika ISSN: 2301-6515 Vol. 1, No. 1, Juli 2012

Lai, D., Guo, D., Hou, Y., Lin, C. and Chen, Q., 2014. Studies of outdoor thermal comfort in northern China. *Building and Environment*, 77, pp.110–118. https://doi.org/10.1016/j.buildenv.2014.03.026

Lin, T.P. and Matzarakis, A., 2011. Tourism climate information based on human thermal perception in Taiwan and Eastern China. *Tourism Management*, 32(3), pp.492–500. https://doi.org/10.1016/j.tourman.2010.03.017

Matzarakis, A. and Matzarakis, A., 2016. Weather- and Climate-Related Information for Tourism. *Weather- and Climate-Related Information for Tourism*, 3, pp.99–115.

Matzarakis, A., Endler, C. and Nastos, P.T., 2014. Quantification of climate-tourism potential for Athens, Greece - Recent and future climate simulations. *Global Nest Journal*, 16(1), pp.43–51. https://doi.org/10.30955/gnj.001264

Mayer, H. and Höppe, P., 1987. Thermal comfort of man in different urban environments. *Theoretical and Applied Climatology*, 38(1), pp.43–49. https://doi.org/10.1007/BF00866252

Park, S., Tuller, S.E. and Jo, M., 2014. Application of Universal Thermal Climate Index (UTCI) for microclimatic analysis in urban thermal environments. *Landscape and Urban Planning*, 125, pp.146–155. https://doi.org/10.1016/j.landurbplan.2014.02.014

Spagnolo, J. and de Dear, R., 2003. A field study of thermal comfort in outdoor and semi-outdoor environments in subtropical Sydney, Australia. *Building and Environment*, 38(5), pp.721–738. https://doi.org/10.1016/S0360-1323(02)00209-3

Sudiar, N.Y. and Gautama, M.I., 2023. Visitors Perceptions of the Climate Comfort at the Padang Coastal Tourism Area, Indonesia. *Nature Environment and Pollution Technology*, 22(2), pp.929–935. https://doi.org/10.46488/NEPT.2023.v22i02.036

Sudiar, N.Y., Koesmaryono, Y., Perdinan, P. and Arifin, H.S., 2019. Karakteristik dan Kenyamanan Iklim Lokasi Wisata Berbasis Alam di Eco-Park Ancol, Kebun Raya Bogor dan Kebun Raya Cibodas. *EnviroScienteae*, 16, p.75. https://doi.org/10.20527/es.v15i2.6967

Original Research Paper https://doi.org/10.46488/NEPT.2025.v24i01.D1670 **Open Access Journal**

Using *Azospirillum* Bacteria Isolated from Soil as Bioremediation Agent in Wastewater Contaminated with Cadmium in Iraq

Z. R. Abbas[1†], A. M. Al-Ezee[1], B. T. Al-Shandah[2] and M. A. Shafeeq[1]

[1]Department of Biology, College of Science, Mustansiriyah University, Baghdad, Iraq
[2]Department of Biology, College of Science, Tikrit University, Iraq
†Corresponding author: Z. R. Abbas; zaid2024ra@hotmail.com; Zaidraad91@uomustansiriyah.edu.iq

ABSTRACT

Bioremediation is an important technique to remove heavy metals from wastewater. The current research aimed to use *Azospirillum* bacteria in removing cadmium ions from wastewater. The source of *Azospirillum* bacteria was the soil of Al-Mishkhab in Al-Najaf province, Iraq (rice fields), while the source of wastewater was taken from the Al-Rustamia wastewater treatment plant, in Baghdad in October 2020. All the experiments were carried out in Soil and Water Research Center, Ministry of Science and Technology. After collecting the soil, the microorganisms were isolated through the Immunomagnetic beads (IMB) process and were incubated on a certain synthesized medium. The concentration of cadmium ion was determined through the Absorption Spectrophotometer (AAS) technique. The *Azospirillum* colonies were identified and characterized as white colonies while the concentration of cadmium ion ranged from 0.03-1.6 mg/L and applying the microorganism on the wastewater will decrease the concentration up to 99.9% in a process called biosorption. Treatment time was also studied for 24, 48, 72, and 168 hours. The statistical analysis shows that increasing time will enhance the removal of cadmium. Cadmium is one of the heavy metals responsible for soil contamination; bacteria play a crucial role in bioremediation, demonstrating stability in decomposing various compounds and materials. *Azospirillum* is employed for soil decontamination purposes; increasing incubation time will enhance the removal of the trace element; also further investigate the effect of other factors such as temperature, pH, and the effect of using other microorganisms.

INTRODUCTION

Bioremediation is a method used to take out pollutants and remove them using microorganisms such as bacteria. However, due to the development of civilization and industry, as well as the huge increase in the activities of human beings, consequently, it has a bad reflection on the environment and increased the rate of pollution which mostly ends and accumulates in water as water pollutants (Manisalidis et al. 2020).

Bacteria and sometimes fungi are used in bioremediation due to their ability to decompose compounds and materials and devour them as well which ultimately detoxifies the surroundings such as water or soil and makes it not hazardous to the environment and all living creatures (Bala et al. 2022), this indicates its microbiological activity. In this, the microorganism can behave as an agent that can store the pollutants after devouring them in a very accurate procedure (Kraemer et al. 2019). Bacteria are the most common microorganisms that are used as a bioremediation agent that performed as a considerable agents to remove pollutants from sediments, water, and soil (Quintella et al. 2019).

Heavy metals, which are non-biodegradable contaminants, pose severe threats to the environment, particularly impacting water and soil (Al-Shammari et al. 2022, Al-Shammari et al. 2023). These metals originate from various sources,

including automobile exhaust, storage batteries, industrial activities, mining, pesticides, fertilizers, and more. Some of the most common and highly toxic heavy metals that adversely affect human health and the well-being of flora and fauna include nickel, gold, silver, cadmium, arsenic, selenium, mercury, and chromium. Numerous approaches and methods have been proposed to eliminate these metals from the environment (Priya et al. 2023).

Microorganisms used in bioremediation can be classified into two categories: aerobic and anaerobic. Aerobic microorganisms, such as *Mycobacterium*, *Rhodococcus*, and *Pseudomonas*, are reported to be effective in degrading hydrocarbons and pesticides. On the other hand, anaerobic microorganisms are utilized for the bioremediation of polychlorinated biphenyls (PCBs) and the dechlorination of river sediments, as evidenced by various bacterial species (Sayqal & Ahmed, 2021). Additionally, *Trichoderma* has been used by Ali et al. (2023) for the removal of toxic dyes from aqueous mediums.

Many researchers studied how to involve microorganisms like; algae, yeast, fungi, and bacteria in the process of bioremediation they used *P. aeruginosa*, *Streptomyces*, and *Pseudomonas* (Azadi & Shojaei 2020, Al-Thukair et al. 2020, Qutob et al. 2022), it was noticed that certain types of bacteria have the ability to bind with the heavy metals through their thick lipo-wall forming a coordination bonds with the toxic heavy metal in a process called biosorption, among these microorganisms are *Saccharomyces*, *Streptoverticullum*, *Aspergillus*, and the genera of *Rhizopus* (Abdel-Raouf et al. 2022). Furthermore, *Azospirillumsp.* is renowned for its role as a promoter of plant growth across diverse cultures. Yet, its adaptive traits in challenging environments position it as a promising candidate for investigating remediation processes in environments contaminated with hydrocarbons and heavy metals (Cruz-Hernández et al. 2022).

In 2023, Zulfiqar et al. mentioned in their review article that microorganisms, such as bacteria, fungi, and algae, are known for their remarkable metal tolerance, exhibiting an impressive 98% capacity for bioremediation.

The current study, aimed to use *Azospirillum* bacteria isolated from soil in wastewater treatment via removing heavy metals, in particular, cadmium.

MATERIALS AND METHODS

Collection!of!Soil!Samples

The samples of soil were collected from a rice field in Al-Mishkhab/Al-Najafprovince, Iraq, this place was chosen as a source for the soil in the current research. The samples of the soil were collected in October 2020 because this month the humidity percentage increased. However, the samples of the soil were gathered at a depth of 35 cm, mixed, and then stored in the lab at room temperature (around 21 °C), the procedure was previously explained by (Dickman et al. 1984).

All the tests of soil and wastewater and the experiments were carried out in Soil and Water Research Center, Ministry of Science and Technology, Baghdad-Iraq.

Wastewater Samples

The wastewater samples were collected from the Al-Rustamia wastewater treatment plant in Baghdad City, Iraq. This location was chosen because it is expected it contain a lot of heavy metals due to the presence of a lot of industrial and chemical activities in the area which increases the presence of pollutants, especially, heavy metals.

Determination of Cadmium

The determination of the cadmium concentration in wastewater was done on both 7850ICP-MS according to SFS-EN ISO 17294-2 standard (Gray & Cunningham 2019), and Shimadzu AA - 6650 Atomic Absorption Spectrophotometer, the protocols were explained by (Costley & Wallis 2001, Sarker et al. 2015).

Serial Dilution Method

The method of serial dilution was carried out according to (Kanimozhi & Panneerselvam 2017, Damo et al. 2022), five grams of the soil were placed in a test tube, and 45 milliliters of SW (sterilized water) was added and mixed carefully, and thoroughly. After good mixing, the mixture was subjected to a process called Immunomagnetic beads [IMB] as explained by (Han & New 1998) after the IMB, only one milliliter of the solution was taken and placed in another test tube, and 9 mL of SW were added to complete the volume to 10 mL (dilution process DP). The DP was repeated for 10 times of dilution (10 folds in a process called serial dilution), however, the solutions that came out from the serial dilution were plated on culture repopulation ability (CRA) and incubated for 5 days at 32°C on NFb agar as described by (Rathore 2014).

Isolation of *Azospirillum*

NFb agar is a suitable medium was used for isolation of *Azospirillum* from the following components (gm/L):

Part A: Agar (1.75) g, $CaCl_2$ (0.02) g, Na Molybdate (0.002) g, Bromothymol blue (0.002) g, NaCl (0.1) g, $MgSO_4$ (0.2) g, $MnSO_4$ (0.01) g, $FeSO_4$ (0.5) g, Dipotassium phosphate (0.5) g (as a buffering reagent), and Malic acid (5.0) g (which is used particularly to grow *Azospirillum* only and not used by other NFb).

Part B. (4.0) g/L of KOH

Part **A** and Part **B** were mixed well together, and the pH was adjusted finally to around (6.9 ± 0.1), the well-mixed result in the medium was placed in an autoclave for 20 minutes and the temperature should be fixed at 121°C. The incubation is carried out for 8 days at 30°C.

Identification of *Azospirillum* Bacteria

Bacterial isolates have been submitted to cultural, microscopical, and biochemical examination as mentioned by (Sulaiman et al. 2019).

Laboratory Experiment

The experiment was carried out by inoculating a test tube containing well-mixed crude wastewater samples with a known concentration of cadmium in it, for the 10 samples that were used in the experiment. They were inoculated by loop via taking a swab of pure bacteria that were grown on NFb agar medium. The tubes were incubated in the incubator at 30°C for a period of specified time (Table 3).

Statistical Analysis

The Statistical Analysis System - SAS (2018) program was used to detect the effect of different factors on study parameters. The least significant difference (LSD) test (Analysis of Variation-ANOVA) was used to significantly compare between means in this study.

Fig. 1: *Azospirillum bacteria*.

Fig. 2: *Azospirillum* colonies in NFb Agar medium after 8 days of incubation.

RESULTS AND DISCUSSION

Isolation and Identification of *Azospirillum* Bacteria

According to Sulaiman et al. (2019), the isolates were identified as members of the genus *Azospirillum* based on their colony shape, Gram staining, and biochemical assays, as detailed in Table 1. On the medium surface, *Azospirillum* colonies appear as dense, white, undulating pellicles approximately 1 mm thick (Fig. 1). The characteristics of *Azospirillum* are listed in Table 1. The observed appearance and identification of *Azospirillum* align with the findings of Mallé et al. (2020) and Sulaiman et al. (2019).

Wastewater samples were collected at different times over ten days. The date, time, and cadmium concentration of these samples are shown in Table 2. It is crucial to specify the time and date accurately, as industrial activities affect the concentration of Cd ions. Nonetheless, the Cd concentration was observed to range from 0.03 to 1.6 mg/L.

According to the World Health Organization (WHO), the concentration of cadmium ions in drinking water should not exceed 0.003 mg/L (Steiner et al. 2011). However, the

Table 1: Biochemical and Morphological characterization of the *Azospirillum* isolates.

No.	Examination	Isolate
1	Characteristic of colonies	Mucous. Large, convex with full edge
2	Microscopic characters	Inflate rods with polymorphic cells from straight to curved
3	Production of acid	Positive
4	Liquefaction of Gelatin	Negative
5	Oxidase	Positive
6	Catalase	Positive
7	Production of Urease	Positive
8	Production of H_2S	Negative
9	Utilization of Citrate	Positive
10	Voges-Proskauer test	Negative
11	Production of Indole	Negative
12	Mannitol	Positive
13	Xylose	Negative
14	Dextrose	Positive
15	Maltose	Positive
16	Lactose	Positive
17	Gram's staining	Gram Negative
18	fermentation of Sucrose	Negative
19	fermentation of Glucose	Positive
20	fermentation of fructose	Positive
21	Pigmentation	Nil

Table 2: Concentration of Cadmium ions in the samples.

Sample No	Date and time	Cd (mg/L)
1.	Saturday 3 Oct. 2020 at 10 am	0.9
2.	Monday 5 Oct. 2020 at 1:30 pm	0.07
3.	Sunday 11 Oct. 2020 at 9:35 am	0.85
4.	Monday 12 Oct. 2020 at 11:45 am	1.02
5.	Wednesday 14 Oct. 2020 at 4:05 pm	1.3
6.	Thursday 15 Oct. 2020 at 10:37 am	1.5
7.	Monday 19 Oct. 2020 at 9:48 am	1.6
8.	Tuesday 20 Oct. 2020 at 11:54 am	0.07
9.	Thursday 22 Oct. 2020 at 2:18 pm	0.06
10.	Friday 23 Oct. 2020 at 3:51 pm	0.03
P-value	-	0.0017 **
** ($P \le 0.01$).		

observed levels significantly exceed this recommended threshold.

Statistical analysis of the values in Table 2 shows significant differences in the cadmium content among the ten samples collected at different times, with a p-value of 0.0017 ($P \le 0.01$).

Azospirillum was used to treat wastewater samples for different durations, as shown in Table 3. Statistical analysis results are also presented in Table 3 and Fig. 2.

Using *Azospirillum* on the contaminated samples revealed the complete removal of Cd traces. Furthermore, a notable correlation was observed between Cd concentrations and time, with the trace element ion being removed by 65% after 24 hours, 99% after 48 hours, and completely after 72 hours. This percentage remains unchanged even after a week, as depicted in Fig. 3.

Research has explored the capability of *Azospirillum*, a bacterium renowned for promoting plant growth, to remove heavy metals such as cadmium from wastewater. Studies indicate that certain strains of *Azospirillum* can enhance the absorption of heavy metals in the soil while preventing cadmium uptake by plants, suggesting a potential role for these microorganisms in bioremediation (Cruz-Hernández et al. 2022). Additionally, another study investigated the use of *Azospirillum* in a mixotrophic culture to eliminate cadmium from wastewater, highlighting its suitability and effectiveness in achieving a 98% bioremediation capacity (Zulfiqar et al. 2023).

Another study indicates that adding *Azospirillum* to plants treated with Cd can positively impact their biomass and root length. It has also been demonstrated to enhance nutrient uptake, stimulate overall plant growth, and mitigate the adverse effects of heavy metals such as Pb and Cd (Cruz-Hernández et al. 2022).

A study on *Pantoea agglomerans* UCP1320's ability to remove cadmium from aqueous solutions found that longer incubation times resulted in higher removal of cadmium (II). The study (Acioly et al. 2018) noted that desorption probabilities typically ranged from 6 to 24 hours during extended incubation times, a conclusion consistent with current research. This finding aligns with the results of Limcharoensuk et al. (2015). It can be concluded, however, that bioremediation cannot eliminate Cd; the maximum removal achieved was 94%, observed after 48 hours. This finding is consistent with the research of Kumar et al. (2021), suggesting that while 48 hours may not suffice for complete removal, longer durations (e.g., 72 hours) may be more effective.

Lipids present in *Azospirillum* membranes may assist in bioremediation by forming organometallic complexes

Table 3: The relationship between the concentration of Cd and treatment time.

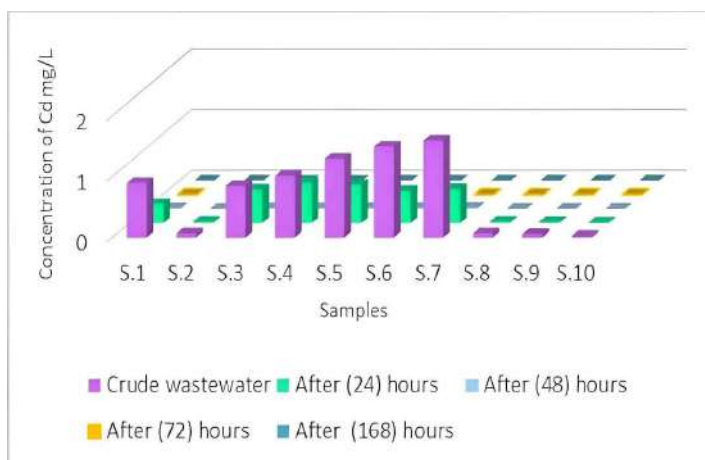| No.	Concentration of Cd (mg/L)					
	Crude wastewater (Not treated)	After (24) hours	After (48) hours	After (72) hours	After one week (168) hours	P-value
1	0.900	0.315 (65%)	0.009 (99%)	0.000 (100%)	0.000 (100%)	0.0001 **
2	0.070	0.025 (65%)	0.000 (99%)	0.000 (100%)	0.000 (100%)	0.0424 *
3	0.850	0.553 (65%)	0.008 (99%)	0.000 (100%)	0.000 (100%)	0.0001 **
4	1.020	0.663 (65%)	0.01 (99%)	0.000 (100%)	0.000 (100%)	0.0001 **
5	1.300	0.631 (65%)	0.013 (99%)	0.000 (100%)	0.000 (100%)	0.0001 **
6	1.500	0.53 (65%)	0.015 (99%)	0.000 (100%)	0.000 (100%)	0.0001 **
7	1.600	0.56 (65%)	0.016 (99%)	0.000 (100%)	0.000 (100%)	0.0001 **
8	0.07	0.024 (65%)	0.000 (99%)	0.000 (100%)	0.000 (100%)	0.0488 *
9	0.06	0.021 (65%)	0.000 (99%)	0.000 (100%)	0.000 (100%)	0.074 NS
10	0.03	0.011 (65%)	0.000 (99%)	0.000 (100%)	0.000 (100%)	0.316 NS
* ($P \le 0.05$), ** ($P \le 0.01$).						

Fig. 3: The relationship between the concentration of Cd and treatment time.

with cadmium ions via biosorption (Haque et al. 2021). The removal process is pH-sensitive. Increasing the pH to alkaline levels (pH 7.8) enhances the release of Cd ions from the medium and strengthens their binding to the microorganisms' cell walls (Javanbakht et al. 2014).

Table 3 reveals notable variations in cadmium concentrations between crude wastewater samples and those treated with bacteria at different time intervals. Statistical analysis indicated significant differences for samples No. 1, 3, 4, 5, 6, and 7 at a significance level of 0.001 ($P \leq 0.01$), while samples No. 2 and 8 showed significant differences at a significance level of 0.005 ($P \leq 0.05$). However, samples No. 9 and 10 did not exhibit significant differences for the same variables.

CONCLUSION

Cadmium is among the heavy metals commonly found in domestic and commercial wastewater. Bacteria, due to their ability to degrade various substances and materials, can be employed in biological treatments to mitigate hazardous levels of this substance in aquatic environments. *Azospirillum* bacteria effectively remove these contaminants from soil. Results indicated that extending the incubation period enhanced the rate of cadmium removal from contaminated water; after 72 hours of incubation, *Azospirillum* bacteria biosynthesized 100% of the cadmium ions. While the study demonstrates the effectiveness of *Azospirillum* bacteria in cadmium removal, further investigation and specific experimental data may be necessary to comprehensively evaluate their efficacy in wastewater treatment. Factors such as temperature, pH, bacterial strain, and their interplay with biological efficiency should also be considered.

REFERENCES

Abdel-Raouf, N., Sholkamy, E.N., Bukhari, N., Al-Enazi, N.M., Alsamhary, K.I., Al-Khiat, S.H.A. and Ibraheem, I.B.M., 2022. Bioremoval capacity of Co²⁺ using *Phormidium tenue* and *Chlorella vulgaris* as biosorbents. *Environmental Research*, 204(Pt B), p.111630. https://doi.org/10.1016/j.envres.2021.111630.

Acioly, L.M., Cavalcanti, D., Luna, M.C., Júnior, J.C.V., Andrade, R.F.S., de Lima e Silva, T.A., La Rotta, C.E. and Campos-Takaki, G.M., 2018. Cadmium removal from aqueous solutions by strain of *Pantoea agglomerans* UCP1320 isolated from laundry effluent. *Open Microbiology Journal*, 12, pp.297-307. https://doi.org/10.2174/1874285801812010297.

Ali, S.S.M., Al-Shammari, R.H.H. and Al-Mamoori, A.M.J., 2023. Removing toxic dyes from aqueous medium by trichoderma-graphain oxide aerogel. *Published Online First*, 20(6), pp.2134-2143. doi: https://dx.doi.org/10.21123/bsj.2023.7773.

Al-Shammari, R.H., Ali, S.S.M. and Hussien, M.S., 2023. Efficient copper adsorption from aqueous solution by *Dictyuchus* sterile pellets. *Nature Environment and Pollution Technology*, 22, pp.905-912. https://doi.org/10.46488/NEPT.2023.v22i02.033.

Al-Shammari, R.H., Alsaady, M.H.M. and Ali, S.S.M., 2022. The efficiency of biosynthesized zinc oxide nanoparticles by *Fusarium* sp. against *Saprolegnia parasitica* isolated from common carp eggs in a fish hatchery. *International Journal of Aquatic Biology*, 10(5), pp.378-383. https://doi.org/10.22034/ijab.v10i5.1741.

Al-Thukair, A.A., Malik, K. and Nzila, A., 2020. Biodegradation of selected hydrocarbons by novel bacterial strains isolated from contaminated Arabian Gulf sediment. *Scientific Reports*, 10(1), p.21846. https://doi.org/10.1038/s41598-020-78733-0.

Azadi, D. and Shojaei, H., 2020. Biodegradation of polycyclic aromatic hydrocarbons, phenol and sodium sulfate by *Nocardia* species isolated and characterized from Iranian ecosystems. *Scientific Reports*, 10(1), p.21860. https://doi.org/10.1038/s41598-020-78821-1.

Bala, S., Garg, D., Thirumalesh, B.V., Sharma, M., Sridhar, K., Inbaraj, B.S. and Tripathi, M., 2022. Recent strategies for bioremediation of

emerging pollutants: a review for a green and sustainable environment. *Toxics*, 10(8), p.484. https://doi.org/10.3390/toxics10080484.

Costley, S.C. and Wallis, F.M., 2001. Bioremediation of heavy metals in a synthetic wastewater using a rotating biological contactor. *Water Research*, 35(15), pp.3715-3723. https://doi.org/10.1016/s0043-1354(01)00072-0.

Cruz-Hernández, M.A., Mendoza-Herrera, A., Bocanegra-García, V. and Rivera, G., 2022. *Azospirillum* spp. from plant growth-promoting bacteria to their use in bioremediation. *Microorganisms*, 10(5), p.1057. https://doi.org/10.3390/microorganisms10051057.

Damo, J.L.C., Ramirez, M.D.A., Agake, S.I., Pedro, M., Brown, M., Sekimoto, H., Yokoyama, T., Sugihara, S., Okazaki, S. and Ohkama-Ohtsu, N., 2022. Isolation and characterization of phosphate solubilizing bacteria from paddy field soils in Japan. *Microbes and Environments*, 37(2), p.ME21085. https://doi.org/10.1264/jsme2.ME21085.

Dickman, L.A., Liberta, A.E. and Anderson, R.C., 1984. Ecological interaction of little bluestem and vesicular–arbuscular mycorrhizal fungi. *Canadian Journal of Botany*, 62(11), pp.2272-2277. https://doi.org/10.1139/b84-309.

Gray, P.J. and Cunningham, W., 2019. Inductively coupled plasma collision cell quadrupole mass spectrometric determination of extractible arsenic, cadmium, chromium, lead, mercury, and other elements in food using microwave-assisted digestion: results from an FDA interlaboratory study. *Journal of AOAC International*, 102(2), pp.590-604. https://doi.org/10.5740/jaoacint.18-0129.

Han, S.O. and New, P.B., 1998. Isolation of *Azospirillum* spp. from natural soils by immunomagnetic separation. *Soil Biology and Biochemistry*, 30(8-9), pp.975-981. https://doi.org/10.1016/S0038-0717(98)00020-0.

Haque, M.M., Mosharaf, M.K., Haque, M.A., Tanvir, M.Z.H. and Alam, M.K., 2021. Biofilm formation, production of matrix compounds and biosorption of copper, nickel and lead by different bacterial strains. *Frontiers in Microbiology*, 12, p.615113. https://doi.org/10.3389/fmicb.2021.615113.

Javanbakht, V., Alavi, S.A. and Zilouei, H., 2014. Mechanisms of heavy metal removal using microorganisms as biosorbent. *Water Science and Technology*, 69(9), pp.1775-1787. https://doi.org/10.2166/wst.2013.718.

Kanimozhi, K. and Panneerselvam, A., 2017. Isolation and characterization of *Azospirillum* sp. from paddy field soil, Thanjavur district, Tamil Nadu. *International Journal of Scientific Research*, 6, pp.1193-1199.

Kraemer, S.A., Ramachandran, A. and Perron, G.G., 2019. Antibiotic pollution in the environment: from microbial ecology to public policy. *Microorganisms*, 7(6), p.180. https://doi.org/10.3390/microorganisms7060180.

Kumar, A., Subrahmanyam, G., Mondal, R., Cabral-Pinto, M.M.S., Shabnam, A.A., Jigyasu, D.K., Malyan, S.K., Fagodiya, R.K., Khan, S.A., Kumar, A. and Yu, Z.G., 2021. Bio-remediation approaches for alleviation of cadmium contamination in natural resources. *Chemosphere*, 268, p.128855. https://doi.org/10.1016/j.chemosphere.2020.128855.

Limcharoensuk, T., Sooksawat, N., Sumarnrote, A., Awutpet, T., Kruatrachue, M., Pokethitiyook, P. and Auesukaree, C., 2015. Bioaccumulation and biosorption of Cd²⁺ and Zn²⁺ by bacteria isolated from a zinc mine in Thailand. *Ecotoxicology and Environmental Safety*, 122, pp.322-330. https://doi.org/10.1016/j.ecoenv.2015.08.013.

Mallé, I., Kassogué, A., Babana, A.H., de Oliveira Paiva, C.A. and Murriel, I.I., 2020. A Malian native *Azospirillum* sp. Az6-based biofertilizer improves growth and yield of both rice (*Oryza sativa* L.) and maize (*Zea mays* L.). *African Journal of Microbiology Research*, 14(7), pp.286-293. https://doi.org/10.5897/AJMR2020.9348.

Manisalidis, I., Stavropoulou, E., Stavropoulos, A. and Bezirtzoglou, E., 2020. Environmental and Health Impacts of Air Pollution: A Review. *Frontiers in Public Health*, 8, p.14. https://doi.org/10.3389/fpubh.2020.00014.

Priya, A.K., Muruganandam, M., Ali, S.S. and Kornaros, M., 2023. Clean-up of heavy metals from contaminated soil by phytoremediation: a multidisciplinary and eco-friendly approach. *Toxics*, 11(5), p.422. https://doi.org/10.3390/toxics11050422.

Quintella, C.M., Mata, A.M.T. and Lima, L.C.P., 2019. Overview of bioremediation with technology assessment and emphasis on fungal bioremediation of oil contaminated soils. *Journal of Environmental Management*, 241, pp.156-166. https://doi.org/10.1016/j.jenvman.2019.04.019.

Qutob, M., Rafatullah, M., Muhammad, S.A., Alosaimi, A.M., Alorfi, H.S. and Hussein, M.A., 2022. A review of pyrene bioremediation using mycobacterium strains in a different matrix. *Fermentation*, 8(6), p.260. https://doi.org/10.3390/fermentation8060260.

Rathore, P., 2014. Isolation, biochemical characterization and inoculation effect of *Azospirillum* on the growth of wheat. *International Journal of Scientific Research*, 3(6), pp.626-628.

Sarker, B.C., Baten, M.A., Eqram, M., Haque, U., Das, A.K., Hossain, A. and Hasan, M.Z., 2015. Heavy metals concentration in textile and garments industries' wastewater of Bhaluka industrial area, Mymensingh, Bangladesh. *Current World Environment*, 10(1), p.61. http://dx.doi.org/10.12944/CWE.10.1.07.

SAS, 2018. *Statistical Analysis System, User's Guide. Statistical*. Version 9.6th ed. SAS Inst. Inc. Cary, N.C., USA.

Sayqal, A. and Ahmed, O.B., 2021. Advances in heavy metal bioremediation: an overview. *Applied Bionics and Biomechanics*, 2021, p.1609149. https://doi.org/10.1155/2021/1609149.

Şenol, H., 2021. Effects of NaOH, thermal, and combined NaOH-thermal pretreatments on the biomethane yields from the anaerobic digestion of walnut shells. *Environmental Science and Pollution Research International*, 28(17), pp.21661-21673. https://doi.org/10.1007/s11356-020-11984-6.

Steiner, T.J., Birbeck, G.L., Jensen, R., Katsarava, Z., Martelletti, P. and Stovner, L.J., 2011. The global campaign, world health organization and lifting the burden: collaboration in action. *Journal of Headache and Pain*, 12(3), pp.273-274. https://doi.org/10.1007/s10194-011-0342-4.

Sulaiman, K.H., Al-Barakah, F.N., Assafed, A.M. and Dar, B.A.M., 2019. Isolation and identification of *Azospirillum* and *Azotobacter* species from Acacia spp. at Riyadh, Saudi Arabia. *Bangladesh Journal of Botany*, 48(2), pp.239-251. https://doi.org/10.3329/bjb.v48i2.47546.

Zulfiqar, U., Haider, F.U., Maqsood, M.F., Mohy-Ud-Din, W., Shabaan, M., Ahmad, M., Kaleem, M., Ishfaq, M., Aslam, Z. and Shahzad, B., 2023. Recent advances in microbial-assisted remediation of cadmium-contaminated soil. *Plants (Basel)*, 12(17), p.3147. https://doi.org/10.3390/plants12173147.

Original Research Paper   https://doi.org/10.46488/NEPT.2025.v24i01.D1682   **Open Access Journal**

The Circular Economy of the Food Bank Supply Chain in Bandung City, West Java

Sri Widiyanesti[1,2][†] and Bintang Mahardhika[1]

[1]School of Economics and Business, Telkom University, Jl. Telekomunikasi No. 1 Ters. Buah Batu, Bandung-40257, Indonesia

[2]Center of Excellent Digital Business Ecosystem, Jl. Telekomunikasi No. 1 Ters. Buah Batu, Bandung-40257, Indonesia

†Corresponding author: Sri Widiyanesti; widiyanesti@telkomuniversity.ac.id

ABSTRACT

Food banks play a crucial role in reducing food waste and addressing food vulnerability. Their operations involve an efficient supply chain that collects surplus food, processes it, and distributes it to those in need. This aligns with the goals of a circular economy, aiming to minimize food crises. This research aims to understand the supply chain of the Food Bank Bandung and analyze the implementation of circular economy principles within its supply chain. The study employs qualitative methods, with data gathered through interviews conducted with representatives from the Food Bank located in Bandung City. The collected information was used to design a comprehensive supply chain model, which was then meticulously analyzed. The analysis reveals that the Food Bank in Bandung effectively implements a circular economy by transforming surplus food, which would otherwise go to waste, into consumable items. Furthermore, the food bank adopts circular economy concepts by providing inedible food to Black Soldier Fly (BSF) cultivation for maggot consumption, which then can be used as an alternative source of protein for animal feed. The findings of the study show how circular economy practices can be integrated into food bank operations. By analyzing the circular economy approach in the Food Bank of Bandung, this research contributes to the existing body of knowledge and provides a foundation for future studies, offering a more extensive dataset for researchers and practitioners in the field.

INTRODUCTION

Food banks play a significant role in implementing circular economy principles to reduce waste and decrease food vulnerability (Syalianda & Kusumastuti 2023). According to research conducted by Syalianda & Kusumastuti (2023), the government plays an important role in addressing hunger-reduction issues and enhancing food security within the implementation of circular economy goals within food banks. The association between the supply chain and the standards of the circular economy is vital and must be adjusted, as highlighted by Montag (2022). An exceedingly viable and effective supply chain can minimize nourishment emergency dangers, as demonstrated by Tan et al. (2022).

Currently, society has adopted supply chain systems in everyday life, businesses, and organizations, both consciously and unconsciously. According to Frederico (2021), the supply chain involves all parties, from suppliers, manufacturers, transporters, warehouses, and retailers to customers. As a real example, food banks, as explained by Syalianda & Kusumastuti (2023), are organizations that apply the concept of the supply chain. Food banks collect food waste from donors, process it, and distribute it to various institutions that provide food to the community in need. The processing of food waste reduces waste and maximizes resource utilization (Dewilda et al. 2021, Studnička 2021). This is closely related to the circular economy system.

Circular economy (CE) involves the circulation of materials and energy, with the primary goal of reducing waste (Arruda et al. 2021). CE supports an economic system that prioritizes the reduction of resource use and mitigates environmental impact (Montag 2022). The implementation of the circular economy is particularly beneficial in countries with high levels of waste production, as noted by Waluyo & Kharisma (2023).

According to the report from the United Nations Environment Programme (UNEP) titled "Food Waste Index 2021" (Forbes et al. 2021), Indonesia has the highest waste production in Southeast Asia, reaching 20,938,252 tons per year. Moreover, the waste composition graph published by SIPSN (National Waste Management Information System) in 2023 indicates that 41.6% of Indonesia's total waste is food waste, followed by wood at 12.5%, paper at 11.5%, plastic at 17.3%, and others 17.1%, emphasizing that the majority of waste in Indonesia is food waste (SIPSN 2023).

Given the prevailing waste conditions in Indonesia, this research aims to confirm that the Food Bank Bandung has implemented a circular economy to address the issue of food waste in Indonesia. Moreover, food banks in other cities can adopt a similar system to what has been implemented in Bandung to assist in addressing food waste in Indonesia.

In the introduction, we delineate the pivotal role of food banks in addressing food waste and hunger reduction. Additionally, we expound on the significance of implementing an effective and efficient supply chain to adhere to the principles of circular economy. The material and methods section provides a detailed explanation of supply chains, food banks, and circular economy. Furthermore, we articulate various insights derived from interviews with Food Bank experts in Bandung and process this information to formulate a supply chain design. The results and discussion section scrutinizes the supply chain of the Food Bank Bandung concerning circular economy principles. In the conclusion, we draw conclusions based on the preceding discussions.

MATERIALS AND METHODS

A. Supply Chain

The supply chain is defined as a flow encompassing individuals, organizations, technology, activities, information, and resources. Various entities are involved in producing and delivering a product from its initial stage to the end user (Bigliardi et al. 2022). To meet consumer demand for products and services, the concept of the supply chain refers to the integration of material and information flows across all supply chain entities (Coyle et al. 2021). This involves coordination among entities such as distributors, suppliers, manufacturers, wholesalers, and customers (Wieland & Durach 2021). For example, Rivera et al. (2023) describe several supply chain models from food banks in Fig. 1.

Food banks occasionally directly distribute food to individual institutions (Network A), but institutions are often aggregated and visited along routes to enhance transportation efficiency (Network B). Additionally, it is possible to introduce food distribution points to share the distribution effort between food banks and institutions (Network C).
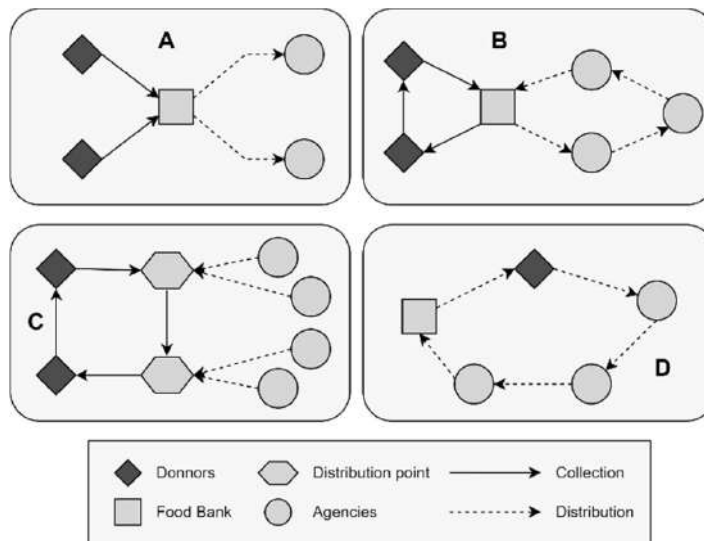
Source: Rivera et al. (2023)

Fig. 1. Several food bank supply chains reported in the literature.

Furthermore, in Network D, food banks visit donors and institutions by organizing pickup locations and distribution flows. From the supply chain model above, we know that a good supply chain will simplify all actions in each process.

A well-managed supply chain can reduce costs, enhance efficiency, and ensure timely product delivery (Zhao et al. 2023). Ensuring the smooth flow of materials, information, and resources efficiently from the initial processes to product delivery to the end user is crucial. Supply chain management involves coordination and integration in every process and activity within the supply chain (Solaimani & Van Der Veen 2021). This encompasses relationship management and processes within the supply chain, aiming to achieve a competitive advantage for all entities in the supply chain (Storer et al. 2014). The multidisciplinary nature of supply chain management integrates concepts from various fields, such as strategic management, marketing, and organizational behavior (Solaimani & Van Der Veen 2021). Researches by (Wieland & Durach 2021, Zhao et al. 2023, and Solaimani & Van Der Veen 2021) emphasize the integration of the supply chain can minimize resources required, waste generated, emissions emitted, and adverse environmental effects throughout the whole supply chain, achieving a balance of internal sustainable efficiency. These are certainly closely related to.

B. Circular Economy

The idea of the circular economy has drawn a lot of attention lately. According to Tapia et al. (2021), the circular economy is a system in which items that reach the end of their useful life are converted into resources for others, closing the circle within the industrial ecosystem and minimizing waste. According to the European Commission (EC), the circular economy is a type of economy where the value of products, materials, and resources is maintained for as long as possible by minimizing the amount of waste produced (Kirchherr et al. 2023). This definition aligns with the broad definition issued by the Joint Research Centre of the European Commission, emphasizing the rotational use of resources, including energy and materials (Mies & Gold 2021). A circular economy can be implemented in the FnB (Food and Beverage) sector. According to Liaros (2021), studies have shown that the food industry has prioritized circular economy principles such as reducing waste and pollution. The food industry can develop self-sustaining production systems that leverage supply chain management and circular economy business models to reduce waste and environmental impact (Montag 2022).

In addition to being a theoretical idea, the circular economy is a workable strategy for advancing a sustainable economy, environment, and society (Roberts et al. 2021). It's

critical to take into account a variety of sector- and region-specific tactics and practices in order to make an efficient transition to a circular economy. The implementation of a closed-loop system is a crucial component of the circular economy, focusing on reducing the use of non-renewable and toxic raw materials, reusing goods and services through better design, and recycling waste into new resources that can be further used and consumed (Patwa et al. 2021). Additionally, the application of circular economy principles requires a deep understanding of the potential of the supply chain and its entities, emphasizing the importance of recycling and expanding sustainability services (Kalemkerian et al. 2022).

To realize the implementation of the circular economy, the application of practices is essential, and it is crucial to develop strategies in the form of a circular business model as a complex and flexible system (Grabowski 2021). This strategy contributes to the formation and development of the circular economy by ensuring that materials and resources in the economy function for as long as possible (Khomenko et al. 2021). By combining these strategies and frameworks, entrepreneurs and policymakers can achieve a transition to the circular economy by generating value for the environment and society (Beccarello & Foggia 2022).

C. Food Bank

The food bank is a non-profit organization that assists low-income communities in obtaining food and distributes it through various non-profit social solidarity institutions (Akkerman et al. 2023). Responding to the urgent needs of those facing food insecurity, this system functions as an essential emergency food supply system (Akkerman et al. 2023). Food banks play a crucial role in addressing food insecurity and poverty by providing long-term supplies to many individuals experiencing severe food insecurity (Berti et al. 2021).

In addition to addressing food insecurity, food banks also play an important role in combating food waste by effectively redistributing food stocks to those in need, thus reducing the environmental impact of food waste (Penalver & Aldaya 2022). By collecting surplus edible food from various sources, food banks contribute to reducing food waste (Akkerman et al. 2023).

Typically, food banks do not directly provide food to end consumers but operate as intermediaries between food suppliers and institutions serving individuals in need (Blackmon et al. 2021). Food banks distribute food to communities in need to address food insecurity. The organization requests, stores, and delivers food from various donors, including local producers, retail food stores, federal commodity distribution programs, and the food industry (Rao

et al. 2021). Functioning as wholesalers, food banks store and manage food obtained from donors before distributing it to charitable organizations addressing food insecurity (Akkerman et al. 2023). Subsequently, the food provided to charitable organizations is distributed to communities in need (Montoli et al. 2023).

This research uses qualitative methods and data collection is carried out by interview. Interview participants are food bank experts (Top level management), and the number of interview participants was 3 people. Our research process includes several steps to ensure the reliability of our results. First, we interviewed the food bank expert to understand the supply chain flow from an initial product to an end product. Next, we process the information from the sample to create a supply chain design, and we ensure that the supply chain design aligns with the one depicted in Fig. 1. Data Collection:

A. Information Collection and Interview

The sample we use here is a Food Bank located in Bandung City, West Java. In these interviews, we collected important data and information from the Food Bank supply chain that can help us to understand how the Food Bank supply chain actually works. Here is some information we obtained from the food bank:

Several donors send food to food banks, but sometimes, food banks pick up food from another donor before there is an agreement between the food bank and donors. Some donors are farms, industrial hotels, bakeries, distributor warehouses, and communities.

1. The food bank only accepts surplus food.

2. The food management standards at the food bank are already in accordance with BAPANAS (National Food Agency of

3. Indonesia) standards. Additionally, the food bank has established a Memorandum of Understanding (MOU) with the NHI Bandung Polytechnic to ensure the safety of the processed food.

4. The food bank will deliver food to charitable institutions and schools, but the priority is charitable institutions, which will later distribute it to people in need.

5. Some non-processable food will be provided to BSF (Black Soldier Fly) cultivation to be used as a food source.

RESULTS AND DISCUSSION

After obtaining various pieces of information from the food bank, we processed the data to formulate a supply chain design, as illustrated in Fig. 2.

The supply chain depicted in Fig. 2 can be aligned with the Model A supply chain illustrated in Fig. 1. In this context, the food bank sources food from various sources, including farms, industrial hotels, bakeries, distributor warehouses, and
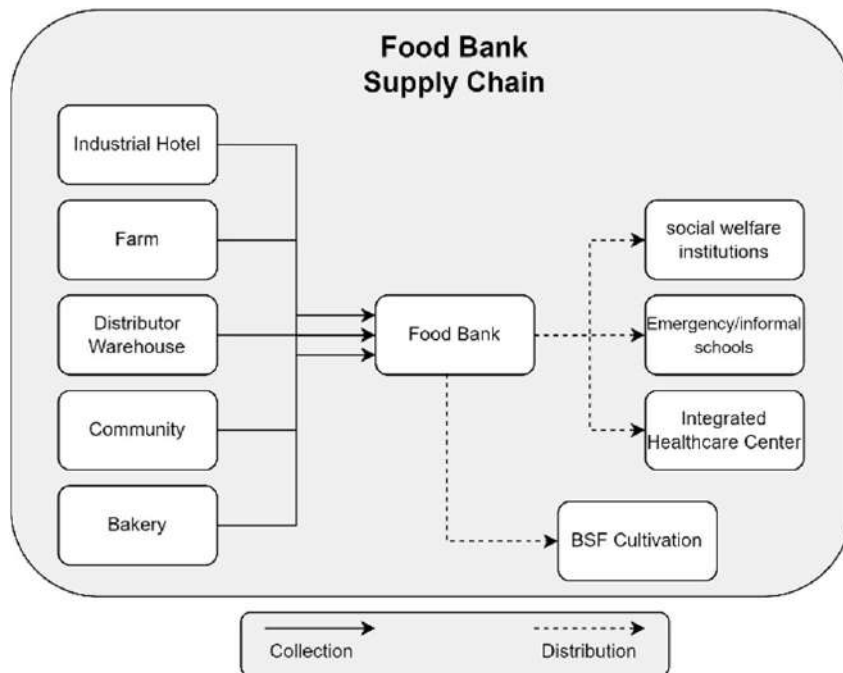

Fig. 2. Food Bank Supply Chain.

the community. Subsequently, the food bank processes the acquired food for distribution to social welfare institutions, emergency/informal schools, integrated health care centers, and BSF Cultivation, where they all act as agencies. The provision of food to BSF Cultivation is only executed when there is food deemed unsuitable for consumption.

If we compare the supply chain at Bandung Food Bank with (Syalianda & Kusumastuti 2023), we will find slight differences in the middle-to-end loop. Bandung Food Bank has a partner in the form of BSF cultivation, which has the benefit of dealing with food that cannot be passed on to beneficiaries. This has a big impact because food that cannot be eaten will not become waste and will be reused as food for maggots.

Examining the food bank supply chain illustrated in Fig. 2, it can be asserted that the food bank has successfully implemented the concept of a circular economy. Firstly, by processing and distributing surplus food from various donors, food banks have turned surplus food that would be wasted into many varieties of food that can be consumed by many people.

Then, Food Bank Bandung provides unprocessable food to BSF Cultivation. In this process, the food serves as consumption for maggots. On the other hand, magot can bring several advantages such as processing organic waste, valuable protein-rich for livestock and fish, and also contributing to economic resilience (Supena et al. 2021, Indrasari 2021). Those are aligned with the circular economy concept when the value of products, materials, and resources is maintained for as long as possible by minimizing the amount of waste produced (Kirchherr et al. 2023).

CONCLUSIONS

The Food Bank Bandung has successfully implemented a circular economy within its supply chain, as evidenced by the detailed analysis of its processes. The supply chain design, illustrated in Fig. 2, begins with the collection of surplus food, processing of food, and distribution of prepared food to agencies. Furthermore, the Food Bank Bandung implements a circular economy in the process of delivering inedible food to BSF cultivation. This food serves as feed for maggots, and these maggots have the potential to create new value by processing organic waste and providing protein-rich food for fish and livestock. Additionally, this initiative contributes to economic resilience.

This study has several limitations. Firstly, the Food Bank Bandung is insufficient to represent all the food banks throughout Indonesia. Therefore, we recommend for future research to do the inclusion of a larger dataset. Additionally,

this study does not compare all food banks in Indonesia. Despite these limitations, the research makes a valuable contribution by validating the ability of Food Bank Bandung to implement a circular economy in its supply chain. (SIPSN 2023). For practice, we recommend adding an entity that can close the loop on food that cannot be given to beneficiaries. This will be beneficial because if food that cannot be eaten is not managed it will become waste and can damage the environment. For policy, we recommend facilitating and establishing good cooperation with food banks in the area so that food surpluses can be resolved effectively and efficiently.

REFERENCES

Akkerman, R., Buisman, M., Cruijssen, F., De Leeuw, S. and Haijema, R., 2023. Dealing with donations: Supply chain management challenges for food banks. *International Journal of Production Economics*, 262, p.108926. https://doi.org/10.1016/j.ijpe.2023.108926

Arruda, E.H., Melatto, R.A.P.B., Levy, W. and Conti, D.M., 2021. Circular economy: A brief literature review (2015–2020). *Sustainable Operations and Computers*, 2, pp.79-86.

Beccarello, M. and Di Foggia, G., 2022. A circularity mapping framework for urban policymaking. *Journal of Politics and Law*, 16(1), p.11.

Berti, G., Giordano, C. and Mininni, M., 2021. Assessing the transformative potential of food banks: The case study of Magazzini Sociali (Italy). *Agriculture*, 11(3), p.249. https://doi.org/10.3390/agriculture11030249

Bigliardi, B., Filippelli, S., Petroni, A. and Tagliente, L., 2022. The digitalization of supply chain: A review. *Procedia Computer Science*, 200, pp.1806–1815. https://doi.org/10.1016/j.procs.2022.01.381

Blackmon, L., Chan, R., Carbral, O., Chintapally, G., Dhara, S., Felix, P., Jagdish, A., Konakalla, S., Labana, J., McIlvain, J.D., Stone, J.D., Tang, C.S., Torres, J. and Wu, W., 2021. Rapid development of a decision support system to alleviate food insecurity at the Los Angeles Regional Food Bank amid the COVID-19 pandemic. *Production and Operations Management*, 30(10), pp.3391-3407.

Coyle, J.J., Novack, R.A., Gibson, B.J. and Langley, C.J., 2021. Supply chain management: A logistics perspective. *SSRN*, 11, p.49

Dewilda, Y., Silvia, S., Riantika, M. and Z., 2021. Food waste composting with the addition of cow rumen using the Takakura method and identification of bacteria that play a role in composting.

Forbes, H., Quested, T. and O'Connor, C., 2021. UNEP - UN Environment Programme. Retrieved 14 November 2023 from https://www.unep.org/resources/report/unep-foodwaste-index-report-2021.

Frederico, G.F., 2021. From Supply Chain 4.0 to Supply Chain 5.0: Findings from a Systematic Literature Review and Research Directions. *Logistics*, 5(3), pp.49. https://doi.org/10.3390/logistics5030049

Indrasari, M., 2021. Maggot BSF cultivation development strategy as economic resilience during a pandemic. *Sinergi: Jurnal Ilmiah Ilmu Manajemen*, 11(2), pp.18-20.

Khomenko, I., Vuychenko, M., Gomeniuk, M., Mazur, Y. and Haidai, O., 2021. Imperatives for the formation and development of the circular economy and global waste management. *E3S Web of Conferences*, 2021.

Kirchherr, J., Yang, N.N., Schulze-Spüntrup, F., Heerink, M.J. and Hartley, K., 2023. Conceptualizing the Circular Economy (Revisited): An analysis of 221 definitions. *Resources, Conservation and Recycling*, 194, p.107001. https://doi.org/10.1016/j.resconrec.2023.107001

Liaros, S., 2021. Circular food futures: What will they look like? *Circular Economy and Sustainability*, 1(4), pp.1193-1206.

Mies, A. and Gold, S., 2021. Mapping the social dimension of the circular economy. *Journal of Cleaner Production*, 321, p.128960. https://doi.org/10.1016/j.jclepro.2021.128960

Montag, L., 2022. Circular economy and supply chains: Definitions, conceptualizations, and research agenda of the Circular Supply Chain Framework. *Circular Economy and Sustainability*, 3(1), pp.35-75. https://doi.org/10.1007/s43615-022-00172-y

Montoli, P., Ares, G., Aschemann-Witzel, J., Curutchet, M.R. and Giménez, A., 2023. Food donation as a strategy to reduce food waste in an emerging Latin American country: a case study in Uruguay. *Nutrire*, 48(1), p.22.

Patwa, N., Sivarajah, U., Seetharaman, A., Sarkar, S., Maiti, K. and Hingorani, K., 2021. Towards a circular economy: An emerging economies context. *Journal of Business Research*, 122, pp.725-735. https://doi.org/10.1016/j.jbusres.2020.05.015

Penalver, J.G. and Aldaya, M.M., 2022. The Role of the food banks in saving freshwater resources through reducing food waste: The Case of the Food Bank of Navarra, Spain. *Foods*, 11(2), p.163.

Rao, M., Bilić, L., Duwel, J., Herentrey, C., Lehtinen, E., Lee, M., Calixto, M.A.D., Bast, A. and De Boer, A., 2021. Let Them Eat Fish!—Exploring the possibility of utilizing unwanted catch in food bank parcels in the Netherlands. *Foods*, 10(11), p.2775. https://doi.org/10.3390/foods10112775

Rivera, A.F., Smith, N.R. and Ruíz, Á., 2023. A systematic literature review of food banks' supply chain operations with a focus on optimization models.

Journal of Humanitarian Logistics and Supply Chain Management, 13(1), pp.1025.

Roberts, T., Williams, I., Preston, J., Clarke, N., Odum, M. and O'Gorman, S., 2021. A Virtuous Circle? Increasing Local Benefits from Ports by Adopting Circular Economy Principles. *Sustainability*, 13(13), p.7079.

SIPSN, 2023. Sistem Informasi Pengelolaan Sampah Nasional. Available at: https://sipsn.menlhk.go.id/sipsn/. [Accessed 12 November 2023].

Solaimani, S. and Van Der Veen, J., 2021. Open supply chain innovation: an extended view on supply chain collaboration. *Supply Chain Management*, 27(5), pp.597-610. https://doi.org/10.1108/scm-09-2020-0433

Storer, M., Hyland, P., Ferrer, M., Santa, R. and Griffiths, A., 2014. Strategic supply chain management factors influencing agribusiness innovation utilization. *The International Journal of Logistics Management*, 25(3), pp.487-521.

Studnička, P., 2021. Possibilities of waste reduction in gastronomy.

Supena, M.H., Wiryati, A.S.S.G. and Subagio, A.A., 2021. Business analysis of black soldier flies (BSF) as an alternative feed for fish cultivation in Bogor City, West Java. *E3S Web of Conferences*, 2, p.21.

Syalianda, R. and Kusumastuti, R.D., 2023. Analysis of an Indonesian d bank sustainability using system dynamics simulation. *Community Engagement, and Social Environment*, pp.5.

Tan, Y., Feng, H., Popp, J. and Oláh, J., 2022. Minimizing waste in the food supply chain: Role of information system, supply chain strategy, and network design. *Sustainability*, 14(18), p.11515.

Tapia, C., Bianchi, M., Pallaske, G. and Bassi, A.M., 2021. Towards a territorial definition of a circular economy: exploring the role of territorial factors in closed-loop systems. *European Planning Studies*, pp.1-20.

Waluyo, B. and Kharisma, D., 2023. Circular economy and food waste problems in Indonesia: Lessons from the policies of leading countries. *Cogent Social Sciences*, 9(1), pp.1-23.

Wieland, A. and Durach, C.F., 2021. Two perspectives on supply chain resilience. *Journal of Business Logistics*, 42(3), pp.315–322. https://doi.org/10.1111/jbl.12271

Zhao, N., Hong, J. and Lau, K.H., 2023. Impact of supply chain digitalization on supply chain resilience and performance: A multi-mediation model. *International Journal of Production Economics*, 259, p.108817. https://doi.org/10.1016/j.ijpe.2023.108817

The Benefit of Biodegradable Plastics for Supporting Sustainable Development: A Case Study of Willingness to Pay in Surakarta City, Indonesia

B. R. M. Jati[1†], Suranto[1], Pranoto[1], Suryanto[2] and E. Gravitiani[2]

[1]Department of Environmental Sciences, University of Sebelas Maret, Ir. Sutami Road No.36A Kentingan, Surakarta, Indonesia
[2]Faculty of Economics and Business, University of Sebelas Maret, Ir. Sutami Road No.36A Kentingan, Surakarta, Indonesia
†Corresponding author: Benedictus Raditya Mustika Jati; raditya_mj@student.uns.ac.id

ABSTRACT

Plastic pollution is a global concern affecting water, soil, and air quality. Urgent action is needed to address this issue. This study aims to identify factors influencing the use of biodegradable plastic to reduce its negative impacts. Data were collected from 269 households-129 in Punggawan and 140 in Mojosongo, Surakarta, and analyzed using multiple regression analysis to study the determinants of WTP *(Willingness to Pay)* for biodegradable plastic with STATA software. The results show that the average WTP for biodegradable plastic is IDR 2,214. Most people in Surakarta are already environmentally conscious. Age, knowledge, occupation, interaction of sex and location, education, and marital status influence WTP for biodegradable plastic. It is hoped that the implications of the research will be used as a recommendation for government policies to reduce the amount of plastic waste generation, which is a danger to human beings and the environment.

INTRODUCTION

In recent years, the issue of environmental pollution resulting from the use of plastic bags has become a matter of great concern (Chandegara et al. 2015, Fischbach et al. 2022, Schuermann & Woo 2022). Researchers in several developed and developing countries have been working hard to reach Sustainable Development Goals (SDGs), especially goal 12 related to sustainable consumption and production (Arora & Mishra 2019, Barcena 2018, Basavaraddi et al. 2012). Data on population and waste generation in Indonesia from 2016 – 2021 shows that the highest population growth rate occurred in 2019, at a rate of 1.08%, from a population of 268 million people in 2018 to a population of 271 million in 2019. The high increase in population in 2019 had a significant influence on the increase in waste generation, which rose from 65.8 million tons per year in 2018 to 67.1 million tons per year in 2019, or an increase in waste generation of 1.99% (Badan Pusat Statistik 2021). The problem of waste is not only a national focus but also the focus of smaller urban areas, including the City of Surakarta. Data from the Surakarta City Environmental Services Department in 2021 shows that the amount of waste produced was 299 tons per day, with the following classification: 185.23 tons per day (61.95%) of organic waste and 113.77 tons per day (38.05%) of inorganic waste (Dinas Lingkungan Hidup Kota Surakarta 2021).

The composition and properties of plastic, which make it difficult to break down, harm the living environment, including soil pollution, water pollution, and air pollution (Gironi & Piemonte 2011, Sharma & Holmberg 2019, Wright et al. 2013). Therefore, progressive environmental policies are urgently needed to achieve

environmental sustainability, even though the improvement of ecological quality is regarded as a luxury for poor people (Song et al. 2022, Suparno et al. 2024). Many researchers are looking for ways to measure the willingness to pay for public goods such as clean air or clean water for personal use by gathering information from property values (Griliches 1971). However, one of the problems with using the Contingent Valuation Method (CVM) is the numerous errors that exist in the different interview methods (Song et al. 2022).

Nowadays, a large number of people are already familiar with various kinds of plastic bags that are made from environmentally friendly materials and can be used instead of single-use (non-environmentally friendly) plastic bags (Ahamed et al. 2021, Angriani et al. 2021, Harianja et al. 2019, Lad et al. 2024, Lutfi et al. 2017). Numerous studies have found that households with a supportive attitude toward the environment tend to be willing to pay premium prices for environmentally friendly products (Ketelsen et al. 2020, Laroche et al. 2001). Further to this, it is extremely important to discover the household determinants for using environmentally friendly plastic. Caplan (2012) believes that people with a high income often prefer to allocate some of their money to buying more plastic bags rather than carrying reusable bags, even though they have a higher awareness than people with a low income. This is because they dislike the inconvenience of bringing their plastic bags from home. In addition, it has been found that socioeconomic factors of society influence willingness to pay, and income level, in particular, is one of the variables that has a significant impact (Madigele et al. 2017, Nattapat et al. 2019, Schuermann & Woo 2022).

Research by Song et al. (2022) investigates WTP for reducing the use of plastic bags in the district of Linh Nam. This study confirms that 85.29% of households are willing to pay IDR 31,500, with variables of income, education, sex, and willingness to protect the environment having a significant positive influence on WTP. The variables of household size and age have been found to have a significant negative influence on WTP. In addition, Wang & Li (2021) emphasize the importance of awareness in reducing the use of plastic bags. Policies to ban plastic have also been effective in changing consumer behavior significantly. Research by Nattapat et al. (2019) also studies willingness to pay for plastic bag waste management in Bangkok, Thailand. This study confirms that the average willingness to pay for plastic bag waste management in Bangkok is IDR 620, with attitude assessment and support for plastic bag retribution having a significant influence on WTP. The results of research by Madigele et al. (2017) show that the variable with a positive influence on WTP is income, while variables with a negative influence are education, tax offers, and plastic bag recycling.

A study by Mogomotsi et al. (2018) presents an optimistic outcome in reducing plastic bag use. It states that 80.7% of a total of 367 people surveyed agreed that they would reduce plastic bag use and start using other bags that are more environmentally friendly. Research has also shown that plastic tax is not too effective because it is difficult to collect. These are some of the reasons why it is important to increase public awareness about environmental protection.

Based on the discussion above, a study is needed about efforts to reduce non-environmentally friendly plastic bag use in daily life through factors that influence the use of biodegradable plastic, which is more environmentally friendly. This can help to design policies that are adapted to suit the location of the study. Therefore, this study aims to analyze people's behavior and to estimate people's willingness to pay, as well as identify the factors that influence willingness to pay for biodegradable plastic.

MATERIALS AND METHODS

The data collection used a survey which was carried out in the Districts of Punggawan and Mojosongo. The reason for choosing these two research locations was that Mojosongo is an example of a district in Surakarta with successful plastic waste management, and this district could be compared with Punggawan, a district that has not yet started to implement plastic waste management. The survey was conducted through a questionnaire containing many prepared questions. The study employs the Contingent Valuation Method (CVM), a versatile and straightforward non-market evaluation technique extensively utilized in cost-benefit analysis and environmental impact assessment (Fauzi 2014, Venkatachalam 2004). In this research, the CVM was used to find the willingness to pay for biodegradable plastic in Surakarta. The WTP data were then estimated with multiple linear regression using STATA software. In measuring willingness to pay, however, it was important to make certain during the interview process that all the respondents had correctly understood the information in the questionnaire.

Data Collection

The total number of households in the two research locations is 1,050 in Punggawan District and 17,712 in Mojosongo District. The sample calculations were made according to the formula of Isaac and Michael (1995) in Vionalita (2020), as follows:

$$s = \frac{X^2.N.P.Q}{d^2(N-1) + X^2.P.Q} \qquad ...(1)$$

Where s is the number of samples, is chi-squared, for the degree of freedom=1, level of error 7.5% = 3.17, N is

the size of the population, P is the chance of being right (0.5), Q is chance of being wrong (0.5), and d is difference between the sample average and population average at 0.05. A random selection of 269 households was chosen, with 129 from Punggawan and 140 from Mojosongo.

Parametric Design of Willingness to Pay Estimate

After all the data had been collected, the next step was to analyze each independent variable that would influence the dependent variable (Table 1).

This resulted in an empirical model of willingness to pay (WTP). The empirical model of WTP is as follows:

$$\ln_{wtp}{}_i = \alpha_i + \beta_{1i}sex + \beta_{2i}age + \beta_{3i}educ + \beta_{4i}knowledge + \beta_{5i}occupation + \beta_{6i}income + \beta_{7i}status + \beta_{8i}location + \varepsilon$$

...(2)

For the equation above: ln_wtp is the Dependent Variable, is the constant, β is the coefficient (which may have either positive or negative value), sex, age, education, knowledge, occupation, income, marital status, and location are the independent variables, ε is the residual, i is the individual number. A comprehensive explanation of the research variables is presented below.

RESULTS AND DISCUSSION

Respondent Survey

The results of the research showed that the total number of respondents was 278, with proportion of 148 (53.24%) from households in Mojosongo and 130 (46.76%) from households in Punggawan (Fig. 1).

Of these respondents, 146 (52.52%) were male and 132 (47.48%) were female. In terms of age, the majority of the respondents were 18-25 years old, with a proportion of 33.09%, followed by 29.14% in the 41-57 age group, 26.98% in the 26-40 age group, and the remaining 10.79% in the age category of 57 and above (Fig. 1a). The majority of the respondents had a Bachelor's degree, with a proportion of 35.61%, followed by 31.29% in the high school category, 16.91% in the diploma category, 8.63% in the junior high school category, 4.32% in the elementary school category, and 3.24% in the postgraduate category (Fig. 1b). In terms of income, almost 32.01% of the respondents earned an income of IDR 1,000,000 to IDR 1,999,999, followed by 23.74% with an income of IDR 2,000,000 to IDR 2,999,999, 14.75% with an income of IDR 3,000,000 to IDR 3,999,999, 7.19% with an income of less than IDR 1,000,000, 6.83% with an income of over IDR 6,000,000, and the remaining 4.68% with an income of IDR 5,000,000 to IDR 5,999,999

Table 1: Explanation of research variables.

Variables	Description
ln_wtp	ln_wtp is the natural logarithm of the value of the willingness to pay for each household in IDR
Sex	The dummy variable of sex, where 1 means female and 0 means male
Age	The age variable is categorized as a dummy variable with 4 groups:
	age_1 for the age category 18-25 years, where 1 if 18-25 years, and 0 if another age
	age_2 for the age category 26-40 years, where 1 if 26-40 years, and 0 if another age
	age_3 for the age category 41-57 years, where 1 if 41-57 years, and 0 if another age
	age_4 for the age category over 57 years, where 1 is over 57 years, and 0 if another age
Education	The education variable is categorized as a dummy variable with 6 groups:
	Elementary school, where 1 if the final education level is Elementary School or the equivalent thereof, and 0 if another education category.
	Junior high school, where 1 if the final education level is Junior High School or the equivalent thereof, and 0 if another education category.
	Senior high school, where 1 if the final education level is Senior High School or the equivalent thereof, and 0 if another education category.
	Diploma, where 1 if the final education level is a Diploma or the equivalent thereof, and 0 if another education category.
	Bachelor, where 1 if the final education level is a Bachelor's degree or the equivalent thereof, and 0 if another education category.
	Postgraduate, where 1 if the final education level is a Master's degree or the equivalent thereof and 0 if another education category.
Knowledge	The dummy variable of knowledge where 1 if there is existing knowledge of biodegradable plastic and 0 if there is no knowledge of biodegradable plastic.
Occupation	The dummy variable of occupation, where 1 if work is in the formal or informal sector, and 0 if otherwise (homemaker, student, etc.)
Income	The variable of income, is calculated with a natural logarithm from the income of household members in Rupiah.
Status	The variable of marital status, where 1 if the respondent is married and 0 if unmarried
Location	The variable of location of the respondent's house, where 1 if the respondent is from Mojosongo, and 0 if the respondent is from Punggawan.

Fig. 1: Distribution of age (a), education (b), and household income (c).

Fig. 2: Respondents' WTP for biodegradable plastic based on location (a), sex (b), and age (c).

(Fig. 1c). Furthermore, it was found that the overall willingness to pay for biodegradable plastic in the two districts was IDR 2,214. If this average Fig. was compared with the results for the separate locations, the WTP of respondents in Mojosongo was higher, at R 3,104 (See Fig. 2a). Other results showed that females had a higher

willingness to pay (Rp 2,597) than males (Rp 1,867) (Fig. 2b).

It was also found that the older the age of the respondents, the lower the tendency to pay for biodegradable plastic (respondents over the age of 41 years had a WTP less than or equal to IDR 2,000), compared with respondents in the younger age group (respondents below the age of 40 years had a WTP higher than IDR 2,000), as seen in Fig. 2c. In addition, the higher the level of education of the respondents, the higher their willingness to pay. This is shown in Fig. 2d, where it can be seen that respondents with an education level of high school and above had a WTP over IDR 2,000, which is higher than those with an education level of junior high school and below, whose WTP was IDR 1,500.

Respondents' Behavior

The majority of respondents already had an existing concern for the environment. This is evident from the respondents' behavior, which can be seen by comparing the level of knowledge and use of biodegradable plastic in Surakarta (See Fig. 3).

Fig. 3 shows that a total of 70.86% of respondents were already environmentally conscious, which was indicated by their knowledge of biodegradable plastic and, subsequently, their use of this type of plastic. The next largest group was the 16.91% of respondents who knew about biodegradable plastic but did not use it, followed by 11.51% of respondents who were not concerned for the environment and showed a minimal response to the existence of plastic waste, and the remaining 0.72% of respondents who already used biodegradable plastic but had no previous knowledge of the existence of this type of plastic before they were told about it when the survey was carried out.

Willingness to Pay Estimation

The results of the regression analysis show that WTP for biodegradable plastic is influenced by the variables of age, knowledge, and occupation, while the interaction of sex and location, and interaction of education level and marital status (See Table 2). Based on the level of education, respondents with the education level diploma, whether married or unmarried, had the strongest influence on WTP for biodegradable plastic, with a significance of ($p < 0.05$), with an increase of 1.77% for those who were unmarried, and 0.94% for those who were married, compared with other levels of education. Respondents in the education category of junior high school who were married also had a strong influence on WTP for biodegradable plastic with a significance of ($p < 0.05$), with an increase of 0.82% compared with other levels of education. Furthermore, respondents in the education category of senior high school
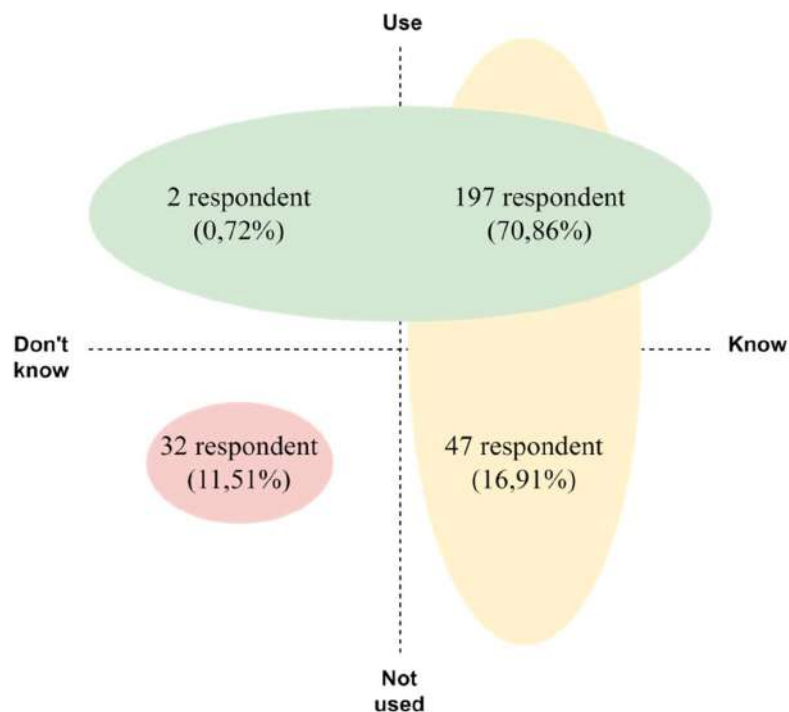
Fig. 3: Mapping of respondents' behavior toward biodegradable plastic.

who were married also had a strong influence on WTP for biodegradable plastic, with a significance of (p <0.10), with an increase of 0.72% compared with other levels of education. Respondents in the education category of Bachelor who were married also had an influence on WTP for biodegradable plastic, with a significance of (p <0.10), with an increase of 0.68% compared with other levels of education.

Females living in Mojosongo were found to have the most significant influence (p<0.01), with an increase of 0.82% compared with both males living in Mojosongo

Table 2: Regression results of WTP for biodegradable plastics.

| Variable	β	S.E	Sig.
Constanta	0.46	1.91	0.81
Age			
18-25 years old (age_1)	-1.01	0.62	0.10
26-40 years old (age_2)	-0.81	0.58	0.16
41-57 years old (age_3)	-1.08	0.58	0.06*
More than 57 years old (age_4)	-1.39	0.60	0.06*
Knowledge	0.41	0.14	0.00***
Occupation	-0.39	0.18	0.03**
Income	0.41	0.10	0.00***
Interaction Variable			
Sex#Location			
Male#Mojosongo	0.63	0.17	0.00***
Female#Punggawan	-0.21	0.19	0.25
Female#Mojosongo	0.82	0.18	0.00***
Education#Status			
Elementary school#Status			
Elementary school#Marriage	-1,04	1.49	0.49
Other#Single	0.26	1.08	0.81
Other#Marriage	-1.39	1.83	0.45
Junior high school#Status			
Junior high school#Marriage	0.82	0.43	0.05**
Other#Single	1.72	1.23	0.16
Senior high school#Status			
Senior high school#Marriage	0.72	0.39	0.07*
Other#Single	1.43	1.01	0.16
Diploma#Status			
Diploma#Marriage	0.94	0.43	0.02**
Other#Single	1.77	1.04	0.09*
Bachelor#Status			
Bachelor#Marriage	0.68	0.38	0.07*
Other#Single	0.97	1.04	0.34

Note: Coefficient (β), Standard Error (S.E), Significance (Sig.). A coefficient is statistically significant at either 1 percent (***), 5 percent (**), or 10 percent (*) of the confidence intervals.

and females living in Punggawan. Respondents who had knowledge of biodegradable plastic were willing to pay 0.41% more for this type of plastic, with a significance of (p <0.01). In addition, an increase in income of 1% had an influence on respondents' willingness to pay 0.41% more for biodegradable plastic. Age had a significant negative influence on WTP for biodegradable plastic. This means that the older the respondent was, the lower their willingness to use biodegradable plastic. This is evident from the results of respondents in the 41-57 year age group and the over 57 age group, who showed a decrease in willingness to pay for biodegradable plastic, at a level of 1.08% for the 41-57 year age category and 1.39% for the over 57 age category. Respondents who had a job were 0.39% less willing to pay for biodegradable plastic compared with homemakers, students, and fresh graduates.

DISCUSSION

Various different models about the importance of biodegradable plastic have confirmed that the preference for strategies for using biodegradable plastic is influenced by socio-economic characteristics and knowledge. From the model used, the explanatory variable estimates have the same signs. Females (seen from the coefficient of "sex") are generally willing to pay "more" for biodegradable plastic compared with males, even though both have an equally significant value. This result is in line with the work of Abate et al. (2020), who state that male respondents have a lower level of concern and attention for environmental issues and are less convinced about the effectiveness of proposed initiatives, which subsequently influences their WTP (Abate et al. 2020). Mainieri et al. (1997) note that this difference in attitude may be because women more frequently shop for household needs than men, and as a result, they are more aware of environmental problems related to various products, including plastic bags, that harm the environment. It is interesting to point out that, in general, the knowledge of females about the environment is usually not as broad as their male counterparts, but females tend to be more emotionally involved, more concerned about environmental degradation, less trusting in technological solutions, and more willing to change or accept environmentally friendly solutions (Kollmuss & Agyeman 2002). This can be linked to their subconscious psychosocial factors, such as emotion, bearing in mind that women are more emotional than males. It has been observed that emotion can also have a significant and direct impact on assessment and choice related to environmental problems (Loewenstein & Lerner 2003).

Age has a negative and significant influence on WTP. This means that the older the respondent, the lower their

wish to pay for newer management strategies, as found in the research of Ojea & Loureiro (2007), which states that older respondents have a lower probability of giving a positive response to WTP compared with their younger counterparts because they have fewer economic resources and, in general, have less concern for the environment (Ojea & Loureiro 2007). Education is expected to have a positive effect on WTP. Education level in relation to environmental management is a strong predictor of the willingness to pay for green, sustainable, and/or environmentally friendly products or initiatives, as found in (Fischbach et al. 2022), a study that focuses on counseling and education efforts as a form of environmental awareness.

Income has a positive and significant influence, and it can be seen statistically that all respondents with similarly high incomes are more inclined to be willing to pay for biodegradable plastic bags than those with a low income. Dunn (2012) believes that respondents with a high income are more willing to pay for new biodegradable plastic rather than have the inconvenience of carrying a reusable bag, even though they have a higher level of environmental awareness than respondents with a low income (Dunn 2012). The fact that a plastic bag is a convenient option, which costs very little when compared with the total cost of the other purchases, makes people more inclined to buy it than to bring their bag from home (Angriani et al. 2021). Therefore, they have no objection to paying for this type of environmentally friendly plastic.

The results of newer research show that knowledge has a positive influence on WTP for biodegradable plastic. This is in line with the findings of Janardan et al. (2023), which state that a high level of general knowledge about plastic pollution influences awareness and knowledge of environmental threats caused by plastic (Coco Chin et al. 2023). In addition, pollution caused by non-environmentally friendly plastic can be reduced by targeting the attitudes of individuals through an educational campaign that aims to improve knowledge and awareness about plastic alternatives and recycling (Oguge et al. 2021). In the same way, an increased understanding and awareness can influence people's convictions concerning the way other people feel about their decision to stop using single-use plastic.

CONCLUSIONS

Biodegradable plastic is plastic that can help reduce the occurrence of environmental pollution if used on a massive scale by the general public. The findings of this research show that there is a positive result regarding people's willingness to pay (WTP) for biodegradable plastic, with an average amount of IDR 2,214. This can be seen in both of the samples from the Districts of Mojosongo and Punggawan. The reason for this is that the majority of people in Surakarta (78.86%) already know about the benefits of biodegradable plastic. Therefore, they do not object to buying and using this type of plastic, even though they have to pay a higher price than for non-environmentally friendly plastic. The results of the analysis show that WTP for biodegradable plastic is influenced by the variables of age, knowledge, and occupation, the interaction of sex and location, and the interaction of education level and marital status. The education level of diploma for both unmarried and married respondents was found to have the strongest influence on WTP for biodegradable plastic. It is hoped that this research can be used as a recommendation for government policies to reduce the amount of plastic waste generation, which presents a danger to human beings and the environment.

ACKNOWLEDGEMENTS

REFERENCES

Abate, T.G., Börger, T., Aanesen, M., Falk-Andersson, J., Wyles, K.J. and Beaumont, N., 2020. Valuation of marine plastic pollution in the European Arctic: Applying an integrated choice and latent variable model to contingent valuation. *Ecological Economics*, 169(October 2019), p.106521. doi: 10.1016/j.ecolecon.2019.106521.

Ahamed, A., Vallam, P., Iyer, N.S., Veksha, A., Bobacka, J. and Lisak, G., 2021. Life cycle assessment of plastic grocery bags and their alternatives in cities with confined waste management structure: A Singapore case study. *Journal of Cleaner Production*, 278, p.123956. doi: 10.1016/j.jclepro.2020.123956.

Angriani, P., Muhaimin, M., Hastuti, K.P., Adyatma, S. and Saputra, A.N., 2021. Ban on plastic bags usage: Consumer perception of single-use plastic bags in traditional market. *Proceedings of the 2nd International Conference on Social Sciences Education (ICSSE 2020)*, 525, pp.226–32. doi: 10.2991/assehr.k.210222.036.

Arora, N.K. and Mishra, I., 2019. United Nations Sustainable Development Goals 2030 and environmental sustainability: Race against time. *Environmental Sustainability*, 2(4), pp.339–42. doi: 10.1007/s42398-019-00092-y.

Badan Pusat Statistik, 2021. *Statistik Lingkungan Hidup Indonesia 2021*. Vol. 21.

Barcena, A., 2018. *The 2030 Agenda and the Sustainable Development Goals: An Opportunity for Latin America and the Caribbean*. ECLAC Publication.

Basavaraddi, S.B., Kousar, H. and Puttaiah, E.T., 2012. Fluoride toxicity in groundwater and its chronic effect on human health: A study in Tiptur town and its surrounding areas in Karnataka State, India. *Nature Environment and Pollution Technology*, 11(2), pp.271–76.

Caplan, A., 2012. Estimating willingness to pay for continued use of plastic grocery bags and willingness to accept switching completely to reusable bags. *Applied Economics Applied Ec (Paper 1282)*, p.59.

Chandegara, V.K., Cholera, S.P., Nandasana, J.N., Kumpavat, M.T. and Patel, K.C., 2015. Plastic packaging waste impact on climate change and its mitigation. In: Subbaiah, R. and Prajapati, G.V., eds. *Water Management and Climate Smart Agriculture*. Gyan Publishing House, New Delhi, India, pp.404–415.

Chin, K.C., Mahanta, J. and Nath, T.K., 2023. Knowledge, attitude, and practices toward plastic pollution among Malaysians: Implications for minimizing plastic use and pollution. *Sustainability (Switzerland)*, 15(2). doi: 10.3390/su15021164.

Dinas Lingkungan Hidup Kota Surakarta, 2021. *Laporan Akhir Inventarisasi Gas Rumah Kaca Kota Surakarta Tahun 2021*.

Dunn, J., 2012. Estimating willingness to pay for continued use of plastic grocery bags and willingness to accept switching completely to reusable bags. *Utah State University*.

Fauzi, A., 2014. *Economic Valuation and Assessment of Damage to Natural Resources and the Environment*. IPB Press.

Fischbach, E., Sparks, E., Hudson, K., Lio, S. and Englebretson, E., 2022. Consumer concern and willingness to pay for plastic alternatives in food service. *Sustainability (Switzerland)*, 14(10), pp.1–23. doi: 10.3390/su14105992.

Gironi, F. and Piemonte, V., 2011. Bioplastics and petroleum-based plastics: Strengths and weaknesses. *Energy Sources, Part A: Recovery, Utilization and Environmental Effects*, 33(21), pp.1949–59. doi: 10.1080/15567030903436830.

Griliches, Z., 1971. *Price Indexes and Quality Change*. Harvard University Press.

Harianja, A.H., Saragih, G.S. and Fauzi, R., 2019. Replacing single-use plastic bags with compostable carriers: Socio-economic approach. *IOP Conference Series: Earth and Environmental Science*, 407(1), p.12001. doi: 10.1088/1755-1315/407/1/012001.

Ketelsen, M., Janssen, M. and Hamm, U., 2020. Consumers' response to environmentally-friendly food packaging - A systematic review. *Journal of Cleaner Production*, 254, p.120123. doi: https://doi.org/10.1016/j.jclepro.2020.120123.

Kollmuss, A. and Agyeman, J., 2002. Mind the gap: Why do people act environmentally, and what are the barriers to pro-environmental behavior? *Environmental Education Research*, 8(3), pp.239–260. doi: 10.1080/13504620220145401.

Lad, A.A., Gaikwad, V.D., Gaikwad, S.V., Kulkarni, A.D. and Kanekar, S.P., 2024. Extraction of environment-friendly biodegradable poly-hydroxy butyrate using novel hydrodynamic cavitation method. *Nature Environment and Pollution Technology*, 23(1), pp.475–483. doi: 10.46488/NEPT.2024.v23i01.043.

Laroche, M., Bergeron, J. and Barbaro-Forleo, G., 2001. Targeting consumers who are willing to pay more for environmentally friendly products. *Journal of Consumer Marketing*, 18(6), pp.503–520. doi: 10.1108/EUM0000000006155.

Loewenstein, G. and Lerner, J.S., 2003. *Handbook of Affective Sciences*. Oxford University Press, pp.619–642.

Lutfi, M., Sumarlan, S.H., Susilo, B., Wignyanto, Zenata, R. and Perdana, L.P.R., 2017. The glycerol effect on the mechanical behavior of biodegradable plastic from the Walur (*Amorphophallus Paenifolius* var. *Sylvestris*). *Nature Environment and Pollution Technology*, 16(4), pp.1121–1124.

Madigele, P.K., Mogomotsi, G.E.J. and Kolobe, M., 2017. Consumer willingness to pay for plastic bags levy and willingness to accept eco-friendly alternatives in Botswana. *Chinese Journal of Population Resources and Environment*, 15(3), pp.255–261. doi: 10.1080/10042857.2017.1369243.

Mogomotsi, G., Gondo, R., Mogomotsi, P. and Madigela, T., 2018. Youth and environmentally responsible consumer behavior: The case of plastic bag usage in Botswana. *Botswana Journal of African Studies*, 32(1), pp.2018.

Nattapat, P., Chanathip, P. and Jun, N., 2019. Estimating willingness to pay for plastic bag waste management in Bangkok, Thailand. *International Journal of Advances in Science Engineering and Technology*, 7(2321–9009), p.5.

Oguge, N., Oremo, F. and Adhiambo, S., 2021. Investigating the knowledge and attitudes towards plastic pollution among the youth in Nairobi, Kenya. *Social Sciences*, 10(11), p.408. doi: 10.3390/socsci10110408.

Ojea, E. and Loureiro, M. L., 2007. Altruistic, egoistic, and biospheric values in willingness to pay (WTP) for wildlife. *Ecological Economics*, 63(4), pp.807–814. doi: https://doi.org/10.1016/j.ecolecon.2007.02.003.

Schuermann, H. and Woo, J. R., 2022. Estimating consumers' willingness to pay for reusable food containers when ordering delivery food: A contingent valuation approach. *Journal of Cleaner Production*, 366(July), p.133012. doi: 10.1016/j.jclepro.2022.133012.

Sharma, S., 2019. *Plastic Packaging: Principles of Design for Recycling*. (Ph.D. Thesis). Available at: https://www.theseus.fi/handle/10024/167495

Song, N.V., Hieu, N.M., Huyen, V.N., Que, N.D., Huong, N.V. and Nguyet, B. T. M., 2022. Households' willingness-to-pay to reduce the use of plastic bags: A case study in Viet Nam. *Journal of Environmental Protection*, 13(03), pp.289–98. doi: 10.4236/jep.2022.133018.

Suparno, S., Deswati, D., Fitri, W.E., Pardi, H. and Putra, A., 2024. Microplastics in the Water of Batang Anai Estuary, Padang Pariaman Regency, Indonesia: Assessing effects on riverine plastic load in the marine environment. *Environment and Natural Resources Journal*, 22(1), pp.55–64. doi: 10.32526/ennrj/22/20230191.

Venkatachalam, L., 2004. The contingent valuation method: a review. *Environmental Impact Assessment Review*, 24(1), p.138. doi: 10.1016/S0195-9255(03)00138-0.

Vionalita, G., 2020. *Benelli's Kunitatibi module methodology*. A. Ungul University, pp.0–17.

Wang, B. and Li, Y., 2021. Plastic Bag Usage and the Policies: A Case Study of China. Waste Management, 126, pp.163–69. doi: 10.1016/j.wasman.2021.03.010.

Wright, S.L., Thompson, R.C. and Galloway, T.S., 2013. The physical impacts of microplastics on marine organisms: A review. *Environmental Pollution*, 178, pp.483–92. doi: 10.1016/j.envpol.2013.02.031.

Original Research Paper | https://doi.org/10.46488/NEPT.2025.v24i01.B4103 | **Open Access Journal**

Geostatistical Appraisal to Comprehend Hydrogeochemical Environment of Major Ions and Depiction of Groundwater Suitability from Part of Balaghat District (M.P.), Central India

Y. A. Murkute† and A. P. Pradhan

Postgraduate Department of Geology, Nagpur University, Law College Square, Nagpur-440001, India
†Corresponding author: Y. A. Murkute; yogmurkute@rediffmail.com

ABSTRACT

The key observations on the study concerning the geostatistical appraisal, hydrogeochemical environment of major ions (cations and anions) as well as groundwater suitability from the part of Balaghat District (MP) latitude 21°31'42": 21°43'11" N and longitude 79°50'30":80°11'30" E., Central India are presented here. The pH (7.3 to 8.6) of the groundwater samples and range of EC values (50-5080 $\mu S.cm^{-1}$) typically clarify the alkaline nature and the involvement of diverse processes (geogenic as well as anthropogenic) deciding the hydrogeochemical environment of groundwater. This prominent behavior is the result of the conductivity in groundwater, which is the consequence of ion exchange along with the solubilization processes during the rock-water interaction and also represents anthropogenic activity. The abundance succession of cations is $Ca^{2+} > Na^+ > Mg^{2+} > K^+$, while the profusion sequence of anions is $HCO_3^- > Cl^- > NO_3^- > SO_4^{2-} > F^-$. The positive correlation among the pair of Ca^{2+} with Mg^{2+} (r = 0.657), Na^+ (r = 0.691), and HCO_3^- (r = 0.842) as well as the high positive association between K^+ and SO_4^{2-} (r = 0.856), plus K^+ and NO_3^- (r = 0.779) unravels the derivation of ions from the geogenic origin and the agro-chemical derivation of ions respectively. The three factors (1:6.350, 2:2.732, and 3:2.697), having a total variance of 87.923%, correspond with the geogenic factor, anthropogenic factor, and alkalinity factor, respectively. The groundwater from the study area is suitable for drinking and irrigation purposes with a slight threat of exchangeable sodium.

INTRODUCTION

The rock-water interface is the common intersection where the physical and chemical properties of both rocks, as well as groundwater, interact for the numerous crucial and decisive hydrogeochemical processes that directly govern the long-lasting chemistry of groundwater and hence also express the typical geogenic changes in the groundwater system (Sreedevi 2004, Nagaraju et al. 2006, Wen et al. 2008, Si et al. 2009, Deshpande & Murkute 2023). At this interface, distinct ions from the mineral suites get released from the aquifer rocks and also combine concurrently to give specific characteristics to the groundwater regime (Jalali 2006, Gupta et al. 2008, Murkute 2014a, Nayak & Hota 2023). Similarly, human interventions, which are also referred to as anthropogenic activities, add non-natural contents, which again deteriorate the groundwater quality (Si et al. 2009, Li et al. 2011, Ravikumar & Somashekhar, 2011, Agoubi et al. 2011, Rajesh et al. 2012, Omran et al. 2012, Bauder et al. 2014, Amiri et al. 2015, Xu et al. 2018, Ahada & Suthar 2018, Wagh et al. 2018, Zhang et al. 2019, Eyankware et al. 2020, Murkute 2014b).

Groundwater contamination poses an immense threat to human health, and hence the unfailing examinations have been expanding the apprehension of the hydrogeochemical environment through statistical investigations and other related

issues (Li et al. 2012, Brindha & Elango 2013, Wu et al. 2015, Hirojeet et al. 2015, Thilagavathi et al. 2015, Duraisamy et al. 2018, Sreedevi et al. 2018, Li et al. 2018, Xu et al. 2018, Adimalla & Qian 2019, Wang et al. 2019, Singh et al. 2019, Eyankware et al. 2020, Gogulothu et al. 2022). Nowadays, the interrelated studies give a hand in devising policies for planning, remedial measures, and regulations to cope with groundwater contamination.

The study area represents the western-south part of Balaghat district, latitude 21°31′42″: 2143′11″ N and longitude 79°50′30″: 80°11′30″ E, Madhya Pradesh, Central India. The study area also corresponds to five watersheds, wherein all these watersheds cover the rural part of the district, in which groundwater is the sole source of water for drinking and irrigation purposes. Seldom public water supply scheme provides tap water, but again the source of water is groundwater from shallow as well as deep aquifers. There is very little information available on the quality, statistical as well as geochemical characteristics of groundwater from this area. It is. Therefore, an endeavor has been made to investigate the hydrogeochemical behavior of groundwater by emphasizing the statistical methods, which would provide significant on groundwater quality. Hence, the statistical tools, namely factor, principal component, and cluster analyses, have been commenced to understand the various leading processes of groundwater chemistry (Hegeu & Kshetrimayum 2019, Ravish et al. 2020, Naidu et al. 2021, Natesan et al. 2022, Nayak & Hota 2023).

STUDY AREA

The Balaghat district is located in the southeastern part of Madhya Pradesh, Central India, and is bounded by Mandla, Rajnandgaon, and Seoni districts in the north, east, and west, respectively. The study area covers the western-south part of Balaghat district. It falls in degree sheet numbers 64B, 64C, 55O, and 55N between latitude 21°15' and 22°30' N and longitude 79°30' and 81°00' E (Fig.1). It represents the undulating area, where the semi-arid climatic condition prevails. In summer seasons, the utmost temperature blazes up to 45°C and drops down in winter to 8°C. The average annual rainfall is 1167 mm in the monsoon season, and humidity varies from 11 to 78%. The small streams of various orders delineate the dendritic-drainage pattern and drain out towards the northern part of the study area.

GEOLOGY AND HYDROGEOLOGY

The Archaean gneisses form the base of the geological set-up. These gneisses are coarse- to medium-grained and are composed mainly of plagioclase, quartz, and microcline with seldom biotite and hornblende mineral suites. The borewells located in this lithological unit have normal depth and diameters up to 60 meters below ground level (mbgL) and from 4 to 8 inches, respectively. The groundwater discharge is measured at 90 to 150 $m^3.day^{-1}$.

MATERIALS AND METHODS

In total, 77 groundwater samples were collected from preferred borewells, and the procedures precisely suggested by APHA (2012) were used for analytical measures. Respective field meters were utilized to measure the temperature, pH, and electrical conductivity (EC) at the borewell locations. The Ca^{2+}, Mg^{2+}, Cl^-, and HCO_3^- were counted by the titration method and the Na^+ K^+ concentrations were noted from the flame photometer. SO_4^{2-}, F^- and NO_3^- were determined by
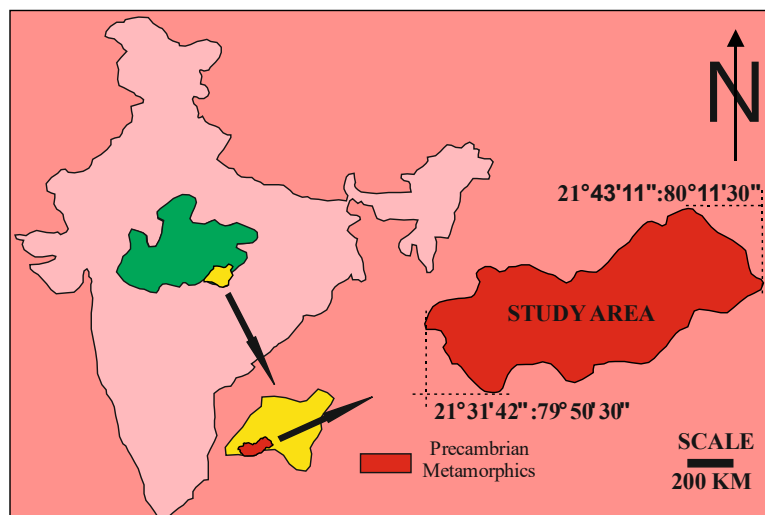

Fig. 1: Location map and geological map of the study area.

the UV-visible spectrophotometer. Total dissolved solids (TDS), as well as total hardness (TH), were worked out from mathematical expressions, and the concentrations of various ions have been presented in Table 1. The chloro-alkaline indices (CAI-1 and CAI-2) were determined after Schoeller (1977). The Principal Component Analysis (PCA) through Kaiser Normalization has been carried out after the standard procedure laid down by Hussain et al. (2016). Cluster analysis ramifies the variables into sets of comparatively homogeneous and distinct groups. Cluster analysis is carried out from correlation coefficient and Euclidean distances. The correlation coefficient method has been followed to group the groundwater parameters of the study area.

RESULTS AND DISCUSSION

Hydrogeochemistry of Ions

The pH and EC values were found to vary from 7.3 to 8.6 and 50 to 5080 $\mu S.cm^{-1}$ (Table 1), unraveling the alkaline nature and partaking of a multifarious series of processes in groundwater characterization (Subba Rao 2017). This highly elevated conductivity in groundwater is due to the ion exchange along with the solubilization processes during the rock-water interaction and may represent anthropogenic activity also (Sanchez-Perez & Tremolieres 2003, Choi et al. 2005). The high TDS (up to 3098 $mg.L^{-1}$, average value - 847.5 $mg.L^{-1}$) certainly represents the Geogenic as well as non-geogenic sources that contribute to salinity in the groundwater (Subba Rao et al. 2012).

In the groundwater samples of the study area, Ca^{2+} is found as the dominant constituent of the abundance succession of cations ($Ca^{2+} > Na^+ > Mg^{2+} > K^+$). The concentration of Ca^{2+} varies from 8.0-493.0 $mg.L^{-1}$, while the Na^+ content ranges from 4.2-540.0 $mg.L^{-1}$ (Table 1). The calcic plagioclases present in host rocks are the chief sources of Ca^{2+}, and the dissolution of calcium-affluent mineral suites is the significant geogenic process responsible for the derivation of Ca^{2+} content in groundwater (Subba Rao & Chaudhary 2019, Murkute 2014b). Moreover, the loss of carbon dioxide as a result of changes in temperature and pressure conditions, reverse ion exchange as well and changes in precipitation cause the behavioral alteration in Ca^{2+} content in groundwater (Ahada & Suthar 2018, Nayak & Hota 2023). The preponderance of Na^+ cation in groundwater points to the exhaustible weathering and dissolution of the host rocks as well as anthropogenic inputs. Also, the intake of such excessive concentration of Na^+ than the permissible limit always poses a threat to the human body, causing the in-taker to be prone to cardiac, renal, and circulatory diseases (Mor et al. 2006). The concentration of Mg^{2+} varies from

4.9-332.9 $mg.L^{-1}$, while the K^+ content ranges from 0.3-5.8 $mg.L^{-1}$. The Mg^{2+} is released from the mineral suites like mica, pyroxenes, amphiboles, magnesium calcite, traces of dolomite, and the gypsum resulting through the ion exchange processes (Thivya et al. 2018, Gogulothu et al. 2022). The at-par dominance of Mg^{2+} content conceivably points out the intense weathering of Mg-rich minerals from the host, suggesting the geogenic origin, contrary to the surplus use of fertilizers, pesticides, domestic wastes, septic tank spillages contribute to the anthropogenic inputs of Mg^{2+} in groundwater regime (Roy et al. 2018, Mgbenu & Egbueri 2019, Subba Rao 2021). The sodic plagioclases and potash feldspars (orthoclase and microcline) are the geogenic, while the potassium-based fertilizers, household wastes as well and irrigation-return-flows are the anthropogenic sources of K^+ (Subba Rao et al. 2020).

HCO_3^- is the dominant anion with concentration varying from 20.0-516.0 $mg.L^{-1}$, and $HCO_3^- > Cl^- > NO_3^- > SO_4^{2-} > F^-$ is the order of abundance of the anions. HCO_3^- is formed by the release of CO_2 into the soil zone by the weathering of minerals, the influence of atmospheric CO_2, and the decay of organic matter. Nevertheless, a higher concentration of HCO_3^- suggests the prevalence of mineral dissolution in the groundwater system (Subba Rao et al. 2021, Subba Rao 2018). The anthropogenic sources like domestic wastes, septic tank leakage, and irrigation-return-flow are the usual sources of Cl^- (8-1250.0 $mg.L^{-1}$) in the groundwater of the study area (Laxman et al. 2019).

The NO_3^- contents (0.8 – 541.9 $mg.L^{-1}$) have probably been released from the sewage waste, septic pool leakages, agricultural left-overs and decay of animal bodies (Subrahmanyam & Yadaiah 2000, Schilling & Wolter 2007, Raju et al. 2009, He et al. 2019). The SO_4^{2-} contents in groundwater of the present study area (0.6 – 184.0 $mg.L^{-1}$) possibly have been released through soil conditioners used in agricultural practices and from oxidation of sulfide minerals supplementary in fertilizers (Min et al. 2003, Chae et al. 2004, Subba Rao et al. 2012, Murkute 2014a). The F^- content varies from 0.5 - 1.5 $mg.L^{-1}$ with an average value of 1.0 $mg.L^{-1}$. The weathering of fluoride minerals like apatite, fluorite, biotite, hornblende, and phosphatic fertilizers are the chief sources of F^- in groundwater (Murkute 2014a, 2014b, Nayak & Hota 2023).

Geogenic and Non-Geogenic Source Genesis

The natural as well as human-induced processes are accountable for the generation of solute changes in the concentration of cations and anions, and the responsible processes may be categorized as rock weathering, evaporation as well and precipitation (Gibbs, 1970). Such Gibbs plots

Table 1: Range of cations and anions with desirable and permissible limits.

Sample No.	pH	EC	TDS	TA	TH	Ca^{2+}	Mg^{2+}	Na^+	K^+	HCO_3^-	Cl^-	SO_4^{2-}	F^-	NO_3^-	CAI-1	CAI-2
AP-1	7.70	488.00	312.00	160.00	236.1	64.10	18.50	23.00	1.60	160.00	35.00	8.20	0.820	6.23	0.3	0.0512
AP-2	7.80	284.00	186.00	128.00	99.8	24.00	9.70	14.40	1.50	128.00	10.00	1.80	0.760	5.83	-0.6	-0.042
AP-3	8.30	350.00	214.00	136.00	150.0	38.50	13.10	28.60	0.90	128.00	20.00	5.40	1.040	5.99	-0.5	-0.059
AP-4	8.20	2060.00	1214.00	516.00	598.6	56.10	111.80	144.00	1.60	516.00	225.00	120.00	1.180	26.64	0.4	0.0922
AP-5	7.60	2450.00	1520.00	408.00	1248.1	192.40	187.10	280.00	3.50	408.00	400.00	132.00	0.520	27.12	0.3	0.1239
AP-6	8.00	806.00	484.00	232.00	249.9	59.30	24.80	55.00	1.10	232.00	69.00	29.20	0.940	28.93	0.2	0.0391
AP-7	7.50	1160.00	672.00	344.00	459.7	85.00	60.30	62.00	1.80	344.00	90.00	62.40	1.040	51.24	0.3	0.0528
AP-8	7.70	1667.00	984.00	356.00	639.7	128.30	77.800	130.00	1.30	356.00	240.00	65.20	1.16	92.62	0.5	0.1644
AP-9	8.30	390.00	242.00	196.00	199.8	41.70	23.30	8.20	1.40	180.00	10.00	4.80	1.500	8.67	0.0	0.0019
AP-10	7.90	2050.00	1190.00	320.00	1018.7	176.40	140.90	214.00	1.80	320.00	300.00	104.40	0.940	34.29	0.3	0.1162
AP-11	8.40	773.00	510.00	364.00	299.4	48.10	43.70	25.60	1.60	348.00	38.00	7.80	1.320	34.21	0.3	0.0264
AP-12	7.30	3250.00	1982.00	360.00	1452.5	373.70	126.40	390.00	3.10	360.00	480.00	150.00	0.840	159.23	0.2	0.0878
AP-13	7.50	1321.00	792.00	280.00	540.2	160.30	34.00	120.00	2.40	280.00	160.00	56.40	0.660	85.72	0.2	0.0757
AP-14	7.90	950.00	560.00	220.00	400.2	112.20	29.20	66.00	1.80	220.00	110.00	32.80	0.740	50.76	0.4	0.1163
AP-15	8.20	1766.00	1024.00	320.00	839.4	168.30	102.10	130.00	1.50	320.00	220.00	80.60	0.860	126.12	0.4	0.1426
AP-16	8.30	709.00	460.00	344.00	363.3	62.50	50.50	19.50	2.00	336.00	26.00	8.80	1.120	5.52	0.2	0.0119
AP-17	7.90	1980.00	1228.00	380.00	839.5	176.40	97.20	190.00	3.60	380.00	260.00	65.40	0.800	94.59	0.3	0.0941
AP-18	8.40	858.00	498.00	200.00	320.3	112.20	9.70	72.00	2.50	176.00	95.00	28.00	1.160	37.68	0.2	0.0635
AP-19	7.90	247.00	160.00	88.00	140.1	25.70	18.50	13.80	0.80	88.00	20.00	7.80	0.940	9.10	0.3	0.0466
AP-20	7.80	50.00	34.00	20.00	40.1	8.00	4.90	4.20	0.30	20.00	8.00	0.60	0.700	1.97	0.4	0.1224
AP-21	8.60	683.00	396.00	260.00	300.1	80.20	24.30	22.20	1.20	236.00	35.00	24.20	1.300	15.57	0.3	0.0363
AP-22	7.80	1517.00	924.00	364.00	599.5	112.20	77.80	170.00	2.90	364.00	210.00	34.20	1.360	65.43	0.2	0.061
AP-23	8.20	1420.00	880.00	336.00	480.2	128.30	38.90	160.00	2.40	336.00	210.00	37.60	1.220	25.62	0.2	0.0816
AP-24	7.50	143.00	92.00	44.00	79.8	22.40	5.80	5.90	0.50	44.00	8.00	10.40	1.080	1.14	0.2	0.0256
AP-25	8.20	2160.00	1254.00	352.00	999.8	240.50	97.20	210.00	4.40	352.00	325.00	55.60	0.950	111.54	0.3	0.0512
AP-26	8.40	1235.00	766.00	240.00	519.3	96.20	68.00	110.00	3.40	224.00	150.00	32.80	1.180	86.71	-0.6	-0.042
AP-27	7.50	1160.00	684.00	368.00	459.8	104.20	48.60	76.00	2.40	368.00	110.00	11.40	1.250	29.32	0.3	0.151
AP-28	7.80	935.00	618.00	344.00	320.0	96.20	19.40	42.00	2.50	344.00	66.00	8.20	0.780	23.02	0.2	0.0866
AP-29	7.60	2740.00	1590.00	312.00	1019.4	224.40	111.80	270.00	4.80	312.00	550.00	108.00	1.220	20.89	0.3	0.0646
AP-30	7.70	2770.00	1690.00	352.00	1138.7	224.40	140.90	330.00	3.60	352.00	500.00	78.00	1.340	104.05	0.3	0.0514
AP-31	8.50	661.00	416.00	204.00	289.7	59.30	34.50	36.00	0.90	172.00	50.00	13.80	0.950	13.68	0.5	0.2837

Sample No.	pH	EC	TDS	TA	TH	Ca^{2+}	Mg^{2+}	Na^+	K^+	HCO_3^-	Cl^-	SO_4^{2-}	F^-	NO_3^-	CAI-1	CAI-2
AP-32	8.20	1085.00	630.00	384.00	439.9	88.20	53.50	62.00	1.80	384.00	80.00	12.40	0.880	3.94	0.3	0.1789
AP-33	8.20	1241.00	732.00	320.00	479.6	101.00	55.40	82.00	2.40	320.00	122.00	32.60	0.620	49.19	0.3	0.0489
AP-34	7.80	579.00	354.00	280.00	239.9	49.70	28.20	64.00	1.60	280.00	50.00	3.40	0.940	1.58	0.2	0.034
AP-35	8.20	700.00	448.00	360.00	289.7	72.10	26.70	7.20	1.20	360.00	10.00	4.80	1.200	4.97	0.3	0.0792
AP-36	8.40	843.00	488.00	352.00	335.6	60.10	45.20	26.50	0.80	344.00	38.00	9.20	1.140	14.27	-0.3	-0.047
AP-37	8.20	670.00	402.00	260.00	319.7	57.70	42.80	16.70	0.70	260.00	23.00	8.20	1.380	7.88	0.2	0.0043
AP-38	8.20	670.00	402.00	260.00	319.7	57.70	42.80	16.70	0.70	260.00	23.00	8.20	1.380	7.88	0.3	0.0268
AP-39	8.10	447.00	260.00	88.00	180.0	49.70	13.60	36.50	0.50	88.00	53.00	6.60	0.780	12.22	0.2	0.0192
AP-40	7.70	688.00	440.00	280.00	335.7	64.90	42.30	18.60	1.40	280.00	25.00	8.80	0.640	8.91	0.2	0.0192
AP-41	7.90	1326.00	796.00	280.00	460.0	113.80	42.80	120.00	2.00	280.00	180.00	66.80	1.340	0.99	0.3	0.1084
AP-42	8.20	806.00	476.00	364.00	301.7	64.10	34.50	14.50	0.90	364.00	22.00	5.40	1.440	6.70	0.2	0.0159
AP-43	7.90	1610.00	966.00	320.00	723.3	129.90	97.20	144.00	2.80	320.00	196.00	40.00	0.920	68.38	0.3	0.1101
AP-44	8.00	1165.00	688.00	288.00	491.7	97.80	60.30	96.00	2.30	288.00	156.00	13.20	0.620	13.72	0.3	0.0169
AP-45	8.20	1525.00	886.00	276.00	240.1	65.70	18.50	82.00	3.10	276.00	125.00	32.00	0.720	2.56	0.3	0.0885
AP-46	7.40	1240.00	782.00	360.00	599.3	102.60	83.60	66.00	0.80	360.00	94.00	30.00	0.840	37.05	0.4	0.1262
AP-47	7.60	810.00	528.00	252.00	260.0	62.50	25.30	40.00	1.50	252.00	63.00	9.00	1.020	19.23	0.3	0.0921
AP-48	7.70	3440.00	1996.00	320.00	1496.3	200.00	243.00	360.00	3.50	320.00	550.00	120.00	0.740	382.30	0.3	0.0562
AP-49	7.60	3990.00	2354.00	360.00	1997.4	332.70	284.30	540.00	4.80	360.00	800.00	136.40	1.090	266.43	0.3	0.0664
AP-50	8.20	780.00	490.00	320.00	347.0	24.00	70.00	28.40	0.90	320.00	45.00	5.80	0.820	3.23	0.3	0.1884
AP-51	7.80	3510.00	2106.00	324.00	1298.0	200.40	194.40	390.00	4.50	324.00	600.00	62.60	1.260	226.23	0.3	0.1969
AP-52	7.90	5080.00	3098.00	340.00	1699.4	380.80	182.30	520.00	5.80	340.00	875.00	126.00	1.320	541.93	0.3	0.0423
AP-53	8.40	2690.00	1668.00	420.00	1047.6	80.20	206.60	260.00	3.20	412.00	350.00	92.40	0.900	119.81	0.3	0.2083
AP-54	8.20	688.00	400.00	288.00	249.8	41.70	35.50	22.80	2.50	288.00	30.00	6.20	0.740	5.91	0.4	0.2604
AP-55	8.00	3920.00	2274.00	288.00	1997.6	335.10	282.90	190.00	3.40	288.00	280.00	184.00	0.980	294.02	0.2	0.1006
AP-56	8.50	507.00	308.00	160.00	250.0	57.70	25.80	14.80	2.10	128.00	23.00	11.60	0.700	15.92	0.2	0.0145
AP-57	8.30	1804.00	1156.00	352.00	823.1	160.30	103.00	176.00	3.80	344.00	325.00	48.40	1.180	19.71	0.3	0.1152
AP-58	8.30	2920.00	1694.00	360.00	1098.9	224.40	131.20	292.00	4.20	352.00	525.00	130.20	1.220	117.84	0.3	0.0313
AP-59	8.10	4980.00	2938.00	300.00	2597.4	493.00	332.90	520.00	5.30	300.00	1250.00	180.00	0.820	219.92	0.4	0.2002
AP-60	8.30	1680.00	1024.00	236.00	619.5	120.20	77.80	210.00	2.20	228.00	325.00	54.60	0.600	29.95	0.4	0.2254
AP-61	8.50	520.00	328.00	228.00	250.0	52.10	29.20	8.10	0.80	204.00	10.00	4.20	0.860	0.79	0.6	0.4189
AP-62	8.30	890.00	544.00	268.00	359.4	65.70	47.60	72.00	1.40	260.00	95.00	14.60	0.880	3.78	0.3	0.1832
AP-63	8.20	313.00	204.00	100.00	189.7	32.10	26.70	12.50	0.60	100.00	17.00	7.00	0.700	12.65	0.1	0.0045

Table Cont....

Sample No.	pH	EC	TDS	TA	TH	Ca^{2+}	Mg^{2+}	Na^+	K^+	HCO_3^-	Cl^-	SO_4^{2-}	F^-	NO_3^-	CAI-1	CAI-2
AP-64	7.80	729.00	482.00	316.00	369.4	70.50	47.10	17.20	2.20	316.00	29.00	5.40	0.900	4.73	0.2	0.0572
AP-65	8.10	743.00	446.00	320.00	323.5	49.70	48.60	19.60	1.60	320.00	28.00	7.40	1.040	5.12	0.2	0.0315
AP-66	8.10	2760.00	1628.00	428.00	718.3	64.10	136.10	310.00	3.40	428.00	450.00	138.00	0.920	137.16	0.3	0.0274
AP-67	8.30	796.00	494.00	364.00	283.8	48.10	39.90	19.20	2.00	348.00	28.00	7.60	0.720	0.79	0.2	0.0191
AP-68	8.40	792.00	476.00	320.00	369.7	72.10	46.20	31.60	1.40	304.00	48.00	13.00	0.940	24.12	0.3	0.1344
AP-69	8.10	2410.00	1494.00	444.00	749.1	136.30	99.60	270.00	2.80	444.00	400.00	100.40	0.980	58.53	0.2	0.017
AP-70	8.40	626.00	388.00	240.00	239.9	43.30	32.10	25.00	1.40	216.00	33.00	12.60	1.240	9.77	0.3	0.0394
AP-71	8.10	623.00	374.00	260.00	247.6	44.10	33.50	17.80	0.60	260.00	25.00	11.80	0.740	3.15	0.3	0.1347
AP-72	8.50	1353.00	786.00	328.00	415.8	80.20	52.50	120.00	0.80	296.00	170.00	31.30	1.160	39.26	0.2	0.0231
AP-73	8.20	565.00	334.00	220.00	229.7	48.10	26.70	18.40	0.40	220.00	27.00	9.80	0.940	6.70	0.3	0.0222
AP-74	7.90	3050.00	1770.00	312.00	1159.8	288.60	106.90	320.00	1.80	312.00	480.00	24.40	0.820	299.54	0.3	0.093
AP-75	8.20	651.00	392.00	280.00	267.5	40.10	40.80	14.60	0.30	280.00	18.00	7.00	0.950	4.10	0.3	0.0319
AP-76	8.40	609.00	372.00	240.00	295.6	56.10	37.90	10.20	0.80	216.00	15.00	10.80	1.240	11.08	0.3	0.1938
AP-77	8.40	617.00	390.00	180.00	299.8	62.50	35.00	28.50	0.60	164.00	40.00	7.60	1.100	16.83	0.2	0.0102
Min	7.3	50.0	34.0	20.0	40.1	8.0	4.9	4.2	0.3	20.0	8.0	0.6	0.5	0.8	-	-
Max	8.6	5080.0	3098.0	516.0	2597.4	493.0	332.9	540.0	5.8	516.0	1250.0	184.0	1.5	541.9	-	-
Avg	8.0	1408.8	847.6	288.2	579.8	112.2	73.0	118.9	2.1	283.3	184.2	42.2	1.0	58.8	-	-
STDEV	0.3	1113.6	659.5	92.0	490.9	93.8	68.5	134.0	1.3	94.1	231.2	47.4	0.2	96.0	-	-
COV	3.9	79.0	77.8	31.9	84.7	83.6	93.8	112.7	62.4	33.2	125.5	112.4	23.7	163.2	-	-

Ions values are presented in mg.L⁻¹ . SD – standard deviation, CV – covariance. DL – Desirable limit, PL – Permissible limit
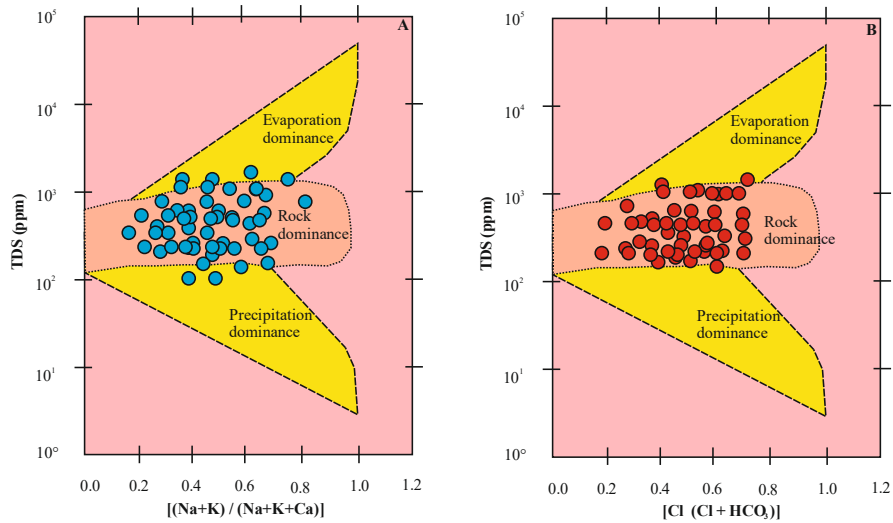
Fig. 2: Gibbs diagrams. a) TDS with [(Na+K) / (Na+K+Ca)], b) TDS with [(Cl/Cl+HCO$_3$)].

have been considered to discover the aforementioned responsible processes of the groundwater character from the study area (Fig. 2A, 2B). The Gibbs plots have been generated by plotting TDS with [(Na$^+$+K$^+$)/(Na$^+$+K$^+$+Ca^{2+})] (Fig.2A) and TDS with [(Cl$^-$/Cl$^-$+HCO$_3^-$)] (Fig.2B) to assess the controlling sources of dissolved hydrogeochemical organization. The data points from these diagrams enumerate that the chemical weathering of rock-forming mineral suites is the key contributing feature in the evolution of the chemical composition of groundwater, which is secondarily influenced by anthropogenic activities (Gibbs 1970, Ravikumar et al. 2010).

The silicate weathering, revealed through reverse ion exchange or cation exchange, is the predominant process, which is governing the groundwater chemistry as revealed through the Cl$^-$ vs. Na$^+$ plot (Fig. 3), wherein Na$^+$ < Cl$^-$ indicates reverse ion exchange, while Na$^+$ > Cl$^-$ suggests cation exchange (Subba Rao et al. 2019). This suggests

that the silicate weathering resulting in cation exchange is the principal factor, while the reverse ion exchange is also an additional contributing factor to solute generation in the groundwater of the study area. For judging the sources of ions in groundwater, the chloro-alkaline indices (CAI-1) and (CAI-2) have been calculated, wherein the values of index CAI-1vary from -0.6 to 0.6, while the values of index CAI-2 range from -0.1 to 0.4 (Table 1). The inter-correlation of CAI-1 vs CAI-2 (Fig. 4) signifies the prevalence of cation exchange over reverse ion exchange.

The NO$_3^-$ + Cl$^-$/HCO$_3^-$ vs. TDS scatter diagram (Fig. 5) demonstrates a linear trend with a positive correlation, supporting the impact of non-geogenic sources
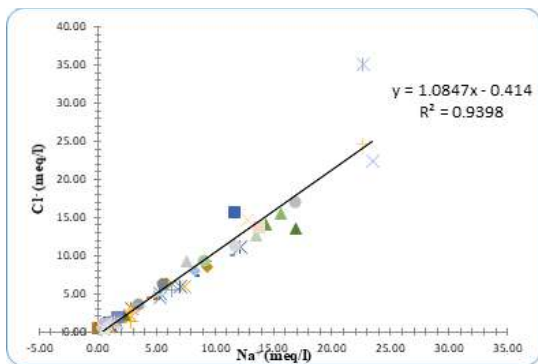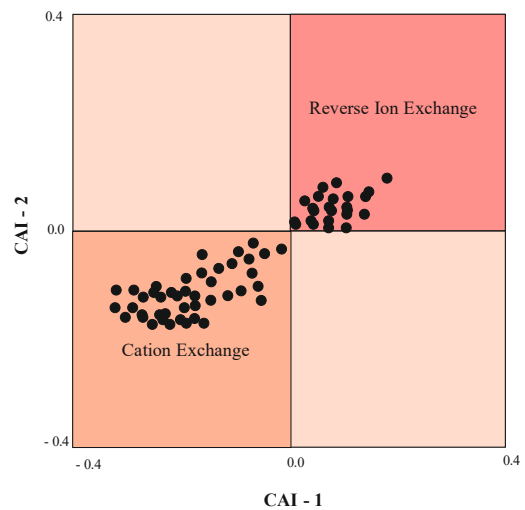

Fig. 3: Interrelation of Cl$^-$ vs. Na$^+$ plot.

Fig. 4: Plot of CAI-1 vs. CAI-2 values calculated for groundwater samples from study area.
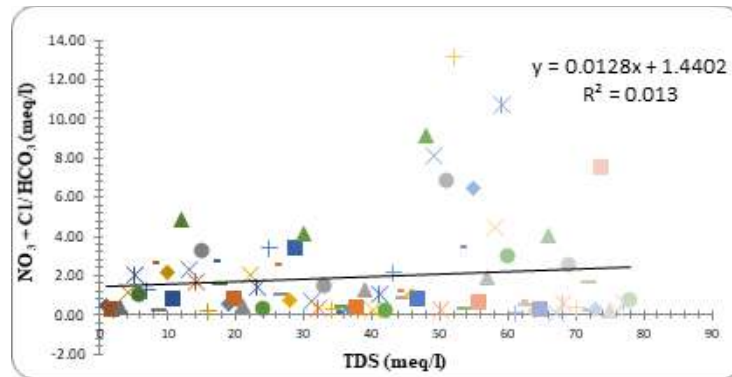
Fig. 5: plot of TDS vs. $NO_3^- + Cl^-/HCO_3^-$ for groundwater samples from the study area.

Table 2: Pearson's bivariate correlation coefficients (r) between pairs of groundwater parameters.

	pH	TDS	TA	TH	Ca^{2+}	Mg^{2+}	Na^+	K^+	HCO_3^-	Cl^-	SO_4^{2-}	NO_3^-	F^-
pH	1.000	0.107	0.872**	0.048	0.198	-0.059	0.223	-0.011	0.127	0.192	-0.102	-0.183	0.878**
TDS		1.000	0.091	0.888**	0.856**	0.782**	0.877**	0.376*	0.876**	0.856**	0.481**	0.466**	0.174
TA			1.000	0.129	0.192	0.065	0.144	-0.167	0.221	0.117	-0.191	-0.252	0.808**
TH				1.000	0.879**	0.927**	0.679**	0.214	0.853**	0.689**	0.376*	0.345*	0.171
Ca^{2+}					1.000	0.657**	0.691**	0.189	0.842**	0.711**	0.265	0.166	-0.323*
Mg^{2+}						1.000	0.563**	0.184	0.709**	0.548**	0.446**	0.383*	0.071
Na^+							1.000	0.213	0.726**	0.945**	0.264	0.347*	0.314*
K^+								1.000	-0.063	0.214	0.856**	0.779**	-0.018
HCO_3^-									1.000	0.672**	0.013	0.019	0.231
Cl^-										1.000	0.285	0.264	0.294
SO_4^{2-}											1.000	0.799**	-0.061
NO_3^-												1.000	-0.167
F^-													1.000

on the groundwater chemistry of the study area (Li et al. 2019, Subba Rao et al. 2021). The important non-geogenic sources are unplanned irrigation-return-flow and the animal wastes sprawled throughout the study area, as well as the use of chemical fertilizers, soil conditioners, and manures in patchy agricultural fields.

Statistical Appraisal

The positive correlation of pH with TA (r = 0.872) and also with F^- (r = 0.878) discern strong involvement of the alkaline character of groundwater from the study area and the fluoride ion concentration (Table 2).

Such a positive phenomenon of TDS interrelationship with other ions suggests these ions are definitely the derived products of weathering and dissolution of mineral suites from the lithology and also the impact of anthropogenic activities (Subba Rao et al. 2020, 2021). The positive correlation

among the Ca^{2+} with Mg^{2+} (r = 0.657), Na^+ (r = 0.691), and HCO_3^- (r = 0.842) conveys the derivation of these ions from the similar lithological (geogenic) origin while the high positive correlations between K^+ and SO_4^{2-} (r = 0.856), as well as K^+ and NO_3^- (r = 0.779), puts on the derivation of these ions from the agro-chemical background (Nayak & Hota 2023).

In the factor analysis through Kaiser Criterion (Kaiser 1958), the 03 statistically significant factors out of all the variables have been found (Table 3), wherein three factors have eigenvalues of 6.350, 2.732, and 2.697, which account for 47.339%, 20.393% and 20.131% of variances respectively, with the total variance 87.923%. The factor-1, which is regarded as the geogenic factor, has very strong positive loadings on TDS (0.937), TH (0.923), Ca^{2+} (0.946), Mg^{2+} (0.906), Na^+ (0.838), HCO_3^- (0.947) and Cl^- (0.853), also corroborating the involvement of TDS, TH with

Table 3: Factor analysis data of groundwater parameters from the study area.

Groundwater parameters	Factor -1	Factor - 2	Factor - 3
pH	0.062	-0.031	**0.957**
TDS	**0.937**	0.315	0.072
TA	0.097	-0.192	**0.819**
TH	**0.923**	0.143	0.025
Ca^{2+}	0.946	0.077	0.151
Mg^{2+}	**0.906**	0.167	-0.101
Na^+	**0.838**	0.189	0.176
K^+	0.041	**0.961**	0.019
HCO_3^-	**0.947**	-0.182	0.068
Cl^-	0.853	0.151	0.134
SO_4^{2-}	0.168	**0.912**	-0.082
NO_3^-	0.217	**0.859**	-0.163
F^-	0.148	-0.051	**0.921**
Eigenvalues	6.350	2.732	2.697
Percentage of total variance	47.399	20.393	20.131
Cumulative percentage of total variance	47.399	67.791	87.923

three cations and two anions present in mineral suites of the host rocks. The ions in factor-2 loaded on K^+ (0.961), SO_4^{2-} (0.912), and NO_3^- (0.859) are specifically present in fertilizers and soil conditioners used to enhance crop production and hence clearly be regarded as anthropogenic. The factor-3 strongly loaded with pH (0.957), TA (0.819), and F^- (0.921), is the alkalinity factor. The factor loadings in three-dimensional rotated space, evaluated for the present investigation, exemplify the ions-assemblage (Fig. 6)

intimately resemble the findings of the factor analysis.

Groundwater Suitability

The suitability of groundwater for various purposes (drinking, as well as irrigation) has direct control on human health, household utility, furthermore agricultural soil, and crop fitness. The 69 % samples of the study area have EC values less than the permissible limit of 1500 mg.L^{-1} (WHO (2017), suggesting suitability for drinking purposes. Considering TA (except sample 4: TA = 516 mg.L^{-1}) and TH content (31%), all the groundwater samples are suitable for drinking purposes. 55% of the samples from the study area have NO_3^- content more than the approved limits (WHO 2017, BIS 2020), hence specifying the need for proper sanitation measures as well as water purification. Sodium Adsorption Ratio (SAR), a test of irrigation suitability, represents the soil permeability, where in cations like Na^+, Ca^{2+} and Mg^{2+} ions are scientifically interconnected (SAR = $Na^+/\sqrt{[(Ca^{2+}+Mg^{2+})/2]}$). The SAR values pertaining to sodium hazard are compared with the salinity hazard (Fig. 7) in the US Salinity Laboratory's diagram (US Salinity Laboratory Staff 1954).

The bunch of plots of the samples in C_3-S_1 type denotes the water of medium to high salinity with medium sodium type. The 65% groundwater points corresponding to the C_3-S_2 and C_3-S_1 type unravel the medium salinity - medium sodium type. Both the above categories express the suitability of groundwater for irrigation purposes with a slight threat of exchangeable sodium. The other two minor clusters (C_4-S_2-10%, C_4-S_1 -5%) point out groundwater suitability for salt-tolerant or semi-tolerant crops.
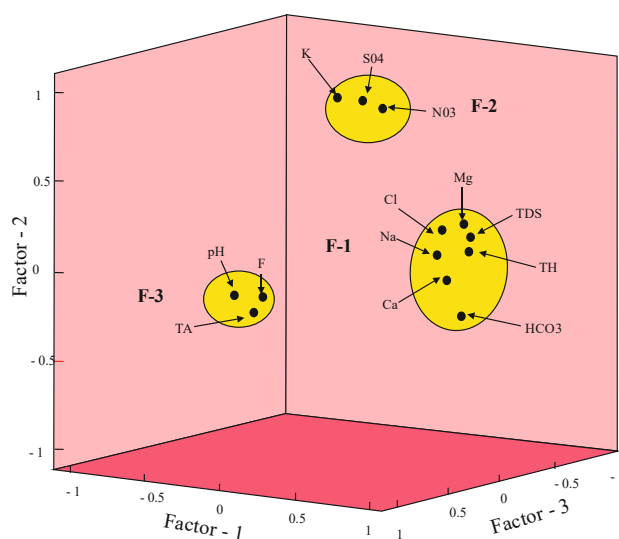

Fig. 6: Factor loadings in three-dimensional rotated space for groundwater samples from the study area.
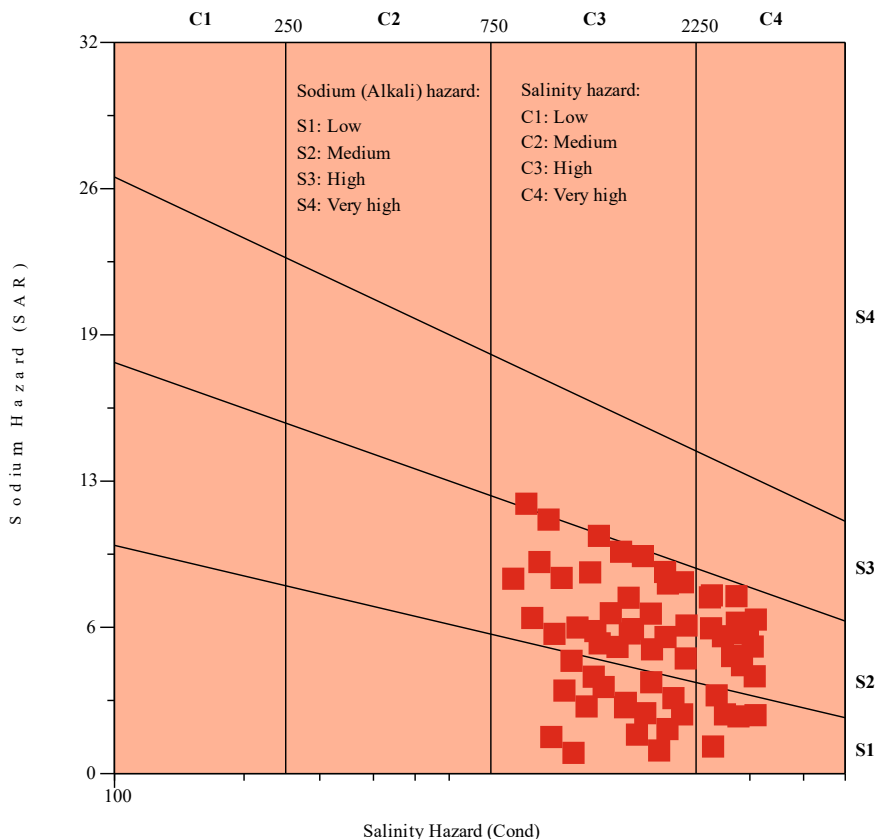
Fig. 7: US Salinity diagram for groundwater samples from the study area.

CONCLUSIONS

The key conclusions of the present study involving geostatistical appraisal, hydrogeochemical environment of major ions, and groundwater suitability from the part of Balaghat District (MP), Central India, are as follows:

i) The pH and EC values (7.3 to 8.6 and 50 to 5080 $\mu S.cm^{-1}$) illuminate the alkaline nature and multifarious processes in groundwater characterization. The prominent conductivity in groundwater represents the ion exchange along with the solubilization processes during the rock-water interaction and may represent anthropogenic activity also.

ii) The abundance succession of cations is $Ca^{2+} > Na^+ > Mg^{2+} > K^+$, while HCO_3^- is dominant anion and abundance succession is $HCO_3^- > Cl^- > NO_3^- > SO_4^{2-} > F^-$. The calcic plagioclases present in host rocks are the chief sources of Ca^{2+}. The anthropogenic sources like domestic wastes, septic tank leakage, and irrigation-return-flow are the usual sources of Cl^- (8 – 1250.0 $mg.L^{-1}$) in the groundwater of the study area.

iii) The positive correlation among the Ca^{2+} with Mg^{2+} (r = 0.657), Na^+ (r = 0.691), and HCO_3^- (r = 0.842) unravels

the derivation of ions from the geogenic origin, whereas the high positive association between K^+ and SO_4^{2-} (r = 0.856) as well as K^+ and NO_3^- (r = 0.779) suggests agro-chemical derivation of ions.

iv) The eigenvalues of three factors (6.350, 2.732, and 2.697) have a total variance of 87.923%. The factor-1, factor-2, and factor-3 correspond with the geogenic factor, anthropogenic factor, and alkalinity factor, respectively.

v) The 69 % samples of the study area having EC values less than the permissible limit of 1500 $mg.L^{-1}$ suggests suitability for drinking purposes. The 65% groundwater points corresponding to the C_3-S_2 and C_3-S_1 types unravel the suitability of groundwater for irrigation purposes with a slight threat of exchangeable sodium.

ACKNOWLEDGMENTS

REFERENCES

Adimalla, N. and Qian, H., 2019. Groundwater quality evaluation using water quality index (WQI) for drinking purposes and human health risk (HHR) assessment in an agricultural region of Nanganur, South India. *Ecotoxicology and Environmental Safety*, 176, pp.153–161.

Agoubi, B., Kharroubi, A. and Abida, H., 2011. Hydrochemistry of groundwater and its assessment for irrigation purposes in the coastal Jeffara aquifer, southeastern Tunisia. *Arabian Journal of Geosciences*, 6, pp.1163–1172.

Ahada, C.P.S. and Suthar, S., 2018. Assessing groundwater hydrochemistry of Malwa Punjab, India. *Arabian Journal of Geosciences*, 4, pp.11–17.

Amiri, V., Rezaei, M. and Sohrabi, N., 2014. Groundwater quality assessment using entropy weighted water quality index (EWQI) in Lenjanat, Iran. *Environmental Earth Sciences*, 72, pp.3479–3490.

APHA, 2012. WPCF, Standard methods for examination of water and wastewater. American Public Health Association/American Water Works Association/Water Environment Federation, Washington DC.

Bauder, T.A., Waskom, R.M., Sutherland, P.L. and Davis, J.G., 2014. *Irrigation Water Quality Criteria*. Colorado State University, p.506.

BIS, 2020. Indian standard drinking water specifications. IS: 10500, Edition 2.2 (2003-2009). Bureau of Indian Standards, New Delhi.

Brindha, K. and Elango, L., 2013. Geochemistry of fluoride-rich groundwater in a weathered granitic rock region, Southern India. *Water Quality Exposure and Health*, 5(3), pp.127–138.

Chae, G.T., Kim, K., Yun, S.T., Kim, K.H., Kim, S.O., Choi, B.Y., Kim, H.S. and Rhee, C.W., 2004. Hydrogeochemistry of alluvial groundwaters in an agricultural area: an implication for groundwater contamination susceptibility. *Chemosphere*, 55, pp.369–378.

Choi, B.Y., Yun, S.T., Yu, S.Y., Lee, P.K., Park, S.S., Chae, G.T. and Mayer, B., 2005. Hydrochemistry of urban groundwater in Seoul, South Korea: effect of land use and pollutant recharge. *Environmental Geology*, 48, pp.979–990.

Deshpande, S.S. and Murkute, Y.A., 2023. Hydrogeochemical characteristics and suitability of groundwater for drinking and irrigation from shallow aquifers of PG1 Watershed in Chandrapur District of Maharashtra. *Nature Environment and Pollution Research*, 22(2), pp.755–765.

Duraisamy, S., Govindhaswamy, V., Duraisamy, K., Krishinaraj, S., Balasubramanian, A. and Thirumalaisamy, S., 2018. Hydrogeochemical characterization and evaluation of groundwater quality in Kangayam taluk, Tirupur district, Tamil Nadu, India, using GIS tech. *Environmental Geochemistry and Health*, 18, p.183. https://doi.org/10.1007/s10653-018-0183-z.

Eyankware, M.O., Aleke, C.G., Selemo, A.O.I. and Nabo, P.N., 2020. Groundwater for sustainable development: hydrogeochemical studies and suitability assessment of groundwater quality for irrigation at Warri and environs, Niger delta basin, Nigeria. *Groundwater for Sustainable Development*, 10, pp.100293.

Gibbs, R.J., 1970. Mechanism controlling world water chemistry. *Science*, 17, pp.1088–1090.

Gogulothu, S., Subba Rao, N., Das, R. and Dhakate, R., 2022. Geochemical evaluation and suitability of groundwater quality for irrigation purposes in an agricultural region of South India. *Applied Water Science*, 12, p.142. https://doi.org/10.1007/s13201-022-01583-w.

Gupta, S., Mahato, A., Roy, P., Datta, J.K. and Saha, R.N., 2008. Geochemistry of groundwater, Burdwan district, West Bengal, India. *Environmental Geology*, 53, pp.1271–1282.

He, X., Wu, J. and He, S., 2019. Hydrochemical characteristics and quality evaluation of groundwater in terms of health risks in Luohe aquifer in Wuqi County of the Chinese Loess Plateau, Northwest China. *Human Ecology Risk Assessment*, 25, pp.32–51.

Hegeu, H. and Kshetrimayum, K.S., 2019. Hydrochemical characterization of groundwater in geomorphic units using graphical and multivariate statistical methods in Dimapur Valley, Northeast India. *Groundwater for Sustainable Development*, 8, pp.484–500.

Herojeet, R., Rishi, M.S. and Kishore, N., 2015. Integrated approach of heavy metal pollution indices and complexity quantification using chemometric models in the Sirsa Basin, Nalagarh valley, Himachal Pradesh, India. *Chinese Journal of Geochemistry*, 34, pp.620–633.

Hussin, N.H., Yusoff, I., Tahir, W., Mohamed, I., Ibrahim, A.I.N. and Rambli, A., 2016. Multivariate statistical analysis for identifying water quality and hydrogeochemical evolution of shallow groundwater in Quaternary deposits in the Lower Kelantan River Basin, Malaysian Peninsula. *Environmental Earth Sciences*, 75, p.1081. https://doi.org/10.1007/s12665-016-5705-3.

Jalali, M., 2009. Geochemistry characterization of groundwater in an agricultural area of Razan, Hamadan, Iran. *Environmental Geology*, 56, pp.1479–1488.

Kaiser, H.F., 1958. The varimax criterion for analytic rotation in factor analysis. *Psychometrika*, 23, pp.187–200.

Laxman, D.K., Satyanarayana, E., Dhakate, R. and Saxena, P.R., 2019. Hydrochemical characteristics concerning fluoride contamination in groundwater of Maheshwaram Mandal, RR District, Telangana state, India. *Groundwater for Sustainable Development*, 8, pp.474–483.

Li, P., Wu, Q. and Wu, J., 2011. Groundwater suitability for drinking and agricultural usage in Yinchuan area, China. *International Journal of Environmental Science*, 1(6), pp.1241–1249.

Li, P., Wu, J. and Qian, H., 2012. Groundwater quality assessment based on rough sets attribute reduction and TOPSIS method in a semi-arid area, China. *Environmental Monitoring and Assessment*, 184, pp.4841–4854.

Li, P., Wu, J., Tian, R., He, S., He, X., Xue, C. and Zhang, K., 2018. Geochemistry, hydraulic connectivity and quality appraisal of multilayered groundwater in the Hongdunzi coal mine, Northwest China. *Mine Water and the Environment*, 37, pp.222–237.

Li, P., He, X. and Guo, W., 2019. Spatial groundwater quality and potential health risks due to nitrate ingestion through drinking water: a case study in Yan'an City on the Loess Plateau of northwest China. *Human Ecology Risk Assessment*, 25, pp.11–31. https://doi.org/10.1080/10807039.2018.1553612.

Mgbenu, C.N. and Egbueri, J.C., 2019. The hydrogeochemical signatures, quality indices and health risk assessment of water resources in Umunya district, Southeast Nigeria. *Applied Water Science*, 9, pp.1–19.

Min, J.H., Yun, S.T., Kim, K., Kim, H.S. and Kim, D.J., 2003. Geologic controls on the chemical behavior of nitrate in riverside alluvial aquifers, Korea. *Hydrological Processes*, 17, pp.1197–1211.

Mor, S.K., Ravindra, R.P., Dahiya, P. and Chandra, A., 2006. Leachate characterization and assessment of groundwater pollution near municipal solid waste landfill site. *Environmental Monitoring and Assessment*, 118, pp.435–456.

Murkute, Y.A., 2014a. Hydrogeochemical characterization and quality assessment of groundwater around Umrer Coal Mine area, Nagpur District, Maharashtra, India. *Environmental Earth Sciences*, 72, pp.4059–4073.

Murkute, Y.A., 2014b. Hydrogeochemical behavior and groundwater suitability of Vislon Area, part of WRD Watershed, Chandrapur District, Maharashtra, India. *Pollution Research*, 42(1), pp.94–104.

Nagaraju, A., Arveti, M.R.S., Sarma, J.A., Aitkendead-Peterson, K. and Sunil, 2011. Fluoride incidence in groundwater: a case study from Talupula, Andhra Pradesh, India. *Environmental Monitoring and Assessment*, 172, pp.427–443.

Naidu, S., Gupta, G., Singh, R., Tahama, K. and Erram, V.C., 2021. Hydrogeochemical processes regulating the groundwater quality and its suitability for drinking and irrigation purpose in parts of coastal Sindhudurg district, Maharashtra. *Journal of the Geological Society of India*, 97, pp.173–185.

Natesan, D., Sabarathinam, C., Kamaraj, P., Mathivanan, M., Haji, M., Viswanathan, P.M., Chandrasekaran, T. and Rajendran, T., 2022. Impact of monsoon shower on the hydrogeochemistry of groundwater along

the lithological contact: a case study from South India. *Applied Water Science*, 12, pp.1–20.

Nayak, M. and Hota, R.N., 2023. Statistical evaluation of major ion chemistry of premonsoon groundwater of Kantapara Block, Cuttack District, Odisha. *Vist Geological Research*, 19, pp.46–56.

Omran, E.S.E., 2012. A proposed model to assess and map irrigation water well suitability using geospatial analysis. *Water*, 4, pp.545–567.

Rajesh, R., Brindha, K., Murugan, R. and Elango, L., 2012. Influence of hydrogeochemical processes on temporal changes in groundwater quality in a part of Nalgonda district, Andhra Pradesh, India. *Environmental Earth Sciences*, 65, pp.1203–1213.

Raju, N.J., Ram, P. and Dey, S., 2009. Groundwater quality in the lower Varuna River basin, Varanasi district, Uttar Pradesh, India. *Journal of the Geological Society of India*, 73, pp.178–192.

Ravikumar, P. and Somashekar, R.K., 2011. A geochemical assessment of coastal groundwater quality in the Varahi river basin, Udupi District, Karnataka State, India. *Arabian Journal of Geosciences*, 6, pp.1855–1870. https://doi.org/10.1007/s12517-011-0470-9.

Ravikumar, P., Venkatesharaju, K., Prakash, K.L. and Somashekhar, R.K., 2010. Geochemistry of groundwater and groundwater prospects evaluation, Anekal Taluk, Bangalore urban district, Karnataka, India. *Environmental Monitoring and Assessment*, DOI: 10.1007/s10661-010-1721-z.

Ravish, S., Setia, B. and Deswal, S., 2020. Groundwater quality analysis of northeastern Haryana using multivariate statistical techniques. *Journal of the Geological Society of India*, 95, pp.407–416.

Roy, A., Keesari, T., Mohokar, H. and Bitra, S., 2018. Assessment of groundwater quality in hard rock aquifer of central Telangana state for drinking and agriculture purposes. *Applied Water Science*. https://doi.org/10.1007/s13201-018-0761-3.

Sanchez-Perez, J.M. and Tremolieres, M., 2003. Change in groundwater chemistry as a consequence of suppression of floods: The case of the Rhine floodplain. *Journal of Hydrology*, 270, pp.89–104.

Schilling, K.E. and Wolter, C.F., 2007. A GIS based groundwater travel time model to evaluate stream nitrate concentration reductions from land use change. *Environmental Geology*, 53, pp.433–443.

Schoeller, H., 1977. Geochemistry of groundwater. In Brown, R.H., Konoplyantsev, A.A., Ineson, J., Kovalevsky, V.S. (eds.), Groundwater studies—An international guide for research and practice, Chapter 15, UNESCO, Paris, pp.1–18.

Si, J., Feng, Q., Wen, X., Su, Y., Xi, H., Chang, Z. and Li, Y., 2009. Major ion chemistry of groundwater in the extreme arid region northwest China. *Environmental Geology*, 57, pp.1079–1087.

Singh, G., Rishi, M.S., Herojeet, R., Kaur, L., Sharma, K. and Gupta, A., 2019. Evaluation of groundwater quality and human health risks from fluoride and nitrate in the semi-arid region of northern India. *Environmental Geochemistry and Health*. https://doi.org/10.1007/s10653-019-00449-6.

Sreedevi, P.D., 2004. Groundwater quality of Pageru River basin, Cuddapah District, Andhra Pradesh. *Journal of the Geological Society of India*, 64, pp.619–636.

Sreedevi, P.D., Sreekanth, P.D., Ahmed, S., Reddy, D.V. and Kumar, P., 2018. Appraisal of groundwater quality in a crystalline aquifer: A chemometric approach. *Arabian Journal of Geosciences*. https://doi.org/10.1007/s12517-018-3480-z.

Subba Rao, N. and Chaudhary, M., 2019. Hydrogeochemical processes regulating the spatial distribution of groundwater contamination, using pollution index of groundwater (PIG) and hierarchical cluster analysis (HCA): A case study. *Groundwater for Sustainable Development*. https://doi.org/10.1016/j.gsd.2019.100238.

Subba Rao, N., Subrahmanyam, A., Ravi Kumar, S., Srinivasulu, N., Babu Rao, G., Surya Rao, P. and Venktram Reddy, G., 2012. Geochemistry and quality of groundwater of Gummanampadu Sub-basin, Guntur District, Andhra Pradesh, India. *Environmental Earth Sciences*, 67, pp.1451–1471.

Subba Rao, N., Srihari, B., Spandana, D., Sravanthi, M., Kamalesh, T. and Abraham Jayadeep, V., 2019. Comprehensive understanding of groundwater quality and hydrogeochemistry for the sustainable development of suburban area of Visakhapatnam, Andhra Pradesh, India. *Human Ecological Risk Assessment*. https://doi.org/10/1080/10807039/1571403.

Subba Rao, N., 2017. *Hydrogeology - Problems with solutions*. PHI Learning Pvt. Ltd., Delhi, 265p.

Subba Rao, N., 2018. Groundwater quality from a part of Prakasam district, Andhra Pradesh, India. *Applied Water Science*, 8, p.30. https://doi.org/10.1007/s13201-018-0665-2.

Subba Rao, N., Ravindra, B., Wu, J. and Liu, Q., 2020. Geochemical and health risk evaluation of fluoride-rich groundwater in Sattenapalle Region, Guntur district, Andhra Pradesh, India. *Human Ecological Risk Assessment*, 26, pp.316–348.

Subba Rao, N., Dinakar, A., Sravanthi, M., Kumari, B.K. and Reddy, R., 2021. Geochemical characteristics and quality of groundwater evaluation for drinking, irrigation, and industrial purposes from a part of hard rock aquifer of South India. *Environmental Science and Pollution Research*, 28, pp.31941–31961.

Subrahmanyam, K. and Yadaiah, P., 2000. Assessment of the impact of industrial effluents on water quality in Patancheru and environs, Medak district, Andhra Pradesh, India. *Hydrogeology Journal*, 9(3), pp.297–312.

Thilagavathi, N., Subramani, T., Suresh, M., Karunanidhi, D. and Ramasamy, R., 2015. Mapping of groundwater potential zones in Salem Chalk Hills, Tamil Nadu, India, using remote sensing and GIS techniques. *Environmental Monitoring and Assessment*, 10, p.65. https://doi.org/10.1007/s10661-015-4376-y.

Thivya, C., Chidambaram, S., Thilagavathi, R., Venkatraman, G., Ganesh, N., Panda, B., Prasanna, M.V. and Kumar, V., 2018. Short-term periodic observation of the relationship of climate variables to groundwater quality along the KT boundary. *Journal of Climate Change*, 4, pp.77–86.

US Salinity Laboratory Staff, 1954. *Diagnosis and Improvements of Saline and Alkali Soils*. US Department of Agriculture Handbook, p.160

Wagh, V., Panaskar, D., Aamalawar, M. and Patil, V., 2018. Hydro-chemical characterization and groundwater suitability for drinking and irrigation uses in the semiarid region of Nashik, Maharashtra, India. *Hydrospatial Analysis*, 2, pp.43–60.

Wang, L., Mei, Y., Yu, K. and Zhang, W., 2019. Anthropogenic effects on hydrogeochemical characterization of the shallow groundwater in an arid irrigated plain in northwestern China. *Water*. 9, p.471. https://doi.org/10.3390/w11112247.

Wen, X.H., Wu, Y.Q., Wu, J. and Yang, X., 2008. Hydrochemical characteristics of groundwater in the Zhangye Basin, Northwestern China. *Environmental Geology*, 55, pp.1713–1724.

WHO, 2017. *Guidelines for Drinking Water Quality, Volume 1: Incorporating the First and Second Addenda, Recommendations*. WHO

Wu, J., Li, P. and Qian, H., 2015. Hydrochemical characterization of drinking groundwater with special reference to fluoride in an arid area of China and the control of aquifer leakage on its concentrations. *Environmental Earth Sciences*, 73, pp.8575–8588.

Xu, Y., Dai, S., Meng, K., Wang, Y., Ren, W., Zhao, L., Christie, P., Teng, Y. and Liu, H., 2018. Occurrence and risk assessment of potentially toxic elements and typical organic pollutants in contaminated rural soils. *Science of the Total Environment*, 630, pp.618–629.

Zhang, Y., Wu, J., Xu, B. and Li, S., 2018. Human health risk assessment of groundwater nitrogen pollution in Jinghui canal irrigation area of the Loess Plateau, northwest China. *Environmental Earth Sciences*, 77, pp. 273–283.

A Review on Biosurfactants with their Broad Spectrum Applications in Various Fields

Nazim Uddin[1] , Jyoti Sarwan[1], Sunny Dhiman[1], Kshitij[1], Komal Mittal[1], Vijaya Sood[1], Md. Abu Bakar Siddique[2] and Jagadeesh Chandra Bose K.[1†]

[1]University Institute of Biotechnology (UIBT), Chandigarh University, Ludhiana Highway, Mohali, 140413, Punjab, India
[2]Nilphamari Government College, Ministry of Education, Bangladesh
†Corresponding author: Jagadeesh Chandra Bose K; jcboseuibltlab@gmail.com

ABSTRACT

Because of the superior qualities of biosurfactants over their equivalents derived from fossil fuels, they have recently attracted more attention. Although production costs are still a major barrier to biosurfactants' superiority over synthetic surfactants, biosurfactants are expected to grow in market share over the next several decades. Glycolipids, a class of low-molecular-weight biosurfactants, are particularly sought-after for a variety of surfactant-related applications due to their effective reduction of surface and interfacial tension. Rhamnolipids, trehalose lipids, sophorolipids, and mannosyl erythritol lipids are the primary types of glycolipids. Glycolipids are made of hydrophilic carbohydrate moieties joined to hydrophobic fatty acid chains by ester bonds. This review addresses the unique glycolipid production and the wide range of goods available in the global market, as well as the present state of the glycolipid industry. Applications include food processing, petroleum refining, biomedical usage, bioremediation, and boosting agricultural productivity. With biosurfactants, their beneficial Ness in releasing oil encased in rock, a need for enhanced oil recovery (EOR). Another crucial biotechnological component in anti-corrosion procedures is biosurfactants, which stop Crude oil transportation in pipelines and are made easier by incrustations and the growth of biofilms on metallic surfaces. They are also employed in the production of emulsifiers and demulsifies and have other cutting-edge uses in the oil sector. Natural surfactants can be used to lessen pollution produced by chemical solvents or synthetic detergents without compromising the oil industry's financial gains. Consequently, it is imperative to invest in biotechnological processes. It is anticipated that natural surfactants will take over the global market in the not-too-distant future and prove to be economically feasible. It is likely possible to substitute synthetic surfactants used in agricultural product composition with biosurfactants. Because biosurfactants can benefit crops without harming the environment, they hold great potential as a useful tool in the fight against pesticide use. Furthermore, by making hazardous and leftover pesticides more soluble and thus accessible for biodegradation by other microbes, their potential as bioremediation agents can help to improve the health of soil systems. This article is based on the explanation of various applications of Biosurfactants.

INTRODUCTION

Sophorolipids are a type of biosurfactant widely used and produced exclusively by microorganisms such as fungi, bacteria, and yeasts. These biosurfactants usually have low molecular weight. Due to their eco-friendly properties, these Sophorolipids are widely accepted in the world market. Compared to chemical surfactants, biosurfactants offer several benefits. For example, biosurfactants are more environmentally friendly than synthetic surfactants because they are readily broken down by microbes in the environment. They are safer to use in a variety of applications since they are often non-toxic to people, animals, and the environment. In comparison to water alone, biosurfactants can penetrate and remove dirt and other impurities more efficiently by lowering the surface tension

of liquids. Biosurfactants are also helpful in a variety of commercial processes, including the manufacturing of food, cosmetics, and pharmaceuticals, because they can create stable emulsions of immiscible liquids. The discovery of certain biosurfactants' antibacterial qualities makes them valuable for the creation of novel antibiotics and other antimicrobial agents (Tajabadi 2023, Bose & Sarwan 2023). When sophorolipids (SLs) made by the yeast *Starmerella bombicola* started to be sold, BS entered the market around 20 years ago, but they currently only account for a minor portion of the surfactant market. Innovation in all facets of BS research is crucial to boost the commercialization of BS. This includes discovering new compounds, creating genetically modified ones, characterizing novel microorganisms that produce BS, and enhancing scale-up and downstream BS production processes. Here, a few current instances of these reports will be shown (Seattle 2023). Surface-active compounds with biological origin, known as biosurfactants, are produced as secondary metabolites by filamentous fungi, bacteria, yeast, or plants. Their biological origin and lack of an additional chemical synthesis step during manufacture set them apart from conventional surfactants. When biosurfactants are in their natural condition, they are usually either neutral or anionic.

On the other hand, substances having amine groups are categorized as cationic. The microbiological source from which biosurfactants are formed, the substrates used for their production, and the particular growth conditions utilized can all be linked to the variations in their structures. Significant studies have been conducted on biosurfactants, such as surfactin, rhamnolipids, sophorolipids, and mannosyl-erythritol lipids (MELs) (Karnwal et al. 2023, Sharma et al. 2023). Among other things, they are used as detergents, foaming agents, wetting agents, emulsifiers, demulsifiers, spreading agents, and functional food ingredients. In the foodservice sector, BSs are used as antiadhesives, emulsion stabilizers, and antimicrobial/antibiofilm agents. Because of their possible benefits for the environment, there is a discernible increase in interest in the use of microbial emulsifying agents (Adetunji 2022).

STRUCTURE OF SOPHOROLIPIDS

SLP are amphiphilic molecules, that are composed of a hydrophilic moiety a (head) sophorose disaccharide (2'-O-β-D-glucopyranosyl-β-D-glucopyranose), linked to the hydrophobic moiety (tail), a long chain of fatty acid, (Fig. 02) and partially acetylated, linked by a β-glycosidic bond to 17-L-hydroxy octadecanoic and 17-L-hydroxy-9-octadecanoic acid. These are produced as a combination of structurally allied molecules, reaching up to 40 patterns,

and associated with isomers. The highest number of various structures originate from different possible combinations of (a) the β-glycosidic bond links the anomeric carbon of the head sophorose (C1') to the ω-carbon (terminal/border) or ω-1 hydroxylated (sub-terminal) from the fatty acid (b) acetylation of the hydroxyl groups of the sugar moiety; sophorose C6' and C6'' carbons can be deacetylated, mono-acetylated or diacetylated; (c) the appearance of acidic or lactonic forms; the *lactonic* form - carboxyl group of the fatty acid (tail) moiety is esterified to the sophorose in C4'', C6' or C6'' (esterification in C4'' is more frequent), acidic form – the carboxyl group of the fatty acid moiety is not esterified ; (d) the fatty acid chain might vary in size (mostly between C16 and C18), with the appearance of unsaturation (saturated, monounsaturated or polyunsaturated) -presence of stereo-isomers and sophorolipids can also consisted in the polymeric as dimeric or trimeric form Biosurfactants are produced from various sources as non-pathogenic microbial strains and they are classified based on their source (Fig. 1) with several oils as substrates and fatty acids sources, sugars, yeast extract used as carbon source, peptone, urea, and ammonium compounds are used for nitrogen sources during the synthesized (fermentation) period (Hernández et al. 2023, Bose & Sarwan 2023, Sharma et al. 2023). Glycolipids, lipopeptides, phospholipids, fatty acids, neutral lipids, polymeric surfactants, polysaccharides, lipopolysaccharides, proteins, and lipoproteins are examples of biosurfactants with a range of chemical structures. These are created by microorganisms grown on soluble (carbohydrates) and insoluble (hydrocarbons, oils, and oily residues) substrates. Vegetable oils and leftover fry oil are examples of substrate combinations that can be utilized to increase the production of biosurfactants. Biosurfactants have molar masses that range from 500 to 1500 Da on average. While biosurfactants with a higher molar mass are more frequently utilized for the stabilization of oil-in-water emulsions, low molar mass biosurfactants are more successful at lowering the surface tension at the air-water interface and the interfacial tension at the oil-water interface. While glycolipids, phospholipids, and lipopeptides have low molar masses and are traditionally referred to as biosurfactants, proteins, lipoproteins, polysaccharides, and lipopolysaccharides have high molar masses and are frequently referred to as emulsifiers (Augusto et al. 2023, Hernández et al. 2023, Seattle 2023).

Fig. 2. shows the molecular structure of biosurfactants and biosurfactants sophorolipids, and the molecular structure of lactonic and acidic forms of microbial-derived biosurfactants sophorolipids; the hexagonal-shaped part is the hydrophilic carbohydrate head sophorose, the hydrophobic part is the acid tail, where R = fatty acids.
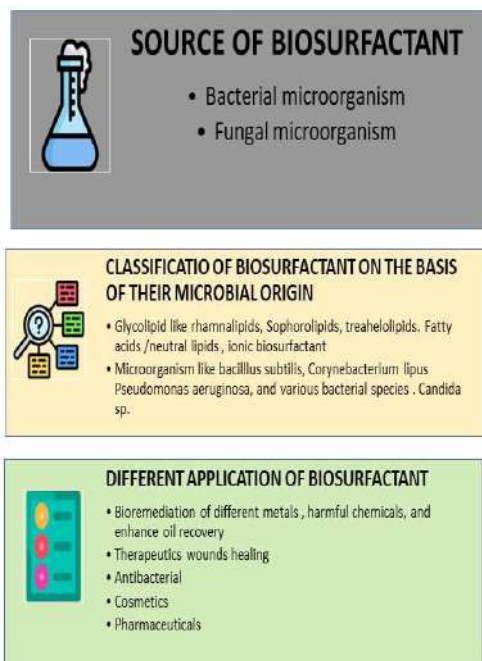
Fig. 1: Represent that the various biosurfactants originated from microorganisms.

Hydrophilic Moiety or
Hydrophilic (Carbohydrates) Head Sophorose.

Hydrophobic Moiety or Fatty Acid Tail.

A. Basic structure of Biosurfactants Sophorolipis.

B. Lactonic Sophorolipid.

SL1: R1=R2=Ac
SL2: R1=H; R2=Ac
SL3: R1=Ac; R2=H
SL4: R1=R2 = Ac

C. Acidic Sophorolipids.

SL5: R1=R2=Ac
SL6: R1=H; R2=Ac
SL7: R1=Ac; R2=H
SL8: R1= R2 = Ac
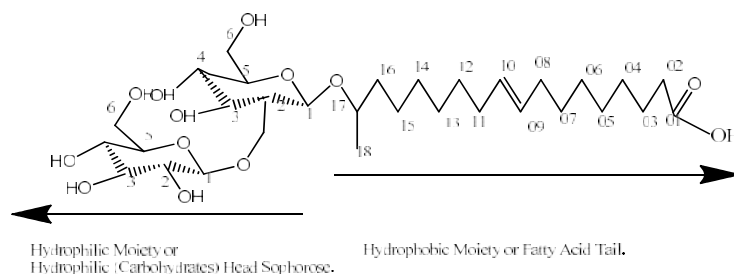
Figure; A. Basic Structure of Sophorolipids, B. Lactonic Sophorolipids, C. Acidic Sophorolipids
Whereas SL is Sophorolipids, and R1..............Rn are Fatty acids.

Fig. 2: Glycolipids biosurfactants (Sophorolipids).

APPLICATIONS OF BIOSURFACTANTS

This section explores some of the key applications of sophorolipids (Fig. 3).

Antimicrobial Applications of Sophorolipids

Organic active compounds sophorolipids with their applications in the healthcare field: Sophorolipids biosurfactant is a bioactive compound capable of building active resistance against a variety of toxic activities such as carcinogenic agents. Due to their adaptable qualities, biosurfactants have garnered a lot of interest in recent decades from a variety of industries, including the environm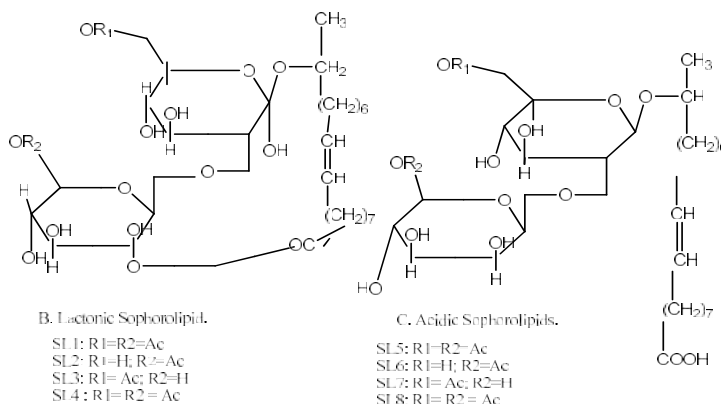ental, oil, agriculture, textile, food, cosmetics, pharmaceutical, and medical (Karnwal et al. 2023). biosurfactants' biocidal and dispersion qualities are used in industrial water systems as anti-biofilm agents, as well as anti-fouling and anti-corrosion agents (Hausmann et al. 2024, McMahan et al. 2021).

Anti-microbial applications of sophorolipids: The growing prevalence of multi-resistant infections and the diminishing efficacy of traditional antimicrobials underscore the pressing need for new strategies. A broad spectrum of pathogenic microorganisms, including Gram-positive and Gram-negative bacteria and fungi, can be successfully inhibited by biosurfactants in their growth. Biosurfactants are a useful tool for developing environmentally conscious and sustainable approaches to combating microbial infections because, unlike synthetic drugs, they can offer unique antimicrobial mechanisms of action such as reducing cell surface hydrophobicity, disrupting membrane integrity, increasing its permeability, altering protein conformation and inhibiting membrane functions (transport and energy generation), or blocking the quorum-sensing system and down-regulating gene expression. Microorganisms find it difficult to overcome and develop resistance to these actions. It is also difficult for microorganisms to overcome and develop resistance to biosurfactants, which makes them a
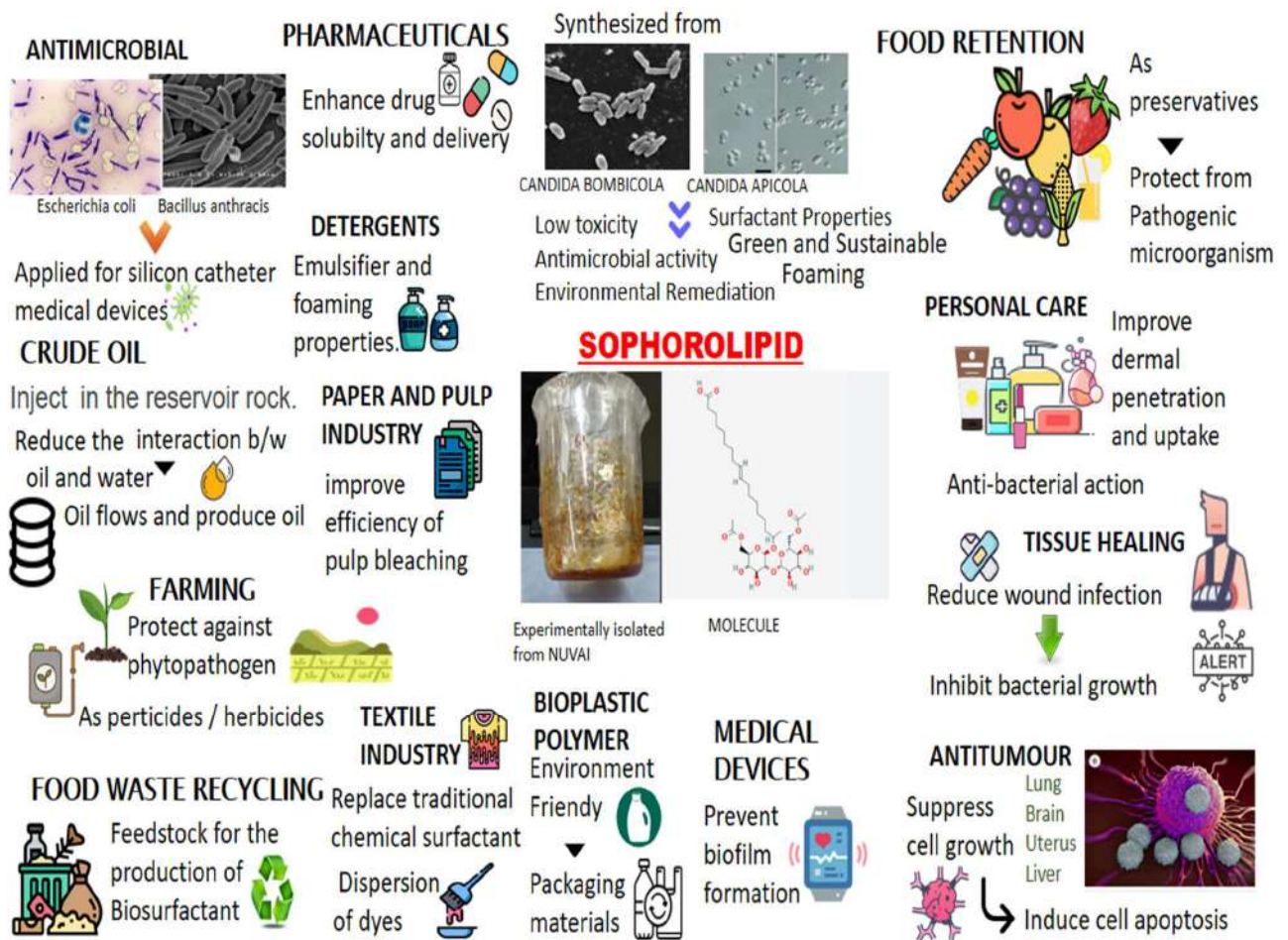

Fig. 3: Applications of biosurfactants sophorolipids in various fields.

Table 1: Different microorganisms and their impacts on the environment and living beings.

Microorganism	Strains	Harmful effects	Activity of SLP on Microorganisms	Ref
Bacteria (+ve)	Bacillus subtilis. Staphylococcus aureus.	food contamination, skin infections, food-poisoning,	Bacteria cells rupture & disengage when treated with SLPiLA	(McMahan et al. 2021)
Bacteria (-ve)	Escherichia coli. Pseudomonas aeruginosa.	Infections of the urinary tract, neonatal meningitis, gastroenteritis, and cross infections in hospitals and clinics.	The bacterial cell wall is severance or contraction or intercept when treated by SLPLA.	(McMahan et al. 2021)
Fungi	Food spoiled, various pathogenic fungi, like *Candida* sp., *Fusarium* p.	Harmful to foods and creates different types of fungal diseases inside and outside of man, plants, and animals.	SLP- creates inhibition against spore germination and growth of mycelial of different fungal species.	(McMahan et al. 2021)
Algae	Creates water impurities, the dead zone in water, harmful to agriculture	The algal bloom changes water color and creates a barrier to entering the sunlight in water. Bloom releases toxins, which cause plants and animals to die.	The SLP has shown cell lysis and different inhibition against various algal species.	(Sun et al. 2004)
Actinomycetes	Dermatophillus congolensis. *Plasmobispora* and *Dactylosporangium*.	These strains are opportunistic. They are caused by dermatophilosis, actiomycosis, and other diseases in the mouth, lungs, and GIT in humans and wild and domestic animals.	The mode of action of SLP on actinomycetes as Cell lysis, cell disruption	(Sun et al. 2004)

valuable tool for developing environmentally conscious and sustainable approaches to combating microbial infections. Moreover, unlike synthetic drugs, these molecules can offer unique antimicrobial mechanisms of action, such as reducing cell surface hydrophobicity, disrupting membrane integrity, increasing its permeability, altering protein conformation and inhibiting membrane functions (transport and energy generation), or blocking the quorum-sensing system and down-regulating gene expression. A multitude of microorganisms that have adapted to survive in harsh environments can be found in the vast and diverse marine ecosystem. These microorganisms may provide a rich source of unique bioactive compounds, some of which, like novel biosurfactants with strong antibacterial and antifungal properties, can effectively fight microbial infections.

Furthermore, using the biosurfactants that marine microorganisms make helps to preserve and investigate marine biodiversity, in addition to providing opportunities for the development of sustainable alternative antimicrobial agents (Ceresa et al. 2023). Surface tension cannot be further reduced by increasing surfactant concentration over a particular point, also referred to as the critical micellar concentration (CMC). Over the CMC, through a process known as micellization, surfactant molecules cluster in the bulk phase to form micelles that can have a variety of geometries, including spherical, cylindrical, discoidal, or even more complicated forms. The rheological and dynamic characteristics of the surfactant solution are influenced by the micelle form. In certain applications, the existence of micelles is essential to the surfactant's ability to operate;

for instance, a study on a household cleaning solution found that foam production increased at concentrations higher than the CMC (Rossini et al. 2024, Karnwal et al. 2023). Table 1 shows the antimicrobial activity of biosurfactants against pathogens.

Except for the exhibition of the anti-bacterial properties, these SLs showed antifungal activities and antibiofilm (Table 2) that are produced by bacterial and fungal strains.

B. Anti-cancerous applications of biosurfactants. Based on the results obtained through more than 1000 nonpathogenic yeast genome sequencing to date, it is certain that the glycolipid (sophorolipids), synthesized from the non-pathogenic yeast *Candida sp. Wickerhamiella Comercial* Y2A species belonging to the class of Saccharomycetales, trychomonascaceae, showed the highest cytotoxicity on various cancer cell lines. These types of cell lines include esophageal cancer cell lines such as KYSE, KYSE-30, KYSE-109, KYSE-150, and KYSE-450. Breast cancer cell line alcohol MDA-MB 231 or BCCL MDA-MB 231, Mouse Skin Cell Line B 16F 10, Lung Cancer Cell Line A 549, etc. A variety of glycolipid biosurfactants, such as lactonic-acidic sophorolipids, glucolipids, and bolalipids, are capable of building the immune system against cancer cells. Treatment with a lactonic sophorolipids-glucolipid combination has shown the highest levels of anticancer activity. This subject has been observed very closely through scratch assay and fluorescence microscopy. Glycolipid surfactants interfere with actin filaments. As a result, the tumor cell's displacement is hampered

Table 2: Biosurfactant sophorolipids producing nonpathogenic yeast and fungal strains, produced SLs, and usage of different concentrations against various pathogenic microorganisms.

Sources of Sophorolipids	Sophorolipids and their structures.	The lethal dosage of sophorolipids and their mode of action on	References
Cryptococcus sp.	Acidic and acetylated	5 mg.mL^{-1} has shown antimicrobial activity and inhibits cell growth against bacteria, and fungal strains like (*S. enterica, and C. albicans*), stabilizers for the production of functionalized NPs.	(Basak et al. 2014)
Candida sp.	Acidic (C$_{18:1}$ NASL) Sophorolipids.	5 to 20 mg.mL^{-1} showed the highest antimicrobial activity against GBP, GNB *S. aureus, P. aeruginosa, and E faecalis*. Adjuvant activity with antibiotics and wound healing of skin	(Lydon et al. 2021)
Candida tropicalis RA1	Lactonic types sophorolipids	At 250 mg.mL^{-1}, the SLs have shown antibacterial against the cell growth of GPB higher than GNB.	(Ankulkar et al. 2022)
Candida sp.	AcSLs, L-SLs	These SLs have shown the MIC 100 µg.mL^{-1} against GPB_GNB (*S. aureus, E. coli*) and adhesion to the abiotic surface of bacteria and inhibition of their biofilm.	(Youssef et al. 2004)
Starmerella / Candida Bombicola	Acidic and lactonic SLs	It shows anti-biofilm activity at 43.7% at the concentration of 50 µg.mL^{-1} SLs against (*P. aeruginosa*) and other bacterial strains	(Gudiña et al. 2010)
	Acidic and lactonic SLs	The MIC of these SLs at the conc. 19.5 µg.mL^{-1} Against the mutual environment of GPB-GNB, and used as surface cleaner and microbial control agents in industries.	(Youssef et al. 2004)
	Acidic: lactonic ratio is 3.8:6.2)	At the conc, 0.1 wt%, it has shown better bacterial anti-biofilm activity against GPB bacterial strains.	(Sun et al. 2004)
	Acidic and lactonic SLs.	At 50 µg.mL^{-1} con. SLs have shown anti-bacterial and anti-biofilm activity and are safely used for silicon catheter medical devices as an antiseptic and biological control agent.	(Soberón-chávez et al. 2010)
	Acidic and lactonic	MIC >5% v/v of these SLs induces cell death of GPB-GNB class planktonic cells.	(Rossini et al. 2024)
	L-SLs	It has shown inhibitory activity at 1 mg.mL^{-1} and 1.3 mg.mL^{-1} conc. Against various oral cariogenic gram (+) bacteria like *L. fermentum and L. acidophilus*.	(Batista et al. 2006)
	L-SLs.	The MIC and MBC of it are at 97.5 mg.mL^{-1}, and 195 mg.mL^{-1} conc. To the oral bacterial (*S. oralis*) strain.	(Muthusamy et al. 2008)
Rhodotorula babjevae	Lc-SLs.	1 mg.mL^{-1} of Sls has shown the MIC 75% on the growth of inhibition of dermatomycosis caused by *T. mentagrophytes* on the witty skin and feet, which are covered by Sox and cloth	(Vijayakumar & Saravanan 2015)
Candida sp.	Ac, -Lc-SLs.	0.1% of these SLs have shown antifungal activity against *T. mentagrophytes*, and it prevents skin and athletes' foot dermatophytosis.	(McMahan et al. 2021)
Starmerella bombicola	Ac, - Lc-SLs.	200 µg.mL^{-1} of SLs has shown antifungal and antibiofilm activity as well as oral, skin, and vaginal candidiasis by *C. albicans*.	(McMahan et al. 2021)
	Ac, - Lc-SLs.	50 µg.mL^{-1} of it has shown inhibitory and preventive activities against various fungal and fungal infections.	(Heyd et al. 2008)

Elshikh et al. 2017

and inhibits migration, resulting in a change in the mitochondrial membrane potential centered around the SLP biosurfactant and its reactive oxygen species, leading to cell necrosis. Hence, cell death or apoptosis occurs. This means that in addition to two specific types of glycolipid surfactants, the combination of two differently formed glycolipids, such as acidic glycolipid or lactonic glycolipid or acidic-lactonic sophorolipids + glucolipid, acts as a potent anti-cancerous prescript. That is, the combination of two sophorolipids from a single sophorolipid is comparatively more effective. For example, the application of such combinations has shown synergistic interactions on the A549 cell line, as well as influencing the connection between the MDA-MB 231 and B16F10 cell lines. Similarly, fluorometric assay analysis shows that the combination application of G-500 ug.mL^{-1} and L-SLP-50 ug.mL^{-1} results in the application after 3 h of observation that all reactive oxygen species are stimulated to produce. However, by increasing the active potential of this glycolipid surfactant, it will be able to demonstrate its ability to produce 100% cell ROS of different cancer cell lines among the sophorolipids synthesized from the *Wickerhamiella* sp. Commercial species, Diacetylated

lactonic sophorolipids human esophageal cancer cell line exhibits severe cytotoxic activity on both KYSE 109 and KYSE 450. That is, as much as monoacetylated lactonic SLP can obstruct in front of these two cell lines, Diacetylated lactonic SLP can create several times more obstruction. The ability of Di-unsaturated SLP in saturated hydroxyl fatty acid-rich sophorolipids to perform inhibition activity across cancer cell lines is much lower than that of monosaturated SLP. Cerasa et al. (2024) examined the mechanism of action of glycolipids, namely glucolipids, bolalipids, and acidic and lactonic sophorolipids, against cancer cells in a recent study. Three distinct cell lines were used in the experiments: A549, which is used for lung cancer, and MDA-MB 231 for breast cancer. And B16F10, which is used for mouse skin melanoma. The findings imply that glucolipids prevent the migration of tumor cells, potentially by interfering with actin filaments, and that reactive oxygen species are produced in cells by both glucolipids and lactonic sophorolipids. Furthermore, these biosurfactants changed the potential of the mitochondrial membrane, which ultimately led to necrosis and cell death. Moreover, pancreatic, breast, cervical, oral, colon, lung, and liver cancers are among the many tumors for which biosurfactants have lately become viable substitute compounds. Their capacity to control certain processes in mammalian cells, which stops the aberrant progression of cancer by inhibiting cell viability, proliferation, and migration, has shown promise for the treatment of cancer. Certain biosurfactants, such as glycolipids and lipopeptides, can decrease tumor cell proliferation and survival. (Ceresa et al. 2023)

C. **Anti-viral application of biosurfactants:** Females that are usually diagnosed with HIV need a female genitalia organ septic microbicidal activating agent for specific protection of their genitals. Sophorolipids synthesized from *Candida bombicola* may be the only promising microbicidal API to carry through the requirements. Individual experiments on the activity of structural analogs of synthesized sophorolipids, synthesized by *C. bombicola*, led to the conclusion that SLP has cytotoxicity activity as well as anti-HIV activity and exceptional spermicidal activity. Structural analysis of the series of derivatives of SLP shows that among the derivatives of SLP, Diacetate Ethyl ester SLP has virucidal and knock-down spermicide activity. Due to the antiviral activity of SLP derivatives, the outer protein lining of HIV-carrying sperm inside HIV is eroded due to the antiviral activity of SLP derivatives The derivative shows a lower application and shorter activity in less

time than the contraceptive pill surfactant Nonoxynol'-9 (N-9) used in the vaginal cavity and rectum region. The sperm in the vaginal cavity and rectum region acts as an inactivating agent (Nagtode et al. 2023). Applying a mixture of Lactonic SLP and Natural SLP in a ratio of 1.0: 0.80 mg.mL^{-1} and observing the sperm by Sander Cromer Assay system, it is seen that 50% of the sperm in just 120 seconds / 2 min. Synthesized Sophorolipids by pure species of non-pathogenic isolated yet also has antibacterial and antifungal activity. Due to the antifungal activity of SLP when applied as an Associate API with APIs used for the treatment of dermatitis, it multiplies the antifungal activity of the particular medicine. When SLP clotrimazole is applied to a certain dose of vaginal candidiasis treatment, the candidiasis patient recovers very quickly. Ethyl 17-L-[(2'-O-β-D-glucopyranosyl-β-D-glucopyranosyl)-oxy]-cis-9-octadecenoate. The pH of seminal fluid is treated with PH <5.0, SLP, which brings down the pH level of the fluid and produces anti-microbial activity against pre-post sexually transmitted pathogens in the female genitalia (Youssef et al. 2004). Analysis of the structural analog of acidic SLPs shows more anti-toxicity was expressed on HIV as a spermicide, but it cannot express the amount. Tests on the structural analogs of lactonic SLps again showed that L-SLps reveal higher virucidal activity (Aparna et al. 2012). Double-strand DNA viruses, such as the herpes simplex virus HSV-1 and HSV-2, infect people of almost ever age group, from infants to the elderly. More frequently acquired by HSV-1, faster than HSV-2. More HSV-2 is transmitted through sexual conjugation. Each year, about 23 million people worldwide are infected by the HSV-2 strain.

D. **Drug and drug delivery system and nanotechnology:** Surfactants are essential molecules in the creation of nanostructures because of their amphiphilic and self-assembly properties. They function as templates, modifiers, growth control agents, and stabilizers. The utilization of biological processes using plants, microorganisms, or their metabolites for the synthesis of nanomaterials is encouraged by the growing need for safe, environmentally friendly alternatives to dangerous chemicals (André et al. 2023). The literature has many papers on the microbial production of nanoparticles (NP). The enzymatic reduction of metal salts such as gold, iron, silver, platinum, and others is the usual process used to create metal nanoparticles (NPs). As a result, microbial metabolism offers an appropriate environment, either intracellularly or extracellularly, to support NP production. Silver NP was synthesized using a lipopeptide BS that was isolated from *Bacillus*

vallimortis, and it showed antibacterial efficacy against Listeria monocytogenes, S. aureus, and E. coli. A different paper explains how a lipopeptide obtained from a Bacillus subtilis CN2 strain is used to prepare stable silver nanoparticles (NP).

In comparison to the NP made without the BS, the addition of the BS decreased the average size, homogeneity, and long-term stability of the NP and produced exceptional antibacterial activity against strains of Bacillus subtilis and *Pseudomonas aeruginosa*. *It* also described how biogenic synthesis by bacteria that produce BS is another method. In this instance, microbial growth is carried out, and after the addition of a metal precursor, the resultant cell-free medium is used as a starting material for NP synthesis. (Ceresa et al. 2023) In comparison to the NP made without the BS, the addition of the BS decreased the average size, homogeneity, and long-term stability of the NP and produced exceptional antibacterial activity against strains of Bacillus subtilis and *Pseudomonas aeruginosa*. It also described how biogenic synthesis by bacteria that produce BS is another method. In this instance, microbial growth is carried out, and after the addition of a metal precursor, the resultant cell-free medium is used as a starting material for NP synthesis. Although there isn't much research on the use of BS in the synthesis of natural organic NP, this method is thought to be more environmentally beneficial since it uses less metal and petrochemicals, both of which can build up in the environment. Recently reported the synthesis of a hybrid biopolymer-biosurfactant NP, which demonstrated that the addition of rhamnolipid increased the antibacterial activity against both planktonic and biofilm S. aureus and decreased the size and polydispersity of chitosan NP. The authors postulated that the hybrid NP's high density of polycationic chitosan enhances electrostatic interactions, promoting the release of RL at the bacterial surface and assisting in the breakdown of the cell membrane, which allows antimicrobials to reach their targets (Rossini et al. 2024, Shakeri et al. 2021, Hernández et al. 2023, Nouri et al. 2023) It was stated that bioactive peptide-loaded rhamnolipid liposomes might be used to create innovative antibacterial systems for use in agriculture and medicine. Nisin was incorporated into rhamnolipid-functionalized liposomes (rhamnosomes) to enhance the antibacterial and antibiofilm properties of the liposomes as well as the effectiveness of nisin. The resultant nanovesicles outperformed liposomes in terms of antibacterial activity, and they also increased nisin's ability to combat L. monocytogenes, S. aureus, E. coli, and P. aeruginosa. Because of its better adherence to the bacterial surface, there was an observed 80% reduction in biofilm biomass.

E. **Application of SLP to enhance immune activity**: Recent studies have also highlighted the potential benefits of biosurfactants for enhancing human health and well-being in the context of wound healing, where they have demonstrated the ability to speed up the healing process and encourage tissue regeneration. Moreover, their antibacterial characteristics provide them with appealing options for battling wound infections. Furthermore, biosurfactants have demonstrated anticancer properties by causing cancer cells to undergo apoptosis and by preventing the formation of tumors. Even with great advancements in cancer treatment, cancer continues to be the second greatest cause of death globally. In particular, the World Health Organization (WHO) released data for 2020 that projected 10 million fatalities and 19.3 million new cases. Over the years, numerous innovative cancer treatments have been created to tackle this deadly disease; nonetheless, chemotherapy and radiotherapy continue to be the primary options.

Notwithstanding several beneficial elements of these treatments, the rising death rates can be linked to anticancer medication's lack of specificity for cancer cells, which causes serious side effects, poor success rates, and the emergence of multidrug resistance in cancer cells. Moreover, they exhibit immuno-modulatory characteristics, which renders them prospective contenders for immunotherapy and immunomodulation tactics (Rossini et al. 2024, Shakeri et al. 2021, Ceresa et al. 2023). Because of its therapeutic qualities, the impact of biosurfactants on wound healing has been studied for more than 15 years. Cheffi et al. (2021) evaluation mentioned the impact of the lipopeptide molecule Bios-PHKT on HEK-293 cells and demonstrated that the migration and proliferation of cells driven by Bios-PHKT could be compared to the controls. It's interesting to note that lower Bios-PHKT concentrations were needed to promote wound healing than to cause cytotoxicity in HEK-293 cells. Regarding their ability to form emulsions, their antitumor and antibacterial qualities, and their impact on the immune system, lipopeptides are among the biosurfactants that have been investigated the most. Using an excision wound model, found that a lipopeptide produced by A. junii B6 can shield mouse cells from damage caused by free radicals, with signs of cell recovery (Ceresa et al. 2023)

Table 3 mentions some of the biosurfactants producing microorganisms to enhance immuno-modulatory activity in humans and animals. In the immune system, biosurfactants follow the path of immune-suppressive drugs, and these can increase wound healing in different inflammations.

Application of sophorolipids for bioremediation: Hydrophobic contaminants from the oil and gas sector can build up in soil. Soil contamination can result from

Table 3: Acidic, Lactonic, acetylated, acidic, and lactonic Sophorolipids mobilized by microorganisms that keep a vital role in the immune system.

Sources of Sophorolipids.	Sophorolipids and their structures.	The sophorolipids and their therapeutic action in the immuno-modulatory system.	References.
Candida, W. Comercial, and various fungi and bacteria.	C18:1DiAL, lactonic, and acidic SLs.	These types of Sophorolipids have shown anti-cancerous activity they showed inhibitory activity against various cancer cell lines at different concentrations.	(McMahan et al. 2021)
Some bacteria and fungi	DiAL, -SLs.	In the immune system, the SLs work as immuno-suppressive drugs; using 25 µg.mL^{-1} of SLs showed the M1 macrophage polarization as an envelope to enhance the execution of typical wound rehabilitation and various inflammations.	(Vijayakumar & Saravanan 2015)

various sources, including storage tank leaks, pipeline leaks, and spills caused by mishaps that occur during the discovery, refining, and transportation of oil. In addition to being hazardous, these contaminants are also recalcitrant and insoluble. Soil remediation techniques include mechanical, chemical, biological, and physical approaches. The biological approach makes use of low-tech materials and renewable resources, such as plants, microbes, and surfactants. Surfactants facilitate the desorption of pollutants from soil particles and promote their mineralization and microbial degradation by reducing the surface and interfacial tensions of the pollutants. Biosurfactants can help in the process of phytoremediation, which is the absorption of toxins by plants to remove contaminants from the environment. Many aspects must be taken into account to effectively use biosurfactants in the bioremediation of petroleum hydrocarbons, particularly in soil systems. Greater efficiency is achieved when low quantities of biosurfactants are administered during the early phases of biodegradation, particularly when the hydrocarbon content is high. High quantities of biosurfactants, on the other hand, cause the bacteria to absorb the biomolecules rather than the pollutant to biodegrade. The oil degradation rate was improved by 10 to 20% by the biosurfactants generated by Bacillus sp. and C. sphaerica UCP0995, showing an improvement in the biodegradation of hydrocarbons in soil. Researchers looked into how well the biosurfactant alasan broke down polyaromatic hydrocarbons in soil. In the presence of the surfactant, it was discovered that fluoranthene was more than 50% and that *Sphingomonas paucimobilis* EPA505

significantly increased the mineralization of phenanthrene. The biosurfactant generated by P. cepacia CCT6659, which was grown in industrial waste, showed promise for use in soil bioremediation. 95% of the contaminants in soil contaminated by hydrophobic organic compounds were degraded in 35 to 60 days by an Indigenous consortia and biosurfactant (Augusto et al. 2023, Fernandes & Dias, 2023, Miao et al. 2024, Rossini et al. 2024)

The following table (Table 4) presents the biodegradation potential of various types of hydrocarbons. Biosurfactant sophorolipids showed their highest biodegradation activity than chemical surfactants by their same concentration on different hydrocarbons.

Oil recovery: Water, gas, and the organic components, together with the proper thermochemical conditions present in sedimentary rock, make up crude oil. There are three processes in the extraction of crude oil. Natural pressure and produced pressure (injection of gas and water) are the first and second processes. Roughly 40% of the trapped oil is extracted by these procedures. Recovering the leftover oil is the third stage. Although it is challenging to remove this oil from rock, enhanced oil recovery, or EOR, uses thermal methods (injection of hot water and carbon dioxide (CO_2), non-thermal methods (flooding with solvents and chemical surfactants), and biological approaches. In this procedure, synthetic surfactants pollute the environment and demand capital. On the other hand, the application of biosurfactants in EOR can create advantageous circumstances and address issues related to environmental contamination. The

Table 4: Biodegradation rates of various hydrocarbon compounds by sophorolipids.

S. No.	Model Compound	Time	SLP	Activity	Reference
1.	Pristan	6 days	10g.L^{-1} -2 ml	85%	(Shekhar et al. 2015)
2.	2-Methylnaphthalene	2 days	10g.L^{-1} -2 ml	95%	(Shekhar et al. 2015)
3.	Hexadecane	6 days	10g.L^{-1} -2 ml	97%	(Priya & Usharani 2009)
4.	Crude oil	56 days	10g.L^{-1} -2 ml	80%	(Priya & Usharani 2009)
5.	Saturates	56 days	10g.L^{-1} -2 ml	80%	(Priya & Usharani 2009)
6.	Phenanthrene	4 days	10g.L^{-1} -2 ml	71%	(Jimoh & Lin 2019)
7.	Aromatics.	56 days	10g.L^{-1} -2 ml	72%	(Jimoh & Lin 2019)

process known as "Microbial Enhanced Oil Recovery" (MEOR) uses microorganisms or the byproducts of their metabolism to extract leftover oil. Typically, this process entails injecting nutrients into the reservoir first, then injecting microorganisms that make biosurfactants (in situ biosurfactant production). Industrial bioreactors can also be used to produce ex-situ biosurfactants, which can then be directly injected into the reservoir using CO_2 (Augusto et al. 2023). According to one study, bacteria produce biosurfactants and can degrade crude oil extracted from an Assamese oil field's reservoir. B. Tequilensis demonstrated optimal biosurfactant synthesis and good oil degradation characteristics. Ex-situ. After obtaining an interfacial tension of 0.32 mN.m^{-1} and eliminating 80% of the oil during washing operations, the crude biosurfactant was determined to be a surfactin.

The microbes' emulsifiers/surfactants cause the surface tension to drop, which releases the contained oil. Biosurfactants change the interfacial behavior of CO_2-brine-rock and the wettability of injected CO_2, improving the flushing efficiency of the injected fluid and CO_2 (Augusto et al. 2023, Hausmann et al. 2024, Miao et al. 2024, Eras-muñoz et al. 2022, Shaikhah et al. 2024, Andreolli et al. 2023, Nagtode et al. 2023, André et al. 2023, Sarwan et al. 2024a, 2024b,)

A list of biosurfactants sophorolipids produced by microorganisms for enhancing oil recovery/bioremediation is listed in Table 5 below. Feedstocks used in the production of biosurfactants and their bioconversion mechanisms in the environment are summarized.

Agricultural application of sophorolipids: It has been shown that biosurfactants can be used to remediate contaminated soil. Achromobacter sp. TMB1 was isolated by Lin (1996) from soils surrounding nearby gas pumps. This bacterium produced ten distinct forms of mono- and dirhamnolipid congeners, with fatty acid carbon lengths ranging from C8 to C12. Subsequent tests revealed that these biosurfactants were stable between 20°C and 100°C in temperature and between 2 and 12 in pH, retaining their structural integrity up to 550°C, suggesting their potential for use in bioremediation. *Gordonia alkanivorans* W33 was shown to be more effective in bioremediating petroleum-contaminated soil when sophorolipids and rhamnolipids were added. Significant breakdown of the petroleum in the soil was seen when the bacteria were combined with sophorolipids and rhamnolipids at a weight ratio of 9:10. With a 20,000 mg.kg^{-1} petroleum content, about 56.3% of the petroleum was broken down, with an average degradation rate of 250.2 mg.d^{-1} (Vandana & Singh 2018)). Sophorolipid and rhamnolipid combination is thought to boost the capacity to create microemulsions from a variety of hydrocarbons; this is supported by a study on the remediation of co-contaminated soil with phenanthrene (PHE) and cadmium (Cd) utilizing enhanced soil washing with biosurfactant. In

Table 5: Sophorolipids and their antimicrobial and oil recovery activity.

Microorganisms	SLs-Biosurfactants.	Density and productivity /Litr And feedstock	SLs, and their mechanisms, bioconversions activity on the environment.	References
Candida floricola	Ac-SLs.	3.5 g.L^{-1} by feed batch fermentation using splurge glycerol as feedstock.	In the future, the SLs will facilitate the broad-spectrum use fields for SLs.	(Nasser et al. 2024)
Starmerella bombicola	DiAc- Lc-LSL (C18:1).	1 g.L^{-1} SLs by solid-state fermentation Winterization oil cake as feedstock	It showed Emulsifying properties, and CMC: 40.1 mg.L^{-1}, it has been used in the displacement of crude oils.	(Aparna et al. 2012, McMahan et al. 2021)
	Ac, -Lc- SLs	41.6 g.L^{-1} by shake flask and 51.5 g.L^{-1} SLs by submerged fermentation, using sunflower oil refinery waste as feedstock.	It has shown emulsifier activity. It is used for various crude oil displacements as bioremediations.	(Sharma et al. 2023)
	Ac, -Lc- SLs.	15.25 g.L^{-1} by feed batch- resting cell methods- using jatropha oil as feedstock.	Its CMC value is 3: 9.5 mg.L^{-1}, so the SLs have been used as a replacement for the synthetic surfactant in detergents, and MIC90 4 value is 300 µg.mL^{-1}. It is used as an antibacterial against GPB.	(Hausmann et al. 2024)
	Lc- SLs.	115.2 g.L^{-1} by feed batch fermentation, using hydrolysate food wastage as feedstock for enhancing SLS production.	The SLS is used for the bioconversion of food and various environmental and industrial waste oils.	(Sun et al. 2004)
	Lc- SLs.	3.7 g.L^{-1} SLs produced by fed-batch fermentation processes using food waste	It is used for bioconversions of food waste and waste streams.	(Sharma et al. 2023)

Table 6: Agricultural applications of sophorolipids.

Sl. No.	Sources of Sophorolipids	Sophorolipids and their structures.	The lethal dosage of sophorolipids and their mode of action in cancer cell lines.	References
1.	*Candida bombicola*	Acidic and lactonic	1 mg.mL^{-1} destabilization, membrane permeability or cell lysis, and inhibition of phytopathogen. 5% v/v of it is capable of disrupting of biofilm of comingle of Staphylococcus aureus ATCC 9144 and Bacillus subtilis BBK006	(Miao et al. 2024)
2.	*Candida kuoi*	Acidic SLs	For the emulsification properties, 1% v/v of SLP has shown phytotoxicity and herbicidal activity against sicklepod and *Senna obtusifolia*	(Miao et al. 2024)
3.	*Stermerella bombicola*	Lactonic SLs	It has shown antimicrobial activity against *Pythium ultimum* and *Moesziomyces sp*. as pesticides and fungicides at 2 mg.mL^{-1} and 1 mg.mL^{-1} concentration.	(Miao et al. 2024)
4.	*Wickerhamiella domercqiae*	Lactonic SLs	The SLs have shown anti-fungal activity against various fungal strains like *F. oxysporum, F. solani P. ultimum* at 10 mg/mL conc. It creates inhibition against the growth of mycelia and germination of spores of fungal strains.	(Miao et al. 2024)

contrast to soils polluted with a single chemical, the presence of both contaminants altered the rhamnolipid micelle and soil structure, resulting in varying clearance rates. The outcomes showed that PHE was successfully ensnared in the rhamnolipid micelles and that Cd complexed with the micelle's exterior carboxyl groups. After the settings were optimized, the removal rates of PHE and Cd were 87.8% and 72.4%, respectively (Miao et al. 2024, Eras-muñoz et al. 2022, Industries et al. 2023, Silva et al. 2024)

The highest number of microorganisms is given below in Table 6. Non-pathogenic yeast strains, not only yeast strains but also bacterial strains, are produced biosurfactants. Both sophorolipids can show antimicrobial, larvicidal, insecticidal, and herbicidal activities against a lot of bacterial and fungal pathogens that are responsible for causing plant disease.

Application in poultry industries: In the poultry industry, there is a widespread influence of artificial emulsifiers and natural sophorolipids biosurfactants on the feed process and quality of pelletized feeds in the broiler diet. In the poultry industry, natural biosurfactant sophorolipids and artificial biosurfactant sophorolipids are being used as natural antibiotics as well as immunoregulators and immunomodulators, along with increasing food quality control and quality(Zhao et al. 2021). In the prescribed ratio of 2 1, oil and water and two types of emulsifiers, such as glycerol polyethylene glycol ricinolate synthetic emulsifiers and lyso-phosphatidylcholine with natural biosurfactant basal diet, mixed with water and emulsifier and natural biosphere. The experiment was performed through 4 treatment processes to determine the effect of unchanged levels of water, oil, natural biosurfactant, and synthetic emulsifiers' compounds with the basal diet, with different ingredients, in water, oil, natural biosurfactant, and synthetic emulsifiers. The effect of emulsifiers on energy

consumed and actual torque displayed in food production has been determined, as the application of emulsifiers as a supplement has been shown to increase the biostability and other quality of poultry and fish feed. Simultaneously, the effect of the emulsifier on mail temperature, moisture, and water activity is determined. The main goals and objectives of conducting this experiment were to determine the quality of the feed palette produced by the application of emulsifiers and biosurfactants based on how the quality of the product is controlled (Zajic et al. 1983). Based on physical (hardness, thickness by pressure ability test of Fr = (Initial weight–Final weight)/Initial weight $\times$ 100 = x.xx%), chemical, biostability, bioavailability, buoyancy, etc., quality of feed palette used in the poultry industry (Adebajo et al. 2020, Nouri et al. 2023, Industries et al. 2023).

Among the microbial strains that have played a role in the production of biosurfactants, *Candida bombicola or Starmerella bombicola* (Table 7) is one of them.

Applications in food industries: Microbial surfactants provide a flexible way to improve a range of food qualities, such as texture improvement, thickening, foaming, emulsification, and preservation. Rhamnolipids, for instance, have been shown to improve the volume, form, and stabilities of dough, therefore improving bread products. Additionally, Ribeiro et al. (2020). investigated the use of biosurfactants from Saccharomyces cerevisiae URM 6670 in place of egg yolk in cookie formulation, with no discernible changes to the dough's physical or physicochemical properties. Cookies with more linoleic acid (C18:2), a source of advantageous polyunsaturated fatty acids (PUFAs) with the potential to reduce cardiovascular disease, were produced as a result of the addition of biosurfactants (Miao et al. 2024, Sundaram et al. 2024, Vigil et al. 2024). Biosurfactants play a vital role in the food business by preventing food spoiling because of

Table 7: Applications of biosurfactants sophorolipids in poultry and poultry feed industries.

Sources of Sophorolipids	Sophorolipids and their structures.	The lethal dosage of sophorolipids and their mode of action on poultry and poultry industries.	References
Starmerella bombicola	Lc-SLs	0.0015%, and 0.5% conc. Using the SLs has shown antimicrobial activity to protect from the effects of Clostridium perfringens and Campylobacter jejune poultry food pathogens in poultry industries.	(Vandana & Singh 2018)
	Lc- SLs	31.25 μg.mL^{-1}, and 62.5 μg.mL^{-1} conc. SLs have been used to give protectants the poultry food affected by different bacterial S. aureus and L. monocytogenes pathogens in poultry.	(Vandana & Singh 2018)
	Ac- SLs	The conc of SLs has been tested at 15.6 to 2,000 μg·mL^{-1} and 78.1 to 10,000 μg·mL^{-1} To protect the poultry food from the harmful effects of gram-positive and gram-negative bacteria.	(Vandana & Singh 2018)

their natural antibacterial and antiadhesive properties. Their versatility in handling many environmental conditions, such as temperature, pH, and salinity, and their biodegradable, non-toxic nature render them appropriate for a range of uses, including food surface cleaning, packaging, coating, transportation, and storage procedures. In light of the possibility of food contamination during food preparation, Listeria monocytogenes is a bacterium that is particularly known to cause serious disease (Sun et al. 2021) examined the potential inhibitory effects of two commercial glycolipid products on L. monocytogenes in milk and cheese, specifically NagardoTM and rhamnolipids. Their research showed that NagardoTM was a better addition to milk at concentrations below 1100 mg.L^{-1}, whereas rhamnolipids caused unwanted color changes and coagulation in whole milk. The minimum bactericidal concentration (MBC) and minimum inhibitory concentration (MIC) values for NagardoTM were 1100 mg.L^{-1} and 800 mg.L^{-1}, respectively. Notably, at a dosage of 1,000 mg.L^{-1}, NagardoTM dramatically reduced cell counts in skim milk, demonstrating more powerful antibacterial actions. Furthermore, it has been shown that glycolipids are excellent at preventing spore germination. The effect on spore-forming bacteria, such as *Viridibacillus arenosi, Bacillus weihenstephanensis*, and *Paenibacillus odorifer*, which are known to withstand pasteurization and induce spoiling during refrigerated storage, was evaluated by Sun et al. (2021a). Their research showed that whereas

dosages of 400 and 200 mg L-1 greatly inhibited the growth of *P. odorifer* and *B. weihenstephanensis* in whole milk, larger concentrations (400 mg.L^{-1}) of glycolipids were required to suppress the germination of *Viridibacillus arenosi* spores. According to), this implies that adding 400 mg.L^{-1} of glycolipids to whole milk may be able to stop spoiling brought on by spore-forming bacteria (Miao et al. 2024, Rossini et al. 2024, Vieira 2023, Nouri et al. 2023)

Below is a list of different microorganisms (bacterial and fungal) in (Tables 8 and 9). With their lethal activity as the applications of sophorolipids bio-surfactant in the food industries. These sophorolipids have shown lethal activity against a lot of bacterial and fungal strains.

Application in cosmetic products of biosurfactants: Another type of glycolipid biosurfactant called sophorolipids is made from the yeast Candida species and is applied to cosmetics. Because of their remarkable ability to reduce surface tension and their emulsifying qualities, sophorolipids are now a necessary component of many cosmetic products. Natural sophorolipids have been shown to lower surface tension from 72 mNm-1 at 25°C to values in the range of 30 to 40 mN m^{-1} at a water-air interface (Develter & Lauryssen 2010). For a certain amount of time, between 500 and 5000 nm, the mean droplet diameters of sophorolipid emulsions show an increase as the percentage of almond oil in an almond oil-water emulsion grows. Pratap et al.

Table 8: Applications of sophorolipids in food industries against a lot of gram-positive and gram-negative bacterial strains.

% Of SLP	Microorganisms	Gram Activity	Lethal time	Rates of Lethality.	References
1% v/v	*Salmonella typhimurium ATCC 23564,*	-ve	10 min	90%	(Vieira, 2023)
1% v/v	*Escherichia coli ATCC 8739*	-ve	10 min	99%	50
1% v/v	*Erwinia chrysanthemi ATCC 11663*	-ve	10 min	100%	50
1% v/v	*Xanthomonas campestris ATCC 13951*	-ve	10 min.	100%	50
1% v/v	*Shigella dysenteriae.*	-ve	30 seconds	100%	(Abu-Ruwaida et al. 1991)
1% v/v	*Salmonella typhi*	-ve	30 seconds	100%	(Abu-Ruwaida et al. 1991)
1% v/v	*Escherichia coli*	-ve	30 seconds	100%	(Abu-Ruwaida et al. 1991)
5% v/v	*Bacillus subtilis*	+ve	30 seconds	100%	(Abu-Ruwaida et al. 1991)

Table 9: Applications of sophorolipids in food industries against a lot of fungal strains.

Microorganisms	Sophorolipids	Types of bioactivities or properties.	Use and their mode of action on the body.	Reference
Rhodotorula babjevae YS3	Ac, - Lc- SLs	Antimicrobial (Antifungal)	A con^c. of 125 µg.mL^{-1} (MIC) of SLs has been used to protect food from food-borne fungal pathogens such as *F. oxysporum* and *F. solani*.	(Sharma et al. 2023a)
Wickerhamiella domercqiae	Lc - SLs	Antimicrobial (Antifungal)	A con^c. of 10 mg.mL^{-1} of SLs has been used to inhibit fungal spore formation and block the mycelial growth of *F. oxysporum* and *P. ultimum*.	(Youssef et al. 2004)
Metschnikowia churdharensis	Ac, - Lc- SLs	Antimicrobial (Antifungal)	SLs at con^c of 49 µg.mL^{-1} and 98 µg.mL^{-1} have been used to protect food from spoilage caused by fungal pathogens such as *F. oxysporum* and *F. solani*.	(Youssef et al. 2004)
Candida glabrata	Ac, - Lc- SLs	Antimicrobial (Antifungal and Antibacterial) Emulsifier.	SLs at con^c of 60 µg.mL^{-1} and 125 µg.mL^{-1} have been used to protect food from spoilage caused by *B. subtilis* (bacteria) and *F. oxysporum* (fungus).	(Youssef et al. 2004)

looked at the surfactant's presence in face wash formulations (Nagtode et al. 2023). These authors concentrated on using non-edible jaggery, maize oil, oleic acid from *Starmerella bombicola*, and waste syrup from a jaggery facility to produce sophorolipids sustainably. It was established that waste-derived sophorolipids could be utilized in face wash formulations in place of chemically generated sodium lauryl sulfate since they exhibited good foam height stability and emulsification index. All skin types, including fair, medium, and dark skin tones, have been demonstrated to experience mild to minimal allergic reactions while using a face wash based on sophorlipids. These results demonstrate the sophorolipids' ability to stabilize emulsions in formulations used in cosmetics. Additionally, sophorolipids exhibit benefits for skin compatibility and moisture that are consistent with important consumer requirements for

contemporary cosmetics. The results of this research indicate that biosurfactants derived from renewable feedstocks have potential use in personal care products, providing a substitute for conventional chemical surfactants. In toothpaste formulations, biosurfactants and chitosan were investigated as potential natural substitutes for sodium lauryl sulfate (Resende et al. 2019, Nasser et al. 2024). It was found that the combination of fungal chitosan and biosurfactants produced by Pseudomonas aeruginosa, Bacillus methylotrophicus, and Candida bombicola showed antibacterial efficacy against Streptococcus mutans without causing cytotoxicity. Similar to commercial fluoride toothpaste, these biosurfactant-chitosan combinations decreased the survival of Streptococcus mutans biofilms. Making use of the complementary properties of chitosan and biosurfactants could offer a viable, long-term strategy for creating toothpastes that work well without the

Table 10: Sophorolipids and their applications in cosmetics industries to produce beauty care products to use and enhance the beauty of the body.

Microorganisms	Sophorolipids	Types of bioactivities or properties.	Use and their mode of action on the body.	References
Starmerella bombicola.	Ac- SLs	It reduces S T.	CAC 2 0.083% showed the highest penetration enhancer.	
	Acidic (C18001 -NASL) 3	Antimicrobial (antibacterial)	Using 4 mg.mL^{-1} with kanamycin or cefotaxime as a synergist has shown MIC against the wounds of *E. faecalis*, *P. aeruginosa*, and cosmetics.	(McMahan et al. 2021)
Candida bombicola	Lactonic-SLP	Emulsifier	Preparation of cream and lotions by the SLP at the 50 µg.mL^{-1} conc. For use in cosmetology.	(Fernandes & Dias 2023)
Candida kuoi	Acidic-SLP	Emulsifier	Pharmaceuticals are formulated drugs for external use.	(Fernandes & Dias 2023)
Pseudohyphozyma bogoriensis. Rhodotorula bogoriensis	Long chain C22-SL 1 SLP.	Antimicrobial (anti-bacterial)	Long-chain SLP has shown antibacterial growth or growth of inhibition against *P. acne as skin care*.	(Fernandes & Dias 2023)
Rhodotorula bogoriensis	Long chain C22-SL 1 sophorolipids	Antimicrobial (anti-bacterial)	At 100 mg.mL^{-1} of the SLP, the colony showed the growth of inhibition against P acne.	(Fernandes & Dias 2023)

use of artificial surfactants. This shows that rhamnolipid biosurfactants have the potential to function as biocompatible detergents and foaming agents in oral hygiene formulations, albeit more clinical research is necessary (Karnwal et al. 2023, Miao et al. 2024, Nasser et al. 2024, Vigil et al. 2024, Adu et al. 2023)

Below is the information in a table of some microorganisms that produced acidic and lactonic sophorolipids (Table 10) with their different bioactive properties in beauty care products and promoting wound healing activity.

Sophorolipids and biosurfactants in the detergent industry: The detergents used in the market have various applications in daily life. In detergent industries, surfactant compounds have been formulated by using byproducts of petrochemical industries. For example, MERS has occurred over the past years and decades during epidemics like COV-1, Evola-V, and ASARCH COV-2, the most commonly used synthetic formed surfactants as detergents, disinfectants, and various antiseptics for preventing the spread of viruses in personal care, households, offices, factories, and populated areas are from various types of petroleum industries derived from by-products. The biodegradation potential of these byproducts is very low, and these synthetic byproducts are the main cause of creating severe toxicity in the ecosystem. To avoid environmental toxicity, instead of petroleum-derived synthetic surfactants, the production and substitution of biodegradable and non-toxic bio-waste or microorganisms-derived molecules (biosurfactants) has become a growing and acceptable commercial option at present. Therefore, by microorganisms, short-length carbon-chained, biodegradable organic compounds should be synthesized and considered to be alternatives to synthetic surfactants and environmentally friendly detergents and disinfectants. Or replacing synthetic surfactants, through technological and product development, with green and biosurfactants (effective in hard water and low temperatures) synergistically. Biosurfactants, due to their emulsifying properties, are capable of exhibiting their activity as detergents, and in addition, due to their unique properties of detergents, they will be popular as laundry and various cleaning agents detergents (Helmy et al. 2020)

In heavy metal binding: Some biosurfactants, such as rhamnolipids, can remove specific components from soil, including Pb, Zn, and Cd. By modifying Cd absorption through their interactions with the cell surface and Cd complexation, rhamnolipids can lessen the toxicity of metals. High-molecular-weight (HMW) polysaccharides in emulsifiers link metals, as demonstrated by the emulsifier Acinetobacter calcoaceticus's ability to link uranium (Shakeri et al. 2021). Lead (Pb), chrome (Cr), mercury (Hg), zinc (Zn), copper (Cu), nickel (Ni), and cobalt (Co) are among the heavy metals that can be found in soil and sediments. To precipitate and be removed from the soil, the heavy metals must form stable complexes with anionic biosurfactants (22). Heavy metal-contaminated soils can be cleaned up by washing with a surfactant solution. Additionally, the biosurfactant can be used repeatedly to remediate polluted soil, allowing the metals to be used again in the battery sector (Augusto et al. 2023).

In pharmaceutical industry: Early neonates experience lung surfactant-related respiratory problems, which can be shown to be normal by a protein-phospholipid complex (PPC). Because this protein is produced fermentatively by cloning the relevant genes into bacteria, it may have therapeutic qualities. One treatment and management option for tobacco mosaic virus (TMV), which mostly affects *Nicotiana glutinosa* and potato virus X (PVX), is 1% rhamnolipid emulsion (Shakeri et al. 2021).

Anti-corrosion activities of biosurfactants: The process of corrosion causes basic qualities used in the application of various materials, including rubber, plastic, wood, cement, and metals, to deteriorate. Metals corrode due to chemical and electrochemical processes, which are influenced by their surroundings. The oxidation of metal atoms on a metal surface leads to corrosion, a natural process that weakens the surface's mineralized structure. This kind of corrosion starts with protons adhering to the metal atoms and progresses through an electrochemical reaction. Surface corrosion can occur when metallic cations react with anions or dissolve in the aqueous phase (Augusto et al. 2023).

CONCLUSIONS

The exceptional qualities of biosurfactants-high biodegradability, low toxicity, and resistance to harsh pH and temperature conditions-have recently attracted more attention, surpassing those of their equivalents derived from fossil fuels. Glycolipids are a type of low molecular weight biosurfactants that are particularly effective at reducing interfacial tension and surface tension among these versatile biomolecules. Particularly, the most notable representations are rhamnolipids, trehalose lipids, sophorolipids, and mannosyl erythritol lipids. Glycolipids have several uses, such as bioremediation, food processing, petroleum refining, biomedical applications, and agriculture, but their production costs continue to be the main barrier to them outperforming synthetic surfactants. While the incorporation of secondary feedstocks offers a viable approach to augmenting the sustainability of glycolipid production, the application of these feedstocks in industrial environments is restricted because of their uneven composition. The incorporation

of secondary feedstocks offers a promising approach to augmenting the sustainability of glycolipid production; nevertheless, the uneven composition of these feedstocks hinders their widespread use in industrial environments. It will take significant work to improve productivity and streamline process flow to address this problem. The appropriate optimization of secondary feedstocks in biosurfactant production is thought to be able to strike a balance between the advantages for the environment, the economy, and society. These developments could lead to more ecologically friendly and sustainable glycolipid synthesis, which would benefit the surfactant sector.

REFERENCES

Abu-Ruwaida, A.S., Banat, I.M., Haditirto, S., Salem, A. and Kadri, M., 1991. Isolation of biosurfactant-producing bacteria, product characterization, and evaluation. *Acta Biotechnologica*, 11(4), pp.315–324. https://doi.org/10.1002/abio.370110405

Adebajo, S.O., Akintokun, P.O., Ojo, A.E., Akintokun, A.K. and Badmos, O.A., 2020. Recovery of biosurfactant using different extraction solvents by rhizospheric bacteria isolated from rice-husk and poultry waste biochar amended soil. *Egyptian Journal of Basic and Applied Sciences*, 7(1), pp.252–266.

Adetunji, C.O., 2022. *Applications of Next Generation Biosurfactants in the Food Sector*. Academic Press.

Adu, S.A., Twigg, M.S., Naughton, P.J., Marchant, R. and Banat, I.M., 2023. Glycolipid biosurfactants in skincare applications: challenges and recommendations for future exploitation. *Plos One*, 11, pp.1–22.

André, M., Dias, M. and Nitschke, M., 2023. Bacterial-derived surfactants: an update on general aspects and forthcoming applications. *Brazilian Journal of Microbiology*, 54(1), pp.103–123.

Andreolli, M., Villanova, V., Zanzoni, S., Onofrio, M.D., Vallini, G., Secchi, N. and Lampis, S., 2023. Characterization of trehalolipid biosurfactant produced by the novel marine strain Rhodococcus sp. SP1d and its potential for environmental applications. *Journal of Cleaner Production*, 5, pp.1–15.

Ankulkar, R., Chavan, S., Aphale, D., Chavan, M. and Mirza, Y., 2022. Cytotoxicity of di-rhamnolipids produced by Pseudomonas aeruginosa RA5 against human cancerous cell lines. *3 Biotech*, 12(11), p.323.

Aparna, A., Srinikethan, G. and Smitha, H., 2012. Production and characterization of biosurfactant produced by a novel Pseudomonas sp. 2B. *Colloids and Surfaces B: Biointerfaces*, 95, pp.23–29. https://doi.org/10.1016/j.colsurfb.2012.01.043

Augusto, A., Filho, P.S., Converti, A., C.R.De, Soares, F. and Sarubbo, L.A., 2023. Biosurfactants as multifunctional remediation agents of environmental pollutants generated by the petroleum industry, *Bioresource Technology*, 81, p.56.

Basak, B., Bhunia, B. and Dey, A., 2014. Studies on the potential use of sugarcane bagasse as carrier matrix for immobilization of Candida tropicalis PHB5 for phenol biodegradation. *International Biodeterioration and Biodegradation*, 93, pp.107–117. https://doi.org/10.1016/j.ibiod.2014.05.012

Batista, S.B., Mounteer, A.H., Amorim, F.R. and Tótola, M.R., 2006. Isolation and characterization of biosurfactant/bioemulsifier-producing bacteria from petroleum-contaminated sites. *Bioresource Technology*, 97(6), pp.868–875. https://doi.org/10.1016/j.biortech.2005.04.020

Bose, K.J. and Sarwan, J., 2023. Multi-enzymatic degradation potential against wastes by the novel isolate of Bacillus. *Biomass Conversion and Biorefinery*, 23, p.789. https://doi.org/10.1007/s13399-023-04620-z

Ceresa, C., Fracchia, L., Sansotera, A.C. and Alejandra, M., 2023.

Harnessing the potential of biosurfactants for biomedical and pharmaceutical applications. *Science*, 21, p.81.

Cheffi, M., Maalej, A., Mahmoudi, A., Hentati, D., Marques, A.M., Sayadi, S. and Chamkha, M., 2021. Lipopeptides production by a newly Halomonas venusta strain: Characterization and biotechnological properties. *Bioorganic Chemistry*, 109, p.104724.

Develter, D.W.G. and Lauryssen, L.M.L., 2010. Properties and industrial applications of sophorolipids. *European Journal of Lipid Science and Technology*, 112(6), pp.628–638.

Eras-Muñoz, E., Farré, A., Sánchez, A., Font, X., Gea, T., Farré, A., Sánchez, A., Font, X. and Gea, T., 2022. Microbial biosurfactants: A review of recent environmental applications. *Bioengineered*, 13(5), pp.12365–12391. https://doi.org/10.1080/21655979.2022.2074621

Fernandes, N. and Dias, D.R., 2023. Biosurfactants and their benefits for seeds. *PLos One*, 16, pp.1412-1423. https://doi.org/10.1007/978-3-031-21682-4

Gudiña, E.J., Teixeira, J.A. and Rodrigues, L.R., 2010. Isolation and functional characterization of a biosurfactant produced by Lactobacillus paracasei. *Colloids and Surfaces B: Biointerfaces*, 76(1), pp.298–304. https://doi.org/10.1016/j.colsurfb.2009.11.008

Hausmann, R., Déziel, E. and Soberón-Chávez, G., 2024. Editorial: Microbial biosurfactants: updates on their biosynthesis, production and applications. *Science*, 11, pp.1–2. https://doi.org/10.3389/fbioe.2024.1433035

Helmy, Q., Gustiani, S. and Mustikawati, A.T., 2020. Application of rhamnolipid biosurfactant for bio-detergent formulation. *IOP Conference Series: Materials Science and Engineering*, 823(1), pp.12104. https://doi.org/10.1088/1757-899X/823/1/012014

Hernández, M.L., Pedersen, J.S. and Otzen, D.E., 2023. Proteins and biosurfactants: Structures, functions, and recent applications. *Current Opinion in Colloid & Interface Science*, 68, p.101746. https://doi.org/10.1016/j.cocis.2023.101746.

Heyd, M., Kohnert, A., Tan, T.H., Nusser, M., Kirschhöfer, F., Brenner-Weiss, G., Franzreb, M. and Berensmeier, S., 2008. Development and trends of biosurfactant analysis and purification using rhamnolipids as an example. *Analytical and Bioanalytical Chemistry*, 391(5), pp.1579-1590. https://doi.org/10.1007/s00216-007-1828-4.

Jagadeesh Chandra Bose, K. and Sarwan, J., 2023. *Nanovaccinology*. Springer, pp. 79–99. https://doi.org/10.1007/978-3-031-35395-6_5.

Jimoh, A.A. and Lin, J., 2019. Biosurfactant: A new frontier for greener technology and environmental sustainability. *Ecotoxicology and Environmental Safety*, 184(June), p.109607. https://doi.org/10.1016/j.ecoenv.2019.109607.

Karnwal, A., Shrivastava, S., Rahman, A., Said, M., Kumar, G., Singh, R., Kumar, A. and Mohan, A., 2023. Microbial biosurfactant as an alternate to chemical surfactants for application in cosmetics industries in personal and skin care products: A critical review. *Journal of Applied and Environmental Microbiology*, 2023. https://doi.org/10.1155/2023/2375223.

Lin, S.C., 1996. Biosurfactants: Recent advances. *Journal of Chemical Technology and Biotechnology*, 66(2), pp.109–120.

Lydon, K.A., Kinsey, T., Le, C., Gulig, P.A. and Jones, J.L., 2021. Biochemical and virulence characterization of *Vibrio vulnificus* isolates from clinical and environmental sources. *Frontiers in Cellular and Infection Microbiology*, 11, p.637019.

McMahan, K., Yu, J., Mercado, N.B., Loos, C., Tostanoski, L.H., Chandrashekar, A., Liu, J., Peter, L., Atyeo, C., Zhu, A., Bondzie, E.A., Dagotto, G., Gebre, M.S., Jacob-Dolan, C., Li, Z., Nampanya, F., Patel, S., Pessaint, L., Van Ry, A. and Barouch, D.H., 2021. Correlates of protection against SARS-CoV-2 in rhesus macaques. *Nature*, 590(7847), pp.630–634. https://doi.org/10.1038/s41586-020-03041-6.

Miao, Y., To, M.H., Siddiqui, M.A., Wang, H., Chopra, S.S., Kaur, G., Roelants, S.L.K.W., Sze, C. and Lin, K., 2024. Sustainable biosurfactant production from secondary feedstock—recent advances, process

optimization, and perspectives. *Frontiers in Chemistry*, 17, p.16. https://doi.org/10.3389/fchem.2024.1327113.

Muthusamy, K., Gopalakrishnan, S., Ravi, K., Sivachidambaram, P., Muthusamy, K. and Gopalakrishnan, S., 2008. Biosurfactants: Properties, commercial production and application. *Current Science*, 94(6), pp.736–747.

Nagtode, V.S., Cardoza, C., Khader, H., Yasin, A., Tambe, S.M., Roy, P., Singh, K., Goel, A., Amin, P.D., Thorat, B.R., Cruz, J.N. and Pratap, A.P., 2023. Green surfactants (biosurfactants): A petroleum-free substitute for sustainability—comparison, applications, market, and prospects. *ACS Omega*, 11, p.591. https://doi.org/10.1021/acsomega.3c00591.

Nasser, M., Sharma, M. and Kaur, G., 2024. Advances in the production of biosurfactants as green ingredients in home and personal care products. *Frontiers in Chemistry*, 3, pp.1–9. https://doi.org/10.3389/fchem.2024.1382547.

Nouri, H., Moghimi, H. and Lashani, E., 2023. Fungal biosurfactants and their applications. *Fungal Biosurfactants and Their Applications*, 16, pp.1–14. https://doi.org/10.1007/978-3-031-31230-4.

Priya, T. and Usharani, G., 2009. Comparative study for biosurfactant production by using *Bacillus subtilis* and *Pseudomonas aeruginosa*. *International Journal of Microbiological Research*, 2(4), pp.284–287.

Resende, A.H.M., Farias, J.M., Silva, D.D.B., Rufino, R.D., Luna, J.M., Stamford, T.C.M. and Sarubbo, L.A., 2019. Application of biosurfactants and chitosan in toothpaste formulation. *Colloids and Surfaces B: Biointerfaces*, 181, pp.77–84.

Ribeiro, B.G., Guerra, J.M.C. and Sarubbo, L.A., 2020. Biosurfactants: production and application prospects in the food industry. *Biotechnology Progress*, 36(5), p.e3030.

Rossini, C., Willian, M., Fernandes, R., Souza, D., Hacha, R.R. and Silvas, C., 2024. Biosurfactants: An overview of their properties, production, and application in mineral flotation. *Minerals Engineering*, 15, pp.1–23.

Sarwan, J., Bose, J.C., Kumar, S., Bhargav, S.S., Dixit, S.K., Sharma, M., Mittal, K., Kumar, G. and Uddin, N., 2024a. Biodegradation of cellulosic wastes and deinking of colored paper with isolated novel cellulolytic bacteria. *Nature Environment and Pollution Technology*, 23(2), pp.761–773. https://doi.org/10.46488/nept.2024.v23i02.013.

Sarwan, J., Uddin, N. and Bose, J.C., 2024b. Enhanced production of microbial cellulases as an industrial enzyme: A short review. *Journal of Microbial Biotechnology*, 2(1), pp.59–70.

Seattle, W., 2023. *Biosurfactants and their Role in Environmental Sustainability*. Springer, pp.1–14. https://doi.org/10.1016/B978-0-323-91697-4.00002-8.

Shaikhah, D., Loise, V., Angelico, R., Porto, M., Calandra, P., Abe, A.A., Testa, F., Bartucca, C., Rossi, C.O. and Caputo, P., 2024. New trends in biosurfactants: From renewable origin to green enhanced oil recovery applications. *Current Trends in Chemical Engineering*, 41, pp.1–34.

Shakeri, F., Babavalian, H., Amoozegar, M.A., Ahmadzadeh, Z., Zuhuriyanizadi, S. and Afsharian, M.P., 2021. Production and application of biosurfactants in biotechnology. *Biotechnology Reports*, 11(3), pp.10446–10460.

Sharma, H., Rana, N., Sarwan, J., Bose, J.C., Devi, M. and Chugh, R., 2023. Nano-material for wastewater treatment. *Materials Today: Proceedings*, 16, p.258. https://doi.org/10.1016/j.matpr.2023.02.258.

Sharma, H., Rana, N., Sarwan, J., Bose, J.C., Devi, M. and Chugh, R., 2023.

Nano-material for wastewater treatment. *Materials Today: Proceedings*, xxxx. https://doi.org/10.1016/j.matpr.2023.02.258

Shekhar, S., Sundaramanickam, A. and Balasubramanian, T., 2015. Biosurfactant producing microbes and their potential applications: A review. *Critical Reviews in Environmental Science and Technology*, 45(14), pp.1522–1554. https://doi.org/10.1080/10643389.2014.955631

Silva, C., Medeiros, A.O., Converti, A., Almeida, F.C.G. and Sarubbo, L.A., 2024. Biosurfactants: Promising biomolecules for agricultural applications. *Biosurfactants,* 19, p.54

Soberón-chávez, G., Abdel-mawgoud, A.M., Hausmann, R. and Le, F., 2010. Biosurfactants and bioengineering of production. *International Journal of Scientific Research,* 17, p.1–11. https://doi.org/10.1007/978-3-642-14490-5

Sun, S., Zeng, H., Robinson, D.B., Raoux, S., Rice, P.M., Wang, S.X. and G.L., 2004. Controlled synthesis of MFe_2O_4 (M = Mn, Fe, Co, Ni and Zn) nanoparticles. *Journal of Chemical Science,* 126(1), pp.273–279.

Sun, W., Zhu, B., Yang, F., Dai, M., Sehar, S., Peng, C., Ali, I. and Naz, I., 2021. Optimization of biosurfactant production from Pseudomonas sp. CQ2 and its application for remediation of heavy metal contaminated soil. *Chemosphere*, 265, p.129090.

Sundaram, T., Govindarajan, R.K., Vinayagam, S., Krishnan, V., Nagarajan, S., Gnanasekaran, G.R., Baek, K., Kumar, S. and Sekar, R., 2024. Advancements in biosurfactant production using agro-industrial waste for industrial and environmental applications. *Plos One,* 12, p.36. https://doi.org/10.3389/fmicb.2024.1357302

Tajabadi, M.T., 2023. Review article: Biosurfactant-producing microorganisms: Potential for bioremediation of organic and inorganic pollutants. *Journal of Bioremediation*, 2(2), pp.18–23. https://doi.org/10.58803/rbes.v2i2.13

Vandana, P. and Singh, D., 2018. Review on biosurfactant production and its application. *International Journal of Current Microbiology and Applied Sciences*, 7(08), pp.4228–4241. https://doi.org/10.20546/ijcmas.2018.708.443

Vieira, R.S., 2023. Biosurfactant production by Acinetobacter venetianus and its application in bioremediation. *Bioremediation*, 91, pp.456-467. https://doi.org/10.1002/ceat.202200540

Vigil, T.N., Felton, S.M., Fahy, W.E., Kinkeade, M.A., Visek, A.M., Janiga, A.R., Jacob, S.G. and Berger, B.W., 2024. Biosurfactants as templates to inspire new environmental and health applications. *Journal of Cleaner Production,* 71, pp.1–9. https://doi.org/10.3389/fsybi.2024.1303423

Vijayakumar, S. and Saravanan, V., 2015. Biosurfactants-types, sources and applications. *Research Journal of Microbiology*, 10(5), pp.181–192. https://doi.org/10.3923/jm.2015.181.192

Youssef, N.H., Duncan, K.E., Nagle, D.P., Savage, K.N., Knapp, R.M. and McInerney, M.J., 2004. Comparison of methods to detect biosurfactant production by diverse microorganisms. *Journal of Microbiological Methods*, 56(3), pp.339–347. https://doi.org/10.1016/j.mimet.2003.11.001

Zhao, F., Zhu, H., Cui, Q., Wang, B., Su, H. and Zhang, Y., 2021. Anaerobic production of surfactin by a new Bacillus subtilis isolate and the in situ emulsification and viscosity reduction effect towards enhanced oil recovery applications. *Journal of Petroleum Science and Engineering*, 201, p.108508.

Woody Species Diversity and Conservation Status of Tumauni Watershed Natural Park, Isabela, Philippines

Rocel S. Galicia[1] and Hannie T. Martin[2]

[1]College of Forestry and Environmental Management, Isabela State University, Philippines
[2]Apayao State College, Philippines
†Corresponding author: Rocel S. Galicia; rocel.s.galicia@isu.edu.ph

ABSTRACT

The study was conducted within the Protected Area of the Tumauini Watershed Natural Park located in the municipality of Tumauini province of Isabela along the western part of the Northern Sierra Madre Natural Park. The protected areas in the Philippines cover 39% of the total forest cover. Protection and conservation of protected areas is significant due to the increasing habitat loss and biodiversity loss. The main objective of the study is to assess the tree diversity of the park using the modified belt-transect method adopted by the Department of Environment and Natural Resources (DENR). The transect line has a distance of 2 kilometers and a total of 9 stations. A Nested Quadrat was established along the transect line for tree identification. Results of the assessment show that the park has a species richness of 34 tree species in eight families and 26 genera. Species diversity indicates low (2.4) to very low (1.12) based on the Shannon-Weiner Diversity Index despite the high number of individuals found in the watershed area. The low diversity of the watershed is affected by the rampant anthropogenic activities and naturally-induced hazards occurring in the protected area. Shorea polysmerma is the most dominant and the most important species, with an Importance Value index of 38.78. Three species of trees were recorded as generalists in the area such as *Calophyllum blancoi, Shorea palosapis*, and *Ficus* sp.

INTRODUCTION

The Tumauini Watershed Natural Park was identified as a natural park through the Republic Act 11038, otherwise known as the "Expanded Natural Integrated Protected Areas System Act of 2018" from the previously Tumauini Watershed Forest Reserve. The park has a total land area of 6,509.38 hectares and is currently exposed to various anthropogenic activities. The Tumauini River within the watershed is one of the tributaries of the Cagayan River, which is identified as the longest river in the Philippines. The park was established across the municipalities of Tumauini and Cabagan in the northernmost part of the province of Isabela (Fig. 1).

Various rehabilitation projects were implemented in the lowland and upland areas of the watershed. Some of the projects in the area are the establishment of bamboo plantations along the riverbanks of the Tumauini River of the watershed and the National Greening Program under the Department of Environment and Natural Resources.

Several wildlife species, both flora and fauna, are found in the forest habitat types. The water resources of the watershed are primarily used for irrigation in the lowland agricultural areas of the municipality.

According to Malabrigo et al. (2015), the condition of a watershed is vital to its provision of goods and services. Unfortunately, a lot of watersheds in the Philippines are degraded due to various causes like deforestation and mining. Most of the threats observed in the TWNP are driven by unsustainable farming
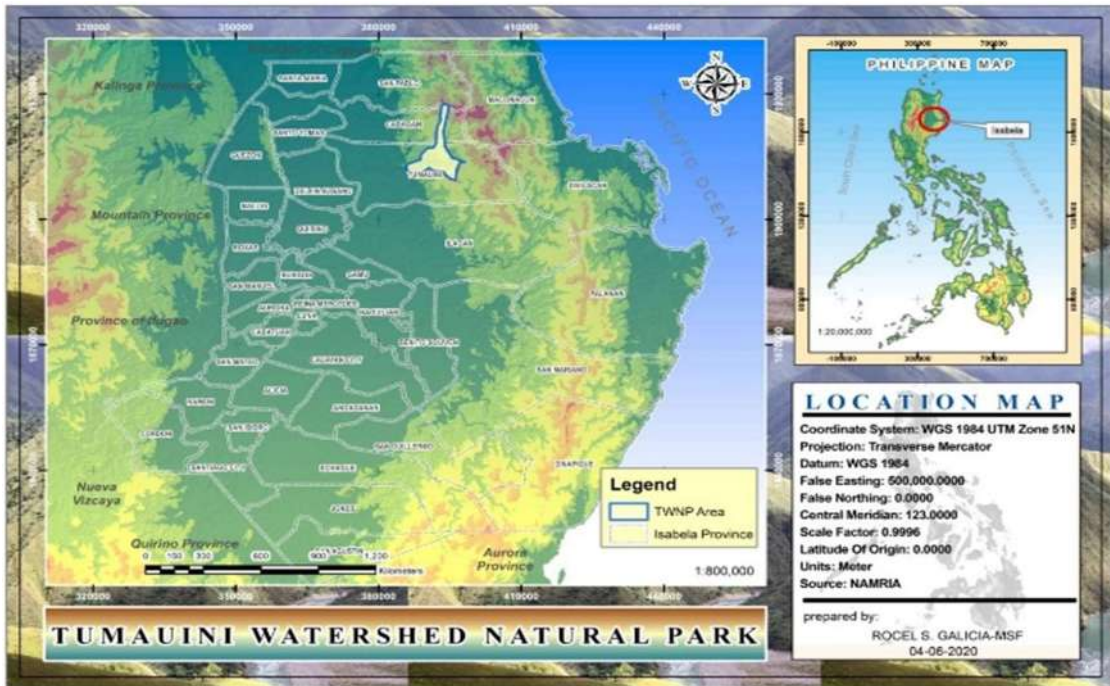
Fig. 1: Location map of the study area.

practices encroaching on the forest zones of the watershed. The TWNP area is relatively large, consisting of various plant communities and land use patterns. Quantification and identification of the tree species within the secondary forest of the watershed is a very challenging task for the management, considering the vast area to quantify. The presence of threatened, invasive, native, and economically important tree species is just a few of the characteristics/ status of species sought to discover in the study.

Nowadays, there is a rapid degradation of watersheds in the municipality due to the increase in population, continuous conversion of kaingin with a monoculture of banana production, as well as the expansion of corn-based farming with rampant use of agrochemicals and timber poaching. In addition, it is also vulnerable to hazards like typhoons and drought that lead to soil erosion and landslides, as well as quality and supply of water. If these conditions continually persist, the use of watershed natural resources will eventually be depleted.

Tree diversity assessment is an activity to monitor biodiversity status and ecosystem changes which is an important tool for managing important watershed and biodiversity conservation areas sustainably (Castillo et al. 2020). The tree diversity assessment in the TWNP serves as baseline data in the region of the watershed where the study was conducted. It is important to monitor forest areas such as declared protected critical watersheds to note any development or improvements

that have happened since the declaration as a protected area.

The natural park's general goal is to protect outstanding natural and scenic areas of national or international significance for scientific, educational, and recreational use (eNIPAS Act 2018). One way to protect the park is through the enhanced restoration of forest cover in the denuded watershed area.

The outputs of the study were presented to the Protected Area Management Board of the TWNP for the awareness of the stakeholders. The data gathered, and findings of the research were turned over to the data manager of the board for its utilization. The output of the study is relevant for the updating of management plans, input for policy formulation, and for the appropriate conservation efforts to be implemented in the protected area.

The main objective of the study is to assess the tree diversity of the Tumauini Watershed Natural Park. The study specifically aimed to assess the Importance Value (IV) of trees, tree diversity, and conservation status of trees in the protected area.

MATERIALS AND METHODS

The study was conducted within the secondary forest of the Tumauini Watershed Natural Park located in the upland barangays of the municipality of Tumauini, province of Isabela in the northern part of the Philippines (Fig. 2). The
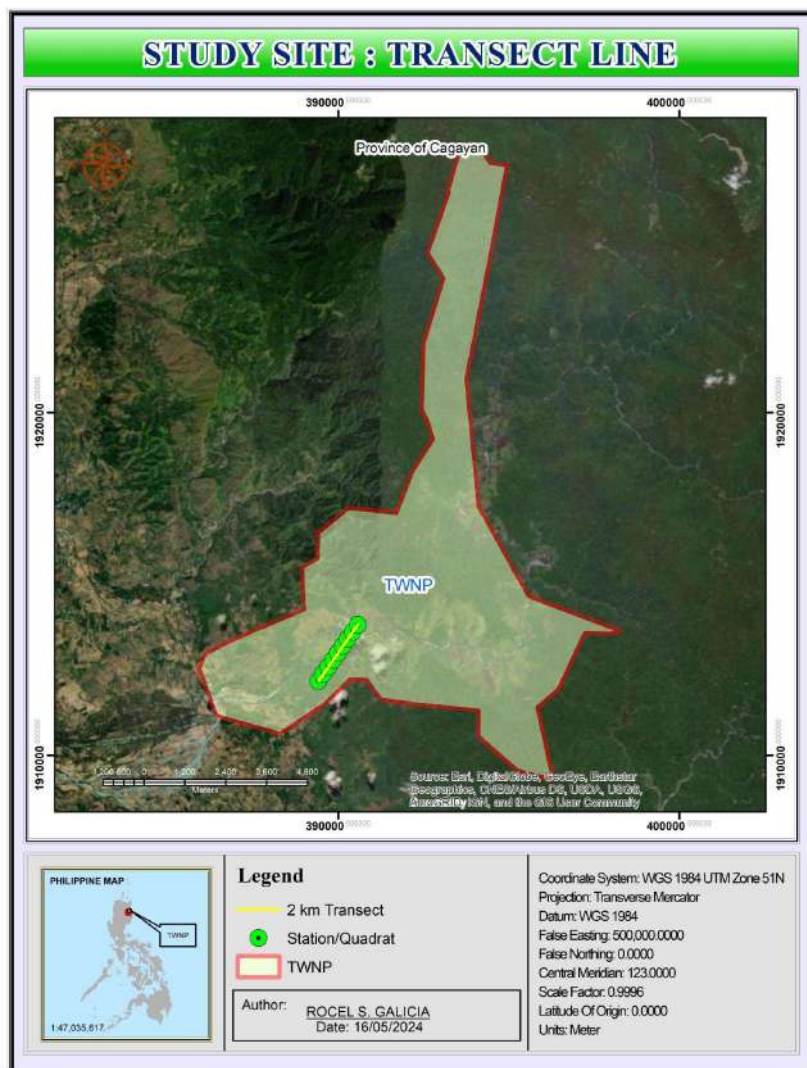
Fig. 2: Transect Line.

Northern Sierra Madre Natural Park, one of the largest Dipterocarp forests in the country is found on the eastern side of the TWNP.

A modified belt transect method with a 2 km transect line) was established for the tree diversity assessment (DENR-BMB, 2018-02). Quadrats were established every 250m interval in alternate positions (Fig. 3). A total of 8 plots with dimensions 20m x 20m. A transect line was established across the different elevation levels (258-462 masl) to represent different plant communities. Opportunistic Sampling was conducted along the transect to record some species outside the sampling areas, particularly along the transect, trails, riverbanks, grassland, and other areas. The data recorded during the opportunistic sampling was not part of the data analysis but listed as additional species that are relevant to the planning and management of the protected area.

All trees within the quadrats along the transect line with DBH of ≥ 10 cm were measured and identified. For the Upper Canopy Diversity Assessment, Diameter at Breast Height (DBH), Merchantable Height (MC), and Total Height (TH) were determined. Trees with ≤10cm diameters were identified within the 5m x 5m quadrat for the assessment of Understorey Diversity. Ground Cover diversity assessment was conducted within the 1m x 1m quadrat for the percent estimation of grasses and other ground cover species. All quadrats were assessed with a total area of 3,200 square meters or 400 square meters per quadrat.

The nested sampling is practically used in heterogeneous stratum, wherein the inventory site of the study is within a
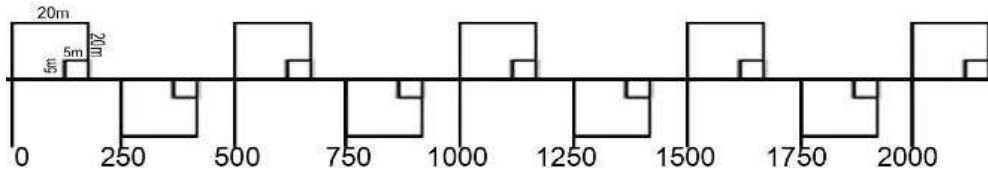
(source: DENR-BMB, 2018-02)

Fig. 3: A 2-km Belt transect.

secondary forest. The forest is composed of different species of plants of various ages and biometry. The belt transect was used to represent the different land use patterns, elevation, soil fertility level, and other topographic characteristics of the site.

Photographs of fruit, flowers, leaves, and bark of trees were taken for verification and identification of unidentified species. Photographs were compared with the sample specimens in the Isabela State University Cabagan Herbarium and other online websites such as iNaturalist.org, Pl@antNet.org, Philippineplants.org, and The Catalogue of Plants 2021 for the verification and identification of unidentified species.

Data Analysis

Importance Value

$$Density = \frac{Number\ of\ individuals}{Area\ sampled}$$

$$Relative\ Density = \frac{Density\ for\ a\ Species}{total\ density\ for\ all\ species} \times 100$$

$$Frequency = \frac{number\ of\ Quadrats\ where\ species\ A\ occurs}{total\ number\ of\ sample\ Quadrats} \times 100$$

$$Relative\ Frequency = \frac{frequency\ of\ species\ A}{total\ frequency\ value\ of\ all\ species} \times 100$$

$$Dominance = \frac{basal\ area\ or\ volume\ for\ species\ A}{total\ area\ sampled} \times 100$$

$$Relative\ Dominance = \frac{dominance\ of\ species\ A}{total\ dominance\ value\ of\ all\ species} \times 100$$

Importance Value = Relative Frequency + Relative Dominance + Relative Density

Diversity Index

$$Diversity\ Index\ (H') = -\sum_{i=1}^{n} (pi * LN\ pi)$$

The Diversity Index is analyzed based on the Classification scheme by Fernando et al. (1998)

Simpson Diversity Index

The Simpson Diversity Index of the protected area was computed using the formula

$$D = \Sigma ni(ni-1)/N(N-1)$$

where:

ni: The number of organisms that belong to species i

N: The total number of organisms

The value for Simpson's Diversity Index ranges between 0 and 1. The higher the value, the lower the diversity.

RESULTS AND DISCUSSION

The study area is within the secondary forest of the protected area with an elevation ranging from 258 meters to 462 meters above sea level. The location of the study is the transition zone of the Molave and Dipterocarp forests. Sporadic patches of natural grasslands and agricultural lands as a result of land conversion were observed in the area.

The transect line was established, representing the different elevations of the watershed, starting from Quadrat One (Q1) with an elevation of 258 meters above sea level to 462 m above sea level of Quadrat Eight (Q8). The transect line from Q1 to Q4 is along the creek while Q5 to Q8 are along the old logging road of the area.

A total of 34 tree species belong to 19 families and 26 genera (Table 2).

Moraceae was found to be the most speciose among the 19 families with five species, followed by Euphorbiaceae (4 spp.), Dipterocarpaceae (4 spp.), Fabaceae (3 spp.), and Lauraceae (3 spp.), as shown in Table 2.

Table 1: Classification scheme for diversity index by Fernando et al. 1998 (as cited in Baliton et al. 2017).

Relative Values	Shannon (H') Index
Very High	3.5 and above
High	3.0-3.49
Moderate	2.5-2.99
Low	2.0-2.49
Very Low	1.9 and below

Table 2: Identified Tree Species.

Scientific Name	Family Name
Calophyllum blancoi Planch. &Triana	Callophylaceae
Canarium ovatum Engl.	Burseraceae
Celtis luzonica Warb.	Cannabaceae
Chisocheton pentandrus (Blanco) Merr.	Meliaceae
Dillenia luzoniensis (S.Vidal) Martelli	Dilleniaceae
Dracontomelon dao (Blanco) Merr.	Anacardiaceae
Endospermum peltatum Merr.	Euphorbiaceae
Fagraea racemosa Jack ex Wall	Gentianaceae
Ficus minahasse (Teijsm. &Vriese) Miq.	Moraceae
Ficus nota (Blanco) Merr.	Moraceae
Ficus septica Burm.f.	Moraceae
Ficus sp.	Moraceae
Ficus variegata Blume	Moraceae
Gomphandra luzoniensis (Merr.) Merr.	Stemonuraceae
Goniothalamus elmeri Merr.	Annonaceae
Kleinhovia hospita L.	Malvaceae
Lithocarpus castellarnauianus (S.Vidal) A.Camus	Malvaceae
Litsea cordata (Jack) Hook. f.	Lauraceae
Litsea glutinosa (Lour.) C.B. Rob.	Lauraceae
Macaranga tanarius (L.) Müll. Arg.	Euphorbiaceae
Mallotus echinatus Elm.	Euphorbiaceae
Mangifera altissima Blanco	Anacardiaceae
Neonauclea bartlingii (DC.) Merr.	Rubiaceae
Neotrewia cumingii (Müll.Arg.) Pax&K. Hoffm.	Euphorbiaceae
Ormosia calavensis Blanco	Fabaceae
Palaquium lanceolatum Blanco	Sapotaceae
Phoebe sterculioides (Elmer) Merr.	Lauraceae
Pouteria macrantha (Merr.) Baehni	Sapotaceae
Pterocarpus indicus Willd.	Fabaceae
Shorea contorta S.Vidal	Dipterocarpaceae
Shorea guiso (Blanco) Blume	Dipterocarpaceae
Shorea palosapis (Blanco) Merr.	Dipterocarpaceae
Shorea polysperma (Blanco) Merr.	Dipterocarpaceae
Syzygium simile (Merr.) Merr.	Myrtaceae

The study on the floristic diversity of the Binaba Watershed (Sarmiento & Mercado 2019) showed a similar result where Moraceae is the most dominant family, followed by Euphorbiaceae. Guingab's (2019) study on the diversity and species composition of the Northern Sierra Madre Natural Park revealed that Euphorbiaceae, Moraceae, Fabaceae, and Lauraceae were among the top ten most speciose families in all forest types. Similar studies on the diversity and species composition of the world's tropical forests revealed that Euphorbiaceae is one of the most dominant families (Pahlevani et al. 2017). These qualitative data indicate similarities in the species composition of tropical forests in the Pacific region, including the Tumauini Watershed Natural Park.

The abundance of Moraceae and Euphorbiaceae in the area indicates that TWNP is a secondary forest, and the presence of Dipterocapaceae indicates the type of forest, which is a mixed dipterocarp forest. The findings of the study are similar to the study of Aureo et al. (2021) conducted within the secondary-growth forest of Mt. Bandila-an Forest Reserve in the Philippines. Moraceae and Euphorbiaceae are among the 6 families dominant in the area.

Quadrats One (Q1) to Q3 were all established along the creek, while the rest were established along the old logging trail. The genus Ficus of the family Moraceae is mostly found in riparian areas in the country (Malabrigo et al. 2014) and is a good indicator of water quantity in a particular area. These species include *Ficusmina hassae, Ficus nota, Ficus septica, Ficus variegata*, and unidentified *Ficus*. Species of Euphorbiaceae, like the *Macaranga,* are pioneer species in the secondary forest.

Relative Density

Results of the study showed that the highest relative density among the 34 tree species identified is *Ficus nota,* with a value of 10.71% (Fig. 4). Relative density shows the numerical strength of the species in relation to the total.

Malabrigo et al. (2014) stated that Ficus nota (Fig. 5) is one of the most important species in riparian areas. It was observed particularly in the Kaliwa River Watershed, a portion of the Sierra Madre Mountain Range with a relative density of 9.35%; the result of the study in the TWNP is much higher than the Relative Density of Kaliwa River of about 1.36%. Similar to other watersheds, *Ficus nota* are usually observed and dispersed, especially along the water bodies and moist areas of the watersheds.

Relative Frequency

Result of this study shows that *Shorea palosapis*, Ficus sp., and *Calophyllum blancoi* have the highest relative frequency value of 7.25% among the 34 species within the quadrats (Fig. 6). These three species of trees frequently appeared in the different quadrats established. This indicates good regeneration performance in the area despite the presence of natural and man-made threats.
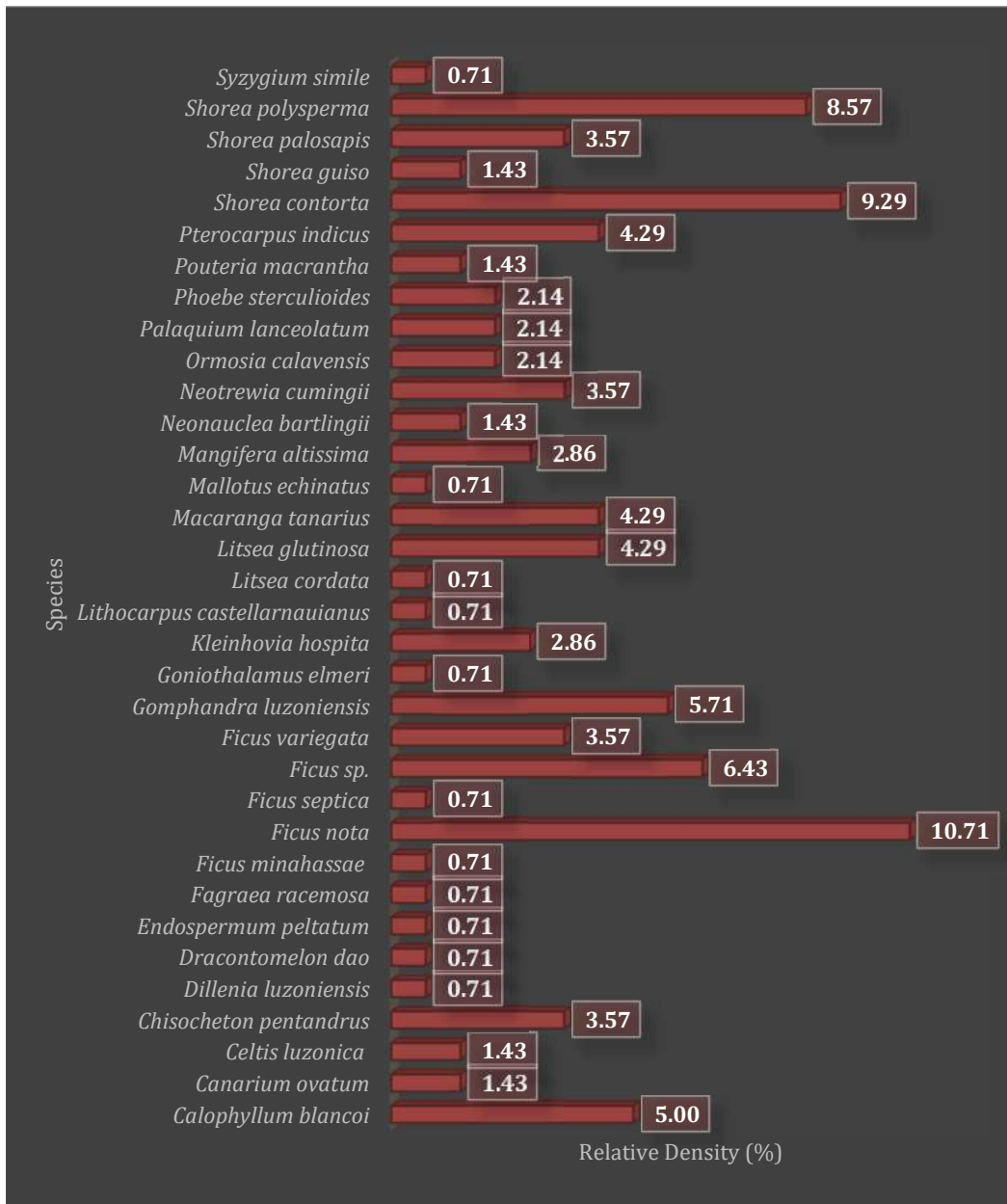
Fig. 4: Relative Density.

Calophyllum blancoi (commonly known as bitanghol) is a generalist species (Fig. 7). According to Guingab (2018), the most widespread species in the NSMNP is bitanghol, which occurs in all forest types except in mangrove forests. The same species was recorded as a generalist in the western slope of Mt. Pangasugan in Leyte Island as it occurred in all altitudinal vegetation zones (Gerhard & Belonias 2011).

Dipterocarps were expected to occur in all quadrats because the vegetation type of the area is a mixed dipterocarp forest but only *Shorea palosapis* gave the highest relative frequency among four dipterocarp species. This means that other dipterocarps are specialists in the area. The wide dispersal of Ficus species in the area is an indicator of the presence of fruit bats, which play an important role in the reproduction of the species in natural forests (Preciado
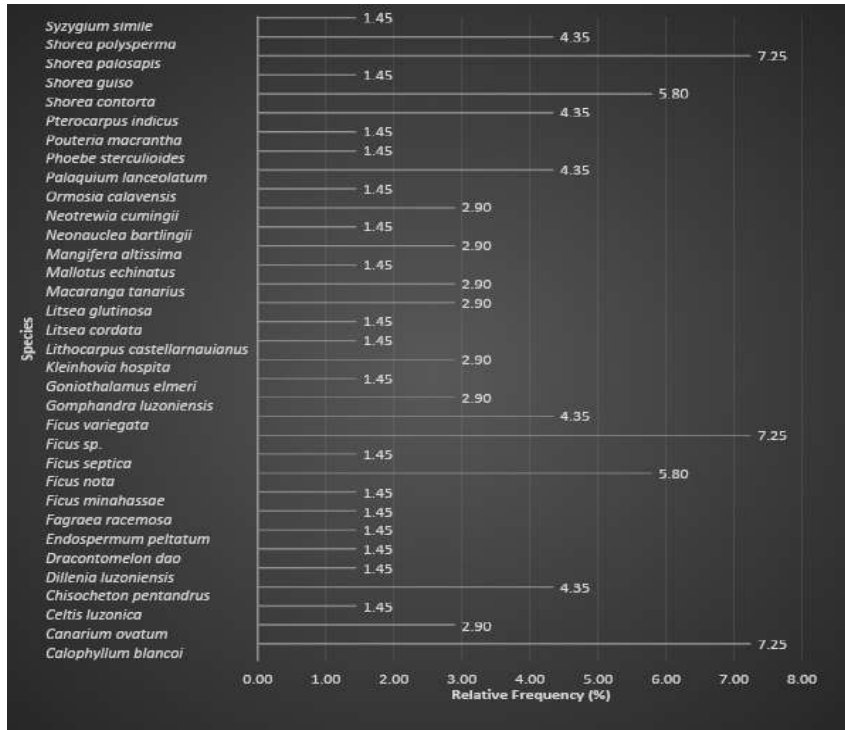
Fig. 5: *Ficus nota*.

Fig. 6: Relative Frequency.

Benítez et al. 2015). Likewise, the presence of this genus indicates the possible presence of other wildlife species, like birds, which adds to the ecological value of the area.

Moraceae, specifically Ficus spp. found to be significant in secondary forests in the tropics, large Ficus species of trees are more effective restoration agents than other remnant trees in disturbed landscapes (Cottee-Jones et al. 2016). The occurrence of generalists such as Ficus sp., *Calophyllum blancoi*, and *Shorea palosapis* with high relative frequency value can contribute to the immediate rehabilitation of the fragmented areas of the park. The management board of the protected area can use these species of trees as the main commodity for reforestation because it is proven to have the

Fig. 7: *Calophyllum blancoi*.

Fig. 8: *Shorea polysmerma*.

capacity to spread and survive in the different elevations of the park.

Relative Dominance

Based on this study, *Shorea polysmerma* (Fig. 8) has the highest relative dominance index of 25.86% among the other 34 species of trees within the sampling area.

The dominance value of the species is influenced by the basal area covered. In this study, *S. polysperma* found in Quadrat 8 showed dominance with a diameter class ranging from 90cm to 110cm.

Shorea polysperma is one of the two most abundant species in five watersheds in Samar (Quimo 2016). The dominance of this species in TWNP (Fig. 9) indicates a high economic value of the forest, specifically the timber produced, and needs to be monitored and protected for the risk of illegal timber harvesting.

Importance Value (IV)

The result of this study revealed that *Shorea polysperma* has the highest IV of 38.78 among the 34 species of trees, followed by *Chisocheton pentandrus* with an IV of 22.18 (Fig. 10).

The species with the least IV is *Litsea cordata*, with a value of 2.30. This species has a DBH of 12cm, a total height of 10m, and one individual. It was located at Quadrat 5. Among the 34 species identified within the eight quadrats, *S. polysperma* is the most important species. It was
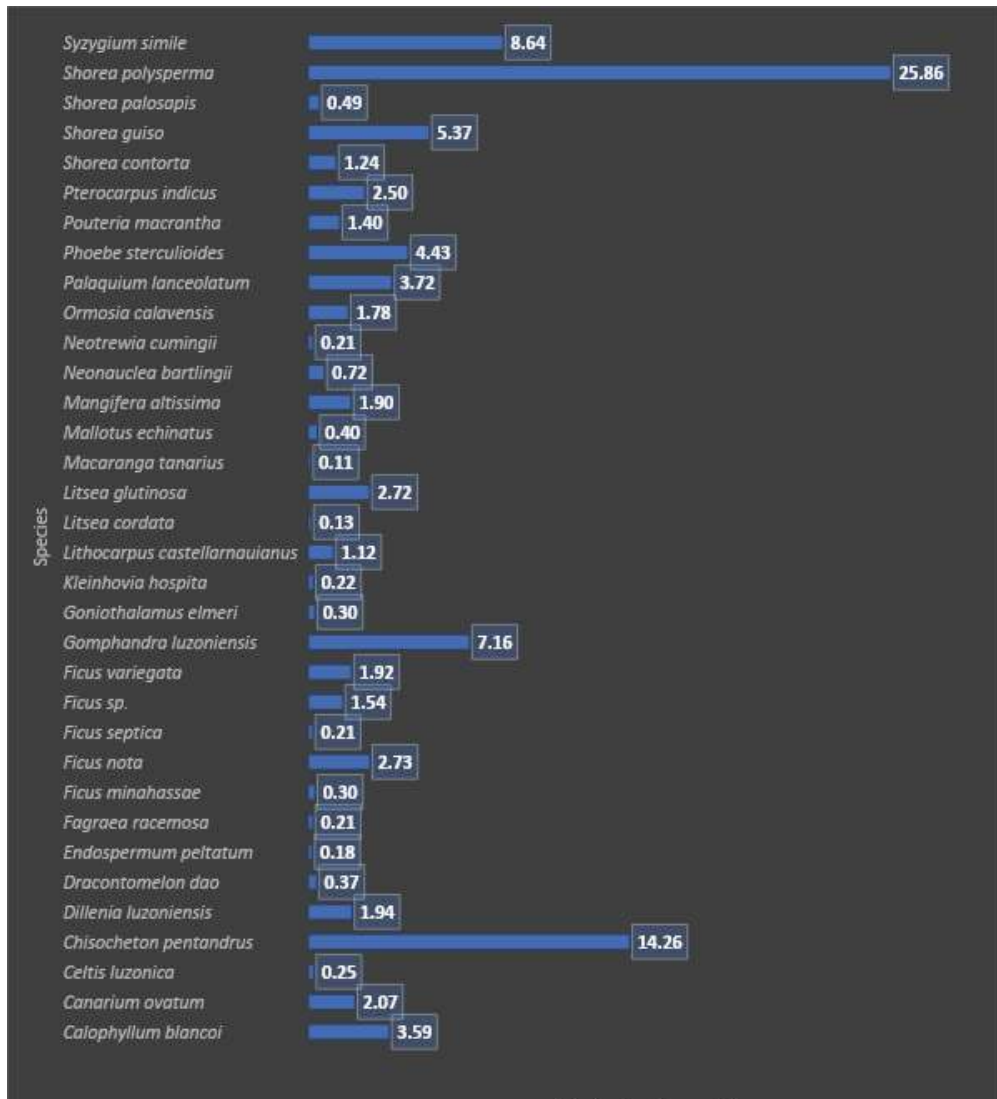
Fig. 9: Relative Dominance Index %.

previously classified as a Critically Endangered species in the 2013 IUCN Red List. The two species having a high IV are influenced by the DBH gained, basal area, number of individuals/count, and frequency. The Importance Value can reach a maximum value of 300, which is the total value of the three indices: Relative Density, Relative Frequency, and Relative Dominance.

Shannon-Wiener Diversity Index

The result of the study shows that Quadrat 8 is the most diverse among all quadrats, with a diversity index of 2.40, while the least is Quadrat 1, with a diversity index of 1.12 (Fig. 11).

Among the quadrats, the highest in terms of species richness and number of individuals was found in Quadrat 8 and it is the factor that influenced the diversity index of the area.

However, based on the classification scheme cited in the Manual on Biodiversity Assessment and Monitoring System for Terrestrial Ecosystems of the DENR (Table 1), Quadrat 1 and Quadrat 6 have "Very Low" values, while the others have "Low" values.

The result indicates immediate protection and rehabilitation of the protected area. Enrichment planting can arrest the status of tree diversity. The scenario is similar in other areas of the Philippines, which is commonly due to the rampant anthropogenic activities in protected areas, such as timber poaching and land conversion, among others (Alaman et al. 2019).
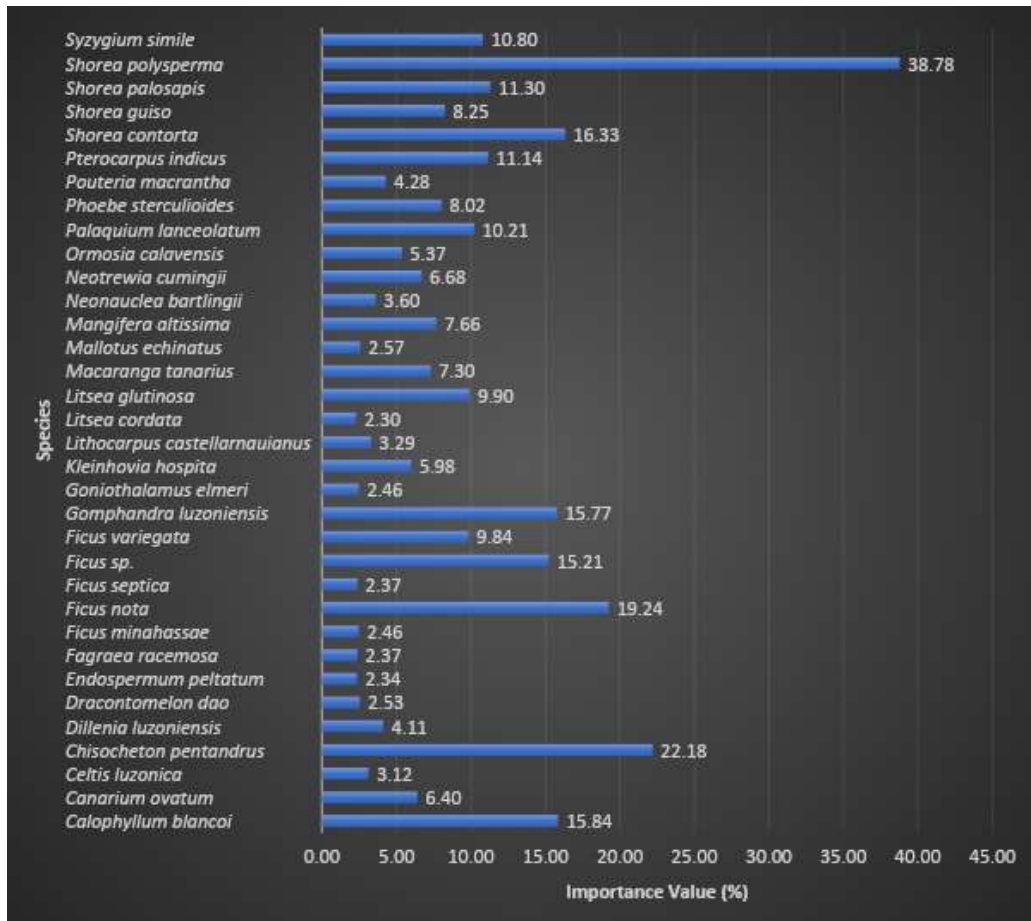
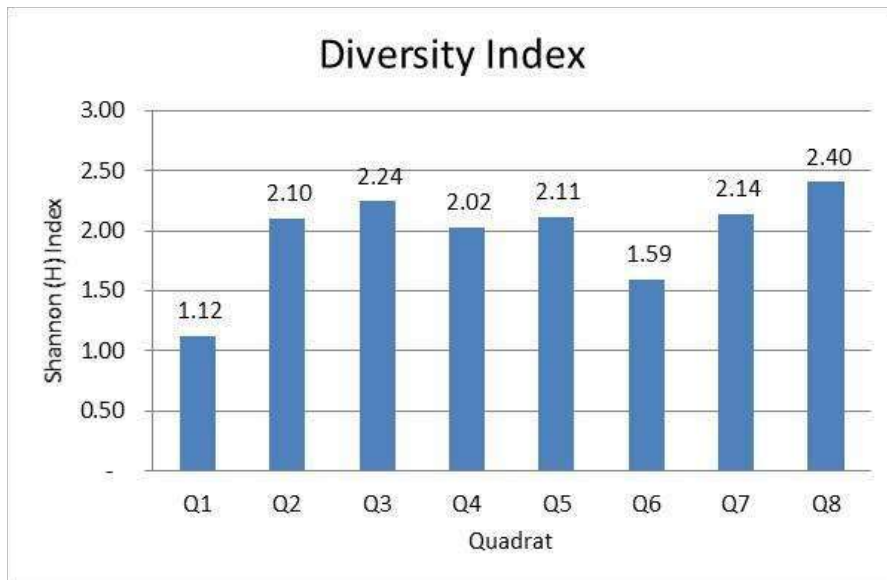Fig. 10: Importance Value.

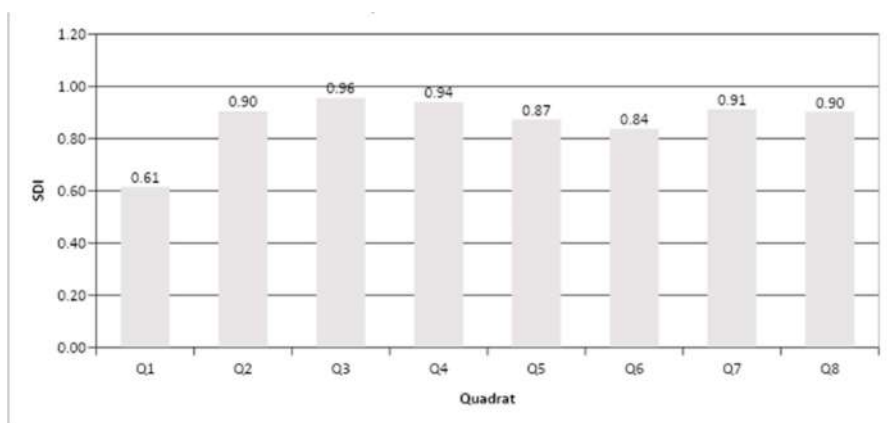Fig. 11: Shannon-Wiener diversity index in TWNP.

Fig. 12: Simpson's Diversity Index.

Fig. 13: Species samples through opportunistic sampling.

Quadrat 1 had the least diversity among all quadrats. The trees have a smaller diameter, less than 10cm dbh, which is outside the range of a diameter class criteria for the 20 x 20 m quadrat. The trees, however, were identified and recorded on the opportunistic sampling classification.

Simpsons Diversity Index

Results of the study showed that among all quadrats, Q3 with the highest SDI value of 0.96, followed by Q4 (0.94) and Q7 (0.91), as shown in (Fig. 12).

Opportunistic Sample Collections

Although opportunistic sample collection outside the

quadrats was not a part of the study, this may contribute to the overall understanding of the diversity of the area. Species of woody and non-woody plants were collected and identified outside the sampling area, some of these are species found along the trails, riverbanks, grassland, and other areas (Fig. 13).

An aggregate of 49 species of trees, shrubs, herbs, and grasses were identified (Table 3). The result of the opportunistic sampling showed a high diversity of flora in comparison to the area sampled.

Conservation Status

Based on the 2021 IUCN Red List and Department

Table 3: Identified plant species within the opportunistic sampling.

Common Name	Scientific Name	Family Name
Bogus	*Acalypha amentaceae*	Euphorbiaceae
Putian	*Alangium javanicum*	Cornaceae
Langil	*Albizia lebbeck*	Fabaceae
	Alseodaphne sp.	Lauraceae
Binayuyu	*Antidesma ghaesambilla*	Phyllanthaceae
Kamansi	*Artocarpus altilis*	Moraceae
Antipolo	*Artocarpus blancoi*	Moraceae
Balinghasai	*Buchanania arborescens*	Anacardiaceae
Ilang ilang	*Cananga odorata*	Annonaceae
Pagsahingin	*Canarium asperum*	Burseraceae
Piling Liitan	*Canarium luzonicum*	Burseraceae
	Carica papaya	Caricaceae
Pugahan	*Caryota cumingii*	Areacaceae
Kalingag	*Cinnamomum mercadoi*	Lauraceae
Bakayau	*Cleistanthus myrianthus*	Phyllanthaceae
	Clerodendrum sp.	Verbenaceae
Kape	*Coffea Arabica*	Rubiaceae
	Dysoxylum parasiticum	Meliaceae
Malakaniue	*Elattostachys verrucosa*	Sapindaceae
Gubas	*Endospermum peltatum*	Euphorbiaceae
	Eschweilera sp.	Lecythidaceae
Bugauak	*Evodia confuse*	Rutaceae
Balatbuaia	*Fagraea racemose*	Loganiaceae
Aplas	*Ficus irisana*	Moraceae
Tabgun	*Ficus ruficaulis*	Moraceae
	Flamingia sp.	Fabaceae
Gmelina	*Gmelina arborea*	Lamiaceae
	Goniothalamus macrophyllus/elmeri	Annonaceae
	Hydnocarpus sp.	Salicaceae
	Kayea sp.	Clusiaceae
Amamali	*Leea aculeate*	Leeaceae
	Leptospermum amboinense	Myrtaceae
	Lithocarpus castellarnauianus	
Bangulo	*Litsea garciae*	Lauraceae
	Litsea varians	Lauraceae
	Macaranga stonei	Euphorbiaceae
Bangkal	*Nauclea orientalis*	Rubiaceae
Malauisak	*Neonauclea reticulate*	Rubiaceae
mamalis	*Pittosporum pentandrum*	Pittosporaceae
Litid	*Poikilospermum erectum*	Urticaceae
Galamay amo	*Schefflera elliptica*	Araliaceae
	Selaginella delicatula	Selaginellaceae

Common Name	Scientific Name	Family Name
Ligas	*Semecarpus cuneiformis*	Anacardiaceae
	Sida rhombifolia	Malvaceae
	Solanum sp.	Solanaceae
	Trametes versicolor	Polyporaceae
	Trema micrantha	Cannabaceae
	Trigonostemon villosus	Euphorbiaceae
Salagong sibat	*Wilkstroemia lanceolata*	Thymelaeaceae

Administrative Order 2017-11 of the DENR, 15 species of trees are classified as Least Concern, 1 Endangered, 5 Vulnerable, 1 Other Threatened Species, and 1 Near Threatened among the 34 species identified in the TWNP (Table 4).

Table 4: Conservation Status of Species in TWNP.

Scientific Name	Category
Calophyllum blancoi Planch. &Triana	
Canarium ovatum Engl.	OTM
Celtis luzonica Warb.	VU
Chisocheton pentandrus (Blanco) Merr.	LC
Dillenia luzoniensis (S.Vidal) Martelli	VU
Dracontomelon dao (Blanco) Merr.	VU
Endospermum peltatum Merr.	LC
Fagraea racemosa Jack ex Wall	
Ficus minahasse (Teijsm. &Vriese) Miq.	
Ficus nota (Blanco) Merr.	LC
Ficus septica Burm.f.	LC
Ficus sp.	
Ficus variegata Blume	LC
Gomphandra luzoniensis (Merr.) Merr.	
Goniothalamus elmeri Merr.	LC
Kleinhovia hospita L.	LC
Lithocarpus castellarnauianus (S.Vidal) A.Camus	NT
Litsea cordata (Jack) Hook. f.	LC
Litsea glutinosa (Lour.) C.B. Rob.	LC
Macaranga tanarius (L.) Müll. Arg.	LC
Mallotus echinatus Elm.	
Mangifera altissima Blanco	
Neonauclea bartlingii (DC.) Merr.	LC
Neotrewia cumingii (Müll.Arg.) Pax&K. Hoffm.	
Ormosia calavensis Blanco	
Palaquium lanceolatum Blanco	
Phoebe sterculioides (Elmer) Merr.	
Pouteria macrantha (Merr.) Baehni	
Pterocarpus indicus Willd.	EN
Shorea contorta S.Vidal	LC
Shorea guiso (Blanco) Blume	VU
Shorea palosapis (Blanco) Merr.	LC
Shorea polysperma (Blanco) Merr.	VU
Syzygium simile (Merr.) Merr.	

Note: OTM- Other Threatened Species; VU- Vulnerable; EN- Endangered; LC- Least Concern; NT-Near Threatened.

Recording of the species with Conservation Status is very significant both for the government and interested groups, particularly for the possibility of propagation and conservation, as mentioned by Chan (2019). The EN and VU species found in the area have known potential timber value used for construction and furniture-making. This is the main reason for the declining quantity in the wild.

CONCLUSION

Results of the study showed that the TWNP has a total of 34 species from 26 genera of the eight families of trees within the 2-km transect line. Among the eight tree families, Moraceae has the highest number of species, such as *Ficus minahassae*, *Ficus nota*, *Ficus septica*, *Ficus variegata,* and an unidentified Ficus sp. Among 34 species, Ficus nota has the highest relative density with a value of 10.71%, followed by *Shorea contorta* with a value of 9.29%. Three species have the same relative frequency of 7.25%, which is the highest among all species, namely, *Shorea palosapis*, *Ficus* sp., and *Calophyllum blancoi*. The most dominant and important species is *Shorea polysperma*, with an Importance Value of 38.78%. The study also revealed that quadrat 8 has the highest diversity index of 2.40. All quadrats, however, indicated "low" diversity indexes. Results showed that Quadrat 3 has the highest Dominance Index of 0.96 among the rest of the quadrats.

The study reveals the need to regulate the harvesting and trading of *Pterocarpus indicus,* an endangered tree species found in the area. By all counts and with proven valid and reliable results, the secondary forest of the protected area is generally low in tree diversity. The status of the tree diversity area is affected by the rampant anthropogenic activities and naturally induced hazards occurring in the protected area, as observed during the assessment along the trails.

In conclusion, it is clear that *Shorea polysperma* is the most important tree species in the area; this tree belongs to the Philippine Mahogany group having high-quality timber and high economic value. Therefore, the forest areas of the watershed need constant monitoring to protect the economically significant native species of trees from the risk of extraction.

RECOMMENDATIONS

The transect method has been used in the assessment of flora and fauna of protected areas. The method is designed to cover the various ecosystems and vegetation of the protected area. Due to the diversified cover, forest types, and land uses of the study area, more transect lines are recommended to increase the sampling intensity for future assessment and research initiatives in the area. This is to provide a more comprehensive output.

An inclusive and intensive assessment of the flora is highly recommended, as observed in the opportunistic sampling wherein a greater number of species were listed outside the sampling area. Future research initiatives in the area shall include the fauna species for a better appreciation of the overall biodiversity of the watershed.

ACKNOWLEDGMENT

REFERENCES

Aleman, B., Calago, J., Pito, E., Tomatao, H., Villanueva, G., Garrido, A., Jr., Alfredo, F., Rey, F. and Villantes, Y., 2019. Species abundance, importance, conservation status, and regenerative potential of the Philippine endemic dipterocarp trees in the southern portion of Mt. Malindang Range Natural Park, Mindanao, Philippines. *Journal of Mindanao Development*, 8(1), p.1467. https://doi.org/10.7828/jmds.v8i1.1467

Aureo, W.A., Reyes, T.D. and Jose, R.P., 2021. Floristic assessment of the Mt. Bandila-an forest reserve in Siquijor, Philippines. 10.21203/rs.3.rs-863087/v1.

Baliton, R.S., Wulandari, C., Landicho, L.D., Budiono, P., Herwanti, S., Rusita, R., Paelmo, R., Cabahug, R.E., Comia, R.A., Visco, R.A. and Castillo, A.K., 2017. Ecological services of agroforestry landscapes in selected watershed areas in the Philippines and Indonesia. *Biotropia*, *24*(1), pp.71-84. DOI: 10.11598/btb.2017.24.1.621.

Biodiversity Management Bureau, 2015. *Guidebook to protected areas of the Philippines*. Biodiversity Management Bureau – Department of Environment and Natural Resources, The Philippines. Retrieved March 6, 2024, from https://issuu.com/oslegarda/docs/guidebook_to_protected_areas_of_the

BMB Technical Bulletin, 2018. Technical Bulletin 2018-02. Biodiversity Management Bureau – Department of Environment and Natural Resources. Retrieved May 6, 2024, from https://elibrary.bmb.gov.ph/elibrary/laws-and-policies/technical-bulletins/

Castillo, L.A., Bantayan, N.C., Canceran, M.S., Barua, L.D., Alegre, A.C., Gonzalvo, K.J.P., Gestiada, E.C., Parducho, V.B., Limpiada, A.A. and Castillo, M.L., 2021. Tree composition, diversity, and stand structure of mid-montane forest in Sipit watershed, Mount Makiling forest reserve ASEAN heritage park, Philippines. *Philippine Journal of Science*, *150*(S1), pp.257-269.

Chan, J., 2019. Saving a Philippine tree last seen a century ago. Retrieved from https://news.mongabay.com/2019/12/saving-a-philippine-tree-last-seen-a-century-ago/. Access date April 3, 2024.

Cottee-Jones, H.E.W., Bajpai, O., Chaudhary, L.B. and Whittaker, R.J., 2016. The importance of Ficus (Moraceae) trees for tropical forest restoration. *Biodiversity and Conservation*, 12, p.304. DOI: https://doi.org/10.1111/btp.12304

Department of Environment and Natural Resources, 2017. DENR Administrative Order 2017-11: Updated national list of threatened Philippine plants and their categories. Retrieved May 6, 2024, from https://leap.unep.org/en/countries/ph/national-legislation/denr-order-no-11-2017-updated-national-list-threatened-plants-and

eNIPAS Act, 2018. Expanded National Integrated Protected Areas System (ENIPAS) Act. Retrieved April 3, 2024, from https://lawphil.net/statutes/repacts/ra2018/ra_11038_2018.html

Guingab, M.V.D., 2019. Floral diversity of the lowland ultrabasic forest in the Northern Sierra Madre Natural Park, Isabela, Luzon, Philippines. *Journal of Biodiversity and Environmental Sciences (JBES)*, 15(5), pp.113-124. DOI: https://innspub.net/jbes/floral-diversity-lowland-ultrabasic-forest-northern-sierra-madre-natural-park-isabela-luzon-philippines/

International Union for Conservation of Nature. 2021. The IUCN Red List of Threatened Species. Version 2021-1. Retrieved May 6, 2024, from https://www.iucnredlist.org/en

Langenberger, G. and Belonias, B.S., 2011. The status of floristic analysis of Mt. Pangasugan, Leyte, Philippines–a conservation priority area classified as "Extremely High Critical". *Annals of Tropical Research*, *33*(2), pp.1-21. DOI: 10.32945/atr3321.2011

Malabrigo, P.L., Umalia, A.A. and Elec, J.P., 2014. Riparian flora of Kaliwa River watershed in the Sierra Madre mountain range, Philippines. *Ecosystems & Development Journal*, 5(1), pp.11-22.

Pahlevani, A.H., 2017. *Diversity of the genus Euphorbia (Euphorbiaceae) in SW Asia* (Doctoral dissertation).

Preciado Benítez, O., Gómez y Gómez, B. B., Navarrete Gutiérrez, D.A. and Horváth, A.. 2015. The use of commercial fruits as attraction agents may increase seed dispersal by bats to degraded areas in Southern Mexico. *Tropical Conservation Science*, 8(2), pp.301-317.

Quimo, J., 2016. Floral composition and timber stock of forest in the Samar Island Natural Park. *Annals of Tropical Research*, 38(23), p. 32945. DOI: https://doi.org/10.32945/atr3823.2016

Sarmiento, R. and Mercado, J.A., 2019. Land use changes and their influence in the conservation of plant diversity within a small Binaba Watershed. *Journal of Biodiversity and Environmental Sciences (JBES)*, 14(1), pp.139-150.

Optimizing Landfill Site Selection and Solid Waste Management in Urbanizing Regions: A Geospatial Analysis of Rewari City, Haryana, India

A. Yadav, P. Kumar and A. Kumar†

Department of Geography, Maharshi Dayanand University, Rohtak, Haryana, India
†Corresponding author: A. Kumar; abhishek.rs.geo@mdurohtak.ac.in

ABSTRACT

Improper disposal of solid waste obstructs drainage systems and pollutes surface water. Additionally, the dumping of unsorted garbage generates emissions and leachate, which harm local ecosystems and contribute to climate change. With Rewari City's growing population, effective municipal solid waste management, including landfill site selection, is crucial. This study employs Geographic Information System (GIS), Analytical Hierarchical Process (AHP), and Weighted Linear Combination (WLC) methodologies to determine appropriate sites for landfills. The FAO, ALOS PALSAR DEM, Sentinel 2B images, Google Earth Pro, and interviews were employed to gather data. The results of the Analytic Hierarchy Process (AHP) indicate that 35.4% of the parameters under consideration are associated with Land Use Land Cover (LULC), whereas roads rank as the second most significant criterion, accounting for 24.0%. The WLC technique determined that 4.65 square kilometers were inappropriate for dump sites, while 0.11 square kilometers were extremely favorable. These findings can assist decision-makers in determining the order of importance for variables when selecting a landfill location.

INTRODUCTION

Solid waste refers to the range of garbage materials arising from human activities that are discarded as unwanted and useless. It encompasses various items, including discarded food, paper, plastics, metals, glass, and other industrial substances that pose significant environmental and health risks if not managed effectively (Al Arni & Elwaheidi 2020, Chandrappa & Das 2012, Cheremisinoff 2003). Annually, around 11.2 billion tonnes of solid trash is gathered globally, and the decomposition of the organic element of this waste is responsible for roughly 5 percent of total greenhouse gas emissions worldwide (UNEP, 2017). Individuals in metropolitan cities in India generate an average of 0.8 kilograms of waste per person every day. The annual municipal solid waste (MSW) generated in metropolitan India is projected to be 68.8 million tonnes (0.573 million metric tonnes per day) in 2008 (Hasan & Ghosal 2023, Karmakar et al. 2023). The composition of MSW generally consists of 51% organic waste, 17% recyclables, 11% hazardous waste, and 21% inert waste. Approximately 40% of all MSW remains uncollected, accumulating in urban areas and contaminating neighboring drains and water bodies. MSW not only causes blockages but also pollutes surface water. Failure to separate waste during collection and transportation results in the disposal of waste in open areas, which produces leachate and gaseous emissions while also generating disturbances in the nearby ecosystem. The leachate pollutes both the groundwater and surface water nearby, while the gaseous emissions add to the phenomenon of global warming. Thus, effective solid waste management is crucial to mitigate these risks and safeguard human health and the environment. Municipal solid waste, originating from households and commercial establishments, requires systematic collection, transportation, treatment, and disposal to prevent pollution and public health hazards (Hong et al. 2017, Narayana 2009, Singh 2019). Proper solid waste management is paramount, emphasizing the need for appropriate landfill site selection and waste

disposal practices. This study explores the various aspects of solid waste management and the importance of landfill site selection in promoting sustainable waste management practices and protecting the environment.

Landfill site selection is critical in municipal solid waste management, which aims to mitigate environmental pollution, protect human health, and ensure urban development. Proper site selection for landfills is essential to minimize the negative impacts of waste disposal on the environment and local communities, including the prevention of water contamination, disease transmission, and other health hazards (Ampofo et al. 2022, Rawal 2019). The selection process involves evaluating multiple criteria, such as environmental, social, technical, and economic factors, to identify locations that are both environmentally sound, economically feasible, and socially acceptable. The complexity of this decision-making problem is compounded by the need to comply with regulations and to consider the long-term implications of landfill operations (Unal et al. 2020).

The Analytical Hierarchy Process (AHP) method and Weighted Linear Combination (WLC) technique are valuable tools in the identification of solid waste disposal sites, offering structured approaches to decision-making (Rahmat et al. 2017, Shahabi et al. 2014). AHP involves breaking down the decision criteria into a hierarchical structure, comparing them pairwise to determine their relative importance, and synthesizing these comparisons to obtain the final ranking of alternatives. This method helps decision-makers consider various factors such as environmental impact, proximity to residential areas, and cost-effectiveness. On the other hand, the WLC technique assigns weights to different criteria based on their importance and combines these weighted criteria to create a composite score for each potential site (Zarin et al. 2021). By integrating these two methods, decision-makers can comprehensively evaluate potential waste disposal sites, leading to more informed and sustainable decisions in solid waste management.

Geographic Information System (GIS) is critical in the landfill site selection process to enable a methodical and scientific approach (Isalou et al. 2013, Jamshidi-Zanjani & Rezaei 2017, Sekulovic & Jakovljevic 2016). GIS facilitates the visualization of spatial data through maps, aiding in interpreting complex relationships and patterns. Multicriteria decision analysis techniques, such as the Analytical Hierarchical Process (AHP) and Weighted Linear Combination (WLC), improve decision-making by taking into account multiple criteria and stakeholder input (Islam et al. 2018, Mousavi et al. 2022, Rezaeisabzevar et al. 2020). Contemporary techniques emphasize the importance of merging indigenous knowledge with advanced spatial

data to improve the analysis of site appropriateness (Mussa & Suryabhagavan 2021, Yildirim et al. 2018, Yousefi et al. 2018). The importance of this selection process is underscored by the need for sustainable waste management practices that align with environmental protection goals, urban life quality, and economic considerations (Hussien & Meaza 2019, Unal et al. 2020, Wayessa et al. 2021).

MATERIALS AND METHODS

The Study Area

Rewari is a municipal city located in the state of Haryana. It is situated between 28°10'25.48'' to 28°13'33.99'' North latitudes and 76°34'23.45'' to 76°39'30.29'' East longitudes (Fig. 1). The city has a total land area of 25.49 square kilometers. The climate of Rewari is predominantly tropical steppe, semi-arid, and hot. Dry conditions, with scorching summers and chilly winters, characterize it. Four distinct seasons occur in a single year. The hot weather season commences in mid-March and extends until the last week of June, after which it is succeeded by the southwest monsoon, which persists until September. The onset of the southwest monsoon occurs in the final week of June and concludes at the end of September, accounting for around 88% of the total annual precipitation. Due to the city's fast industrialization, the number of emigrants has been rising, causing the population to undergo an inflow at various times. The requirement to process household garbage has increased and will continue to increase with the population. To make the city a better place to live, the current waste collection system needs to be updated or replaced with something more modern.

Data Sets

The current study focuses on the identification of landfill sites using Geographic Information System (GIS) techniques. The study utilizes several datasets from various sources to analyze and identify suitable locations for landfill sites. The Land Use Land Cover (LULC) data is sourced from Sentinel 2B satellite imagery having a resolution of 10 meters, which provides detailed information on land cover types. Data on roads, water bodies, canals, and sensitive places are digitized from Google Earth Pro images, aiding in understanding the environmental and social context of the area. Soil data is sourced from the Food and Agriculture Organization of the United Nations (FAO), providing information on soil types and characteristics. The slope data, crucial for identifying suitable landfill sites, is derived from the ALOS PALSAR Digital Elevation Model (DEM) with a resolution of 12.5 meters. The outer boundary of the city, a key reference for

the study area, is obtained from the Department of Town and Country Planning, Haryana. Additional information was collected through interviews with environmental protection officers and citizens near current dumps. The input datasets were georeferenced to the UTM Zone 43N coordinate system and classed with assigned weights. These classed datasets were used to build new maps within the GIS environment.

The shapefiles were transferred to the respective feature datasets, and the raster files were transferred as separate raster datasets within the geodatabase. Integrating these datasets, the study aims to identify suitable locations for landfill sites, considering environmental, social, and infrastructural factors. All the data sets are summarized in Table 1.
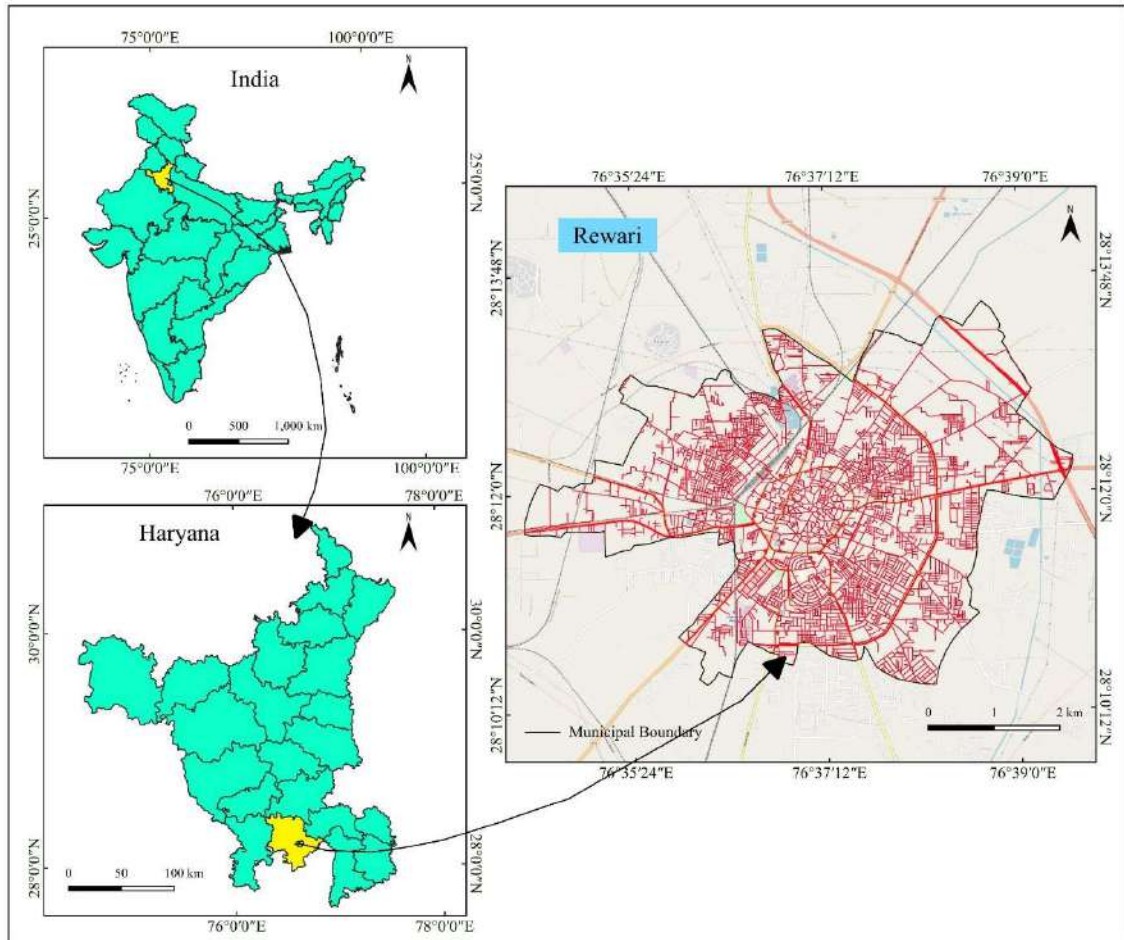

Fig. 1: Study area map.

Table 1: Details of the dataset used to identify landfill sites.

Data	Data Source	Year	Web Access
LULC	Sentinel 2B	2024	https://scihub.copernicus.eu/
Roads	Google Earth Pro	2024	https://earth.google.com/
Water Bodies	Google Earth Pro	2024	https://earth.google.com/
Canal	Google Earth Pro	2024	https://earth.google.com/
Sensitive Places	Google Earth Pro	2024	https://earth.google.com/
Soil	Food and Agriculture Organization UN	1961	https://www.fao.org/soils-portal/
Slope	ALOS PALSAR DEM	2007	https://search.asf.alaska.edu/

Selection of Criteria

Seven criteria, namely LULC, roads, water bodies, canals, sensitive places, soil, and slope were selected to identify suitable landfill sites. The Land Use Land Cover (LULC) data provides insights into the current land cover types, which are essential for understanding the existing landscape and its compatibility with landfill operations. Road networks are vital in determining accessibility to potential landfill sites, ensuring efficient waste transportation and management. Water bodies' data is important to avoid contamination and ensure compliance with environmental regulations. Similarly, canal data helps assess potential impacts on water resources and the surrounding environment. Information on sensitive places such as schools, hospitals, and parks is critical to avoid adverse impacts on human health. Soil data provides insights into the soil characteristics, which influence the suitability of a site for landfill operations. Lastly, slope data is essential for identifying suitable areas with minimal slope, as steep slopes can lead to erosion and instability.

Selection of Buffers for Each Criterion

According to the "Solid Waste Management Rules, 2016", issued by the Ministry of Environment, Forest and Climate Change, India, certain buffer zones are mandated for landfill site construction to protect sensitive areas. Roads require a buffer zone of 500 meters, while water bodies necessitate a 200-meter buffer, and canals require a 30-meter buffer zone. Similarly, sensitive places such as schools, hospitals, and residential areas should have a buffer zone of 500 meters to prevent adverse impacts from landfill operations. In addition to these buffer zones, land suitability for landfill construction is determined by the Land Use Land Cover (LULC) classification, where barren land is considered most suitable due to minimal environmental impact. Low slope gradients are preferred for landfill sites, as they reduce the risk of erosion and instability. Sandy soil is also considered ideal for landfill construction, as it allows for better drainage and reduces the risk of groundwater contamination. By adhering to these guidelines and considering these factors, the construction of landfill sites can be planned to minimize environmental and social impacts, ensuring sustainable waste management practices.

Methods

The methodology for identifying suitable landfill sites begins with the acquisition of data from various sources, including satellite imagery, government records, and field surveys. This data is essential for understanding the environmental and socio-economic context of the study area. Once obtained, the data is processed and projected to the UTM 43N coordinate system using QGIS to ensure consistency in analysis across different datasets. Digitization is carried out where necessary, such as for roads, canals, and other features, to create digital
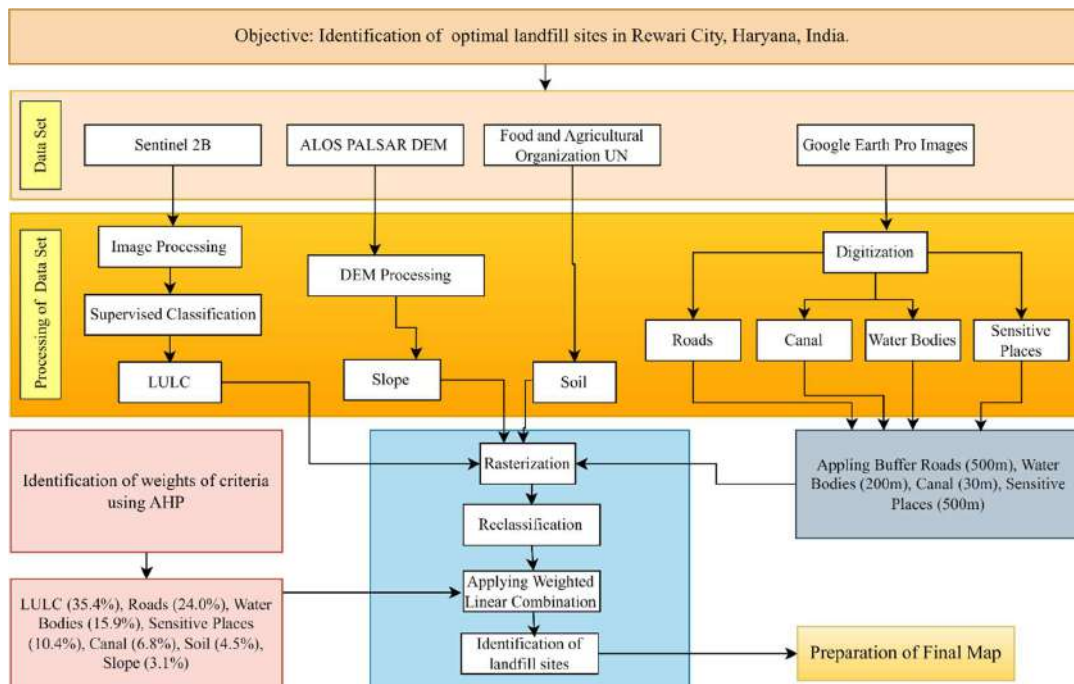

Fig. 2: Flow chart of the methodology used in this study.

representations of these elements. Thematic maps are then prepared for seven Criteria viz. Land Use Land Cover (LULC), Roads, Water Bodies, Canal, Sensitive Places, Soil, and Slope. These maps provide detailed information on the characteristics of the study area, helping to identify suitable locations for landfill sites. Boolean Constraints are applied using different buffer values specified earlier to determine areas where landfill construction is prohibited. For example, a buffer of 500 meters is applied to roads and sensitive places, while a buffer of 200 meters is applied to water bodies. These buffers help to delineate areas where construction should be avoided due to potential environmental or social impacts. Each thematic layer is then rasterized to convert them into raster datasets, which can be more easily analyzed and manipulated. For the purpose of landfill site selection, the AHP method is used to give each thematic layer a weight according to its relative value. Lastly, a comprehensive landfill site suitability map is generated by combining all the criteria using the Weighted Linear Combination technique. The methodology is depicted in Fig. 2.

Analytic Hierarchy Process (AHP)

The AHP is a method for making decisions based on several criteria. It involves defining important criteria for prioritization, such as land-suitability variables, morphometric characteristics, and flood susceptibility factors (Arulbalaji et al. 2019, Hembram & Saha 2020). These criteria are subsequently compared in pairs to determine their relative significance, using a scale ranging from 1 to 9 based on Saaty's fundamental scale. The comparisons' reliability is assessed by evaluating the consistency of these judgments using consistency ratios. The criteria weights are determined by combining the pairwise comparison matrices using the eigenvector approach. These weights are utilized to compute the comprehensive scores of the criteria, hence establishing their priority levels for Landfill Suitable Sites (Ali et al. 2023, Beskese et al. 2015, Mahammad & Islam 2021).

Dividing the consistency index (RI) by the random index yields the consistency ratio (Eq. 1 & Eq. 2). The random index depends on the size of the matrix being compared and is used to determine the acceptable level of inconsistency based on the number of criteria or alternatives. The consistency ratio should ideally be less than 0.1 (10%) for the judgments to be considered consistent. If the consistency ratio exceeds 0.1, it indicates that the judgments are not sufficiently consistent.

$$\text{Consistency Ratio (CR)} = \frac{\text{Consistency Index (CI)}}{\text{Random Index (RI)}} \qquad \dots(1)$$

where the Consistency Index (CI) is calculated as:

$$\text{Consistency Index (CI)} = \frac{\lambda \max - n}{n - 1} \qquad \dots(2)$$

Here, $\lambda_{\max}$ is the maximum eigenvalue of the pairwise comparison matrix, and n is the number of criteria or alternatives being compared.

Weighted Linear Combination

The weighted linear combination (WLC) model is a highly prevalent decision-making approach in Geographic Information Systems (GIS) (Mahini & Gholamalifard 2006, Salman 2006). The technique is commonly utilized in the investigation of land use suitability, site selection, and resource appraisal problems (Al-Hanbali et al. 2011, He et al. 2014, Malczewski 2000, Moeinaddini et al. 2010, Yin et al. 2020). The main factor contributing to its widespread use is the method's simplicity in implementation inside the GIS environment through the utilization of map algebra operations and cartographic modeling (Dhakal & Sharma 2024, Ghosh & Lepcha 2019). The WLC technique for identifying landfill sites involves several key steps. Firstly, the objectives of the analysis are defined, and attribute map layers representing different study area characteristics, such as land use and slope, are identified. Feasible alternatives representing different locations within the study area are then identified. The commensurate attribute maps are created by transforming the original attribute values into a common scale, i.e., from 1 to 5. This transformation ensures that all criteria are comparable and can be combined effectively. After this, the combination of attribute maps and weights is done using a weighted sum approach, where each normalized attribute map is multiplied by its corresponding weight and then added together to obtain the overall suitability score for each alternative cell Eq. 3.

$$S = \sum_{i=1}^{n} W_i X f_i \qquad \dots(3)$$

S = overall suitability score, Wi = weight of the ith evaluation factor, fi = suitability score of the ith evaluation factor.

According to Eastman et al. (1993, 1995), the WLC model can be adjusted for GIS applications by including constraint maps using Eq. 4. In this equation, r[jk] represents the value assigned to the jth cell on the kth constraint map layer. A value of 1 is given to feasible cells, while a value of 0 is assigned to cells that are not feasible.

$$S = \sum_{i=1}^{n} (W_i f_i) \prod_{j=1}^{m} r_{jk} \qquad \dots(4)$$

Finally, the alternatives are ranked based on their suitability scores, with higher scores indicating greater suitability for landfill site selection. The WLC method provides a systematic and transparent approach to decision-making, allowing for a more informed and defensible selection of landfill sites.

RESULTS AND DISCUSSION

Criteria

Land Use Land Cover (LULC): Land Use Land Cover (LULC) is the classification of the earth's surface based on human activities and natural features. It is a critical Criteria in landfill site selection as it helps in identifying areas that are already in use or have a certain cover, such as agricultural, residential, or industrial zones, which may not be suitable for landfilling due to potential conflicts with existing land uses (Rahmat et al. 2017a, Sekulovic & Jakovljevic 2016). The study area's suitable landfill sites were identified using a land use land cover (LULC) map prepared from Sentinel 2 satellite imagery. The map was generated using supervised classification in GIS software, categorizing the land cover into agricultural land, vegetation, built-up area, water bodies, and barren land (Fig. 3a). Barren land was identified as suitable for landfill sites. Because barren land typically has low ecological value, it is often flat and devoid of vegetation, and placing landfills on barren land can minimize conflicts with other land uses and reduce the risk of contamination of nearby water bodies or agricultural areas.

Roads: Roads are considered in landfill site selection due to the need for accessible transportation routes for waste collection vehicles. Proximity to roads can reduce transportation costs and environmental impacts but must be balanced against the potential for traffic congestion and accidents (MAlanbari et al. 2014a, 2014b). The road network map was created using Open Street Maps as the base data source. To assess the suitability of different areas for landfill sites based on their proximity to roads, buffers were applied at intervals of 200, 300, 400, 500, and greater than 500 meters around the road network (Fig. 4). These buffer zones were then reclassified into distance zones, ranked from 1 to 5, to indicate their suitability for landfill sites. In the reclassification scheme, distance zone 1 represents areas within 0 to 200 meters of roads, which are considered less suitable for landfill sites due to potential proximity to roads (Table 2). Conversely, distance zone 5 represents areas located more than 500 meters away from roads, indicating higher suitability for landfill sites.

Water Bodies: Water Bodies, including lakes, rivers, and streams, are important to consider because landfills must be situated at a safe distance to prevent contamination of these water sources through leachate migration (Rahmat et al. 2017, Şener et al. 2011). The water bodies in the study area were demarcated using images from Google Earth Pro in order to evaluate their proximity to prospective landfill locations. Buffers were implemented at regular intervals of 50, 100, 150, 200, and beyond 200 meters surrounding the water bodies (Fig. 4). These buffer zones were then categorized into distance zones ranging from 1 to 5 (Table 2). The suitability of zone 1, which encompasses locations within a 0 to 50-meter radius of water bodies, is lower due to the heightened probabilities of water contamination, adverse effects on aquatic ecosystems, and environmental effects. In contrast, distance zone 5, which encompasses lands situated over 200 meters distant from water bodies, was deemed extremely appropriate for dump sites due to the diminished likelihood of water contamination and ecological damage.

Canals: Canals, like other water bodies, must be protected from potential landfill pollution. They are also part of the infrastructure that may need to be considered for the management of stormwater and leachate from the landfill site (Sk et al. 2020). The study area's canal network was mapped using Google Earth Pro images (Fig 3c). Buffer zones were established at 30-meter intervals and beyond 30 meters from the canals (Fig. 4). The reclassed distance zone 1 denotes areas within 0 to 30 meters from the canals, which are deemed less suitable for landfill sites due to heightened risks of water contamination and environmental impact (Table 2). Conversely, distance zone 5 signifies areas located more than 30 meters away from the canals, which are considered highly suitable for landfill sites due to reduced risks of water pollution and environmental harm.

Sensitive Places: Sensitive Places refer to areas such as schools, hospitals, and protected natural habitats. Landfills should not be located near these places to avoid adverse effects on human health and the environment (Mohsin et al. 2021, Sekulovic & Jakovljevic 2016). The map of sensitive places, which includes schools, hospitals, and parks, was created using Google Earth Pro image (Fig. 3e). Buffers were applied at intervals of 200, 300, 400, 500, and greater than 500 meters around these sensitive locations and then reclassified into distance zones, ranging from 1 to 5, where distance zone 1 represents areas within 0 to 200 meters from sensitive places (Fig. 4) (Table 2), which are considered less suitable for landfill sites due to potential impacts on public health, safety, and quality of life. On the other hand, distance zone 5 represents areas located more than 500 meters away from sensitive places, which are deemed highly suitable for landfill sites due to minimized disturbance to these areas, enhanced public health and safety by reducing environmental hazards, and improved community relations.

Soil: Soil is a key factor in landfill site selection due to its role in the natural attenuation of contaminants and support for the landfill structure. Soil type affects the permeability and stability of the site, which are crucial for preventing leachate migration and ensuring structural Ramu integrity (Ramu et al. 2023).
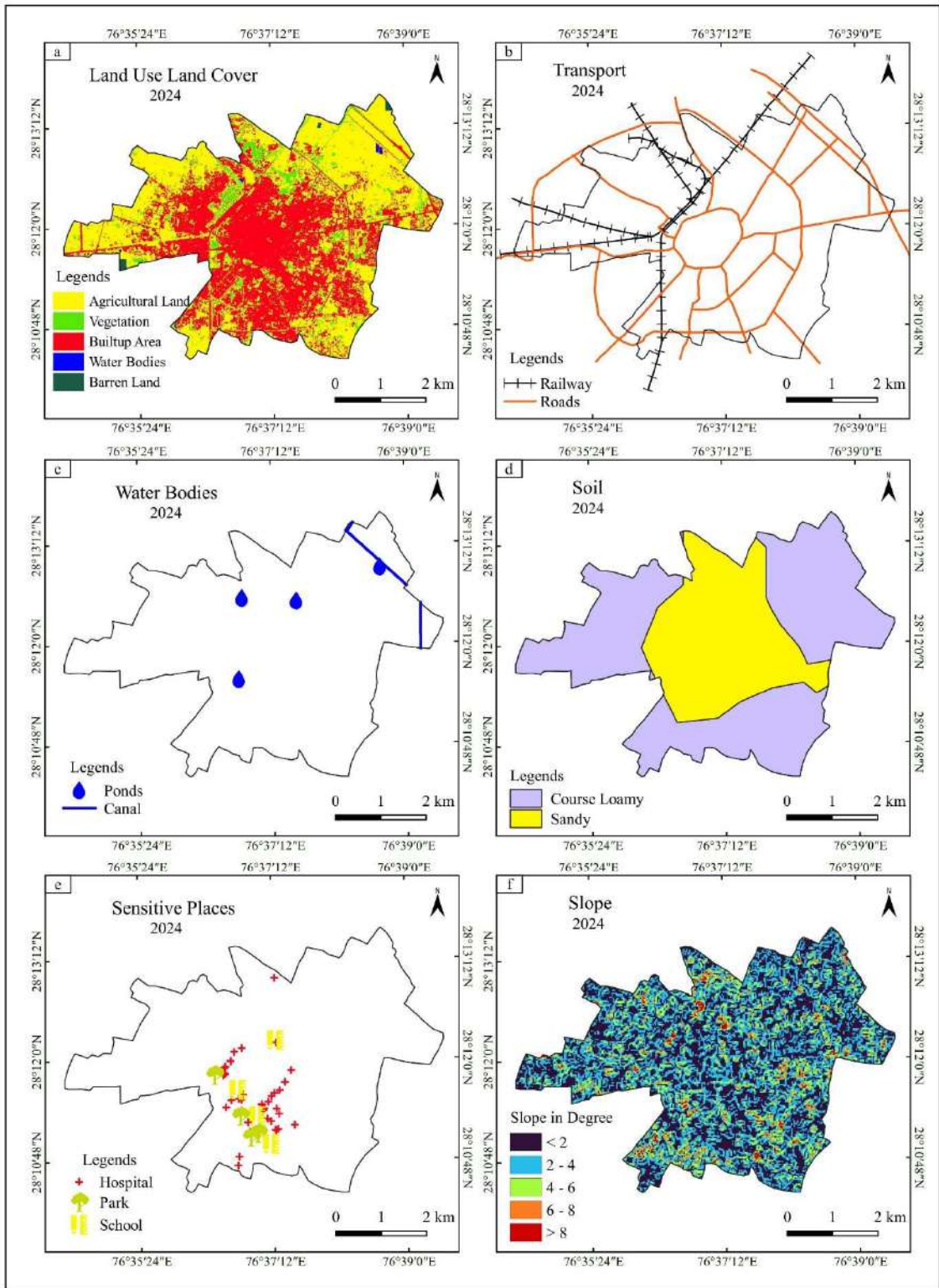
Fig. 3: Map showing the distribution of criteria in the Rewari City, namely LULC (a), roads (b), water bodies (c), canals (c), soil (d), sensitive places (e), and slope (f).
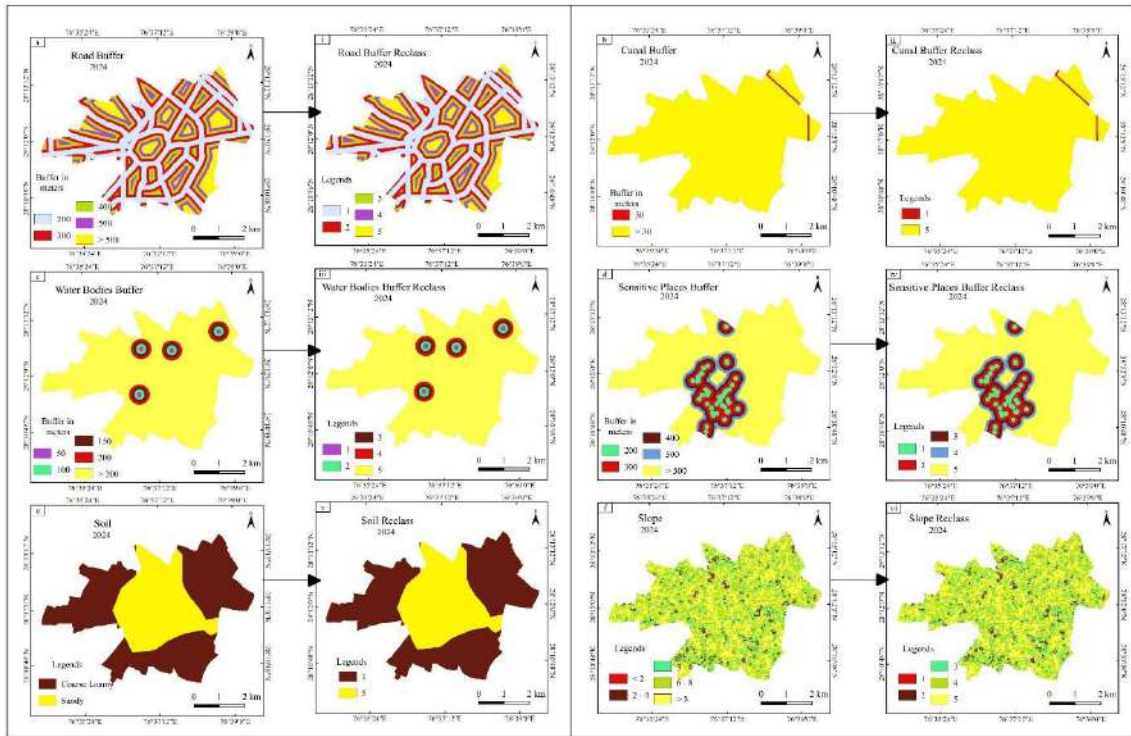
Fig. 4: Map showing the buffer applied on each criterion and their respective ranking from 1 to 5.

The soil map was developed using data from the FAO to assess its suitability for landfill sites based on soil types. The soil was classified into two main categories, Course Loamy and Sandy (Fig. 3d). These classifications were further reclassified into Zone 1, representing Course Loamy soil, considered less suitable, and Zone 5, representing Sandy soil, considered highly suitable for landfill sites (Fig. 4) (Table 2). Advantages of locating landfill sites in sandy soil include enhanced drainage, lower environmental impact due to reduced contaminant spread, and easier construction. However, disadvantages include the risk of leachate migration, the potential for subsidence, and limited soil stability, which can pose challenges for landfill infrastructure.

Slope: The slope is relevant because steep slopes can complicate landfill construction and operation, increase erosion risks, and affect the stability of the landfill. Flatter areas are generally preferred to minimize these issues (Ramu et al. 2023, Şener et al. 2011). The slope map was generated using the ALOS PALSAR Digital Elevation Model to evaluate its suitability for landfill sites based on the degree of slope. The slope was classified into five categories: slopes less than 2 degrees, slopes between 2-4 degrees, slopes between 4-6 degrees, slopes between 6-8 degrees, and slopes greater than 8 degrees (Fig. 3f). These categories were

reclassified into distance zones ranging from 1 to 5, with zone 1 representing slopes greater than 8 degrees, considered less suitable, and zone 5 representing slopes less than 2 degrees, considered highly suitable for landfill sites (Fig. 4) (Table 2).

Identification of Suitable Sites

The identification of landfill sites is a multifaceted process that incorporates various criteria, and both the AHP and WLC are prominent methods used in this context. AHP is advantageous for its ability to handle multiple criteria and its simplicity in dealing with both qualitative and quantitative data, which is crucial for prioritizing landfill siting alternatives (Moeinaddini et al. 2010). The results of AHP indicate that Land Use Land Cover (LULC) was assigned the highest weightage, comprising 35.4% of the decision-making process (Table 2, Table 3 and Table 4). This suggests that the composition and characteristics of the land, including its current use and cover types, are deemed crucial in site selection. Roads were deemed the second most important criterion, with a weightage of 24.0%, highlighting the significance of accessibility and transportation infrastructure in landfill site planning. Water Bodies followed closely behind, with a weightage of 15.9%, emphasizing the need to consider environmental factors and potential impacts on water resources. Sensitive Places,

Table 2: Criteria for Landfill site selection suitability and their rank.

Sr. No.	Factor	Sub-criteria/alternatives	Suitability index (ranking)	Area in sq. km	Area (%)
1	LULC	Agricultural Land	3	12.6	49.41
		Vegetation	4	1.96	7.69
		Builtup	1	10.78	42.27
		Water Bodies	2	0.08	0.31
		Barren Land	5	0.08	0.31
2	Roads	200	1	9.87	38.71
		300	2	6.62	25.96
		400	3	4.31	16.90
		500	4	2.55	10.00
		> 500	5	2.16	8.47
3	Canal	30	1	0.19	0.75
		> 30	5	25.31	99.25
4	Water Bodies	50	1	0.12	0.47
		100	2	0.37	1.45
		150	3	0.62	2.43
		200	4	0.87	3.41
		> 200	5	23.49	92.12
5	Soil	Course Loamy	1	16	62.75
		Sandy	5	9.5	37.25
6	Sensitive Places	200	1	1.1	4.31
		300	2	1.75	6.86
		400	3	1.53	6.00
		500	4	1.45	5.69
		> 500	5	19.67	77.14
7	Slope	< 2	5	0.25	0.98
		2 to 4	4	0.81	3.18
		4 to 6	3	3.34	13.10
		6 to 8	2	10.67	41.84
		> 8	1	10.42	40.86

Table 3: Pairwise comparison matrix for Criteria for solid waste management.

	LULC	Roads	Water Bodies	Sensitive Places	Canal	Soil	Slope
LULC	1	2	3	4	5	6	7
Roads	1/2	1	2	3	4	5	6
Water Bodies	1/3	1/2	1	2	3	4	5
Sensitive Places	1/4	1/3	1/2	1	2	3	4
Canal	1/5	1/4	1/3	½	1	2	3
Soil	1/6	1/5	1/4	1/3	1/2	1	2
Slope	1/7	1/6	1/5	¼	1/3	1/2	1

including schools, hospitals, and parks, were assigned a weightage of 10.4%, indicating the importance of minimizing the impact on these areas. Canals and Soil were assigned weightage of 6.8% and 4.5%, respectively, suggesting that

Table 4: Principal eigenvector of the pairwise comparison matrix.

Sr. No.	Criterion	Weights	Error (+/-)
1	LULC	35.4%	9.7%
2	Roads	24.0%	5.4%
3	Water Bodies	15.9%	3.5%
4	Sensitive Places	10.4%	2.4%
5	Canal	6.8%	1.6%
6	Soil	4.5%	1.1%
7	Slope	3.1%	1.0%

λ_{max} = 7.19, CI = 0.09, RI = 1.32, CR = 2.4% i.e. less than 10%.

while they are considered in site selection, their influence is relatively lower compared to other factors (Table 4). The slope was assigned the lowest weightage of 3.1%, indicating that while terrain characteristics are considered, they are of lesser importance compared.

WLC, on the other hand, is frequently employed for the initial identification of suitable sites by integrating multiple criteria into a composite index (Rezaeisabzevar et al. 2020). It is a multicriteria decision-making approach used to derive composite maps in Geographic Information Systems (GIS) and to evaluate based on multiple criteria in various fields. The fundamental formula for WLC is given by the sum of the products of the criteria values and their corresponding {(LULC × 35.4) + (Roads × 24) + (Water Bodies × 15.9) + (Sensitive Places 10.4) + (Canal × 6.8) + (Soil × 4.5) + (Slope × 3.1)} (Malczewski 2000, Mateo 2012, Sivaji et al. 2022). The results indicate that out of the total study area, the largest proportion was classified as "Less Suitable," covering an area of 12.58 square kilometers (Fig. 5, Fig. 6). This suggests that a significant portion of the study area meets the criteria set for less suitability for landfill sites. The second-largest category was "Unsuitable," with an area of 4.65 square kilometers, indicating areas that do not meet the criteria for landfill site suitability. "Moderately suitable" sites covered an area of 3.46 square kilometers, suggesting areas that may require further evaluation or mitigation
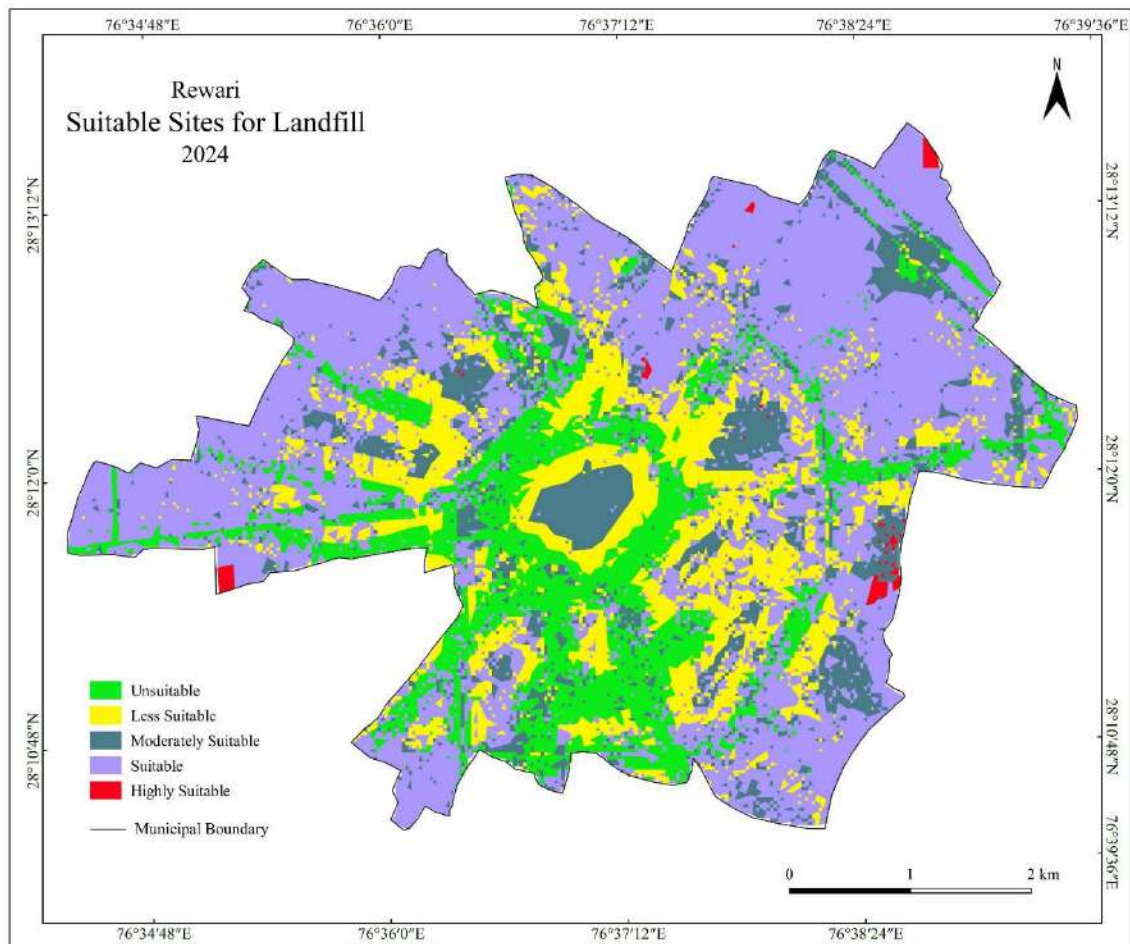

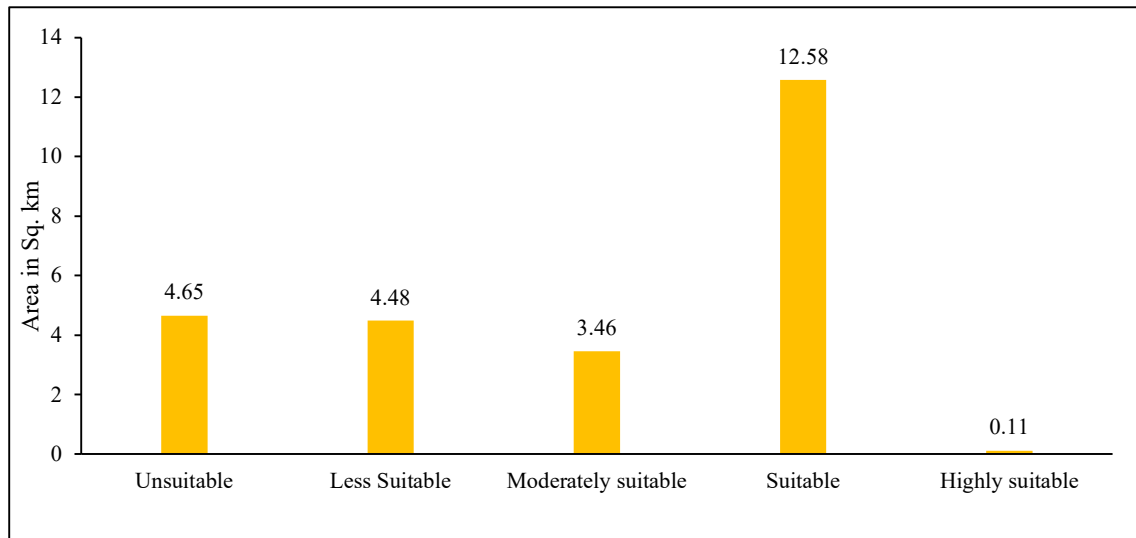Fig. 5: Final map of landfill site suitability.

Fig. 6: Area under landfill site suitability classes.

measures before being considered suitable. Interestingly, a small area of 0.11 square kilometers was classified as "Highly suitable," indicating a small but potentially ideal location for landfill development (Fig. 5, Fig. 6).

Both the AHP and WLC are valuable in the landfill site selection process. Their integration within a GIS environment is particularly effective. The combination of AHP and WLC within a GIS framework is also recommended for its ability to minimize public health risks and environmental degradation (Saleh et al. 2020). The findings of this work provide valuable insights for decision-makers and planners in identifying appropriate sites for landfill development while considering various environmental and socio-economic factors.

CONCLUSIONS

The study focuses on identifying landfill sites using Geographic Information Systems (GIS) techniques. It uses various datasets from various sources, including Sentinel 2B satellite imagery, Google Earth Pro images, water bodies, canals, and sensitive places data, soil data from the FAO, slope data from ALOS PALSAR Digital Elevation Model (DEM), and interviews with environmental protection officers and citizens. Each of these criteria plays a significant role in landfill site selection. LULC ensures compatibility with existing land uses, roads provide necessary access, water bodies and canals must be protected from contamination, sensitive places require a buffer from landfill impacts, soil properties are crucial for containment and stability, and slope affects the feasibility of construction and operation. The AHP and WLC are prominent methods used in this context. AHP is advantageous for its ability to handle multiple criteria and

its simplicity in dealing with both qualitative and quantitative data. The results indicate that Land Use Land Cover (LULC) is the highest weightage, comprising 35.4% of the decision-making process. Roads are the second most important criterion, with 24.0% emphasizing the significance of accessibility and transportation infrastructure in landfill site planning. Water Bodies follow closely behind, with 15.9%, emphasizing the need to consider environmental factors and potential impacts on water resources. Sensitive Places, including schools, hospitals, and parks, are assigned 10.4%, emphasizing the importance of minimizing their impact. Canals and Soil are assigned 6.8% and 4.5%, respectively, suggesting that while they are considered in site selection, their influence is relatively lower compared to other factors. Notably, a compact region measuring 0.11 square kilometers was designated as "Highly suitable," suggesting a modest yet possibly optimal site for landfill expansion. The findings provide valuable insights for decision-makers and planners in identifying appropriate sites for landfill development while considering various environmental and socio-economic factors. The combination of AHP and WLC within a GIS framework is recommended for its ability to minimize public health risks and environmental degradation.

REFERENCES

Al Arni, S.S. and Elwaheidi, M.M., 2020. Solid Waste Management. In: *Concise Handbook of Waste Treatment Technologies*, pp.29–37. https://doi.org/10.1201/9781003112266-6

Alanbari, M.A., Al-Ansari, N. and Jasim, H.K., 2014a. GIS and multicriteria decision analysis for landfill site selection in AL-HashimyahQadaa. *Natural Science*, 6(5), pp.282–304.

Alanbari, M., Al-Ansari, N., Jasim, H. and Knutsson, S., 2014b. Al-Mseiab

Qadaa landfill site selection using GIS and multicriteria decision analysis. *Engineering*, 6(9), pp.526–549.

Al-Hanbali, A., Alsaaideh, B. and Kondoh, A., 2011. Using GIS-based weighted linear combination analysis and remote sensing techniques to select optimum solid waste disposal sites within Mafraq City, Jordan. *Journal of Geographic Information System*, 3(04), pp.267.

Ali, I., Islam, A., Ali, S.M. and Adnan, S., 2023. Identification and selection of suitable landfill sites using GIS-based multi-criteria decision analysis in the Peshawar District, Pakistan. *Waste Management & Research*, 41(3), pp.608–619.

Ampofo, S., Sackeyb, I., Danaaa, L. and Kusibua, M.M., 2022. Multi-criteria assessment (Mca) and selection of a solid waste disposal site within Wa Municipality, Upper West Region, Ghana. *Journal of Wastes and Biomass Management (JWBM)*, 4(2), pp.83–91.

Arulbalaji, P., Padmalal, D. and Sreelash, K., 2019. GIS and AHP techniques based delineation of groundwater potential zones: A case study from southern Western Ghats, India. *Scientific Reports*, 9(1), pp.2082.

Beskese, A., Demir, H.H., Ozcan, H.K. and Okten, H.E., 2015. Landfill site selection using fuzzy AHP and fuzzy TOPSIS: a case study for Istanbul. *Environmental Earth Sciences*, 73(7), pp.3513–3521. https://doi.org/10.1007/S12665-014-3635-5

Chandrappa, R. and Das, D.B., 2012. *Solid Waste Management*. Springer, p.681. https://doi.org/10.1007/978-3-642-28681-0

Cheremisinoff, N.P., 2003. *Handbook of Solid Waste Management and Waste Minimization Technologies*. Oxford Publications, pp.34–95. https://doi.org/10.1016/B978-075067507-9/50004-8

Dhakal, D. and Sharma, K., 2024. QWLCPM: A Method for QoS-Aware Forwarding and Caching Using Simple Weighted Linear Combination and Proximity for Named Data Vehicular Sensor Network. *Electronics*, 13(7), p.1183.

Ghosh, P. and Lepcha, K., 2019. Weighted linear combination method versus grid-based overlay operation method–A study for potential soil erosion susceptibility analysis of Malda district (West Bengal) in India. *The Egyptian Journal of Remote Sensing and Space Science*, 22(1), pp.95–115.

Hasan, M.S. and Ghosal, S., 2023. Informal plastic waste recycling firms in rural eastern India: Implications for livelihood and health. *Clinical Epidemiology and Global Health*, 21, p.1286. https://doi.org/10.1016/J.CEGH.2023.101286

He, X., Hong, Y., Yu, X., Cerato, A.B., Zhang, X. and Komac, M., 2014. *Landslide Science for a Safer Geoenvironment: Methods of Landslide Studies*. Springer, pp.371–377.

Hembram, T.K. and Saha, S., 2020. Prioritization of sub-watersheds for soil erosion based on morphometric attributes using fuzzy AHP and compound factor in Jainti River basin, Jharkhand, Eastern India. *Environment, Development and Sustainability*, 22(2), pp.1241–1268. https://doi.org/10.1007/S10668-018-0247-3

Hong, J., Chen, Y., Wang, M., Ye, L., Qi, C., Yuan, H., Zheng, T. and Li, X., 2017. Intensification of municipal solid waste disposal in China. *Renewable and Sustainable Energy Reviews*, 69, pp.168–176.

Hussien, K. and Meaza, H., 2019. A GIS-based multi-criteria evaluation approach location suitability modeling for solid waste disposal: Dire Dawa City, East Hararghe, Ethiopia. *Papers in Applied Geography*, 5(3–4), pp.272–293.

Isalou, A.A., Zamani, V., Shahmoradi, B. and Alizadeh, H., 2013. Landfill site selection using integrated fuzzy logic and analytic network process (F-ANP). *Environmental Earth Sciences*, 68(6), pp.1745–1755. https://doi.org/10.1007/S12665-012-1865-Y

Islam, A., Ali, S.M., Afzaal, M., Iqbal, S. and Zaidi, S.N.F., 2018. Landfill site selection through analytical hierarchy process for twin cities of Islamabad and Rawalpindi, Pakistan. *Environmental Earth Sciences*, 77(3), p.314. https://doi.org/10.1007/S12665-018-7239-3

Jamshidi-Zanjani, A. and Rezaei, M., 2017. Landfill site selection using a combination of fuzzy logic and a multi-attribute decision-making

approach. *Environmental Earth Sciences*, 76(13), pp.16-28. https://doi.org/10.1007/S12665-017-6774-7

Karmakar, A., Daftari, T., Sivagami, K., Chandan, M.R., Shaik, A.H., Kiran, B. and Chakraborty, S., 2023. A comprehensive insight into Waste to Energy conversion strategies in India and its associated air pollution hazard. *Environmental Technology and Innovation*, 29, p.301. https://doi.org/10.1016/j.eti.2023.103017

Mahammad, S. and Islam, A., 2021. Evaluating the groundwater quality of Damodar Fan Delta (India) using fuzzy-AHP MCDM technique. *Applied Water Science*, 11(7). https://doi.org/10.1007/S13201-021-01408-2

Mahini, A.S. and Gholamalifard, M., 2006. Siting MSW landfills with a weighted linear combination methodology in a GIS environment. *International Journal of Environmental Science & Technology*, 3, pp.435–445.

Malczewski, J., 2000. On the use of weighted linear combination method in GIS: common and best practice approaches. *Transactions in GIS*, 4(1), pp.5–22.

Moeinaddini, M., Khorasani, N., Danehkar, A. and Darvishsefat, A.A., 2010. Siting MSW landfill using weighted linear combination and analytical hierarchy process (AHP) methodology in GIS environment (case study: Karaj). *Waste Management*, 30(5), pp.912–920.

Mohsin, M., Ali, S.A., Shamim, S.K. and Ahmad, A., 2021. A GIS-based novel approach for sustainable sanitary landfill site selection using integrated fuzzy AHP and machine learning algorithms. *Research Square*, 71, p. 64

Mousavi, S.M., Darvishi, G., Mobarghaee Dinan, N. and Naghibi, S.A., 2022. Optimal landfill site selection for solid waste of three municipalities based on boolean and fuzzy methods: A case study in Kermanshah Province, Iran. *Land*, 11(10), pp.1779. https://doi.org/10.3390/land11101779

Mussa, A. and Suryabhagavan, K.V., 2021. Solid waste dumping site selection using GIS-based multi-criteria spatial modeling: A case study in Logia town, Afar region, Ethiopia. *Geology, Ecology, and Landscapes*, 5(3), pp.186-198. https://doi.org/10.1080/24749508.2021.1950535

Narayana, T., 2009. Municipal solid waste management in India: From waste disposal to recovery of resources? *Waste Management*, 29(3), pp.1163-1166. https://doi.org/10.1016/j.wasman.2008.11.020

Rahmat, Z.G., Niri, M.V., Alavi, N., Goudarzi, G., Babaei, A.A., Baboli, Z. and Hosseinzadeh, M., 2017. Landfill site selection using GIS and AHP: A case study: Behbahan, Iran. *KSCE Journal of Civil Engineering*, 21(1), pp.111-118. https://doi.org/10.1007/S12205-016-0296-9

Ramu, P., Santosh, B.S. and Praveen, S., 2023. An Integrated GIS-AHP Approach for Municipal Solid Waste Landfill Siting in Srikakulam District, Andhra Pradesh. *Nature Environment & Pollution Technology*, 22(1), pp.163-180.

Rawal, N., 2019. An approach for selection of solid waste disposal sites by rapid impact assessment matrix and environmental performance index analysis. *International Journal of Environment and Pollution*, 66(1–3), pp.127-142. https://doi.org/10.1504/IJEP.2019.100282

Rezaeisabzevar, Y., Bazargan, A. and Zohourian, B., 2020. Landfill site selection using multi-criteria decision making: Influential factors for comparing locations. *Journal of Environmental Sciences*, 93, pp.170-184. https://doi.org/10.1016/j.jes.2020.01.001

Saleh, S.K., Aliani, H. and Amoushahi, S., 2020. Application of modeling based on fuzzy logic with multi-criteria method in determining appropriate municipal landfill sites (case study: Kerman City). *Arabian Journal of Geosciences*, 13(22). https://doi.org/10.1007/S12517-020-06213-W

Salman, S.M., 2006. Siting MSW landfills with a weighted linear combination methodology in a GIS environment. *International Journal of Environment Science and Technology*, 3(4), p.53

Sekulovic, D. and Jakovljevic, G., 2016. Landfill site selection using GIS

technology and the analytic hierarchy process. *Vojnotehnicki Glasnik*, 64(3), pp.769-783. https://doi.org/10.5937/VOJTEHG64-9578

Şener, Ş., Sener, E. and Karagüzel, R., 2011. Solid waste disposal site selection with GIS and AHP methodology: A case study in Senirkent-Uluborlu (Isparta) Basin, Turkey. *Environmental Monitoring and Assessment*, 173(1–4), pp.533-554. https://doi.org/10.1007/S10661-010-1403-X

Shahabi, H., Keihanfard, S., Ahmad, B. Bin and Amiri, M.J.T., 2014. Evaluating Boolean, AHP, and WLC methods for the selection of waste landfill sites using GIS and satellite images. *Environmental Earth Sciences*, 71, pp.4221-4233. https://doi.org/10.1007/s12665-013-2864-2

Singh, A., 2019. Managing the uncertainty problems of municipal solid waste disposal. *Journal of Environmental Management*, 240, pp.259-265. https://doi.org/10.1016/j.jenvman.2019.02.022

Sk, M.M., Ali, S.A. and Ahmad, A., 2020. Optimal sanitary landfill site selection for solid waste disposal in Durgapur city using geographic information system and multi-criteria evaluation technique. *KN-Journal of Cartography and Geographic Information*, 70, pp.163-180. https://doi.org/10.1007/s42419-020-00039-0

Unal, M., Cilek, A. and Guner, E.D., 2020. Implementation of fuzzy, Simos and strengths, weaknesses, opportunities and threats analysis for municipal solid waste landfill site selection: Adana City case study. *Waste Management & Research*, 38(1_suppl), pp.45-64. https://doi.org/10.1177/0734242X20908159

UNEP, 2017. Solid waste management | UNEP - UN Environment Programme. Available at https://www.unep.org/explore-topics/resource-efficiency/what-we-do/cities/solid-waste-management.   Accessed on May 13, 2024.

Wayessa, S.G., Duresa, J.N., Beyene, A.A. and Regasa, M.S., 2021. Suitable Site Selection and Location Allocation of Solid Waste Collection Bin by Using Geographic Information Systems: A Case of Nekemte Town. *Journal of Building Material Science*, 3(1), pp.22-30.

Yildirim, V., Memisoglu, T., Bediroglu, S. and Colak, H.E., 2018. Municipal solid waste landfill site selection using multi-criteria decision making and GIS: case study of Bursa province. *Journal of Environmental Engineering and Landscape Management*, 26(2), pp.107-119. https://doi.org/10.3846/16486897.2018.1493137

Yin, S., Li, J., Liang, J., Jia, K., Yang, Z. and Wang, Y., 2020. Optimization of the weighted linear combination method for agricultural land suitability evaluation considering current land use and regional differences. *Sustainability*, 12(23), pp.10134-10145. https://doi.org/10.3390/su122310134

Yousefi, H., Javadzadeh, Z., Noorollahi, Y. and Yousefi-Sahzabi, A., 2018. Landfill site selection using a multi-criteria decision-making method: A case study of the salafcheghan special economic zone, Iran. *Sustainability (Switzerland)*, 10(4), pp.1107-1120. https://doi.org/10.3390/SU10041107

Zarin, R., Azmat, M., Naqvi, S.R., Saddique, Q. and Ullah, S., 2021. Landfill site selection by integrating fuzzy logic, AHP, and WLC method based on multi-criteria decision analysis. *Environmental Science and Pollution Research*, 28(16), pp.19726-19741. https://doi.org/10.1007/S11356-020-11975-7

Environmental Assessment Methods for Dissolution of Soil

Deepanjali Sahu[1][†] , **M. K. Tiwari**[1] **and Arunachal Sahu**[2]

[1]Dr. C. V. Raman University, Kota Bilaspur, C.G., India

[2]Chhattisgarh Swami Vivekanand Technical University, Bhilai, C.G., India

†Corresponding author: Deepanjali Sahu; deepanjalisahu23@gmail.com

ABSTRACT

Water plays a crucial role in the environment and in the process of liquefaction, which can occur during moderate to major earthquakes and cause significant structural damage. Liquefaction is defined as the transformation of granular material from a solid state to a liquid state, a process driven by increased pore water pressure and reduced effective stress within the soil. When an earthquake strikes, the shaking causes the pore water pressure between the sand grains to rise, which in turn reduces the contact forces between the grains. As a result, the sand loses its effective shear strength and starts to behave more like a fluid, leading to instability and potential collapse of structures built on such ground. Liquefaction can occur in moderate to major earthquakes, resulting in severe damage to structures. The transformation of granular material from a solid state to a liquid state due to increased pore pressure and reduced effective stress is defined as liquefaction. When this happens, the sand grains lose their effective shear strength and will behave more like a fluid. This phenomenon of dissolution of soil damages trees' stability and disturbs the formation of the earth's surface. Liquefaction resistance of soil depends on the initial state of soil to the state corresponding to failure. The liquefaction resistance can be evaluated based on tests on laboratory and in situ tests. For this research, liquefaction resistance using in-field tests based on SPT N values is attempted. Cyclic resistance ratio (CRR) is found based on the corrected N value. About 16 bore logs have been selected for the factor of safety calculation. The factor of safety for soil was arrived at by taking into account of corresponding corrected SPT N values. The liquefaction hazard map is prepared for the moment magnitude of 7.5-7.6 M w. It is also found that the areas close to water bodies and streams have the factor of safety less than unity. The bore log of locations having a factor of safety less than one indicates that up to a depth of about 6 m, very loose silty sand with clay and sand is present, which are defined as medium to fine sand having low field N values.

INTRODUCTION

An in-situ dynamic penetration test called the standard penetration test (SPT) is used to collect information on the soil's soil mechanics characteristics. The most common subsurface soil exploration test carried out globally is this one.

The primary goal of the test is to give a general idea of the relative density of granular deposits, including sand and gravel, from which it is nearly difficult to get undisturbed samples. The test's simplicity and low cost are its greatest strengths and the key factors behind its mass acceptance. The soil strength parameters that can be determined are approximate, but they may serve as a valuable reference in ground conditions, including gravels, sands, silts, clay that contains sand or gravel, and weak rock where it may not be practical to get borehole samples of appropriate quality.

Only soils that have filled in voids between grains of sand are liquefied. These soils are called water-saturated soils. The pressure that the water applies to the particles affects how tightly they are packed together. Before an earthquake, the pressure of water is low and stable. Yet, the water pressure may rise significantly

during the dynamic shaking, allowing the particles to freely pass one another. As that occurs, the soil deteriorates and becomes a slick, sticky liquid.

Recent geologic layers and sandy soils are the most susceptible to liquefaction in thorough field research (Fig. 1). They have also offered a database from which significant connections with engineering practices have been generated. They've demonstrated, for instance, that deposits that liquefy after one earthquake might do so once more during future ones.

Due to sandy soils, this type of liquefaction is called boiling of sand. Generally safe results of this liquefaction are "sand boils," which resemble miniature mud volcanoes (Fig. 2). Sand erupts from the soil with the same force as
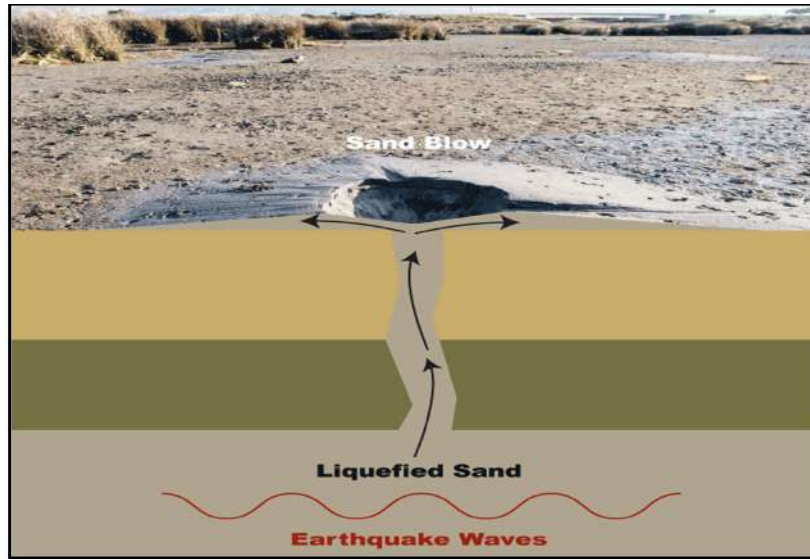

Fig. 1: Schematic vertical section showing where sills form by liquefaction during an earthquake. Reproduced from Obermeier (1996). Paleoseismic analysis of liquefaction-induced and other soft-sediment features. In: McCalpin, J.P. (Ed.), Paleoseismology. Second ed., Academic Press, Burlington, MA, pp. 497–564.
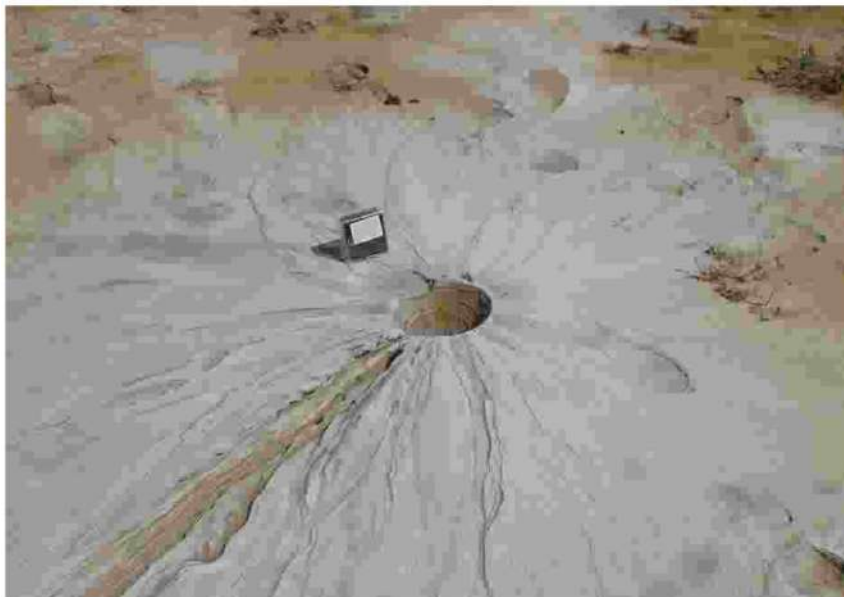

Fig. 2: One typical sand boil from Runn of Kutch's liquefied region, measuring 6 to 8 meters in diameter and 20 centimeters in height by Indian Institute of Technology, Kanpur, (https://www.iitk.ac.in/nicee/EQ_Reports/Bhuj/lique1.htm).

lava does from a volcano due to internal overpressure. A building might sink into the ground, as our feet did at the beach when soil liquefaction takes place underneath it. The structure might potentially collapse.

Some of the data used in this manuscript was obtained from an in-situ dynamic penetration test in an earthquake-affected area of Gujarat. The objective of the SPT is to determine the SPT N-value, which is an indication of the criteria governing soil strength, especially in granular soils. The SPT N-value can be correlated with soil properties for geotechnical engineering analysis and design. This value is also applicable for predicting the susceptibility of the soils to liquefaction.

A largely used liquefaction method of Standard Penetration Test (Fig. 3) of soil has been given by (Broichsitter et al. 2023, Guan et al. 2022, Zhu et al. 2021, Ordaz et al. 2023).

According to a consideration of the dynamic loading test, the cyclic pair in the cyclic load method analysis passes a high-risk zone right after it causes cyclic instability. Development-affected terrain with thick layers of soft soil and low groundwater levels is more prone to liquefaction. Results of cyclic, undrained tests on loose soils show that partially saturated soils display increased resistance at saturation levels that are only a tiny percentage below 100 (Pietruszczak et al. 2003). The triaxial tests showed how liquefaction pore pressure forms at low strains, and the fixed-base and free-top resonant column tests yielded specimens with dimensions similar to those of those tests.

The triaxial tests, which showed how liquefaction pore pressure forms at low strains, yielded specimens with dimensions similar to those of the fixed-base and free-top resonant column tests. The range of the effective stress ratios
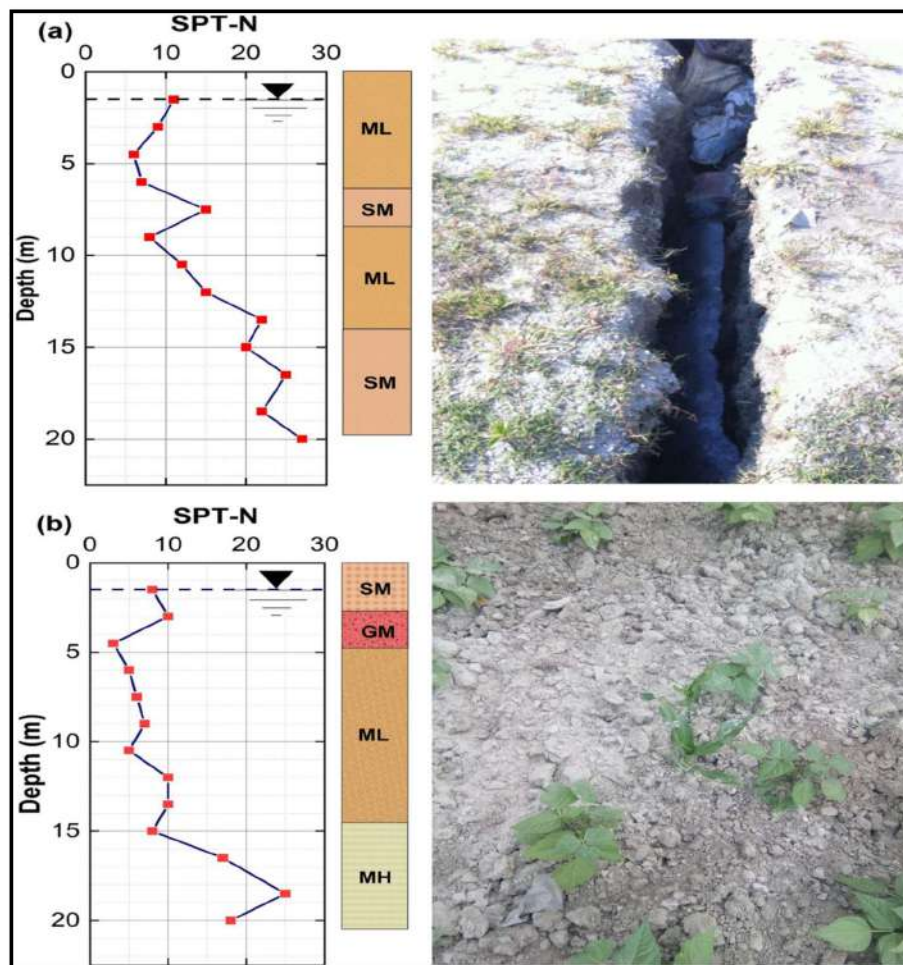

Fig. 3: Standard drill records show evidence of liquefaction in Manamaiju and Imadol during the 2015 Gorkha Earthquake (Subedi & Acharya 2022). Liquefaction hazard assessment and ground failure probability analysis in the Kathmandu Valley of Nepal, Geoenvironmental Disasters, Volume 9, Article No.: 1.

Table 1: Overview of the reviewed literature.

S. No.	Author	Methods of Analysis	Justification
1	Jethwa et al. (2018)	Deterministic In-situ analysis software	This report provides an overview of an alternative approach to assessing the liquefaction potential. The soil's back study demonstrates that there is liquefied dirt at the foundation level.
2	Liao & Whitman (1986)	Factors for Overburden Correction in SPT	Overburden factors have been analyzed over a variety of intermediate soil types, and normalizations of penetration resistance under overburden and cycle resistance ratios were performed. Overburden normalization of penetration resistances is based on either a permanent state factor or a steady void ratio.
3	Al-Jabban (2013)	Estimation of standard Penetration test (SPT)	SPT can offer dependable and practical data, the most used for geotechnical characterization tools a site mostly because of its simplicity and affordable price
4	Uprety & Lal (2021)	Standard penetration test	In this research, experiments are based on finding the N-value, or the resistance the soil presents to a sampler going inside it, which is the fundamental goal of doing SPT. Determine different soil qualities. These correlations and the field N-value help figure out the properties of the soil, but we should be aware that the tests and the empirical equations that produce the correlation have certain flaws.
5	Yusof & Zabidi (2018)	Standard penetration test (SPT) in predicting Properties of soil.	This manuscript defines test outcomes like the SPT number is significantly impacted by the shear strength parameter. Although SPT was conducted in the field on disturbed soil, it is sufficient to use SPT rather than laboratory testing to calculate the shear strength parameter. It is accurate to anticipate the shear strength parameter by taking into account the standard penetration test. The SPT number is greatly influenced by the depth of the soil, and the Atterberg limits have no impact on it because they depend on the mechanical and physical characteristics of the soil particles.
6	Skempton (1986)	Standard penetration Test with analysis of overburden	This paper analyzes soil at a given overburden pressure and constant relative density. N values might vary between various sands. By transforming the results into a conventional rod energy ratio, this impact can be completely removed. When the impacts of aging, particle size, and over-consolidation are taken into consideration, the variations that remain are fundamental to a characterization of the sands being studied and fall into a predictable pattern.
7	Gutierrez (2016)	Geostatistical data analysis of the standard penetration test (SPT)	The collection of SPT data into a single database turns out to be quite beneficial since it makes it possible to more readily spot commonalities and to combine different pieces of information for a better understanding of the soils. The usage of the geostatistics standard approach proved successful. The behavior of soils with respect to other variables that are presenting spatial variability enables us to discover potential relationships between their geomorphological traits and properties.
8	Yimsiri (2005)	Energy ratio of SPT practice	The impacts of friction, friction losses, parasitic effects of the borehole, and rod type have been analyzed for liquefaction.
9	Aggour and Radding (2001)	Standard penetration Test (SPT) correction	Different types of hammers, drill rigs, drill rod lengths, drill rod types, hammer blow rates, energy delivery systems with varying degrees of effectiveness, multiple borehole fluids, and various sampling tubes are used to measure the standard penetration resistance.
10	Kumar et al. (2016)	SPT using random number generation	In this paper, as a result, two distinct connections for cohesiveness are proposed for essentially two types of soils. Even though there are typical values for soil in the case of the angle of friction, a dramatic change in the plot's characteristics of randomly produced data is seen. Two distinct relationships for the friction angle are presented for various ranges of SPT N value as a result of this abrupt change in the plot. There are four distinct, discontinuous ranges of usual values for both the shear wave velocity and the Poisson's ratio.
11	Wazoh & Mallo (2014)	Standard penetration test	The N-value, which is essentially the resistance provided by the soil to the sampler entering inside it, is what SPT is measuring. Together with the N-value, SPT also gives us access to an SPT sample (Undisturbed Sample), which can be examined in a lab to ascertain different soil parameters. The usage of SPT is not limited to just determining N-value because it can be associated with many other soil parameters to aid in understanding the soil at the site. These correlations and the field N-value help figure out the properties of the soil, but we should be aware that the tests and the empirical equations that produce the correlation have certain flaws.

that lead to instability was shown to highlight the degree of uncertainty in that specific region.

Table 1 presents a summary of the reviewed literature on soil liquefaction analysis, outlining different methods and their justifications. Jethwa et al. (2018) employed deterministic in-situ analysis software to evaluate liquefaction potential, revealing the presence of liquefied soil at the foundation level. Liao & Whitman (1986) investigated overburden correction factors in the Standard Penetration Test (SPT), focusing on the normalization of penetration resistance. Al-Jabban (2013) highlighted SPT as a widely used, reliable, and cost-effective tool for geotechnical site characterization. Uprety & Lal (2021) conducted experiments to determine N-values, correlating them with soil properties while acknowledging the limitations of empirical correlations. These studies contribute to the broader understanding of seismic soil behavior, as discussed in prior research by (Agea et al. 2021), (Ahmadi 2015), (Ahmed et al. 2014), (Baki et al. 2012), (Bhattacharya et al. 2011), and (Bolton et al. 1985).

Positioning of Studies in Terms of Theory

Liquefaction is the loss of strength in saturated and cohesion-less soils due to increasing pore water pressures and reduced effective stresses caused by dynamic loading. It is a process in which earthquake shaking (seismic effect) or other quick loading reduces soil's strength and rigid properties.

Past Records of Liquefaction

It is important to assess the possibility of seismic hazard given the recent industrial expansion in Kutch-Gujarat, especially in the largest growing regions like Mundra, Kutch, and Bhuj. The worst earthquake to hit Kutch occurred in 2001. Also, we have seen an upsurge in seismic activity in recent months. So, the crucial requirement to reduce liquefaction is the assessment of liquefaction and the appropriate selection of foundation.

The liquefaction phenomenon is one of the main findings of an earthquake's secondary effects. The liquefaction caused by the 2001 Bhuj earthquake resulted in catastrophic failures in the form of lateral spreading, sudden settlements, etc. It is necessary to comprehend the causes and modes of these failures as well as the calculation of the factor of safety, total liquefaction potential, and cumulative settlement before planning and researching mitigation strategies for such failures.

To comprehend different failure kinds and reasons, this study has examined many events, including the following-

- Bhuj Earthquake (Mag. M_w =7.7) 2001
- Kutch Earthquake (Mag. M_w = 7.5) 2001

Seismic Liquefaction Hazard in Kathmandu and Nepal

Kathmandu Valley is highly susceptible to seismic liquefaction due to its alluvial deposits, loose sandy soils, and high groundwater levels. Studies, including (KC et al. 2020) and (Pokhrel et al. 2022), confirm moderate to high liquefaction risks, exacerbated by strong seismic activity like the 2015 Gorkha earthquake (Okamura et al. 2015). Liquefaction causes differential settlement, foundation failures, and building collapses, as observed by (Sharma et al. 2016) and (Setiawan et al. 2017). Critical infrastructure, including roads and pipelines, also suffer significant damage, disrupting lifeline services.

Probabilistic models, such as those by (Sianko et al. 2020), aid in assessing earthquake hazards and mitigating risks. To reduce vulnerability, enhanced building codes, soil stabilization, and hazard-resistant planning are essential. Future research should focus on site-specific ground improvement techniques to enhance resilience against liquefaction hazards in Kathmandu Valley.

Maps of Earthquake Hazard in Gujarat

The GSDMA started a study to create a Composite Hazard Risk and Security Vulnerabilities Map for the State, which would cover six natural and man-made hazards as well as the physical, social, and economic vulnerability of its citizens, assets, and economy at the taluka level. This would serve as a framework for undertaking mitigation investments and activities. The following hazards have been thoroughly studied using sophisticated computer-aided GIS models, probabilistic analysis, and thorough field studies: seismic tremor (between a 25 and 50-year return period), and crucially for Gujarat, drought over a century.

Two earthquake hazard risk maps (for 25 and 50-year return periods) were generated based on the earthquake risk event space probability information at PGA values calculated based on IS: 1893 (Part 1) 2002 classes (Fig. 4 & 5). Where PGA is Peak ground acceleration (PGA) is the maximum ground acceleration experienced at a spot during an earthquake's shaking. PGA is defined as the maximum absolute acceleration measured on an accelerogram at a location during a specific earthquake, expressed as amplitude.

Gujarat has faced several major earthquakes causing damage due to liquefaction. Notably, the Bhuj earthquake on January 26, 2001 (Mw=7.7), led to over 13,823 fatalities and widespread destruction, while another Mw=7.5 quake on the same day devastated Kutch, destroying Bhuj and critical infrastructure (Gujarat State Disaster Management Authority). Table 2 summarizes these past events, including the October 20, 2011 (Mw=5.0) Sasangir earthquake, which
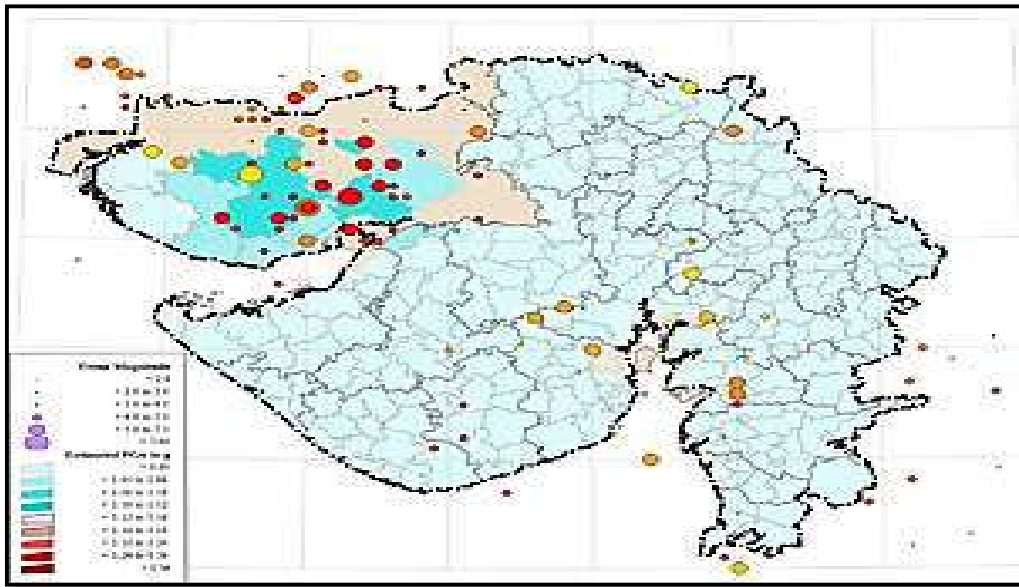
Fig. 4: The estimated mean Taluka PGA (in g) zonation for a 25-year Return period is presented [Provided by Gujarat State Disaster Management Authority, An Initiative of Government of Gujarat] assessed on dated 17/3/2024.
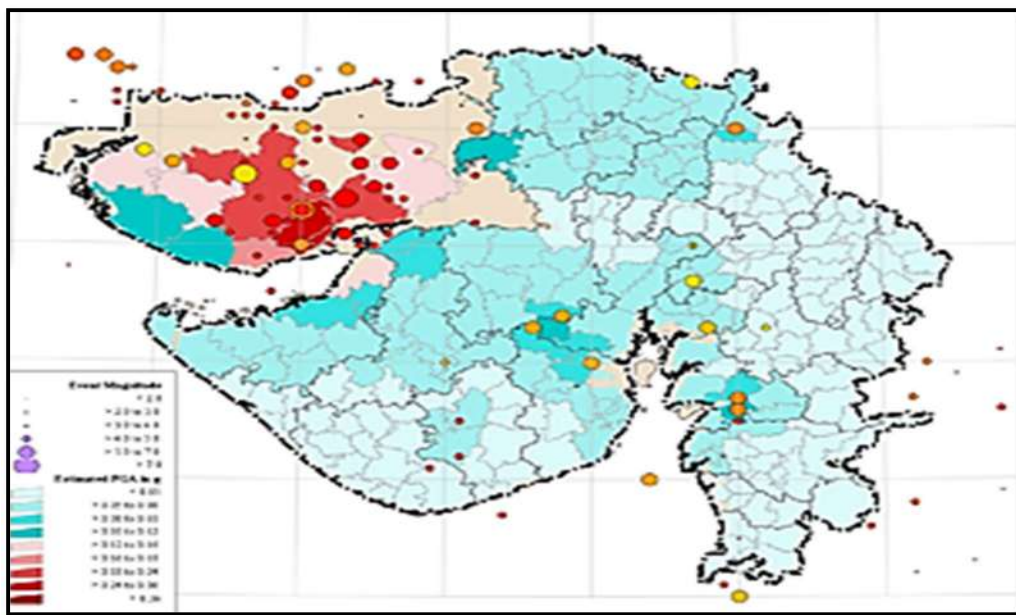

Fig. 5: The estimated mean Taluka PGA (in g) zonation for a 50-year Return period is presented [Provided by Gujarat State Disaster Management Authority, An Initiative of Government of Gujarat] assessed on dated 17/3/2024.

caused injuries and damage in Junagarh, and the August 5, 2003 (Mw=5.0) Suvi earthquake, which triggered panic across Gujarat. These incidents align with research on soil liquefaction and seismic impacts by Akin et al. (2011), (Amanta & Dasaka 2021), (Anagnostopoulos et al. 2003), (Broichsitter et al. 2023), (Chang et al. 2014), and (Chatterjee & Choudhury 2013).

MATERIALS AND METHODS

One of the in situ tests performed for coastal and near-coastal soil analysis initiatives is the Standard Penetration Test (SPT). SPT test data is often used to estimate the soil design parameters required for geotechnical analysis. However, the quality and reliability of SPT results are often unsatisfactory

Table 2: Records of events of damages in Gujarat due to liquefaction.

S. No.	Date	Place	Magnitude (Richter Scale)	Seismic Zone	Areas affected	Scale of Damage	References
1	20 Oct. 2011	Sasan Gir region, Gujarat	5.0	III	District of Junagarh, Gujarat, India	On October 20, 2011, at 22:48 local time, a mild earthquake struck the Gir National Park area of Gujarat's Saurashtra region in India. It was felt widely throughout the Kathiawar peninsula and as far away as Bombay, with a magnitude of Mw=5.0. In the district of Junagarh, there were numerous injuries and significant damage.	Gujarat State Disaster Management Authority
2	05 Aug. 2003	Suvi area, Gujarat	5.0	III	Suvi area, Gujarat, India	On August 5, 2003, at 16:38 local time, a moderate earthquake rocked Gujarat, India. It caused modest damage in eastern Kachchh and significant panic throughout Gujarat. The earthquake was Mw=5.0 in size.	National Center for Seismology Ministry of Earth Sciences, Government of India
3	26 Jan. 2001	Bhachau-Chobari (Bhuj) area, Gujarat	7.7	IV	Bhachau-Chobari, Gujarat, India	At 8:46 AM local time, a significant earthquake struck Gujarat, leaving over 13,823 people dead and significant property damage. A lower degree of damage was also sustained in the neighboring Indian states of Madhya Pradesh, Maharashtra, and Rajasthan, as well as the Pakistani province of Sindh.	Gujarat State Disaster Management Authority
4	26 Jan. 2001	Kutch, Gujarat	7.5	IV	Gujarat, Pakistan India	The price in the Kutch area was 13,000. About 20 kilometers separated the earthquake's epicenter from Bhuj, which was destroyed. In addition to four-hundredths of homes, eight colleges, two hospitals, and four kilometers of roads in Bhuj, the historic Swami Narayan Mandir, Praag Bhawan, and Aaina Mahal and forts were all severely damaged by the earthquake.	Gujarat State Disaster Management Authority
5	12 Sept. 2000	Bhavnagar area, Gujarat	3.8	III	Bhavnagar, Gujarat, India	The greatest shock in a seismic wave that started in 1999 and peaked in August 2000 left 1 person injured and a large no. of buildings destroyed. During the swarm, many more citizens fled Bhawnagar, and transportation services leaving the city were overrun by evacuees.	National Center for Seismology Ministry of Earth Sciences, Government of India
6	23 Mar. 1970	Ankleshwar-Bharuch area, Gujarat	5.4	III	Ankleshwar, Bhavnagar, Surat, and Vadodara	In Bharuch and the nearby villages, this earthquake resulted in 26 fatalities and 200 injuries. Bharuch City sustained significant damage. A 20-kilometer stretch of the ground was reported to have fissures, and considerable amounts of sand and water were released from them. Also, Ankleshwar, Bhavnagar, Surat, and Vadodara felt the tremor.	Avadh Ram, Broach (Gujarat) earthquake of March 23, 1970, Pure and Applied Geophysics

S. No.	Date	Place	Magnitude (Richter Scale)	Seismic Zone	Areas affected	Scale of Damage	References
7	21 July 1956	Anjar in Kutch	6.0	IV	Bhuj, Keira, Bhachaau, Gandhi-dham and the port town of Kandla	The area, particularly in and around the Indian city of Anjar, suffered significant damage and several fatalities. The perceptible radius was 300 km2, and the largest damaged area was 2000 km2.	The Rann of Cutch Earthquake of 21 July 1956, India Meteorological Department
8	27 Nov. 1945	Makran coast, Pakistan and kachchh	8.0	IV	Makran coast, Pakistan and kachchh	At least 2,000 deaths were reported from Iran and southern Pakistan. Twelve-meter-high tsunamis hit the Makran coast. Ormara area also suffered damage. Tsunamis with heights of more than 6 meters have also been recorded in Kachchh.	S.P. Prizomwala et al. (1922), Geological footprints of the 1945 Makran tsunami from the west coast of India, Marine Geology
9	23 July, 1938	Dhandhulka-Limbdi area, Gujarat, India	6.9	IV	Vikramgad, Morbi and Rajkot	Earthquakes were felt in Vikramgad, Morbi, and Rajkot. Southwest of Ahmedabad lies this region. felt in Vikramgad, Morbi and Rajkot. The Paliyad earthquake is another name for this event.	Seismological features of the Satpura earthquake, Indian Academy of Sciences
10	15 Aug. 1906	North of Bakhasara, Rajasthan, India	6.2	IV	Rajputana, Jodhpur, Ahmedabad, India	Gujarat, Sindh, and the India-Pakistan border all heavily felt this seismic effect. Rajputana, Jodhpur, Ahmedabad, and the area around the Gulf of Khambaat also experienced it for a few seconds.	Gujarat State Disaster Management Authority
11	16 June 1819	Rann of Kachchh, Gujarat	8.2	IV	Kachchh and nearby southern Pakistan regions	In Kachchh and nearby southern Pakistani regions, several towns and villages were destroyed, and 2,000 people died. The earthquake caused significant surface deformation, including the elevation of the Allah Bund, a 90-kilometer stretch of land, by several meters.	M. G. Thakkar et al. (1912), Terrain response to the 1819 Allah Bund earthquake in western Great Rann of Kachchh, Gujarat, India, Current Science Association

for a variety of reasons, including varying hammer drop height, drive rod tilting, and erroneous hammer firing resulting in incomplete energy transfer.

Introduction of SPT (Standard Penetration Test)

This test was primarily used to correlate soil-specific gravity, but today, it is used to build foundations based on load calculations. Numerous studies have been conducted to link the SPT N value of different soil properties. Various modifications are made to the SPT N-value fields since these correlations cannot be exact.

In this area, (Kumar et al. 2006) found that there are significant fault lines near Mumbai that are close to the area of Mumbai where liquefaction was studied.

The two variables used for the liquefaction estimation or calculations, which are determined using cyclic stress techniques, are as follows:

1. Cyclic Resistance Ratio (CRR): The cyclic resistance ratio is a measure of a soil's ability to resist liquefaction. Using the information from the SPT test, the most commonly used method of calculating liquefaction resistance,

2. CSR or cyclic stress ratio: The cyclic stress ratio serves as a representation of the seismic stress on the soil layers. Liquefaction could occur during an earthquake if the cyclic stress ratio induced by the earthquake is higher than the cyclic resistance ratio of the soil in situ.

Liquefaction assessment methods include the Cone Penetration Test (CPT) and Shear Wave Velocity (Vs) techniques, as compared by (Robertson 2015), and cyclic liquefaction evaluation via CPT (Robertson & Wride 1998). The Standard Penetration Test (SPT) is another common method, though it has limitations as discussed by (Sermalai et al. 2022), and can be improved using correlations with

other metrics (Ulmer et al. 2020). Surface analysis techniques for liquefaction evaluation have been explored by Shelley et al. (2014). Mitigation strategies, such as using gravel and geosynthetics, have been studied by (Setiawan et al. 2018), while seismic spectral acceleration estimations for risk assessment were analyzed by (RaghuKanth & Iyengar 2007). Kumar & Choudhary (2016) explored engineering property estimations from SPT results. Probabilistic models, such as those by (Sianko et al. 2020), aid in assessing earthquake hazards and mitigating risks. To reduce vulnerability, enhanced building codes, soil stabilization, and hazard-resistant planning are essential.

A flowchart shown in Fig. 6 presents the Standard Penetration Test (SPT) procedure, covering key steps such as sample collection, data filtering based on distance criteria, data interpretation, statistical analysis, correlation between DPT, and comparison with literature review before concluding with result analysis. The process highlights key considerations in evaluating soil properties through SPT. This study aligns with previous research on SPT and soil liquefaction assessment, as discussed in works by (Anbazhagan et al. 2013, 2012), (Fang et al. 2023), (Ghorbani & Rajab 2020), (Bolton et al. 1985) and (Atalic et al. 2021).

Flow Chart of Standard Penetration Test

Sample Collection

A borehole must be dug to the specified sampling depth for this test. The test uses a 650mm long, heavy-walled sample
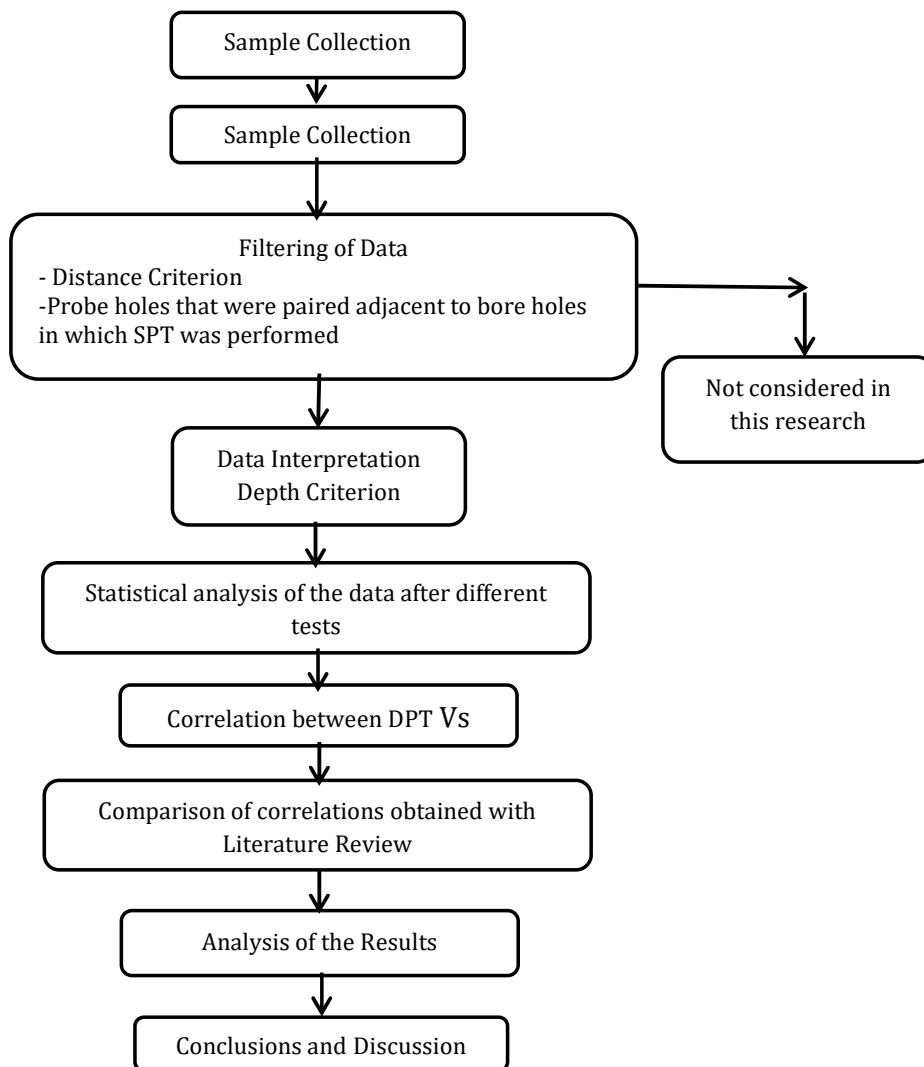

Fig. 6: Flowchart of the Standard Penetration Test (SPT) Procedure, illustrating key steps from sample collection to result analysis.

Fig. 7: The image shows the borehole location and Sample collection location by SPT at B.H. no.–1, Geomorphic features, and selected profiles in the study area, 2001 Bhuj earthquake Mw 7.5. Assessedby site of Kandla.

Fig. 8 (a)

Fig. 8 (b)

Fig. 8 (a) and (b): Photograph of the appearance of the soil sample of B.H. No. -1 (Between 3-5, 5-7, 10-12, and 12-15 m depth) of Kandla, Bhuj, Gujrat.

tube with an outer diameter of 50.8mm and an inner diameter of 35mm. The spoon sampler connected to the drill pipe is set down at the examination site.

The sampler is driven into the ground to a depth of 15 cm by continuously striking a hammer weighing 63.5 kg (140 lbs (long drill distance)) from a height of 76 cm (30 in) (6 in). It is noted how many strokes are necessary. This process is repeated two more times for a total insertion of 45 cm (18 inches).

Fig. 7 illustrates the borehole location and sample collection process using the Standard Penetration Test (SPT) at B.H. No. 1, highlighting geomorphic features and selected profiles in the study area. This location was assessed in relation to the 2001 Bhuj earthquake (Mw 7.5), specifically at the Kandla site.

Fig. 8(a) and 8(b) depict the retrieved soil samples from B.H. No. 1 at various depths (3-5 m, 5-7 m, 10-12 m, and 12-15 m) in Kandla, Bhuj, Gujarat, providing crucial insights into the subsoil characteristics of the earthquake-affected region.

RESULTS AND DISCUSSION

Data Interpretation

The usual penetration tests were carried out in accordance with the IS Code. However, the measured SPT-N value is affected by many variables, including the hammer, sampler, drilling techniques, rod types used in drilling, and hole size. All drill holes and samples shown in Fig. 6, 7, and 8 were subjected to standard penetration testing to 7m by 150mm diameter. For a geotechnical investigation, soil samples were taken from both damaged and undisturbed areas during drilling. At shallow depths, STP-N values are often low. However, there are more punches at deeper levels. No strike counts greater than 50 were observed, even at depths of 67 m, indicating liquefied behavior in the shallow layer of the study area. The estimated CRR is used to correct the SPT-N values.

Table 3 outlines the borehole data and soil classification for the study area, providing Standard Penetration Test (SPT) values and soil types at varying depths across locations including Bhuj, Mundra, Kutch, and Kandla. This data is essential for understanding the soil composition and its resistance characteristics, which are critical in evaluating the potential for soil liquefaction in earthquake-prone areas. In Bhuj, the soil predominantly consists of silty sand and coarse sand, with SPT values increasing from 5 (at 3-5 m) to 15 (at 13-15 m), indicating a shift from relatively loose to moderately dense conditions. Similarly, both Mundra and Kutch feature a mixture of coarse sand, silty sand, and silt, with SPT values ranging from 9 to 22, suggesting varying levels of compaction. Kandla, however, exhibits notably lower SPT values (4-6) across all depths, with soils primarily composed of silt and clay, which are more prone to deformation under seismic stress.

This analysis underscores the importance of site-specific soil characterization, as variations in soil properties

Table 3: Borehole data and type of soil of the study area.

B.H. No.	Location	Depth [m]	SPT Values (No. of blows)	Type of soil
1	Bhuj	3-5	5	Coarse sand
		5-7	9	Silty sand
		10-12	11	Silty sand and coarse sand
		13-15	15	Silty sand and coarse sand
2	Mundra	3-5	12	Coarse sand with silt
		5-7	9	Coarse sand
		10-12	13	Coarse sand with silt
		13-15	21	Silty sand
3	Kutch	3-5	12	Coarse sand with silt
		5-7	9	Coarse sand
		10-12	12	Coarse sand with silt
		13-15	22	Silty sand
4	Kandla	3-5	4	Silt and clay
		5-7	4	Silt and clay
		10-12	5	Silt and clay
		13-15	6	Silt and clay

play a crucial role in assessing seismic risks and foundation stability. Studies such as (Aude et al. 2022), (Audemard et al. 2005), (Ayele et al. 2021), (Chaulagain et al. 2016), (Chenjia et al. 2023), and (Chopra et al. 2012) have similarly emphasized the need for detailed soil analysis in earthquake-prone regions to better understand the potential for soil liquefaction and its impact on infrastructure stability.

Correlations for Fines Content and Soil Plasticity

Another change was the quantification of the fines correction to better fit the empirical data (Table 4) and support spreadsheet calculations. In the original development, (Seed et al. 1985) found that, for a given $(N_1)60$, CRR increases with increasing fines fraction. However, it is not clear whether the increase in CRR is due to greater resistance
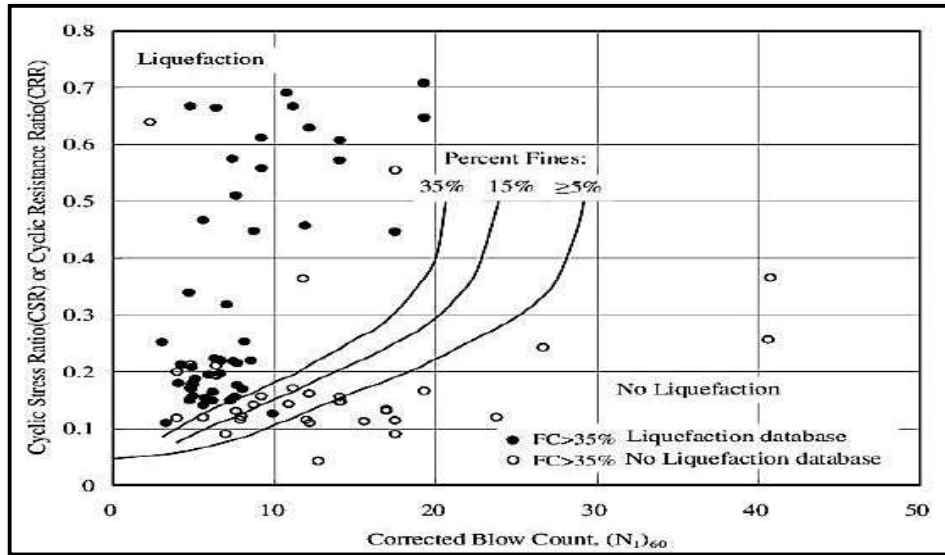

Fig. 9: Simplified baseline recommended for calculating CRR from SPT data together with empirical liquefaction data modified from (Seed et al. 1985).

Table 4: Correlation between soil sample and particle size distribution.

B.H. No.	Location	Fines Content (FC)[%]	D50 [mm]	Class of Soil	Depth of water table
1	Bhuj	4	0.50	SM	5 m
		25	0.30	SP	
		26	0.27	SP	
		26	0.27	SP	
2	Mundra	3	0.40	SP	3 m
		6	0.30	SP	
		3	0.41	SP	
		12	0.23	SM	
3	Kutch	3	0.40	SP	3 m
		6	0.30	SP	
		3	0.40	SP	
		11	0.21	SM	
4	Kandla	-	-	CH	At G.L.
		-	-	CH	
		-	-	CH	
		-	-	CH	

to liquefaction or less resistance to penetration as a result of the general increase in compressibility and decrease in permeability with increasing fines. Based on the available empirical data, Seed et al. (1985) developed CRR curves for different fines, as shown in Fig. 9.

Referring to Table 4, where, GW (Graded Gravel), GP (Poorly graded Gravel), SW (Well graded Sand), SP (Poorly graded Sand), SM (Silty Sand), GM (Silty Gravel), SC (Clayey Sand), GC are some of the different types of coarse-grained soils that are categorized (Clayey Gravel), CH (fat clays, inorganic clays with great plasticity) and D50 is the average particle diameter or mean particle size.

When the total percentage of gains reaches 50%, the appropriate particle size is D50. The term "median particle diameter" or "median particle size" is also used to refer to D50. For instance, if the D50 value for a soil sample is 5 m, this indicates that 50% of the particles are larger than 5 m and 50% are smaller than 5 m.

Due to the presence of fat clay as provided in Table 4 soil in the study area of B.H. No. 4, Kandla (Gujarat), no correlation has been found. A soil type known as "fat clays" is cohesive, elastic, and highly flexible, with a high percentage of elements that give the soil a viscous feel. When wet, difficult to deal with; when dry, strong.

Table 5 and Table 6 provide critical parameters and correlation values used in the liquefaction analysis for the study area. Table 5 outlines the key calculation parameters derived from the case study, considering an earthquake magnitude of 7.6 Mw and a peak ground acceleration (PGA) of 0.36g, based on the seismic zone classification for Kutch (Zone IV) as per IS-1893 (2002). The liquefaction potential was evaluated using the Idriss & Boulanger (2014) method, with soil sampling performed using a standard sampler in boreholes of 150mm diameter. Additionally, the lateral displacement assumptions indicate that the ground is flat across all boreholes, with no slope influence, and a 1.00m rod length was considered above ground.

Further, Table 6 presents the Cyclic Resistance Ratio (CRR) and Cyclic Stress Ratio (CSR) correlations for different borehole depths, which are essential for assessing liquefaction susceptibility. The CRR values, which indicate soil resistance against cyclic loading, vary across depths, with Borehole 1 showing a range from 0.117 at 4m to 0.165 at 9m, suggesting moderate resistance. Similarly, CSR values, representing the cyclic stress imposed by the earthquake, range from 0.215 to 0.539 in Borehole 1, highlighting variations in soil behavior at different depths. Notably, Borehole 3 exhibits a high CRR value of 0.291 at 9m, while Borehole 2 demonstrates relatively lower CRR values, suggesting different levels of soil susceptibility to liquefaction. Borehole 4 does not contain CRR and CSR data, indicating a potential lack of relevant testing or unsuitable soil conditions for analysis.

The Problem Stems from the CH Soil Type

High-plasticity clay has microscopic mineral grains that are particularly attractive to water. Although clay can usually absorb large amounts of water and still retain its strength, it expands in volume. It only takes one bad event, such as a broken water line or a major leak, for the bottom to become wet and the expansion process to begin. Once the swelling starts, it can last for years.

Table 5: Calculation parameters taken from case study.

Earthquake Magnitude	7.6 M_w
Peak ground acceleration (PGA)	0.36g (Kutch-Zone IV) (Zone factors based on Intensity of shaking IS-1893, 2002)
Calculation method	Idriss & Boulanger 2014
Sampling method	Standard Sampler
Borehole diameter	150mm
Lateral Displacement	The earth is flat for every borehole and there is no slope present.
Length of Rod	1.00m (above ground)

Table 6: Correlations for SPT using CSR and CRR.

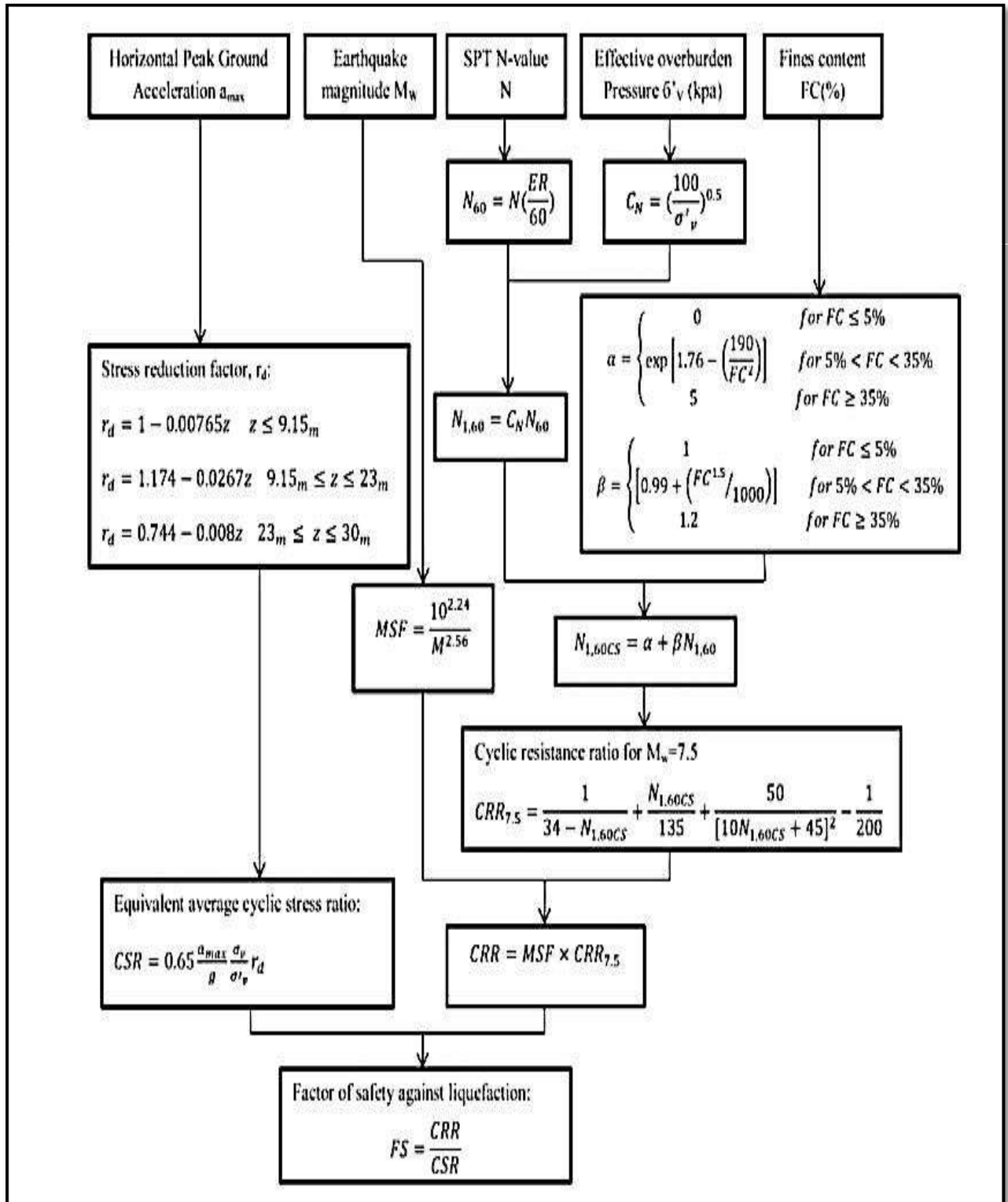| B.H. No.	CRR				CSR			
	1 m	4 m	9 m	14 m	1 m	4 m	9 m	14 m
1	0.17	0.117	0.165	0.135	0.215	0.493	0.539	0.498
2	0.08	0.098	0.098	0.078	0.458	0.443	0.443	0.368
3	0.173	0.158	0.291	0.233	0.244	0.326	0.891	0.708
4	-	-	-		-	-	-	-

Fig. 10: Assessment of the possibility for liquefaction, using the cyclic stress method, a summary flowchart of Seed and Idriss (1971) SPT-based method with modifications in the workshops by NCEER and NSF.

Table 7: Factors of safety against liquefaction.

B.H. No.	Ration of CRR and CSR			
	1 m	4 m	9 m	14 m
1	0.79	0.24	0.31	0.27
2	0.17	0.22	0.22	0.21
3	0.71	0.48	0.33	0.33
Avg. FOS	0.6	0.3	0.3	0.3
Liquefaction Severity Index	Very Critical	Very Critical	Very Critical	Very Critical

Fig. 10 presents a systematic flowchart for calculating the Factor of Safety (FS) against liquefaction, integrating various geotechnical and seismic parameters. The process begins with the Horizontal Peak Ground Acceleration (a_max), Earthquake Magnitude (M_w), SPT N-value (N), Effective Overburden Pressure (σ›v), and Fines Content (FC%), all of which influence the soil's resistance to liquefaction.

Table 7 presents the Factors of Safety (FS) against liquefaction, determined by calculating the ratio of the Cyclic Resistance Ratio (CRR) to the Cyclic Stress Ratio (CSR) at different depths across the boreholes. The results indicate that FS values remain consistently below 1.0, highlighting a significant susceptibility to liquefaction in the study area. Borehole 2 exhibits the lowest FS values, ranging from 0.17 at 1m depth to 0.22 at 9m, suggesting extreme vulnerability to seismic-induced soil failure. Similarly,

the average FS values across all boreholes at 1m, 4m, 9m, and 14m depths are 0.6, 0.3, 0.3, and 0.3, respectively, indicating that deeper layers remain highly susceptible to liquefaction. The Liquefaction Severity Index classifies all depths as "Very Critical," reinforcing the potential risk of ground deformation, excessive settlement, and structural instability during an earthquake. The findings emphasize the necessity for implementing liquefaction mitigation strategies, such as soil densification, deep foundations, or stabilization techniques, particularly in areas around Borehole 2, where the risk is most severe.

Clean Sand Base Curve

The simplified base curve's path is first changed to a low $(N_1)60$ curve with an estimated CRR intercept of roughly 0.05. With this change, the base curve is reshaped to be consistent with CRR curves.
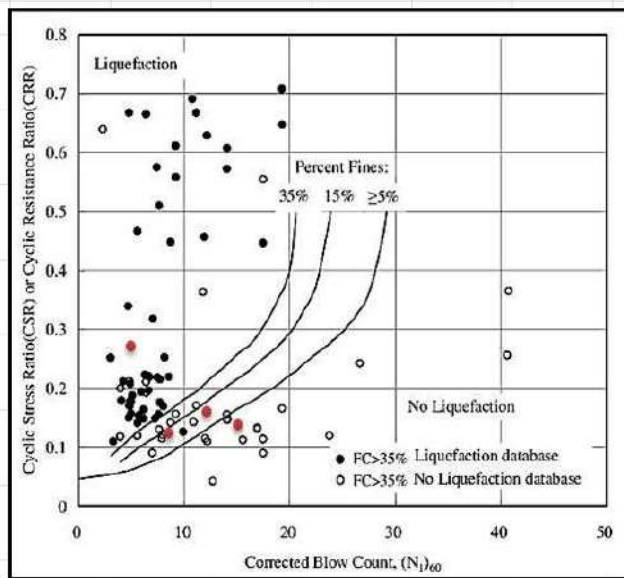

Fig. 11: Simplified Base Curve Recommended For Calculation of CRR from SPT Data along with Empirical Liquefaction Data Modified From (Seed et al. 1985) B.H.–2 mag. 7.5.
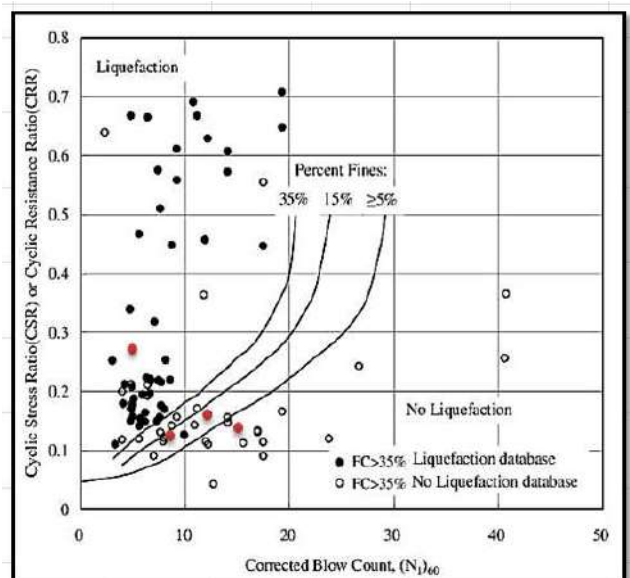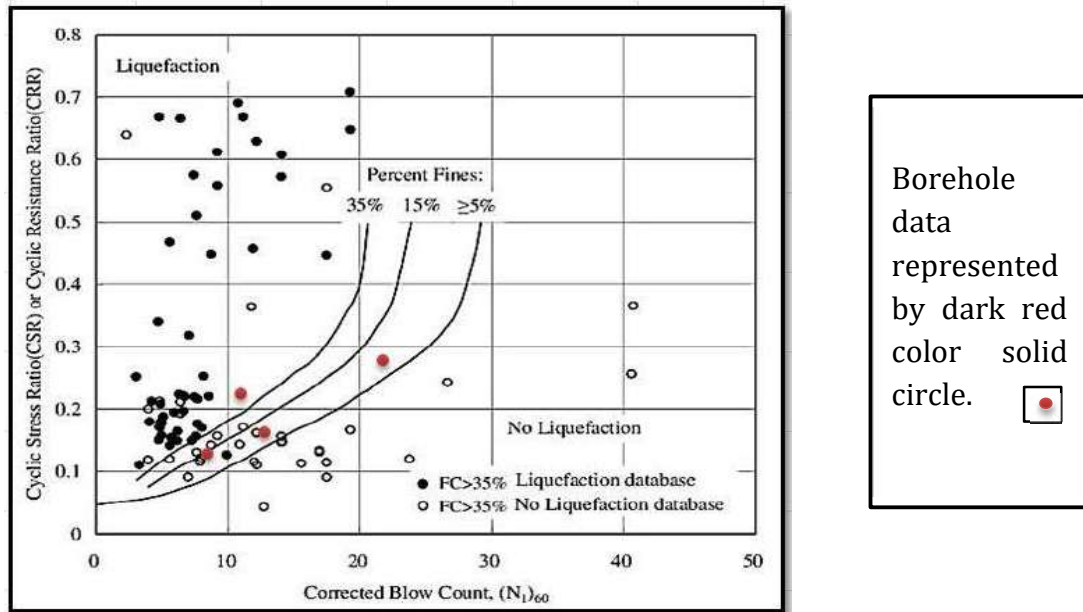
Fig. 12: Simplified Base Curve Recommended Calculation of CRR from SPT Data along with Empirical Liquefaction Data Modified From (Seed et al. 1985) B.H.–1 mag. 7.5.

Fig. 13: Simplified Base Curve Recommended for Calculation of CRR from SPT Data along with Empirical Liquefaction Data modified from (Seed et al. 1985) B.H.–1 mag. 7.5.

Fig. 11, 12, and 13 illustrate the Simplified Base Curve recommended for the calculation of the Cyclic Resistance Ratio (CRR) from Standard Penetration Test (SPT) data, incorporating empirical liquefaction data modified from (Seed et al. 1985). These figures are critical in evaluating the liquefaction resistance of soil deposits, as they provide a graphical approach for estimating CRR based on SPT values under seismic loading conditions. Fig. 11 represents the base curve for Borehole 1 under a magnitude 7.5 earthquake, while Fig. 12 presents a similar base curve for Borehole 2, reinforcing the applicability of empirical correlations for liquefaction assessment. Fig. 13 further confirms the recommended base curve for Borehole 1, emphasizing the significance of SPT-based correlations in determining soil stability during earthquakes. These graphical interpretations align with previous studies, such as (Seed and Idriss 1971) and (Ishihara 1977), who developed simplified procedures to evaluate soil liquefaction potential using SPT data. Additionally, research by (Ishihara et al. 1976) and (Nath et al. 2018) has demonstrated the effectiveness of these methods in predicting liquefaction risks in various seismic regions. Ibrahim (2014) further highlighted the role of alluvial soil deposits in liquefaction behavior, which is particularly relevant for regions with loose, saturated sands. The consistency of these findings with the historical studies of (Seed et al. 1985) affirms the reliability of SPT-based empirical models in liquefaction hazard assessment. By integrating these methodologies, engineers can refine their liquefaction risk evaluation, leading to safer foundation design and improved soil stabilization techniques in earthquake-prone areas.

CONCLUSION

Using the findings of other tests for the calculation of shear wave velocity is very helpful because geophysical studies are frequently expensive and time-consuming. This work focuses on establishing and providing a link between the findings of the standard penetration test (SPT), a factor of safety (severity Index), and the shear wave velocity of soil. To achieve this, many boreholes of varying depths were dug in several liquefied areas, especially near coastal cities, and SPT was conducted there.

Concentrating on the important characteristics of soil liquefaction caused by earthquakes and evaluating areas of agreement and disagreement using the Standard Penetration Test, although it has a great focus on earthquake engineering concerns. However, there are major uncertainties in the liquefaction assessment results based on the study and experimental area. Out of four areas (Bhuj, Kutch, Mundra, and Kandla), due to the presence of fat clay soil in the study area of Kandla (Gujarat), no CSR and CRR correlation has been found. Whereas the other three areas are approaching a very critical severity index for liquefaction. Only 75% of all sites, according to liquefaction research, have a safety factor of less than one. A quarter of the sites have fat clay soil, which could reduce soil tension during an earthquake. At 1.2 meters above ground level,

a modest water table has also been observed in these areas.

After testing and analyzing various borehole soil samples from four different depths, identified the behavior of soil:

- Mostly parallel to the stream of water sources where sandy soil or muddy clay would be present, lateral spread extension has a set direction.

- The technique shows its capacity to capture the geographical distribution of liquefaction potential and quantify the liquefaction likelihood at each position of a cross-section by analyzing actual data from liquefaction from the soil of different earthquake zones.

- Technical demand parameters were also utilized to explore this method, with the aid of the soil model and its characteristics. This manuscript evaluates the effects of soil material damping on the seismic analysis of systems with soil for MDOF (multi-degree of freedom) structures.

This report provides an overview of an alternative approach to assessing the liquefaction potential. The soil's back study demonstrates that there is liquefied dirt at the foundation level up to 14 meters for all three areas, excluding Kandla; the factor of safety can be employed in this paper. It is also found that areas close to water bodies and streams have the factor of safety less than unity. The bore log of locations having a factor of safety less than one indicates that up to a depth of about 6 m, very loose silty sand with clay and sand is present, which are classified as medium to fine sand having very low field N values.

REFERENCES

Agea, A., Medina, R. and Risk, P., 2021. Risk-targeted hazard maps for Spain. *Bulletin of Earthquake Engineering*, 19, pp.5369–5389.

Aggour, M. and Radding, W., 2001. *Standard penetration test (SPT) correction*. University of Maryland, Department of Civil and Environmental Engineering; Maryland Department of Transportation, State Highway Administration.

Ahmadi, E., 2015. Importance of soil material damping in seismic responses of soil-MDOF structure systems. *Soils and Foundations*, 55(1), pp.35-44.

Ahmed, S.M., Agaiby, S.W. and Rahman, A.H., 2014. A unified CPT–SPT correlation for noncrushable and crushable cohesionless soils. *Ain Shams Engineering Journal*, 5(1), pp.63-73.

Akin, M.K., Kramer, S.L. and Topal, T., 2011. Empirical correlations of shear wave velocity (Vs) and penetration resistance (SPT-N) for different soils in an earthquake-prone area (Erbaa-Turkey). *Engineering geology*, 119(1-2), pp.1-17.

Al-Jabban, A., 2013. Estimation of standard penetration test (SPT) of Hilla City - Iraq by using GPS coordination. *Jordan Journal of Civil Engineering*, 7(2).

Amanta, A.S. and Dasaka, S.M., 2021. Air injection method as a liquefaction countermeasure for saturated granular soils. *Transportation Geotechnics*, 30, p.100622.

Anagnostopoulos, A., Koukis, G., Sabatakis, N. and Tsiambaos, G., 2003. Empirical correlations of soil parameters based on cone penetration tests for Greek soils. *Geotechnical and Geological Engineering*, 21, pp.377–387.

Anbazhagan, P., Kumar, A. and Sitharam, T.G., 2013. Seismic site classification and correlation between standard penetration test N value and shear wave velocity for Lucknow City in Indo-Gangetic Basin. *Pure and applied geophysics*, 170, pp.299-318.

Anbazhagan, P., Parihar, A. and Rashmi, H.N., 2012. Review of correlations between SPT-N and shear modulus: a new correlation applicable to any region. *Soil Dynamics and Earthquake Engineering*, 36, pp.52–69.

Atalic, J., Uroš, M., Novak, M.S., Demšić, M. and Nastev, M., 2021. The Mw5.4 Zagreb (Croatia) earthquake of March 22, 2020: impacts and response. *Bulletin of Earthquake Engineering*, 19, pp.3461–3489.

Aude, S.A., Mahmood, N.S., Sulaiman, S.O., Hasan Hussain Abdullah, H.H. and Ansari, N.A., 2022. Slope stability and soil liquefaction analysis of earth dams with a proposed method of geotextile reinforcement. *International Journal of Geomate*, 22(94), pp.102-112.

Audemard, F.A., Gomez, J.C., Tavera, H.J. and Orihuela, N., 2005. Soil liquefaction during the Arequipa Mw 8.4, June 23, 2001 earthquake, southern coastal Peru. *Engineering Geology*, 78(3–4), pp.237-255.

Ayele, A., Woldearegay, K. and Meten, M., 2021. A review on the multi-criteria seismic hazard analysis of Ethiopia: with implications for infrastructural development. *Geoenvironmental Disasters*, 8(1), pp.1–22.

Baki, Md. A.L., Rahman, M.M. and Gnanendran, C.T., 2012. Linkage between static and cyclic liquefaction of loose sand with a range of fines contents. *Canadian Geotechnical Journal*, 49(6), pp.891–906.

Bhattacharya, S., Hyodo, M., Goda, K., Tazoh, T. and Taylor, C.A., 2011. Liquefaction of soil in the Tokyo Bay area from the 2011 Tohoku (Japan) earthquake. *Soil Dynamics and Earthquake Engineering*, 31(11), pp.1618-1628.

Bolton, S.H., Tokimatsu, K., Harder, L.F. and Chung, R.M., 1985. Influence of SPT procedures in soil liquefaction resistance evaluations. *Journal of Geotechnical Engineering*, 111(12), pp.1425–1445.

Broichsitter, S.B., Schroeder, R., Mordhorst, A., Fleige, H. and Horn, R., 2023. Soil water diffusivity as a function of the pore size distribution and pre-compression stress. *Soil and Tillage Research*, 229, p.105675.

Chang, D.W., Cheng, S.H. and Wang, Y.L., 2014. One-dimensional wave equation analyses for pile responses subjected to seismic horizontal ground motions. *Soils and Foundations*, 54(3), pp.313–328.

Chatterjee, K. and Choudhury, D., 2013. Variations in shear wave velocity and soil site class in Kolkata city using regression and sensitivity analysis. *Natural Hazards*, 69(3), pp.2057–2082.

Chaulagain, H., Rodrigues, H., Silva, V., Spacone, E. and Varum, H., 2016. Earthquake loss estimation for the Kathmandu Valley. *Bulletin of Earthquake Engineering*, 14(1), pp.59–88.

Chopra, S., Kumar, D., Rastogi, B.K., Choudhury, P. and Yadav, R.B.S., 2012. Estimation of seismic hazard in Gujarat region, India. *Natural Hazards*, 65(2), pp.1157–1178.

Fang, Y., Idriss, J. and Pirhadi, N., 2023. Neural transfer learning for soil liquefaction tests. *Computers & Geosciences*, 171, p.105282.

Ghorbani, E. and Rajab, A.M., 2020. A review on SPT-based liquefaction potential evaluation to assess the possibility of performing a risk management. *Transactions on Civil Engineering*, 27(2), pp.639-656.

Guan, Y., Liu, H., Zhang, L. and Xu, Y., 2022. Efficient three-dimensional soil liquefaction potential and reconsolidation settlement assessment from limited CPTs considering spatial variability. *Soil Dynamics and Earthquake Engineering*, 163, p.107518.

Gutierrez, L., 2016. Análise geoestatística de dados do ensaio a percussão SPT e correlações com o relevo para a cidade de Maringá-PR. *Universidade Estadual de Maringá, Centro de Tecnologia, Departamento de Engenharia Civil, Pós-Graduação em Engenharia Civil – Mestrado*.

Ibrahim, M., 2014. Liquefaction analysis of alluvial soil deposits in Bedsa southwest of Cairo. *Ain Shams Engineering Journal*, 5(3), pp.647–655.

Ishihara, K., 1977. Simple method of analysis for liquefaction of sand deposits during earthquakes. *Soils and Foundations*, 17(3), pp.1–14.

Ishihara, K., Yoshimoto, N. and Matsuo, O., 1976. Prediction of liquefaction of sand deposits during earthquake. *Soils and Foundations*, 16(1), pp.1–16.

Jethwa, A., Pandya, H. and Sharma, R., 2018. Liquefaction analysis for Kutch region using deterministic in-situ analysis software. *International Research Journal of Engineering and Technology (IRJET)*, 5(4), pp.2395–0056.

KC, A., Joshi, S., and Paudel, S., 2020. Probabilistic seismic liquefaction hazard assessment of Kathmandu Valley, Nepal. *Geomathematics and Natural Hazards Risk*, 11(1), pp.259–271.

Kumar, P., Ranjan, R., and Sharma, V., 2016. Simulation of rock subjected to underground blast using FLAC3D. *Japanese Geotechnical Society Special Publication*, 2, pp.508–511.

Kumar, R. and Choudhary, D., 2016. Estimation of engineering properties of soils from field SPT using random number generation. *INAE Letters*, 1, pp.77–84.

Kumar, S., Singh, S. and Nandini, D., 2006. Method for regulated expression of single-copy efflux pump genes in a surrogate Pseudomonas aeruginosa strain: identification of the BpeEF-OprC chloramphenicol and trimethoprim efflux pump of Burkholderia pseudomallei 1026b. *Antimicrobial Agents and Chemotherapy*, 50(10), pp. 3460–3463.

Liao, S. and Whitman, R.V., 1986. Overburden correction factors for SPT in sand. *Journal of Geotechnical Engineering*, 112(3), pp. 373–377.

Nath, S., Saha, S., Pati, P. and Sahoo, S., 2018. Earthquake induced liquefaction hazard, probability, and risk assessment in the city of Kolkata, India: Its historical perspective and deterministic scenario. *Journal of Seismology*, 22(1), pp. 35–68.

Obermeier, S.F., 1996. Use of liquefaction-induced features for paleo seismic analysis: An overview of how seismic liquefaction features can be distinguished from other features and how their regional distribution and properties of source sediment can be used to infer the location and strength of Holocene paleo-earthquakes. *Engineering Geology*, 44(1–4), pp. 1–76.

Okamura, H., Yamada, T., Matsumoto, S. and Ueda, S., 2015. Report on a reconnaissance survey of damage in Kathmandu caused by the 2015 Gorkha Nepal earthquake. *Soils and Foundations*, 55(5), pp. 1015–1029.

Ordaz, M., Yegian, M.K., Lin, L. and Giardini, D., 2023. Event-based probabilistic liquefaction hazard analysis for defining soil acceptance criteria. *Soil Dynamics and Earthquake Engineering*, 166, p. 107781.

Pietruszczak, S., Tatsuoka, F. and Zienkiewicz, O.C., 2003. Mitigation of risk of liquefaction. *Geotechnique*, 53(9), pp.833–838.

Pokhrel, R.M., Gilder, C.E., Vardanega, P.J., De Luca, F., De Risi, R., Werner, M.J. and Sextos, A., 2022. Liquefaction potential for the Kathmandu Valley, Nepal: a sensitivity study. *Bulletin of Earthquake Engineering*, 20(1), pp.25-51.

Prizomwala, S.P., Vedpathak, C., Tandon, A., Das, A., Makwana, N. and Joshi, N., 2022. Geological footprints of the 1945 Makran tsunami from the west coast of India. *Marine Geology*, 446, p.106773.

RaghuKanth, S.T.G. and Iyengar, R.N., 2007. Estimation of seismic spectral acceleration in Peninsular India. *Journal of Earth System Science*, 116, pp. 199–214.

Robertson, P.K. and Wride, C., 1998. Evaluating cyclic liquefaction potential using the cone penetration test. *Canadian Geotechnical Journal*, 35, pp. 442–459.

Robertson, P.K., 2015. Comparing CPT and Vs liquefaction triggering methods. *Journal of Geotechnical and Geo-environmental Engineering*, 2015.

Seed, H.B. and Idriss, I.M., 1971. Simplified procedure for evaluating soil liquefaction potential. *Journal of the Soil Mechanics and Foundations Division, ASCE*, 97(SM9), pp. 1249–1273.

Seed, H.B., Idriss, I.M. and Arango, I., 1985. Influence of SPT procedure in soil liquefaction resistance evaluations. *Journal of Geotechnical Engineering, ASCE*, 111(12), pp. 1425–1445.

Sermalai, S., Mukundan, M. and Alagirisamy, S., 2022. Standard Penetration Test (SPT) pitfalls and improvements. In: Reddy, C.N.V., Muthukkumaran, K., Satyam, N., Vaidya, R., eds. *Ground Characterization and Foundations*. *Civil Engineering*, vol. 167.

Setiawan, H., Serikawa, Y., Nakamura, M., Miyajima, M. and Yoshida, M., 2017. Structural damage to houses and buildings induced by liquefaction in the 2016 Kumamoto earthquake, Japan. *Geoenviron Disasters*, 4(1), pp. 1–12.

Setiawan, H., Serikawa, Y., Sugita, W., Kawasaki, H. and Miyajima, M., 2018. Experimental study on mitigation of liquefaction-induced vertical ground displacement by using gravel and geosynthetics. *Geoenviron Disasters*, 5(1), pp. 1–9.

Sharma, K., Deng, L. and Noguez, C.C., 2016. Field investigation on the performance of building structures during the April 25, 2015, Gorkha earthquake in Nepal. *Engineering Structures*, 121, pp. 61–74.

Shelley, E.O., Mussio, V., Rodriguez, M. and Chang, A., 2014. Evaluation of soil liquefaction from surface analysis. *Geofísica Internacional*, 54(1), pp. 95–109.

Sianko, I., Ozdemir, Z., Khoshkholghi, S., Garcia, R., Hajirasouliha, I., Yazgan, U. and Pilakoutas, K., 2020. A practical probabilistic earthquake hazard analysis tool: case study Marmara region. *Bulletin of Earthquake Engineering*, 18, pp. 2523–2555.

Skempton, A.W., 1986. Standard penetration test procedures and the effect in sands of overburden pressure, relative density, particle size, aging, and over-consolidation. *Geotechnique*, 36, pp. 425–447.

Subedi, S. and Acharya, L., 2022. Liquefaction hazard assessment and ground failure probability analysis in the Kathmandu Valley of Nepal. *Geoenviron Disasters*, 9(1).

Thakkar, M.G., Ngangom, M., Thakker, P.S. and Juyal, N., 2012. Terrain response to the 1819 Allah Bund earthquake in western great rann of Kachchh, Gujarat, India. *Current Science*, pp.208-212.

Ulmer, K.J., Green, R.A. and Marek, A.R., 2020. Consistent correlation between Vs, SPT, and CPT metrics for use in liquefaction evaluation procedures. *Geo-Congress*, February 2020.

Uprety, S. and Lal, R., 2021. Standard penetration test in geotechnical engineering site investigations. *Journal of Emerging Technologies and Innovative Research*, 8(4).

Wazoh, S.A. and Mallo, S.P., 2014. Standard penetration test in engineering geological site investigations – A review. *The International Journal of Engineering and Science (IJES)*.

Yimsiri, S., 2005. Distinct element analysis of soil-pipeline interaction in sand under upward movement at deep embedment condition. In *Proceedings of the 16th International Conference on Soil Mechanics and Geotechnical Engineering*, vol. 3.

Yusof, N. and Zabidi, M.A., 2018. Reliability of using standard penetration test (SPT) in predicting properties of soil. *Journal of Physics: Conference Series*, 1082, p. 012094.

Zhu, Z., Liu, J., Yang, H. and Zhang, L., 2021. Assessment of tamping-based specimen preparation methods on static liquefaction of loose silty sand. *Soil Dynamics and Earthquake Engineering*, 143, p. 106592.

... Continued from inner front cover

- The text of the manuscript should run into Abstract, Introduction, Materials & Methods, Results, Discussion, Acknowledgement (if any) and References or other suitable headings in case of reviews and theoretically oriented papers. However, short communication can be submitted in running with Abstract and References. The references should be in full with the title of the paper and mentioning names of all the authors.

- The figures should preferably be made on a computer with high resolution and should be capable of withstanding a reasonable reduction with the legends provided separately outside the figures. Photographs may be black and white or colour.

- Tables should be typed separately bearing a short title, preferably in vertical form. They should be of a size, which could easily be accommodated in the page of the Journal.

- References in the text should be cited by the authors' surname and year. In case of more than one reference of the same author in the same year, add suffix a,b,c,.... to the year. For example: (Thomas 1969, Mass 1973a, 1973b, Madony et al. 1990, Abasi & Soni 1991).

List of References

The references cited in the text should be arranged alphabetically by authors' surname in the following manner: (Note: The titles of the papers should be in running 'sentence case', while the titles of the books, reports, theses, journals, etc. should be in 'title case' with all words starting with CAPITAL letter). The references should be given in the **"Harvard Pattern"** as exemplified below.

- Dutta, A. and Chaudhury, M., 1991. Removal of arsenic from groundwater by lime softening with powdered coal additive. *Journal of Water Supply: Research and Technology—Aqua*, 40(1), pp.25-29. **(For Papers Published in Journals)**

- Goel, P.K., 2006. *Water pollution: Causes, Effects and Control*. New age international, New Delhi. **(For Authored Books)**

- Environmental Protection Agency (EPA), 2023. Air Quality and Pollution Data. Retrieved June 25, 2024, from https://www.epa.gov/air-quality-and-pollution-data **(For Data Retrieved from a Website)**

- Hammer, D.A. (ed.), 1989. *Constructed Wetlands for Wastewater Treatment-Municipal, Industrial and Agricultural*. Lewis Publishers Inc., pp.831. **(For Edited Book)**

- Haynes, R.J., 1986. Surface mining and wetland reclamation. In: J. Harper and B. Plass (eds.) *New Horizons for Mined Land Reclamation*. Proceedings of a National Meeting of the American Society for Surface Reclamation, Princeton, W.V. **(For Papers published in Edited Books)**

Submission of Papers

- The papers have to be submitted online in a single WORD file through the online submission portal of journal's website: **www.neptjournal.com**

Attention

1. Any change in the authors' affiliation may please be notified at the earliest.
2. Please make all the correspondence by e-mail, and authors should always quote the manuscript number.

Note: In order to speed up the publication, authors are requested to correct the galley proof immediately after receipt. The galley proof must be checked with utmost care, as publishers owe no responsibility for mistakes. The papers will be put on priority for publication only after receiving the processing and publication charges.

For further details of the Journal, please visit the website. All the papers published on a particular subject/topic or by any particular author in the journal can be searched and accessed by typing a keyword or name of the author in the 'Search' option on the Home page of the website. All the papers containing that keyword or author will be shown on the home page from where they can be directly downloaded.

www.neptjournal.com